Appendix F

CENRAP Technical Support Document

Draft Report

Technical Support Document for CENRAP Emissions and Air Quality Modeling to Support Regional Haze State Implementation Plans

Prepared for:
Central Regional Air Planning Association
10005 S. Pennsylvania, Suite C
Oklahoma City, OK 73159

Prepared by:
ENVIRON International Corporation
101 Rowland Way, Suite 220
Novato, CA 94945

and

University of California at Riverside
College of Engineering Center for
Environmental Research and Technology
Riverside, Ca 92517

September 12, 2007

TABLE OF CONTENTS

Page

APPENDICES

TABLES

FIGURES

1.0 INTRODUCTION

This Technical Support Document (TSD) describes the Central Regional Air Planning Association (CENRAP) regional emissions and air quality modeling to support the central states Regional Haze Rule (RHR) State Implementation Plans (SIPs). The CENRAP 2002 annual emissions and air quality modeling was performed by the contractor team of ENVIRON International Corporation (ENVIRON) and the University of California at Riverside (UCR).

1.1 Background

The 1977 Clean Air Act Amendments (CAAA) added a new Section 169A for the protection of visibility in Federal Class I areas (specific national parks, wilderness areas and wildlife refuges). Section 169A(a)(1) of the CAAA established the national goal for visibility protection: "Congress hereby declares as a national goal the prevention of any future, and the remedying of any existing, impairment of visibility in mandatory class I Federal areas which impairment results from manmade air pollution." The CAAA require States to submit SIPs containing emission limits, schedules of compliance and to "promulgate regulations to assure reasonable progress toward meeting the national goal" (Section 169A(a)(4)). In response to these mandates EPA promulgated the Regional Haze Rule (RHR) on July 1, 1999 that requires States to "establish goals (expressed in deciviews) that provide for reasonable progress towards achieving natural visibility conditions" at Class I areas. The States' RHR SIPs are due December 17, 2007 and an important component of the SIP will be the 2018 Reasonable Progress Goals (RPGs) toward achieving natural conditions in 2064. Regional air quality models are used to project visibility to 2018 to determine the level of visibility improvement that is expected to be achieved in 2018. This information, along with other sources, can be used by the states to assist in setting their 2018 RPGs.

CENRAP is one of five Regional Planning Organizations (RPOs) that have responsibility for coordinating development of SIPs and Tribal Implementation Plans (TIPs) in selected areas of the U.S. to address the requirements of the RHR. CENRAP is a regional partnership of states, tribes, federal agencies, stakeholders and citizen groups established to initiate and coordinate activities associated with the management of regional haze and other air quality issues within the CENRAP states. The CENRAP region includes states and tribal lands located within the boundaries of Arkansas, Iowa, Kansas, Louisiana, Minnesota, Missouri, Nebraska, Oklahoma and Texas.

The CENRAP Emissions and Air Quality Modeling Team is composed of staff from ENVIRON and UCR, with assistance and coordination from the CENRAP states, tribes, federal agencies and stakeholders. The ENVIRON/UCR Team performs the emissions and air quality modeling simulations for states and tribes within the CENRAP region, providing analytical results used in developing implementation plans under the RHR. Figure 1-1 shows the states included in each of the five RPOs in the U.S., including CENRAP. Table 1-1 lists the Class I areas within the CENRAP states.

CENRAP is performing emissions and air quality modeling to project visibility to 2018. The modeling results will be used to determine the level of visibility improvement expected in 2018

under various emission scenarios. States will use these results to assist in determining their 2018 RPGs toward achieving natural conditions in 2064.

Figure 1-1. Regional Planning Organizations engaged in Regional Haze Modeling.

Table 1-1. Federal Mandated Class I Areas in the CENRAP States.

Class I Area	Acreage	Federal Land Manager	Public Law
Arkansas			
Caney Creek Wilderness Area	14,460	USDA-FS	93-622
Upper Buffalo Wilderness Area	12,018	USDA-FS	93-622
Louisiana			
Breton Wilderness Area	5,000+	USDI-FWS	93-632
Minnesota			
Boundary Waters Canoe Area Wilderness	810,088	USDA-FS	99-577
Voyageurs National Park	114,964	USDI-NP	99-261
Missouri			
Hercules-Glade Wilderness Area	12,314	USDA-FS	94-557
Mingo Wilderness Area	8,000	USDI-FWS	95-557
Oklahoma			
Wichita Mountains Wilderness	8,900	USDI-FWS	91-504
Texas			
Big Bend National Park	708,118	USDI-NP	74-157
Guadalupe Mountains National Park	76,292	USDI-NP	89-667

1.2 CENRAP Organizational Structure and Work Groups

The governing body of CENRAP is the Policy Oversight Group (POG) that is made up of voting members representing states and tribes within the CENRAP region and non-voting members representing local agencies, the EPA and other federal agencies. The work of CENRAP is accomplished through five standing workgroups:

- Monitoring;
- Emissions Inventory;
- Modeling;
- Communications; and
- Implementation and Control Strategies.

Participation in workgroups is open to all interested parties and the POG may form additional ad hoc workgroups to address specific issues (e.g., a Data Analysis workgroup was formed).

The RHR requires the states, and the tribes that may elect to, submit the first SIPs and TIPs that address progress toward natural conditions at federally mandated Class I areas by December 17, 2007. 40 CFR 51.308 (Section 308) discusses the following four core requirements to be included in SIPs/TIPs and Best Available Retrofit Technology (BART) requirements:

1. Reasonable progress goals;
2. Calculations of baseline and natural visibility conditions;
3. A Long-term strategy for regional haze;
4. A Monitoring strategy and other implementation plan requirements; and
5. BART requirements for regional haze visibility impairment.

One of CENRAP's goals is to provide support to states and tribes to meet each of these requirements of the RHR and to develop scientifically supportable, economical and effective control strategies that the states and tribes may adopt to reduce anthropogenic effects on visibility impairment at Class I areas. One component of CENRAP's support to states and tribes as part of compliance with the RHR is performing emissions and air quality modeling. These activities were implemented to:

- obtain a better understanding of the causes of visibility impairment and to identify potential mitigation measures for visibility impairment at Class I areas;
- to evaluate the effects of alternative control strategies for improving visibility; and
- to project future-year air quality and visibility conditions.

In October 2004, CENRAP selected the team of ENVIRON and UCR to perform their Emissions and Air Quality Modeling.

The CENRAP Emissions and Air Quality Modeling Team performs regional haze analyses by operating regional scale, three-dimensional air quality models that simulate the emissions, chemical transformations, and transport of gaseous and particulate matter (PM) species and consequently the effects on visibility in Class I Areas in the central U.S. A key element of this work includes the integration of emissions inventories and emissions models with regional transport models. The general services provided by the CENRAP Emissions and Air Quality Modeling Team include, but are not limited to:

- Emissions processing and modeling;
- Air quality and visibility modeling simulations;
- Analysis, display, and reporting of modeling results; and
- Storage/quality assurance of the modeling input and output files.

The CENRAP 2002 annual Emissions and Air Quality Modeling Team performs work for the CENRAP Modeling Workgroup through direction from the CENRAP Technical Director and CENRAP Executive Director.

1.3 Overview of 2002 Annual Emissions and Air Quality Modeling Approach

The CENRAP 2002 annual emissions and air quality modeling was initiated on October 16, 2004 and involved the preparation of numerous databases, model simulations, presentations and reports. Much of the modeling analyses have been posted to the CENRAP modeling website at: http://pah.cert.ucr.edu/aqm/cenrap/index.shtml. There were numerous versions and iterations of the modeling and interim results. The results presented in this TSD focus on the final modeling results and key findings in their development. The reader is referred to the modeling website for interim products.

1.3.1 Modeling Protocol

A Modeling Protocol was prepared at the outset of the study to serve as a road map for performing the CENRAP emissions and air quality modeling and to communicate the modeling

plans to the CENRAP participants. The Modeling Protocol was prepared following EPA guidance for preparation at the time it was prepared (EPA, 1991; 1999, 2001) and took into account CENRAP's long-term plan (CENRAP, 2003) and the modeling needs of the RHR SIPs. The first version (Version 1.0) of the Modeling Protocol was dated November 19, 2004. Based on comments received from CENRAP, the Modeling Protocol was updated to the current Version 2.0 (Morris et al., 2004a) that was dated December 8, 2004. This Modeling Protocol can be found on the CENRAP modeling Website at:

http://pah.cert.ucr.edu/aqm/cenrap/docs/CENRAP_Draft2.0_Modeling_Protocol_120804.pdf

1.3.2 Quality Assurance Project Plan (QAPP)

A Quality Assurance Project Plan (QAPP) was prepared for the CENRAP emissions and air quality modeling study that described the quality management functions performed by the modeling team. The QAPP was prepared and was based on the national consensus standards for quality assurance (ANSI/ASQC, 1994), followed EPA's guidelines for quality assurance project plans for modeling (EPA, 2002) and for QAPPs (EPA, 2001) and took into account the recommendations from the North American Research Strategy for Tropospheric Ozone (NARSTO) Quality Handbook for modeling projects (NARSTO, 1998). The EPA and NARSTO guidance documents were developed specifically for modeling projects, which have different quality assurance concerns than environmental monitoring data collection projects. The work performed in this project involves modeling at the basic research level and for regulatory/planning applications. In order to use model outputs for these purposes, it must be established that each model is scientifically sound, robust, and defensible. This is accomplished by following a project planning process that incorporates the following elements as described in the EPA modeling guidance document:

- A systematic planning process including identification of assessments and related performance criteria;
- Peer reviewed theory and equations;
- A carefully designed life-cycle development process that minimizes errors;
- Documentation of any changes from original plans;
- Clear documentation of assumptions, theory, and parameterization that is detailed enough so others can understand the model output;
- Input data and parameters that are accurate and appropriate for the analysis; and
- Output data that can be used to help inform decision makers.

The CENRAP QAPP can be found at:

http://pah.cert.ucr.edu/aqm/cenrap/docs/CENRAP_QAPP_Nov_24_2004.pdf).

A key component of the CENRAP emissions and air quality modeling QAPP was the graphical display of model inputs and outputs and multiple peer-review of each step of the modeling process. This was accomplished through use of the CENRAP modeling website where modelers posted displays of work products (e.g., emissions plots, model outputs, etc.) for review by the CENRAP modeling team, modeling workgroup and others. This website can be found at: http://pah.cert.ucr.edu/aqm/cenrap/index.shtml.

1.3.3 Model Selection

The selection of the meteorological, emissions and air quality models for the CENRAP regional haze modeling was based on a review of previous regional haze modeling studies performed in the CENRAP region (e.g., Pitchford et al., 2004; Pun, Chen and Seigneur, 2004; Tonnesen and Morris 2004) as well as elsewhere in the United States (e.g., Morris et al, 2004a; Tonnesen et al., 2003; Baker, 2004). The CENRAP emissions and air quality Modeling Protocol (Morris et al., 2004a) provides details on the justification for model selection and the formulation of the different models. Based on previous work (e.g., CENRAP, WRAP, VISTAS, MRPO, BRAVO and EPA), CENRAP selected the following models for use in modeling PM and regional haze in the central states:

- **MM5:** The Pennsylvania State University/National Center for Atmospheric Research (PSU/NCAR) Mesoscale Meteorological Model (MM5 Version 3.6 MPP) is a non-hydrostatic, prognostic meteorological model routinely used for urban- and regional-scale photochemical, fine particulate, and regional haze regulatory modeling studies (Anthes and Warner, 1978; Chen and Dudhia, 2001; Stauffer and Seaman, 1990, 1991; Xiu and Pleim, 2000).

- **SMOKE**: The Sparse Matrix Operator Kernel Emissions (SMOKE) modeling system is an emissions modeling system that generates hourly gridded speciated emission inputs of mobile, non-road, area, point, fire and biogenic emission sources for photochemical grid models. (Coats, 1995; Houyoux and Vukovich, 1999). As with most 'emissions models', SMOKE is principally an *emission processing system* and not a true *emissions modeling system* in which emissions estimates are simulated from 'first principles'. This means that, with the exception of mobile and biogenic sources, its purpose is to provide an efficient tool for converting an existing base emissions inventory data into the hourly, gridded, speciated, and formatted emission files required by an air quality model.

- **CMAQ:** EPA's Models-3/Community Multiscale Air Quality (CMAQ) modeling system is a 'One-Atmosphere' photochemical grid model capable of addressing ozone, PM, visibility and acid deposition at a regional scale for extended periods of time (Dennis, et al., 1996; Byun et al., 1998a; Byun and Ching, 1999, Pleim et al., 2003).

- **CAMx:** ENVIRON's Comprehensive Air Quality Model with Extensions (CAMx) modeling system is also a state-of-science 'One-Atmosphere' photochemical grid model capable of addressing ozone, PM, visibility and acid deposition at a regional scale for extended periods of time. (ENVIRON, 2006).

1.3.3.1 MM5 Meteorological Model Configuration for CENRAP Annual Modeling

Application of the MM5 for the 2002 annual modeling on a 36 km grid for the continental US was performed by the Iowa Department of Natural Resources (IDNR; Johnson, 2007). Details of the 2002 36 km MM5 model application and evaluation procedures carried out by IDNR may be found in Johnson, 2007. Application of the MM5 model on a 12 km grid covering the Central States for portions of 2002 was performed by EPA Region VII and the Texas Commission on Environmental Quality (TCEQ).

The MM5 (Version 3.63) configuration used in the generation of the meteorological modeling datasets consists of the following (see Table 1-2 for more details):

- 36 km grid with 34 vertical layers;
- 12 km nested grid for episodic modeling;
- For 12 km runs use two way nesting (without feedback) within the 36 km grid;
- Initialization and boundary conditions from Eta analysis fields;
  - Eta 3D and surface analysis data (ds609.2);
  - Not using NCEP global tropospheric SST data (ds083.0) ;
  - Observational enhancement (LITTLE_R)
    - NCEP ADP surface obs (ds464.0)
    - NCEP ADP upper-air obs (ds353.4)
- Pleim-Xiu (P-X) land-surface model (LSM);
- Pleim-Chang Asymmetric Convective Mixing (ACM) PBL model;
- Kain-Fritsch 2 cumulus parameterization;
- Mixed phase (Reisner 1) cloud microphysics;
- Rapid Radiative Transfer Model (RRTM) radiation;
- No Shallow Convection (ISHALLO=0);
- Standard 3D FDDA analysis nudging outside of PBL; and
- Surface nudging of the winds only.

1.3.3.2 SMOKE Emissions Model Configuration for CENRAP Annual Modeling

SMOKE supports area, mobile, fire and point source emission processing and includes biogenic emissions modeling through a rewrite of the Biogenic Emission Inventory System, version 3 (BEIS3) (see, http://www.epa.gov/ttn/chief/software.html#pcbeis). SMOKE has been available since 1996, and has been used for emissions processing in a number of regional air quality modeling applications. In 1998 and 1999, SMOKE was redesigned and improved with the support of the U.S. Environmental Protection Agency (EPA), for use with EPA's Models-3/CMAQ (http://www.epa.gov/asmdnerl/models3). The primary purposes of the SMOKE redesign were support of: (a) emissions processing with user-selected chemical mechanisms and (b) emissions processing for reactivity assessments.

As an emissions processing system, SMOKE has far fewer 'science configuration' options compared with the MM5 and CMAQ models. Table 1-3 summarizes the version of the SMOKE system that was used and the sources of data that were employed in constructing the required modeling inventories.

1.3.3.3 CMAQ Air Quality Model Configuration for CENRAP Annual Modeling

CENRAP used CMAQ Version 4.5 with the "SOAmods enhancement", described below, and used the model configuration as shown in Table 1-4. The model was set up and exercised on the same 36 km grid that was used by WRAP and VISTAS, the 36 km RPO national grid. CENRAP performed 12 km CMAQ sensitivity tests and found little change in model performance with a large penalty in computation time. Consequently, at the February 7, 2006 CENRAP Modeling

Workgroup Meeting a decision was made to proceed with the CENRAP emissions and air quality modeling using just the 36 km national RPO grid (Morris et al., 2006a).

Initial CMAQ 2002 simulations performed by VISTAS found that the model greatly underestimates organic mass carbon (OMC) concentrations, especially in the summer. A review of the CMAQ formulation found that it failed to treat Secondary Organic Aerosol (SOA) formation from sesquiterpenes and isoprene and also failed to account for the fact that SOA can become polymerized so that it is no longer volatile and stays in the particle form. Thus, VISTAS updated the CMAQ SOA module to include these missing processes and found much improved OMC model performance (Morris et al., 2006c). CENRAP tested the CMAQ Version 4.5 with SOAmods enhancement and found it performed much better for OMC than the standard versions of CMAQ Version 4.5. Therefore, CMAQ Version 4.5, with the enhanced SOAmods (Morris et al., 2006c), was adopted for the CENRAP modeling. CMAQ Version 4.5 is available from the CMAS center (www.cmascenter.org).

1.3.3.4 CAMx Air Quality Model Configuration for CENRAP Annual Modeling

CAMx Version 4.40 was applied using similar options as used by CMAQ. CAMx was used initially in side-by-side comparisons with CMAQ. Comparative model performance results and other factors for CAMx V4 and CMAQ V4.4 with SOAmods were presented at the February 7, 2006 CENRAP modeling workgroup meetings that found (Morris et al., 2006b):

- No one model was consistently performing better than the other over all species and averaging times.
- Both models performed well for sulfate.
- CMAQ's winter nitrate over-prediction tendency not as large as CAMx's.
- CAMx performed slightly better than CMAQ for elemental carbon (EC).
- CMAQ performed much better than CAMx for organic mass carbon (OMC).
- Both models over-predicted Soil and under-predicted coarse mass (CM).
- CMAQ ran faster than CAMx due to MPI multi-processing capability.
- CAMx required much less disk space than CMAQ.

Based on these factors, CMAQ was selected as the lead air quality model for the CENRAP regional haze modeling with CAMx the secondary corroborative model. However, CAMx also contained a PM Source Apportionment Technology (PSAT) capability that was used widely in the CENRAP modeling. Table 1-4 lists the main CAMx configuration used for the CENRAP annual modeling that was selected, in part, to be consistent with the CMAQ model configuration (Table 1-4). One exception to this was that the CAMx PSAT simulations used the Bott advection solver rather than the PPM advection solver. The PPM advection solver is typically used in the standard CAMx and CMAQ runs. Bott, however, is more computationally efficient and the high computational requirements of the CAMx PSAT runs dictated this choice.

Table 1-2. MM5 Meteorological Model Configuration for CENRAP 2002 Annual Modeling (Johnson, 2007).

Science Options	Configuration	Details/Comments
Model Code	MM5 version 3.63	Grell et al., 1994
Horizontal Grid Mesh	36 km	
36 km grid	165 x 129 dot points	RPO MM5 Grid
Vertical Grid Mesh	34 layers	Vertically varying; sigma pressure coordinate system
Grid Interaction	No Feedback	IFEED=0
Initialization	Eta first guess fields/LittleR	
Boundary Conditions	Eta first guess fields/LittleR	
Microphysics	Reisner I Mixed Ice	Look up table
Cumulus Scheme	Kain-Fritsch 2	On 36 and 12 km Grids
Planetary Boundary Layer	ACM PBL	
Radiation	RRTM	
Vegetation Data	USGS	24 Category Scheme
Land Surface Model	Pleim-Xiu Land Surface Model (LSM)	
Shallow Convection	None	
Sea Surface Temperature	Eta Skin	Spatially varying
Thermal Roughness	Garratt	
Snow Cover Effects	None	
4D Data Assimilation	Analysis Nudging on 36 and 12	
Surface Nudging	Wind Field Only	
Integration Time Step	90 seconds	
Simulation Periods	Annual 2002 for 36 km	12 km episodic only
Platform	Linux Cluster	Done at IDNR[1]

[1] Twelve km episodic modeling completed by EPA Region VII and the Texas Commission on Environmental Quality.

Table 1-3. SMOKE Emissions Model Configuration for CENRAP Annual Modeling.

Emissions Component	Configuration	Details/Comments
Emissions Model	SMOKE Version 2.3	Several versions of SMOKE used during course of the study
Horizontal Grid Mesh	36 km	
36 km grid	148 x 112 cells	RPO National Grid
Area Source Emissions	CENRAP Domain: CENRAP State 2002 EI	Updated '02 developed by CENRAP states (Pechan, 2005d,e)
	Other States: '02 NEI augmented with other 2002	Generated from EPA NEI02 v.1 and RPO interaction (Pechan, 2005c)
On-Road Mobile Sources	CENRAP Domain: CENRAP VMT data	Updated '02 developed by CENRAP states (Reid et al., 2004a)
	Other States: EPA '02 NEI augmented with other 2002	Generated from EPA NEI02 v.1 and RPO interaction (Pechan, 2005c)
Point Sources	CENRAP Domain: CENRAP State 2002 EI	Updated '02 developed by CENRAP states and stakeholders (Pechan, 2005a,b)
	Other States: EPA '02 NEI augmented with other 2002	Generated from EPA NEI02 v.1 and RPO interaction (Pechan, 2005c)
Off-Road Mobile Sources	CENRAP Domain: CENRAP State 2002 EI	Updated '02 developed by CENRAP states (Pechan, 2005d,e)
	Other States: EPA '02 NEI augmented with other 2002	Generated from EPA NEI02 v.1 and RPO interaction (Pechan, 2005c)
Biogenic Sources	SMOKE BEIS-3	BELD3 vegetative database
Mexican Sources	1999 Emissions for 2002 and 2018	http://www.epa.gov/ttn/chief/net/mexico.html; (ERG, 2006)
Canadian Sources	2000 Emissions for 2002 and 2020 Emissions for 2018	http://www.epa.gov/ttn/chief/net/canada.html
Temporal Adjustments	Seasonal, day, hour	Based on latest collected information and CEM-based profiles
Chemical Speciation	Revised CBM-IV Chemical Speciation	Updated January 2004
Gridding	Revised EPA Spatial Surrogates Used	Gridding of surrogates from http://www.epa.gov/ttn/chief/emch/spatial/
Growth and Controls	CENRAP developed	Pechan (2005a,b)
Quality Assurance	QA Tools in SMOKE 2.0	Follow QAPP (Morris and Tonnesen, 2004) and QA refinements (Morris and Tonnesen, 2006)
Simulation Periods	Annual 2002 for 36 km	Episodic periods at 12 km

Table 1-4. CMAQ Air Quality Model Configuration for CENRAP Annual Modeling.

Science Options	Configuration	Details/Comments
Model Code	CMAQ Version 4.5 w/ SOAmods	Secondary Organic Aerosol enhancements as described by Morris et al., (2006c)
Horizontal Grid Mesh	36 km annual	36 km covering continental U.S; some episodic 12 km sensitivity runs were also performed
36 km grid	148 x 112 cells	RPO National Grid
Vertical Grid Mesh	19 Layers	First 17 layers sync'd w/ MM5
Grid Interaction	One-way nesting	
Initial Conditions	~15 days full spin-up	Separately run 4 quarters of 2002
Boundary Conditions	2002 GEOS-CHEM day-specific	2002 GEOS-CHEM day specific 3-hour average data
Emissions		
Baseline Emissions Processing	See SMOKE model configuration	MM5 Meteorology input to SMOKE, CMAQ
Sub-grid-scale Plumes	No Plume-in-Grid (PinG)	
Chemistry		
Gas Phase Chemistry	CBM-IV	
Aerosol Chemistry	AE3/ISORROPIA	
Secondary Organic Aerosols	Secondary Organic Aerosol Model (SORGAM) w/ SOAmods update	Schell et al., (2001); Morris et al., (2006c)
Cloud Chemistry	RADM-type aqueous chemistry	Includes subgrid cloud processes
N2O5 Reaction Probability	0.01 – 0.001	
Meteorological Processor	MCIP Version 2.3	Includes dry deposition and snow cover updates
Horizontal Transport		
Numerical Scheme	PPM advection solver	
Eddy Diffusivity Scheme	K-theory with Kh grid size dependence	Multiscale Smagorinsky (1963) approach
Vertical Transport		
Eddy Diffusivity Scheme	K-theory	
Diffusivity Lower Limit	Kzmin = 0.1 to 1.0	Land use dependent Kzmin
Deposition Scheme	M3dry	Directly linked to Pleim-Xiu Land Surface Model parameters
Numerics		
Gas Phase Chemistry Solver	Euler Backward Iterative (EBI) solver	
Horizontal Advection Scheme	Piecewise Parabolic Method (PPM) scheme	
Simulation Periods	Annual 2002 for 36 km	Episodic periods at 12 km
Integration Time Step	Calculated Internally	15 minute coupling time step

Table 1-5. CAMx Air Quality Model Configuration for CENRAP Annual Modeling.

Science Options	Configuration	Details
Model Code	CAMx Version 4.40	Available at: www.camx.com
Horizontal Grid Mesh	36 km annual	36 km covering continental U.S
36 km grid	148 x 112 cells	
Vertical Grid Mesh	19 Layers	17 Layers sync'd w/ MM5
Grid Interaction	Two-way nesting	
Initial Conditions	~15 days full spin-up	Separately run 4 quarters of 2002
Boundary Conditions	2002 GEOS-CHEM day-specific	2002 GEOS-CHEM day specific 3-hour average data
Emissions		
Baseline Emissions Processing	See SMOKE model configuration	MM5 Meteorology input to SMOKE, CAMx
Sub-grid-scale Plumes	No Plume-in-Grid (PinG)	Consistent with CMAQ
Chemistry		
Gas Phase Chemistry	CBM-IV	with Isoprene updates
Aerosol Chemistry	ISORROPIA equilibrium	Dynamic and hybrid also available but not used
Secondary Organic Aerosols	SOAP	
Cloud Chemistry	RADM-type aqueous chemistry	Alternative is CMU multi-section aqueous chemistry
N2O5 Reaction Probability	None	
Meteorological Processor	MM5CAMx	
Horizontal Transport		
Eddy Diffusivity Scheme	K-theory with Kh grid size dependence	
Vertical Transport		
Eddy Diffusivity Scheme	K-Theory	
Diffusivity Lower Limit	Kzmin = 0.1 to 1.0	Land use dependent Kzmin
Planetary Boundary Layer	No Patch	
Deposition Scheme	Wesely	
Numerics		
Gas Phase Chemistry Solver	CMC Fast Solver	
Horizontal Advection Scheme	Piecewise Parabolic Method (PPM) scheme. PSAT w/ Bott scheme.	
Simulation Periods	Annual 2002 at 36 km	
Integration Time Step	Wind speed dependent	

1.3.4 Modeling Domains

The CENRAP emissions and air quality modeling was conducted on the 36 km national RPO domain as depicted in Figure 1-2. This domain consists of a 148 by 112 array of 36 km by 36 km grid cells and covers the continental United States. Sensitivity simulations were also performed for episodes on a 12 km modeling domain covering the central states, however the results were very similar to the 36 km results so CENRAP elected to proceed with the 2002 annual modeling using the 36 km domain for computational efficiency (Morris et al., 2006a).

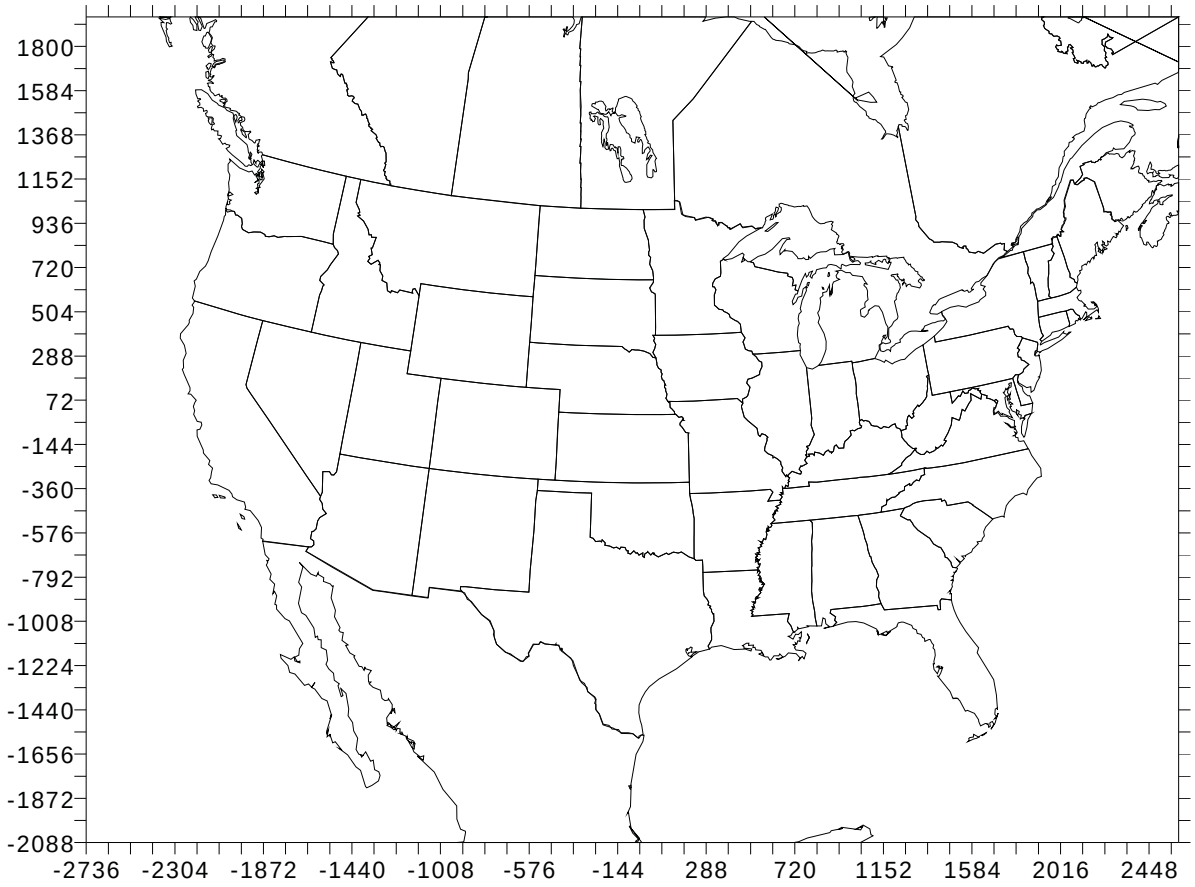

Figure 1-2. National Inter-RPO 36 km modeling domain used for the CENRAP 2002 annual SMOKE, CMAQ and CAMx modeling.

1.3.5 Vertical Structure of Modeling Domain

The MM5 meteorological model was exercised using 34 vertical layers from the surface to a pressure level of 100 mb (approximately 15 km above ground level). Both the CMAQ and CAMx air quality models can employ layer collapsing in which vertical layers in the MM5 are combined in the air quality model, which improves computational efficiency. The sensitivity of the CMAQ model estimates to the number of vertical layers was evaluated by the Western Regional Air Partnership (WRAP) and Visibility Improvements State and Tribal Association of the Southeast (VISTAS) (Tonnesen et al., 2005; 2006; Morris et al., 2004a). CMAQ model simulations were performed with no layer collapsing (i.e., the same 34 layers as used by MM5) and with various levels of layer collapsing. These studies found that using 19 vertical layers up

to 100 mb (i.e., same model top as MM5) and matching the eight lowest MM5 vertical layers near the surface produced nearly identical results as with no layer collapsing. They also found that very aggressive layer collapsing (e.g., 34 to 12 layers) produced results with substantial differences compared to no layer collapsing. Therefore, based on the WRAP/VISTAS sensitivity analysis, CENRAP adopted the 19 vertical layer configuration up to the 100 mb model top. Figure 1-3 displays the definition of the 34 MM5 vertical layers and how they were collapsed to 19 vertical layers in the air quality modeling performed by CENRAP.

MM5					CMAQ 19L				
Layer	Sigma	Pres(mb)	Height(m	Depth(m)	Layer	Sigma	Pres(mb)	Height(m)	Depth(m)
34	**0.000**	**100**	**14662**	**1841**	**19**	**0.000**	**100**	**14662**	**6536**
33	0.050	145	12822	1466		0.050	145		
32	0.100	190	11356	1228		0.100	190		
31	0.150	235	10127	1062		0.150	235		
30	0.200	280	9066	939		0.200	280		
29	**0.250**	**325**	**8127**	**843**	**18**	**0.250**	**325**	**8127**	**2966**
28	0.300	370	7284	767		0.300	370		
27	0.350	415	6517	704		0.350	415		
26	0.400	460	5812	652		0.400	460		
25	**0.450**	**505**	**5160**	**607**	**17**	**0.450**	**505**	**5160**	**1712**
24	0.500	550	4553	569		0.500	550		
23	0.550	595	3984	536		0.550	595		
22	**0.600**	**640**	**3448**	**506**	**16**	**0.600**	**640**	**3448**	**986**
21	0.650	685	2942	480		0.650	685		
20	**0.700**	**730**	**2462**	**367**	**15**	**0.700**	**730**	**2462**	**633**
19	0.740	766	2095	266		0.740	766		
18	**0.770**	**793**	**1828**	**259**	**14**	**0.770**	**793**	**1828**	**428**
17	0.800	820	1569	169		0.800	820		
16	**0.820**	**838**	**1400**	**166**	**13**	**0.820**	**838**	**1400**	**329**
15	0.840	856	1235	163		0.840	856		
14	**0.860**	**874**	**1071**	**160**	**12**	**0.860**	**874**	**1071**	**160**
13	0.880	892	911	158	**11**	**0.880**	**892**	**911**	**158**
12	**0.900**	**910**	**753**	**78**	**10**	**0.900**	**910**	**753**	**155**
11	0.910	919	675	77		0.910	919		
10	**0.920**	**928**	**598**	**77**	**9**	**0.920**	**928**	**598**	**153**
9	0.930	937	521	76		0.930	937		
8	**0.940**	**946**	**445**	**76**	**8**	**0.940**	**946**	**445**	**76**
7	**0.950**	**955**	**369**	**75**	**7**	**0.950**	**955**	**369**	**75**
6	**0.960**	**964**	**294**	**74**	**6**	**0.960**	**964**	**294**	**74**
5	**0.970**	**973**	**220**	**74**	**5**	**0.970**	**973**	**220**	**74**
4	**0.980**	**982**	**146**	**37**	**4**	**0.980**	**982**	**146**	**37**
3	**0.985**	**986.5**	**109**	**37**	**3**	**0.985**	**986.5**	**109**	**37**
2	**0.990**	**991**	**73**	**36**	**2**	**0.990**	**991**	**73**	**36**
1	**0.995**	**995.5**	**36**	**36**	**1**	**0.995**	**995.5**	**36**	**36**
0	**1.000**	**1000**	**0**	**0**	**0**	**1.000**	**1000**	**0**	**0**

Figure 1-3. MM5 34 vertical layer definitions and scheme for collapsing the 34 layers down to 19 layers for the CENRAP CMAQ and CAMx 2002 annual modeling.

1.3.6 2002 Calendar Year Selection

The calendar year 2002 was selected for CENRAP regional haze annual modeling as described in the CENRAP Modeling Protocol (Morris et al., 2004a). EPA's applicable guidance on $PM_{2.5}$/Regional Haze modeling at that time (EPA, 2001) identified specific goals to consider when selecting modeling periods for use in demonstrating reasonable progress in attaining the regional haze goals. However, since there is much in common with the goals for selecting episodes for annual and episodic $PM_{2.5}$ attainment demonstrations as well as regional haze, EPA's current guidance addresses all three in a common document. (EPA, 2007) At the time of the modeling period selection EPA had also published an updated summary of $PM_{2.5}$ and Regional Haze Modeling Guidance (Timin, 2002) that served, in some respects, as an interim placeholder until the final guidance was issued as part of the $PM_{2.5}$/regional haze NAAQS implementation process that was ultimately published in April 2007 (EPA, 2007). The interim EPA modeling guidance for episode selection (EPA, 2001; Timin, 2002) was consistent with the final EPA regional haze modeling guidance (EPA, 2007).

EPA recommends that the selection of a modeling period derive from three principal criteria:

- A variety of meteorological conditions should be covered that includes the types of meteorological conditions that produce the worst 20 percent and best 20 percent visibility days at Class I areas in the CENRAP States during the 2000-2004 baseline period;

- To the extent possible, the modeling data base should include days for which enhanced data bases (i.e. beyond routine aerometric and emissions monitoring) are available; and

- Sufficient days should be available such that relative response factors (RRFs) can be based on several (i.e., $\geq$ 15) days.

For regional haze modeling, the guidance goes further by suggesting that the preferred approach is to model a full, *representative* year (EPA, 2001, pg. 188). Moreover, the required RRF values should be based on model results averaged over the 20 percent worst and 20 percent best visibility days determined for each Class I area based on monitoring data from the 2000 – 2004 baseline period. More recent EPA guidance (Timin, 2002) suggests that states should model at least 10 worst and 10 best visibility days at each Class 1 area. EPA also lists several 'other considerations' to bear in mind when choosing potential PM/regional haze episodes including: (a) choose periods which have already been modeled, (b) choose periods which are drawn from the years upon which the current design values are based, (c) include weekend days among those chosen, and (d) choose modeling periods that meet as many episode selection criteria as possible in the maximum number of nonattainment or Class I areas as possible.

Due to limited available resources CENRAP was restricted to modeling a single calendar year. The RHR uses the five-year baseline of 2000-2004 period as the starting point for projecting future-year visibility. Thus, the modeling year should be selected from this five-year baseline period. The 2002 calendar year, which lies in the middle of the 2000-2004 Baseline, was selected for the following reasons:

- Based on available information, 2002 appears to be a fairly typical year in terms of meteorology for the 5-year Baseline period of 2000-2004;

- 2003 and 2004 appeared to be colder and wetter than typical in the eastern US;
- The enhanced IMPROVE and IMPROVE Protocol and Supersites PM monitoring data were fully operational by 2002. Much less IMPROVE monitoring data was available during 2000-2001, especially in the CENRAP region;
- IMPROVE data for 2003 and 2004 were not yet available at the time that the CENRAP modeling was initiated; and
- 2002 was being used by the other RPOs.

1.3.7 Initial Concentrations and Boundary Conditions

The CMAQ and CAMx models were operated separately for each of four quarters of the 2002 year using a ~15 day spin up period (i.e., the models were started approximately 15 days before the first day of interest in each quarter in order to limit the influence of the assumed initial concentrations, e.g., start June 15 for quarter 3 whose first day of interest is July 1). Sensitivity simulations demonstrated that with ~15 initialization days, the influence of initial concentrations (ICs) was minimal using the 36 km Inter-RPO continental U.S. modeling domain. Consequently, clean ICs were specified in the CMAQ and CAMx modeling using a ~15 day spin up period.

Boundary Conditions (BCs) (i.e., the assumed concentrations along the later edges of the 36 km modeling domain, see Figure 1-2) were based on a 2002 simulation by the GEOS-CHEM global circulation/chemistry model. GEOS-CHEM is a three-dimensional global chemistry model driven by assimilated meteorological observations from the Goddard Earth Observing System (GEOS) of the NASA Global Modeling and Assimilation Office. It is applied by research groups around the world to a wide range of atmospheric composition problems, including future climates and planetary atmospheres using general circulation model meteorology to drive the model. Central management and support of the model is provided by the Atmospheric Chemistry Modeling Group at Harvard University.

A joint RPO study was performed, coordinated by VISTAS, in which Harvard University applied the GEOS-CHEM global model for the 2002 calendar year (Jacob, Park and Logan, 2005). The University of Houston (UH) was retained to process the 2002 GEOS-CHEM output into BCs for the CMAQ model (Byun, 2004). The GEOS-CHEM simulations for the RPOs used GEOS meteorological observations for the year 2002. These were obtained from the Global Modeling and Assimilation Office(GMAO) as a 6-hourly archive (3-hour for surface quantities such as mixing depths). The data through August 2002 were from the GEOS-3 assimilation, with horizontal resolution of 1^{o}x1^{o} and 55 vertical layers. The data after August 2002 were from the updated GEOS-4 assimilation, with horizontal resolution of 1^{o}x1.25^{o} and 48 vertical layers (note 1^{o} latitude is equal to approximately 110 km). The GEOS-CHEM output was processed by mapping the GEOS-CHEM chemical compounds to the species in the CBM-IV chemical mechanism used by CMAQ/CAMx and mapping the GEOS-CHEM vertical layers to the 19 layer vertical layer structure used by CMAQ/CAMx in the CENRAP modeling (Byun, 2004). The results were day-specific three-hourly BC inputs for the CMAQ model. The CMAQ2CAMx processor was then used to transform the CMAQ day-specific 3-hourly BCs to the format used by CAMx.

There were several quality assurance (QA) checks of the BCs generated from the 2002 GEOS-CHEM output. The first QA/QC check was a range check to assure reasonable values. The BCs were compared against the GEOS-CHEM outputs to assure the mapping and interpolation was performed correctly. The code used to map the GEOS-CHEM output to the CMAQ BC format was obtained from UH, reviewed and the BC generation duplicated for several time periods during 2002.

1.3.8 Emissions Input Preparation

The CENRAP SMOKE emissions modeling was based on an updated 2002 emissions data for the U.S. (Pechan, 2005c,e; Reid et al., 2004a,b), 1999 emissions data for Mexico (ERG, 2006), and 2000 emissions data for Canada. These data were used to generate a final base 2002 Base G Typical (Typ02G) annual emissions database. Numerous iterations of the emissions modeling were conducted using interim databases before arriving at the final Base G emission inventories (e.g., Morris et al., 2005). The 2018 Base G base case emissions (Base18G) for most source categories in the U.S. were based on projections of the 2002 inventory assuming growth and control (Pechan, 2005d). 2018 EGU emissions were based on the run 2.1.9 of the Integrated Planning Model (IPM) updated by the CENRAP states. Canadian emissions for the Base18G scenario were based on a 2020 inventory, whereas the Mexican 1999 inventory was held constant for 2018.

The Typ02G and Base18G emission inventories represent significant improvements to the preliminary emissions modeling performed by CENRAP (Morris et al., 2005). While the preliminary 2002 modeling served its purpose to develop the infrastructure for modeling large emissions data sets and producing annual emissions simulations, much of the input data (both as inventories and ancillary data) were placeholders for actual 2002 data that were being prepared through calendar year 2005. As these actual 2002 data sets became available, they were integrated into the SMOKE modeling and QA system that was developed during the preliminary modeling, to produce a high-quality emissions data set for use in the final CMAQ and CAMx modeling. The addition of entirely new inventory categories, like marine shipping, added complexity to the modeling. By the end of the emissions data collection phase, there were 23 separate emissions processing streams covering a variety of sources categories necessary to general model-ready emission inputs for the 2002 calendar year.

Details on the emissions modeling are provided in Chapter 2 with additional information contained in Appendix B.

1.3.9 Meteorological Input Preparation

The 2002 36 km MM5 meteorological modeling was conducted by the Iowa Department of Natural Resources (IDNR) who also performed a preliminary model performance evaluation (Johnson, 2007). CENRAP performed an additional MM5 evaluation of the CENRAP 2002 36 km MM5 simulation that included a comparative evaluation against the final VISTAS 2002 36 km MM5 and an interim WRAP 2002 36 km simulation (Kemball-Cook et al., 2004). Kemball-Cook and co-workers (2004) found the following in the comparative evaluation of the CENRAP, WRAP and VISTAS 2002 36 km MM5 simulations, (details are provided in Appendix A):

Surface Meteorological Performance within the CENRAP Region

- The three MM5 simulations (CENRAP, VISTAS and WRAP) obtained comparable model performance for winds and humidity that were within model performance benchmarks.
- The WRAP MM5 simulation obtained better temperature model performance than the other two simulations due to the use of surface temperature data assimilation.
    - In the final WRAP MM5 simulation the use of surface temperature assimilation was dropped because it introduced instability in the vertical structure of the atmosphere.
- For all three runs, the Northern CENRAP domain had a cold bias in winter and a warm bias in summer.

Surface Meteorological Performance outside the CENRAP Region

- All three runs had similar surface wind model performance in the western U.S. that was outside the model performance benchmarks
- For temperature, the WRAP MM5 simulation had the best performance overall due to the surface temperature data assimilation that was dropped in the final WRAP run.
- The three runs had comparable humidity performance, although WRAP exhibited a larger wet bias in the summer and the southwestern U.S.

Upper-Air Meteorological Performance

- The VISTAS and CENRAP MM5 simulations were better able to reproduce the deep convective summer boundary layers compared to the WRAP MM5 simulations, which exhibited a smoother decrease in temperature with increase in altitude.
- CENRAP and VISTAS MM5 simulations better simulated the surface temperature inversions than WRAP.
- WRAP was better able to simulate the surface temperature.
- All three models exhibited similar vertical wind profiles.

Precipitation Performance

- In winter, all three MM5 simulations exhibited similar, fairly good, performance in reproducing the spatial distribution and magnitudes of the monthly average observed precipitation.
- In summer, all runs had a wet bias, particularly in the desert southwest where the interim WRAP run had the largest wet bias.

In conclusion, the VISTAS simulation appeared to perform best, the CENRAP MM5 model performance was generally between the VISTAS and WRAP performance, with performance more similar to VISTAS than WRAP. Although the interim WRAP MM5 simulation performed best for surface temperature due to the surface temperature data assimilation, the surface temperature assimilation degraded the MM5 upper-air performance including the ability to assimilate surface inversions and was ultimately dropped from the final WRAP MM5 simulations (Kemball-Cook et al., 2005).

The IDNR 12 km[2] MM5 simulations were also evaluated and compared with the performance of the 36 km MM5 simulation (Johnson et al., 2007). The IDNR 36 km and 12 km MM5 model performance was similar (Johnson, 2007), which supported the findings of the CMAQ and CAMx 36 and 12 km sensitivity simulations that there was little benefit of using a 12 km grid for simulating regional haze at rural Class I areas (Morris et al., 2006a). However, as noted by Tonnesen and co-workers (2005; 2006) and EPA modeling guidance (1991; 1999; 2001; 2007) this finding does not necessarily hold for 8-hour ozone and $PM_{2.5}$ modeling that is characterized by sharper concentration gradients and frequently occurs in the urban environment as compared to the more rural nature of regional haze.

1.3.10 Photolysis Rates Model Inputs

Several chemical reactions in the atmosphere are initiated by the photodissociation of various trace gases. To accurately represent the complex chemical transformations in the atmosphere, accurate estimates of these photodissociation rates must be made. The Models-3/CMAQ system includes the JPROC processor, which calculates a table of clear-sky photolysis rates (or J-values) for a specific date. JPROC uses default values for total aerosol loading and provides the option to use default ozone column data or to use measured total ozone column data. These data come from the Total Ozone Mapping Spectrometer (TOMS) satellite data. TOMS data that is available at 24-hour averages was obtained from http://toms.gsfc.nasa.gov/eptoms/ep.html. Day-specific TOMS data was used in the CMAQ radiation model (JPROC) to calculate photolysis rates. The TOMS data were missing or erroneous for several periods in 2002: August 2-12; June 10; and November 18-19. Thus, the TOMS data for August 1, 2002 was used for August 2-7 and TOMS data for August 13 was used for August 8-12. Similarly, TOMS data for June 9 was used for June 10 and data for August 17 was used for August 18-19. Note that the total column of ozone in the atmosphere is dominated by stratospheric ozone which has very little day-to-day variability so the use of TOMS data within a week or two of an actual day introduces minimal uncertainties in the modeling analysis.

JPROC produces a "look-up" table that provides photolysis rates as a function of latitude, altitude, and time (in terms of the number of hours of deviation from local noon, or hour angle). In the current CMAQ implementation, the J-values are calculated for six latitudinal bands (10º, 20º, 30º, 40º, 50º, and 60º N), seven altitudes (0 km, 1 km, 2 km, 3 km, 4 km, 5 km, and 10 km), and hourly values up to ∀8 hours of deviation from local noon. During model calculations, photolysis rates for each model grid cell are estimated by first interpolating the clear-sky photolysis rates from the look-up table using the grid cell latitude, altitude, and hour angle, followed by applying a cloud correction (attenuation) factor based on the cloud inputs from MM5.

The photolysis rates input file was prepared as separate look-up tables for each simulation day. Photolysis files are ASCII files that were visually checked for selected days to verify that photolysis are within the expected ranges.

[2] The IDNR twelve 12 km annual simulation domain was not sufficient for CENRAP's needs, thus Bret Anderson with EPA Region 7 in cooperation with Texas completed an episodic 12km simulation on a larger domain.

The Tropospheric Ultraviolet and Visible (TUV) Radiation Model (http://cprm.acd.ucar.edu/Models/TUV/) is used to generate the photolysis rates input file for CAMx. TOMS ozone data and land use data were used to develop the CAMx Albedo/Haze/Ozone input file for 2002. As for CMAQ, the missing TOMS data period in the fall of 2002 was filled-in using observed TOMS data on either side of the missing period using the same procedures as described above for CMAQ. Default land use specific albedo values were used and a constant haze value used, corresponding to rural conditions over North America.

1.3.11 Air Quality Input Preparation

Air quality data used with the CMAQ and CAMx modeling systems include: (1) Initial Concentrations (ICs) that are the assumed initial three-dimensional concentrations throughout the modeling domain.; (2) the Boundary Conditions (BCs) that are the concentrations assumed along the lateral edges of the RPO national 36 km modeling domain; and (3) air quality observations that are used in the model performance evaluation (MPE). The MPE is discussed in Section 3 and Appendix C of this TSD.

As noted in Section 1.3.7, CMAQ default clean Initial Concentrations (ICs) were used along with an approximately 15 day spin up (initialization) period to eliminate any significant influence of the ICs on the modeled concentrations for the days of interest. The same ICs were used with CAMx as well. Both CMAQ and CAMx were run for each quarter of the year. Each quarter's model run was initialized 15 days prior to the first day of interest (e.g., for quarter 3, Jul-Aug-Sep, the model was initialized on June 15, 2002 with the first modeling day of interest July 1, 2002). The CMAQ Boundary Conditions (BCs) for the Inter-RPO 36 km continental U.S. grid (Figure 1-2) were based on day-specific 3-hour averages from the output of the GEOS-CHEM global simulation model of 2002 (Jacob, Park and Logan, 2005). The 2002 GEOS-CHEM output was mapped to the species and vertical layer structure of CMAQ and interpolated to the lateral boundaries of the 36 km grid shown in Figure 1-2 (Byun, 2004).

Table 1-6 summarizes the surface air quality monitoring networks and the number of sites available in the CENRAP region that were used in the model performance evaluation. Data from these monitoring networks were also used to evaluate the CMAQ and CAMx models outside of the CENRAP region.

Table 1-6. Ground-level ambient data monitoring networks and stations available in the CENRAP states for calendar year 2002 used in the model performance evaluation.

Monitoring Network	Chemical Species Measured	Sampling Frequency; Duration	Approximate Number of Monitors
IMPROVE	Speciated $PM_{2.5}$ and PM_{10}	1 in 3 days; 24 hr	11
CASTNET	Speciated $PM_{2.5}$, Ozone	Hourly, Weekly; 1 hr, 1 Week	3
NADP	WSO4, WNO3, WNH4	Weekly	23
EPA-STN	Speciated $PM_{2.5}$	Varies; Varies	12
AIRS/AQS	CO, NO, NO_2, NO_x, O_3	Hourly; Hourly	25

1.3.12 2002 Base Case Modeling and Model Performance Evaluation

The CMAQ and CAMx models were evaluated against ambient measurements of PM species, gas-phase species and wet deposition. Table 1-6 summarizes the networks used in the model evaluation, the species measured and the averaging times and frequency of the measurements. Numerous iterations of CMAQ and CAMx 2002 base case simulations and model performance evaluations were conducted during the course of the CENRAP modeling study, most of which have been posted on the CENRAP modeling website (http://pah.cert.ucr.edu/aqm/cenrap/cmaq.shtml) and presented in previous reports and presentations for CENRAP (e.g., Morris et al., 2005; 2006a,b). Details on the final 2002 Base F 36 km CMAQ base case modeling performance evaluation are provided in Chapter 3 and Appendix C (because of the similarity between 2002 Base F and 2002 Base G and resource constraints the model evaluation was not re-conducted for Base G). In general, the model performance of the CMAQ and CAMx models for sulfate (SO4) and elemental carbon (EC) was good. Model performance for nitrate (NO3) was variable, with a summer underestimation and winter overestimation bias. Performance for organic mass carbon (OMC) was also variable, with the inclusion of the SOAmods enhancement in CMAQ Version 4.5 greatly improving the CMAQ summer OMC model performance (Morris et al., 2006c). Model performance for Soil and coarse mass (CM) was generally poor. Part of the poor performance for Soil and CM is believed to be due to measurement-model incommensurability. The IMPROVE measured values are due, in part, to local fugitive dust sources that are not captured in the model's emission inputs and the 36 km grid resolution is not conducive to modeling localized events.

1.3.13 2018 Modeling and Visibility Projections

Emissions for the 2018 base case were generated following the procedures discussed in Section 1.3.8 and Chapter 2. 2018 emissions for Electrical Generating Units (EGUs) were based on simulations of the Integrated Planning Model (IPM) that took into the account the effects of the Clean Air Interstate Rule (CAIR) on emissions from EGUs in CAIR states using an IPM realization of a CAIR cap-and-trade program. Emissions for on-road and non-road mobile sources were based on activity growth and emissions factors from the EPA MOBILE6 and NONROAD models, respectively. Area sources and non-EGU point sources were grown to 2018 levels (Pechan, 2005d). The Canadian year 2000 emissions inventory was replaced by a Canadian 2020 emissions inventory for the 2018 CMAQ/CAMx simulations. The following sources were assumed to remain constant between the 2002 and 2018 base case simulations:

- Biogenic VOC and NOx emissions from the BEIS3 biogenic emissions model;
- Wind blown dust associated with non-agricultural sources (i.e., natural wind blown fugitive dust);
- Off-shore emissions associated with off-shore marine and oil and gas production activities;
- Emissions from wildfires;
- Emissions from Mexico; and
- Global transport (i.e., emissions due to BCs from the 2002 GEOS-CHEM global chemistry model.

The results from the 2002 and 2018 CMAQ and CAMx simulations were used to project 2018 PM levels from which 2018 visibility estimates were obtained. The 2002 and 2018 modeling results were used in a relative sense to scale the observed PM concentrations from the 2000-2004 Baseline and the IMPROVE monitoring network to obtain the 2018 PM projections. The 2018/2002 modeled scaling factors are called Relative Response Factors (RRFs) and are constructed as the ratio of modeling results for the 2018 model simulation to the 2002 model simulation. Two important regional haze metrics are the average visibility for the worst 20 percent and best 20 percent days from the 2000-2004 five-year Baseline. For the 2018 visibility projections, EPA guidance recommends developing Class I area and PM species specific RRFs using the average modeling results for the worst 20 percent days during the 2002 modeling period and the 2002 and 2018 emission scenarios. The results of the CENRAP 2018 visibility projections following EPA guidance procedures (EPA, 2007a) are provided in Chapter 4 and Appendix D. CENRAP has also developed alternative procedures for visibility projections that are discussed in Chapter 5 and Appendix D. For example, much of the coarse mass (CM) impacts at Class I area IMPROVE monitors is believed to be natural and primarily from local sources that are subgrid-scale to the modeled 36 km grid so are not represented in the modeling. So, one alternative visibility projection approach is to set the RRF for CM to 1.0. That is, the CM impacts in 2018 are assumed to be the same as in the observed 2000-2004 Baseline. Similarly, the Soil impacts at IMPROVE monitors are likely mainly due to local dust sources so another alternative approach is to set the RRFs for both CM and Soil to 1.0.

The 2018 visibility projections for the worst 20 percent days are compared against a 2018 point on the Uniform Rate of Progress (URP) glidepath or the "2018 URP point". The 2018 URP point is obtained by constructing a linear visibility glidepath in deciviews from the observed 2000-2004 Baseline (EPA, 2003a) for the worst 20 percent days to the 2064 Natural Conditions (EPA, 2003b; Pitchford, 2006). Where the linear glidepath crosses the year 2018 is the 2018 URP point. States may use the modeled 2018 visibility to help define their 2018 RPG in their RHR SIPs. The 2018 URP point is used as a benchmark to help judge the 2018 modeled visibility projections and the state's RPG. However, as noted in EPA's RPG guidance "The glidepath is not a presumptive target, and States may establish a RPG that provides for greater, lesser, or equivalent visibility improvement as that described by the glidepath" (EPA, 2007b). Chapter 4 and Appendix D present the 2018 visibility projections for the CENRAP Class I areas and their comparisons with the 2018 URP point using EPA default visibility projection procedures (EPA, 2007a) and EPA default URP glidepaths (EPA, 2003a,b; 2007b).

Various techniques have been developed to display the 2018 visibility modeling results including "DotPlots" that display the 2018 visibility projections as a percentage of meeting the 2018 point on the URP glidepath. A value of 100% on the DotPlot indicates that the Class I area is predicted to meet the 2018 point on the URP glidepath. Over 100% means the 2018 visibility projection obtains more visibility improvements (reductions) than required to meet the 2018 point on the URP glidepath (i.e., projected value is below the glidepath). And less than 100% indicates that fewer visibility improvements are projected than are needed to meet the 2018 point URP on the glidepath (i.e., above the glidepath). Figure 1-4 displays a DotPlot that compares the 2018 visibility projections from the CENRAP 2018 Base G CMAQ simulation with the 2018 URP point using the EPA default RRFs and alternative RRFs that set the CM and Soil RRFs to unity (i.e., assume CM and Soil are natural so remain unchanged from the 2000-2004 Baseline). For these results, the 2018 visibility projections at the Hercules Glade (HEGL1) Class I area meets the 2018 point on the URP glidepath (100%), whereas the 2018 visibility projections at Caney

Creek (CACR), Mingo (MING) and Upper Buffalo (UPBU) achieve more visibility improvements than needed to meet the 2018 URP point so are below the 2018 URP glidepath. However, the 2018 visibility projections at Breton Island comes up slightly short (~5%) of meeting the 2018 point on the URP glidepath and Wichita Mountains (WIMO) comes up approximately 40% short of meeting the 2018 point on the URP glidepath. Class I areas at the northern (e.g., VOYA, BOWA and ISLE) and southern (e.g., BIBE and GUMO) boundaries of the U.S. also fall short of achieving the 2018 URP point. High contributions of international transport and/or natural sources (e.g., wind blown dust) affect the ability of these Class I areas to be on the URP glidepath. These issues are discussed in more detail in Chapters 4 and 5.

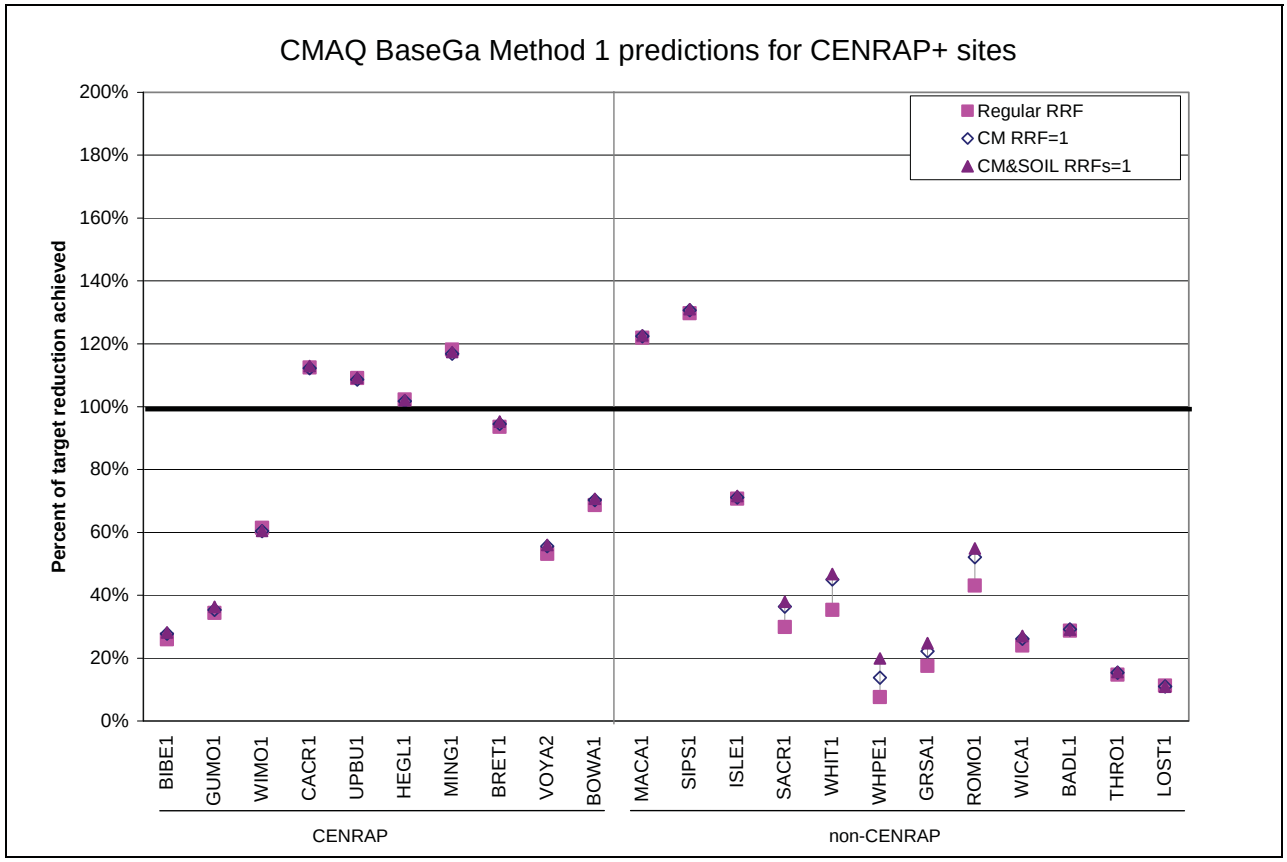

Figure 1-4. 2018 visibility projections expressed as a percent of meeting the 2018 URP point for the 2018 BaseG CMAQ base case simulation using the EPA default (EPA, 2007) Regular RRF and alternative projections procedures that set the RRFs for CM=1.0 and CM&SOIL=1.0.

1.3.14 Additional Supporting Analysis

CENRAP performed numerous supporting analyses of its modeling results including analyzing alternative glidepaths and 2018 projection Approaches and performing confirmatory analysis of the 2018 visibility projections. Details on the additional supporting analysis are contained discussed in Chapter 5, which include:

- The CENRAP 2018 visibility projections were compared with those generated by VISTAS and MRPO. There was close agreement between the CENRAP and VISTAS 2018 visibility projections at almost all common Class I areas. With the only exception being Breton Island where the CENRAP's projections were slightly more optimistic than VISTAS'. The MRPO 2018 visibility projections were less optimistic than CENRAP's at the four Arkansas-Missouri Class I area that may have been due to CENRAP's BART emission controls in CENRAP states not included in the 2018 MRPO inventory.
- Extinction based glidepaths were developed and the CENRAP 2018 visibility projections were shown to produce nearly identical estimates of achieving the 2018 URP point when using total extinction glidepaths as when the linear deciview glidepaths were used. With the extinction based glidepaths the analysis of 2018 URP could be made on a PM species-by-species basis where it was shown that 2018 extinctions due to SO4 and, to a lesser extent, NO3 and EC, achieve the URP, but the other species do not and in fact extinction due to Soil and CM is projected to get worse.
- 2018 visibility projections were made using EPA's new Modeled Attainment Test Software (MATS) program and the CENRAP Typ02G and Base18G modeling results. The CENRAP 2018 visibility projections exactly agreed with those generated by MATS with three exceptions: Breton Island, Boundary Waters and Mingo Class I areas, At these three Class I areas MATS did not produce any 2018 visibility projections due to insufficient data in the raw IMPROVE database to produce a valid observed 2000-2004 Baseline. CENRAP used filled data for these three Class I areas.
- PM Source Apportionment Technology (PSAT) modeling was conducted to estimate the contributions to visibility impairment at Class I areas by source region (e.g., states) and major source category. Source contributions were obtained for a 2002 and 2018 base case and the PSAT modeling results were implemented in a PSAT Visualization Tool that was provided to CENRAP states and others. Major findings from the PSAT source apportionment modeling include the following:
    - Sulfate from elevated point sources was the highest source category contribution to visibility impairment at CENRAP Class I areas for the worst 20 percent days.
    - International transport contributed significantly to visibility impairment at CENRAP Class I areas on the southern (BIBE and GUMO) and northern (BOWA and VOYA) borders of the U.S. and to a lesser extent at WIMO as well.
- Alternative visibility projections were made assuming that coarse mass (CM) alone and CM and Soil were natural in origin that confirmed the original 2018 visibility projections.
- Visibility projections were made using an alternative model (CAMx) that verified the projections made by CMAQ.
- The effects of International Transport were examined several ways and found that the inability of the 2018 visibility projections to achieve the 2018 URP point at the northern and southern border Class I areas was due to high contributions due to International Transport.

- Visibility trends for the worst 20 percent days, best 20 percent days and all monitored days were analyzed at CENRAP Class I areas using the period of record IMPROVE observations. At most Class I areas there was insufficient years of data to produce a discernable trend. In addition, there was significant year-to-year variability in visibility impairment with episodic events (e.g., wildfires and wind blown dust) confounding the analysis.

1.4 Organization of the Report

Chapter 1 of this TSD presents background, an overview of the approach and summary of the results of the CENRAP meteorological, emissions and air quality modeling. Appendix A contains more details on the meteorological model evaluation discussed in Chapter 1. Details on the emissions modeling are provided in Chapter 2 and Appendix B. The model performance evaluation is given in Chapter 3 and Appendix C. The 2018 visibility projections and comparisons with the 2018 URP point are provided in Chapter 4 with more details given in Appendix D. Chapter 5 contains additional supporting analysis with details on the PM source apportionment modeling and alternative projections provided in Appendices E and F, respectively. Chapter 6 lists the references cited in the report.

2.0 EMISSIONS MODELING

2.1 Emissions Modeling Overview

For the emissions modeling work conducted in support of CENRAP air quality modeling, we used updated 2002 emissions data for the U.S., 1999 emissions data for Mexico, and 2000 emissions data for Canada to generate a final base 2002 Base G Typical (Typ02G) annual emissions database. Numerous iterations of the emissions modeling were conducted using interim databases before arriving at the final Base G emission inventories. The 2002 and 2018 emissions inventories and ancillary modeling data were provided by CENRAP emissions inventory contractors (Pechan and CEP, 2005c,e; Reid et al., 2004a,b; Coe and Reid, 2003), other Regional Planning Organizations (RPOs) and EPA. Building from the CENRAP preliminary 2002 database (Pechan and CEP. 2005e) and 2018 projections (Pechan, 2005d), we integrated several updates to the inventories and ancillary data to create final emissions input files; the final simulations are referred to as 2002 Typical and 2018 Base G, or Typ02G and Base18G. We used the Sparse Matrix Operator Kernel Emissions (SMOKE) version 2.1 processing system (CEP, 2004) to prepare the inventories for input to the air quality modeling systems. The SMOKE simulations documented in this report include emissions generated for annual CMAQ and CAMx simulations at a 36-km model grid resolution, and a short-term CMAQ test simulation at a 12-km model grid resolution. We performed the modeling and quality assurance (QA) work based on the CENRAP modeling Quality Assurance Project Plan (QAPP; Morris and Tonnesen, 2004) and Modeling Protocol (Morris et al., 2004a).

The Typ02G and Base18G emission inventories represent significant improvements to the preliminary emissions modeling performed by CENRAP (Morris et al., 2005). While the preliminary 2002 modeling served its purpose to develop the infrastructure for modeling large emissions data sets and producing annual emissions simulations, much of the input data (both as inventories and ancillary data) were placeholders for actual 2002 data that were being prepared through calendar year 2005. As these actual 2002 data sets became available, they were integrated into the SMOKE modeling and QA system that was developed during the preliminary modeling, to produce a high-quality emissions data set for use in the final CMAQ and CAMx modeling. The addition of entirely new inventory categories, like marine shipping, added complexity to the modeling. By the end of the emissions data collection phase, there were 23 separate emissions processing streams covering a variety of sources categories necessary to general model-ready emission inputs for the 2002 calendar year.

2.1.1 SMOKE Emissions Modeling System Background

The purpose of SMOKE (or any emissions processor) is to process the raw emissions reported by states and EPA into gridded hourly speciated emissions required by the air quality model. Emission inventories are typically available as an annual total emissions value for each emissions source, or perhaps with an average-day emissions value. The air quality models, however, typically require emissions data on an hourly basis, for each model grid cell (and perhaps model layer), and for each model species. Consequently, emissions processing involves (at a minimum) transformation of emission inventory data by temporal allocation, chemical speciation, spatial allocation, and perhaps layer assignment, to achieve the input requirements of the air quality model. For the CENRAP modeling effort, all of these steps were needed. In

addition, CENRAP processing requires special MOBILE6 processing and growth and control of emissions for the future-year inventories. Finally, the biogenic emission processing using BEIS2 includes additional processing steps. SMOKE formulates emissions modeling in terms of sparse matrix operations. Figure 2-1 shows an example of how the matrix approach organizes the emissions processing steps for anthropogenic emissions, with the final step that creates the model-ready emissions being the merging of all the different processing streams of emissions into a total emissions input file for the air quality model. Figure 2-1 does not include all the potential processing steps, which can be different for each source category in SMOKE, but does include the major processing steps listed in the previous paragraph, except the layer assignment. Specifically, the inventory emissions are arranged as a vector of emissions, with associated vectors that include characteristics about the sources such as its state and county or source classification code (SCC). SMOKE also creates matrices that will apply the gridding, speciation, and temporal factors to the vector of emissions. In many cases, these matrices are independent from one another, and can therefore be generated in parallel. The processing approach ends with the merge step, which combines the inventory emissions vector (now an hourly inventory file) with the control, speciation, and gridding matrices to create model-ready emissions.

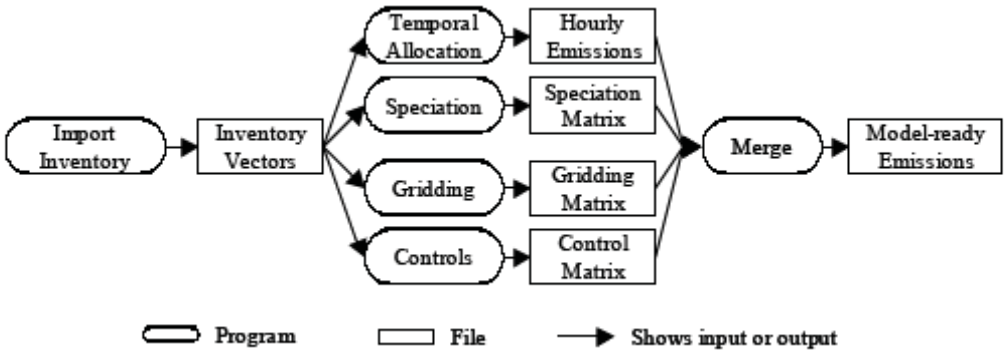

Figure 2-1. Flow diagram of major SMOKE processing steps needed by all source categories.

Temporal processing includes both seasonal or monthly adjustments and day-of-week adjustments. Emissions are known to be quite different for a typical weekday versus a typical Saturday or Sunday. For the day-of-week temporal processing step, emissions may be processed using representative Monday, weekday, Saturday, and Sunday for each month; we refer to this type of processing here as MWSS processing (note that because SMOKE operates in Greenwich Mean Time [GMT] then Monday would include some of local time Sunday so needs to be processed separately from the typical weekday). This approach significantly reduces the number of times the temporal processing step must be run. In the sections below, we have identified the cases in which we have used the MWSS processing approach. Figure 2-2 provides a schematic diagram of SMOKE/BEIS2 processing steps used in this project to generate biogenic emissions rates for Volatile Organic Compounds (VOCs) and oxides of nitrogen (NOx). Because biogenic emissions are temperature sensitive, they are generated for each day of 2002 using day-specific meteorological conditions from the MM5 meteorological model.

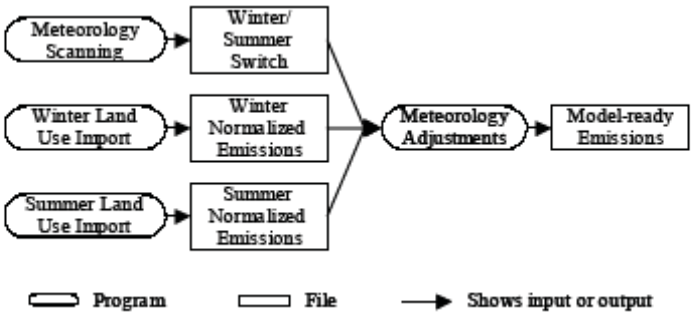

Figure 2-2. Flow diagram of SMOKE/BEIS2 processing steps.

2.1.2 SMOKE Scripts

The scripts are the interface that emissions modelers use to run SMOKE and define the set up and databases used in the emissions modeling so are important for anyone wishing to reproduce the CENRAP SMOKE emissions modeling. Many iterations of the CENRAP SMOKE emissions modeling were performed using updated and corrected emissions data and assumptions resulting in the creation of numerous SMOKE modeling scripts during the course of the study. For the CENRAP annual 2002 SMOKE emissions modeling, the default SMOKE script set up, which is based on source categories, was used to configure the scripts. We made several modifications to the default SMOKE scripts to modularize them, add error checking loops, and break up the report and logs directories by source category. The result is one script for each major source category being modeled that calls all of the SMOKE programs required for simulating that source category. 16 major source categories were modeled by SMOKE for CENRAP. An addition seven SMOKE scripts were also run to set up the emissions modeling. Table 2-1 lists all of the SMOKE scripts used for the 2002 base year modeling and the SMOKE programs called by each script. In addition to the source-specific scripts listed in Table 2-1, we also listed the SMOKE utility scripts that actually call executables, manage the log files, and manage the configuration of the SMOKE simulations.

Table 2-1. Summary of SMOKE scripts.

Source Category	Script Name	SMOKE Programs/Functions
Area	/home/aqm2/edss2/cenrap02f/subsys/smoke/scripts/run/36km/smk_ar_base02f.csh	smkinev, grdmat, spcmat, temporal, smkmerge, smkreport
Area fire	/home/aqm2/edss2/cenrap02f/subsys/smoke/scripts/run/36km/smk_arf_base02f.csh	smkinev, grdmat, spcmat, temporal, smkmerge, smkreport
Offshore Area	/home/aqm2/edss2/cenrap02f/subsys/smoke/scripts/run/36km/smk_ofsar_base02f.csh	smkinev, grdmat, spcmat, temporal, smkmerge, smkreport
Non-road* Mobile	/home/aqm2/edss2/cenrap02f/subsys/smoke/scripts/run/36km/smk_nr_base02f.csh	smkinev, grdmat, spcmat, temporal, smkmerge, smkreport
Fugitive dust	/home/aqm2/edss2/cenrap02f/subsys/smoke/scripts/run/36km/smk_fd_base02f.csh	smkinev, grdmat, spcmat, temporal, smkmerge, smkreport
Road dust	/home/aqm2/edss2/cenrap02f/subsys/smoke/scripts/run/36km/smk_rd_base02f.csh	smkinev, grdmat, spcmat, temporal, smkmerge, smkreport
Ammonia*	/home/aqm2/edss2/cenrap02f/subsys/smoke/scripts/run/36km/smk_nh3_base02f.csh	smkinev, grdmat, spcmat, temporal, smkmerge, smkreport
On-road Mobile (non-VMT-based)	/home/aqm2/edss2/cenrap02f/subsys/smoke/scripts/run/36km/smk_mb_base02f.csh	smkinev, grdmat, spcmat, temporal, smkmerge, smkreport
On-road non-US Mobile (non-VMT-based)	/home/aqm2/edss2/cenrap02f/subsys/smoke/scripts/run/36km/smk_nusm_base02f.csh	smkinev, grdmat, spcmat, temporal, smkmerge, smkreport
On-road Mobile (VMT-based)	/home/aqm2/edss2/cenrap02f/subsys/smoke/scripts/run/36km/smk_mbv_base02f.csh	smkinev, mbsetup, grdmat, spcmat, premobl, emisfac, temporal, smkmerge, smkreport
WRAP Oil and Gas	/home/aqm2/edss2/cenrap02f/subsys/smoke/scripts/run/36km/smk_wog_base02f.csh	smkinev, grdmat, spcmat, temporal, smkmerge, smkreport
Point	/home/aqm2/edss2/cenrap02f/subsys/smoke/scripts/run/36km/smk_pt_base02f.csh	smkinev, grdmat, spcmat, laypoint, temporal, smkmerge, smkreport
Offshore point	/home/aqm2/edss2/cenrap02f/subsys/smoke/scripts/run/36km/smk_ofs_base02f.csh	smkinev, grdmat, spcmat, laypoint, temporal, smkmerge, smkreport
Canadian Point fires	/home/aqm2/edss2/cenrap02f/subsys/smoke/scripts/run/36km/smk_bsf_base02f.csh	smkinev, grdmat, spcmat, laypoint, temporal, smkmerge, smkreport
All point fires	/home/aqm2/edss2/cenrap02f/subsys/smoke/scripts/run/36km/smk_alf_base02f.csh	smkinev, grdmat, spcmat, laypoint, temporal, smkmerge, smkreport
Biogenec	/home/aqm2/edss2/cenrap02f/subsys/smoke/scripts/run/36km/smk_bg_base02f.csh	Normbies3, tmpbies3, smkmerge
n/a	/home/aqm2/edss2/cenrap02f/subsys/smoke/scripts/run/make_invdir.csh	builds output file names and directories
n/a	/home/aqm2/edss2/cenrap02f/subsys/smoke/scripts/run/smk_run.csh	Calls SMOKE executables for everything but projection, controls, and QA
n/a	/home/aqm2/edss2/cenrap02f/subsys/smoke/scripts/run/qa_run.csh	Calls the SMOKE executables for running QA program & names the input/output directories for reports
n/a	/home/aqm2/edss2/cenrap02f/subsys/smoke/scripts/run/36km/smoke_calls.csh	Calls smk_run.csh, qa_run.csh, configuration and management
n/a	/home/aqm2/edss2/cenrap02f/subsys/smoke/Assignes/ASSIGNES.cenrap_base02f.cmaq.cb4p25	Sets up the environment variables for use of SMOKE
n/a	/home/aqm2/edss2/cenrap02f/subsys/smoke/Assignes/smk_mkdir	Creates the input/output directories
n/a	/home/aqm2/edss2/cenrap02f/subsys/smoke/Assignes/setmerge_files.scr	Sets up the output environment variables for the smkmerge program

* The nr and nh3 where farther divided to nrm and nry and nh3m and nh3y for the monthly/seasonal and yearly inventories

2.1.3 SMOKE Directory Structures

The SMOKE directories can be divided into three broad categories:

1. Program Directories: These directories contain the model source code, assigns files, scripts and executables needed to run SMOKE.
2. Input Directors: These directories contain the raw emissions inventories, the meteorological data and the ancillary input files.
3. Output Directories: These directories contain all of the output from the model. Also, the output directories contain the MOBILE6 input files.

The directories are described in the Table 2-2. The final pre-merged emission file names and sources of the data re provided in Appendix B.

Table 2-2. Summary of SMOKE directories.

Category	Directory Location	Directory Contents
Program	/home/aqm2/edss2/ cenrap02f/subsys/smoke/src	SMOKE source code
	/home/aqm2/edss2/ cenrap02f/subsys/smoke/assigns	SMOKE assigns files
	/home/aqm2/edss2/ cenrap02f/subsys/smoke/scripts	SMOKE make and run scripts
	/home/aqm2/edss2/ cenrap02f/subsys/smoke/Linux2_x86pg	SMOKE executables
Input	/home/aqm2/edss2/ cenrap02f/data/met	MCIP out metrology files
	/home/aqm2/edss2/ cenrap02f/data/ge_dat	SMOKE ancillary input files
	/home/aqm2/edss2/ cenrap02f/data/inventory/cenrap2002	Raw emissions inventory files
Output	/home/aqm2/edss2/ cenrap02f/data/run_base02f/static	Non-time dependent SMOKE intermediate outputs and MOBILE6 inputs
	/home/aqm2/edss2/ cenrap02f/ data/run_base02f/scenario	Time dependent SMOKE intermediate outputs
	/home/aqm2/edss2/ cenrap02f/data/run_base02f/outputs	Model-ready SMOKE outputs
	/home/aqm2/edss2/ cenrap02f/data/reports	SMOKE QA reports

2.1.4 SMOKE Configuration

SMOKE was configured to generate emissions for all months of 2002 on the 36-km unified RPO modeling domain (Figure 1-2). For the anthropogenic emissions sources that use hourly meteorology and daily or hourly data (i.e., on-road mobile sources, point sources with CEM data, point source fires and biogenic sources) we configured SMOKE to represent the daily emissions explicitly. For the non-meteorology dependent emissions, we used a representative Saturday, Sunday, Monday, and weekday for each month as surrogate days for the entire month's emissions (we refer to this as the MWSS processing approach). For these non-meteorology dependent emissions sources we explicitly represented the holidays as Sundays. Table 2-3 lists the days that we modeled as representative days in the months that we simulated for the 2002 base year modeling. Table 2-4 lists the holidays in 2002 that were modeled as Sundays.

Table 2-3: Representative model days for 2002 base year simulation.

Saturday	Sunday	Monday	Weekday
January 5	January 6	January 7	January 4
February 2	February 3	February 4	February 5
March 2	March 3	March 4	March 5
April 6	April 7	April 8	April 2
May 4	May 5	May 6	May 7
June 8	June 9	June 3	June 4
July 6	July 7	July 8	July 3
August 3	August 4	August 5	August 6
September 7	September 8	September 9	September 10
October 5	October 6	October 7	October 8
November 2	November 3	November 4	November 5
December 7	December 8	December 9	December 10

Table 2-4: 2002 modeled holidays.

Holiday	Date
New Years	January 1, 2002 January 2, 2002
Good Friday	March 29, 2002 March 30, 2002
Memorial Day	May 27, 2002 May 28, 2002
Independence Day	July 4, 2002 July 5, 2002
Labor Day	September 2, 2002 September 3, 2002
Thanksgiving Holiday	November 28-30, 2002
Christmas Holiday	December 24-26, 2002

We used the designations in Table 2-5 to determine which months fell into each season when temporally allocating the seasonal emissions inventories. Some of the inventories for the Electrical Generating Units (EGUs) were received for Winter and Summer. Table 2-6 determines which months fell into each season

Table 2-5. Assignments of months to four seasons for use of seasonal inventory files in SMOKE.

Month	Season
January	Winter
February	Winter
March	Spring
April	Spring
May	Spring
June	Summer
July	Summer
August	Summer
September	Fall
October	Fall
November	Fall
December	Winter

Table 2-6. Assignments of months to two seasons for use of seasonal inventory files in SMOKE.

Month	Season
January	Winter
February	Winter
March	Winter
April	Winter
May	Summer
June	Summer
July	Summer
August	Summer
September	Summer
October	Winter
November	Winter
December	Winter

2.1.5 SMOKE Processing Categories

Emissions inventories are typically divided into area, on-road mobile, non-road mobile, point, and biogenic source categories. These divisions arise from differing methods for preparing the inventories, different characteristics and attributes of the categories, and how the emissions are processed through models. Generally, emissions inventories are divided into the following source categories, which we refer to later as "SMOKE processing categories."

- Stationary Area Sources: Sources that are treated as being spread over a spatial extent (usually a county or air district) and that are not movable (as compared to non-road mobile and on-road mobile sources). Because it is not possible to collect the emissions at each point of emission, they are estimated over larger regions. Examples of stationary

area sources are residential heating and architectural coatings. Numerous sources, such as dry cleaning facilities, may be treated either as stationary area sources or as point sources.

- On-Road Mobile Sources: Vehicular sources that travel on roadways. These sources can be computed either as being spread over a spatial extent or as being assigned to a line location (called a link). Data in on-road inventories can be either emissions or activity data. Activity data consist of vehicle miles traveled (VMT) and, optionally, vehicle speed. Activity data are used when SMOKE will be computing emission factors via another model, such as MOBILE6 (U.S. EPA, 2005). Examples of on-road mobile sources include light-duty gasoline vehicles and heavy-duty diesel vehicles.

- Non-Road Mobile Sources: These sources are engines that do not always travel on roadways. They encompass a wide variety of source types from lawn and garden equipment to locomotives and airplanes. Emission estimates for most non-road sources come from EPA's NONROAD model (OFFROAD in California). The exceptions are emissions for locomotives, airplanes, pleasure craft and commercial marine vessels.

- Point Sources: These are sources that are identified by point locations, typically because they are regulated and their locations are available in regulatory reports. In addition, elevated point sources will have their emissions allocated vertically through the model layers, as opposed to being emitted into only the first model layer. Point sources are often further subdivided into electric generating unit (EGU) sources and non-EGU sources, particularly in criteria inventories in which EGUs are a primary source of NO_x and SO_2. Examples of non-EGU point sources include chemical manufacturers and furniture refinishers. Point sources are included in both criteria and toxics inventories.

- Biogenic Land Use Data: Biogenic land use data characterize the types of vegetation that exist in either county-total or grid cell values. The biogenic land use data in North America are available using two different sets of land use categories: the Biogenic Emissions Landcover Database (BELD) version 2 (BELD2), and the BELD version 3 (BELD3) (CEP, 2004b).

In addition to these standard SMOKE processing categories, we have added other categories either to represent specific emissions processes more accurately or to integrate emissions data that are not compatible with SMOKE. Examples of emissions sectors that fall outside of the SMOKE processing categories include emissions generated from process-based models for representing windblown dust and agricultural ammonia (NH_3) sources. An emissions category with data that are not compatible with SMOKE is one with gridded emissions data sets, such as commercial marine sources. Another nonstandard emissions category that we modeled was emissions from fires. All of the emissions categories that we used to build CENRAP simulations are described in detail in the following sections.

Continuing the enhancement of the emissions source categories that we initiated during the preliminary 2002 modeling, we further refined the categories from the standard definitions listed above to include more explicit emissions sectors. The advantage of using more detailed definitions of the source categories is that it leads to more flexibility in designing control strategies, substituting new inventory or profile data into the modeling, managing the input and output data from SMOKE and conducting QA of the SMOKE outputs. The major drawback to defining more emissions source categories is the increased level of complexity and computational requirements (run times and disk space) that results from having a larger number of input data sets. Another motivation behind separating the various emissions categories is related to the size and flexibility of the input data. Some data sets, like the CENRAP on-road

mobile inventory, were so large that we had to process them separately from the rest of the sources in the on-road sector due to computational constraints. We also separated the non-road mobile and ammonia sectors into yearly and monthly inventories to facilitate the application of uniform monthly temporal profiles to the monthly data. Additional details about how we prepared the emissions inventories and ancillary data for modeling are described in Sections 2.2 through 2.16. Table 2-7 summarizes the entire group of source sectors that composed simulation Typ02G. Each emissions sector listed in the table represents an explicit SMOKE simulation. As discussed in Section 2.1.2 below, after finishing all of the source-specific simulations, we used SMOKE to combine all of the data into a single file for each day for input to the air quality modeling systems. Each subsection on the emissions sectors describes each sector in terms of the SMOKE processing category, the year covered by the inventory, and the source(s) of the data.

Additional details about the inventories are also provided, including any modifications that we made to prepare them for input into SMOKE.

Table 2-7. CENRAP Typ02G emissions categories.

Emissions Sector	Abbreviation*
Fires as Point Sources (WRAP, CENRAP, VISTAS)	Alf
Area Sources (All domain)	ar
CENRAP area fires	arf
Area fires, Anthropogenic (All domain, excluding WRAP and CENRAP)	arfa
Area fires, Wild (All domain, excluding WRAP)	arfw
Biogenic	b3
Ontario, Canada, point-source fires	bsf
Fugitive dust	fd
WRAP on-road mobile	mb
CENRAP on-road mobile	mbv_CENRAP
Other US on-road mobile	mbv
Monthly CENRAP/MRPO anthropogenic NH_3	nh3m
Ammonia from annual inventory (CENRAP)	nh3y
WRAP anthropogenic NH_3	nh3
Seasonal/Monthly non-road mobile (WRAP, CENRAP, MW)	nrm
Annual non-road mobile	nry
On-road Mobile (Non-US)	nusm
Offshore shipping (Gulf, Atlantic)	ofs
Offshore area (Gulf)	ofsar
Stationary point (All domain, including offshore)	pt
Road dust	rd
Windblown dust (All domain)	wb_dust
WRAP oil and gas	wog

*These abbreviations are used in the file naming of the SMOKE output files for each sector.

Emissions models such as SMOKE are computer programs that convert annual or daily estimates of emissions at the state or county level to hourly emissions fluxes on a uniform spatial grid that are formatted for input to an air quality model. For the Typ02G and Base18G emission inventories we prepared emissions for CMAQ version 4.5 using SMOKE version 2.1 on the UCR Linux computing cluster. SMOKE integrates annual county-level emissions inventories with source-based temporal, spatial, and chemical allocation profiles to create hourly emissions fluxes on a predefined model grid. For elevated sources that require allocation of the emissions to the vertical model layers, SMOKE integrates meteorology data to derive dynamic vertical profiles. In addition to its capacity to represent the standard emissions processing categories, SMOKE is also instrumented with the Biogenic Emissions Inventory System, version 3 (BEIS3) model for estimating biogenic emissions fluxes (U.S. EPA, 2004) and the MOBILE6 model for estimating on-road mobile emissions fluxes from county-level vehicle activity data (U.S. EPA, 2005a).

SMOKE uses C-Shell scripts as user interfaces to set configuration options and call executables. SMOKE is designed with flexible QA capabilities to generate standard and custom reports for checking the emissions modeling process. After modeling all of the source categories individually, including those categories generated outside of SMOKE, we used SMOKE to merge all of the categories together to create a single CMAQ input file per simulation day. Also, for use in the CAMx modeling, we converted the CMAQ-ready emissions estimates to CAMx-ready files using the CMAQ2CAMx converter. Additional technical details about the version of SMOKE used for final simulations are available from CEP (2004b). All scripts, data, and executables used to generate the Typ02G and Base18G emissions for CMAQ and CAMx are archived on the CENRAP computing cluster.

2.1.6 2002 and 2018 Data Sources

This section describes the procedures that the CENRAP followed to collect and prepare all emissions data for Typ02G and Base18G simulations. We discuss the sources of all inventory and ancillary data used for simulations. CENRAP worked with emissions inventory contractors, other RPOs, and EPA to collect all of the data that constitute the simulation. Table 2-8 lists all of the contacts for the various U.S. anthropogenic emission inventories we used. For the CENRAP inventories, this table lists the contacts for the contractors who prepared the inventories; for the non-CENRAP inventories it lists the contacts at the RPOs who provided us inventory data. We obtained the emissions inventories for Canada and Mexico from the U.S. EPA Emissions Factors and Inventory Group (EFIG) via the Clearinghouse for Inventories and Emissions Factors (CHIEF) website (http://www.epa.gov/ttn/chief/index.html).

Table 2-8. CENRAP anthropogenic emissions inventory contacts.

Source Category	Emissions Data Contact
WRAP	
All	Tom Moore, Western Governors' Association Phone: (970) 491-8837 Email: mooret@cira.colostate.edu
CENRAP	
2002 Consolidated Inventory	Randy Strait, E.H. Pechan & Assoc., Inc. Phone: 919-493-3144 Email: rstrait@pechan.com
NH3 Inventory, Prescribed and Agricultural Fires, and On-road mobile emissions	Dana Sullivan, Sonoma Technology, Inc. Phone: 707-665-9900 Email: dana@sonomatech.com
Gulf Off-shore platform and support vessel emissions	Holly Ensz, Minerals Management Service Phone: (504) 736-2536 Email: holli.ensz@mms.gov
VISTAS	
All	Greg Stella, Alpine Geophysics, LLC, Phone: 828-675-9045 Email: gms@alpinegeophysics.com
MANE-VU	
All	Megan Schuster, MARAMA, Baltimore, MD USA Phone: 410-467-0170 Email: mschuster@marama.org
MRPO	
All	Mark Janssen, LADCO, Des Plaines, IL, USA Phone: 847-296-2181 Email:janssen@ladco.org

As mentioned above, the refinement of these inventories involved splitting some of the inventory files into more specific source sectors. As the stationary-area-source emissions sector has traditionally been a catch-all for many types of sources, this is the inventory sector that required the greatest amount of preparation. Upon receiving all stationary-area-source inventories we extracted fugitive dust, road dust, anthropogenic NH_3, and for the non-WRAP U.S. inventories, stage II refueling sources. We retained the dust sources as separate categories that we would further refine with the application of transport factors (see Section 2.8).

We collected the ancillary data used for SMOKE modeling from several sources. SMOKE ancillary modeling data include:

- Temporal and chemical allocation factors by state, county, and source classification code (SCC);
- Spatial surrogates and cross-reference files for allocating county-level emissions to the model grid;
- Hourly gridded meteorology data;
- Stack defaults for elevated point sources;
- MOBILE6 configuration files;
- A Federal Implementation Standards (FIPS) codes (i.e., country/state/county codes) definition file;

- A Source Category Classification (SCC) codes definition file;
- A pollutant definition file; and
- Biogenic emission factors.

Except for the meteorology data and the MOBILE6 configuration files, we used default data sets provided by EPA as the basis for all of the ancillary data except for temporal profiles used for Electric Generating Units (EGUs). These profiles were developed based on CEM data from 2000 through 2003 (Pechan and CEP, 2005c). CENRAP provided the meteorology data for the simulations at 36-km and 12-km grid resolutions (Johnson, 2007). The inventory contractor who prepared the MOBILE6 inventories provided the MOBILE6 configuration files either directly or via an RPO representative; details about the sources of the MOBILE6 inputs are provided in Section 2.4. We made minor modifications to the chemical allocation, pollutant definition, and country/state/county codes files for new sources, pollutants, or counties contained in the inventories that we had not previously modeled. We made major modifications to the temporal and spatial allocation inputs, as described below.

2.1.7 Temporal Allocation

Temporally allocating annual, daily, or hourly emissions inventories in SMOKE involves combining a temporal cross-reference file and a temporal profiles file.

- Temporal cross-reference files associate monthly, weekly, and diurnal temporal profile codes with specific inventory sources, through a combination of a FIPS (country/state/county) code, an SCC, and sometimes for point sources, facility and unit identification codes.
- Temporal profiles files contain coded monthly, weekly, and diurnal profiles in terms of a percentage of emissions allocated to each temporal unit (e.g., percentage of emissions per month, weekday, or hour).

As a starting point for the temporal allocation data for simulations, we used the files generated by emission inventory contractors (Pechan and CEP, 2005c). Based on guidance from the developers of some of the inventory files, we enhanced the temporal profiles and assignments for some source categories (Pechan, 2005b).

We modified the temporal allocation data for the simulations to improve the representation of temporal emissions patterns for certain source categories. We implemented the adjusted profiles in SMOKE by modifying the temporal cross-reference file for the applicable FIPS and SCC combinations.

Updated temporal profiles for EGUs were made available for MRPO in the MRPO Base K inventory. Since the non-road emissions for IA and MN were monthly emissions developed by MRPO, new temporal profiles were created for all the SCCs in these emissions files for these two states only. The monthly profile was uniform and the weekly and diurnal profiles were kept the same as were modeled for the rest of the country.

An updated temporal profile, profile 485, based on NOAA 1971-2000 population weighted average heating degree days for home heating area source emissions was obtained from

VISTAS. This profile provided state specific updates for home heating emissions and was applied to the full inventory in place of profile 17XX.

Other additions to the Base02G temporal allocation data included updates that made by other RPOs that are applicable to their inventories. These other updates to the temporal allocation files included

- VISTAS continuous emissions monitoring (CEM)-specific profiles for EGUs in the VISTAS states;
- VISTAS agricultural burning profiles;
- Wildfire and prescribed fire profiles developed by VISTAS for the entire U.S.;
- MANE-VU on-road mobile profiles;
- WRAP weekly and diurnal road dust profiles;
- WRAP diurnal wildfire, agricultural fire, and prescribed fire profiles; and
- WRAP on-road mobile weekly and diurnal profiles.

Finally, for all of the monthly and seasonal emissions inventories, we modified the temporal cross-reference files to apply uniform monthly profiles to the sources contained in these inventories. The monthly variability is inherent in monthly and seasonal inventories and does not need to be reapplied through the temporal allocation process in SMOKE. The inventories to which we applied uniform monthly temporal profiles included:

- WRAP, CENRAP, and MRPO non-road mobile sources;
- WRAP on-road mobile sources;
- WRAP road dust; and
- CENRAP anthropogenic ammonia.

2.1.8 Spatial Allocation

SMOKE uses spatial surrogates and SCC cross-reference files to allocate county-level emissions inventories to model grid cells. Geographic information system (GIS)-calculated fractional land use values define the percentage of a grid cell that is covered by standard sets of land use categories. For example, spatial surrogates can define a grid cell as being 50% urban, 10% forest, and 40% agricultural. In addition to land use categories, spatial surrogates can also be defined by demographic or industrial units, such as population or commercial area. Similar to the temporal allocation data, an accompanying spatial cross-reference file associates the spatial surrogates (indexed with a numeric code) to SCCs. Spatial allocation with surrogates is applicable only to area and mobile sources that are provided on a county level basis. Point sources are located in the model grid cells by SMOKE based on the latitude-longitude coordinates of each source. Biogenic emissions are estimated based on 1-km^2 gridded land use information that is mapped to the model grid using a processing program such as the Multimedia Integrated Modeling System (MIMS) Spatial Allocator (CEP, 2004).

We used various sources of spatial surrogate information for the U.S., Canada, and Mexico inventories in the simulations. For the U.S. and Canadian sources, we used the EPA unified

surrogates available through the EFIG web site (EPA, 2005c). For the 36-km grid, EPA provides these data already formatted for SMOKE on the RPO Unified 36-km domain that we used for the simulations. We modified the spatial surrogates for Canada on the RPO Unified 36-km domain by adopting several surrogate categories that were enhanced by the WRAP. Table 2-9 provides details about the new Canadian spatial surrogates that were developed by the WRAP and used for CENRAP simulations. For modeling Mexico, we used Shapefiles developed for the Big Bend Regional Aerosol and Visibility Observations Study (BRAVO) modeling to create surrogates for Mexico on the RPO Unified 36-km domain (EPA, 2005c).

Table 2-9. New Canadian spatial surrogates.

Attribute	Base02a Code	Shapefile	Reference
Land area	950	can_land93_land	Natural Resources Canada (1993) AVHRR land cover data
Water area	951	can_land93_water	Natural Resources Canada (1993) AVHRR land cover data
Forest land area	952	can_land93_forest	Natural Resources Canada (1993) AVHRR land cover data
Agricultural land area	953	can_land93_agri	Natural Resources Canada (1993) AVHRR land cover data
Urban land area	954	can_land93_urban	Natural Resources Canada (1993) AVHRR land cover data
Rural land area	955	can_land93_rural	Natural Resources Canada (1993) AVHRR land cover data
Airports	956	can_airport	U.S. DOT Bureau of Transportation Statistics (2005) NORTAD 1:1,000,000 scale data
Ports	957	can_port	U.S. DOT Bureau of Transportation Statistics (2005) NORTAD 1:1,000,000 scale data
Roads	958	can_road1m	Natural Resources Canada (2001) National Scale Frameworks data
Rail	959	can_rail1m	Natural Resources Canada (1999) National Scale Frameworks data

2.2 Stationary Point Source Emissions

Stationary-point-source emissions data for SMOKE consist of (1) Inventory Data Analyzer (IDA)-formatted inventory files; (2) ancillary data for allocating the inventories in space, time, and to the Carbon Bond-IV chemistry mechanism used in CMAQ and CAMx; and (3) meteorology data for calculating plume rise from the elevated point sources. This section describes where CENRAP obtained these data, how we modeled them, and the types of QA that we performed to ensure that SMOKE processed the data as expected.

2.2.1 Data Sources

For the stationary-point-source inventories in Typ02G and Base18G, we used actual 2002 data developed by the RPOs for the U.S., version 2 of the year 2000 Canadian inventory, and the BRAVO 1999 Mexican inventory. The BRAVO inventory was updated with entirely new inventories for the six northern states of Mexico for stationary area, as well as stationary point, on-road mobile, and off-road mobile sources. Emissions for the southern states of Mexico were included for the first time in CENRAP simulations Typ02G and Base18G. These data were provided by ERG, Inc., who completed an updated 1999 emissions inventory for northern Mexico (ERG, 2006b) and delivered these data to the WRAP. The CENRAP stationary-point inventory consisted of annual county-level and tribal data provided in August of 2005 (Pechan and CEP, 2005e). The WRAP (ERG, 2006a) and VISTAS Base G (MACTEC, 2006) stationary-point inventories consisted of an annual data set and monthly CEM data for selected EGUs. The WRAP and VISTAS provided these data directly to CENRAP. We downloaded the MANE-VU stationary-point inventories from the MANE-VU web sites. MRPO base K data was downloaded and processed for SMOKE modeling by Alpine Geophysics under contract from MARAMA. UCR entered into a nondisclosure agreement with Environment Canada to obtain version 2 of the 2000 Canadian point-source inventory. This inventory represented a major improvement over the version of the data that we had used in the preliminary 2002 modeling.

Reductions anticipated from BART controls for electric generating units (EGU) in Oklahoma, Arkansas, Kansas, and Nebraska were included in projections of 2018 emissions. These anticipated reductions were based on actual operating conditions and estimated control efficiencies from utilities.

Newly permitted coal-fired utilities were included in 2018 projections. Conservatively, no IPM projected new units were removed from the simulation with the addition of the permitted facilities.

Due to missing or clearly erroneous stack parameters, several facilities in CENRAP states were relegated to default stack profiles based on SCC in the NEI QA process. Prioritizing for the largest emissions sources, these default parameters were corrected by CENRAP States and updated files were provided to modeling contractors. Final IDA input files Typ02G and Base18G for point sources reflect State corrections.

For coal-fired point and area sources, The EPA Office of Air Quality and Planning Standards (OAQPS) determined that the organic carbon fraction in the speciation profile code "NCOAL" was not representative of most coal combustion occurring in the U.S. This profile has an organic carbon fraction of 20%, which includes an adjustment factor of 1.2 to account for other atoms (like oxygen) attached to the carbon. OAQPS has reverted back to the profile code "22001" for coal combustion, which has an organic carbon fraction of 1.07% (again including the 1.2 factor adjustment). This is the same profile that EPA used for previous rulemaking efforts including the Heavy Duty Diesel Rule and Non-Road Rule, which were proposed (and publicly reviewed) prior to the introduction of the NCOAL profile.

The consensus in OAQPS is that the NCOAL profile has a high organic carbon percentage because it is based on measurements of combustion of lignite coal. With the exception of Texas, lignite is not widely used in the U.S.. Thus, OAQPS staff stopped relying on this profile as a national default profile. A new coal speciation profile developed based on Eastern bituminous

coal combustion (since much of the coal burned in the U.S. is of this type) is being developed by EPA's Office of Research and Development but was not completed for this study.

The profile recently developed for MRPO by Carnegie Mellon was provided to CENRAP and is representative of combustion of eastern bituminous coal. This profile is a more appropriate profile for most facilities in the U.S. than the default NCOAL profile.

Additionally, the "22001" profile has been flagged as problematic because of the apparent inadvertent switching of the organic carbon and elemental carbon fractions, which are 1.07% and 1.83% respectively. The report discovering the discrepancy in the profile did not offer a clear alternative to correct the problem (MACTEC, 2003).

CENRAP has continued to use the NCOAL factor for facilities burning lignite in North Dakota and Texas. For the remainder of the U.S., the MRPO profile, CMU, was used. The NCOAL factor was modified reducing the organic carbon by half and assigning the remainder to $PM_{2.5}$. The modification was at the request of Texas and was reflective of the original study for the NCOAL factor conducted in Texas (Chow, 2005). Table 2-10 summarizes the $PM_{2.5}$ speciation profiles for the NCOAL, 2201 and CMU speciation profiles for coal burning sources.

Table 2-10. PM 2.5 speciation profiles for coal-burning sources.

Profile	POC	PEC	PNO3	PSO4	PM2.5
NCOAL	0.1000	0.0100	0.0050	0.1600	0.7250
22001	0.0107	0.0183	0.0000	0.1190	0.8520
CMU	0.0263	0.0315	0.0036	0.0447	0.8938

Final simulations used improved temporal allocation and speciation information relative to the preliminary 2002 modeling; the rest of the ancillary data for modeling stationary point sources stayed the same (Mansell et al., 2005).

2.2.2 Emissions Processing

For Typ02G and Base18G simulations we configured SMOKE to process the annual inventories for the U.S., Canada, and Mexico and process hourly CEM data for the VISTAS. We configured SMOKE to allocate these emissions up to model layer 15 (approximately 2,500 m AGL), which roughly corresponds to the maximum planetary boundary layer (PBL) heights across the entire domain throughout the year. As coarse particulate matter (PMC) is not an inventory pollutant but is required by the air quality models as input species, we used SMOKE to calculate PMC during the processing as (PM_{10} - $PM_{2.5}$). With the SMOKE option WKDAY_NORMALIZE set to "No," we treated the annual inventories based on the assumption that they represent average-day data based on a seven-day week, rather than average weekday data. We also assumed that all of the volatile organic compound (VOC) emissions in the inventories are reactive organic gas (ROG), and thus used SMOKE to convert the VOC to total organic gas (TOG) before converting the emissions into CB-IV speciation for the air quality models. To capture the differences in diurnal patterns that are contained in the CEM temporal profiles for VISTAS and CENRAP states (Base02F), we configured SMOKE to generate daily temporal matrices, as opposed to using a Monday-weekday-Saturday-Sunday (MWSS) temporal allocation approach.

To QA the stationary-point emissions, we used the procedures in the CENRAP emissions modeling QA protocol (Morris and Tonnesen, 2004) and a suite of graphical summaries. We used tabulated summaries of the input data and SMOKE script settings to document the data and configuration of SMOKE for all simulations. These QA graphics are available on the web site at: http://pah.cert.ucr.edu/aqm/cenrap/emissions.shtml

2.2.3 Uncertainties and Recommendations

There were issues with the stationary-point emissions that we left unresolved at the completion of the Typ02G and Base18G emissions modeling either because we did not feel they would have a major impact on the modeling results in CENRAP states or because we did not have alternative approaches and they represented the best available information. Canadian emissions for 2000 were found to have a significant number of missing stack parameters. These stacks when modeled with default parameters frequently resulted in lower plume heights. Stack parameters for 2000 were corrected based on cross referencing sources with the 2005 Canadian inventory for the largest emitting points. Stack parameters for many of the sources with lower emissions remain incorrect, but are assumed to have a less significant impact on CENRAP Class I areas. The 2020 projected emissions for Canada were obtained as air quality model-ready files from EPA. EPA has not confirmed that missing stack parameters were corrected for the projected inventory. It is assumed that they were not corrected and default parameters were used instead. Given confidentiality issues that surround Canadian inventories, EPA processed emissions represent the best available data.

2.3 Stationary Area Sources

Stationary-area-source emissions data for SMOKE consist of IDA-formatted inventory files and ancillary data for allocating the inventories in space, time, and to the Carbon Bond-IV chemistry mechanism used in CMAQ and CAMx. This section describes where we obtained these data, how we modeled them, and the types of QA that we performed to ensure that SMOKE processed the data as expected.

2.3.1 Data Sources

For the stationary area source inventories in the Typ02G and Base18G simulations, we used actual 2002 data developed by the RPOs for the U.S., version 2 of the year 2000 Canadian inventory, and the updated Mexican inventory, http://www.epa.gov/ttn/chief/net/mexico.html. The BRAVO inventory was updated with entirely new inventories for the six northern states of Mexico for stationary area, as well as stationary point, on-road mobile, and off-road mobile sources. Emissions for the southern states of Mexico were included for the first time in CENRAP simulations Typ02G and Base18G. The CENRAP stationary-area inventory consisted of annual county-level and tribal data provided by in August of 2005 (Pechan and CEP, 2005e). The WRAP (ERG, 2006a) and VISTAS Base G (MACTEC, 2006) stationary-area inventories consisted of an annual data set. We downloaded the MANE-VU stationary-area inventories from the MANE-VU web sites. MRPO base K data was downloaded and processed for SMOKE modeling by Alpine Geophysics under contract from MARAMA.

To prepare the stationary-area inventories for modeling, we made several modifications to the files by removing selected sources either to model them as separate source categories or to omit them from simulations completely. Using guidance provided by EPA (EPA, 2004b), we extracted fugitive and road dust sources from all stationary-area inventories for adjustment by transport factors and modeling as separate source categories (see Section 2.8). We also extracted and discarded the stage II refueling sources (Table 2-11) from the U.S. inventories; we modeled these sources with MOBILE6 as part of the on-road mobile-source emissions. We left the stage II refueling emissions in the WRAP stationary-area inventory because the on-road mobile inventory that we received for this region did not contain these emissions.

Table 2-11. Refueling SCCs removed from the non-WRAP U.S. stationary-area inventory.

SCC	Description
2501060100	Storage and Transport Petroleum and Petroleum Product Storage Gasoline Service Stations Stage 2: Total
2501060101	Storage and Transport Petroleum and Petroleum Product Storage Gasoline Service Stations Stage 2: Displacement Loss/Uncontrolled
2501060102	Storage and Transport Petroleum and Petroleum Product Storage Gasoline Service Stations Stage 2: Displacement Loss/Controlled
2501060103	Storage and Transport Petroleum and Petroleum Product Storage Gasoline Service Stations Stage 2: Spillage
2501070100	Storage and Transport Petroleum and Petroleum Product Storage Diesel Service Stations Stage 2: Total
2501070101	Storage and Transport Petroleum and Petroleum Product Storage Diesel Service Stations Stage 2: Displacement Loss/Uncontrolled
2501070102	Storage and Transport Petroleum and Petroleum Product Storage Diesel Service Stations Stage 2: Displacement Loss/Controlled
2501070103	Storage and Transport Petroleum and Petroleum Product Storage Diesel Service Stations Stage 2: Spillage

Other steps that we took to prepare the stationary-area inventories included confirming that there is no overlap between the anthropogenic NH_3 inventory (Section 2.9) and stationary area sources, and moving area-source fires in each regional inventory to separate files. In addition to these inventory modifications we made a few changes to the ancillary data files for simulation Typ02G, as described next.

Simulation Typ02G used improved temporal and spatial allocation information relative to the preliminary 2002 modeling; the rest of the ancillary data for modeling stationary area sources stayed the same as in the preliminary 2002 modeling (Mansell et al., 2005). We adopted enhanced spatial allocation data with additional area-based surrogates for Canada (Table 2-9), and added surrogates for a missing county in Colorado (Broomfield) from WRAP modeling and QA work. The WRAP had noticed when looking at the Canadian data for the preliminary 2002 modeling that forest fire emissions from the Canadian area-source inventory, which are relatively large sources of CO, NO_x, and $PM_{2.5}$, were being allocated to a surrogate for logging activities. They found similar discrepancies for other area and non-road SCCs in Canada. To improve the representation of the Canadian emissions, we adopted several land-area-based surrogates developed by the WRAP, such as forested land area, urban land area, and rural land area, and made the accompanying additions to the spatial cross-reference file to associate inventory SCCs with these surrogates. We also added spatial surrogates for Broomfield County, CO; this county was included in the inventory but was not included in the base EPA surrogates (this county was recently created from portions of other counties).

Improvements to the temporal allocation data for simulation Typ02G included the addition of several FIPS-specific profiles provided by VISTAS and CENRAP contractors (Pechan 2005b). These temporal profiles listed in Table 2-12 targeted mainly fire and agricultural NH_3 sources, such as open burning and livestock operations, respectively.

Table 2-12. New Temporal Profile Assignments for CENRAP Area Source SCCs.

SCC	Description	Month	Week	Diurnal	Recommendation Based on Profile Data for SCC	Description of Similar SCC used to Recommend Profiles
2310001000	Industrial Processes; Oil and Gas Production: SIC 13;All Processes : On-shore; Total: All Processes	262	7	26	2310000000	Industrial Processes;Oil and Gas Production: SIC 13;All Processes;Total: All Processes
2310002000	Industrial Processes;Oil and Gas Production: SIC 13;All Processes : Off-shore;Total: All Processes	262	7	26	2310000000	Industrial Processes;Oil and Gas Production: SIC 13;All Processes;Total: All Processes
2461870999	Solvent Utilization;Miscellaneous Non-industrial: Commercial;Pesticide Application: Non-Agricultural;Not Elsewhere Classified	258	7	26	2461800000	Solvent Utilization;Miscellaneous Non-industrial: Commercial;Pesticide Application: All Processes;Total: All Solvent Types
2805009200	Miscellaneous Area Sources;Agriculture Production - Livestock;Poultry production - broilers;Manure handling and storage	1500	7	26	2805009300	Miscellaneous Area Sources;Agriculture Production - Livestock;Poultry production - broilers;Land application of manure
2805021100	Miscellaneous Area Sources;Agriculture Production - Livestock;Dairy cattle - scrape dairy;Confinement	1500	7	26	2805021300	Miscellaneous Area Sources;Agriculture Production - Livestock;Dairy cattle - scrape dairy;Land application of manure
2805021200	Miscellaneous Area Sources;Agriculture Production - Livestock;Dairy cattle - scrape dairy;Manure handling and storage	1500	7	26	2805021300	Miscellaneous Area Sources;Agriculture Production - Livestock;Dairy cattle - scrape dairy;Land application of manure
2805023100	Miscellaneous Area Sources;Agriculture Production - Livestock;Dairy cattle - drylot/pasture dairy;Confinement	1500	7	26	2805023300	Miscellaneous Area Sources;Agriculture Production - Livestock;Dairy cattle - drylot/pasture dairy;Land application of manure
2805023200	Miscellaneous Area Sources;Agriculture Production - Livestock;Dairy cattle - drylot/pasture dairy;Manure handling and storage	1500	7	26	2805023300	Miscellaneous Area Sources;Agriculture Production - Livestock;Dairy cattle - drylot/pasture dairy;Land application of manure
2810020000	Miscellaneous Area Sources;Other Combustion;Prescribed Burning of Rangeland;Total	3	11	13	2810015000	Miscellaneous Area Sources;Other Combustion;Prescribed Burning for Forest Management;Total

2.3.2 Emissions Processing

For simulations Typ02G and Base18G we configured SMOKE to process the annual stationary-area-source inventories for the U.S., Canada, and Mexico. As PMC is not an inventory pollutant but is required by the air quality models as input species, we used SMOKE to calculate PMC during the processing as (PM_{10} - $PM_{2.5}$). With the SMOKE option WKDAY_NORMALIZE set to "Yes," we treated the annual stationary-area inventories based on the assumption that they represent average weekday data, causing SMOKE to renormalize the data to a seven-day estimate before applying any temporal adjustments. We also assumed that all of the VOC emissions in the inventories are ROG and thus used SMOKE to convert the VOC to TOG before converting the emissions into CB-IV speciation for the air quality models. We configured SMOKE to use a MWSS temporal allocation approach, as opposed to a daily temporal approach.

To QA the stationary-area emissions, we used the procedures in the CENRAP modeling QAPP and Modeling Protocol (Morris and Tonnesen, 2004; Morris et al., 2004a) and a suite of graphical summaries. We used tabulated summaries of the input data and SMOKE script settings to document the data and configuration of SMOKE for all simulations. The graphical QA summaries include, for all emissions output species, daily spatial plots summed across all model layers, daily time-series plots, and annual time-series plots. These QA graphics are available on the UCR/CENRAP web site at http://pah.cert.ucr.edu/aqm/cenrap/emissions.shtml .

2.3.3 Uncertainties and Recommendations

Most of the issues that we encountered with the stationary area sources related to the removal of certain SCCs from the base inventories for inclusion as other source categories or complete omission from simulations. We spent considerable effort on ensuring that we did not have overlap between the area inventory and the other sectors that explicitly represent sources traditionally contained in the area inventory, such as NH_3 and dust.

Both the Canadian and Mexican inventories presented minor problems that we resolved for simulation Typ02G but that can be addressed more thoroughly in future simulations. The Canadian inventory we used contained data only at the province level, essentially equivalent to a statewide rather than county-level inventory. A higher resolution inventory would have allowed us to use higher-resolution and more accurate spatial allocation data. Future modeling that uses Canadian data should move to the newly released municipality-level year 2000 inventories for Canada.

There was a discrepancy between the state and county coding in the Mexican inventory and the SMOKE file that defines acceptable FIPS codes. Differences in the ordering of the Mexican state names between these two data sets led to some of the Mexican inventory sources being mislabeled in the SMOKE QA reports. The state codes in the inventory and spatial surrogate files for two Mexican states were changed to be consistent with the SMOKE country/state/county codes file.

2.4 On-Road Mobile Sources

On-road mobile-source emissions data for SMOKE consist of IDA-formatted emissions and vehicle activity inventory files, and ancillary data for allocating the inventories in space, time, and to the Carbon Bond-IV chemistry mechanism used in CMAQ and CAMx. This section describes where we obtained these data, how we modeled them, and the types of QA that we performed to ensure that SMOKE processed the data as expected.

2.4.1 Data Sources

The SMOKE processing for CENRAP included two approaches for processing on-road mobile sources depending on the source of the data provided. The first approach was to compute mobile emissions values prior to providing them to SMOKE; we call this the pre-computed emissions approach. The second approach was to provide SMOKE with VMT data, meteorology data, and MOBILE6 inputs, and let the SMOKE/MOBILE6 module compute the mobile emissions based on these data; we call this the VMT approach. These approaches are not mutually exclusive for a single SMOKE run; therefore, we performed single SMOKE runs in which both approaches were used as follows:

- Annual VMT for computing CO, NO_x, VOC, SO2, NH3 and PM using MOBILE6 for all CENRAP States.
- Pre-computed, seasonal MOBILE6-based emissions of all pollutants for the 13 WRAP states that included pre-speciated $PM_{2.5}$ data.
- Annual VMT for computing CO, NO_x, VOC, SO2, NH3 and PM using MOBILE6 for the rest of the United States (VISTAS, MRPO and MANE-VU).
- Pre-computed, annual 1999 emissions of all pollutants for Mexico.
- Pre-computed, annual 2000 emissions of all pollutants for Canada.

For the CENRAP states, STI provided VMT data and MOBILE6 input files for all counties in the CENRAP region (Reid et al., 2004a). MOBILE6 input files were provided only for the months of January and July for 2002. MOBILE6 input files for the remaining months of 2002 had to be generated. These data were then processed within SMOKE. Using one set of MOBILE6 input files for each county in the CENRAP states resulted in compute memory requirements that were to large to process all CENRAP states together. Therefore the on-road mobile processing for the CENRAP states was split into two groups for SMOKE processing. The resulting gridded emissions data files were then merged together to obtain an on-road mobile source emissions file for the entire CENRAP region.

For the WRAP states we used actual 2002 data split into California and non-California seasonal inventories that were provided by the WRAP (Pollack et al., 2006). In addition to the standard criteria pollutants, these files contained pre-speciated $PM_{2.5}$ emissions. For the rest of the U.S. we used annual county-level activity and speed inventories with monthly, county-level MOBILE6 inputs, and hourly meteorology to estimate the hourly emissions with the SMOKE/MOBILE6 module. For the non-U.S. inventories, we used version 2 of the year 2000 Canadian inventory and the updated 1999 Mexican inventory pre-computed mobile source emissions.

2.4.2 Emissions Processing

For the Typ02G emissions modeling we configured SMOKE to process the annual on-road mobile emissions inventory data for the WRAP, Canada, and Mexico as pre-computed inventories. For the non-WRAP states, we used the SMOKE/MOBILE6 integration to process the annual activity inventories and monthly, county-based roadway information. The WRAP inventories contained pre-computed speciated PM emissions (Pollack et al, 2006) so the SMOKE PM speciation module was not used. The WRAP on-road mobile inventories were developed to represent seven-day (weekly) average emissions (as compared to the area source inventory, which represented average weekday emissions). As actual weekly average emissions, we configured SMOKE to process the WRAP on-road mobile source emissions by setting WKDAY_NORMALIZE to "No" in which case the emissions are adjusted to represent weekday and Saturday and Sunday emissions (as in contrast to the area sources where the emissions are just adjusted for Saturday and Sunday). We also assumed that all of the VOC emissions in the inventories are ROG and used SMOKE to convert the VOC to TOG before converting the emissions into CB-IV speciation for the air quality models. We configured SMOKE to create day-of-week specific rather than MWSS, temporal profiles because the WRAP on-road mobile temporal profiles contain weekly profiles that vary across the weekdays.

As noted previously, the large number of county roadway inputs for MOBILE6 processed for the non-WRAP portion of the U.S. required us to split the states mobile-source processing into three subsets because of computer memory limitations. Separate MOBILE6 input files were used for each separate county for CENRAP states, where as one MOBILE6 input file was used for several counties outside of the CENRAP region. The three subsets consisted of two sets of SMOKE/MOBILE6 simulations for the CENRAP and a simulation that computed on-road mobile emissions for the MRPO, VISTAS, and MANE-VU states. We configured MOBILE6 to use weekly temperature averaging for computing these emissions within SMOKE.

To QA the on-road mobile emissions, we used the CENRAP emissions modeling QA protocol (Morris and Tonnesen, 2004; Morris et al., 2004a) and a suite of graphical summaries. We used tabulated summaries of the input data and SMOKE script settings to document the data and configuration of SMOKE for simulations Typ02G and Base18G. The graphical QA summaries include, for all emissions output species, daily spatial plots, daily time-series plots, and annual time-series plots. These graphics are available at http://pah.cert.ucr.edu/aqm/cenrap/qa_base02b36.shtml#mb

2.4.3 Uncertainties and Recommendations

We approached the on-road mobile emissions preparation for simulation Typ02G from three different directions, which were based on the form of the input inventories and ancillary emissions data for different regions of the modeling domain:

- The WRAP region used emissions estimates pre-computed with EMFAC for California and MOBILE6 for the rest of WRAP states and processed like area sources with SMOKE adjusted from weekly to day-of-week emissions.
- The CENRAP, VISTAS, MRPO, and MANE-VU states used county-level activity data to compute emissions with the SMOKE/MOBILE6 module.

- The non-U.S. parts of the domain also had pre-computer on-road mobile source emissions so used an area-source approach for processing with SMOKE.

Different approaches for modeling a single emissions sector adds complexity and additional sources of error and inconsistencies to the modeling because of the different assumptions that went into the preparation of the input data. For example, refueling emissions from the on-road mobile sector are represented in the WRAP area-source sector but are computed with MOBILE6 for the rest of the U.S. Not using MOBILE6-based emissions for the non-U.S. portion of the domain neglects the effects of the actual 2002 meteorology on these emissions. Applying MOBILE6 outside of the U.S. is currently not possible because MOBILE6 is instrumented only for calculating emissions for the U.S. automotive fleet. The result of using MOBILE6 to calculate U.S. emissions and not using it to calculate the non-U.S. on-road mobile emissions estimates is that the non-U.S. emissions are not specific to this modeling year and the 2002 meteorological conditions, whereas the U.S. emissions are 2002-specific.

While we used the best available information to compute the on-road mobile emissions for the various portions of the modeling domain, inconsistent approaches for representing these emissions may lead to unnatural emissions gradients along political boundaries. We recommend for future work a unified approach for at least the U.S. inventories, where either we use MOBILE6 in SMOKE for the entire domain (or alternative emissions model such as CONCEPT), or we calculate the emissions with MOBILE6 outside of SMOKE and then use the resulting county-based emissions inventories.

2.5 Non-Road Mobile Sources

Non-road mobile source emissions data for SMOKE consist of annual, seasonal, and monthly IDA-formatted emission inventory files and ancillary data for allocating the inventories in space, time, and to the Carbon Bond-IV chemistry mechanism used in CMAQ and CAMx. This section describes where we obtained these data, how we modeled them, and the types of QA that we performed to ensure that SMOKE processed the data as expected.

2.5.1 Data Sources

The non-road mobile-source inventories in the Typ02G and Base18G emissions modeling used actual 2002 data developed by the RPOs for the U.S., version 2 of the year 2000 Canadian inventory and the improved 1999 Mexican inventory. The U.S. inventories consisted of annual, seasonal, and monthly inventories; the non-U.S. inventories were annual data. Pechan provided the CENRAP inventories divided between annual data for aircraft, locomotive, and commercial marine and annual files for all other non-road sources (Pechan and CEP, 2005e). Minnesota substituted the monthly MRPO Base K non-road inventory for the CENRAP inventory in their state. Iowa substituted the monthly estimates for non-road agricultural sources from the MRPO base K inventory for the CENRAP inventory. Texas provided estimates for 2002 non-road emissions in lieu of the CENRAP prepared inventory. WRAP provided non-road inventories divided between California and non-California seasonal inventories, further subdivided into aircraft, locomotives, shipping, and all other non-road mobile sources (Pollack et al., 2006). Note that the California Air Resources Board uses their own OFFROAD model for California non-

road emissions, whereas the EPA NONROAD model is used for the rest of the states (with the exception of locomotives, aircraft and shipping). With these data WRAP also provided temporal adjustments to apply to the inventories to split them between weekday and weekend emissions. We used these weekday/weekend splits to derive new weekly temporal profiles for the WRAP sources. The MRPO base K monthly non-road inventories were obtained from MRPO in NIF format and were converted to SMOKE format by Wendy Vit of the Missouri DNR. The VISTAS Base G and MANE-VU non-road mobile inventories consisted of annual county-level data (Pechan and CEP, 2005c). We received these inventories directly from the respective RPO inventory representatives. We received the Canadian 2000 inventory version 2 from the U.S. EPA EFIG (EPA, 2005d). For Mexico we used the improved 1999 inventory available at http://www.epa.gov/ttn/chief/net/mexico.html.

Along with adding the WRAP weekday/weekend emissions splits to the temporal allocation files, we also created temporal input files that apply a flat, uniform monthly profile to the monthly and seasonal non-road inventories. With the monthly and seasonal variability inherent in these inventories, we avoided applying redundant monthly profiles by splitting the inventories into seasonal/monthly and annual data. We applied the uniform monthly temporal profiles to the seasonal/monthly inventories and non-uniform monthly temporal profiles to the annual inventories. How the non-road emissions inventory data were split into those with monthly/seasonal emission and those with annual emissions is provided in Table 2-13.

Table 2-13. Non-road mobile-source inventory temporal configuration.

Region	Source	Temporal Coverage
WRAP (non-CA)	Non-road mobile	Seasonal
WRAP (CA)	Non-road mobile	Seasonal
WRAP	Aircraft	Seasonal
WRAP	Locomotive	Annual
WRAP	In-port and near-shore shipping	Annual
CENRAP	All non-road	Annual
CENRAP, IA	Non road Ag.	Monthly
VISTAS	All non-road	Annual
MRPO and MN	All non-road	Monthly
MANE-VU	All non-road	Annual
Canada	All non-road	Annual
Mexico	All non-road	Annual

Iowa elected to use the CENRAP-sponsored inventory for all of the non-road categories except for the agricultural equipment categories provided in Table 2-14. For these agricultural equipment categories, Iowa elected to use the Midwest RPO Base K inventory because this inventory provided improvements to the temporal allocation of emissions for the agricultural sector. The Base K inventory includes monthly emissions. The monthly emissions are used in the SMOKE IDA files for modeling.

Table 2-14. Non-road agricultural emissions categories where the MRPO Base K inventory was used instead of the CENRAP inventory in Iowa.

SCC	SCC Description
22600050xx	Off-highway Vehicle Gasoline, 2-Stroke: Agricultural Equipment (2 SCCs);
22650050xx	Off-highway Vehicle Gasoline, 4-Stroke: Agricultural Equipment (11 SCCs);
22670050xx	LPG : Agricultural Equipment (3 SCCs);
22680050xx	CNG : Agricultural Equipment (3 SCCs); and
22700050xx	Off-highway Vehicle Diesel : Agricultural Equipment (11 SCCs).

Texas provided annual and daily emissions for CO, CO_2, NO_x, VOC, SO_2, PM10-FIL, and PM25-FIL for several oil and gas field equipment non-road categories (Table 2-15). Texas provided authorization to change the pollutant codes from PM10-FIL to PM10-PRI and PM25-FIL to PM25-PRI.

Table 2-15. Non-road oil and gas development equipment categories that Texas provided emissions to be used instead of the CENRAP inventory.

SCC	SCC Description
2265010010	Off-highway Vehicle Gasoline, 4-Stroke : Industrial Equipment: Other Oil Field Equipment;
2268010010	CNG : Industrial Equipment : Other Oil Field Equipment; and
2270010010	Off-highway Vehicle Diesel : Industrial Equipment : Other Oil Field Equipment

Lancaster County Nebraska provided its own non-road inventory for SCC 2260000000 (Off-highway Vehicle Gasoline, 2-Stroke : 2-Stroke Gasoline except Rail and Marine: All). The CENRAP-sponsored inventories for SCCs starting with 226 in Lancaster County were removed to correct double-counting of emissions. This adjustment was made by Pechan for Base02b modeling.

2.5.2 Emissions Processing

We configured SMOKE to process all of the non-road mobile emissions inventory data as area-like inventories using spatial surrogates to grid the county-level emissions. As the WRAP inventories contained pre-computed PM emissions, we did not have to use SMOKE to compute coarse mass PM (PMC). The WRAP non-road mobile inventories represented seven-day average emissions (different from the area inventory, which represented weekday average emissions). As actual weekly average emissions, we configured SMOKE to process them by setting WKDAY_NORMALIZE to "No." For the rest of the non-road mobile inventories we processed the data as weekday average data by setting WKDAY_NORMALIZE to "Yes." We also assumed that all of the VOC emissions in the inventories are ROG and used SMOKE to convert the VOC to TOG before converting the emissions into CB-IV speciation for the air quality models. We configured SMOKE to create MWSS temporal intermediates rather than daily temporal files because the non-road mobile sources do not use weekly temporal profiles that vary across the weekdays, but do have very different emissions on weekdays versus weekend days.

We divided the non-road mobile emissions modeling based on whether the data were annual or seasonal/monthly inventories. This split facilitated the application of uniform monthly temporal profiles to the seasonal/monthly inventories. After processing the non-road emissions as two separate categories, non-road yearly and non-road monthly, we combined them with the rest of the emissions sectors to create model-ready emissions for CMAQ and CAMx.
To QA the non-road mobile emissions we used the procedures in the CENRAP emissions modeling QAPP (Morris and Tonnesen, 2004) and Modeling Protocol (Morris et al., 2004a) and a suite of graphical summaries. We used tabulated summaries of the input data and SMOKE script settings to document the data and configuration of SMOKE for simulations. The graphical QA summaries include, for all emissions output species, daily spatial plots, daily time-series plots, and annual time-series plots. These QA graphics are available at
http://pah.cert.ucr.edu/aqm/cenrap/qa_base02f36.shtml#nr

2.5.3 Uncertainties and Recommendations

We prepared non-road mobile emissions using a combination of inventories having different temporal resolutions and various forms of ancillary data. These different combinations of information may lead to inconsistencies in how these emissions are represented across the modeling domain. In addition, the Canadian inventories contain only province-level information and thus have low-resolution spatial and temporal profiles applied to them. The Mexican non-road emissions are deficient in the number of different SCCs contained in the inventory and the availability of spatial surrogates that are applicable to non-road mobile sources. Improvements to the temporal profiles and spatial surrogates could provide a more consistent approach to representing the non-road emissions across the entire modeling domain.

2.6 Biogenic Sources

Biogenic emissions data for SMOKE consist of input files to the BEIS3 model (EPA, 2004a). BEIS3 is a system integrated into SMOKE for deriving emissions estimates of biogenic gas-phase pollutants from land use information, emissions factors for different plant species, and hourly, gridded meteorology data. The results of BEIS3 modeling are hourly, gridded emissions fluxes formatted for input to CMAQ or CAMx. This section describes the sources of the BEIS3 input data that we used for the Typ02G and Base18G emissions, how we modeled these data and the types of QA that were performed to ensure that SMOKE processed the data as expected.

2.6.1 Data Sources

The BELD3 land use data and biogenic emissions factors that were developed during the WRAP preliminary 2002 modeling were used for the CENRAP biogenic emissions modeling (Tonnesen et al., 2005). These data included BELD3 1-km resolution land use estimates and version 0.98 of the BELD emissions factors. Since the WRAP and CENRAP use the same 36 km Inter-RPO continental U.S. modeling domain, CENRAP was able to leverage of the WRAP work performed previously.

2.6.2 Emissions Processing

We used BEIS3.12 integrated in SMOKE to prepare emissions for the simulations. Most of the preparation for the biogenic emissions processing was completed during the preliminary 2002 modeling (Morris et al., 2005). As the modeling domains did not change from the preliminary 2002 to the final modeling, we re-used the gridded land use data and vegetation emissions factors that we prepared for the preliminary simulations.

To QA the biogenic emissions, we used the CENRAP emissions modeling QAPP (Morris and Tonnesen, 2004) and Modeling Protocol (Morris et al., 2004a) and a suite of graphical summaries. We used tabulated summaries of the input data and SMOKE script settings to document the data and configuration of SMOKE for simulation Base02b. The graphical QA summaries include, for all emissions output species, daily spatial plots, daily time-series plots, and annual time-series plots. These QA graphics are available at http://pah.cert.ucr.edu/aqm/cenrap/qa_base02b36.shtml#b3

2.6.3 Uncertainties and Recommendations

The use of newer versions of BEIS (BEIS3.13) and the new MEGAN biogenic emissions models should be considered in future modeling.

2.7 Fire Emissions

Fire emissions data for SMOKE have traditionally been represented as county-level area-source inventories that were placed in only the first vertical model layer. We advanced the representation of fire emissions for air quality modeling by preparing portions of the inventory data as point sources with specific latitude-longitude coordinates for each fire centroid and pre-computed plume rise parameters that were derived from individual fire characteristics. These new inventories were based on the fire data products prepared by a CENRAP emission contractor (Reid et al., 2004b) and modified by the project team to be properly modeled as point sources. These data consist of annual, daily, and hourly IDA-formatted emissions inventory files and ancillary data for allocating the inventories in space, time, and to the Carbon Bond-IV chemistry mechanism used in CMAQ and CAMx. This section describes where we obtained these data, how we modeled them, and the types of QA performed to ensure that SMOKE processed the fire emissions data as expected.

2.7.1 Data Sources

The fire inventories in the Typ02G emissions inventory were held constant through Base18G. We used actual 2002 fire data developed by the RPOs for the U.S., version 2 of the year 2000 Canadian inventory fire data, and actual 2002 fire data for Ontario, Canada. The inventories used consisted of both area and point source data for the U.S., Canada, and Mexico. Sonoma Technology, Inc. provided the fire emissions for the CENRAP states (Reid et al., 2004b). Air Sciences provided us with the WRAP inventories divided among six different fire categories: wildfires, agricultural fires, wildland fire use, natural prescribed, anthropogenic prescribed, and non-Federal rangeland fires (Air Sciences, 2007a). These inventories consisted of annual, daily, and hourly IDA-formatted files with information on daily emissions totals and hourly plume characteristics for each fire. We received similar fire emission inventories for the other RPOS (Air Sciences, 2007b). We modeled these sources with the rest of the stationary-area-source sector.

CENRAP received data for 54 fires that occurred in Ontario during the year 2002. Information on the data code abbreviations, data definitions, and data units used in the raw data files was obtained from Mr. Rob Luik (Data Management Specialist) at the Ontario Ministry of Natural Resources (Rob.Luik@MNR. gov.on.ca). Emissions for each fire were estimated using the Emission Production Model (EPM)/CONSUME within the BlueSky framework. A fire identification code is needed to track individual fires throughout the processing. The unique fire identification code was created for each fire by concatenating the FIRE_NUMBER and CUR_DIST fields of the original data. The fire identification code also contains the FIPS code of the fire; this information is not used by BlueSky but is needed by BlueSky2Inv, the utility program that converts the BlueSky output to the SMOKE inventory format. The FIPS code 135000 was used for all fires with longitudes east of –90°, and FIPS code 135059 was used for

fires west of –90°. These FIPS codes were used to ensure that the fires would be assigned the correct time zones in later SMOKE processing. Some of the dates provided in the original data included hourly information. In all cases, the hourly information was not used leaving all data at a daily resolution.

2.7.2 Emissions Processing

SMOKE is instrumented to distribute point-source-formatted fire inventories to the vertical model layers either by using a pre-computed plume rise approach or by computing the plume rise dynamically using actual 2002 meteorology. We applied both approaches for modeling point-source fire emissions in simulation Typ02G. For the pre-computed plume rise approach, SMOKE reads an annual inventory file with information on fire locations, a daily inventory file with daily emission totals for each fire, and an hourly inventory file with hourly plume bottom, plume top, and layer 1 fractions for each fire. SMOKE uses this information to locate the fires on the horizontal model grid and to distribute the plume of each fire vertically to the model layers. Because some of these fires have plumes that reach the model top, we set the number of emissions layers for processing these inventories to the full 19 layers of the meteorology. We applied this approach to the point-source fires for the WRAP, CENRAP and VISTAS regions.
The alternative plume rise approach uses information on fuel loading and the heat flux of the fires to distribute the fires vertically to the model layers. The data are provided to SMOKE in the form of an annual inventory with information on fire locations and a daily inventory with daily emission totals for each fire, daily heat flux, and daily fuel loading. We applied this approach to the point-source fires for Ontario, Canada.

All of the point-source fires used diurnal temporal profiles and speciation profiles for VOC and $PM_{2.5}$ developed by Air Sciences (2007a) during the preliminary 2002 modeling (Morris et al., 2005).

We modeled the area-source fires for U.S. and Canada as standard stationary area sources. We applied monthly temporal profiles provided by RPOs, flat weekly temporal profiles, and the diurnal profiles developed by Air Sciences for WRAP fires (Air Sciences, 2007a), and for the rest of the RPOs we used diurnal profiles that were provided by them (Air Sciences, 2007b). We used the forestland area surrogate to distribute these emissions from the county or province level in the inventories to the model grid cells.

To QA the fire emissions, we used the procedure in the CENRAP emissions modeling QA protocol (Environ, 2004) and a suite of graphical summaries. We used tabulated summaries of the input data and SMOKE script settings to document the data and configuration of SMOKE for simulation Typ02G. The graphical QA summaries include, for all emissions output species, daily spatial plots, daily time-series plots, annual time-series plots, and vertical profiles. These QA graphics are available at: http://pah.cert.ucr.edu/aqm/cenrap/qa_typ02g36.shtml.

2.7.3 Uncertainties and Recommendations

We used forestland spatial surrogates to distribute these county level (province level for Canada) data to the model grid. Using spatial surrogates to locate fires is a crude approach that results in the artificial smearing of the emissions over too large an area. This issue can be remedied by

moving to a point-source approach for representing these fires, similar to the approach used by Air Sciences for preparing the WRAP fire inventories.

2.8 Dust Emissions

Dust emissions data for SMOKE have traditionally taken the form of county-level stationary-area-source inventories. As these emissions are correlated to meteorology, land use, and vegetative cover, we made several changes to how dust emissions are simulated by SMOKE to take these parameters into consideration. This section describes where we obtained data for windblown, fugitive, and road dust sources, how we modeled them, and the types of QA performed to ensure that SMOKE processed the data as expected.

2.8.1 Data Sources

For the fugitive dust and road dust inventories in the Typ02G emission scenario, we used actual 2002 data developed by the RPOs for the U.S., version 2 of the year 2000 Canadian inventory, and the BRAVO 1999 Mexican inventory. We extracted the fugitive dust inventories from the stationary-area inventories for each of the RPOs, Mexico, and Canada. Before modeling these data we further divided them into construction/mining sources and agricultural sources. We defined the fugitive dust sources in the Base02f modeling based on guidance provided by EPA (2004b). WRAP provide road dust emission inventories (Pollack et al., 2006). For the rest of the RPOs and Canada, we extracted the road dust SCCs from the stationary-area-source inventories. The BRAVO 1999 Mexico inventory did not contain any road dust SCCs. Table 2-16 lists the SCCs for the various fugitive and road dust sources that we modeled in the Base02f and Typ02G inventories. We applied near-source capture transport factors that are based on county-level vegetative cover to the fugitive and road dust inventories to prepare them for input to the air quality models.

For windblown dust, we used gridded emissions prepared outside of SMOKE using a land use and meteorology-based model developed under funding from the WRAP by ENVIRON and UC-Riverside (Mansell, 2005; Mansell et al., 2005).

Table 2-16. Fugitive and road dust SCCs.

Dust Category	SCCs
Fugitive dust (construction and mining)	2275085000, 2311000000, 2311010000, 2311010070, 2311020000, 2311030000, 2325000000, 2305070000, 2530000020, 2530000100, 2530000120
Fugitive dust (agricultural)	2801000003, 2801000005, 2801000008, 2805001000
Road dust	2294000000, 2296000000

2.8.2 Emissions Processing

We modeled the fugitive and road dust inventories through SMOKE using an area-source approach. We modeled these data on the assumption that they represented weekday, rather than seven-day week, emissions and thus used the SMOKE setting WKDAY_NORMALIZE to convert the data to a seven-day average. We configured SMOKE to compute PMC during the

processing as (PM_{10} - $PM_{2.5}$). Usually the records with dust do not include any other pollutants such as VOC, and NOx. For the few records that did include pollutants other than the PM we

split the records where the PMs processed with dust and the non PMs processed with the area. We configured SMOKE to create MWSS temporal intermediates rather than daily temporal files because the dust sources do not use weekly temporal profiles that vary across the weekdays.
As noted above, we used SMOKE to apply near-source transport factors to the raw fugitive and road dust inventories to prepare them for input to the air quality models. We used U.S. transport factors from work done by Pace (2005) and a 2001 land use/land cover database to develop a SMOKE input file of county and SCC-based transport factors for the U.S., Canada, and Mexico. We applied these factors to create a new set of inventories adjusted for these transport factors for all regions except VISTAS; the VISTAS dust sources that we received already had the transport factors applied to them.

We calculated the windblown dust emissions outside of SMOKE using an internally developed, process-based model. By "process-based" we refer to an emissions model that integrates information about the processes that lead to the emissions of interest, in this case windblown dust. The process-based windblown dust model developed by the WRAP considers wind speeds, precipitation history, and soil types to derive gridded dust fluxes resulting from wind disturbances for the modeling domain. More information on this model, its modes of operation, and the configuration used for simulation Base02a are available in Mansell et al. (2005).
To QA the fire emissions, we used the procedures in the CENRAP emissions modeling QAPP (Morris and Tonnesen, 2004) and Modeling Protocol (Morris et al., 2004a) and a suite of graphical summaries. We used tabulated summaries of the input data and SMOKE script settings to document the data and configuration of SMOKE for Base02f emissions. The graphical QA summaries include, for all emissions output species, daily spatial plots, daily time-series plots, and annual time-series plots. These QA graphics are available at http://pah.cert.ucr.edu/aqm/cenrap/qa_base02f36.shtml#fd for fugitive dust, http://pah.cert.ucr.edu/aqm/cenrap/qa_base02f36.shtml#rd for road dust, and http://pah.cert.ucr.edu/aqm/cenrap/qa_base02b36.shtml#wbd for windblown dust.

2.8.3 Uncertainties and Recommendations

There are several improvements that should be made to the dust emissions modeling in future simulations. We will expand the list of fugitive dust SCCs that we extract from the stationary-area-source inventories for application of transport factors. This expanded list is based on recent work by EPA (2004b). We will also explore improvements to the assumptions that we used for generating emissions with the WRAP windblown dust model. Areas of improvement in the windblown dust model include refinements to the land use data and soil characteristics, additional information about agricultural activities in the WRAP and CENRAP regions, detailed model evaluation on targeted windblown dust case studies, and the application of snow-cover and vegetative transport factors to these emissions (Mansell et al., 2005).

2.9 Ammonia Emissions

Ammonia (NH_3) emissions from agricultural activities are a major source of ammonia and are dependent on many different environmental parameters, such as meteorology, crop and soil

types, and land use. CENRAP developed NH_3 emissions for the CENRAP states (Pechan and CEP, 2005e). Ammonia emissions were estimated for 13 source categories using the Carnegie Mellon University (CMU) model and supplemental technical work; 80% of technical work was dedicated to improving emissions estimates for two source categories—livestock production and fertilizer use. For these two categories, as well as biogenic sources, improvements were made to the activity data and/or emission factors used by the CMU model. For four other source categories (industrial point sources, landfills, ammonia refrigeration, and non-road mobile sources), emissions estimates were prepared independently of the CMU model, and for the remaining six source categories (publicly owned treatment works, wildfires, domestic animals, wild animals, human respiration, and on-road mobile sources), emissions estimates were derived by running the CMU model with no alterations.

CENRAP NH_3 model emissions estimates were combined with data provided by the other RPOs to represent agricultural NH_3 emissions in simulations Typ02G and Base18G.

2.9.1 Data Sources

The WRAP provided NH_3 emissions using the WRAP NH_3 model (Mansell et al, 2005) that generated emissions for the following sectors: domestic sources, wild animals, fertilizers, soils, and livestock. MWRPO provided monthly IDA-formatted inventories reflective of base K to CENRAP that they produced from process-based models of their own, along with temporal profiles and spatial cross-reference information for these sources. Iowa elected to use the MWRPO estimates of NH_3 emissions for fertilizer application, livestock, and wastewater treatment or SCC 28017XXXXX, 28050XXXXX, and 2630020000 respectively. Minnesota reviewed the MWRPO inventory and chose to move forward with the CENRAP developed data set. The rest of the U.S., Canada, and Mexico had agricultural NH_3 emissions contained within their annual stationary-area-source inventories.

2.9.2 Emissions Processing

The WRAP NH_3 emissions were processed outside of SMOKE using the WRAP NH_3 model and provided to CENRAP as gridded, hourly emissions in network common data form (NetCDF) files. CENRAP and MWRPO provided monthly IDA-formatted, county-level NH_3 inventories that were developed separately with process-based models. We modeled these emissions like area sources with SMOKE, applying the temporal profiles and the spatial cross-referencing developed for CENRAP that we received from the MWRPO. The agricultural NH_3 emissions for the rest of the RPOs, Canada, and Mexico are contained within their stationary-area inventories. We applied the SMOKE default temporal profiles and spatial surrogates to all non-process-based NH_3 emissions.

To QA the NH_3 emissions, we used the procedures in the CENRAP modeling QAPP (Morris and Tonnesen, 2004) and Modeling Protocol (Morris et al., 2004a) and a suite of graphical summaries. We used tabulated summaries of the input data and SMOKE script settings to document the data and configuration of SMOKE for simulations Typ02G and Base18G. The graphical QA summaries include, for all emissions output species, daily spatial plots, daily time-series plots, and annual time-series plots. These QA graphics are available at http://pah.cert.ucr.edu/aqm/cenrap/index.shtml

2.9.3 Uncertainties and Recommendations

Like the other emissions categories that have traditionally been represented as stationary area sources, the agricultural NH_3 emissions sector is affected by interregional inconsistencies in the way these emissions are represented.

During the QA of the Base02a emissions, the WRAP discovered a problem with their soil NH_3 estimates. The emission factor for soil NH_3 that were used in developing these data produced too high an emission estimate from this sector. For simulations Base02B through Typ02G, we therefore removed the soil NH_3 sector completely from the WRAP domain. In future simulations we will include these emissions with a revised emission factor for NH_3 emissions from soils.

2.10 Oil and Gas Emissions

Emissions from oil and gas development activities have been poorly characterized in the past. Simulations These emissions have been sporadically reported by some states in their stationary-area-source inventories, but for the most part were missing from our preliminary modeling. In the Typ02G and Base18G simulations, significant effort was made to better represent oil and gas production emissions explicitly as both area and point sources.

2.10.1 Data Sources

Emissions from oil and gas production activities for the CENRAP states were included with the other CENRAP state emission source categories (Pechan and CEP, 2005e). We received oil and gas production emissions inventories for the WRAP states and for tribal lands in the WRAP region as stationary-area-source and stationary-point-source IDA-formatted inventories. ERG, Inc. provided the point-source inventories with the rest of the stationary-point data (ERG, 2006a). ENVIRON provided the area-source oil and gas inventories for non-CA WRAP states and for tribal lands in the WRAP region, along with spatial surrogates for allocating these data to the model grid (Russell and Pollack. 2005). Oil and gas production emissions data for outside of the WRAP region are contained in the stationary-area inventories.

2.10.2 Emissions Processing

We modeled the WRAP point-source oil and gas production emissions in combination with the rest of the stationary-point-source emissions. We modeled the WRAP area-source oil and gas production emissions explicitly as a separate category that included WRAP and tribal inventories. These data represent weekly average emissions and did not require any renormalization within SMOKE. We used spatial surrogates generated by ENVIRON to allocate these annual county-level emissions to the model grid. For all oil and gas emissions, we applied flat temporal profiles to create hourly inputs to CMAQ and CAMx.

2.10.3 Uncertainties and Recommendations

In future 2002 modeling California oil and gas production emissions should be replaced with revised data provided by the California Air Resources Board (CARB). In addition, WRAP has

updated their oil and gas production inventory for the base and future years in a Phase II work effort that substantially improved the emissions inventory estimates (Bar-Ilan et al., 2007).

2.11 MMS Off-shore Gulf of Mexico Emissions

Offshore area point source emissions include emissions in the Gulf of Mexico and off the coast of California that are associated with oil and gas drilling platforms.

2.11.1 Data Sources

We obtained year 2000 IDA-formatted point-source inventories for oil and gas platforms in the Gulf of Mexico from the Minerals Management Service (MMS) web site: http://www.gomr.mms.gov/homepg/regulate/environ/airquality/gulfwide_emission_inventory/2000GulfwideEmissionInventory.html

We combined these with point-source data for coastal California provided to us by CARB during the preliminary 2002 modeling. We also obtained gridded area source emissions for platforms in the Gulf of Mexico from the MMS that we converted to the CENRAP 36-km model grid.

The 2000 MMS Gulf wide Emission Inventory was updated as of June 2006 to account for a change in vessel emissions in the non-point source (non-platform) database file. The point source (platform) emission inventory database file has not changed from the original version. Area source emissions from offshore activities in the Gulf of Mexico were developed from the latest estimates provided by the Minerals Management Service (MMS). The MMS inventory includes both platform and non-platform sources. The non-platform area source emissions estimates are spatially allocated to lease blocks and protraction units throughout the Gulf of Mexico. Temporal and spatial allocation cross-reference data were developed from the MMS inventory data and formatted for input to the SMOKE emissions model by Carolina Environmental Programs. These data were provided to the CENRAP emissions modeling team for implementation within SMOKE. The spatial allocation surrogates were provided for 4-km grid cells. The UCR team used these surrogates and developed surrogates for 36-km grid cells. Because these data are references to lease blocks/protraction units, rather than counties, this source category was processed separately form all other emissions using a customized reference data and SMOKE run scripts.

We modeled the offshore point and area sources as separate categories in the simulations. We used SMOKE to locate the offshore point sources on the model grid and to vertically allocate them into 15 model layers.

To QA the offshore platform emissions, we used the procedures in the CENRAP modeling QAPP (Morris and Tonnesen, 2004) and Modeling Protocol (Morris et al., 20042) and a suite of graphical summaries. We used tabulated summaries of the input data and SMOKE script settings to document the data and configuration of SMOKE for simulation Base02a. The graphical QA summaries include, for all emissions output species, daily spatial plots, daily time-series plots, and annual time-series plots. These QA graphics are available at http://pah.cert.ucr.edu/aqm/cenrap/index.shtml for the point and area sources.

2.11.2 Uncertainties and Recommendations

While the MMS data that we used were an improvement over previously modeled Gulf of Mexico platform inventories, the data were developed for a different modeling application that covered only the extreme northwestern portion of the Gulf, so they are missing large areas of the region of the Gulf that contain drilling platforms. The California offshore inventory represents an initial attempt at compiling an emission inventory for this area and contains very few sources. Future simulations will focus on improving these emissions by expanding the coverage of the offshore platform inventories for both the Gulf of Mexico and the Pacific Coast.

2.12 Off-shore Shipping Emissions

Emission inventory development for regional- and continental-scale air quality modeling has historically neglected offshore emissions sources beyond 25 miles offshore. Concern over the environmental effects of commercial shipping emissions in the Pacific on the coastal states in the WRAP region led to the development of a commercial marine shipping inventory for the Pacific. This inventory of off-shore marine vessels emissions made a substantial difference in some of the coastal western PM estimates (e.g., SO4). VISTAS developed an off-shore marine vessels inventory for the entire modeling domain that included the Pacific and Atlantic Oceans and the Gulf Of Mexico. For Typ02G and Base18G emission inventories CENRAP adopted the offshore shipping inventories developed by VISTAS.

2.12.1 Data Sources

Initially we obtained gridded annual commercial marine shipping emissions for the Pacific on the 36-km model grid from WRAP for inclusion in CENRAP simulations in the Base F modeling (Pollack et al., 2006). The commercial marine inventory contains all of the criteria pollutants contained in the non-road mobile-source inventory: CO, NO_x, VOC, NH_3, SO_2, PM_{10}, and $PM_{2.5}$. This inventory was subsequently updated in the Typ02G and Base18G modeling with the VISTAS off-shore commercial marine emissions inventory that covered the Gulf of Mexico and the Atlantic and Pacific Oceans and was based on the EPA/ARB SOx Emissions Control Area (SECA) program. Dr. James Corbett (University of Delaware) analyzed off-shore marine vessel data and worked with ENVIRON/ICF to convert to gridded emissions for the SECA grid. ENVIRON then provided SO_2, NO_X, PM and VOC emissions for the RPO 36-km grid.

2.12.2 Emissions Processing

The commercial marine shipping inventory was not processed through SMOKE. VISTAS provided the data to the as gridded text files on the 36-km model grid. These data were reformatted to the NetCDF CMAQ input format with a utility developed by UCR. The VOC inventory was converted to CB-IV speciation and the NO_x and $PM_{2.5}$ inventory pollutants to CMAQ input species with SMOKE chemical profiles for commercial shipping sources. No temporal adjustments were applied to these emissions; they use uniform monthly, daily, and diurnal profiles. An SCC for commercial marine vessels within the MMS inventory (SCC CM80002200) was accounted for in the commercial marine inventory developed for VISTAS. The duplicate emissions were removed from the MMS inventory prior to processing emissions

for Base G simulations. The duplicated emissions amounted to 19,000 TPY of NO_X and 3,184 TPY of SO_2. For simulation Typ02G and Base18G we received binary netCDF file from ENVIRON for one day and that day was used for every day of the year.
To QA the commercial marine shipping emissions, we used the procedures in the CENRAP modeling QAPP (Morris and Tonnesen, 2004) and Modeling Protocol (Morris et al., 2004a) and a suite of graphical summaries. The graphical QA summaries include, for all emissions output species, daily spatial plots, daily time-series plots, and annual time-series plots. These QA graphics are available at http://pah.cert.ucr.edu/aqm/cenrap/index.shtml.

2.12.3 Uncertainties and Recommendations

As a first attempt at representing shipping emissions in the Pacific in international waters, the WRAP and VISTAS 2002 commercial shipping inventory is a breakthrough in a historically neglected emissions category. As the RPOs evaluate the effects of these emissions on the air quality modeling, we anticipate that there will be refinements to the temporal profiles and to the vertical allocation of the emissions. Many of the stacks of large commercial ships contained in this inventory extend vertically above the first model layer. Future versions of this inventory should use higher-resolution temporal adjustments and should allocate the emissions to the appropriate model layers. Off-shore marine shipping activity is projected to increase. However, there are also the potential for emission controls on this source category (e.g., SECA program). Given these two off setting activities, the 2002 off-shore marine shipping emissions were assumed to be unchanged going from 2002 to 2018. Better estimates of 2018 marine emissions are being developed that should be considered in future modeling activities.

2.13 2018 Growth and Control

Base18G was based on grown inventories assuming on-the-books control strategies. CENRAP contracted with Pechan to deliver growth and control data for CENRAP and to consolidate growth and control information for other RPOs where available (Pechan, 2005d). The data are applicable to all source categories and pollutants included in the CENRAP 2002 emission inventory. This includes the following pollutants: sulfur oxides (SO_x), oxides of nitrogen (NO_x), volatile organic compounds (VOC), carbon monoxide (CO), ammonia (NH_3), and primary PM_{10} and $PM_{2.5}$. Some source categories were held constant between 2002 and 2018 because either stagnant growth was deemed appropriate or insufficient data was available to adequately project future growth or controls. These source categories include the following:

- Wind Blown Dust from non-agricultural land use categories.
- Emissions from wildfires.
- Emissions from Mexico.
- Global transport sources (i.e., the 2002 GEOS-CHEM boundary conditions).

2.13.1 Data Sources

CENRAP contracted with Pechan to provide growth and control factors to be applied with SMOKE for the CENRAP region (Pechan, 2005d). These growth and control parameters were based on growth estimates derived from EGAS 5.0 and control estimates assumed for

implementation of federal regulations and on-the-books state and local control programs. Emissions projections for electric generating units were developed for the RPOs with the Integrated Planning Model (IPM). The RPO 2.1.9 IPM results were subsequently modified by VISTAS, MRPO and CENRAP to reflect planned new construction and controls. The WRAP provided 2018 EGU estimates developed in coordination with State and Industry stakeholders. VISTAS, MWRPO and the WRAP provided emissions for 2018, having applied growth and control factors outside of SMOKE processing. EPA provided SMOKE processed emissions, applying both growth and controls, for Canada for the year 2020. These emissions were provided on the RPO 36-km grid. However, emissions were inexplicably processed for an alternative vertical structure. Alpine Geophysics, under contract to VISTAS reallocated the emissions through the vertical layers to more accurately reflect the vertical structure applied uniformly by the RPOs. The modified data was obtained directly from Alpine Geophysics. Emissions from Mexico were held constant between the inventory year 1999 and modeled 2002 and 2018. Improvements to the Mexican inventory have been continuously made between generation of the original BRAVO inventory and the present improved 1999 inventory. However, given the continued uncertainties in the improved inventory, no future year projections where attempted by CENRAP.

2.13.2 Emissions Processing

Growth and control factors developed by Pechan (2005d) for Arkansas did not match the final delivered inventory for Arkansas. Arkansas underwent major revisions to point and facility IDs in mid-2005. These updates were not available by the delivery date of the growth and control parameters. In coordination with Arkansas, a cross-walk was developed to correct the point and facility IDs.

The assumptions that went into the development of controls for engines covered under the RICE MACT were not consistent with the final rule. Rule penetration values for CENRAP states were adjusted to more accurately reflect the impact of the final rule.

The impact of the refinery global settlements was not incorporated into CENRAP modeling until the base G simulations. Control assumptions provided by EPA and referenced in EPA CAIR modeling were applied to the 2018 inventory. These reductions primarily impacted SO_2 emissions; however, NO_X reductions were applied in Oklahoma, Louisiana, and Minnesota.

2.13.3 Uncertainties and Recommendations

The impact of control programs is an area of uncertainty that will need continued review as the programs are implemented. Development of growth and control assumptions for Mexico will be necessary for continued refinement of the impact of international transport. CENRAP obtained estimates of increased prescribed burn activity for the Forest Service after processing of the base G simulations was underway. These estimates of increased activity should be reviewed for inclusion in future simulations. EPA developed 2020 estimates of Canadian emissions are assumed to include erroneous stack parameters previously addressed in the 2000 emissions processing. Further review of this data set is recommended.

2.14 2018 Base G C1 Control Sensitivity

CENRAP conducted a control sensitivity evaluating the impact of point source reductions given a maximum dollar per ton control level. The intent of the control sensitivity was to generate information on the impact of possible control strategies in support of the consultation process. The strategies were grouped together under a common set of criteria and not specifically identified by the states. The results of the modeling were not intended to be prescriptive; instead, they were intended to be a starting point for control discussions that would require much greater refinement.

2.14.1 Data Sources

CENRAP contracted with Alpine Geophysics to provide an evaluation of possible additional controls for the 2018 CENRAP point source inventory. These controls were in addition to on-the-books and BART controls assumed in the development of Base18F and Base18G emission scenarios. Base18F IDA files were enhanced with additional information on base level controls. The enhanced dataset was then linked with the control data contained in the 2006 release of EPA's AirControlNet software. Alpine developed cost curves for NO_X and SO_2 in 2005 dollars for the Base18F CENRAP point source inventory. Staff from Iowa DNR and Kansas DHE worked in conjunction to add area of influence data (Alpine Geophysics, 2006) and distance calculations to each Class I area in CENRAP. A variety of dollar per ton control levels were evaluated. CENRAP elected to base the sensitivity on a maximum control cost of $5,000 per ton. This selection was made with the understanding that the cost data under-represented the true cost of retrofit controls and did not take in to consideration more recent market fluctuations impacting costs of controls and construction. CENRAP refined the selection by applying controls to only those sources that met the criteria that the ratio of their emissions in tons per year to their distance to any Class I area in kilometers be less than 5. This distance weighting criteria allowed the sensitivity to focus on those sources with the greatest impact. Additional controls for other RPOs were not considered in this evaluation.

2.14.2 Emissions Processing

Sources considered for control were removed from the IDA files. Growth and control assumptions were applied outside of SMOKE and delivered to UCR as 2018 emissions. Stack parameter changes as a result of additional controls were not considered in this analysis.

2.14.3 Uncertainties and Recommendations

Given uncertainties in control costs more refined analyses should include an evaluation of retrofit control costs under present values.

2.15 Emissions Summaries

Appendix B provides details on the source of the emission files used in the CENRAP Typ02G and Base18G modeling. Also in Appendix B are sample emission summary plots, additional plots are available on the CENREAP modeling website: http://pah.cert.ucr.edu/aqm/cenrap/emissions.shtml.

CENRAP has contracted with E.H. Pechan and Associates to provide emissions summaries used in the final Typ02G and Base18G modeling in Excel spreadsheets and in an Access database that are available on the CENRAP website (http://www.cenrap.org/projects.asp#). Figures 2-3 through 2-9 display the, respectively, SO2, NOx, VOC, PM2.5, PM10, NH3 and CO anthropogenic emissions for the CENRAP states and the Typ02G and Base18G emission scenarios. Emissions are broken down by major source sector. For the state of Texas the emissions are broken by three groups, northeast Texas, southeast Texas and remainder of Texas (west Texas).

For most states, EGUs are the largest contributor to SO2 emissions (Figure 2-3). As EGU SO2 emissions are generally projected to be reduced in the future, most states show a reduction in total SO2 emissions from 2002 to 2018. One exception to this is Louisiana for which non-EGU point source SO2 emissions are greater than for EGU and are projected to increase from 2002 to 2018. The reasons for these increases are unclear, but the growth factors for non-EGU points should be examined more carefully.

NOx emissions are fairly evenly distributed across non-EGU point, EGU point, non-road mobile, on-road mobile and area sources for the 2002 Typ02G emissions scenario (Figure 2-4). In 2018, the contributions of on-road mobile source NOx emissions is reduced dramatically, with some states also showing reductions in EGU NOx emissions as well, resulting in all states exhibiting lower NOx emissions in 2018 than 2002.

VOC emissions are dominated by area, non-road mobile, on-road mobile and non-EGU point sources in both 2002 and 2018 (Figure 2-5). VOC emissions from on-road and non-road mobile source are projected to go down in the future, whereas VOC emissions from non-EGU point and, especially, area sources are projected to increase. Thus, whether a state's total VOC emissions increase or decrease depends on the relative contributions of mobile versus area sources and the level of increase in area source VOC emissions. Note that the VOC emissions listed in Figure 2-5 do not include biogenic VOC emissions that would be greater than the anthropogenic VOC emissions shown in Figure 2-5. Note that because biogenic VOC emissions are processed using the SMOKE/BEIS module on the 36 km grid, state-wide biogenic VOC emissions summaries are not readily available.

Primary $PM_{2.5}$ emissions are primarily from road dust and fugitive dust, and for some states fires (Figure 2-6). Kansas, Oklahoma, Louisiana and Texas all have large contributions from fires not seen in the other states. Road dust and fugitive dust are the most dominate source categories for coarse particulate as well (Figure 2-7).

CENRAP developed a separate ammonia emissions for 13 categories using the CMU model including livestock and fertilizer that dominates the ammonia emissions across the CENRAP

states (Figure 2-8). Several states also have significant ammonia contributions from non-EGU point sources, whereas others do not.

CO emissions are dominated by the on-road and non-road mobile source sectors (Figure 2-9). However, states with fires also see large CO contributions from them as well. On-road mobile source CO emissions are projected to go down substantially from 2002 to 2018, whereas the other source categories are flat.

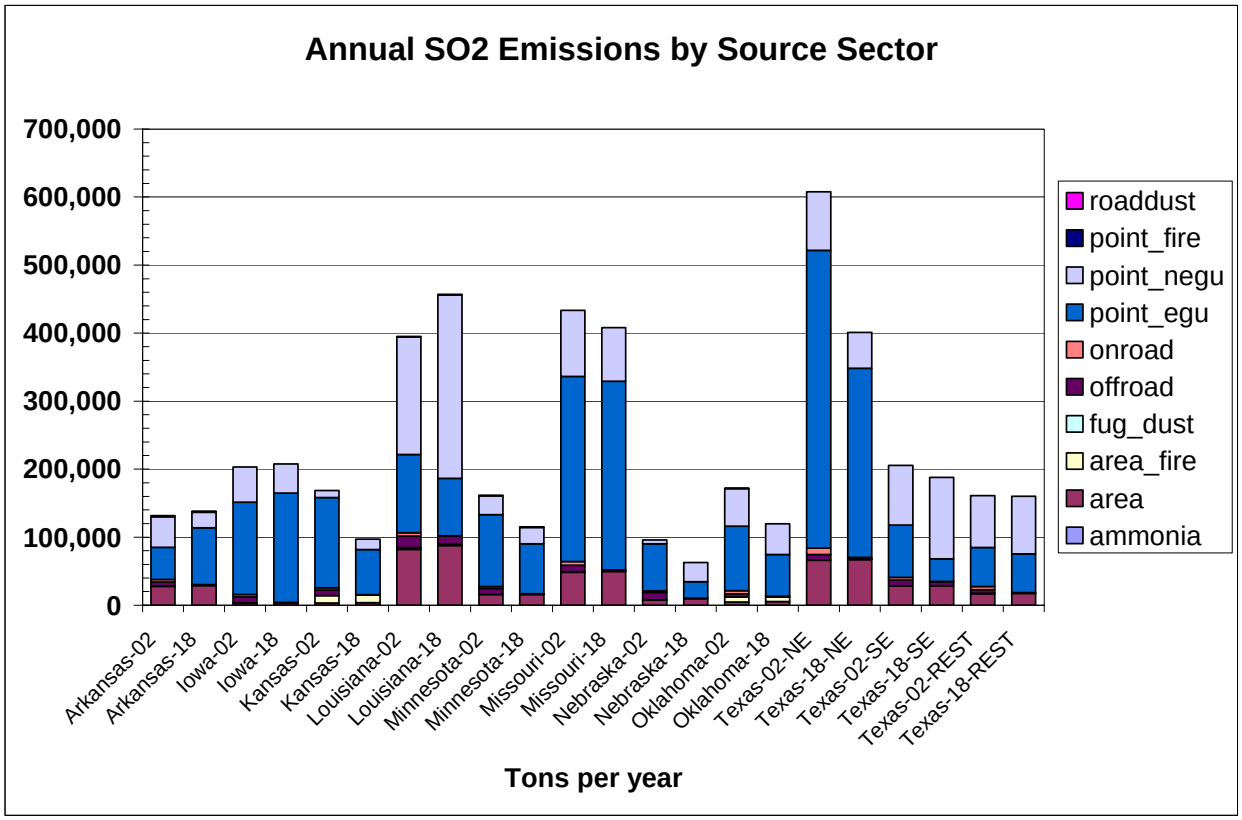

Figure 2-3. Summary of Typ02G and Base18G SO2 emissions by CENRAP state and major source sector (tons per year).

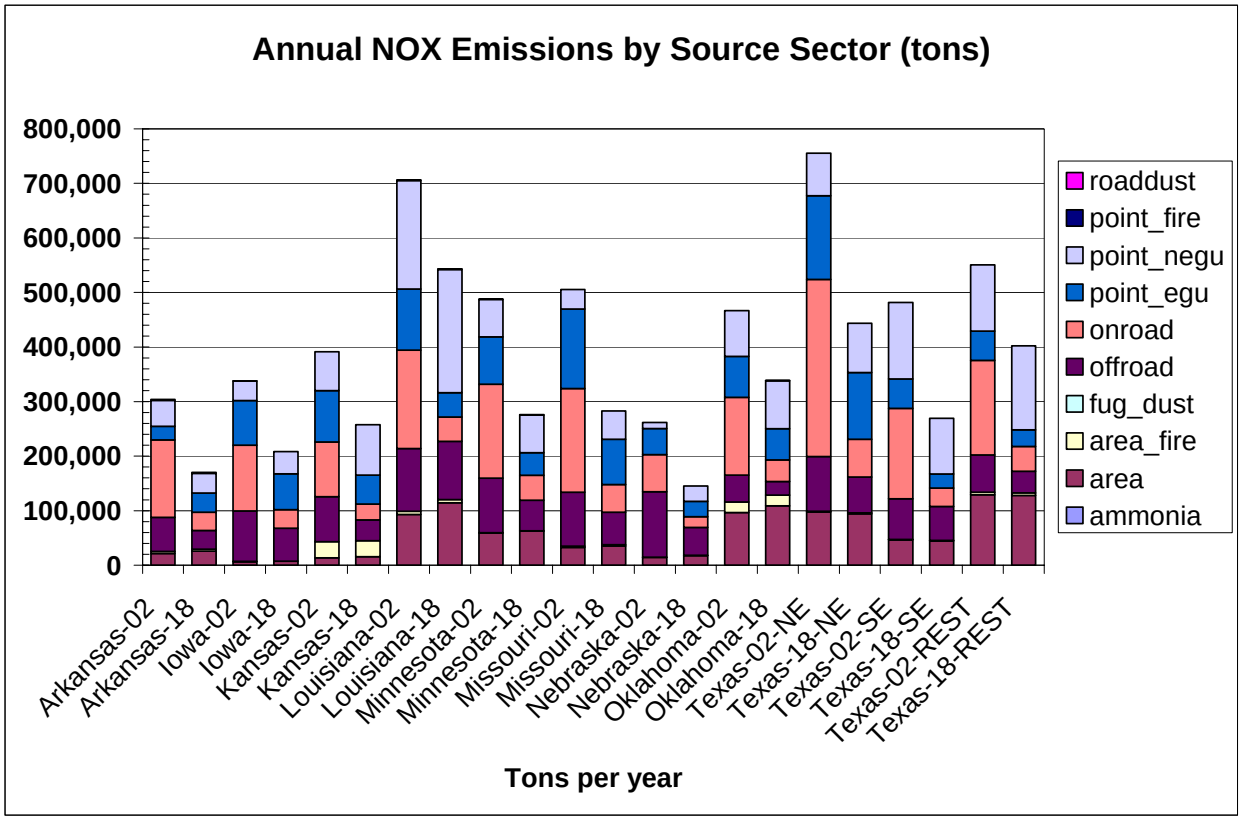

Figure 2-4. Summary of Typ02G and Base18G NOx emissions by CENRAP state and major source sector (tons per year).

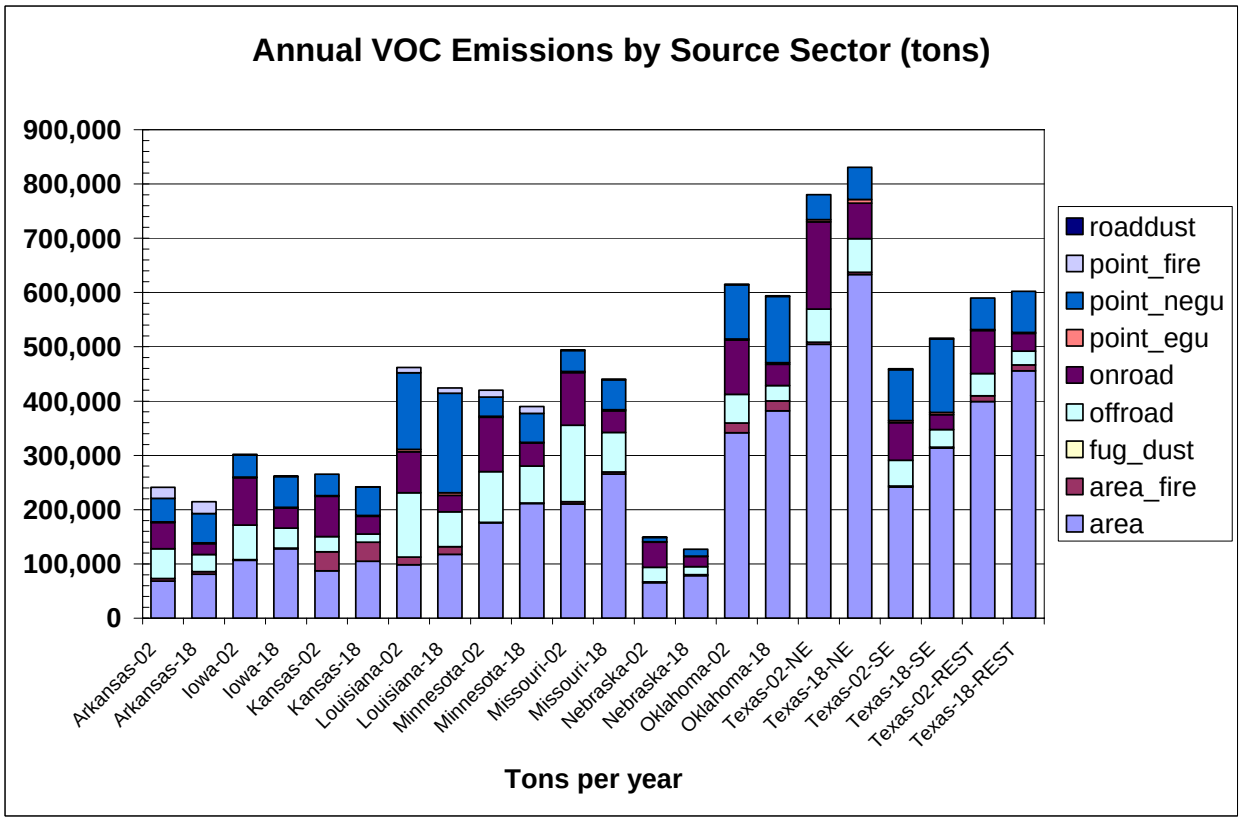

Figure 2-5. Summary of Typ02G and Base18G VOC emissions by CENRAP state and major source sector (tons per year).

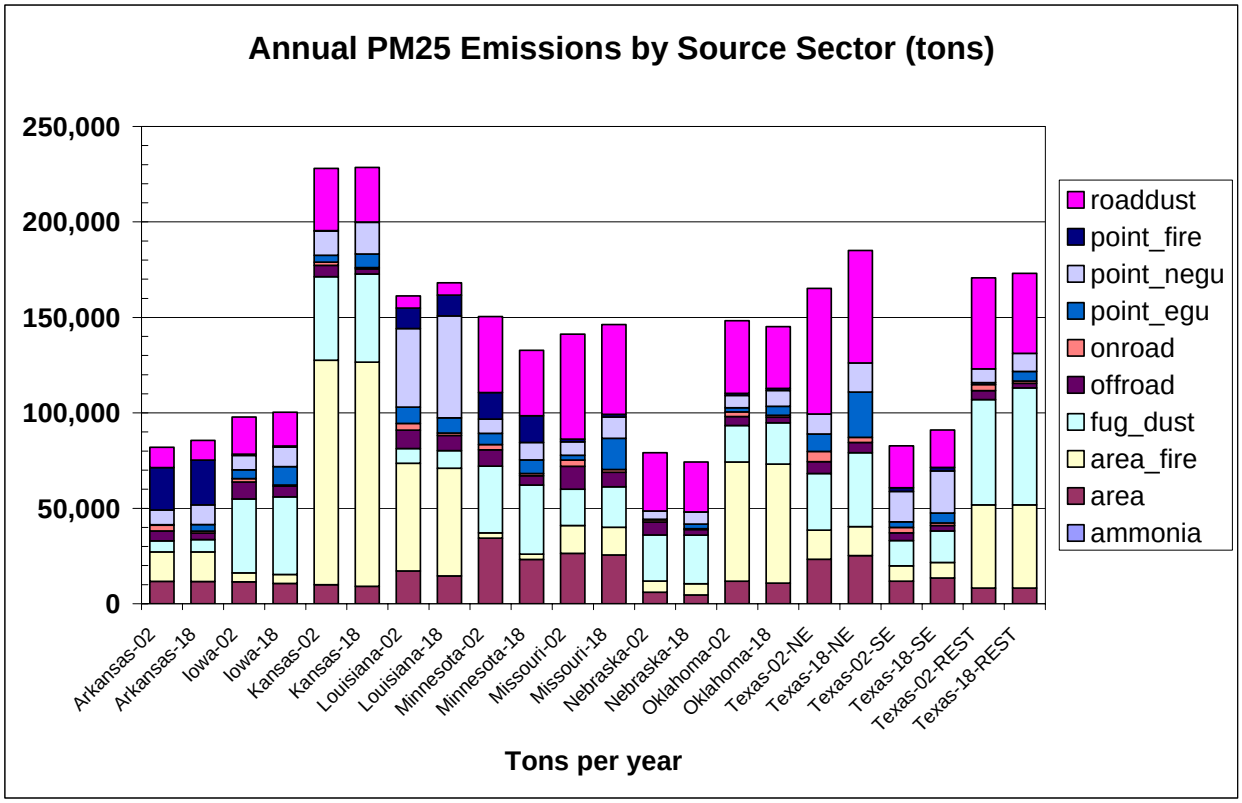

Figure 2-6. Summary of Typ02G and Base18G PM2.5 emissions by CENRAP state and major source sector (tons per year).

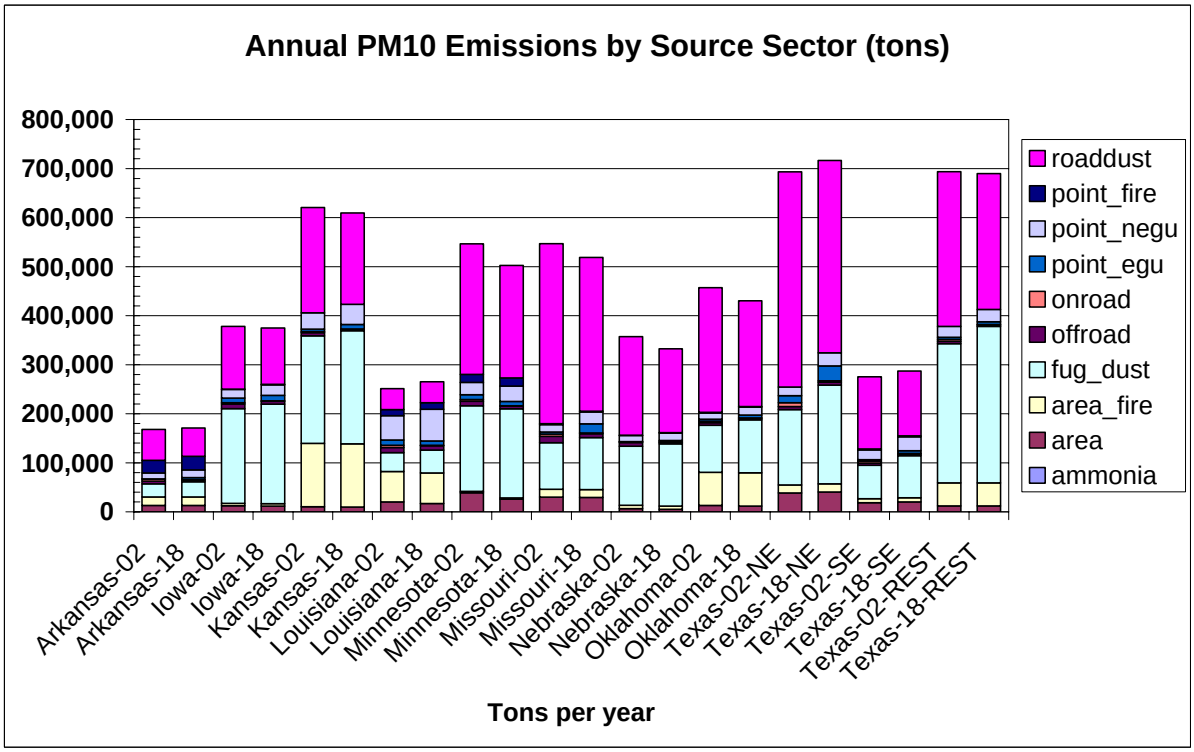

Figure 2-7. Summary of Typ02G and Base18G PM10 emissions by CENRAP state and major source sector (tons per year).

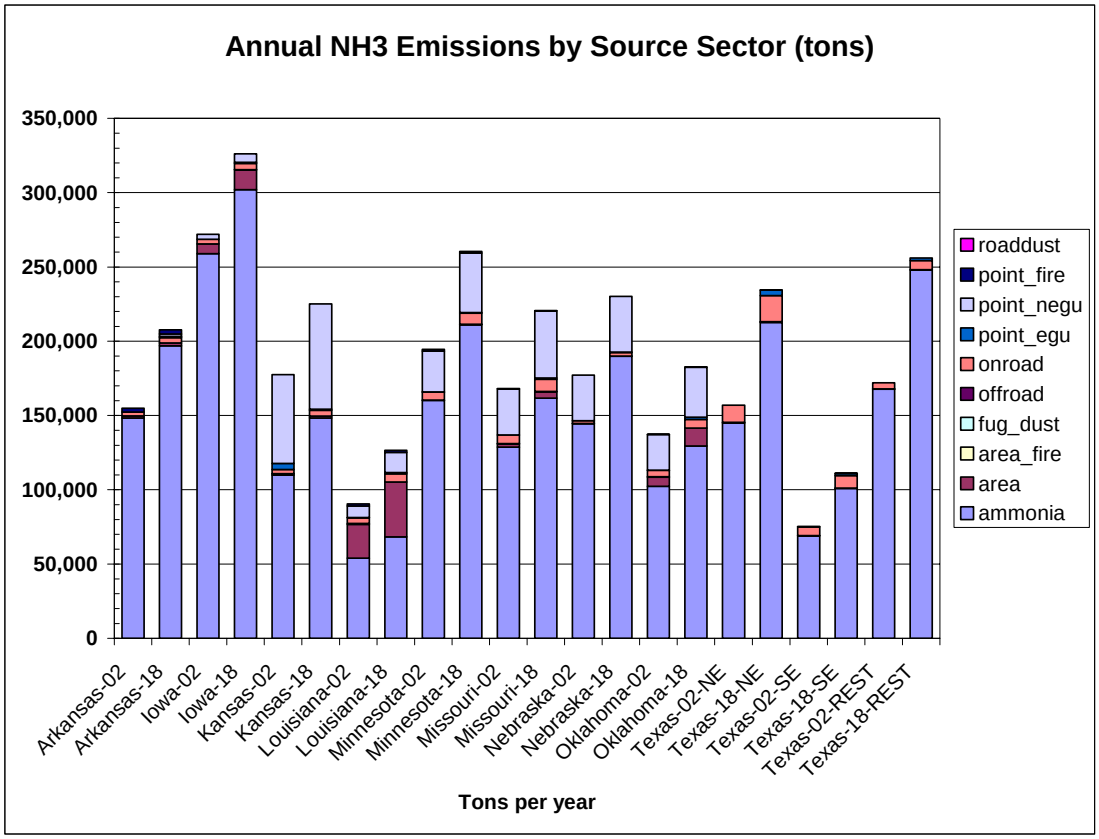

Figure 2-8. Summary of Typ02G and Base18G NH3 emissions by CENRAP state and major source sector (tons per year).

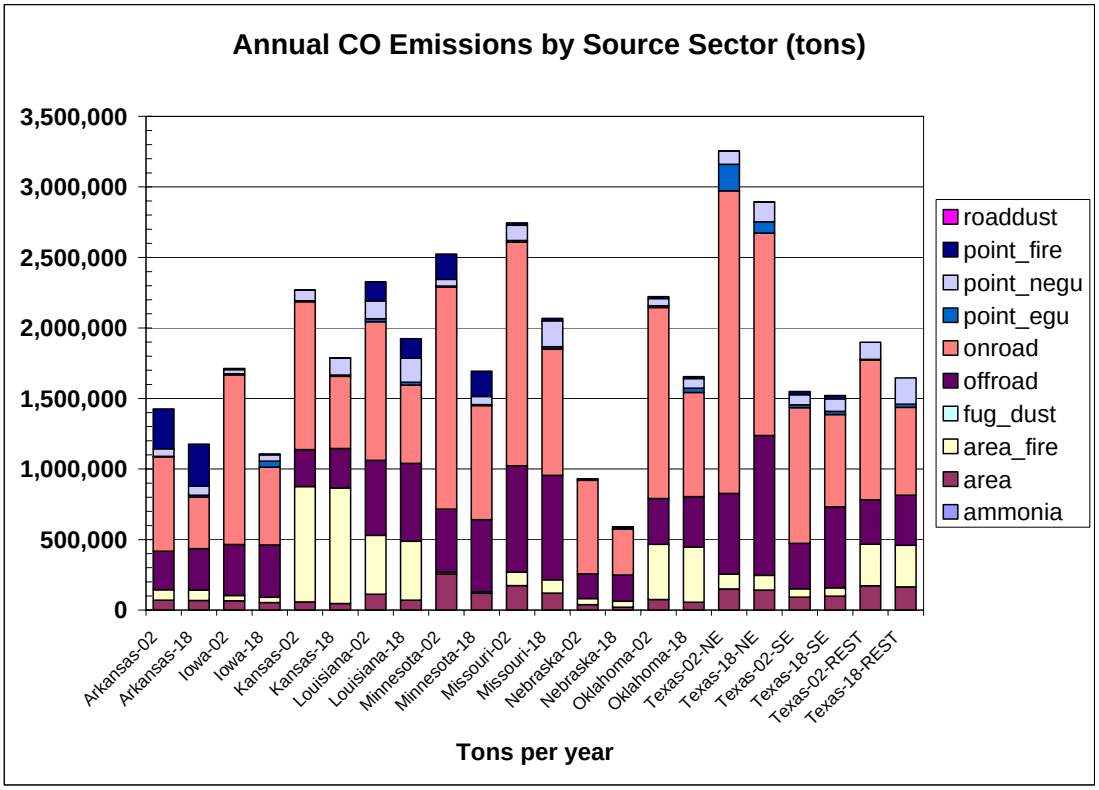

Figure 2-9. Summary of Typ02G and Base18G CO emissions by CENRAP state and major source sector (tons per year).

3.0 MODEL PERFORMANCE EVALUATION

In this Chapter we summarize the CMAQ model performance for the final 2002 36 km Base F base case simulation. Because the 2002 Base F CMAQ simulation produced nearly identical results in the U.S. as the final 2002 Base G simulation and limited resource availability, CENRAP elected not to redo the model evaluation for the 2002 Base G case. This model performance focuses on the ability of the model to predict PM species within the CENRAP region. Details on the model performance are provided in Appendix C. Previously we have documented model performance of interim versions of model base case simulations in reports (Morris et al., 2005) and presentations to the CENRAP Work Groups and POG (e.g., Morris et al., 2006a,b).

3.1 Evaluation Methodology

EPA's integrated ozone, $PM_{2.5}$ and regional haze modeling guidance calls for a comprehensive, multi-layered approach to model performance testing, consisting of the four major components: operational, diagnostic, mechanistic (or scientific) and probabilistic (EPA, 2007). The CMAQ model performance evaluation effort focused on the first two components, namely:

- **Operational Evaluation**: Tests the ability of the model to estimate PM concentrations (both fine and coarse) and the components at PM_{10} and $PM_{2.5}$ including the quantities used to characterize visibility (i.e., sulfate, nitrate, ammonium, organic carbon, elemental carbon, other $PM_{2.5}$, and coarse matter ($PM_{2.5-10}$). This evaluation examines whether the measurements are properly represented by the model predictions but does not necessarily ensure that the model is getting "the right answer for the right reason"; and

- **Diagnostic Evaluation:** Tests the ability of the model to predict visibility and extinction, PM chemical composition including PM precursors (e.g., SOx, NOx, and NH_3) and associated oxidants (e.g., ozone and nitric acid); PM size distribution; temporal variation; spatial variation; mass fluxes; and components of light extinction (i.e., scattering and absorption).

In this final model performance evaluation for the 2002 Typical Base F CMAQ simulation, the operational evaluation has been given the greatest attention since this is the primary thrust of EPA's modeling guidance. However, we have also examined certain diagnostic features dealing with the model's ability to simulate sub-regional, monthly, diurnal, gas phase and aerosol concentration distributions. In the course of the CENRAP air quality modeling and other modeling processes, numerous diagnostic sensitivity tests were performed to investigate and improve model performance. Key diagnostic tests that were performed and the results are discussed on the CENRAP modeling website: http://pah.cert.ucr.edu/aqm/cenrap/index.shtml.

3.2 Ambient Air Quality Data used in the Evaluation

The ground-level model evaluation database for 2002 was compiled by the modeling team using several routine and research-grade databases. The first is the routine gas-phase concentration measurements for ozone, SO_2, NO_2 and CO archived in EPA's Aerometric Information Retrieval System (AIRS) Air Quality System (AQS) database. Other sources of observed information come from the various PM monitoring networks in the U.S. These include the Interagency Monitoring of Protected Visual Environments (IMPROVE); Clean Air Status and Trends Network (CASTNET); EPA Speciation Trends Network (STN) of $PM_{2.5}$ species; and National Acid Deposition Program (NADP). During the course of the CENRAP modeling, the numerous base case simulations were evaluated across the continental U.S. (e.g., Morris et al., 2005). In this section and in Appendix C we focus our evaluation on model performance within the CENRAP region.

3.2 Operational Model Evaluation Approach

The CENRAP modeling databases will be used to develop the visibility State Implementation Plan (SIP) as required by the Regional Haze Rule (RHR). Accordingly, the primary focus of the operational evaluation in this report is on the six components of fine particulate ($PM_{2.5}$) and coarse mass ($PM_{2.5-10}$) within the CENRAP region that are used to characterize visibility at Class I areas:

- Sulfate (SO4);
- Particulate Nitrate (NO3);
- Elemental Carbon (EC);
- Organic Mass Carbon (OMC);
- Other inorganic fine particulate (IP or Soil); and
- Coarse Mass (CM).

The model performance for ozone, precursors, and product species (e.g., SO_4 , NO_3, NH_4 and HNO_3) is also evaluated to build confidence that the modeling system is sufficiently reliable to project future-year visibility.

3.3 Model Performance Goals and Criteria

The issue of model performance goals for PM species is an area of ongoing research and debate. For ozone modeling, EPA has established performance goals for 1-hour ozone: normalized mean bias and gross error of #±15% and #35%, respectively (EPA, 1991). EPA's draft fine particulate modeling guidance notes that performance goals for ozone should be viewed as upper bounds of model performance that PM models may not be able to always achieve and that we should demand better model performance for PM components that make up a larger fraction of the PM mass than those that are minor contributors (EPA, 2001). EPA's final modeling guidance does not list any specific model performance goals for PM and visibility modeling and instead provides a summary of PM model performance across several historical applications that can be used for comparisons, if desired. Measuring PM species is not as precise as ozone monitoring. In fact, the uncertainty in measurement techniques for some PM species is likely to

exceed the more stringent model performance goals, such as those for ozone. For example, recent comparisons of the PM species measurements using the IMPROVE and STN measurement technologies found uncertainties of approximately ∀20% (SO4) to ∀50% (EC) (Solomon et al., 2004).

For the CENRAP modeling we have adopted three levels of model performance goals and criteria for bias and gross error as listed in Table 3-1. Note that we are not suggesting that these performance goals be adopted as guidance. Rather, we are just using them to frame and put the PM model performance into context and to facilitate model performance intercomparison across episodes, species, models and sensitivity tests.

Table 3-1. Model performance goals and criteria used to assist in interpreting modeling results.

Fractional Bias	Fractional Gross Error	Comment
#∀15%	#35%	Ozone model performance goal for which PM model performance would be considered "good" – note that for many PM species measurement uncertainties may exceed this goal.
#∀30%	#50%	Proposed PM model performance goal that we would hope each PM species could meet
#∀60%	#75%	Proposed PM criteria above which indicates potential fundamental problems with the modeling system.

As noted in EPA's PM modeling guidance, less abundant PM species should have less stringent performance goals (EPA, 2001; 2007). Accordingly, we are also using performance goals that are a continuous function of average concentrations, as proposed by Dr. James Boylan at the Georgia Department of Natural Resources (GA DNR), that have the following features (Boylan, 2004):

- Asymptotically approaching proposed performance goals or criteria (i.e., the ∀30%/50% and ∀60%/75% bias/error levels listed in Table 3-1) when the mean of the observed concentrations are greater than 2.5 ug/m^3.

- Approaching 200% error and ∀200% bias when the mean of the observed concentrations are extremely small.

Bias and error are plotted as a function of average concentrations. As the mean concentration approaches zero, the bias performance goal and criteria flare out to ∀200% creating a horn shape, hence the name "Bugle Plots". Dr. Boylan has defined three Zones of model performance: Zone 1 meets the ∀30%/50% bias/error performance goal and is considered "good" model performance; Zone 2 lies between the ∀30%/50% performance goal and ∀60%/75% performance criteria and is an area where concern for model performance is raised; and Zone 3 lies above the ∀60%/75% performance criteria and is an area of questionable model performance.

3.4 Key Measures of Model Performance

Although we have generated numerous statistical performance measures (see Table C-2 in Appendix C) that are available on the CENRAP modeling website, when comparing model performance across months, subdomains, networks, grid resolution, models, studies, etc. it is useful to have a few key measurement statistics to be used to facilitate the comparisons. It is also useful to have a subset of months within the 2002 year that can represent the entire year so that a more focused evaluation can be conducted. We have found that the Mean Fractional Bias and Mean Fractional Gross Error appear to be the most consistent descriptive measure of model performance (Morris et al., 2004b; 2005). The Fractional Bias and Error are normalized by the average of the observed and predicted value (see Table C-2) because it provides descriptive power across different magnitudes of the model and observed concentrations and is bounded by -200% to +200%. This is in contrast to the normalized bias and error (as recommended for ozone performance goals, EPA, 1991) that is normalized by just the observed value so can "blow up" to infinity as the observed value approaches zero. In Appendix C we perform a focused evaluation of model performance for PM and gaseous species and four months of the 2002 year that are used to represent the seasonal variation in performance:

- January
- April
- July
- October

Scatter plots of model predictions and observations for each PM species are presented for each of the four months along with performance statistics and predicted and observed time series plots at each CENRAP Class I area. Summary plots of monthly fractional bias and error are also presented.

3.5 Operational Model Performance Evaluation

A summary of the operational evaluation is presented below. Just the monthly fractional bias performance metrics for each PM species using bar charts and Bugle Plots are presented in this section. The reader is referred to Appendix C for the complete model performance evaluation.

3.5.1 Sulfate (SO4) Model Performance

Figure 3-1 compares the monthly SO4 fractional bias across the CENRAP region for the IMPROVE, STN and CASTNet monitoring networks. An underprediction bias is clearly evident the first 8-10 months of the year. This underestimation bias is greatest across the CASTNet network which persists throughout the year. The SO4 underprediction is not as severe for the STN network and it is minimal by August becoming a slight overprediction in September. For the IMPROVE network, the SO4 fractional bias is < ±20% for the first 2 and last 3 months of the year and ranges from -30% to -50% for the late Spring and Summer months.

Figure 3-1 also includes a Bugle Plot of monthly SO4 fractional bias statistics (for Bugle Plot of fractional gross error see Appendix C) and compares them against the proposed PM model

performance goal and criteria (see Table 3-1). For the STN network, SO4 model performance meets the proposed performance goal for all months. For the IMPROVE network, approximately half of the months achieve the proposed PM performance goal with the other half outside of the goal, but within the performance criteria. Across the CASTNet network, most months are outside of the proposed goal but are within the criteria. The CASTNet fractional bias for some months is right at the performance criteria (≤±60%). With the exception of two IMPROVE months, the monthly SO4 fractional bias performance statistics achieve the proposed PM model performance goal.

3.5.2 Nitrate (NO3) Model Performance

Monthly NO3 model performance across the CENRAP region is characterized by a summer underestimation and winter overestimation bias (Figure 3-2). The summer underestimation bias is more severe, exceeding -100%. Whereas, the winter overestimation bias is approximately 50%. So based on statistics alone, it appears the summer underestimation bias is a bigger concern than the winter overestimation bias. However, the Bugle Plots in the bottom part of Figure 3-2 show that the summer underestimation bias occurs when NO3 is very low and is not an important component of PM and visibility impairment. These summer values occur in the flared horn part of the Bugle Plot and the summer NO3 performance, in most cases, achieves the model performance goal and always achieves the performance criteria. Whereas, the winter overstated NO3 performance for the most part doesn't meet the performance goal and there are some months/networks that also don't meet the performance criteria.

3.5.3 Organic Matter Carbon (OMC) Model Performance

The OMC monthly fractional bias across IMPROVE and STN sites in the CENRAP region are shown in Figure 3-3. The fractional bias for OMC at the IMPROVE sites is quite good throughout the year with values generally within ±20%, albeit with a slight winter overestimation and summer underestimation bias. At the urban STN sites, the model exhibits an underestimation bias throughout the year that ranges from -20% to -50%. The urban underestimation of OMC is a fairly common occurrence and suggests there may be missing sources of organic aerosol emissions in the modeling inventory.

The good performance of the model for OMC at the IMPROVE sites is also reflected in the Bugle Plot (Figure 3-3, bottom) with the bias achieving the proposed PM model performance goal for all months of the year. At the STN sites, however, the OMC bias falls between the proposed PM model performance goal and criteria, with error right at the goal for most months.

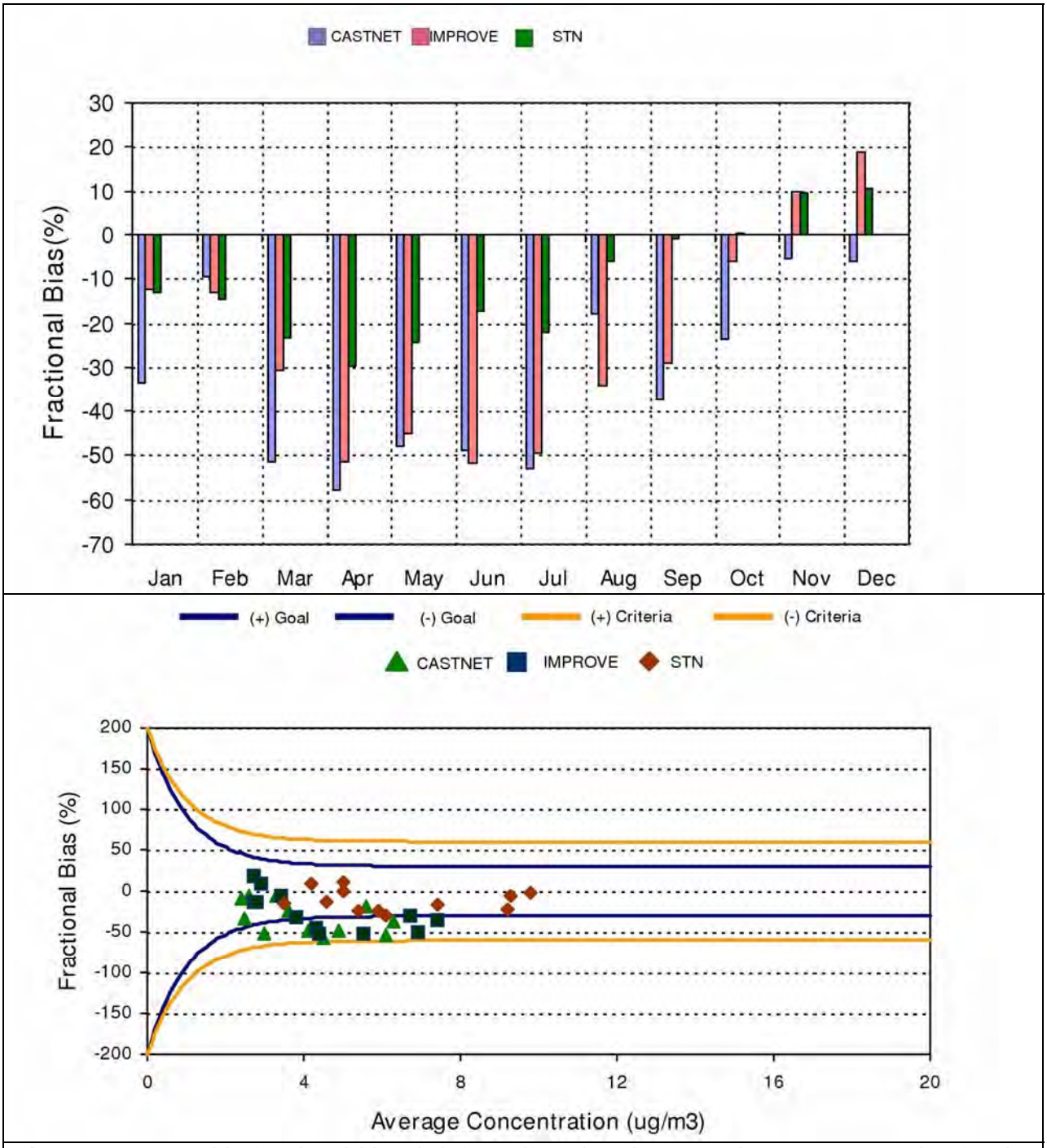

Figure 3-1. Monthly fractional bias (%) for sulfate (SO4) across the CENRAP region for the CMAQ 2002 36 km Base F base case simulation.

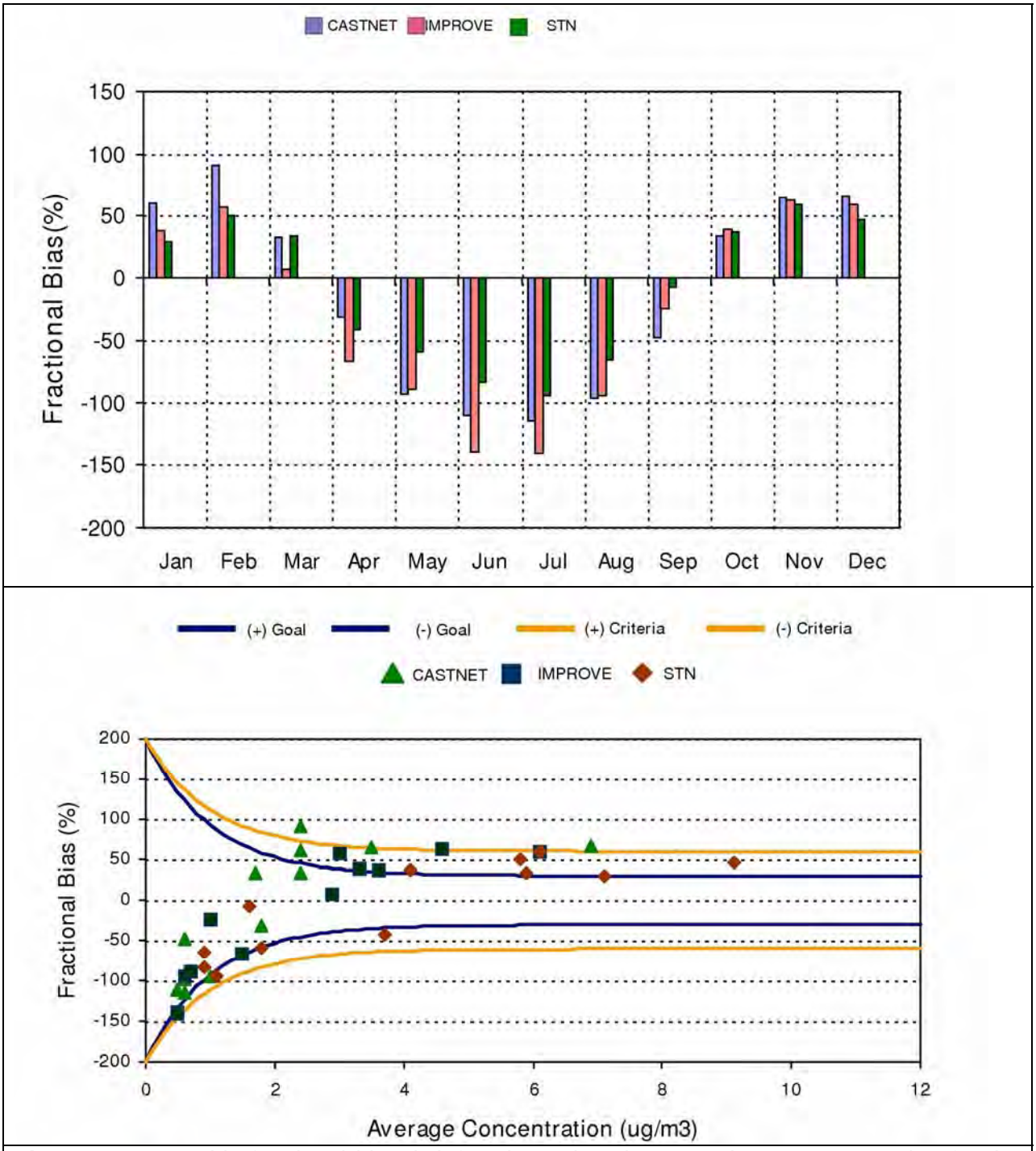

Figure 3-2. Monthly fractional bias (%) for nitrate (NO3) across the CENRAP region for the CMAQ 2002 36 km Base F base case simulation.

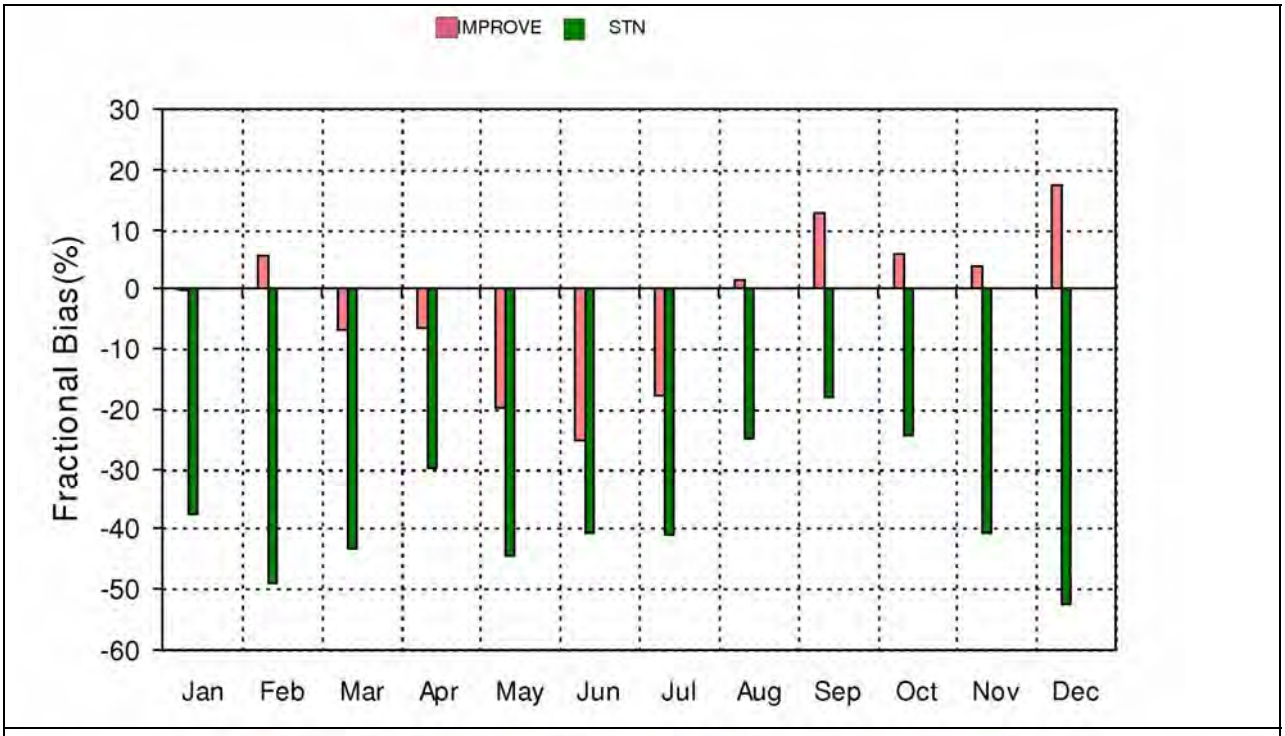

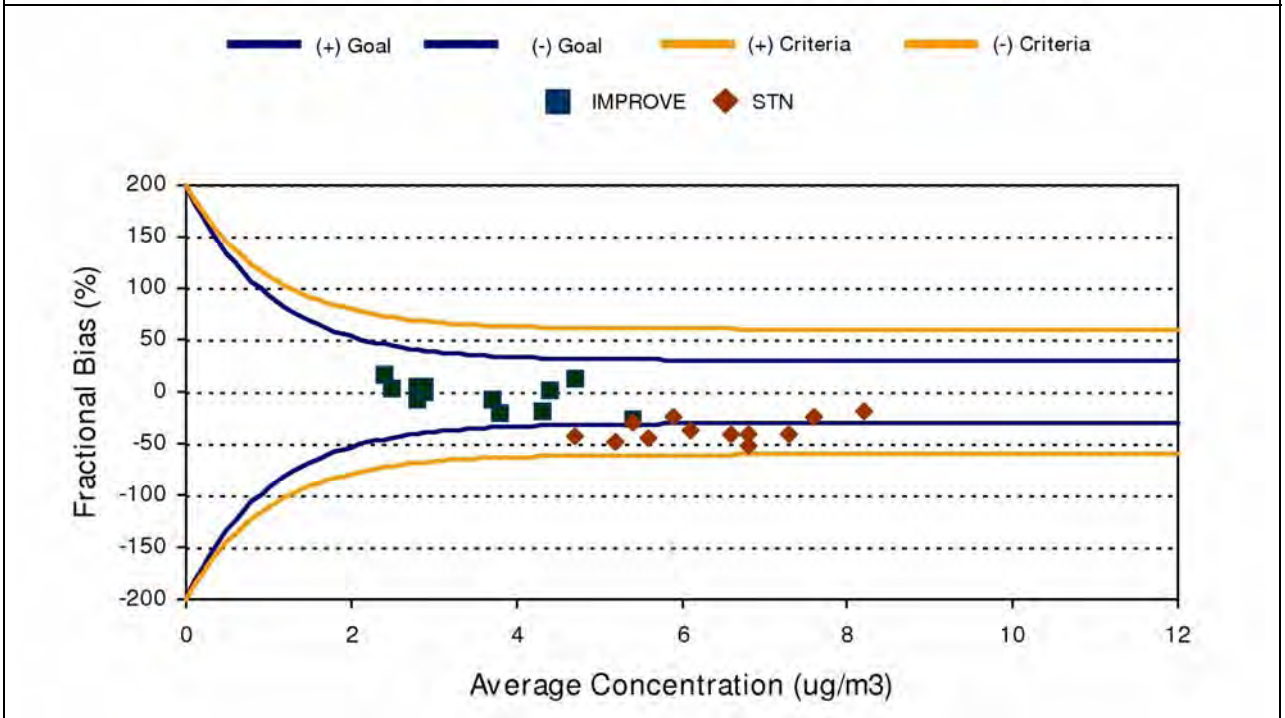

Figure 3-3. Monthly fractional bias (%) for organic matter carbon (OMC) across the CENRAP region for the CMAQ 2002 36 km Base F base case simulation.

3.5.4 Elemental Carbon (EC) Model Performance

The monthly average bias for EC across the IMPROVE and STN monitors in the CENRAP region are shown in Figure 3-4. The STN network exhibits small fractional bias year round, whereas the IMPROVE monitoring network exhibits a large underprediction bias in the summer months (-40% to -70%) and much smaller bias in the winter. The Bugle Plot puts the EC performance in context. The low EC concentrations at the IMPROVE sites results in bias values in the horn of the Bugle Plot. Thus, EC bias achieves the proposed PM performance goal for all months of the year.

3.5.5 Other $PM_{2.5}$ (Soil) Model Performance

Figure 3-5 displays the monthly variation in the Soil fractional bias using IMPROVE measurements in the CENRAP region. During the winter months, the model exhibits a very large (> 100%) overestimation bias. With the exception of July, the summer monthly bias is toward a slight overprediction but generally less than 20%. The July underestimation bias appears to be driven by impacts of high Soil values from wind blown dust events (e.g., see July 2002 discussion in Appendix C). The Bugle Plot indicates that the summer Soil performance achieves the PM performance goal, a few months in the Spring/Fall period fall between the performance goal and criteria and the winter Soil performance exceeds the model performance criteria. Thus, the Soil performance is a cause for concern.

3.5.6 Coarse Mass (CM) Model Performance

The monthly average fractional bias values for CM are shown in Figure 3-6. In the winter the underprediction bias is typically in the -60% to -80% range. In the late Spring and Summer the underprediction bias ranges from -120% to -160%. As this underprediction bias is nearly systematic (i.e., an underprediction almost always occurs), then the fractional errors are the same magnitude as the bias.

The Bugle Plots clearly show that the CM model performance is a problem. The monthly bias exceeds both the performance goal and criteria for almost every month of the year.

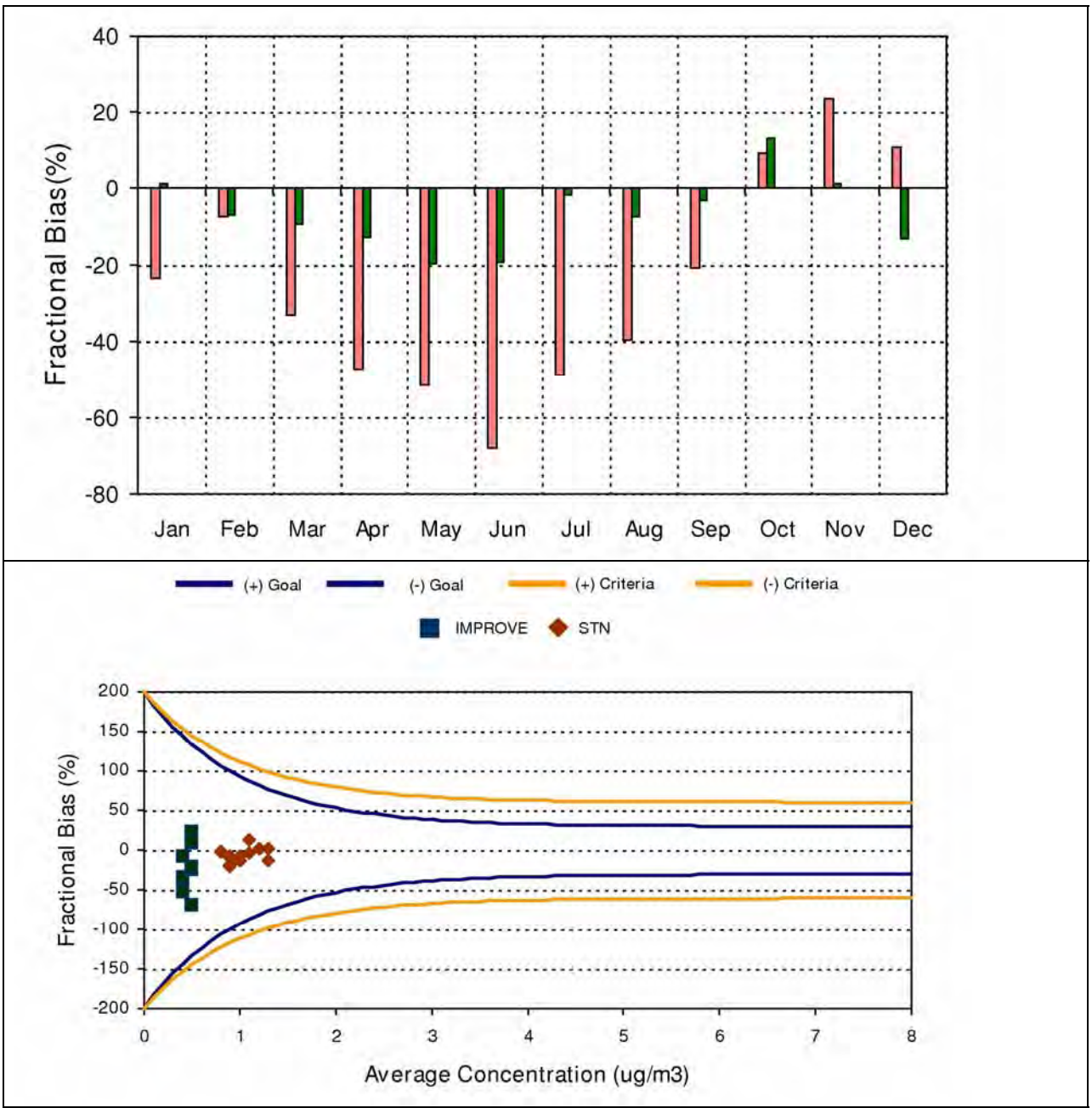

Figure 3-4. Monthly fractional bias (%) for elemental carbon (EC) across the CENRAP region for the CMAQ 2002 36 km Base F base case simulation.

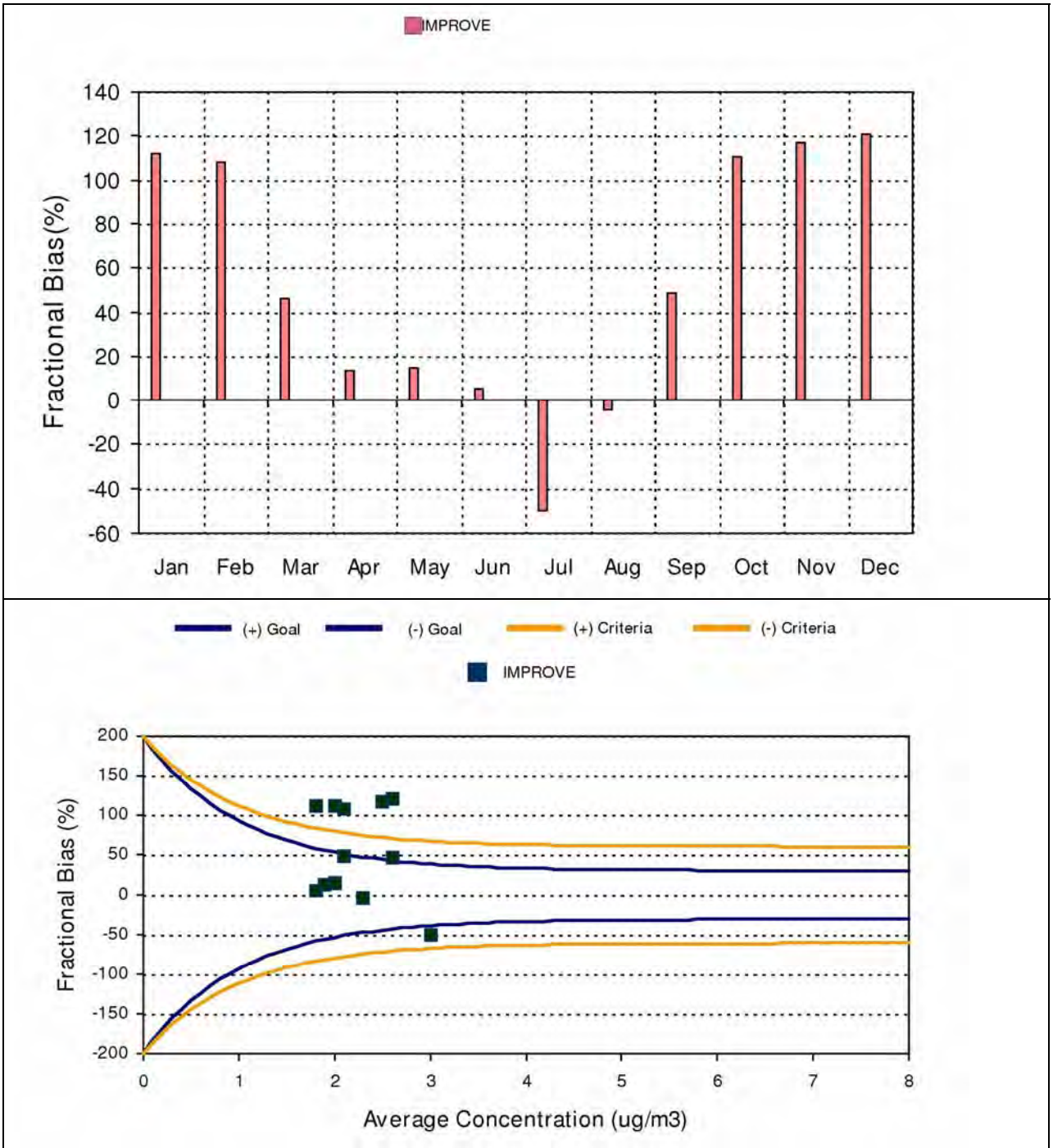

Figure 3-5. Monthly fractional bias (%) for other $PM_{2.5}$ (Soil) across the CENRAP region for the CMAQ 2002 36 km Base F base case simulation.

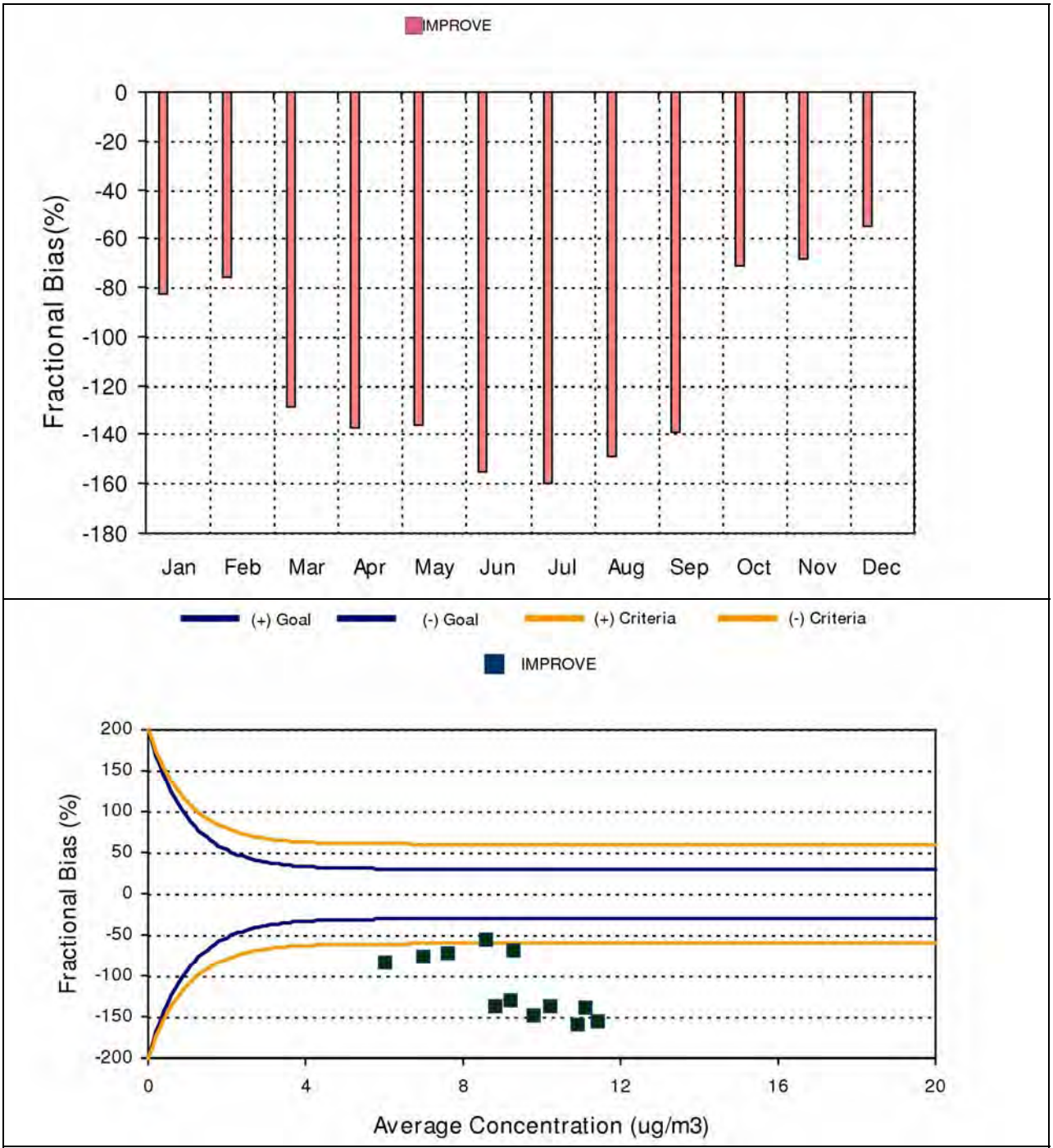

Figure 3-6. Monthly fractional bias (%) for coarse mass (CM) across the CENRAP region for the CMAQ 2002 36 km Base F base case simulation.

3.6 Diagnostic Model Performance Evaluation

The CASTNet and AQS networks also measure gas-phase species that are PM precursor or related species. The diagnostic evaluation of the 2002 36 km Base F CMAQ base case simulation for these compounds and the four seasonal months are presented in Appendix C. The displays for January are provided below as an example; the reader is referred to Appendix C for the rest of the monthly displays.

The CASTNet network measures weekly average samples of SO2, SO4, NO2, HNO3, NO3 and NH4. The AQS network collects hourly measurements of SO2, NO2, O3 and CO. A comparison of the SO2 and SO4 performance provides insight into whether the SO4 formation rate may be too slow or fast. For example, if SO4 is underestimated and SO2 is overestimated that may indicate chemical conversion rates that are too slow. Analyzing the performance for SO4, HNO3, NO3, Total NO3 and NH4 provides insight into the equilibrium of these species. For example, if Total NO3 performs well but HNO3 and NO3 do not, then there may be issues associated with the partitioning between the gaseous and particulate phases of nitrate. Causes for incorrect HNO3/NO3 partitioning could include inadequate ammonia emissions and/or poorly characterized meteorological conditions (e.g., temperature).

3.6.1 Diagnostic Model Performance in January 2002

In January, SO2 is overstated across both the CASTNet and AQS sites with fractional bias values of 38% (Figure 3-7) and 31% (Figure 3-8), respectively. SO4 is understated by -34% across the CASTNet monitors (Figure 3-7) and -12% and -13% for the IMPROVE and STN networks (Figure C-4a). Wet SO4 deposition is also overstated in January (+40%, Figure C-4a). Given that SO2 emissions are well characterized, these results suggest that the January SO4 underestimation may be partly due to understated transformation rates of SO2 to SO4 and overstated wet SO4 deposition.

Total NO3 is overestimated by 35% on average across the CASTNet sites in the CENRAP region in January (Figure 3-7). HNO3 is underestimated (-34%) and particle NO3 is overestimated (+61%) suggesting there are gas/particle equilibrium issues. An analysis of the time series of the four CASTNet stations reveals that NO3, HNO3 and NH4 performance is actually very reasonable at the west Texas site and the HNO3 underestimation and NO3 overestimation bias is coming from the east Kansas, central Arkansas and northern Minnesota CASTNet sites (see Figure C-3 for site locations). One potential contributor for this performance problem could be overstated NH3 emissions. However, the Total NO3 overestimation bias suggests that the model estimated NOx oxidation rate may be too high in January.

The SO2, NO2, O3 and CO performance across the AQS sites in January is shown in Figure 3-8. The AQS monitoring network is primarily an urban-oriented network. So, it is not surprising that the model is underestimating concentrations of primary emissions when a 36 km grid is used. NO2 is underestimated by approximately 5%, and CO by approximately 67%. Ozone is also underestimated on average, especially the maximum values above 60 ppb.

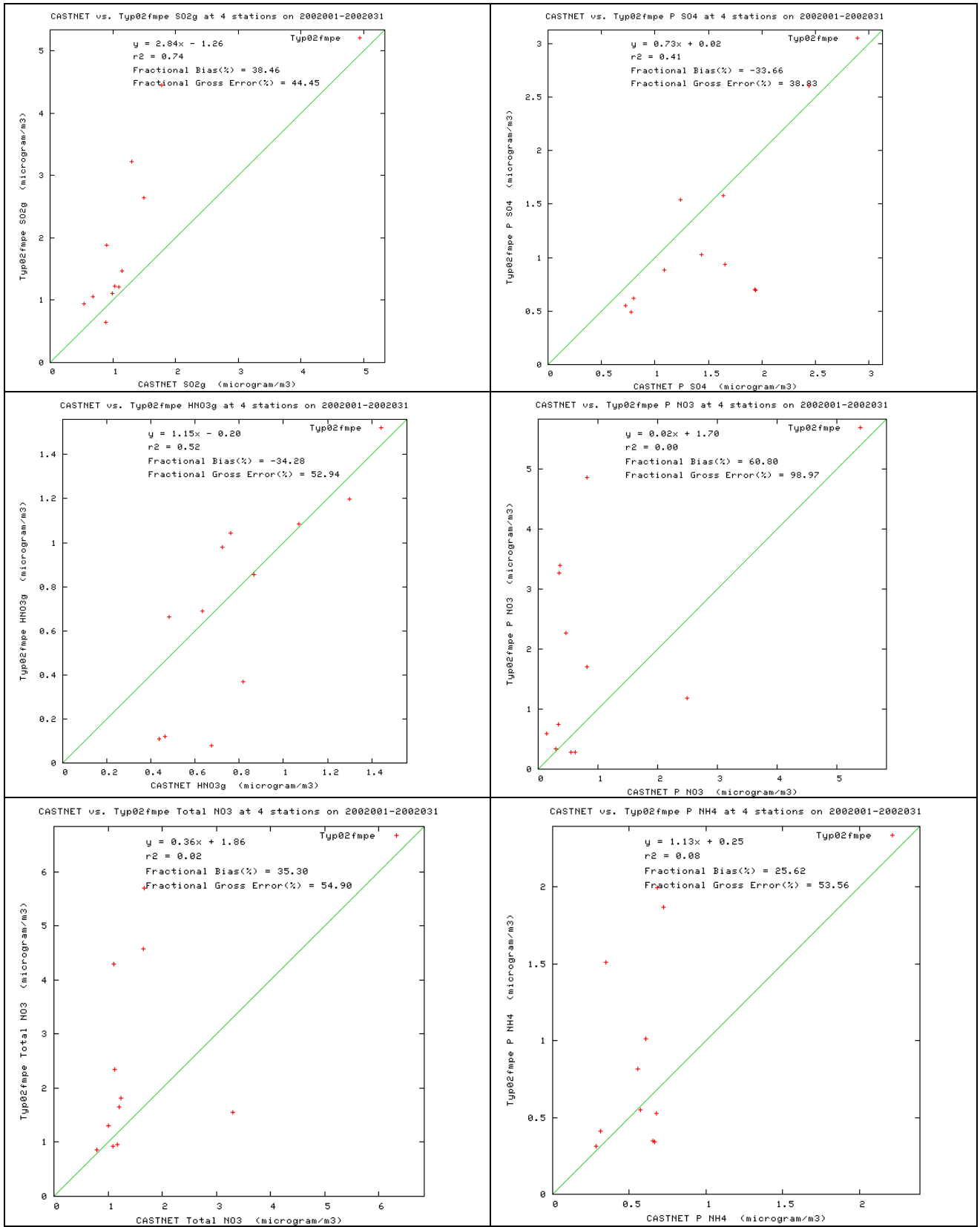

Figure 3-7. January 2002 performance at CENRAP CASTNet sites for SO2 (top left), SO4 (top right), HNO3 (middle left), NO3 (middle right), Total NO3 (bottom left) and NH4 (bottom right).

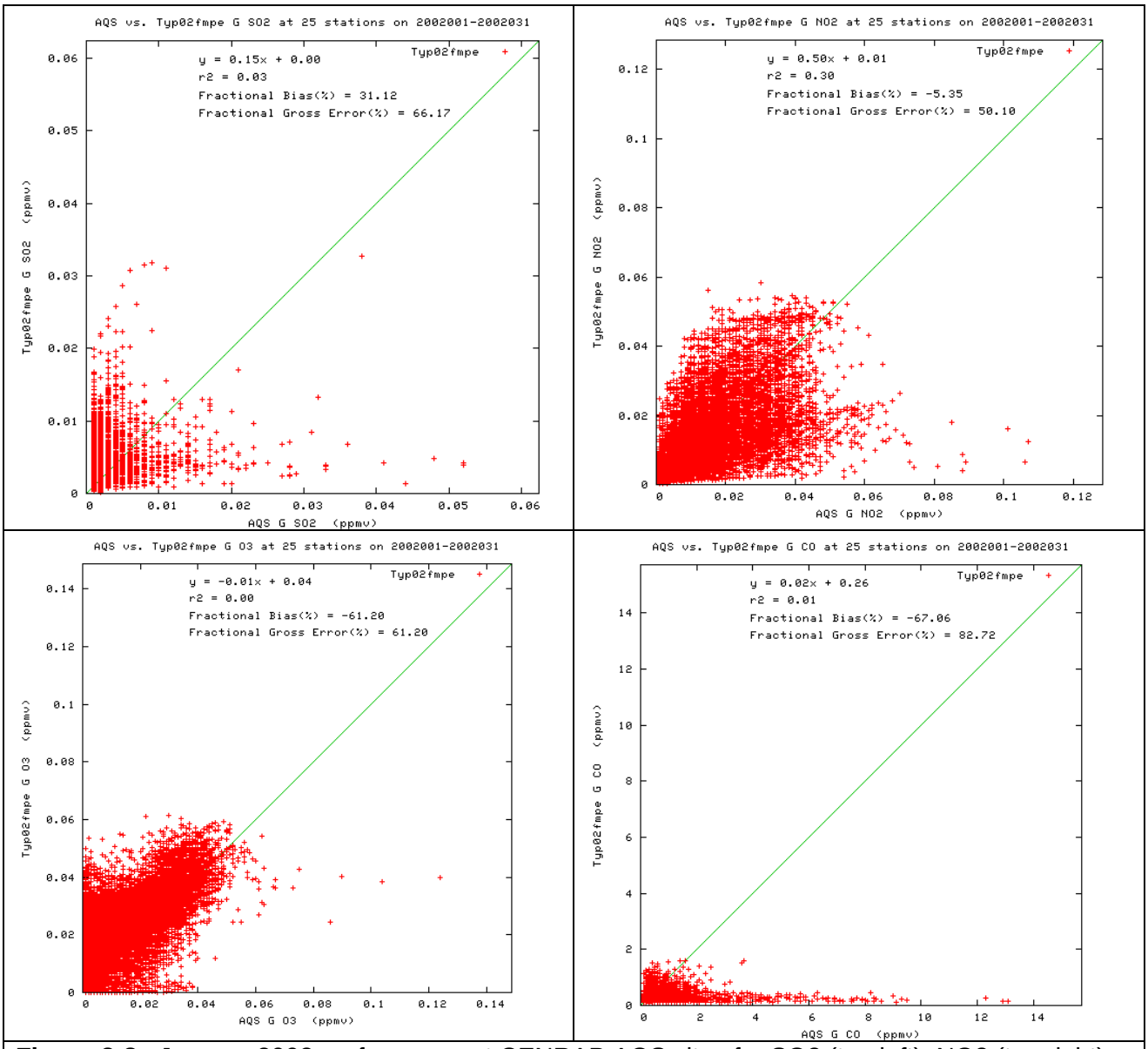

Figure 3-8. January 2002 performance at CENRAP AQS sites for SO2 (top left), NO2 (top right), O3 (bottom left) and CO (bottom right).

3.6.2 Diagnostic Model Performance In April

In April there is an average SO2 overestimation bias across the CASTNet (+15%) and underestimation bias across the AQS (-10%) networks (Figures C-42 and C-43). SO4 is underestimated across all networks by -30% to -58% (Figure C-5a). The wet SO4 deposition bias is near zero. Both SO2 and SO4 are underestimated at the west Texas CASTNet monitor in April suggesting SO2 emissions in Mexico are likely understated.

The HNO3 performance in April is interesting with almost perfect agreement except for 5 modeled-observed comparisons that drives the average underprediction bias of -29% (Figure C-42). On Julian Day 102 there is high HNO3 at the MN, KS and OK CASTNet sites that is not captured by the model. Given that HNO3, NO3 and Total NO3 are all underestimated by about the same amount (-30%), then part of the underestimation bias is likely due to too slow oxidation of NOx.

There is a lot of scatter in the NO2 and O3 performance that is more or less centered on the 1:1 line of perfect agreement with bias values of -8% and -21%, respectively (Figure C-43). CO is underestimated by -72% with the model unable to predict CO concentrations above 1 ppm due to the use of the coarse 36 km grid spacing. Mobile sources produce a vast majority of the CO emissions. So, AQS monitors for CO compliance are located near roadways, which are not simulated well using a 36 km grid.

3.6.3 Diagnostic Model Performance In July

In July SO2 is slightly underestimated across the CASTNet (-5%) and AQS (-12%) networks (Figures C-44 and C-45). SO4 is more significantly underestimated across all networks (-22% to -53%, as shown in Figure C-6a). Since wet deposition SO4 is also underestimated, it is unclear why all sulfur species are underestimated.

The nitrate species are also all underestimated with the Total NO3 bias (-56%) being between the HNO3 bias (-35%) and NO3 bias (-115%). The modeled NO3 values are all near zero with little correlation with the observations, whereas the observed HNO3 and Total NO3 is tracked well with correlation coefficients of 0.74 and 0.76. These results suggest that the July NO3 model performance problem is partly due to insufficient formation of Total NO3, but mainly due to incorrect partitioning of the Total NO3.

Again, there is abundant scatter in the AQS NO2 scatter plot for July (Figure C-45) resulting in a low bias (0%) but high error (65%). Ozone performance also exhibits a low bias (-15%) and error (20%), but the model is incapable of simulating ozone above 100 ppb. Although CO performance in July is better than the previous months, it still has a large underestimation bias of 82%.

3.6.4 Diagnostic Model Performance In October

SO2 is overstated in October across the CASTNet (+28%) and AQS (+33%) sites (Figures C-46 and C-47). Although SO4 is understated across the CASTNet sites (-24%), the bias across the IMPROVE (-6%) and STN (0%) sites are near zero (Figure C-7a).

Performance for HNO3 is fairly good with a low bias (+12%) and error (30%). But NO3 is overstated (+34%) leading to an overstatement of Total NO3 (+37%). The overstatement of NO3 leads to an overstatement of NH4 as well (Figure C-46)

As seen in the other months, NO2 exhibits a lot of scatter resulting in a low correlation (0.22) and high error (61%) but low bias (12%). The model tends to underpredict the high and overpredict the low O3 observations resulting in a -29% bias and low correlation coefficient. CO is also underpredicted (-76%) for the reasons discussed previously.

3.7 Performance at CENRAP Class I Areas for the Worst and Best 20 Percent Days

In this section, and in section C.5 of Appendix C, we present the results of the model performance evaluation at each of the CENRAP Class I areas for the worst and best 20 percent days. Performance on these days is critical since they are the days used in the 2018 visibility projections discussed in Chapter 4. For each Class I area we compared the predicted and observed extinction of the worst and best 20 percent days below. In Appendix C the PM species-specific extinction is also compared for the worst 20 percent days.

3.7.1 Caney Creek (CACR) Arkansas

The ability of the CMAQ model to estimate visibility extinction at the CACR Class I area on the 2002 worst and best 20 percent days is provide in Figures 3-9 and C-48. On most of the worst 20 percent days at CACR total extinction is dominated by SO4 extinction with some extinction due to OMC. On four of the worst 20 percent days extinction is dominated by NO3. The average extinction across the worst 20 percent days is underestimated by -33% (Figure 3-9), which is primarily due to a -51% underestimation of SO4 extinction combined with a 6% overestimation of NO3 extinction (Figure C-48). Performance for OMC extinction at CACR on the worst 20 percent days is pretty good with a -20% bias and 36% error. EC extinction is systematically underestimated. Soil extinction has low bias (-19%) buts lots of scatter and high error (74%), while CM extinction is greatly underestimated (bias of -153%).

On the best 20 percent days at CACR the observed extinction ranges from 20 to 40 Mm^{-1}. Whereas, the modeled extinction has a much larger range from 15 to 120 Mm^{-1}. Much of the modeled overestimation of total extinction on the best 20% days (+44% bias) is due to NO3 overestimation (+94% bias).

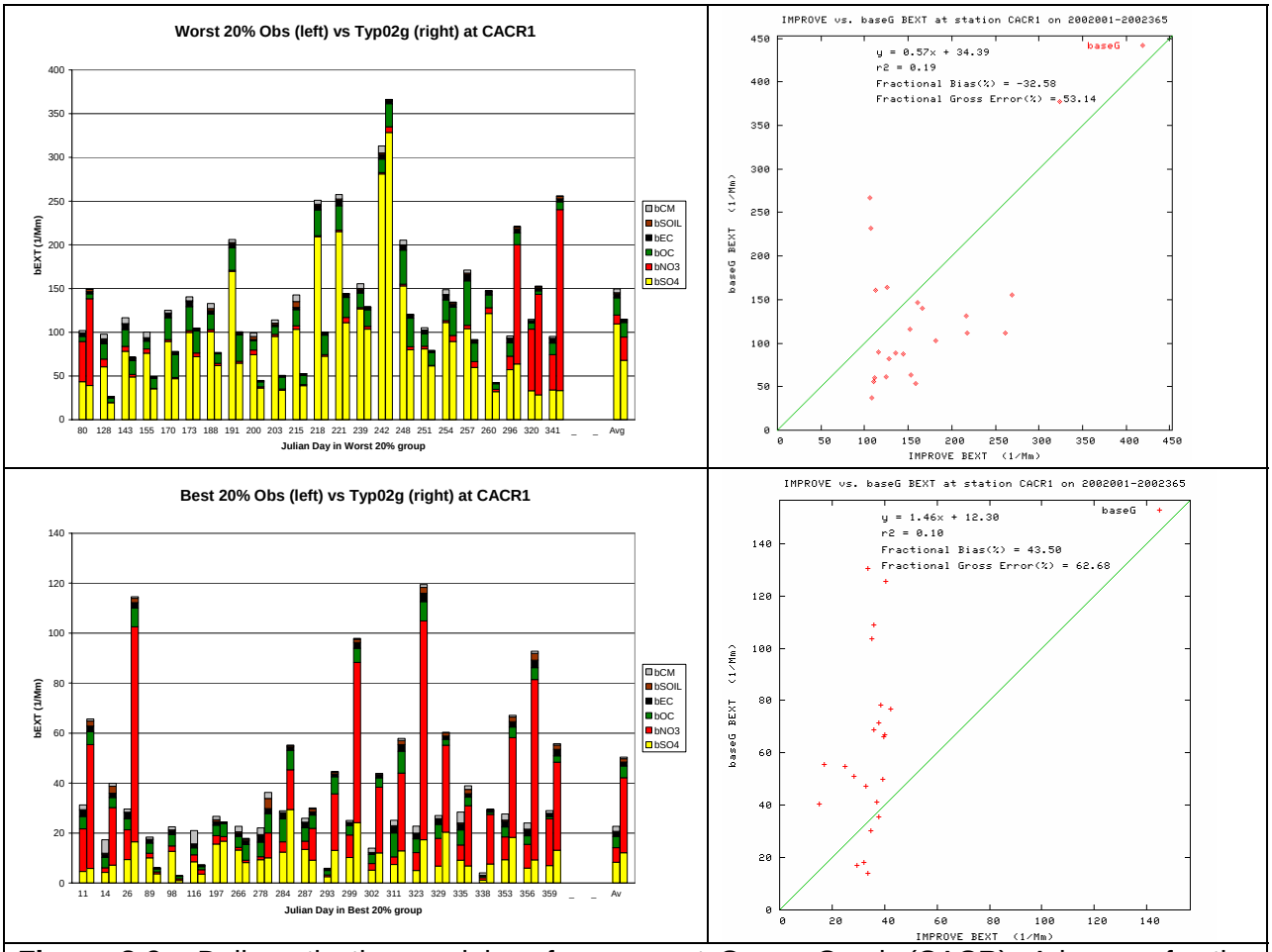

Figure 3-9. Daily extinction model performance at Caney Creek (CACR), Arkansas for the worst (top) and best (bottom) 20 percent days during 2002.

3.7.2 Upper Buffalo (UPBU) Arkansas

Model performance at the UPBU Class I area for the worst and best 20 percent days is shown in Figures 3-10 and C-49. On most of the worst 20 percent days at UPBU, visibility impairment is dominated by SO4, although there are also two high NO3 days. The model underestimates the average of the total extinction on the worst 20 percent days at UPBU by -40% (Figure 3-10), which is due to an underestimation of extinction due to SO4, OMC and CM by -46%, -33% and -179%, respectively.

On the best 20 percent days at UPBU, the model performs reasonably well with a low bias (2%) and error (42%). But again, the model has a much wider range in extinction values across the best 20 percent days (15 to 120 Mm^{-1}) than observed (20 to 45 Mm^{-1}). There are five days in which the modeled NO3 overprediction is quite severe and when those days are removed the range in the modeled and observed extinction on the best 20 percent days is quite similar to the observed, although the model gets much cleaner on the very cleanest modeled days.

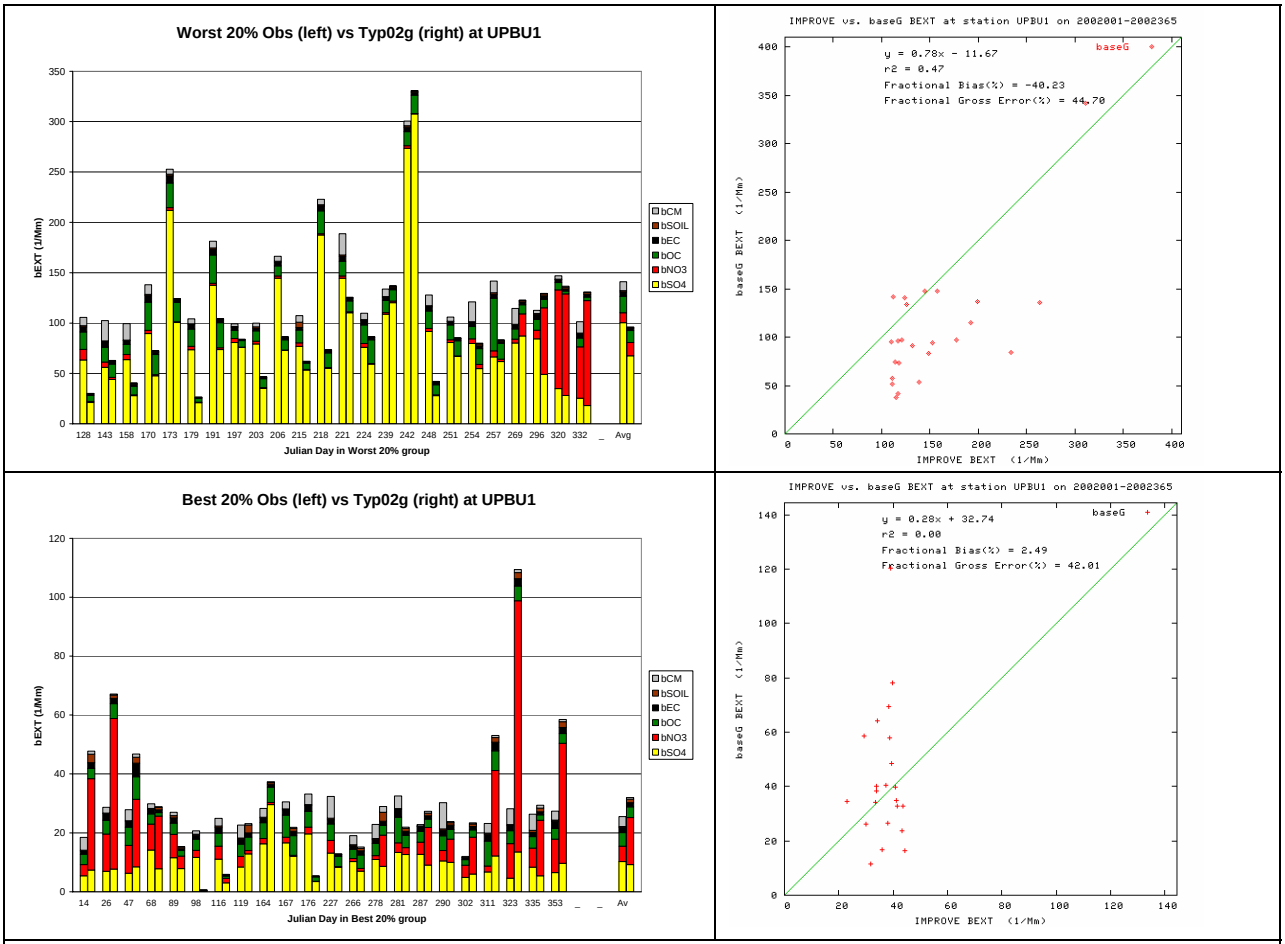

Figure 3-10. Daily extinction model performance at Upper Buffalo (UPBU), Arkansas for the worst (top) and best (bottom) 20 percent days during 2002.

3.7.3 Breton Island (BRET), Louisiana

The observed total extinction on the worst 20 percent days at Breton Island is underestimated by -71% (Figure 3-11), which is due to an underestimation of each component of extinction (Figure C-50) by from -50% to -70% (SO4, OMC and Soil) to over -100% (EC and CM). The observed extinction on the worst 20 percent days ranges from 90 to 170 Mm^{-1}, whereas the modeled values drop down to as low as approximately 15 Mm^{-1}. On the best 20 percent days the range of the observed and modeled extinction is similar (roughly 10 to 50 Mm^{-1}) that results in a reasonably low bias (-22%), but there is little agreement on which days are higher or lower resulting in a lot of scatter and high error (54%).

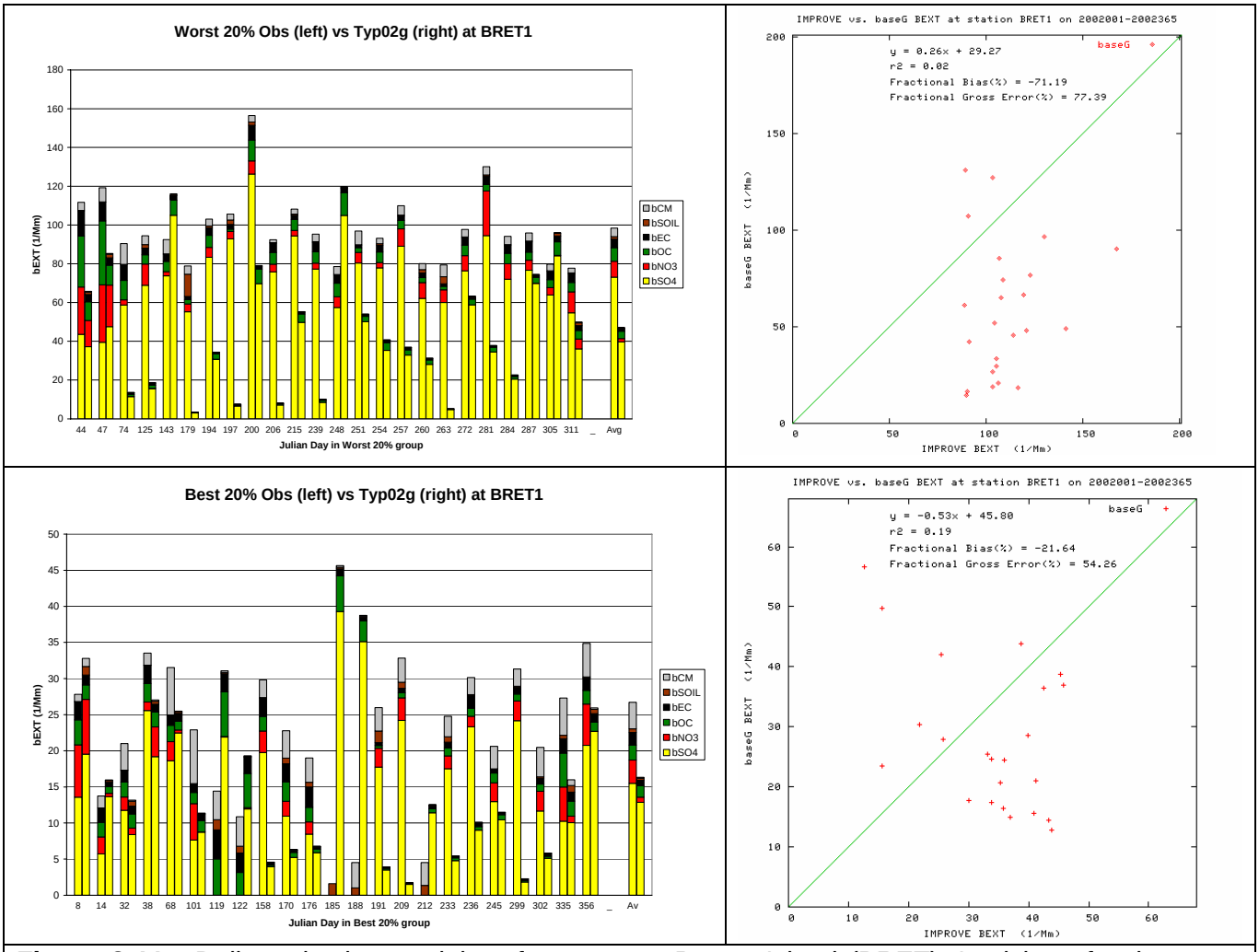

Figure 3-11. Daily extinction model performance at Breton Island (BRET), Louisiana for the worst (top) and best (bottom) 20 percent days during 2002.

3.7.4 Boundary Waters (BOWA), Minnesota

There are three types of days during the worst 20 percent days at BOWA: SO4 days, OMC days and NO3 days (Figure 3-12). The two high OMC days are likely fire impact events that the model captures to some extent on one day and not on the other. On the five high (> 20 Mm^{-1}) NO3 extinction days the model predicts the observed extinction well on three days and overestimates by a factor of 3-4 on the other two high NO3 days. SO4 is underestimated by -43% on average across the worst 20 percent days at BOWA.

With the exception of two days, the model reproduces the total extinction for the best 20 percent days at BOWA quite well with a bias and error value of +14% and 22% (Figure 3-12). Without these two days, the modeled and observed extinction both range between 15 and 25 Mm^{-1}.

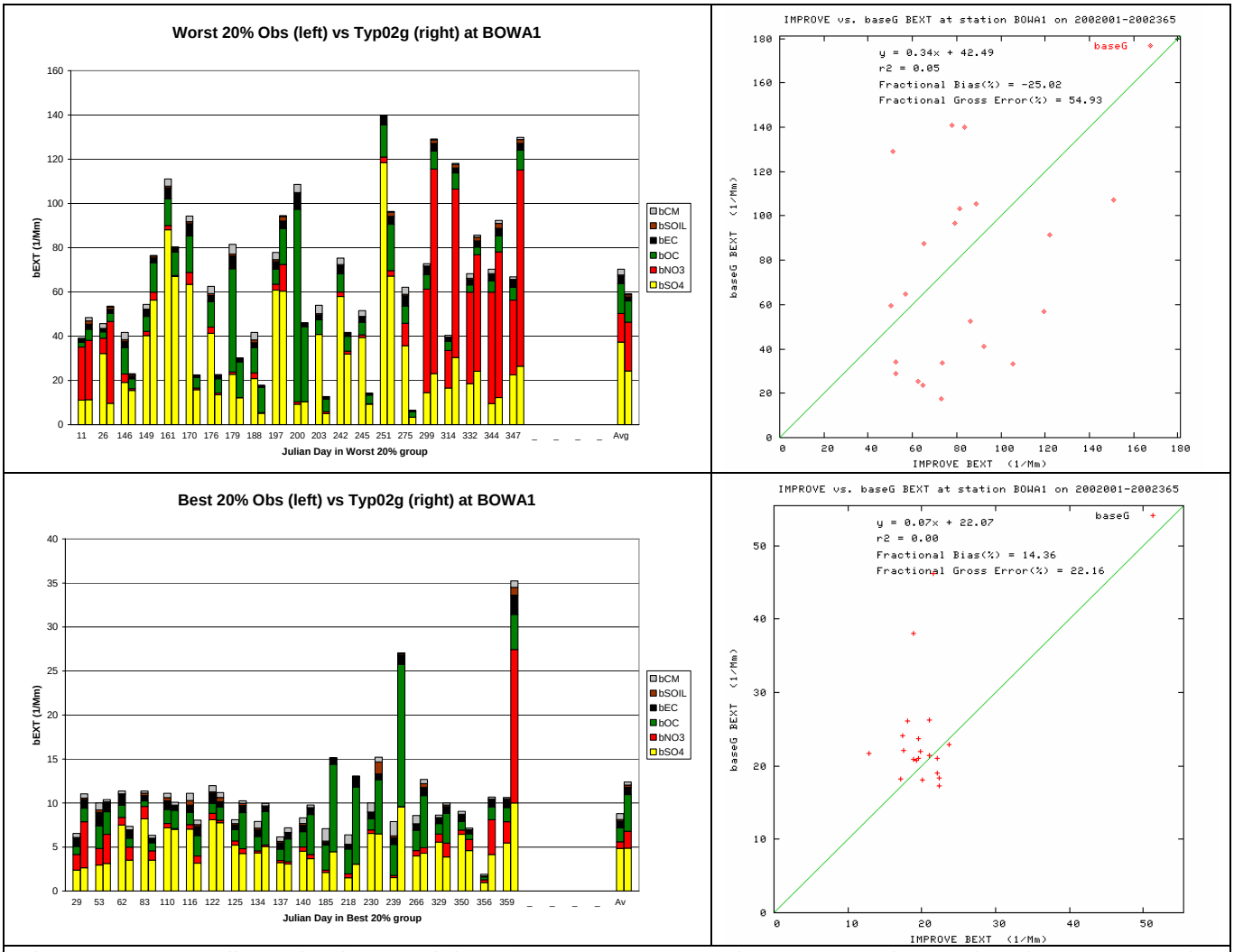

Figure 3-12. Daily extinction model performance at Boundary Waters (BOWA), Minnesota for the worst (top) and best (bottom) 20 percent days during 2002.

3.7.5 Voyageurs (VOYA) Minnesota

VOYA is also characterized by SO4, NO3 and OMC days (Figure 3-13). Julian Days 179 and 200 are high OMC days that were also high OMC days at BOWA again indicating impacts from fires in the area that is not fully captured by the model. SO4 and NO3 performance is fairly good and, without the fire days, OMC performance looks good as well (Figure C-52). On the best 20 percent days there is one day the modeled extinction is much higher than observed and a few others that are somewhat higher, but for most of the best 20 percent days the modeled extinction is comparable to the observed values.

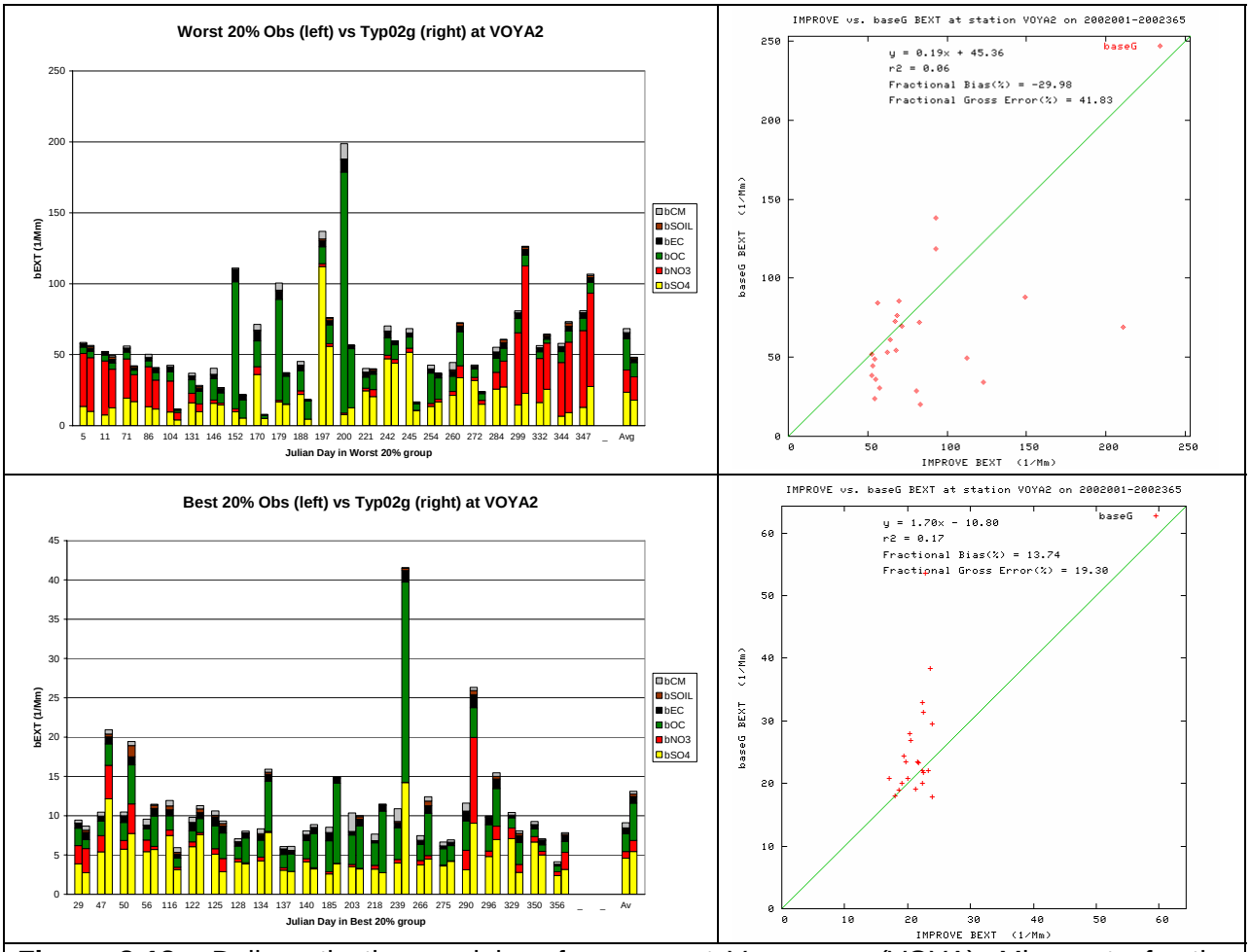

Figure 3-13. Daily extinction model performance at Voyageurs (VOYA), Minnesota for the worst (top) and best (bottom) 20 percent days during 2002.

3.7.6 Hercules Glade (HEGL) Missouri

On most of the worst 20 percent days at HEGL the observed extinction ranges from 120 to 220 Mm^{-1} whereas model extinction ranges from 50 to 170 Mm^{-1} (Figure 3-14). However, there is one extreme day with extinction approaching 400 Mm^{-1} that the model does a very good job in replicating. Over all the days there is a modest underestimation bias in SO4 (-39%) and OMC (-39%) extinction, larger underestimation bias in EC (-62%) and CM (-118%) extinction and overestimation bias in Soil (+30%) extinction (Figure C-53).

On the best 20 percent days there is one day where the model overstates the observed extinction by approximately a factor of four and a handful of other days that the model overstates the extinction by a factor of 2 or so, but most of the days both the model and observed extinction sites are around 40 Mm^{-1} ±10 Mm^{-1}. On the best 20 percent days, when the observed extinction is overstated, it is due to overstatement of the NO3.

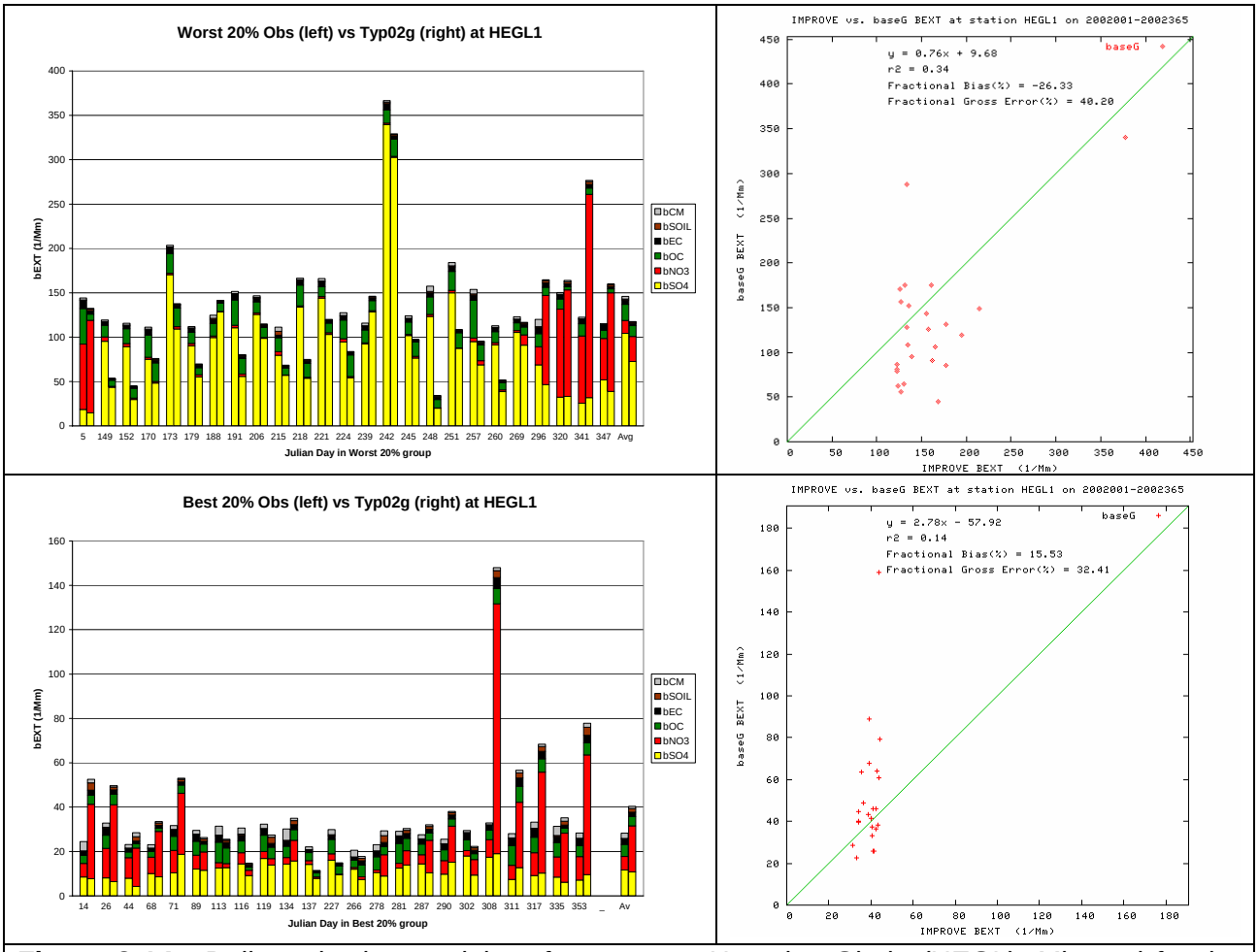

Figure 3-14. Daily extinction model performance at Hercules Glade (HEGL), Missouri for the worst (top) and best (bottom) 20 percent days during 2002.

3.7.7 Mingo (MING) Missouri

The worst 20 percent days at MING are mainly high SO4 days with a few high NO3 days that the model reproduces reasonably well resulting in low bias (+10%) and error (38%) for total extinction (Figure 3-15). The PM species specific performance is fairly good with low bias for SO4 (+4%), good agreement with NO3 on high NO3 days except for one day, low OMC (+23%) and EC (+3%) bias and larger bias in EC (+37%) and CM (-105%) extinction (Figure C-54).

For the best 20 percent days, there is one day the model is way too high due to overstated NO3 extinction and a few other days the model overstates the observed extinction that is usually due to overpredicted NO3, but on most of the best 20 percent days the modeled extinction is comparable to the observed values. This results in low bias (+12%) and error (36%) for total extinction at MING for the best 20 percent days.

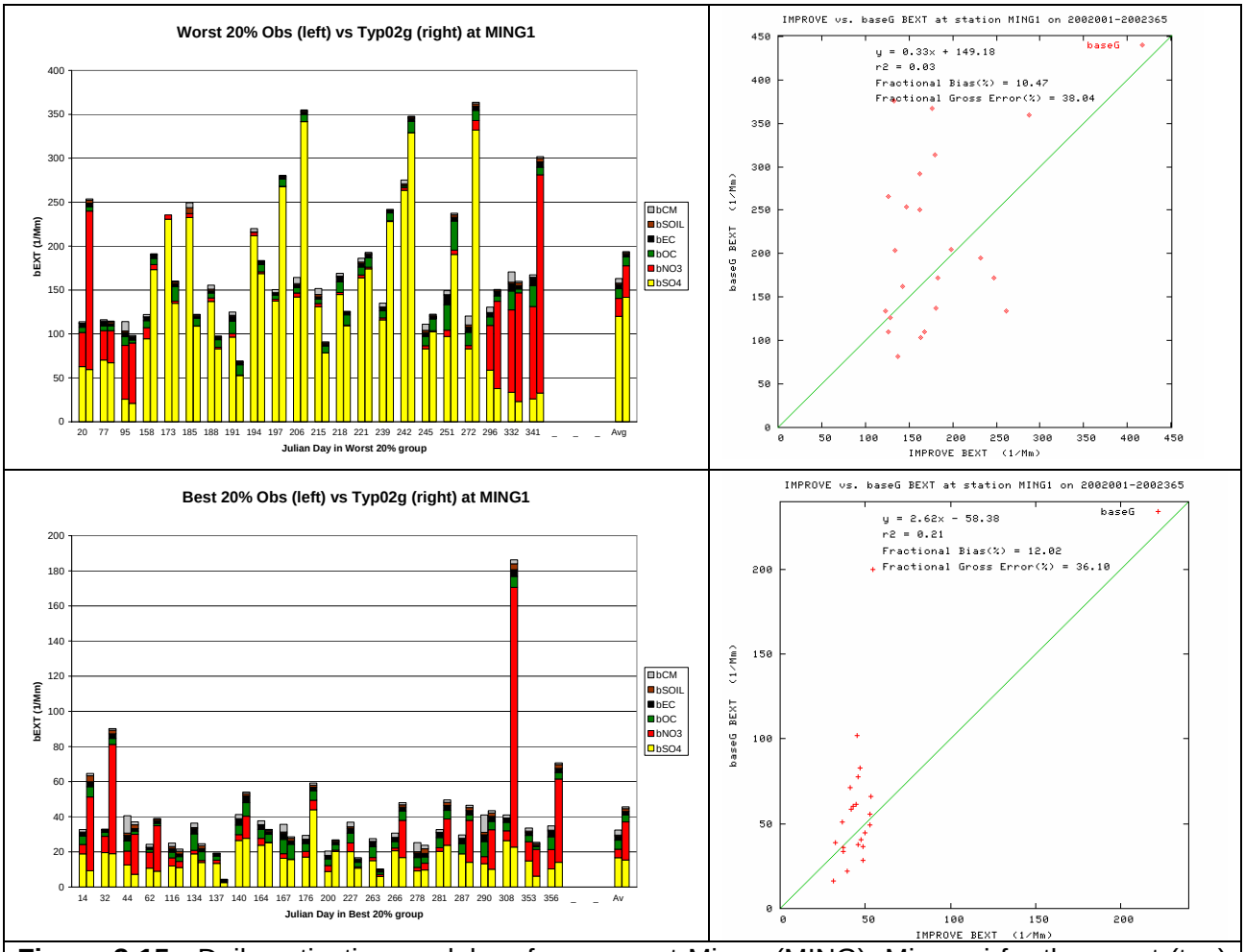

Figure 3-15. Daily extinction model performance at Mingo (MING), Missouri for the worst (top) and best (bottom) 20 percent days during 2002.

3.7.8 Wichita Mountains (WIMO), Oklahoma

With the exception of an overprediction on day 344 due to NO3, observed total extinction on the worst 20 percent days at WIMO is understated with a bias of -42% (Figure 3-16) that is primarily due to an underestimation of extinction due to SO4 (-48%) and OMC (-69%) (Figure C-55).

CMAQ total extinction performance for the average of the best 20 percent days at WIMO is characterized by an overestimation bias (+21%) on most days that is primarily due to NO3 overprediction on several days. Again the modeled range of extinction on the best 20 percent days (12-60 Mm^{-1}) is much greater than observed (20-35 Mm^{-1}).

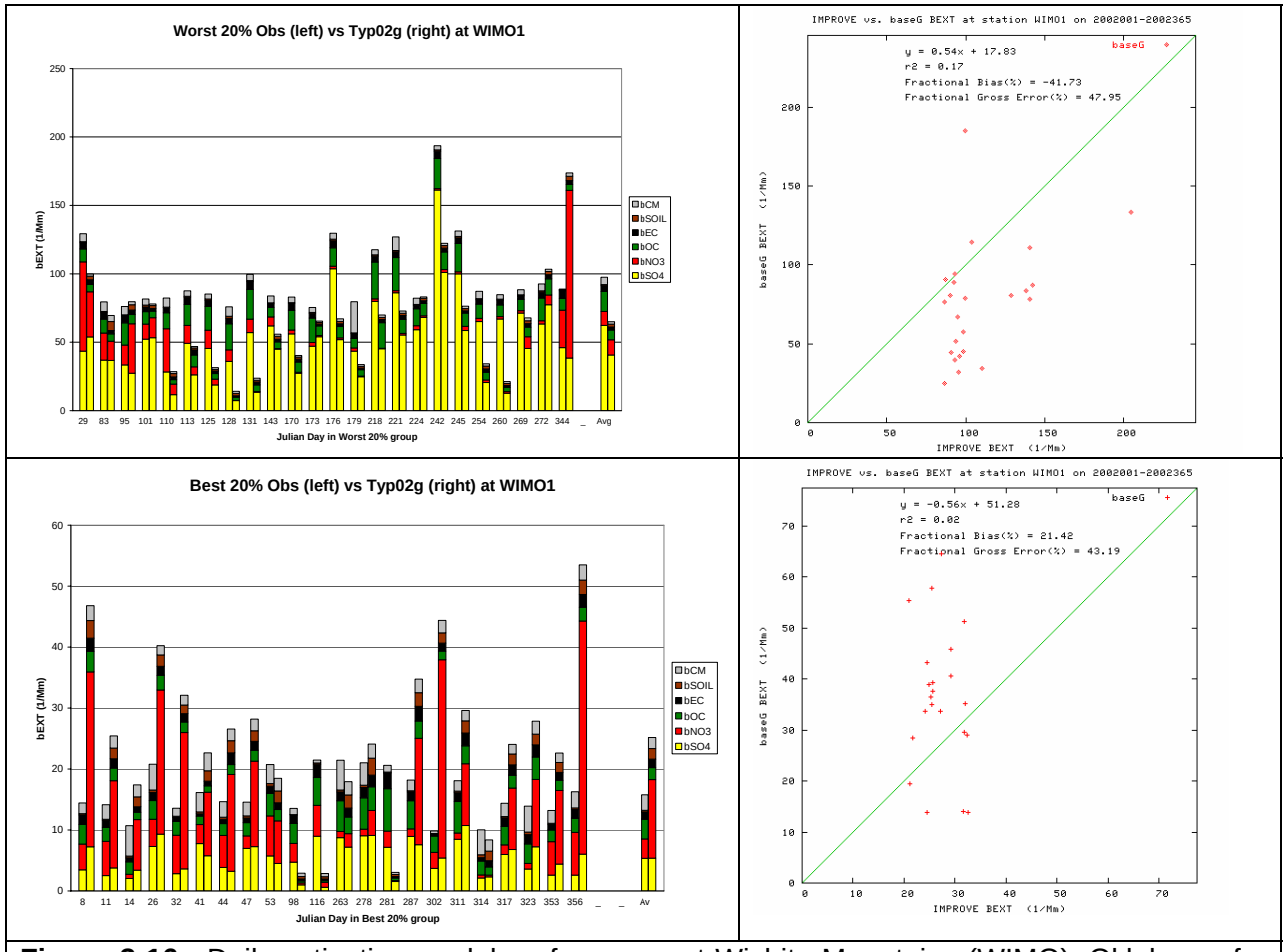

Figure 3-16. Daily extinction model performance at Wichita Mountains (WIMO), Oklahoma for the worst (top) and best (bottom) 20 percent days during 2002.

3.7.9 Big Bend (BIBE) Texas

The observed extinction on the worst 20 percent days at BIBE is underpredicted on almost every day resulting in a fractional bias value of -72% (Figure 3-17). Every component of extinction is underestimated on average for the worst 20 percent days (Figure C-56) with the underestimation bias ranging from -24% (OMC) to -162% (CM). SO4 extinction, that typically represents the largest component of the total extinction is understated by -94%.

The model does a better job in predicting the total extinction at BIBE for the best 20 percent days with average fractional bias and error values of +13% and 19% (Figure 3-17). With the exception of one day that the observed extinction is overestimated by approximately a factor of 2, the modeled and observed extinction on the best 20 percent days at BIBE are both within 12 to 25 Mm^{-1}. However, there are some mismatches with the components of extinction with the model estimating much lower contributions due to Soil and CM.

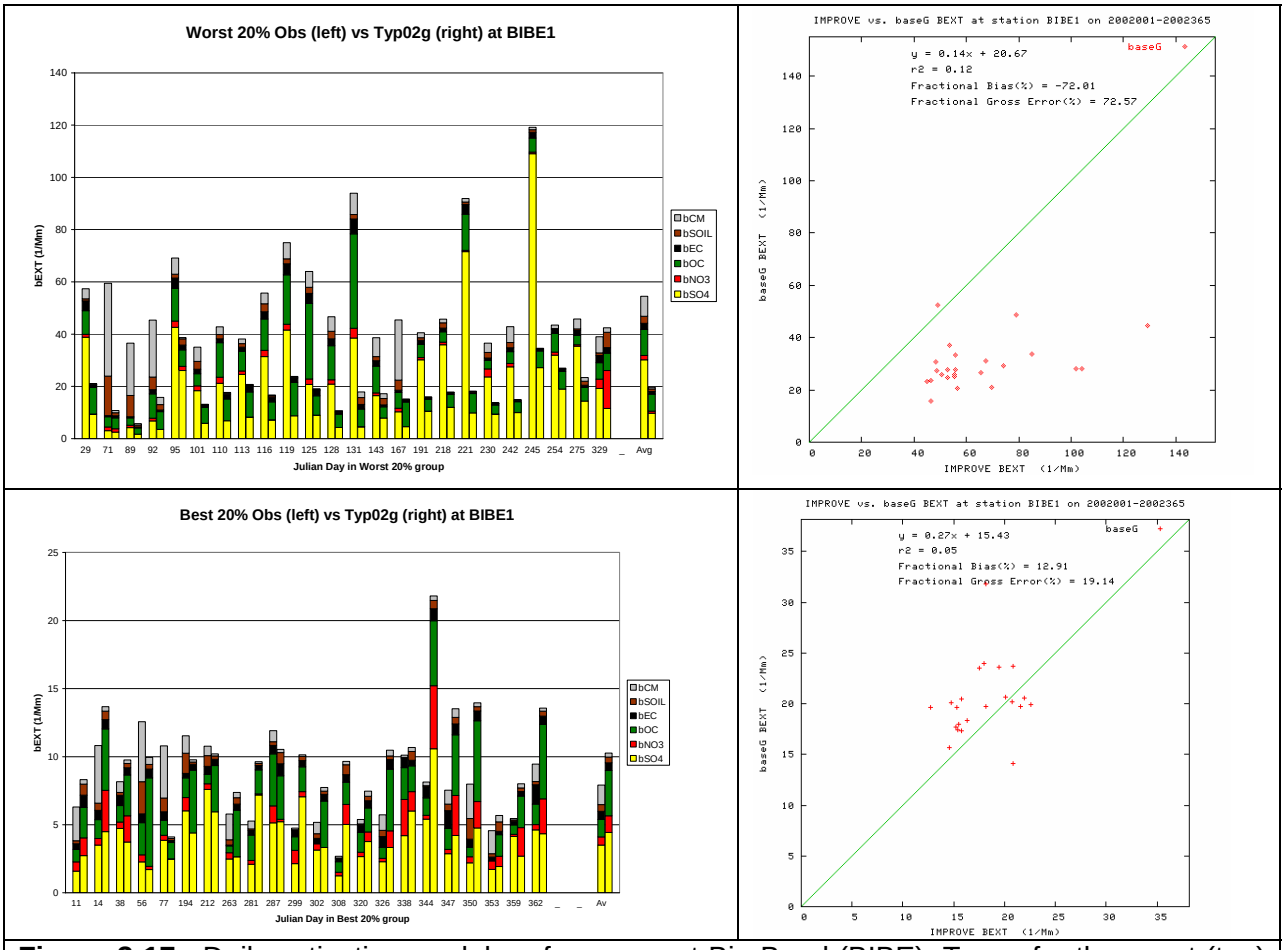

Figure 3-17. Daily extinction model performance at Big Bend (BIBE), Texas for the worst (top) and best (bottom) 20 percent days during 2002.

3.7.10 Guadalupe Mountains (GUMO) Texas

Most of the worst 20 percent days at GUMO are high dust days with high Soil and CM that is not captured by the model (Figure 3-18). Extinction due to Soil and CM on the worst 20 percent days is underestimated by -105% and -191%, respectively (Figure C-57). Better performance is seen on the best 20 percent days with bias and error for total extinction of 8% and 21%, but the model still understates Soil and CM.

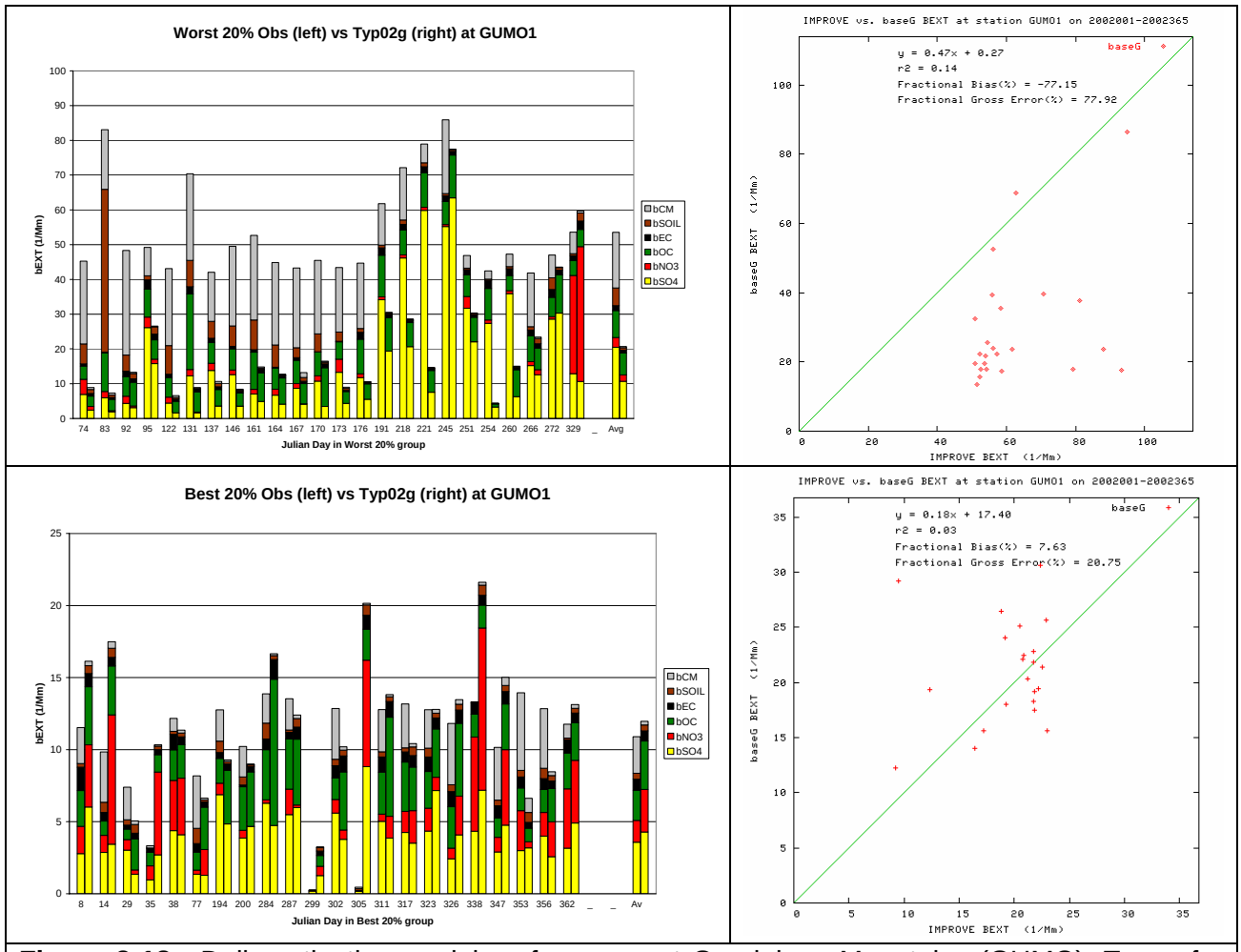

Figure 3-18. Daily extinction model performance at Guadalupe Mountains (GUMO), Texas for the worst (top) and best (bottom) 20 percent days during 2002.

3.8 Model Performance Evaluation Conclusions

The model performance evaluation reveals that the model is performing best for SO4, OMC and EC. Soil performance is mixed with a winter overestimation bias with lower bias and higher error in the summer. CM performance is poor year round. The operational evaluation reveals that SO4 performance usually achieves the PM model performance goal and always achieves the model performance criteria, although it does have an underestimation bias that is greatest in the summer. NO3 performance is characterized by a winter overestimation bias with an even greater summer underestimation bias. However, the summer underestimation bias occurs when NO3 is very low and when it is not an important component of the observed or predicted PM mass concentrations or component of visibility impairment. Performance for OMC meets the model performance goal year round at the IMPROVE sites, but is characterized by an underestimation bias at the more urban STN sites. EC exhibits very low bias at the STN sites and a summer underestimation bias at the IMPROVE sites, but meets the model performance goal throughout the year. Soil has a winter overestimation bias that is outside of the model performance goal and criteria raising questions whether the model should be used for this species. Finally, CM performance is extremely poor with an underprediction bias that is outside of the performance goal and criteria. We suspect that much of the CM concentrations measured at the IMPROVE sites is due to highly localized emissions from fugitive dust sources that are not included in the emissions inventory and would be difficult to simulate using 36 km regional modeling.

Performance for the worst 20 percent days at the CENRAP Class I areas is generally characterized by an underestimation bias. Performance at the BRET, BIBE and GUMO Class I areas for the worst 20 percent days is particularly suspect and care should be taken in the interpretation of the visibility projections at these three Class I areas.

The CMAQ 2002 36 km model appears to be working well enough to reliably make future-year projections for changes in SO4, NO3, EC and OMC at the rural Class I areas. Performance for Soil and especially CM is suspect enough that care should be taken in interpreting these modeling results. The model evaluation focused on the model's ability to predict the components of light extinction mainly at the Class I areas. Additional analysis would have to be undertaken to examine the model's ability to simulate ozone and fine particulate to address 8-hour ozone and $PM_{2.5}$ attainment issues.

4.0 VISIBILITY PROJECTIONS

This section presents the future-year visibility projections for Class I areas within and near the CENRAP states and their comparison with the 2018 Uniform Rate of Progress (URP) point. As noted in Chapter 1, the Regional Haze Rule (RHR) requires states with Class I areas to develop State Implementation Plans (SIPs) that include reasonable progress goals (RPGs) for improving visibility in each Class I area and emission reduction measures to meet those goals. For the initial SIPs due in December 2007, states are required to adopt RPGs for improving visibility from Baseline Conditions. The 2000-2004 five-year period is used to define Baseline Conditions and the first future progress period is 2018. A state is required to set RPGs for each Class I area in the state for two visibility metrics:

- Provide for an improvement in visibility for the most impaired visibility days (i.e., the worst 20 percent days); and

- Ensure no degradation in visibility for the least impaired visibility days (i.e., the best 20 percent days).

The goal of the RPGs is to provide for a rate of improvement sufficient to be on a course to attain "Natural Conditions" by 2064. States are to define controls to meet RPGs every 10 years, starting in 2018, which defines progress periods ending in 2018, 2028, 2038, 2048, 2058 and finally 2064. States will determine whether they are meeting their goals by comparing visibility conditions from one five-year period to another (e.g., 2000-2004 to 2013-2017). As stated in 40 CFR 51.308 (d) (1), baseline visibility conditions, reasonable progress goals, and changes in visibility must be expressed in terms of deciview (dv) units. The haze index (HI) metric of visibility impairment, in deciviews, is derived from light extinction (b_{ext}) as follows:

$$HI = 10 \ln (b_{ext}/10),$$

Where light extinction (b_{ext}) is expressed in terms of inverse megameters ($Mm^{-1} = 10^{-6}\ m^{-1}$). Light extinction ($b_{ext}$) is calculated using the observed fine particulate concentrations from the IMPROVE monitors using either the original or the new IMPROVE aerosol extinction equation. Both equations are discussed below.

4.1 Guidance for Visibility Projections

EPA has published several guidance documents that relate to how modeling results should be used to project future-year visibility and how states should define RPGs:

"Guidance on the Use of Models and Other Analyses for Demonstrating Attainment of Air Quality Goals for Ozone, $PM_{2.5}$ and Regional Haze" (EPA, 2007a).

"Guidance for Tracking Progress Under the Regional Haze Rule" (EPA, 2003a).

"Guidance for Estimating Natural Visibility Conditions Under the Regional Haze Rule" (EPA, 2003b).

"Guidance for Setting Reasonable Progress Goals Under the Regional Haze Program" (EPA, 2007b).

The first EPA modeling guidance document listed above (EPA, 2007) discusses the use of modeling results to project future-year visibility. The second EPA guidance document (EPA, 2003a) focuses on monitored visibility, how to define the visibility Baseline Conditions and how to track visibility goals. The third EPA guidance document discusses procedures for defining Natural Conditions for a Class I area. Natural Conditions are the visibility goal for 2064. Although states may propose alternative approaches for defining Natural Conditions, in this section we use the default Natural Conditions at Class I areas (EPA, 2003b; Pitchford, 2006). The final EPA guidance document discusses how states should define their RPGs and their relationship to the 2018 URP point.

The EPA documents discussed above are followed for the visibility projections presented in this section with one notable exception. Some of the EPA documents are based on the original IMPROVE equation (e.g., EPA, 2003a, b). The CENRAP visibility projections are based on the new IMPROVE equation, although projections based on the original IMPROVE equation are also presented as an alternative approach in Chapter 5. EPA guidance allows for using either the original or the new IMPROVE equation (EPA, 2007a; Timin, 2007). CENRAP, along with the other RPOs, have elected to use the new IMPROVE equation for their visibility projections.

4.2 Calculation of Visibility and 2018 URP Point from IMPROVE Measurements

EPA guidance recommends using the model in a relative sense to project future-year visibility conditions (EPA, 2007a). This projection is made using Relative Response Factors (RRFs) that are defined as the ratio of the future-year modeling results to the base-year modeling results. The RRFs are applied to the baseline visibility conditions to project future-year visibility. The major features of EPA's recommended visibility projection approach are as follows (EPA, 2003a,b; 2007a):

- Monitored data are used to define current visibility Baseline Conditions using IMPROVE monitoring data from the 2000-2004 five-year base period.

- Monitored concentrations of PM_{10} are divided into six major components, the first five of which are assumed to be $PM_{2.5}$ and the sixth is coarse mass (CM or $PM_{2.5-10}$).
  - SO4 (sulfate) that is assumed to be ammonium sulfate [$(NH_4)_2SO_4$];
  - NO3 (particulate nitrate) that is assumed to be ammonium nitrate [NH_4NO_3];
  - OC (organic carbon) that is assumed to be total organic mass carbon (OMC)
  - EC (elemental carbon);
  - IP (other fine inorganic particulate or Soil); and
  - CM (coarse mass).

- Models are used in a relative sense to develop RRFs between baseline and future predicted concentrations of each component.

- PM component-specific RRFs are multiplied by observed Baseline monitored values to estimate future-year PM component concentrations.

- Estimates of future-year component concentrations are consolidated to provide an estimate of future-year air quality and visibility using either the original or new IMPROVE equation.

- Future-year model projected visibility is compared with the 2018 point on the URP glidepath to assist in evaluating the visibility improvements.

- It is assumed that all measured sulfate is in the form of ammonium sulfate [$(NH_4)_2SO_4$] and all particulate nitrate is in the form of ammonium nitrate [NH_4NO_3].

In order to facilitate tracking visibility progress, three important visibility concepts are required for each Class I area:

Baseline Conditions: Baseline Conditions represent visibility for the 20 percent best (B20%) and 20 percent worst (W20%) visibility days for the initial five-year baseline period of the regional haze program. Baseline Conditions are calculated using IMPROVE monitor data collected during the 2000-2004 five-year period and are the starting point in 2004 for the URP glidepath and 2018 visibility projections.

Natural Conditions: Estimates of natural visibility conditions for the best 20 percent and worst 20 percent days at a Class I area (i.e., visibility conditions that would be experienced in the absence of human-caused impairment). EPA has defined a set of default Natural Conditions for the original IMPROVE equation (EPA, 2003b) that has been updated to the new IMPROVE equation by the Natural Haze Levels II Committee (Pitchford, 2006) that we have used in this Chapter.

2018 URP Point: The 2018 Uniform Rate of Progress (URP) point is defined by defining a linear glidepath in deciviews starting with the 2000-2004 Baseline Conditions in 2004 and ending at Natural Conditions in 2064. Where the linear glidepath passes through 2018 is the 2018 URP point in deciviews.

4.2.1 Calculation of Visibility from IMPROVE PM Measurements

Baseline Conditions for Class I areas are calculated using the procedures in EPA's guidance document (EPA, 2003a) and fine and coarse particulate matter concentrations measured at IMPROVE monitors (Malm et al, 2000; Debell et al., 2006). Currently, each Class I area in the CENRAP domain has an associated IMPROVE monitor. The IMPROVE monitors do not directly measure visibility, but instead measure speciated fine particulate ($PM_{2.5}$) and total $PM_{2.5}$ and PM_{10} mass concentrations from which visibility is obtained through the IMPROVE equation.

Visibility conditions are estimated starting with the IMPROVE 24-hour average mass measurements for six PM species:

- Sulfate [$(NH_4)_2SO_4$];
- Particulate Nitrate [$(NH_4NO_3$];
- Organic Matter Carbon or Organic Mass by Carbon [OMC];
- Elemental Carbon [EC] or Light Absorbing Carbon [LAC];
- Other fine particulate [Soil]; and
- Coarse Matter or Coarse Mass [CM].

The IMPROVE monitors do not directly measure some of these species so assumptions are made as to how the IMPROVE measurements can be adjusted and combined to obtain these six components of light extinction. For example, in the IMPROVE equation sulfate and particulate nitrate are assumed to be completely neutralized by ammonium. In addition, only the fine mode ($PM_{2.5}$) of PM is speciated by the IMPROVE monitor to obtain sulfate and nitrate measurements (that is, any coarse mode sulfate and nitrate in the real atmosphere may be present in the CM IMPROVE measurement). Concentrations for the above six components of light extinction in the IMPROVE equation are obtained from the IMPROVE measured species using the mappings shown in Table 4-1:

Table 4-1. Definition of IMPROVE PM Components from Measured IMPROVE Species.

IMPROVE Component	IMPROVE Measured Species
Sulfate	1.375 x (3 x S)
Nitrate	1.29 x NO_3^-
OMC	1.4*OC (original IMPROVE) and 1.8*OC (new IMPROVE)
LAC	EC
Soil	2.2*AL + 2.49*SI + 1.63*CA + 2.42*FE + 1.94*TI
CM	MT – MF

Where:

- S is elemental sulfur as determined from proton induced x-ray emissions (PIXE) analysis of the IMPROVE Module A[1]. To estimate the mass of the sulfate ion ($SO_4^=$), S is multiplied by 3 to account the presence of oxygen. If S is missing then the sulfate (SO_4) measured by ion chromatography analysis of the Module B is used to replace (3 x S). For the IMPROVE aerosol extinction calculation, Sulfate is assumed to be completely neutralized by ammonium (1.375 x SO_4).
- NO_3^- is the particulate nitrate measured by ion chromatography analysis of the Module B. For the IMPROVE aerosol extinction calculation, it is assumed to be completely neutralized by ammonium (1.29 x NO_3^-).
- The IMPROVE Organic Carbon (OC) measurements are multiplied by 1.4 to obtain Organic Mass Carbon (OMC) using the original IMPROVE equation and multiplied by 1.8 for the new IMPROVE equation. This adjustment of the measured OC accounts for mass due to other elements in the OMC besides Carbon.
- Elemental Carbon (EC) is also referred to as Light Absorbing Carbon (LAC).

[1] The IMPROVE sampler consists of four independent modules (A, B, C and D). Each module incorporates a separate inlet, filter pack and pump assembly and are controlled by a common timing mechanism. Module A measures fine PM mass and elements. Module B measures sulfate and nitrate ions. Module C measures EC and OC. Module D measures PM_{10} mass. (see http://vista.cira.colostate.edu/improve/ for more details).

- Soil is determined as a sum of the masses of those elements (measured by PIXE) predominantly associated with soil (Al, Si, Ca, Fe, K and Ti), adjusted to account for oxygen associated with the common oxide forms. Since K and FE are products of the combustion of vegetation, they are both represented in the formula by 0.6 x Fe and K is not shown explicitly.
- MT and MF are total PM_{10} and $PM_{2.5}$ mass, respectively.

4.2.1.1 Original and New IMPROVE Equations

Associated with each PM species is an extinction efficiency that converts concentrations (in $\mu g/m^3$) to light extinction (in inverse megameters, Mm^{-1}). Sulfate and nitrate are hygroscopic which means that they can absorb water from the atmosphere which changes their extinction efficiency. This is accounted for through relative humidity adjustment factors [f(RH)] that increase the particle's extinction efficiency with increasing RH to account for the particles taking on water Note that some OMC may also have hygroscopic properties, but the IMPROVE equations assume OMC is non-hygroscopic.

There are currently two IMPROVE equations that are used to convert the measured PM concentrations to light extinction, the original (or old) and the new IMPROVE equations.

4.2.1.1.1 Original IMPROVE Equation

The original IMPROVE equation that converts PM species concentrations to light extinction is given as follows:

$b_{Sulfate}$ = 3 x f(RH) x [Sulfate]
$b_{Nitrate}$ = 3 x f(RH) x [Nitrate]
b_{EC} = 10 x [EC]
b_{OMC} = 4 x [OMC]
b_{Soil} = 1 x [Soil]
b_{CM} = 0.6 x [CM]

Monthly average f(RH) factors are used as recommended in EPA's guidance (EPA, 2003a). These values are available in the final EPA guidance document (EPA, 2003a) and at: ftp://ftp.saic.com/raleigh/RegionalHaze_2002FRHcurve/fRH_analysis/.

The total light extinction (b_{ext}) is assumed to be the sum of the light extinction due to the six PM species listed above plus Rayleigh (blue sky) background (b_{Ray}) that is assumed to be 10 Mm^{-1}.

$$b_{ext} = b_{Ray} + b_{Sulfate} + b_{Nitrate} + b_{EC} + b_{OMC} + b_{Soil} + b_{CM}$$

The total light extinction (b_{ext}) in Mm^{-1} is related to visual range (VR) in km using the following relationship:

$$VR = 3912 / b_{ext},$$

for b_{ext} in Mm^{-1}.

The Regional Haze Rule requires that visibility be expressed in terms of a haze index (HI) in units of deciviews (dv), which is calculated as follows:

$$HI = 10 \ln(b_{ext}/10)$$

4.2.1.1.2 New IMPROVE Equation

The new IMPROVE equation is nonlinear in SO4, NO3 and OMC concentrations accounting for the different light scattering efficiency characteristics as a function of concentrations for these three species. It is expressed as follows:

$b_{Sulfate}$ = 2.2 x f_S(RH) x [Small Sulfate] + 4.8 f_S(RH) x [Large Sulfate]
$b_{Nitrate}$ = 2.4 x f_S(RH) x [Small Nitrate] + 5.1 f_S(RH) x [Large Nitrate]
b_{EC} = 10 x [Elemental Carbon]
b_{OMC} = 2.8 x [Small Organic Mass] + 6.1 x [Large Organic Mass]
b_{Soil} = 1 x [Fine Soil]
b_{CM} = 0.6 x [Coarse Mass]
b_{NaCl} = 1.7 x f_{SS}(RH) x [Sea Salt]
b_{NO2} = 0.33 x [NO_2 (ppb)]

The total Sulfate, Nitrate and OMC are each split into two fractions, representing small and large size distributions of those components. As noted in Table 4-1, the OMC is 1.8 times the IMPROVE OC measurement in the new IMPROVE algorithm, compared to 1.4 times the IMPROVE OC measurement in the original IMPROVE equation. New terms have been added for Sea Salt (important for coastal areas and possibly other areas)and for light absorption by NO2 (only used where NO2 observations are available). As none of the CENRAP Class I area IMPROVE sites measure NO2 concentrations, then this component of the new IMPROVE equations was not used. Site-specific Rayleigh scattering for each IMPROVE monitoring site is used in the new IMPROVE equation, as compared to a constant 10 Mm^{-1} value assumed in the original IMPROVE equation.

The apportionment of the Small and Large components of Sulfate, Nitrate and Organic Mass is done as follows:

[Large Sulfate] = [Total Sulfate] / 20 x [Total Sulfate], for [Total Sulfate] < 20 $\mu g/m^3$

[Large Sulfate] = [Total Sulfate], for [Total Sulfate] $\geq$ 20 $\mu g/m^3$

[Small Sulfate] = [Total Sulfate] – [Large Sulfate]

The same equations are used to apportion Total Nitrate and Total OMC among their Large and Small components.

The total extinction (b_{ext}) in the new IMPROVE equations is the sum of all the extinction components associated with each PM species. The new IMPROVE equation adds Sea Salt and

NO_2 as noted above. In addition, site-specific Rayleigh background is used with the new IMPROVE equation:

$$b_{ext} = b_{Ray} + b_{Sulfate} + b_{Nitrate} + b_{EC} + b_{OMC} + b_{Soil} + b_{CM} + b_{NaCl} + b_{NO2}$$

The Haze Index (HI) and Visual Range (VR) are calculated from the total extinction from the new IMPROVE equation using the same formulas as given above for the original IMPROVE equation.

4.2.1.1.3 Justification for Using the New IMPROVE Equation

The new IMPROVE equation was developed using the latest scientific information on PM species extinction properties combined with fitting reconstructed light extinction based on IMPROVE measured PM and NO2 concentrations with actual co-located measured light extinction (e.g., nephelometer measurements). Figure 4-1 displays example comparisons of 24-hour light extinction using the original and new IMPROVE equations compared against 24-hour nephelometer measurements of light extinction at the Great Smoky Mountains Class I area IMPROVE monitor. The original IMPROVE equation has a bias toward understating light extinction at the high end and overstating it at the low end, whereas the new IMPROVE equation does a better job in estimating light extinction from measured PM at all extinction levels. Because the new IMPROVE equation is based on more recent science and fits the observed light extinction values better, the CENRAP states have elected to perform their primary visibility projections using the new IMPROVE equation. Results using the original IMPROVE equation are presented in Section 5 as an alternative approach.

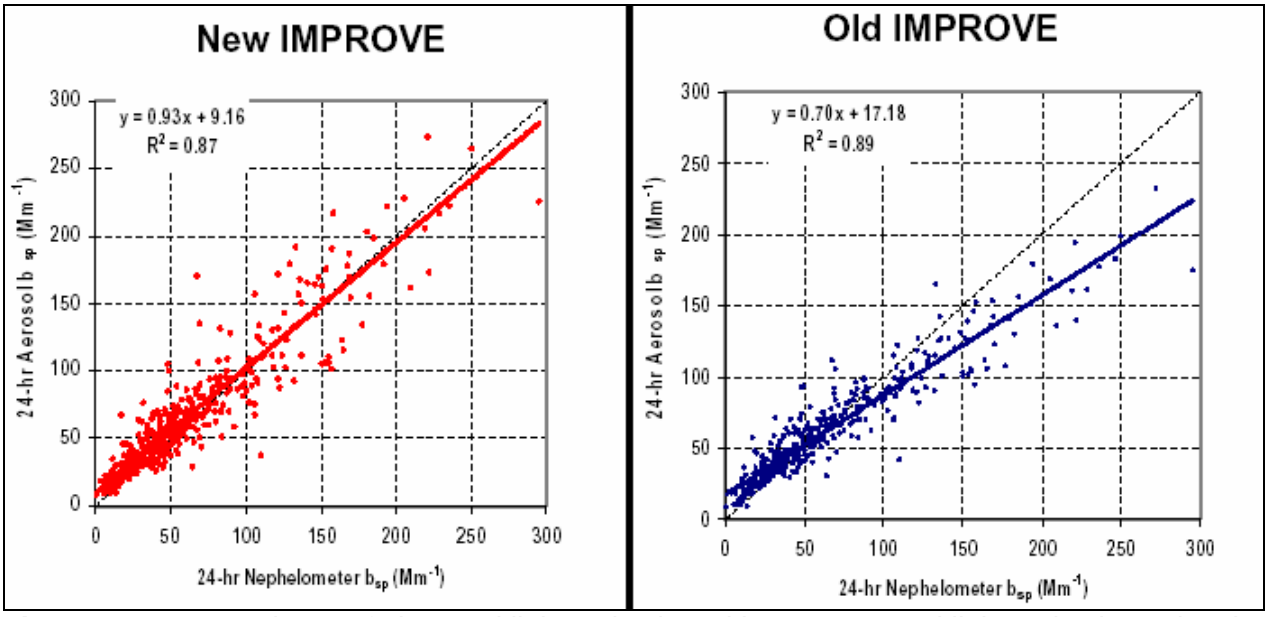

Figure 4-1. Comparisons of observed light extinction with reconstructed light extinction using the new (left) and original (right) IMPROVE equations at the Great Smoky Mountains National Park.

4.2.2 Calculation of the Baseline Conditions

The visibility Baseline Conditions for the worst 20 percent and best 20 percent days is calculated from the IMPROVE observations from the 2000-2004 period for each Class I area following EPA's guidance (EPA, 2003a). The basic procedures for calculating the Baseline Conditions are as follows:

1. Determine whether the observed IMPROVE data for each site and year satisfies EPA's minimal data capture criteria (EPA, 2003a). If there are less than three years with valid data capture for the 2000-2004 Baseline then the Baseline Conditions can not be calculated and data filling is needed.
2. For each year in the 2000-2004 period with sufficient valid data, rank the visibility in terms of extinction or deciview using either the original or new IMPROVE equation and monthly average f(RH) factors (EPA, 2003a).
3. For the worst 20 percent days, extract the 20% most impaired visibility days for each year (similarly for best 20 percent days extract 20% cleanest days). With a complete yearly data capture of IMPROVE 1:3 day sampling frequency this would result in 24 worst 20 percent and 24 best 20 percent days in a year.
4. For each worst 20 percent (or best 20 percent) day in each year, calculate 24-hour average visibility extinction using the IMPROVE measurements and either the original and new IMPROVE equation, convert the daily extinction to daily deciview and then average across each year to get yearly average deciview extinction for the worst 20 percent (or best 20 percent) days for each valid year from the 2000-2004 period.
5. Average the annual average deciview worst 20 percent (or best 20 percent) days deciview across each valid year in the 2000-2004 period (minimum of 3 valid years required) to get the worst 20 percent (or best 20 percent) Baseline Conditions.

4.2.3 Data Filling for Sites with Insufficient Valid Data to Calculate Baseline Conditions

Three CENRAP Class I areas did not contain sufficient IMPROVE observations during the five-year 2000-2004 Baseline to have three valid years of data from which Baseline Conditions could be constructed: Breton Island (BRET), Louisiana; Boundary Waters (BOWA), Minnesota and Mingo (MING), Missouri. For these three Class I areas, data filling was used to obtain sufficient data so that at least three-years of valid data were available from which Baseline Conditions could be calculated. These data filled IMPROVE databases were prepared and made available on the VIEWS website. More information on the data filling procedures can be found at the VIEWS website: (http://vista.cira.colostate.edu/views/).

4.2.4 Natural Conditions

EPA has published default Natural Conditions for Annual Average and the worst 20 percent and best 20 percent days based on the original IMPROVE equation (EPA, 2003b). These default Natural Conditions have been updated to the new IMPROVE equation by the Natural Haze Levels II Committee (Pitchford, 2006). These default Natural Conditions are used as the anchor point for the glidepaths in 2064 and are provided in Appendix D for the CENRAP Class I areas.

4.2.5 2018 URP Point

The 2018 point on the Uniform Rate of Progress (URP) glidepath is constructed by generating a linear glidepath in deciviews from the Baseline Conditions in 2004 to Natural Conditions in 2064. Where the linear glidepath crosses 2018 is the 2018 point on the URP glidepath or the 2018 URP point. Figure 4-2 displays an example linear glidepath for the Caney Creek Class I area in Arkansas. There are three years of sufficient valid IMPROVE data during the 2000-2004 Baseline (2002, 2003 and 2004) with values of 27.21, 26.52 and 25.34 dv resulting in worst 20 percent Baseline Conditions of 26.36 dv that is placed as the starting point in 2004 for the glidepath. The ending point for the glidepath is 11.58 dv which is the default Natural Conditions for the worst 20 percent days (EPA, 2003b; Pitchford, 2006). The linear glidepath crosses 2018 at 22.91 dv which becomes the 2018 URP point.

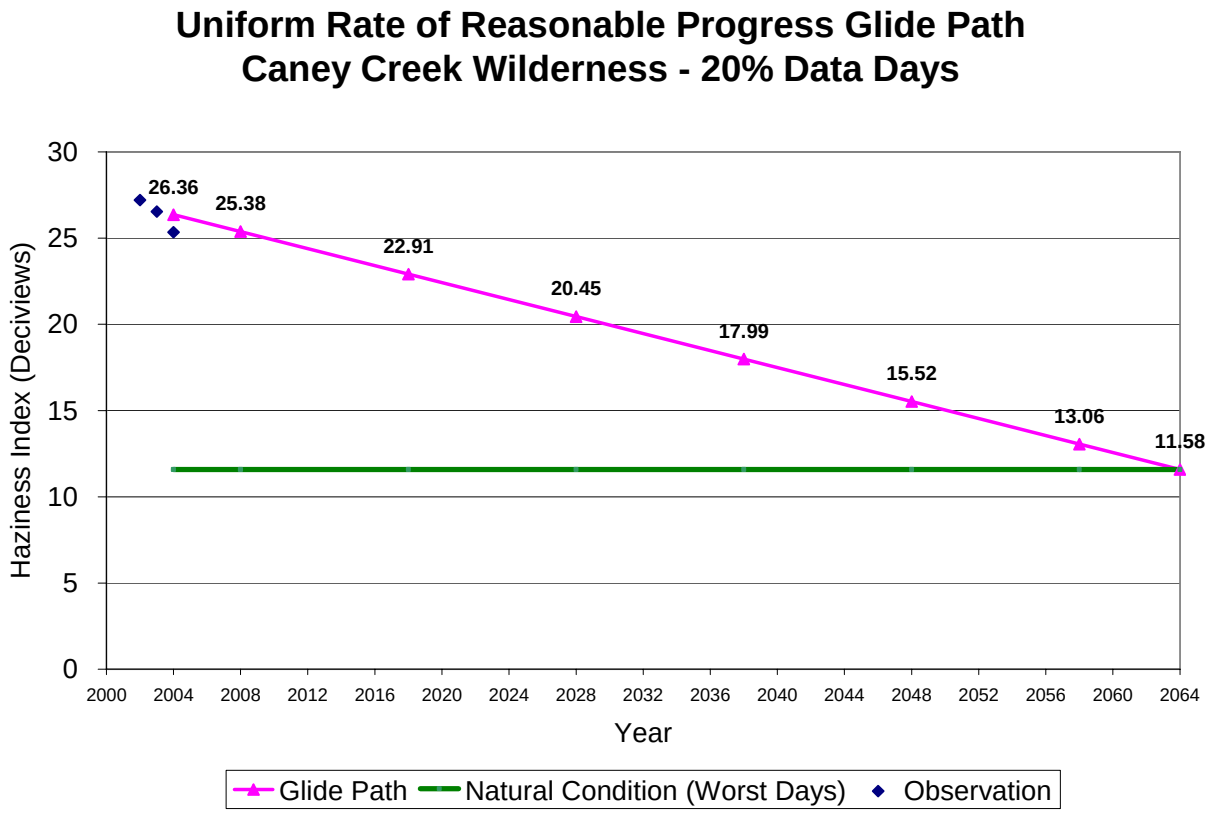

Figure 4-2. Linear Glidepath for Caney Creek (CACR), Arkansas that linearly connects the 26.36 dv Baseline Conditions in 2004 with the 11.58 dv Natural Conditions in 2064 resulting in a 22.91 dv 2018 URP Point.

4.3 EPA Default Approach to Visibility Projections

For CENRAP's model application for a single year (2002), EPA's regional haze modeling guidance recommends developing Class I area-specific and PM species-specific RRFs based on the average concentrations for the worst 20 percent days from 2002 (EPA, 2007). Thus, this is

the methodology used to project 2018 visibility estimates in this section. For example, if $SO4(2002)_i$ and $SO4(2018)_i$ are the model estimated sulfate concentrations for the 2002 worst 20 percent days (i=1…N) at a given Class I area for the 2002 and 2018 emission scenarios then the RRF for sulfate and this Class I area is given by:

$$RRF(SO4)_i = \sum SO4(2018)_i / \sum SO4(2002)_i$$

4.3.1 Mapping of Modeling Results to the IMPROVE Measurements

As noted above, to project future-year visibility at Class I areas the modeling results are used in a relative sense to scale current observed visibility for the worst 20 percent and best 20 percent visibility days using RRFs that are the ratio of modeling results for the future-year to current-year. This scaling is done separately for each of the six components of light extinction in the IMPROVE equations. The CMAQ modeled species do not necessarily exactly match up with the IMPROVE PM species, thus assumptions must be made to map the modeled species to the IMPROVE PM species for the purpose of projecting visibility improvements. For example, CMAQ explicitly simulates ammonium and sulfate may or may not be fully neutralized in the model by ammonium, whereas the IMPROVE equations assume sulfate is fully neutralized by ammonium. For the CMAQ Version 4.5 (September 15, 2005 release) model, the mapping of modeled species to IMPROVE equation PM species is listed in Table 4-2.

Table 4-2. Mapping of CMAQ V4.5 modeled species concentrations to IMPROVE PM components.

IMPROVE Component	CMAQ V4.3 Species
Sulfate	1.375 x (ASO4J + ASO4I)
Nitrate	1.29 x (ANO3J + ANO3I)
LAC	AECJ + AECI
OMC	AORGAJ + AORGAI + AORGPAJ + AORGPAI + AORGBJ + AORGBI
Soil	A25J + A25I
CM	ACORS + ASEAS + ASOIL

For the CENRAP visibility projections using the 2002 Typical and 2018 base case Base G emission scenarios, the secondary organic aerosol (SOA) module in CMAQ V4.5 was modified (SOAmods) to include additional processes related to the generation of SOA from biogenic emissions. In particular, three new species have been added that represent SOA products from biogenic emission compounds that is not included in the standard version of CMAQ V4.5 (Morris et al., 2006c):

- ASOC1 – SOA from biogenic sources (e.g., terpenes and isoprene) that has become polymerized so is no longer volatile.
- ASOC2 – SOA from biogenic sesquiterpene and higher reactivity and higher yield monoterpene emissions.
- ASOC3 – SOA from biogenic isoprene emissions.

Thus, the species mapping for Organic Mass Carbon (OMC) and the CMAQ V4.5 SOAmods version of the model used in CENRAP 2018 visibility projections is as given in Table 4-2 only with the addition of the three new biogenic SOA species to OMC as follows:

OMC = AORGAJ + AORGAI + AORGPAJ + AORGPAI + AORGBJ + AORGBI + ASOC1 + ASOC2 + ASOC3

4.3.2 Using Modeling Results to Project Changes in Visibility

Modeling results are used in a relative fashion to project future-year visibility using relative response factors (RRFs). RRFs are expressed as the ratio of the modeling results for the future-year to the results of the base year (2018/2002) and are Class I area and PM species specific. RRFs are applied to the Baseline Condition observed PM species to project future-year PM levels from which visibility can be assessed using the IMPROVE equations listed above. The following six steps are used to project future-year visibility for the worst 20 percent and best 20 percent visibility days (discussion is for worst 20 percent days but also applies to best 20 percent days):

1. For each Class I area and each monitored day, daily visibility is ranked using IMPROVE data and IMPROVE equation (either original or new IMPROVE equation) for each year from the five-year baseline period (2000-2004) to identify the worst 20 percent visibility days for each year from the five-year baseline (see Baseline Conditions discussion above).

2. Use an air quality model to simulate a base year period (ideally the five-year Baseline period of 2000-2004, but for CENRAP just the 2002 annual period was simulated) and a future-year (e.g., 2018) and use the resulting information to develop Class I area-specific RRFs for each of the six components of light extinction in the IMPROVE equation (SO4, NO3, EC, OMC, Soil and CM).

3. Multiply the RRF times the measured 24-hour PM concentration data for each day from the worst 20 percent days in each year from the five-year Baseline period to obtain projected future-year 24-hour PM concentrations for the worst 20 percent days and the five-year Baseline.

4. Compute the future-year daily extinction using the IMPROVE equation and the projected PM concentrations for each of the worst 20 percent days in the five-year baseline from Step 3.

5. For each of the worst 20 percent days within each year of the five-year baseline, convert the future-year daily extinction to deciview and average the daily deciview values within each of the five years separately to obtain five-years (or as many years with valid data in the 2000-2004 Baseline) of average deciview visibility for the worst 20 percent days.

6. Average the five-years of average deciview visibility to obtain the future-year visibility Haze Index estimate that is the future-year estimated visibility.

In calculating the RRFs, EPA draft guidance recommends selecting estimated PM species concentrations "near" the monitor by taking a spatial average of PM concentrations across a grid cell resolution dependent NX by NY array of cells centered on the grid containing the monitor. The NX x NY array of cells is grid resolution specific with EPA recommending that NX=NY=1 for 36 km grids, NX=NY=3 for 12 km grids and NX=NY=7 for 4 km grids (EPA, 2007). For the CENRAP 2002 36 km modeling, just the model estimates for the grid cell containing the monitor was used (i.e., NX=NY=1).

4.4 EPA Default 2018 Visibility at CENRAP and Nearby Class I areas and Comparisons to 2018 URP Goals

Using the EPA default visibility projection procedure described in Section 4.3 and the CENRAP 2002 Typical Base G and 2018 Base Case Base G CMAQ modeling results, 2018 visibility projections were made for CENRAP and nearby Class I areas. Appendix D details the 2018 Base G visibility projections for each Class I area in the CENRAP region using the new IMPROVE equation. Results for the Caney Creek (CACR), Arkansas Class I area are discussed in Section 4.4.1 below Displays for other CENRAP Class I areas are provided in Appendix D and summarized in Section 4.4.2

4.4.1 Example 2018 Base G Visibility Projections for Caney Creek, Arkansas

The 2018 visibility projections for the Caney Creek (CACR), Arkansas Class I area given in Figure D-1 in Appendix D are reproduced in Figure 4-3 and described below.

4.4.1.1 EPA Default 2018 Visibility Projections

The 2018 Base G visibility projection using the EPA default method (EPA, 2007a) and comparison with the 2018 URP point for the worst 20 percent days and the CACR Class I area is shown in Figure 4-3a. The 2000-2004 Baseline Conditions for CACR is 26.36 dv and the 2018 URP point is 22.91 dv so that a 3.45 dv reduction in visibility for the worst 20 percent days is needed to meet the 2018 URP point. The 2018 Base G CMAQ projected visibility is 22.48 dv so that the modeling predicts more visibility improvements (3.88 dv reduction) than required to meet the 2018 URP point (3.45 dv reduction). When looking at visibility projections across several Class I areas, it has been useful to present the 2018 visibility projections as a percentage of meeting the 2018 URP point; where 100% is meeting the point, greater than 100% surpassing the point (i.e., below the glidepath) and less than 100% means that less visibility improvement is achieved than needed to meet the 2018 URP point. For 2018 Base G CMAQ modeling at CACR, we achieve 112% of the visibility reduction needed to meet the 2018 URP point. Note that meeting the 2018 URP point is not a requirement of the RHR SIPs, rather it just serves as a benchmark to compare progress toward Natural Conditions in 2064 and is designed to help states in selecting their 2018 RPGs. As clearly stated in EPA guidance "The glidepath is not a presumptive target, and States may establish a RPG that provides for greater, lesser, or equivalent improvement as that described by the glidepath" (EPA, 2007b).

The 2018 Base G CMAQ visibility projections for the best 20 percent days and CACR is shown in Figure 4-3b. Recall the RHR goal for this visibility metric is no worsening of the visibility for the best 20 percent days. The Baseline Conditions for the best 20 percent days at CACR is 11.24 dv. The 2018 Base G projected visibility for the best 20 percent days is 10.35 dv, which represents a 0.89 dv visibility improvement for the best 20 percent days at CACR and demonstrating no worsening in visibility for the best 20 percent days.

Figure 4-3c displays "StackedBar Chart" plots of observed and model estimated extinction for each of the worst 20 percent days in 2002 and the 2002 Typical Base G CMAQ simulation and the average across the worst 20 percent days. This figure allows a comparison of how well the model is reproducing the observed extinction at CACR for the worst 20 percent days in 2002 and the breakdown of the PM components that are contributing to visibility impairment (more details on model performance were presented in Chapter 3). The 2002 worst 20 percent days at CACR are dominated by SO4 days (yellow), although during the winter there are also three days dominated by NO3 (Julian Days 80, 320 and 341). For most of the worst 20 percent days at CACR, the model reproduces the observed extinction reasonably well, although it does tend to understate SO4 on a few days and overstate NO3 on the four winter days. The observed average extinction across the 2002 worst 20 percent days at CACR is 150 Mm^{-1}, compared to a modeled value that is 23% lower (115 Mm^{-1}).

Figure 4-3d displays "Boxplots" of differences in modeled extinction for the 2002 worst 20 percent days between the 2018 Base G and 2002 Typical Base G CMAQ simulations. On most days SO4 is the largest component of the extinction that is estimated to be reduced at CACR on the worst 20 percent days. The exception to this is for the winter NO3 days where NO3 is the largest component of extinction that is reduced. The modeling results are not used directly in the visibility projections, rather they are used to develop the PM-species specific RRFs. That is, an important attribute in Figures 4-3c and 4-3d is the relative changes in the modeled PM species averaged across the worst 20 percent days that are represented by the last bar in each figure and provide insight into the RRFs used in the visibility projections. These results are summarized in Table 4-3 below. Table 4-3 compares the average extinction across the 2002 worst 20 percent days at CACR from the measured IMPROVE data, the modeled values and the modeled change in extinction between the 2018 and 2002 emissions scenarios. Although the results in Table 4-3 are not RRFs (RRFs are based on ratios of concentrations not extinction) they do show how the RRFs may magnify or deflate the importance of a modeled PM species. For example, the model estimates that approximately 23% (26.66 Mm^{-1}) of the visibility extinction average across the worst 20 percent days is due to NO3, whereas it is only 7% in the observed values (10.22 Mm^{-1}). So the modeled ~40% reduction in NO3 between the 2018 and 2002 scenarios is applied to the smaller observed NO3 value to obtain the 2018 projected NO3 value making NO3 a smaller portion of the 2018 projected visibility than the 2018 modeled visibility. On the other hand, the modeled SO4 extinction is less than observed so that its importance in the 2018 projections is much greater than in the modeled 2018 SO4 values.

Table 4-3. Observed and Modeled Extinction by Species Averaged Across the Worst 20 Percent Days in 2002 at CACR.

	2002 Average Observed W20% (Mm^{-1})	2002 Average Modeled W20% (Mm^{-1})	2018-2002 Reduction (Mm^{-1})	2018-2002 Reduction (%)
bSO4	109.50	67.90	-24.47	-36%
bNO3	10.22	26.66	-10.90	-41%
bOMC	19.65	16.68	-2.12	-13%
bEC	4.38	2.32	-0.67	-29%
bSOIL	1.43	1.04	+0.21	+20%
bCM	4.30	0.37	-0.01	-3%

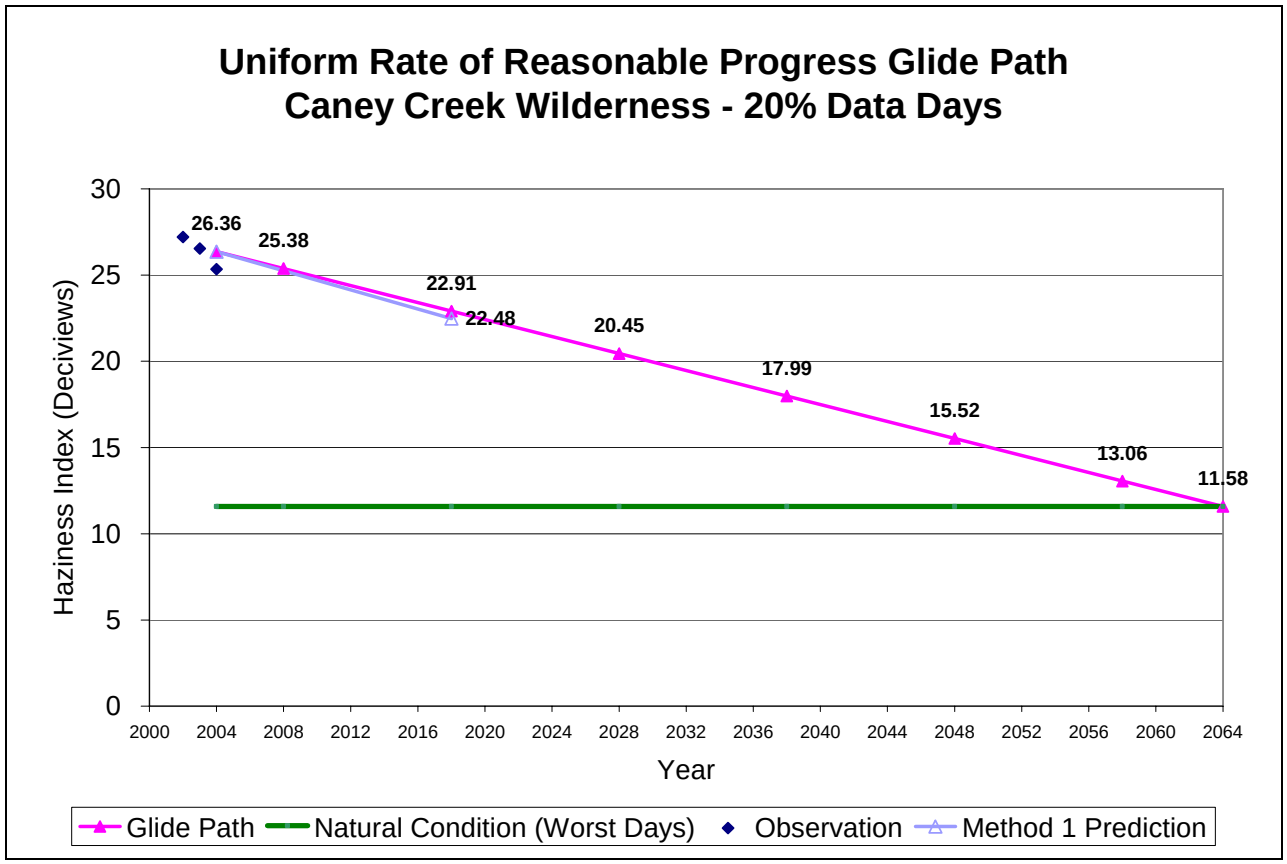

Figure 4-3a. 2018 Visibility Projections and 2018 URP Glidepaths in Deciview for Caney Creek (CACR), Arkansas and Worst 20 Percent (W20%) days Using 2002/2018 Base G CMAQ 36 km Modeling Results.

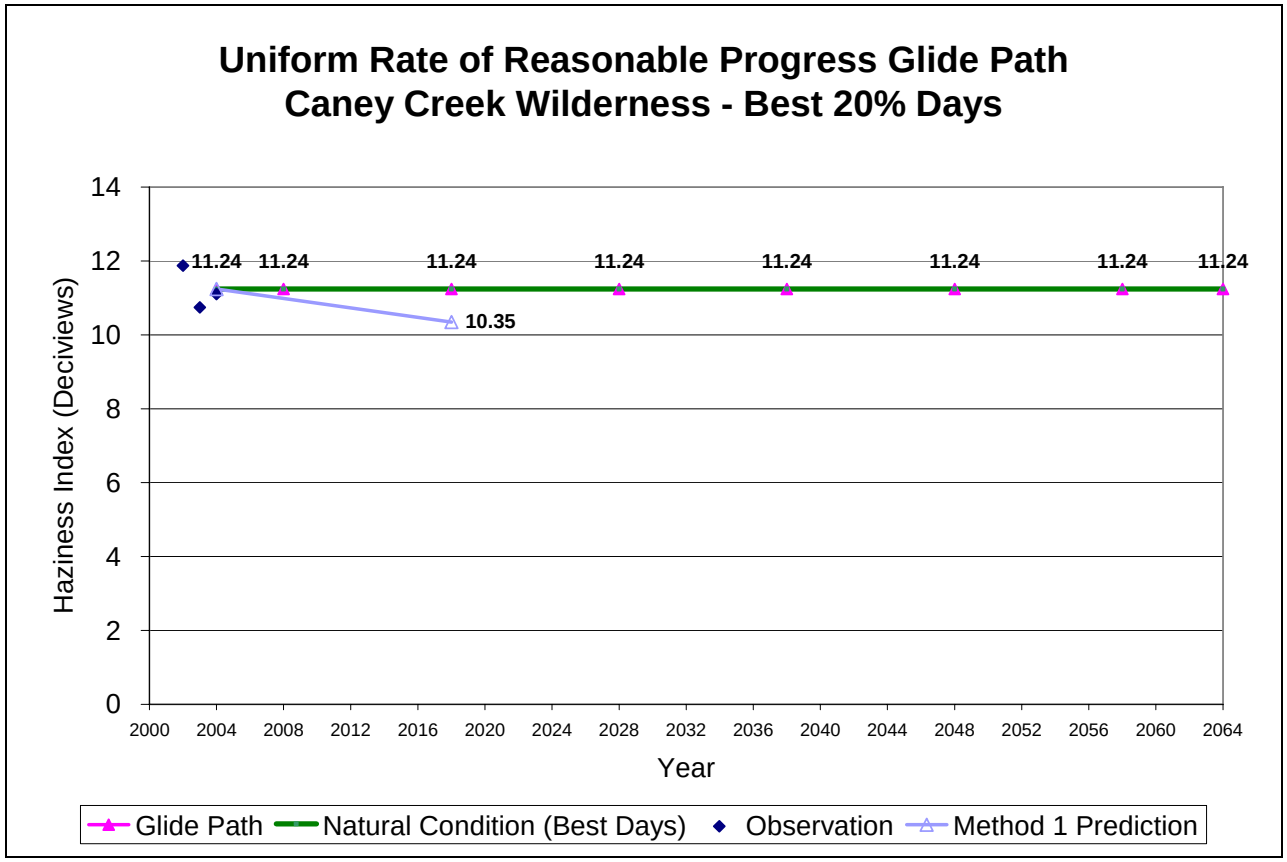

Figure 4-3b. 2018 Visibility Projections and 2018 URP Glidepaths in Deciview for CACR, Arkansas and Best 20 Percent (B20%) days Using 2002/2018 Base G CMAQ 36 m Modeling Results.

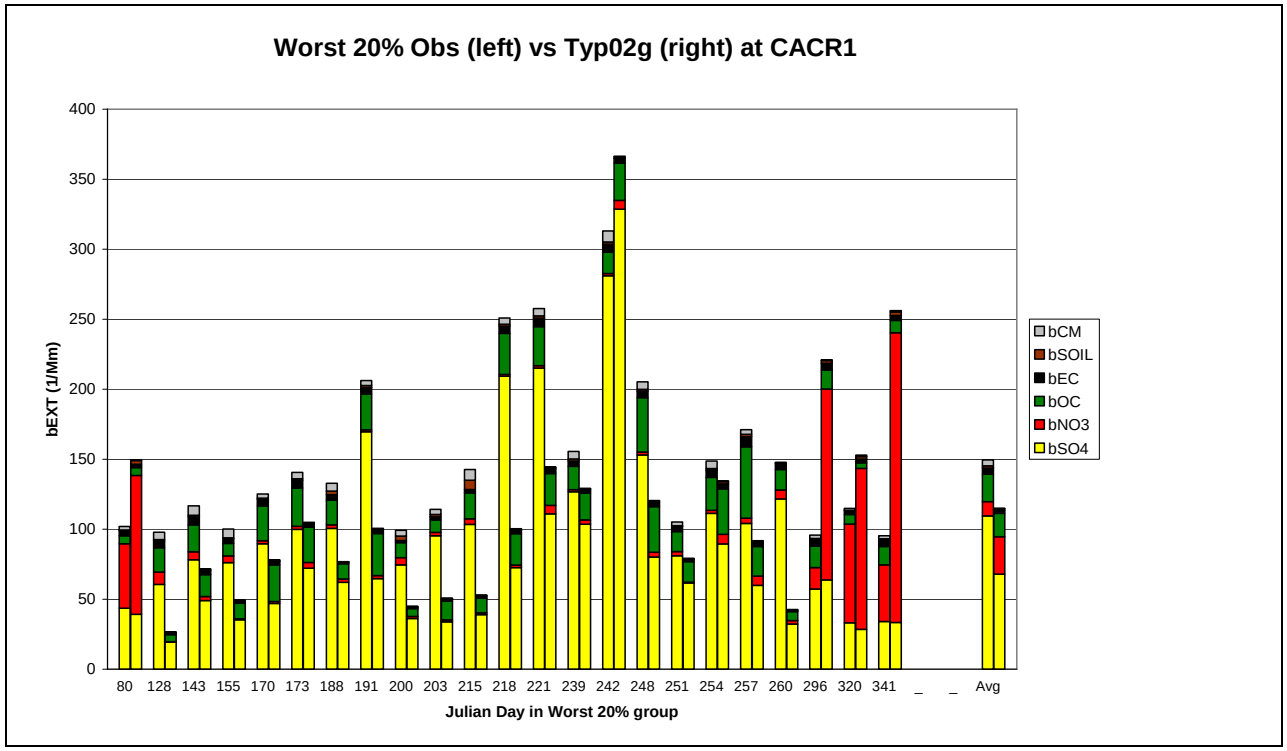

Figure 4-3c. Comparison of Observed (left) and 2002 Base G Modeled (right) Daily Extinction for Caney Creek (CACR), Arkansas and Worst 20 Percent (W20%) days in 2002.

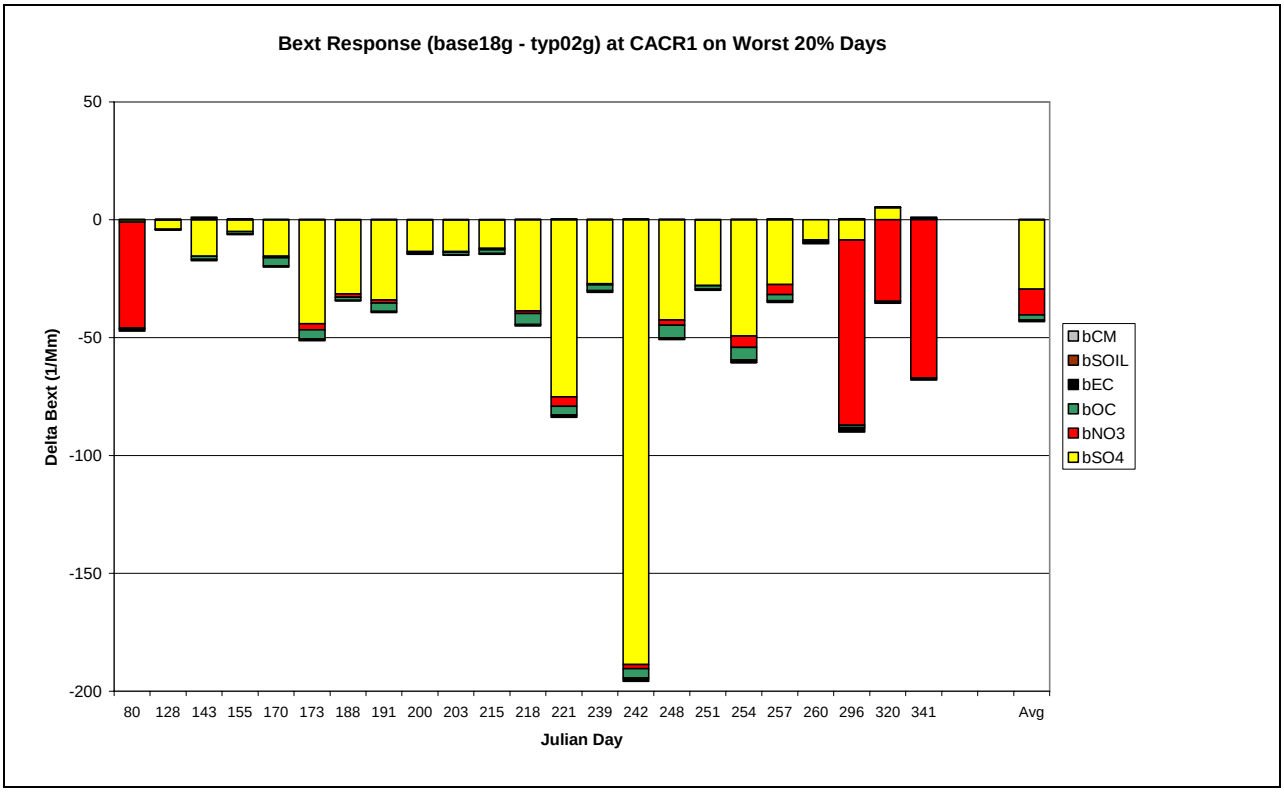

Figure 4-3d. Differences in Modeled 2002 and 2018 Base G CMAQ Results (2018-2002) Daily Extinction for Caney Creek (CACR), Arkansas and Worst 20 Percent (W20%) Days in 2002.

4.4.2 Summary 2018 Visibility Projections Across Class I Areas

Figure 4-4 displays a "DotPlot" of 2018 visibility projections using the 2002 Typical and 2018 base case Base G CMAQ 36 km modeling results. DotPlots present the 2018 visibility projections as a percentage of meeting the 2018 URP point. For example, at CACR the 2018 Base G modeling achieved 112% of the visibility reduction needed to meet the 2018 URP point so the dot under CACR is plotted at 112%. Class I areas' with dots above 100% surpass the 2018 URP point (i.e., are below the glidepath), whereas Class I areas' with dots that are under 100% fail to meet the 2018 URP point. Figure 4-4 summarizes the 2018 visibility projections using the EPA default "Regular RRF" and the two alternatives where CM is assumed to be natural (CM RRF=1) and both CM and Soil are assumed to be natural (CM&SOIL RRF=1). When CM or CM&SOIL are assumed to be natural that means that we assume the same CM or CM&SOIL occurs in the 2018 future-year as in the 2000-2004 Baseline Conditions. For the CENRAP sites, the EPA default and alternative projection, assuming CM alone or CM and Soil are natural, techniques produced similar results.

At the four eastern CENRAP Class I area sites close to the Mississippi River (CACR, UPBU, HEGL and MING), the 2018 visibility projections meet (HEGL) or surpass the 2018 URP point. Breton Island Class I area (BRET) comes up 6% short of meeting the 2018 URP point (i.e., 94% of the URP point). Wichita Mountains Class I area (WIMO) comes up approximately 40% short of the 2018 URP point. The two northern Class I areas (BOWA and VOYA) also come up about 40% short of meeting the 2018 URP point (i.e., achieve 69% and 53% of the visibility improvement needed to meet the 2018 URP point). The two Texas Class I areas only achieve

26% (BIBE) and 34% (GUMO) of the visibility improvement needed to meet the 2018 URP point for the worst 20 percent days. As discussed in more detail in Chapter 5, much of the difficulty for the Texas and some of the other CENRAP Class I areas in meeting the 2018 URP point is due to large contributions due to international transport, much of which (e.g., Mexico and global transport) is assumed to remain unchanged from 2002 to 2018.

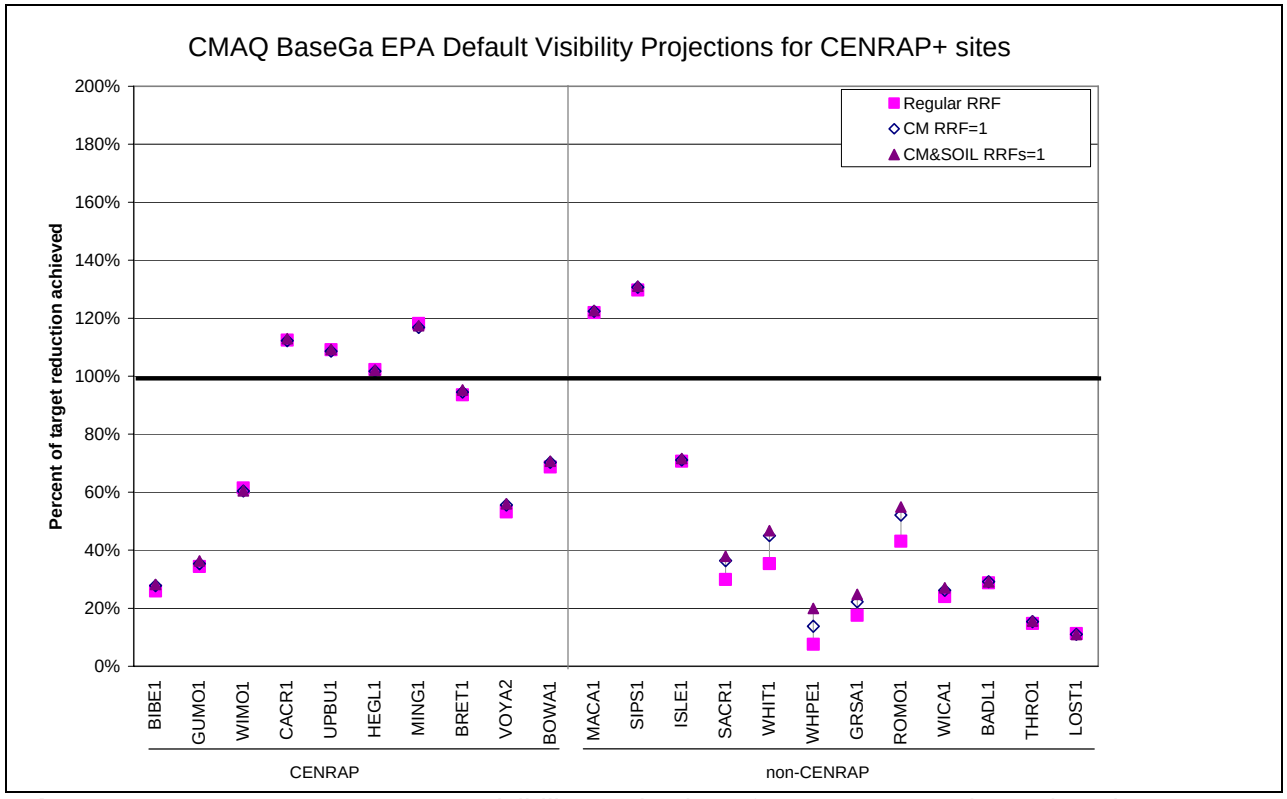

Figure 4-4. 2018 Base G CMAQ Visibility Projections for CENRAP and Nearby Class I areas Using DotPlots that Express 2018 Visibility as a Percentage of Meeting the 2018 URP Point On the Deciview Linear Glidepath.

Figure 4-5 displays the model estimated absolute change in extinction (Mm^{-1}) averaged across the 2002 worst 20 percent days at Class I areas in and near the CENRAP region. The largest modeled reductions are in SO4 extinction. Figure 4-6 displays the percent change in the projected PM extinction by PM species for each CENRAP and nearby Class I area average across the worst 20 percent days (i.e., the relative modeled change). The four CENRAP Class I areas that meet the 2018 URP point (CACR, UPBU, HEGL and MING) are characterized by large SO4, NO3 and EC extinction reductions (30-40%) with small Soil increases. At the other CENRAP Class I areas, however, there are lower levels of SO4, NO3 and EC extinction reductions and even some NO3 increases (BIBE). At the non-CENRAP Class I areas, the two VISTAS Class I areas (MACA and SIPS) have large reductions in SO4 extinction (~50%), whereas the WRAP Class I areas SO4 extinction reductions are much smaller.

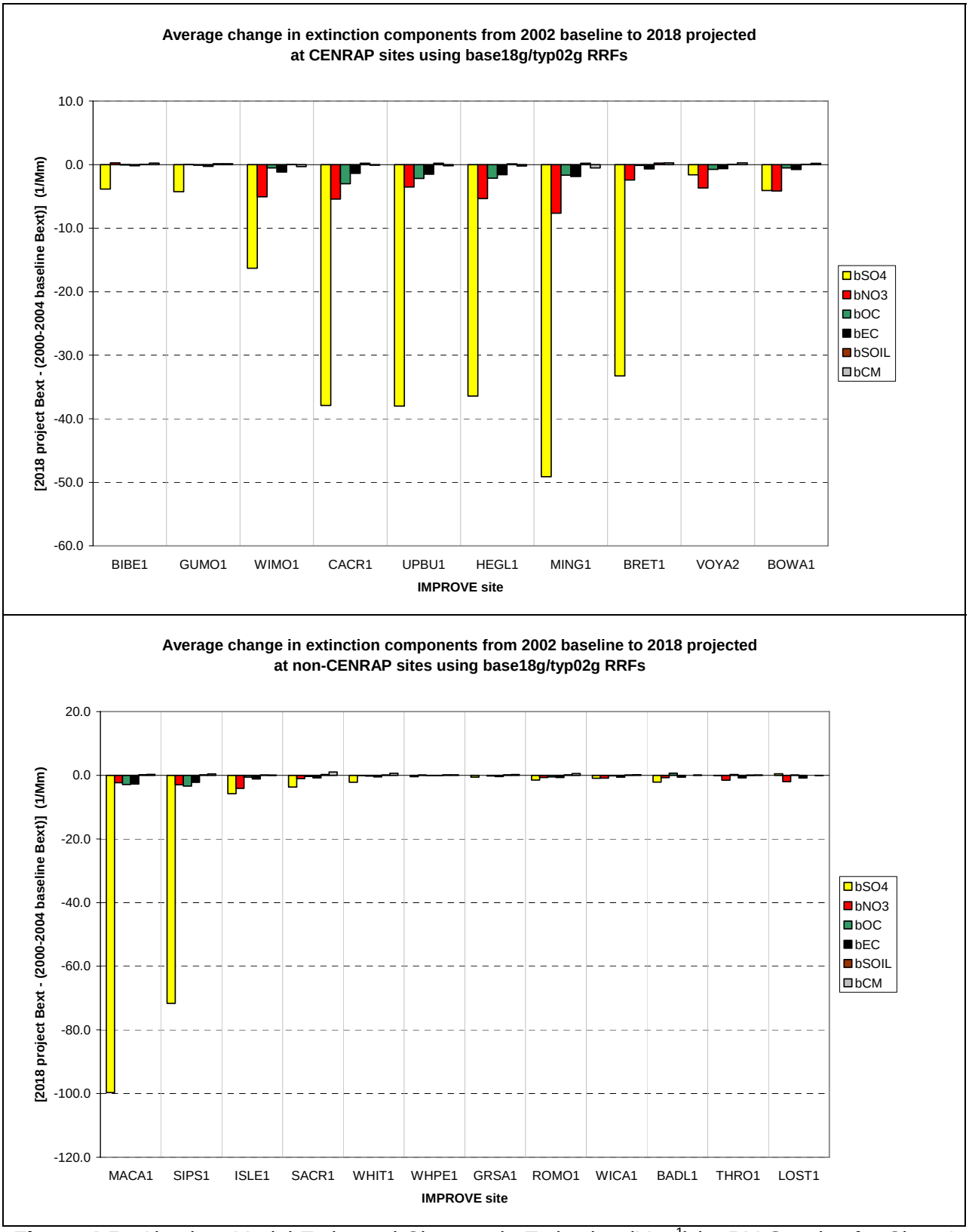

Figure 4-5. Absolute Model Estimated Changes in Extinction (Mm^{-1}) by PM Species for Class I Areas in the CENRAP region (top) and Near the CENRAP region (bottom).

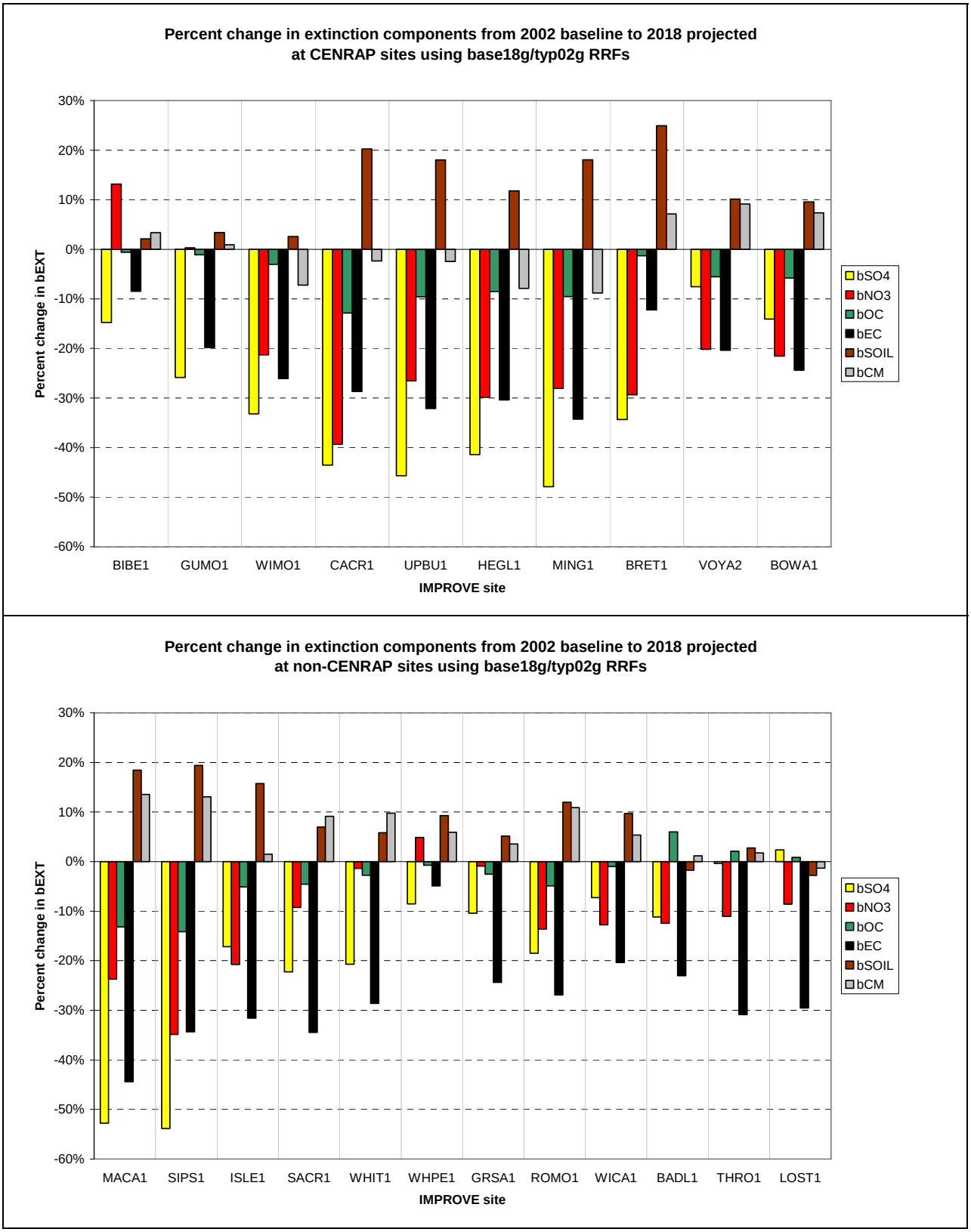

Figure 4-6. Percent Change In Modeled Extinction by PM Species Averaged Across the 2002 Worst 20 Percent Days for Class I areas in the CENRAP region (top) and Near the CENRAP region (bottom).

4.5 2018 Visibility Projections for Base G C1 Control Scenario

The 2018 visibility projections based on the CMAQ simulations for the 2018 Base G C1 Control Strategy simulations are presented in this section. The C1 Control Strategy results in reductions mainly in SO2 and NOx emissions from point sources in the CENRAP states. Consequently, PM improvements are limited to mainly SO4 and NO3 concentration reductions in the CENRAP states. Figure 4-7 displays the differences in CMAQ-estimated annual average SO4 and NO3 concentrations between the 2018 Base G base case and the 2018 Base G C1 Control Strategy case; the differences in all other PM species (with the exception of NH4) were negligible (see: http://pah.cert.ucr.edu/aqm/cenrap/cmaq.shtml#base18gc1vsbase18g). Annual average SO4 concentration reductions of over a quarter of a $\mu g/m^3$ are estimated to occur in northeast Texas, east Oklahoma, Missouri, northeast Arkansas and up into Iowa and Illinois. There are much lower reductions in NO3 that cover a similar area.

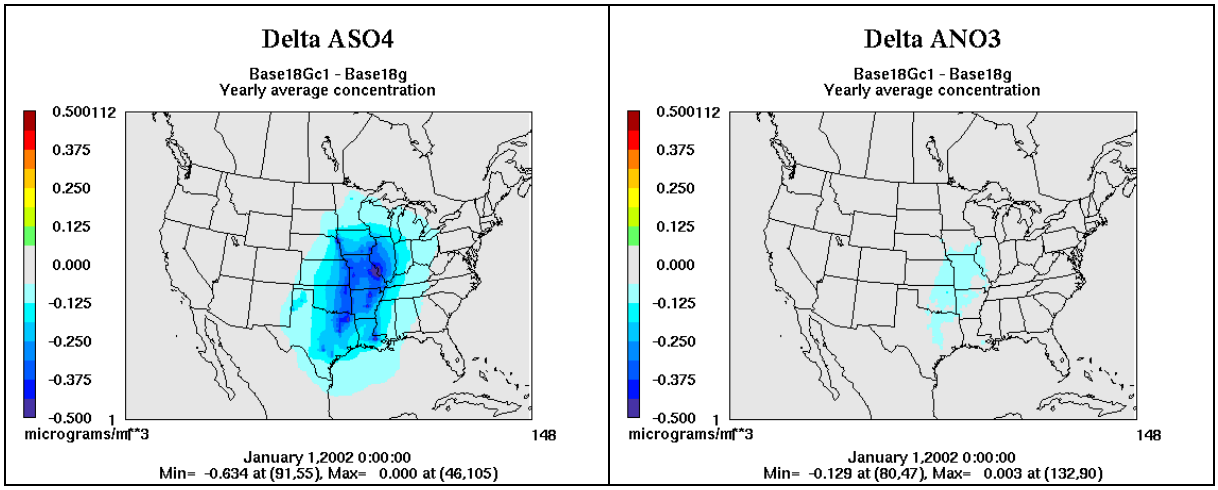

Figure 4-7. CMAQ-Estimated Reductions in Annual Average SO4 (left) and NO3 (right) Fine Particle Concentrations Between the 2018 Base G Base Case and 2018 Base G C1 Control Strategy Case.

Figure 4-8 displays the DotPlot comparisons of the 2018 visibility projections for 2018 Base G and 2018 Base G C1 Control Strategy emission scenarios. The additional controls in the C1 Control Strategy are projected to result in visibility improvements for the worst 20 percent days at Class I areas throughout and near the CENRAP region. Sites are closer to being on the glide path by 10 to 30 percent. For Breton Island this makes a difference of not meeting the 2018 URP point in 2018 Base G (94%) to surpassing the URP point in the C1 Control Strategy (106%).

Table 4-4 presents a tabular summary of the information presented in Figure 4-8, including the Baseline, 2018 URP point, and 2018 projected visibility for the Base G and C1 Control Strategy simulations.

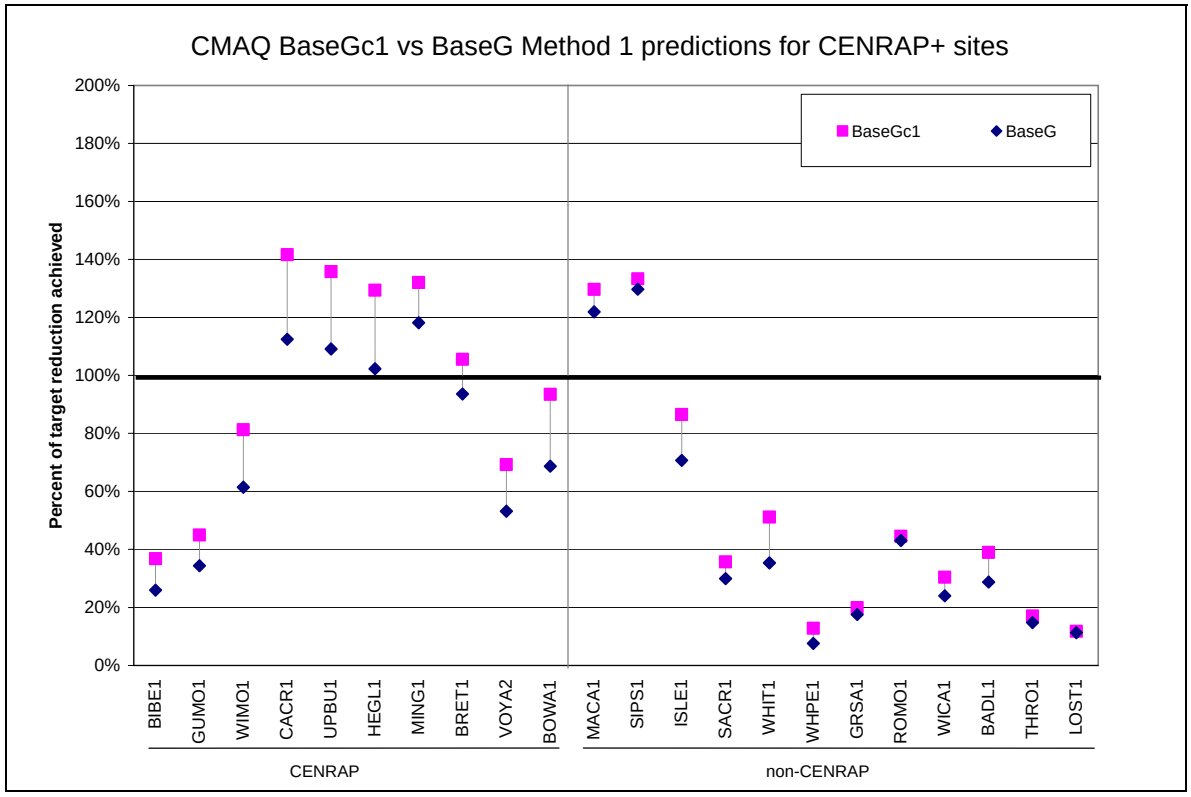

Figure 4-8. 2018 Visibility Projections as a Percentage of Meeting the 2018 URP Point (i.e., DotPlot) for the 2018 Base G and 2018 Base G C1 Control Strategy Emission Scenarios.

Table 4-4. 2000-2004 Baseline, 2018 URP Point, and Projected 2018 Visibility and Percent of Meeting the 2018 URP Point for the 2018 Base G and 2018 C1 Control Strategy CMAQ Simulations.

Class I Area Name	State	ID	Lat.	Lon.	00/04 Baseline Condit.	2018 URP Point	2018 Base G Base Case		2018 Base G C1 Control Strategy	
			(deg)	(deg)	(dv)	(dv)	(dv)	(%)	(dv)	(%)
Badlands NP	SD	BADL1	43.81	-102.36	17.14	15.02	16.53	29%	16.31	39%
Big Bend NP	TX	BIBE1	29.33	-103.31	17.30	14.93	16.69	26%	16.43	37%
Boundary Waters Canoe Area	MN	BOWA1	48.06	-91.43	19.58	17.72	18.30	69%	17.84	93%
Breton	LA	BRET1	29.87	-88.82	25.73	22.51	22.72	94%	22.34	106%
Caney Creek Wilderness	AR	CACR1	34.41	-94.08	26.36	22.91	22.48	112%	21.48	142%
Great Sand Dunes NM	CO	GRSA1	37.77	-105.57	12.78	11.35	12.53	18%	12.49	20%
Guadalupe Mountains NP	TX	GUMO1	31.91	-104.85	17.19	14.74	16.35	34%	16.09	45%
Hercules-Glades Wilderness	MO	HEGL1	36.68	-92.9	26.75	23.14	23.06	102%	22.09	129%
Isle Royale NP	MI	ISLE1	48.01	-88.83	20.74	18.78	19.36	71%	19.05	87%
Lostwood	ND	LOST1	48.59	-102.46	19.57	16.87	19.27	11%	19.26	12%
Mammoth Cave NP	KY	MACA1	37.20	-86.15	31.37	26.64	25.60	122%	25.23	130%
Mingo	MO	MING1	37.00	-90.19	28.02	24.37	23.71	118%	23.21	132%
Rocky Mountain NP	CO	ROMO1	40.35	-105.7	13.83	12.29	13.17	43%	13.14	45%
Salt Creek	NM	SACR1	33.6	-104.41	18.03	15.41	17.25	30%	17.10	36%
Sipsey Wilderness	AL	SIPS1	34.32	-87.44	29.03	24.82	23.57	130%	23.42	133%
Theodore Roosevelt NP	ND	THRO1	46.96	-103.46	17.74	15.42	17.40	15%	17.34	17%
Upper Buffalo Wilderness	AR	UPBU1	36.17	-92.41	26.27	22.84	22.52	109%	21.61	136%
Voyageurs NP	MN	VOYA2	48.47	-92.8	19.27	17.58	18.37	53%	18.10	69%
White Mountain Wilderness	NM	WHIT1	33.48	-105.85	13.70	12.11	13.14	35%	12.89	51%
Wheeler Peak Wilderness	NM	WHPE1	36.57	-105.4	10.41	9.49	10.34	8%	10.30	13%
Wind Cave NP	SD	WICA1	43.58	-103.47	15.84	13.94	15.39	24%	15.26	30%
Wichita Mountains	OK	WIMO1	34.75	-98.65	23.81	20.01	21.47	61%	20.72	81%

5.0 ADDITIONAL SUPPORTING ANALYSIS

This Chapter presents additional supporting analysis to the modeled 2018 visibility projections provided in Chapter 4. This supporting analysis may be used by the states in their RHR SIPs, along with their factor analysis, to assist in setting their 2018 RPGs for the worst 20 percent days and best 20 percent days.

5.1 Comparison of CENRAP 2018 Visibility Projections with Other Groups

2018 visibility projections for CENRAP and nearby Class I area have also been performed by the other RPOs. Thus, it is useful to compare the CENRAP 2018 visibility projections with those from the other RPOs as a quality assurance (QA) check and to foster confidence in the CENRAP modeling results.

5.1.1 Comparison of CENRAP, VISTAS, MRPO and WRAP Visibility Projections

The CENRAP 2018 Base G visibility projections were compared to the following other RPO visibility projections:

- VISTAS 2018 visibility projections based on their CMAQ 12 km 2002 annual modeling results for the 2002 Base G and 2018 Base G2a emissions scenarios.
- MRPO 2018 visibility projections based on their CAMx 36 km 2002 annual modeling for the Run 4 Scenario 1a (R4S1a) emissions scenario.
- WRAP 2018 visibility results based on their Plan02b and Base18b CMAQ 36 km modeling of the 2002 calendar year.

Figure 5-1 displays a DotPlot comparison of the four RPO visibility projections expressed as a percentage of achieving the 2018 URP point at CENRAP and nearby Class I areas. For the four CENRAP Class I areas just west of the Mississippi River in Arkansas and Missouri (CACR, UPBU, HEGL and MING), 2018 visibility projections are available from the CENRAP, VISTAS and MRPO RPOs. At HEGL, the three RPOs 2018 visibility projections are in close agreement with each other (estimated to achieve 99%, 101% and 95% of the 2018 URP point). The CENRAP and VISTAS 2018 visibility projections are also very close at the other three Arkansas-Missouri CENRAP Class I areas: CACR (112% and 116%), UPBU (109% and 112%) and MING (118% and 114%). But the MRPO 2018 visibility projections are approximately 12 to 25 percentage points lower than the CENRAP and VISTAS projections at these three Class I areas, with values of 97% to 100%. The reasons why the MRPO 2018 visibility projections are less optimistic than CENRAP and VISTAS are unclear. However, the MRPO focused on visibility projections at their northern Class I areas and likely did not use the latest CENRAP emission estimates. In addition, the CENRAP 2018 visibility projections included BART controls on several sources in CENRAP states not included in the MRPO projections. Such BART controls are even more important in those states not covered by CAIR.

For the Breton Island (BRET) Class I area, 2018 visibility projections are available from CENRAP and VISTAS. CENRAP estimates that BRET will achieve 94% of the URP point and

VISTAS is slightly less optimistic with an 84% value. One potential contributor to this is that emissions from off-shore marine vessel emissions in the oil and gas production areas of the Gulf of Mexico are double counted in the VISTAS Base G modeling. As these emissions were assumed to remain unchanged between 2002 and 2018, the double counting of their emissions will result in stiffer RRFs than there should be and consequently less visibility benefits in 2018. This double counting also occurred in the CENRAP Base F modeling but was corrected in Base G. The double counting occurred because off-shore marine vessels were present in both the MMS off-shore oil/gas development inventory for the Gulf of Mexico and the VISTAS off-shore marine vessel inventory for the Pacific and Atlanta Oceans and the Gulf of Mexico. VISTAS intends to correct this double counting in their next round of modeling.

At the two northern Minnesota Class I areas (BOWA and VOYA), the MRPO 2018 visibility projections (93% and 92%) exhibit more visibility improvements than CENRAP's (69% and 53%). This is believed to be due to higher contributions to visibility impairment from Canada in the CENRAP modeling. Figure 5-2 displays the CENRAP 2002 Base F total SO2 emissions and their differences with the 2018 Base F SO2 emissions. The SO2 emissions in Alberta Canada appear to be much higher and more wide spread when compared to the other provinces in Canada and emissions in the U.S. states. Also, there is a very large SO2 source in northern Manitoba (> 10^5 tons/year). The Alberta SO2 emissions may be overstated in the CENRAP modeling, which would overstate the Canadian contribution to visibility impairment. The western boundary of the MRPO modeling domain was east of the Rocky Mountains so did not include Alberta. CENRAP confirmed that the Alberta emissions and the source in Manitoba were present in the emissions provided by Canada. Air parcels from Canada are generally associated with clean visibility conditions at the northern Minnesota Class I areas with the worst 20 percent days generally occurring under conditions with a southerly wind component. However, in 2002 some of the worst 20 percent days did occur with transport out of Canada. For example, Figure 5-3 displays back trajectories off of the VIEWS website for two of the worst 20 percent days at Voyageurs National Park (Julian Days 347 and 332). These back trajectories suggest that the potentially overstated emissions in Alberta would have an impact at VOYA during the worst 20 percent days in 2002.

At the VISTAS Mammoth Cave (MACA), Kentucky Class I area, VISTAS, CENRAP and the MRPO estimated that 2018 visibility for the worst 20 percent days will achieve, respectively, 122%, 123% and 102% of the 2018 URP point. The close agreement between the VISTAS (122%) and CENRAP (123%) 2018 visibility projections for MACA is encouraging. Why MRPO is 20 percentage points lower is unclear, but may be due to using earlier versions of the VISTAS and CENRAP emissions. The 2018 visibility projections at Sipsey (SIPS), Alabama estimated by VISTAS (127%) and CENRAP (130%) are also extremely close.

Both the CENRAP and WRAP 2018 visibility projections agree that the WRAP Class I areas fail to achieve the 2018 URP point by a wide margin, with values achieving only ~40% or less of the 2018 URP point. The CENRAP 2018 visibility projections agrees well with the WRAP values at Great Sands (GRSA), Colorado (18% vs. 15%), Badlands (BADL), South Dakota (24% vs. 31%), Theodore Roosevelt, North Dakota (15% vs. 11%) and Lostwood (LOST), Montana (11% vs. 14%). There is also reasonable agreement between CENRAP and WRAP 2018 visibility projections at Salt Creek (SACR), New Mexico (30% vs. 12%), Rocky Mountain (ROMO), Colorado (43% vs. 30%), and Wind Cave (WICA), South Dakota (24% vs. 6%). There are two WRAP Class I areas, White Mountains (WHIT) and Wheeler Peak (WEPE), where the WRAP

2018 visibility projections estimate that visibility will degrade for the worst 20 percent days (i.e., negative percent of achieving the 2018 URP point), whereas CENRAP estimates visibility improvements. The reasons for these differences are unclear.

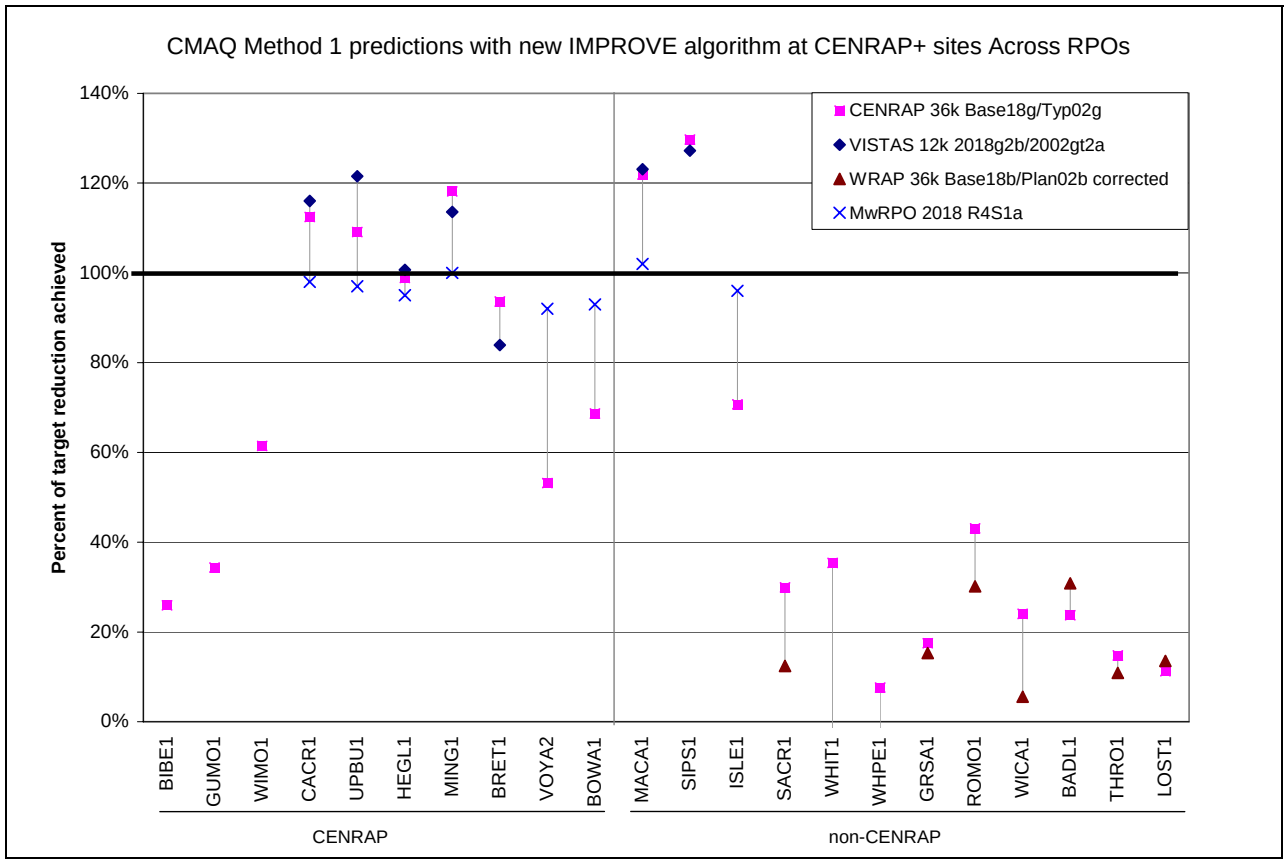

Figure 5-1. DotPlot comparing the CENRAP, VISTAS, MRPO and WRAP 2018 visibility projections expressed as a percentage of achieving the 2018 URP goal.

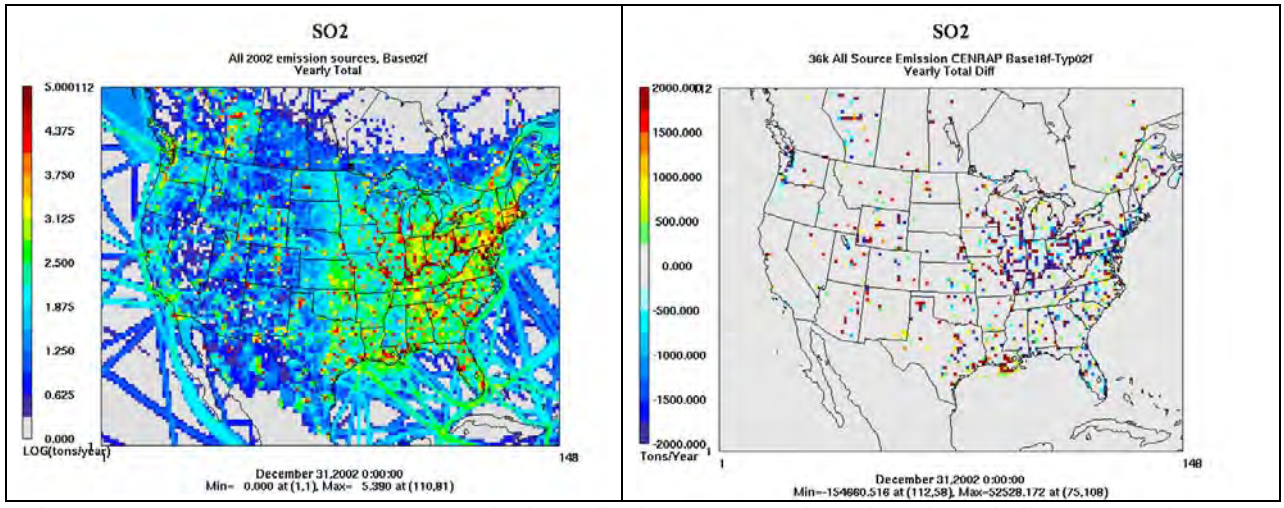

Figure 5-2. 2002 Base F SO2 emissions (left) as LOG10(tons/year) and differences in 2018 and 2002 Base F SO2 emissions (tons/year).

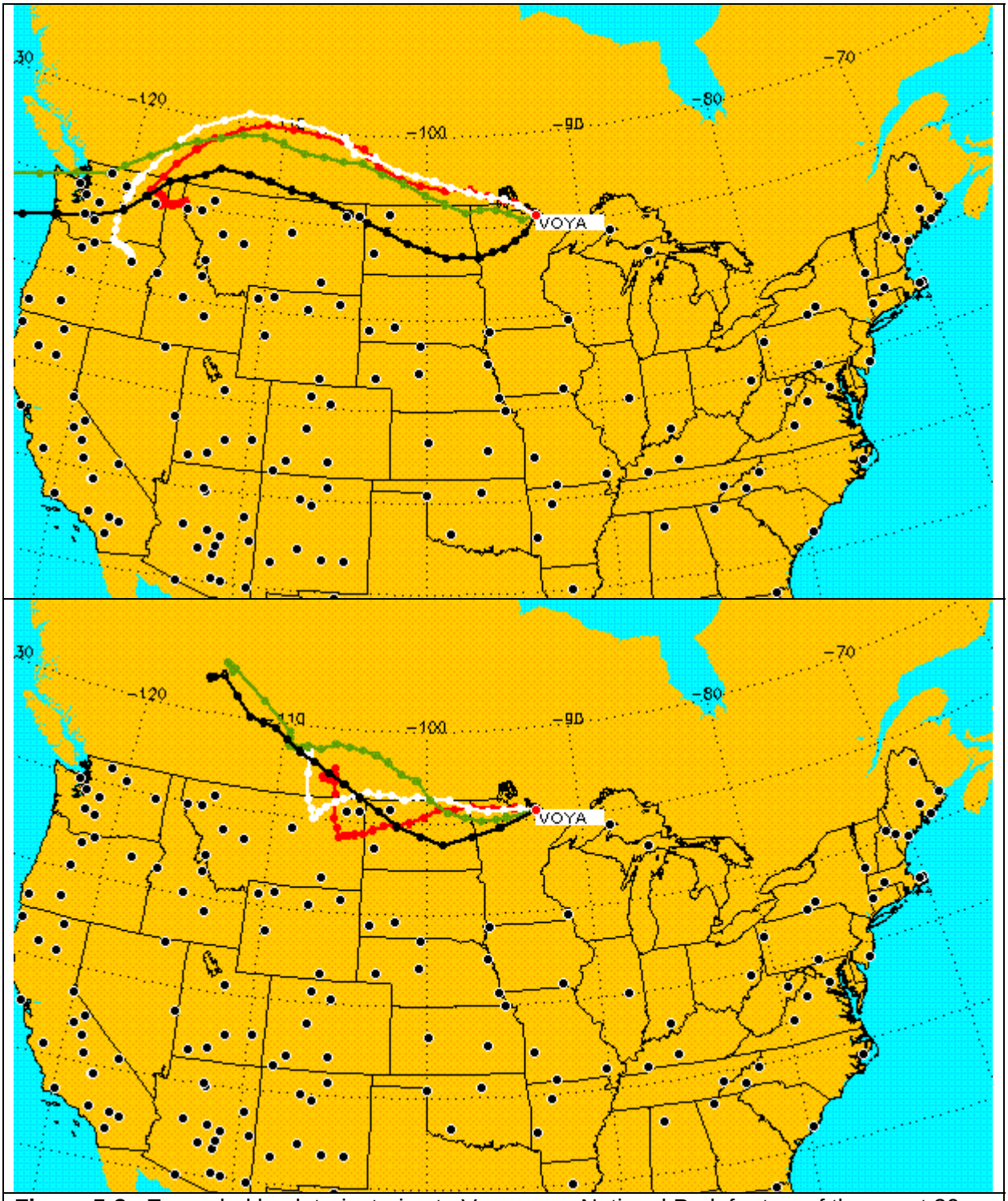

Figure 5-3. Exampled back trajectories to Voyageurs National Park for two of the worst 20 percent days from 2002: December 13, 2002 (Julian Day 347) and November 28, 2002 (Julian Day 332).

5.2 Extinction and PM Species Specific Visibility Projections and Comparisons to 2018 URP Point

It is useful to examine 2018 visibility projections by PM species to determine how each PM component of visibility is changing as both a diagnostic analysis of the visibility projections as well as whether species that are associated more with anthropogenic emissions (e.g., SO4 and NO3) are being reduced substantially compared to those that are less influenced by anthropogenic emissions (e.g., Soil and CM). However, because deciview is the natural logarithm of total extinction, such comparisons can not be made using the deciview scale and must be made using extinction. The linear glidepath from which the 2018 URP points are derived are based on deciview, thus to examine corresponding glidepath using extinction the curvature associated with the logarithmic transformation of the linear deciview glidepath to extinction must be accounted for in the extinction glidepath.

5.2.1 Total Extinction Glidepaths

Figure 5-4 displays a total extinction based glidepath for Caney Creek that is based on the EPA default deciview linear glidepath counterpart shown in Figure 4-3a. That is, the deciview linear glidepath defined by the line connecting the 26.36 dv Baseline Conditions at 2004 to the 11.58 dv Natural Conditions in 2064. The glidepath points in 2008, 2018, 2028, etc. from the linear deciview glidepath (Figure 4-3a) are turned into extinction (Bext) [Bext = 10 exp(dv/10)] to create the curved extinction glidepath that exactly match the linear deciview glidepath points. Note that the 2000-2004 Baseline using the curved extinction glidepath is slightly different than if you just converted the deciview baseline to extinction because the logarithm relationship is performed before the averaging, but they are extremely close. Using the extinction curved glidepath, the 2018 URP point is a reduction of the Baseline 145.10 Mm^{-1} to 98.88 Mm^{-1} (a 46.22 Mm^{-1} reduction). The modeled 2018 visibility projection in extinction is 97.54 Mm^{-1}, a 47.56 Mm^{-1} reduction, which achieves 103% of the reduction needed to achieve the 2018 URP point. Note that this compares with achieving 112% of the 2018 URP reduction point when using the deciview linear glidepath. The percent of achieving the 2018 URP point using the linear deciview and curved extinction glidepaths will rarely be the same due to the logarithmic relationship between the two visibility metrics and the fact that averaging within and across years in the deciview calculations occur after the logarithms have been applied. The greater the difference in extinction across the worst 20 percent days in a year and averaged across the years in the 2000-2004 Baseline and the greater number of years available from the 2000-2004 Baseline may result in greater differences in the 2018 URP points using the linear deciview and the curved extinction glidepaths.

Appendix F contains total extinction curved glidepaths for all the CENRAP Class I areas and Figure 5-5 contains a DotPlot that compares the percent of achieving the 2018 URP point at each CENRAP Class I area using the 2018 Base G modeling results and the linear deciview and curved extinction glidepaths. At most CENRAP Class I areas the ability of the 2018 modeling results to achieve the 2018 URP point is the same using either the deciview or extinction glidepaths. There are some differences at GUMO, BOWA and VOYA Class I areas which are due to these Class I areas having more complete data during the 2000-2004 Baseline period and therefore more years in the Baseline than other Class I areas as well as having variations in extinction across the worst 20 percent days and years (Appendix F). In any event, the closeness of the ability of the model to achieve the 2018 URP point using either the extinction or deciview

glidepath verifies the validity of the extinction based glidepaths and allows for the construction of PM species specific glidepaths in extinction to gain insight into how each component of extinction is being reduced to achieve a uniform rate of progress toward natural conditions in 2064.

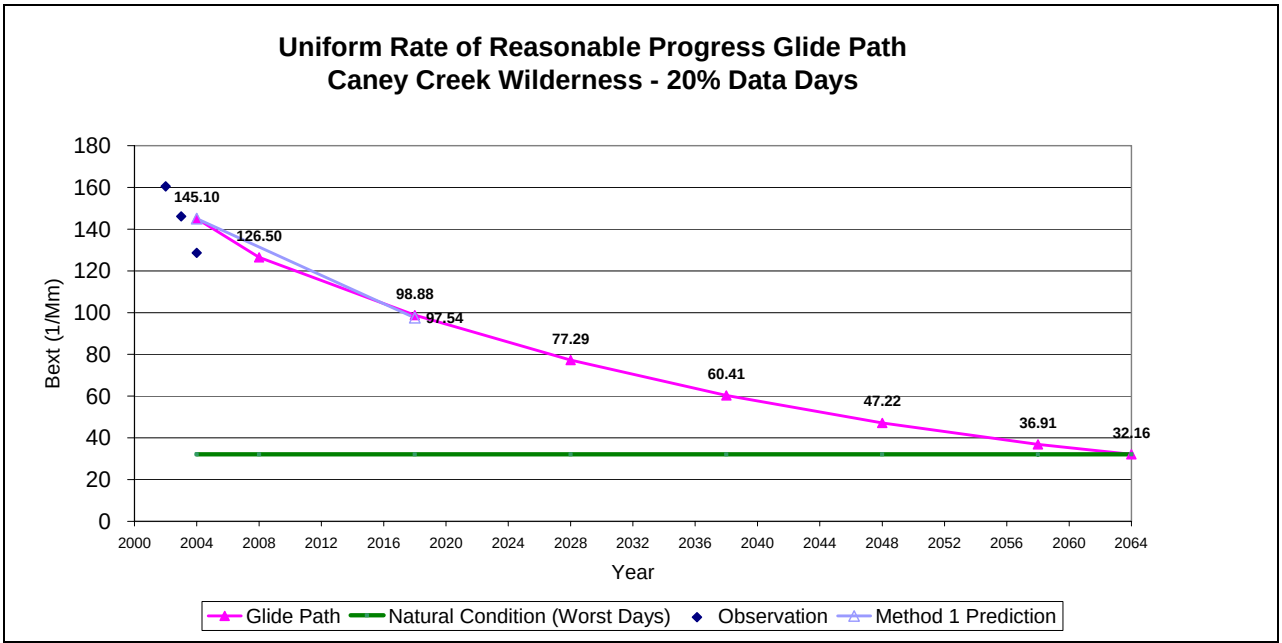

Figure 5-4. 2018 Visibility Projections and 2018 URP Glidepaths in extinction (Mm^{-1}) for Caney Creek (CACR), Arkansas and Worst 20% (W20%) days using 2002/2018 Base G CMAQ 36 km modeling results.

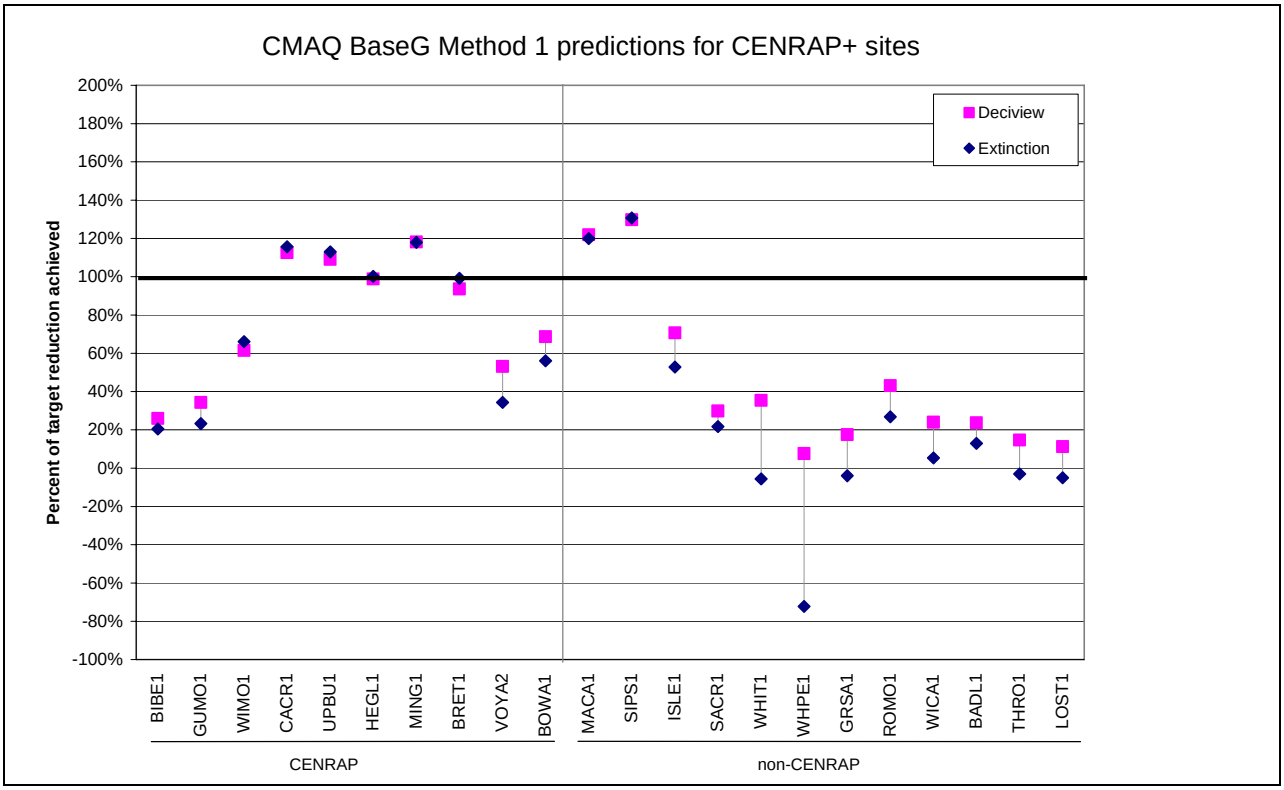

Figure 5-5. CMAQ 2018 Base G visibility projections and comparison of ability to achieve the 2018 URP point using the EPA default deciview and alternative total extinction Glidepaths.

5.2.2 PM Species specific Glidepaths

The VIEWS website (http://vista.cira.colostate.edu/views/) has posted PM species specific Natural Conditions based on the new IMPROVE equation. Using these PM species specific Natural Conditions and the curved extinction glidepaths we can evaluate how well visibility extinction achieves the 2018 URP point on a species-by-species basis. The PM species specific glidepaths are constructing starting with a Baseline at 2004 averaging the extinction for each PM species measured using the 2000-2004 IMPROVE observations and ending with the Natural Conditions in 2064 from the VIEWS website. Points in the glidepath for the years in between 2004 and 2064 are constructed based on the relative differences in the 2004 Baseline and 2064 Natural Conditions PM species extinction such that the total extinction due to all PM species at each interim year adds up to the same as the total extinction on the extinction-based glidepath (e.g., Figure 5-3). For example, for the CACR SO4 extinction glidepath the 2018 URP point is generated from the 2004 and 2064 SO4 extinction (BSO4) and the 2004, 2018 and 2064 total extinction (BTOT) as follows:

$$
\begin{aligned}
BSO4\_2018 &= BSO4\_2004 - [(BSO4\_2004 - BSO4\_2064)/ \\
&\quad (BTOT\_2004 - BTOT\_2064)] \times (BTOT\_2004 - BTOT\_2018) \\
&= 87.05 - [(87.05 - 3.20)/(145.10 - 32.16)] \times (145.10 - 98.88) \\
&= 52.73\ Mm^{-1}
\end{aligned}
$$

Note that the SO4 2018 URP point in Figure 5-5 and F-1b (52.77 Mm-1) does not exactly match the 52.73 Mm^{-1} calculated due to round off error in the above calculation that only used numbers with precision to the nearest hundredth.

As there are larger differences between the Baseline and Natural PM species extinction for some species, then the rate of improvement to achieve a species specific 2018 URP point will vary across PM species. For example, current Baseline extinction values for Soil and CM tend to be closer to Natural Conditions than extinction due to SO4 and NO3. Consequently the rate of progress to achieve the 2018 URP point for Soil and CM will be less than for SO4 and NO3.

Appendix F contains the PM species specific glidepaths compares them to the modeled 2018 projections for all CENRAP Class I areas. The species specific results for the CACR Class I area in Figure F-1 are reproduced in Figure 5-6. The modeled rate of SO4 and NO3 extinction reduction is greater than the PM species specific glidepaths and both achieve the species specific 2018 URP point by achieving 111% and 104% of the reduction needed to achieve the 2018 URP point. The modeled rate of extinction improvement at CACR for EC and OC is less than the species specific glidepath achieving only 65% and 75% of the reduction needed to achieve the species specific 2018 URP point. The PM species specific glidepath for Soil is flat because the Baseline and Natural Conditions (1.12 Mm^{-1}) are the same. This does not mean that anthropogenic emissions of Soil do not contribute on worst 20 percent days at CACR. It just points to a mismatch between the current set of worst 20 percent days and those in 2064 under Natural Conditions. The worst 20 percent days in 2064 under Natural Conditions will be dominated by wind blown dust days when Soil and CM may be higher than during the current set of worst 20 percent days that are dominated by SO4, NO3 and OMC. Thus, the Soil and CM glidepaths tend to be flatter and in some cases may even have an upward trend for some Class I areas (see Appendix F). Soil is projected to increase at CACR in 2018 so does not achieve its species specific URP point. Little reduction in CM is also seen by 2018. As discussed

previously, this is due in part to incompatibilities between the measured Soil and CM values at the IMPROVE monitor and the modeled Soil and CM species. In the model, a large component of the Soil and CM in the inventory is due to paved and unpaved road dust. These emissions are directly related to Vehicles Miles Traveled (VMT). VMT is projected to increase in future-years resulting in increases in road dust emissions. At the IMPROVE monitor, much of the measured Soil and CM is likely due to local dust events that are not simulated by the model using a 36 km grid resolution. Thus, the 2018 projections for Soil and CM are likely applying modeled changes due to road dust to local Soil and CM concentrations that in reality are likely natural and should remain unchanged in the future year. This is why alternative 2018 modeled projection approaches have been developed that assume that CM and CM and Soil are natural so remain unchanged in the future-year (see Section 5.5).

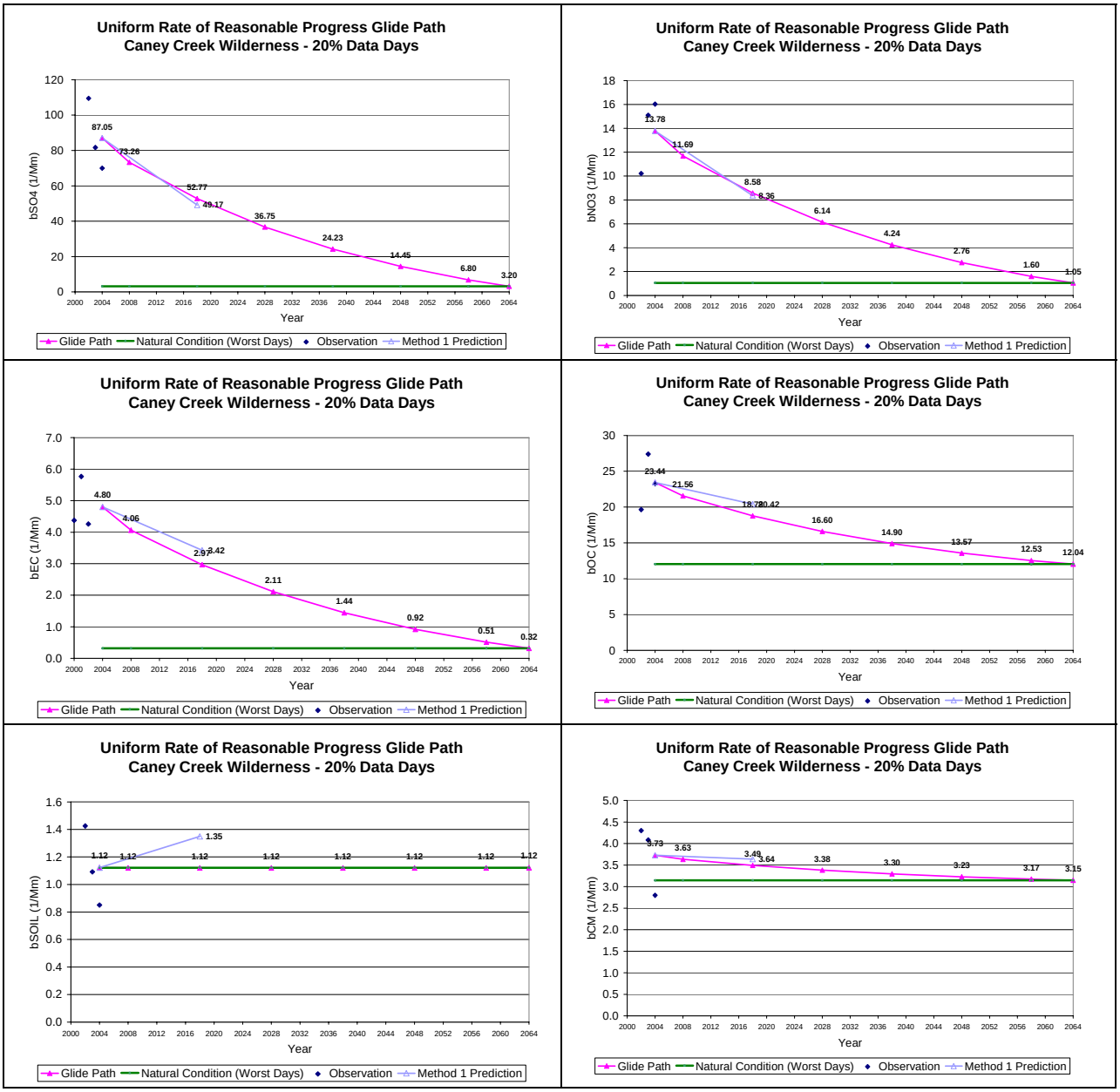

Figure 5-6. 2018 Visibility Projections and 2018 URP Glidepaths for SO4 (top left), NO3 (top right), EC (middle left), OMC (middle right), Soil (bottom left) and CM (bottom right) in extinction (Mm^{-1}) for Caney Creek (CACR), Arkansas and Worst 20 Percent Days using 2002/2018 Base G CMAQ 36 km modeling results.

Figure 5-7 displays a DotPlot that compares the 2018 projected total and PM species specific extinction with the 2018 URP points. These results show that SO4 is most frequently achieving its 2018 URP point at those Class I areas that achieve the deciview URP point. Reductions in NO3 and EC also sometimes achieve their species specific URP point.

There are some anomalies in the species specific projections and glidepaths that bear mention and point to areas where better estimates of emissions growth and Natural Conditions are needed needed. The increase in 2018 Soil projections is not an isolated incident at CACR and occurs at other CENRAP Class I areas. There are three CENRAP Class I areas that "achieve" the Soil specific 2018 URP point (HEGL, BOWA and VOYA). An examination of these glidepaths and visibility projections (Figures F-4f, F-5f and F-6f) reveals that the current Baseline Conditions Soil at these three Class I areas is actually less than the 2064 Natural Conditions so that the glidepath is an accent rather than reduction (Figures F-4g, F-5g and F-6g). In these three cases to "achieve" the 2018 URP point the modeling results must increase the projected Soil extinction, which is why these three Class I areas "achieve" their 2018 URP point for Soil. Clearly, the 2018 URP point for Soil is not very meaningful under these conditions. The current Baseline Conditions for OMC at BRET and BOWA is also less than the Natural Conditions resulting in anomalous glidepaths (Figure F-3e and F-4e).

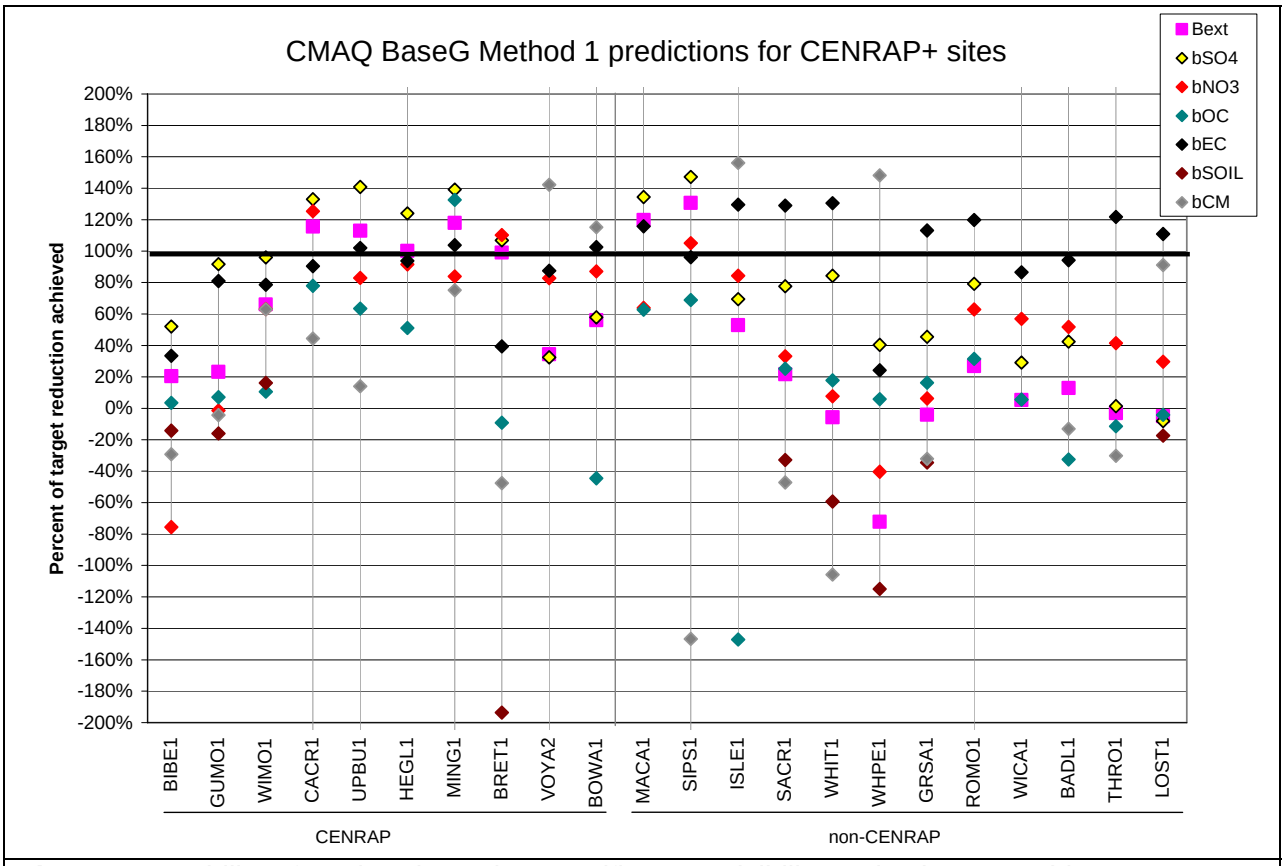

Figure 5-7. Ability of total and species specific 2018 visibility projections to achieve 2018 URP points.

5.3 Alternative 2018 Visibility Projection Software

The CENRAP 2018 visibility projections were made using software developed by the CENRAP modeling team. PM concentrations in the 36 km grid cells containing each of the Class I area IMPROVE monitoring sites were extracted using the UCR Analysis Tool. These modeling data were then ported into Excel spreadsheets that also include the filled RHR IMPROVE database available from the VIEWS website along with the EPA default Natural Conditions (EPA, 2003b). Excel macros are then used to perform the visibility projections using the EPA default procedures described in Chapter 4 and alternative procedures described in this Chapter.

EPA is developing a Modeled Attainment Test Software (MATS) program that codifies the 8-hour ozone, $PM_{2.5}$ and visibility projection procedures given in EPA's latest air quality modeling guidance (EPA, 2007a). The June 2007 release of the beta version of MATS is capable of performing 8-hour ozone and visibility projections; MATS is still under development for making $PM_{2.5}$ projections. The June 2007 beta versions of MATS was applied to the CENRAP 2002 and 2018 Base G 36 km CMAQ results and the resultant 2018 visibility projections were compared with the CENRAP values using the EPA default projection approach (see Chapter 4) at CENRAP and nearby Class I areas. The projected 2018 visibility estimates using the CENRAP and EPA MATS software are shown in Table 5-1. The biggest differences in the two 2018 visibility projections are for the Boundary Waters (BOWA). Breton Island (BRET), and Mingo (MING) Class I areas where MATS produces no 2018 visibility projections. This is because there is insufficient capture of valid IMPROVE PM measurements within the 2000-2004 five-year baseline to generate three years of annual visibility estimates that is the minimum needed to develop the Baseline Conditions following EPA's guidance (EPA, 2003a). For the CENRAP projections, data filling was used to fill out the IMPROVE measurements with sufficient data so that Baseline Conditions could be calculated at these three Class I areas. At 14 of the remaining 17 Class I areas, the CENRAP and MATS 2018 visibility projections agree exactly to within a hundredth of a deciview. At the three sites that are different (BIBE, GUMO and ISLE) the difference is 0.01 dv, which is 0.06 percent or less. These differences are likely due to round off errors in the calculations and are not significant. These results verify the consistency with the CENRAP spreadsheet based and EPA MATS software for projecting future-year visibility estimates.

Table 5-1. Comparison of CENRAP and EPA MATS 2018 visibility projections at CENRAP and nearby Class I areas.

	2018 Visibility Projections		2000-2004 Baseline Conditions	
Site	MATS (dv)	CENRAP (dv)	MATS (dv)	CENRAP (dv)
BADL	16.53	16.53	17.14	17.14
BIBE	16.70	16.69	17.30	17.30
BOWA	NA	18.30	NA	19.58
BRET	NA	22.72	NA	25.73
CACR	22.48	22.48	26.36	26.36
GRSA	12.53	12.53	12.78	12.78
GUMO	16.36	16.35	17.19	17.19
HEGL	23.06	23.06	26.75	26.75
ISLE	19.35	19.36	20.74	20.74
LOST	19.27	19.27	19.57	19.57
MACA	25.60	25.60	31.37	31.37
MING	NA	23.71	NA	28.02
ROMO	13.17	13.17	13.83	13.83
SACR	17.25	17.25	18.03	18.03
SIPS	23.57	23.57	29.03	29.03
THRO	17.40	17.40	17.74	17.74
UPBU	22.52	22.52	26.27	26.27
VOYA	18.37	18.37	19.27	19.27
WHIT	13.14	13.14	13.70	13.70
WHPE	10.34	10.34	10.41	10.41
WICA	15.39	15.39	15.84	15.84
WIMO	21.47	21.47	23.81	23.81

NA = Not Available

5.4 PM Source Apportionment Modeling

The PM Source Apportionment Technology (PSAT) was used to obtain PM source apportionment by geographic regions and major source category for the CENRAP 2002 and 2018 Base E base case conditions. PSAT uses reactive tracers that operated in parallel to the CAMx host model using the same emissions, transport, chemical transformation and deposition rates as the host model to account for the contributions of user specified source regions and categories to PM concentrations throughout the modeling domain. Details on the formulation of the CAMx PSAT source apportionment can be found in the CAMx user's guidance (ENVIRON, 2006; www.camx.com).

5.4.1 Definition of CENRAP 2002 and 2018 PM Source Apportionment Modeling

PSAT calculated PM source apportionment for user defined source groups. Source groups are usually defined by specifying a source region map of geographic regions where source contributions are desired and providing source categories as input so that source group would

consist of a geographic region plus source category (e.g., on-road mobile source emissions from Oklahoma). Although other source group configurations and even individual sources may be specified. For the CENRAP PSAT application, a source region map was used that divided up the modeling domain into 30 geographic source regions as shown in Figure 5-8. The 2002 and 2018 emissions inventories were divided into six source categories. The 30 geographic source regions consisted of CENRAP and nearby states, with Texas divided into 3 regions, remainder of the western and eastern States, Gulf of Mexico, Canada and Mexico. The original intent of the CENRAP PSAT analysis was to obtain separate contributions due to on-road mobile, non-road mobile, area, natural, EGU point and non-EGU point sources. However, the CAMx emissions for the PSAT runs were based on the CMAQ pre-merged 3-D emission files. Since all point sources were contained in a single CMAQ pre-merged emissions file, then the separate source apportionment modeling of EGU and non-EGU point sources was not possible. The six source categories that were separately tracked in the PSAT PM source apportionment modeling were:

- Elevated point sources;
- Low-level point sources (i.e., point source emissions emitted into layer 1 of the model);
- On-Road Mobile Sources;
- Non-Road Mobile Sources;
- Area Sources; and
- Natural Sources.

Natural Sources included biogenic VOC and NOx emissions from the BEIS3 biogenic emissions model, emissions from wildfires and emissions from wind blown dust due to non-agriculture land use types.

PM source apportionment in PSAT is available for five families of PM tracers: (1) Sulfate; (2) Nitrate and Ammonium; (3) Secondary Organic Aerosols (SOA); (4) Primary PM; and (5) mercury. The CENRAP PSAT 2002 and 2018 applications used three of the PSAT families of tracers and did not use the SOA and mercury families. For SOA, the standard CAMx model output was used that partitions SOA into an anthropogenic (SOAA) and biogenic (SOAB) components.

The PSAT results were extracted at the CENRAP and nearby Class I areas and the contributions for the average of the worst 20 percent and best 20 percent days were processed. A PSAT Visualization Tool was developed that can be used by States, Tribes and others to generate displays of the contributions of source regions and categories to visibility impairment for the average of the worst 20 percent and best 20 percent days at each CENRAP and nearby Class I areas.

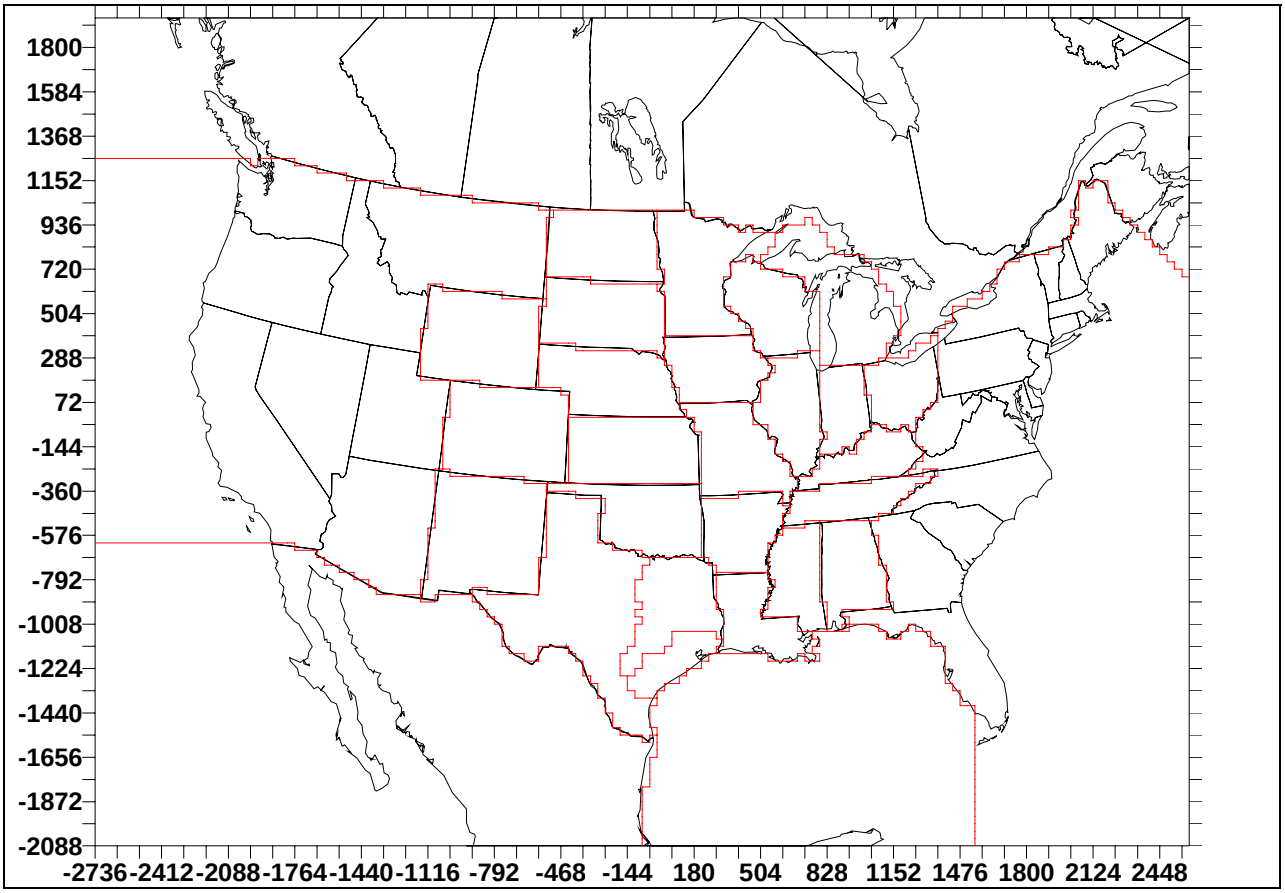

Figure 5-8. 30 source regions used in the CENRAP 2002 and 2018 CAMx PSAT PM source apportionment modeling.

5.4.2 CENRAP PSAT Visualization Tool

The PSAT Visualization Tool allows CENRAP States, Tribes and others to visualize the CENRAP 2002 and 2018 PSAT modeling results and identify which source regions, categories and PM species are contributing to visibility impairment at Class I areas for the average of the worst 20 percent and best 20 percent visibility days. The Visualization Tool is currently available on the CENRAP website (http://www.cenrap.org) under Projects. The Tool can generate bar charts of source contributions at Class I areas. It can be run in a receptor oriented mode where it identifies the contributions of PM species and source regions and categories to visibility impairment on the worst and best 20 percent days. It can also be run in a source oriented mode to examine an individual source region's (State's) contribution to visibility impairment at downwind Class I areas on the worst and best 20% days. The original IMPROVE equation is used to convert the PM species concentrations to extinction.

There are 14 air quality analysis metrics in the Tool:

W20% Modeled Bext: The source region, source category and PM species contributions to the extinction (Bext) at a Class I area estimated by the model averaged across the worst 20 percent days in 2002.

W20% Projected Bext: The source region, source category and PM species contributions to the extinction (Bext) at a Class I area projected by the model averaged across the worst 20 percent days in the 2000-2004 Baseline.

W20% Modeled USAnthro: The source region, source category and PM species contributions to the extinction (Bext) at a Class I area for just U.S. anthropogenic emission source categories estimated by the model averaged across the worst 20 percent days in 2002.

W20% Projected USAnthro: The source region, source category and PM species contributions to the extinction (Bext) at a Class I area for just U.S. anthropogenic emission source categories projected by the model averaged across the worst 20 percent days in the 2000-2004 Baseline.

Emissions: Emissions by source region, source category and PM precursor. Precursors include SOx, NOx, primary organic aerosol (POA), primary elemental carbon (PEC) other primary fine particulate (FCRS+FPRM) and coarse mass (CCRS+CPRM). Emissions for four days have been extracted and implemented in the Tool.

Control Effectiveness: Control effectiveness is defined as the PM contribution divided by the emissions of the primary precursor. For example the SO4 contribution divided by the SO2 emissions.

Visualization Tool results are available for visibility contributions on both an absolute (Mm^{-1}) and percentage basis. When looking at contributions at a given Class I area, contributions can be examined in terms of PM species, source regions and/or source categories. Results are available for both the current year (2002 modeled or 2000-2004 projected) and future year (2018). The "2002 W20% Project Bext" metric applies the 2002 PSAT modeled source apportionment to the observed 2000-2004 Baseline extinction keeping the relative contributions of source groups to each PM species (e.g., SO4, NO3, etc.) the same averaged across the 2002 worst 20 percent days but scaling their magnitudes up or down based on the ratio of the 2000-2004 Baseline to the 2002 modeling results. Similarly, the "2018 W20% Projected" metric uses the relative contributions of the 2018 PSAT results from each source group and scales them according to the differences in the 2018 projected PM species to the 2018 modeled PM species for the average of the worst 20 percent days. The US Anthropogenic metrics just include source groups associated with U.S. man-made emissions (i.e., non-Natural source categories from states and Gulf of Mexico source regions) so excludes contributions from Canada and Mexico, Boundary Conditions, SOA from biogenic sources and the natural source category (biogenic NOx, wildfires and wind blown dust).

5.4.3 Source Contributions to Visibility Impairment at Class I Areas

Appendix E displays example contributions of PM species, source regions and source categories to visibility impairment for the worst and best 20 percent days at the CENRAP Class I areas. Some of the results from Figure E-1 for the CACR Class I area are reproduced in Figures 5-9, 5-10 and 5-11 below.

5.4.3.1 Caney Creek (CACR) Arkansas

2002 visibility impairment for the worst 20 percent days at CACR is primarily due to SO4 from elevated point sources that contributes over half (66.3 Mm^{-1}) of the total extinction of 118.8 Mm^{-1} (Figure E-1a and 5-8 left). By 2018, the total extinction at CACR for the worst 20 percent days is reduced by approximately one third (38.5 Mm^{-1}) which is primarily due to reductions in SO4 extinction from elevated point sources (from 66.3 to 37.3 Mm^{-1}) as well as reductions in visibility impairment from on-road and non-road mobile sources. Even with such large reductions in SO4 from point sources in 2018, extinction due to elevated point sources is still the highest contributor to visibility impairment on the worst 20 percent days contributing over half (41.8 Mm^{-1}) of the total extinction in 2018 of 80.3 Mm^{-1}, with area sources the next most important source category contributing 16.0 Mm^{-1} (~20%).

The geographic source apportionment for the worst 20 percent says at CACR is shown in Figures 5-10, E-1c and E-1d. Elevated point sources from the eastern source region is the largest contributor in 2002 contributing almost 18 Mm^{-1} that is reduced by over a factor of three in 2018 to approximately 5 Mm^{-1}. By 2018, Arkansas is the largest contributor to extinction at CACR for the 20 percent worst days followed by East Texas, the large Eastern U.S. region and then SOA due to biogenic sources. Figures E-1e ranks the source group contributions to extinction on the worst 20 percent days at CACR with Elevated Point Sources from East Texas being the highest contributor to total extinction, similar results are seen when examining extinction at CACR for the worst 20 percent days due to just SO4 and NO3 (Figure E-1f).

For the best 20 percent days at CACR (Figures 5-11, E-1g-j), SO4 is still a major contributor but no where near as dominate as seen for the worst 20 percent days, but elevated point is still the largest contributing source category Local contributions from within Arkansas contribute the most to the average of extinction across the best 20 percent days at CACR.

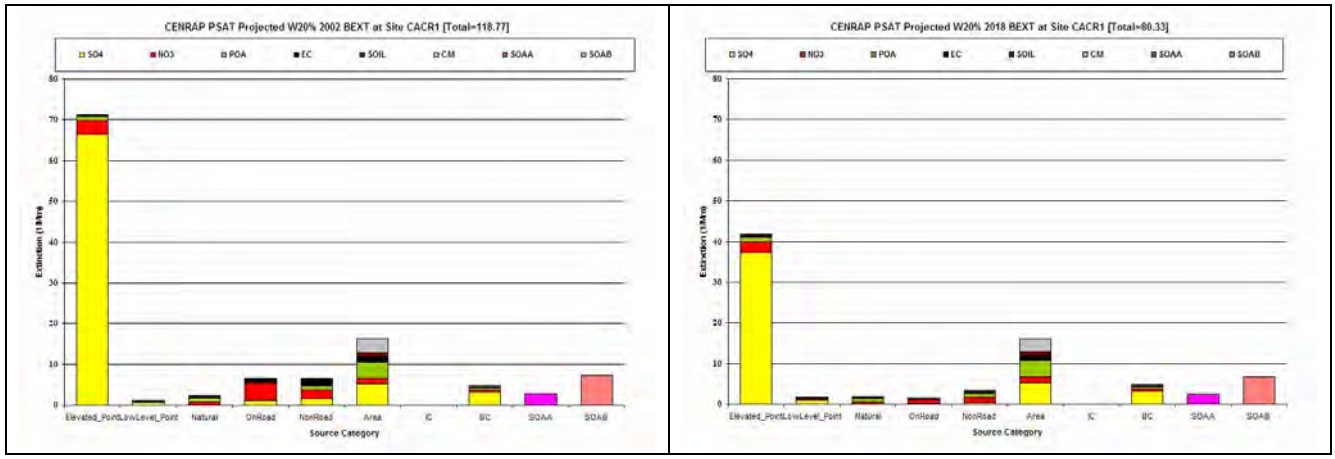

Figure 5-9. PSAT source category by PM species contributions to the average 2000-2004 Baseline and 2018 projected extinction (Mm^{-1}) for the worst 20 percent visibility days at Caney Creek (CACR), Arkansas.

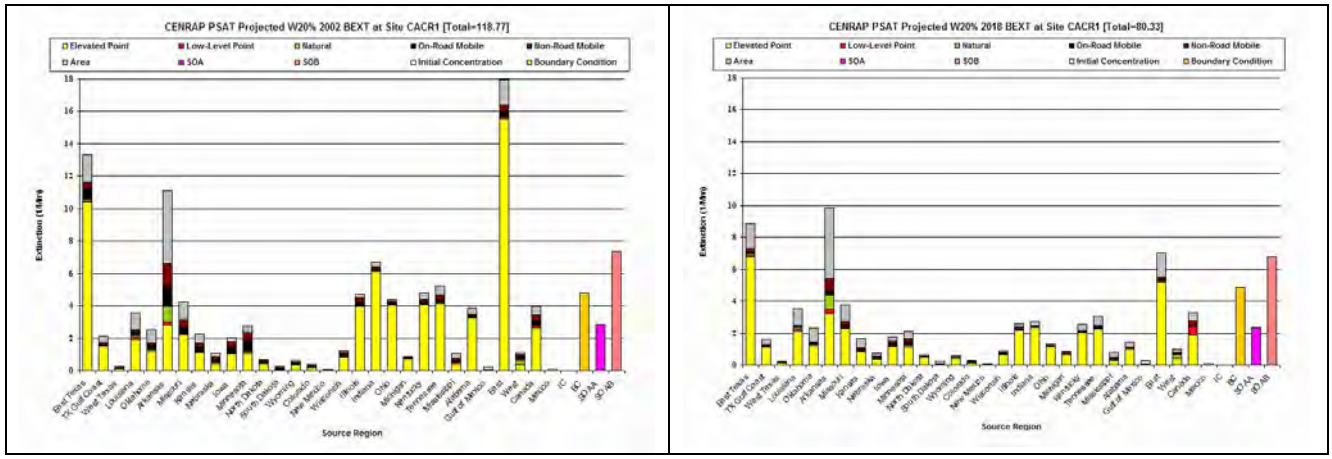

Figure 5-10. PSAT source region by source category contributions to the average 2000-2004 Baseline and 2018 projected extinction (Mm^{-1}) for the worst 20 percent visibility days at Caney Creek (CACR), Arkansas.

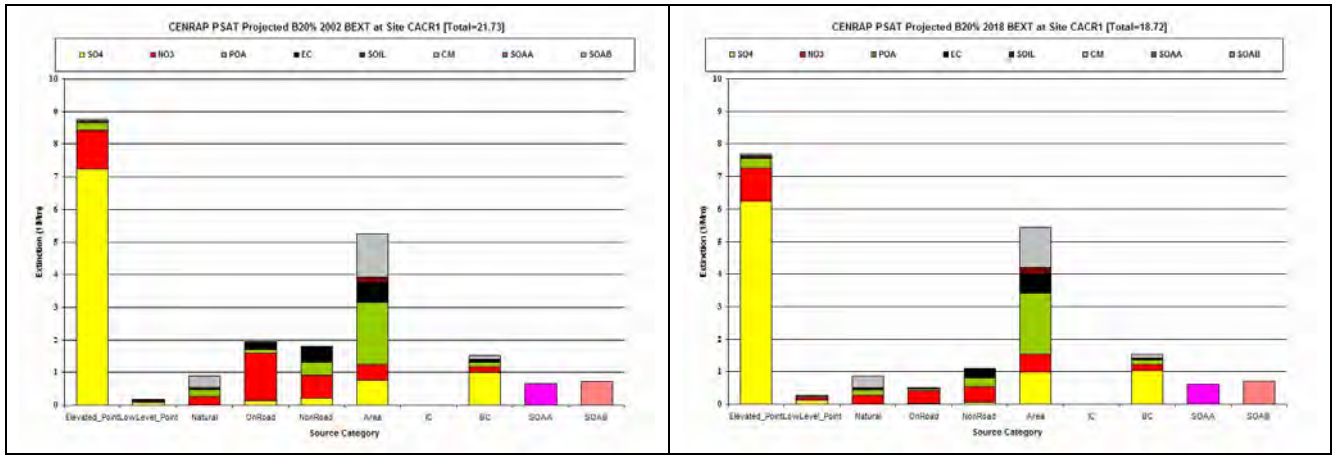

Figure 5-11. PSAT source category by PM species contributions to the average 2000-2004 Baseline and 2018 projected extinction (Mm^{-1}) for the best 20 percent visibility days at Caney Creek (CACR), Arkansas.

5.4.3.2 Upper Buffalo (UPBU) Arkansas

The contributions to extinction on the worst 20 percent days at UPBU (Figure E-2) is similar to CACR only with less contributions from East Texas and more from Missouri, Illinois and Indiana. By 2018, the top five highest contributing source groups to the average extinction on the worst 20 percent days are as follows: Arkansas Elevated Point; SOA from biogenics; Boundary Conditions, East Elevated Points, and Illinois Elevated Points (Figure E-2e). On the best 20 percent days at UPBU visibility impairment is primarily due to Arkansas and adjacent states Oklahoma, Missouri, and Kansas).

5.4.3.3 Breton Island (BRET) Missouri

Visibility impairment for the worst 20 percent days at Breton Island is primarily (69%) due to elevated point sources that contribute 77.7 Mm^{-1} out of a total of 122.2 Mm^{-1} (Figure E-3a). Although the contribution of elevated point sources is reduced substantially by 2018, they still contribute over half of the total extinction (101.1 Mm^{-1}) on the worst 20 percent days at BRET (Figure E-3b). The top five contributing source groups to 2018 visibility impairment at BRET for the worst 20 percent days are: Louisiana Elevated Point Sources; Boundary Conditions; East Elevated Point Sources; Gulf of Mexico Area Sources and Louisiana Area Sources. Gulf of Mexico Area sources includes off shore shipping and oil and gas development emissions; note that for the PSAT simulation the off-shore marine shipping emissions were double counted which was corrected in the Base G emission scenarios used in the 2018 visibility projections discussed in Chapter 4.

5.4.3.4 Boundary Waters (BOWA) Minnesota

As seen for the other Class I areas, elevated point sources contribute the largest amount (47%) to visibility impairment at BOWA for the worst 20 percent days in 2002 (Figure E-4a). However, unlike many of the other Class I areas, there is little reductions (~10%) in the elevated point source contributions going from 2002 (29.0 Mm^{-1}) to 2018 (26.2 Mm^{-1}) (Figures E-4a and E-4b). This is because there is a slight increase in the contributions of elevated point sources in Minnesota from 2002 to 2018 (Figures E-4c and E-4d) that is the highest contributing source group (Figure E-4e). Note that the 2018 emission scenario includes growth and CAIR controls but no BART controls. For the best 20 percent days, the largest contributing source group by far is Boundary Conditions (i.e., global transport) followed by Minnesota and Canada (Figures E-4g-j).

5.4.3.5 Voyageurs (VOYA) Minnesota

Results for VOYA are similar to BOWA with Minnesota, Canada and Boundary Conditions contributing the most to visibility impairment on the worst and best 20 percent days (Figure E-5).

5.4.3.6 Hercules Glade (HEGL) Missouri

Elevated point sources contribute over half to the total extinction for the worst 20 percent days at HEGL in 2002 (Figures E-6a and E-6b). Going from 2002 to 2018 the contributions due to elevated point sources, on-road mobile and non-road mobile are reduced substantially, but the contributions due to the other sources remain unchanged. The largest source group contributing to visibility impairment on the worst 20 percents days is area sources from Missouri in both 2002 and 2018 (Figures E-6c and E-6d). Since area emissions are not reduced much between 2002 and 2018 and Missouri elevated point sources are mostly unchanged because the IPM model assumed Missouri CAIR sources would buy credits, then the Missouri contributions is only reduced a little going from 2002 to 2018 (from ~18 Mm-1 to ~16 Mm-1). However, the contributions due to the Eastern U.S., Illinois and Indiana are reduced substantially. Missouri is by far the largest contribution to visibility impairment at UPBU on the best 20 percent days as

well with area sources from Missouri being the largest source category (Figures E-6h through E-6j).

5.4.3.7 Mingo (MING) Missouri

The substantial improvements in visibility impairment at MING for the worst 20 percent days from 2002 (141 Mm^{-1}) to 2018 (96 Mm^{-1}) is primarily due to reductions in SO4 from non-Missouri elevated point sources (Figures E-7a through E-7d). Even so, with the exception of the top contributing Missouri area sources the largest contributing source groups to 2018 visibility impairment for the worst 20 percent days are still elevated point sources from several CAIR states (Illinois, Indiana, Missouri, East; Figure E-7e). Missouri is the largest contributor to visibility on the best 20 percent days followed by Boundary Conditions and Illinois (Figure E-7i-j).

5.4.3.8 Wichita Mountains (WIMO) Oklahoma

Elevated point sources are the largest contributors to visibility impairment on the worst 20 percent days at WIMO in both 2002 and 2018 (Figures E-8a and E-8b). East Texas followed closely by Oklahoma are the largest contributing source regions in 2002, but by 2018 the reverse is true (Figures E-8c and E-8d). By 2018 the largest contributing source group to visibility impairment on the worst 20 percent days at WIMO is global transport (i.e., boundary conditions) followed by Oklahoma Area Sources and East Texas Elevated Point sources (Figure E-8e). Oklahoma Area Sources is the largest contributor to visibility impairment on the best 20 percent days at WIMO (Figures E-8g-j).

5.4.3.9 Big Bend (BIBE) Texas

Elevated point sources (~17 Mm^{-1}) followed by Boundary Conditions (~12 $Mm^{-}1$) are the largest contributions to total extinction (46 Mm^{-1}) on the worst 20 percent days at BIBE in 2002 (Figure E-9a). In 2018 there is very little (~2 Mm^{-1}) reduction in the contributions of elevated point sources and no reductions in global transport resulting in little reductions (~7%) in visibility impairment on the worst 20 percent days from 2002 (46 Mm^{-1}) to 2018 (43 Mm^{-1}). This is due to the extremely large contributions of emissions from Mexico in both 2002 (Figure E-9c) and 2018 (Figure E-9d). In fact, the four highest contributing source groups to visibility impairment at BIBE for the worst 20 percent days are assumed to be unchanged from 2002 to 2018: Boundary Conditions, Mexico Elevated Points, West Texas Natural and Mexico Natural (Figure E-9e). For the best 20 percent days at BIBE, West Texas, Mexico and Boundary Conditions are the highest three contributors to visibility impairment (Figures E-9g-j).

5.4.3.10 Guadalupe Mountains (GUMO) Texas

The large contribution of CM to visibility impairment at GUMO is clearly evident in the source apportionment modeling results (Figures E-10a-b). These sources are about evenly divided in the modeling between natural sources and area sources. Since these source categories are not reduced in the future year then there is little reduction in extinction from 2002 to 2018 (50 to 45

Mm^{-1}) and what reductions there are come from Elevated Point Sources. Sources in West Texas, Mexico, Boundary Conditions and New Mexico are the largest contributing source regions for both the worst 20 percent days (Figure E-10c-e) and best 20 percent days (Figures E-10g-j).

5.5 Alternative Visibility Projection Procedures

In this section we analyze several alternative visibility projection procedures from the EPA's default approach (EPA, 2007a) used in Chapter 4.

5.5.1 Treatment of Coarse Mass and Soil

As noted previously, much of the coarse mass (CM) and, to a lesser extent, Soil measured at the IMPROVE monitor is likely due to local wind blown dust that is natural in origin and not captured by the model. Consequently, even using the modeling results in a relative sense with the RRFs may not be appropriate for projecting CM and Soil. If CM and Soil are in fact local impacts due to wind blown dust from natural lands, then it would be appropriate to assume they are natural and remain unchanged from the 2000-2004 Baseline to 2018. This is probably certainly appropriate for CM because CM is primarily due to fugitive dust and it has a very short transport distance that is subgrid-scale to the model. In fact the model evaluation discussed in Chapter 3 and Appendix C clearly shows a large underprediction bias for CM that is likely due to local fugitive dust impacts at the IMPROVE monitor. For Soil this is less clear as fine particles can be transported over longer distances and is produced by anthropogenic sources, such as combustion and road dust, as well as natural sources. We initially performed two CM and Soil sensitivity tests, the first assumed CM was all natural so remains unchanged from the 2000-2004 Baseline to 2018 (i.e., set the RRF for CM equal to 1.0). The second sensitivity test assumed both CM and Soil were natural so set RRFs for both of them to 1.0. A comment from an FLM noted that we know some of the Soil is likely anthropogenic in origin. So it was suggested to subtract the 2002 base case modeled Soil from the observed values for the 2002 worst 20 percent days and assume that the remainder (if any) was natural so hold the rest of the Soil constant in 2018 and add to the 2018 modeled Soil values.

The results of the CM and Soil visibility projection sensitivity analysis are shown in the DotPlot in Figure 5-12. The CM and Soil visibility projection sensitivity analysis has little effect on the 2018 visibility projections at the CENRAP Class I areas. Even GUMO, which has a large CM and Soil component, shows very little sensitivity. This is probably because the CM at GUMO is likely dominated by wind blown dust that was assumed constant from 2002 to 2018 so the RRF calculated using the default EPA method is near 1.0 anyway. Some larger sensitivity is seen at several WRAP Class I areas. It is encouraging that CENRAP 2018 visibility projections are not sensitive to the CM and Soil components of the modeling which are highly uncertain.

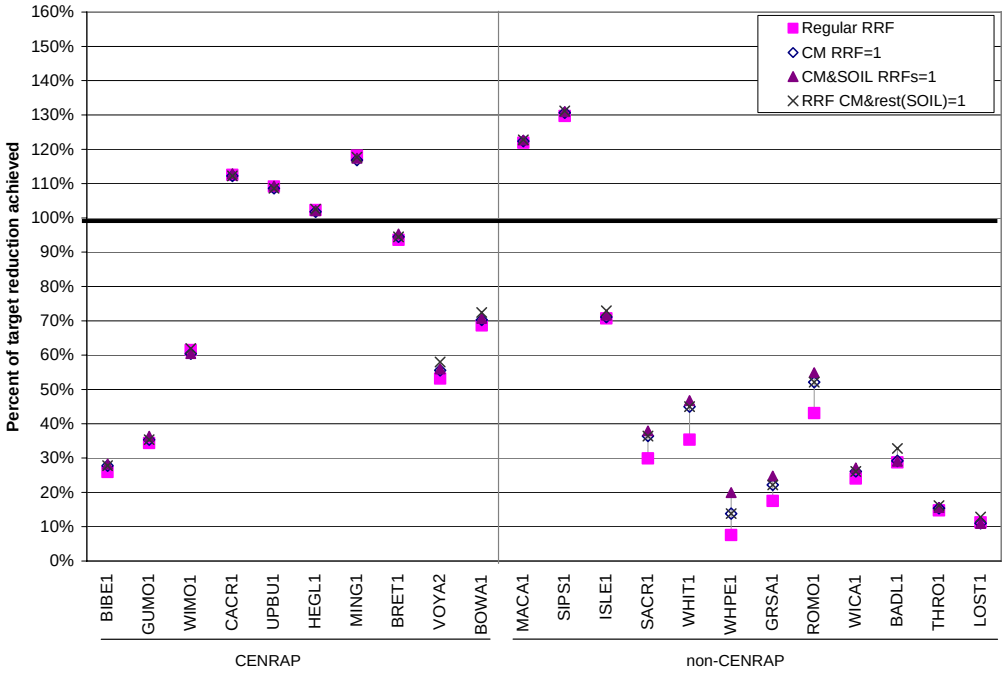

Figure 5-12. Sensitivity of 2018 visibility projections to various methods that assume all CM, all CM and Soil and all CM and part of the Soil is natural.

5.6 Alternative Model

The CAMx model was also run for a 2002 and 2018 base case scenarios with earlier versions of the CENRAP emissions (Base E modified to eliminate double counting of some area fire emissions) than the final CMAQ 2002 Base G modeling. The CAMx 2002 and 2018 output was processed the same way that the CMAQ results were to generate 2018 visibility projections at the CENRAP and nearby Class I areas that were compared with the 2018 URP point. Figure 5-13 summarizes the CAMx 2018 visibility projections using the new IMPROVE algorithm (NIA) in a DotPlot and compares them with the CMAQ 2018 Base G results (from Figure 5-12). The CMAQ and CAMx 2018 visibility projections are remarkably similar. The four Arkansas and Missouri Class I areas are projected to achieve the 2018 URP point by almost the exact same amount by the two models. The two Texas Class I areas are projected to come up short of achieving the 2018 URP point by the same amount by the two models. The largest differences are seen at BRET, and to a lesser extent BOWA and VOYA. At BRET the CAMx 2018 visibility projections are much less optimistic (< 80%) in achieving the 2018 URP point than CMAQ (> 90%). And CMAQ is slightly less optimistic than CAMx in achieving the 2018 URP point for the two northern Minnesota Class I areas. The reasons for these differences are unclear but could be partially due to the emissions updates in the final CMAQ Base G run that included eliminating the double counting of off-shore marine emissions in the Gulf of Mexico that was present in the CAMx simulation, which makes it more difficult to get visibility improvements at BRET since it is influenced by sources in the Gulf. Corrections to stack parameters for Canadian point sources were also made for the final Base G. The general close agreement of the CAMx 2018 visibility projections to the final CMAQ values is encouraging and good QA check.

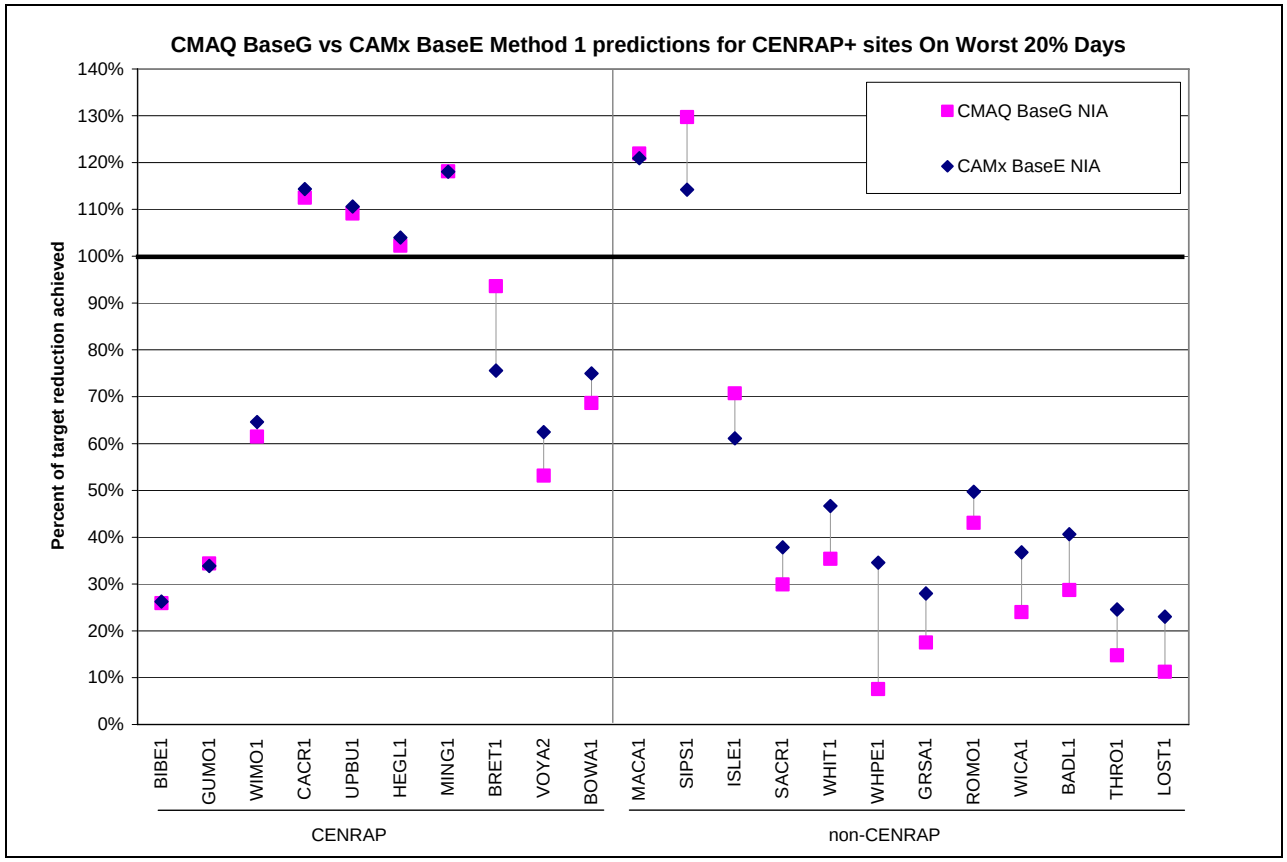

Figure 5-13. Comparison of CAMx 2018 visibility projections with 2018 URP points for CENRAP and nearby Class I areas.

5.7 Effects of International Transport on 2018 Visibility Projections

As seen in the PM source apportionment modeling discussed in Section 5.4, there is significant contributions of international sources to visibility impairment at many CENRAP Class I areas for the worst 20 percent days. With the exception of Canada, where we used a year 2000 inventory for the 2002 base case modeling and a 2020 inventory for the 2018 inventory, international sources were assumed to be constant between 2002 and 2018. Thus, Class I areas that are heavily impacted by contributions of international transport will have a difficult time achieving the 2018 URP point since international sources are assumed to remain constant. The CAMx PSAT runs discussed previously provide a framework for quantitatively assessing the contributions of international transport to the visibility projections and whether reasonable progress toward natural conditions is being achieved in the 2018 modeling.

There are several source regions (Figure 5-8) and source categories in the PSAT modeling that include international sources:

- Mexico Anthropogenic Sources (assumed all international);
- Canada Anthropogenic Sources (assumed all international);
- Gulf of Mexico (assumed all U.S. sources);
- Pacific and Atlanta Ocean (assumed all U.S. sources); and
- Boundary Conditions (assumed half international and half natural sources).

Although it can be argued that Mexico and Canada are not truly international due to the presence of numerous U.S. corporations in Mexico along with free trade among the two countries, states and federal government have no jurisdiction to regulate industry in these two countries so they are considered international in these calculations. The Gulf of Mexico includes off-shore oil and gas production facilities, support vessels and aircraft and off-shore marine shipping. Given that emissions from the oil and gas production can be regulated by the U.S., then the Gulf of Mexico is not considered an international source. Emissions from off-shore shipping in the Pacific and Atlantic Oceans are also currently not regulated by the U.S. government. However, there are current efforts to apply some regulations to these emissions so for these calculations they were not assumed to be international sources. Finally, the Boundary Conditions (BCs) for the CENRAP modeling were generated from a 2002 simulation of the GEOS-CHEM global chemistry model and held constant in 2018. These BCs would include contributions from international sources as well as natural sources, so need to be split. For the sensitivity calculations discussed below we assumed that the BCs were half due to natural and half due to international sources. This results in international sources being defined as follows:

International Contribution = Mexico Anthro + Canada Anthro + ½ BCs

Two methods were examined to see what the effects of international sources on 2018 visibility projections and a Class I areas ability to achieve the 2018 URP point:

Elimination of International Contributions to 2018 Visibility Projections: In this method the contribution of international emissions is taken out of the 2018 visibility projections and examined to see whether the new visibility projection achieves the URP point. If so, then international sources are hindering a Class I area in achieving the 2018 URP point, which suggests that the 2018 URP point is not a reasonable value for an RPG.

Visibility Projections and Glidepaths Based on Controllable Visibility Impairment: The second method would look at the visibility projections for just the U.S. controllable portion of the visibility impairment. The glidepath end point in 2064 would be to eliminate the U.S. man-made contributions to visibility impairment on the worst 20 percent days.

Note that this analysis is performed solely for providing states and others additional information on which Class I areas the modeling suggest are unduly influenced by International Transport.

5.7.1 Elimination of International Contributions to 2018 Visibility Projections

This method was also discussed in a recent technical brief prepared by the Electric Power Research Institute (EPRI), only in EPRI's analysis they used results from a global chemistry model and VISTAS CMAQ runs with no global anthropogenic emissions (EPRI, 2007). Thus, before discussing our results of this analysis using PSAT, we discuss EPRI's analysis.

5.7.1.1 EPRI's Analysis of Effects of International Contributions

EPRI funded Harvard University to perform annual simulations of the GEOS-Chem global chemistry model (http://www-as.harvard.edu/chemistry/trop/geos/) for annual simulations with and without non-U.S. anthropogenic emissions to determine the contributions of international transport to PM and visibility. The EPRI Harvard GEOS-Chem simulations were performed for 2001. Figure 5-14 and 5-15 compare the annual average ammonium sulfate, ammonium nitrate organic mass carbon (OMC, also called OCM) and elemental carbon (EC) due to the GEOS-Chem global modeling and the CAMx PSAT source apportionment modeling. The similarity of the results for ammonium sulfate is remarkable (Figure 5-14). Both methods estimate that the annual average ammonium sulfate contribution due to international sources ranges from 0.4 to 1.0 $\mu g/m^3$ across the Class I areas. There is less agreement between the two methods for ammonium nitrate due in part to a CAMx overestimation issue that is likely due in part to how ammonia emissions were classified as being anthropogenic or not in the no U.S. anthropogenic emissions simulations (Figure 5-15). Better agreement is seen between the two methods international contributions of OMC and EC, although CAMx estimates higher contributions than GEOS-Chem.

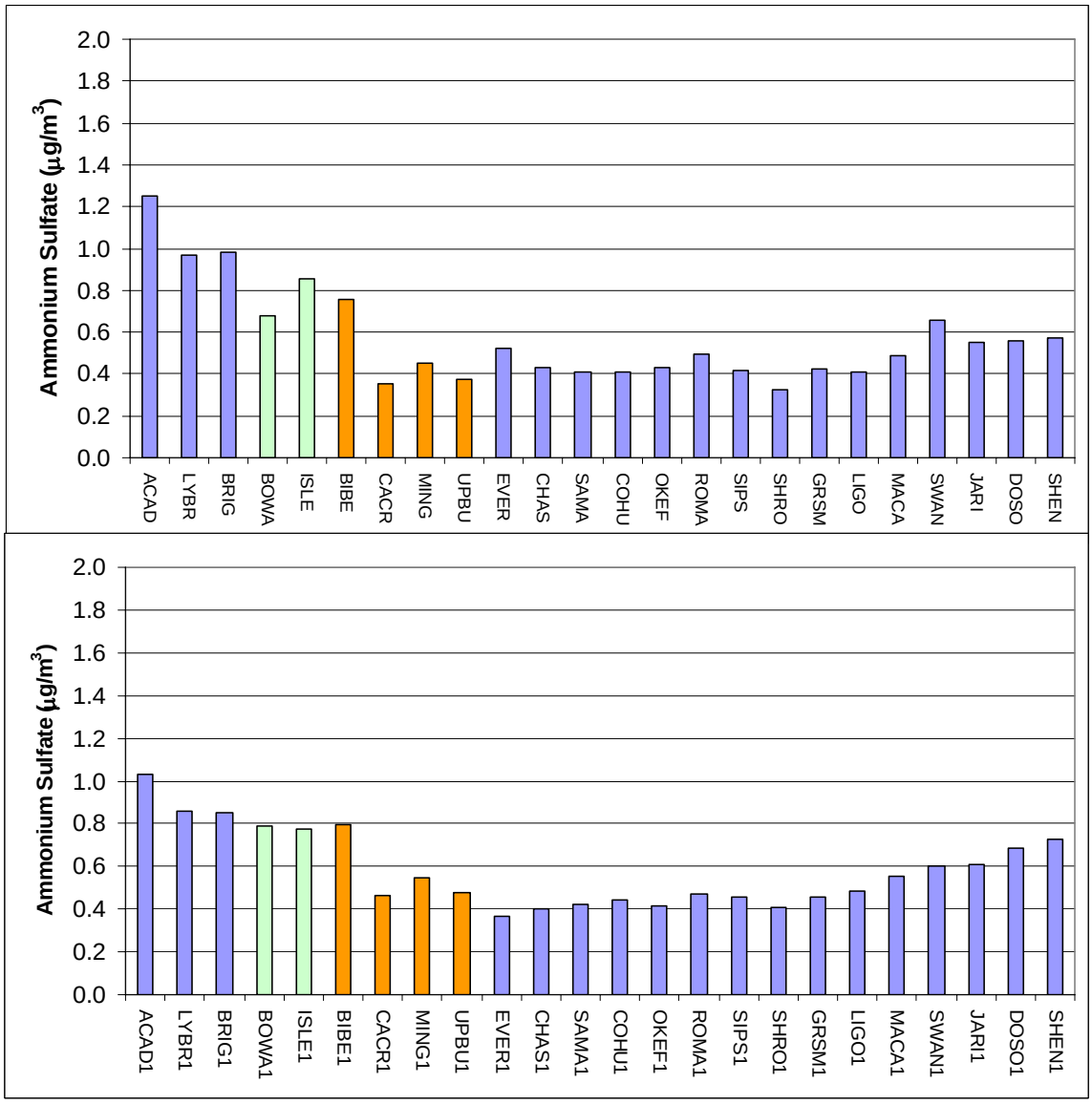

Figure 5-14. Comparison of EPRI Harvard GEOS-Chem global chemistry (top) and CENRAP PSAT (bottom) international source contributions to ammonium sulfate at Class I areas.

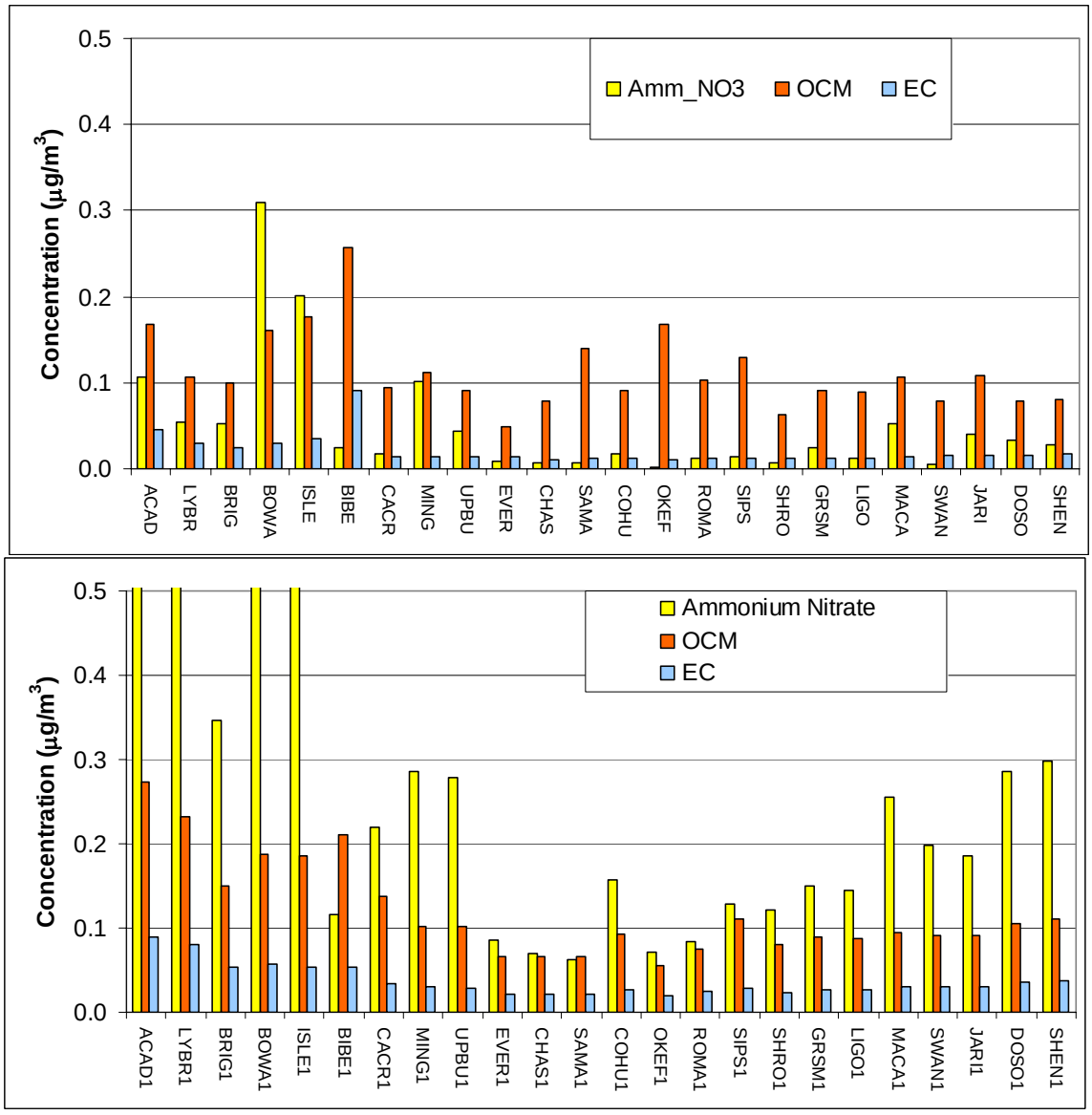

Figure 5-15. Comparison of EPRI Harvard GEOS-Chem global chemistry (top) and CENRAP PSAT (bottom) international source contributions to ammonium nitrate, organic carbon mass (OCM or OMC) and elemental carbon (EC) at Class I areas.

The EPRI technical brief used the VISTAS CMAQ runs to adjust the modeled 2018 visibility projections to eliminate the effect of international transport and compared them to the 2018 URP point. For the Boundary Waters, Voyageurs, Isle Royal and Seney Class I areas the standard 2018 visibility projections did not achieve the 2018 URP point. However, when the effect of transboundary pollutions was removed the 2018 URP point was essentially achieved or more than achieved at all four Class I areas.

5.7.1.2 CENRAP Results From Elimination International Transport

Because the elimination of the international sources from the 2018 visibility projections results in a portion of the total light extinction, then these comparisons with the 2018 URP points were done using extinction glidepaths and projections rather than deciview. In Section 5.2.1 we demonstrated that the level of achieving the 2018 URP point was almost identical at CENRAP Class I areas whether the linear deciview or curved extinction glidepaths were used. The PSAT source apportionment was used to determine the contribution to the projected extinction in 2018 due to international sources. As noted above, international sources were assumed to be due to anthropogenic emissions in Mexico and Canada and half of the Boundary Conditions.

Figure 5-16 shows the standard CAMx extinction glidepaths and 2018 visibility projections and the 2018 visibility projections when the contributions of international sources is eliminated. CACR, which achieved the 2018 URP point by 104%, achieves it by even more when international sources are eliminated (117%). UPBU that barely achieved the 2018 URP point by 102% achieves it by 116% without international emissions.

BRET comes up short of achieving the 2018 URP point when international emission are included (76%) as well as when they are eliminated (92%), although it is much closer (recall contributions of Gulf of Mexico to visibility impairment at BRET that is assumed in this analysis to be of U.S. origin). Eliminating international transport emissions makes of difference of meeting the 2018 URP point without them (120%) to not meeting it with them (64%) at BOWA. Similarly at VOYA the standard 2018 visibility projections do not achieve the 2018 URP point (54%), whereas it is achieved by a far margin when international sources are eliminated (132%).

HEGL comes up short achieving the 2018 URP point when international sources are included (95%), but achieves it when they are eliminated (107%). Recall the standard CAMx deciview visibility projections barely achieved the URP point even when international emissions are included (Figure 5-13). MING achieves the 2018 URP point with (106%) and without (116%) international sources. WIMO does not achieve the 2018 URP point when international contributions are eliminated.

International sources have by far the largest effect at BIBE. Whereas the standard 2018 visibility projections only achieved 27% of the reductions needed to achieve the 2018 URP point, elimination of the international source contributions achieves 172% of the reduction needed. GUMO comes up short in achieving the 2018 URP point when international sources are included (31%), but achieves it when they are not (107%).

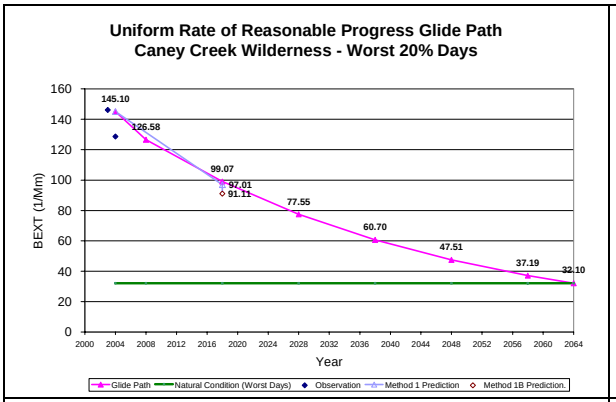
Uniform Rate of Reasonable Progress Glide Path
Caney Creek Wilderness - Worst 20% Days
BEXT (1/Mm)
Year
145.10
126.58
99.07
97.01
91.11
77.55
60.70
47.51
37.19
32.10
Glide Path
Natural Condition (Worst Days)
Observation
Method 1 Prediction
Method 1B Prediction.

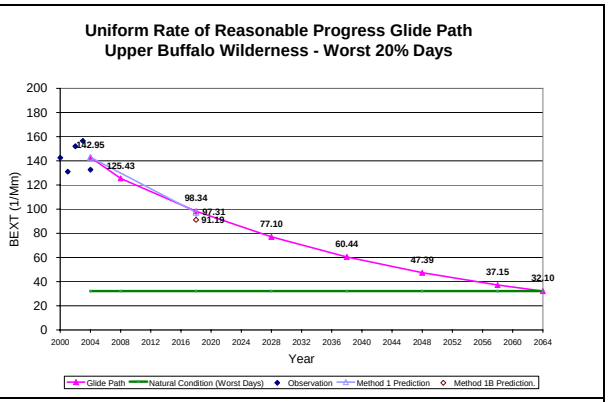
Uniform Rate of Reasonable Progress Glide Path
Upper Buffalo Wilderness - Worst 20% Days
BEXT (1/Mm)
Year
142.95
125.43
98.34
97.31
91.19
77.10
60.44
47.39
37.15
32.10
Glide Path
Natural Condition (Worst Days)
Observation
Method 1 Prediction
Method 1B Prediction.

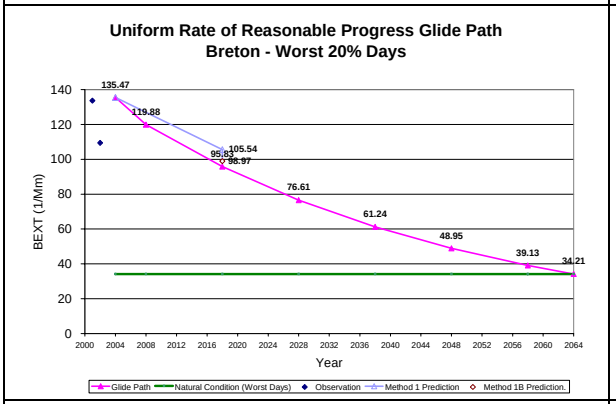
Uniform Rate of Reasonable Progress Glide Path
Breton - Worst 20% Days
BEXT (1/Mm)
Year
135.47
119.88
105.54
95.83
98.97
76.61
61.24
48.95
39.13
34.21
Glide Path
Natural Condition (Worst Days)
Observation
Method 1 Prediction
Method 1B Prediction.

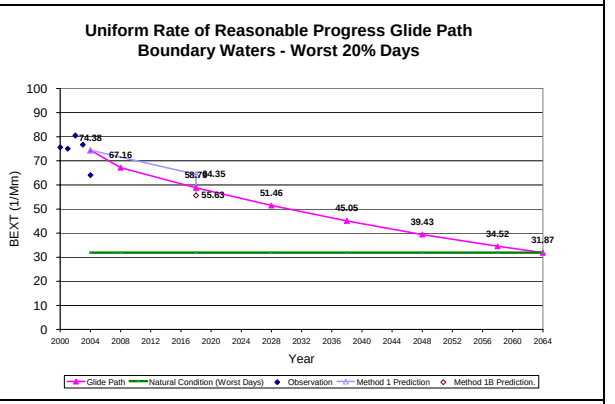
Uniform Rate of Reasonable Progress Glide Path
Boundary Waters - Worst 20% Days
BEXT (1/Mm)
Year
74.38
67.16
58.76
64.35
55.63
51.46
45.05
39.43
34.52
31.87
Glide Path
Natural Condition (Worst Days)
Observation
Method 1 Prediction
Method 1B Prediction.

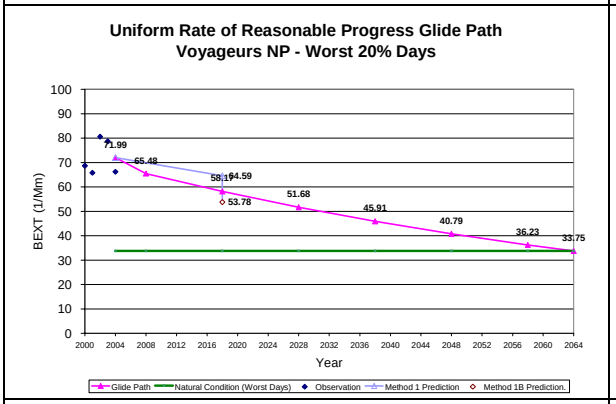
Uniform Rate of Reasonable Progress Glide Path
Voyageurs NP - Worst 20% Days
BEXT (1/Mm)
Year
71.99
65.48
58.19
64.59
53.78
51.68
45.91
40.79
36.23
33.75
Glide Path
Natural Condition (Worst Days)
Observation
Method 1 Prediction
Method 1B Prediction.

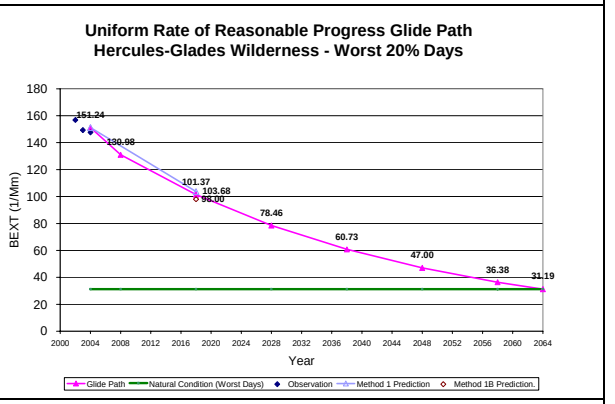
Uniform Rate of Reasonable Progress Glide Path
Hercules-Glades Wilderness - Worst 20% Days
BEXT (1/Mm)
Year
151.24
130.98
101.37
103.68
98.00
78.46
60.73
47.00
36.38
31.19
Glide Path
Natural Condition (Worst Days)
Observation
Method 1 Prediction
Method 1B Prediction.

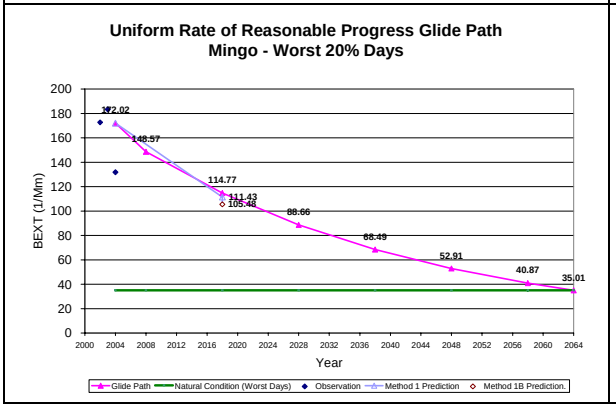
Uniform Rate of Reasonable Progress Glide Path
Mingo - Worst 20% Days
BEXT (1/Mm)
Year
172.02
148.57
114.77
111.43
105.48
88.66
68.49
52.91
40.87
35.01
Glide Path
Natural Condition (Worst Days)
Observation
Method 1 Prediction
Method 1B Prediction.

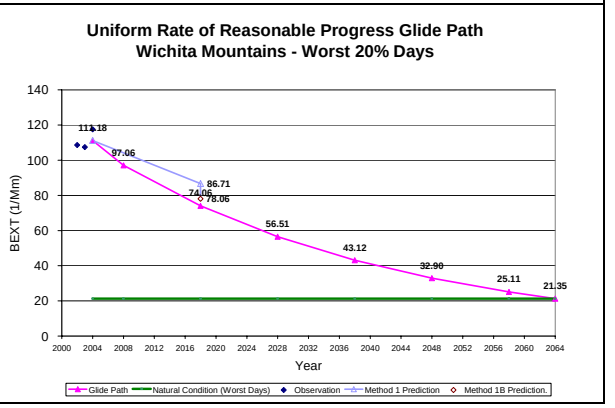
Uniform Rate of Reasonable Progress Glide Path
Wichita Mountains - Worst 20% Days
BEXT (1/Mm)
Year
111.18
97.06
86.71
74.06
78.06
56.51
43.12
32.90
25.11
21.35
Glide Path
Natural Condition (Worst Days)
Observation
Method 1 Prediction
Method 1B Prediction.

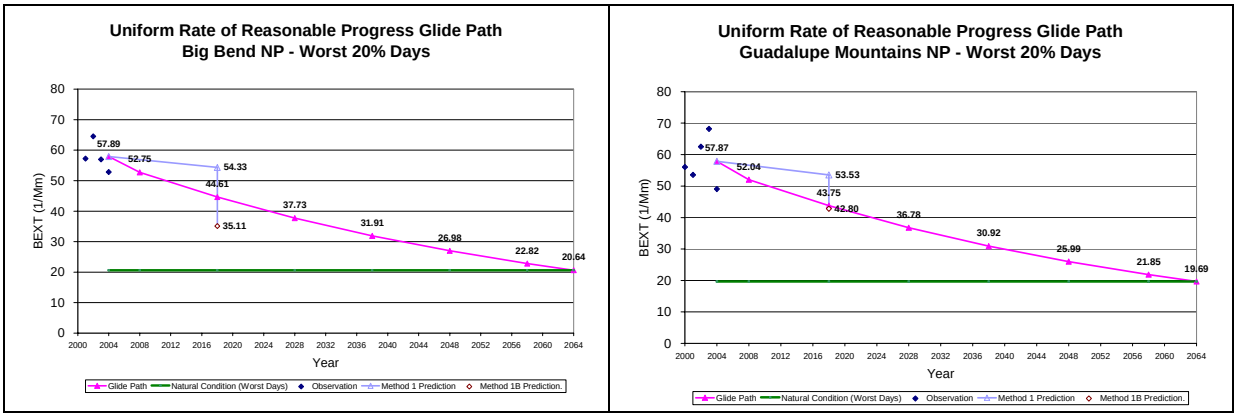

Figure 5-16. Elimination of international sources from 2018 visibility projections and comparison with 2018 URP point at CENRAP Class I areas.

5.7.2 Glidepaths Based on Controllable Extinction

Another alternative glidepath that was examined using the CAMx PSAT source apportionment results was based on the U.S. anthropogenic emissions contributions to visibility impairment on the worst 20 percent days at the CENRAP Class I areas. The RHR strives to achieve "natural visibility conditions" by 2064 and defines natural conditions as conditions that would exist "in the absence of human caused impairment". As shown above, anthropogenic emissions from international sources contribute significantly to visibility impairment at many of the CENRAP Class I areas making the RHR objective not practical if contributions from such sources are not reduced. Given that states and EPA have no jurisdiction over international sources, then we can not assume they will be controlled and have therefore held most of them constant at 2002 levels. For such Class I areas with high contributions from international sources, the comparison with the 2018 URP point is not very meaningful since the 2018 URP assumes such sources will be reduced. A more meaningful comparison would be to focus on the U.S. man-made contributions to visibility impairment at the Class I areas and develop a URP glidepath and 2018 URP point that is aimed at eliminating the U.S. anthropogenic emissions contributions to visibility impairment at Class I areas for the worst 20 percent days in 2064.

The CAMx 2002 base case PSAT PM source apportionment results were processed to identify the portion of the 2000-2004 Baseline extinction that was due to U.S. anthropogenic emissions (i.e., man-made sources). The contributions of source groups that included on-road mobile, non-road mobile, elevated point sources, low-level point sources and area sources from the PSAT source regions covering the U.S. states and Gulf of Mexico (Figure 5-8) were assumed to make up the U.S. anthropogenic contributions (i.e., excluding the Natural source category, all sources from the Mexico and Canada source regions and boundary conditions). Note that off-shore marine emissions in the Pacific and Atlantic Oceans and Gulf of Mexico were included in the U.S. anthropogenic emissions definition because they were in source regions associated with states or the Gulf of Mexico. As off-shore marine emissions may not be controllable by U.S. agencies and they were assumed to remain unchanged going from 2002 to 2018, then the 2018 visibility projections for the U.S. anthropogenic component are overstated.

The 2064 objective for the U.S. anthropogenic emissions glidepath would be no contributions on the worst 20 percent days. This does not mean the 2064 U.S. anthropogenic extinction objective

is zero, rather the U.S. anthropogenic plus natural background is less than the Natural Conditions for the worst 20 percent days. The PSAT results were used to define the natural background contributions on the current worst 20 percent days which was subtracted from the EPA default Natural Conditions to obtain the 2064 objective for the U.S. anthropogenic emissions contributions. Here the PSAT derived natural background was defined as the sum of the contributions from the Natural source category, secondary organic aerosol from biogenic sources (SOAB) and half of the boundary conditions. For example, Figure 5-17 top left displays the US anthropogenic emissions glidepath for CACR. The PSAT natural sources contribution (=Natural Source Category + SOAB + ½ BC) is approximately 13 Mm^{-1} so that is subtracted from the 2064 Natural Background (~32 Mm^{-1}, see figure 5-16) to obtain a 2064 end point of ~19 Mm^{-1} for the glidepath. The 2002 PSAT results applied to the 2000-2004 Baseline extinction estimates that 111 Mm^{-1} of the extinction is due to U.S. anthropogenic emissions which form the starting point for the glidepath. The curvature in the US anthropogenic glidepath is introduced the same way as for the extinction based glidepath to account for the logarithmic relationship between extinction and deciview.

Figure 5-17 displays the U.S. anthropogenic emissions extinction glidepaths and comparison with the 2018 visibility projections for extinction due to U.S. anthropogenic emissions on the worst 20 percent days. As seen by the standard linear deciview glidepaths discussed in Chapter 4, the U.S. anthropogenic emissions 2018 URP point is achieved by a wide margin at the four Class I areas in Arkansas and Missouri (CACR, UPBU, HRGL and MING). BRET that achieved 94% of the 2018 URP point obtains similar results using the U.S. anthropogenic emissions glidepath achieving 96% of the 2018 URP point. As discussed above, the inclusion of the off-shore marine emissions in the U.S. anthropogenic emissions will greatly affect the BRET Class I area so that actual reduction in U.S. anthropogenic emissions extinction would be greater and may even achieve the 2018 URP point if off-shore marine vessels were classified as not being part of the U.S..

The BOWA and VOYA northern Minnesota Class I areas achieved, respectively, 69% and 53% of the 2018 URP point using the standard EPA default deciview glidepaths and projection techniques (Figure 4-4). Using the U.S. anthropogenic glidepaths BOWA and VOYA achieve 92% and 86% of the 2018 point, respectively (Figure 5-17). WIMO that came up approximately 40% short of achieving the 2018 URP point using the deciview glidepath comes up under 20% short using the U.S. anthropogenic emissions glidepath.

The two Texas Class I areas also come up short in achieving the 2018 URP point using the U.S. anthropogenic emissions glidepaths, but not as short as when the linear deciview glidepaths are used. BIBE increases from 26% to 67% and GUMO increases from 34% to 49%. One reason these two Class I areas fail to achieve the 2018 point for U.S. anthropogenic emissions is because of the high contributions of Soil and CM and little change in precursor emissions of these species between 2002 and 2018.

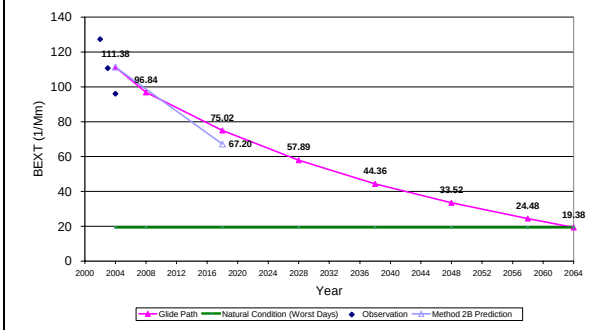
Uniform Rate of Reasonable Progress Glide Path
Caney Creek Wilderness - Worst 20% Days
BEXT (1/Mm)
Year
111.38
96.84
75.02
67.20
57.89
44.36
33.52
24.48
19.38
Glide Path
Natural Condition (Worst Days)
Observation
Method 2B Prediction

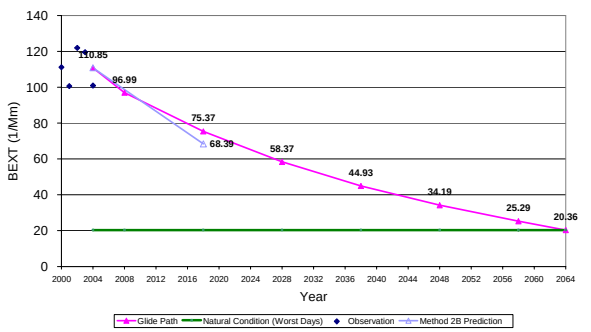
Uniform Rate of Reasonable Progress Glide Path
Upper Buffalo Wilderness - Worst 20% Days
BEXT (1/Mm)
Year
110.85
96.99
75.37
68.39
58.37
44.93
34.19
25.29
20.36
Glide Path
Natural Condition (Worst Days)
Observation
Method 2B Prediction

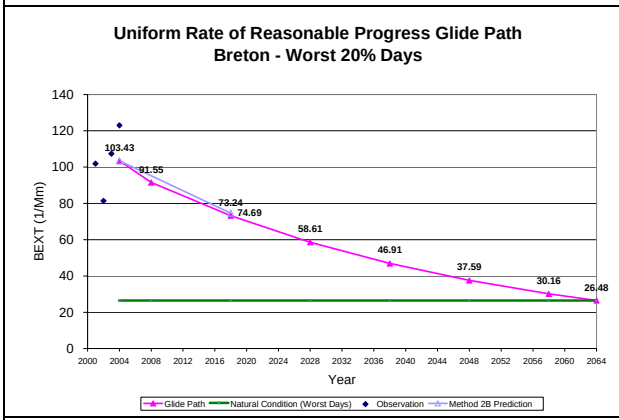
Uniform Rate of Reasonable Progress Glide Path
Breton - Worst 20% Days
BEXT (1/Mm)
Year
103.43
91.55
73.24
74.69
58.61
46.91
37.59
30.16
26.48
Glide Path
Natural Condition (Worst Days)
Observation
Method 2B Prediction

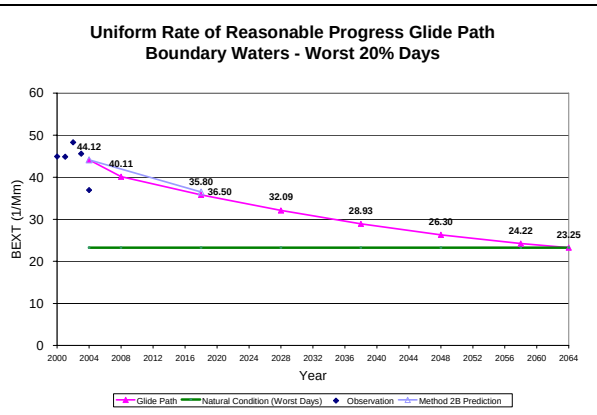
Uniform Rate of Reasonable Progress Glide Path
Boundary Waters - Worst 20% Days
BEXT (1/Mm)
Year
44.12
40.11
35.80
36.50
32.09
28.93
26.30
24.22
23.25
Glide Path
Natural Condition (Worst Days)
Observation
Method 2B Prediction

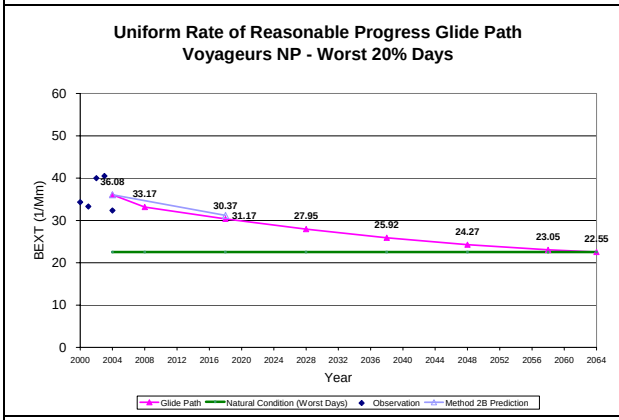
Uniform Rate of Reasonable Progress Glide Path
Voyageurs NP - Worst 20% Days
BEXT (1/Mm)
Year
36.08
33.17
30.37
31.17
27.95
25.92
24.27
23.05
22.55
Glide Path
Natural Condition (Worst Days)
Observation
Method 2B Prediction

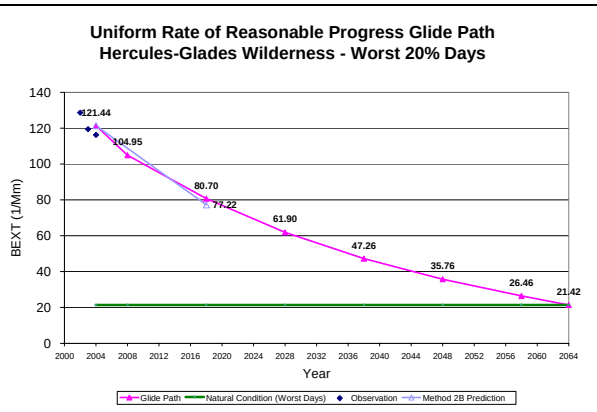
Uniform Rate of Reasonable Progress Glide Path
Hercules-Glades Wilderness - Worst 20% Days
BEXT (1/Mm)
Year
121.44
104.95
80.70
77.22
61.90
47.26
35.76
26.46
21.42
Glide Path
Natural Condition (Worst Days)
Observation
Method 2B Prediction

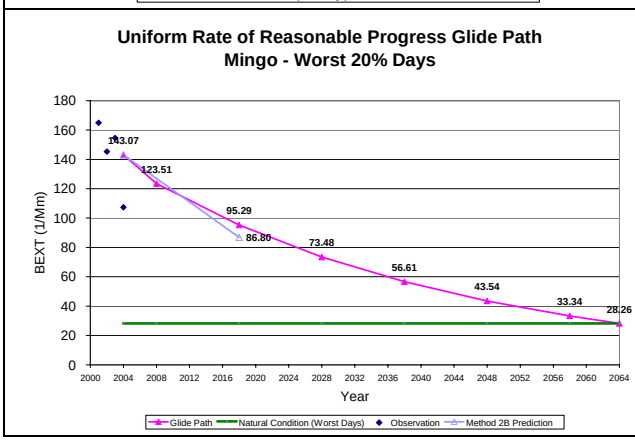
Uniform Rate of Reasonable Progress Glide Path
Mingo - Worst 20% Days
BEXT (1/Mm)
Year
143.07
123.51
95.29
86.80
73.48
56.61
43.54
33.34
28.26
Glide Path
Natural Condition (Worst Days)
Observation
Method 2B Prediction

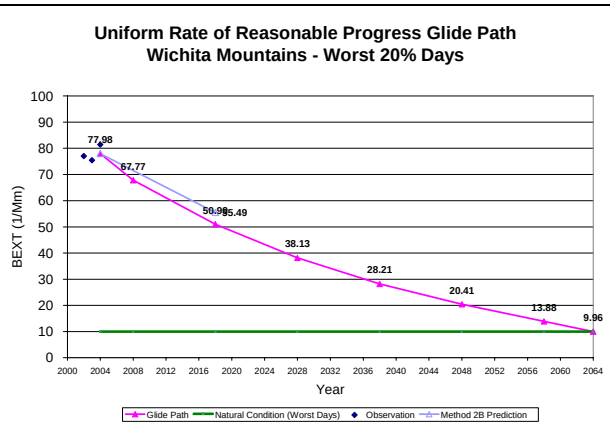
Uniform Rate of Reasonable Progress Glide Path
Wichita Mountains - Worst 20% Days
BEXT (1/Mm)
Year
77.98
67.77
50.98
45.49
38.13
28.21
20.41
13.88
9.96
Glide Path
Natural Condition (Worst Days)
Observation
Method 2B Prediction

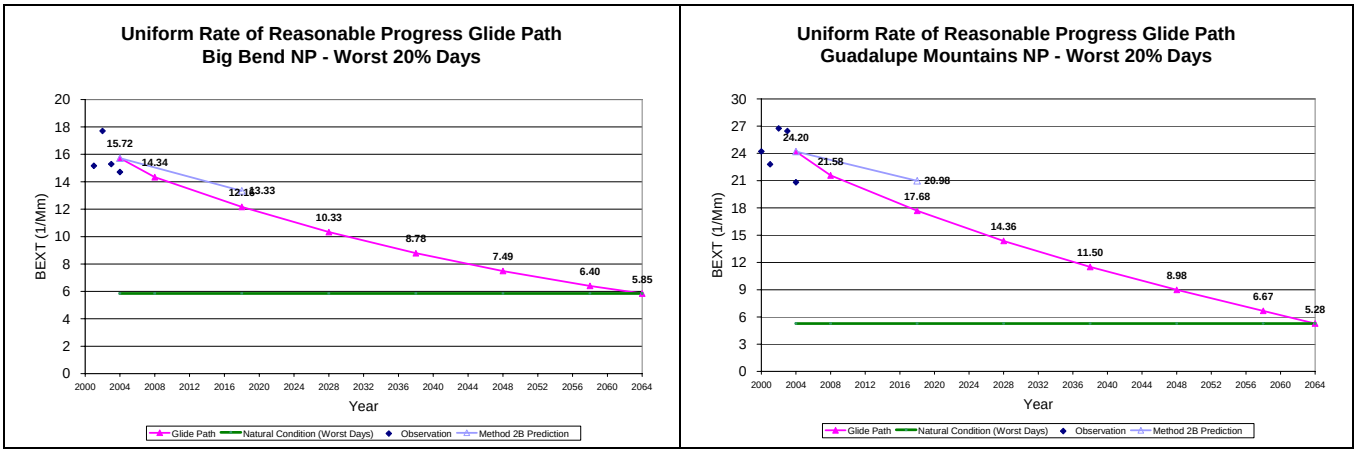

Figure 5-17. Glidepaths and 2018 visibility projections based on visibility due to U.S. anthropogenic emissions at CENRAP Class I areas.

5.8 Use of Original IMPROVE Equation

2018 visibility projections were also made using the CENRAP Typ02g and Base18g CMAQ modeling results and the original (old) IMPROVE equation. Figure 5-18 displays a DotPlot that compares the 2018 Base G visibility projections using the new IMPROVE algorithm (NIA) and the original IMPROVE algorithm (OIA). In general the new IMPROVE equation results in more optimistic 2018 visibility projections than the original IMPROVE equation. For the Texas and WRAP Class I areas, the 2018 visibility projections are nearly identical using the two IMPROVE equations. For the four Class I areas in Arkansas and Missouri the 2018 visibility projections using the new IMPROVE equation are from 7 to 21 percentage points more optimistic than the original IMPROVE equation. In the case of UPBU, HEGL and MING the 2018 visibility projections go from not achieving to achieving the 29018 URP point when switching from the old to new IMPROVE equation.

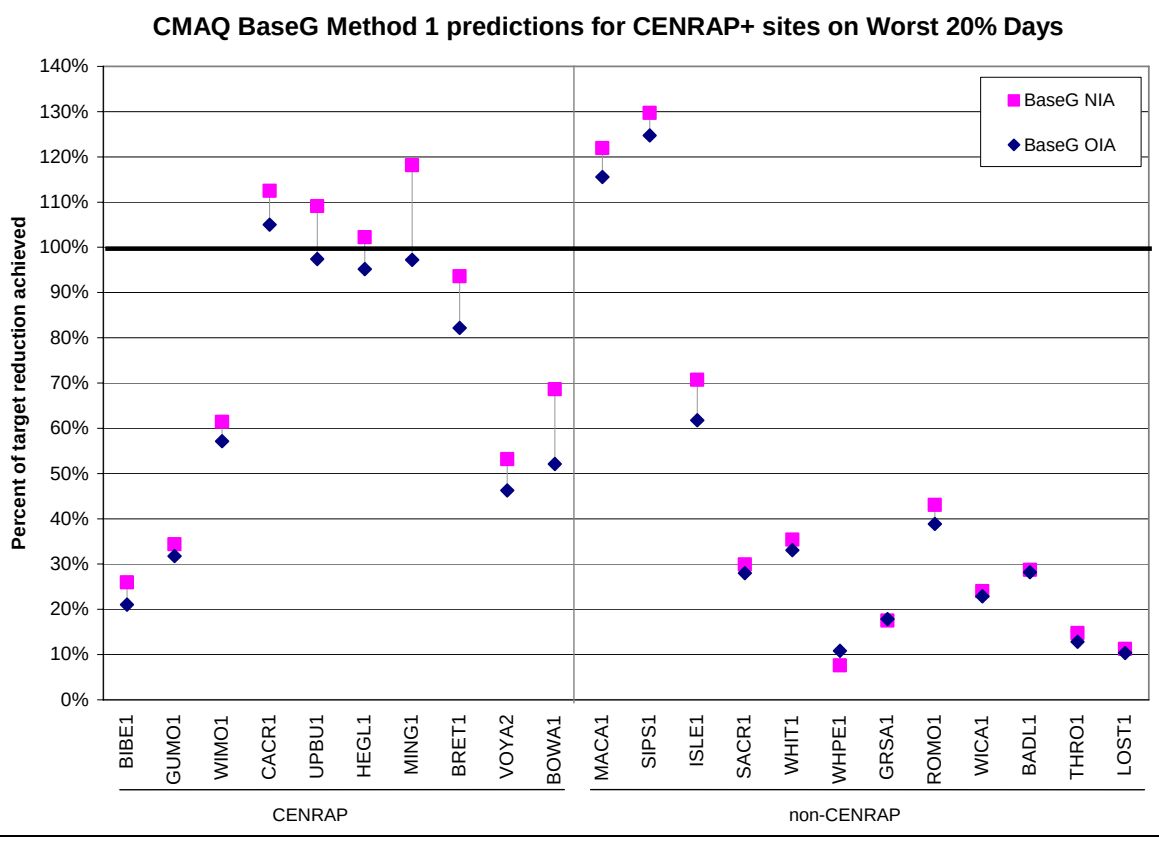

Figure 5-18. Comparison of 2018 Base G visibility projections using the New (NIA) and Old (OIA) IMPROVE algorithms expressed as a percentage of achieving the 2018 URP point visibility improvements.

5.9 Visibility Trends

Figure 5-19 displays trends in visibility impairment at the CENRAP Class I areas using the period of record of measurements at the associated IMPROVE monitor and the new IMPROVE equation. These trends include trends for the worst 20 percent days, the best 20 percent days and all IMPROVE sampled days during a year. The EPA guidance procedures were used to construct the worst and best 20 percent days that includes a minimum data capture requirement (EPA, 2003a), whereas no such minimum data capture was applied when looking at the "annual average" of all IMPROVE sampled days trends. So care must be taken when analyzing trends for the all sampled IMPROVE days trends as there could be large missing periods with high or low extinction that are not being account for. The WRAP Technical Support System (TSS) website was used to calculate the visibility trends at the CENRAP Class I areas that includes IMPROVE data from start of recording through 2004 and includes no data filling (see: http://vista.cira.colostate.edu/TSS/Default.aspx) .

Trends in visibility at CACR has three years of data (2002-2004) for the worst and best 20 percent days and fives years for the IMPROVE sampled days trends. Although it is hard to come to any conclusions regarding trends with just three years of data, there does seem to be a general downward trend, that is also supported by the five year trend in the IMPROVE sampled days.

A much longer trend plot is available for UPBU that includes 12 years of data for the worst and best 20 percent days (Figure 5-19b). Although there is a lot of a year-to-year variation in the visibility trends with cleaner years occurring in 1997, 2001 and 2004, there does appear to be a slight trend toward improved visibility at UPBU.

There is insufficient data to calculate the worst or best 20 percent days visibility for any year at the BRET Class I area so only the IMPROVE sampled days trends are presented (Figure 5-19c). The trends at BRET are inconclusive and given the large amounts of missing data at this site it is difficult to interpret the results.

There is also a lot of missing years in the worst and best 20 percent days for the BOWA Class I area making it difficult to interpret (Figure 5-19d). But visibility appears to be more impaired in the early 1990s than in more current years so improvements have been seen. VOYA has five years of valid data and shows worsening visibility for 2000-2003, and then improved visibility in 2004. It is unclear whether the 2004 improved visibility is a trend or just due to variations in meteorology so no conclusions can be drawn.

Although a downward trend in visibility impairment appears to be occurring at the two Missouri Class I areas (Figure 5-19f-g), given that there are only three years available for HEGL and lots of missing data for MING these trends are inconclusive.

Three years (2002-2004) of visibility trends for the worst and best 20 percent days are available for WIMO (Figure 5-19h). The most impaired year from the three years for the worst 20 percent days is the most recent (2004). Again, the time period is too short to draw any conclusions on trends in visibility at WIMO.

The two Texas Class I areas have a relatively long period of record. There is a lot of year-to-year variability in the visibility measurements that make interpreting the trends difficult. 1998 appears to be an anomalously high visibility impairment year at BIBE and due to the much higher OMC extinction indicates that the year was likely impacted by smoke from fires. GUMO has lots of year to year variability in CM and Soil which are likely due to occurrences of impacts due to wind blown dust. Even taking Soil and CM out of the interpretation it is difficult to interpret ay trend in visibility at the two Texas Class I areas. The higher visibility impairment in 1998 and 1999 suggests a downward trend but that may be just due to more adverse meteorological and natural emissions (e.g., wildfires) in these two years than any real long term trend.

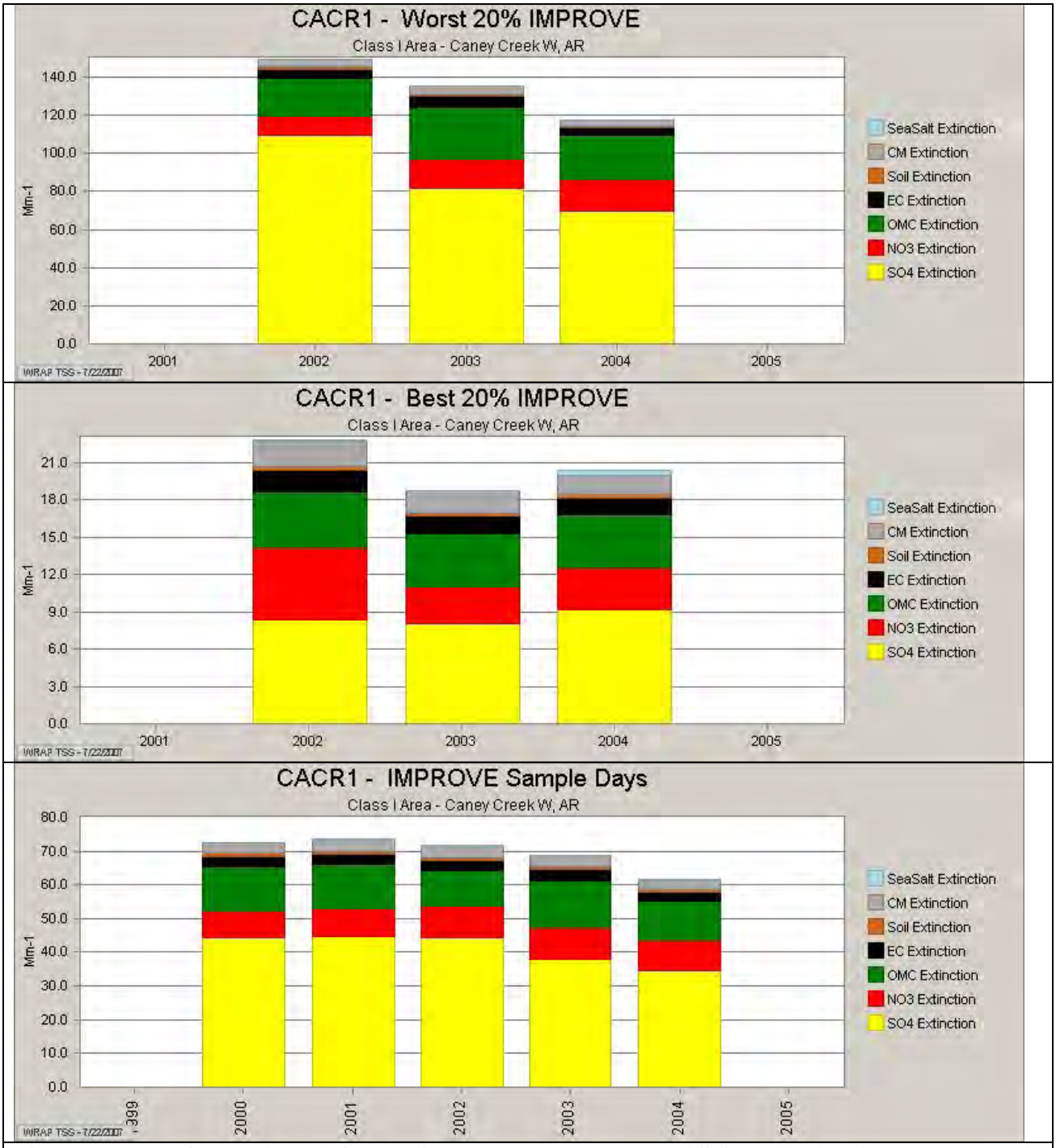

Figure 5-19a. Time series of observed IMPROVE reconstructed light extinction (New IMPROVE) at Caney Creek (CACR), Arkansas for the average of the Worst 20 Percent days (top), Best 20 Percent days (middle) days and all IMPROVE sampling days during the period of record.

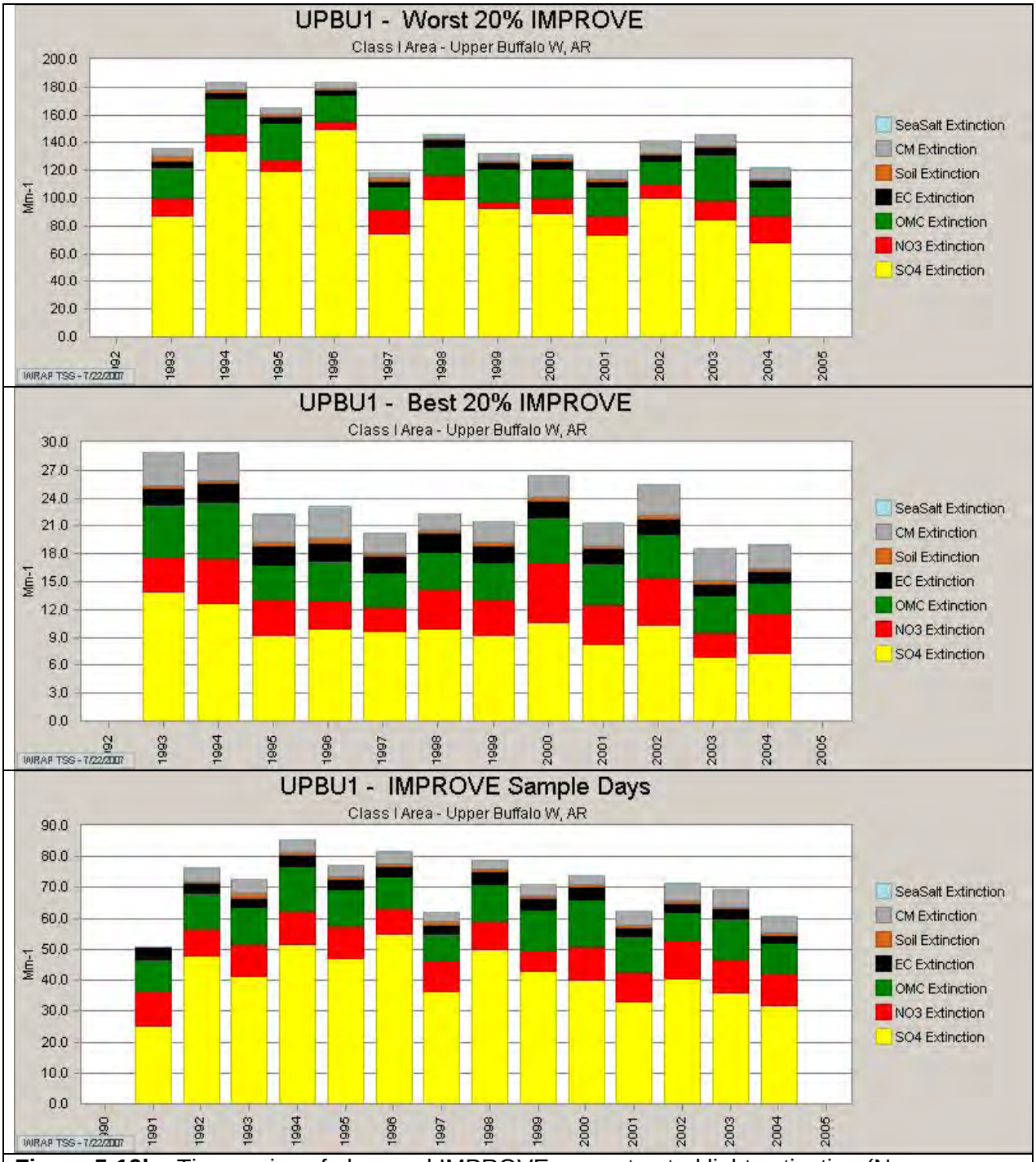

Figure 5-19b. Time series of observed IMPROVE reconstructed light extinction (New IMPROVE) at Upper Buffalo (UPBU), Arkansas for the average of the Worst 20 Percent days (top), Best 20 Percent days (middle) days and all IMPROVE sampling days during the period of record.

Insufficient Data to Calculate Best 20 Percent days at BRET

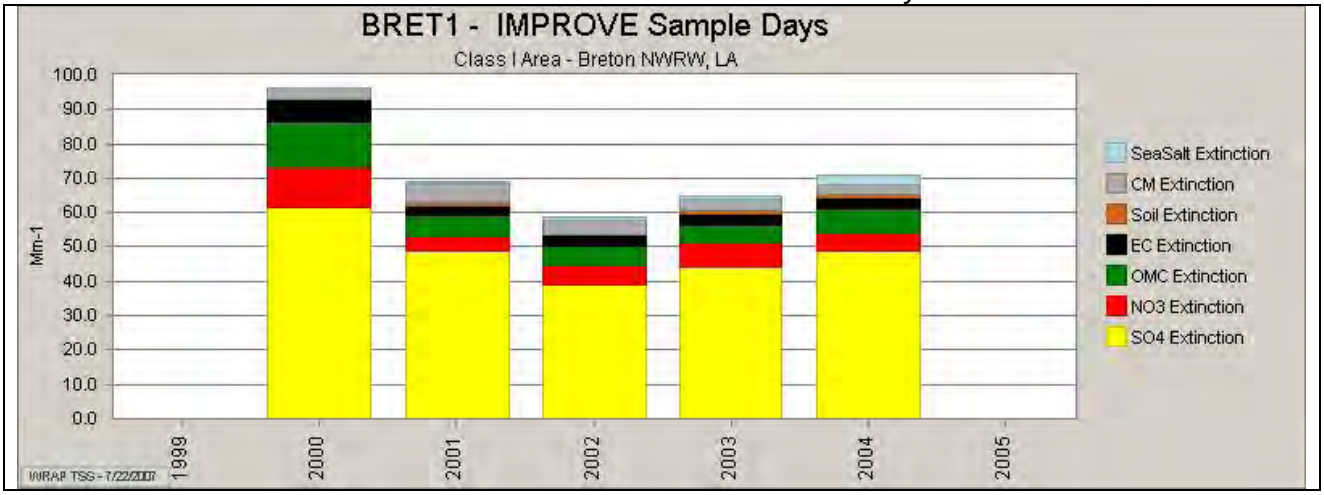

Figure 5-19c. Time series of observed IMPROVE reconstructed light extinction (New IMPROVE) at Breton Island (BRET), Louisiana for the average of the Worst 20 Percent days (top), Best 20 Percent days (middle) days and all IMPROVE sampling days during the period of record.

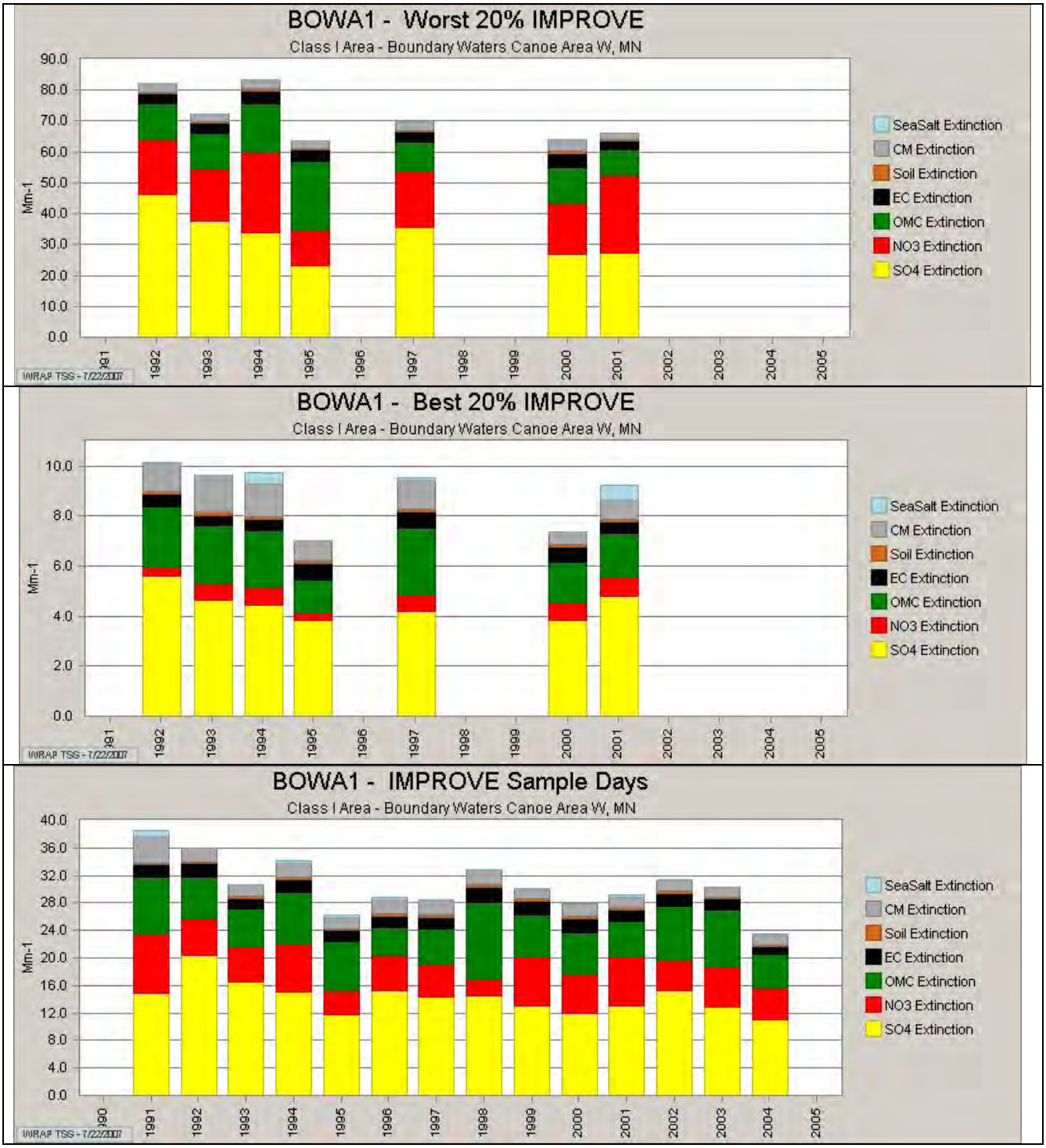

Figure 5-19d. Time series of observed IMPROVE reconstructed light extinction (New IMPROVE) at Boundary Waters (BOWA), Minnesota for the average of the Worst 20 Percent days (top), Best 20 Percent days (middle) days and all IMPROVE sampling days during the period of record.

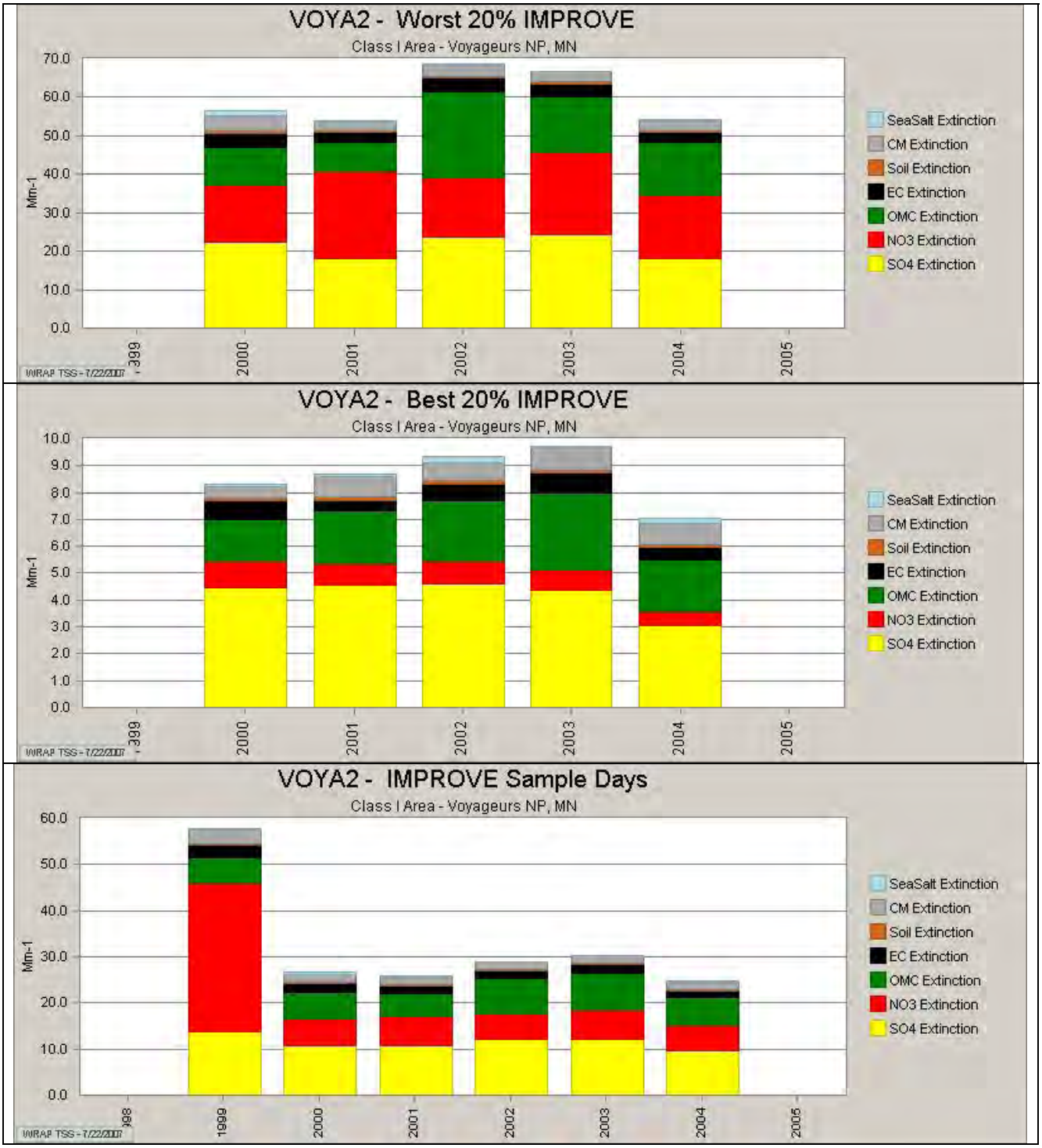

Figure 5-19e. Time series of observed IMPROVE reconstructed light extinction (New IMPROVE) at Voyageurs (VOYA), Minnesota for the average of the Worst 20 Percent days (top), Best 20 Percent days (middle) days and all IMPROVE sampling days during the period of record.

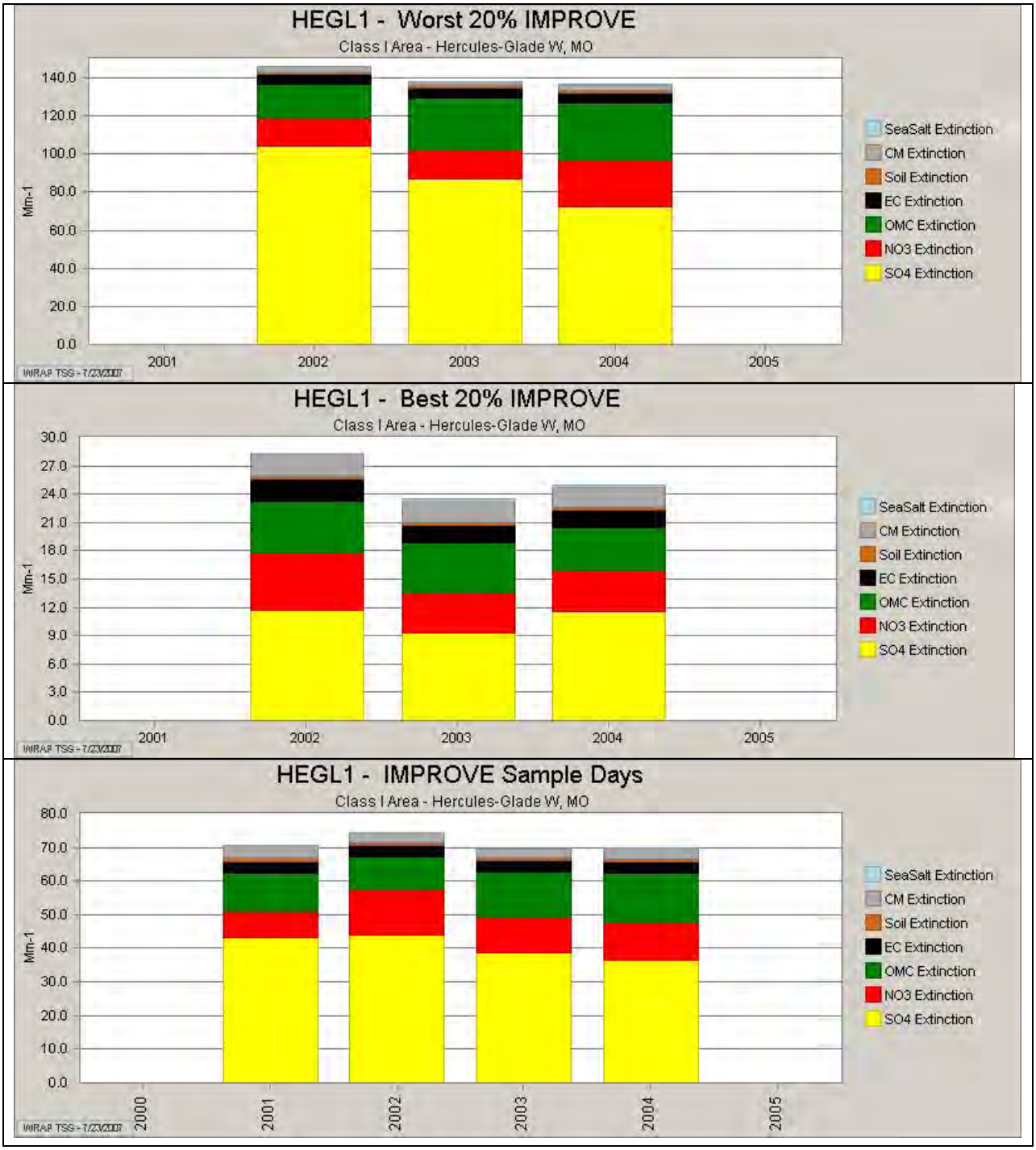

Figure 5-19f. Time series of observed IMPROVE reconstructed light extinction (New IMPROVE) at Hercules Glade (HEGL), Missouri for the average of the Worst 20 Percent days (top), Best 20 Percent days (middle) days and all IMPROVE sampling days during the period of record.

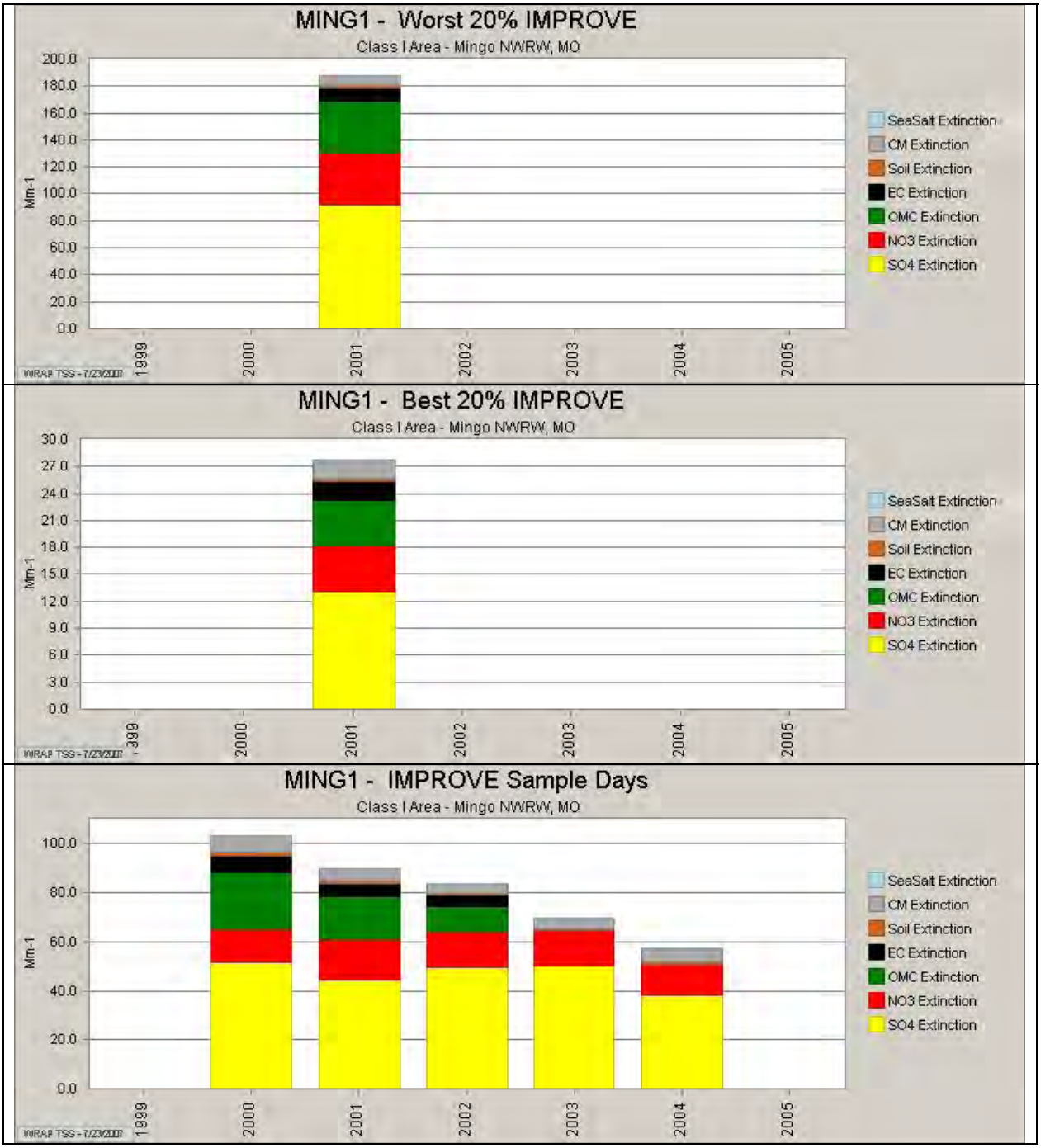

Figure 5-19g. Time series of observed IMPROVE reconstructed light extinction (New IMPROVE) at Mingo (MING), Missouri for the average of the Worst 20 Percent days (top), Best 20 Percent days (middle) days and all IMPROVE sampling days during the period of record.

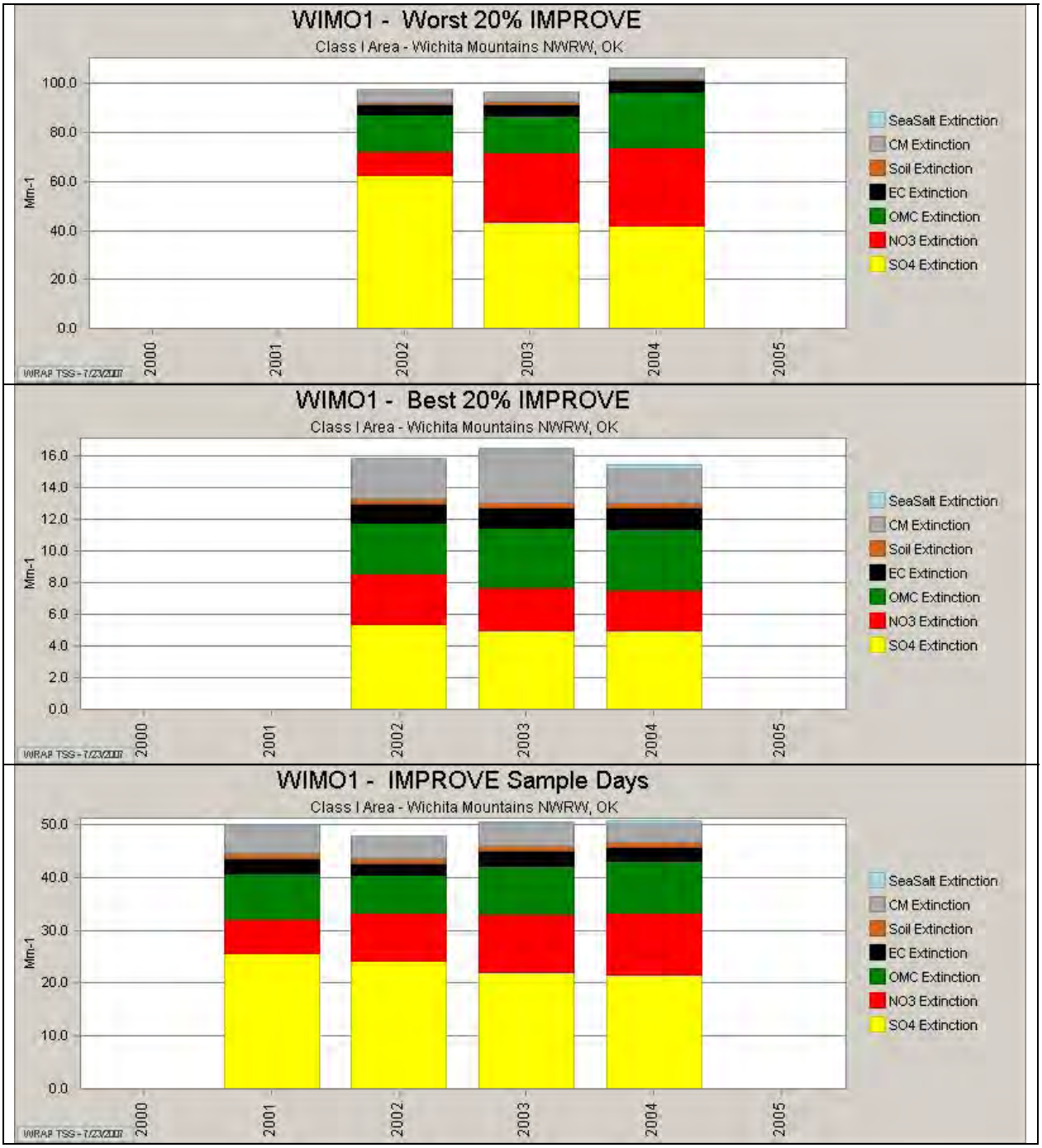

Figure 5-19h. Time series of observed IMPROVE reconstructed light extinction (New IMPROVE) at Wichita Mountains (WIMO), Oklahoma for the average of the Worst 20 Percent days (top), Best 20 Percent days (middle) days and all IMPROVE sampling days during the period of record.

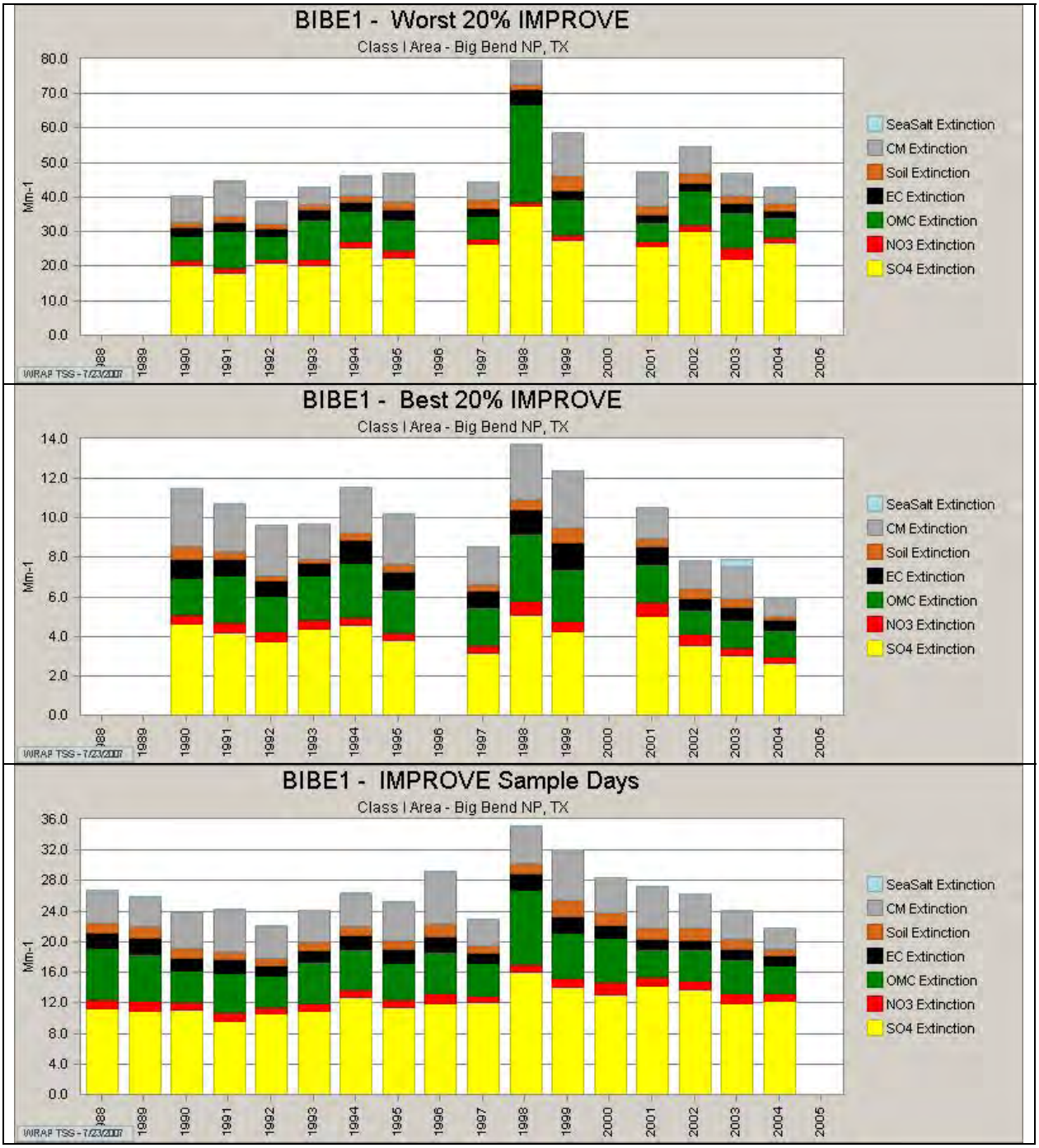

Figure 5-19i. Time series of observed IMPROVE reconstructed light extinction (New IMPROVE) at Big Bend (BIBE), Texas for the average of the Worst 20 Percent days (top), Best 20 Percent days (middle) days and all IMPROVE sampling days during the period of record.

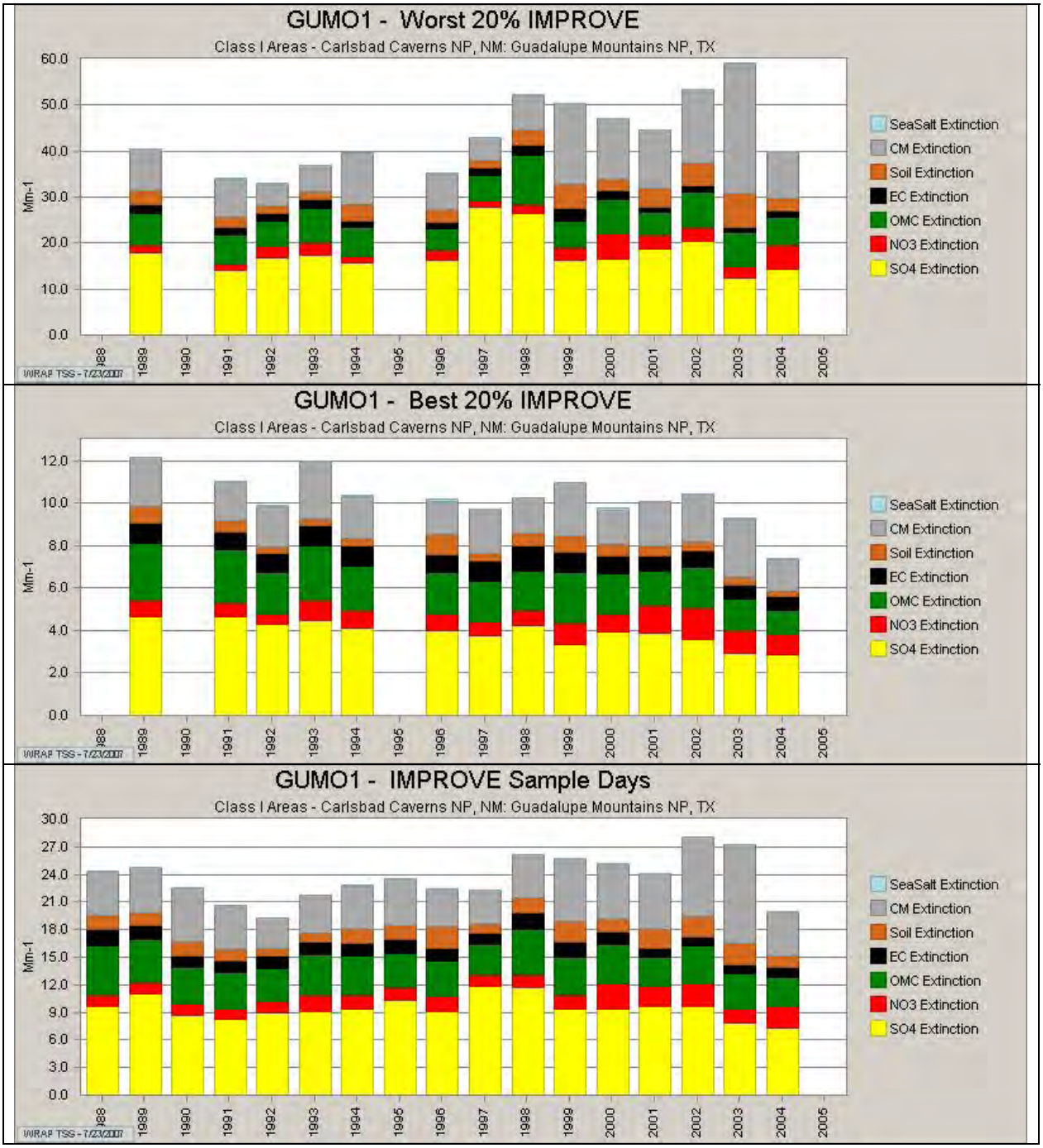

Figure 5-19j. Time series of observed IMPROVE reconstructed light extinction (New IMPROVE) at Guadalupe Mountains (GUMO), Texas for the average of the Worst 20 Percent days (top), Best 20 Percent days (middle) days and all IMPROVE sampling days during the period of record.

6.0 REFERENCES

Air Sciences. 2007a. Development of 2000-04 Baseline Period and 2018 Projection Year Emission Inventories. Air Sciences, Denver, Colorado and ECR, Inc., North Carolina. May. (http://www.wrapair.org/forums/fejf/documents/task7/Phase3-4EI/WRAP_Fire_Ph3-4_EI_Report_20070515.pdf).

Air Sciences. 2007. Inter-RPO 2002 National Wildfire Emission Inventory. Air Sciences, Denver, Colorado and ECR, Inc., North Carolina. May. (http://www.wrapair.org/forums/fejf/documents/task7/InterRPO_02WildFire_EI/Inter-RPO_2002_WF_EI%20Report_rev_20070515.pdf).

Alpine Geophysics. 2006. CENRAP Regional Haze Control Strategy Analysis Plan. Alpine Geophysics, LLC, Burnsville, North Carolina. May.

Bar-Ilan, A., R. Friesen, A. Pollack and A. Hoats. 2007. WRAP Area Source Emissions Inventory Projections and Control Strategy Evaluation Phase II. ENVIRON International Corporation, Novato, California. July. (http://www.wrapair.org/forums/ssjf/documents/eictts/OilGas/2007-07_Phase%20II_O&G_Draft_Final_Report-v7-23.pdf).

Boylan, J. W. 2004. "Calculating Statistics: Concentration Related Performance Goals", paper presented at the EPA PM Model Performance Workshop, Chapel Hill, NC. 11 February.

Byun, D.W., and J.K.S. Ching. 1999. "Science Algorithms of the EPA Models-3 Community Multiscale Air Quality (CMAQ) Modeling System", EPA/600/R-99/030.

Byun, D.W. 2004. Quality Assurance Activities for VISTAS BC Processing. University of Houston. December 31.

Chow, J et al. 2004. Source Profiles for Industrial, Mobile, and Area Sources in the Big Bend Regional Aerosol Visibility and Observational Study. 2003

Chow, J. 2005. Memorandum: EPA Chemical Profiles for Coal Fired Power Station Emissions. Prepared for TCEQ. July 2005

Coe, D.L. and S.B. Reid. 2003. Research and Development of Ammonia Emission Inventories for the Central States Regional Air Planning Association. Sonoma Technology, Inc., Petaluma, California. (available at http://cenrap.sonomatech.com/index.cfm). October 30.

ENVIRON. 2002. "User's Guide Comprehensive Air Quality Model With Extensions (CAMx) Version 3.10." ENVIRON International Corporation, Novato, California (available at www.camx.com) April.

ENVIRON. 2003a. "VISTAS Emissions and Air Quality Modeling – Phase I Task 2 Report: Recommended Model Configurations and Evaluation Methodology for Phase I Modeling." Prepared by ENVIRON International Corporation, Alpine Geophysics, LLC and University

of California at Riverside. Novato, California. (available at: http://pah.cert.ucr.edu/vistas/docs.shtml). August 4.

ENVIRON, Alpine Geophysics, UC Riverside and UC Davis. 2003b. "VISTAS Emissions and Air Quality Modeling – Phase I Task 4a/b Report: Review of Model Sensitivity Simulations and Recommendations of Initial CMAQ Model Configurations and Sensitivity Tests." Revised Draft July 25.

ENVIRON. 2003d. "Development of an Advanced Photochemical Model for Particulate Matter: PMCAMx." ENVIRON International Corporation, Novato, CA. Prepared for Coordinating Research Council, Inc. Project A-30 (available at www.crcao.com).

EPA. 1991. "Guidance for Regulatory Application of the Urban Airshed Model (UAM), "Office of Air Quality Planning and Standards, U.S. Environmental Protection Agency, Research Triangle Park, N.C.

EPA. 1999. "Draft Guidance on the Use of Models and Other Analyses in Attainment Demonstrations for the 8-hr Ozone NAAQS". Draft (May 1999), U.S. Environmental Protection Agency, Office of Air Quality Planning and Standards, Research Triangle Park, N.C

EPA. 2001. "Guidance for Demonstrating Attainment of Air Quality Goals for $PM_{2.5}$ and Regional Haze", Draft Report, U.S. Environmental Protection Agency, Research Triangle Park, NC.

EPA. 2003a. "Guidance for Tracking Progress Under the Regional Haze Rule", U.S. Environmental Protection Agency, Research Triangle Park, NC.

EPA. 2003b. "Guidance for Estimating Natural Visibility Conditions Under the Regional Haze Rule", U.S. Environmental Protection Agency, Research Triangle Park, NC.

EPA. 2003c. *A Conceptual Model to Adjust Fugitive Dust Emissions to Account for Near Source Particle Removal in Grid Model Applications*, prepared by Tom Pace, U.S. EPA, August 22, 2003. http://www.epa.gov/ttn/chief/emch/invent/statusfugdustemissions_082203.pdf.

EPA. 2007a. Guidance on the Use of Models and Other Analyses for Demonstrating Attainment of Air Quality Goals for Ozone, $PM_{2.5}$ and Regional Haze. U.S. Environmental Protection Agency, Research Triangle Park, NC. EPA-454/B-07-002. April.

EPA. 2007b. Guidance for Setting Reasonable Progress Goals Under the Regional Haze Program. U.S. Environmental Protection Agency, Office of Air Quality and Planning Standards, Air Policy Division, Geographic Strategies Group, Research Triangle Park, NC. June 1. (http://epa.gov/ttn/oarpg/t1/memoranda/reasonable_progress_guid071307.pdf).

ERG. 2006a. WRAP Point and Area Source Emissions Projections for the 2018 Base Case. Eastern Research Group, Inc., Sacramento, California. January 25. (http://www.wrapair.org/forums/ssjf/documents/eictts/docs/WRAP_2018_EI-Version_1-Report_Jan2006.pdf).

ERG. 2006b. Mexico National Emissions Inventory, 1999. Eastern Research Group, Inc, Sacramento, California and TransEngineering, El Paso, Texas. October 11. (http://www.epa.gov/ttn/chief/net/mexico/1999_mexico_nei_final_report.pdf).

FLAG. 2000. Federal Land Manager's Air Quality Related Values Workgroup (FLAG) Phase I Report. (http://www2.nature.nps.gov/ard/flagfiee/AL.doc).

Jacob, D.J., R. Park and J.A. Logan. 2005. Documentation and Evaluation of the GEOS-CHEM Simulation for 2002 Provided to the VISTAS Group. Harvard University. June 24.

Johnson, M. 2007. Meteorological Model Performance Evaluation of an Annual 2002 MM5 (Version 3.6.3) Simulation. Iowa Department of natural Resources, Air Quality Bureau. November. (http://www.iowadnr.gov/air/prof/progdev/modeling.html).

Johnson, J., Y. Jia, C. Emery, R. Morris, Z. Wang and G. Tonnesen. 2006. Comparison of CENRAP 36 km and 12 km MM5 Model Runs for 2002. Prepared for CENRAP Modeling Work Group. May 23. (http://pah.cert.ucr.edu/aqm/cenrap/ppt_files/CENRAP_2002_36km_vs_12km_MM5_May22_2006.ppt).

Kemball-Cook, S., Y. Jia, C. Emery, R. Morris, Z. Wang and G. Tonnesen. 2004a. Comparison of CENRAP, VISTAS and WRAP 36 km MM5 Model Runs for 2002, Task 3: Meteorological Gatekeeper Report. (http://pah.cert.ucr.edu/aqm/cenrap/ppt_files/CENRAP_VISTAS_WRAP_2002_36km_MM5_eval.ppt). December 14.

Kemball-Cook, S., Y. Jia, C. Emery, R. Morris, Z. Wang and G. Tonnesen. 2005. Annual 2002 MM5 Meteorological Modeling to Support Regional Haze Modeling of the Western United States. Western Regional Air Partnership (WRAP), Regional Modeling Center (RMC). (http://pah.cert.ucr.edu/aqm/308/reports/mm5/DrftFnl_2002MM5_FinalWRAP_Eval.pdf). March.

Lindhjem, C. and Hoats, A. 2006. Memorandum: Description of Spatial Allocation of Marine Vessel Emissions. September 2006.

MACTEC. 2003. Memorandum: Expansion of Existing $PM_{2.5}$ Split Factor Background Documentation. Prepared for EPA. September 2003.

MACTEC. 2006. Documentation of the Base G 2002 Base Year, 2009 and 2018, Emission Inventories for VISTAS. Prepared for Visibility Improvement State and Tribal Association of the Southeast (VISTAS). MACTEC, Inc., Gainesville, Florida.

Malm, W.C.; Pitchford, M.L; Scruggs, M.; Sisler, J.F.; Ames, R.; Cepeland, S.; Gebhart, K.; Day, D.E. 2000. *Spatial and Seasonal Patterns and Temporal Variability of Haze and Its Constituents in the United States. Report III.* Cooperative Institute for Research in the Atmosphere, May.

Mansell, G.; Hoats, A.; Rao, S.; Omary, M. 2005. Air Quality Modeling Analysis for CENRAP, Development of the 2002 Base Case Modeling Inventory. April 2005

Mansell, G., S. Lau, J. Russell and M. Omary. Fugitive Wind Blown Dust Emissions and Model Performance Evaluation – Phase II. ENVIRON International Corporation, Novato Californisa and University of California at Riverside. May 5. (http://www.wrapair.org/forums/dejf/documents/WRAP_WBD_PhaseII_Final_Report_050506.pdf).

MMS. 2006. Gulfwide Emission Inventory Study for the Regional Haze and Ozone Modeling Effort. May 2006

Morris, R.E. and G. Tonnesen. 2004. Quality Assurance Project Plan (Draft) for Central Regional Air Planning Association (CENRAP) Emissions and Air Quality Modeling. (http://pah.cert.ucr.edu/aqm/cenrap/docs/CENRAP_QAPP_Nov_24_2004.pdf). December 23.

Morris, R.E., G.E. Mansell, B. Koo, G. Tonnesen, M. Omary and Z. Wang. 2004a. Modeling Protocol for the CENRAP 2002 Annual Emissions and Air Quality Modeling, Draft 2.0. (http://pah.cert.ucr.edu/aqm/cenrap/docs/CENRAP_Draft2.0_Modeling_Protocol_120804.pdf). December 8.

Morris, R.E., B. Koo, S. Lau, T.W. Tesche, D. McNally, C. Loomis, G. Stella, G. Tonnesen and Z. Wang. 2004b. "VISTAS Emissions and Air Quality Modeling – Phase I Task 4cd Report: Model Performance Evaluation and Model Sensitivity Tests for Three Phase I Episodes", prepared for the VISTAS Technical Analysis Committee, prepared by ENVIRON International Corporation, Alpine Geophysics, LLC, and the University of California, Riverside (CE-CERT).

Morris, R.E., A. Hoats, S. Lau, B. Koo, G. Tonnesen, C-J. Chien and M. Omary. 2005. Air Quality Modeling Analysis for CENRAP – Preliminary 2002 Base Case CMAQ and CAMx Modeling of the Continental US 36 km Domain and Model Performance Evaluation. ENVIRON International Corporation, Novato, California. April 30.

Morris, R.E., G. Mansell, B. Koo, A. Hoats, G. Tonnesen, M. Omary, C-J. Chien and Y. Wang. 2006a. CENRAP Modeling: Need for 36 km versus 12 km Grid Resolution. Presented at CENRAP Modeling Work Group Meeting, Baton Rouge, Louisiana. (http://pah.cert.ucr.edu/aqm/cenrap/ppt_files/414,1,CENRAP Modeling: Need for 36 km versus 12 km Grid Resolution). February 7.

Morris, R.E., G. Mansell, B. Koo, A. Hoats, G. Tonnesen, M. Omary, C-J. Chien and Y. Wang. 2006b. CENRAP Modeling Update: CMAQ versus CAMx Model Performance Evaluation. Presented at CENRAP Modeling Work Group Meeting, Baton Rouge, Louisiana. (http://pah.cert.ucr.edu/aqm/cenrap/ppt_files/414,1,CENRAP Modeling Update: CMAQ versus CAMx Model Performance Evaluation). February 7.

Morris, R.E., B. Koo, A. Guenther, G. Yarwood, D. McNally, T.W. Tesche, G. Tonnesen, J. Boylan and P. Brewer. 2006c. Model Sensitivity Evaluation for Organic Carbon using Two Multi-

Pollutant Air Quality Models that Simulate Regional Haze in the Southeastern United States. *Atmos. Env.* 40 (2006) 4960-4972.

Pechan and CEP. 2004. Methods for Consolidation of Emissions Inventories (Schedule 9; Work Item 3). Prepared for CENRAP Emissions Inventory Workgroup. E.H. Pechan and Associates, Inc. Durham, North Carolina. Carolina Environmental Program, University of North Carolina, Chapel, Hill, North Carolina.

Pechan. 2005a. Electric Generating Unit (EGU) Growth Factor Comparison. Prepared for CENRAP Emissions Inventory Workgroup. E.H. Pechan and Associates, Inc. Durham, North Carolina. January.

Pechan. 2005b. Technical Memorandum: Updates to Source Classification Code (SCC) to Speciation Profile Cross-Reference Table. Prepared for CENRAP Emissions Inventory Workgroup. E.H. Pechan and Associates, Inc. Durham, North Carolina. April.

Pechan and CEP. 2005c. Consolidated of Emissions Inventories (Schedule 9; Work Item 3). E.H. Pechan and Associates, Inc. Durham, North Carolina. Carolina Environmental Program, University of North Carolina, Chapel, Hill, North Carolina. April 28.

Pechan 2005d. Development of Growth and Control Inputs for CENRAP 2018 Emissions, Draft Technical Support Document. E.H. Pechan and Associates, Inc. Durham, North Carolina. Carolina Environmental Program, University of North Carolina, Chapel, Hill, North Carolina. May.

Pechan and CEP. 2005e. Refinements of CENRAP's 2002 Emissions Inventories (Schedule 9; Work Item 3). E.H. Pechan and Associates, Inc. Durham, North Carolina. Carolina Environmental Program, University of North Carolina, Chapel, Hill, North Carolina. August 23.

Pitchford, M. 2006. Natural Haze Levels II: Application of the New IMPROVE Algorithm to Natural Species. Final Report by the Natural Haze Levels II Committee to the RPO Monitoring/Data Analysis Workgroup. (Marck.Pitchford@NOAA.gov).

Pollack, A.K, L. Chan, P. Chandraker, J. Grant, C. Lindhjem, S. Rao, J. Russell and C. Tran. 2006. WRAP Mobile Source Emission Inventories Update. ENVIRON International Corporation, Novato, California. May. (http://www.wrapair.org/forums/ef/UMSI/0606_WRAP_Mobile_Source_EI_Final_Report.pdf)

Reid, S.B., D.C. Sullivan, B.M. Penfold, T.H. Funk, T.M Tamura, P.S. Stiefer, S.M. Raffuse and H.L. Arkinson. 2004a. Emission Inventory Development for Mobile Sources and Agricultural Dust Sources for the Central States. Sonoma Technology, Inc., Petaluma, California. (available at http://cenrap.sonomatech.com/index.cfm). October 28.

Reid, S.B., S.G. Brown, D.C. Sullivan, H.L. Arkinson, T.H. Funk and P.S. Stiefer. 2004b. Research and Development of Planned Burning Emission Inventories for the Central States

Regional Air Planning Association. Sonoma Technology, Inc., Petaluma, California. (available at http://cenrap.sonomatech.com/index.cfm). July 30.

Russell, J., C. Lindhjem, B. Koo, R. Morris, C. Loomis, and G. Stella. 2006. Addition of Off-shore Marine Emissions to VISTAS Modeling. May 2006.

Russell, J. and A. Pollack. 2005. Oil and Gas Emission Inventories for the Western States. ENVITON International Corporation, Novato, California. December 27.

Seigneur, C., et al. 2000. "Guidance for the Performance Evaluation of Three-Dimensional Air Quality Modeling Systems for Particulate Matter and Visibility", *J. Air & Waste Manage. Assoc.* Vol. 50, pp. 588-599.

Solomon, P.S., T. Klamser-Williams, P. Egeghy, D. Crumpler and J. Rice. 2004. "STN/IMPROVE Comparison Study Preliminary Results". Presented at PM Model Performance Workshop. Chapel Hill, NC. February 10.

Stella, G. 2007. Memorandum: Cost Curve Comments and Actions Taken. Prepared for CENRAP. February 2007.

Timin, B. 2002. "$PM^{-}_{2.5}$ and Regional Haze Modeling Guidance". Prepared by the U.S. EPA/OAQPS. April 24.

Timin, B. 2004. "$PM_{2.5}$ Model Performance Evaluation: Purpose and Goals". Presented at PM Model Evaluation Workshop, Chapel Hill, NC. February.

Timin, B. 2007. Final Ozone/PM2.5/Regional Haze Modeling Guidance Summary. Presented at Region IV Modeling Workshop. U.S. Environmental Protection Agency, Office of Air Quality and Planning Standards, RTP, NC. March 28. (http://www.epa.gov/region04/air/modeling/Wed%203-28-07/Timin%20-%20Final-guidance-summary-R4-v2.pdf)

Tonnesen, G., Z. Wang, M. Omary, C-J. Jung, R. Morris, G. Mansell, S. Kemball-Cook, G. Yarwood, Z. Adelman, A. Holland and K. Hanisak. 2005. Final Report for the Western Regional Air Partnership (WRAP) Regional Modeling Center (RMC) for the Project Period March 1, 2004 through February 28, 2005. University of California at Riverside, Riverside, California. August 16. (http://pah.cert.ucr.edu/aqm/308/reports/final/2004_RMC_final_report_main_body.pdf).

Tonnesen, G., Z. Wang, M. Omary, C-J. Jung, Y. Wang, R. Morris, S. Kemball-Cook, Y. Jia, S. Lao, B. Koo, Z. Adelman, A. Holland and J. Wallace. 2006. Final Report for the Western Regional Air Partnership (WRAP) 2002 Visibility Model Performance Evaluation. University of California at Riverside, Riverside, California. February 24. (http://pah.cert.ucr.edu/aqm/308/reports/final/2002_MPE_report_main_body_FINAL.pdf).

Xiu, A., and J.E. Pleim. 2000. Development of a land surface model. Part I: Application in a mesoscale meteorology model. *Journal of Applied Meteorology*, 40, 192-209.

APPENDIX A

Model Performance Evaluation of the 2002 36 km MM5 Meteorological Model Simulation used in the CENRAP Modeling and Comparison to VISTAS Final 2002 36 km MM5 and WRAP Interim 2002 36 km MM5 Simulations

The CENRAP 2002 36 km MM5 simulation (Johnson, 2007) was evaluated against observed surface and upper-air meteorological observations and observed precipitation amounts and its performance was compared against the VISTAS final and the WRAP interim 2002 36 km MM5 simulations. The CENRAP, VISTAS and WRAP 2002 36 km MM5 simulations used several common science options:

- Lambert Conformal Projection with center at (97°, 40°) and standard parallels at (33°, 45°).
- 164 by 128 36 km by 36 km horizontal grids covering the continental U.S. and adjacent regions.
- 34 vertical layers up to 100 mb (~15 km AGL).
- Pleim-Xiu Land Surface Module (LSM).
- Asymmetric Convective Mixing (ACM) Planetary Boundary Layer (PBL) model.
- RRTM long-wave radiation.
- Dudhia short-wave radiation.
- No Shallow convection.

However, there were some differences in the choice of science options:

- VISTAS and CENRAP MM5 simulations used the Kain Fritsch 2 cumulus parameterization, whereas WRAP MM5 used Kain Fritsch 1.
- VISTAS and CENRAP MM5 simulations used the Reisner 1 moist physics while WRAP MM5 used Reisner 2.
- All three MM5 simulations used Four Dimensional Data Assimilation (FDDA analysis nudging at the surface for winds, but WRAP also used surface analysis nudging to temperature and moisture.
- All three MM5 simulations used analysis nudging FDDA above the PNL to winds, temperature and moisture.

Much of the difference in the model performance for the three MM5 simulations was related to the surface temperature and moisture analysis nudging used in the interim WRAP MM5 simulations that resulted in better surface temperature model performance, but caused instabilities resulting in degradation in meteorological model performance above the surface. The final WRAP 2002 36 km MM5 simulation did not use the surface temperature and moisture FDDA and used the Betts-Miller cumulus scheme instead of Kain Fritsch that resulted in much improved meteorological model performance in the western States (Kemball-Cook et al., 2005).

A.1 Surface Meteorological Model Performance

The performance of the three MM5 simulations at the surface was evaluated through comparisons against observed surface wind, temperature and humidity measurements from the ds472 observational database. The METSTAT program was used to evaluate the MM5 simulations for each month of 2002 and across the 11 subdomains shown in Figure A-1. These subdomains are as follows:

1 = Pacific NW
2 = SW
3 = North
4 = Desert SW
5 = CenrapN
6 = CenrapS
7 = Great Lakes
8 = Ohio Valley
9 = SE
10 = NE
11 = MidAtlantic

Emery and Tai (2001) have developed model performance benchmarks by analyzing over 30 MM5RAMS meteorological model simulations and tabulating the typical level of performance that a good meteorological model achieves. These performance benchmarks are not intended to be pass/fail grades; rather they provide a framework to evaluate the model performance against past applications. Since many of the past MM5/RAMS meteorological model simulations that the benchmarks were developed from were in support of urban ozone modeling that are typically fairly stagnant conditions with little or no precipitation and involved multiple iterations to achieve the final base case simulation. Thus, we may not expect the 2002 annual MM5 simulations to achieve a similar level of performance given the complicating factors of precipitation and complex terrain associate with many Class I areas in the west. Table A-1 lists the meteorological model performance benchmarks for wind speed, wind direction, temperature and humidity.

Table A-1. Meteorological model performance benchmarks (Source: Emery et al., 1999).

Statistic	Wind Speed	Wind Direction	Temperature	Humidity
RMSE	≤ 2 m/s			
Mean Bias	≤ ±0.5 m/s	≤ ±10°	≤ ±0.5 K	≤ ±1.0 g/kg
Index of Agreement	≤ 0.6		≤ 0.8	≤ 0.6
Gross Error		≤ 30°	≤ 2.0 K	≤ 2.0 g/kg

Below we present the evaluation of the CENRAP, VISTAS and interim WRAP 2002 36 km MM5 simulations against surface meteorological observations for the four seasonal months of January, March, July and October and the CENRAP North (CenrapN) and CENRAP South (CenrapS) subdomains (i.e., subdomains 5 and 6 in Figure A-1). The surface evaluation of the three MM5 2002 36 km simulations outside of the CENRAP subdomains can be found in Kemball-Cook et al., (2004).

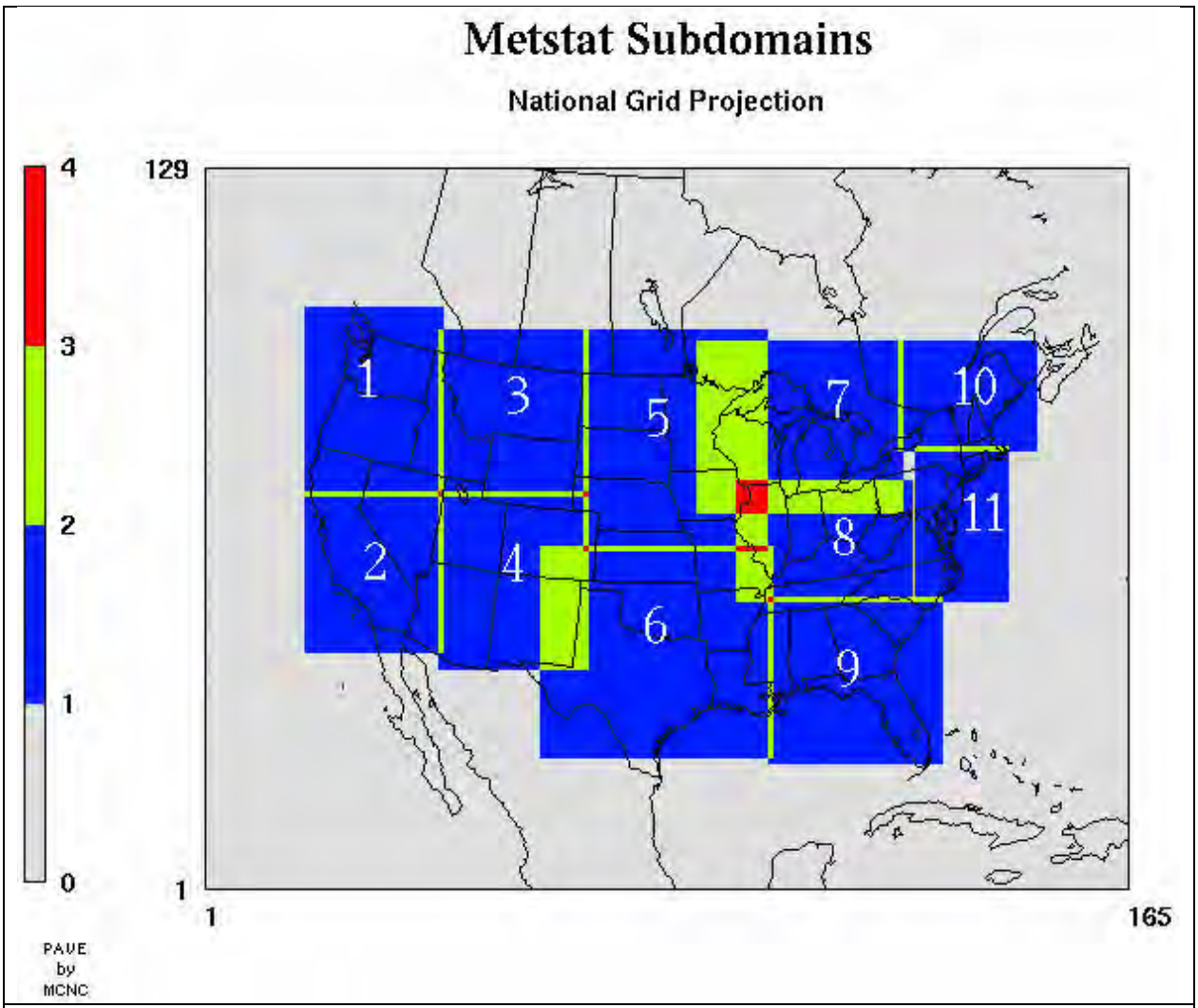

Figure A-1. Eleven subdomains where monthly evaluation of the MM5 simulations surface model performance was evaluated.

A.1.1 Temperature

Figure A-2 displays the surface temperature model performance for the CENRAP, VISTAS and WRAP 2002 36 km MM5 simulations in the CenrapN and CenrapS subdomains and the months of January, March, July and October. The WRAP MM5 simulations are performing best for January temperature in both CENRAP domains exhibiting low bias and the lowest error that are within the benchmark. The VISTAS MM5 rum is performing next best with bias well within the benchmark and error within but close to the error benchmark. The CENRAP MM5 simulation performs well for the CenrapS domain with zero bias and error within, but approaching the benchmark. However, the CENRAP performance for the CenrapN domain does not achieve the performance benchmarks due to a too cold bias.

The temperature performance in March is similar to January with both the VISTAS and WRAP MM5 simulations achieving the benchmark for both CENRAP subdomains. Again the CENRAP MM5 simulation has a near zero bias and achieves the error benchmark in the CenrapS subdomain, but is too cold in the CenrapN domain falling out of the bias benchmark range.

In July the three simulations achieve the temperature benchmark in both CENRAP subdomains, although the WRAP MM5 simulations is cooler with the CenrapS bias right at the -0.5 K lower bound benchmark. The CENRAP MM5 simulation is slightly warmer than the VISTAS MM5 simulation.

In October, all three MM5 simulations achieve the temperature performance benchmarks. The WRAP MM5 simulation performs best with near zero bias and lower error than either the VISTAS or CENRAP simulations. The VISTAS and CENRAP MM5 simulations exhibit nearly identical temperature performance in October with a near zero bias for the CenrapS subdomain and a cool bias for the CenrapN subdomain.

In conclusion, the WRAP MM5 simulation is always performing best for surface temperature with the lowest bias and usually the lowest error. The VISTAS MM5 simulations is performing next best as the CENRAP MM5 simulations exhibits a cool bias for the CenrapN subdomain in January and March that exceed the performance benchmarks.

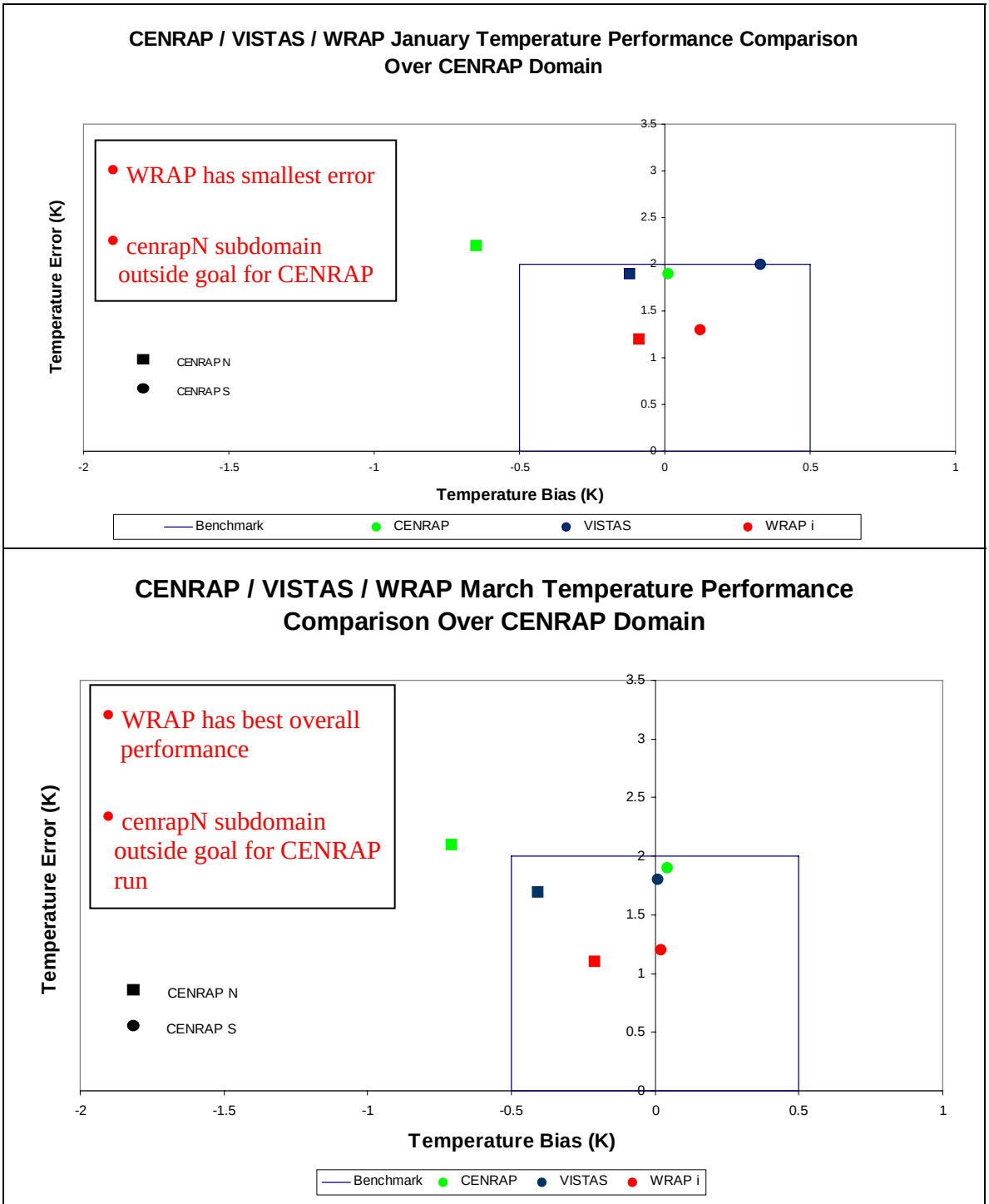

Figure A-2a. Temperature performance for the CENRAP, VISTAS and interim WRAP 2002 36 km MM5 simulations, the CenrapN and CenrapS subdomains and January (top) and March (bottom).

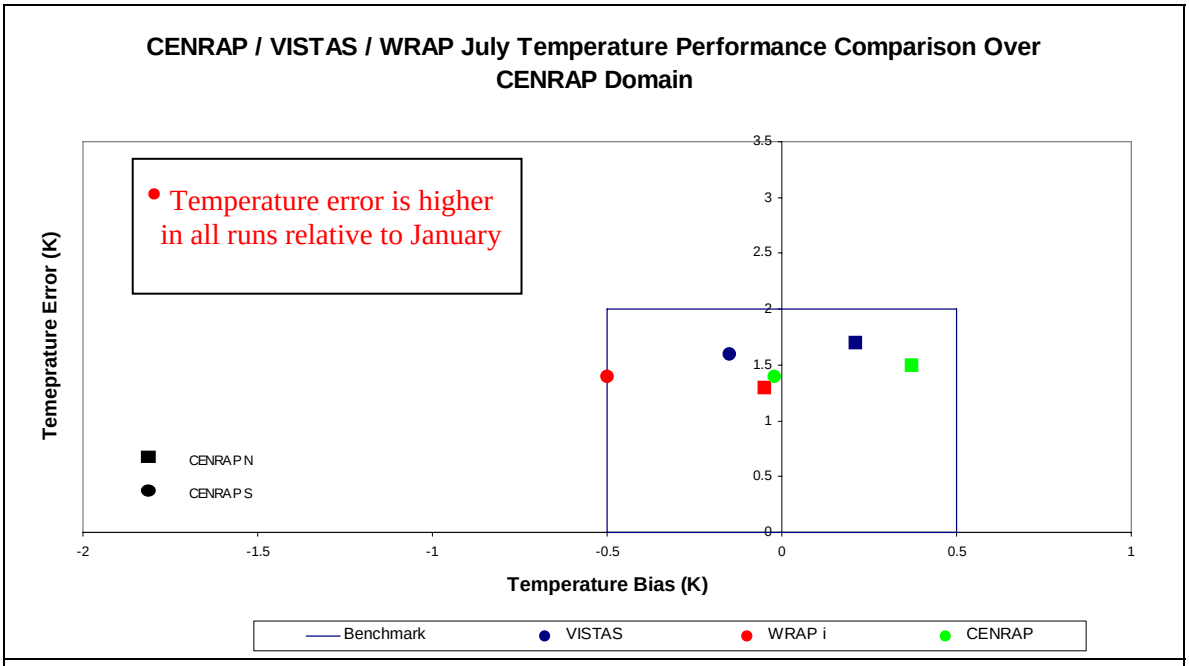

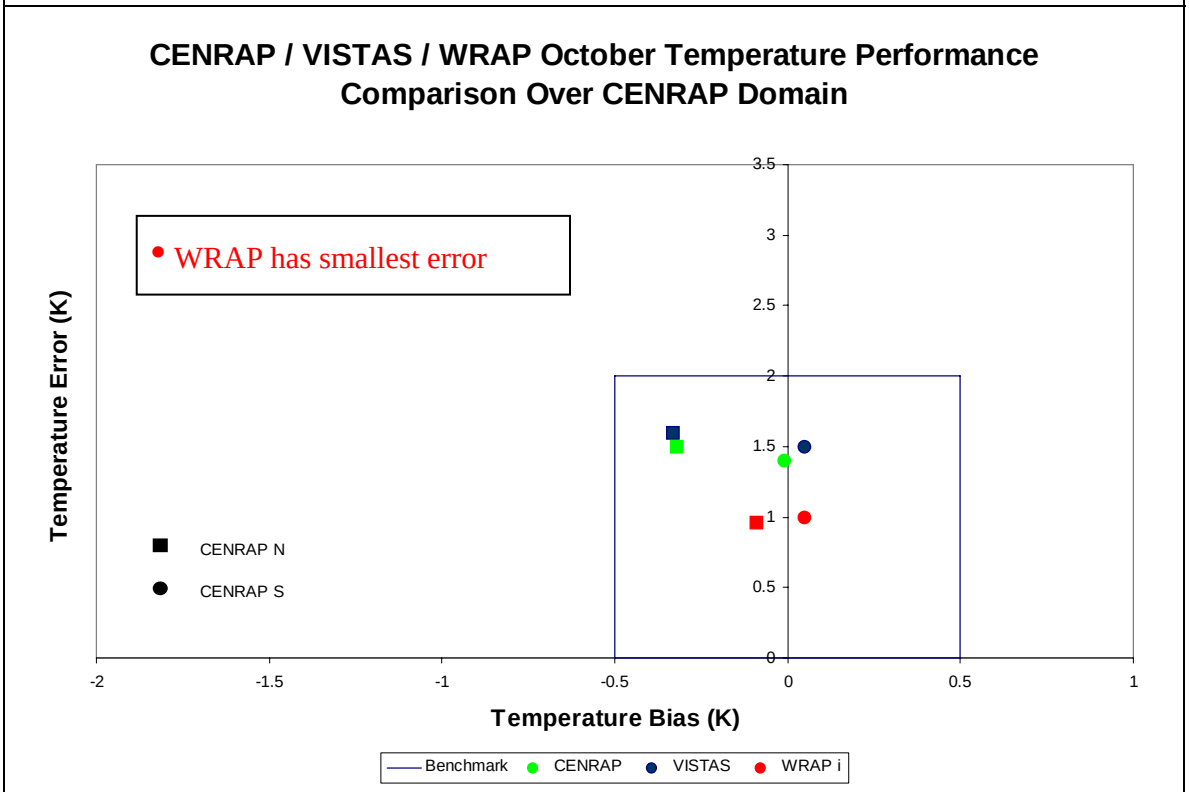

Figure A-2b. Temperature performance for the CENRAP, VISTAS and interim WRAP 2002 36 km MM5 simulations, the CenrapN and CenrapS subdomains and July (top) and October (bottom).

A.1.2 Humidity

The humidity performance for the three MM5 simulations is comparable and always achieves the performance benchmarks. The humidity bias is always near zero for all three runs and four months. In January, March and October the humidity error is at or less than half of the 2.0 g/kg benchmark. However, in July there is more error in the humidity with it within but approaching the benchmark value for all three models.

In conclusion, all three MM5 simulations achieved the humidity benchmark performance goals for all months studied. No model simulation exhibited superior performance over another.

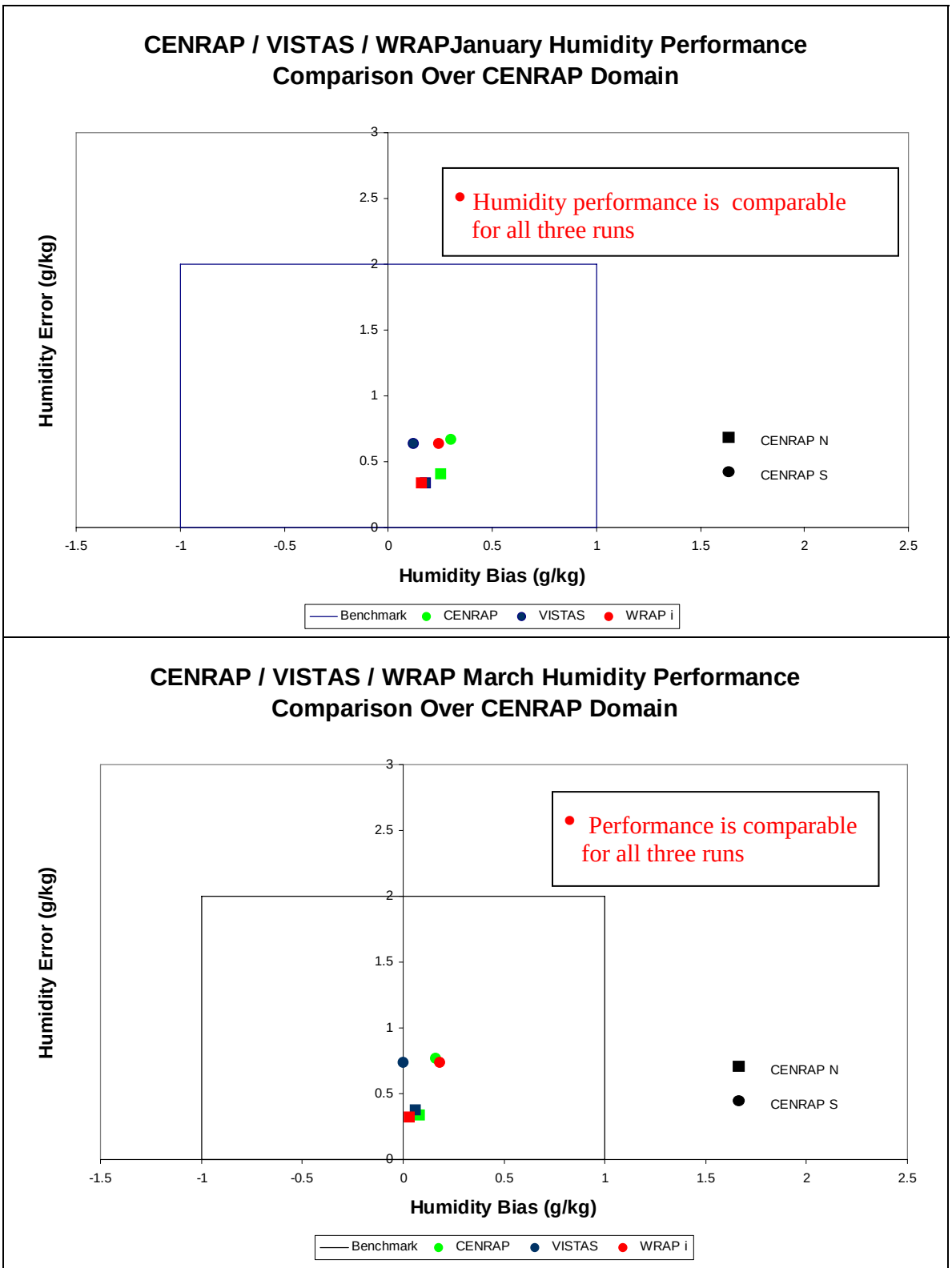

Figure A-3a. Humidity performance for the CENRAP, VISTAS and interim WRAP 2002 36 km MM5 simulations, the CenrapN and CenrapS subdomains and January (top) and March (bottom).

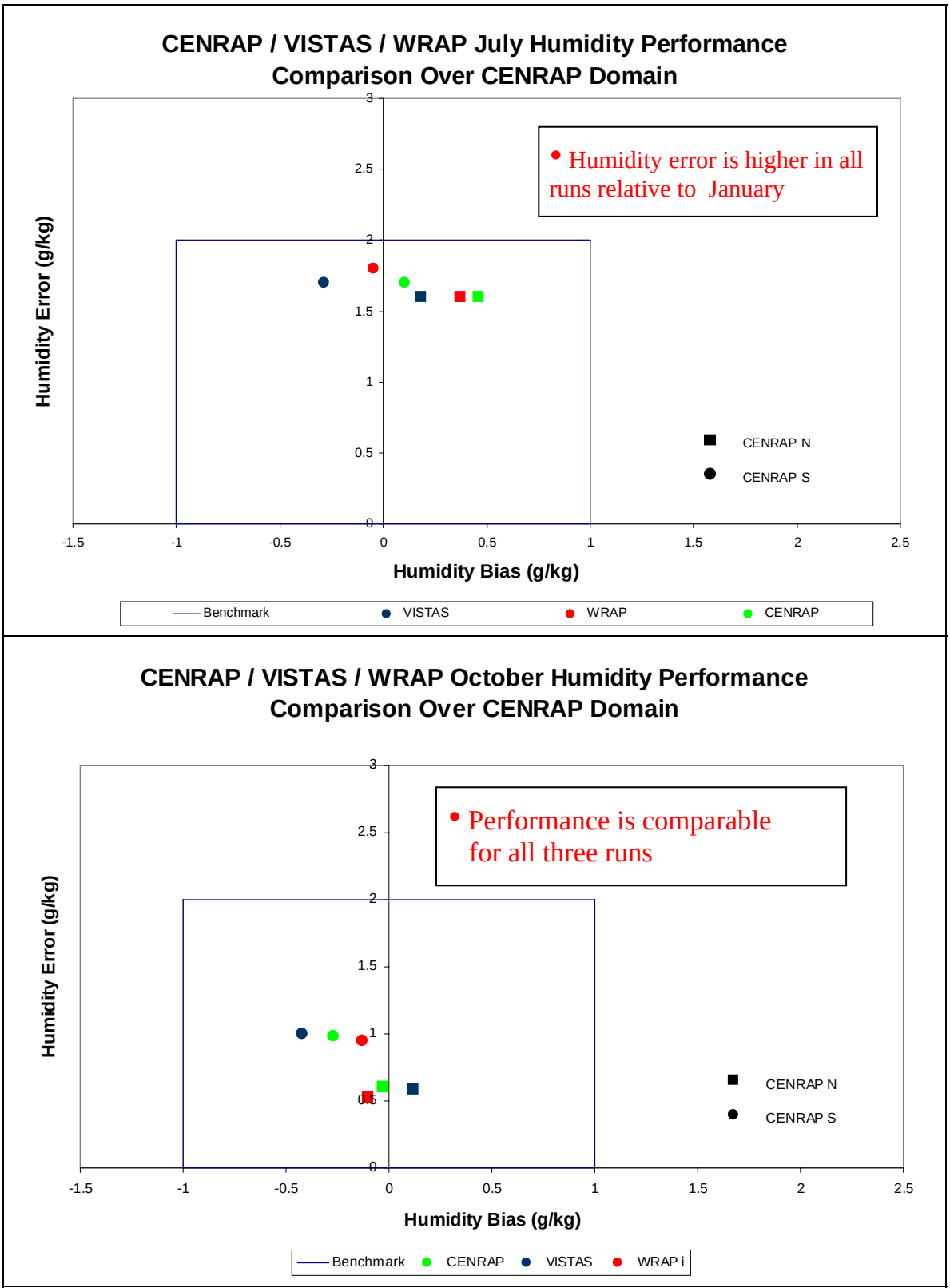

Figure A-3b. Humidity performance for the CENRAP, VISTAS and interim WRAP 2002 36 km MM5 simulations, the CenrapN and CenrapS subdomains and July (top) and October (bottom).

A.1.3 Winds

The model performance for wind speed and direction and January is almost identical and within the benchmarks for all three models and both CENRAP subdomains. In fact, the performance is so close the CenrapS symbols are plotted over and obliterate the CenrapN performance symbols.

In March, the wind performance is within the benchmark for all three MM5 simulations, which exhibit similar performance statistics. The wind performance in the CenrapS subdomain is slightly better than CenrapN with the CENRAP MM5 simulations showing the largest wind speed RMSE in the CenrapN subdomain, although still within the benchmarks.

Slight degraded wind direction performance is seen in July with the error increases to just below 20 degrees to just below the 30 degree benchmark value for all three models. Similar wind speed RMSE is seen for all three models.

The October wind performance is within the benchmarks for all three models with performance between that seen for January/March and July.

In summary, the models exhibited similar model performance for surface wind speed and direction.

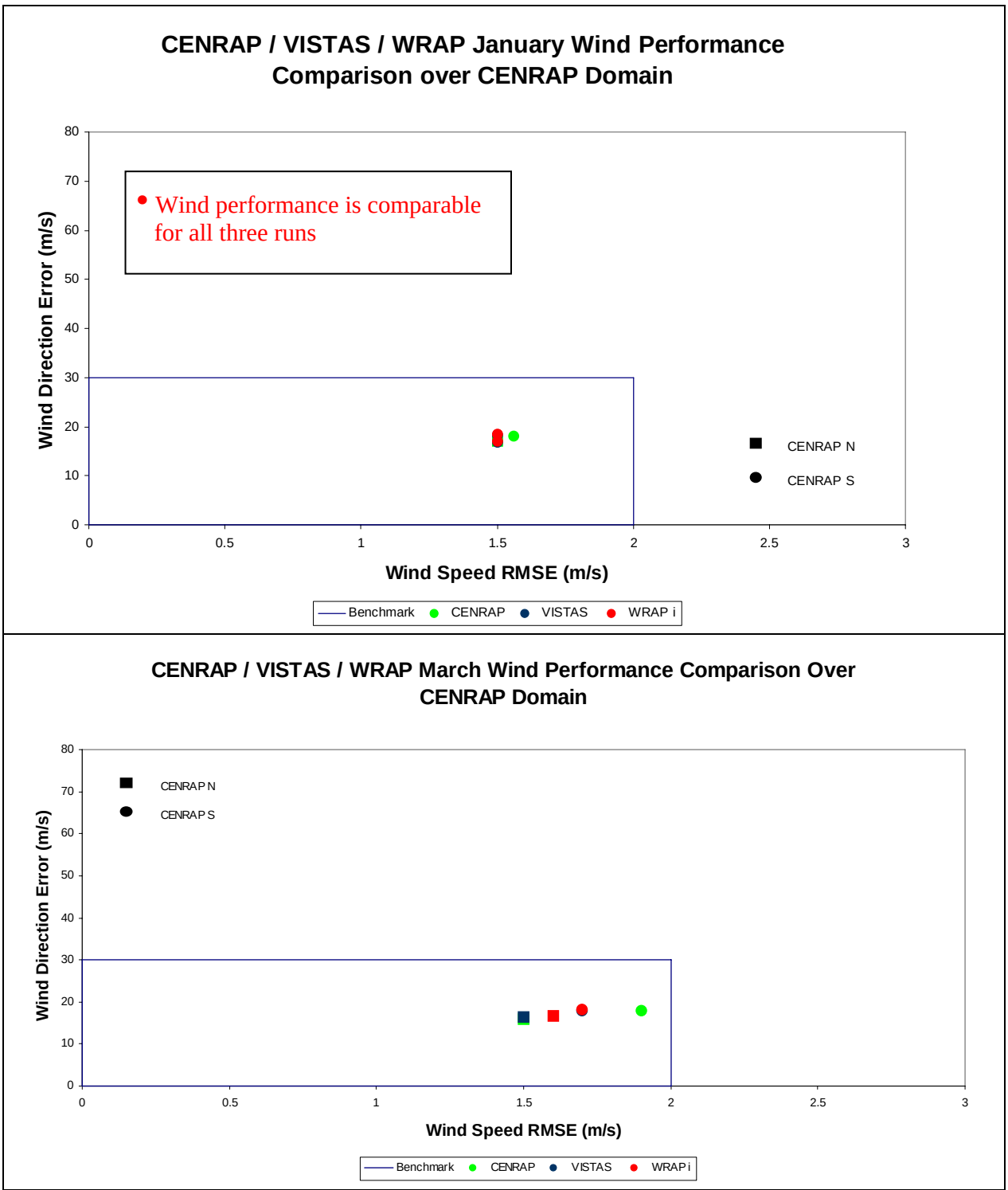

Figure A-4a. Wind Speed and Wind Direction performance for the CENRAP, VISTAS and interim WRAP 2002 36 km MM5 simulations, the CenrapN and CenrapS subdomains and January (top) and March (bottom).

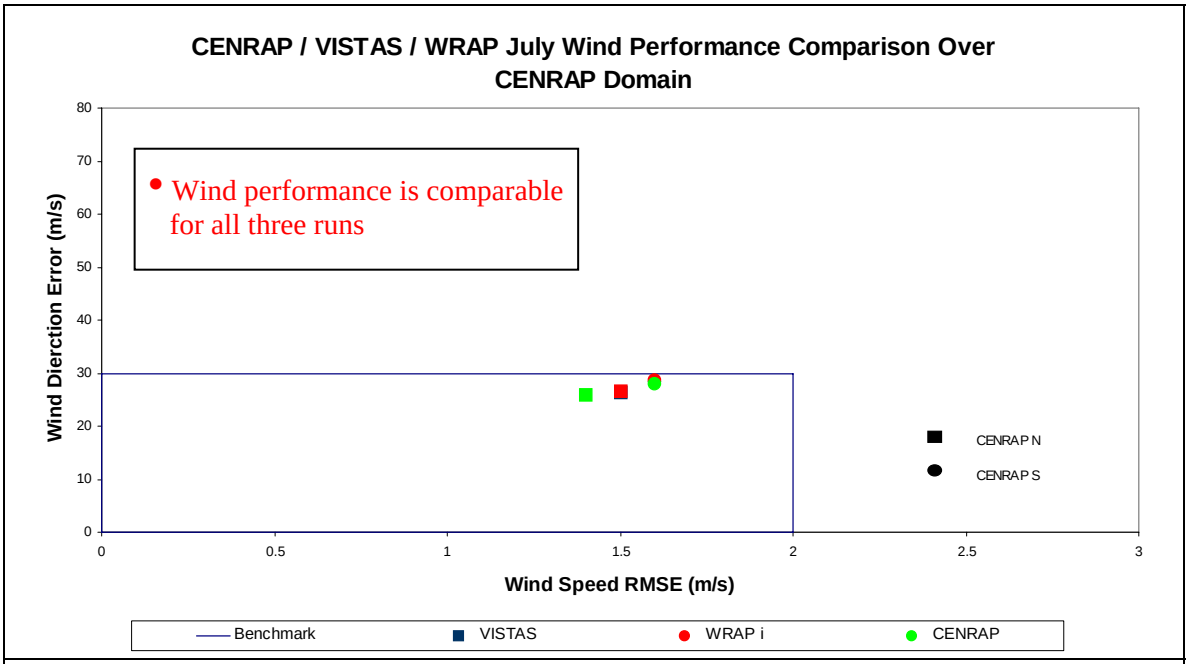

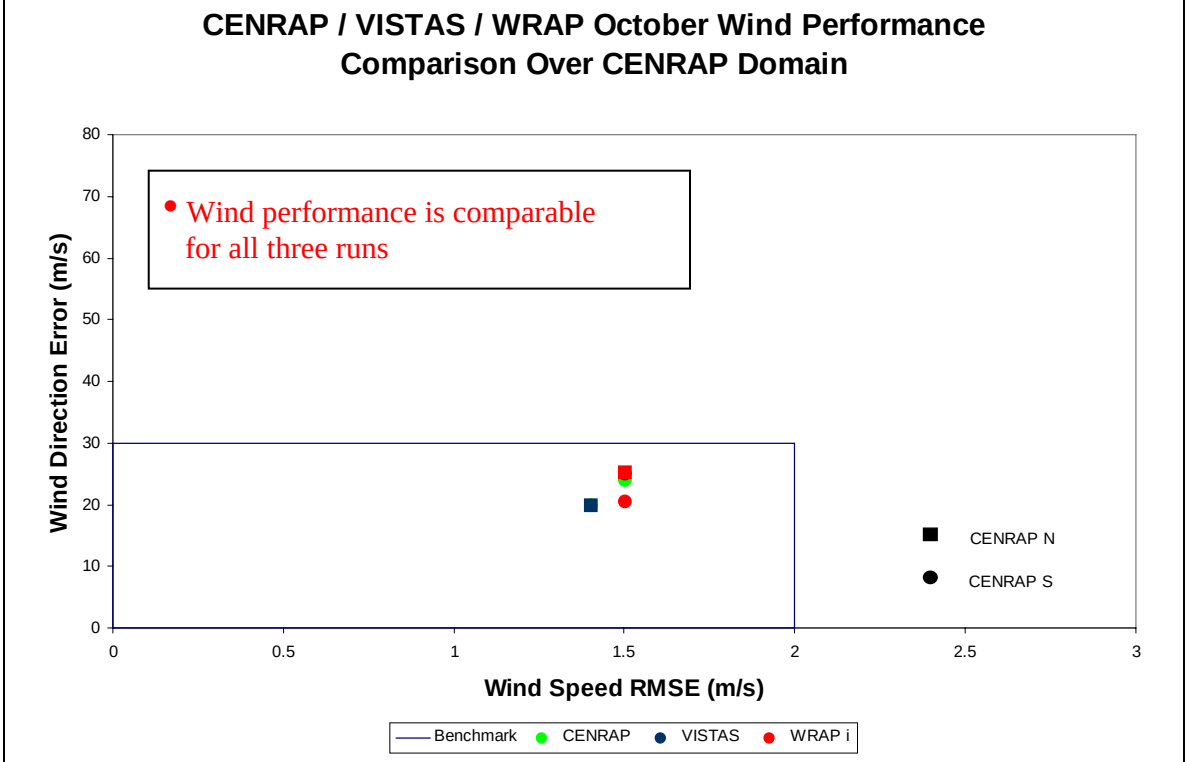

Figure A-4b. Wind Speed and Wind Direction performance for the CENRAP, VISTAS and interim WRAP 2002 36 km MM5 simulations, the CenrapN and CenrapS subdomains and July (top) and October (bottom).

A.2 Upper-Air Meteorological Evaluation

Figure A-5 displays an example comparison of the vertical profile of predicted and observed winds and temperature for Midland, Texas and January 7 2002 at 12 GMT (6am LST) and for July 16, 2002 at 00 GMT (6pm LST). Above the surface, all three models do a good job in replicating the observed temperature, dew point temperature and winds at 6a on January 7, 2002. Although the WRAP MM5 simulation predicts the surface temperature better than the other two simulations, the vertical structure of the temperature and the surface temperature inversion is not reproduced as well.

All three models understate the afternoon PBL depth on July 16, 2002 at Midland Texas. This phenomenon was seen at other sites as well.

The upper-air meteorological model evaluation found that all three models had difficulty reproducing the observed nocturnal inversion. The day time convective mixing depths were also typically underestimated.

Although the WRAP MM5 simulation reproduced the surface temperature the best of the three models, it was worst at reproducing the observed vertical temperature structure and resultant level of mixing. These results are likely due to the surface data assimilation of temperature employed by the WRAP interim MM5 simulation and resulted in WRAP eliminating the surface temperature and humidity FDDA in their final simulation.

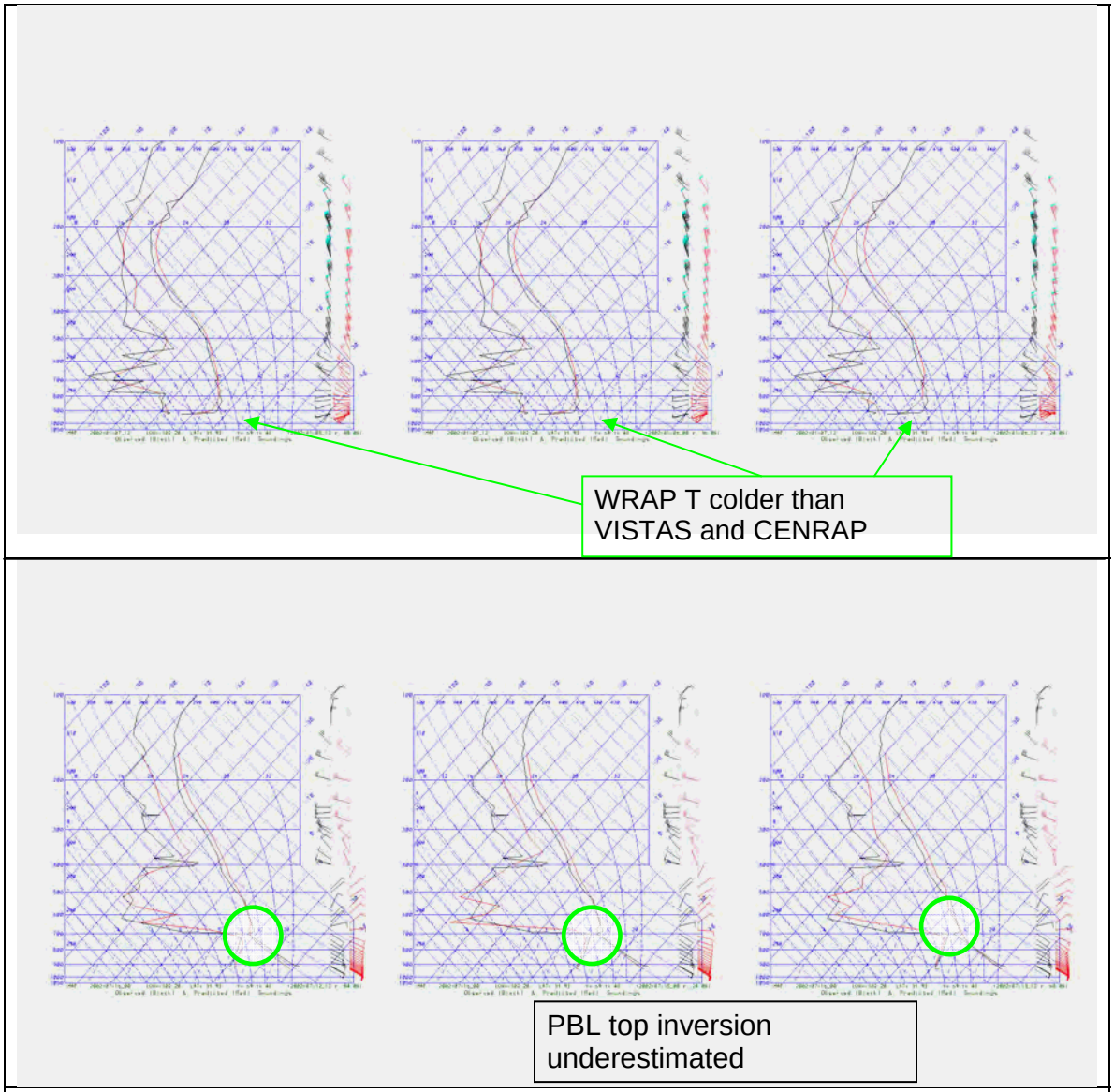

Figure A-5. Comparison of predicted and observed vertical temperature, dew point and winds profiles for the CENRAP (left), VISTAS (middle) and WRAP (right) at Midland Texas on January 7, 2002 at 12 GMT (top) and July 16, 2002 at 00 GMT (bottom).

A.4 Precipitation Model Performance Evaluation

The three MM5 model simulation precipitation estimates were evaluated by comparing the monthly average spatial distributions and amounts with observed values from the observed CPC 0.25 by 0.25 degree (approximately 28 km by 28 km) gridded analysis fields. The CPC analysis fields are gridded from on U.S. land-based observations, consequently the gridded observed fields are not available over the oceans and Canada and Mexico. The CPC observed monthly average precipitation fields were displayed using the MM5 modeling domain. The MM5 total precipitation estimates were accumulated for a month and plotted. Here total precipitation includes both explicit large scale synoptic precipitation as well as the subgrid-scale convective precipitation from the cumulus parameterization (Kain Fritsch 1 or 2).

Figures A-6 through A-9 display the monthly average precipitation fields for the months of January, March, July and October and the CPC observed and CENRAP, VISTAS and interim WRAP MM5 simulations. In January (Figure A-6), all three models reproduce the observed monthly average precipitation well with enhanced predicted and observed precipitation over the Pacific Northwest and the Appalachian Mountains. The MM5 simulations also estimated enhanced precipitation in off-shore areas north of Seattle, over the Atlantic Ocean and in the Gulf of Mexico that can not be either confirmed or refuted by the CPC observations. MM5 does overstate the amount of precipitation in January over the northern CENRAP region including over Minnesota, Iowa and Nebraska.

The three models also do a good job in reproducing the observed spatial distribution and amounts of the precipitation in March 2002 (Figure A-7). Elevated precipitation areas in the Pacific Northwest and across the lower Midwest from Arkansas and up into the Ohio River Valley and adjacent areas. The MM5 simulations do understate the highest observed precipitation amounts in Arkansas. The MM5 simulations also overstate the amount of precipitation in the desert southwest (Four Corners) area in March.

The MM5 monthly average precipitation performance is dramatically worse in July 2002 (Figure A-8). Precipitation is overstated by all three MM5 simulations throughout the U.S. and particularly in the southern states, from Arkansas across Texas to the southeastern U.S. particularly Florida South and North Carolina. This over-prediction bias is due to convective precipitation from the cumulus parameterization (either Kain Fritsch 1 or 2). This overactive precipitation is the result of the over-prediction bias I humidity seen in many subdomains (see Table A-3b and Kemball-Cook et al., 2004a).

In October 2002, the three MM5 simulations reproduced the observed monthly average rainfall fairly well across the U.S. (Figure A-9). The models predict the location of the maximum precipitation in southern Louisiana well, but under-predict the magnitude, which may be due to a slight spatial displacement offshore in the Gulf of Mexico. The MM5 simulations understate the precipitation over the CENRAP region, which explains the dry humidity bias in the CenrapS subdomain in October (Figure A-3b).

In conclusion, the three MM5 simulations do a good job in simulating the observed precipitation when it is due to synoptic weather systems. However, when precipitation is due to convective activity as seen in July that is simulated by the MM5 cumulus parameterization, MM5 greatly overstates the precipitation amounts. This is particularly pronounced in the southern states from the Four Corners area to Florida with the interim WRAP simulation exhibiting the largest over-prediction bias. In the final WRAP MM5 simulation the Betts-Miller cumulus parameterization was used that greatly reduced the convective precipitation amounts resulting in better model performance (Kemball-Cook et al., 2005). However, an overestimation bias under convective precipitation conditions still was present.

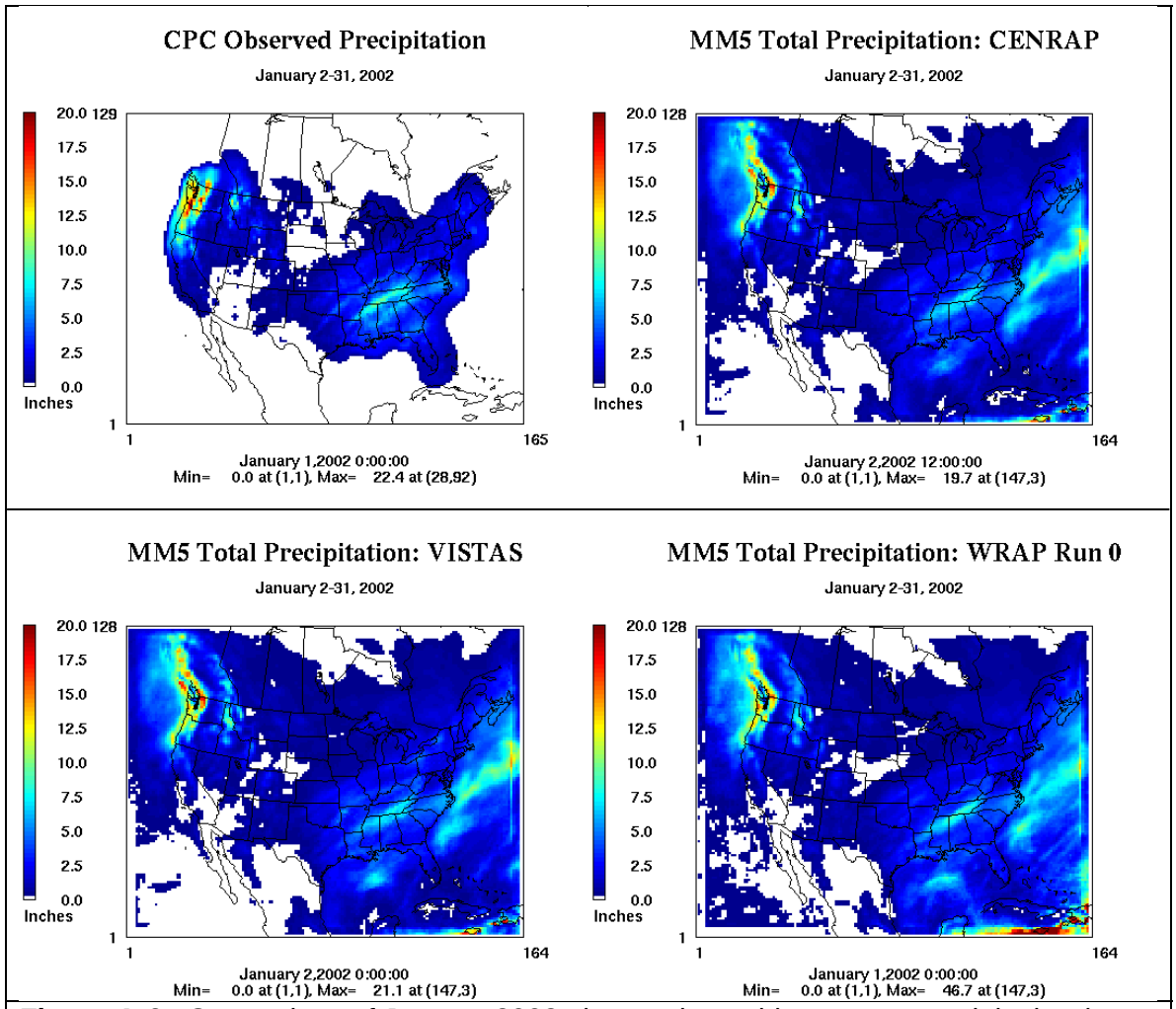

Figure A-6. Comparison of January 2002 observed monthly average precipitation (top left) with predicted values for the CENRAP (top right), VISTAS (bottom left) and WRAP (bottom right January 2002 simulation (note: observed precipitation not valid over water due to lack of measurements).

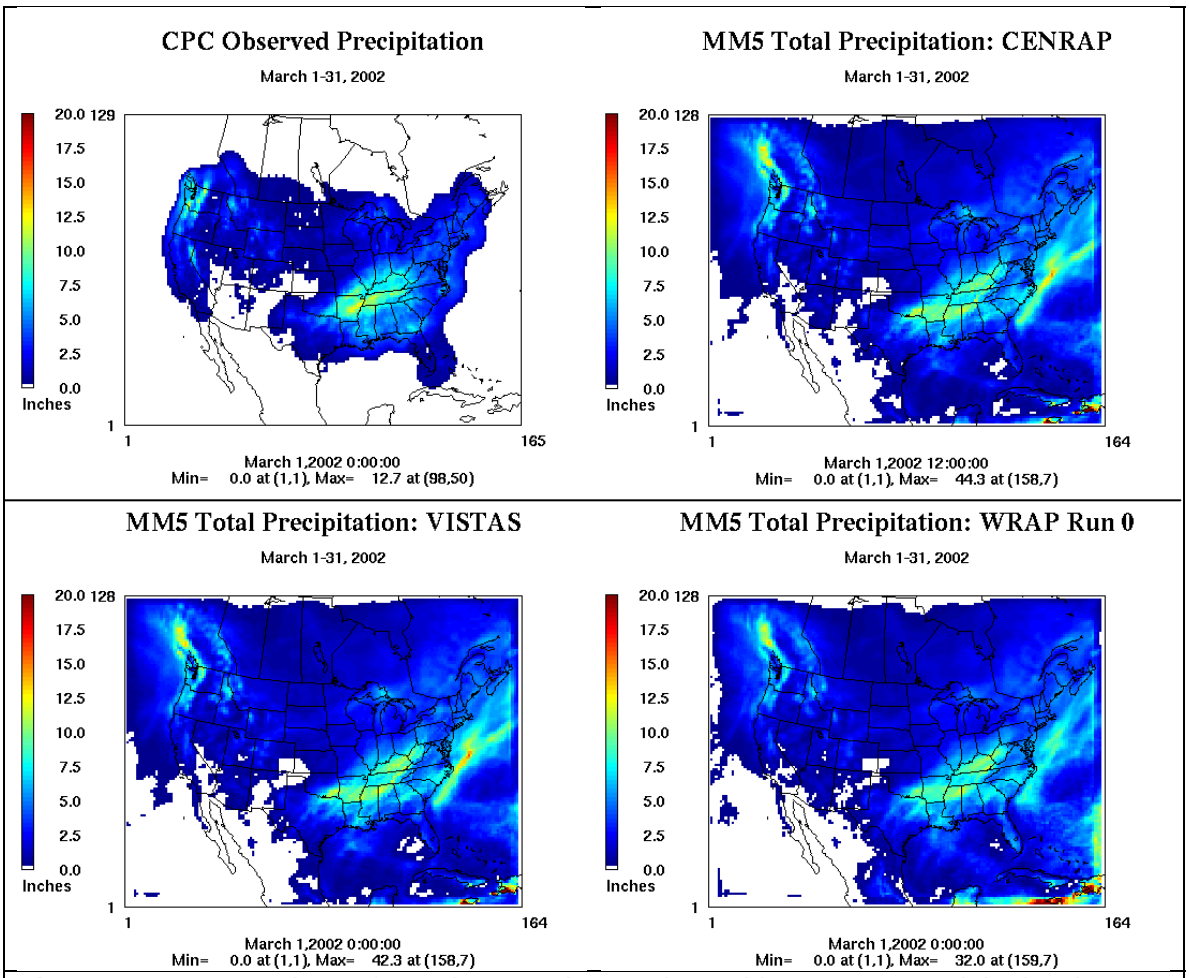

Figure A-7. Comparison of March 2002 observed monthly average precipitation (top left) with predicted values for the CENRAP (top right), VISTAS (bottom left) and WRAP (bottom right January 2002 simulation (note: observed precipitation not valid over water due to lack of measurements).

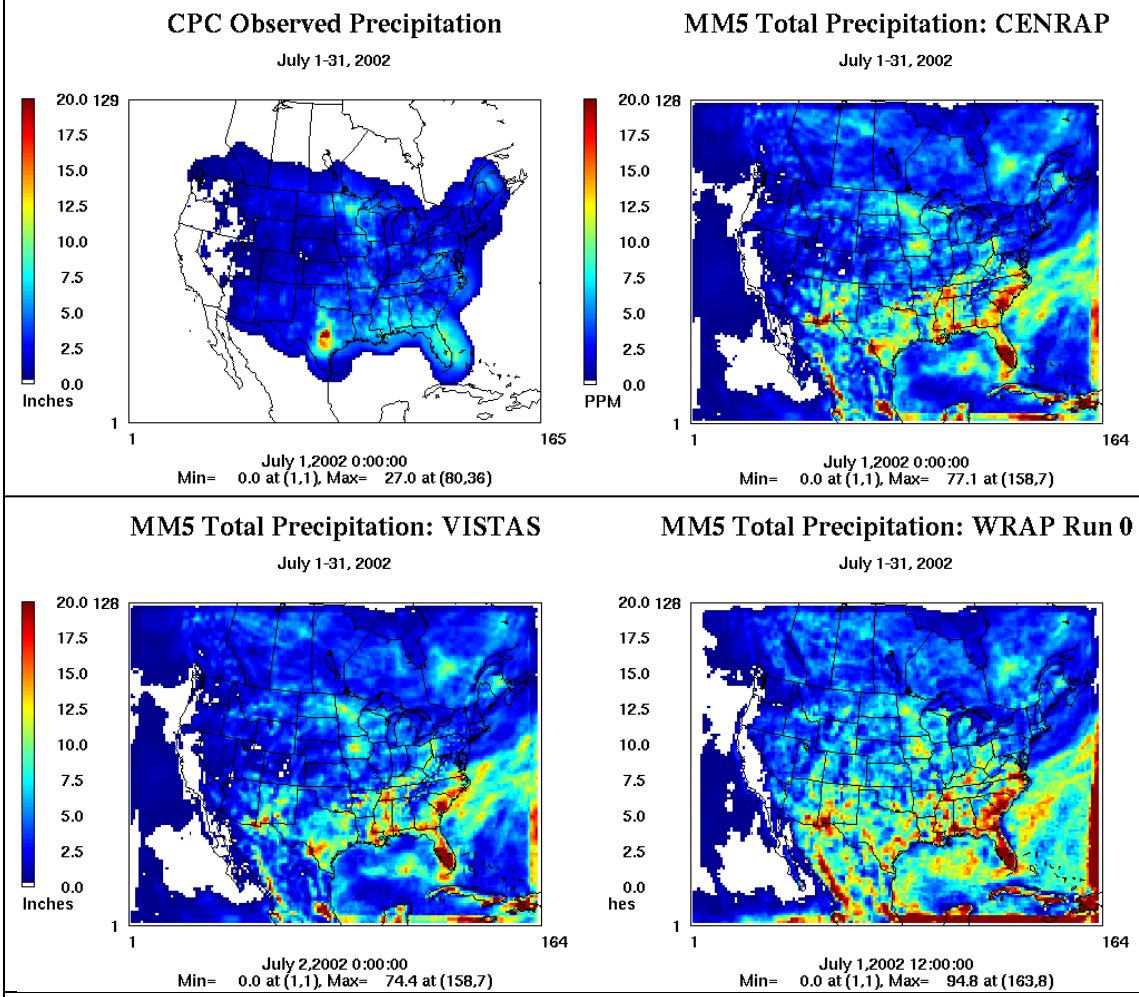

Figure A-8. Comparison of July 2002 observed monthly average precipitation (top left) with predicted values for the CENRAP (top right), VISTAS (bottom left) and WRAP (bottom right) (note: observed precipitation not valid over water due to lack of measurements).

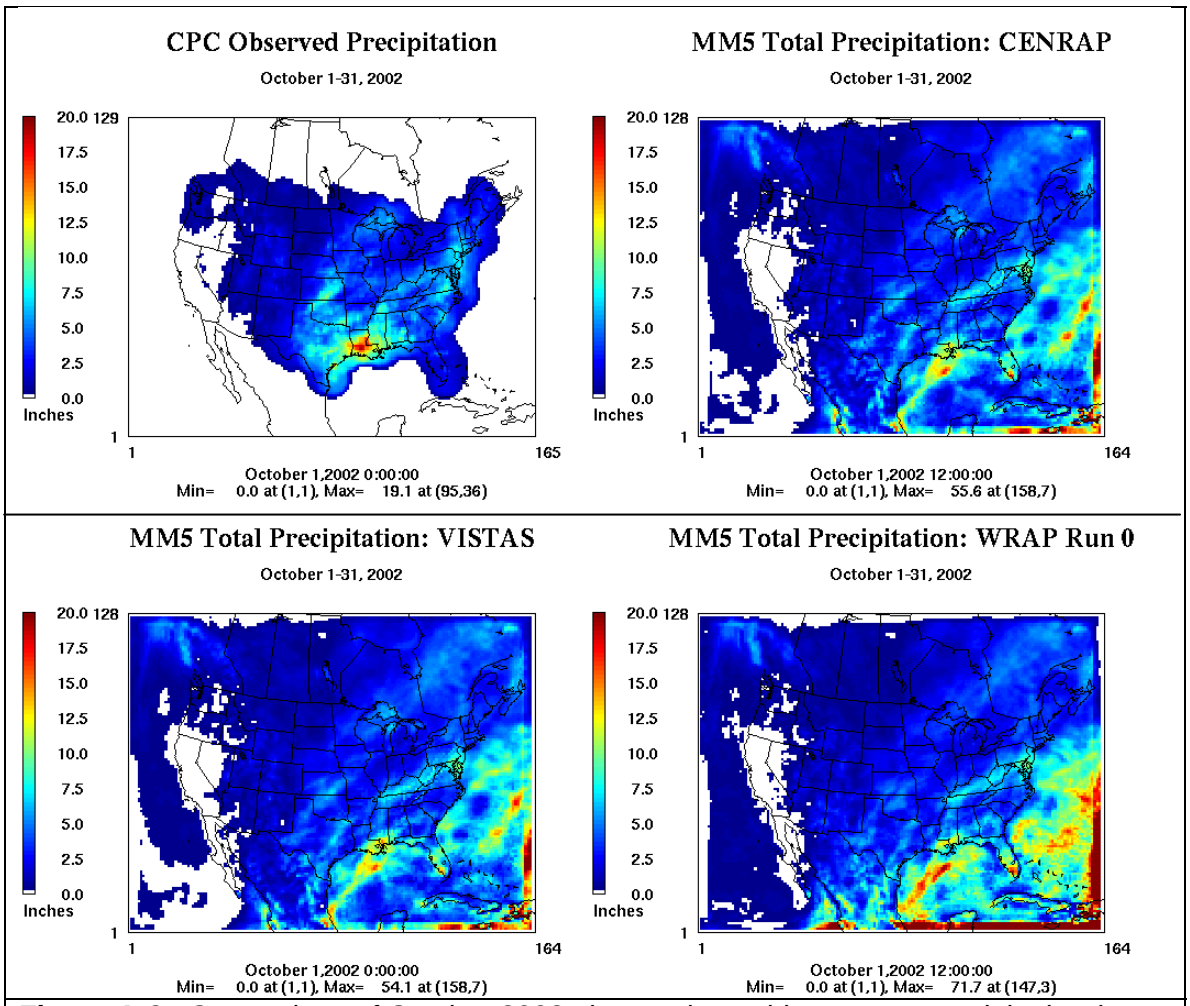

Figure A-9. Comparison of October 2002 observed monthly average precipitation (top left) with predicted values for the CENRAP (top right), VISTAS (bottom left) and WRAP (bottom right) (note: observed precipitation not valid over water due to lack of measurements).

APPENDIX B

File Names, Data Source and Type and Description of Emissions Used in the 2002 Typical and 2018 Base G Emissions Inventories

Table A-1. CENRAP 2002 Typical Base G (Typ02G) emissions inventory.

Filename	Source	Data type	Description
1 Stationary Area Sources			
arinv_Mexico99phase3_border_20051027v4_noDust_noFire.ida	**ERG**	**Text**	**1999 BRAVO Mexico inventory for the six Northern states; annual**
arinv_Mexico99phase3_interior_ERG_Oct06_noDust_noFire.ida	**ERG**	**Text**	**1999 BRAVO Mexico inventory for the Southern states; annual**
arinv_nodust_noOilGas_CA2002_111105.ida	**ERG**	**Test**	**California 2002 inventory; annual**
arinv_noDUST_noREF_vistas_2002g_2453908.ida	**Alpine Geophysics**	**Test**	**VISTAS 2002 inventory; annual**
arinv_nodust_wrap2002_v1_noCAWANDORUT_081205.ida	**ERG**	**Text**	**WRAP 2002 inventory for AZ, CO, ID, MT, NM, NV, SD, and WY ; annual**
arinv_nodust_wrap2002_v2_WANDORUT_102105.ida	**ERG**	**Text**	**WRAP 2002 inventory for ND, OR, UT, and WA; annual**
arinv_NoFire_CANADA2000_v2.ida	**Environment, Canada 011205**		**2000 Canada inventory; annual**
arinv_NoFire_noDUST_noREF_mrpok_2002_20jun2006.ida	**Alpine Geophysics**	**Text**	**MWRPO 2002 inventory; annual**
arinv_NoFire_nodust_ref_mane-vu2002_011705.ida	**MARAM web site**	**Text**	**MANE_VU 2002 inventory, annual**
arinv_NoFire_nodust_ref_nh3_cenrap2002_081705.ida	**Pechan**	**Text**	**CENRAP 2002 inventory; annual**
arinv_vistas2002_TypicalFires2610000_112704.ida	**Alpine Geophysics**	**Text**	**VISTAS 2002 inventory for SCC 2610000500**
2 Fugitive Dust			
fdinv1_CA2002_v2_wfac_111105.ida	**ERG**	**Text**	**CA 2002 inventory; extracted from stationary area inventory using initial list of SCCs; transport fractions applied; annual**
fdinv1_CANADA2000_v2_wfac.ida	**Environment Canada**	**Text**	**Canada 2000 inventory; extracted from stationary area inventory using initial list of SCCs; transport fractions applied; annual**
fdinv1_cenrap2002_wfac_081705.ida	**Pechan**	**Text**	**CENRAP 2002 inventory; extracted from stationary area inventory using initial list of SCCs; transport fractions applied; annual**
fdinv1_manevu2002_wfac_011705.ida	**MARMA web site**	**Text**	**MANE-VU2002 inventory; extracted from stationary area inventory using initial list of SCCs; transport fractions applied; annual**
fdinv1_Mexico99phase3_border_20051027v4_wTfac.ida	**MARMA web site**	**Text**	**Mexico Northern states 1999 inventory; extracted from stationary area inventory using initial list of**

Filename	Source	Data type	Description
			SCCs; transport fractions applied; annual
fdinv1_Mexico99phase3_interior_ERG_Oct06_wo_pmfac.ida	**ERG**	**Text**	**Mexico Southern states 1999 inventory; extracted from stationary area inventory using initial list of SCCs; no transport fractions applied; annual**
fdinv1_mrpok_2002_20jun2006_w_tfrac.ida	**Alpine Geophysics**	**Text**	**MWRPO 2002 inventory; extracted from stationary area inventory using initial list of SCCs; transport fractions applied; annual**
fdinv1_vistas_2002g_2453908_w_pmfac.ida	**Alpine Geophysics**	**Text**	**VISTAS 2002 inventory; extracted from stationary area inventory using initial list of SCCs; transport fractions applied; annual**
fdinv1_wrap2002_wfac_noCAWANDORUT_081205.ida	**ERG**	**Text**	**WRAP 2002 inventory; extracted from stationary area inventory using initial list of SCCs; transport fractions applied; annual**
fdinv1_wrap2002_wfac_WANDORUT_102105.ida	**ERG**	**Text**	**WRAP 2002 inventory; extracted from stationary area inventory using initial list of SCCs; transport fractions applied; annual**
fdinv2_CA2002_111105.w_tfrac.ida	**ERG**	**Text**	**CA 2002 inventory; extracted from stationary area inventory using extended list of SCCs; transport fractions applied; annual**
fdinv2_CANADA_v2.w_tfrac.ida	**Environment Canada**	**Text**	**Canada 2000 inventory; extracted from stationary area inventory using extended list of SCCs; transport fractions applied; annual**
fdinv2_cenrap2002_081705.w_tfrac.ida	**Pechan**	**Text**	**CENRAP 2002 inventory; extracted from stationary area inventory using extended list of SCCs; transport fractions applied; annual**
fdinv2_mane-vu2002_011705.w_tfrac.ida	**MARAMA web site**	**Text**	**MANE-VU2002 inventory; extracted from stationary area inventory using extended list of SCCs; transport fractions applied; annual**
fdinv2_vistas_2002g_2453908_w_pmfac.ida	**Alpine Geophysics**	**Text**	**VISTAS 2002 inventory; extracted from stationary area inventory using extended list of SCCs; transport**

Filename	Source	Data type	Description
			fractions applied; annual
fdinv2_wrap2002_v1_noCAWANDORUT_081205.w_tfrac.ida	**ERG**	**Text**	**WRAP 2002 inventory; extracted from stationary area inventory using extended list of SCCs; transport fractions applied; annual**
fdinv2_wrap2002_v2_WANDORUT_102105.w_tfrac.ida	**ERG**	**Text**	**WRAP 2002 inventory; extracted from stationary area inventory using extended list of SCCs; transport fractions applied; annual**
3 Road Dust			
rdinv_CA2002_v2_wfac_111105.ida	**Environ**	**Text**	**California 2002 inventory; extracted from stationary area inventory; transport fractions applied; annual**
rdinv_CANADA2000_v2_wfac.ida	**Environment Canada**	**Text**	**Canada 2000 inventory; extracted from stationary area inventory; transport fractions applied; annual**
rdinv_cenrap2002_wfac_081705.ida	**Pechan**	**Text**	**CENRAP 2002 inventory; extracted from stationary area inventory; transport fractions applied; annual**
rdinv_manevu2002_wfac.ida	**Alpine Geophysics**	**Text**	**MANE-VU 2002 inventory; extracted from stationary area inventory; transport fractions applied; annual**
rdinv_vistas_2002g_2453908_w_pmfac.txt	**Alpine Geophysics**	**Text**	**VISTAS 2002 inventory; extracted from stationary area inventory; transport fractions applied; annual**
rdinv_wrap2002_wfac_${season}_082205.ida	**ENVIRON**	**Text**	**WRAP 2002 inventory; transport fractions applied; seasonal**
4 Ammonia			
arinv_nh3_2002_mrpok_${month}_3may2006.ida	**Alpine Geophysics**	**Text**	**MWRPO 2002 agricultural ammonia inventory; monthly**
arinv_nh3_cenrap02_082406__${month}.ida	**Pechan**	**Text**	**CENRAP 2002 xxxx inventory; monthly**
CENRAP_AREA_MISC_SMOKE_INPUT_NH3_MONTH_ ${month}_072805_NoBio.txt	**Pechan**	**Text**	**CENRAP 2002 xxxx inventory; monthly**
NH3_CENRAP_ANN.082506.txt	**Pechan**	**Text**	**CENRAP 2002 xxxx inventory; annual**
CENRAP_AREA_MISC_SMOKE_INPUT_ANN_STATE_071905.txt	**Pechan**	**Text**	**CENRAP 2002 xxxx inventory; annual**
5 WRAP Ammonia			
nh3gts_l.2002###.1.WRAP36.base02b_nosoil.ncf	**Environ**	**Binary, netCDF**	**Includes domestic, livestock, fertilizer, and wild life gridded inventory; daily**
6 Area Anthropogenic Fires			
arfinv_anthro_cenrap2002_081705.ida	**Pechan**	**Text**	**CENRAP 2002 inventory; extracted**

Filename	Source	Data type	Description
			from stationary area inventory; annual
AREA_BURNING_SMOKE_INPUT_ANN_TX_NELI_071905.txt	**Pechan**	**Text**	**CENRAP 2002 inventory; extracted from stationary area inventory; annual**
arfinv_anthro_CANADA2000_v2.ida	**Environment Canada**	**Text**	**Canada 2000 inventory; extracted from stationary area inventory; annual**
arfinv_anthro_mane-vu2002_011705.ida	**MARAM web site**	**Text**	**MANE-VU2002 inventory; extracted from stationary area inventory; annual**
arfinv_anthro_Mexico99phase3_border_20051027v4.ida	**ERG**	**Text**	**Mexico 1999 inventory for Northern states; extracted from stationary area inventory; annual**
arfinv_anthro_Mexico99phase3_interior_ERG_Oct06.ida	**ERG**	**Text**	**Mexico 1999 inventory for Southern states inventory; extracted from stationary area inventory; annual**
arfinv_anthro_mrpok_2002_20jun2006.ida	**Alpine Geophysics**	**Text**	**MWRPO 2002 inventory; extracted from stationary area inventory; annual**
arfinv_anthro_vistas2002_TypicalFires_No2610000_112704.ida	**Alpine Geophysics**	**Text**	**VISTAS 2002 inventory; annual**
7 Area Wild Fires			
arfinv_wf_CANADA2000_v2.ida	**Environment Canada**	**Text**	**Canada 2000 inventory; extracted from stationary area inventory; annual**
arfinv_wf_cenrap2002_081705.ida	**Pechan**	**Text**	**CENRAP 2002 inventory; extracted from stationary area inventory; annual**
arfinv_wf_mane-vu2002_011705.ida	**MARAM web site**	**Text**	**MANE-VU 2002 inventory; extracted from stationary area inventory; annual**
arfinv_wf_Mexico99phase3_border_20051027v4.ida	**ERG**	**Text**	**Mexico 1999 inventory for Northern states inventory; extracted from stationary area inventory; annual**
arfinv_wf_Mexico99phase3_interior_ERG_Oct06.ida	**ERG**	**Text**	**Mexico 1999 inventory for Southern states inventory; extracted from stationary area inventory; annual**
arfinv_wf_mrpok_2002_20jun2006.ida	**Alpine Geophysics**	**Text**	**MWRPO 2002 inventory; extracted from stationary area inventory; annual**
arfinv_wf_vistas2002_TypicalFires_No2610000_112704.ida	**Alpine**	**Text**	**VISTAS 2002 inventory; annual**

Filename	Source	Data type	Description
	Geophysics		
8 Offshore Area Sources (Gulf of Mexico)			
CO_noCM.txt	**MMS**	**Text**	**Commercial marines records were removed; they are modeled in offshore shipping**
NOX_noCM.txt	**MMS**	**Text**	**Commercial marines records were removed; they are modeled in offshore shipping**
PM_noCM.txt	**MMS**	**Text**	**Commercial marines records were removed; they are modeled in offshore shipping**
SO2_noCM.txt	**MMS**	**Text**	**Commercial marines records were removed; they are modeled in offshore shipping**
VOC_noCM.txt	**MMS**	**Text**	**Commercial marines records were removed; they are modeled in offshore shipping**
9 Non Road (Annual Inventory)			
arinv_marine_mrpok_2002_27apr2006.ida	**Alpine Geophysics**	**Text**	**MWRPO 2002 Marine inventory; annual**
marinv_vistas_2002g_2453972.ida	**Alpine Geophysics**	**Text**	**VISTAS 2002 Marine inventory; annual**
nrinv_CANADA2000_v2_aircraft.ida	**Environment Canada**	**Text**	**Canada 2000 aircraft inventory; extracted from non-road inventory; annual**
nrinv_CANADA2000_v2.ida	**Environment Canada**	**Text**	**Canada 2000 inventory; annual**
nrinv_CANADA2000_v2_locomotive.ida	**Environment Canada**	**Text**	**Canada 2000 locomotive inventory; extracted from non-road inventory; annual**
nrinv_CANADA2000_v2_marine.ida	**Environment Canada**	**Text**	**Canada 2000 marine inventory; extracted from non-road inventory; annual**
nrinv_cenrap2002_annual_071305.ida	**Pechan**	**Text**	**CENRAP 2002 inventory; annual**
nrinv_mane-vu2002_052505.ida	**MARAM web site**	**Text**	**MANE_VU 2002 inventory; annual**
nrinv_mane-vu2002_aircraft_052505.ida	**MARAM web site**	**Text**	**MANE-VU 2002 aircraft inventory; extracted from non-road inventory; annual**
nrinv_mane-vu2002_locomotive_052505.ida	**MARAM web site**	**Text**	**MANE-VU 2002 locomotive inventory; extracted from non-road inventory; annual**
nrinv_mane-vu2002_shipping_052505.ida	**MARAM web site**	**Text**	**MANE-VU 2002 marine inventory;**

Filename	Source	Data type	Description
			extracted from non-road inventory; annual
nrinv_Mexico1999_ERG_Aircraft_Locomotive_Rec_102705.ida	**ERG**	**Text**	**Mexico 1999 aircraft and locomotive inventory; annual**
nrinv_Mexico99phase3_border_20061025v4.ida	**ERG**	**Text**	**Mexico 1999 inventory for Northern states; annual**
nrinv_Mexico99phase3_interior_ERG_Oct06.ida	**ERG**	**Text**	**Mexico 1999 inventory for Southern states; annual**
nrinv_vistas_2002g_2453908.ida	**Alpine Geophysics**	**Text**	**VISTAS 2002 inventory; annual**
nrinv_wrap2002_InshoreMarine_annual_tpd_080205.ida	**ENVIRON**	**Text**	**WRAP marine inventory; annual**
nrinv_wrap2002_v2_locomotive_annual_tpd_102705.ida	**ENVIRON**	**Text**	**WRAP locomotive inventory; annual**
11 Non Road (Monthly and Seasonal Inventory)			
nrinv_2002_mrpok_$month_3may2006.ida	**Missouri DNR**	**Text**	**MWRPO 2002 inventory; monthly**
nrinv_CA2002_v2_OffRoad_${season}_103105.ida	**EENVIRON**	**Text**	**California 2002 inventory, seasonal**
nrinv_cenrap2002_$month_082806.ida	**Pechan**	**Text**	**CENRAP 2002 inventory; monthly**
nrinv_wrap2002_nonCA_${season}_060705.ida	**ENVIRON**	**Text**	**WRAP 2002 inventory, monthly**
nrinv_wrap2002_v2_Aircraft_${season}_103105.ida	**ENVIRON**	**Text**	**WRAP 2002 aircraft inventory; seasonal**
12 Stationary Point			
pthour_2002typ_baseg_${month}_28jun2006.ems	**Alpine Geophysics**	**Text**	**VISTAS 2002 hourly inventory for the EGUs; monthly**
egu_ptinv_vistas_2002typ_baseg_2453909.ida	**Alpine Geophysics**	**Text**	**VISTAS 2002 EGUs inventory; annual**
negu_ptinv_vistas_2002typ_baseg_2453909.ida	**Alpine Geophysics**	**Text**	**VISTAS 2002 non EGUs inventory, annual**
ptinv_CA2002_101405.ida	**ERG**	**Text**	**California 2002 inventory; annual**
ptinv_CA2002_CARBofs_v1.ida	**ARB**	**Text**	**California 2002 offshore inventory; annual**
Ptinv_CANADA2000_v2_032407.ida	**Environment Canada**	**Text**	**Canada 2000 inventory; annual**
Ptinv_cenrap2002_033007.ida	**Pechan**	**Text**	**CENRAP 2002 inventory; annual**
ptinv_egu_2002_mrpok_1may2006.ida	**Alpine Geophysics**	**Text**	**MWRPO 2002 EGUs inventory; annual**
ptinv_mane-vu2002_v2_${WINSUM}_041905.ida	**MARAM web site**	**Text**	**MANE-VU 2002 inventory, seasonal; winter summer**
ptinv_Mexico99phase3_border_20061025v4.ida	**ERG**	**Text**	**Mexico 1999 inventory for Northern states; annual**
ptinv_Mexico99phase3_interior_ERG_Oct06.ida	**ERG**	**Text**	**Mexico 1999 inventory for Southern states; annual**
ptinv_negu_2002_mrpok_1may2006.ida		**Text**	**MWRPO 2002 non EGUs inventory;**

Filename	Source	Data type	Description
			annual
ptinv_wrap2002_AKAZMTNMORUTWAWY_102405.ida	**ERG**	**Text**	**WRAP 2002 inventory for AK, AZ, MT, NM, OR, UT, WA, and WY; annual**
tinv_wrap2002_v2_NVIDSDNDCO_090805.ida	**ERG**	**Text**	**WRAP 2002 inventory for NV, ID, SD, ND, and CO; annual**
ptinv_WRAPTribes2002_102005.ida	**ERG**	**Text**	**WRAP/Tribes 2002 inventory; annual**
13 Offshore Point (Gulf)			
CO.afs.gwei2000.20000801.latlong.ida	**MMS**	**Text**	
PM10.afs.gwei2000.20000801.latlong.ida	**MMS**	**Text**	
SO2.afs.gwei2000.20000801.latlong.ida	**MMS**	**Text**	
NOX.afs.gwei2000.20000801.latlong.ida	**MMS**	**Text**	
PM2_5.afs.gwei2000.20000801.latlong.ida	**MMS**	**Text**	
VOC.afs.gwei2000.20000801.latlong.ida	**MMS**	**Text**	
14 On Road Mobile (Emissions)			
mbinv_wrap2002_v2_noCA_${season}_101305.ida	**ENVIRON**	**Text**	**WRAP 2002 inventory; seasonal**
mbinv_CA2002_v2_${season}_102705.ida	**ENVIRON**	**Text**	**California 2002 inventory; seasonal**
mbinv_CANADA2000.ida	**Environment Canada**	**Text**	**Canada 2000 inventory; annual**
mbinv_Mexico99phase3_border_20051021v4.ida	**ERG**	**Text**	**Mexico 1999 inventory for Northern states; annual**
mbinv_Mexico99phase3_interior_ERG_Oct06.ida	**ERG**	**Text**	**Mexico 1999 inventory for Southern states; annual**
15 On Road Mobile (Activities, VMT)			
mbinv#_vmt_cenrap.ida	**STI**	**Text**	**CENRAP 2002 inventory; divided into three files; annual**
mbinv_2002_vmt_mane-vu.ida	**MARAM web site**	**Text**	**MANE-VU 2002 inventory; annual**
mbinv_mrpo_02f_vmt_02may06.ida	**Alpine Geophysics**	**Text**	**MWRPO 2002 inventory; annual**
mbinv_vistas_02g_vmt_12jun06.ida	**Alpine Geophysics**	**Text**	**VISTAS 2002 inventory; annual**
16 Point Fires			
ptday_2002CENRAP_ptfires_mon##.ida	**STI**	**Text**	**CENRAP 2002 prescribed fires; daily emissions; monthly**
ptday_agfires_##_vistas.ida	**Alpine Geophysics**	**Text**	**VISTA 2002 all fire sources; daily emissions; monthly**
PTDAY_200504051315_wrap2002_nfr.mon##.ida	**AirSciences**	**Text**	**WRAP 2002 non federal rangeland fires; daily emissions; monthly**
PTDAY_200507011516_wrap2002_agf_base.mon##.ida	**AirSciences**	**Text**	**WRAP 2002 Ag. Fires; daily emissions; monthly**
PTDAY_200510210936_wrap2002_wild_base.mon##.ida	**AirSciences**	**Text**	**WRAP 2002 wild fires; daily emissions; monthly**

Filename	Source	Data type	Description
PTDAY_200510211022_wrap2002_wfu_base.mon##.ida	**AirSciences**	**Text**	**WRAP 2002 wild fire use; daily emissions; monthly**
PTDAY_200510211029_wrap2002_rx_base.mon##.ida	**AirSciences**	**Text**	**WRAP 2002 prescribed fires; daily emissions; monthly**
pthour_2002CENRAP_ptfires_mon##.ida	**STI**	**Text**	**CENRAP 2002 prescribed fires; hourly plume distribution; monthly**
pthour_agfires_##_vistas.ida	**Alpine Geophysics**	**Text**	**VISTA 2002 all fire sources; hourly plume distribution; monthly**
PTHOUR_200504051315_wrap2002_nfr.mon##.ida	**AirSciences**	**Text**	**WRAP 2002 non federal rangeland; hourly plume distribution; monthly**
PTHOUR_200507011516_wrap2002_agf_base.mon##.ida	**AirSciences**	**Text**	**WRAP 2002 Ag. Fires; hourly plume distribution; monthly**
PTHOUR_200510210936_wrap2002_wild_base.mon##.ida	**AirSciences**	**Text**	**WRAP 2002 wild fires; hourly plume distribution; monthly**
PTHOUR_200510211022_wrap2002_wfu_base.mon##.ida	**AirSciences**	**Text**	**WRAP 2002 wild fire use; hourly plume disributution; monthly**
PTHOUR_200510211029_wrap2002_rx_base.mon##.ida	**AirSciences**	**Text**	**WRAP 2002 prescribed fires; hourly plume distribution; monthly**
ptinv_2002CENRAP_ptfires_mon##.ida	**STI**	**Text**	**CENRAP 2002 prescribed fires; fire location info.; monthly**
ptinv_agfires_##_vistas.ida	**Alpine Geophysics**	**Text**	**VISTA 2002 all fire sourcesfire location info; monthly**
PTINV_200504051315_wrap2002_nfr.mon##.ida	**AirSciences**	**Text**	**WRAP 2002 non federal rangeland fires; fire location info; monthly**
PTINV_200507011516_wrap2002_agf_base.mon##.ida	**AirSciences**	**Text**	**WRAP 2002 Ag. Fires; fire location info.; monthly**
PTINV_200510210936_wrap2002_wild_base.mon##.ida	**AirSciences**	**Text**	**WRAP 2002 wild fires; fire location info.; monthly**
PTINV_200510211022_wrap2002_wfu_base.mon##.ida	**AirSciences**	**Text**	**WRAP 2002 wild fire use; fire location info.; monthly**
PTINV_200510211029_wrap2002_rx_base.mon##.ida	**AirSciences**	**Text**	**WRAP 2002 prescribed fires; fire location; monthly**
ptday.ontario_fires.2002.txt.ida	**Environment Canada**	**Text**	**Ontario/Canada wild fires; daily emissions and fire info.; monthly**
ptinv.ontario_fires.2002.txt.ida	**Environment Canada**	**Text**	**Ontario/Canada wild fires; fire location info.; monthly**
17 Biogenecs			
b3fac.beis3_efac_v0.98.txt	**EPA**	**Text**	**Version 0.98 biogenic emission factors**
b3_a.VISTAS36_148X112.beld3_v2.ncf	**Alpine Geophysics**	**Binary**	**Gridded land use**
b3_b.VISTAS36_148X112.beld3_v2.ncf	**Alpine**	**Binary**	**Gridded land use**

Filename	Source	Data type	Description
	Geophysics		
b3_t.VISTAS36_148X112.beld3_v2.ncf	**Alpine Geophysics**	**Binary**	**Gridded land use**
18 Windblown Dust			
wb_dust_ii_cenrap_cmaq_RPO36_2002###_agadj_tf_b.ncf	**ENVIRON/UCR**	**Binary; netCDF**	**Domain wide wind blown dust emissions from WRAP wind blown dust model; hourly**
19 WRAP Oil and Gas			
arinv_CA2002_v2_OilGas_111105.ida	**ENVIRON**	**Text**	**California 2002 oil and gas inventory; annual**
arinv_wrap2002_v2_OilGas_annual_082505.ida	**ENVIRON**	**Text**	**WRAP 2002 oil and gas inventory; annual**
20 Offshore Shipping			
ofsgts_l.2002###.1.vista36.baseg_2002.shipping.ncf	**ENVIRON/VISTAS**	**Binary; netCDF**	**Pacific, Gulf of Mex. and Atlantic 2002 Offshore shipping inventory; daily**

Table A-2. CENRAP 2018 Base G (Base18G) emissions inventory.

Filename	Source	Data type	Description
1 Stationary Area Sources			
arinv_Mexico99phase3_border_20051027v4_noDust_noFire.ida	**ERG**	**Text**	**1999 BRAVO Mexico inventory for the six Northern states; annual**
arinv_Mexico99phase3_interior_ERG_Oct06_noDust_noFire.ida	**ERG**	**Text**	**1999 BRAVO Mexico inventory for the Southern states; annual**
arinv_CA2018_112205.ida	**ERG**	**Text**	**California 2018 inventory; annual**
arinv_NoDust_NoREF_vistas_2018g_2453922.ida	**Alpine Geophysics**	**Test**	**VISTAS 2018 inventory; annual**
arinv_wrap2018.091205.ida	**ERG**	**Text**	**WRAP 2018 inventory; annual**
arinv_canada_2020_noDust_NoFire.ida	**Environment, Canada**		**Canada 2020 inventory; annual**
arinv_NoFire_NoDust_NoREF_mrpok_2018_22aug2006.ida	**Alpine Geophysics**	**Text**	**MWRPO 2018 inventory; annual**
arinv_mane_vu_2018v3_1_NoDust_NoFire.ida		**Text**	**MANE_VU 2018 inventory, annual**
arinv_NoFire_nodust_ref_nh3_cenrap2002-2018_101606.ida	**UCR; grown from 2002**	**Text**	**CENRAP 2018 inventory; annual**
arinv_vistas_baseg_2018t_lofire_11feb2007_scc2610000500.ida	**Alpine Geophysics**	**Text**	**VISTAS 2018 inventory for SCC 2610000500**
2 Fugitive Dust			
fdinv1.CA2018_wfac.ida	**ERG**	**Text**	**CA 2018 inventory; extracted from stationary area inventory using initial list of SCCs; transport fractions applied; annual**
fdinv1.canada_2020.wTfac.ida	**Environment Canada**	**Text**	**Canada 2000 inventory; extracted from stationary area inventory using initial list of SCCs; transport fractions applied; annual**
fdinv1.cenrap2002_2018_wfac.ida	**UCR; grown from 2002**	**Text**	**CENRAP 2018 inventory; extracted from stationary area inventory using initial list of SCCs; transport fractions applied; annual**
fdinv1.mane_vu2018_wfac.ida	**MARAM web site**	**Text**	**MANE-VU 2018 inventory; extracted from stationary area inventory using initial list of SCCs; transport fractions**

Filename	Source	Data type	Description
			applied; annual
fdinv1_Mexico99phase3_border_20051027v4_wTfac.ida	**ERG**	**Text**	**Mexico Northern states 1999 inventory; extracted from stationary area inventory using initial list of SCCs; transport fractions applied; annual**
fdinv1_Mexico99phase3_interior_ERG_Oct06_wo_pmfac.ida	**ERG**	**Text**	**Mexico Southern states 1999 inventory; extracted from stationary area inventory using initial list of SCCs; no transport fractions applied; annual**
fdinv1_mrpok_2018_22aug2006_wfac.ida	**Alpine Geophysics**	**Text**	**MWRPO 2018 inventory; extracted from stationary area inventory using initial list of SCCs; transport fractions applied; annual**
fdinv1_vistas_2018g_2453922_w_pmfac.ida	**Alpine Geophysics**	**Text**	**VISTAS 2018 inventory; extracted from stationary area inventory using initial list of SCCs; transport fractions applied; annual**
fdinv1.wrap2018_wfac.ida	**ERG**	**Text**	**WRAP 2018 inventory; extracted from stationary area inventory using initial list of SCCs; transport fractions applied; annual**
fdinv2.CA2018_wfac.ida	**ERG**	**Text**	**CA 2018 inventory; extracted from stationary area inventory using extended list of SCCs; transport fractions applied; annual**
fdinv2.canada_2020.wTfac.ida	**Environment Canada**	**Text**	**Canada 2020 inventory; extracted from stationary area inventory using extended list of SCCs; transport fractions applied; annual**
fdinv2.cenrap2002_2018_wfac.ida	**UCR; grown from 2002**	**Text**	**CENRAP 2018 inventory; extracted from stationary area inventory using extended list of SCCs; transport fractions applied; annual**
fdinv2.mane-vu2018_wfac.ida	**MARAM web site**	**Text**	**MANE-VU 2018 inventory;**

Filename	Source	Data type	Description
			extracted from stationary area inventory using extended list of SCCs; transport fractions applied; annual
fdinv2_vistas_2018g_2453922_w_pmfac.ida	**Alpine Geophysics**	**Text**	**VISTAS 2018 inventory; extracted from stationary area inventory using extended list of SCCs; transport fractions applied; annual**
fdinv2_wrap2018.091205_wfac.ida	**ERG**	**Text**	**WRAP 2018 inventory; extracted from stationary area inventory using extended list of SCCs; transport fractions applied; annual**
3 Road Dust			
rdinv.CA2018_wfac.ida	**Environ**	**Text**	**California 2018 inventory; extracted from stationary area inventory; transport fractions applied; annual**
rdinv_canada_2020_wTfac.ida	**Environment Canada**	**Text**	**Canada 2020 inventory; extracted from stationary area inventory; transport fractions applied; annual**
rdinv.cnrap2002_2018.wfac.ida	**UCR; grown from 2002**	**Text**	**CENRAP 2018 inventory; extracted from stationary area inventory; transport fractions applied; annual**
rdinv_mane_vu_2018v3_1_wTfac.ida	**MARAM web site**	**Text**	**MANE-VU 2018 inventory; extracted from stationary area inventory; transport fractions applied; annual**
rdinv_vistas_vistas_2018g_2453922_w_pmfac.ida	**Alpine Geophysics**	**Text**	**VISTAS 2018 inventory; extracted from stationary area inventory; transport fractions applied; annual**
rdinv.wrap2018_wfac_${season}.ida	**ENVIRON**	**Text**	**WRAP 2018 inventory; transport fractions applied; seasonal**
4 Ammonia			
arinv_nh3_2018_mrpok_${month}_22aug2006.ida	**Alpine Geophysics**	**Text**	**MWRPO 2018 agricultural ammonia inventory; monthly**
nh3minv.cenrap2018gr_18.apr.ida	**UCR; grown from 2002**	**Text**	**CENRAP 2018 xxxx inventory; monthly**

Filename	Source	Data type	Description
nh3inv.misc.cnrap2002_2018.feb.ida	**UCR; grown from 2002**	**Text**	**CENRAP 2018 xxxx inventory; monthly**
nh3yinv.annual.cnrap2002_2018.100406.ida	**UCR; grown from 2002**	**Text**	**CENRAP 2018 xxxx inventory; annual**
nh3inv.misc_annual.cnrap2002_2018.ida	**UCR; grown from 2002**	**Text**	**CENRAP 2018 xxxx inventory; annual**
5 WRAP Ammonia			
nh3gts_l.2002###.1.WRAP36.base02b_nosoil.ncf	**Environ**	**Binary, netCDF**	**Includes domestic, livestock, fertilizer, and wild life gridded inventory; daily**
6 Area Anthropogenic Fires			
arfinv_anthro_cenrap2002_081705.ida	**Pechan**	**Text**	**CENRAP 2002 inventory; extracted from stationary area inventory; annual**
AREA_BURNING_SMOKE_INPUT_ANN_TX_NELI_071905.txt	**Pechan**	**Text**	**CENRAP 2002 inventory; extracted from stationary area inventory; annual**
arfinv_anthro_canda2020.ida	**Environment Canada**	**Text**	**Canada 2000 inventory; extracted from stationary area inventory; annual**
arfinv_anthro_mane_vu_2018v3_1.ida	**MARAM web site**	**Text**	**MANE-VU 2018 inventory; extracted from stationary area inventory; annual**
arfinv_anthro_Mexico99phase3_border_20051027v4.ida	**ERG**	**Text**	**Mexico 1999 inventory for Northern states; extracted from stationary area inventory; annual**
arfinv_anthro_Mexico99phase3_interior_ERG_Oct06.ida	**ERG**	**Text**	**Mexico 1999 inventory for Southern states inventory; extracted from stationary area inventory; annual**
arfinv_anthro_mrpok_2018_22aug2006.ida	**Alpine Geophysics**	**Text**	**MWRPO 2018 inventory; extracted from stationary area inventory; annual**
arfinv_anthro_vistas_baseg_2018t_11feb2007_NOscc2610000500.ida	**Alpine Geophysics**	**Text**	**VISTAS 2018 inventory; annual**
7 Area Wild Fires			
arfinv_wf_canada2020.ida	**Environment Canada**	**Text**	**Canada 2020 inventory; extracted from stationary area inventory; annual**
arfinv_wf_cenrap2002-2018_101606.ida	**UCR; grown from 2002**	**Text**	**CENRAP 2018 inventory; extracted from stationary area inventory; annual**

Filename	Source	Data type	Description
arfinv_wf_mane_vu_2018v3_1.ida	**MARAM web site**	**Text**	**MANE-VU 2018 inventory; extracted from stationary area inventory; annual**
arfinv_wf_Mexico99phase3_border_20051027v4.ida	**ERG**	**Text**	**Mexico 1999 inventory for Northern states inventory; extracted from stationary area inventory; annual**
arfinv_wf_Mexico99phase3_interior_ERG_Oct06.ida	**ERG**	**Text**	**Mexico 1999 inventory for Southern states inventory; extracted from stationary area inventory; annual**
arfinv_wf_mrpok_2018_22aug2006.ida	**Alpine Geophysics**	**Text**	**MWRPO 2018 inventory; extracted from stationary area inventory; annual**
arfinv_wf_vistas_baseg_2018t_11feb2007_NOscc2610000500.ida	**Alpine Geophysics**	**Text**	**VISTAS 2018 inventory; annual**
8 Offshore Area Sources (Gulf of Mexico)			
ofsarinv.cnrap2002_2018_noCM.ida	**UCR; grown from 2002**	**Text**	**Commercial marines records were removed; they are modeled in offshore shipping; all pollutants; annual**
9 Non Road (Annual Inventory)			
arinv_mar_mrpok_2018_22aug2006.ida		**Text**	**MWRPO 2018 Marine inventory; annual**
marinv_vistas_2018g_2453972.ida	**Alpine Geophysics**	**Text**	**VISTAS 2018 Marine inventory; annual**
NONROAD2020_Canada.ida	**Environment Canada**	**Text**	**Canada 2020 aircraft inventory; extracted from non-road inventory; annual**
CENRAP_2018_Fnl_Nrd_Emissions091506.ida	**Pecahn**	**Text**	**CENRAP 2018 inventory; annual**
nrinv_mane_vu_2018v3_1.ida	**MARAM web site**	**Text**	**MANE_VU 2018 inventory; annual**
nrinv_Mexico1999_ERG_Aircraft_Locomotive_Rec_102705.ida	**ERG**	**Text**	**Mexico 1999 aircraft and locomotive inventory; annual**
nrinv_Mexico99phase3_border_20061025v4.ida	**ERG**	**Text**	**Mexico 1999 inventory for Northern states; annual**
nrinv_Mexico99phase3_interior_ERG_Oct06.ida	**ERG**	**Text**	**Mexico 1999 inventory for Southern states; annual**
nrinv_vistas_2018g_2453908.ida	**Alpine Geophysics**	**Text**	**VISTAS 2018 inventory; annual**
nrinv_wrap2018_Locomotive_annual_tpd_111805.ida	**ENVIRON**	**Text**	**WRAP 2018 locomotive inventory; annual**

Filename	Source	Data type	Description
11 Non Road (Monthly and Seasonal Inventory)			
nrinv_2018_mrpok_apr_22aug2006.ida	**Alpine Geophysics**	**Text**	**MWRPO 2018 inventory; monthly**
nrinv_CA2018_win_111805.ida	**EENVIRON**	**Text**	**California 2018 inventory, seasonal**
2018NONROAD_AG_IA_${month}.ida	**Missouri DNR**	**Text**	**CENRAP/IA 2018 inventory; monthly**
nrinv.mrpok.minn.apr_2018.011306.ida	**Missouri DNR**	**Text**	**CENRAP/MN 2018 inventory; monthly**
nrinv_WRAP2018_${season}_102105.ida	**ENVIRON**	**Text**	**WRAP 2018 inventory, monthly**
nrinv_WRAP2018_Aircraft_${season}.111805.ida	**ENVIRON**	**Text**	**WRAP 2018 aircraft inventory; seasonal**
12 Stationary Point			
pthour_2018_baseg_sep_2453993.ems	**Alpine Geophysics**	**Text**	**VISTAS 2018 hourly inventory for the EGUs; monthly**
ptinv_egu_18_vistas_g_2453993.ida	**Alpine Geophysics**	**Text**	**VISTAS 2018 EGUs inventory; annual**
ptinv_nonEGU_vistas_2018_baseg_2453957.ida	**Alpine Geophysics**	**Text**	**VISTAS 2018 non EGUs inventory, annual**
pgts3d_l.2002###.1.cmaq.cb4p25.us36b.CANADA_20i01.19L.ncf	**EPA**	**Binary; netCDF**	**Canada 2020 inventory; daily**
Ptinv_cenrap2018_EGU_${WINSUM}_annual_050407.ida	**CENRAP**	**Text**	**CENRAP 2018 EGUs inventory, seasonal; winter summer**
ptinv_o.cenrap2002_2018_nonEGU050307.ida	**UCR; grown from 2002**	**Text**	**CENRAP 2018 non EGUs inventory; annual**
ptinv_cenrapNonegu_2018_050707_refin_new_sources.ida	**CENRAP**	**Text**	**CENRAP 2018 Additional sources; annual**
ptinv_egu_2018_mrpok_11sep006.ida	**Alpine Geophysics**	**Text**	**MWRPO 2002 EGUs inventory; annual**
Ptinv_manevu2018_EGU_${WINSUM}_ANNUAL_080805.ida	**MARAM web site**	**Text**	**MANE-VU 2018 EGUs inventory, seasonal; winter summer**
ptinv_manevu2018_nonEGU_112105.ida		**Text**	**MANE-VU 2018 non EGUs inventory, annual**
ptinv_Mexico99phase3_border_20061025v4.ida	**ERG**	**Text**	**Mexico 1999 inventory for Northern states; annual**
ptinv_Mexico99phase3_interior_ERG_Oct06.ida	**ERG**	**Text**	**Mexico 1999 inventory for Southern states; annual**
ptinv_negu_2018_mrpok_23aug2006.ida	**Alpine Geophysics**	**Text**	**MWRPO 2018 non EGUs inventory; annual**
ptinv_wrap2018_NoOG_050406.ida	**ERG**	**Text**	**WRAP 2018 inventory; no oil and gas; annual**

Filename	Source	Data type	Description
ptinv_wrap2018_OG_091205.ida	**ERG**	**Text**	**WRAP 2018 inventory; oil and gas; annual**
ptinv_WRAPTribes2018_NoOG_091205.ida	**ERG**	**Text**	**WRAP/Tribes 2018 inventory; no oil and gas annual**
ptinv_WRAPTribes2018_OG_091205.ida	**ERG**		**WRAP/Tribes 2018 inventory; oil and gas annual**
13 Offshore Point (Gulf)			
ofsinv_o_CO.cnrap2002_2018.ida	**UCR; grown from 2002 emissions**	**Text**	
ofsinv_o_NOX.cnrap2002_2018.ida	**UCR; grown from 2002 emissions**	**Text**	
ofsinv_o_PM10.cnrap2002_2018.ida	**UCR; grown from 2002 emissions**	**Text**	
ofsinv_o_PM2_5.cnrap2002_2018.ida	**UCR; grown from 2002 emissions**	**Text**	
ofsinv_o_SO2.cnrap2002_2018.ida	**UCR; grown from 2002 emissions**	**Text**	
ofsinv_o_VOC.cnrap2002_2018.ida	**UCR; grown from 2002 emissions**	**Text**	
14 On Road Mobile (Emissions)			
mbinv_WRAP2018_aut_102105.ida	**ENVIRON**	**Text**	**WRAP 2018 inventory; seasonal**
mbinv_CA2018_win_111805.ida	**ENVIRON**	**Text**	**California 2018 inventory; seasonal**
mbinv_CANADA2020.ida	**Environment Canada**	**Text**	**Canada 2020 inventory; annual**
mbinv_Mexico99phase3_border_20051021v4.ida	**ERG**	**Text**	**Mexico 1999 inventory for Northern states; annual**
mbinv_Mexico99phase3_interior_ERG_Oct06.ida	**ERG**	**Text**	**Mexico 1999 inventory for Southern states; annual**
15 On Road Mobile (Activities, VMT)			
mbinv.mbv#_vmt_cenrap2018_072005.ida	**STI**	**Text**	**CENRAP 2018 inventory; divided into tow files; annual**
mbinv_vmt_manevu2018_update.ida	**MARAM web site**	**Text**	**MANE-VU 2018 inventory; annual**
mbinv_mrpo_18f_vmt_11aug06.ida	**Alpine Geophysics**	**Text**	**MWRPO 2018 inventory; annual**
mbinv_vistas_18g_vmt_12jun06.ida	**Alpine Geophysics**	**Text**	**VISTAS 2018 inventory; annual**
16 Point Fires			
ptday_2002CENRAP_ptfires_mon##.ida	**STI**	**Text**	**CENRAP 2002 prescribed fires; daily emissions; monthly**
ptday.plume.vistasG2_2018.##.ida	**Alpine**	**Text**	**VISTA 2018 all fire sources; daily**

Filename	Source	Data type	Description
	Geophysics		**emissions; monthly**
PTDAY_200504051315_wrap2002_nfr.mon##.ida	**AirSciences**	**Text**	**WRAP 2002 non federal rangeland fires; daily emissions; monthly**
PTDAY_200604272314_wrap02_04_agf.mon##.ida	**AirSciences**	**Text**	**WRAP 2002-4 Ag. Fires; daily emissions; monthly**
PTDAY_200510210936_wrap2002_wild_base.mon##.ida	**AirSciences**	**Text**	**WRAP 2002 wild fires; daily emissions; monthly**
PTDAY_200510211022_wrap2002_wfu_base.mon##.ida	**AirSciences**	**Text**	**WRAP 2002 wild fire use; daily emissions; monthly**
PTDAY_200604281056_wrap02_04_arx.mon##.ida	**AirSciences**	**Text**	**WRAP 2002-4 prescribed fires; daily emissions; monthly**
PTDAY_200604281056_wrap02_04_nrx.mon##.ida	**AirSciences**	**Text**	**WRAP 2002-4 natural prescribed fires; daily emissions; monthly**
pthour_2002CENRAP_ptfires_mon##.ida	**STI**	**Text**	**CENRAP 2002 anthro. prescribed fires; hourly plume distribution; monthly**
pthour.plume.vistasG2_2018.##.ida	**Alpine Geophysics**	**Text**	**VISTA 2002 all fire sources; hourly plume distribution; monthly**
PTHOUR_200504051315_wrap2002_nfr.mon##.ida	**AirSciences**	**Text**	**WRAP 2002 non federal rangeland; hourly plume distribution; monthly**
PTHOUR_200604272314_wrap02_04_agf.mon##.ida	**AirSciences**	**Text**	**WRAP 2002 Ag. Fires; hourly plume distribution; monthly**
PTHOUR_200510210936_wrap2002_wild_base.mon##.ida	**AirSciences**	**Text**	**WRAP 2002 wild fires; hourly plume distribution; monthly**
PTHOUR_200510211022_wrap2002_wfu_base.mon##.ida	**AirSciences**	**Text**	**WRAP 2002 wild fire use; hourly plume disributution; monthly**
PTHOUR_200604281056_wrap02_04_arx.mon##.ida	**AirSciences**	**Text**	**WRAP 2002 natural prescribed fires; hourly plume distribution; monthly**
PTHOUR_200604281056_wrap02_04_nrx.mon##.ida	**AirSciences**	**Text**	**WRAP 2002 anthro. prescribed fires; hourly plume distribution; monthly**
ptinv_2002CENRAP_ptfires_mon##.ida	**STI**	**Text**	**CENRAP 2002 prescribed fires; fire location info.; monthly**
ptinv.plume.vistasG2_2018.11.ida	**Alpine Geophysics**	**Text**	**VISTA 2002 all fire sourcesfire location info; monthly**
PTINV_200504051315_wrap2002_nfr.mon##.ida	**AirSciences**	**Text**	**WRAP 2002 non federal rangeland fires; fire location info; monthly**

Filename	Source	Data type	Description
PTINV_200507011516_wrap2002_agf_base.mon##.ida	**AirSciences**	**Text**	**WRAP 2002 Ag. Fires; fire location info.; monthly**
PTINV_200510210936_wrap2002_wild_base.mon##.ida	**AirSciences**	**Text**	**WRAP 2002 wild fires; fire location info.; monthly**
PTINV_200604272314_wrap02_04_agf.mon##.ida	**AirSciences**	**Text**	**WRAP 2002 wild fire use; fire location info.; monthly**
PTINV_200604281056_wrap02_04_arx.mon##.ida	**AirSciences**	**Text**	**WRAP 2002 anthro. prescribed fires; fire location; monthly**
PTINV_200604281056_wrap02_04_nrx.mon##.ida	**AirSciences**		**WRAP 2002 natural prescribed fires; fire location; monthly**
ptday.ontario_fires.2002.txt.ida	**Environment Canada**	**Text**	**Ontario/Canada wild fires; daily emissions and fire info.; monthly**
ptinv.ontario_fires.2002.txt.ida	**Environment Canada**	**Text**	**Ontario/Canada wild fires; fire location info.; monthly**
17 Biogenecs			
b3fac.beis3_efac_v0.98.txt	**EPA**	**Text**	**Version 0.98 biogenic emission factors**
b3_a.VISTAS36_148X112.beld3_v2.ncf	**Alpine Geophysics**	**Binary**	**Gridded land use**
b3_b.VISTAS36_148X112.beld3_v2.ncf	**Alpine Geophysics**	**Binary**	**Gridded land use**
b3_t.VISTAS36_148X112.beld3_v2.ncf	**Alpine Geophysics**	**Binary**	**Gridded land use**
18 Windblown Dust			
wb_dust_ii_cenrap_cmaq_RPO36_2002###_agadj_tf_b.ncf	**ENVIRON/UCR**	**Binary; netCDF**	**Domain wide wind blown dust emissions from WRAP wind blown dust model; hourly**
19 WRAP Oil and Gas			
arinv_CA2018_OilGas_112205.ida	**ENVIRON**	**Text**	**California 2018 oil and gas inventory; annual**
oginv_WRAP2018_annual_tpd_111605.ida	**ENVIRON**	**Text**	**WRAP 2018 oil and gas inventory; annual**
20 Offshore Shipping			
ofsgts_l.2002###.1.vista36.baseg_2002.shipping.ncf	**ENVIRON/VISTAS**	**Binary; netCDF**	**Pacific, Gulf of Mex. and Atlantic 2002 Offshore shipping inventory; daily**

APPENDIX C

Model Performance Evaluation for the CMAQ 2002 Base F Base Case Simulation in the CENRAP Region

C.1 2002 Typical Base F Model Performance Evaluation Scenario

This Appendix presents the operational evaluation of the CMAQ model for the 2002 36 km Typical Base F emissions scenario. The final CENRAP 2002 and 2018 emissions scenarios used in the 2018 visibility projections was Base G. The main differences between Base G and Base F emissions inventories were updated Mexican emissions in the northern states, addition of Mexican emissions in the southern states that were not included in CENRAP's emission inventories prior to Base G and correction of a few point source stack parameters and emissions in the CENRAP states and Canada (see: http://pah.cert.ucr.edu/aqm/cenrap/QA_typ02g36.plots/log_inv_categ_Typ02g.doc). Figure C-1 displays the differences in annual average $PM_{2.5}$ and ozone concentrations between the 2002 Typical Base G and Base F simulations. Most of the differences in the two simulations are concentrations within Mexico where no monitoring data were available for the model evaluation. Thus, given the very small differences between the 2002 Typical Base F and G base case simulations, the model performance evaluation is presented for just the 2002 Typical Base F simulation (for additional comparisons of Base G and F see: http://pah.cert.ucr.edu/aqm/cenrap/cmaq.shtml#typ02gvstyp02f_mpe).

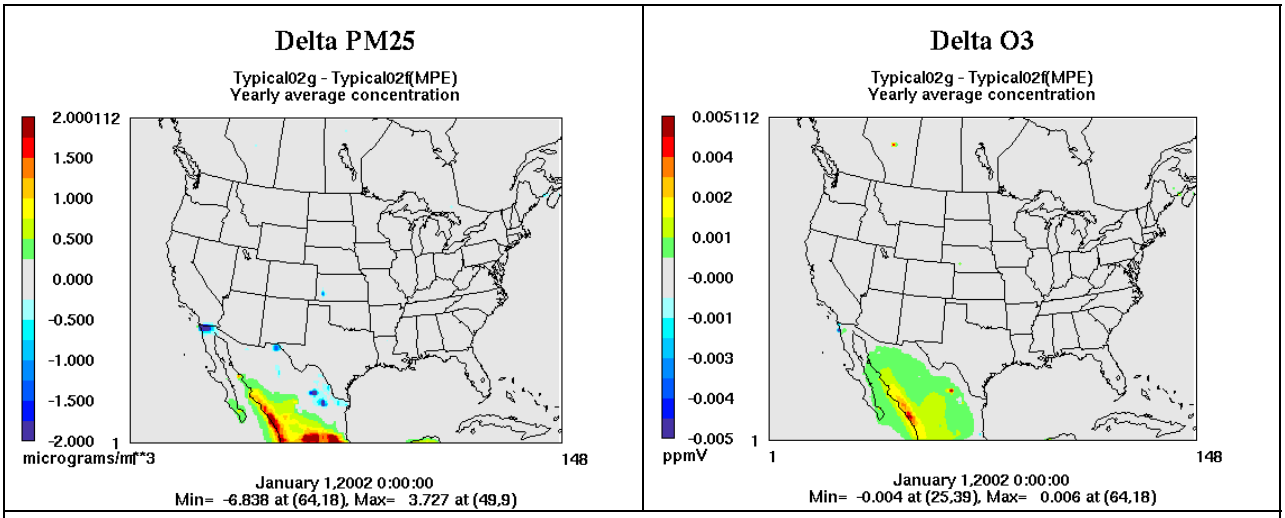

Figure C-1. Comparison of differences in annual average $PM_{2.5}$ (left) and ozone concentrations between 2002 Typical Base G and F (Base G – Base F).

The CENRAP emissions and air quality modeling initially conducted 2002 base case modeling for two 2002 base case emissions scenarios: a 2002 Actual emissions base case; and a 2002 Typical emissions base case. For the 2002 Actual base case, day-specific SO2 and NOx emissions for large stationary point sources were used based on measured continuous emissions monitoring (CEM) data along with actual 2002 fire emissions In the 2002 Typical base case, emissions for large stationary sources and fires were more representative of the 2000-2004 Baseline period. For large stationary sources' typical emissions, 5-years of CEM data were analyzed and typical seasonal and diurnally varying emissions were defined for when the sources where operating For the typical fire emissions, the locations of the 2002 Actual fire emissions were retained, but the intensity was reduced or increased to match the average conditions over the 5-year Baseline. The original intent of the CENRAP modeling of both a 2002 Actual and Typical base cases was to use the 2002 Actual base case for the model performance evaluation and the 2002 Typical base case with the 2018 emission scenario for the 2018 visibility projections.

The need to generate both the 2002 Typical and Actual base case inventories and perform CMAQ model simulations each time an emissions update or correction to the modeling occurred became burdensome and potentially could compromise the CENRAP schedule and available resources. For the Base F vintage emissions database, a model performance evaluation was conducted that compared the model performance of the 2002 Actual and Typical Base F CMAQ base case simulations to determine whether use of the Actual emissions substantially changed the interpretation of the model performance. The maximum change in model performance between the 2002 Actual and Typical base case was for sulfate and occurred during the summer months, when sulfate is the highest. Figure C-2 displays sulfate (SO4), nitrate (NO3), elemental carbon (EC) and organic matter carbon (OMC) performance for July 2002 across IMPROVE sites in the CENRAP region for the 2002 36 km Actual and Typical Base F CMAQ base case simulations. Although differences in predicted 24-hour SO4 concentrations are sometimes discernable in the scatter plot, the basic model performance conclusions remains the same and the difference in fractional bias (-48% vs. -49%) and fraction error (58% vs. 59%) are not significant. Similarly, the difference in NO3 model performance between the Actual and Typical Base F simulations are not significant. The performance of the CMAQ Actual and Typical simulation for EC and OMC is essentially identical. Given the similarity of the 2002 Base F Actual and Typical model performance evaluation, future CENRAP CMAQ model performance analysis were just performed on the Typical simulation.

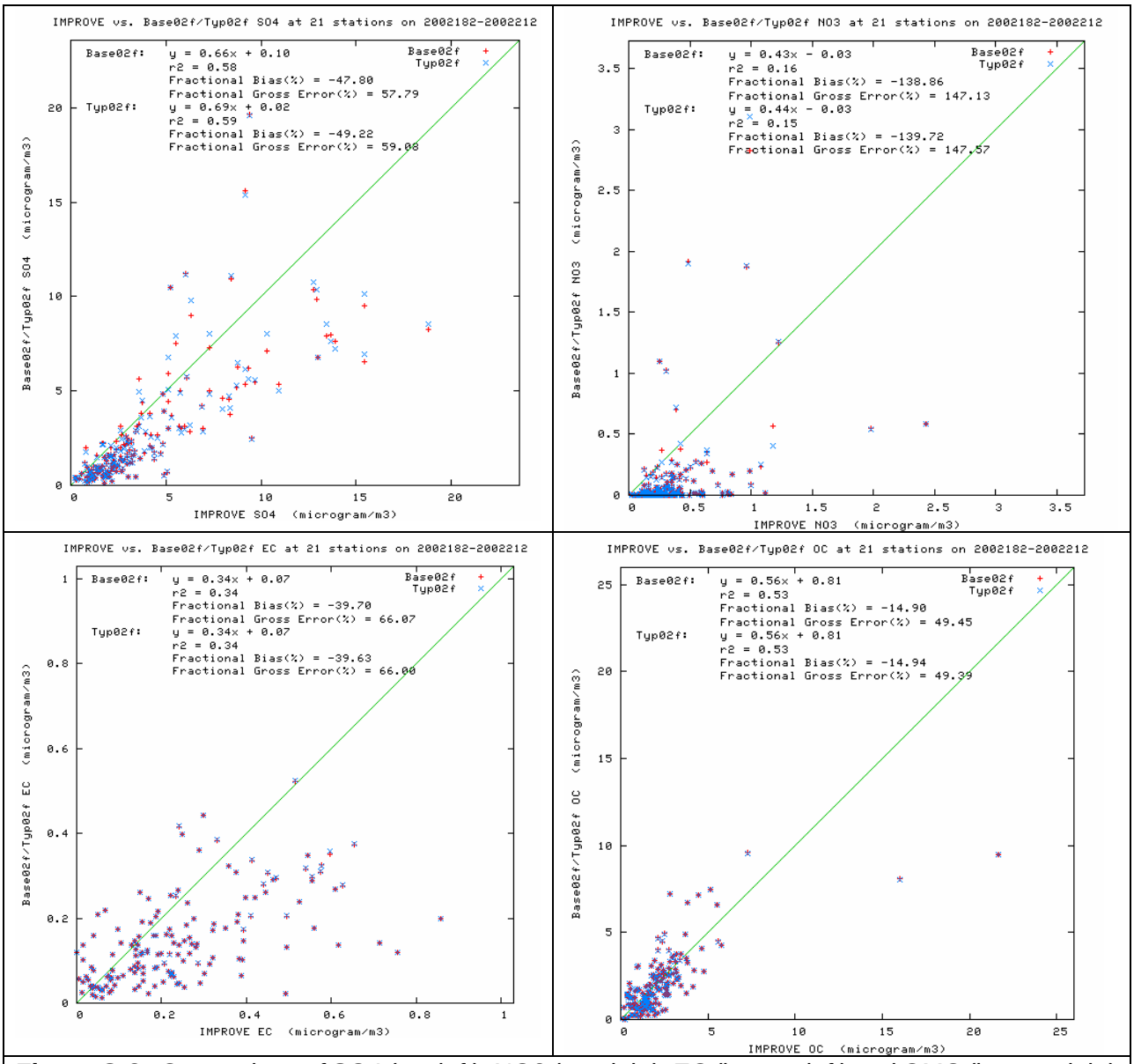

Figure C-2. Comparison of SO4 (top left), NO3 (top right), EC (bottom left) and OMC (bottom right) model performance for July 2002, the CENRAP region and the 2002 36 km Base F Actual (red) and Typical (blue) CMAQ base case simulation.

C.2 CMAQ Evaluation Methodology

EPA's integrated ozone, $PM_{2.5}$ and regional haze modeling guidance calls for a comprehensive, multi-layered approach to model performance testing, consisting of the four major components: operational, diagnostic, mechanistic (or scientific) and probabilistic (EPA, 2007). The CMAQ model performance evaluation effort focused on the first two components, namely:

- **Operational Evaluation**: Tests the ability of the model to estimate PM concentrations (both fine and coarse) and the components at PM_{10} and $PM_{2.5}$ including the quantities used to characterize visibility (i.e., sulfate, nitrate, ammonium, organic carbon, elemental carbon, other $PM_{2.5}$, and coarse matter ($PM_{2.5-10}$). This evaluation examines whether the measurements are properly represented by the model predictions but does not necessarily ensure that the model is getting "the right answer for the right reason"; and

- **Diagnostic Evaluation:** Tests the ability of the model to predict visibility and extinction, PM chemical composition including PM precursors (e.g., SOx, NOx, and NH_3) and associated oxidants (e.g., ozone and nitric acid); PM size distribution; temporal variation; spatial variation; mass fluxes; and components of light extinction (i.e., scattering and absorption).

The diagnostic evaluation also includes the performance of diagnostic tests to better understand model performance and identify potential flaws in the modeling system that can be corrected. The diagnostic evaluation may also includes the use of "probing tools" to understand why the model obtains a given prediction; probing tools include Process Analysis (PA), decoupled direct method (DDM) and source apportionment (SA).

In this final model performance evaluation for the 2002 Typical Base F CMAQ simulation, the operational evaluation has been given the greatest attention since this is the primarily thrust of EPA's modeling guidance. However, we have also examined certain diagnostic features dealing with the model's ability to simulate sub-regional and monthly/diurnal gas phase and aerosol concentration distributions. In the course of the CENRAP and other modeling process numerous diagnostic sensitivity tests were performed to investigate and improve model performance. Key diagnostic tests performed are discussed and the results for the rest are available on the CENRAP modeling website: http://pah.cert.ucr.edu/aqm/cenrap/index.shtml.

C.2.1 Ambient Air Quality Data for CENRAP Model Evaluation

The ground-level model evaluation database for 2002 was compiled by the modeling team using several routine and research-grade databases. The first is the routine gas-phase concentration measurements for ozone, NO, NO_2 and CO archived in EPA's Aerometric Information Retrieval System (AIRS) Air Quality System (AQS) database. Other sources of observed information come from the various PM monitoring networks in the U.S. These include the: (a) Interagency Monitoring of Protected Visual Environments (IMPROVE); (b) Clean Air Status and Trends Network (CASTNET); (c) Southeastern Aerosol Research and Characterization (SEARCH); (d) EPA Federal Reference Method $PM_{2.5}$ and PM_{10} Mass Networks (EPA-FRM); (e) EPA Speciation Trends Network (STN) of $PM_{2.5}$ species; and (f) National Acid Deposition Network (NADP). These PM

monitoring networks may also provide ozone and other gas phase precursors and product species, and visibility measurements at some sites. During the course of the CENRAP modeling, the numerous base case simulations were evaluated across the continental U.S. In this section we focus our evaluation on model performance within the CENRAP region. Table C-1 summarizes the observations collected at each monitoring network within the CENRAP region and their sampling frequency with Figure C-3 displaying the locations of the monitors for the various monitoring networks operating in the CENRAP region during 2002.

Table C-1. Ambient monitoring data available in the CENRAP region during 2002.

Monitoring Network	Chemical Species Measured	Sampling Frequency; Duration
IMPROVE	Speciated $PM_{2.5}$ and PM_{10}	1 in 3 days; 24 hr
CASTNET	Speciated $PM_{2.5}$, Ozone	Hourly, Weekly; 1 hr, Week
SEARCH	24-hr PM_{25} (FRM Mass, OC, BC, SO_4, NO_3, NH_4, Elem.); 24-hr PM coarse (SO_4, NO_3, NH_4, elements); Hourly $PM_{2.5}$ (Mass, SO_4, NO_3, NH_4, EC, TC); and Hourly gases (O_3, NO, NO_2, NO_y, HNO_3, SO_2, CO)	Daily, Hourly;
NADP	WSO_4, WNO_3, WNH_4	Weekly
EPA-FRM	Only total fine mass ($PM_{2.5}$)	1 in 3 days; 24 hr
EPA-STN	Speciated $PM_{2.5}$	Varies; Varies
AIRS/AQS	CO, NO, NO_2, NO_x, O_3	Hourly; Hourly

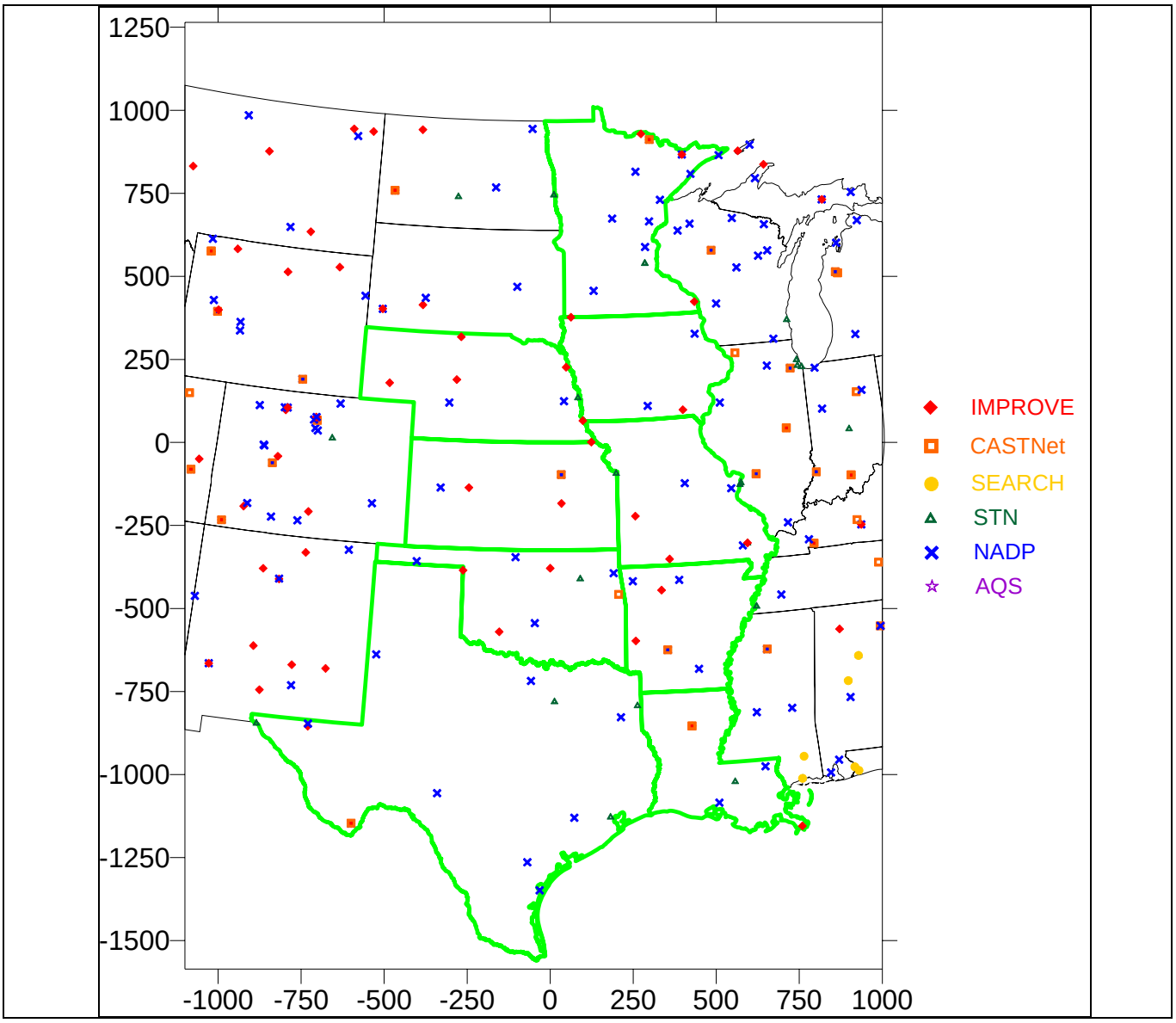

Figure C-3. Locations of surface monitors within the CENRAP states for sites operating during 2002.

C.2.2 Scope of CMAQ Model Performance Evaluation

The primary focus of the CMAQ Base F evaluation is on how well the model is able to replicate observed concentrations gas-phase pollutants and precursors, the various components of $PM_{2.5}$, total observed mass of $PM_{2.5}$, and wet deposition amounts. The CMAQ operational evaluation, model outputs are compared statistically and graphically with observational data obtained from the IMPROVE, CASTNet, STN, NADP and AQS monitoring networks. Because the SEARCH network is located in the southeastern U.S. (VISTAS region) outside of the CENRAP region, it is not a major component of our evaluation. Also, since the EPA-FRM network focuses on just $PM_{2.5}$ mass measurements primarily in $PM_{2.5}$ nonattainment or near nonattainment areas it is not very relevant for simulating regional haze at mainly remote Class I areas so is also not used in our model performance evaluation. The primary focus of the operational evaluation of the CMAQ 2002 Base F simulation is the performance of PM components in the CENRAP region for predicting regional haze at Class I areas.

Many statistical performance measures have been calculated using the different monitoring networks and across the different model performance subdomains (e.g., RPO regions). Table C-2 lists the definitions of the model performance evaluation statistical metrics. These performance metrics are routinely generate by the UCR Analysis Tool and are available on the project website. Many of them are measures of bias and error that are somewhat redundant.

Table C-2. Statistical Measures Used in the CENRAP CMAQ Model Evaluation.

Statistical Measure	Shorthand Notation	Mathematical Expression	Notes
Accuracy of paired peak (***A_p***)	**Paired_Peak**	$\frac{P - O_{peak}}{O_{peak}}$	P_{peak} = paired (in both time and space) peak prediction
Coefficient of determination (***r^2***)	**Coef_Determ**	$\frac{\left[\sum_{i=1}^{N}(P_i - \overline{P})(O_i - \overline{O})\right]^2}{\sum_{i=1}^{N}(P_i - \overline{P})^2 \sum_{i=1}^{N}(O_i - \overline{O})^2}$	P_i = prediction at time and location i; O_i = observation at time and location i; $\overline{P}$ = arithmetic average of P_i, i=1,2,…, N; $\overline{O}$ = arithmetic average of O_i, i=1,2,…,N
Normalized Mean Error (***NME***)	**Norm_Mean_Err**	$\frac{\sum_{i=1}^{N}\lvert P_i - O_i\rvert}{\sum_{i=1}^{N} O_i}$	Reported as %
Root Mean Square Error (***RMSE***)	**Rt_Mean_Sqr_Err**	$\left[\frac{1}{N}\sum_{i=1}^{N}(P_i - O_i)^2\right]^{1/2}$	Reported as %
Fractional Gross Error (***F_E***)	**Frac_Gross_Err**	$\frac{2}{N}\sum_{i=1}^{N}\left\lvert\frac{P_i - O_i}{P_i + O_i}\right\rvert$	Reported as %
Mean Absolute Gross Error (***MAGE***)	**Mean_Abs_G_Err**	$\frac{1}{N}\sum_{i=1}^{N}\lvert P_i - O_i\rvert$	
Mean Normalized Gross Error (***MNGE***)	**Mean_Norm_G_Err**	$\frac{1}{N}\sum_{i=1}^{N}\frac{\lvert P_i - O_i\rvert}{O_i}$	Reported as %
Mean Bias (***MB***)	**Mean_Bias**	$\frac{1}{N}\sum_{i=1}^{N}(P_i - O_i)$	Reported as concentration (e.g., µg/m^3)

Statistical Measure	Shorthand Notation	Mathematical Expression	Notes
Mean Normalized Bias (***MNB***)	**Mean_Norm_Bias**	$\frac{1}{N}\sum_{i=1}^{N}\frac{(P_i - O_i)}{O_i}$	Reported as %
Mean Fractionalized Bias (Fractional Bias, ***MFB***)	**Mean_Fract_Bias**	$\frac{2}{N}\sum_{i=1}^{N}\left(\frac{P_i - O_i}{P_i + O_i}\right)$	Reported as %
Normalized Mean Bias **(*NMB*)**	**Norm_Mean_Bias**	$\frac{\sum_{i=1}^{N}(P_i - O_i)}{\sum_{i=1}^{N}O_i}$	Reported as %
Bias Factor (***BF***)	**Bias Factor**	$\frac{1}{N}\sum_{i=1}^{N}\left(\frac{P_i}{O_i}\right)$	Reported as BF:1 or 1: BF or in fractional notation (BF/1 or 1/BF).

C.2.3 Operational Model Evaluation Approach

The CENRAP modeling databases will be used to develop the visibility State Implementation Plan (SIP) due in December 2007 as required by the Regional Haze Rule (RHR). Accordingly, the primary focus of the operational evaluation is on the six components of fine particulate ($PM_{2.5}$) and Coarse Matter ($PM_{2.5-10}$) within the CENRAP region that are used to characterize visibility at Class I areas:

- Sulfate (SO4);
- Particulate Nitrate (NO3);
- Elemental Carbon (EC);
- Organic Mass Carbon (OMC);
- Other inorganic fine particulate (IP or Soil); and
- Coarse Matter (CM).

The model performance for ozone and precursor and product species (e.g., SO_2 and HNO_3) is also evaluated to build confidence that the modeling system is sufficiently reliable to project future-year visibility.

C.2.5 Performance Evaluation Tools

One of the many challenges in evaluating an annual PM/ozone model simulation is how to synthesize model performance given the shear volume of output from an annual simulation. The model is run on a 148 x 112 x 19 grid with approximately 30 species producing hourly outputs for each day of the year. This results in approximately 90 trillion concentration estimates that are produced for an annual simulation. Thus, the synthesis and interpretation of numerous graphical and tabular displays of model performance into a few concise and descriptive displays that identify the most salient features of model performance is necessary. As part of the CENRAP modeling, as well as work performed by WRAP, VISTAS, MRPO and MANE-VU, several analysis tools and summary displays have been developed and are used:

UCR Analysis Tools: The University of California at Riverside (UCR) Analysis Tools have been used extensively to evaluate the CMAQ and CAMx models for CENRAP (e.g., Morris et al., 2005), WRAP (Tonnesen et al., 2004), VISTAS (Morris et al., 2004) as well as other studies and are run on a Linux platform separately for each network. Numerous graphical displays of model performance are automatically generated using gnuplot. The software generates the following summary and graphical displays of model performance:

- Tabular statistical measures (see Table C-2);
- Time Series Plots for each site and species; and
- Scatter Plots for each species by allsite_allday, allday_onesite and allsite_oneday.

The UCR Analysis Tool is run for a specific subregion (e.g., by RPO region) and for selected monitoring networks. Because each monitoring network has its own measurement artifacts, the model is evaluated separately for each monitoring network.

Summary Bias/Error Plots: The modeling team has developed additional displays of model performance statistics that elucidate model performance in a concise manner: (1) monthly time series plots of average bias and error; (2) soccer plots that display bias versus error and compares them to model performance goals and criteria; and (3) tools to analyze visibility model performance for the worst and best 20 percent visibility days that are used in visibility projections.

GA DNR Analysis Plots: Dr. James Boylan of the Georgia Department of Natural Resources has extended the concept in EPA's draft PM fine particulate and regional haze modeling guidance that model performance for species that make up a major contribution to visibility impairment be subjected to more stringent goals than species that are minor contributors by developing concentration-dependent performance goals and "Bugle Plots" to display them (Boylan, 2004).

The evaluation of the CENRAP 2002 36 km Base F CMAQ simulation used each of the analysis tools listed above taking advantage of their different descriptive and complimentary nature. The use of these analysis tools generated thousands of statistical measures and graphical displays of model performance that cannot all be displayed in this report. The modeling team has gone through the plots and measures using slide shows to identify those displays that are most descriptive in conveying model performance so should be included in this TSD. The complete set of model performance statistics and graphical performance displays can be found on the CENRAP modeling Website at:

http://pah.cert.ucr.edu/aqm/cenrap/cmaq.shtml#cmaq_typ02f_mpe

Note that model performance statistics are calculated separately for each of the monitoring networks. Different PM measurement technology can produce different measurement values even when measuring the same air parcel. Thus, when calculating model performance metrics, measurements in different networks are not mixed.

C.2.4 Subdomains Analyzed

CENRAP has been analyzing model performance in five subdomains corresponding to the states contained in the five RPOs (see Figure 1-1):

- CENRAP
- MRPO
- VISTAS
- MANE-VU
- WRAP

As CENRAP has refined its emissions inventory, the changes in model performance from one 2002 base case to another has diminished to the point where little has changed in the last few iterations. Thus, the CMAQ 2002 36 km Base F evaluation presented in this section was just performed for the CENRAP region and the reader is referred to the modeling Website (http://pah.cert.ucr.edu/aqm/cenrap/cmaq.shtml) and Morris and co-workers (2005) for the evaluation outside of the CENRAP region and the diagnostic model evaluation.

C.2.5 Model Performance Goals and Criteria

The issue of model performance goals for PM species is an area of ongoing research and debate. For ozone modeling, EPA has established performance goals for 1-hour ozone normalized mean bias and gross error of #±15% and #35%, respectively (EPA, 1991). EPA's draft fine particulate modeling guidance notes that performance goals for ozone should be viewed as upper bounds of model performance that PM models may not be able to always achieve and we should demand better model performance for PM components that make up a larger fraction of the PM mass than those that are minor contributors (EPA, 2001). EPA's final modeling guidance does not list any specific model performance goals for PM and visibility modeling and instead provides a summary of PM model performance across several historical applications that can be used for comparisons if desired. Measuring PM species is not as precise as ozone monitoring. In fact, the differences in measurement techniques for some species likely exceed the more stringent performance goals, such as those for ozone. For example, recent comparisons of the PM species measurements using the IMPROVE and STN measurement technologies found differences of approximately ∀20% (SO4) to ∀50% (EC) (Solomon et al., 2004).

For the CENRAP, VISTAS and WRAP modeling we have adopted three levels of model performance goals and criteria for bias and gross error as listed in Table C-3. Note that we are not suggesting that these performance goals be adopted as guidance or that they are the most appropriate goals to use. Rather, we are just using them to frame and put the PM model performance into context and to facilitate model performance intercomparison across episodes, species, models and sensitivity tests.

Table C-3. Model performance goals and criteria used to assist in interpreting modeling results.

Fractional Bias	Fractional Error	Comment
#∀15%	#35%	Ozone model performance goal for which PM model performance would be considered good – note that for many PM species measurement uncertainties may exceed this goal.
#∀30%	#50%	Proposed PM model performance goal that we would hope each PM species could meet
#∀60%	#75%	Proposed PM criteria above which indicates potential fundamental problems with the modeling system.

As noted in EPA's PM modeling guidance, less abundant PM species should have less stringent performance goals (EPA, 2001; 2007). Accordingly, we are also using performance goals that are a continuous function of average concentrations, as proposed by Dr. James Boylan at the Georgia Department of Natural Resources (GA DNR), that have the following features (Boylan, 2004):

- Asymptotically approaching proposed performance goals or criteria (i.e., the ∀30%/50% and ∀60%/75% bias/error levels listed in Table C-1) when the mean of the observed concentrations are greater than 2.5 ug/m^3.
- Approaching 200% error and ∀200% bias when the mean of the observed concentrations are extremely small.

Bias and error are plotted as a function of average concentrations. As the mean concentration approach zero, the bias performance goal and criteria flare out to ∀200% creating a horn shape, hence the name "Bugle Plots". Dr. Boylan has defined three Zones of model performance: Zone 1 meets the ∀30%/50% bias/error performance goal and is considered "good" model performance; Zone 2 lies between the ∀30%/50% performance goal and ∀60%/75% performance criteria and is an area where concern for model performance is raised; and Zone 3 lies above the ∀60%/75% performance criteria and is an area of questionable model performance.

C.2.6 Performance Time Periods

The CMAQ 2002 36 km Base F evaluation, model performance statistics and graphical displays are generated monthly using the native averaging times of each monitoring network (i.e., 24-hour for IMPROVE and STN; weekly for CASTNet and NADP; and hourly for AQS). As the focus of the RHR is on daily average visibility that is calculated from daily average PM species concentrations then the evaluation of the model for 24-hour concentrations is particularly relevant. The RHR places particular emphasis on the Worst 20% (W20%) and Best 20% (B20%) days at Class I areas. Thus, we also place particular emphasis on the model performance for PM species on the W20% and B20% days during 2002 at Class I areas.

C.2.7 Key Measures of Model Performance

Although we have generated numerous statistical performance measures (see Table C-2) that are available on the CENRAP modeling website, when comparing model performance across months, subdomains, networks, grid resolution, models, studies, etc. it is useful to have a few key measurement statistics to be used to facilitate the comparisons. It is also useful to have a subset of the 2002 year that can represent the entire year so that a more focused evaluation can be conducted. We have found that the Mean Fractional Bias and Mean Fractional Gross Error appear to be the most consistent descriptive measure of model performance (Morris et al., 2004b; 2005). The Fractional Bias and Error normalize by the average of the observed and predicted value (see Table C-2) because it provides descriptive power across different magnitudes of the model and observed concentrations and is bounded by -200% to +200%. This is in contrast to the normalized bias and error (as recommended for ozone performance goals, EPA, 1991) that is normalized by just the observed value so can "blow up" to infinity as the observed value approaches zero. Below we perform a focused evaluation of model performance for four months of the 2002 year that are used to represent the seasonal variation in performance:

- January
- April
- July
- October

We also present fractional bias and error for all months of 2002 using time series and bugle plots.

C.3 Operational Model Performance Evaluation in the CENRAP Region

In the following discussions we use selected monthly scatter plots, time series plots and model performance statistical measures from the UCR Analysis Tools application to the 2002 CMAQ Base F base case simulation in an operational evaluation of the model for PM species. We focus on the six main components of PM that are used to project visibility.

C.3.1 Sulfate (SO4) Monthly Model Performance

C.3.1.1 SO4 in January 2002

Figure C-4a displays scatter plots of predicted and observed SO4 concentrations or wet depositions for sites in the CENRAP regions using observations from the IMPROVE, STN, CASTNet and NADP monitoring networks; the IMPROVE and STN SO4 concentrations are 24-hour averages whereas the CASTNet SO4 concentrations and NADP SO4 wet deposition are weekly averages. The January SO4 performance at the IMPROVE and STN networks in the CENRAP region is quite good with low fractional bias (-12% to -13%) and some scatter (fractional error of 42% and 34%) but centered in the 1:1 line of perfect agreement. There is a net SO4 underestimation bias in January across the CASTNet network (fractional bias of -34%) with wet SO4 deposition overstated on average across the NADP sites in the CENRAP region (+40% fractional bias). Whether the overstated SO4 wet deposition is a contributor to the SO4 concentration underestimation bias is unclear, but it is in the correct direction to account for it.

The time series comparisons of predicted and observed 24-hour SO4 concentrations at CENRAP Class I area IMPROVE sites during January 2002 shown in Figure C-4b are quite encouraging. Although there are some days and sites with mismatches (e.g., January 26 at BOWA and VOYA) and sites with systematic performance problems (SO4 underestimated at BIBE), the time series in generally are quite good with the model tracking the observed temp[oral variation in daily sulfate in January and some sites exhibiting remarkable agreement (e.g., MING).

Figure C-4c displays the spatial variations in the predicted and IMPROVE observed SO4 concentrations for January 20, 23, 26 and 29, 2002, which are four consecutive days of IMPROVE monitoring using its 1:3 day monitoring frequency. On January 20 both the model and observations agree on that an elevated sulfate clouds is entering the CENRAP region across southern Illinois and Missouri. There is a sharp SO4 concentration gradient going east to west with both the model and observations estimating relatively clean SO4 values over Colorado. By January 23 the model and observations agree that elevated SO4 exists along a diagonal orientation from Chicago to East Texas. Although there are some SO4 model/observed spatial mismatches on this day (e.g., northern Louisiana and western Arkansas) the model generally reproduces the areas of elevated and low observed SO4. By January 29 the model and observations agree that SO4 has cleaned out of the CENRAP region. Although there are elevated SO4 observations in western North Dakota and northern Minnesota not reflected in the model. On January 29 there is an elevated tongue of SO3 entering the CENRAP region through southern Illinois stretching to the southwest almost to Big Bend in western Texas. Observed SO4 is measured at Big Bend but the modeled high SO4 is slightly east of there. There is very good agreement on this day between the predicted and observed spatial distribution of SO4.

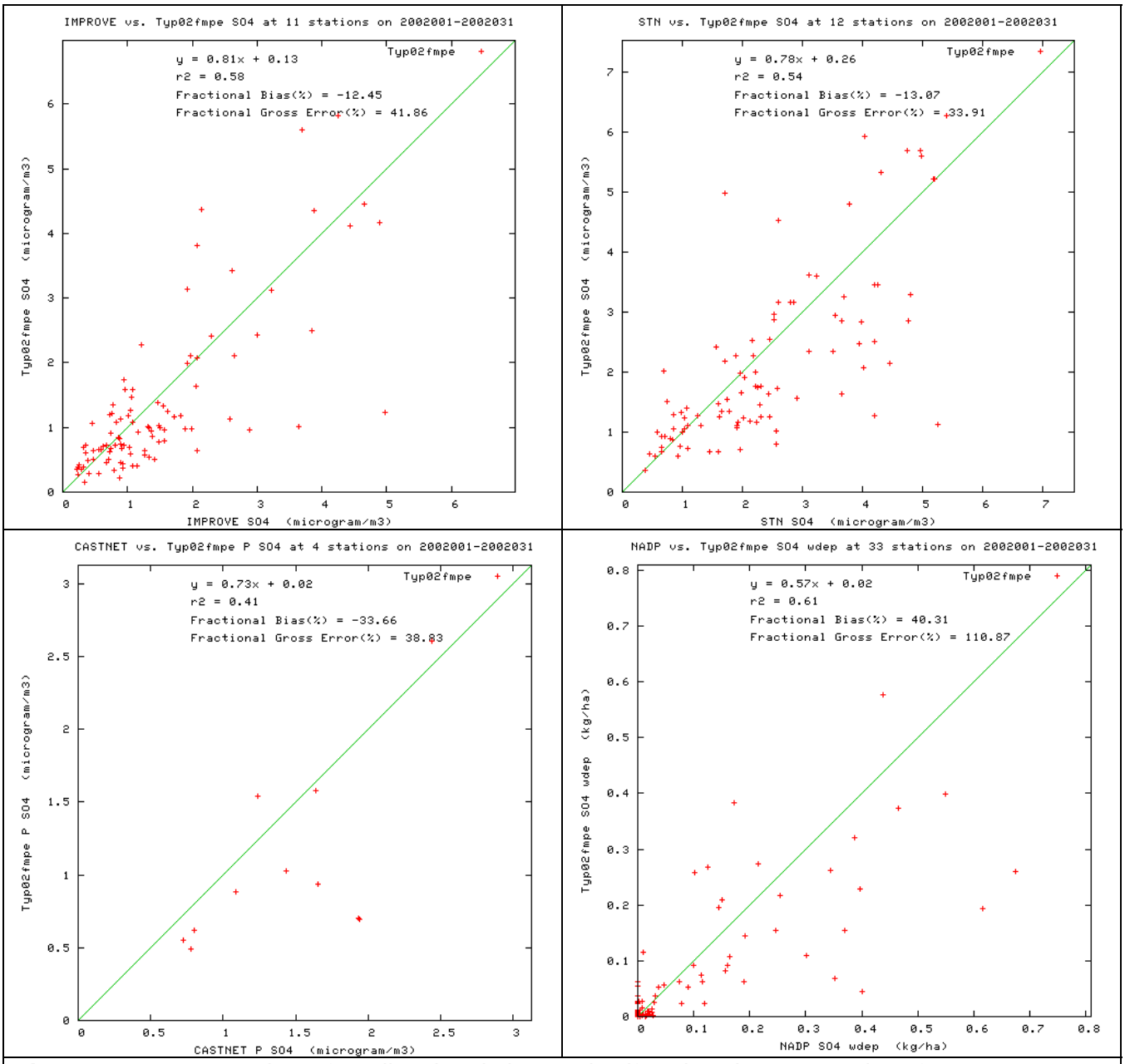

Figure C-4a. Scatter plots of predicted and observed sulfate (SO4) concentrations for January 2002 and sites in the CENRAP region using IMPROVE (top left), STN (top right), CASTNet (bottom left) and NADP monitoring networks using the CMAQ 2002 36 km Base F base case simulation.

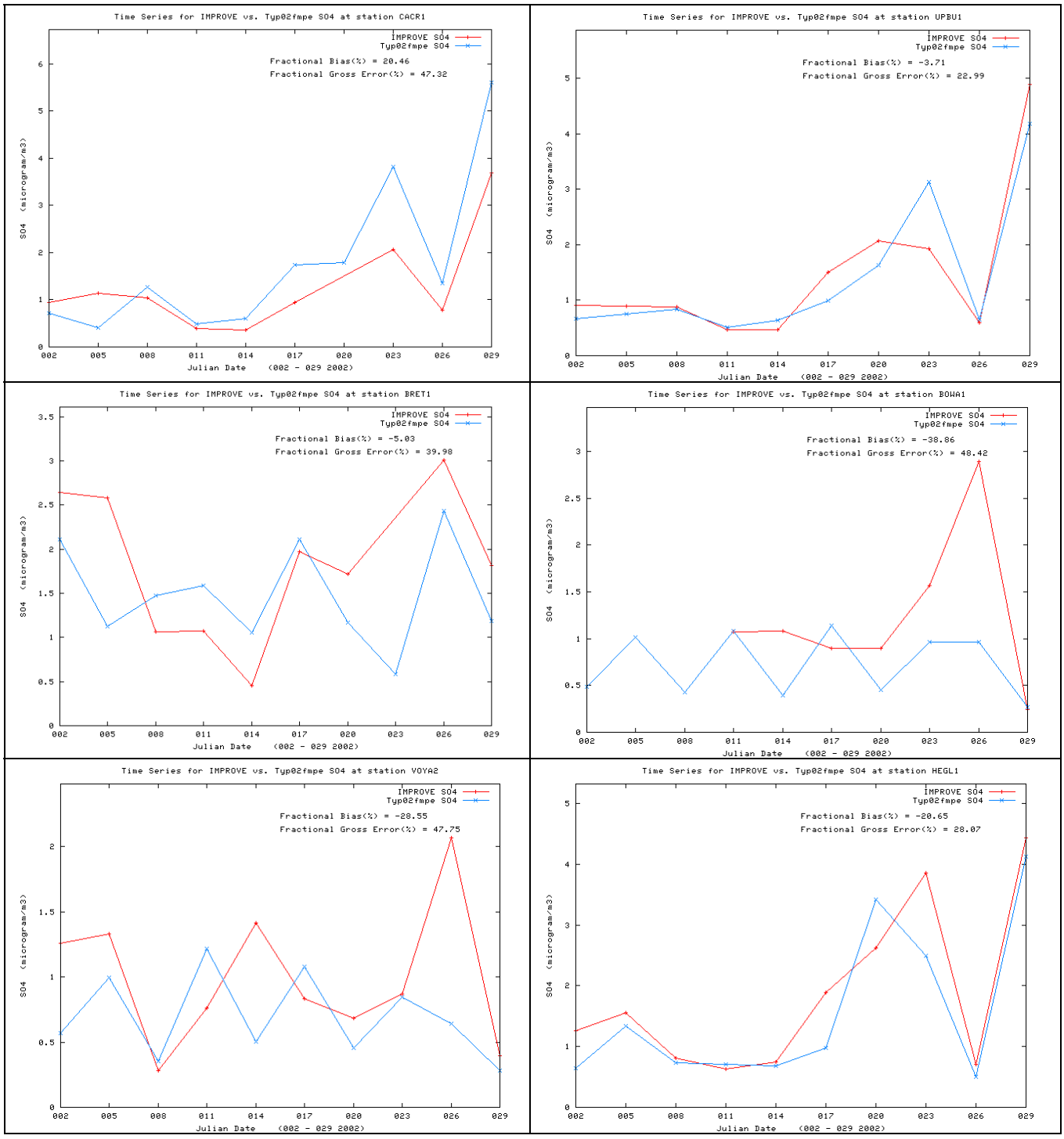
Time Series for IMPROVE vs. Typ02fmpe SO4 at station CACR1
IMPROVE SO4
Typ02fmpe SO4
Fractional Bias(%) = 20.46
Fractional Gross Error(%) = 47.32
SO4 (microgram/m3)
Julian Date (002 - 029 2002)
Time Series for IMPROVE vs. Typ02fmpe SO4 at station UPBU1
IMPROVE SO4
Typ02fmpe SO4
Fractional Bias(%) = -3.71
Fractional Gross Error(%) = 22.99
SO4 (microgram/m3)
Julian Date (002 - 029 2002)
Time Series for IMPROVE vs. Typ02fmpe SO4 at station BRET1
IMPROVE SO4
Typ02fmpe SO4
Fractional Bias(%) = -5.03
Fractional Gross Error(%) = 39.98
SO4 (microgram/m3)
Julian Date (002 - 029 2002)
Time Series for IMPROVE vs. Typ02fmpe SO4 at station BOWA1
IMPROVE SO4
Typ02fmpe SO4
Fractional Bias(%) = -38.86
Fractional Gross Error(%) = 48.42
SO4 (microgram/m3)
Julian Date (002 - 029 2002)
Time Series for IMPROVE vs. Typ02fmpe SO4 at station VOYA2
IMPROVE SO4
Typ02fmpe SO4
Fractional Bias(%) = -28.55
Fractional Gross Error(%) = 47.75
SO4 (microgram/m3)
Julian Date (002 - 029 2002)
Time Series for IMPROVE vs. Typ02fmpe SO4 at station HEGL1
IMPROVE SO4
Typ02fmpe SO4
Fractional Bias(%) = -20.65
Fractional Gross Error(%) = 28.07
SO4 (microgram/m3)
Julian Date (002 - 029 2002)

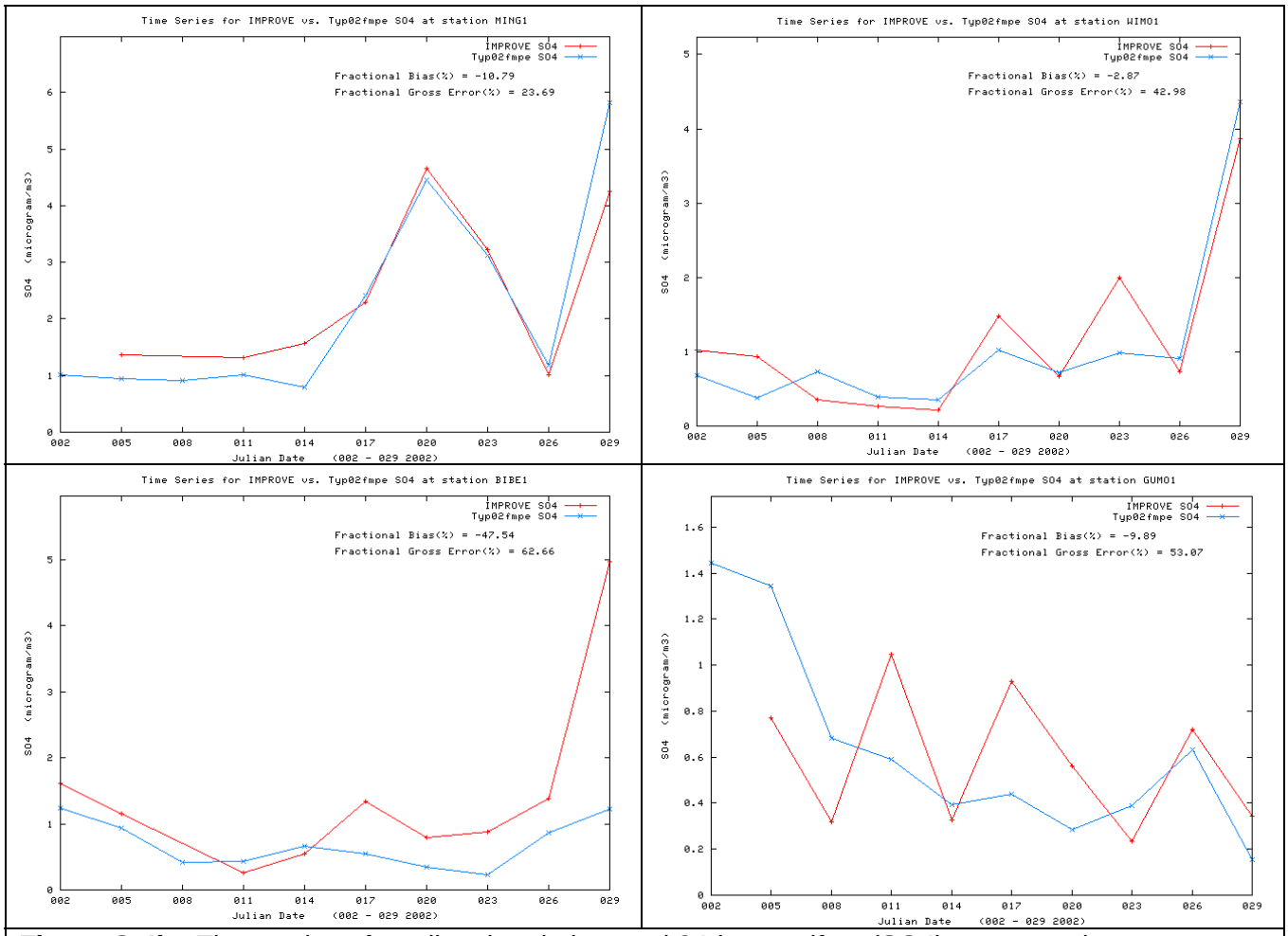

Figure C-4b. Time series of predicted and observed 24-hour sulfate (SO4) concentrations at CENRAP IMPROVE CLASS I AREA sites in January 2002 for CMAQ 2002 36 km Base F base case simulation.

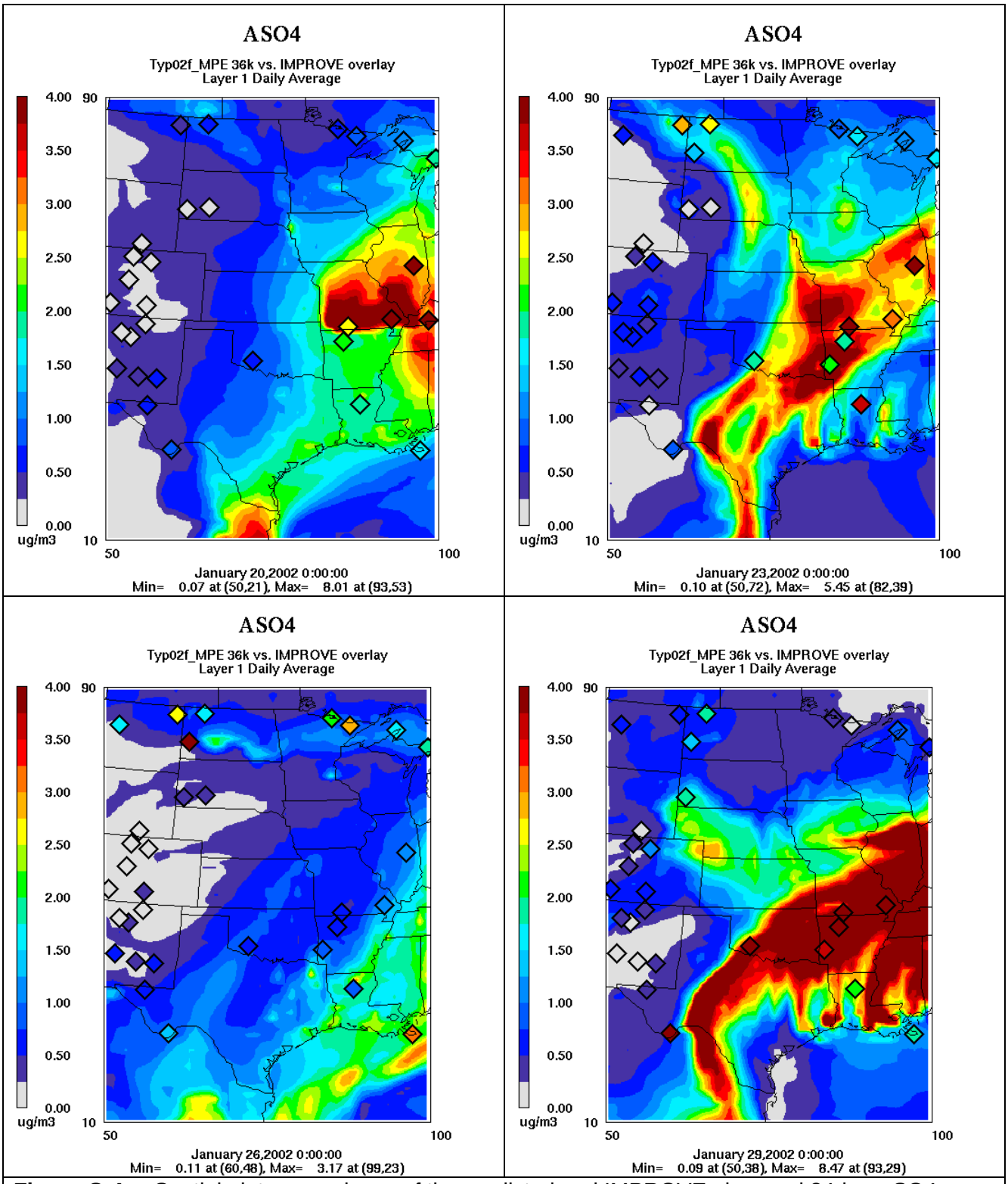

Figure C-4c. Spatial plot comparisons of the predicted and IMPROVE observed 24-hour SO4 concentrations for January 20, 23, 26 and 29, 2002.

C.3.1.2 SO4 in April 2002

In April CMAQ underestimates the observed SO4 in the CENRAP region with fractional bias values of -52%, -30% and -58% across the IMPROVE, STN and CASTNet networks (Figure C-5a). The fractional bias for wet SO4 deposition is quite low (3%) albeit with a lot of scatter which is reflected in high fractional error (78%). The ability of the model to reproduce the temporal variability of the April observed SO4 concentrations at the IMPROVE sites is quite variable. The SO4 under-prediction bias is clearly present at several sites (e.g., HEGL, BIBE and GUMO), whereas there is quite good agreement at others (UPBU, BRET and VOYA). Comparisons of the spatial distributions of the predicted and observed SO4 concentrations on April 5, 8, 11 and 14 are shown in Figure C-5c. On April 5 the model reproduces the half circle of elevated SO4 across Texas-Louisiana, but appears to not be as large an area as observed coming up short from some of the sites (e.g., BIBE and GUMO). Model and observations agree that April 8 is a relatively low SO4 day in the CENRAP region with just a small intrusion of elevated values across Mississippi. On April 14 the model has two separate clouds of elevated SO4, one over East Texas-Louisiana and one over northeastern Illinois and eastward with a clean area in between in southern Missouri. The observations agree except that it has these two elevated SO4 areas connected with the southern Missouri area not as clean as in the model.

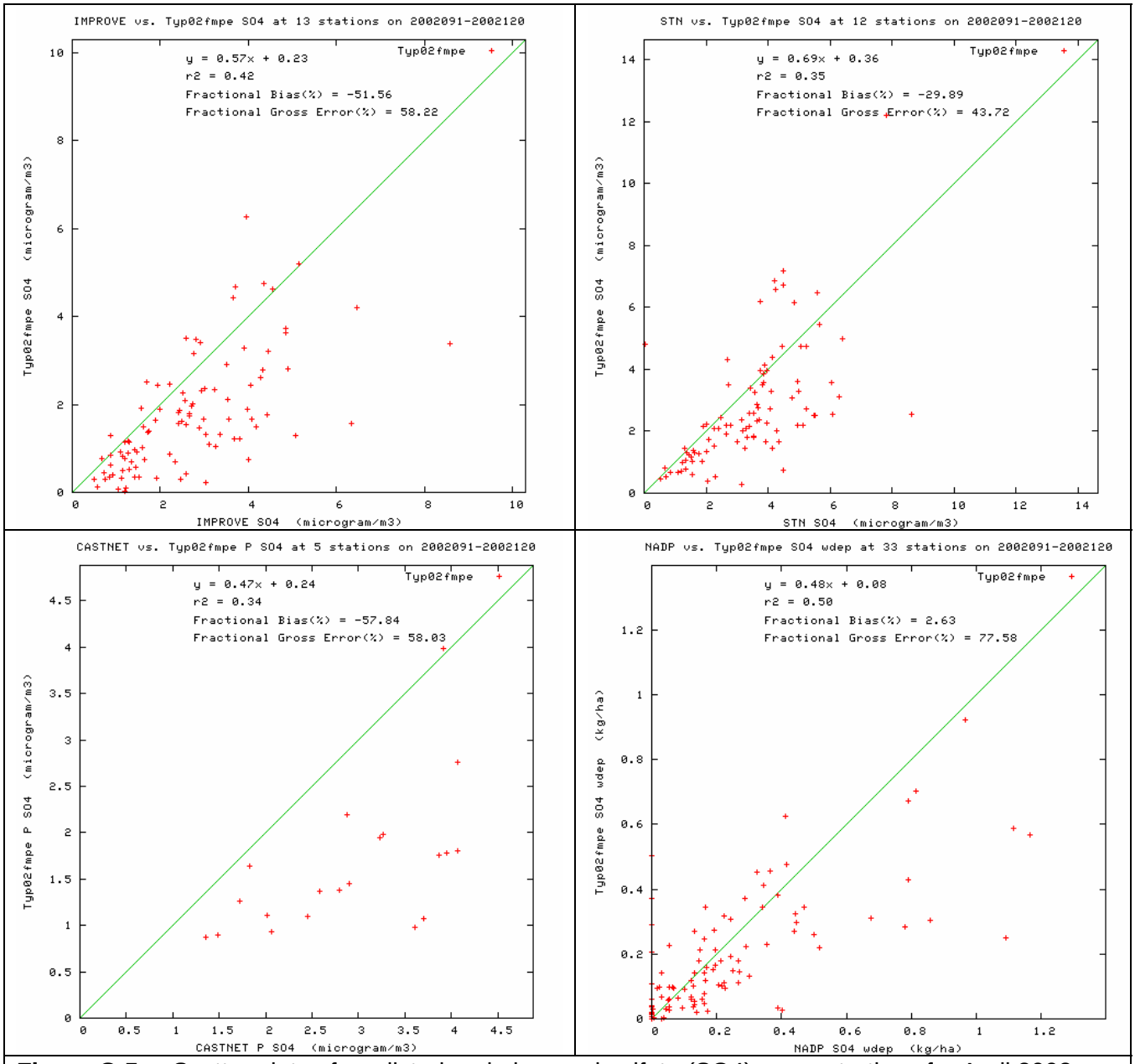

Figure C-5a. Scatter plots of predicted and observed sulfate (SO4) concentrations for April 2002 and sites in the CENRAP region using IMPROVE (top left), STN (top right), CASTNet (bottom left) and NADP monitoring networks using the CMAQ 2002 36 km Base F base case simulation.

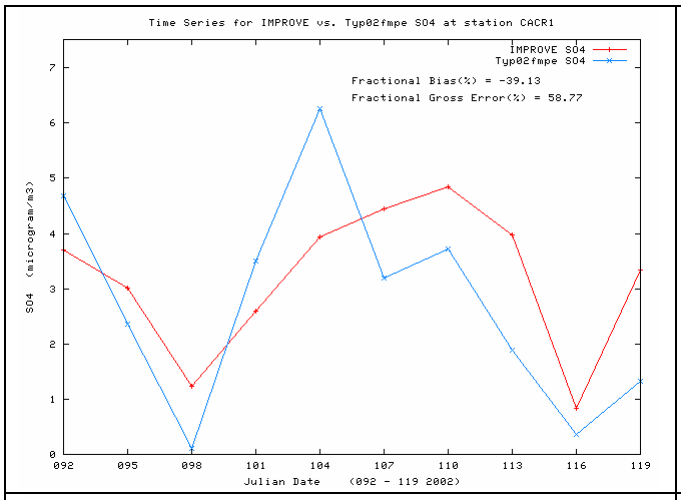
Time Series for IMPROVE vs. Typ02fmpe SO4 at station CACR1
IMPROVE SO4
Typ02fmpe SO4
Fractional Bias(%) = -39.13
Fractional Gross Error(%) = 58.77
SO4 (microgram/m3)
Julian Date (092 - 119 2002)

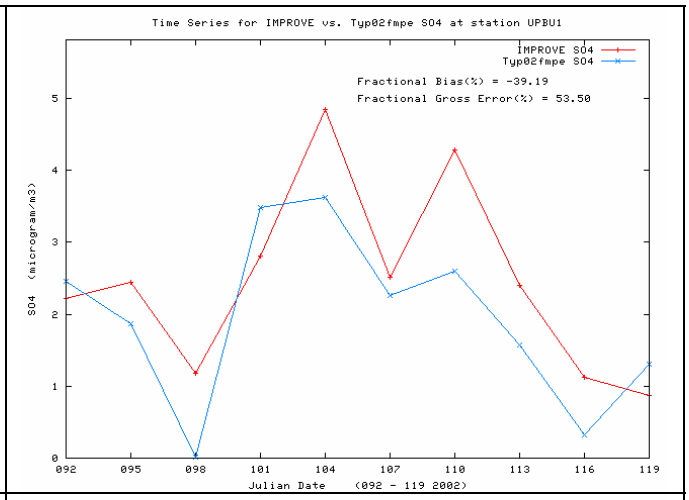
Time Series for IMPROVE vs. Typ02fmpe SO4 at station UPBU1
IMPROVE SO4
Typ02fmpe SO4
Fractional Bias(%) = -39.19
Fractional Gross Error(%) = 53.50
SO4 (microgram/m3)
Julian Date (092 - 119 2002)

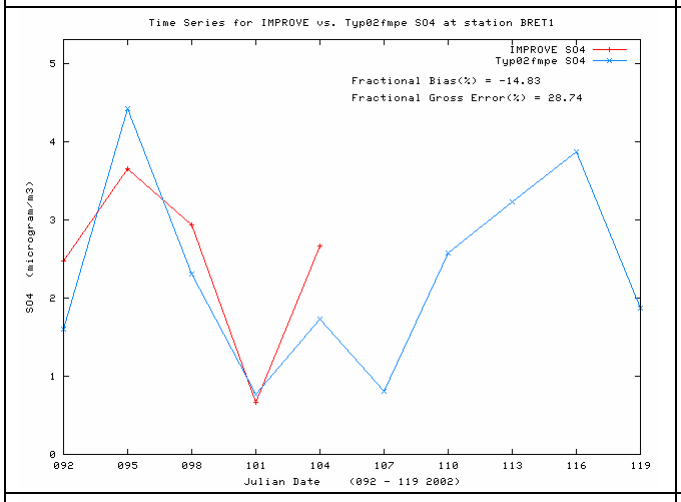
Time Series for IMPROVE vs. Typ02fmpe SO4 at station BRET1
IMPROVE SO4
Typ02fmpe SO4
Fractional Bias(%) = -14.83
Fractional Gross Error(%) = 28.74
SO4 (microgram/m3)
Julian Date (092 - 119 2002)

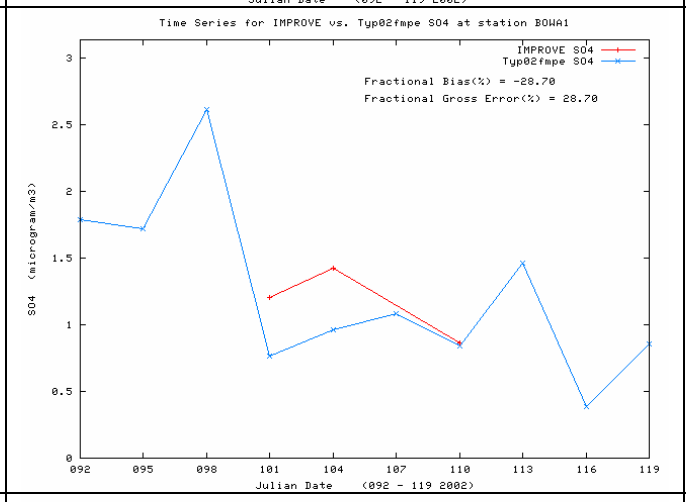
Time Series for IMPROVE vs. Typ02fmpe SO4 at station BOWA1
IMPROVE SO4
Typ02fmpe SO4
Fractional Bias(%) = -28.70
Fractional Gross Error(%) = 28.70
SO4 (microgram/m3)
Julian Date (092 - 119 2002)

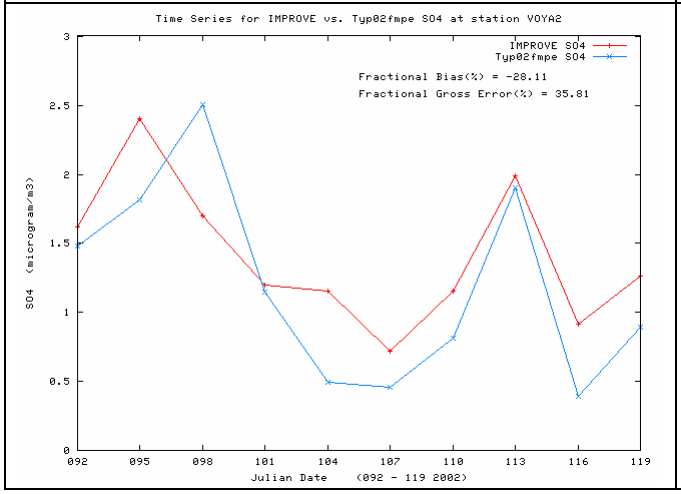
Time Series for IMPROVE vs. Typ02fmpe SO4 at station VOYA2
IMPROVE SO4
Typ02fmpe SO4
Fractional Bias(%) = -28.11
Fractional Gross Error(%) = 35.81
SO4 (microgram/m3)
Julian Date (092 - 119 2002)

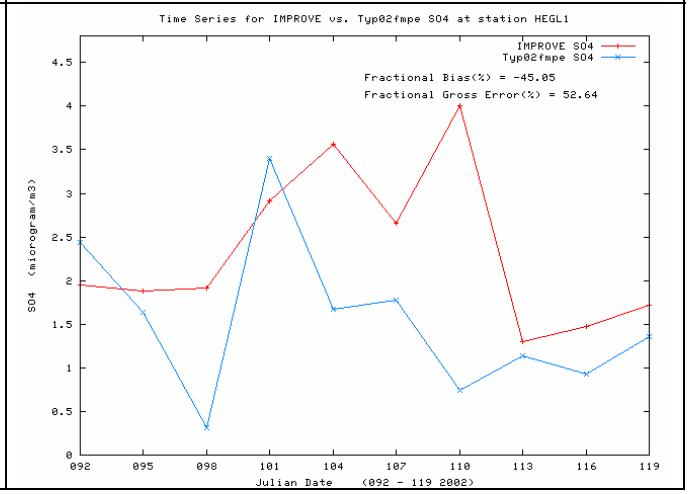
Time Series for IMPROVE vs. Typ02fmpe SO4 at station HEGL1
IMPROVE SO4
Typ02fmpe SO4
Fractional Bias(%) = -45.05
Fractional Gross Error(%) = 52.64
SO4 (microgram/m3)
Julian Date (092 - 119 2002)

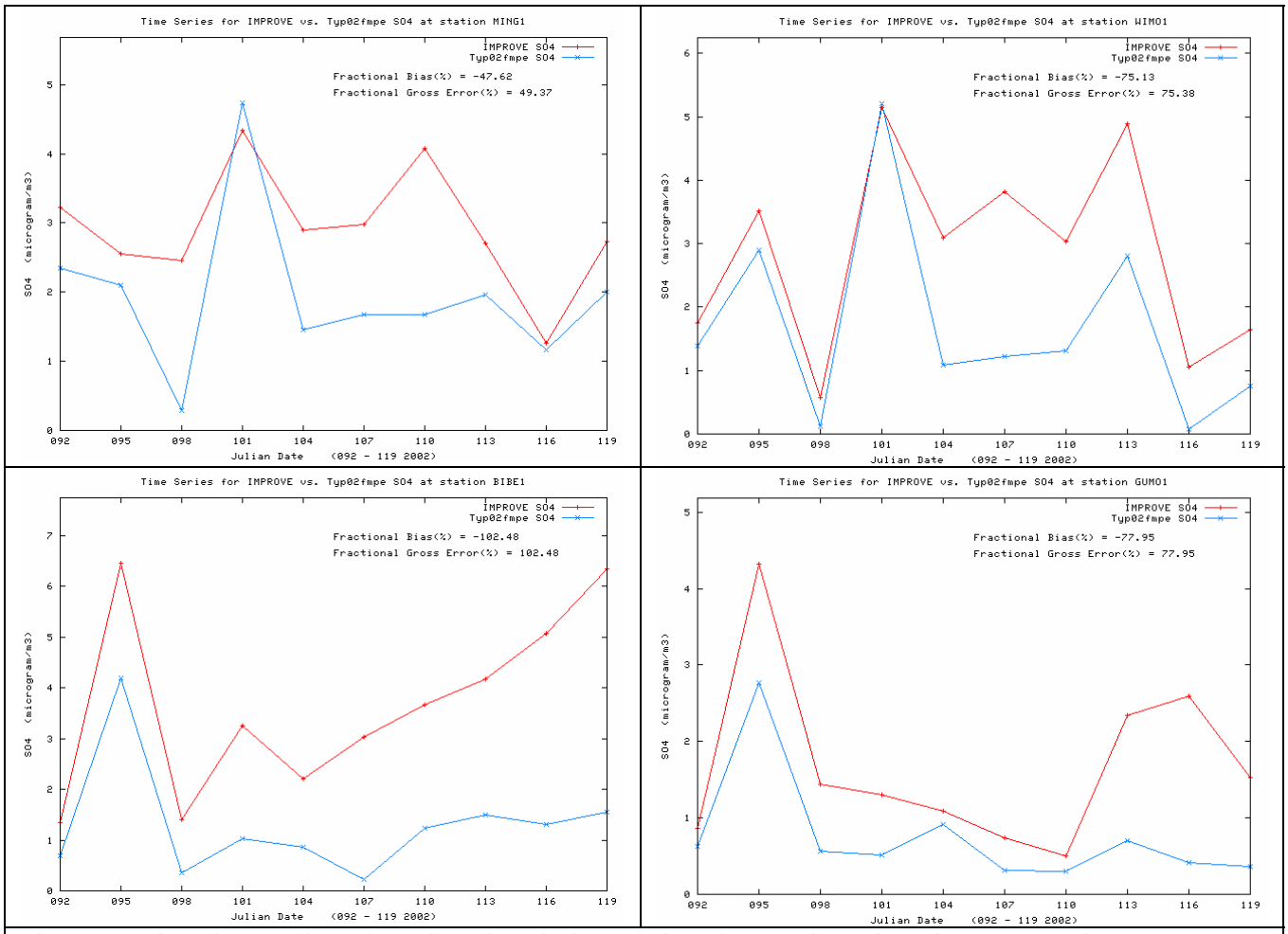

Figure C-5b. Time series of predicted and observed 24-hour sulfate (SO4) concentrations at CENRAP IMPROVE CLASS I AREA sites in April 2002 for CMAQ 2002 36 km Base F base case simulation.

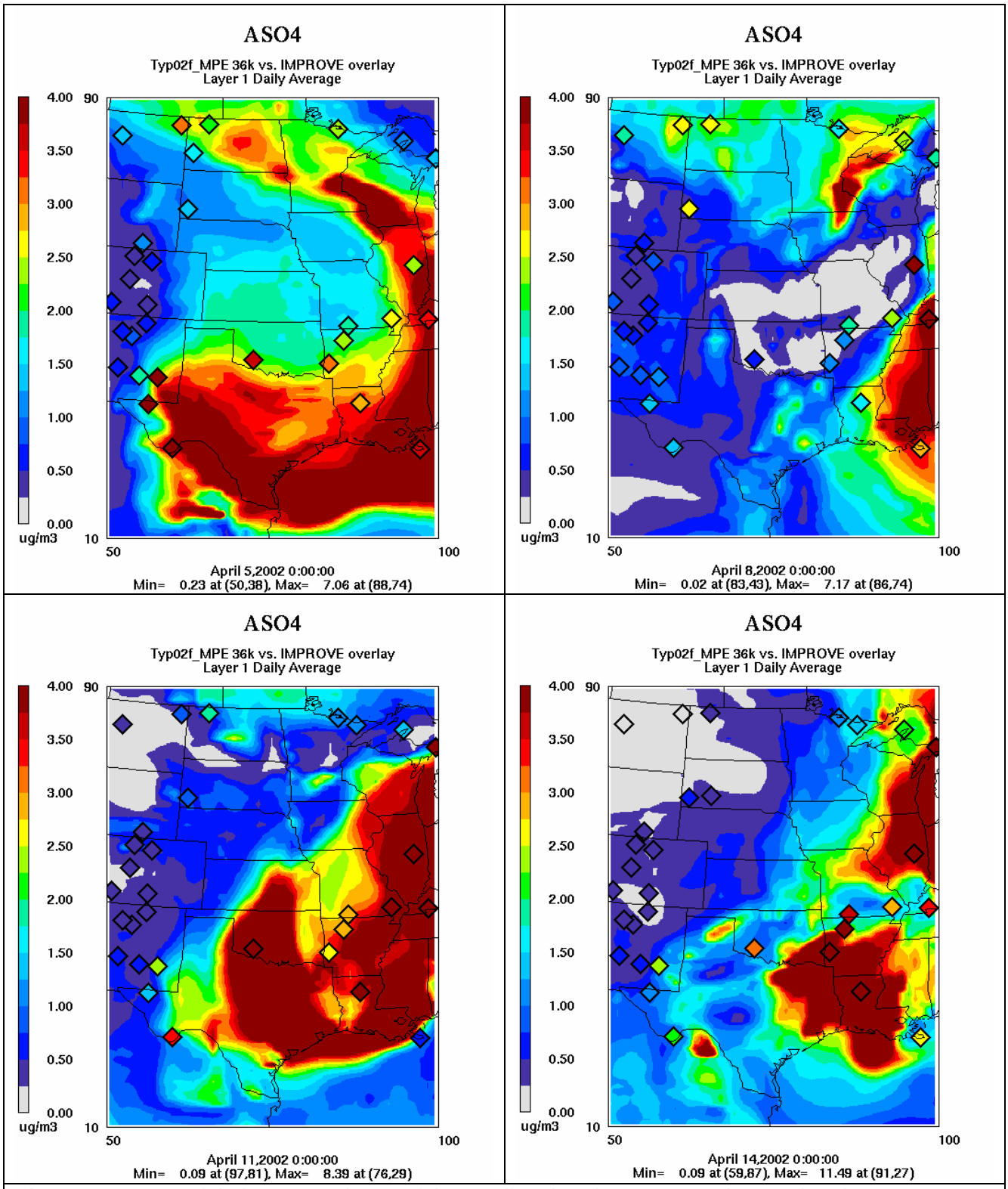

Figure C-5c. Spatial plot comparisons of the predicted and IMPROVE observed 24-hour SO4 concentrations for April 5, 8, 11 and 14, 2002.

C.3.1.3 SO4 in July 2002

SO4 concentrations are also underestimated by CMAQ in July (Figure C-6a) with fractional bias value ranging from -22 to -52%. Wet SO4 deposition is slightly overstated (22%) with a lot of scatter (83% error). The July SO4 under-prediction bias is also reflected in the time series plots (Figure C-6b). Comparisons of the predicted and observed spatial distribution of SO4 in the CENRAP region for July 7, 10, 13 and 16, 2002 are shown in Figure C-6c. In general the model and observations agree on the locations of the elevated SO4, except that the observed extent is somewhat larger so that the modeled elevated SO4 fails to impact some of the sites on the edge of the elevated cloud of SO4 (e.g., Big Bend, Guadalupe Mountains and northwestern Oklahoma).

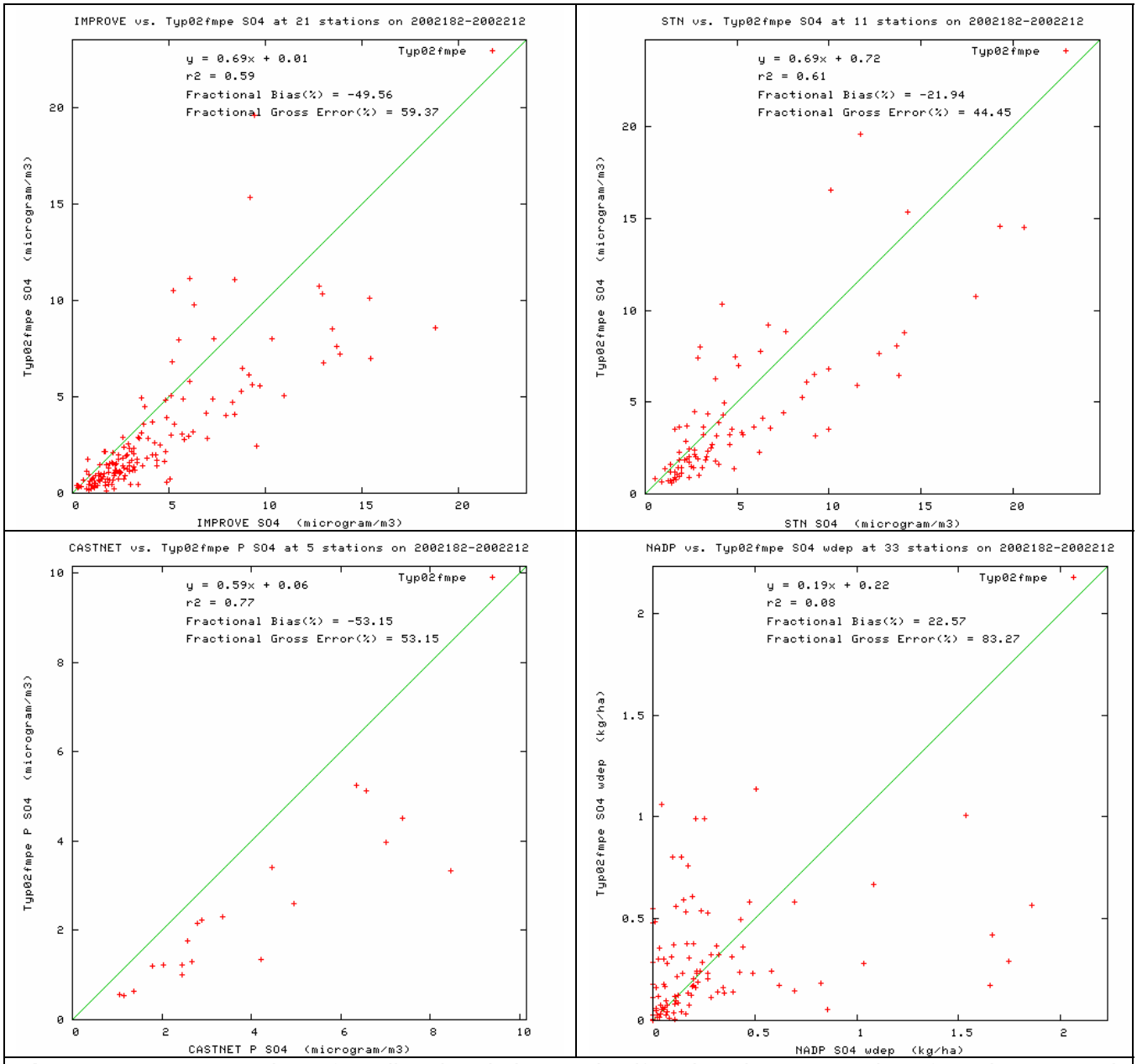

Figure C-6a. Scatter plots of predicted and observed sulfate (SO4) concentrations for July 2002 and sites in the CENRAP region using IMPROVE (top left), STN (top right), CASTNet (bottom left) and NADP monitoring networks using the CMAQ 2002 36 km Base F base case simulation.

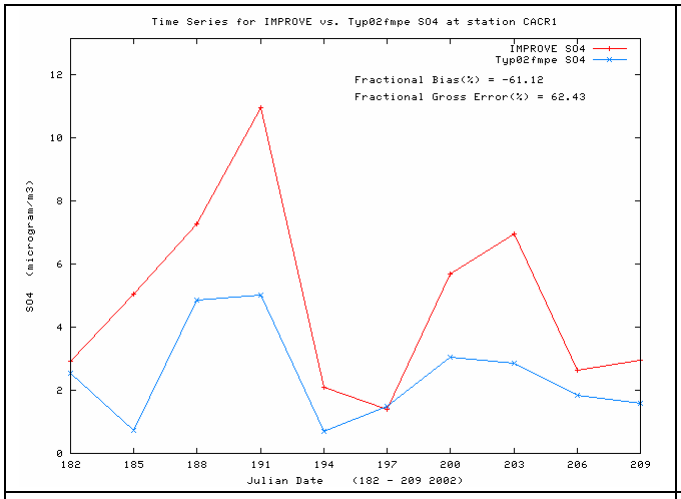
Time Series for IMPROVE vs. Typ02fmpe SO4 at station CACR1
IMPROVE SO4
Typ02fmpe SO4
Fractional Bias(%) = -61.12
Fractional Gross Error(%) = 62.43
SO4 (microgram/m3)
Julian Date (182 - 209 2002)

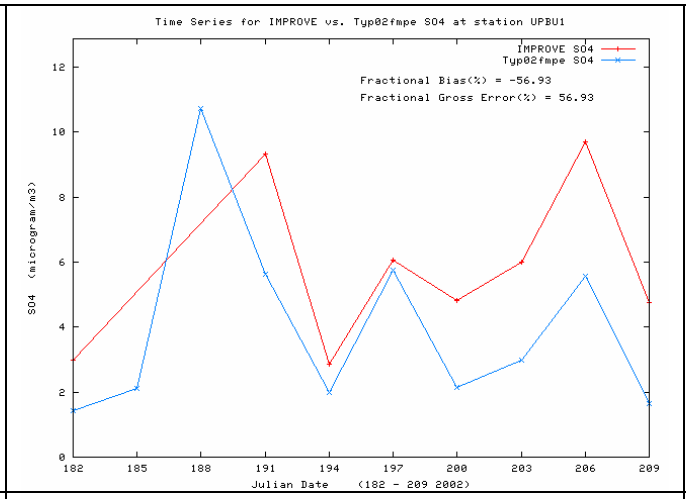
Time Series for IMPROVE vs. Typ02fmpe SO4 at station UPBU1
IMPROVE SO4
Typ02fmpe SO4
Fractional Bias(%) = -56.93
Fractional Gross Error(%) = 56.93
SO4 (microgram/m3)
Julian Date (182 - 209 2002)

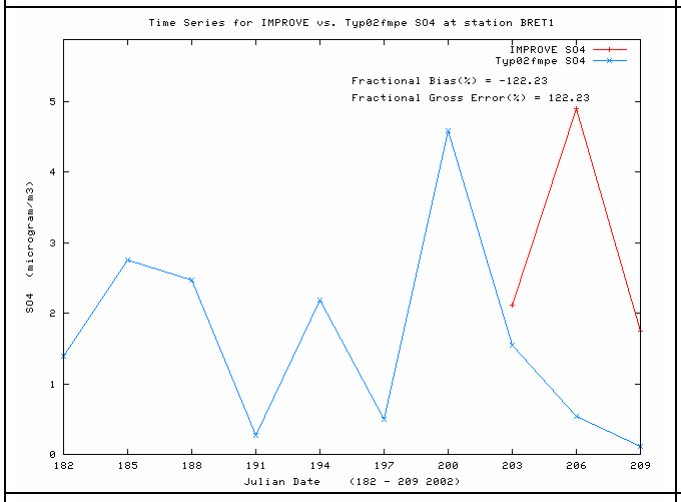
Time Series for IMPROVE vs. Typ02fmpe SO4 at station BRET1
IMPROVE SO4
Typ02fmpe SO4
Fractional Bias(%) = -122.23
Fractional Gross Error(%) = 122.23
SO4 (microgram/m3)
Julian Date (182 - 209 2002)

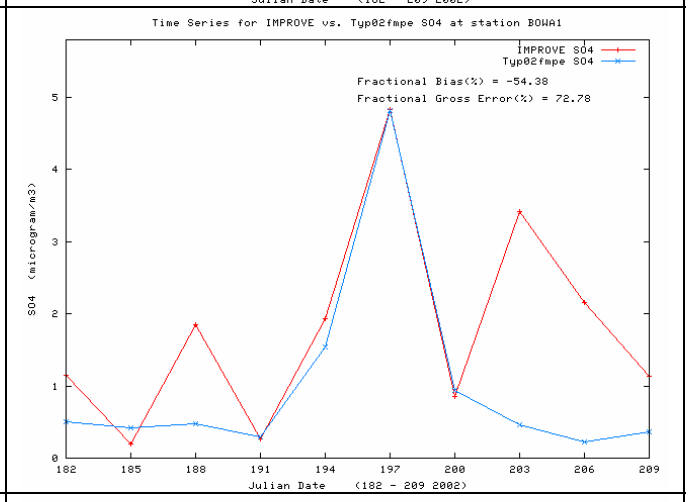
Time Series for IMPROVE vs. Typ02fmpe SO4 at station BOWA1
IMPROVE SO4
Typ02fmpe SO4
Fractional Bias(%) = -54.38
Fractional Gross Error(%) = 72.78
SO4 (microgram/m3)
Julian Date (182 - 209 2002)

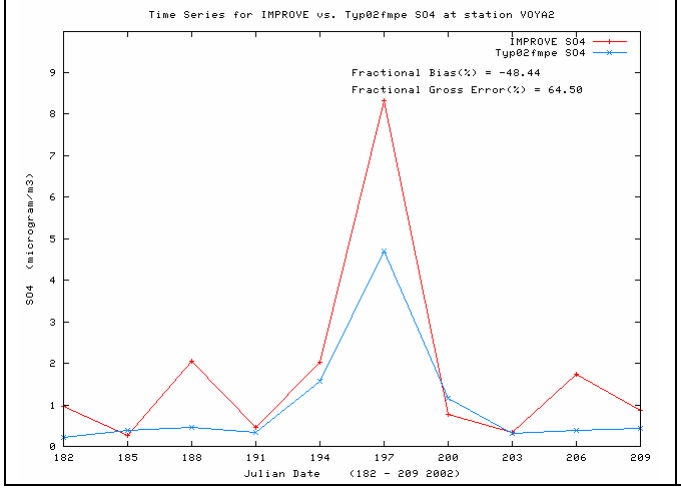
Time Series for IMPROVE vs. Typ02fmpe SO4 at station VOYA2
IMPROVE SO4
Typ02fmpe SO4
Fractional Bias(%) = -48.44
Fractional Gross Error(%) = 64.50
SO4 (microgram/m3)
Julian Date (182 - 209 2002)

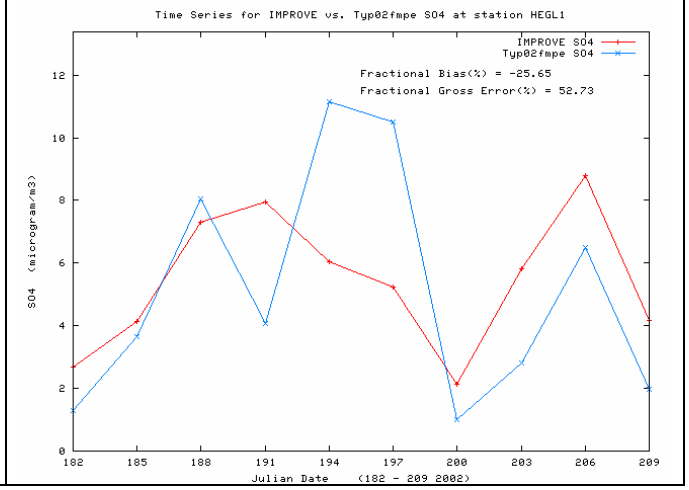
Time Series for IMPROVE vs. Typ02fmpe SO4 at station HEGL1
IMPROVE SO4
Typ02fmpe SO4
Fractional Bias(%) = -25.65
Fractional Gross Error(%) = 52.73
SO4 (microgram/m3)
Julian Date (182 - 209 2002)

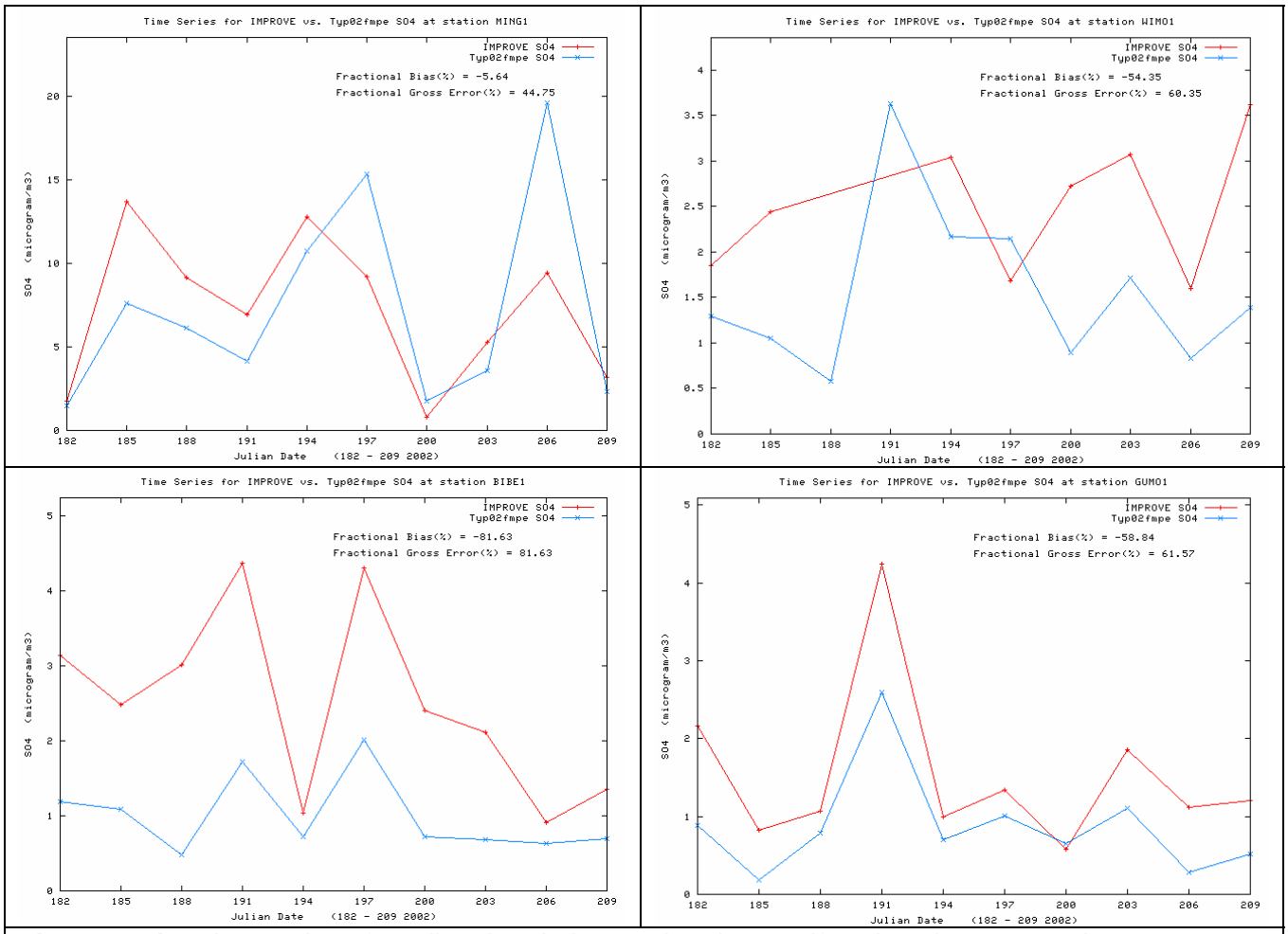

Figure C-6b. Time series of predicted and observed 24-hour sulfate (SO4) concentrations at CENRAP IMPROVE CLASS I AREA sites in July 2002 for CMAQ 2002 36 km Base F base case simulation.

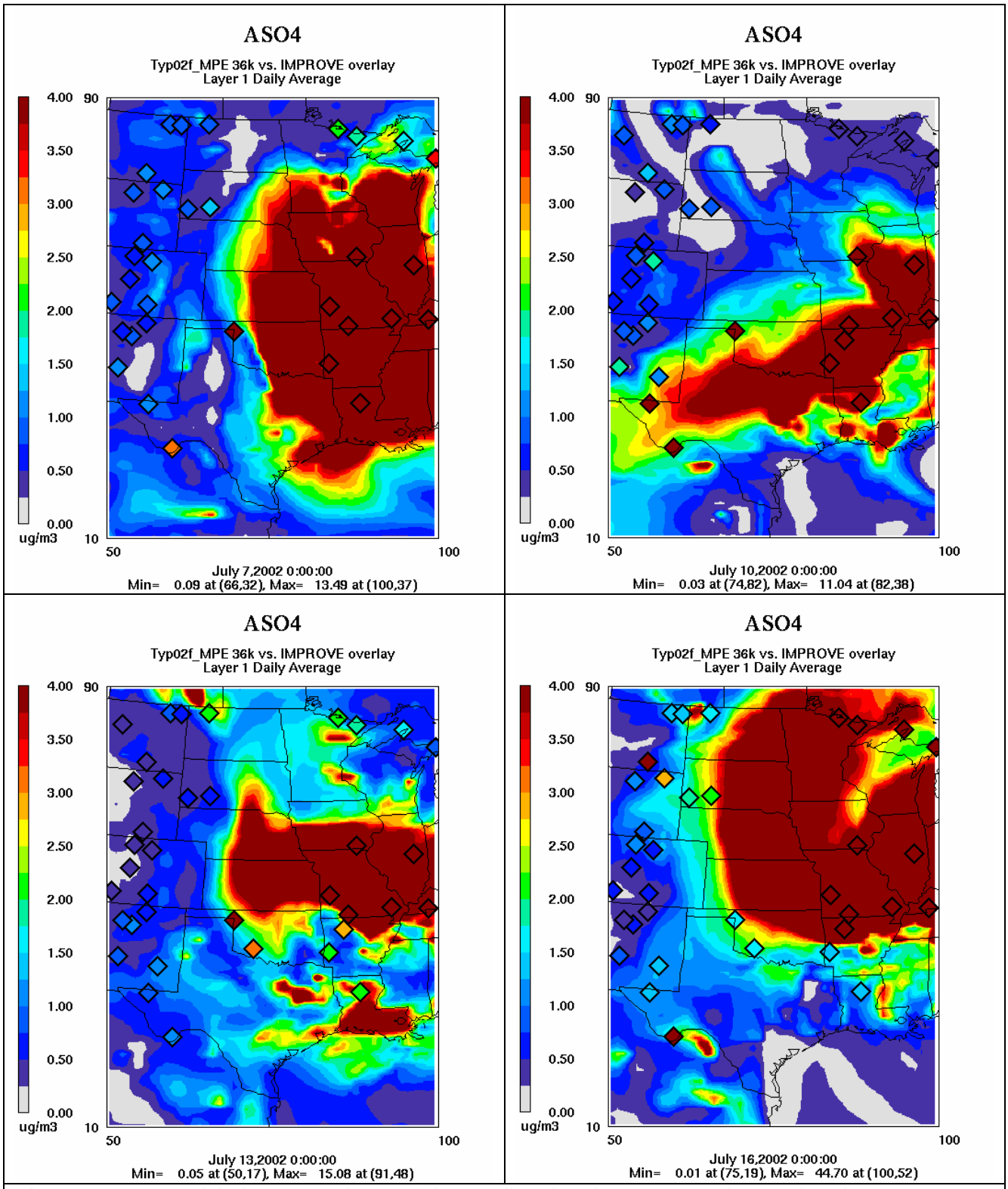

Figure C-6c. Spatial plot comparisons of the predicted and IMPROVE observed 24-hour SO4 concentrations for July 7, 10, 13 and 16, 2002.

C.3.1.4 SO4 in October 2002

In October 2002, CMAQ is doing a better job of reproducing the observed SO4 concentrations with much lower fractional bias values (-6%, 0% and -23%) and fractional errors < 40% (Figure C-7a). The observed SO4 time series are also reproduced well by the model, although an under-prediction bias is clearly evident at Big Bend, Guadalupe Mountains and Wichita Mountains. The model also reproduces the observed spatial distribution of SO4 well in October (Figure C-7c).

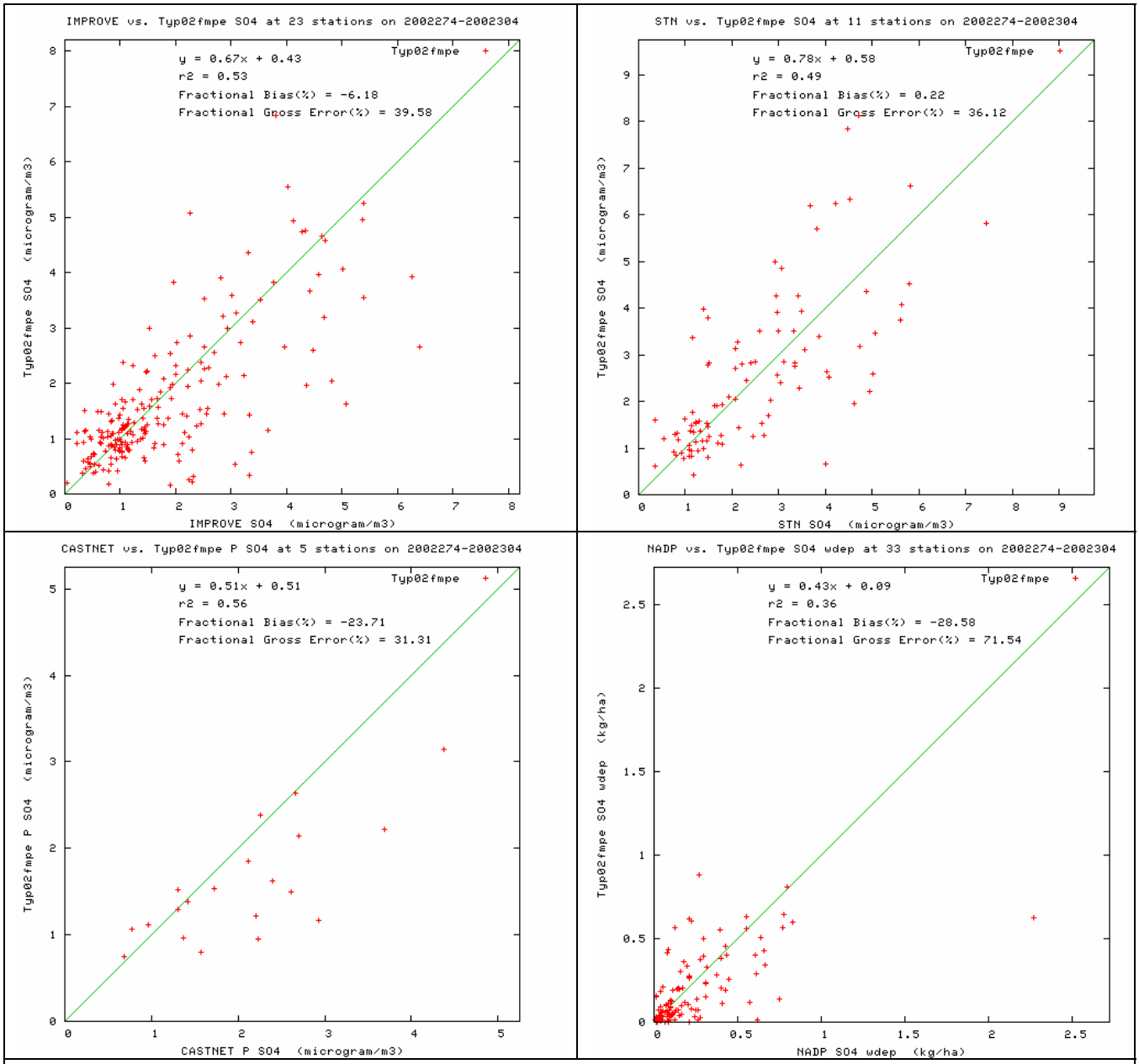

Figure C-7a. Scatter plots of predicted and observed sulfate (SO4) concentrations for October 2002 and sites in the CENRAP region using IMPROVE (top left), STN (top right), CASTNet (bottom left) and NADP monitoring networks using the CMAQ 2002 36 km Base F base case simulation.

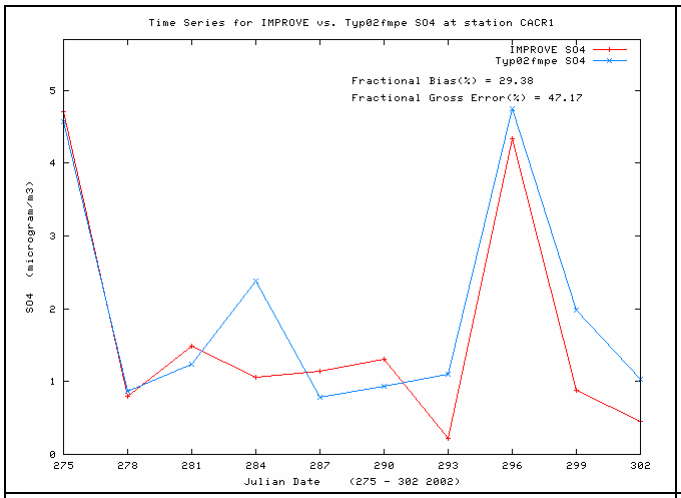
Time Series for IMPROVE vs. Typ02fmpe SO4 at station CACR1
IMPROVE SO4
Typ02fmpe SO4
Fractional Bias(%) = 29.38
Fractional Gross Error(%) = 47.17
SO4 (microgram/m3)
Julian Date (275 - 302 2002)

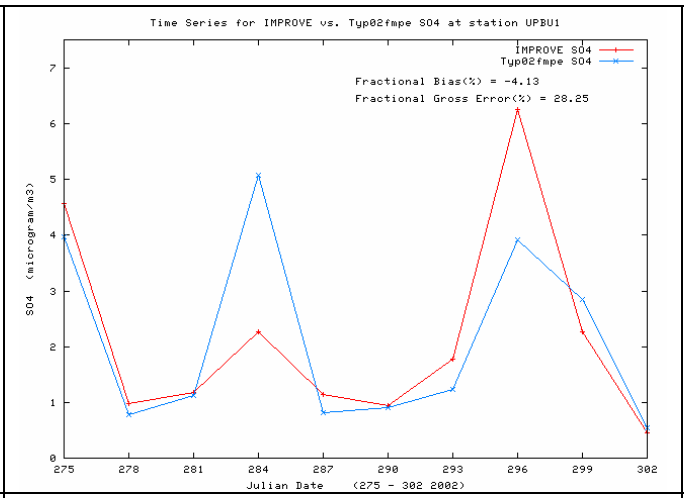
Time Series for IMPROVE vs. Typ02fmpe SO4 at station UPBU1
IMPROVE SO4
Typ02fmpe SO4
Fractional Bias(%) = -4.13
Fractional Gross Error(%) = 28.25
SO4 (microgram/m3)
Julian Date (275 - 302 2002)

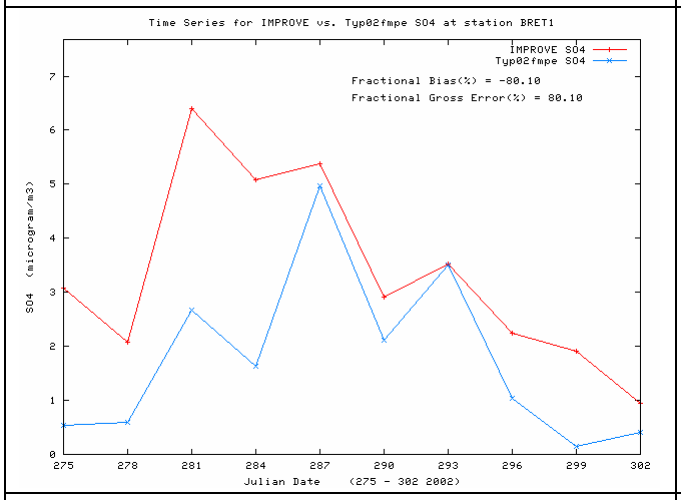
Time Series for IMPROVE vs. Typ02fmpe SO4 at station BRET1
IMPROVE SO4
Typ02fmpe SO4
Fractional Bias(%) = -80.10
Fractional Gross Error(%) = 80.10
SO4 (microgram/m3)
Julian Date (275 - 302 2002)

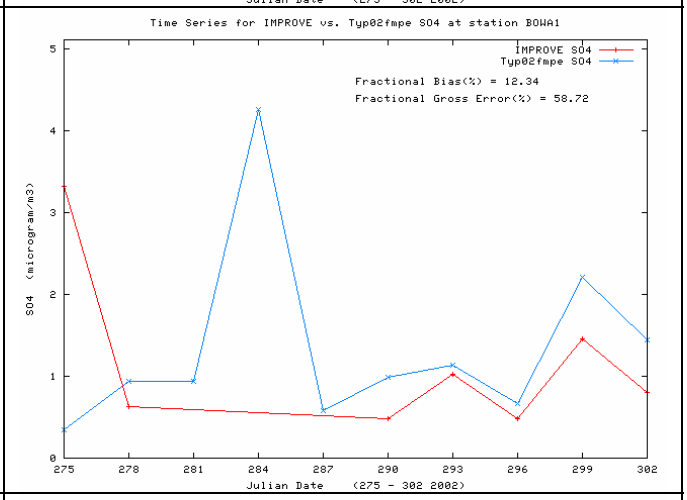
Time Series for IMPROVE vs. Typ02fmpe SO4 at station BOWA1
IMPROVE SO4
Typ02fmpe SO4
Fractional Bias(%) = 12.34
Fractional Gross Error(%) = 58.72
SO4 (microgram/m3)
Julian Date (275 - 302 2002)

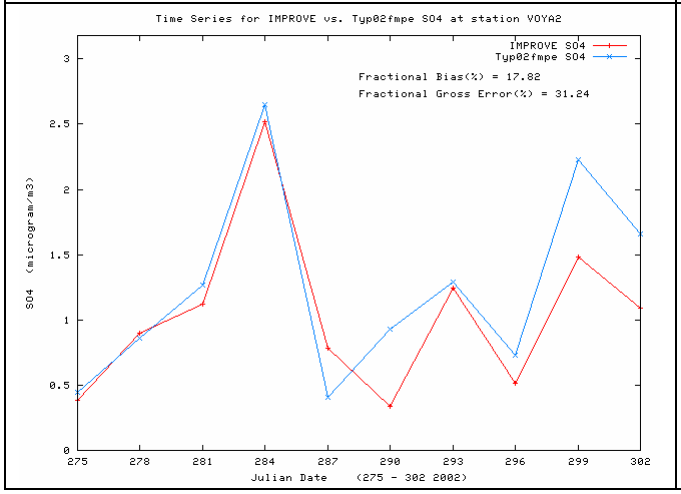
Time Series for IMPROVE vs. Typ02fmpe SO4 at station VOYA2
IMPROVE SO4
Typ02fmpe SO4
Fractional Bias(%) = 17.82
Fractional Gross Error(%) = 31.24
SO4 (microgram/m3)
Julian Date (275 - 302 2002)

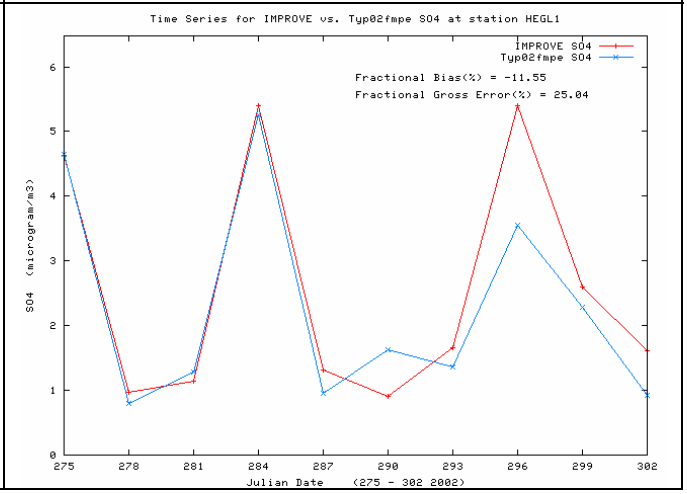
Time Series for IMPROVE vs. Typ02fmpe SO4 at station HEGL1
IMPROVE SO4
Typ02fmpe SO4
Fractional Bias(%) = -11.55
Fractional Gross Error(%) = 25.04
SO4 (microgram/m3)
Julian Date (275 - 302 2002)

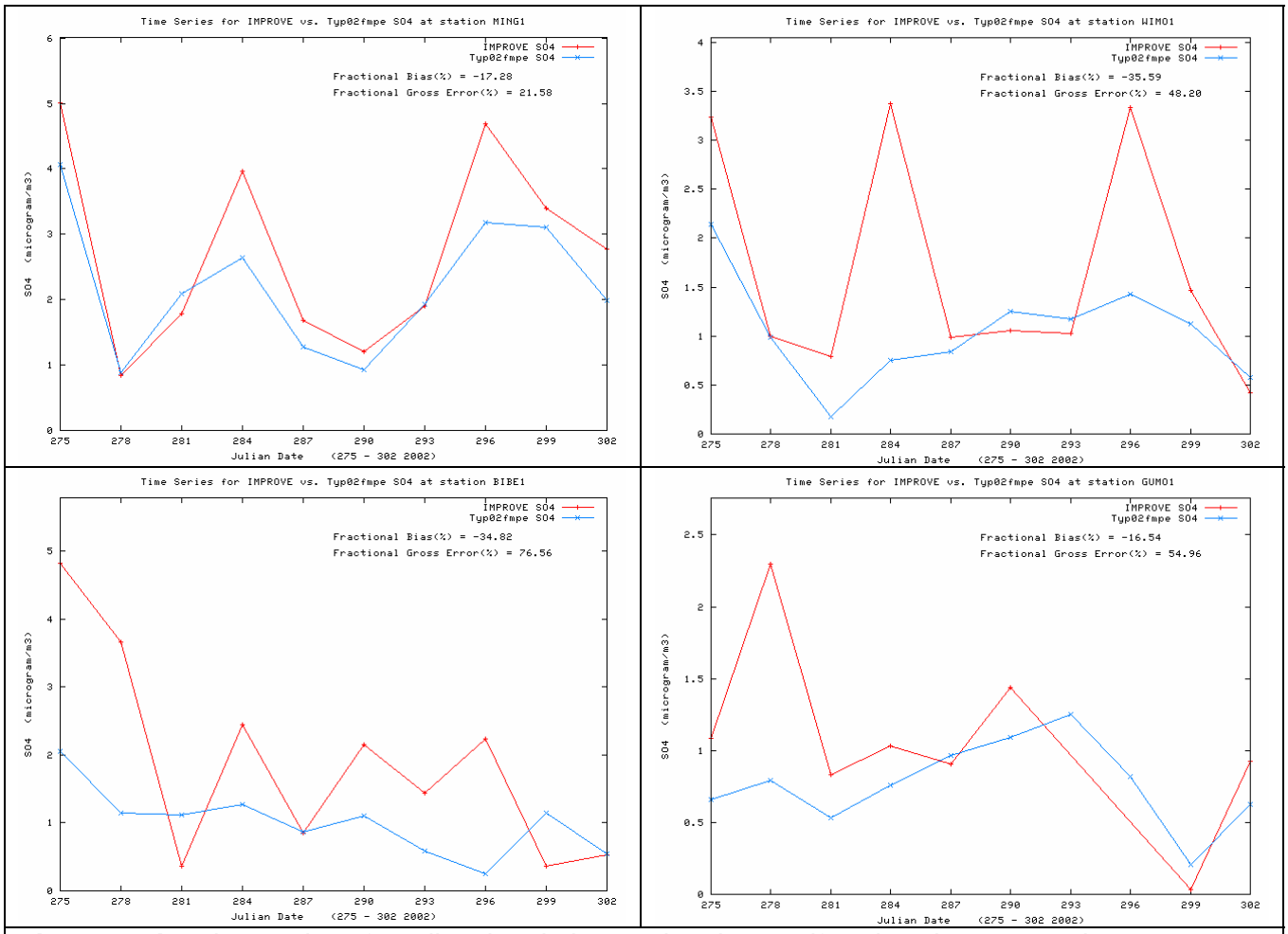

Figure C-7b. Time series of predicted and observed 24-hour sulfate (SO4) concentrations at CENRAP IMPROVE CLASS I AREA sites in October 2002 for CMAQ 2002 36 km Base F base case simulation.

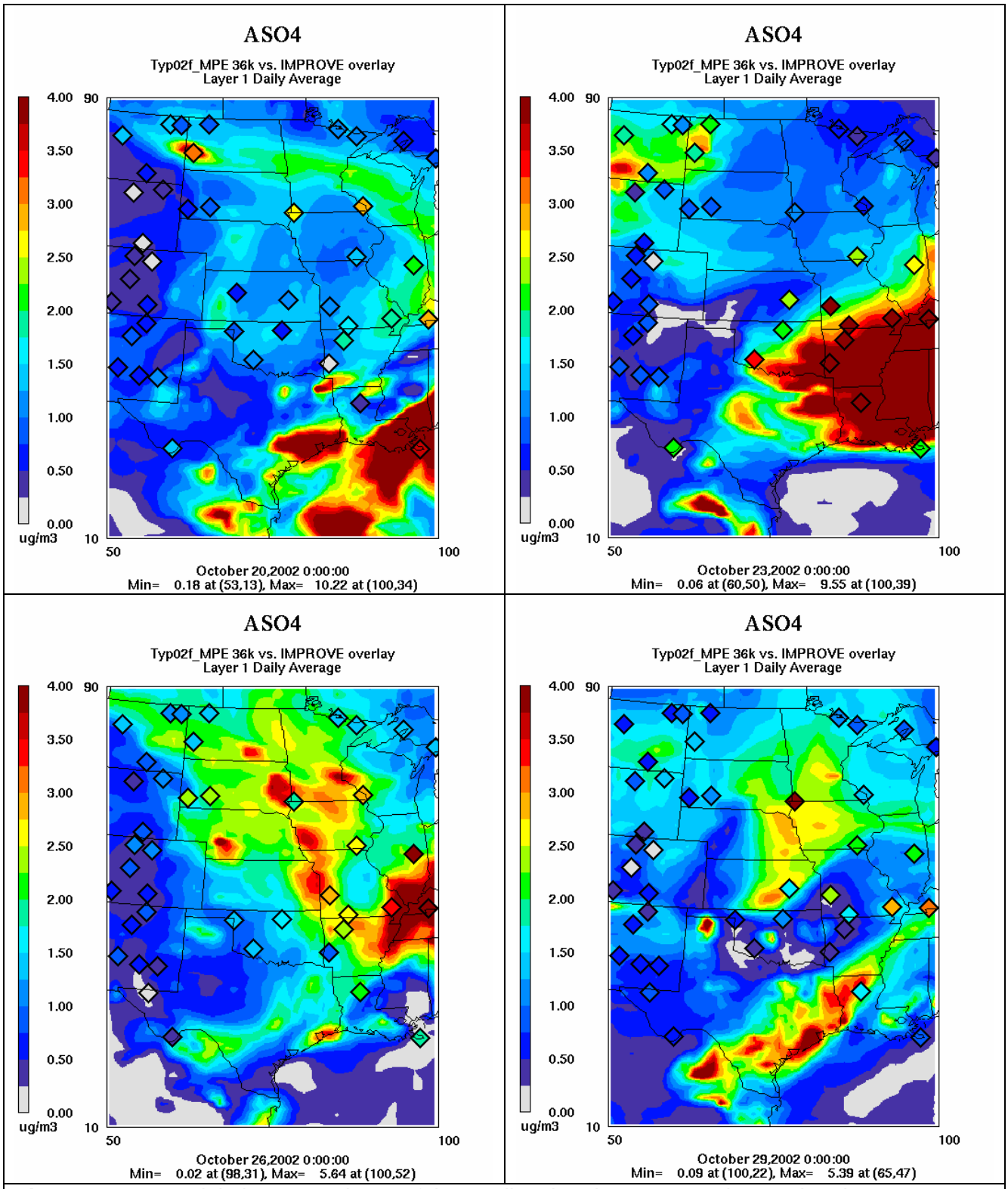

Figure C-7c. Spatial plot comparisons of the predicted and IMPROVE observed 24-hour SO4 concentrations for October 20, 23, 26 and 29, 2002.

C.3.1.5 SO4 Monthly Bias and Error

Figure C-8 compares the monthly SO4 fractional bias and error across the CENRAP region for the three monitoring networks. The under-prediction bias is clearly evident the first 8-10 months of the year. This underestimation bias is greatest across the CASTNet network which persists through out the year and is least for the STN network where it disappears by August-September. The monthly SO4 fractional errors are generally between 30% and 60% and are greatest in the summer when SO4 concentrations are the highest.

Figure C-9 presents a Bugle Plot of monthly So4 fractional bias and error statistics and compares them against the proposed PM model performance goal and criteria (see Table C-3). For the STN network, it appears that SO4 performance for all months achieves the proposed PM model performance goal. For the IMPROVE network, approximately half of the months achieve the proposed PM performance goal with the other half exceed the goal but within the performance criteria. Across the CASTNet network most months exceed the proposed goal and are within the criteria. Although the CASTNet fractional bias for some months is right at the criteria ($\leq \pm 60\%$). With the exception of two IMPROVE months, all of the monthly SO4 fractional error performance statistics achieve the proposed PM model performance goal.

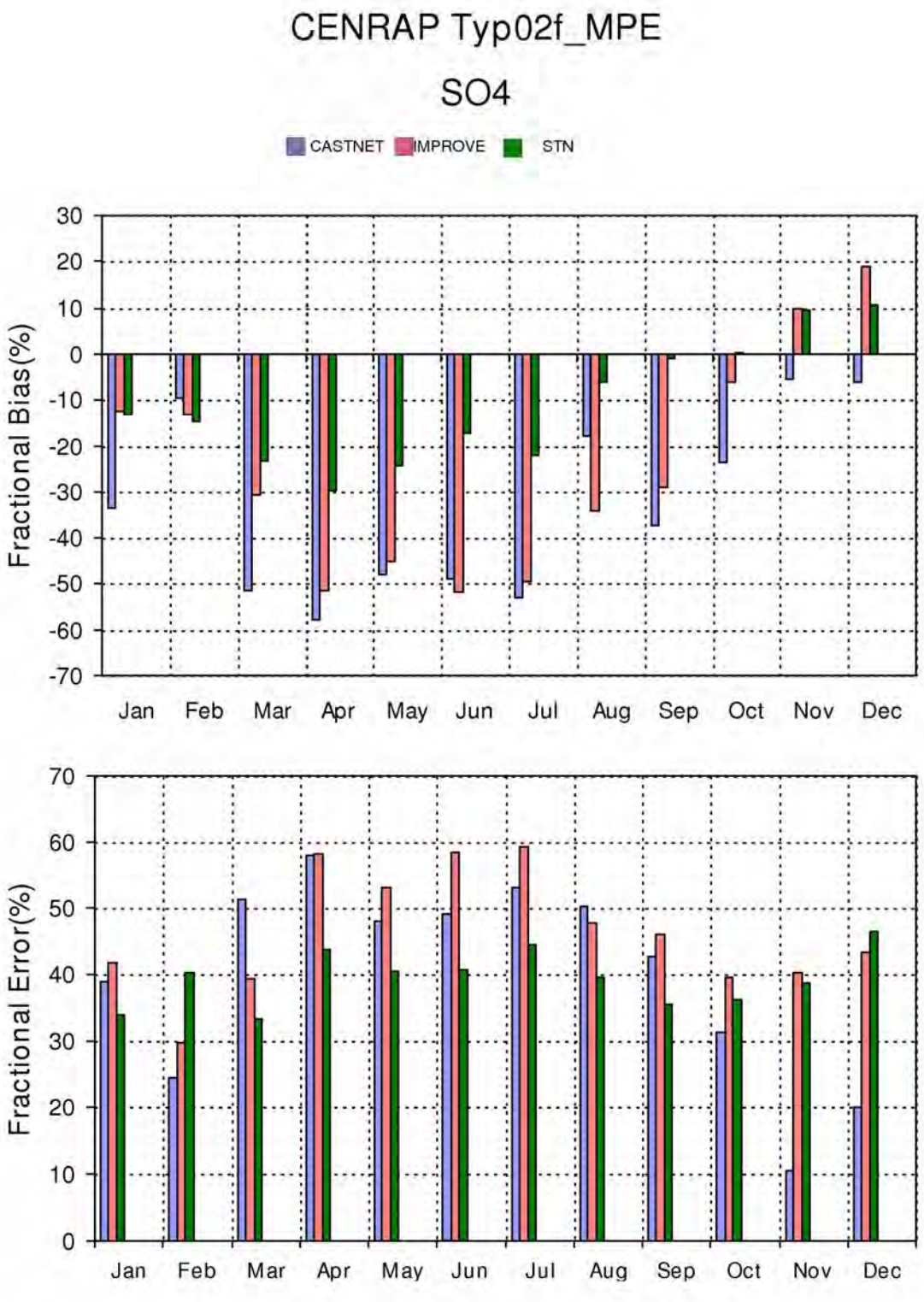

Figure C-8. Monthly SO4 fractional bias (top) and fractional gross error (bottom) statistical measures for IMPROVE, STN and CASTNet monitoring sites in the CENRAP region.

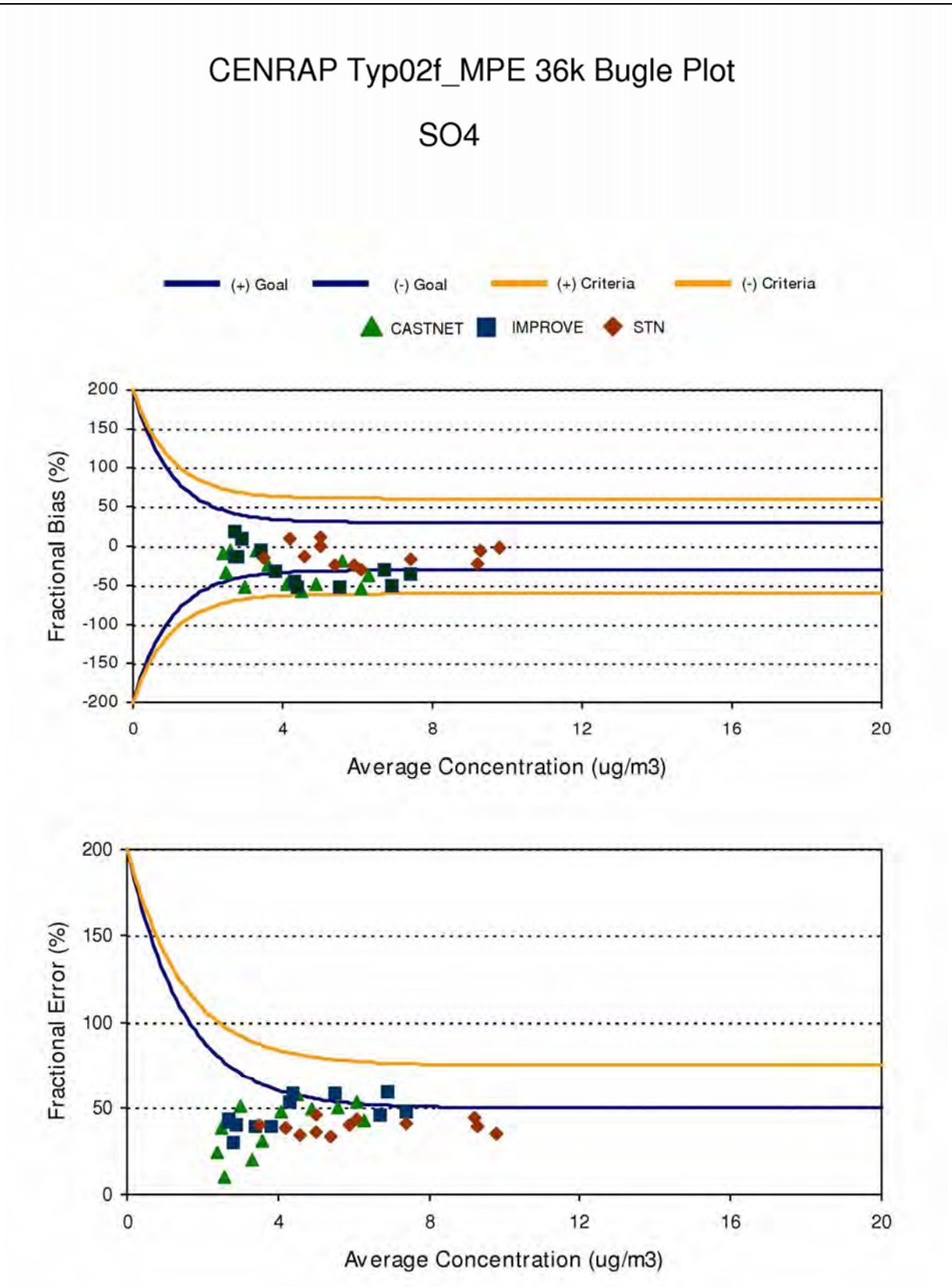

Figure C-9. Bugle Plots of monthly fractional bias (top) and fractional gross error (bottom) and comparisons with model performance goals and criteria for SO4 and IMPROVE, STN and CASTNet monitoring sites in the CENRAP region.

C.3.2 Nitrate (NO3) Monthly Model Performance

The following sections discuss the monthly NO3 model performance across the IMPROVE, STN and CASTNet monitoring networks in the CENRAP region.

C.3.2.1 NO3 in January 2002

January NO3 CMAQ model performance is characterized by an overestimation bias across the CENRAP region (Figure C-10a). The fractional bias values for the IMPROVE, STN and CASTNet networks are 38%, 29% and 61%. Unlike SO4, wet deposition of NO3 is also overstated in January (43%). Fractional errors range from 90%-100% for the IMPROVE and CASTNet networks and are lower (54%) for the STN network and higher (114%) for the NADP network.

With the exception of Breton Island and Big Bend, the model NO3 over-prediction bias occurs at the other 8 CENRAP Class I areas (Figure C-10b). The observed time series is reproduced reasonable well at a couple sites, such as Wichita Mountains and the first half of January for Voyageurs. However, for most sites the observed NO3 time series is not reproduced very well and is extremely poorly reproduced for Breton Island, Big Bend and Guadalupe Mountains.

The model typically estimates a larger area of elevated NO3 concentrations than is observed. This is shown for January 20, 23, 26 and 29 in Figure C-10c. Whereas the model exhibits large areas of brown indicated daily average NO3 concentrations of 4 $\mu g/m^3$ or higher, the observed values of this high rarely occur and are usually limited to the central Illinois site. On January 20 the model estimates the entire eastern half of the CENRAP region should be covered by elevated NO3 concentrations, whereas the observations indicate much lower values. On January 23 the modeled elevated NO3 concentrations lies between the IMPROVE monitoring sites, although the central Illinois site suggests high NO3 did occur in the region. The observations on January 26 also suggest lower NO3 than the model is predicting. On January 29 the model estimates elevated NO3 from the central Illinois site to Wichita Mountains, Oklahoma that is supported by these two observations. In general, the model is estimating more wide-spread elevated NO3 concentrations than observed, whereas the observations suggest that the elevated NO3 occurrences is less frequent and more spotty.

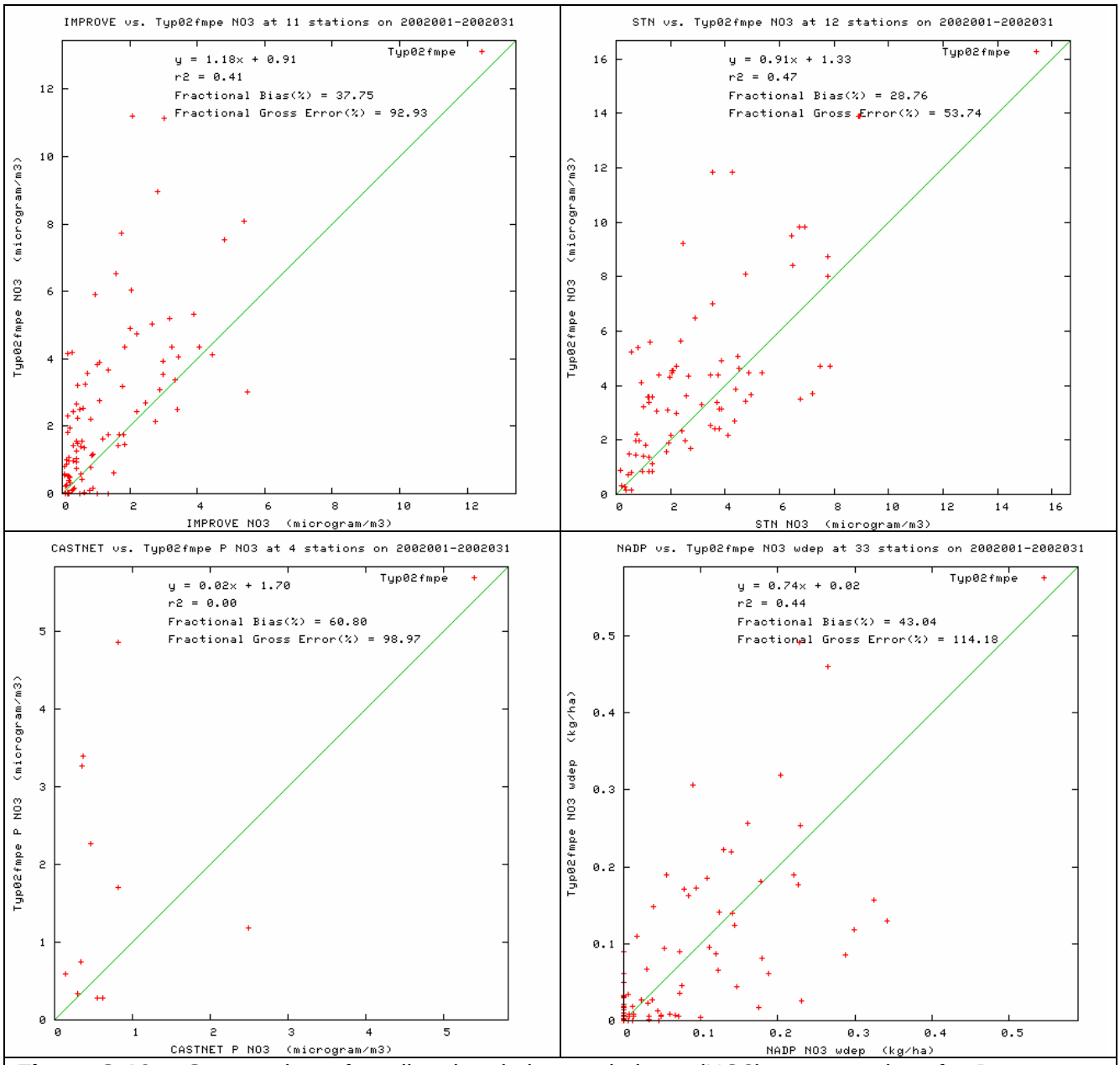

Figure C-10a. Scatter plots of predicted and observed nitrate (NO3) concentrations for January 2002 and sites in the CENRAP region using IMPROVE (top left), STN (top right), CASTNet (bottom left) and NADP monitoring networks using the CMAQ 2002 36 km Base F base case simulation.

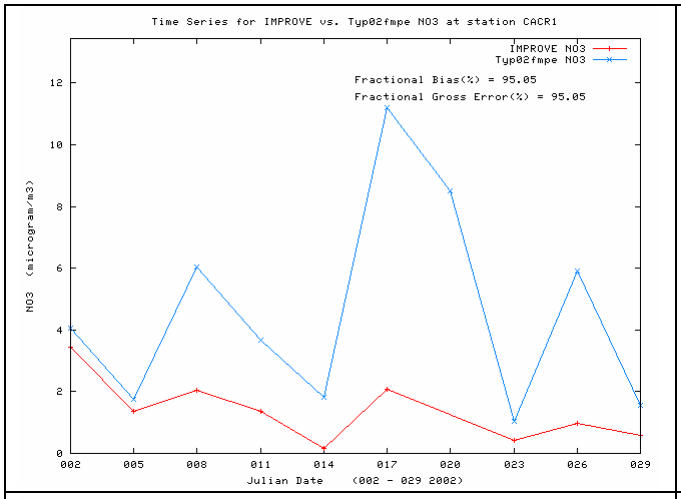
Time Series for IMPROVE vs. Typ02fmpe NO3 at station CACR1
IMPROVE NO3
Typ02fmpe NO3
Fractional Bias(%) = 95.05
Fractional Gross Error(%) = 95.05
NO3 (microgram/m3)
Julian Date (002 - 029 2002)

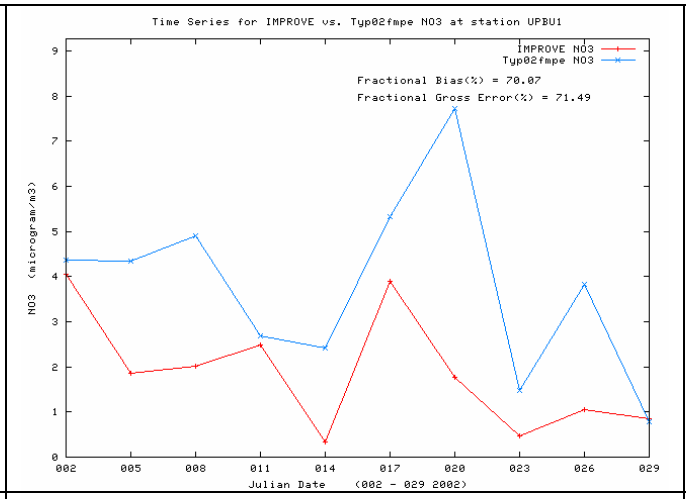
Time Series for IMPROVE vs. Typ02fmpe NO3 at station UPBU1
IMPROVE NO3
Typ02fmpe NO3
Fractional Bias(%) = 70.07
Fractional Gross Error(%) = 71.49
NO3 (microgram/m3)
Julian Date (002 - 029 2002)

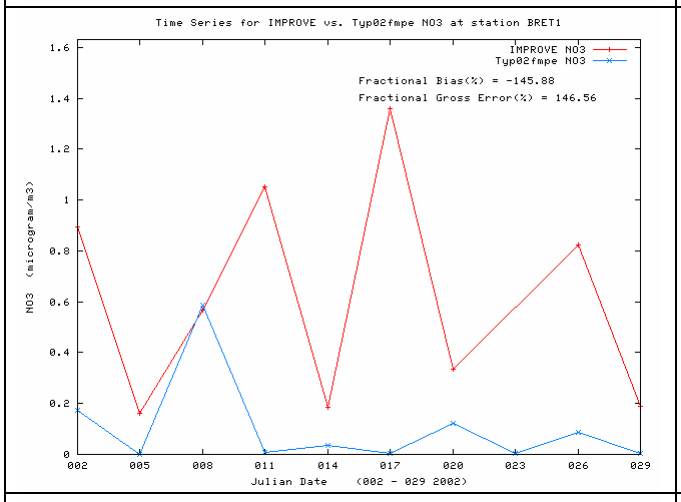
Time Series for IMPROVE vs. Typ02fmpe NO3 at station BRET1
IMPROVE NO3
Typ02fmpe NO3
Fractional Bias(%) = -145.88
Fractional Gross Error(%) = 146.56
NO3 (microgram/m3)
Julian Date (002 - 029 2002)

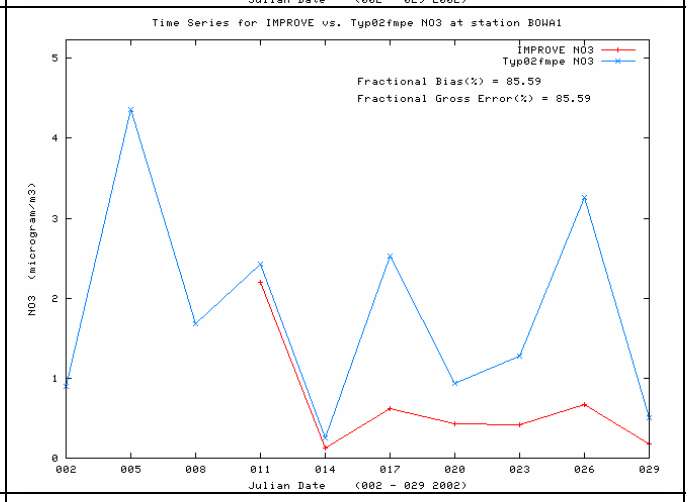
Time Series for IMPROVE vs. Typ02fmpe NO3 at station BOWA1
IMPROVE NO3
Typ02fmpe NO3
Fractional Bias(%) = 85.59
Fractional Gross Error(%) = 85.59
NO3 (microgram/m3)
Julian Date (002 - 029 2002)

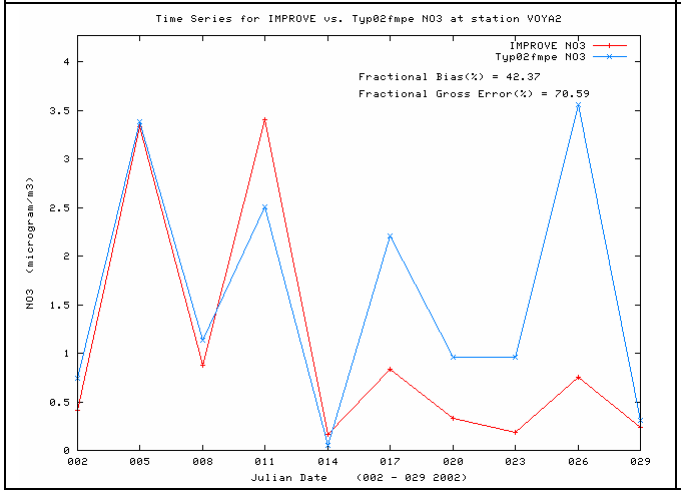
Time Series for IMPROVE vs. Typ02fmpe NO3 at station VOYA2
IMPROVE NO3
Typ02fmpe NO3
Fractional Bias(%) = 42.37
Fractional Gross Error(%) = 70.59
NO3 (microgram/m3)
Julian Date (002 - 029 2002)

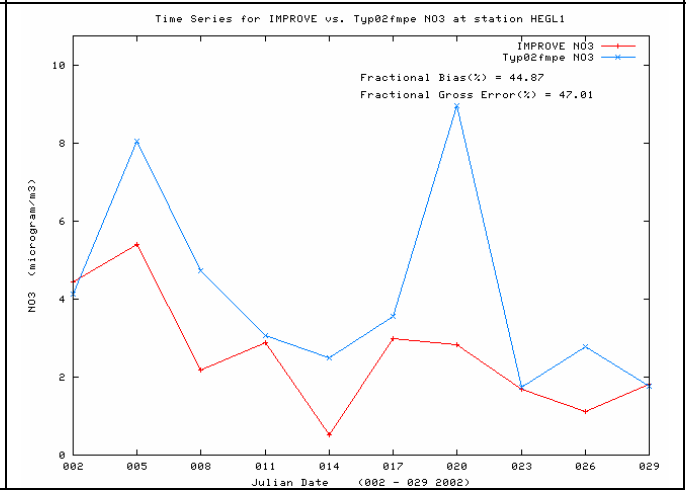
Time Series for IMPROVE vs. Typ02fmpe NO3 at station HEGL1
IMPROVE NO3
Typ02fmpe NO3
Fractional Bias(%) = 44.87
Fractional Gross Error(%) = 47.01
NO3 (microgram/m3)
Julian Date (002 - 029 2002)

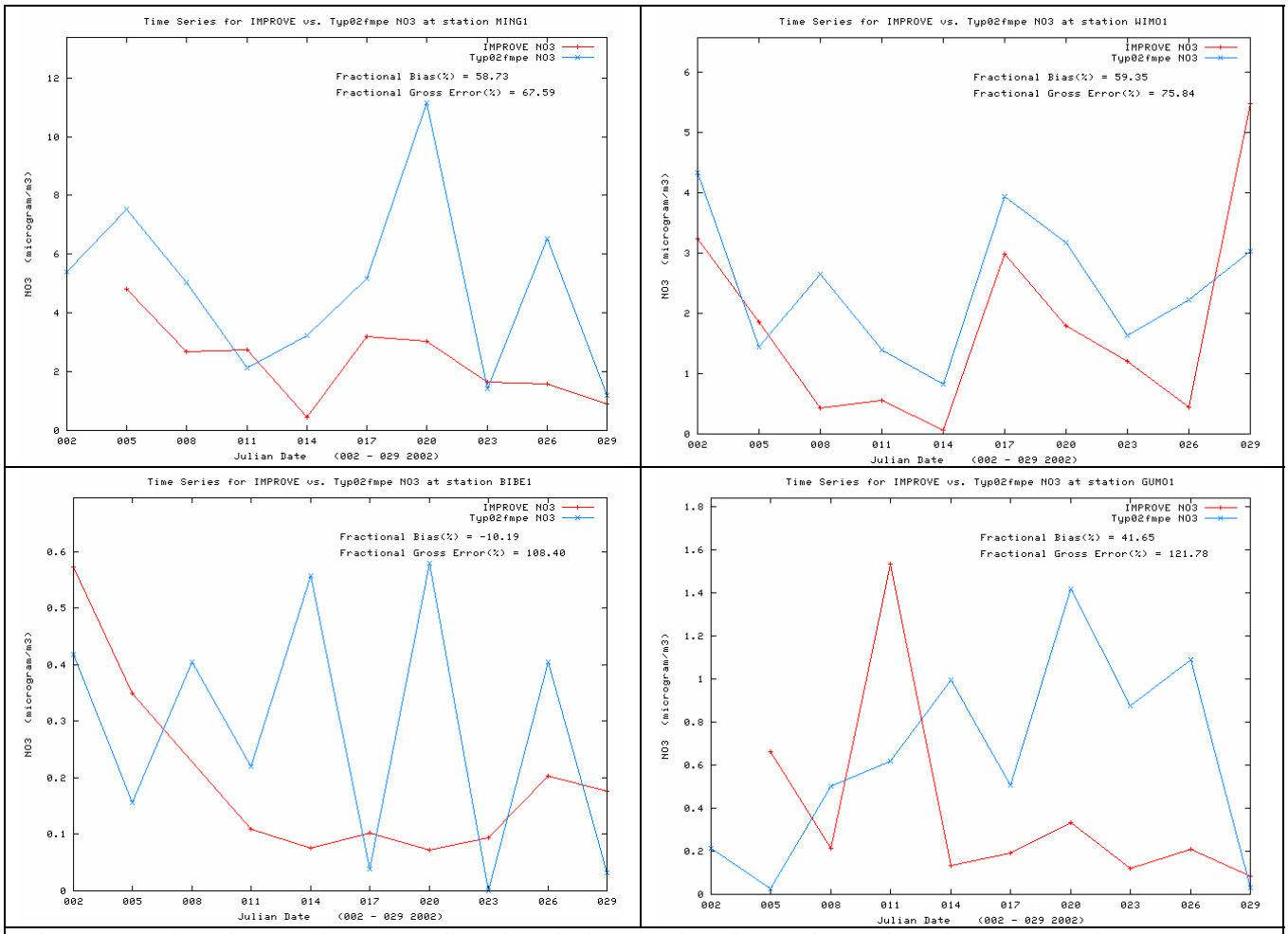

Figure C-10b. Time series of predicted and observed 24-hour nitrate (NO3) concentrations at CENRAP IMPROVE CLASS I AREA sites in January 2002 for CMAQ 2002 36 km Base F base case simulation.

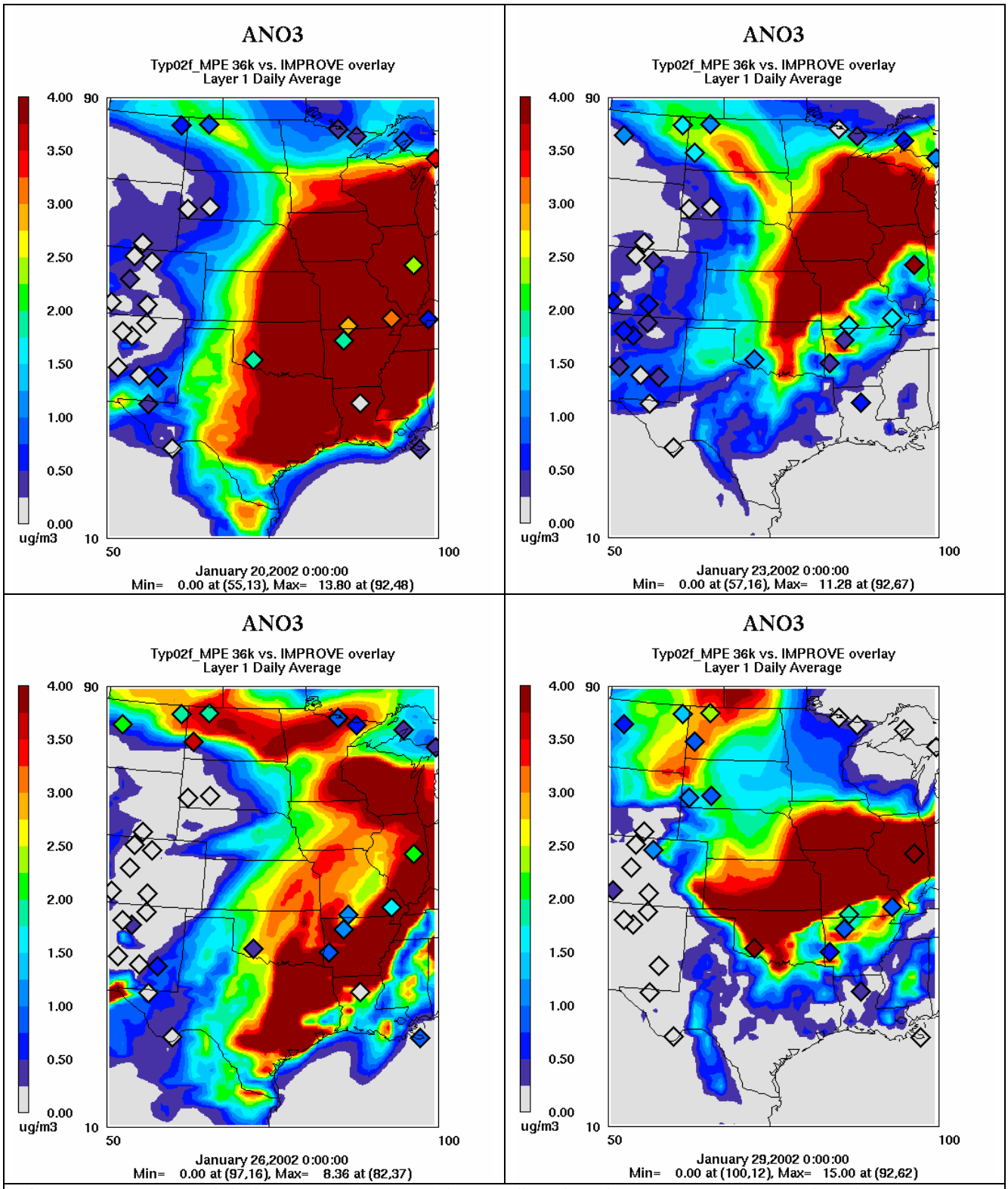

Figure C-10c. Spatial plot comparisons of the predicted and IMPROVE observed 24-hour NO3 concentrations for January 20, 23, 26 and 29, 2002.

C.3.2.2 NO3 in April 2002

Unlike the NO3 overestimation bias of January, the April NO3 performance is characterized by an underestimation bias (Figure C-11a). This under-prediction bias appears to be driven by near zero model predictions when the observed values are small (< 1 $\mu g/m^3$), but positive. This effect is especially noticeable in the NO3 time series (Figure C-11b) where at several sites the modeled NO3 concentrations foes to zero (e.g., BRET, BIBE, GUMO), whereas the observed values has an approximately 0.2 μg/m3 floor. The spatial maps suggest that the large April NO3 under-prediction bias indicated by the performance statistics is not as bad as they suggest (Figure C-11c). Mostly the model is predicting low NO3 values where low values are observed, just that the model approaches zero which results in a large relative difference with the observe values.

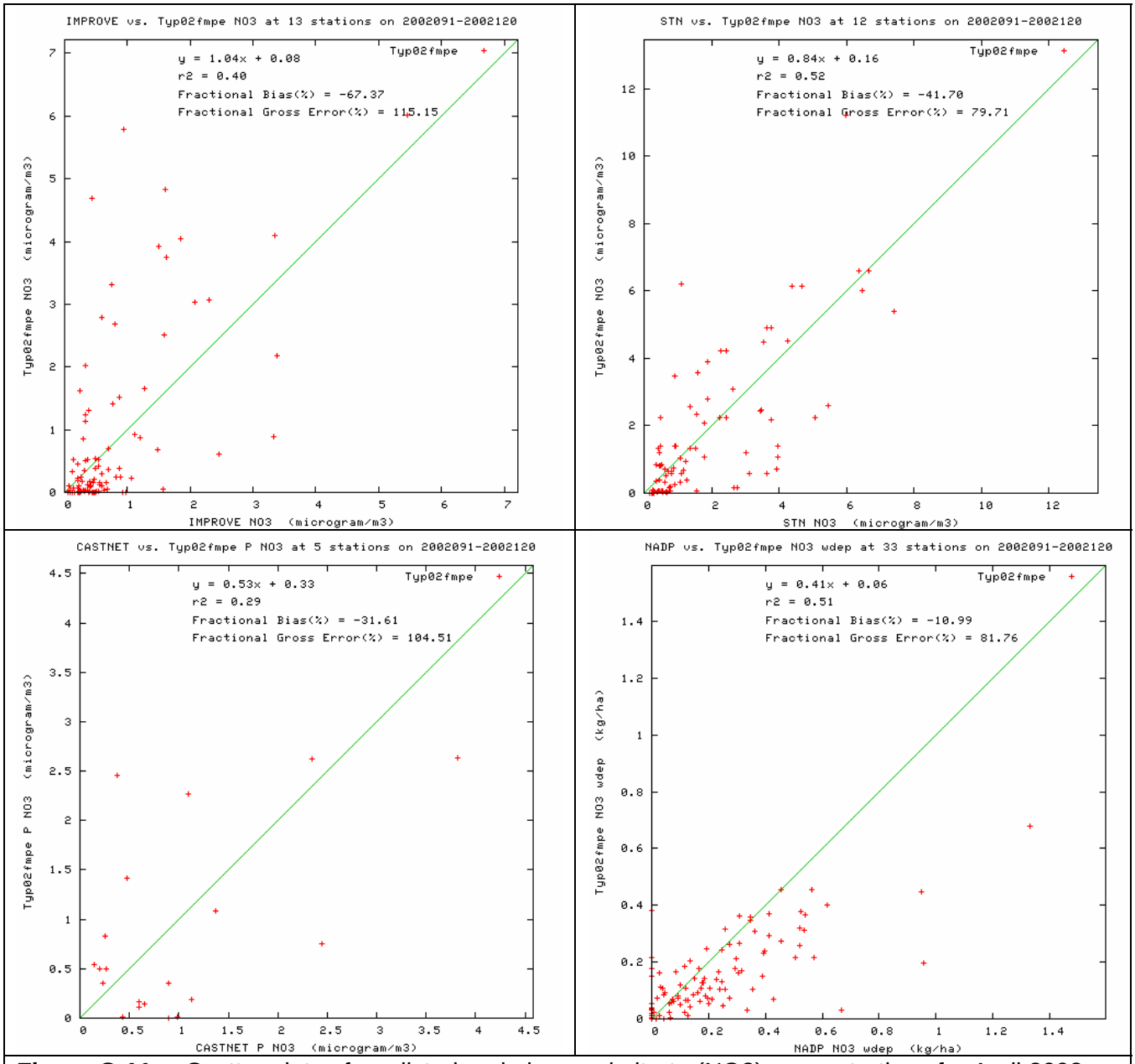

Figure C-11a. Scatter plots of predicted and observed nitrate (NO3) concentrations for April 2002 and sites in the CENRAP region using IMPROVE (top left), STN (top right), CASTNet (bottom left) and NADP monitoring networks using the CMAQ 2002 36 km Base F base case simulation.

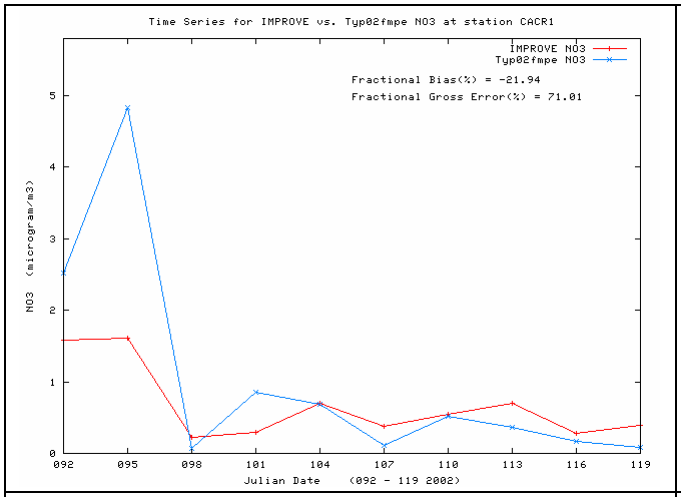
Time Series for IMPROVE vs. Typ02fmpe NO3 at station CACR1
IMPROVE NO3
Typ02fmpe NO3
Fractional Bias(%) = -21.94
Fractional Gross Error(%) = 71.01
NO3 (microgram/m3)
Julian Date (092 - 119 2002)

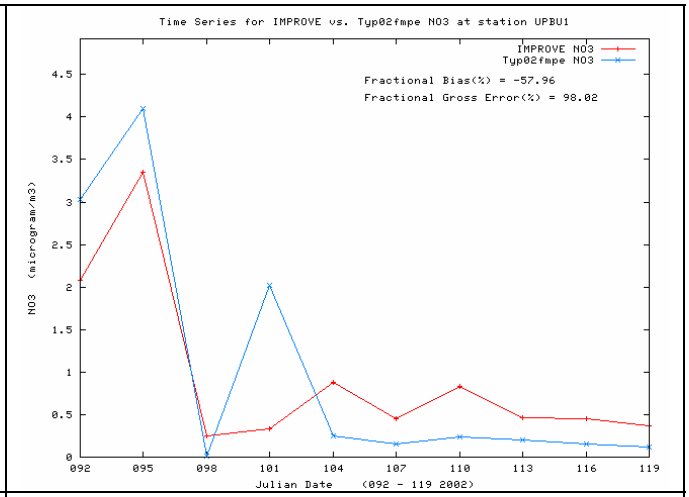
Time Series for IMPROVE vs. Typ02fmpe NO3 at station UPBU1
IMPROVE NO3
Typ02fmpe NO3
Fractional Bias(%) = -57.96
Fractional Gross Error(%) = 98.02
NO3 (microgram/m3)
Julian Date (092 - 119 2002)

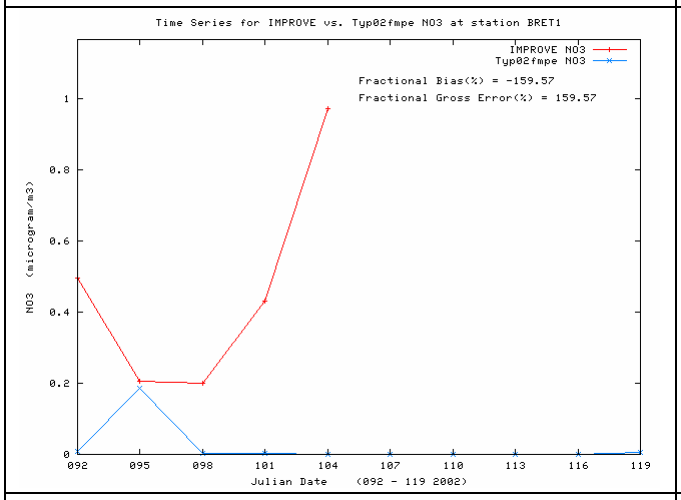
Time Series for IMPROVE vs. Typ02fmpe NO3 at station BRET1
IMPROVE NO3
Typ02fmpe NO3
Fractional Bias(%) = -159.57
Fractional Gross Error(%) = 159.57
NO3 (microgram/m3)
Julian Date (092 - 119 2002)

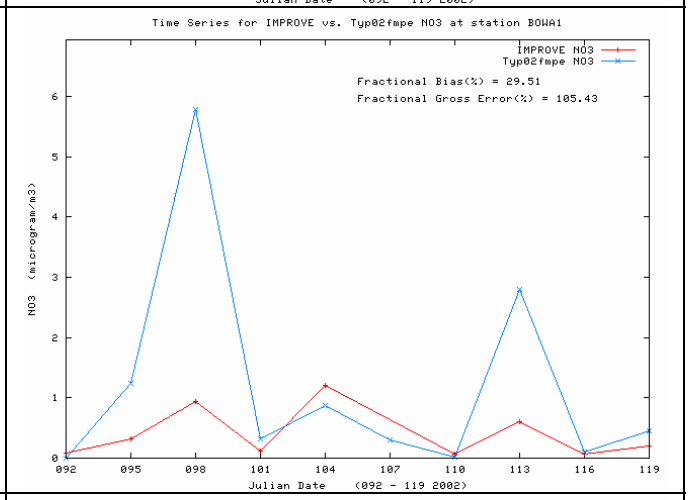
Time Series for IMPROVE vs. Typ02fmpe NO3 at station BOWA1
IMPROVE NO3
Typ02fmpe NO3
Fractional Bias(%) = 29.51
Fractional Gross Error(%) = 105.43
NO3 (microgram/m3)
Julian Date (092 - 119 2002)

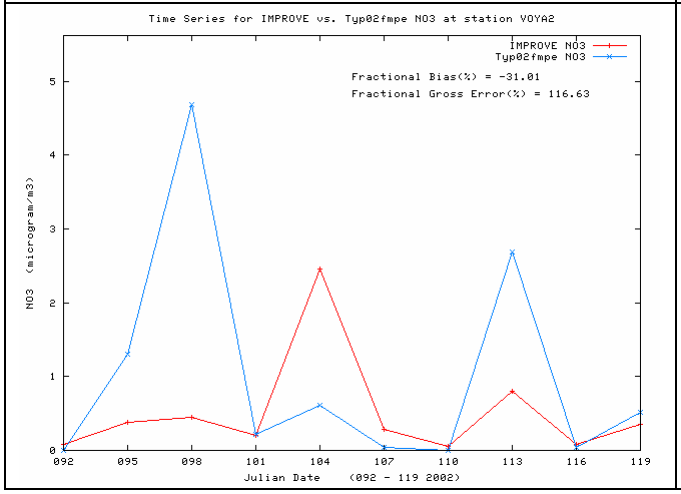
Time Series for IMPROVE vs. Typ02fmpe NO3 at station VOYA2
IMPROVE NO3
Typ02fmpe NO3
Fractional Bias(%) = -31.01
Fractional Gross Error(%) = 116.63
NO3 (microgram/m3)
Julian Date (092 - 119 2002)

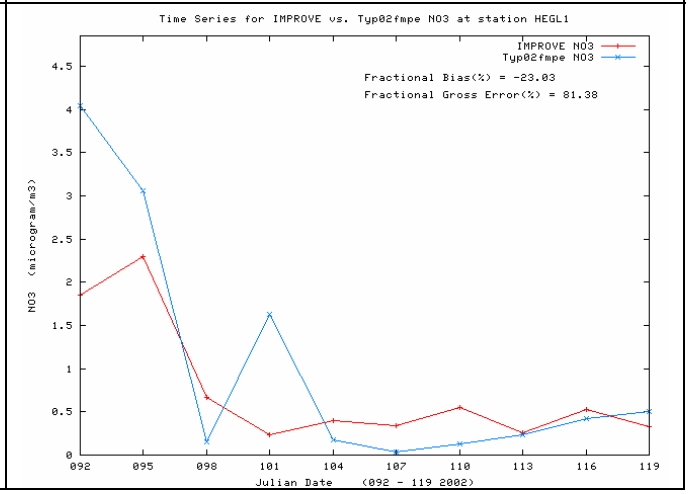
Time Series for IMPROVE vs. Typ02fmpe NO3 at station HEGL1
IMPROVE NO3
Typ02fmpe NO3
Fractional Bias(%) = -23.03
Fractional Gross Error(%) = 81.38
NO3 (microgram/m3)
Julian Date (092 - 119 2002)

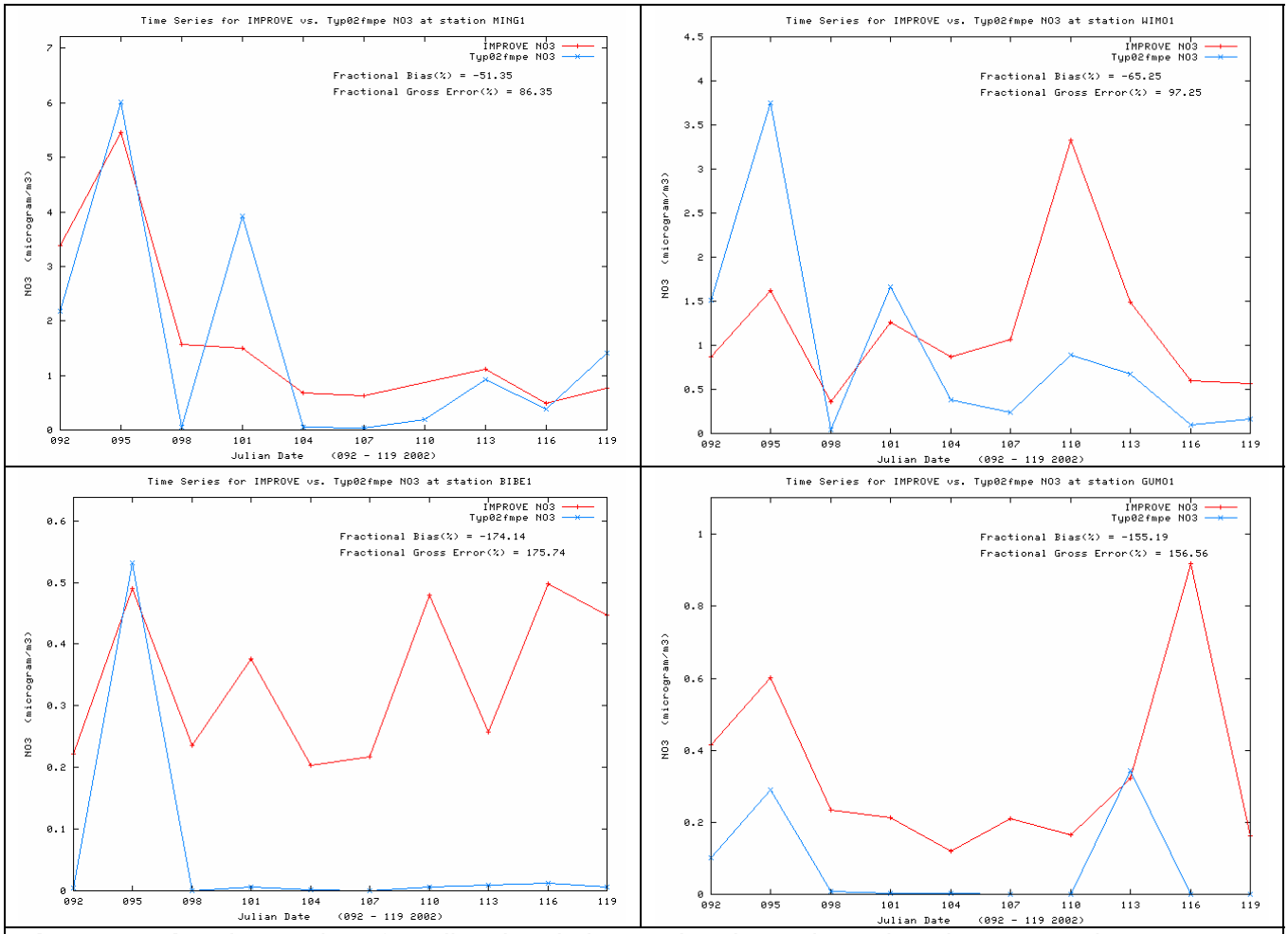

Figure C-11b. Time series of predicted and observed 24-hour nitrate (NO3) concentrations at CENRAP IMPROVE CLASS I AREA sites in April 2002 for CMAQ 2002 36 km Base F base case simulation.

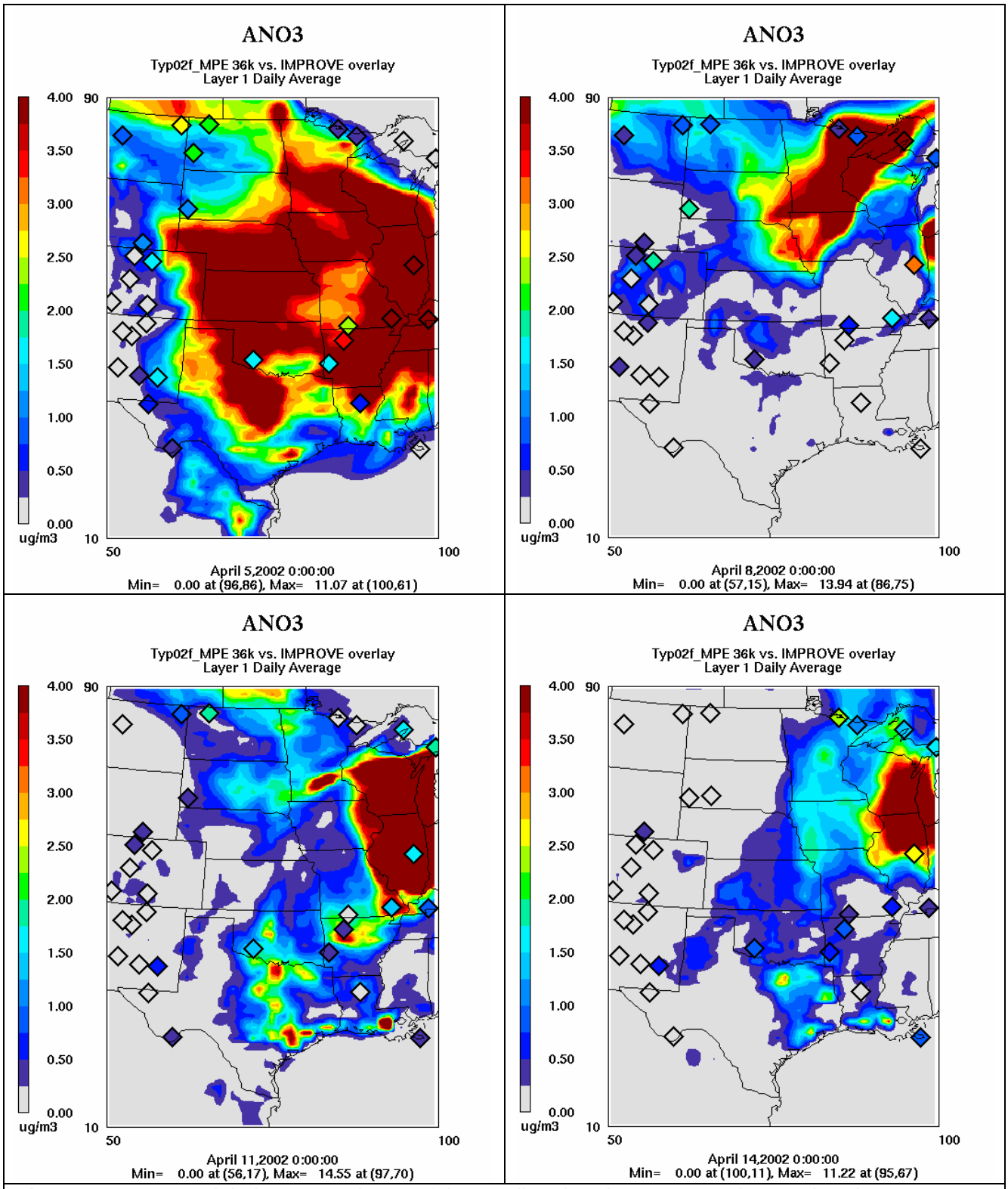

Figure C-11c. Spatial plot comparisons of the predicted and IMPROVE observed 24-hour NO3 concentrations for April 5, 8, 11 and 14, 2002.

C.3.2.3 NO3 in July 2002

NO3 performance in July 2002 is also characterized by a large under-prediction bias that is driven by the frequent occurrence of near zero modeled values (Figure C-12). Both the model and observations agree that NO3 is mostly extremely low in July, just the model produces near zero values and resultant poor performance statistics.

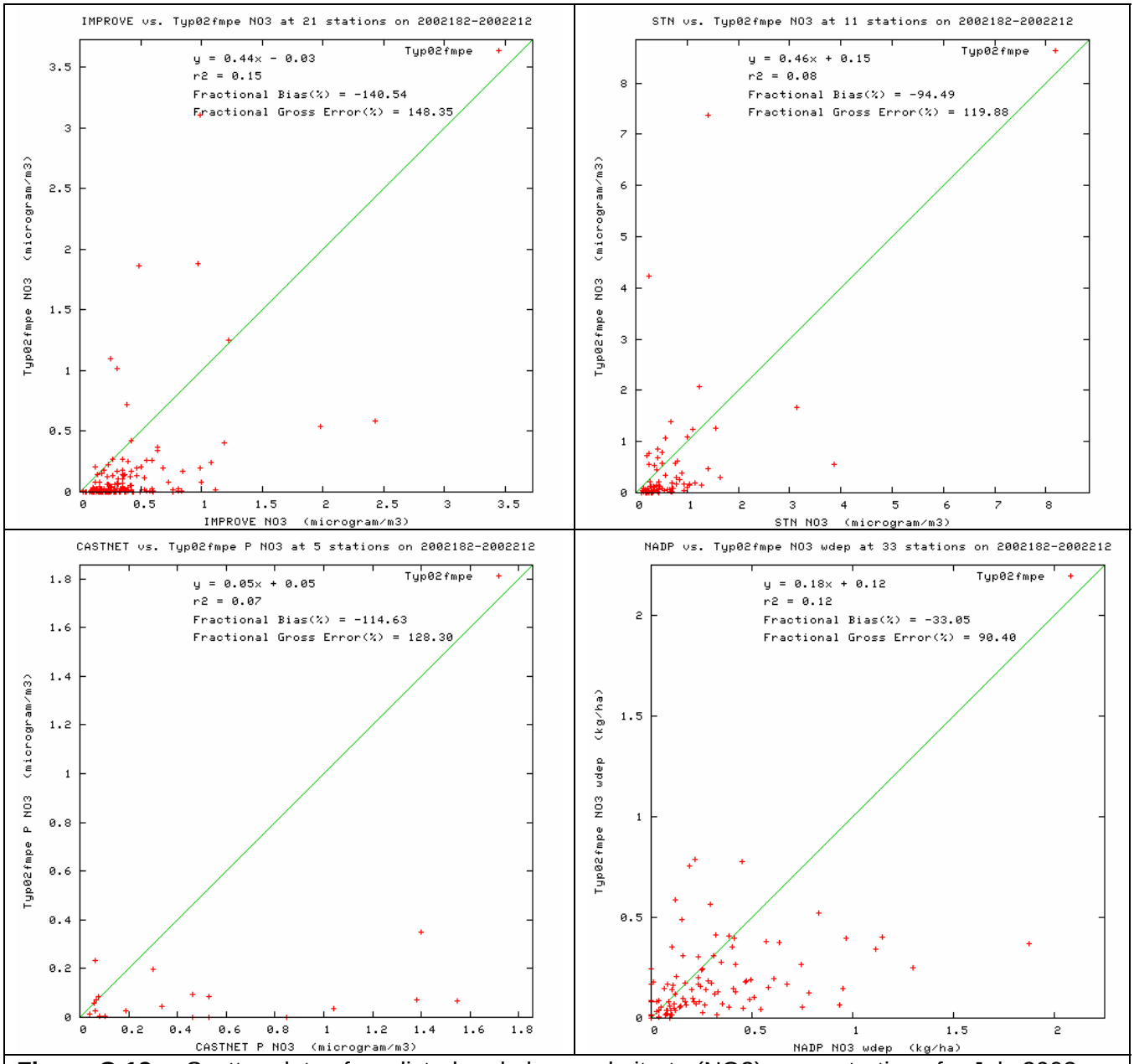

Figure C-12a. Scatter plots of predicted and observed nitrate (NO3) concentrations for July 2002 and sites in the CENRAP region using IMPROVE (top left), STN (top right), CASTNet (bottom left) and NADP monitoring networks using the CMAQ 2002 36 km Base F base case simulation.

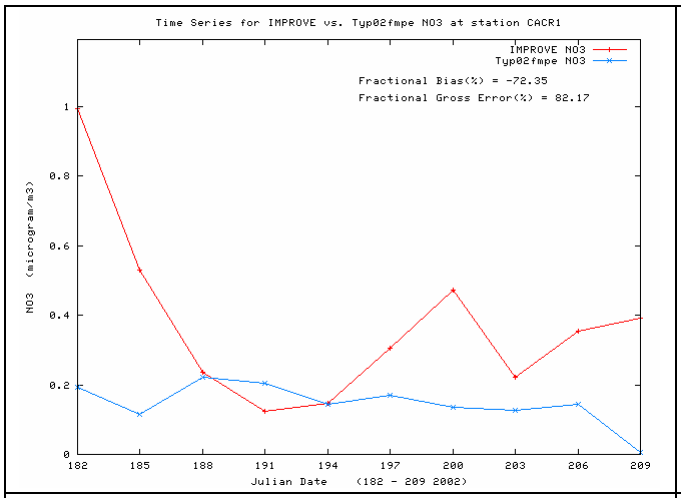
Time Series for IMPROVE vs. Typ02fmpe NO3 at station CACR1
IMPROVE NO3
Typ02fmpe NO3
Fractional Bias(%) = -72.35
Fractional Gross Error(%) = 82.17
NO3 (microgram/m3)
Julian Date (182 - 209 2002)

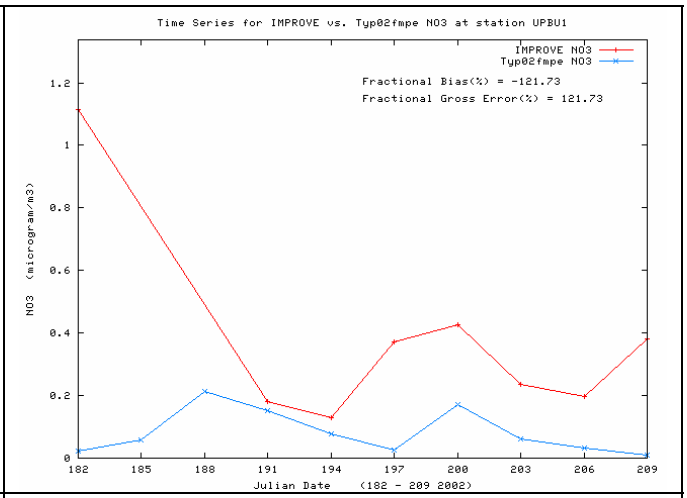
Time Series for IMPROVE vs. Typ02fmpe NO3 at station UPBU1
IMPROVE NO3
Typ02fmpe NO3
Fractional Bias(%) = -121.73
Fractional Gross Error(%) = 121.73
NO3 (microgram/m3)
Julian Date (182 - 209 2002)

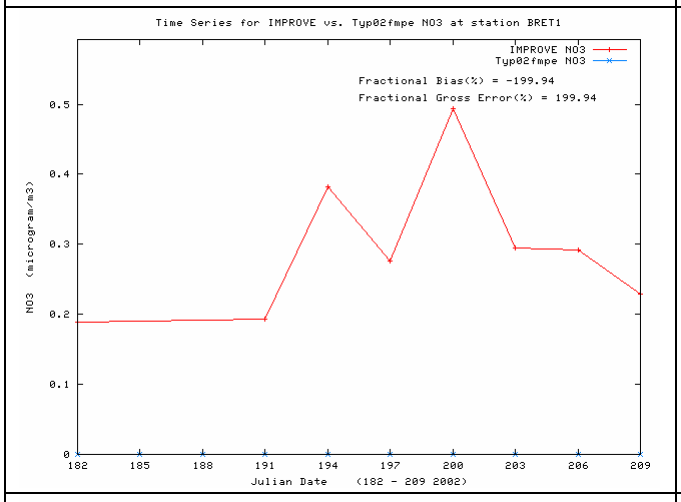
Time Series for IMPROVE vs. Typ02fmpe NO3 at station BRET1
IMPROVE NO3
Typ02fmpe NO3
Fractional Bias(%) = -199.94
Fractional Gross Error(%) = 199.94
NO3 (microgram/m3)
Julian Date (182 - 209 2002)

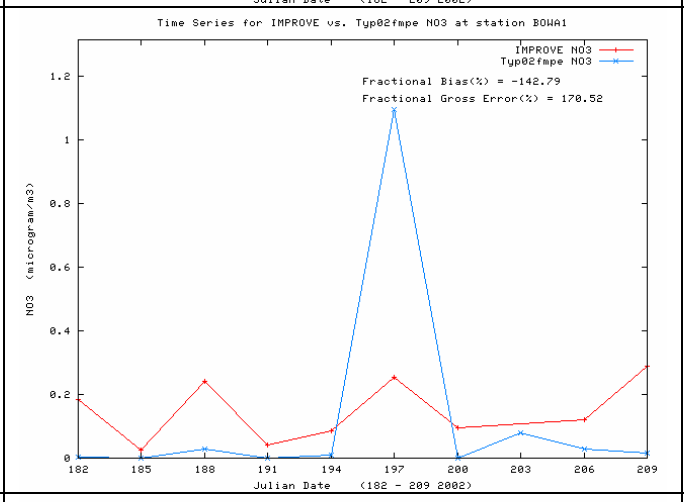
Time Series for IMPROVE vs. Typ02fmpe NO3 at station BOWA1
IMPROVE NO3
Typ02fmpe NO3
Fractional Bias(%) = -142.79
Fractional Gross Error(%) = 170.52
NO3 (microgram/m3)
Julian Date (182 - 209 2002)

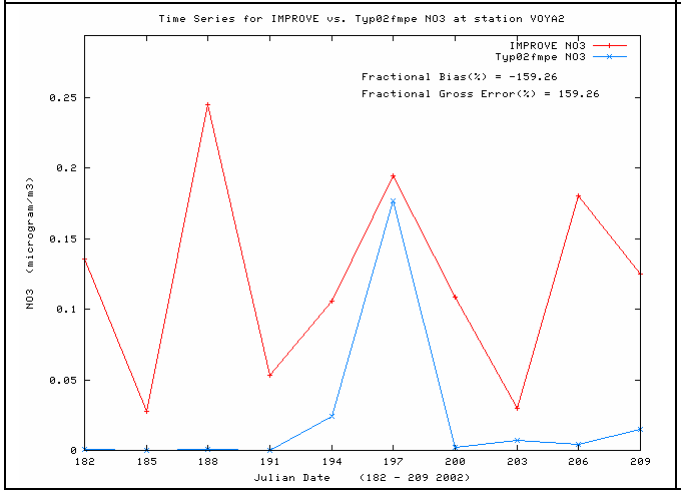
Time Series for IMPROVE vs. Typ02fmpe NO3 at station VOYA2
IMPROVE NO3
Typ02fmpe NO3
Fractional Bias(%) = -159.26
Fractional Gross Error(%) = 159.26
NO3 (microgram/m3)
Julian Date (182 - 209 2002)


Time Series for IMPROVE vs. Typ02fmpe NO3 at station HEGL1
IMPROVE NO3
Typ02fmpe NO3
Fractional Bias(%) = -118.31
Fractional Gross Error(%) = 118.31
NO3 (microgram/m3)
Julian Date (182 - 209 2002)

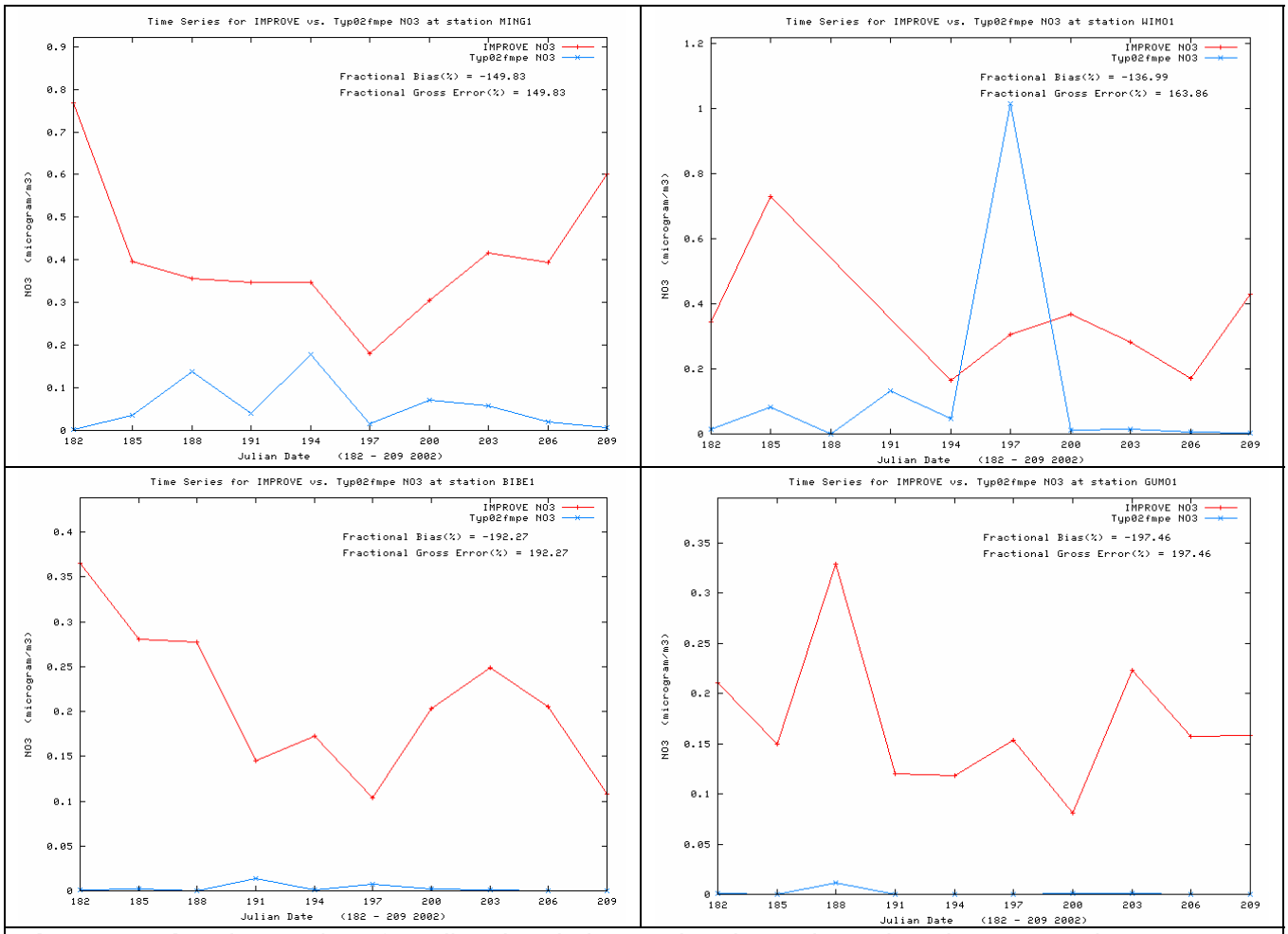

Figure C-12b. Time series of predicted and observed 24-hour nitrate (NO3) concentrations at CENRAP IMPROVE CLASS I AREA sites in July 2002 for CMAQ 2002 36 km Base F base case simulation.

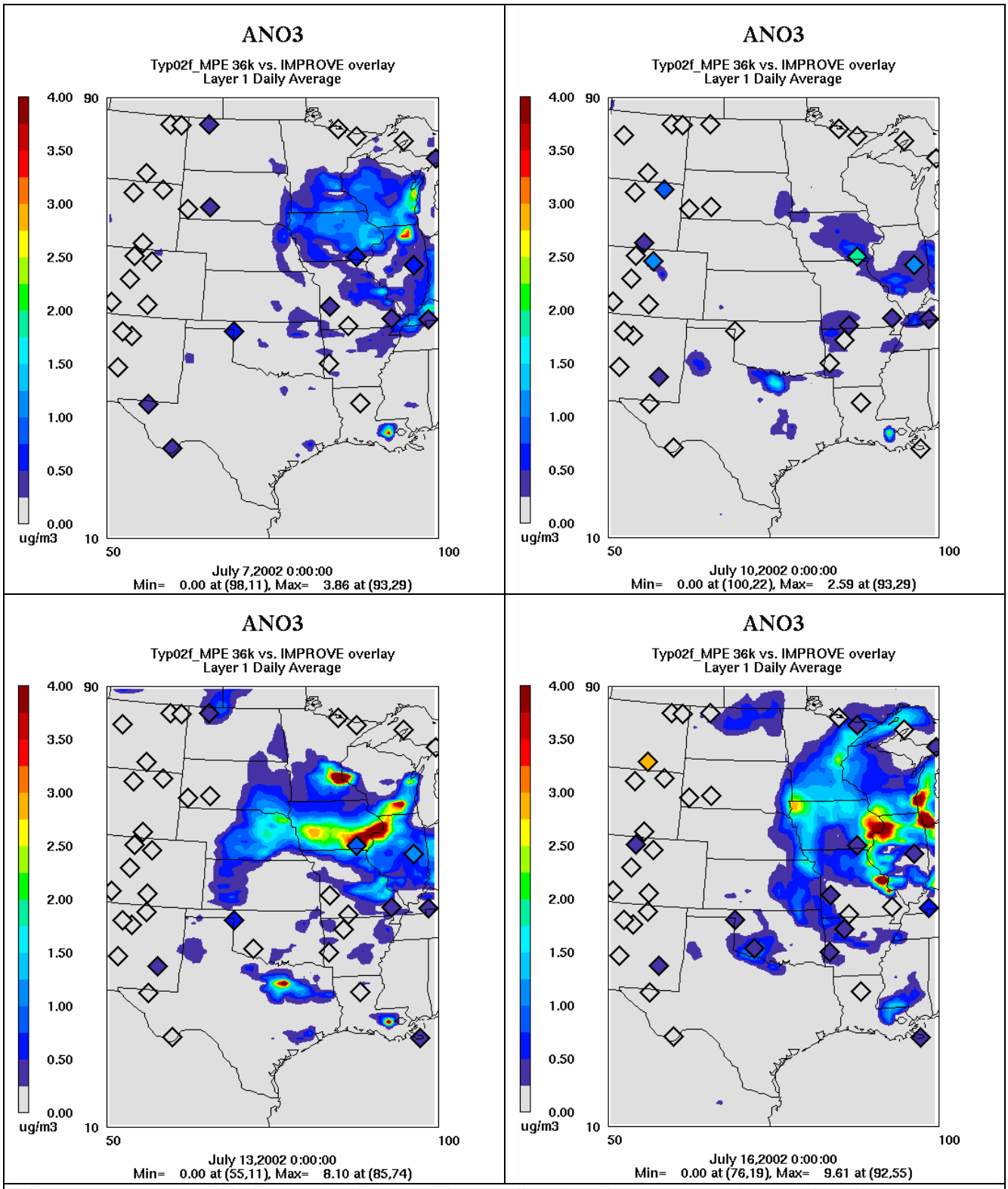

Figure C-12c. Spatial plot comparisons of the predicted and IMPROVE observed 24-hour NO3 concentrations for July 7, 10, 13 and 16, 2002.

C.3.2.4 NO3 in October 2002

Like January and unlike April and July, in October the model has a net NO3 overestimation bias of about 30%-40% (Figure C-13a). This overestimation bias occurs at all sites but BRET, BIBE and GUMO that exhibit a NO3 underestimation bias (Figure C-13b). The spatial maps suggest that the modeled elevated NO3 concentrations are more wide-spread and less spotty than observed.

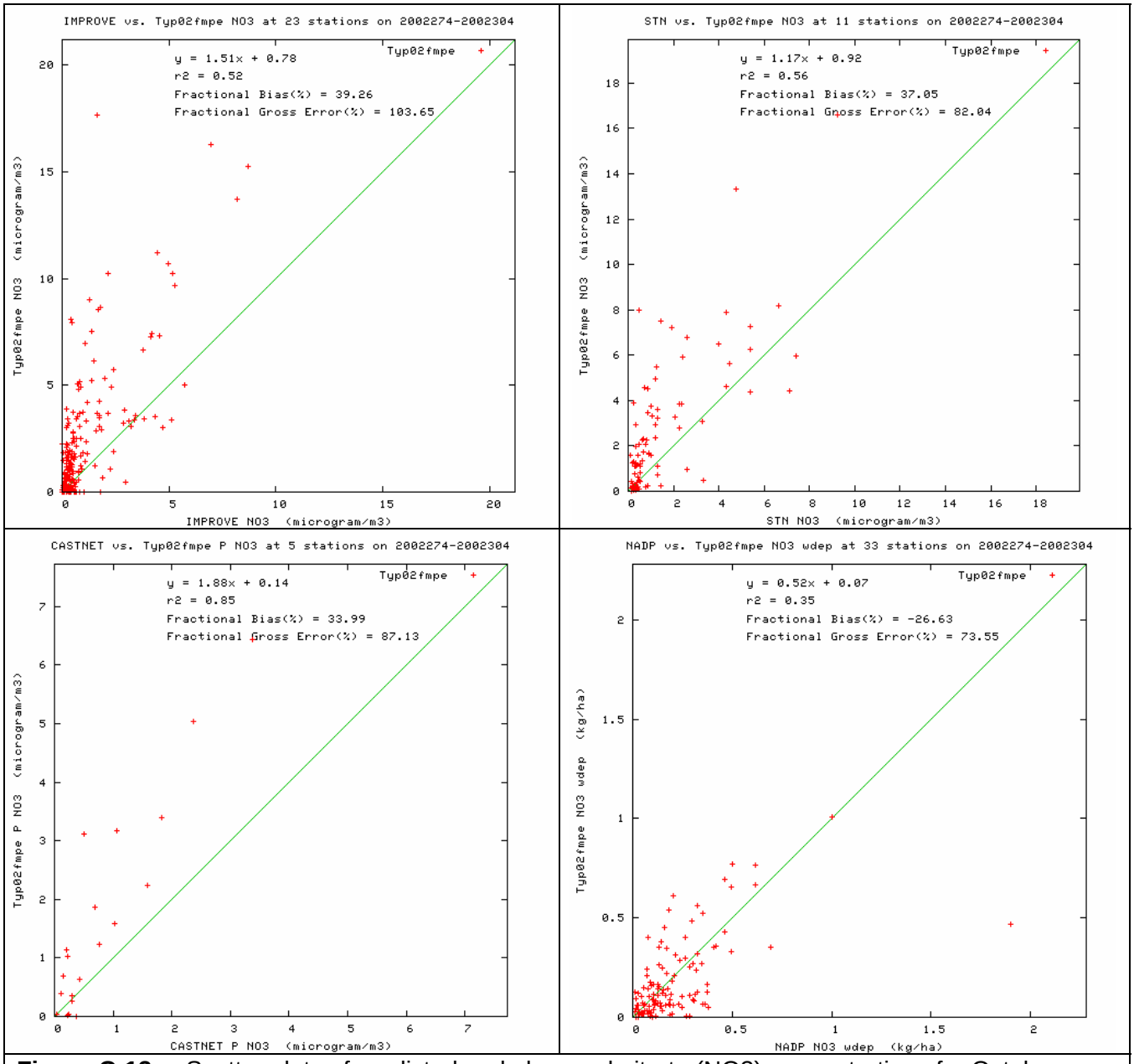

Figure C-13a. Scatter plots of predicted and observed nitrate (NO3) concentrations for October 2002 and sites in the CENRAP region using IMPROVE (top left), STN (top right), CASTNet (bottom left) and NADP monitoring networks using the CMAQ 2002 36 km Base F base case simulation.

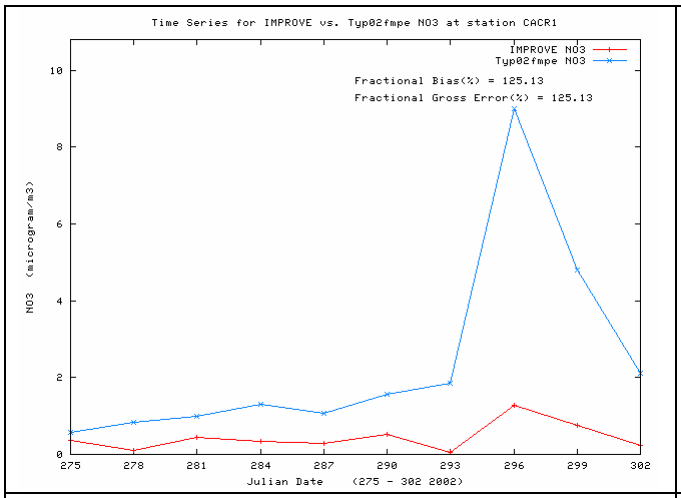
Time Series for IMPROVE vs. Typ02fmpe NO3 at station CACR1
IMPROVE NO3
Typ02fmpe NO3
Fractional Bias(%) = 125.13
Fractional Gross Error(%) = 125.13
NO3 (microgram/m3)
Julian Date (275 - 302 2002)

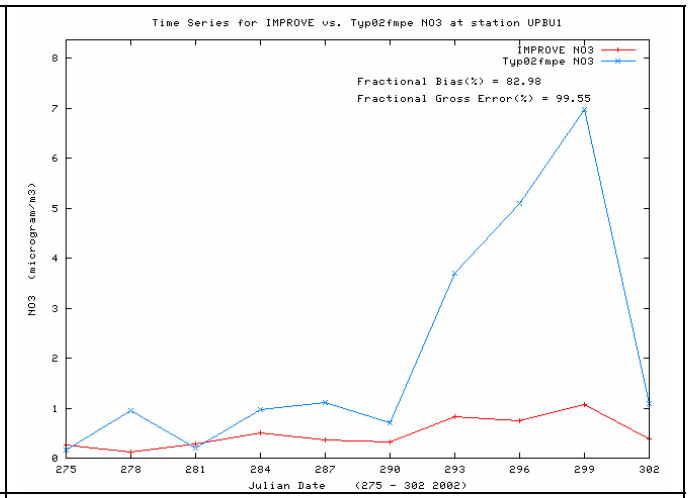
Time Series for IMPROVE vs. Typ02fmpe NO3 at station UPBU1
IMPROVE NO3
Typ02fmpe NO3
Fractional Bias(%) = 82.98
Fractional Gross Error(%) = 99.55
NO3 (microgram/m3)
Julian Date (275 - 302 2002)

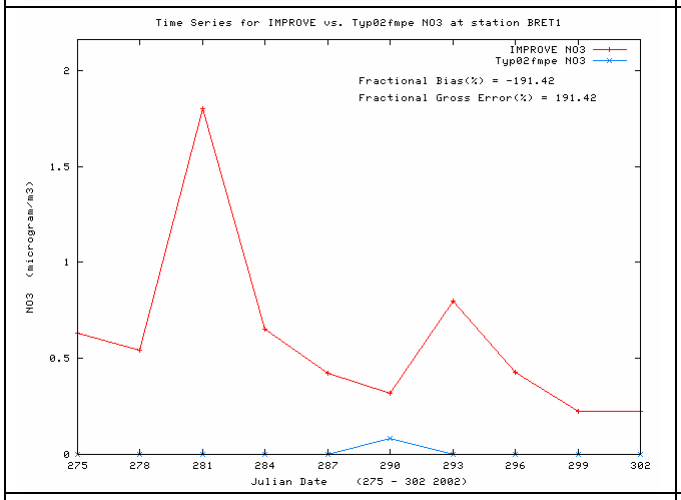
Time Series for IMPROVE vs. Typ02fmpe NO3 at station BRET1
IMPROVE NO3
Typ02fmpe NO3
Fractional Bias(%) = -191.42
Fractional Gross Error(%) = 191.42
NO3 (microgram/m3)
Julian Date (275 - 302 2002)

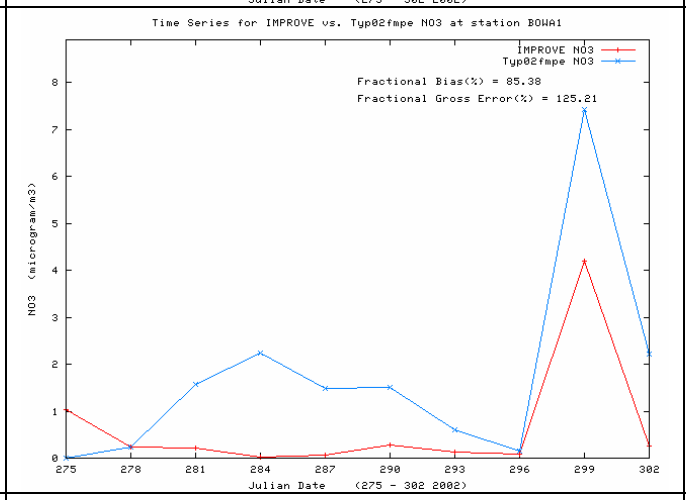
Time Series for IMPROVE vs. Typ02fmpe NO3 at station BOWA1
IMPROVE NO3
Typ02fmpe NO3
Fractional Bias(%) = 85.38
Fractional Gross Error(%) = 125.21
NO3 (microgram/m3)
Julian Date (275 - 302 2002)

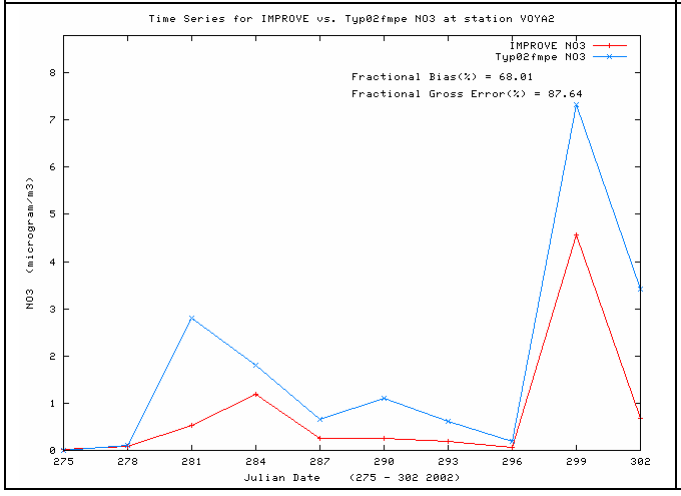
Time Series for IMPROVE vs. Typ02fmpe NO3 at station VOYA2
IMPROVE NO3
Typ02fmpe NO3
Fractional Bias(%) = 68.01
Fractional Gross Error(%) = 87.64
NO3 (microgram/m3)
Julian Date (275 - 302 2002)

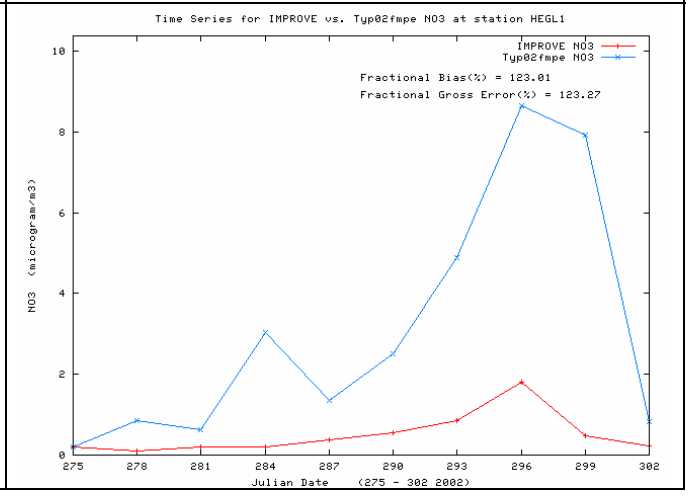
Time Series for IMPROVE vs. Typ02fmpe NO3 at station HEGL1
IMPROVE NO3
Typ02fmpe NO3
Fractional Bias(%) = 123.01
Fractional Gross Error(%) = 123.27
NO3 (microgram/m3)
Julian Date (275 - 302 2002)

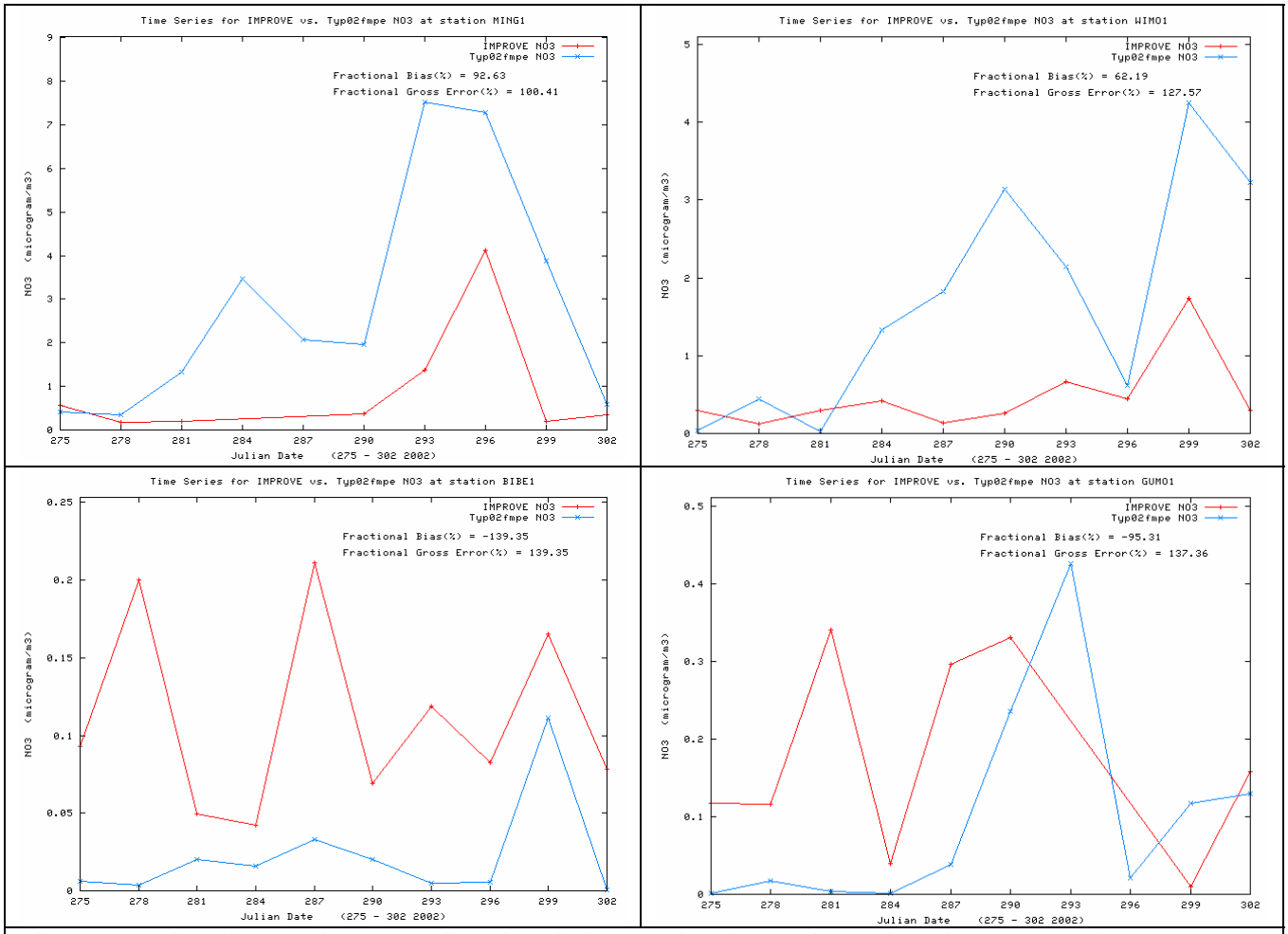

Figure C-13b. Time series of predicted and observed 24-hour nitrate (NO3) concentrations at CENRAP IMPROVE CLASS I AREA sites in October 2002 for CMAQ 2002 36 km Base F base case simulation.

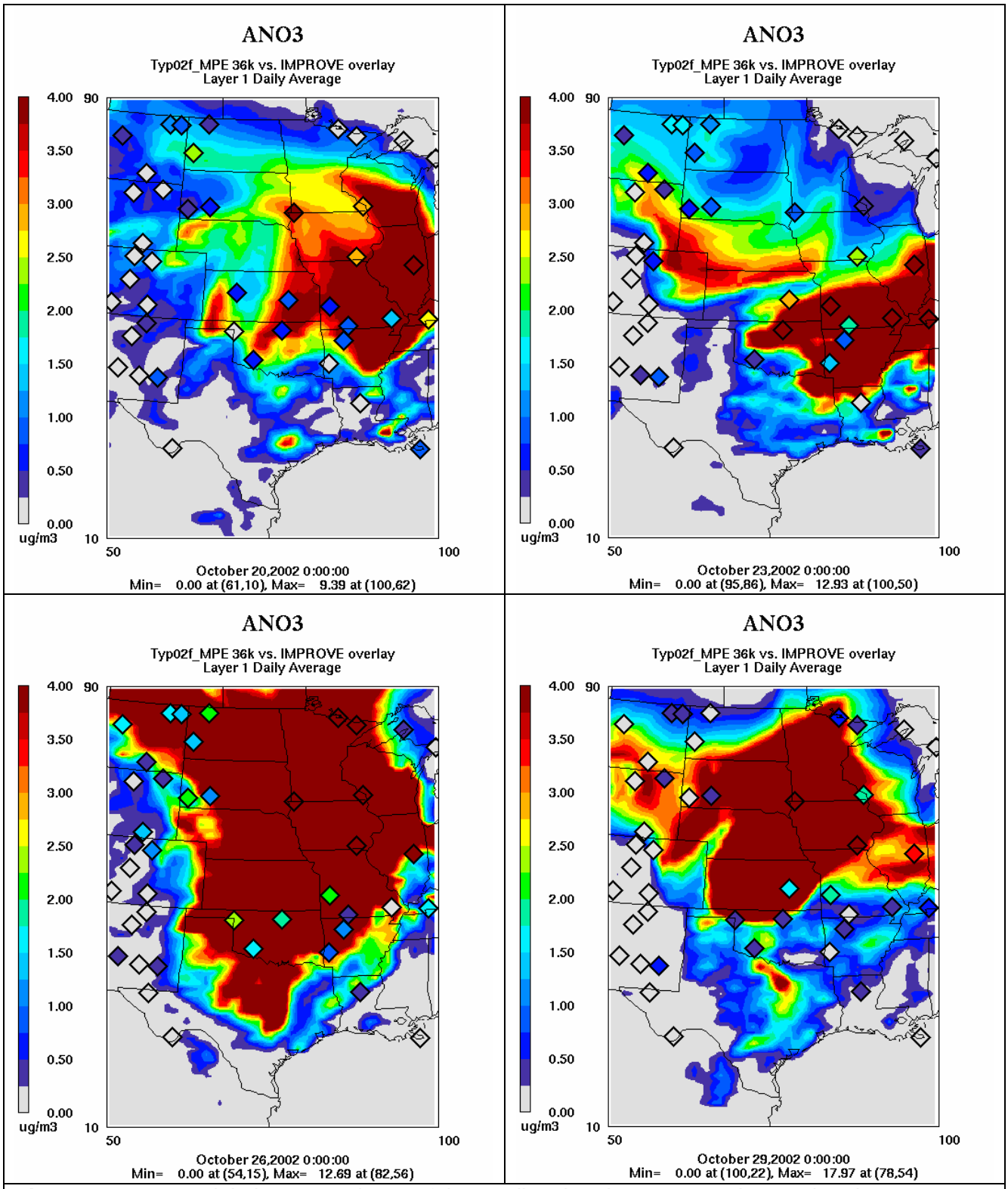

Figure C-13c. Spatial plot comparisons of the predicted and IMPROVE observed 24-hour NO3 concentrations for October 20, 23, 26 and 29, 2002.

C.3.2.5 NO3 Monthly Bias and Error

The monthly fractional bias values for NO3 clearly show the summer underestimation and winter overestimation bias (Figure C-14). The summer underestimation bias is more severe exceeding -100%, whereas the winter overestimation is closer to 50%. The fractional errors in the summer are also greater than in the winter with some values exceeding 100%. So based on statistics alone, it appears the summer underestimation bias is a bigger concern than the winter overestimation bias. However, the Bugle Plots in Figure C-15 paint a different picture entirely. The summer underestimation bias occurred when NO3 is low and is not an important component of PM and visibility impairment. These summer values occur in the flared horn part of the Bugle Plot and in fact the summer NO3 performance mostly achieves the model performance goal and always achieves the performance criteria. Whereas the winter overstated NO3 performance mostly doesn't meet the performance goal and there are even some months/networks that don't meet the performance criteria.

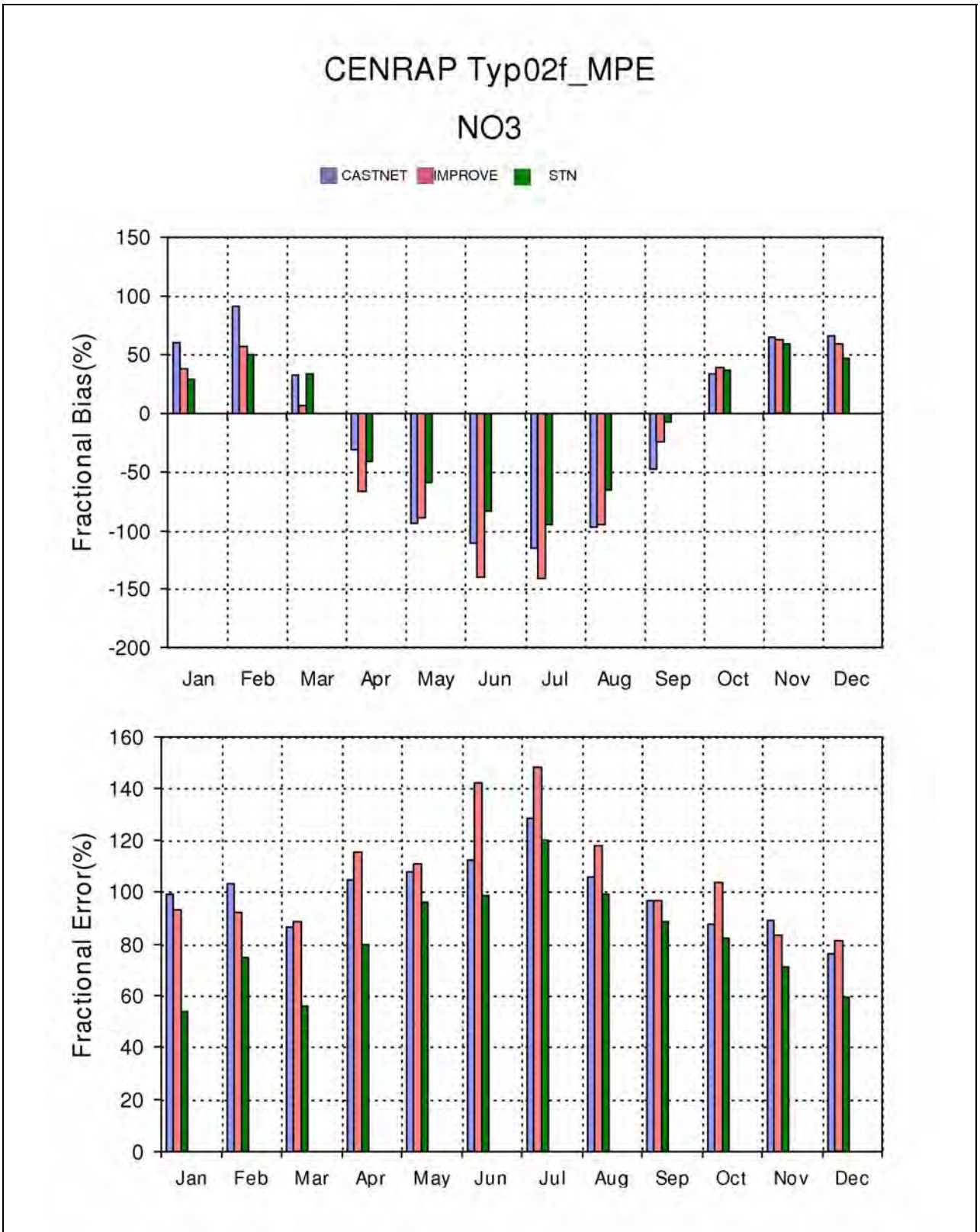

Figure C-14. Monthly NO3 fractional bias (top) and fractional gross error (bottom) statistical measures for IMPROVE, STN and CASTNet monitoring sites in the CENRAP region.

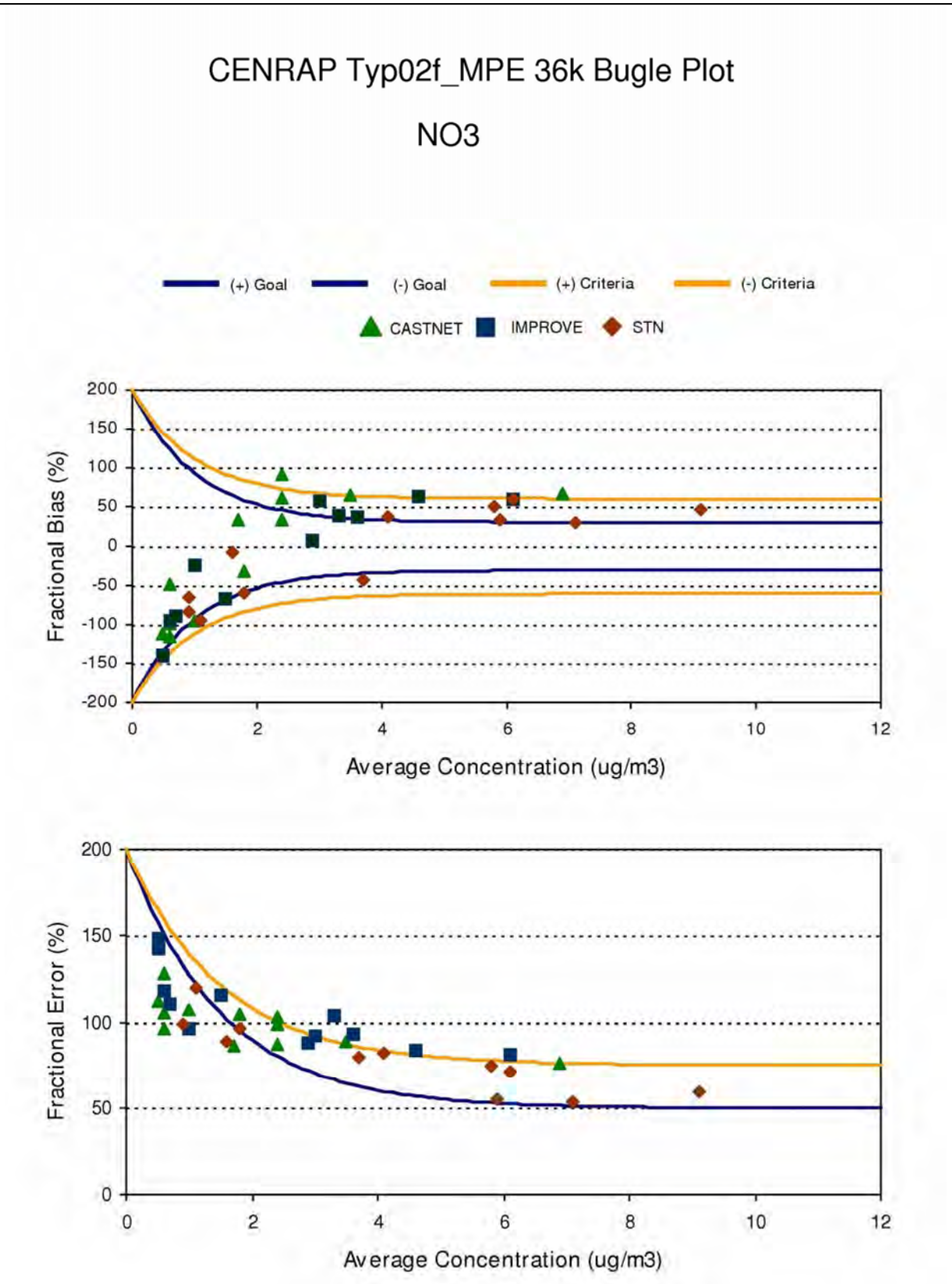

Figure C-15. Bugle Plots of monthly fractional bias (top) and fractional gross error (bottom) and comparisons with model performance goals and criteria for NO3 and IMPROVE, STN and CASTNet monitoring sites in the CENRAP region.

C.3.3 Organic Matter Carbon (OMC) Monthly Model Performance

Organic Matter Carbon (OMC) model performance is presented below. There is incommensurability between the observed and modeled OMC, the model provides estimates of OMC that includes Organic Carbon (OC) as well as other elements attached to the OC (e.g., oxygen), whereas the monitoring networks measure just the carbon component of OMC (i.e., OC). Consequently, the measured OC must be adjusted to OMC for comparison with the model to account for the additional elements attached to the carbon. The OMC/OC ratio is not constant and depends in part on the age of the OMC with fresh OMC having lower OMC/OC ratios than aged OMC. The original IMPROVE equation used an OMC/OC ratio of 1.4 based mainly on urban-oriented measurements. The new IMPROVE equation uses an OMC/OC ratio of 1.8 reflecting the fact that OMC at the more rural IMPROVE monitors is more aged than urban OMC. Thus, selecting a single OMC/OC ratio for adjusting the measured OC to OMC for the model evaluation is somewhat problematic when we have both urban (STN) and rural (IMPPROVE) monitors. In addition, measured OC also has substantial uncertainty with different measurement techniques differing by as much as 50% (Solomon et al., 2005). A 1.4 OMC/OC ratio was used to convert the measured OC to OMC for the model performance evaluation.

C.3.3.1 OMC in January 2002

Figure C-16a displays scatter plots and performance statistics for January OMC model performance across the IMPROVE and STN sites in the CENRAP region. OMC model performance is fairly with near zero bias across the IMPROVE sites, -38% underestimation bias across the STN sites and errors of ~50%. The underestimation of OMC at the urban STN sites is a common occurrence in air quality modeling and may indicate a missing source of urban OMC. With the exception of an underestimation bias at Breton Island and an over-prediction bias at the two Texas IMPORVE sites (BIBE and GUMO), the model reproduces the observed OMC time series in January fairly well. The modeled spatial distribution of OMC is in general agreement with the observations although it sometimes captures the elevated values on some days (e.g., January 29, 2002 in central Illinois) and misses it on others (e.g., January 26, 2002 at Mingo).

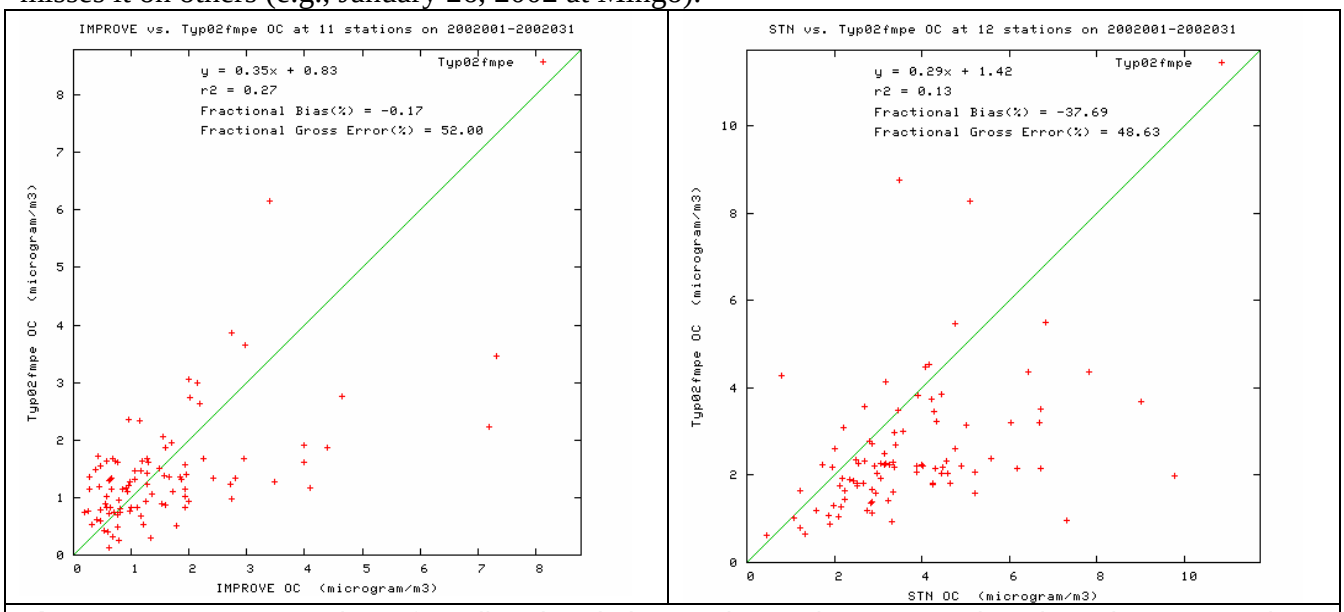

Figure C-16a. Scatter plots of predicted and observed organic matter carbon (OMC) concentrations for January 2002 and sites in the CENRAP region using IMPROVE (left) and STN (right) monitoring networks using the CMAQ 2002 36 km Base F base case simulation.

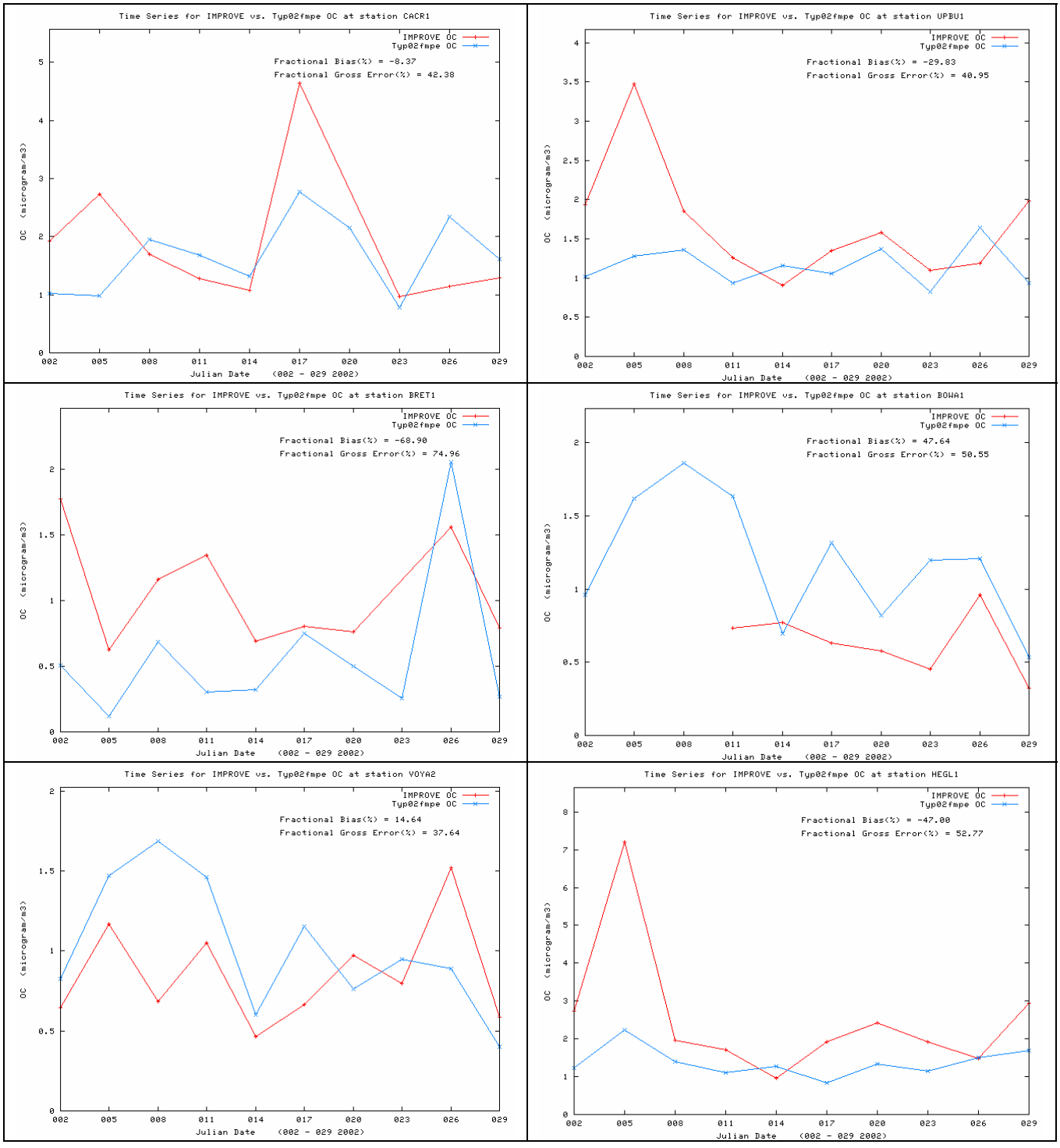
Time Series for IMPROVE vs. Typ02fmpe OC at station CACR1
IMPROVE OC
Typ02fmpe OC
Fractional Bias(%) = -8.37
Fractional Gross Error(%) = 42.38
OC (microgram/m3)
Julian Date (002 - 029 2002)
Time Series for IMPROVE vs. Typ02fmpe OC at station UPBU1
IMPROVE OC
Typ02fmpe OC
Fractional Bias(%) = -29.83
Fractional Gross Error(%) = 40.95
OC (microgram/m3)
Julian Date (002 - 029 2002)
Time Series for IMPROVE vs. Typ02fmpe OC at station BRET1
IMPROVE OC
Typ02fmpe OC
Fractional Bias(%) = -68.90
Fractional Gross Error(%) = 74.96
OC (microgram/m3)
Julian Date (002 - 029 2002)
Time Series for IMPROVE vs. Typ02fmpe OC at station BOWA1
IMPROVE OC
Typ02fmpe OC
Fractional Bias(%) = 47.64
Fractional Gross Error(%) = 50.55
OC (microgram/m3)
Julian Date (002 - 029 2002)
Time Series for IMPROVE vs. Typ02fmpe OC at station VOYA2
IMPROVE OC
Typ02fmpe OC
Fractional Bias(%) = 14.64
Fractional Gross Error(%) = 37.64
OC (microgram/m3)
Julian Date (002 - 029 2002)
Time Series for IMPROVE vs. Typ02fmpe OC at station HEGL1
IMPROVE OC
Typ02fmpe OC
Fractional Bias(%) = -47.00
Fractional Gross Error(%) = 52.77
OC (microgram/m3)
Julian Date (002 - 029 2002)

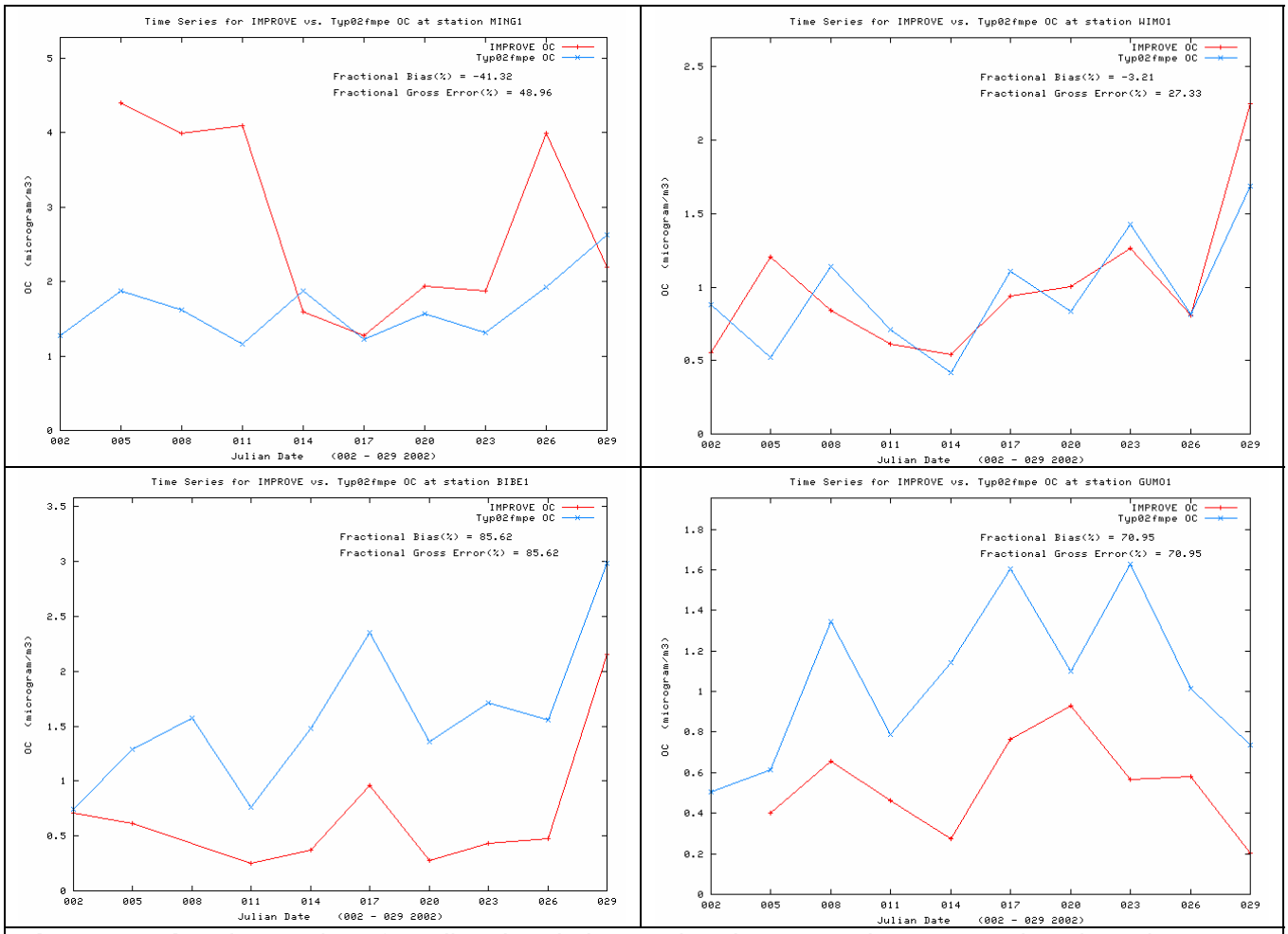

Figure C-16b. Time series of predicted and observed 24-hour organic matter carbon (OMC) concentrations at CENRAP IMPROVE CLASS I AREA sites in January 2002 for CMAQ 2002 36 km Base F base case simulation.

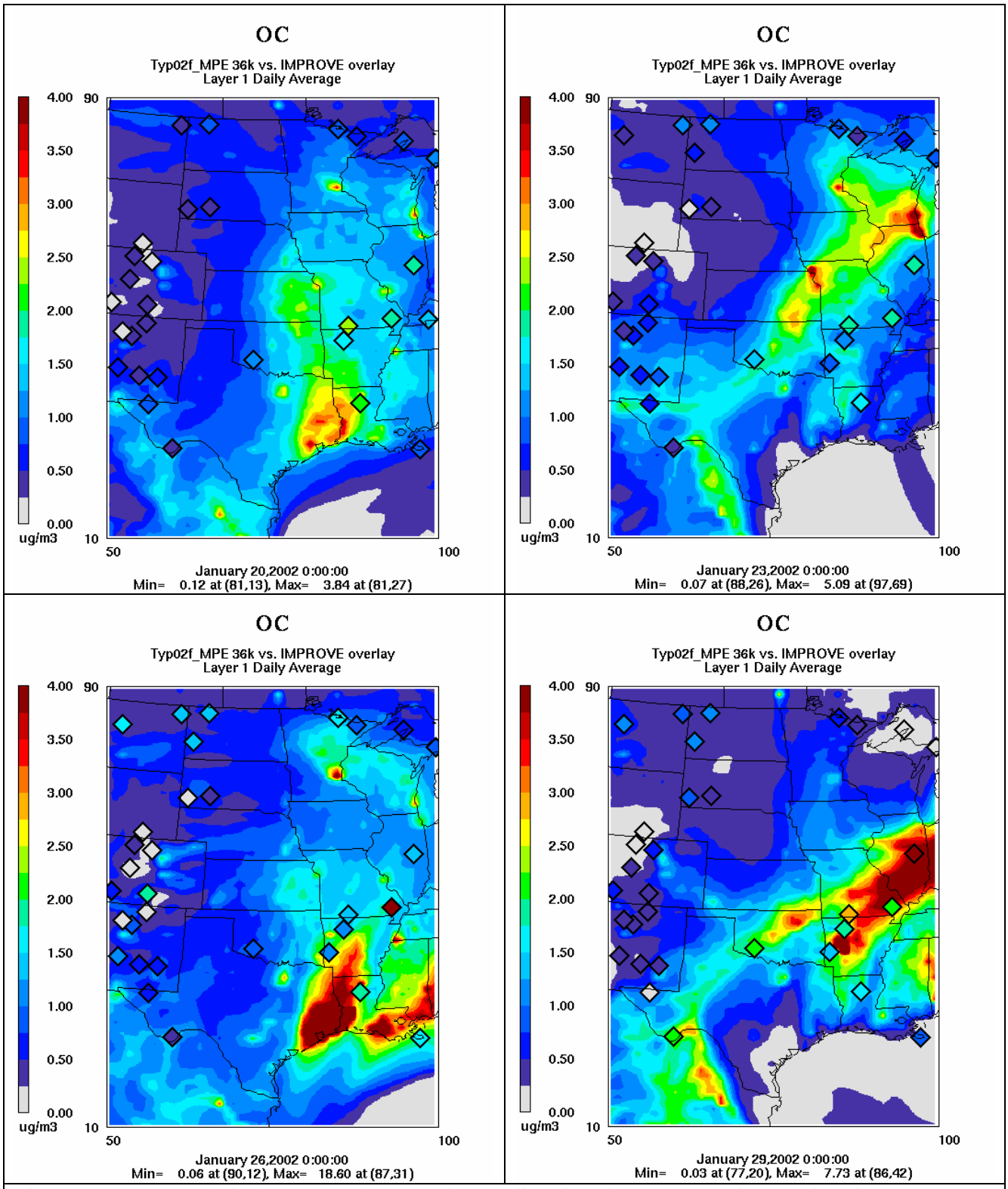

Figure C-16c. Spatial plot comparisons of the predicted and IMPROVE observed 24-hour OMC concentrations for January 20, 23, 26 and 29, 2002.

C.3.3.2 OMC in April 2002

The OMC performance in April is also fairly reasonable, again bias across the IMPROVE monitors is near zero (-7%), an underestimation bias exists across the STN sites (-30%) and errors are near 50% (Figure C-17a). The time series comparisons (Figure C-17b) are also reasonable with the model generally agreeing on the magnitudes of the observed OMC, but with an underestimation bias at several sites (e.g., MING and WIMO). The observed spatial distribution of OMCV appears to be much spottier than predicted (Figure C-17c). Thus, when the model reproduces an elevated observed OMC value like at UPBU on April 5th, it overestimates OMC at neighboring sites that have lower values (e.g., HEGL).

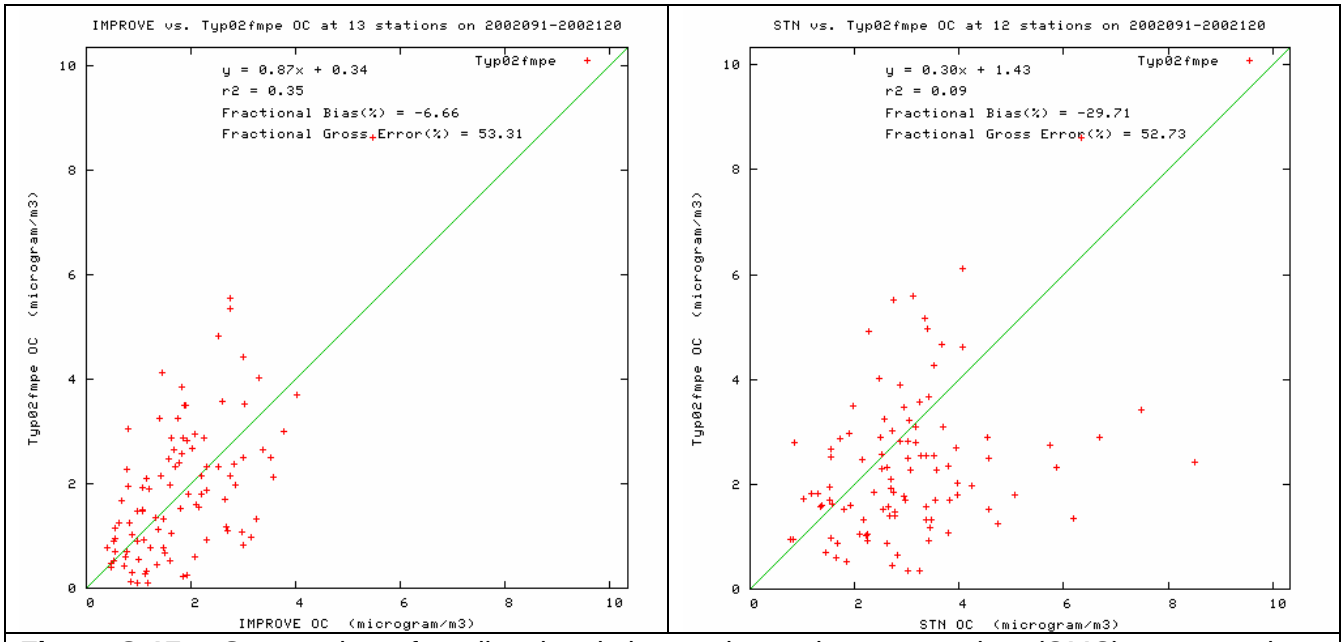

Figure C-17a. Scatter plots of predicted and observed organic matter carbon (OMC) concentrations for April 2002 and sites in the CENRAP region using IMPROVE (left) and STN (right) monitoring networks using the CMAQ 2002 36 km Base F base case simulation.

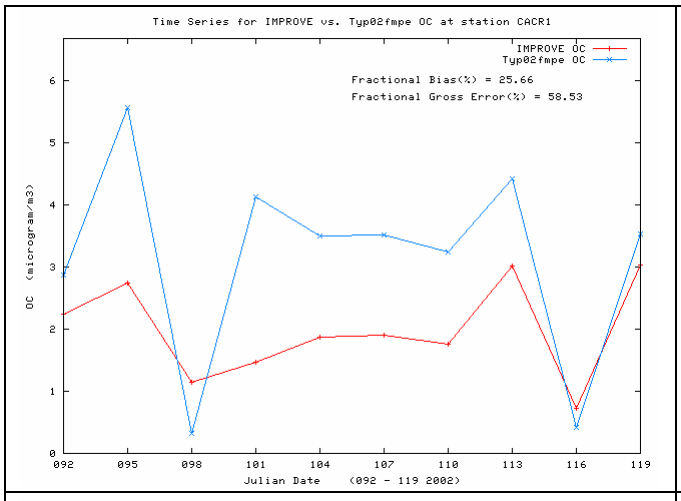
Time Series for IMPROVE vs. Typ02fmpe OC at station CACR1
IMPROVE OC
Typ02fmpe OC
Fractional Bias(%) = 25.66
Fractional Gross Error(%) = 58.53
OC (microgram/m3)
Julian Date (092 - 119 2002)

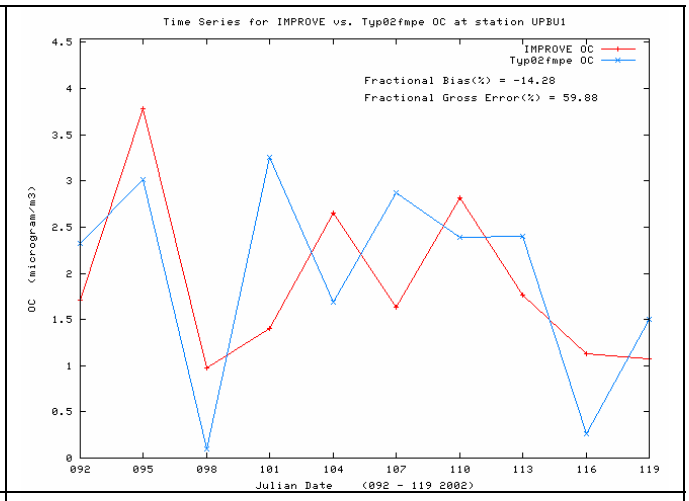
Time Series for IMPROVE vs. Typ02fmpe OC at station UPBU1
IMPROVE OC
Typ02fmpe OC
Fractional Bias(%) = -14.28
Fractional Gross Error(%) = 59.88
OC (microgram/m3)
Julian Date (092 - 119 2002)

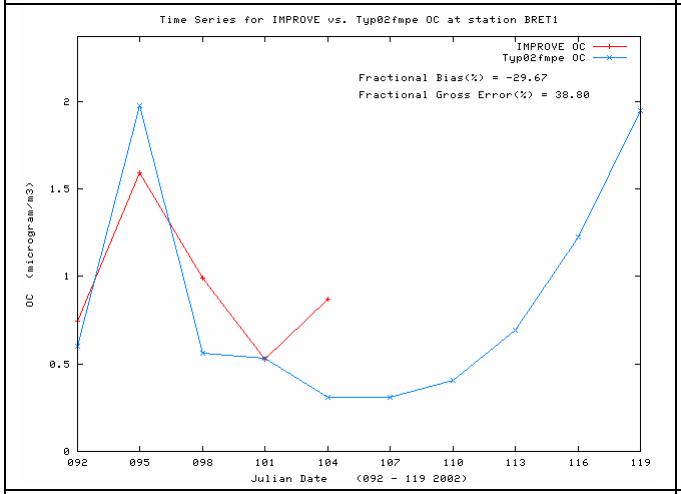
Time Series for IMPROVE vs. Typ02fmpe OC at station BRET1
IMPROVE OC
Typ02fmpe OC
Fractional Bias(%) = -29.67
Fractional Gross Error(%) = 38.80
OC (microgram/m3)
Julian Date (092 - 119 2002)

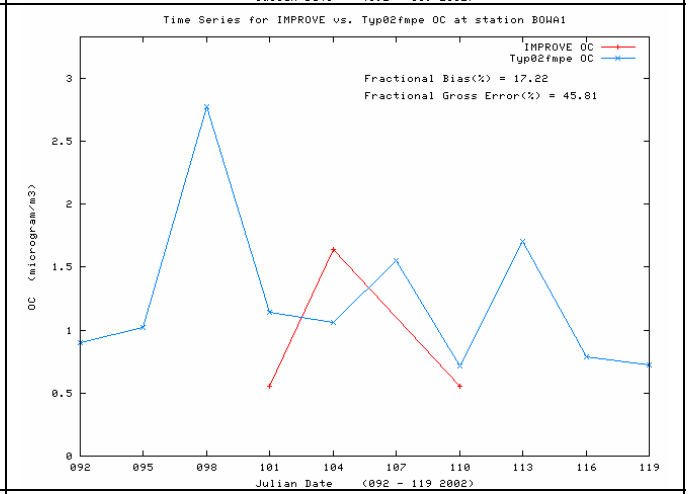
Time Series for IMPROVE vs. Typ02fmpe OC at station BOWA1
IMPROVE OC
Typ02fmpe OC
Fractional Bias(%) = 17.22
Fractional Gross Error(%) = 45.81
OC (microgram/m3)
Julian Date (092 - 119 2002)

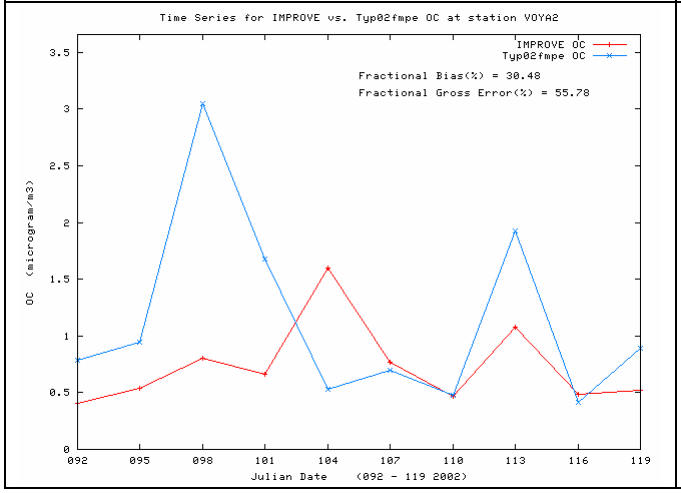
Time Series for IMPROVE vs. Typ02fmpe OC at station VOYA2
IMPROVE OC
Typ02fmpe OC
Fractional Bias(%) = 30.48
Fractional Gross Error(%) = 55.78
OC (microgram/m3)
Julian Date (092 - 119 2002)

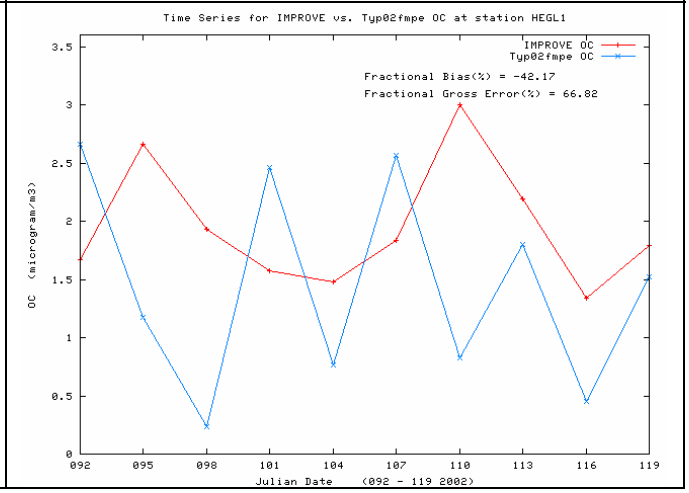
Time Series for IMPROVE vs. Typ02fmpe OC at station HEGL1
IMPROVE OC
Typ02fmpe OC
Fractional Bias(%) = -42.17
Fractional Gross Error(%) = 66.82
OC (microgram/m3)
Julian Date (092 - 119 2002)

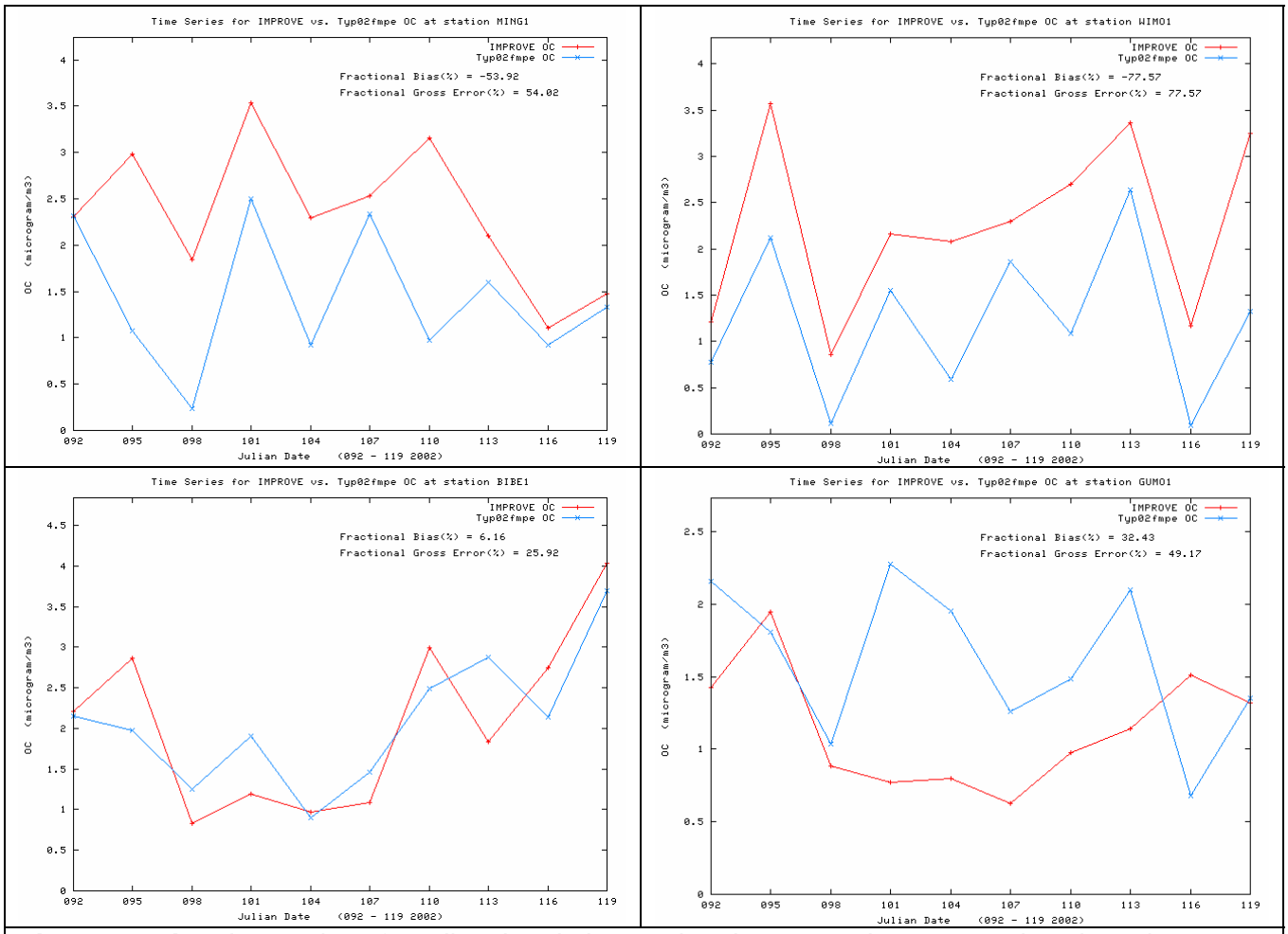

Figure C-17b. Time series of predicted and observed 24-hour organic matter carbon (OMC) concentrations at CENRAP IMPROVE CLASS I AREA sites in April 2002 for CMAQ 2002 36 km Base F base case simulation.

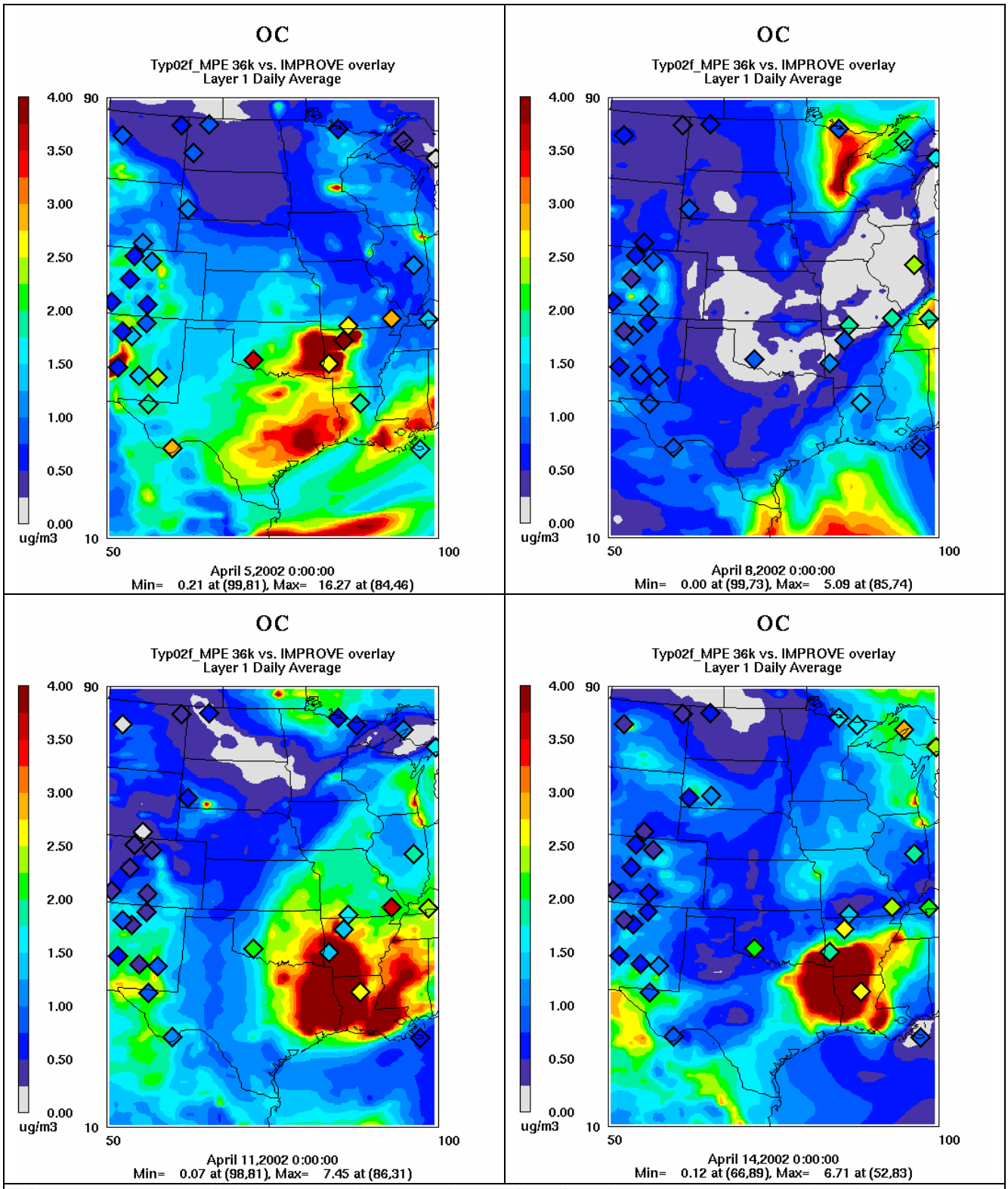

Figure C-17c. Spatial plot comparisons of the predicted and IMPROVE observed 24-hour OMC concentrations for April 5, 8, 11 and 14, 2002.

C.3.3.3 OMC in July 2002

Modeled and observed OMC are higher in July due to the impacts of more secondary organic aerosols (SOA) and fires. OMC bias values of -18% and -41% exist across the IMPROVE and STN networks in July (Figure C-18a). Two of the observed OMC values at the IMPROVE sites are very high (> 15 μg/m^3). An examination of the time series plots (Figure C-18b) reveals that these two values occur on Julian Day 200 and the two northern Minnesota sites (VOYA and BOWA) and are likely due to fire impacts. The model is also estimating elevated OMC at these sites on these two days, but not as high as observed. At most sites the model is racking the temporal variation of the observed OMC reasonably well. OMC data for MING were missing in July 2002. The model reproduces the observed high OMC in northern Minnesota and centered on Louisiana and adjacent areas on July 7 and 10 quite well, but also predicts elevated OMC in the Denver area that is not reflected in the observations (Figure C-18c). The model is exhibiting less skill in predicting the spatial distribution of the observed OMC on July 13 and 16.

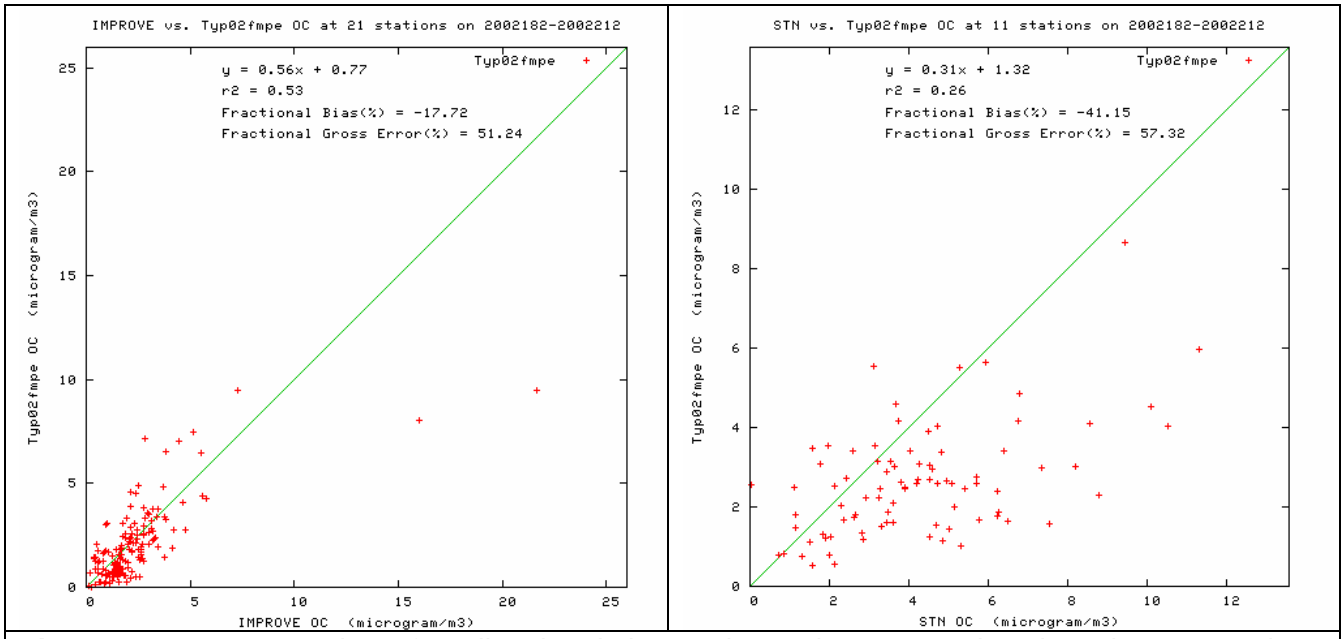

Figure C-18a. Scatter plots of predicted and observed organic matter carbon (OMC) concentrations for July 2002 and sites in the CENRAP region using IMPROVE (left) and STN (right) monitoring networks using the CMAQ 2002 36 km Base F base case simulation.

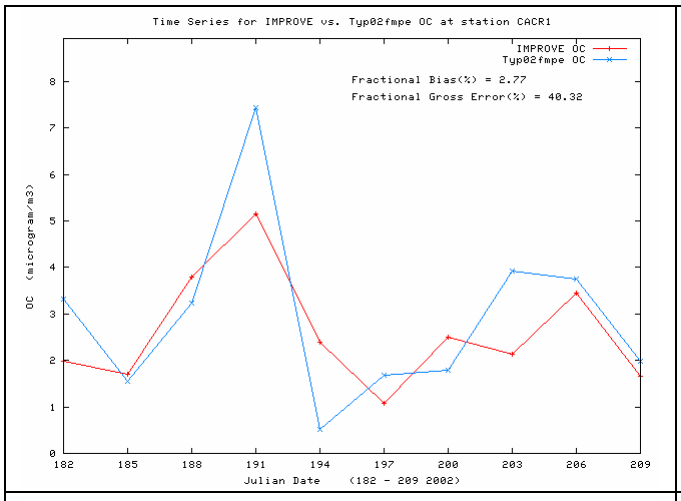
Time Series for IMPROVE vs. Typ02fmpe OC at station CACR1
IMPROVE OC
Typ02fmpe OC
Fractional Bias(%) = 2.77
Fractional Gross Error(%) = 40.32
OC (microgram/m3)
Julian Date (182 - 209 2002)

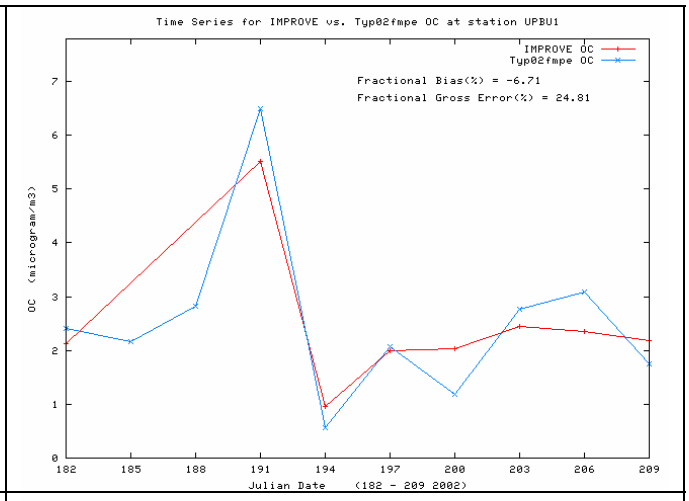
Time Series for IMPROVE vs. Typ02fmpe OC at station UPBU1
IMPROVE OC
Typ02fmpe OC
Fractional Bias(%) = -6.71
Fractional Gross Error(%) = 24.81
OC (microgram/m3)
Julian Date (182 - 209 2002)

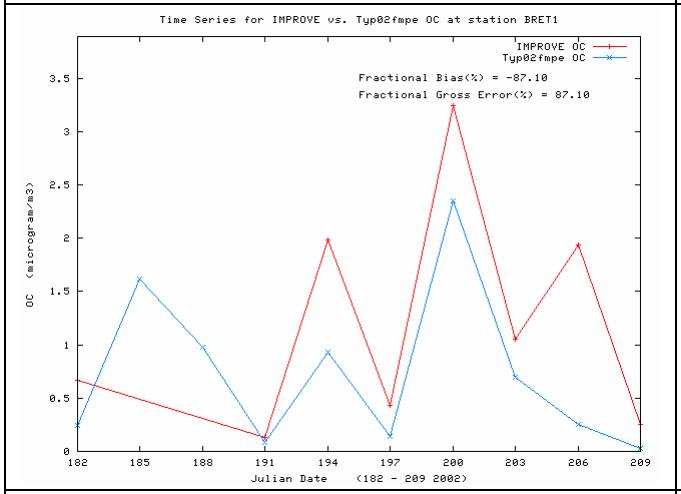
Time Series for IMPROVE vs. Typ02fmpe OC at station BRET1
IMPROVE OC
Typ02fmpe OC
Fractional Bias(%) = -87.10
Fractional Gross Error(%) = 87.10
OC (microgram/m3)
Julian Date (182 - 209 2002)

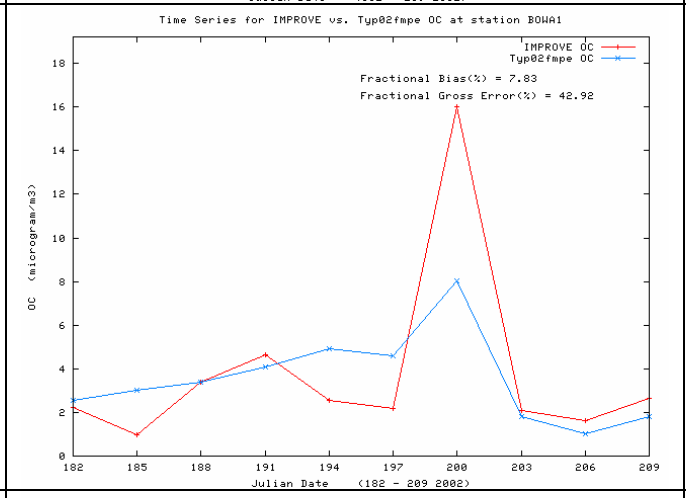
Time Series for IMPROVE vs. Typ02fmpe OC at station BOWA1
IMPROVE OC
Typ02fmpe OC
Fractional Bias(%) = 7.83
Fractional Gross Error(%) = 42.92
OC (microgram/m3)
Julian Date (182 - 209 2002)

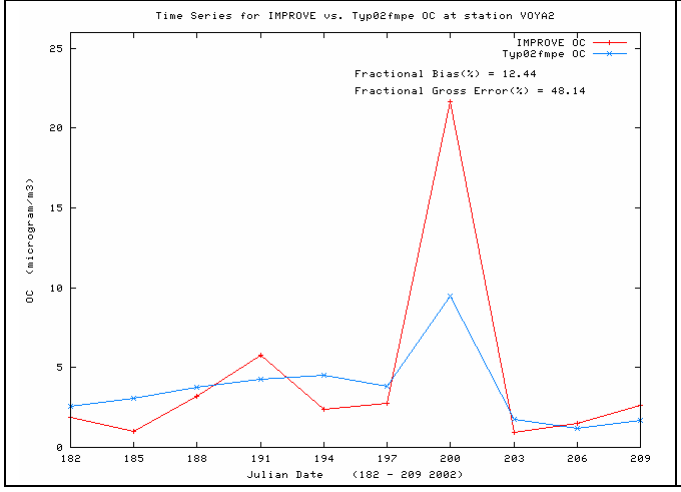
Time Series for IMPROVE vs. Typ02fmpe OC at station VOYA2
IMPROVE OC
Typ02fmpe OC
Fractional Bias(%) = 12.44
Fractional Gross Error(%) = 48.14
OC (microgram/m3)
Julian Date (182 - 209 2002)

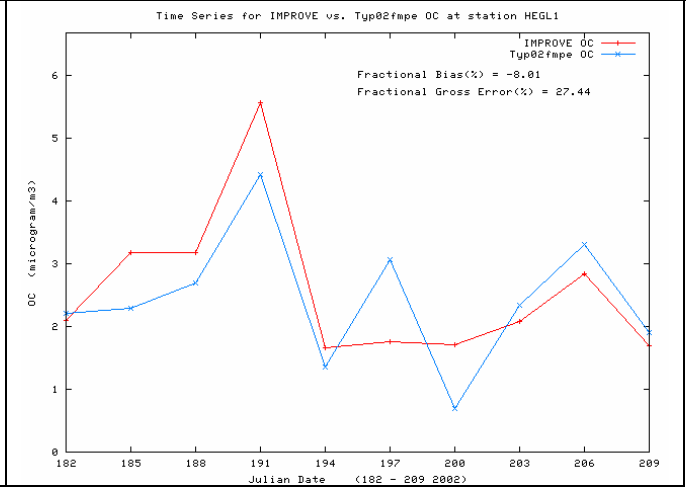
Time Series for IMPROVE vs. Typ02fmpe OC at station HEGL1
IMPROVE OC
Typ02fmpe OC
Fractional Bias(%) = -8.01
Fractional Gross Error(%) = 27.44
OC (microgram/m3)
Julian Date (182 - 209 2002)

No Data for Mingo (MING)

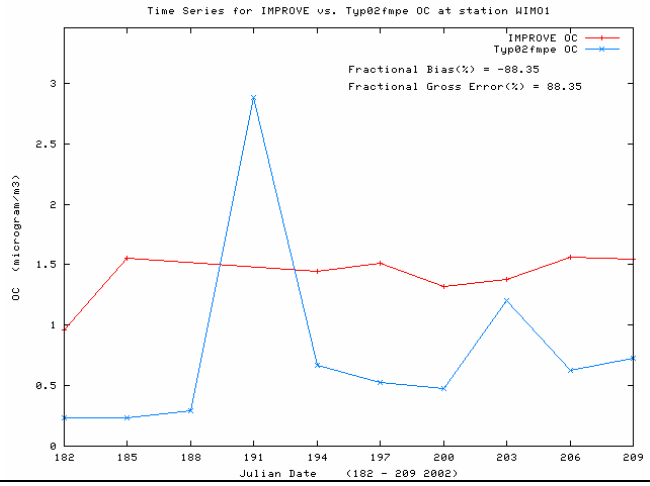

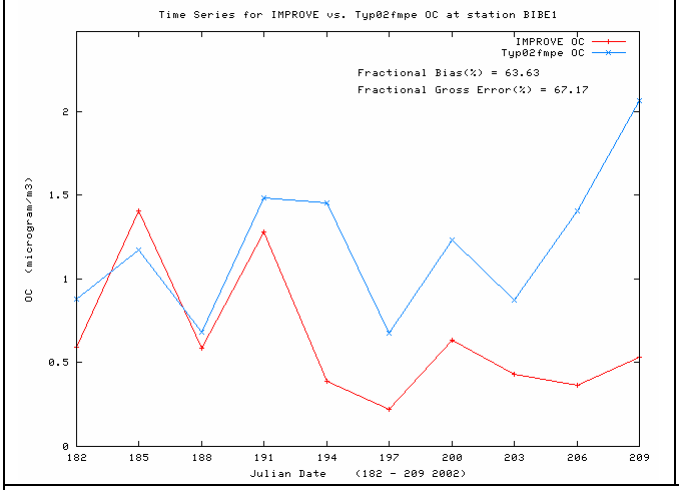

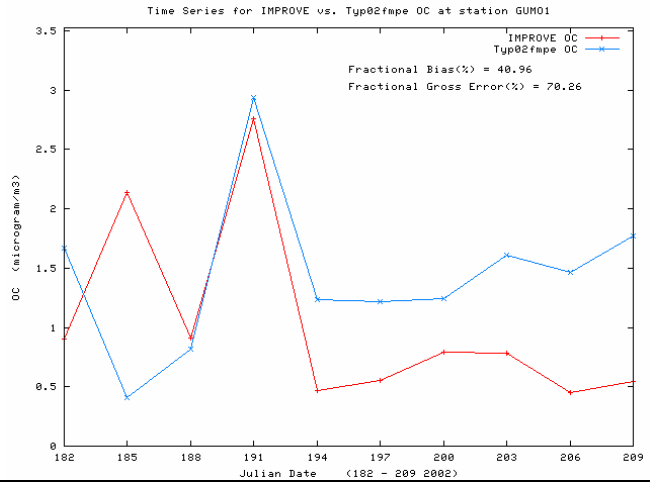

Figure C-18b. Time series of predicted and observed 24-hour organic matter carbon (OMC) concentrations at CENRAP IMPROVE CLASS I AREA sites in July 2002 for CMAQ 2002 36 km Base F base case simulation.

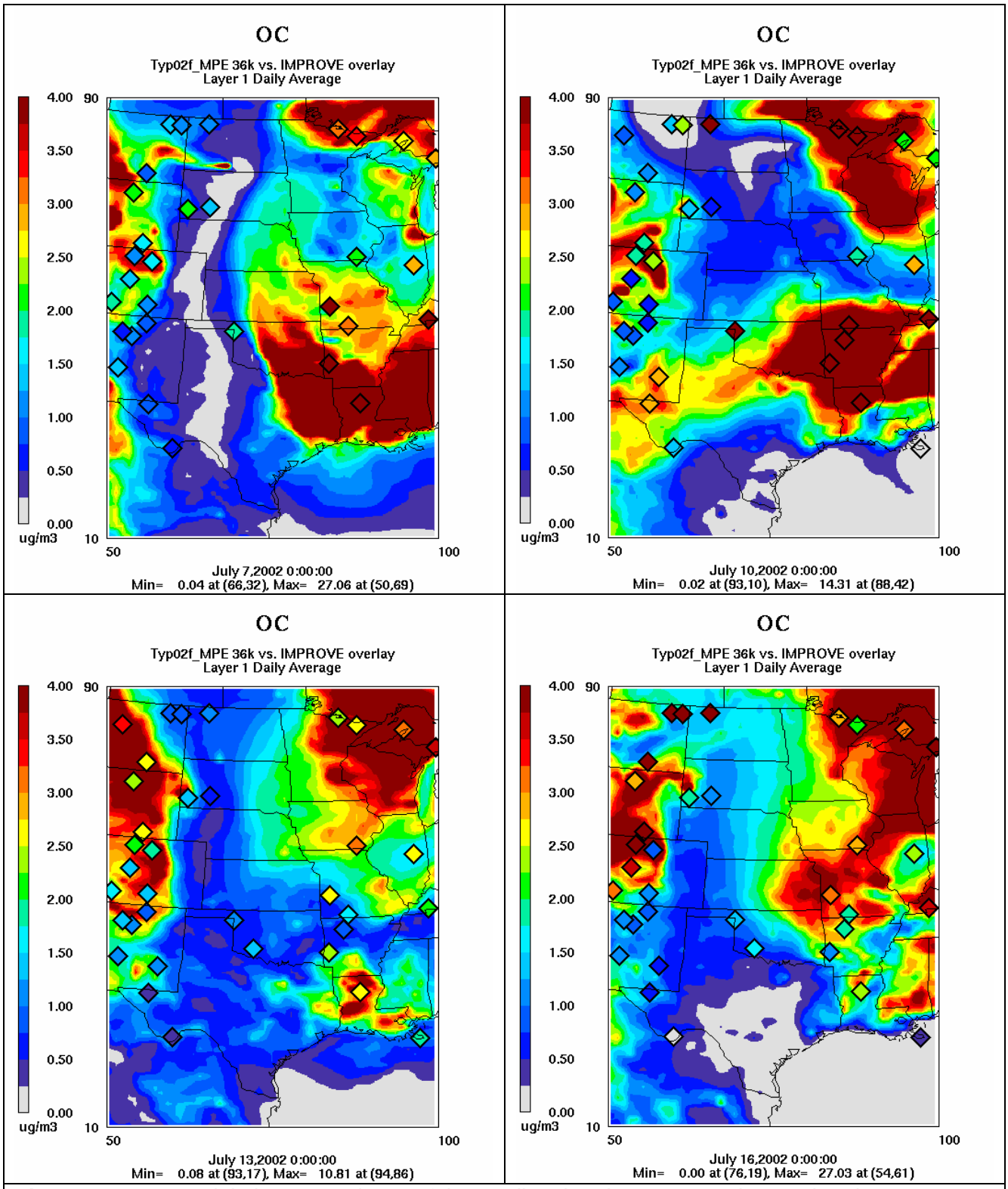

Figure C-18c. Spatial plot comparisons of the predicted and IMPROVE observed 24-hour OMC concentrations for July 7, 10, 13 and 16, 2002.

C.3.3.4 OMC in October 2002

OMC model performance in October 2002 is similar to the other months with near zero bias across the IMPROVE sites and an underestimation bias across the STN sites in the CENRAP region (Figure C-19a). Although OMC overestimation bias occurs at the Texas sites (BIBE and GUMO), the model is exhibiting remarkable ability to reproduce the observed temporal variation in OMC at several of the sites (e.g., CACR, UPBU, VOYA and HEGL; Figure C-19b). The model also performs reasonable well in reproducing the day to day and spatial variability in the observed OMC (Figure C-19c).

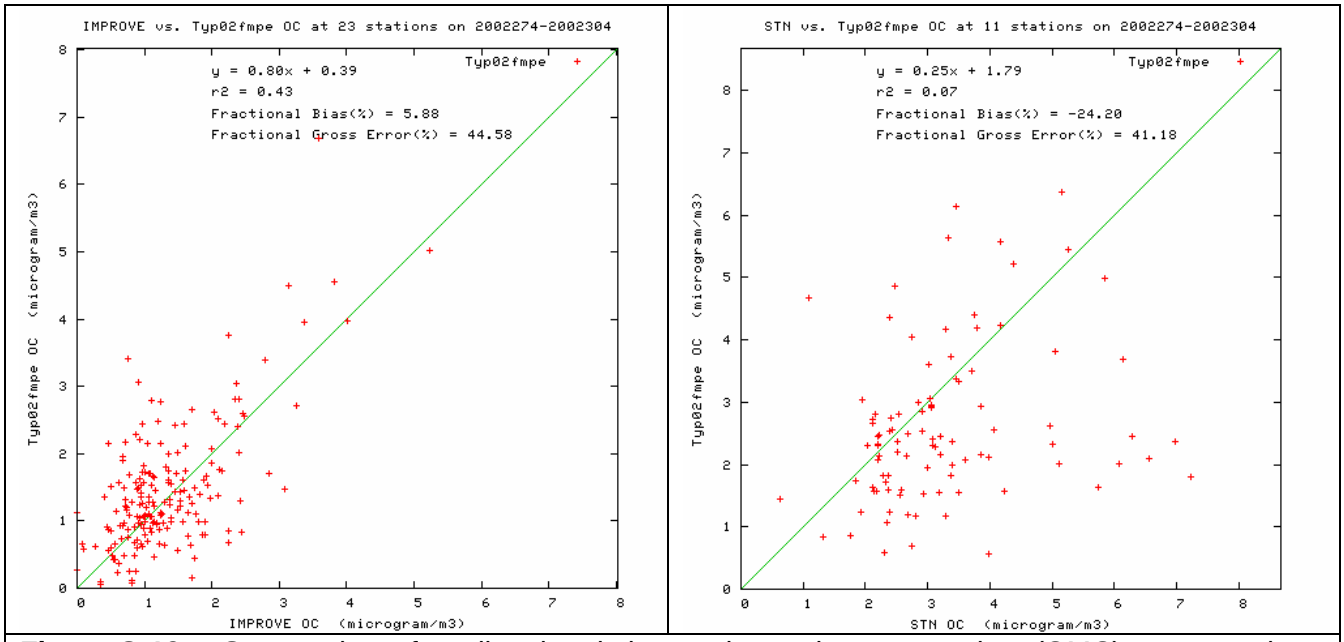

Figure C-19a. Scatter plots of predicted and observed organic matter carbon (OMC) concentrations for October 2002 and sites in the CENRAP region using IMPROVE (left) and STN (right) monitoring networks using the CMAQ 2002 36 km Base F base case simulation.

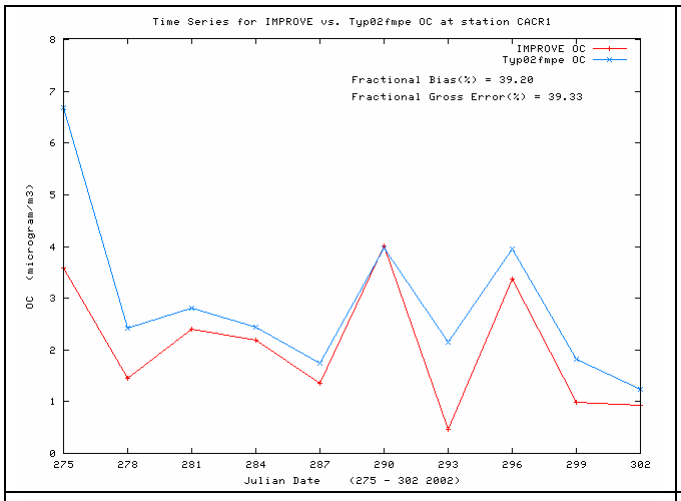
Time Series for IMPROVE vs. Typ02fmpe OC at station CACR1
IMPROVE OC
Typ02fmpe OC
Fractional Bias(%) = 39.20
Fractional Gross Error(%) = 39.33
OC (microgram/m3)
Julian Date (275 - 302 2002)

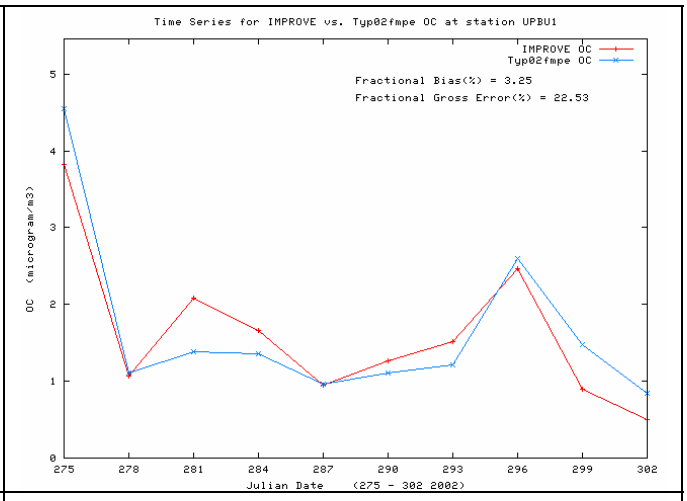
Time Series for IMPROVE vs. Typ02fmpe OC at station UPBU1
IMPROVE OC
Typ02fmpe OC
Fractional Bias(%) = 3.25
Fractional Gross Error(%) = 22.53
OC (microgram/m3)
Julian Date (275 - 302 2002)

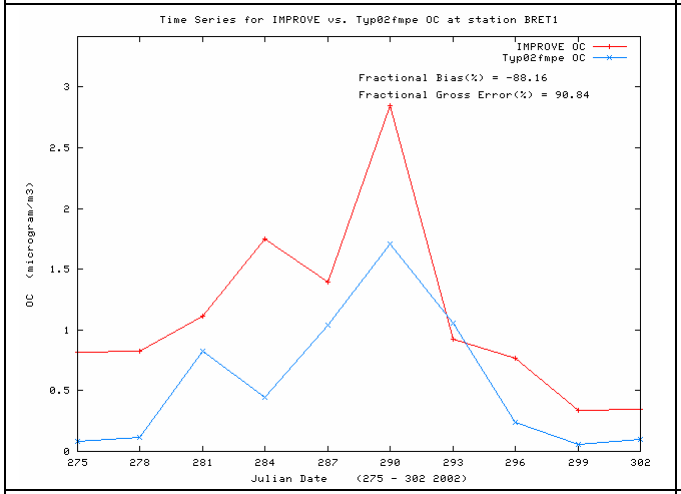
Time Series for IMPROVE vs. Typ02fmpe OC at station BRET1
IMPROVE OC
Typ02fmpe OC
Fractional Bias(%) = -88.16
Fractional Gross Error(%) = 90.84
OC (microgram/m3)
Julian Date (275 - 302 2002)

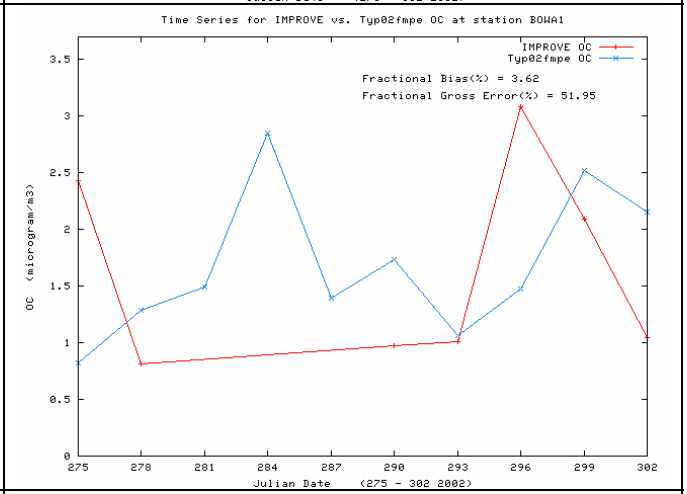
Time Series for IMPROVE vs. Typ02fmpe OC at station BOWA1
IMPROVE OC
Typ02fmpe OC
Fractional Bias(%) = 3.62
Fractional Gross Error(%) = 51.95
OC (microgram/m3)
Julian Date (275 - 302 2002)

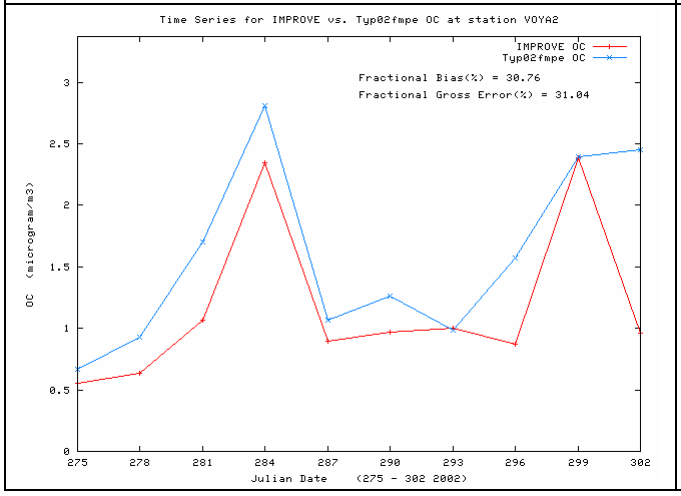
Time Series for IMPROVE vs. Typ02fmpe OC at station VOYA2
IMPROVE OC
Typ02fmpe OC
Fractional Bias(%) = 30.76
Fractional Gross Error(%) = 31.04
OC (microgram/m3)
Julian Date (275 - 302 2002)

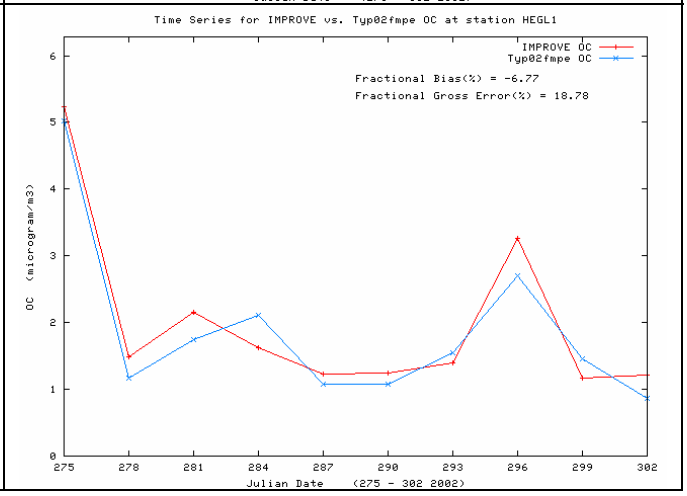
Time Series for IMPROVE vs. Typ02fmpe OC at station HEGL1
IMPROVE OC
Typ02fmpe OC
Fractional Bias(%) = -6.77
Fractional Gross Error(%) = 18.78
OC (microgram/m3)
Julian Date (275 - 302 2002)

No Data for Mingo (MING)

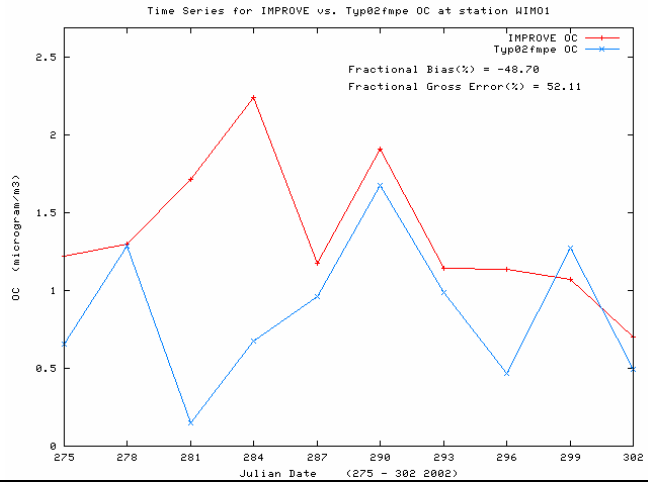

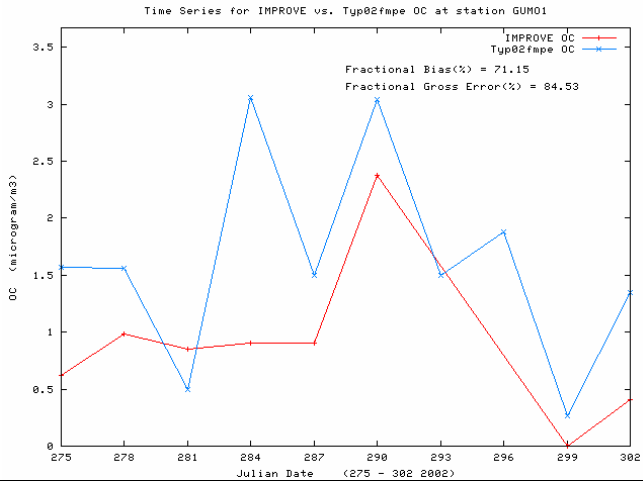

Figure C-19b. Time series of predicted and observed 24-hour organic matter carbon (OMC) concentrations at CENRAP IMPROVE CLASS I AREA sites in October 2002 for CMAQ 2002 36 km Base F base case simulation.

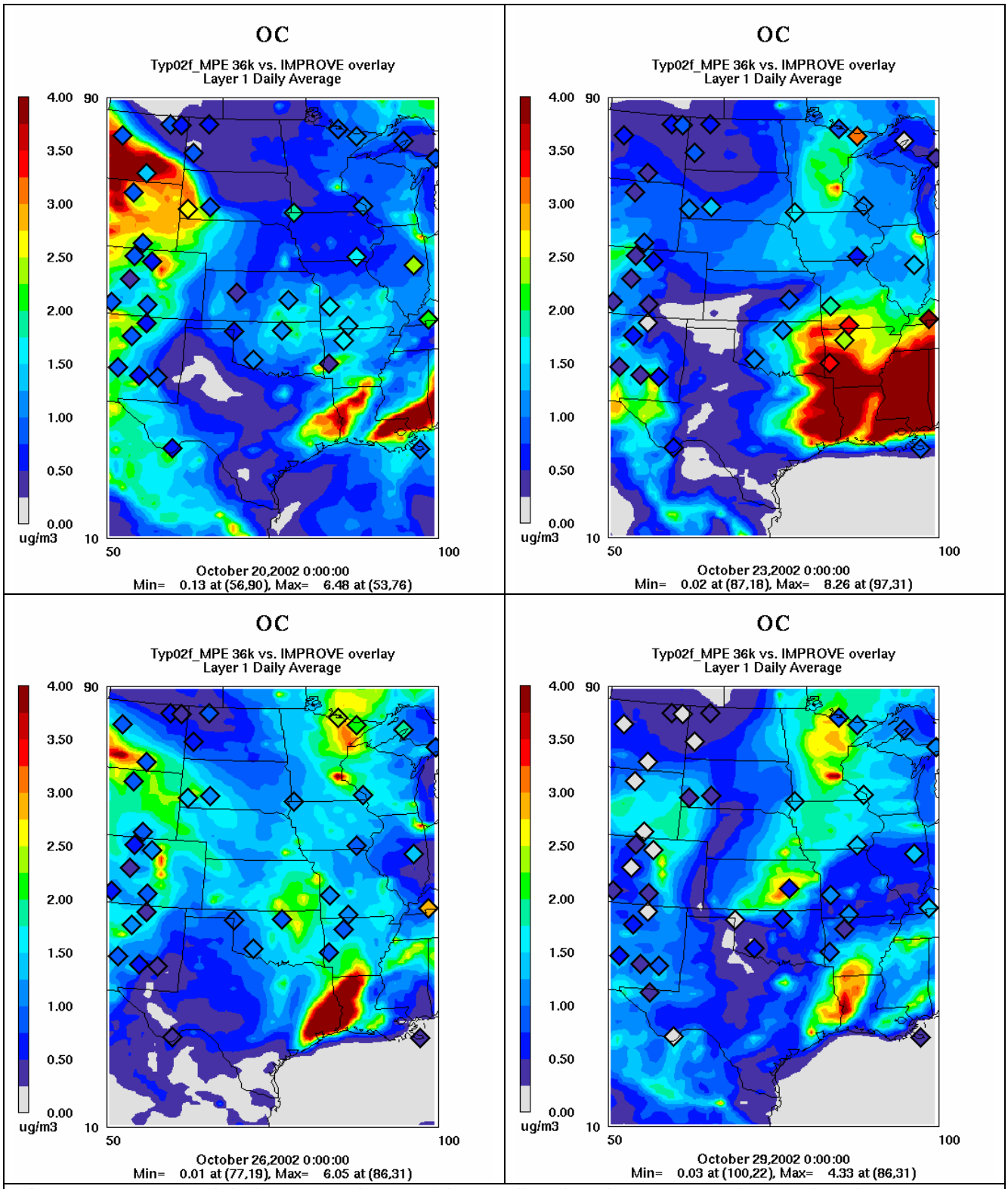

Figure C-19c. Spatial plot comparisons of the predicted and IMPROVE observed 24-hour OMC concentrations for October 20, 23, 26 and 29, 2002.

C.3.3.5 OMC Monthly Bias and Error

The OMC monthly bias and error across IMPROVE and STN sites in the CENRAP region are shown in Figure C-20. The bias performance for OMC at the IMPROVE sites are quite good throughout the year with values generally within ±20%, albeit with a slight winter overestimation and summer underestimation bias. At the urban STN sites the model exhibits an underestimation bias throughout the year that ranges from -20% to -50%. Fractional errors are mostly within 40% to 60% with the STN network generally exhibiting more error than IMPROVE.

The good performance of the model for OMC at the IMPROVE sites is also reflected in the Bugle Plot (Figure C-21) with the bias and error achieving the proposed PM model performance goal for all months of the year. At the STN sites, however, the OMC bias falls between the proposed PM model performance goal and criteria, with error right at the goal for most months.

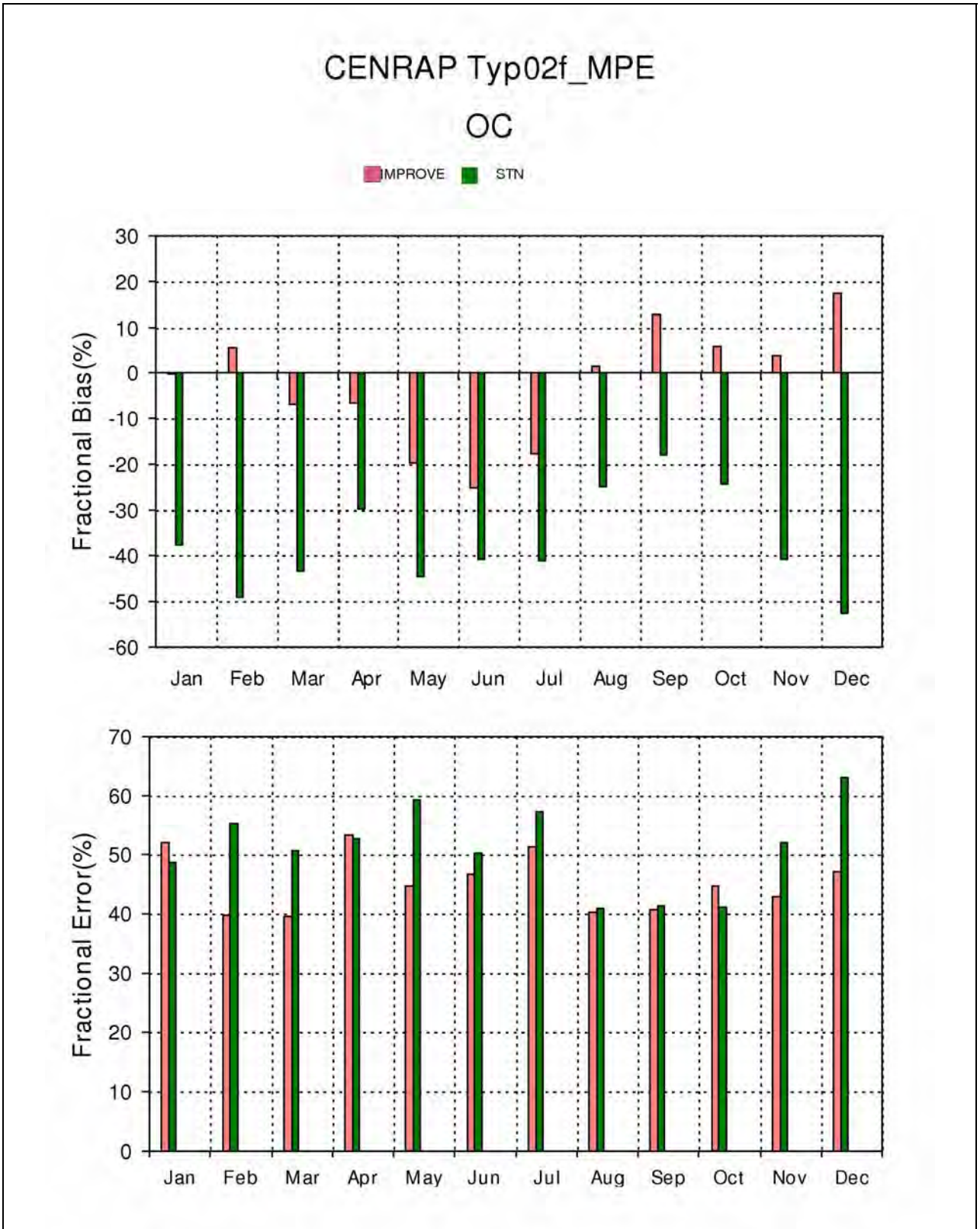

Figure C-20. Monthly OMC fractional bias (top) and fractional gross error (bottom) statistical measures for IMPROVE and STN monitoring sites in the CENRAP region.

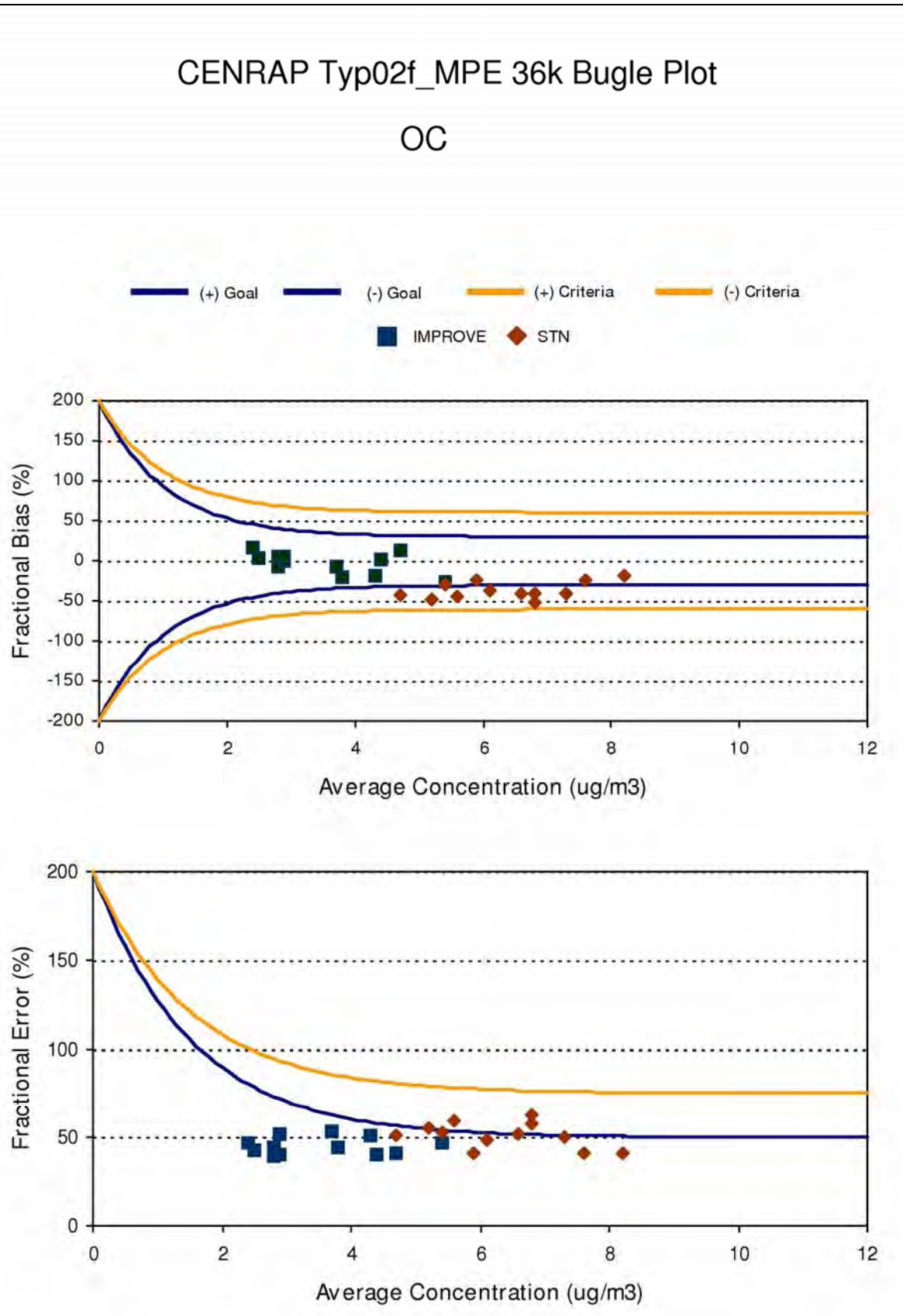

Figure C-21. Bugle Plots of monthly fractional bias (top) and fractional gross error (bottom) and comparisons with model performance goals and criteria for OMC and IMPROVE and STN monitoring sites in the CENRAP region.

C.3.4 Elemental Carbon (EC) Monthly Model Performance

Elemental Carbon (EC) measurements are also uncertain, with the IMPROVE and STN using different measurement technologies with different measurement artifacts.

C.3.4.1 EC in January 2002

Although there is a lot of scatter in the January EC scatter plots at the IMPROVE and STN sites, the bias is fairly low (-24% and 1%) with errors in the 40%-50% range (Figure C-22a). The time series comparisons (Figure C-22b) suggest an EC underestimation bias at BRET and an overestimation bias at the northern Minnesota sites (VOYA and BOWA). The model generally agrees with the observed spatial distribution of EC in January with higher values on the eastern than western portions of the CENRAP region (Figure C-22c).

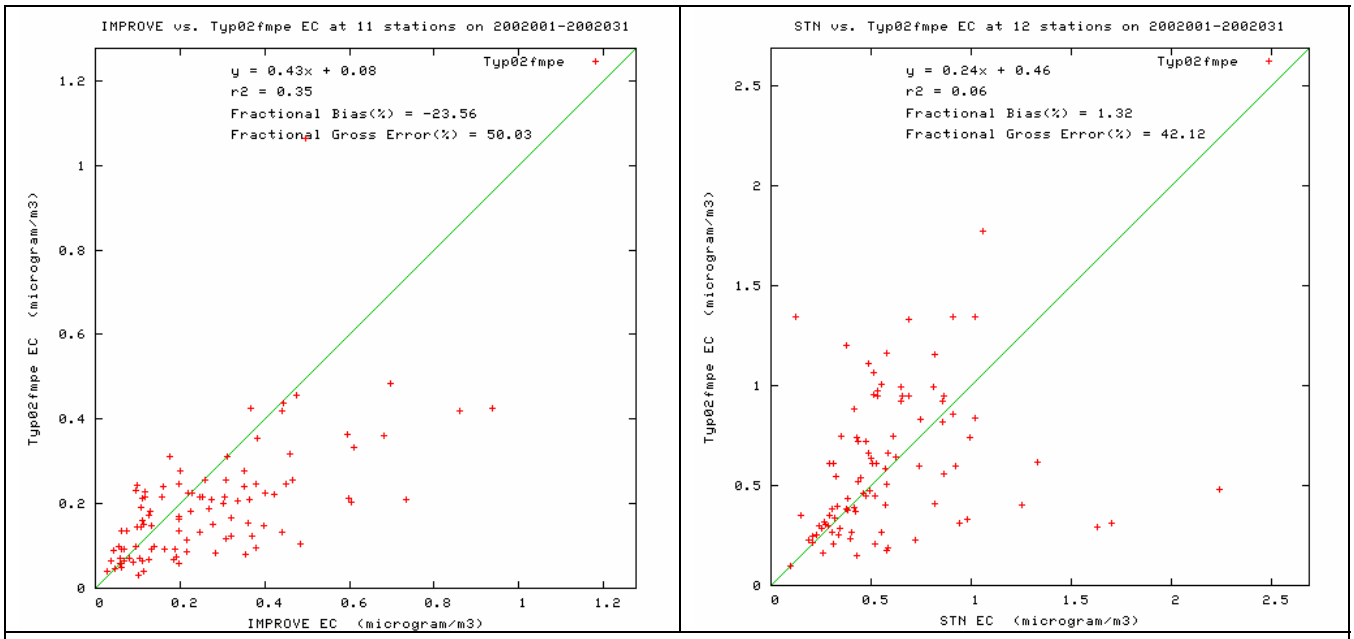

Figure C-22a. Scatter plots of predicted and observed elemental carbon (EC) concentrations for January 2002 and sites in the CENRAP region using IMPROVE (left) and STN (right) monitoring networks using the CMAQ 2002 36 km Base F base case simulation.

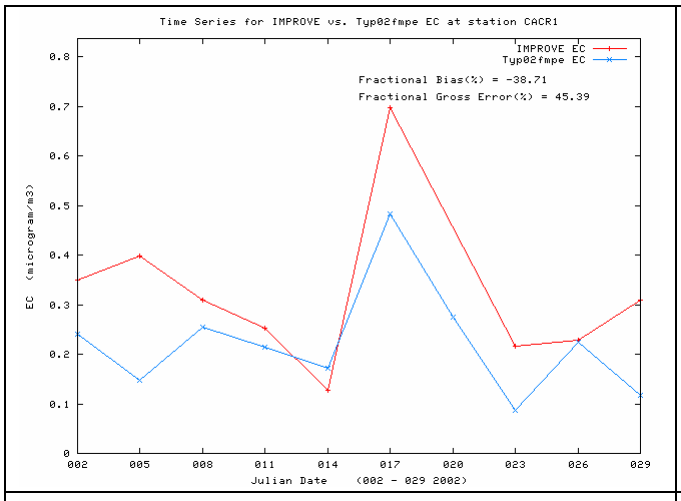
Time Series for IMPROVE vs. Typ02fmpe EC at station CACR1
IMPROVE EC
Typ02fmpe EC
Fractional Bias(%) = -38.71
Fractional Gross Error(%) = 45.39
EC (microgram/m3)
Julian Date (002 - 029 2002)

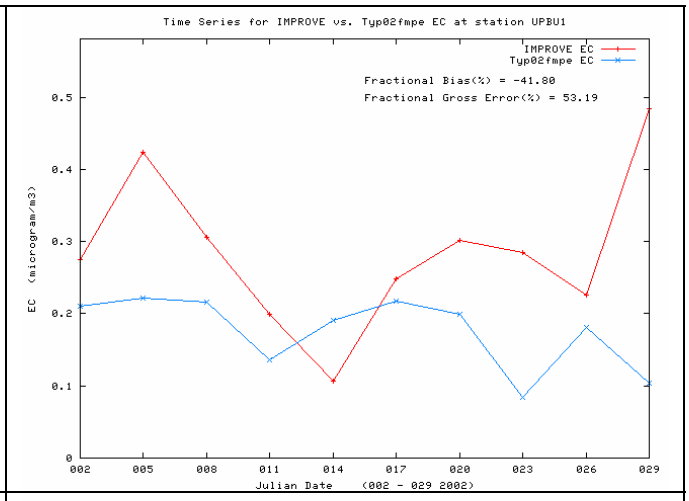
Time Series for IMPROVE vs. Typ02fmpe EC at station UPBU1
IMPROVE EC
Typ02fmpe EC
Fractional Bias(%) = -41.80
Fractional Gross Error(%) = 53.19
EC (microgram/m3)
Julian Date (002 - 029 2002)

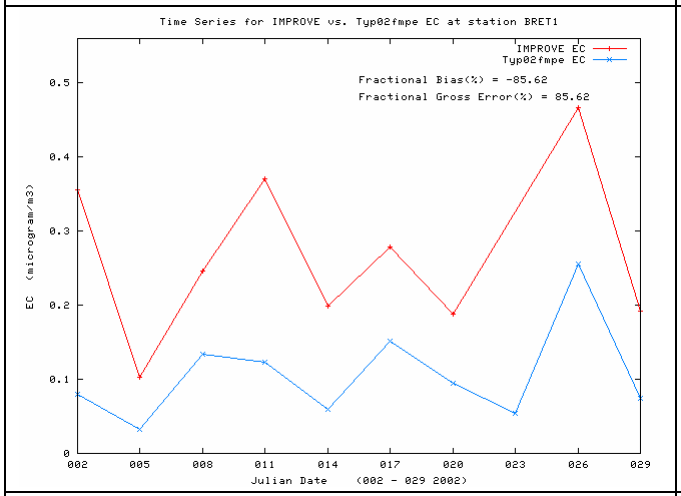
Time Series for IMPROVE vs. Typ02fmpe EC at station BRET1
IMPROVE EC
Typ02fmpe EC
Fractional Bias(%) = -85.62
Fractional Gross Error(%) = 85.62
EC (microgram/m3)
Julian Date (002 - 029 2002)

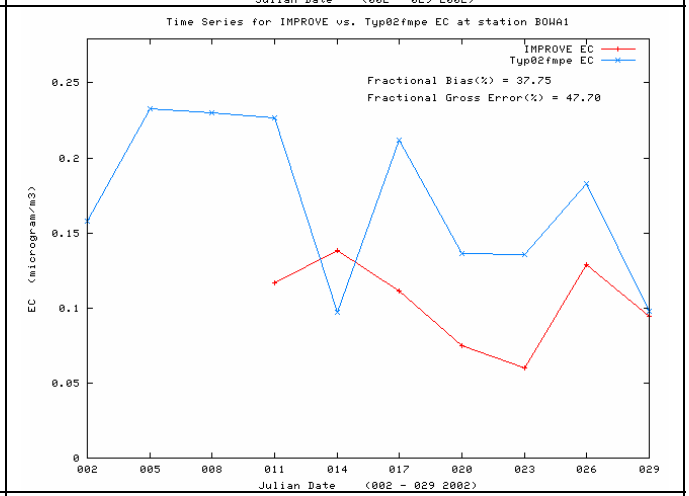
Time Series for IMPROVE vs. Typ02fmpe EC at station BOWA1
IMPROVE EC
Typ02fmpe EC
Fractional Bias(%) = 37.75
Fractional Gross Error(%) = 47.70
EC (microgram/m3)
Julian Date (002 - 029 2002)

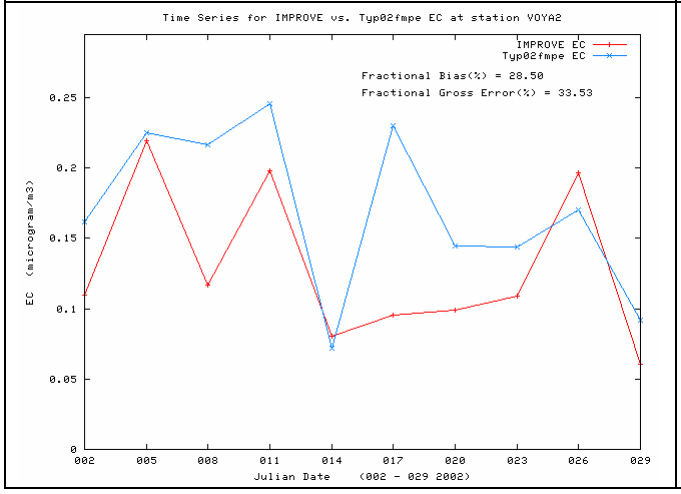
Time Series for IMPROVE vs. Typ02fmpe EC at station VOYA2
IMPROVE EC
Typ02fmpe EC
Fractional Bias(%) = 28.50
Fractional Gross Error(%) = 33.53
EC (microgram/m3)
Julian Date (002 - 029 2002)

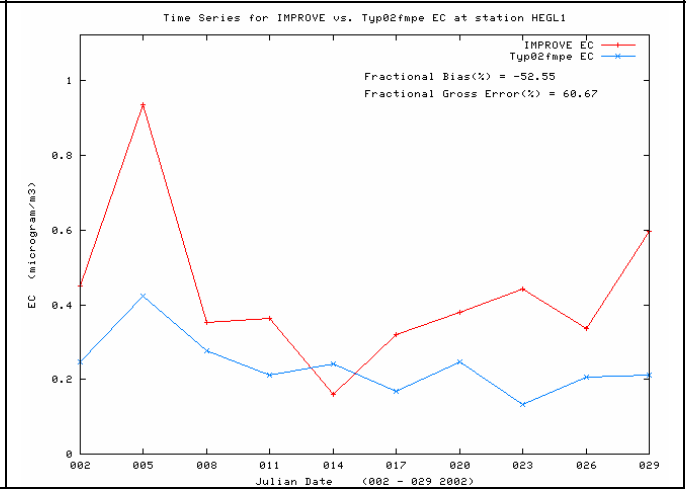
Time Series for IMPROVE vs. Typ02fmpe EC at station HEGL1
IMPROVE EC
Typ02fmpe EC
Fractional Bias(%) = -52.55
Fractional Gross Error(%) = 60.67
EC (microgram/m3)
Julian Date (002 - 029 2002)

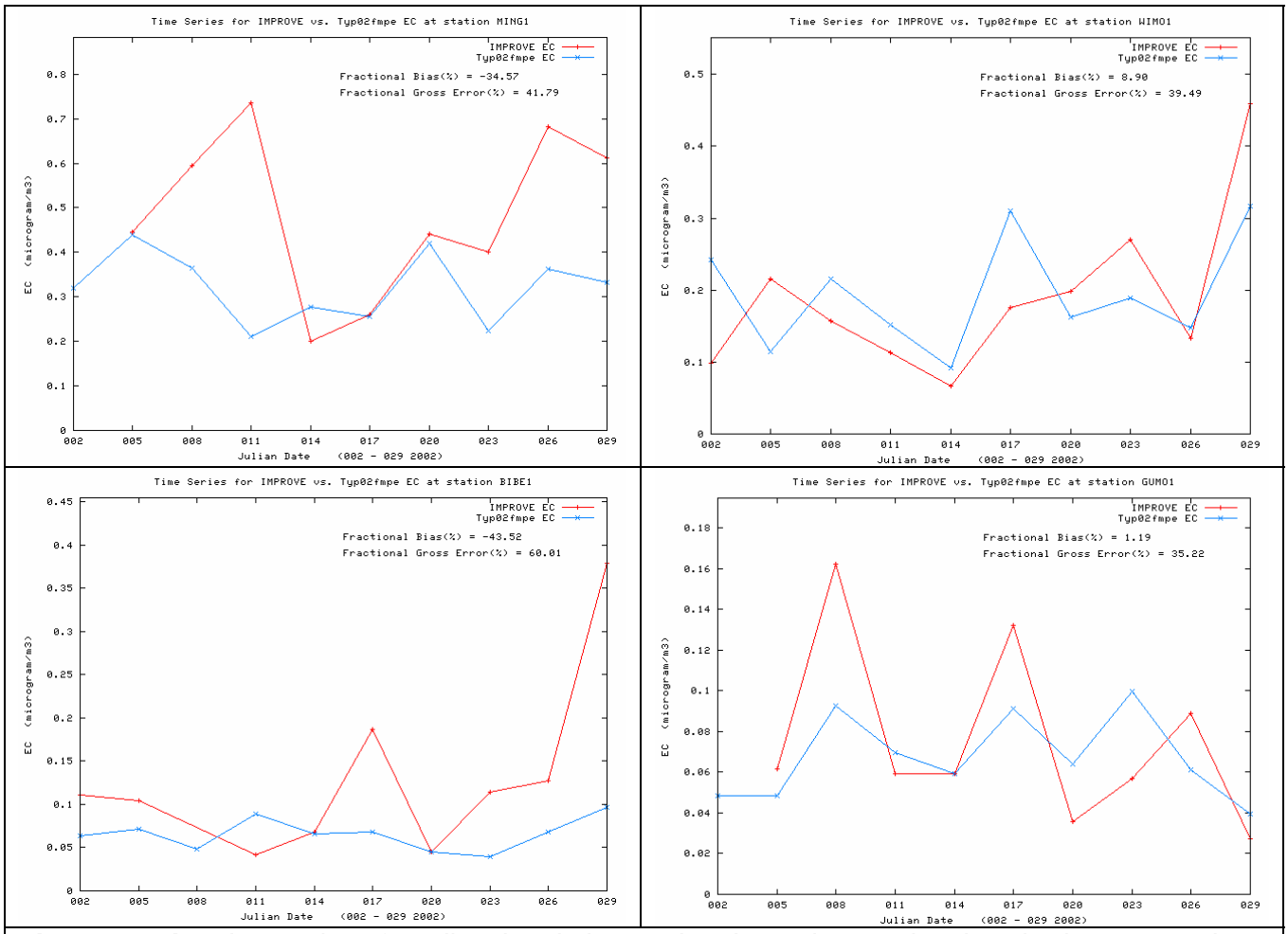

Figure C-22b. Time series of predicted and observed 24-hour elemental carbon (EC) concentrations at CENRAP IMPROVE CLASS I AREA sites in January 2002 for CMAQ 2002 36 km Base F base case simulation.

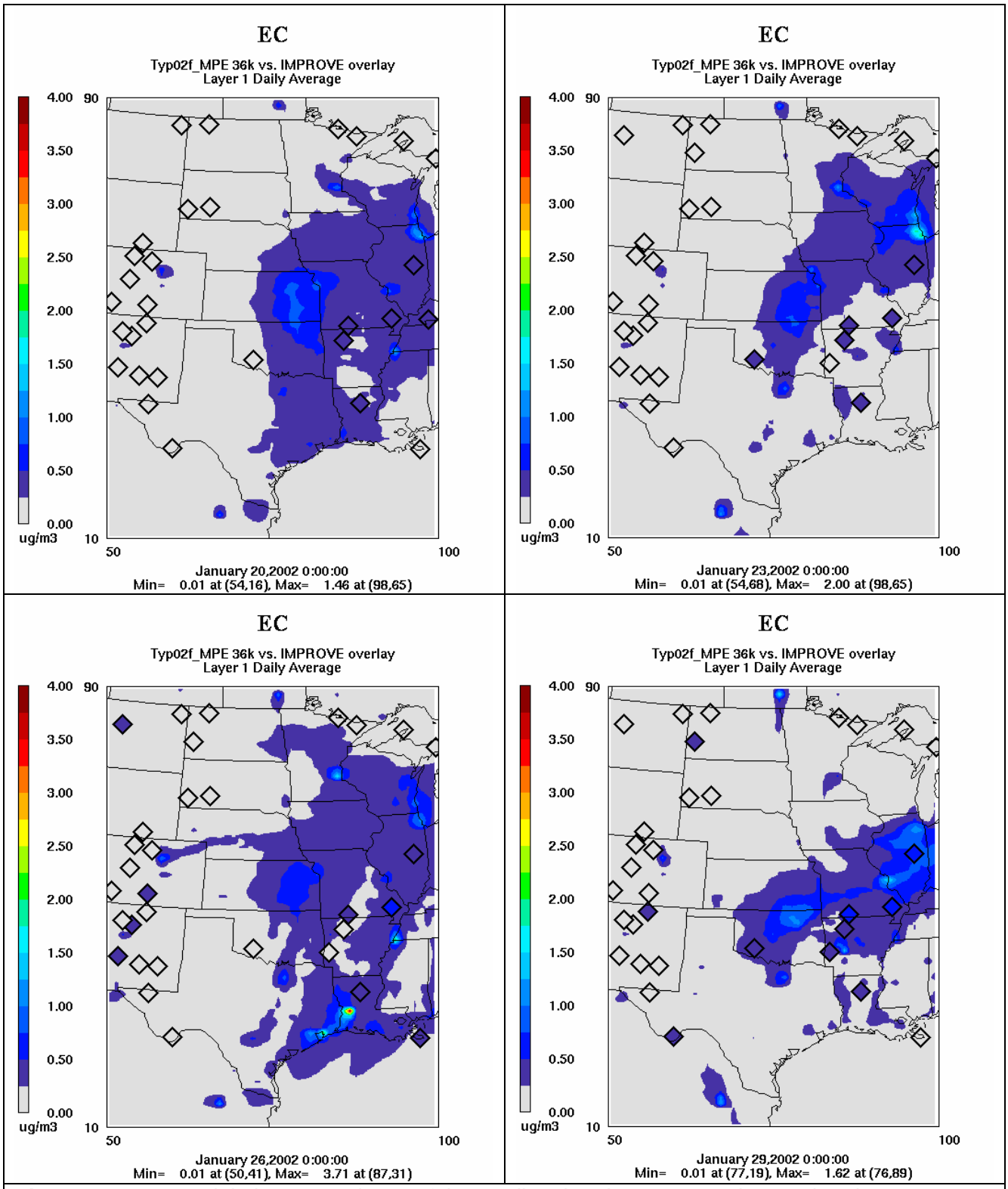

Figure C-22c. Spatial plot comparisons of the predicted and IMPROVE observed 24-hour EC concentrations for January 20, 23, 26 and 29, 2002.

C.3.4.2 EC in April 2002

EC is underestimated at the IMPROVE sites in April (bias of -48%), but reproduced well at the STN sites (bias of -13%). Although EC is underestimated at the IMPROVE sites both the model and observations agree that EC concentrations are very small and not a significant component of the PM budget. The model fails to capture the day-to-day variability in the observed EC at the IMPROVE sites and exhibits a systematic under-prediction tendency at some sites (Figure C-23b). On April 5 and 11 the model reproduces the spatial distribution of the observed EC reasonable well with higher values in the eastern than western portion of the CENRAP region. But on April 8 and 14 the model is much to clean in the eastern portion of the CENRAP region (Figure C-23c).

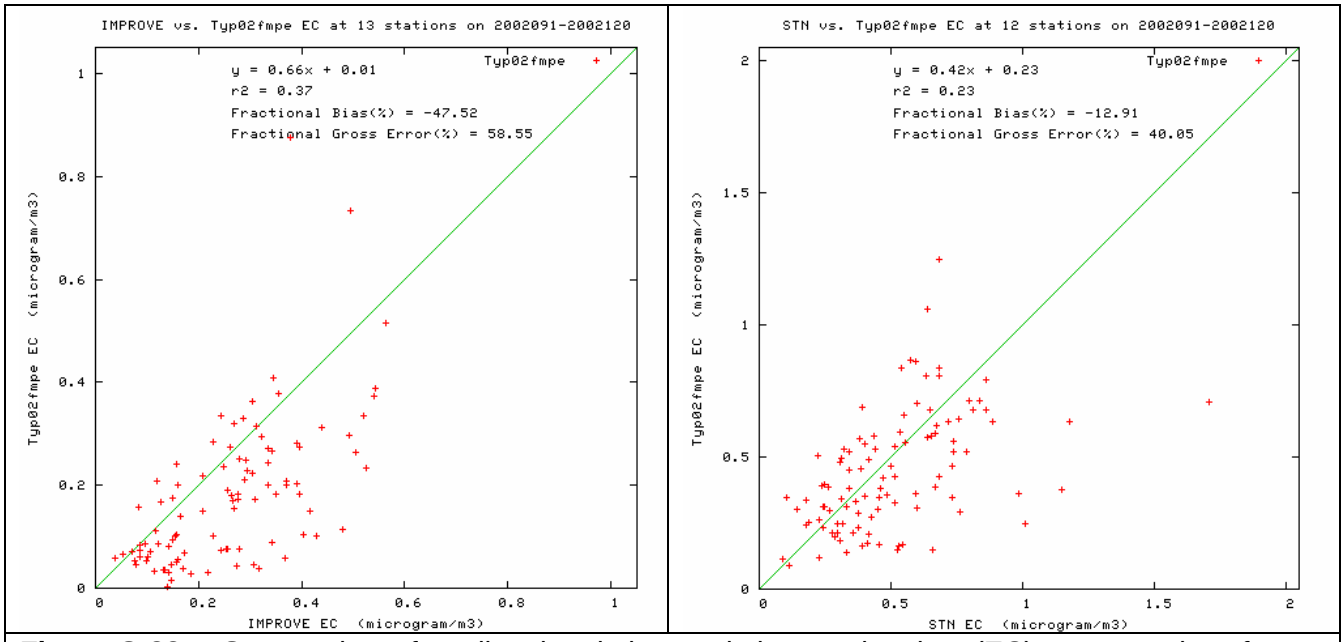

Figure C-23a. Scatter plots of predicted and observed elemental carbon (EC) concentrations for April 2002 and sites in the CENRAP region using IMPROVE (left) and STN (right) monitoring networks using the CMAQ 2002 36 km Base F base case simulation

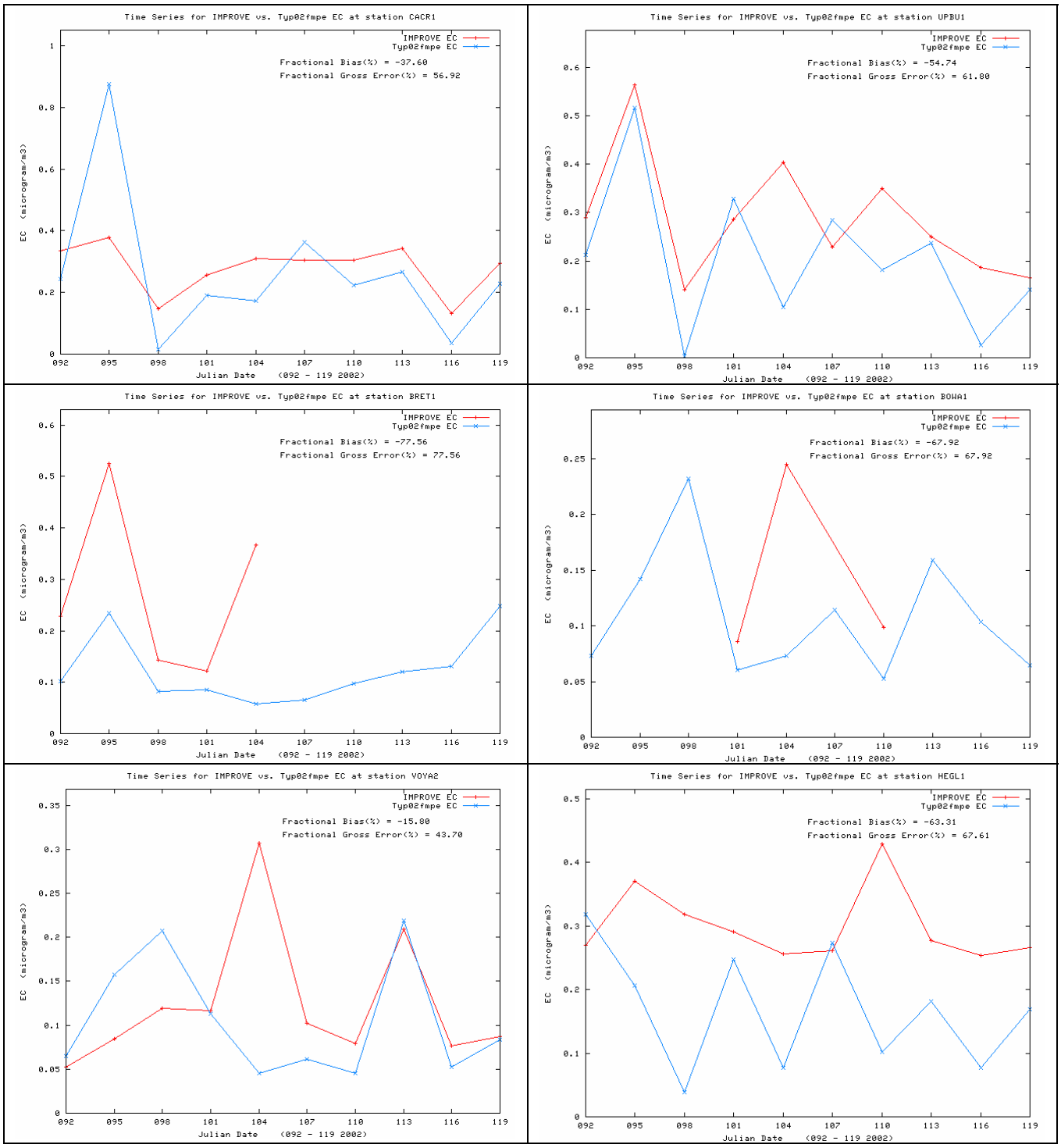
Time Series for IMPROVE vs. Typ02fmpe EC at station CACR1
IMPROVE EC
Typ02fmpe EC
Fractional Bias(%) = -37.60
Fractional Gross Error(%) = 56.92
EC (microgram/m3)
Julian Date (092 - 119 2002)
Time Series for IMPROVE vs. Typ02fmpe EC at station UPBU1
IMPROVE EC
Typ02fmpe EC
Fractional Bias(%) = -54.74
Fractional Gross Error(%) = 61.80
EC (microgram/m3)
Julian Date (092 - 119 2002)
Time Series for IMPROVE vs. Typ02fmpe EC at station BRET1
IMPROVE EC
Typ02fmpe EC
Fractional Bias(%) = -77.56
Fractional Gross Error(%) = 77.56
EC (microgram/m3)
Julian Date (092 - 119 2002)
Time Series for IMPROVE vs. Typ02fmpe EC at station BOWA1
IMPROVE EC
Typ02fmpe EC
Fractional Bias(%) = -67.92
Fractional Gross Error(%) = 67.92
EC (microgram/m3)
Julian Date (092 - 119 2002)
Time Series for IMPROVE vs. Typ02fmpe EC at station VOYA2
IMPROVE EC
Typ02fmpe EC
Fractional Bias(%) = -15.80
Fractional Gross Error(%) = 43.70
EC (microgram/m3)
Julian Date (092 - 119 2002)
Time Series for IMPROVE vs. Typ02fmpe EC at station HEGL1
IMPROVE EC
Typ02fmpe EC
Fractional Bias(%) = -63.31
Fractional Gross Error(%) = 67.61
EC (microgram/m3)
Julian Date (092 - 119 2002)

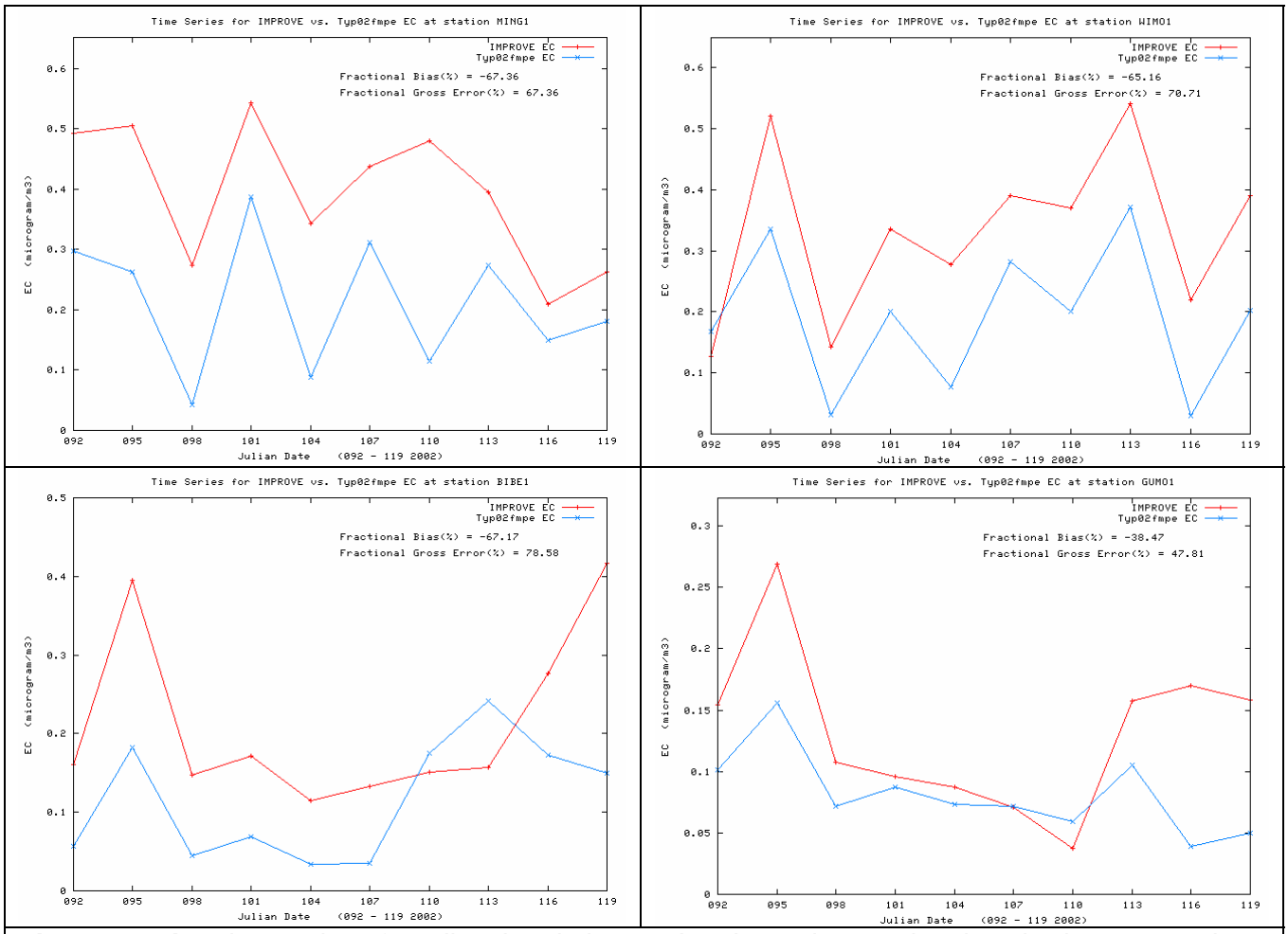

Figure C-23b. Time series of predicted and observed 24-hour elemental carbon (EC) concentrations at CENRAP IMPROVE CLASS I AREA sites in April 2002 for CMAQ 2002 36 km Base F base case simulation.

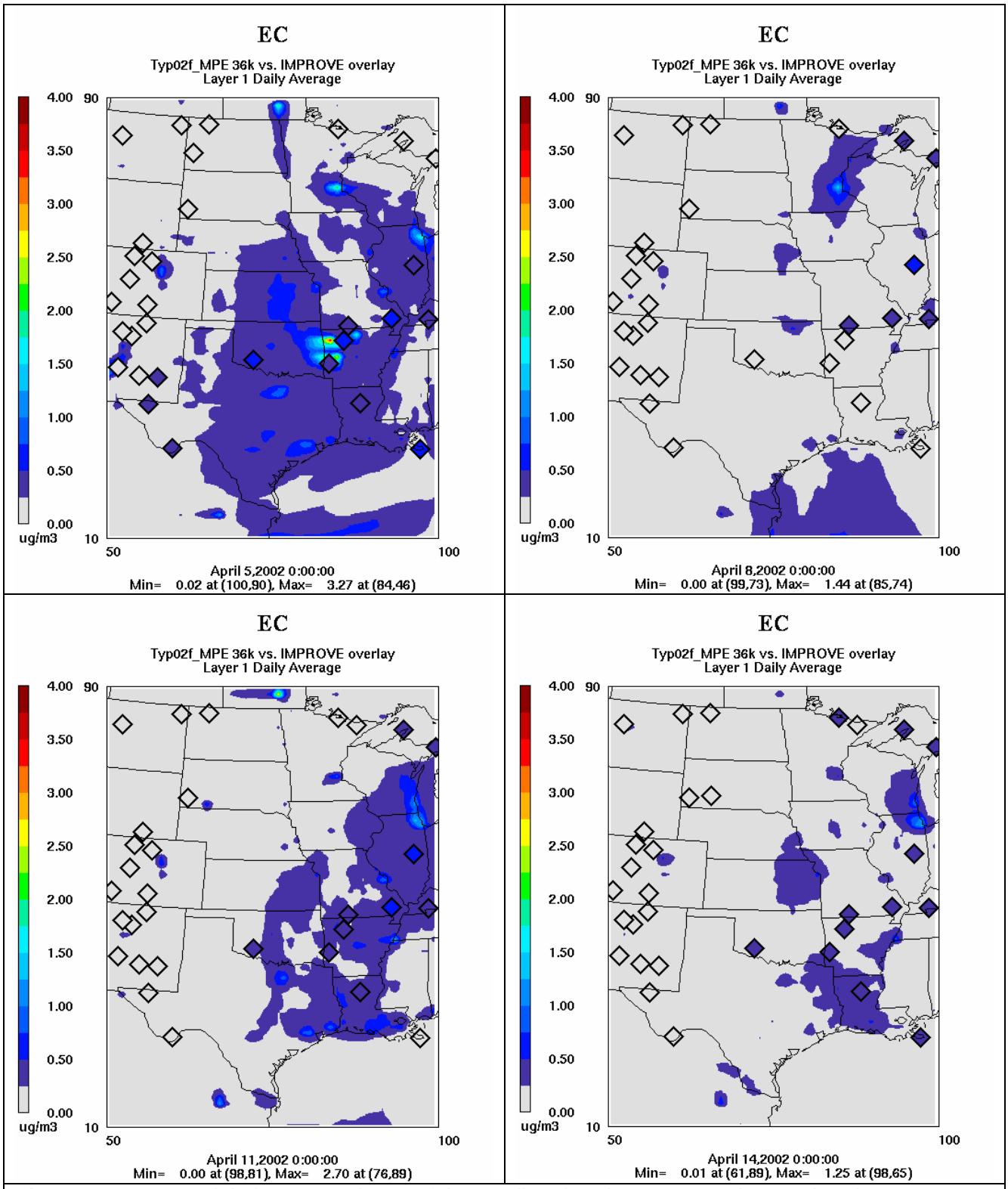

Figure C-23c. Spatial plot comparisons of the predicted and IMPROVE observed 24-hour EC concentrations for April 5, 8, 11 and 14, 2002.

C.3.3.3 EC in July 2002

July EC performance is similar to the other months with near zero bias across he STN sites and an underestimation bias across the IMPROVE sites (Figure C-24). Again the model and observations agree that EC is low in July and not a significant component of visibility impairment.

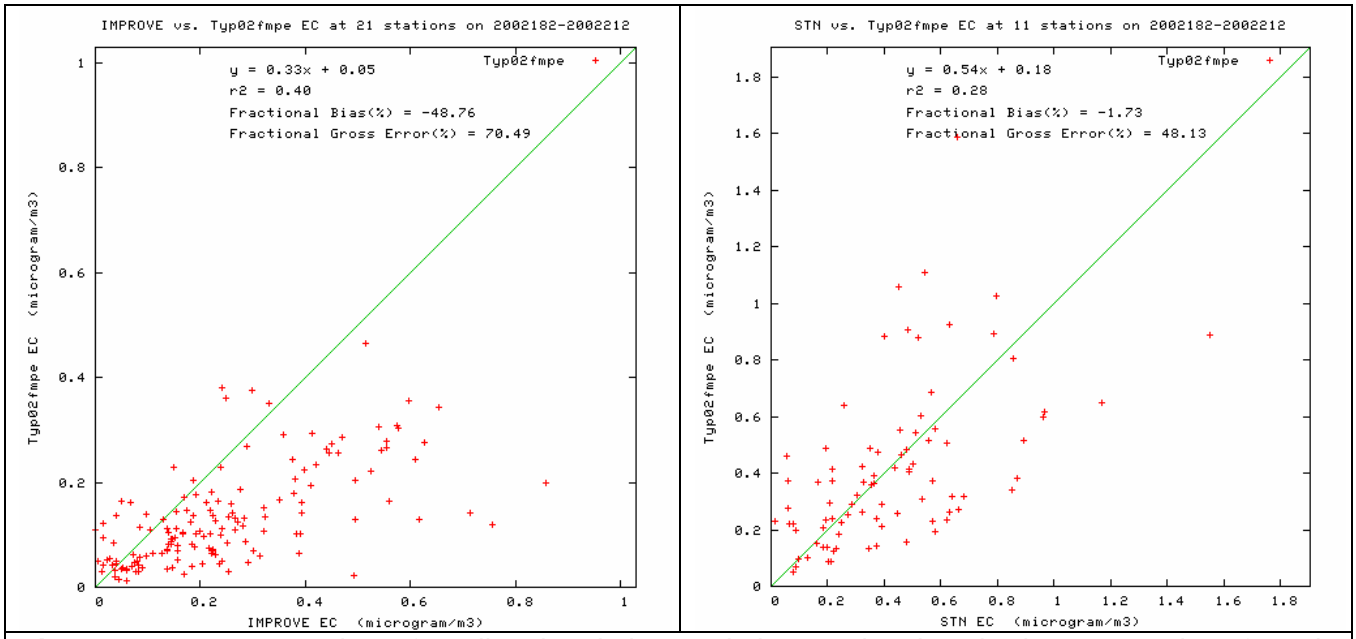

Figure C-24a. Scatter plots of predicted and observed elemental carbon (EC) concentrations for July 2002 and sites in the CENRAP region using IMPROVE (left) and STN (right) monitoring networks using the CMAQ 2002 36 km Base F base case simulation.

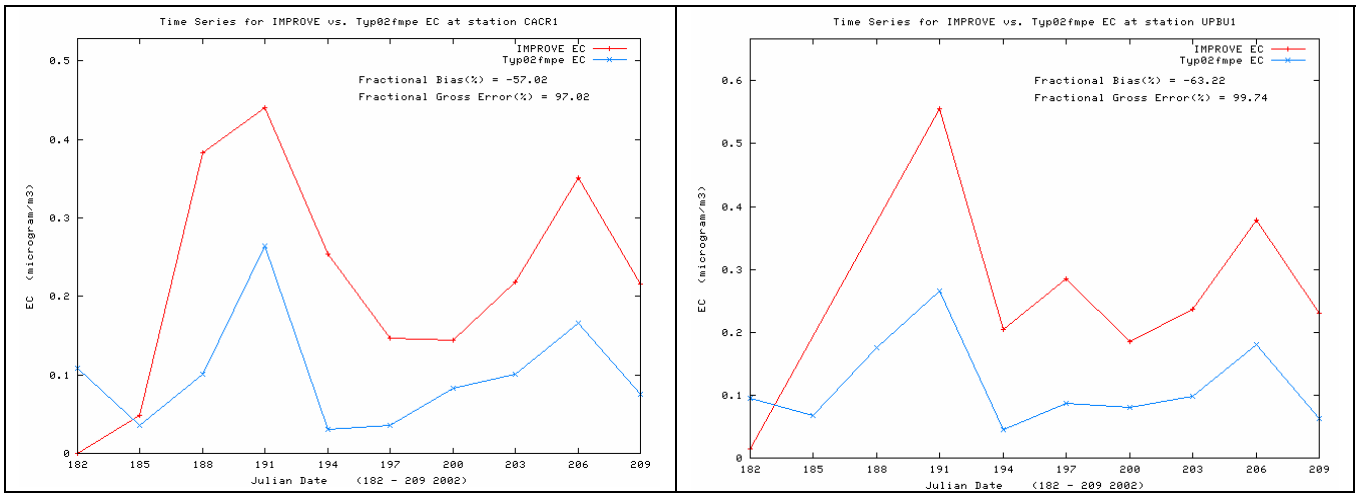

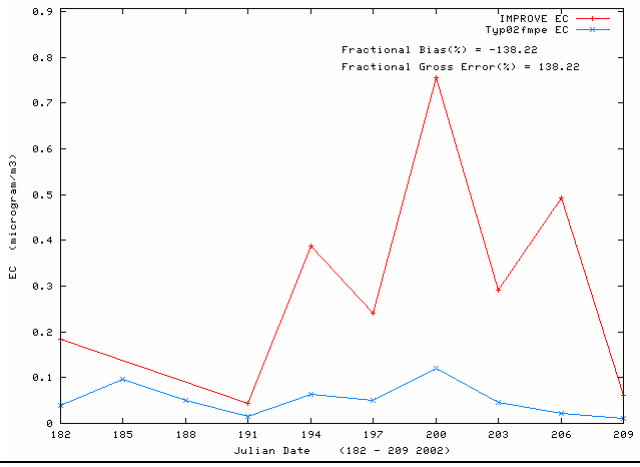

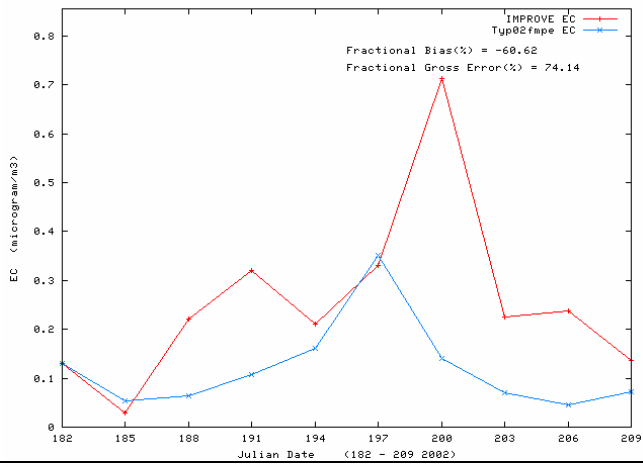

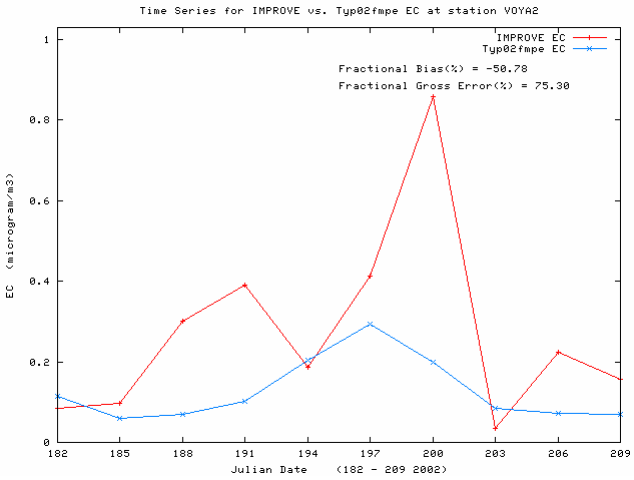

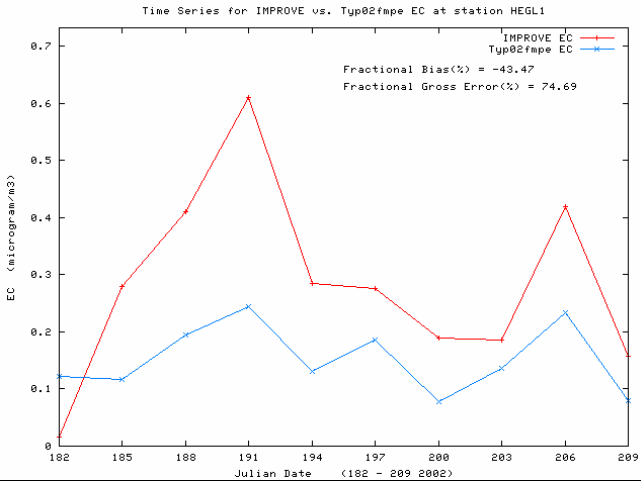

No Data for Mingo (MING)

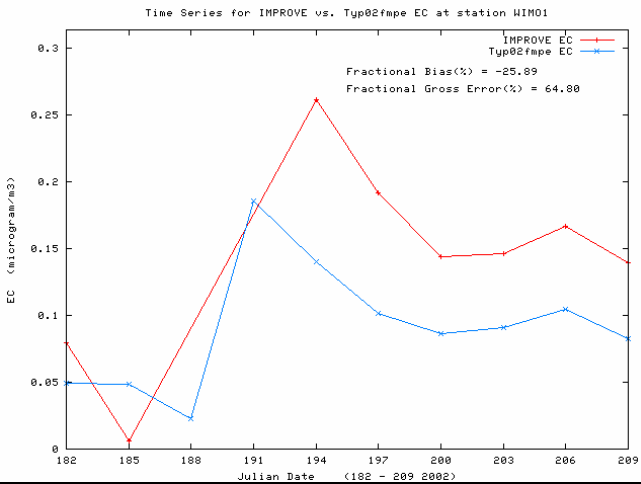

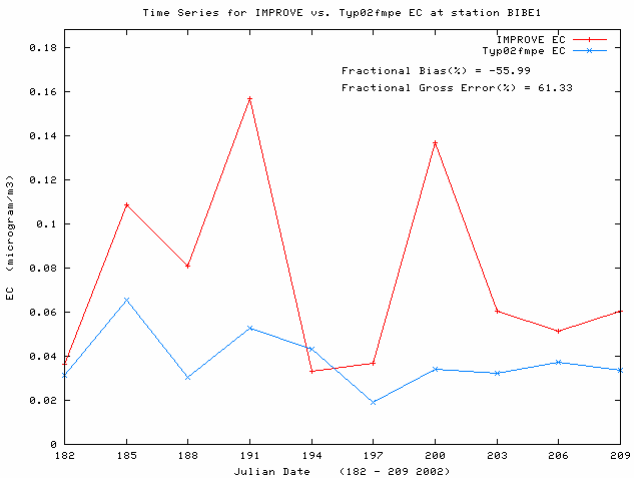

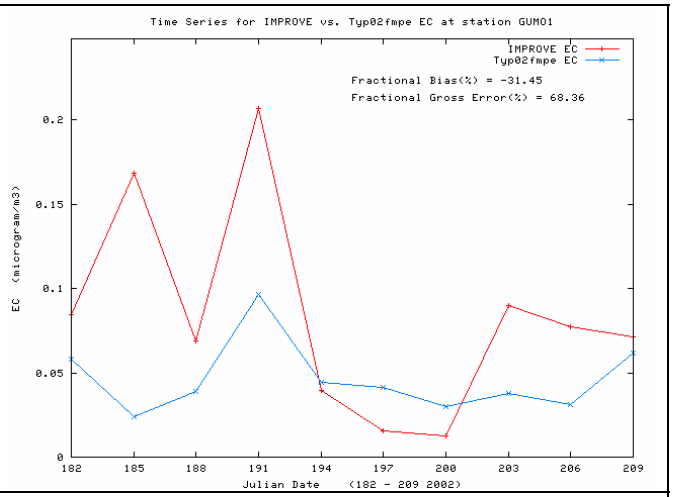

Figure C-24b. Time series of predicted and observed 24-hour elemental carbon (EC) concentrations at CENRAP IMPROVE CLASS I AREA sites in July 2002 for CMAQ 2002 36 km Base F base case simulation.

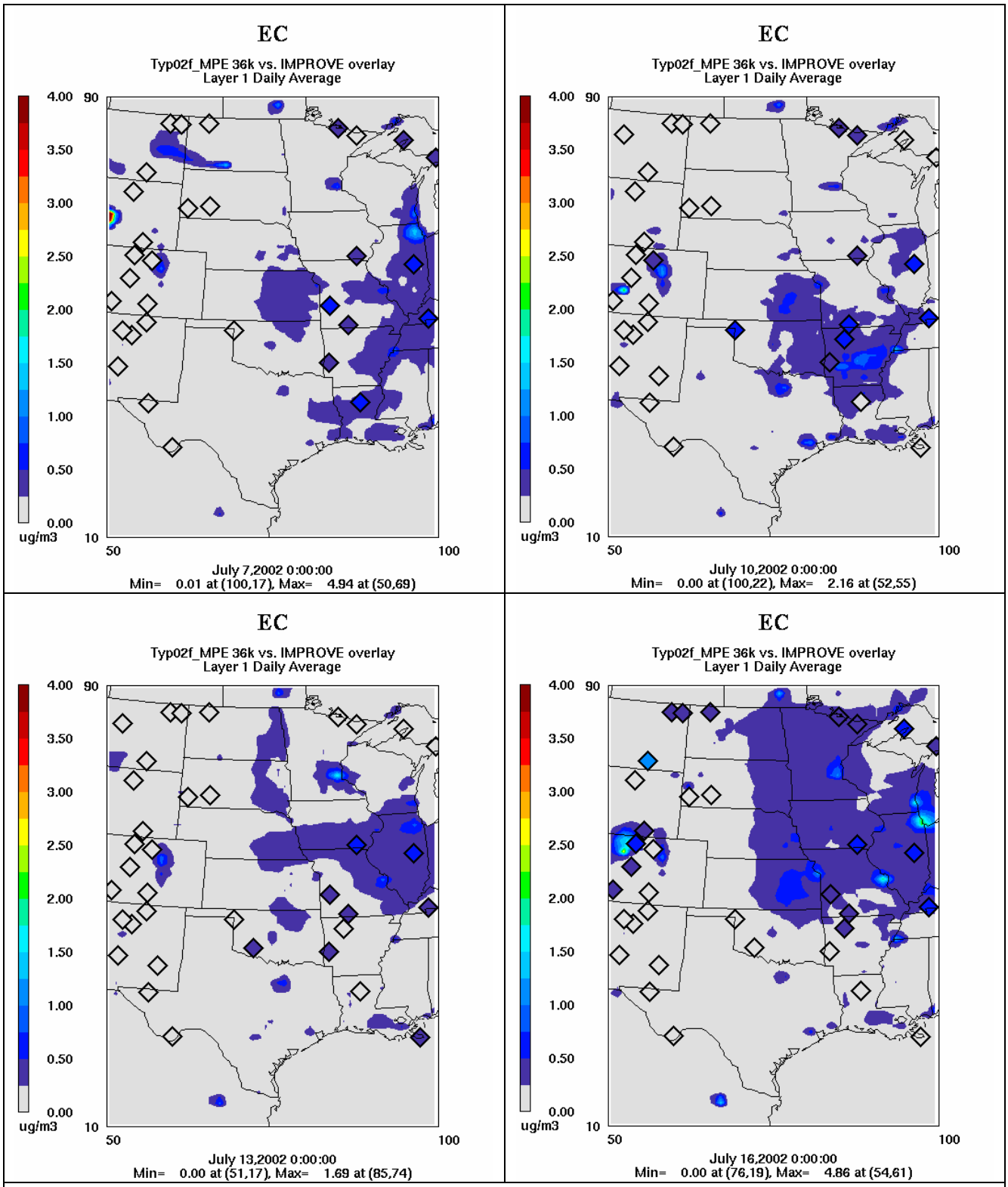

Figure C-24c. Spatial plot comparisons of the predicted and IMPROVE observed 24-hour EC concentrations for July 7, 10, 13 and 16, 2002.

C.3.4.4 EC in October 2002

EC performance is improved at the IMPROVE sites in October with lower bias (9%) than the previous months where an under-prediction tendency was seen (Figure C-25a). EC bias is also fairly low at the STN sites with errors across both networks of approximately 50%. Although there is a systematic underestimation of EC at BRET, the agreement between the predicted and observed October time series (Figure C-25b) is remarkable at several sites (e.g., CACR, UPBU, VOYA and HEGL).

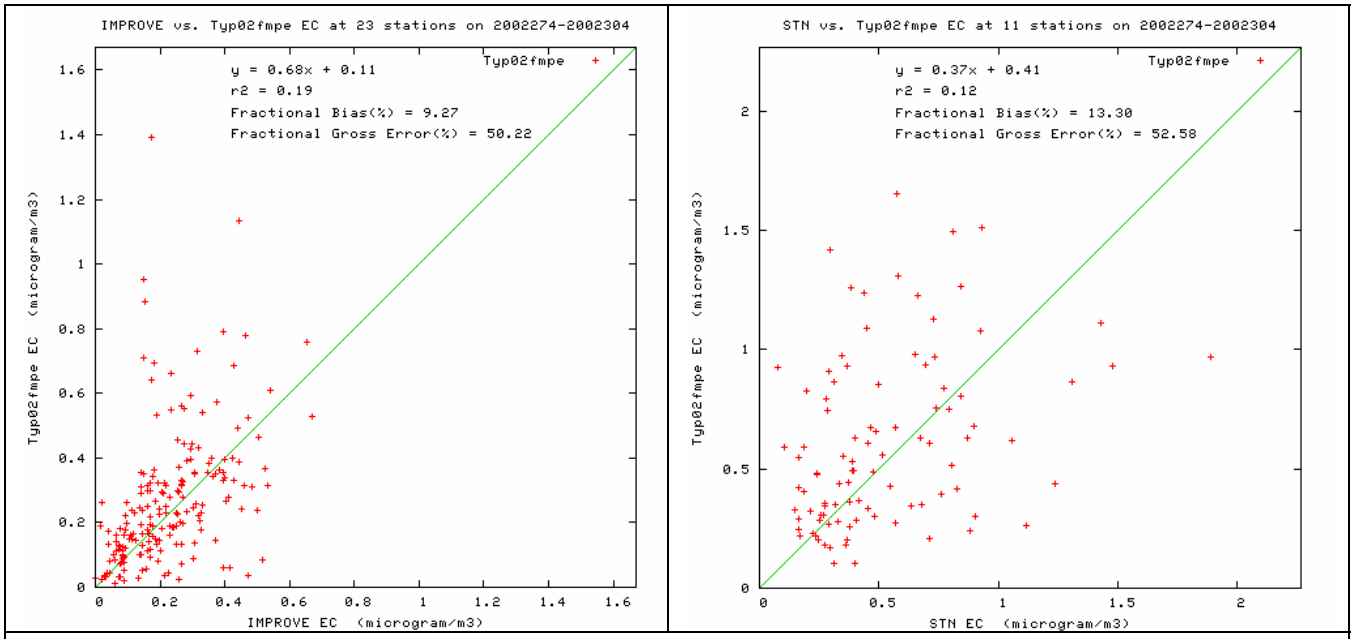

Figure C-25a. Scatter plots of predicted and observed elemental carbon (EC) concentrations for October 2002 and sites in the CENRAP region using IMPROVE (left) and STN (right) monitoring networks using the CMAQ 2002 36 km Base F base case simulation.

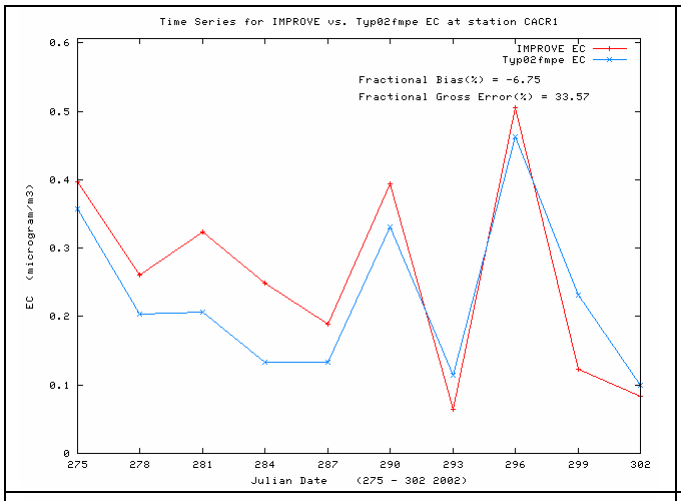
Time Series for IMPROVE vs. Typ02fmpe EC at station CACR1
IMPROVE EC
Typ02fmpe EC
Fractional Bias(%) = -6.75
Fractional Gross Error(%) = 33.57
EC (microgram/m3)
Julian Date (275 - 302 2002)

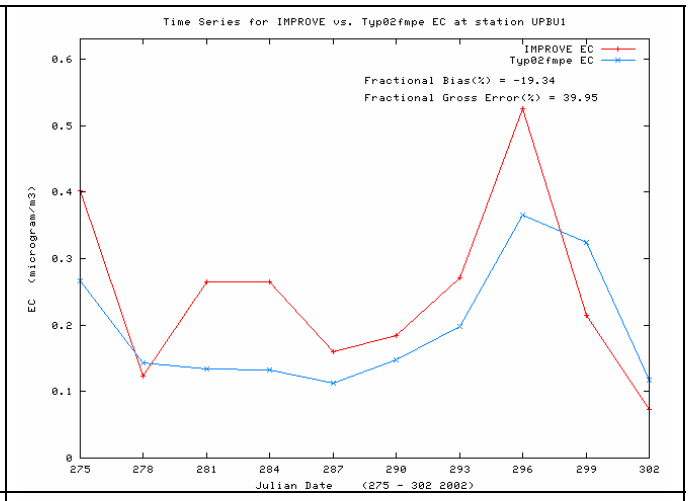
Time Series for IMPROVE vs. Typ02fmpe EC at station UPBU1
IMPROVE EC
Typ02fmpe EC
Fractional Bias(%) = -19.34
Fractional Gross Error(%) = 39.95
EC (microgram/m3)
Julian Date (275 - 302 2002)

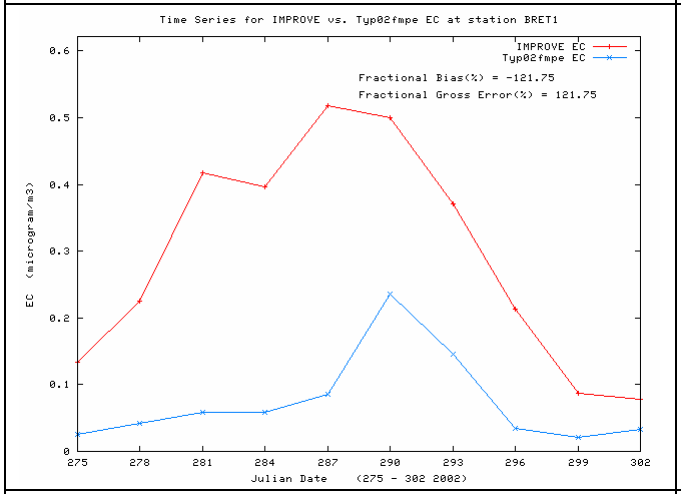
Time Series for IMPROVE vs. Typ02fmpe EC at station BRET1
IMPROVE EC
Typ02fmpe EC
Fractional Bias(%) = -121.75
Fractional Gross Error(%) = 121.75
EC (microgram/m3)
Julian Date (275 - 302 2002)

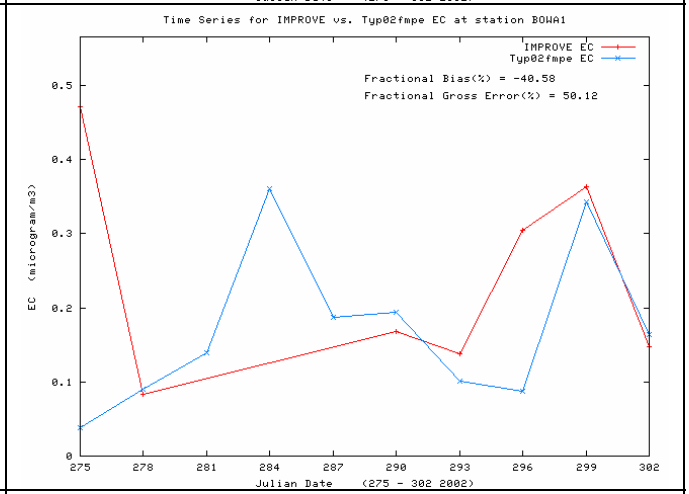
Time Series for IMPROVE vs. Typ02fmpe EC at station BOWA1
IMPROVE EC
Typ02fmpe EC
Fractional Bias(%) = -40.58
Fractional Gross Error(%) = 50.12
EC (microgram/m3)
Julian Date (275 - 302 2002)

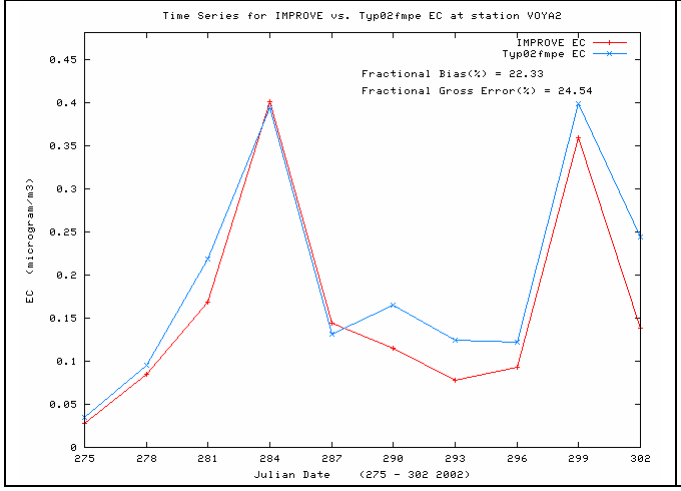
Time Series for IMPROVE vs. Typ02fmpe EC at station VOYA2
IMPROVE EC
Typ02fmpe EC
Fractional Bias(%) = 22.33
Fractional Gross Error(%) = 24.54
EC (microgram/m3)
Julian Date (275 - 302 2002)

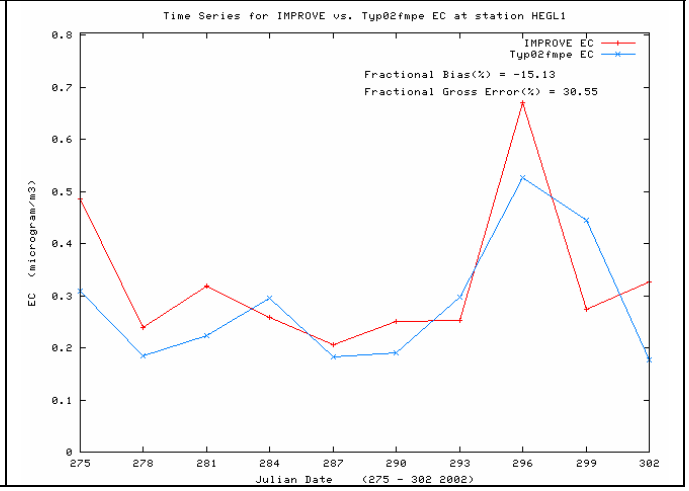
Time Series for IMPROVE vs. Typ02fmpe EC at station HEGL1
IMPROVE EC
Typ02fmpe EC
Fractional Bias(%) = -15.13
Fractional Gross Error(%) = 30.55
EC (microgram/m3)
Julian Date (275 - 302 2002)

No Data for Mingo (MING)

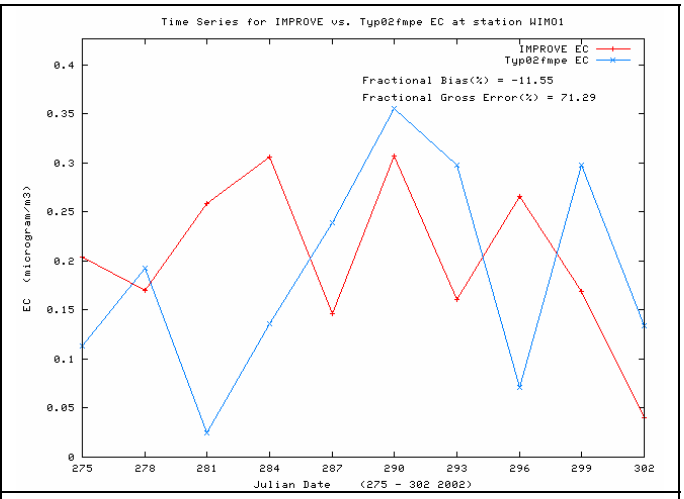

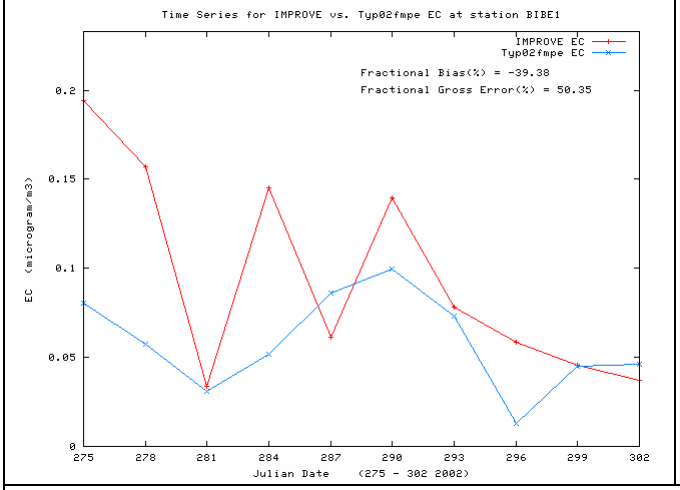

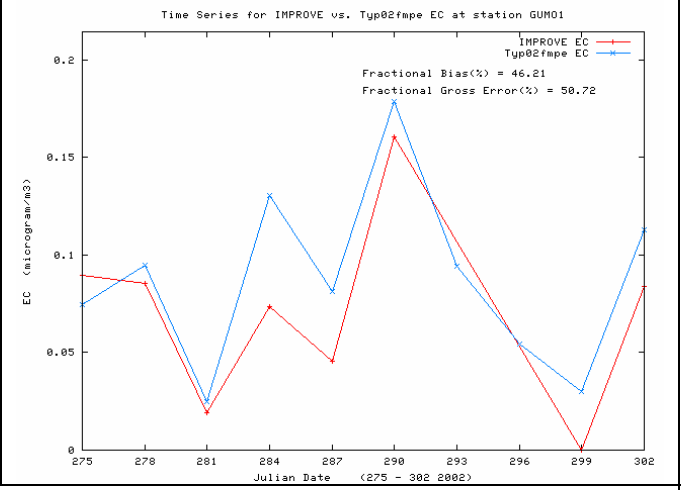

Figure C-25b. Time series of predicted and observed 24-hour elemental carbon (EC) concentrations at CENRAP IMPROVE CLASS I AREA sites in October 2002 for CMAQ 2002 36 km Base F base case simulation.

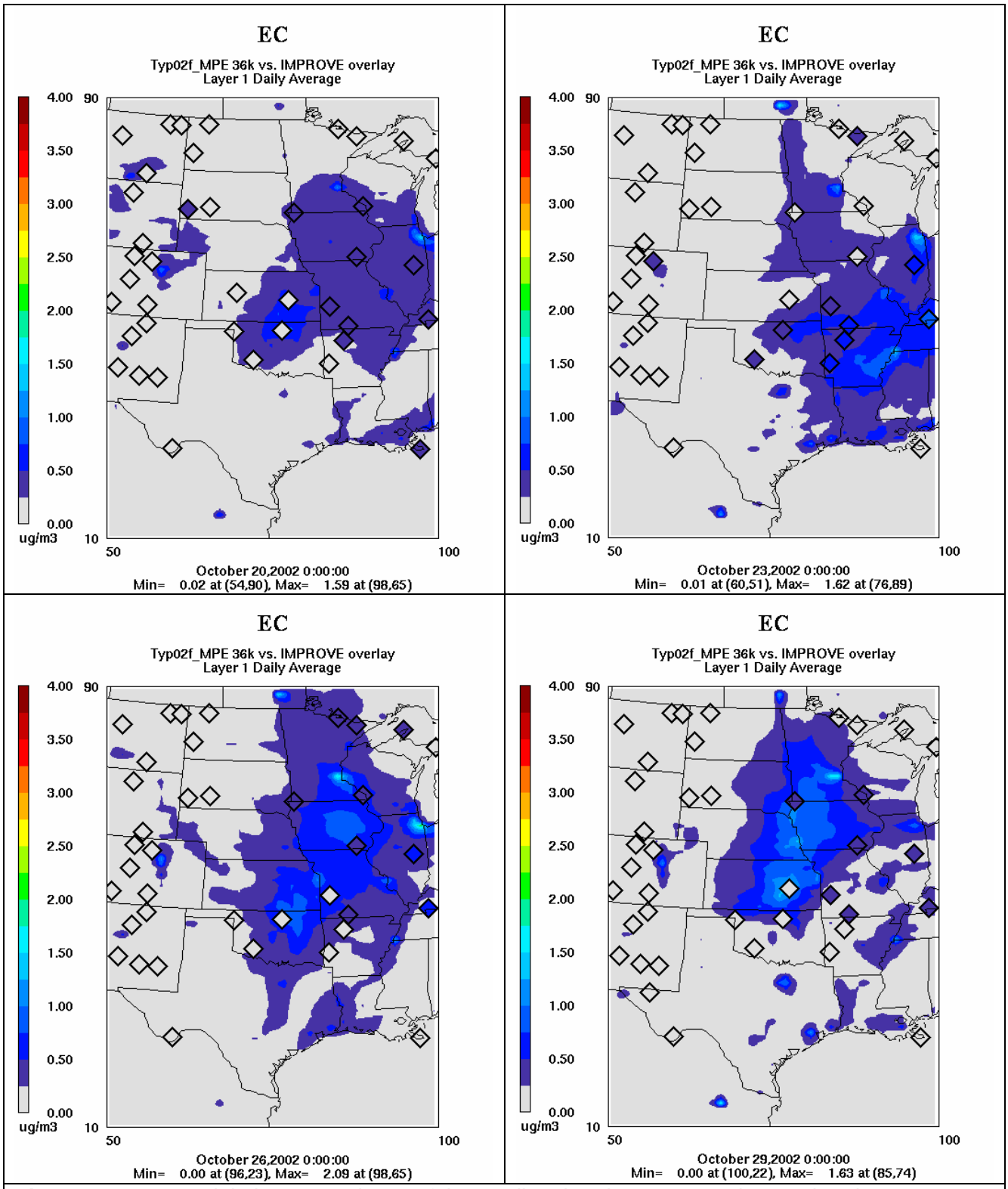

Figure C-25c. Spatial plot comparisons of the predicted and IMPROVE observed 24-hour EC concentrations for October 20, 23, 26 and 29, 2002.

C.3.4.5 EC Monthly Bias and Error

The monthly average bias and error for EC across the IMPROVE and STN monitors in the CENRAP region are shown in Figure C-26. The STN network exhibits low bias year round, whereas the IMPROVE monitoring network exhibits a large under-prediction bias in the summer months (-40% to -60%) and much lower EC bias in the winter. The errors in the IMPROVE summer EC performance are also quite high (60% to 80%), whereas during the winter the IMPROVE errors are in the 40% to 50% range which is also where the STN errors reside year round.

The Bugle Plot puts the EC performance in context (Figure C-27). The low EC concentrations put the IMPROVE EC performance in the horn of the Bugle Plot so that it achieves the proposed PM performance goal for all months of the year.

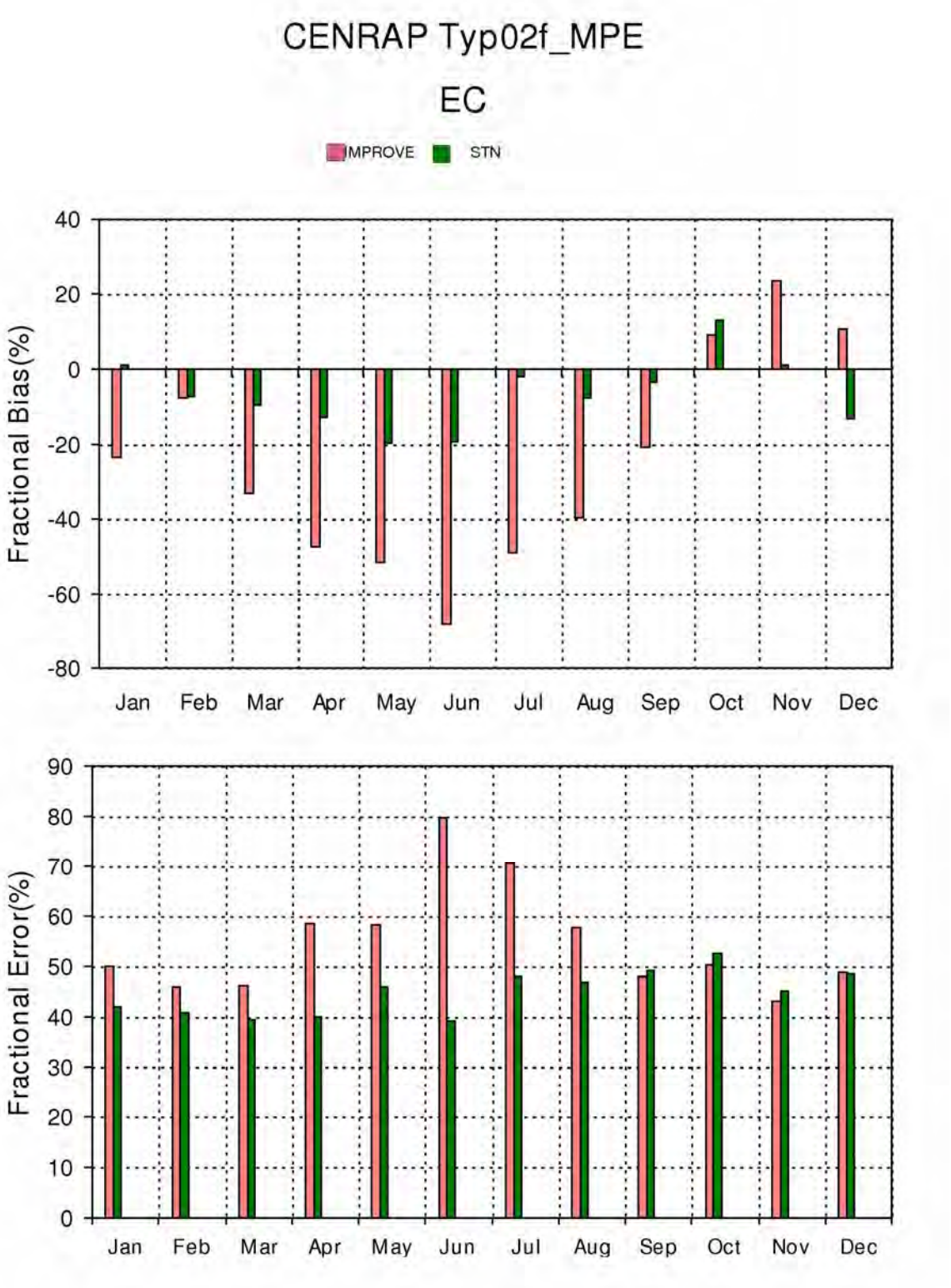

Figure C-26. Monthly EC fractional bias (top) and fractional gross error (bottom) statistical measures for IMPROVE and STN monitoring sites in the CENRAP region.

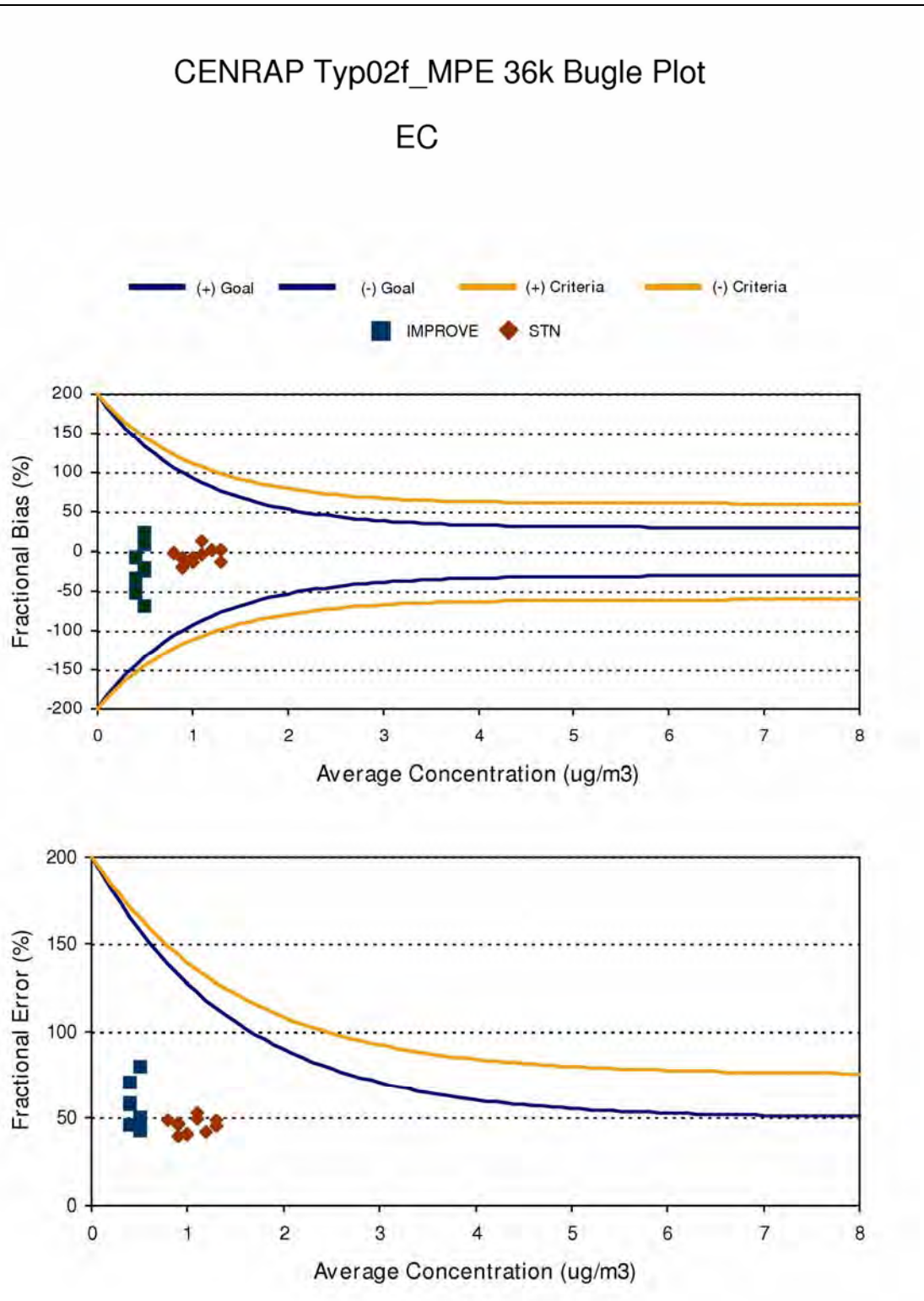

Figure C-27. Bugle Plots of monthly fractional bias (top) and fractional gross error (bottom) and comparisons with model performance goals and criteria for EC and IMPROVE and STN monitoring sites in the CENRAP region.

C.3.5 Other $PM_{2.5}$ (Soil) Monthly Model Performance

There are also model-measurement incommensurability problems with the other $PM_{2.5}$ (Soil) species. Whereas the IMPROVE Soil species is built up from measure elements, the modeled other $PM_{2.5}$ concentrations are based on emissions speciation profiles that likely include other species besides just elements. Soil is only collected at the IMPROVE monitors.

C.3.5.1 Soil in January 2002

The model greatly overestimates the Soil species at IMPORVE sites in January (Figure C-28a). The fractional bias exceeds 100% with errors of almost 130%. With the possible exception of the two Texas sites, the model Soil overestimation bias occurs across all of the CENRAP Class I areas in January (Figure C-28b). The model also does a poor job in reproducing the spatial variability of the observed Soil with a general overestimation tendency except at GUMO where it fails to reproduce the high Soil events.

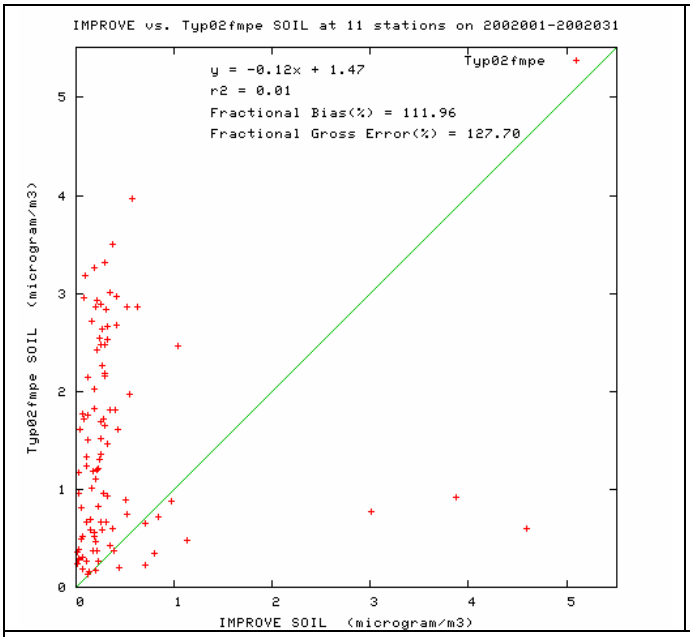

Figure C-28a. Scatter plots of predicted and observed other $PM_{2.5}$ (Soil) concentrations for January 2002 and sites in the CENRAP region using IMPROVE monitoring network and the CMAQ 2002 36 km Base F base case simulation.

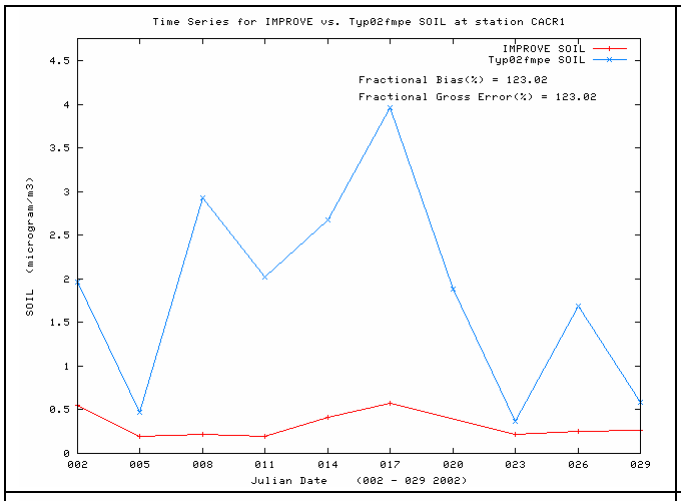
Time Series for IMPROVE vs. Typ02fmpe SOIL at station CACR1
IMPROVE SOIL
Typ02fmpe SOIL
Fractional Bias(%) = 123.02
Fractional Gross Error(%) = 123.02
SOIL (microgram/m3)
Julian Date (002 - 029 2002)

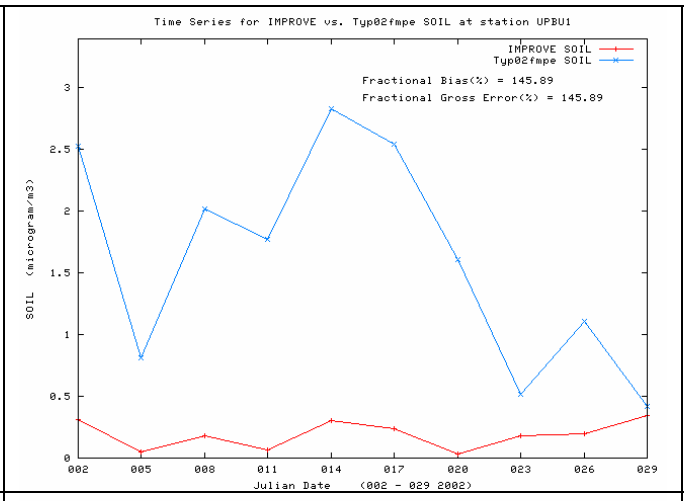
Time Series for IMPROVE vs. Typ02fmpe SOIL at station UPBU1
IMPROVE SOIL
Typ02fmpe SOIL
Fractional Bias(%) = 145.89
Fractional Gross Error(%) = 145.89
SOIL (microgram/m3)
Julian Date (002 - 029 2002)

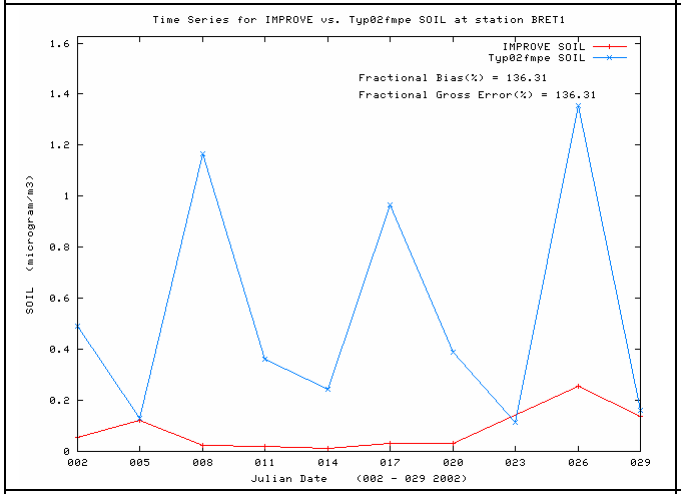
Time Series for IMPROVE vs. Typ02fmpe SOIL at station BRET1
IMPROVE SOIL
Typ02fmpe SOIL
Fractional Bias(%) = 136.31
Fractional Gross Error(%) = 136.31
SOIL (microgram/m3)
Julian Date (002 - 029 2002)

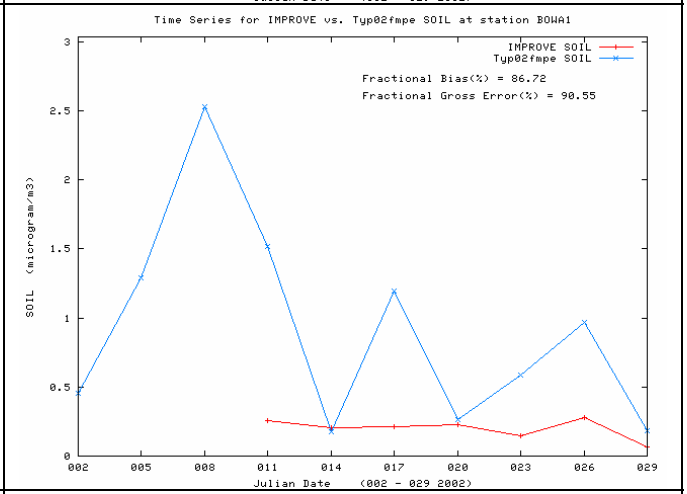
Time Series for IMPROVE vs. Typ02fmpe SOIL at station BOWA1
IMPROVE SOIL
Typ02fmpe SOIL
Fractional Bias(%) = 86.72
Fractional Gross Error(%) = 90.55
SOIL (microgram/m3)
Julian Date (002 - 029 2002)

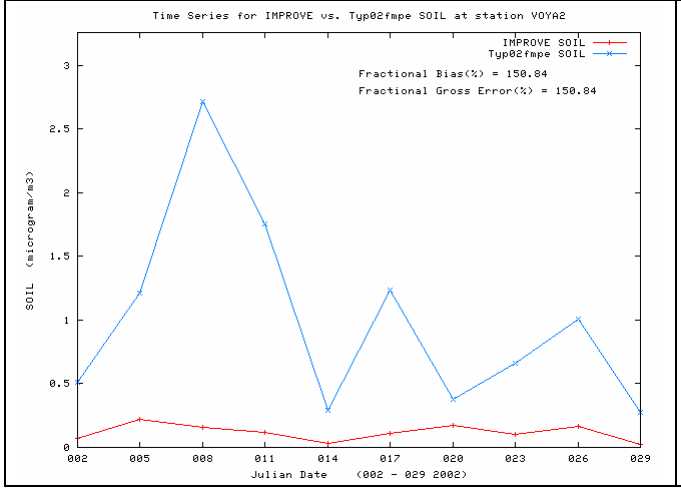
Time Series for IMPROVE vs. Typ02fmpe SOIL at station VOYA2
IMPROVE SOIL
Typ02fmpe SOIL
Fractional Bias(%) = 150.84
Fractional Gross Error(%) = 150.84
SOIL (microgram/m3)
Julian Date (002 - 029 2002)

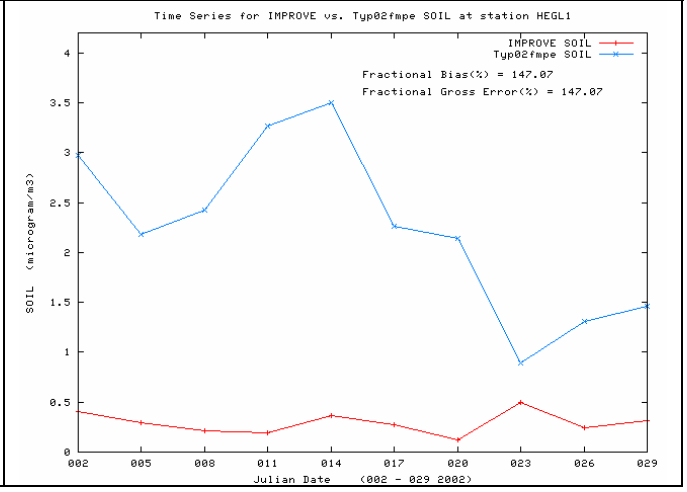
Time Series for IMPROVE vs. Typ02fmpe SOIL at station HEGL1
IMPROVE SOIL
Typ02fmpe SOIL
Fractional Bias(%) = 147.07
Fractional Gross Error(%) = 147.07
SOIL (microgram/m3)
Julian Date (002 - 029 2002)

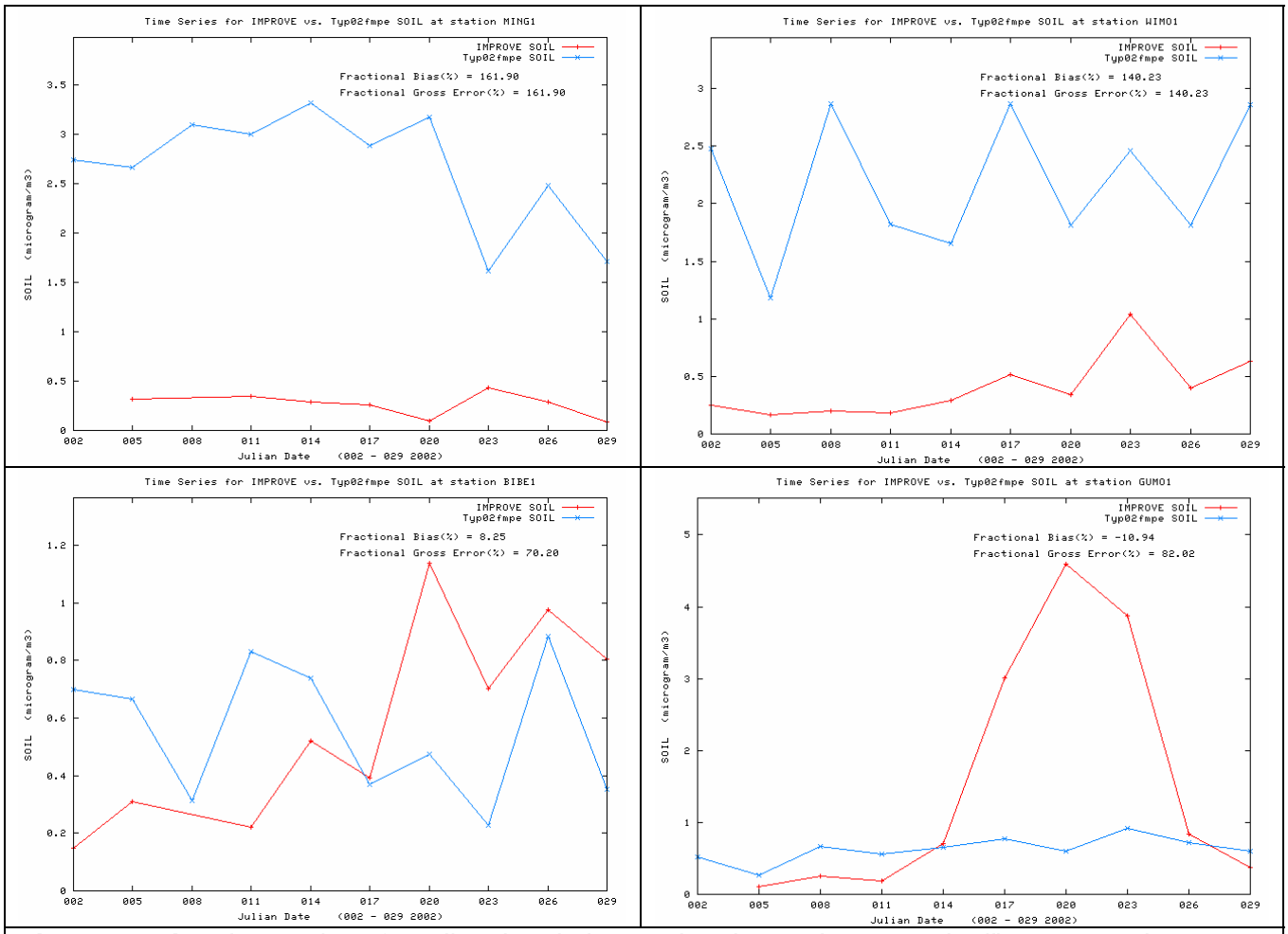

Figure C-28b. Time series of predicted and observed 24-hour other $PM_{2.5}$ (Soil) concentrations at CENRAP IMPROVE CLASS I AREA sites in January 2002 for CMAQ 2002 36 km Base F base case simulation.

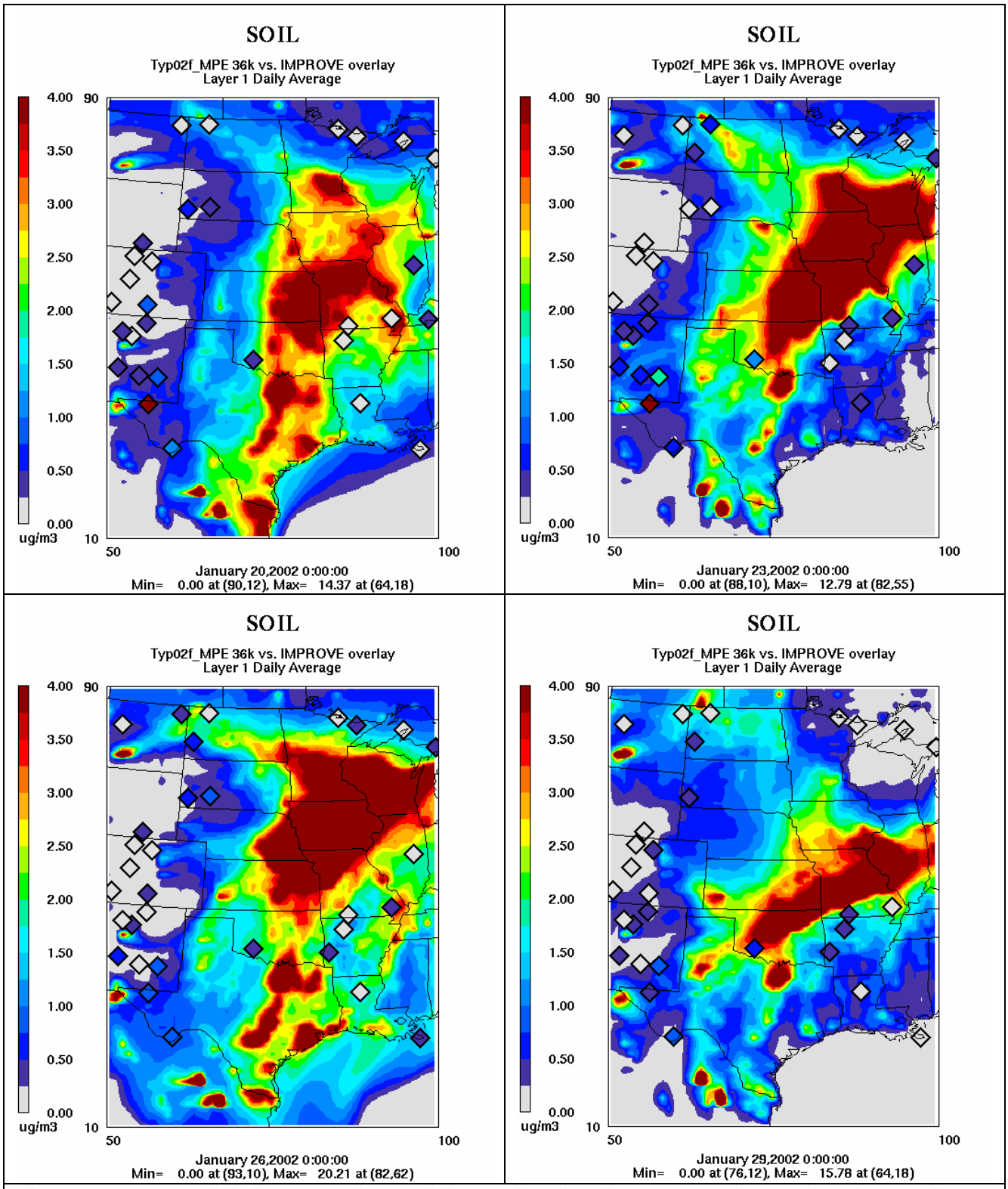

Figure C-28c. Spatial plot comparisons of the predicted and IMPROVE observed 24-hour Soil concentrations for January 20, 23, 26 and 29, 2002.

C.3.5.2 Soil in April 2002

The model does a better job in reproducing the overall magnitude of the Soil measurements in April with a bias of 13% (Figure C-29a). But it exhibits little skill with lots of scatter and an error of 81%. The model is generally exhibiting a lot more day-to-day variability than observed with the observed daily time series much flatter than the modeled values (Figure C-29b). The modeled and observed spatial variability in Soil on April 5, 8, 11 and 14 are shown in Figure C-29c. Although the model exhibits large day-to-day variability, the observations do not reflect what the model predicts.

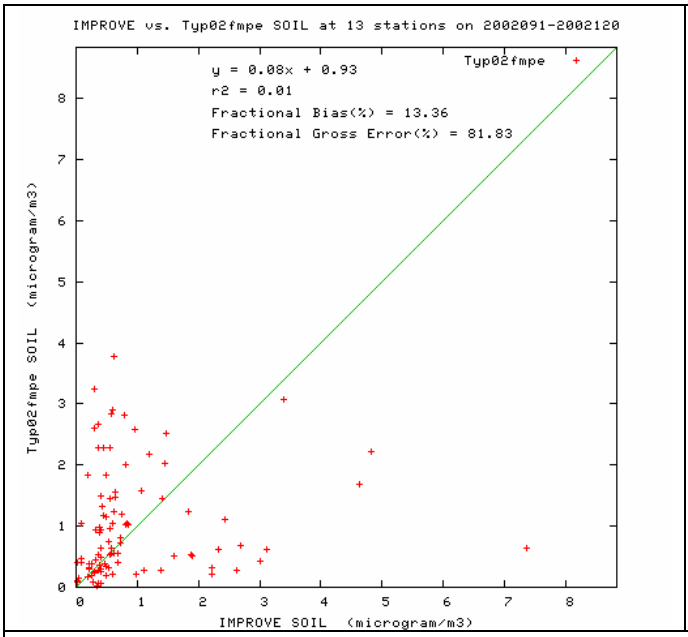

Figure C-29a. Scatter plots of predicted and observed other $PM_{2.5}$ (Soil) concentrations for April 2002 and sites in the CENRAP region using IMPROVE monitoring networks using the CMAQ 2002 36 km Base F base case simulation.

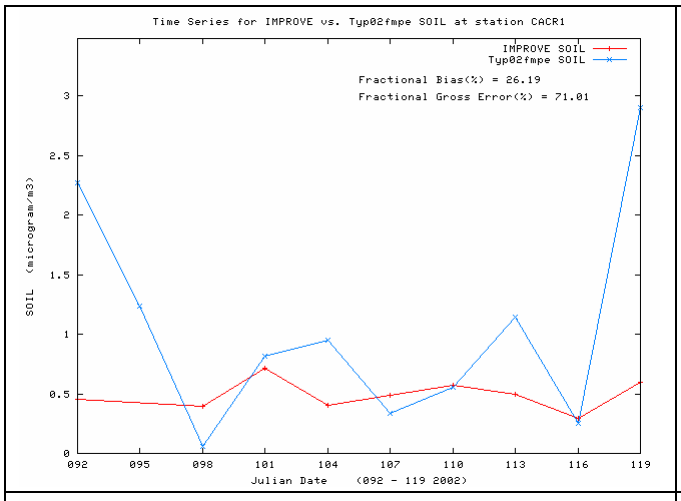
Time Series for IMPROVE vs. Typ02fmpe SOIL at station CACR1
IMPROVE SOIL
Typ02fmpe SOIL
Fractional Bias(%) = 26.19
Fractional Gross Error(%) = 71.01
SOIL (microgram/m3)
Julian Date (092 - 119 2002)

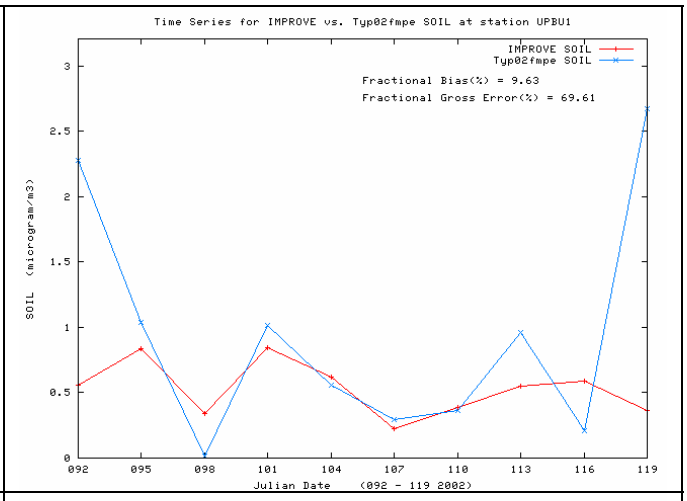
Time Series for IMPROVE vs. Typ02fmpe SOIL at station UPBU1
IMPROVE SOIL
Typ02fmpe SOIL
Fractional Bias(%) = 9.63
Fractional Gross Error(%) = 69.61
SOIL (microgram/m3)
Julian Date (092 - 119 2002)

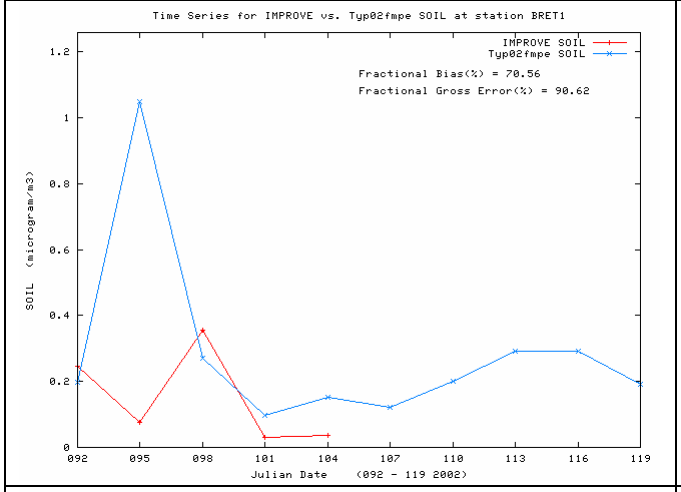
Time Series for IMPROVE vs. Typ02fmpe SOIL at station BRET1
IMPROVE SOIL
Typ02fmpe SOIL
Fractional Bias(%) = 70.56
Fractional Gross Error(%) = 90.62
SOIL (microgram/m3)
Julian Date (092 - 119 2002)

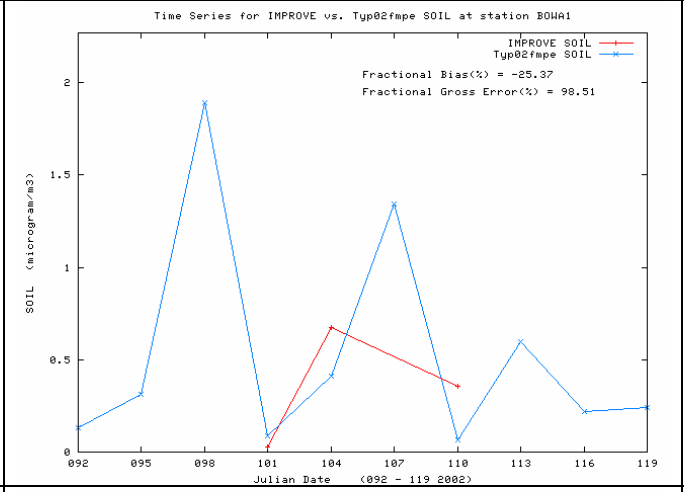
Time Series for IMPROVE vs. Typ02fmpe SOIL at station BOWA1
IMPROVE SOIL
Typ02fmpe SOIL
Fractional Bias(%) = -25.37
Fractional Gross Error(%) = 98.51
SOIL (microgram/m3)
Julian Date (092 - 119 2002)

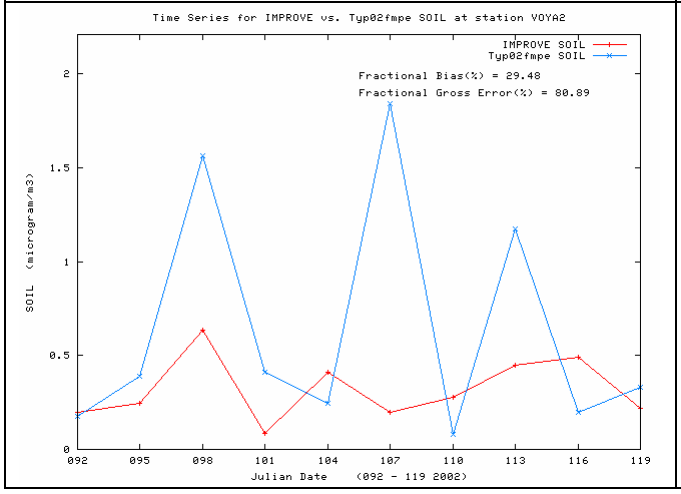
Time Series for IMPROVE vs. Typ02fmpe SOIL at station VOYA2
IMPROVE SOIL
Typ02fmpe SOIL
Fractional Bias(%) = 29.48
Fractional Gross Error(%) = 80.89
SOIL (microgram/m3)
Julian Date (092 - 119 2002)

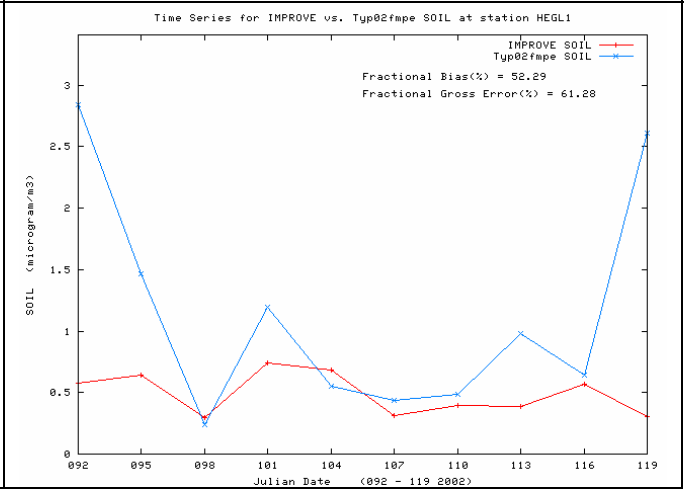
Time Series for IMPROVE vs. Typ02fmpe SOIL at station HEGL1
IMPROVE SOIL
Typ02fmpe SOIL
Fractional Bias(%) = 52.29
Fractional Gross Error(%) = 61.28
SOIL (microgram/m3)
Julian Date (092 - 119 2002)

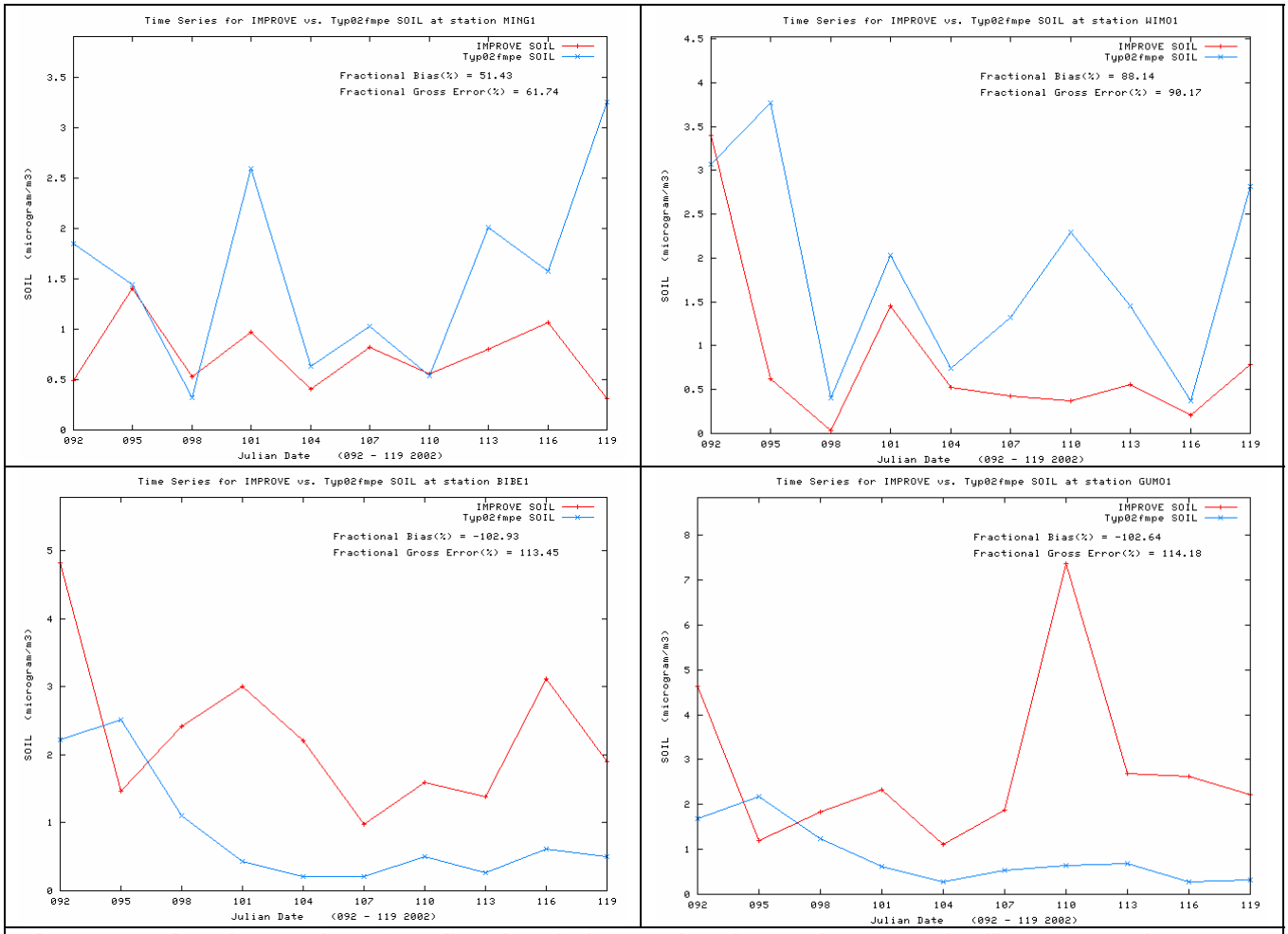

Figure C-29b. Time series of predicted and observed 24-hour other $PM_{2.5}$ (Soil) concentrations at CENRAP IMPROVE CLASS I AREA sites in April 2002 for CMAQ 2002 36 km Base F base case simulation.

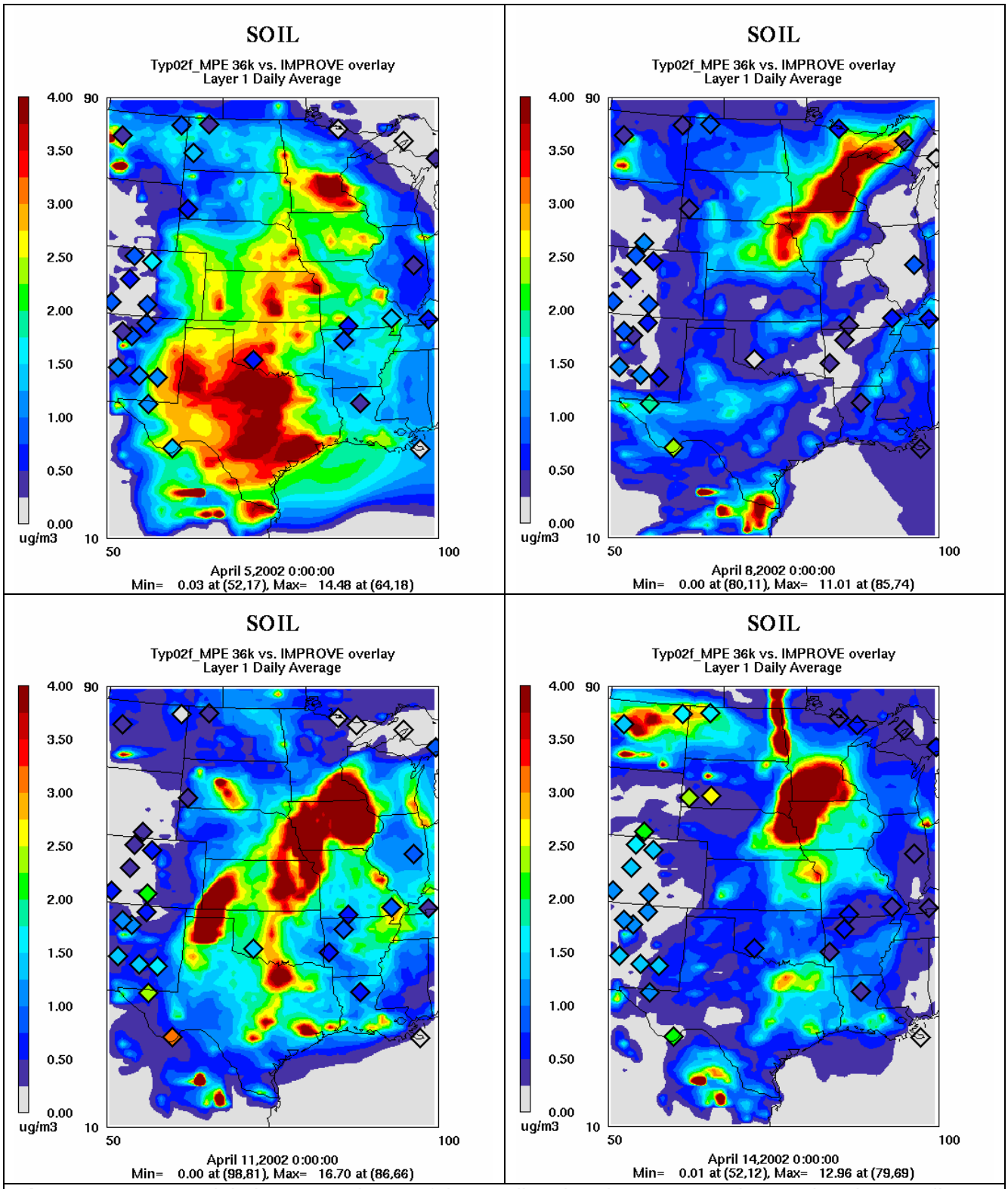

Figure C-29c. Spatial plot comparisons of the predicted and IMPROVE observed 24-hour Soil concentrations for April 5, 8, 11 and 14, 2002.

C.3.5.3 Soil in July 2002

The -50% Soil under-prediction bias seen in July appears to be driven to several high Soil measurements (Figure C-30a). An observed high Soil event took place on July 1 (Julian Day 182) across the Arkansas and Missouri Class I areas that all observed Soil values in excess of 15 μg/m^3. This event was not captured by the model. With the exception of a systematic Soil underestimation bias at the two Texas sites and missing these high Soil events, the model generally reproduces the magnitudes of the Soil observations in July.

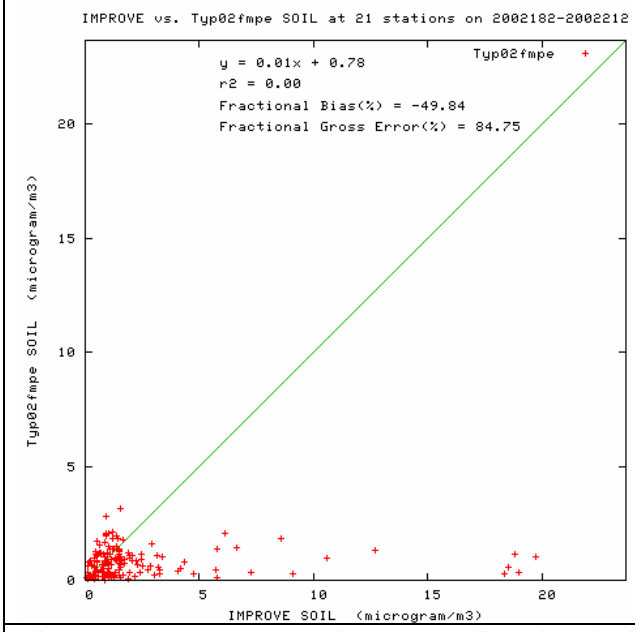

Figure C-30a. Scatter plots of predicted and observed other $PM_{2.5}$ (Soil) concentrations for July 2002 and sites in the CENRAP region using IMPROVE monitoring networks using the CMAQ 2002 36 km Base F base case simulation.

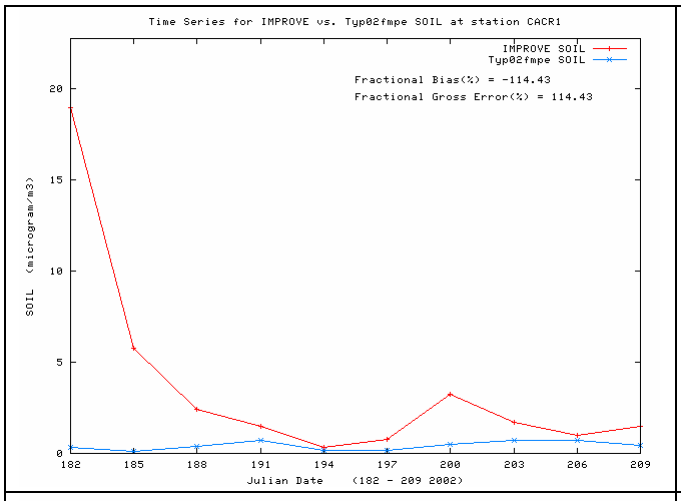
Time Series for IMPROVE vs. Typ02fmpe SOIL at station CACR1
IMPROVE SOIL
Typ02fmpe SOIL
Fractional Bias(%) = -114.43
Fractional Gross Error(%) = 114.43
SOIL (microgram/m3)
Julian Date (182 - 209 2002)

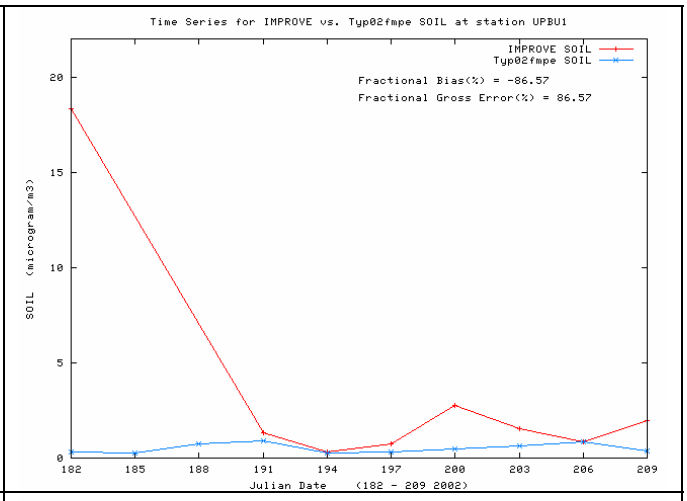
Time Series for IMPROVE vs. Typ02fmpe SOIL at station UPBU1
IMPROVE SOIL
Typ02fmpe SOIL
Fractional Bias(%) = -86.57
Fractional Gross Error(%) = 86.57
SOIL (microgram/m3)
Julian Date (182 - 209 2002)

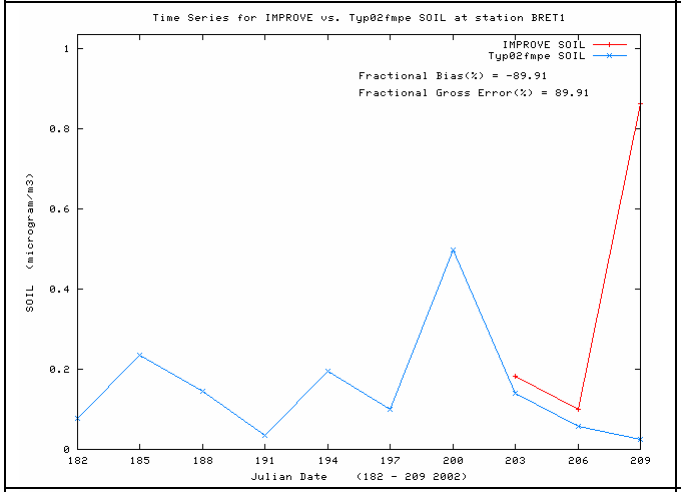
Time Series for IMPROVE vs. Typ02fmpe SOIL at station BRET1
IMPROVE SOIL
Typ02fmpe SOIL
Fractional Bias(%) = -89.91
Fractional Gross Error(%) = 89.91
SOIL (microgram/m3)
Julian Date (182 - 209 2002)

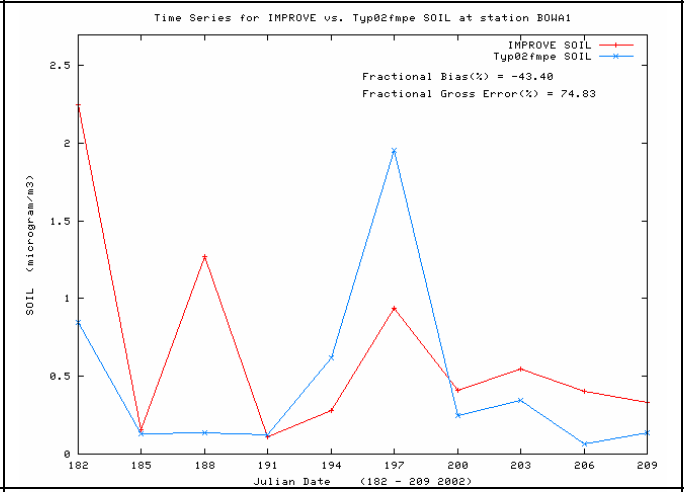
Time Series for IMPROVE vs. Typ02fmpe SOIL at station BOWA1
IMPROVE SOIL
Typ02fmpe SOIL
Fractional Bias(%) = -43.40
Fractional Gross Error(%) = 74.83
SOIL (microgram/m3)
Julian Date (182 - 209 2002)

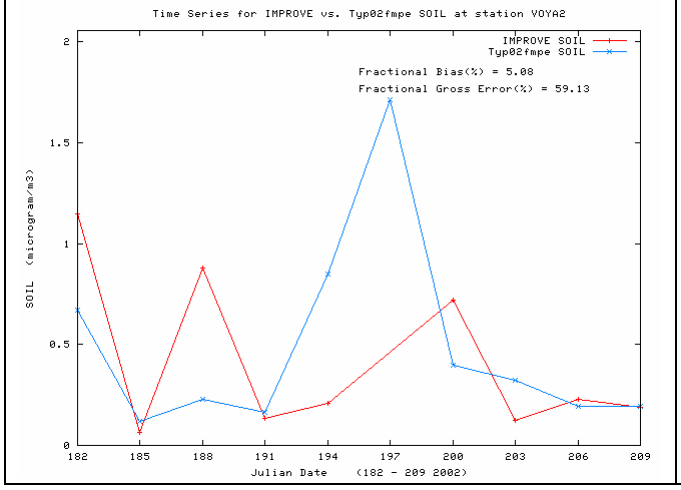
Time Series for IMPROVE vs. Typ02fmpe SOIL at station VOYA2
IMPROVE SOIL
Typ02fmpe SOIL
Fractional Bias(%) = 5.08
Fractional Gross Error(%) = 59.13
SOIL (microgram/m3)
Julian Date (182 - 209 2002)

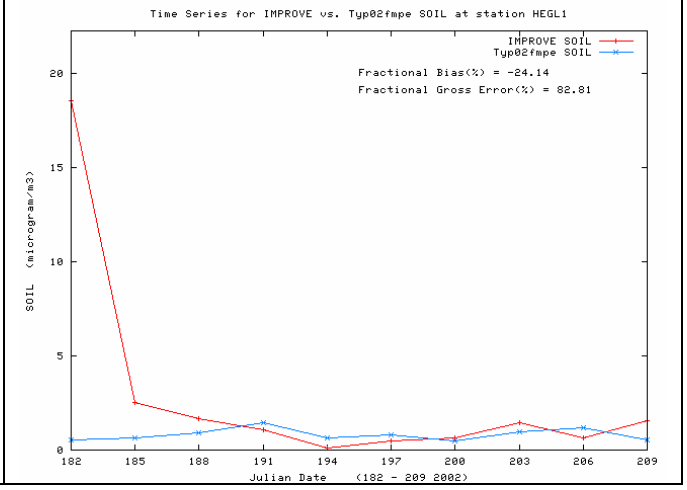
Time Series for IMPROVE vs. Typ02fmpe SOIL at station HEGL1
IMPROVE SOIL
Typ02fmpe SOIL
Fractional Bias(%) = -24.14
Fractional Gross Error(%) = 82.81
SOIL (microgram/m3)
Julian Date (182 - 209 2002)

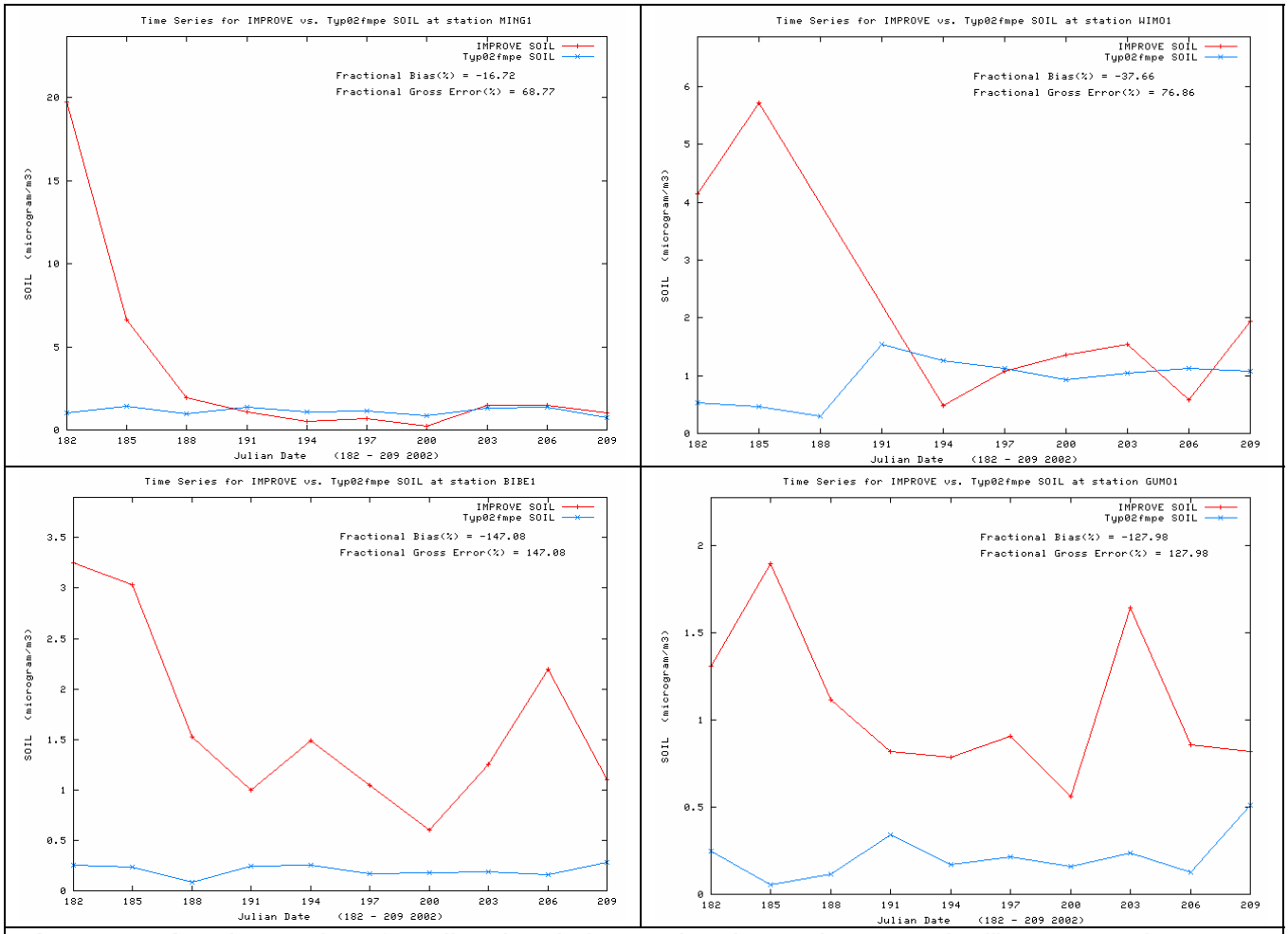

Figure C-30b. Time series of predicted and observed 24-hour other $PM_{2.5}$ (Soil) concentrations at CENRAP IMPROVE sites in July 2002 for CMAQ 2002 36 km Base F base case simulation.

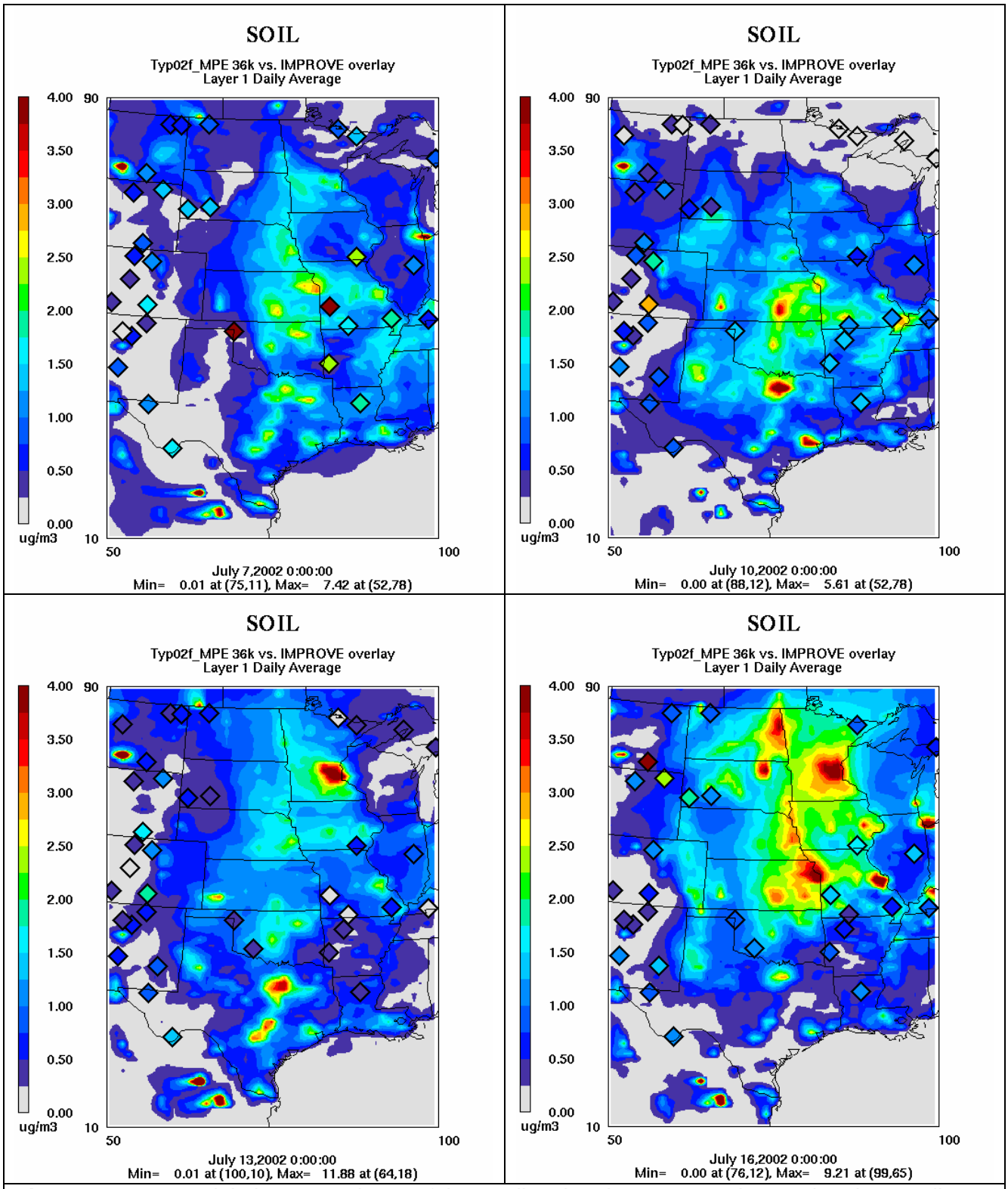

Figure C-30c. Spatial plot comparisons of the predicted and IMPROVE observed 24-hour Soil concentrations for July 7, 10, 13 and 16, 2002.

C.3.5.4 Soil in October 2002

The nearly systematic Soil over-prediction bias seen in January returns in October (Figure C-31a). Except for the two Texas sites, BRET and BOWA, the model overstates the observed Soil during all days of October at the other monitoring sites (Figure C-31b). The model is predicting elevated Soil concentrations in the OK-KS-MO-IA area that is not reflected in the measurements (Figure C-31c).

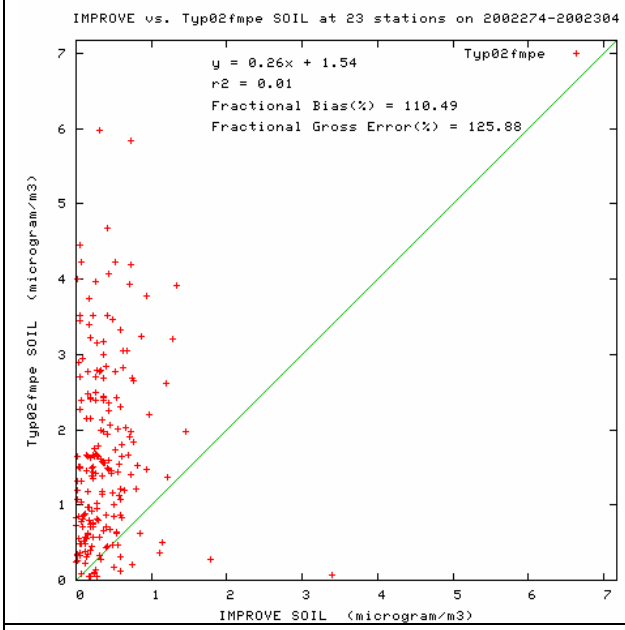

Figure C-31a. Scatter plots of predicted and observed other $PM_{2.5}$ (Soil) concentrations for October 2002 and sites in the CENRAP region using IMPROVE monitoring networks using the CMAQ 2002 36 km Base F base case simulation.

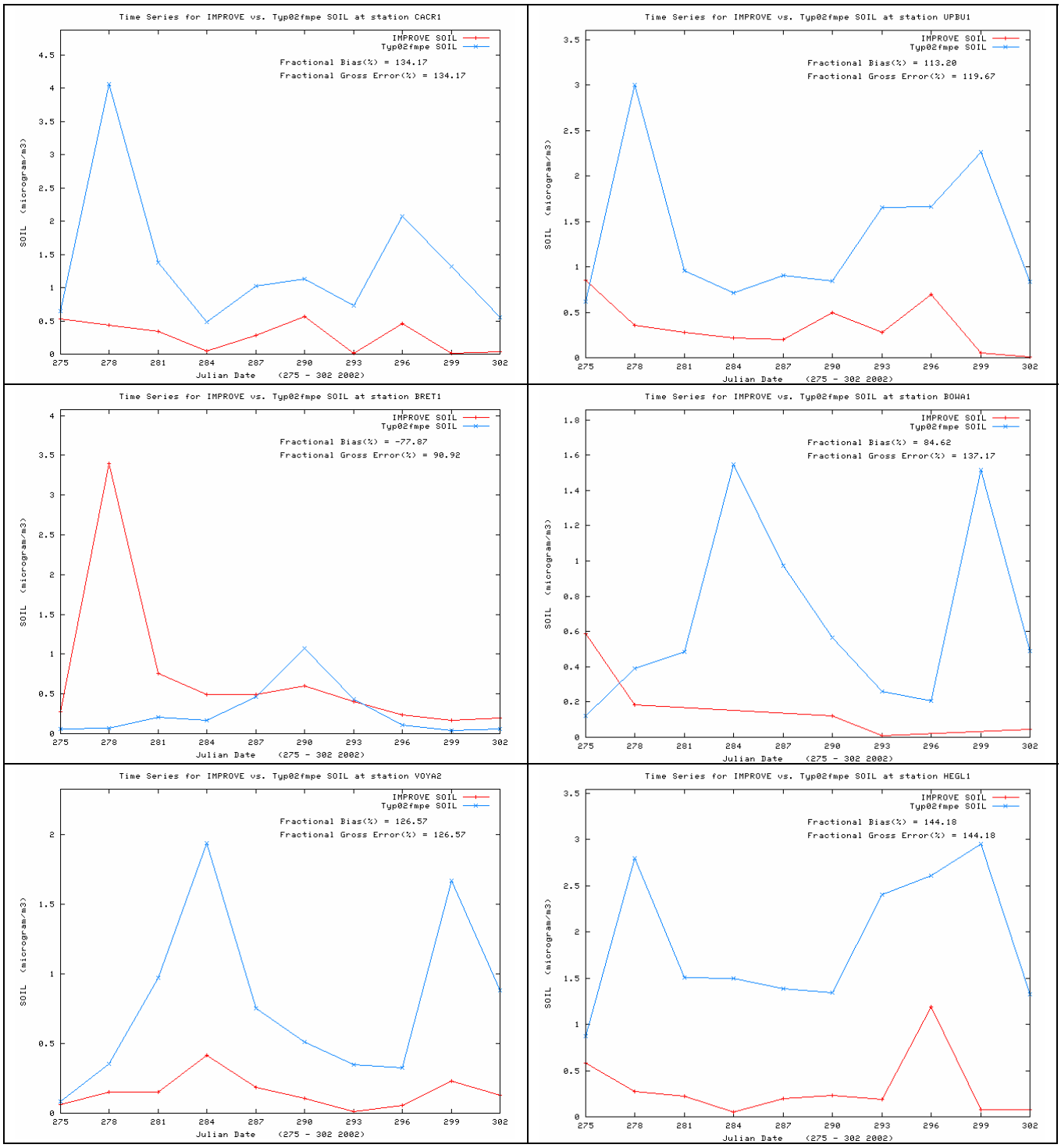
Time Series for IMPROVE vs. Typ02fmpe SOIL at station CACR1
IMPROVE SOIL
Typ02fmpe SOIL
Fractional Bias(%) = 134.17
Fractional Gross Error(%) = 134.17
SOIL (microgram/m3)
Julian Date (275 - 302 2002)
Time Series for IMPROVE vs. Typ02fmpe SOIL at station UPBU1
IMPROVE SOIL
Typ02fmpe SOIL
Fractional Bias(%) = 113.20
Fractional Gross Error(%) = 119.67
SOIL (microgram/m3)
Julian Date (275 - 302 2002)
Time Series for IMPROVE vs. Typ02fmpe SOIL at station BRET1
IMPROVE SOIL
Typ02fmpe SOIL
Fractional Bias(%) = -77.87
Fractional Gross Error(%) = 90.92
SOIL (microgram/m3)
Julian Date (275 - 302 2002)
Time Series for IMPROVE vs. Typ02fmpe SOIL at station BOWA1
IMPROVE SOIL
Typ02fmpe SOIL
Fractional Bias(%) = 84.62
Fractional Gross Error(%) = 137.17
SOIL (microgram/m3)
Julian Date (275 - 302 2002)
Time Series for IMPROVE vs. Typ02fmpe SOIL at station VOYA2
IMPROVE SOIL
Typ02fmpe SOIL
Fractional Bias(%) = 126.57
Fractional Gross Error(%) = 126.57
SOIL (microgram/m3)
Julian Date (275 - 302 2002)
Time Series for IMPROVE vs. Typ02fmpe SOIL at station HEGL1
IMPROVE SOIL
Typ02fmpe SOIL
Fractional Bias(%) = 144.18
Fractional Gross Error(%) = 144.18
SOIL (microgram/m3)
Julian Date (275 - 302 2002)

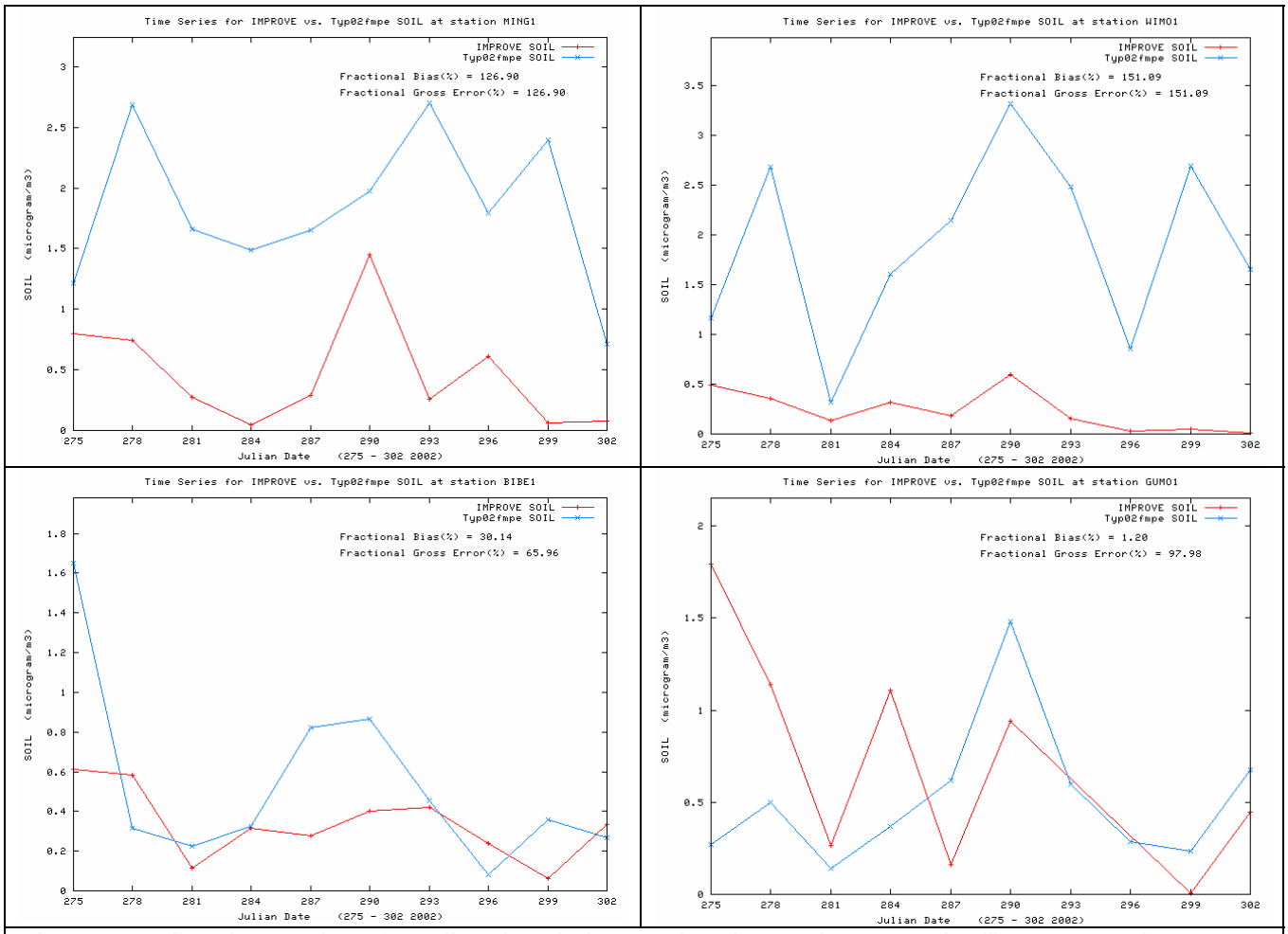

Figure C-31b. Time series of predicted and observed 24-hour other $PM_{2.5}$ (Soil) concentrations at CENRAP IMPROVE CLASS I AREA sites in October 2002 for CMAQ 2002 36 km Base F base case simulation.

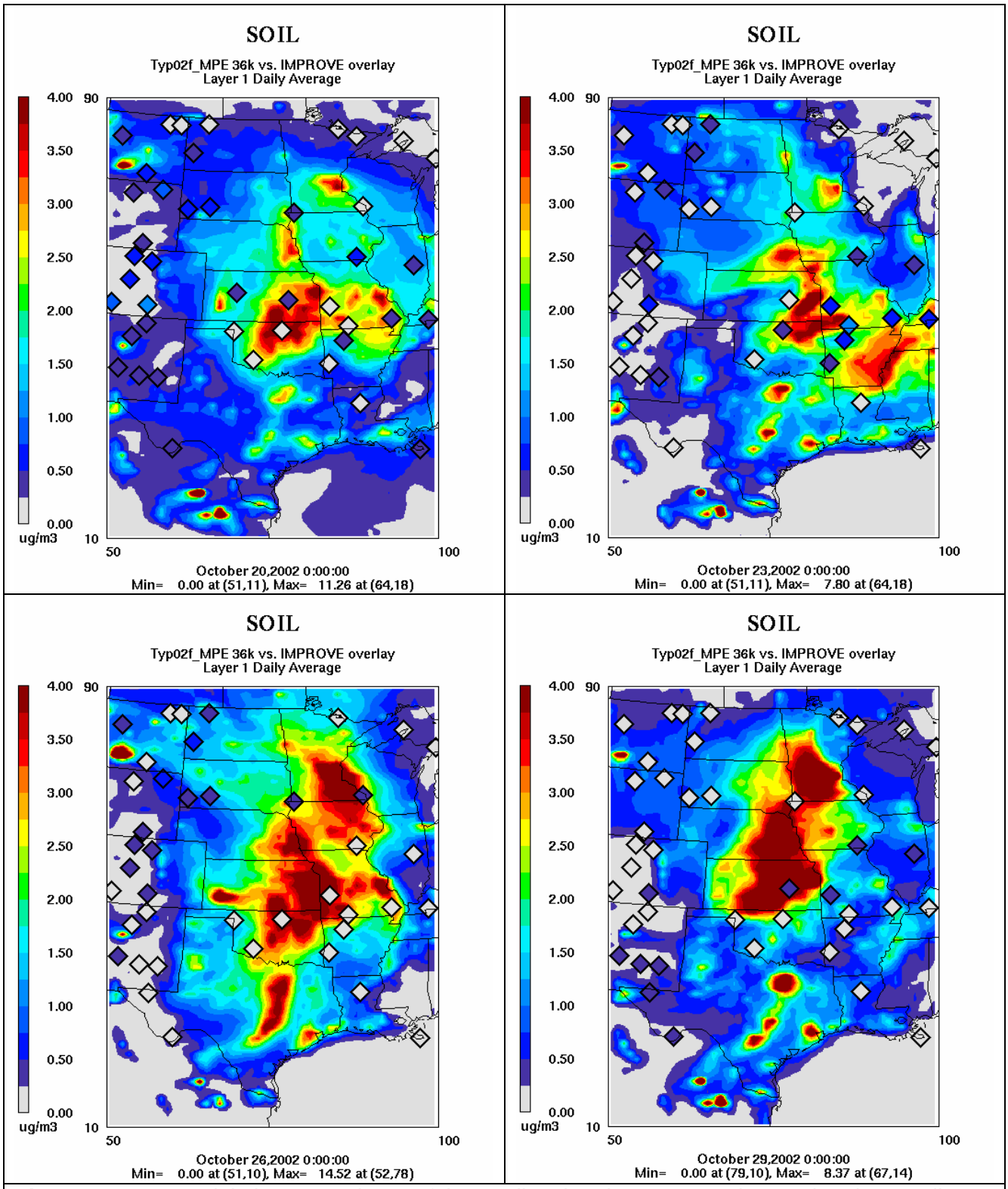

Figure C-31c. Spatial plot comparisons of the predicted and IMPROVE observed 24-hour Soil concentrations for October 20, 23, 26 and 29, 2002.

C.3.5.5 Soil Monthly Bias and Error

Figure C-32 displays the monthly variation in the Soil bias and error. During the winter months the model exhibits a very large (> 100%) overestimation bias with large errors as well. With the exception of July, in the summer the model bias is a slight over-prediction but generally less than 20% with errors of 60% to 80%. The Bugle Plot indicates that the summer Soil performance achieves the PM performance goal, a few months in the Spring/Fall period fall between the performance goal and criteria and the winter Soil performance exceeds the model performance criteria by a far margin. Thus, the Soil performance is a cause for concern.

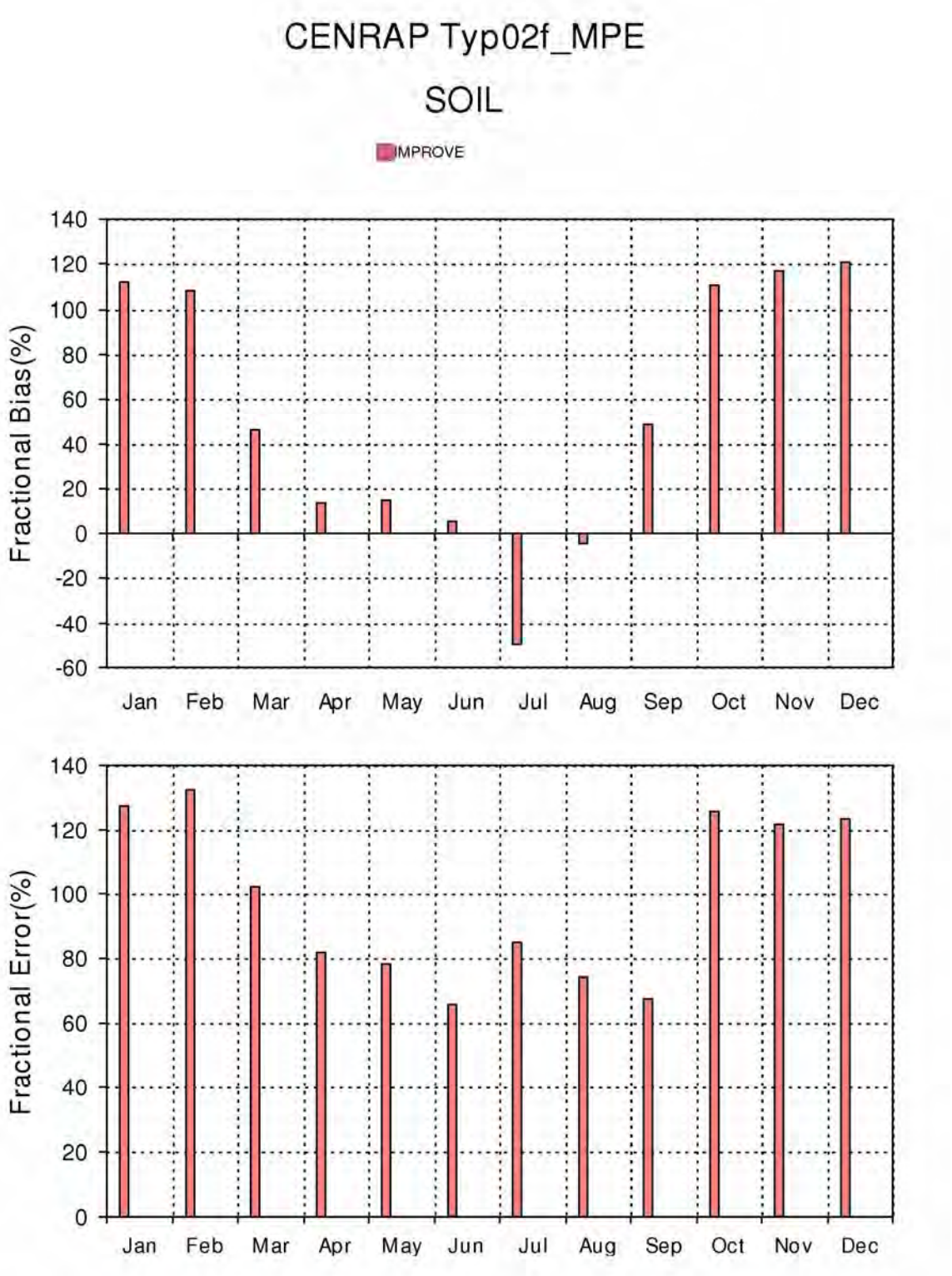

Figure C-32. Monthly Soil fractional bias (top) and fractional gross error (bottom) statistical measures for IMPROVE, STN and CASTNet monitoring sites in the CENRAP region.

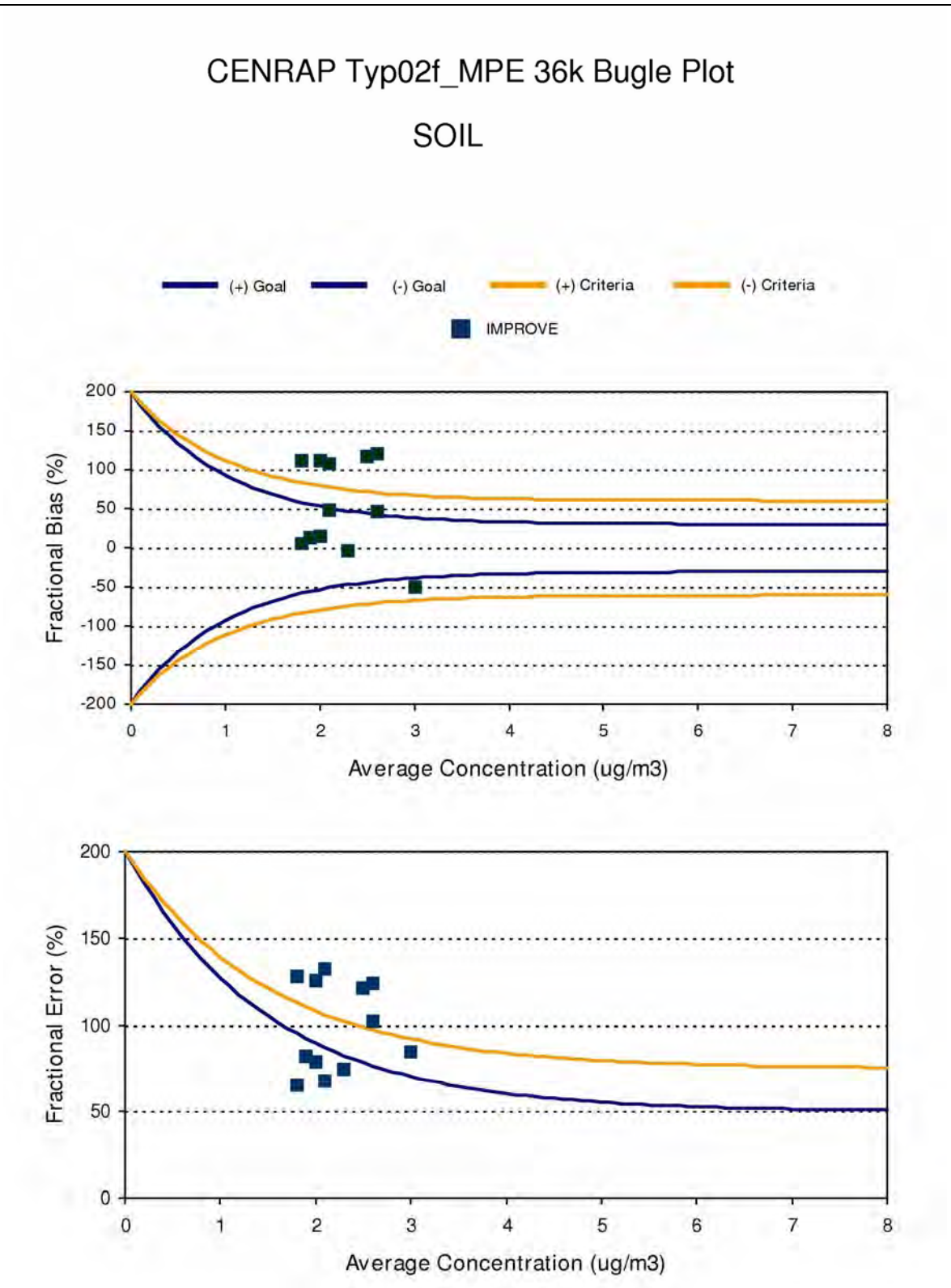

Figure C-33. Bugle Plots of monthly fractional bias (top) and fractional gross error (bottom) and comparisons with model performance goals and criteria for Soil and IMPROVE monitoring sites in the CENRAP region.

C.3.6 Coarse Mass (CM) Monthly Model Performance

The IMPROVE coarse mass (CM) measurement is taken as the difference between the PM_{10} and $PM_{2.5}$ mass measurement. Any SO4 or NO3 in the coarse mode will be in the CM measurement. The model, on the other hand, only includes primary CM. Any coarse SO4 or NO3 will be in the SO4 and NO3 modeled species.

C.3.6.1 CM in January 2002

The model underestimates the observed CM in January with a fractional bias of -83% (Figure C-34a). Although the model appears to reproduce CM at some sites (e.g., VOYA) at the two Texas sites the bias is approximately -150% (Figure C-34b). The observed spatial distribution of CM in January is not reproduced by the model at all (Figure C-34c). Whereas the observations indicate high CM concentrations in the west Texas-New Mexico area, the model estimates elevated CM in northeast Texas, through Oklahoma, Kansas, Iowa and into southern Minnesota. Although the CM measurements at WIMO in this area are also elevated, the rest of the high modeled CM values fall in between the IMPROVE monitors so can not be verified or refuted by the measurements.

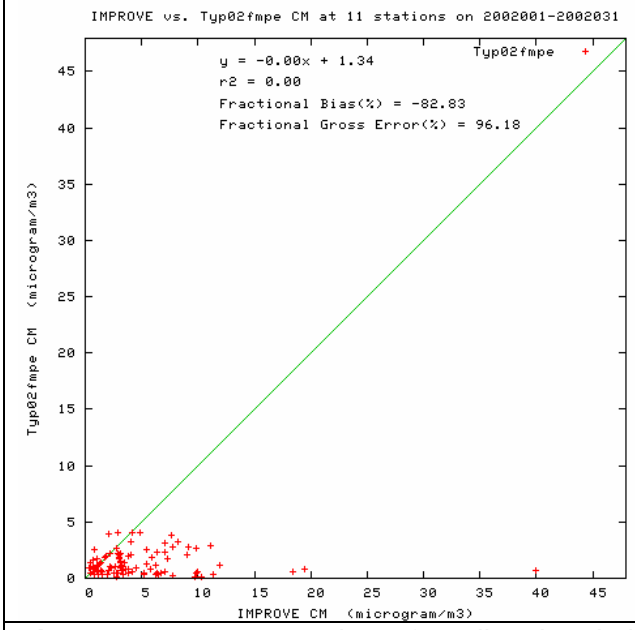

Figure C-34a. Scatter plots of predicted and observed coarse mass (CM) concentrations for January 2002 and sites in the CENRAP region using IMPROVE monitoring networks using the CMAQ 2002 36 km Base F base case simulation.

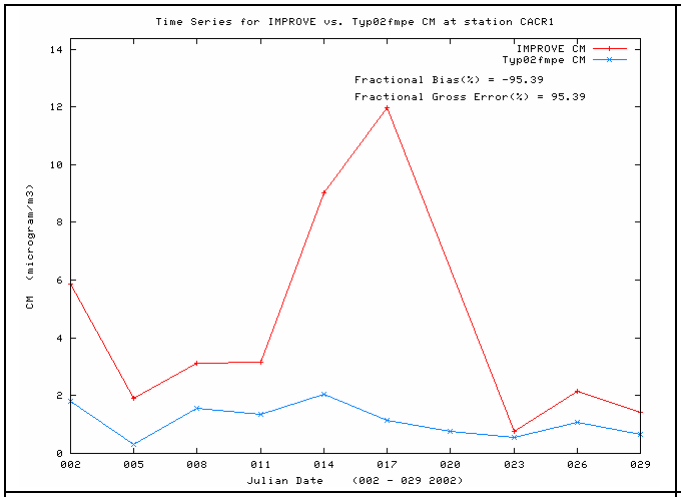
Time Series for IMPROVE vs. Typ02fmpe CM at station CACR1
IMPROVE CM
Typ02fmpe CM
Fractional Bias(%) = -95.39
Fractional Gross Error(%) = 95.39
CM (microgram/m3)
Julian Date (002 - 029 2002)

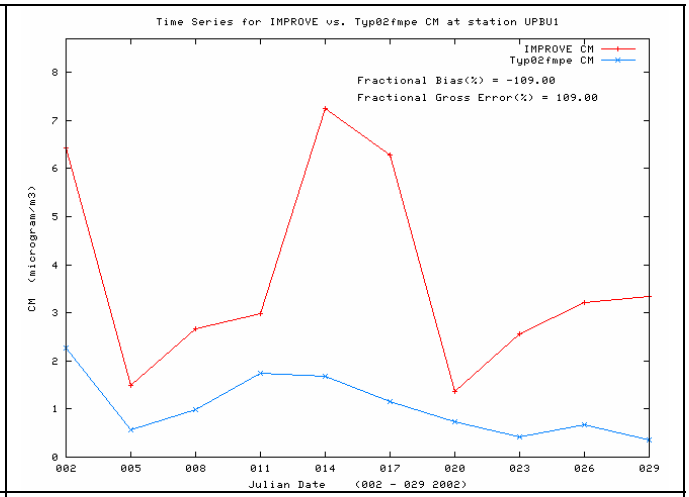
Time Series for IMPROVE vs. Typ02fmpe CM at station UPBU1
IMPROVE CM
Typ02fmpe CM
Fractional Bias(%) = -109.00
Fractional Gross Error(%) = 109.00
CM (microgram/m3)
Julian Date (002 - 029 2002)

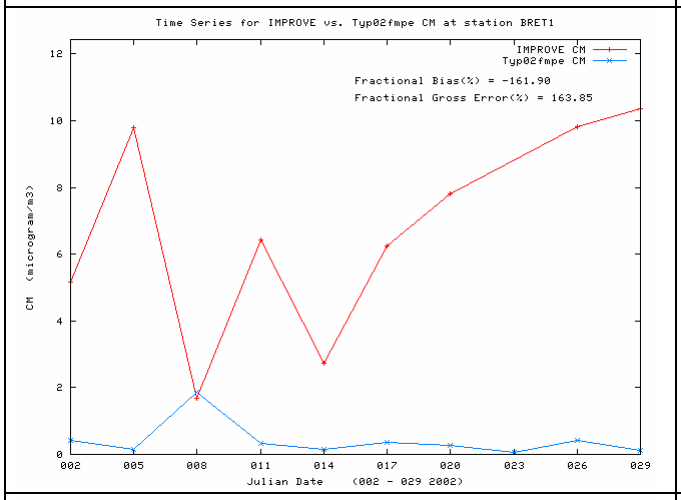
Time Series for IMPROVE vs. Typ02fmpe CM at station BRET1
IMPROVE CM
Typ02fmpe CM
Fractional Bias(%) = -161.90
Fractional Gross Error(%) = 163.85
CM (microgram/m3)
Julian Date (002 - 029 2002)

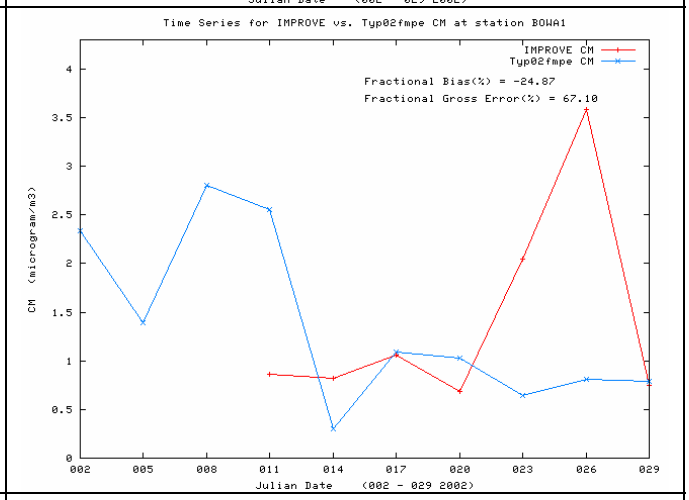
Time Series for IMPROVE vs. Typ02fmpe CM at station BOWA1
IMPROVE CM
Typ02fmpe CM
Fractional Bias(%) = -24.87
Fractional Gross Error(%) = 67.10
CM (microgram/m3)
Julian Date (002 - 029 2002)

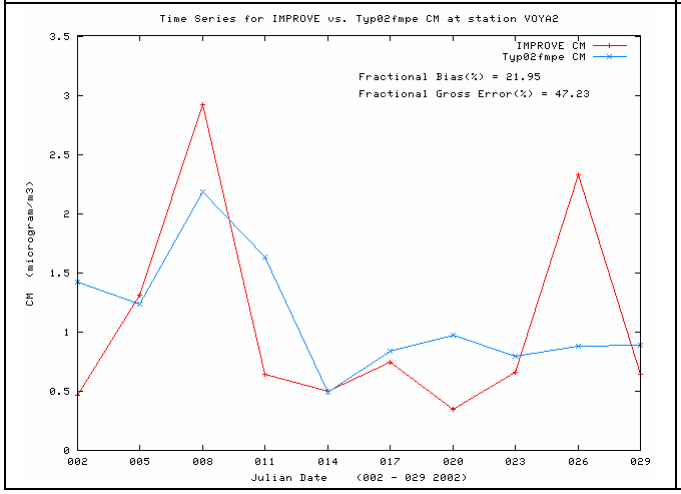
Time Series for IMPROVE vs. Typ02fmpe CM at station VOYA2
IMPROVE CM
Typ02fmpe CM
Fractional Bias(%) = 21.95
Fractional Gross Error(%) = 47.23
CM (microgram/m3)
Julian Date (002 - 029 2002)

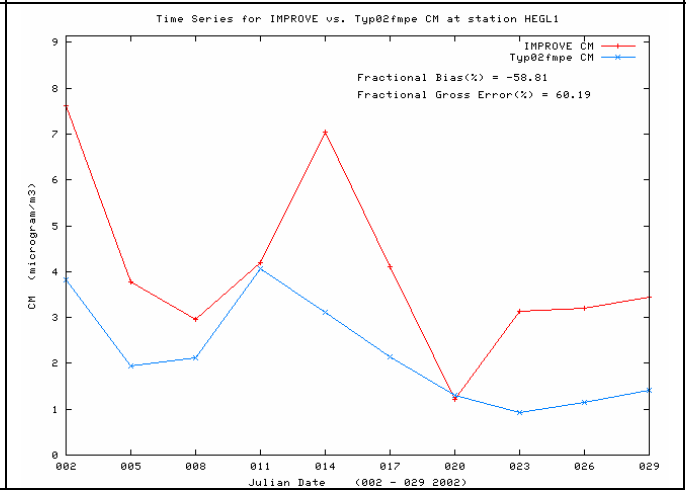
Time Series for IMPROVE vs. Typ02fmpe CM at station HEGL1
IMPROVE CM
Typ02fmpe CM
Fractional Bias(%) = -58.81
Fractional Gross Error(%) = 60.19
CM (microgram/m3)
Julian Date (002 - 029 2002)

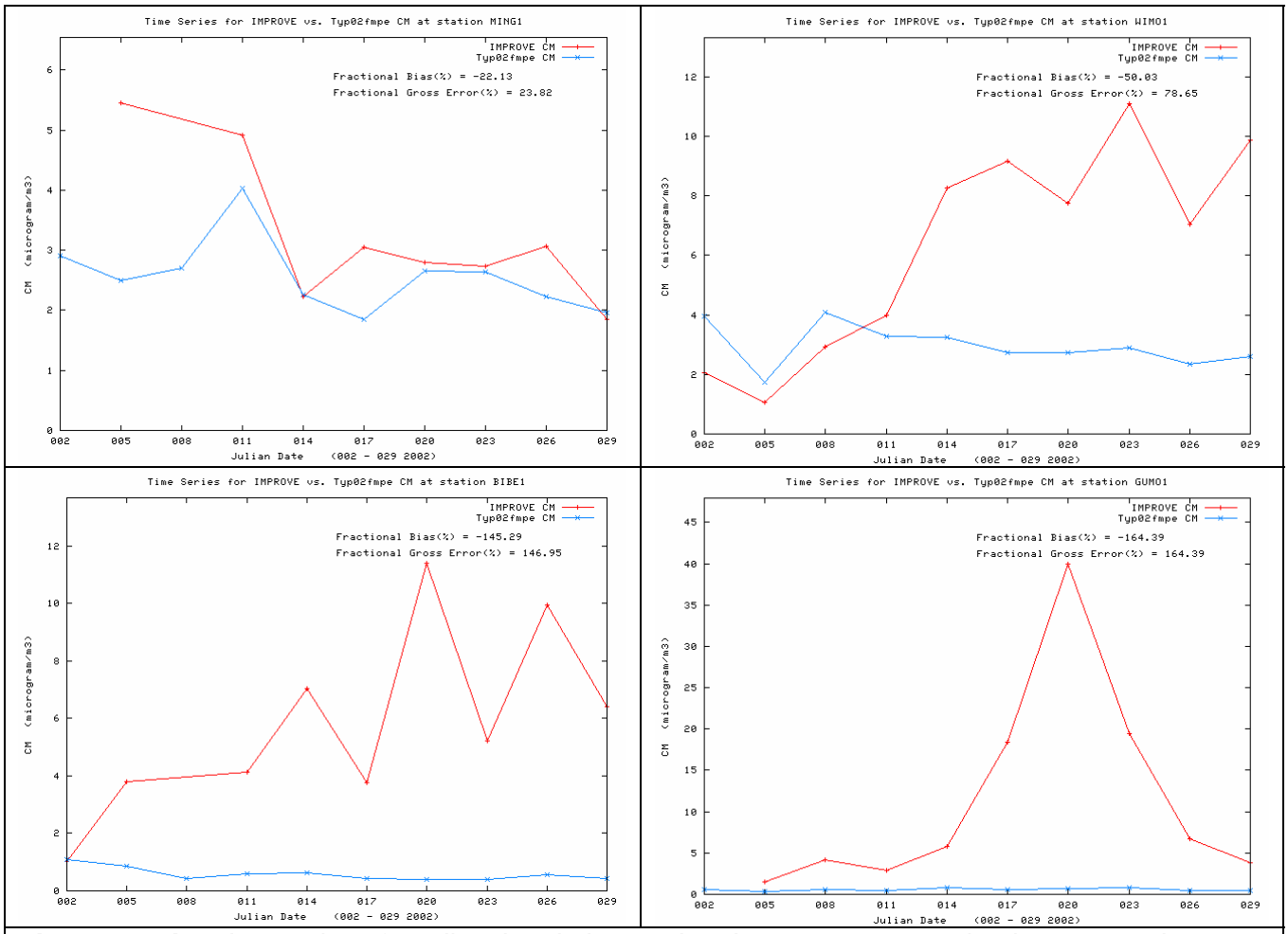

Figure C-34b. Time series of predicted and observed 24-hour coarse mass (CM) concentrations at CENRAP IMPROVE CLASS I AREA sites in January 2002 for CMAQ 2002 36 km Base F base case simulation.

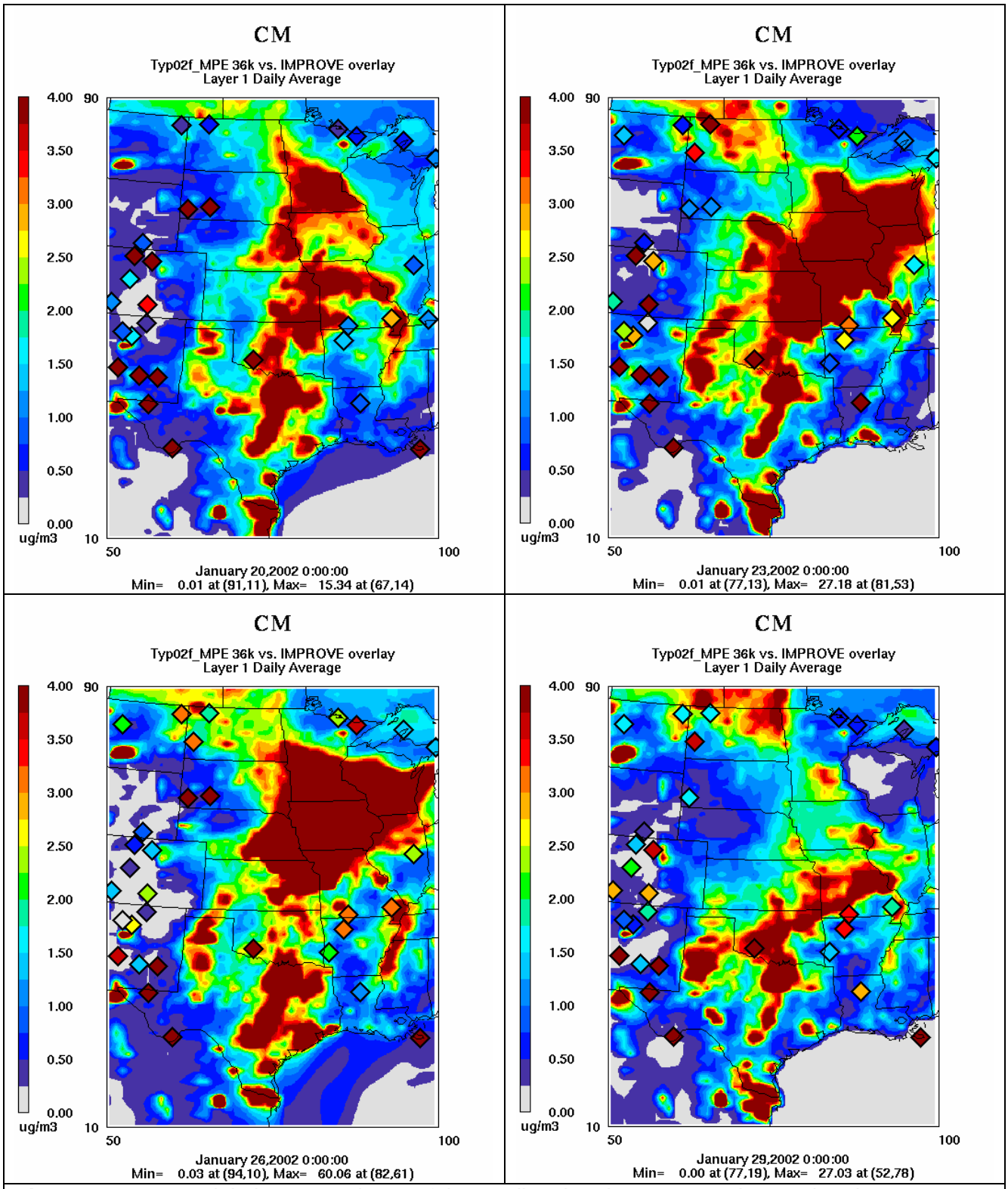

Figure C-34c. Spatial plot comparisons of the predicted and IMPROVE observed 24-hour CM concentrations for January 20, 23, 26 and 29, 2002.

C.3.6.2 CM in April 2002

The CM underestimation bias is even greater in April (-137%) and occurs at all IMPROVE sites (Figure C-35).

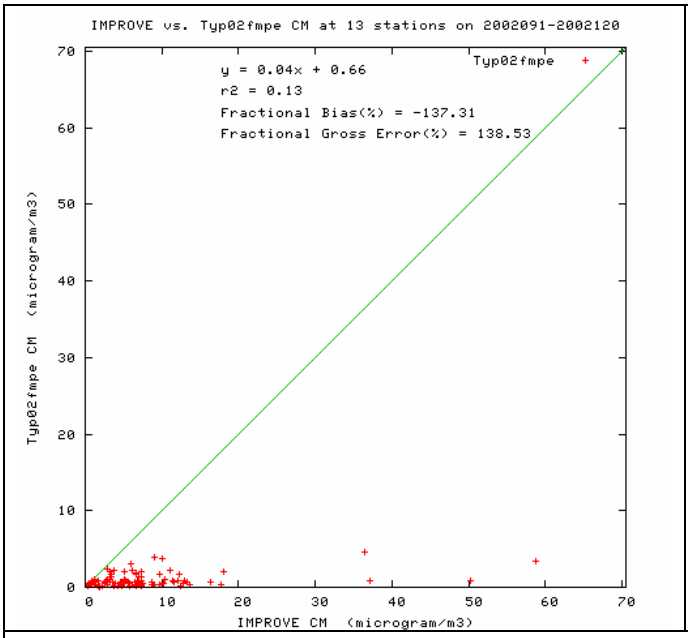

Figure C-35a. Scatter plots of predicted and observed coarse mass (CM) concentrations for April 2002 and sites in the CENRAP region using IMPROVE monitoring networks using the CMAQ 2002 36 km Base F base case simulation.

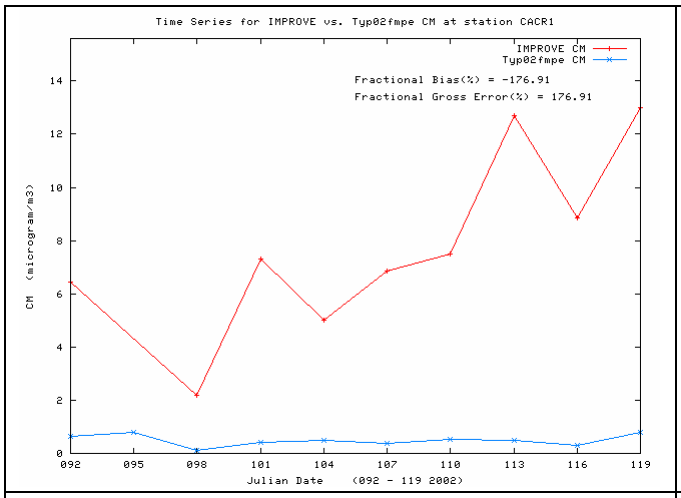
Time Series for IMPROVE vs. Typ02fmpe CM at station CACR1
IMPROVE CM
Typ02fmpe CM
Fractional Bias(%) = -176.91
Fractional Gross Error(%) = 176.91
CM (microgram/m3)
Julian Date (092 - 119 2002)

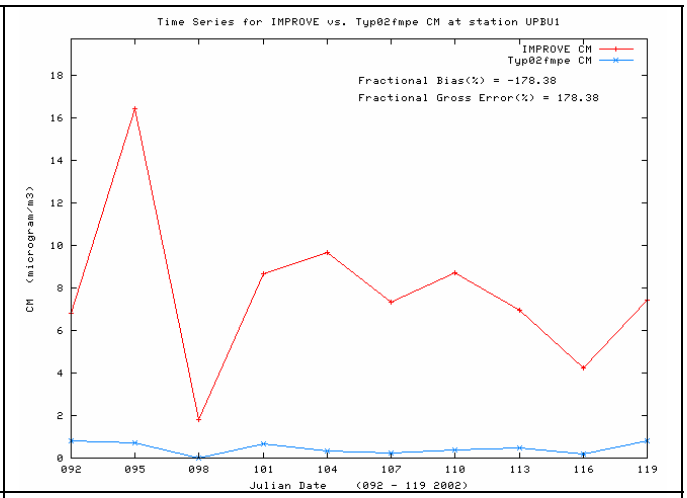
Time Series for IMPROVE vs. Typ02fmpe CM at station UPBU1
IMPROVE CM
Typ02fmpe CM
Fractional Bias(%) = -178.38
Fractional Gross Error(%) = 178.38
CM (microgram/m3)
Julian Date (092 - 119 2002)

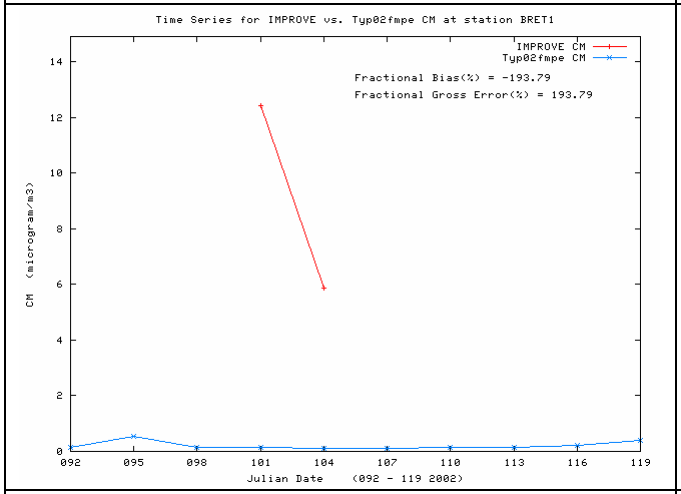
Time Series for IMPROVE vs. Typ02fmpe CM at station BRET1
IMPROVE CM
Typ02fmpe CM
Fractional Bias(%) = -193.79
Fractional Gross Error(%) = 193.79
CM (microgram/m3)
Julian Date (092 - 119 2002)

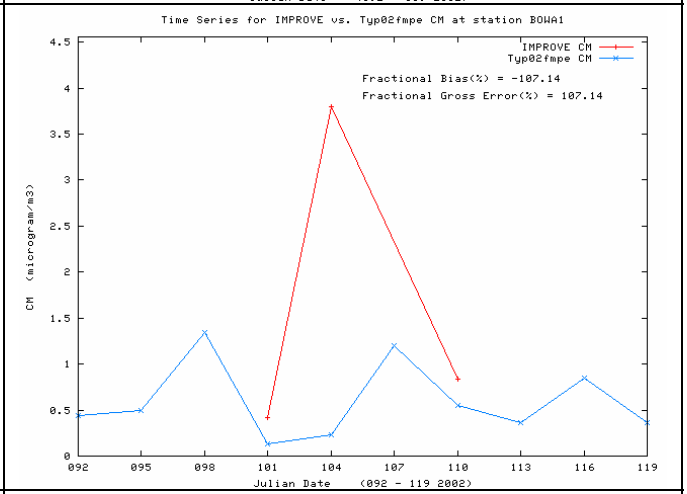
Time Series for IMPROVE vs. Typ02fmpe CM at station BOWA1
IMPROVE CM
Typ02fmpe CM
Fractional Bias(%) = -107.14
Fractional Gross Error(%) = 107.14
CM (microgram/m3)
Julian Date (092 - 119 2002)

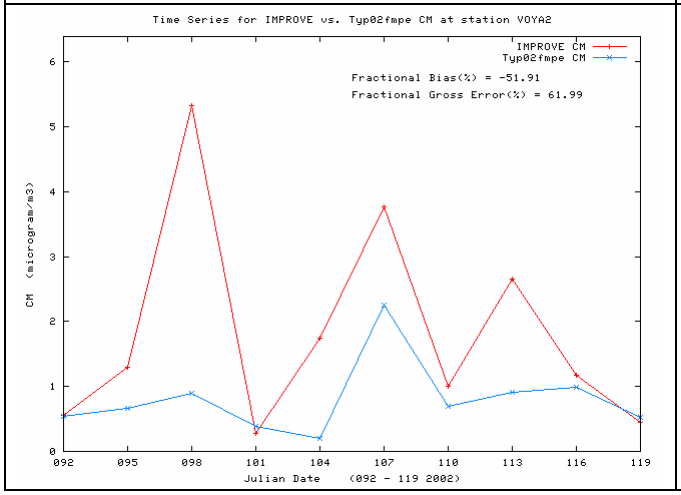
Time Series for IMPROVE vs. Typ02fmpe CM at station VOYA2
IMPROVE CM
Typ02fmpe CM
Fractional Bias(%) = -51.91
Fractional Gross Error(%) = 61.99
CM (microgram/m3)
Julian Date (092 - 119 2002)

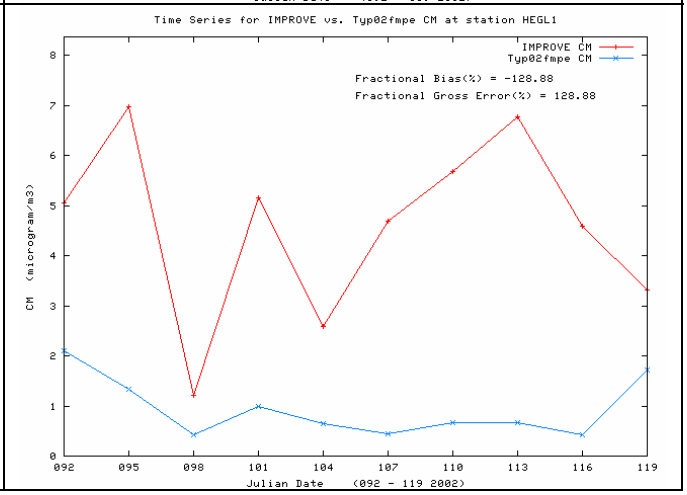
Time Series for IMPROVE vs. Typ02fmpe CM at station HEGL1
IMPROVE CM
Typ02fmpe CM
Fractional Bias(%) = -128.88
Fractional Gross Error(%) = 128.88
CM (microgram/m3)
Julian Date (092 - 119 2002)

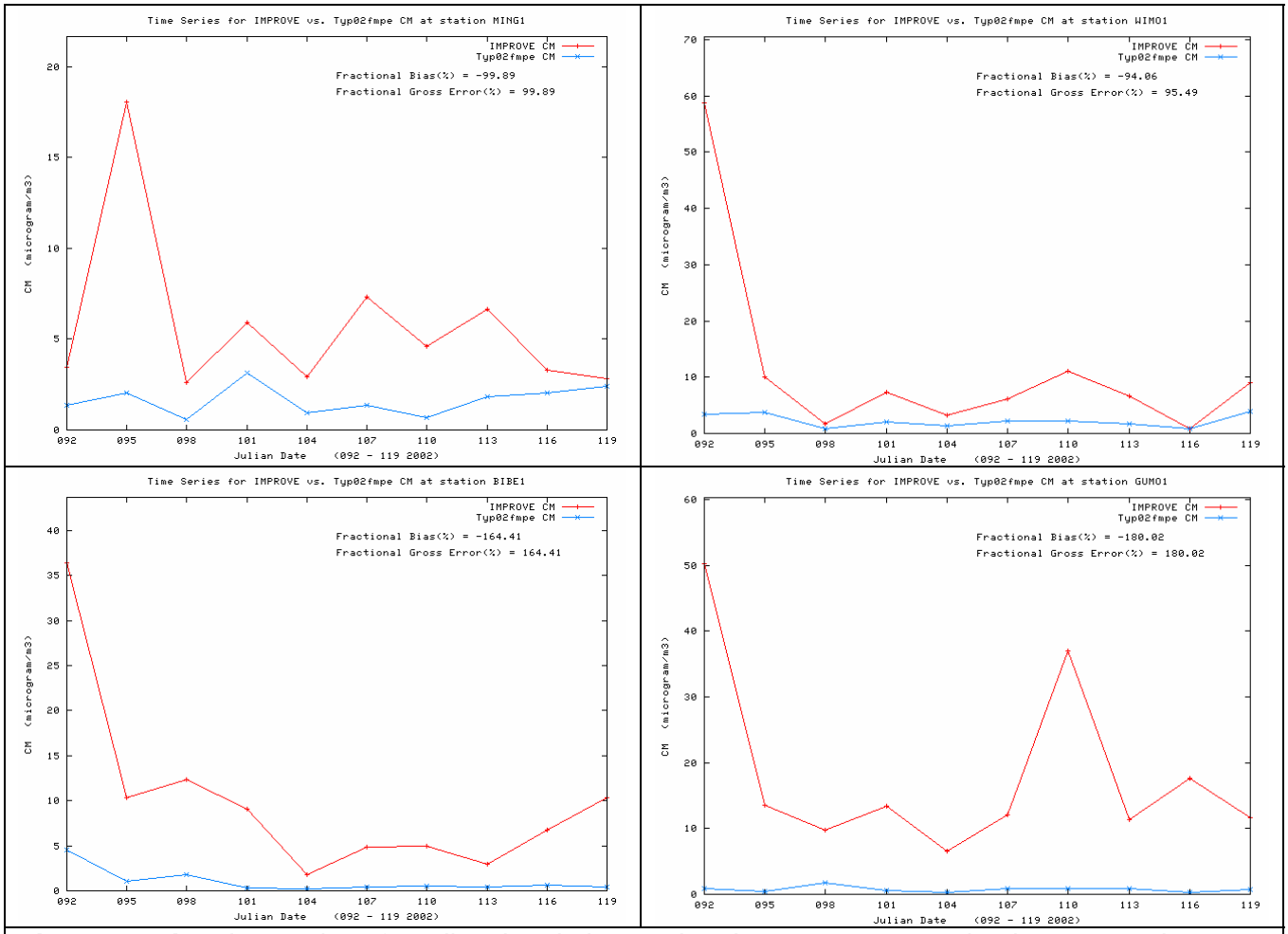

Figure C-35b. Time series of predicted and observed 24-hour coarse mass (CM) concentrations at CENRAP IMPROVE CLASS I AREA sites in April 2002 for CMAQ 2002 36 km Base F base case simulation.

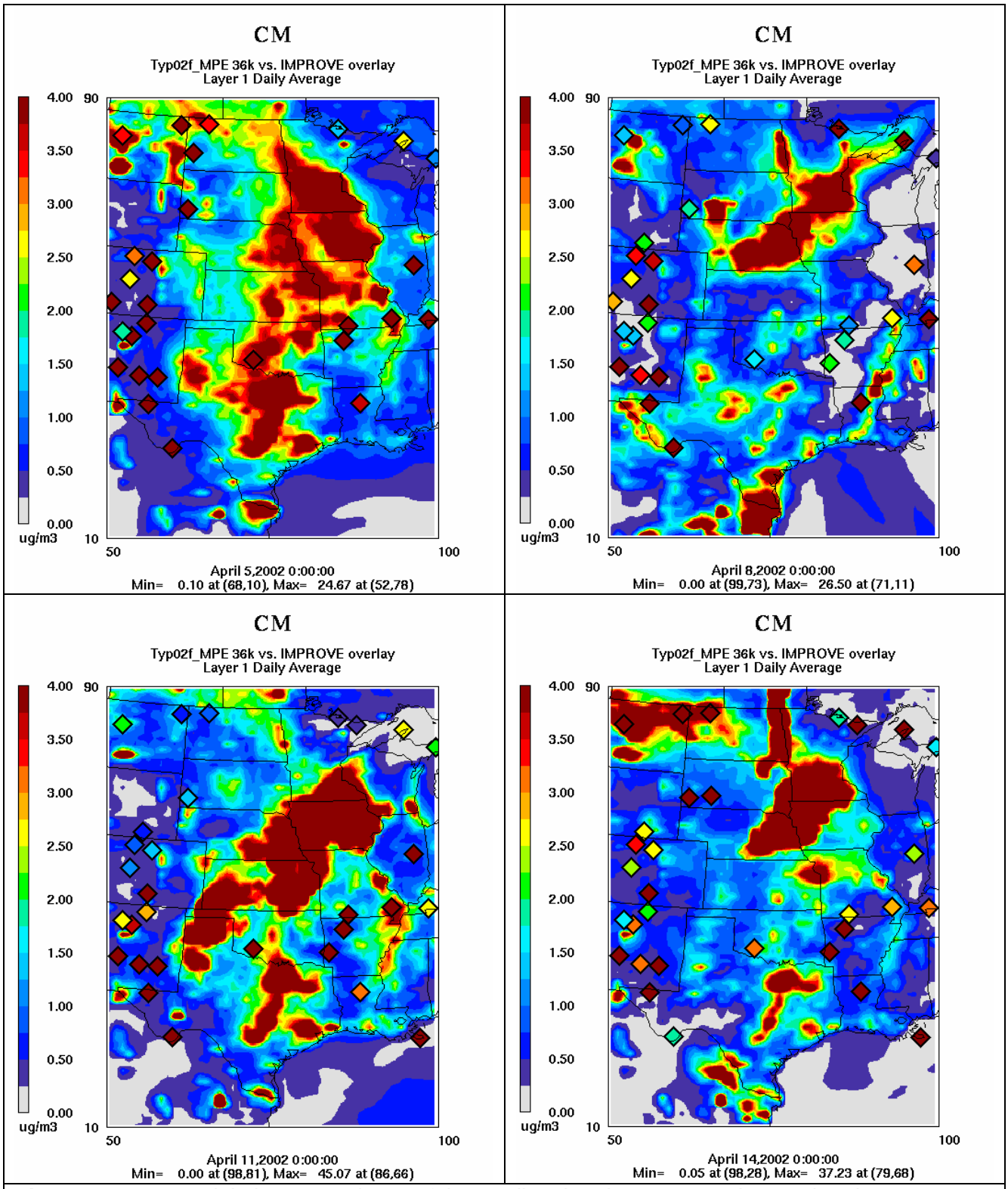

Figure C-35c. Spatial plot comparisons of the predicted and IMPROVE observed 24-hour CM concentrations for April 5, 8, 11 and 14, 2002.

C.3.6.3 CM in July 2002

CM performance in July is also very poor with a fractional bias value of -160% (Figure C-36).

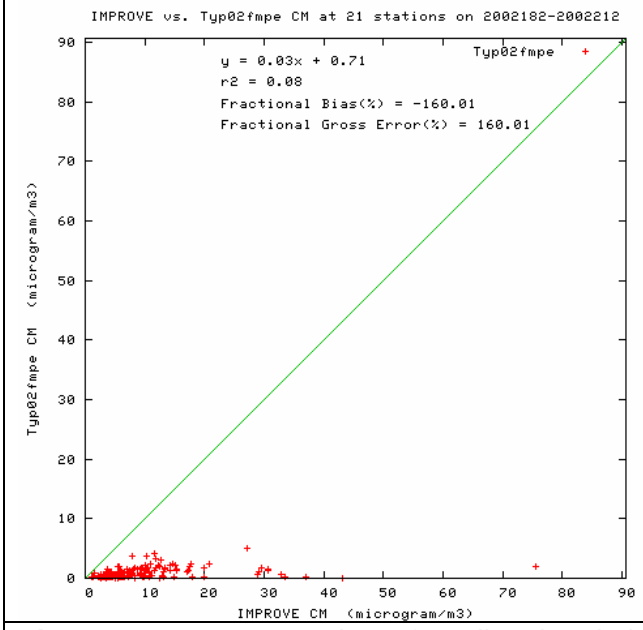

Figure C-36a. Scatter plots of predicted and observed coarse mass (CM) concentrations for July 2002 and sites in the CENRAP region using IMPROVE monitoring networks using the CMAQ 2002 36 km Base F base case simulation.

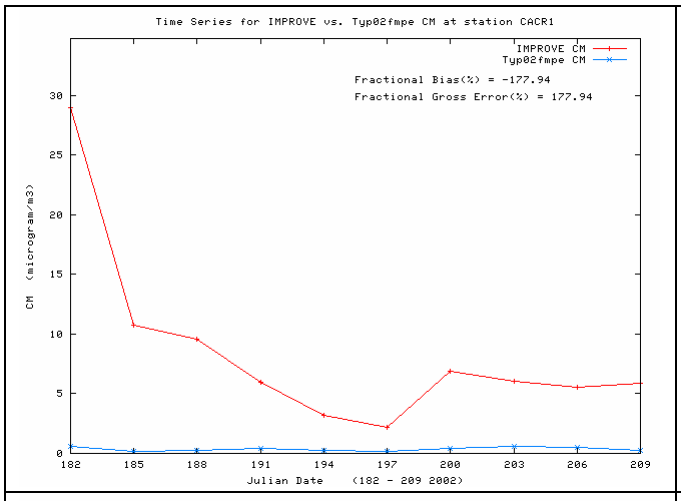
Time Series for IMPROVE vs. Typ02fmpe CM at station CACR1
IMPROVE CM
Typ02fmpe CM
Fractional Bias(%) = -177.94
Fractional Gross Error(%) = 177.94
CM (microgram/m3)
Julian Date (182 - 209 2002)

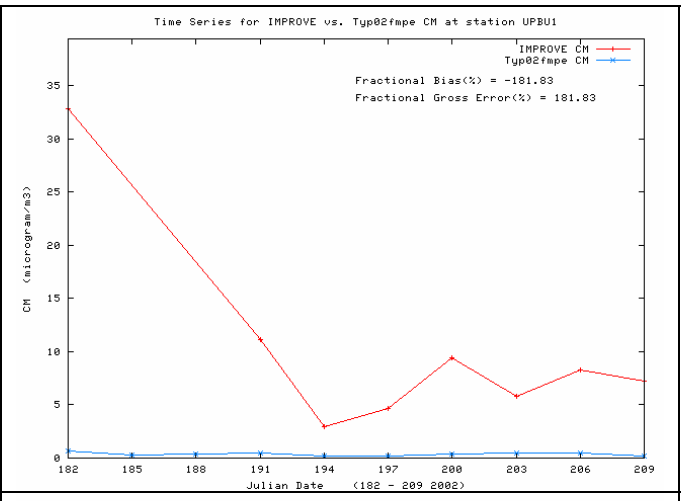
Time Series for IMPROVE vs. Typ02fmpe CM at station UPBU1
IMPROVE CM
Typ02fmpe CM
Fractional Bias(%) = -181.83
Fractional Gross Error(%) = 181.83
CM (microgram/m3)
Julian Date (182 - 209 2002)

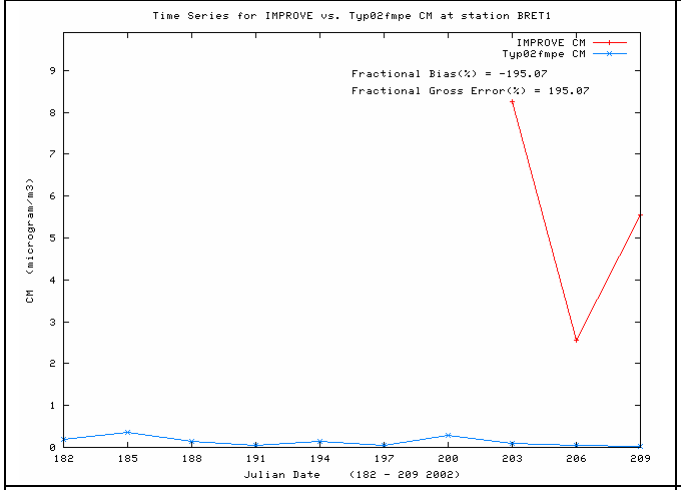
Time Series for IMPROVE vs. Typ02fmpe CM at station BRET1
IMPROVE CM
Typ02fmpe CM
Fractional Bias(%) = -195.07
Fractional Gross Error(%) = 195.07
CM (microgram/m3)
Julian Date (182 - 209 2002)

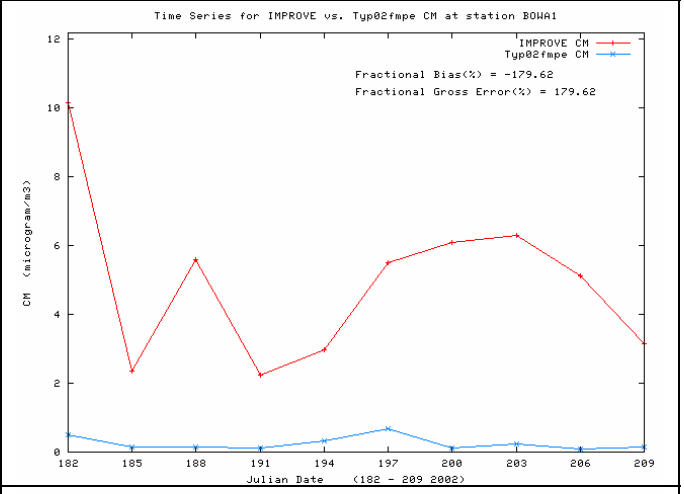
Time Series for IMPROVE vs. Typ02fmpe CM at station BOWA1
IMPROVE CM
Typ02fmpe CM
Fractional Bias(%) = -179.62
Fractional Gross Error(%) = 179.62
CM (microgram/m3)
Julian Date (182 - 209 2002)

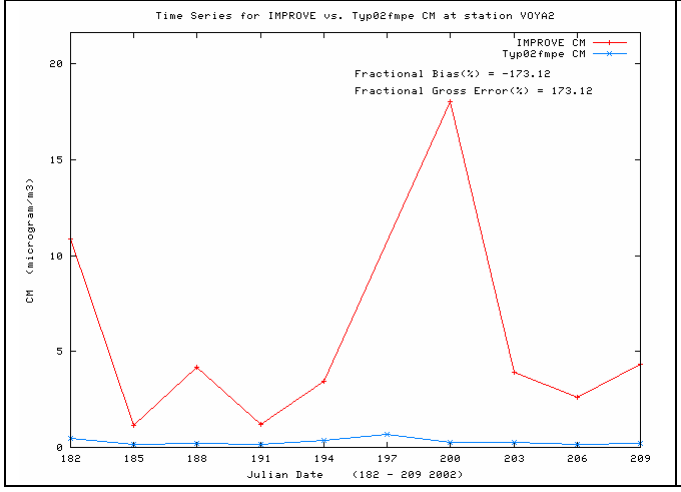
Time Series for IMPROVE vs. Typ02fmpe CM at station VOYA2
IMPROVE CM
Typ02fmpe CM
Fractional Bias(%) = -173.12
Fractional Gross Error(%) = 173.12
CM (microgram/m3)
Julian Date (182 - 209 2002)

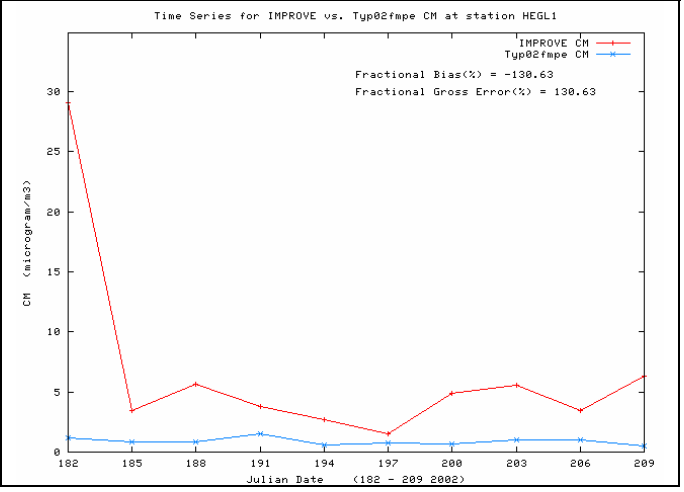
Time Series for IMPROVE vs. Typ02fmpe CM at station HEGL1
IMPROVE CM
Typ02fmpe CM
Fractional Bias(%) = -130.63
Fractional Gross Error(%) = 130.63
CM (microgram/m3)
Julian Date (182 - 209 2002)

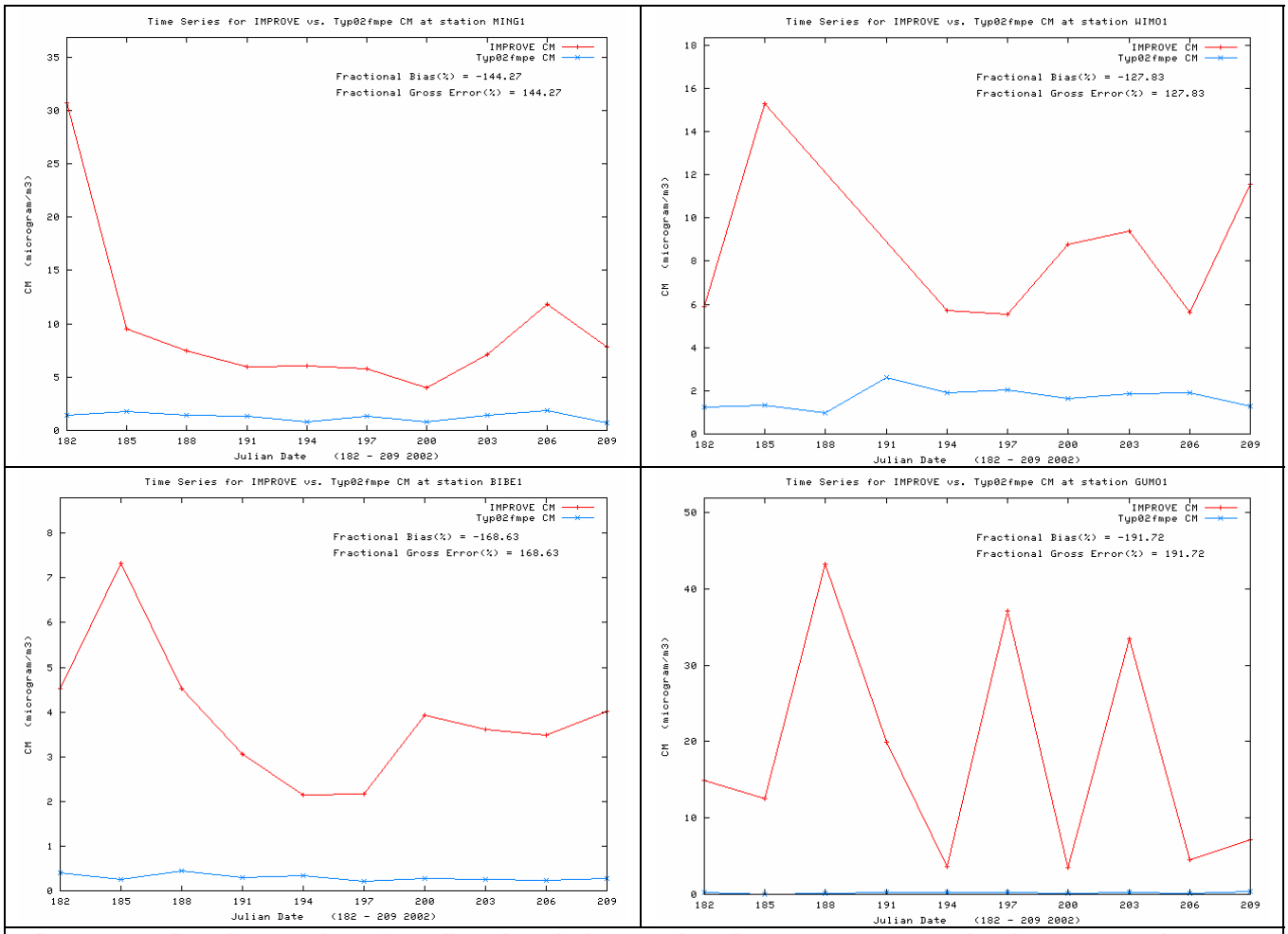

Figure C-36b. Time series of predicted and observed 24-hour coarse mass (CM) concentrations at CENRAP IMPROVE CLASS I AREA sites in July 2002 for CMAQ 2002 36 km Base F base case simulation.

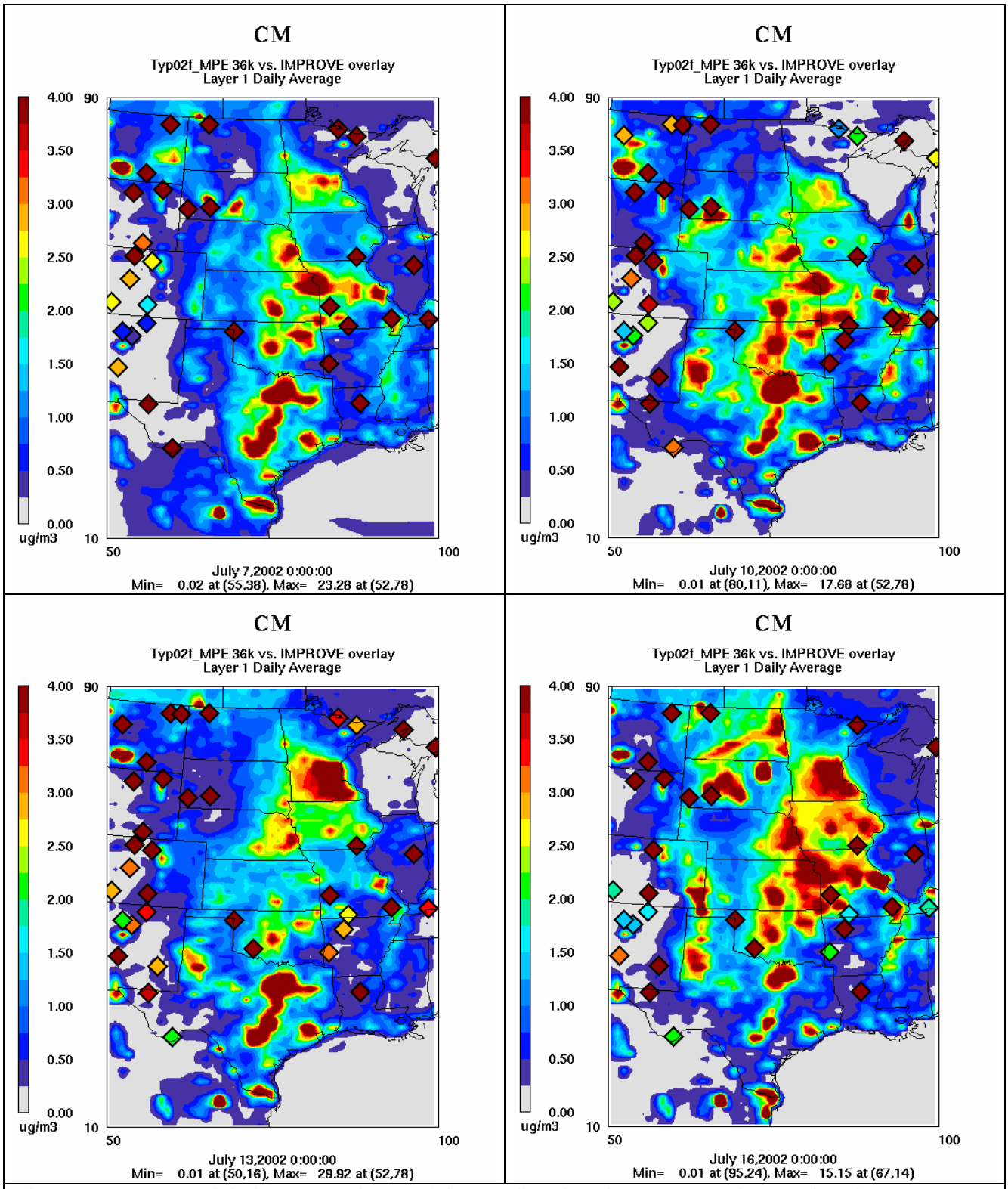

Figure C-36c. Spatial plot comparisons of the predicted and IMPROVE observed 24-hour CM concentrations for July 7, 10, 13 and 16, 2002.

C.3.6.4 CM in October 2002

CM is also underestimated in October, although the overestimation bias (-72%) is not as great as seen in July (Figure C-37).

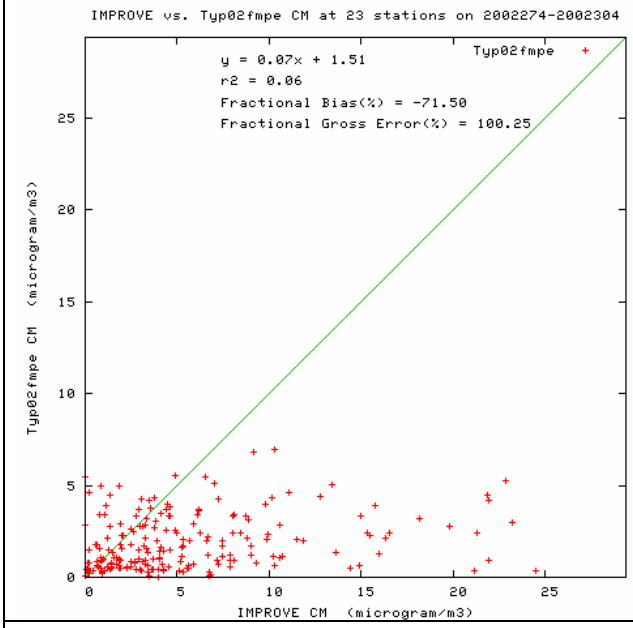

Figure C-37a. Scatter plots of predicted and observed coarse mass (CM) concentrations for October 2002 and sites in the CENRAP region using IMPROVE monitoring networks using the CMAQ 2002 36 km Base F base case simulation.

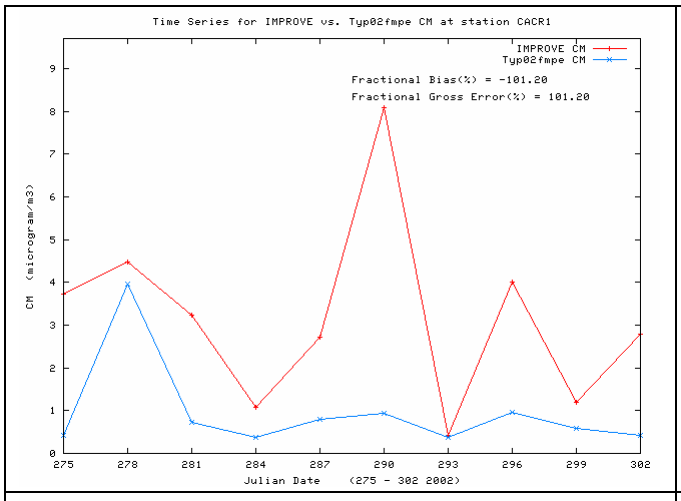
Time Series for IMPROVE vs. Typ02fmpe CM at station CACR1
IMPROVE CM
Typ02fmpe CM
Fractional Bias(%) = -101.20
Fractional Gross Error(%) = 101.20
CM (microgram/m3)
Julian Date (275 - 302 2002)

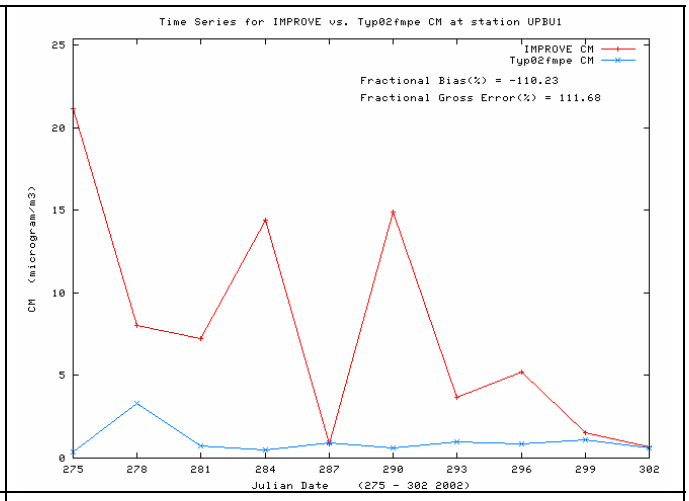
Time Series for IMPROVE vs. Typ02fmpe CM at station UPBU1
IMPROVE CM
Typ02fmpe CM
Fractional Bias(%) = -110.23
Fractional Gross Error(%) = 111.68
CM (microgram/m3)
Julian Date (275 - 302 2002)

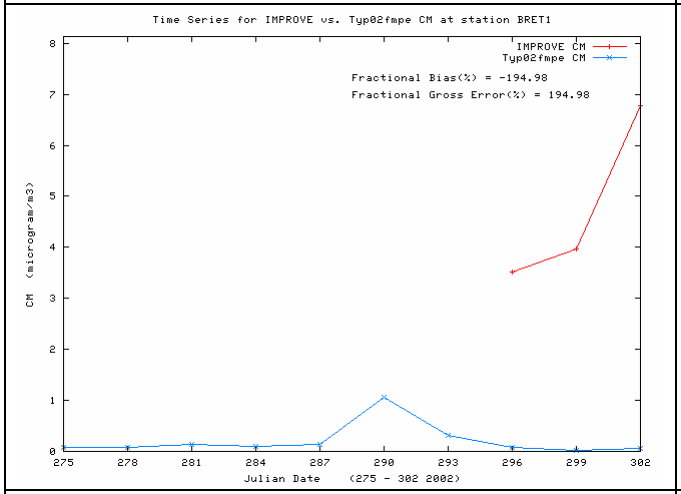
Time Series for IMPROVE vs. Typ02fmpe CM at station BRET1
IMPROVE CM
Typ02fmpe CM
Fractional Bias(%) = -194.98
Fractional Gross Error(%) = 194.98
CM (microgram/m3)
Julian Date (275 - 302 2002)

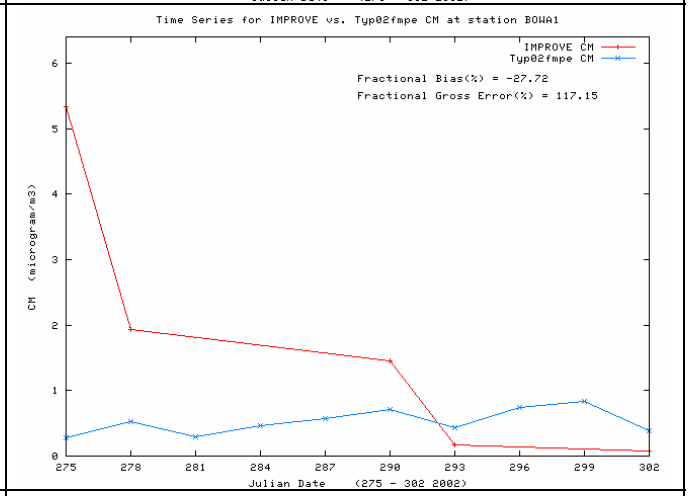
Time Series for IMPROVE vs. Typ02fmpe CM at station BOWA1
IMPROVE CM
Typ02fmpe CM
Fractional Bias(%) = -27.72
Fractional Gross Error(%) = 117.15
CM (microgram/m3)
Julian Date (275 - 302 2002)

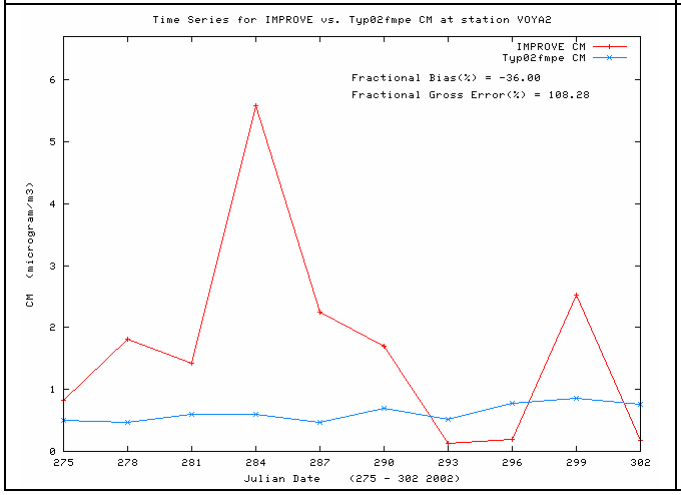
Time Series for IMPROVE vs. Typ02fmpe CM at station VOYA2
IMPROVE CM
Typ02fmpe CM
Fractional Bias(%) = -36.00
Fractional Gross Error(%) = 108.28
CM (microgram/m3)
Julian Date (275 - 302 2002)

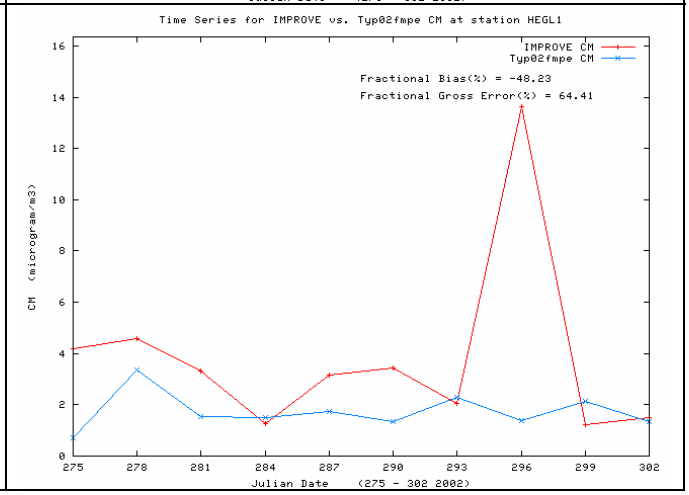
Time Series for IMPROVE vs. Typ02fmpe CM at station HEGL1
IMPROVE CM
Typ02fmpe CM
Fractional Bias(%) = -48.23
Fractional Gross Error(%) = 64.41
CM (microgram/m3)
Julian Date (275 - 302 2002)

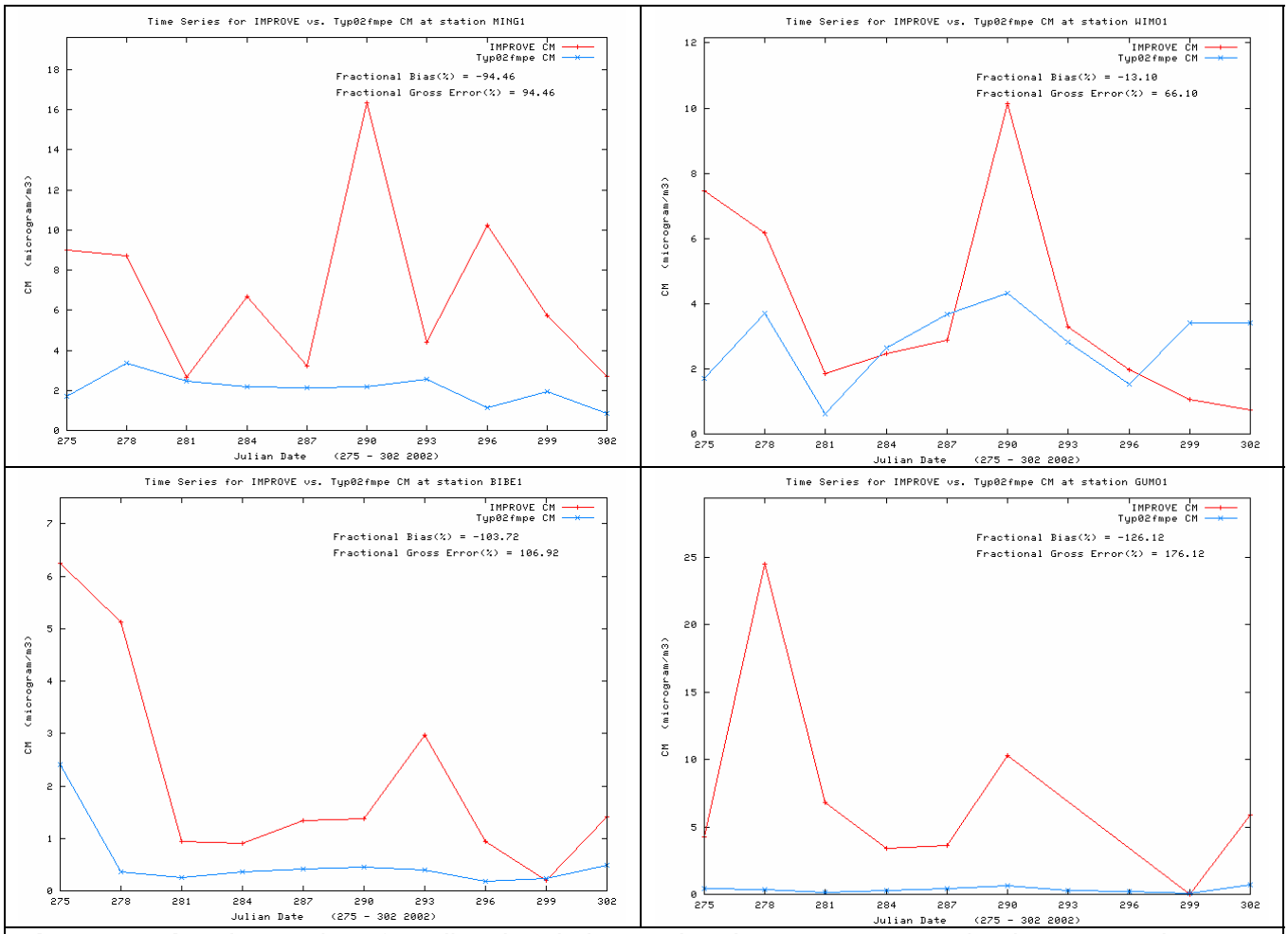

Figure C-37b. Time series of predicted and observed 24-hour coarse mass (CM) concentrations at CENRAP IMPROVE CLASS I AREA sites in October 2002 for CMAQ 2002 36 km Base F base case simulation.

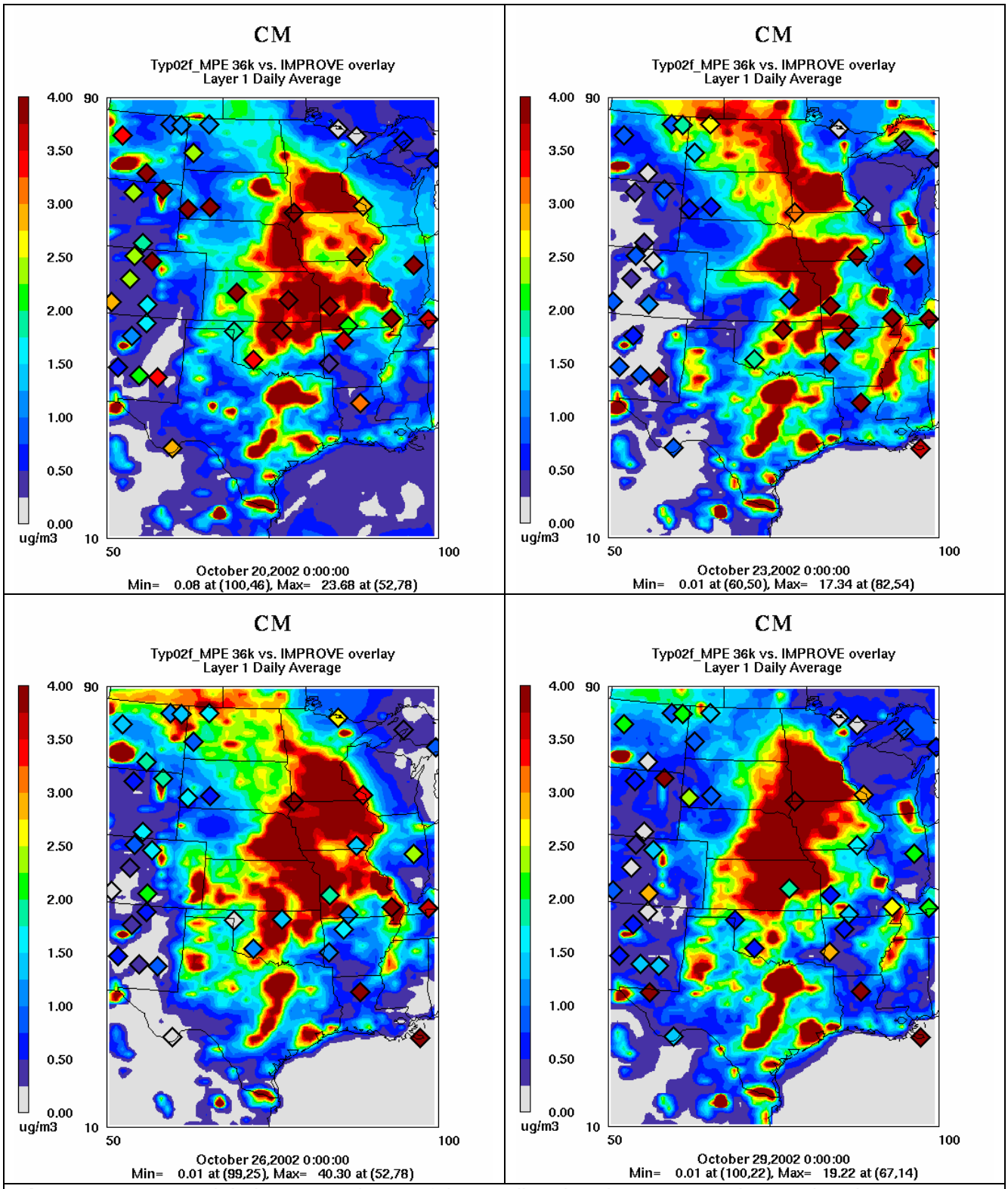

Figure C-37c. Spatial plot comparisons of the predicted and IMPROVE observed 24-hour CM concentrations for October 20, 23, 26 and 29, 2002.

C.3.6.5 CM Monthly Bias and Error

The monthly average fractional bias and error values for CM are shown in Figure C-38. In the winter the under-prediction bias is typically in the -60% to -80% range. In the late Spring and Summer the under-prediction bias ranges from -120% to -160%. As this under-prediction bias is nearly systematic, then the errors are the same magnitude as the bias.

The Bugle Plots clearly show that the CM model performance is a problem. The monthly bias exceeds both the performance goal and criteria for almost every month of the year. The error criteria are also exceeded for all months of the year.

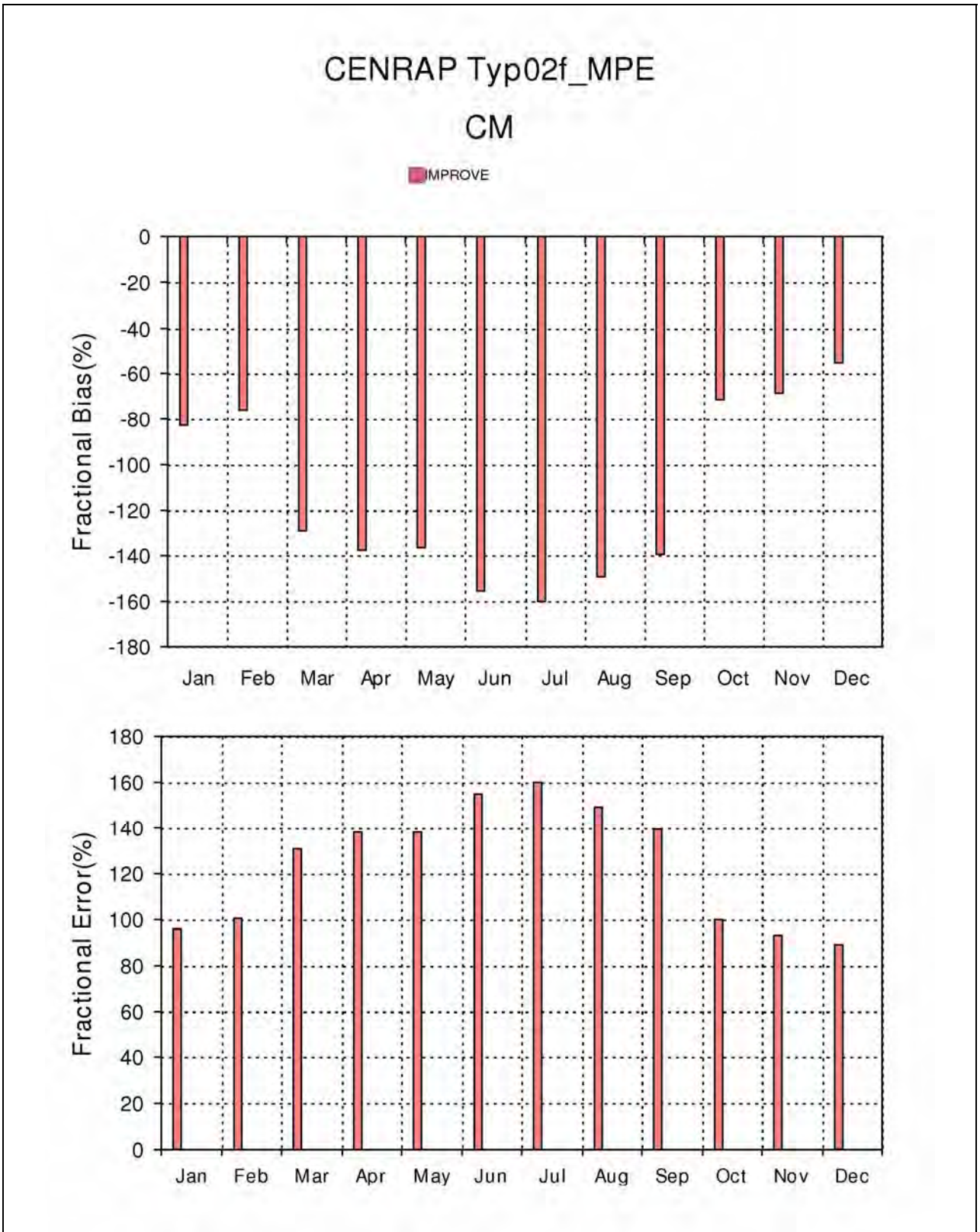

Figure C-38. Monthly CM fractional bias (top) and fractional gross error (bottom) statistical measures for IMPROVE monitoring sites in the CENRAP region.

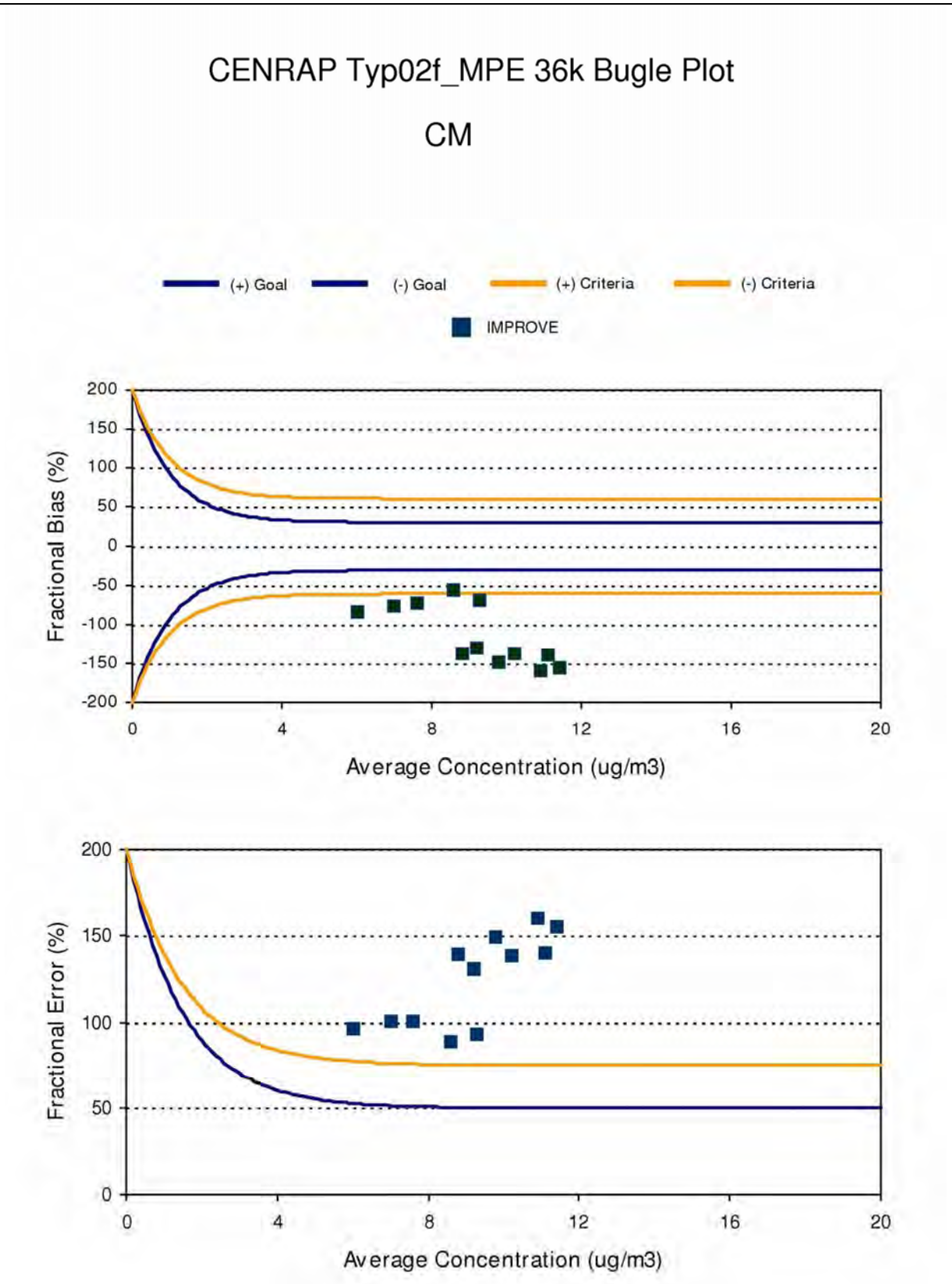

Figure C-39. Bugle Plots of monthly fractional bias (top) and fractional gross error (bottom) and comparisons with model performance goals and criteria for CM and IMPROVE monitoring sites in the CENRAP region.

C.4 Diagnostic Model Evaluation for Gas-Phase and Precursor Species

The CASTNet and AQS networks also measure gas-phase species that are PM precursor or related species. The diagnostic evaluation of the 2002 36 km Base F CMAQ base case simulation for these compounds and the four seasonal months presented previously is provided below.

The CASTNet network measures weekly average samples of SO2, SO4, NO2, HNO3, NO3 and NH4. The AQS network collects hourly measurements of SO2, NO2, O3 and CO. A comparison of the SO2 and SO4 performance provides insight into whether the SO4 formation rate may be too slow or fast. For example, if SO4 is underestimated and SO2 is overestimated that may indicate too slow chemical conversion rate. Analyzing the performance for SO4, HNO3, NO3, Total NO3 and NH4 provides insight into the equilibrium of these species. For example, if Total NO3 performs well but HNO3 and NO3 do not, then there may be issues associated with the partitioning between the gaseous and particle phases of nitrate.

C.4.1 Diagnostic Model Performance in January 2002

In January, SO2 is overstated across both the CASTNet and AQS sites with fractional bias values of 38% (Figure C-40) and 31% (Figure C-41), respectively. SO4 is understated by -34% across the CASTNet monitors (Figure C-40) and -12% and -13% for the IMPROVE and STN networks (Figure C-4a). As noted previously, wet SO4 deposition is also overstated in January (+40%, Figure C-4a). Given that SO2 emissions are well characterized, these results suggest that the January SO4 underestimation may be partly due to understated transformation rates of So2 to SO4 and overstated wet SO4 deposition.

Total NO3 is overestimated by 35% on average across the CASTNet sites in the CENRAP region in January (Figure C-40). HNO3 is underestimated (-34%) and particle NO3 is overestimated (+61%) suggesting there are gas/particle equilibrium issues. An analysis of the time series of the four CASTNet stations reveals that NO3, HNO3 and NH4 performance is actually very reasonable at the west Texas and the HNO3 underestimation and NO3 overestimation bias is coming from the east Kansas, central Arkansas and northern Minnesota CASTNet sites. One potential contributor for this performance problem is overstated NH3 emissions. However the overstated Total NO3 suggests that the model estimated NOx oxidation rate may be too high in January.

The SO2, NO2, O3 and CO performance across the AQS sites in January is shown in Figure C-41. The AQS monitoring network is primarily an urban-oriented network so it is not surprising that the model is underestimating concentrations of primary emissions like NO2 (-5%) and particularly CO (-67%) when a 36 km grid is used. Ozone is also underestimated on average, especially the maximum values above 60 ppb.

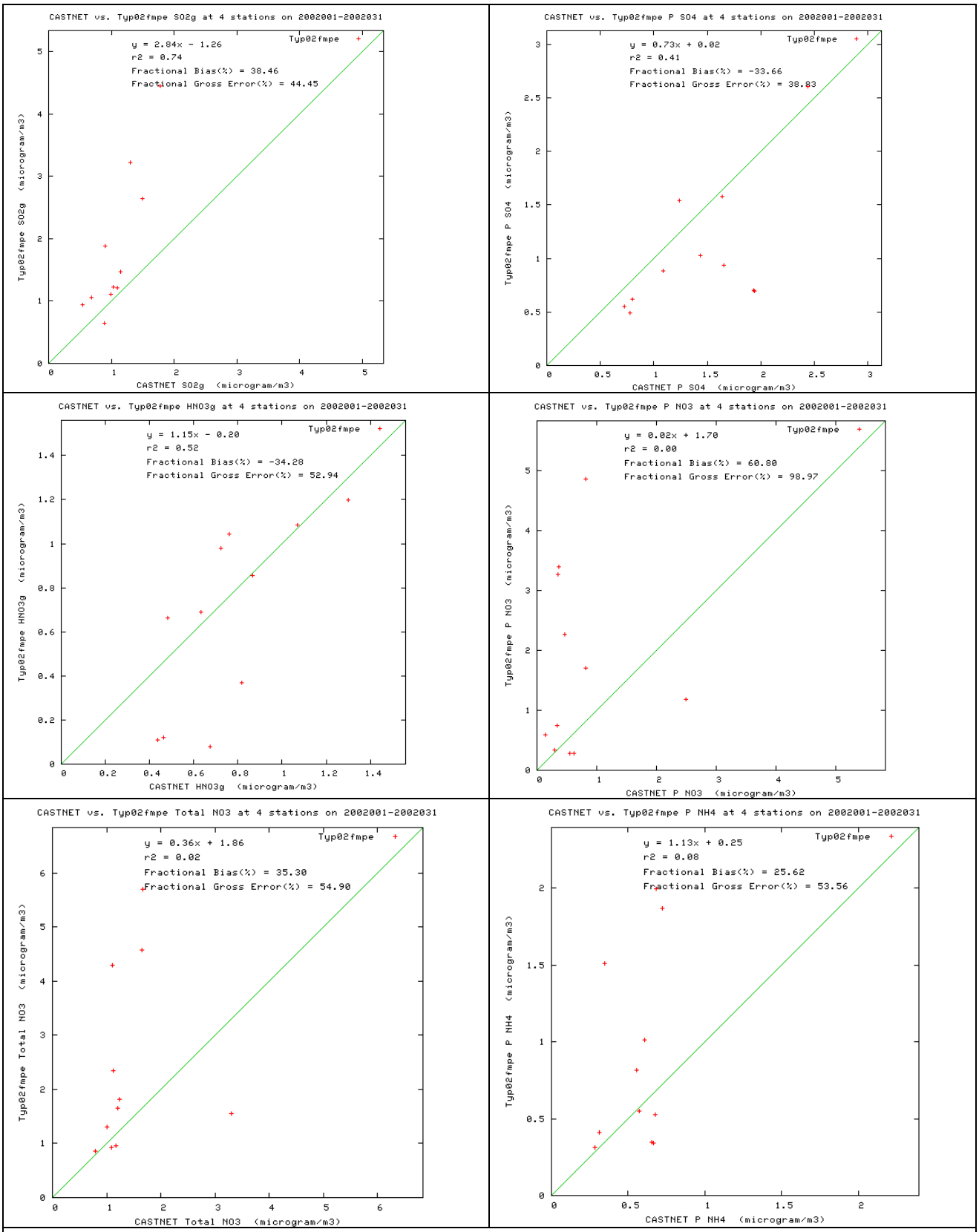

Figure C-40. January 2002 performance at CENRAP CASTNet sites for SO2 (top left), SO4 (top right), HNO3 (middle left), NO3 (middle right), Ttoal NO3 (bottom left) and NH4 (bottom right).

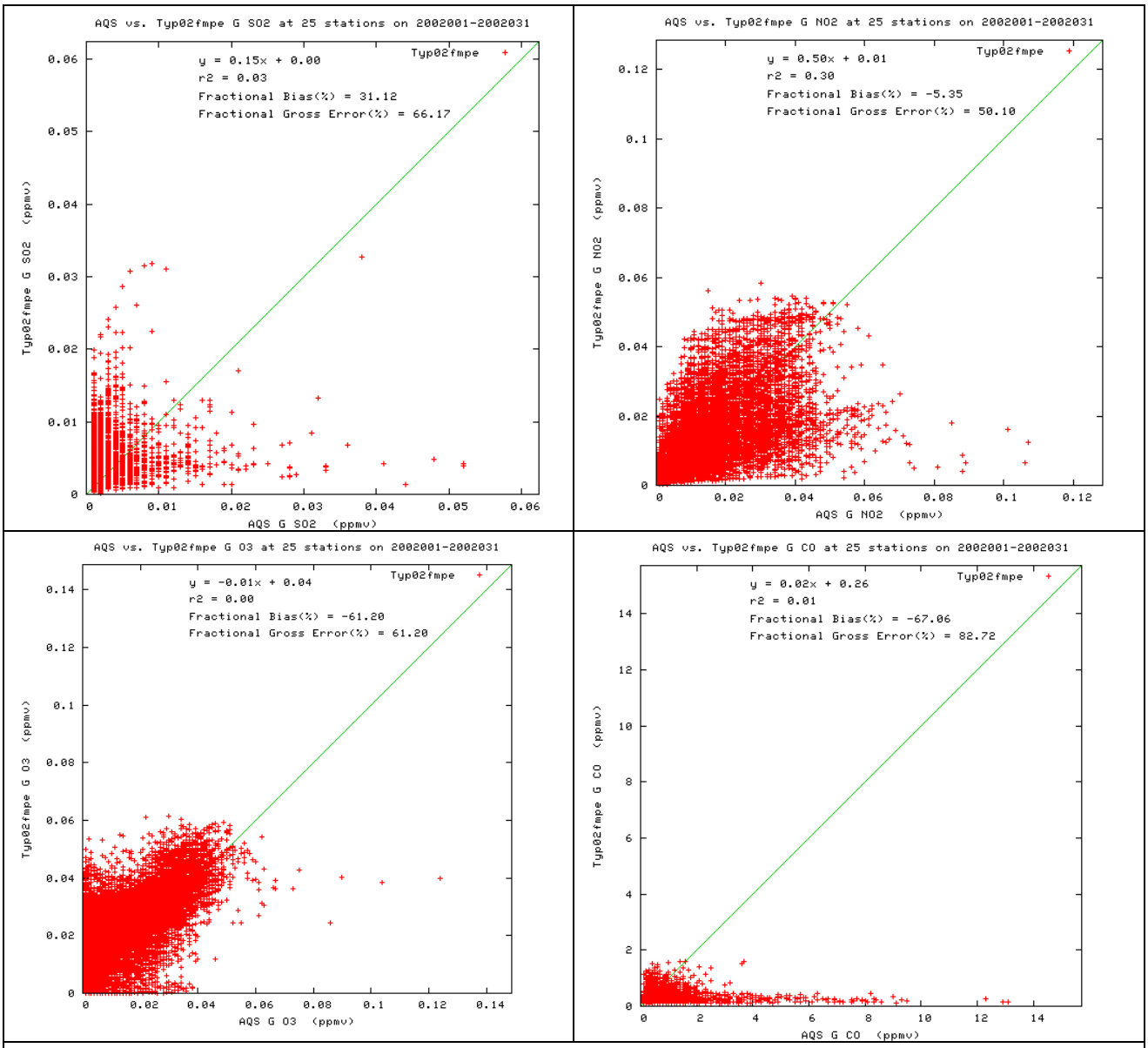

Figure C-41. January 2002 performance at CENRAP AQS sites for SO2 (top left), NO2 (top right), O3 (bottom left) and CO (bottom right).

C.4.2 Diagnostic Model Performance In April

In April there is an average SO2 overestimation bias across the CASTNet (+15%) and underestimation bias across the AQS (-10%) networks (Figures C-42 and C-43). SO4 is underestimated across all networks by -30% to -58% (Figure C-5a). The wet SO4 deposition bias is near zero. Both SO2 and SO4 are underestimated at the west Texas CASTNet monitor in April suggesting SO2 emissions in Mexico are likely understated.

The HNO3 performance in April is interesting with almost perfect agreement except for 5 modeled-observed comparisons that drives the average under-prediction bias of -29%. On Julian Day 102 there is high HNO3 at the MN, KS and OK CASTNet sites that is not captured by the model. Given that HNO3, NO3 and Total NO3 are all underestimated by about the same amount (-30%), then part of the underestimation bias is likely due to too slow oxidation of NOx.

There is a lot of scatter in the NO2 and O3 performance that is more or less centered on the 1:1 line of perfect agreement with bias values of -8% and -21%, respectively (Figure C-43). CO is underestimated by -72% with the model unable to predict CO concentrations above 1 $\mu g/m^3$ due to the use of the coarse 36 km grid spacing. Mobile sources produce a vast majority of the CO emissions so AQS monitors for CO compliance are located near roadways, which are not simulated well using a 36 km grid.

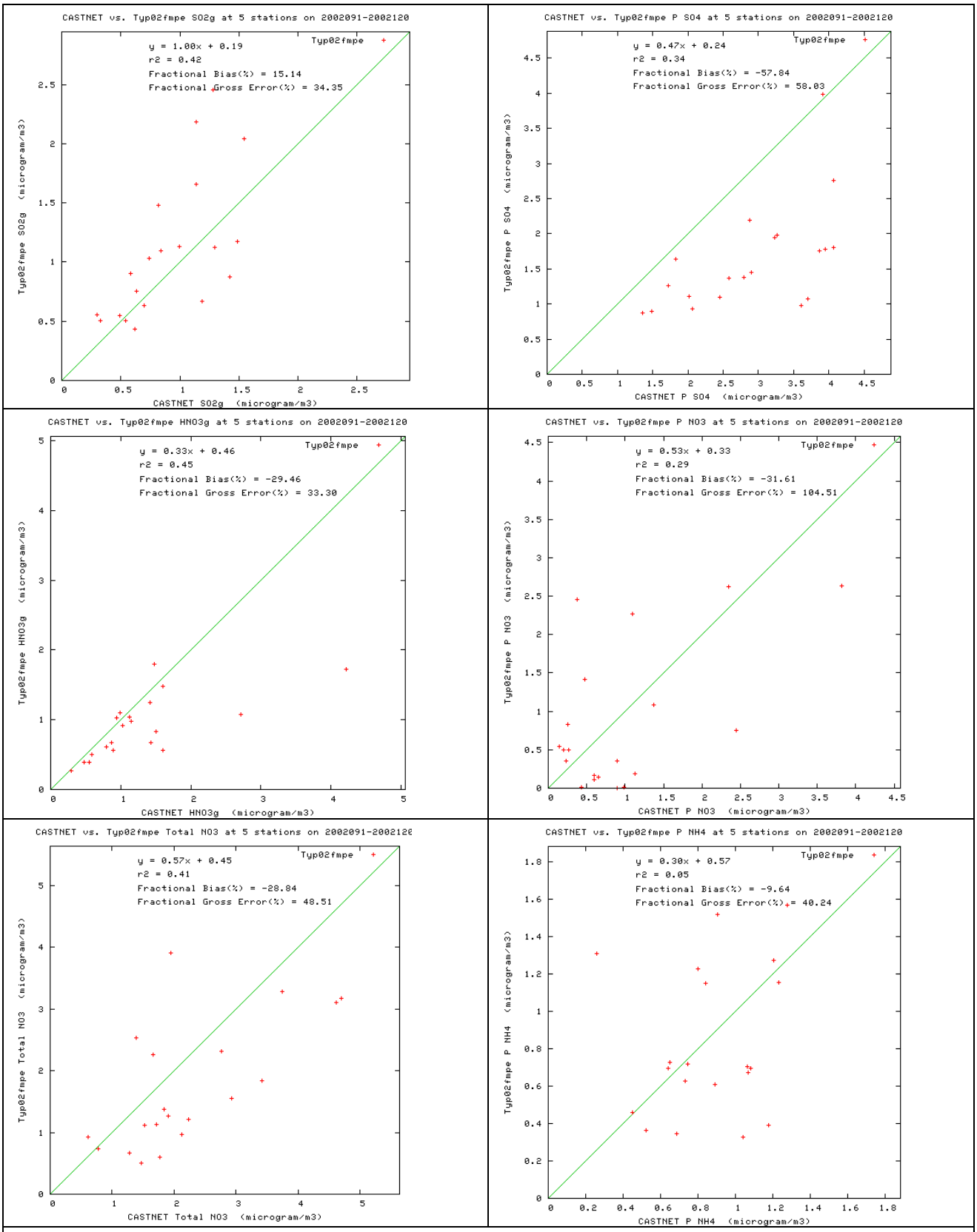

Figure C-42 April 2002 performance at CENRAP CASTNet sites for SO2 (top left), SO4 (top right), HNO3 (middle left), NO3 (middle right), Total NO3 (bottom left) and NH4 (bottom right).

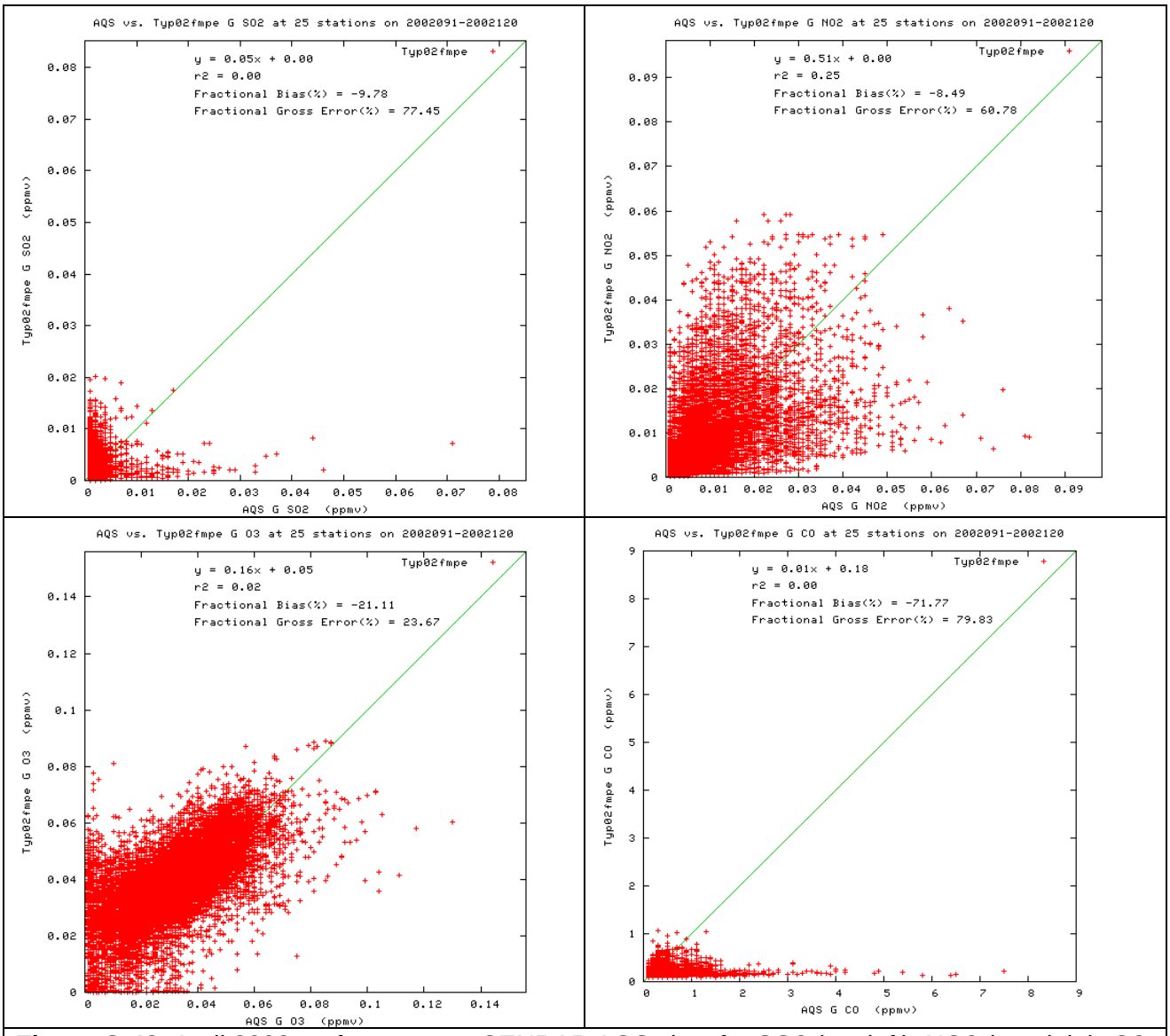

Figure C-43 April 2002 performance at CENRAP AQS sites for SO2 (top left), NO2 (top right), O3 (bottom left) and CO (bottom right).

C.4.3 Diagnostic Model Performance In July

In July SO2 is slightly underestimated across the CASTNet (-5%) and AQS (-12%) networks (Figures C-44 and C-45) and SO4 is more significantly underestimated across all networks (-22% to -53%, Figure C-6a). Since wet SO4 is also underestimated it is unclear the reasons for why all sulfur species are underestimated.

The nitrate species are also all underestimated with the Total NO3 bias (-56%) being between the HNO3 bias (-35%) and NO3 bias (-115%). The modeled NO3 values are all near zero with little correlation with the observations, whereas the observed HNO3 and Total NO3 is tracked well with correlation coefficients of 0.74 and 0.76. These results suggest that the July NO3 model performance problem is partly due to insufficient formation of Total NO3 and mainly due to too little incorrect partitioning of the Total NO3 into the particle NO3.

Again there is lots of scatter in the AQS NO2 scatter plot for July (Figure C-45) resulting in a low bias (0%) but high error (65%). Ozone performance also exhibits a low bias (-15%) and error (20%), but the model is incapable of simulating ozone above 100 ppb. Although CO performance in July is better than the previous months, it still has a large underestimation bias (-82%).

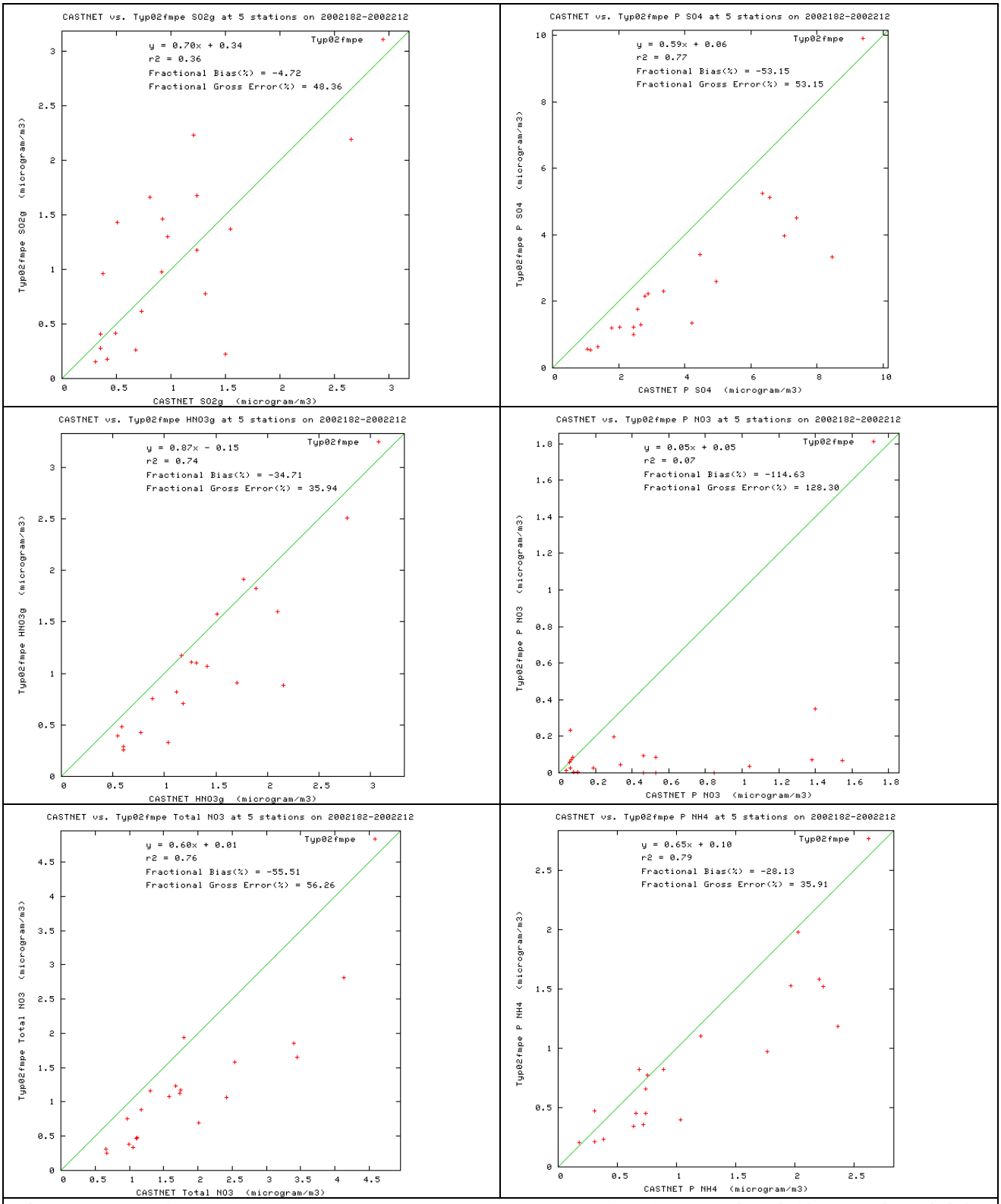

Figure C-44 July 2002 performance at CENRAP CASTNet sites for SO2 (top left), SO4 (top right), HNO3 (middle left), NO3 (middle right), Total NO3 (bottom left) and NH4 (bottom right).

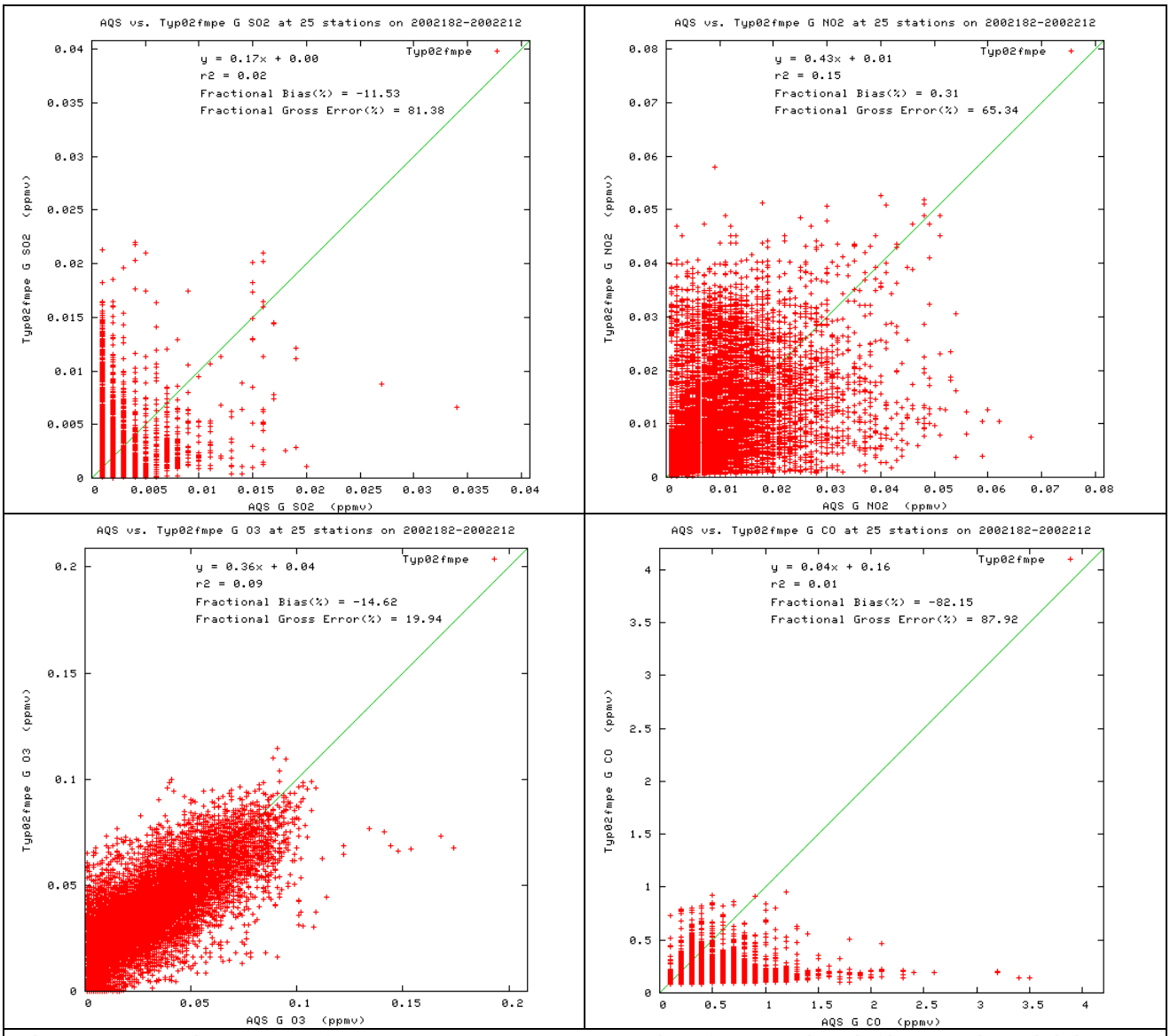

Figure C-45 July 2002 performance at CENRAP AQS sites for SO2 (top left), NO2 (top right), O3 (bottom left) and CO (bottom right).

C.4.4 Diagnostic Model Performance In October

SO2 is overstated in October across the CASTNet (+28%) and AQS (+33%) sites (Figures C-46 and C-47). Although SO4 is understated across the CASTNet sites (-24%), the bias across the IMPROVE (-6%) and STN (0%) sites are near zero (Figure C-7a).

Performance for HNO3 is fairly good with a low bias (+12%) and error (30%). But NO3 is overstated (+34%) leading to an overstatement of Total NO3 (+37%). The overstatement of NO3 leads to an overstatement of NH4 as well (Figure C-46)

As seen in the other months, NO2 exhibits a lot of scatter resulting in a low correlation (0.22) and high error (61%) but low bias (12%). The model tends to under-predict the high and over-predict the low O3 observations resulting in a -29% bias and low correlation coefficient. CO is also under-predicted (-76%) for the reasons discussed previously.

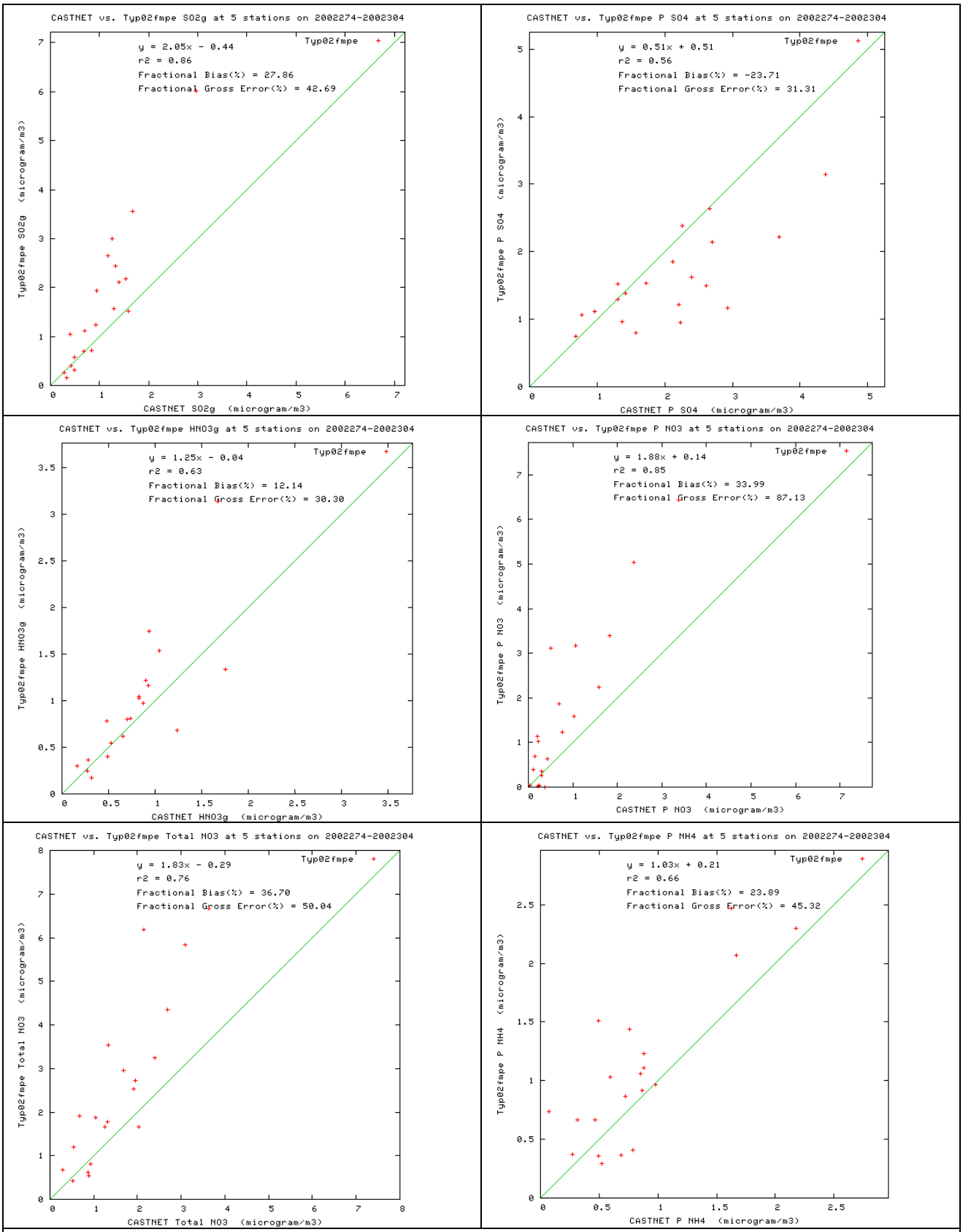

Figure C-46 October 2002 performance at CENRAP CASTNet sites for SO2 (top left), SO4 (top right), HNO3 (middle left), NO3 (middle right), Total NO3 (bottom left) and NH4 (bottom right).

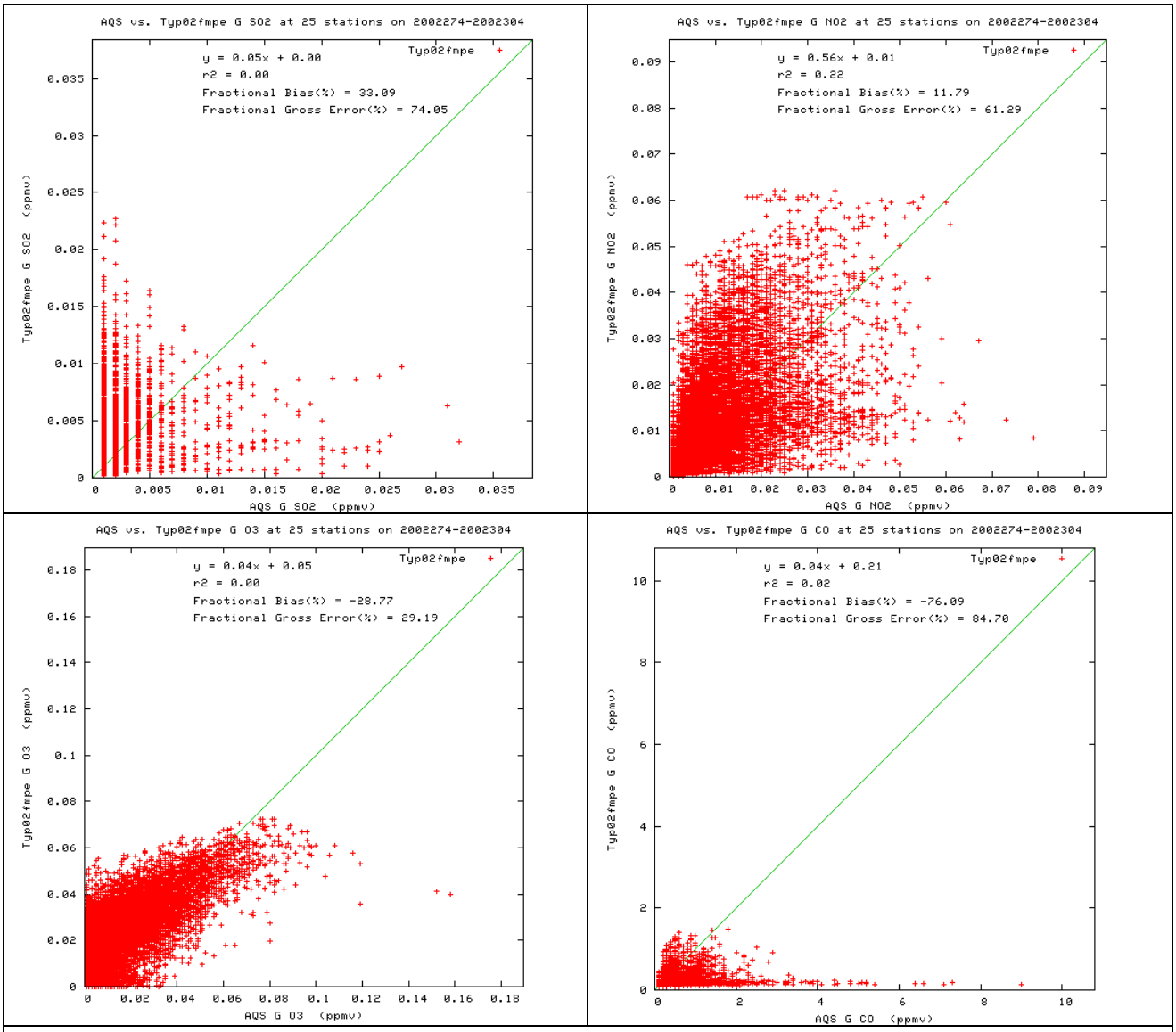

Figure C-47 October 2002 performance at CENRAP AQS sites for SO2 (top left), NO2 (top right), O3 (bottom left) and CO (bottom right).

C.5 Evaluation at Class I Areas for the Worst and Best 20 Percent Days

In this section, and in section C.5 of Appendix C, we present the results of the model performance evaluation at each of the CENRAP Class I areas for the worst and best 20 percent days. Performance on these days is critical since they are the days used in the 2018 visibility projections discussed in Chapter 4. For each Class I area we compared the predicted and observed total extinction (these figures are in Chapter 3) and PM species-specific extinction for the worst and best 20 percent days in 2002.

C.5.1 Caney Creek (CACR) Arkansas

The ability of the CMAQ model to estimate visibility extinction at the CACR Class I area on the 2002 worst and best 20 percent days is provide in Figures 3-9 and C-48. On most of the worst 20 percent days at CACR total extinction is dominated by SO4 extinction with some extinction due to OMC. On four of the worst 20 percent days extinction is dominated by NO3. The average extinction across the worst 20 percent days is underestimated by -33% (Figure 3-9), which is primarily due to a -51% underestimation of SO4 extinction combined with a 6% overestimation of NO3 extinction (Figure C-48). Performance for OMC extinction at CACR on the worst 20 percent days is pretty good with a -20% bias and 36% error, EC extinction is systematically underestimated, Soil extinction has low bias (-19%) buts lots of scatter and high error (74%), while CM extinction is greatly underestimated (bias of -153%).

On the best 20 percent days at CACR the observed extinction ranges from 20 to 40 Mm^{-1}, whereas then modeled extinction has a much larger range from 15 to 120 Mm^{-1}. Much of the modeled overestimation of total extinction on the best 20% days (+44% bias) is due to NO3 overestimation (+94% bias).

C.5.2 Upper Buffalo (UOBU) Arkansas

Model performance at the UPBU Class I area for the worst and best 20 percent days is shown in Figures 3-10 and C-49. On most of the worst 20 percent days at UPBU visibility impairment is dominated by SO4, although there are also two high NO3 days. The model underestimates the average of the total extinction on the worst 20 percent days at UPBU by -40% (Figure 3-10), which is due to an underestimation of extinction due to SO4, OMC and CM by, respectively,

-46%, -33% and -179%.

On the best 20 percent days at UPBU, the model performs reasonably well with a low bias (2%) and error (42%). But again the model has a much wider range in extinction values across the best 20 percent days (15 to 120 Mm^{-1}) than observed (20 to 45 Mm^{-1}). There are five days in which the modeled NO3 over-prediction is quite severe and when those days are removed the range in the modeled and observed extinction on the best 20 percent days is quite similar, although the model gets much cleaner on the very cleanest modeled days.

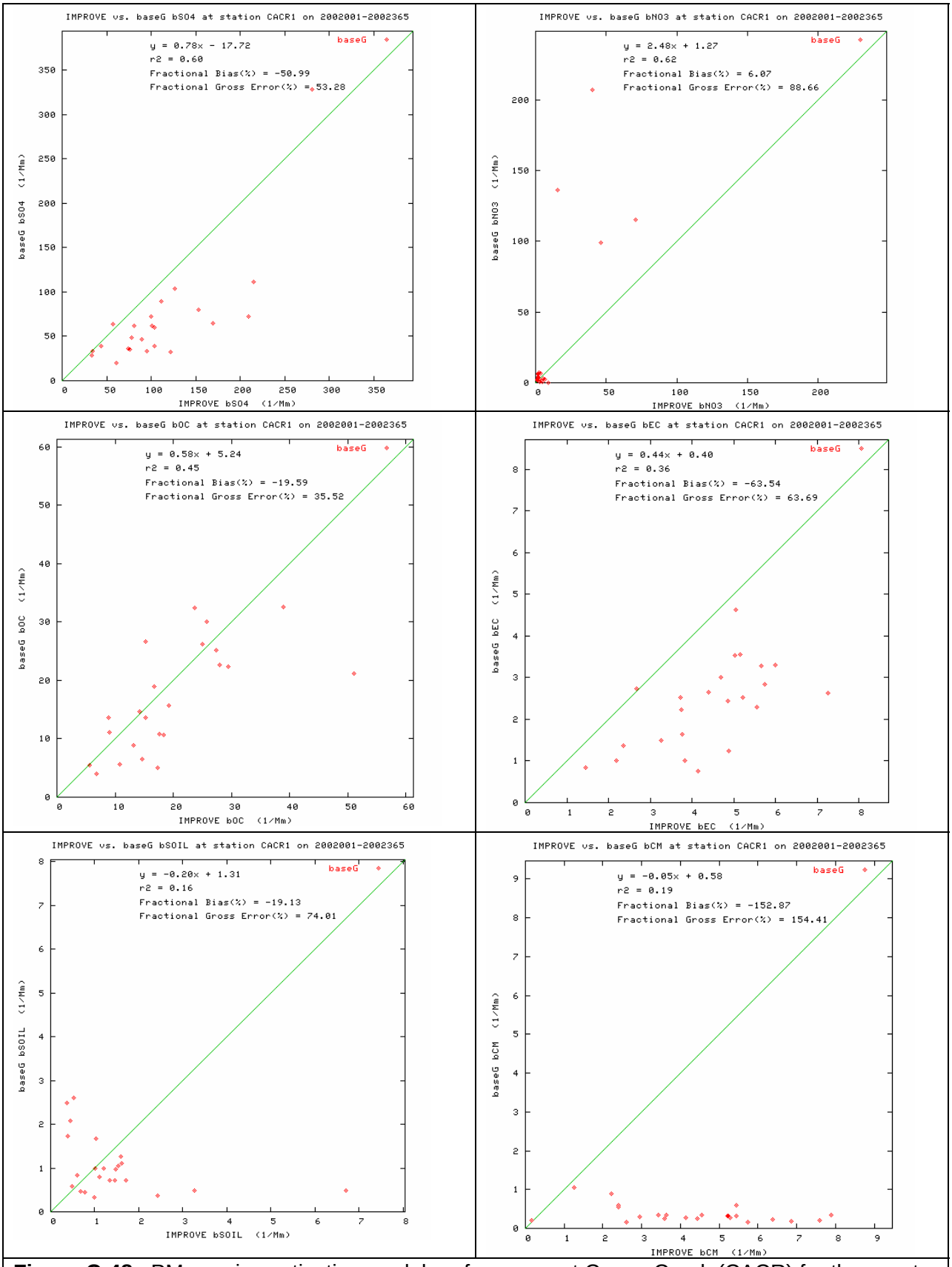

Figure C-48. PM species extinction model performance at Caney Creek (CACR) for the worst 20 percent days during 2002.

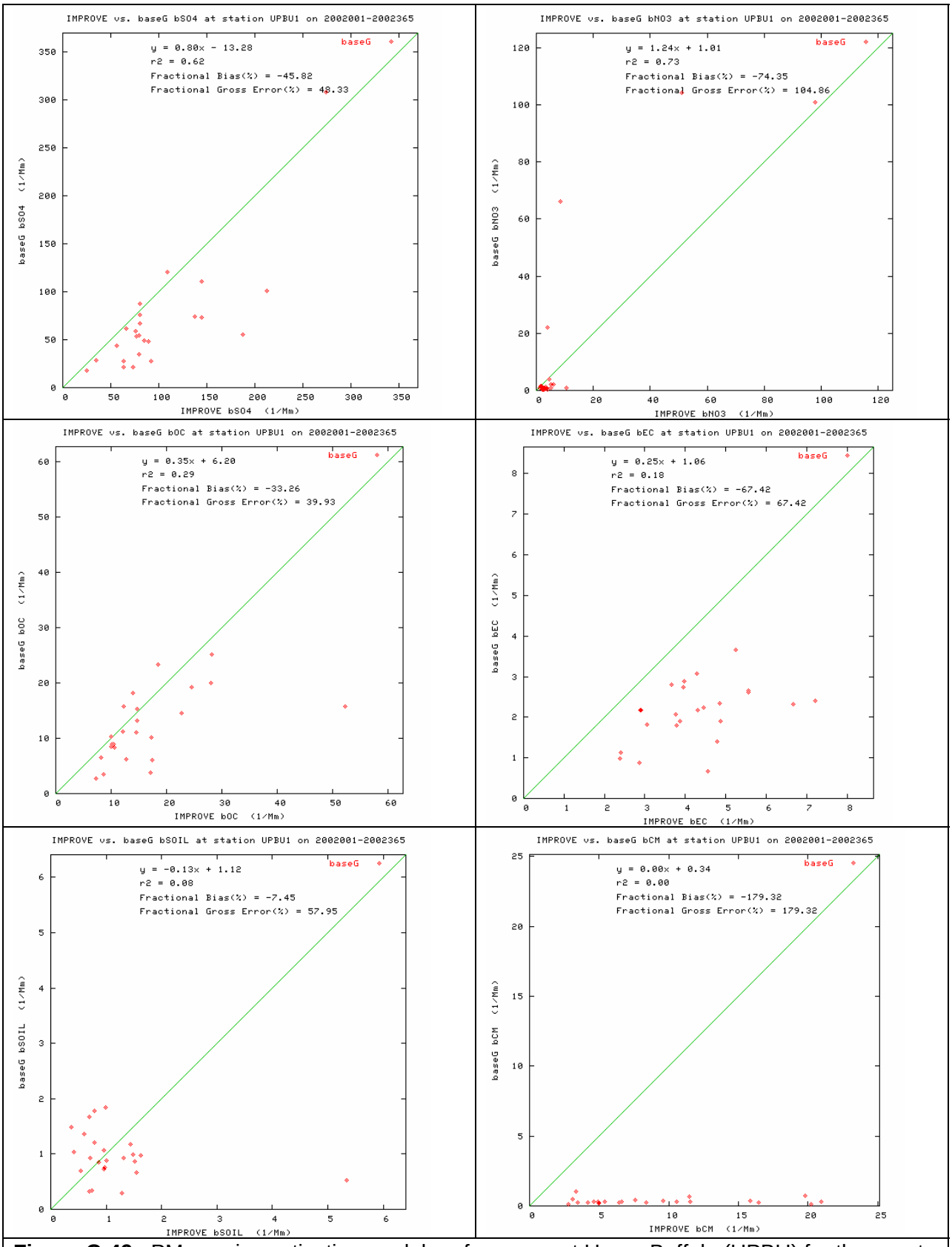

Figure C-49. PM species extinction model performance at Upper Buffalo (UPBU) for the worst 20 percent days during 2002.

C.5.3 Breton Island (BRET), Louisiana

The observed total extinction on the worst 20 percent days at Breton Island is underestimated by -71% (Figure 3-11), which is due to an underestimation of each component of extinction (Figure C-50) by from -50% to -70% (SO4, OMC and Soil) to over -100% (EC and CM). The observed extinction on the worst 20 percent days ranges from 90 to 170 Mm^{-1}, whereas the modeled values drop down to as low as approximately 15 Mm^{-1}. On the best 20 percent days the range of the observed and modeled extinction is similarly (roughly 10 to 50 Mm^{-1}) that results in a reasonably low bias (-22%), but there is little agreement on which days are higher or lower resulting in a lot of scatter and high error (54%).

C.5.4 Boundary Waters (BOWA), Minnesota

There are three types of days during the worst 20 percent days at BOWA, SO4 days, OMC days and NO3 days (Figure 3-12). The two high OMC days are likely fire impact events that the model captures to some extent on one day and not on the other. On the five high (> 20 Mm^{-1}) NO3 extinction days the model predicts the observed extinction well on three days and overestimates by a factor of 3-4 on the other two high NO3 days. SO4 in underestimate by -43% on average across the worst 20 percent days at BOWA.

With the exception of two days, the model reproduces the total extinction for the best 20 percent days at BOWA quite well with a bias and error value of +14% and 22% (Figure 3-12). Without these two days, the modeled and observed extinction both range between 15 and 25 Mm^{-1}.

C.5.5 Voyageurs (VOYA) Minnesota

VOYA is also characterized by SO4, NO3 and OMC days (Figure 3-13). Julian Days 179 and 200 are high OMC days that were also high OMC days at BOWA again indicating impacts from fires in the area that is not fully captured by the model. SO4 and NO3 extinction is fairly good and, without the fire days, OMC performance looks good as well (Figure C-52). On the best 20 percent days there is one day the modeled extinction is much higher than observed and a few others that are somewhat higher, but for most of the best 20 percent days the modeled extinction is comparable to the observed values.

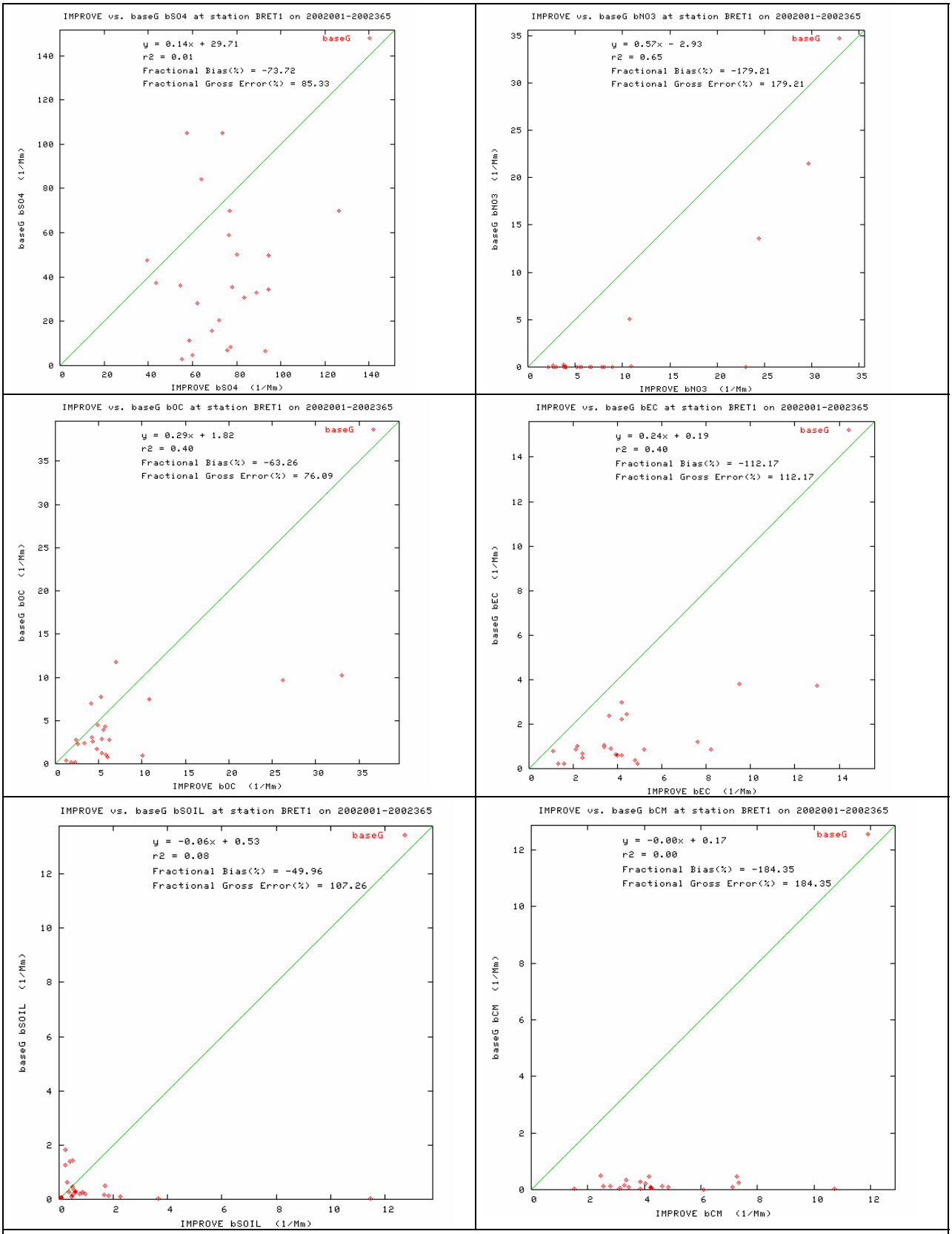

Figure C-50. PM species extinction model performance at Breton Island (BRET) for the worst 20 percent days during 2002.

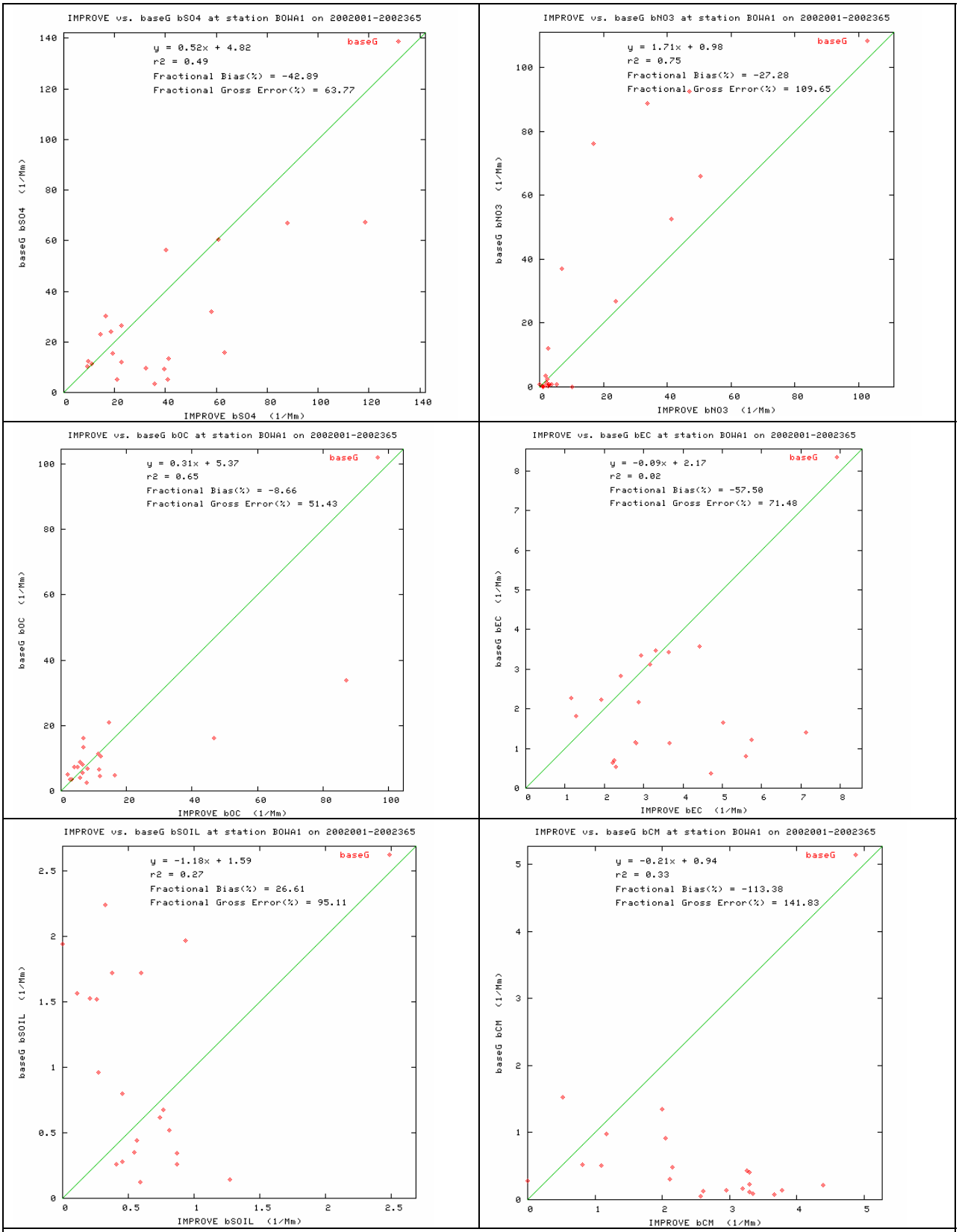

Figure C-51. PM species extinction model performance at Boundary Waters (BOWA) for the worst 20 percent days during 2002.

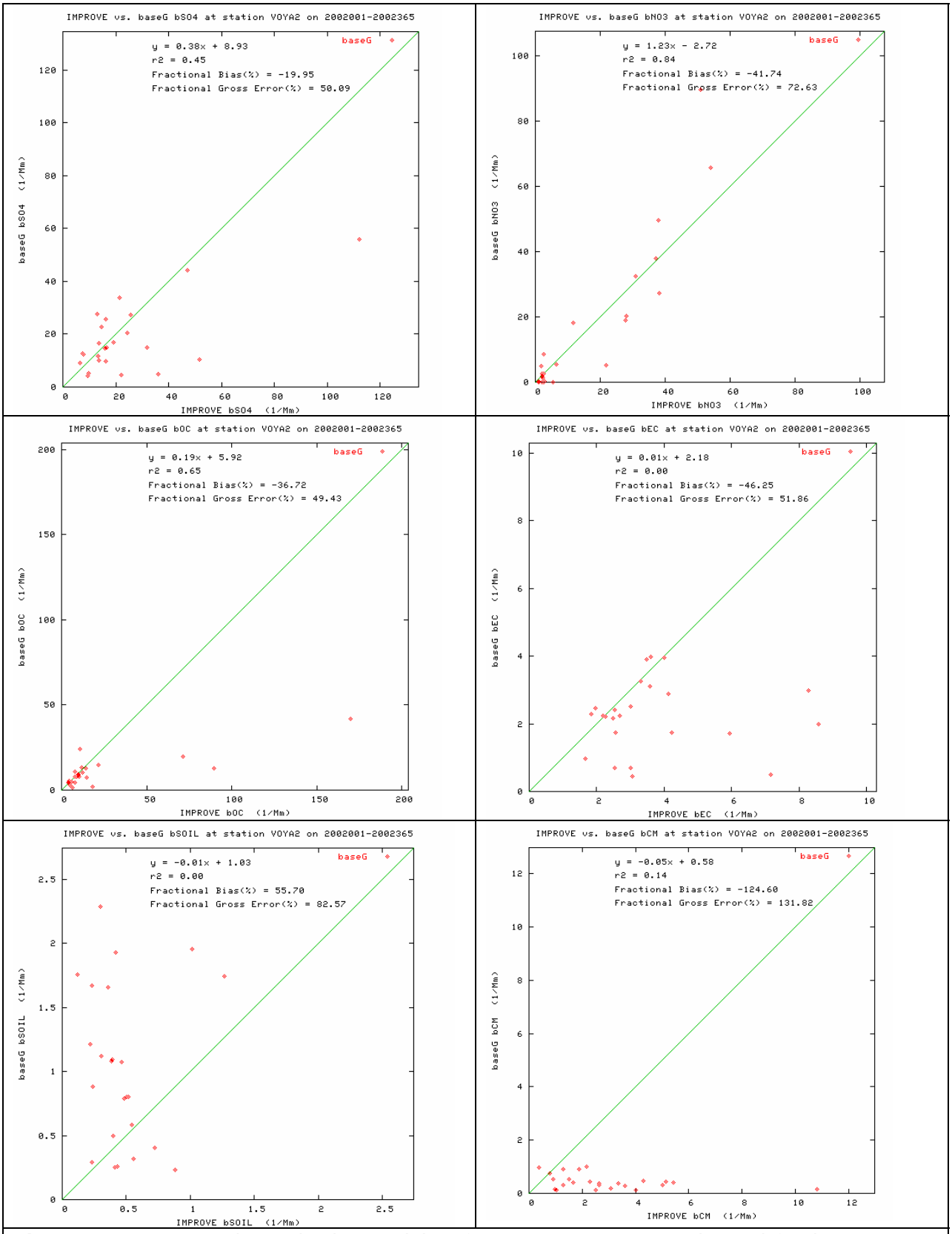

Figure C-52. PM species extinction model performance at Voyageurs (VOYA) for the worst 20 percent days during 2002.

C.5.6 Hercules Glade (HEGL) Missouri

On most of the worst 20 percent days at HEGL the observed extinction ranges from 120 to 220 Mm^{-1} whereas model extinction ranging from 50 to 170 Mm^{-1} (Figure 3-14). However, there is one extreme day with extinction approaching 400 Mm^{-1} that the model does a very good job in replicating. Over all the days there is a modest underestimation bias in SO4 (-39%) and OMC (-39%) extinction, larger underestimation bias in EC (-62%) and CM (-118%) extinction and overestimation bias in Soil (+30%) extinction (Figure C-53).

On the best 20 percent days there is one day where the model overstates the observed extinction by approximately a factor of four and a handful of other days that the model overstates the extinction by a factor of 2 or so, but most of the days both the model and observed extinction sites are around 40 Mm^{-1} plus or minus about 10 Mm^{-1}. On the best 20 percent days when the observed extinction is overstated it is due to overstatement of the NO3.

C.5.7 Mingo (MING) Missouri

The worst 20 percent days at Ming are mainly high SO4 days with a few high NO3 days that the model reproduces reasonably well resulting in low bias (+10%) and error (38%) for total extinction (Figure 3-15). The PM species specific performance is fairly good with low bias for SO4 (+4%), good agreement with NO3 on high NO3 days except for one day, low OMC (+23%) and EC (+3%) bias and larger bias in EC (+37%) and CM (-105%) extinction (Figure C-54).

For the best 20 percent days, there is one day the model is way to high due to overstated NO3 extinction and a few other days the model overstates the observed extinction that is usually due to overrated NO3, but on most of the best 20 percent days the modeled extinction is comparable to the observed values. This results in low bias (+12%) and error (36%) for total extinction at MING for the best 20 percent days.

C.5.8 Wichita Mountains (WIMO), Oklahoma

With the exception of an over-prediction on day 344 due to NO3, observed total extinction on the worst 20 percent days at WIMO is understated with a bias of -42% (Figure 3-16) that is primarily due to an underestimation of extinction due to SO4 (-48%) and OMC (-69%) (Figure C-55).

CMAQ total extinction performance for the average of the best 20 percent days at WIMO is characterized by an overestimation bias (+21%) on most days that is primarily due to NO3 over-prediction on several days. Again the modeled range of extinction on the best 20 percent days (12-60 Mm^{-1}) is much greater than observed (20-35 Mm^{-1}).

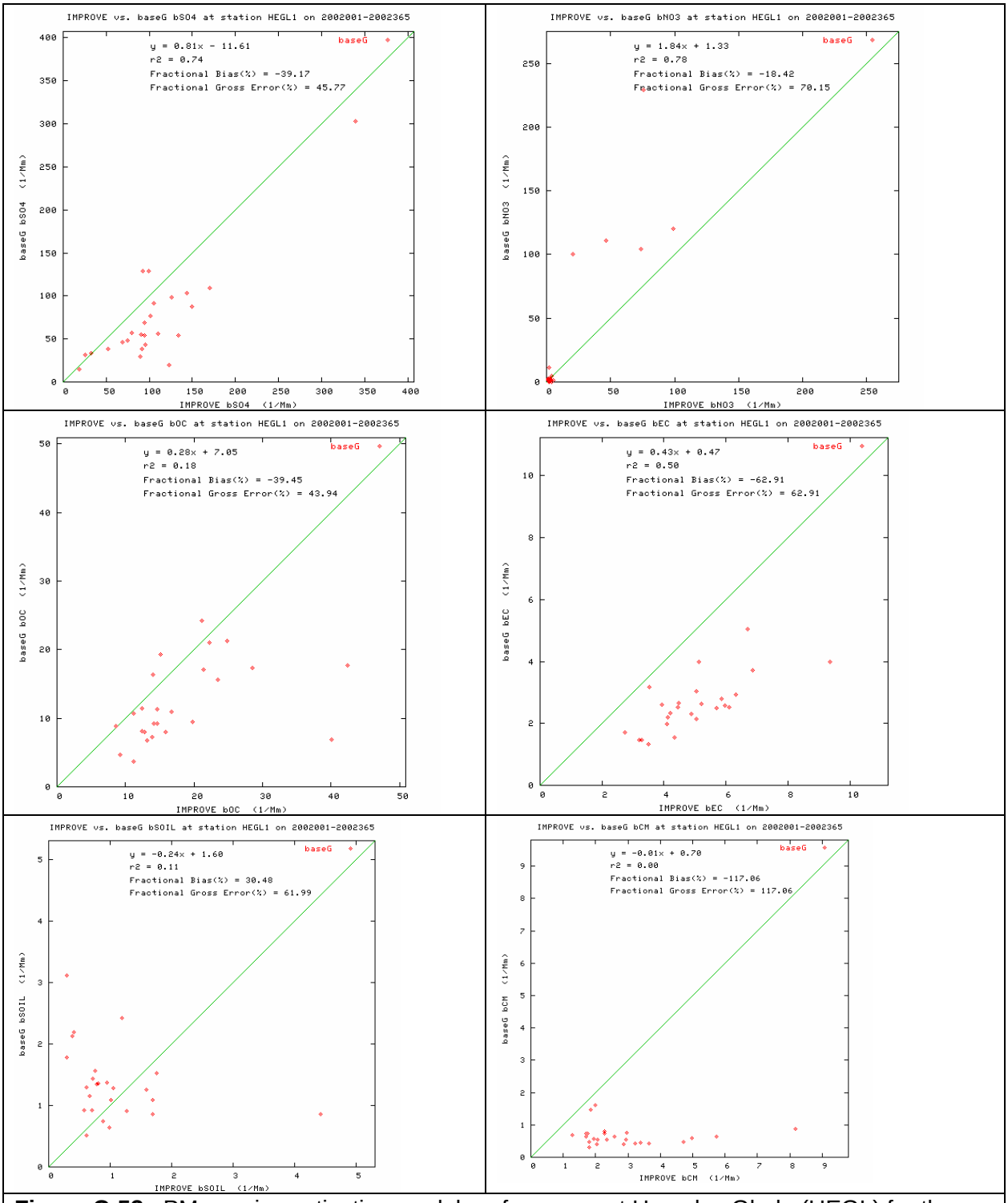

Figure C-53. PM species extinction model performance at Hercules Glade (HEGL) for the worst 20 percent days during 2002.

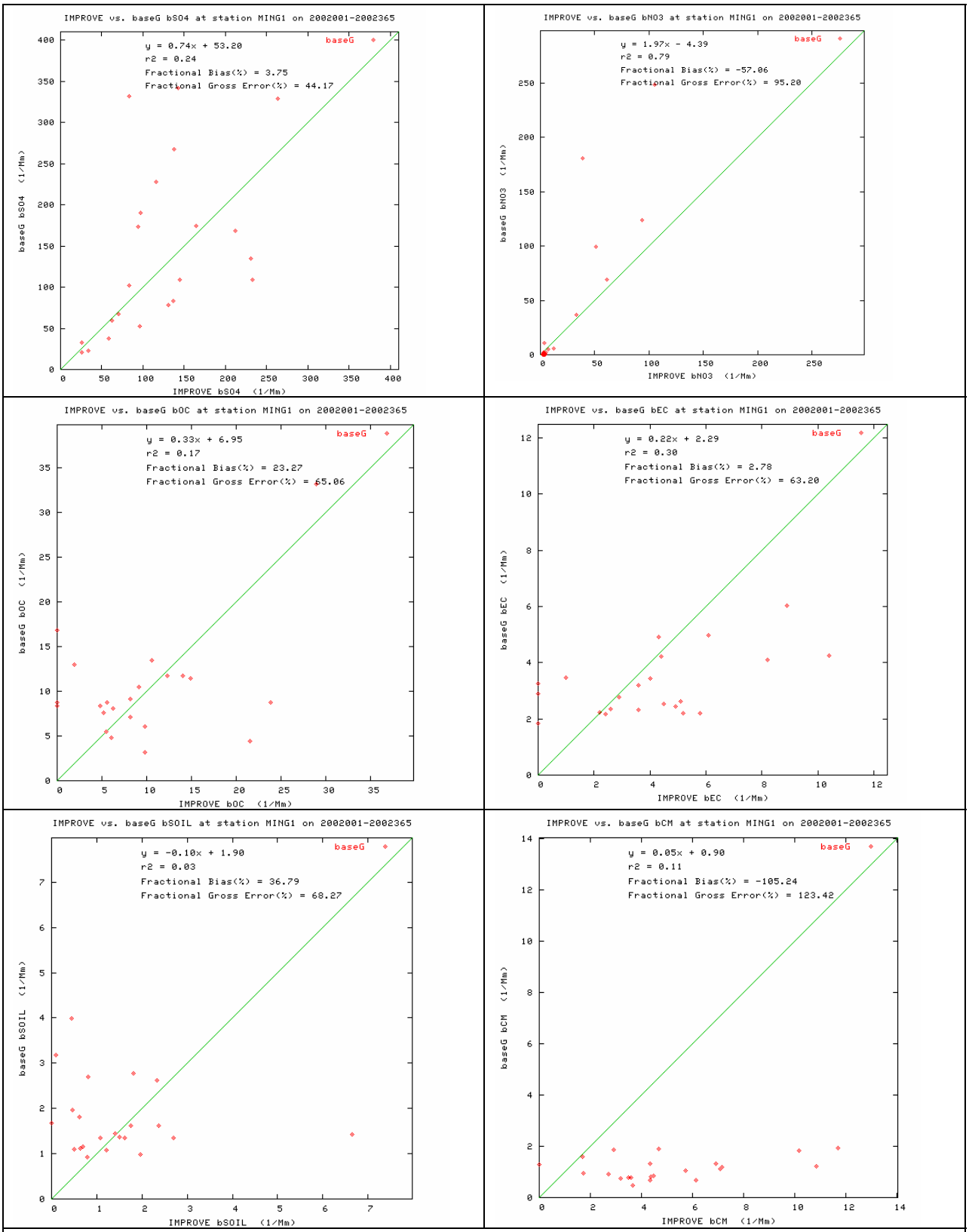

Figure C-54. PM species extinction model performance at Mingo (MING) for the worst 20 percent days during 2002.

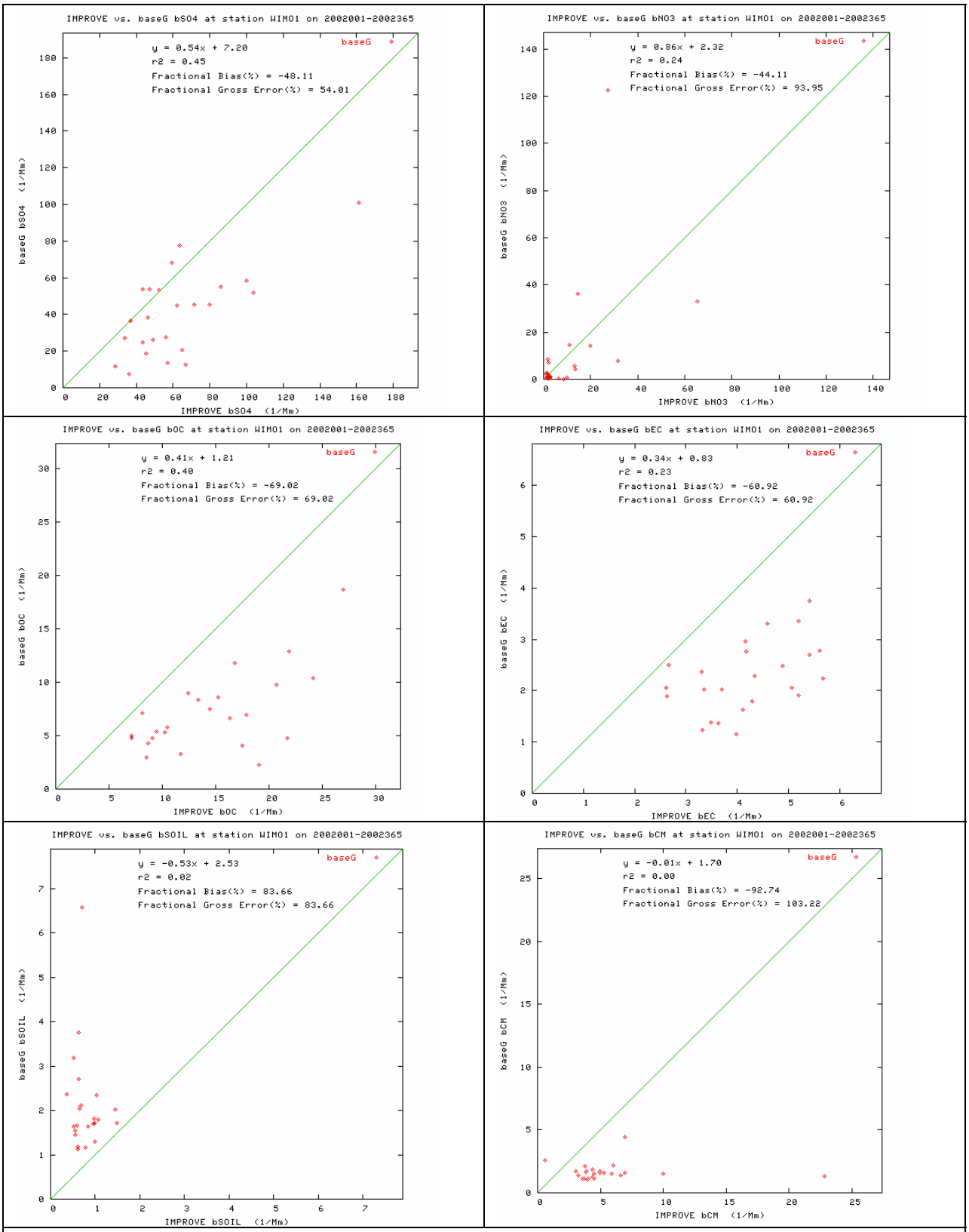

Figure C-55. PM species extinction model performance at Wichita Mountains (WIMO) for the worst 20 percent days during 2002.

C.5.9 Big Bend (BIBE) Texas

The observed extinction on the worst 20 percent days at BIBE is under-predicted on almost every day resulting in a fractional bias value of -72% (Figure 3-17). Every component of extinction is underestimated on average for the worst 20 percent days (Figure C-56) with the underestimation bias ranging from -24% (OMC) to -162% (CM). SO4 extinction, that typically represents the largest component of the total extinction is understated by -94%.

The model does a better job in predicting the total extinction at BIBE for the best 20 percent days with average fractional bias and error values of +13% and 19% (Figure 3-17). With the exception of one day that the observed extinction is overestimated by approximately a factor of 2, the modeled and observed extinction on the best 20 percent days at BIBE are both within 12 to 25 Mm^{-1}. However, there are some mismatches with the components of extinction with the model estimating much lower contributions due to Soil and CM.

C.5.10 Guadalupe Mountains (GUMO) Texas

Most of the worst 30 percent days at GUMO are dust days with high Soil and CM that is not at all captured by the model (Figure 3-18). Extinction due to Soil and CM on the worst 20 percent days is underestimated by -105% and -191%, respectively (Figure C-57). Better performance is seen on the best 20 percent days with bias and error for total extinction of 8% and 21%, but the model still understates Soil and CM.

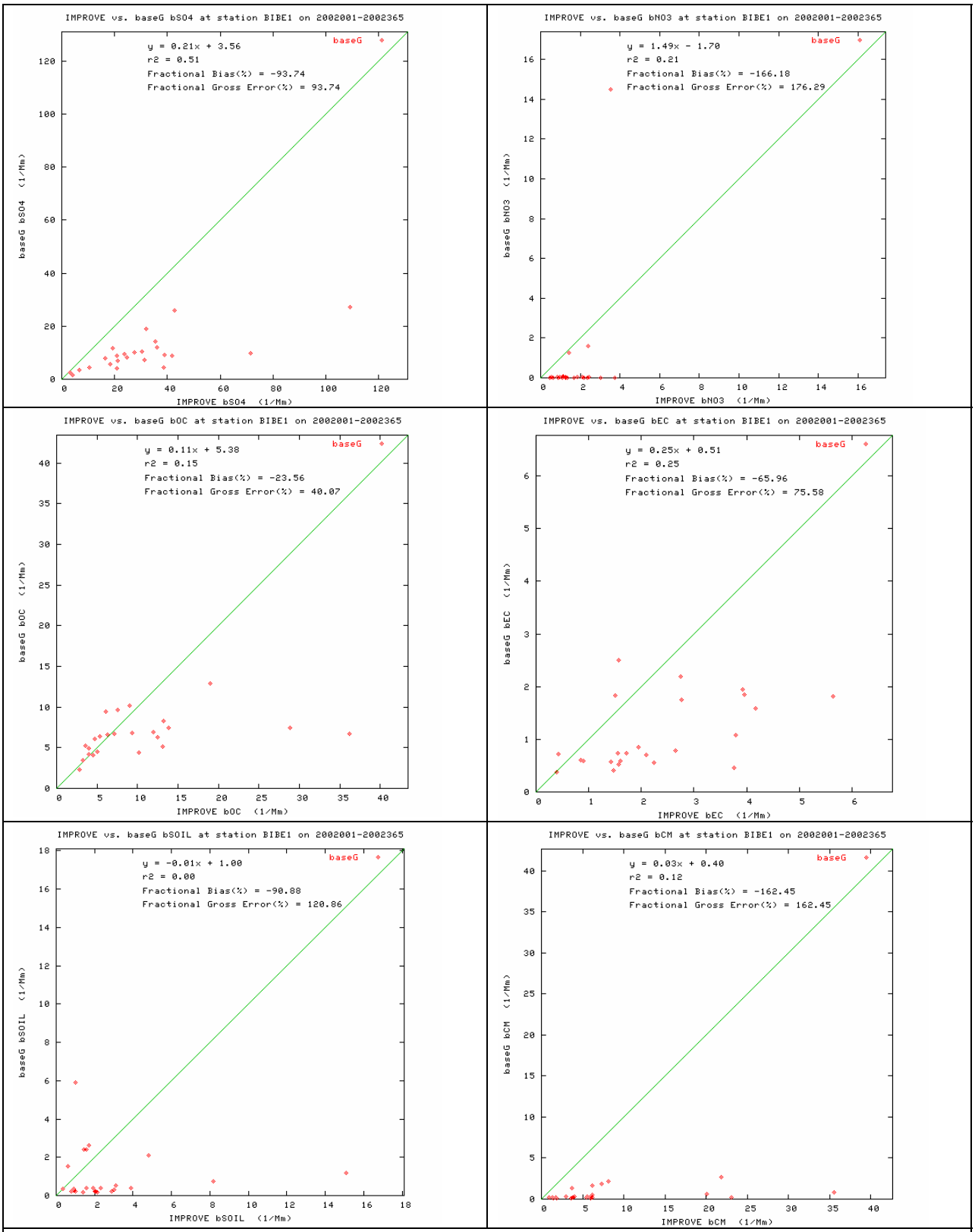

Figure C-56. PM species extinction model performance at Big Bend (BIBE) for the worst 20 percent days during 2002.

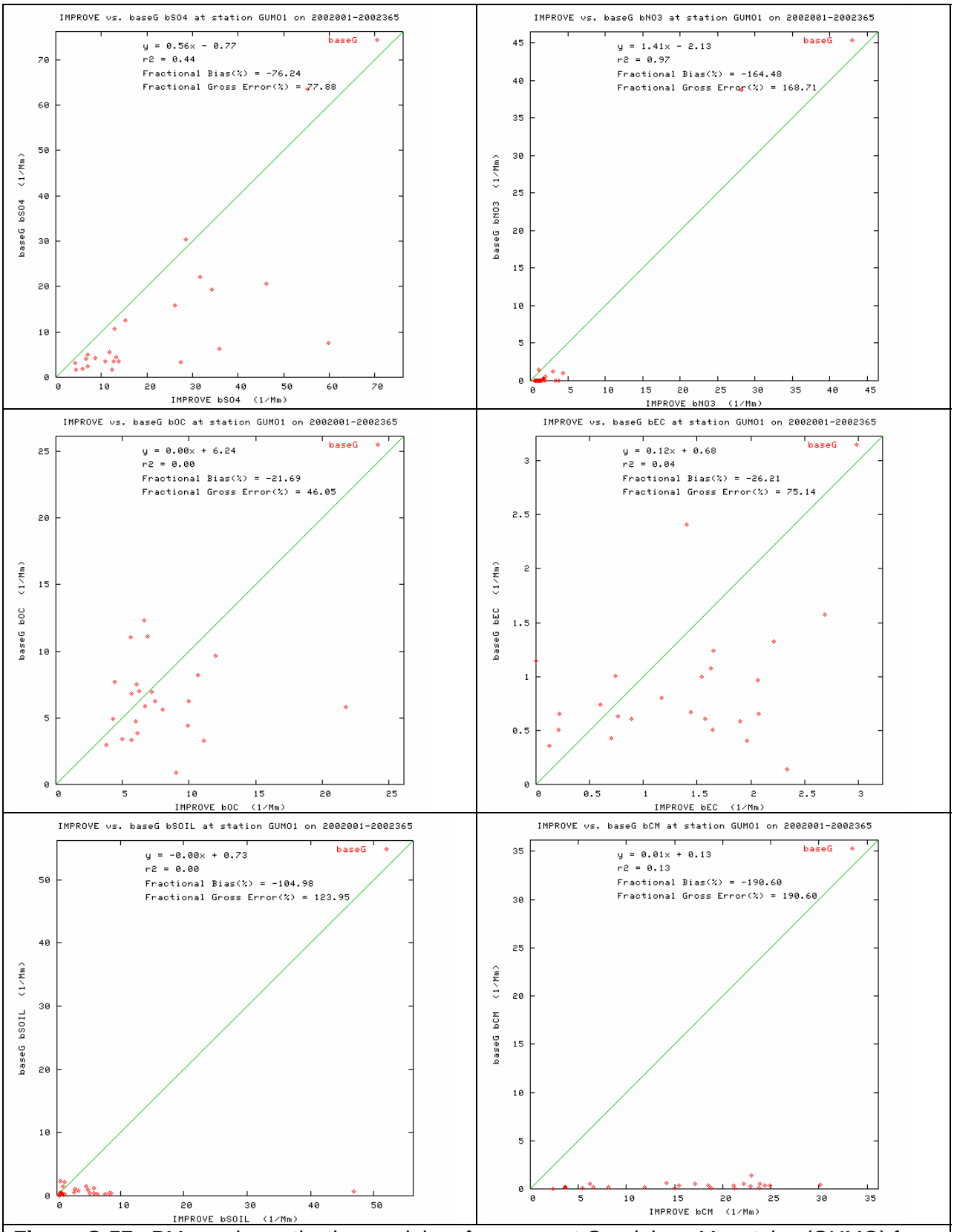

Figure C-57. PM species extinction model performance at Guadalupe Mountains (GUMO) for the worst 20 percent days during 2002.

C.6 Model Performance Evaluation Conclusions

The model performance evaluation reveals that the model is performing best for SO4, OMC and EC. Soil performance is mixed with winter overestimation bias but lower bias but high error in the summer. CM performance is poor year round. The operational evaluation reveals that SO4 performance usually achieves the PM model performance goal and always achieves the model performance criteria, although it does have an underestimation bias that is greatest in the summer. NO3 performance is characterized by a winter overestimation bias with an even greater summer underestimation bias. However, the summer underestimation bias occurs when NO3 is very low and it is not an important component of the observed or predicted PM and visibility impairment. Performance for OMC meets the model performance goal year round at the IMPROVE sites, but is characterized by an underestimation bias at the more urban STN sites. EC exhibits very low bias at the STN sites and a summer underestimation bias at the IMPROVE sites, but meets the model performance goal throughout the year. Soil has a winter overestimation bias that exceeds the model performance goal and criteria raising questions whether the model should be used for this species. Finally, CM performance is extremely poor with an under-prediction bias that exceeds the performance goal and criteria. We suspect that much of the CM concentrations measured at the IMPROVE sites is due to highly localized emissions that can not be simulated with 36 km regional modeling.

Performance for the worst 20 percent days at the CENRAP Class I areas is generally characterized by an underestimation bias. Performance at the BRET, BIBE and GUMO Class I areas for the worst 20 percent days is particularly suspect and care should be taken in the interpretation of the visibility projections at these three Class I areas.

The CMAQ 2002 36 km model appears to be working well enough to reliably make future-year projections for changes in SO4, NO3, EC and OMC at the rural Class I areas. Performance for Soil and especially CM is suspect enough that care should be taken in interpreting these modeling results. The model evaluation focused on the model's ability to predict the components of light extinction mainly at the Class I areas. Additional analysis would have to be undertaken to examine the model's ability to treat ozone and fine particulate to address 8-hour ozone and $PM_{2.5}$ attainment issues.

APPENDIX D

2018 Visibility Projections for CENRAP Class I Areas Using 2002 Typical and 2018 Base Case Base G Emission Scenario CMAQ Results and EPA Default Projection Method and Comparison with 2018 Uniform Rate of Progress (URP) Glidepaths

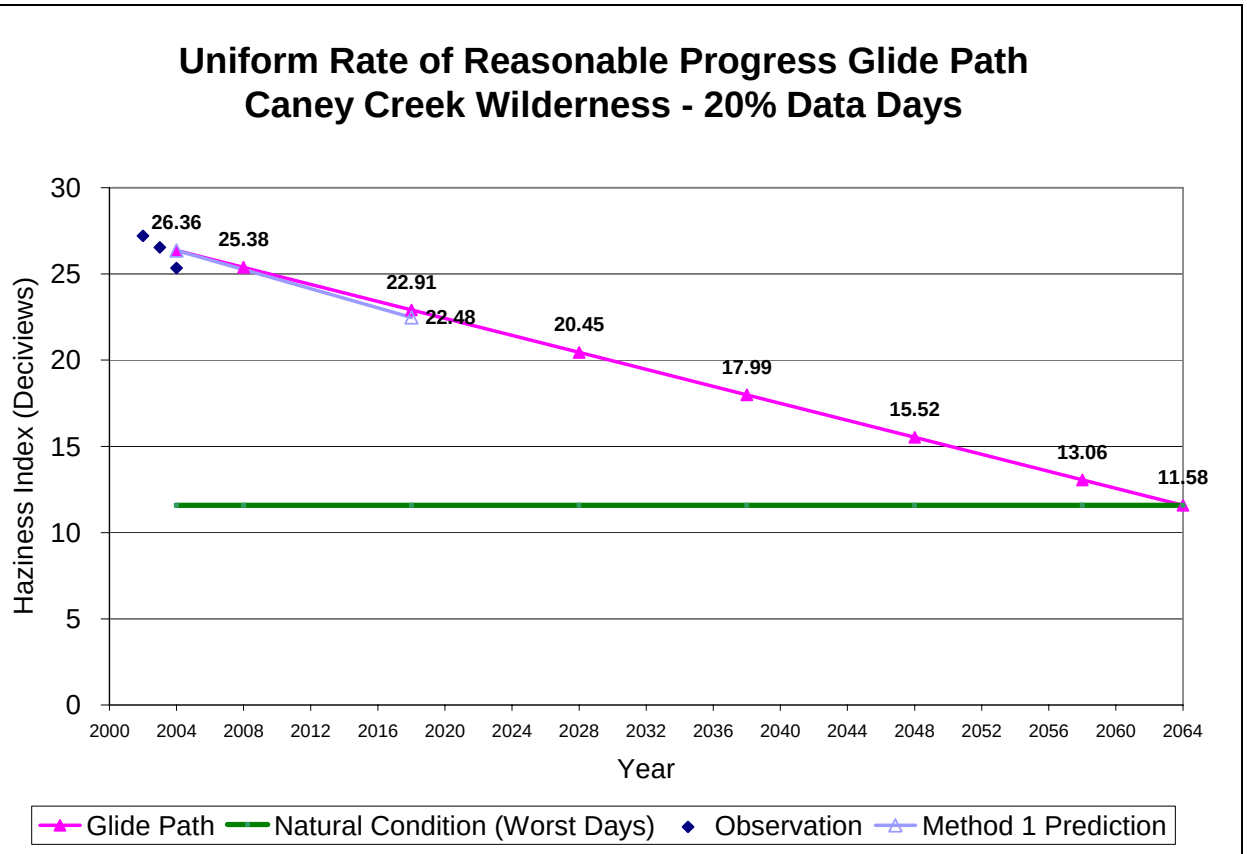

Figure D-1a. 2018 Visibility Projections and 2018 URP Glidepaths in deciview for Caney Creek (CACR), Arkansas and Worst 20% (W20%) days using 2002/2018 Base G CMAQ 36 km modeling results.

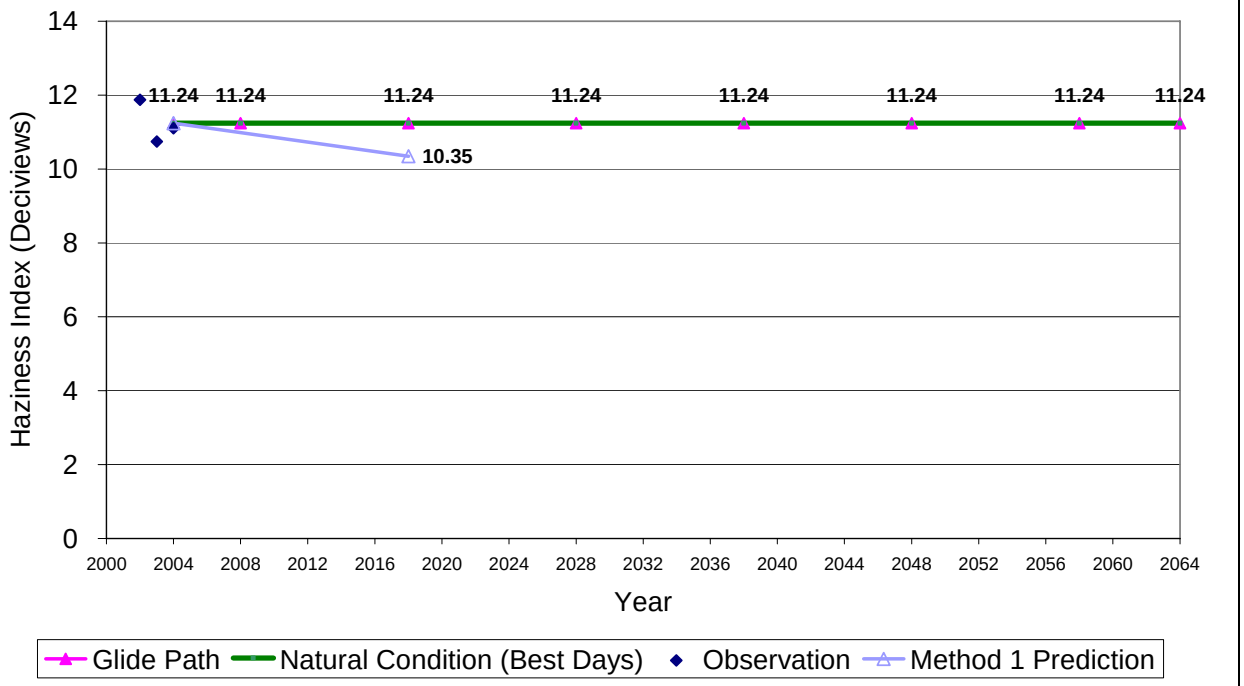

Figure D-1b. 2018 Visibility Projections and 2018 URP Glidepaths in deciview for Caney Creek (CACR), Arkansas and Best 20% (B20%) days using 2002/2018 Base G CMAQ 36 km modeling results.

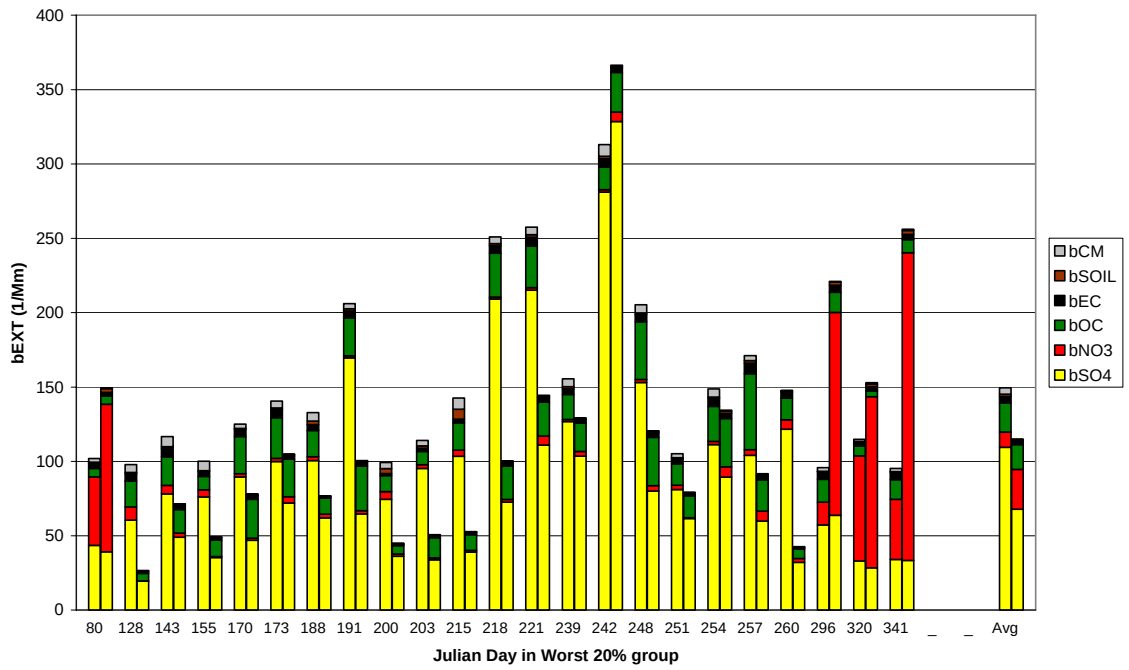

Figure D-1c. Comparison of observed (left) and 2002 Base G modeled (right) daily extinction for Caney Creek (CACR), Arkansas and Worst 20% (W20%) days in 2002.

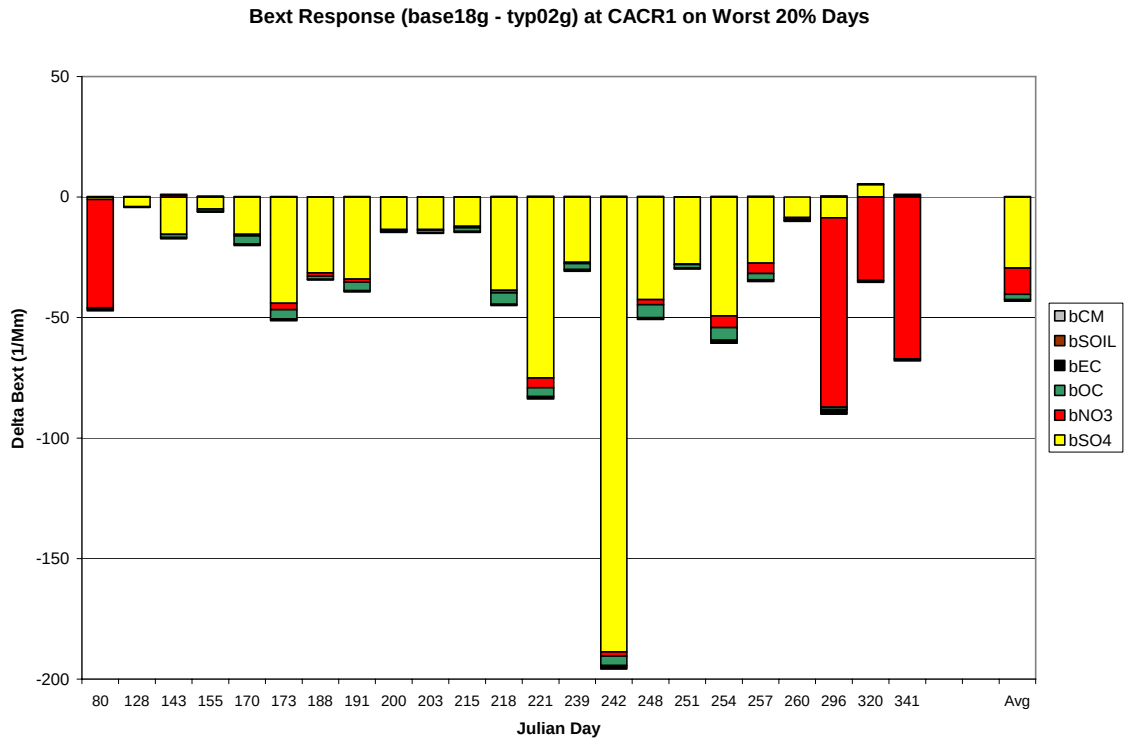

Figure D-1d. Differences in modeled 2002 and 2018 Base G CMAQ results (2018-2002) daily extinction for Caney Creek (CACR), Arkansas and Worst 20% (W20%) days in 2002.

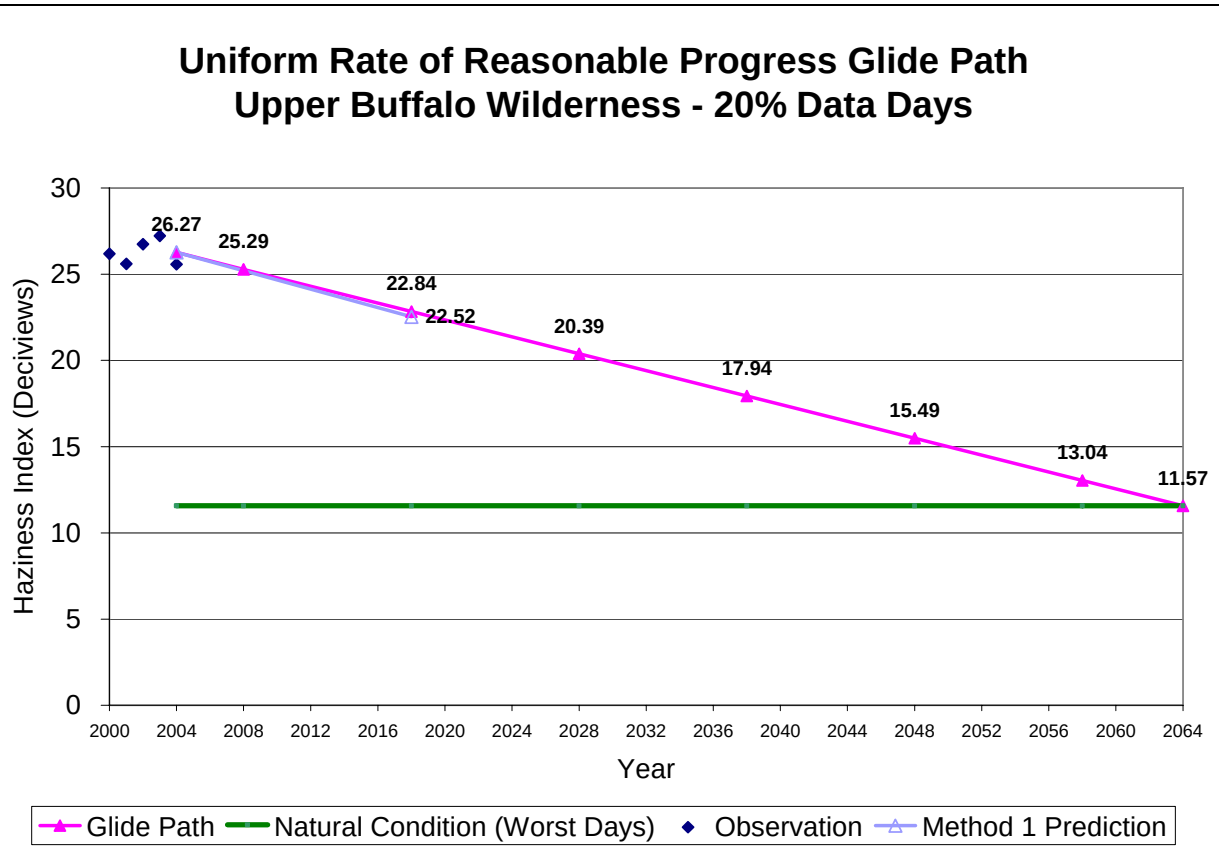

Figure D-2a. 2018 Visibility Projections and 2018 URP Glidepaths in deciview for Upper Buffalo (UPBU), Arkansas and Worst 20% (W20%) days using 2002/2018 Base G CMAQ 36 km modeling results.

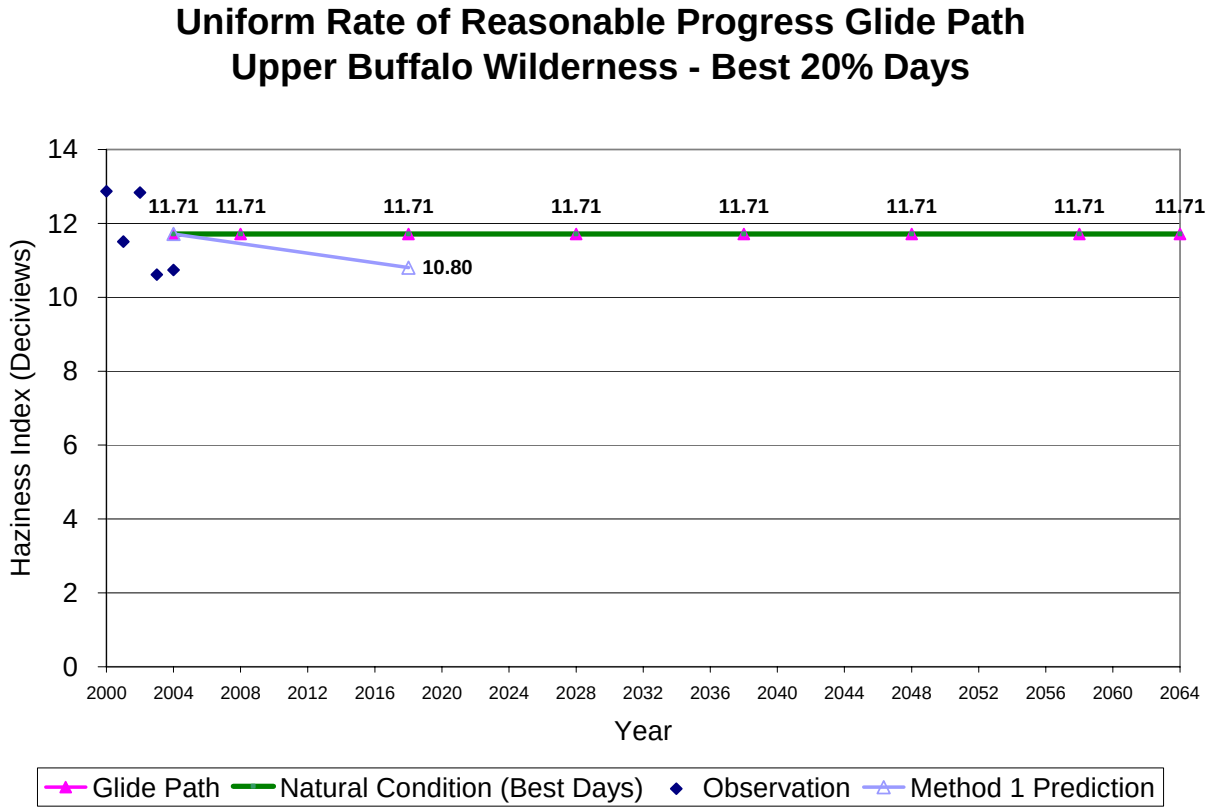

Figure D-2b. 2018 Visibility Projections and 2018 URP Glidepaths in deciview for Upper Buffalo (UPBU), Arkansas and Best 20% (B20%) days using 2002/2018 Base G CMAQ 36 km modeling results.

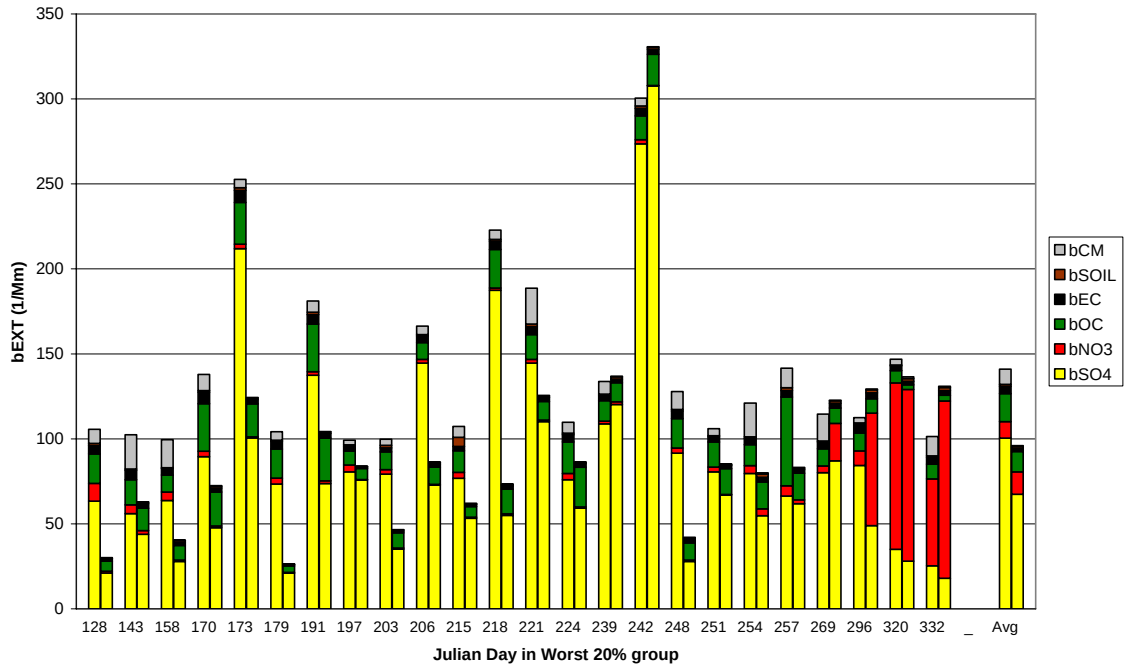

Figure D-2c. Comparison of observed (left) and 2002 Base G modeled (right) daily extinction for Upper Buffalo (UPBU), Arkansas and Worst 20% (W20%) days in 2002.

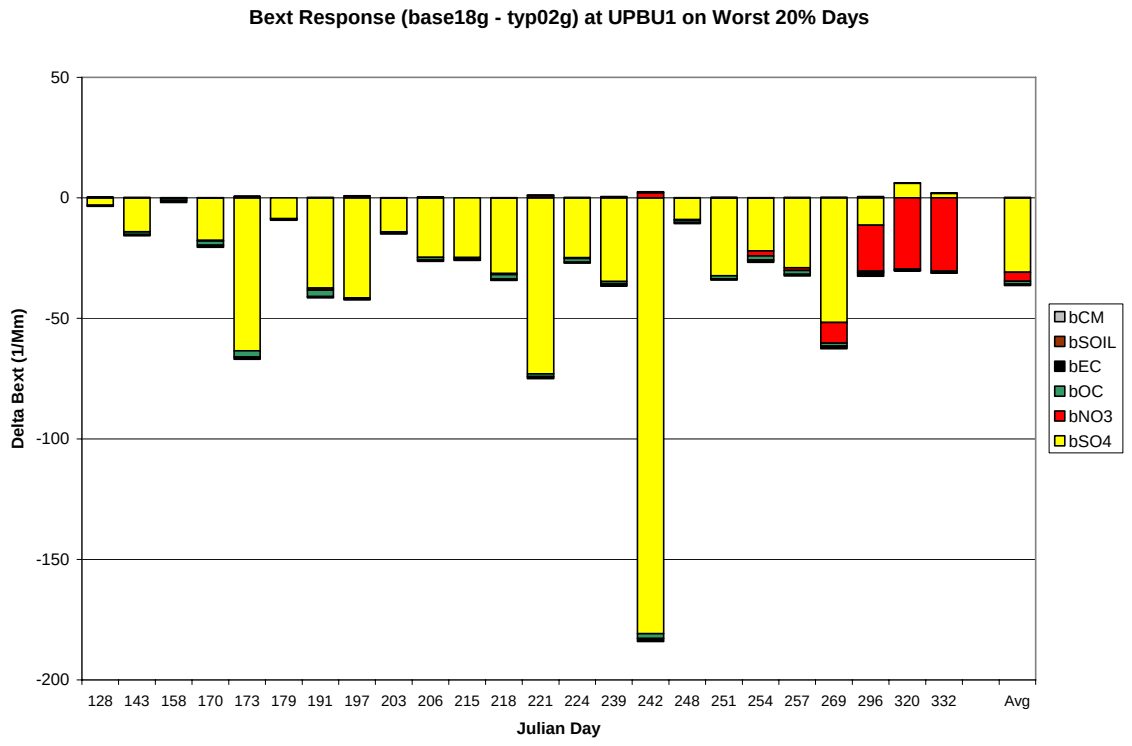

Figure D-2d. Differences in modeled 2002 and 2018 Base G CMAQ results (2018-2002) daily extinction for Upper Buffalo (UPBU), Arkansas and Worst 20% (W20%) days in 2002.

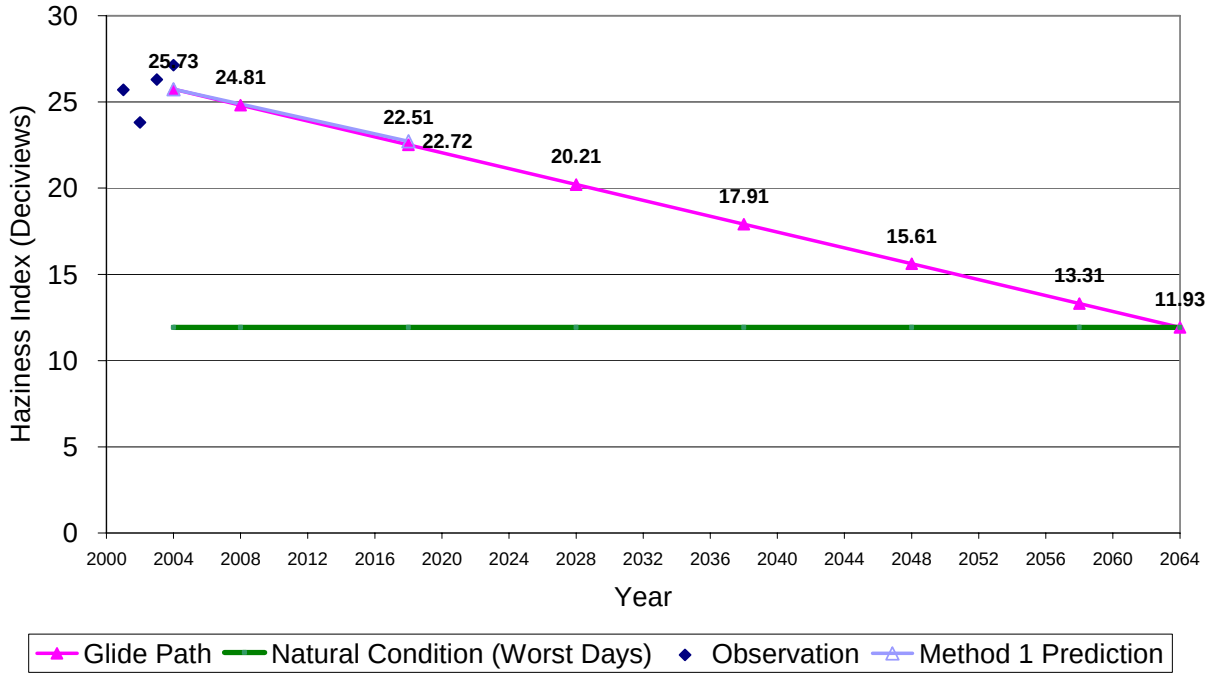

Figure D-3a. 2018 Visibility Projections and 2018 URP Glidepaths in deciview for Breton Island (BRET), Louisiana and Worst 20% (W20%) days using 2002/2018 Base G CMAQ 36 km modeling results.

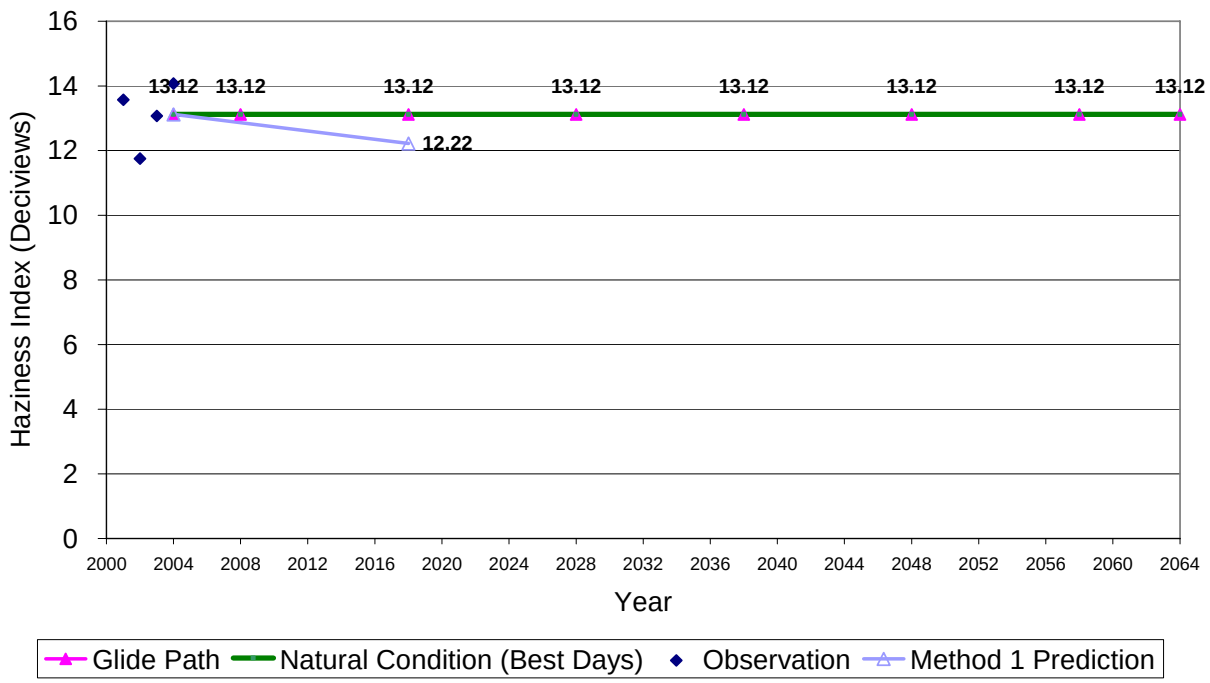

Figure D-3b. 2018 Visibility Projections and 2018 URP Glidepaths in deciview for Breton Island (BRET), Louisiana and Best 20% (B20%) days using 2002/2018 Base G CMAQ 36 km modeling results.

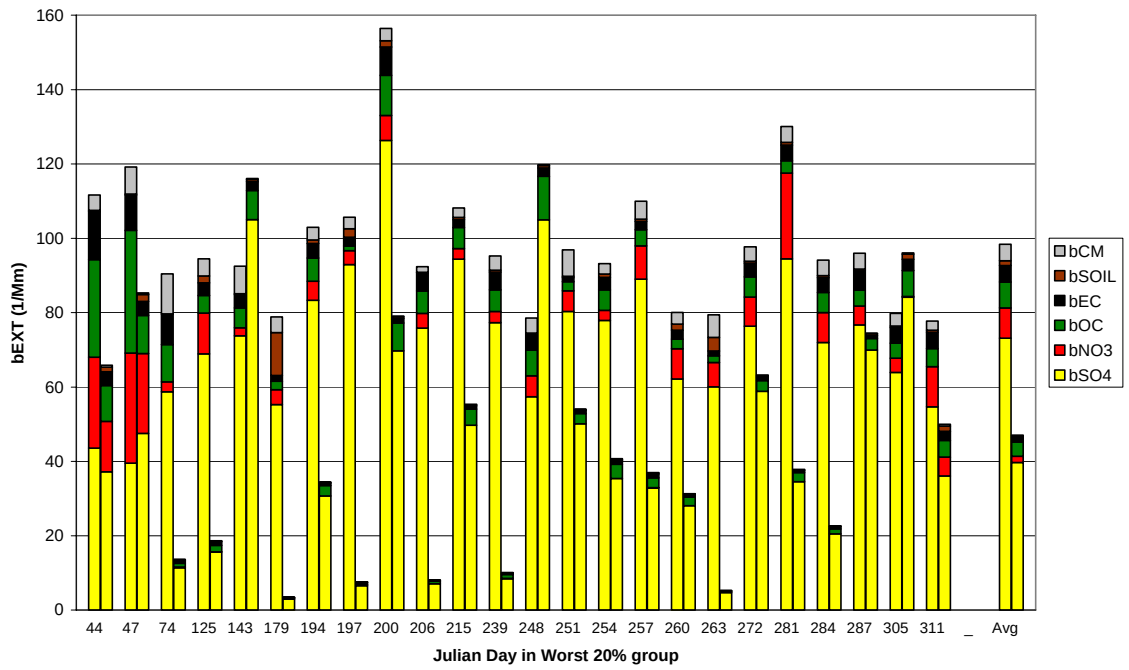

Figure D-3c. Comparison of observed (left) and 2002 Base G modeled (right) daily extinction for Breton Island (BRET), Louisiana and Worst 20% (W20%) days in 2002.

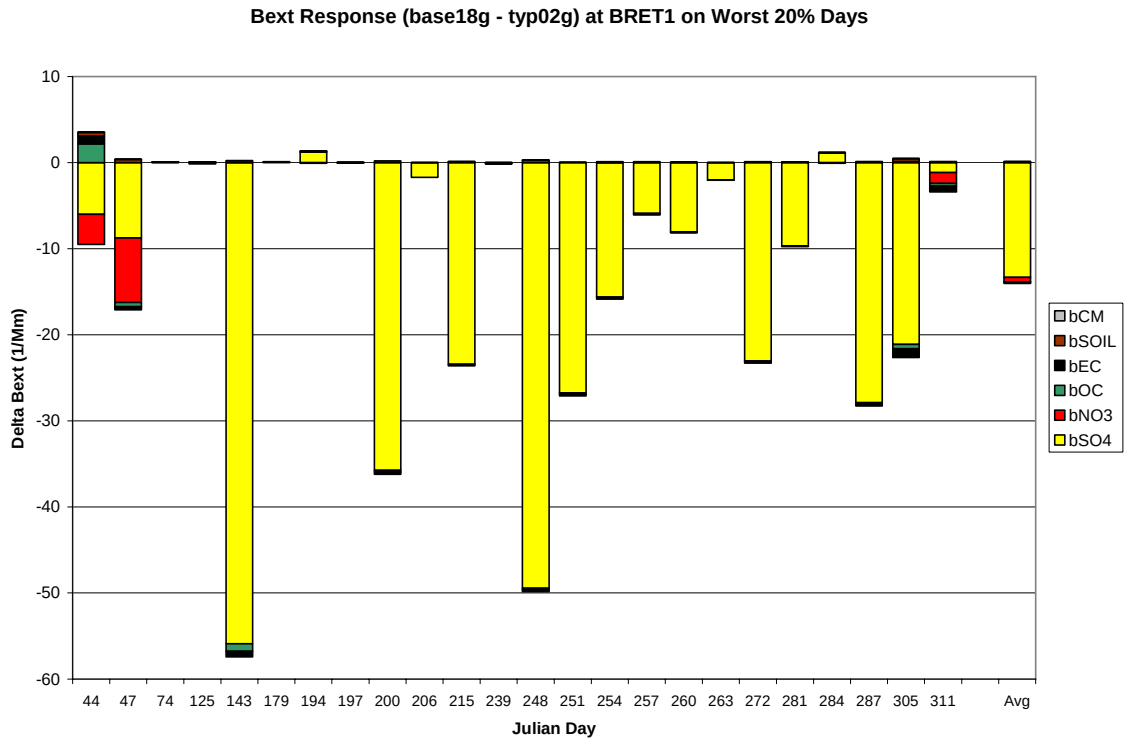

Figure D-3d. Differences in modeled 2002 and 2018 Base G CMAQ results (2018-2002) daily extinction for Breton Island (BRET), Louisiana and Worst 20% (W20%) days in 2002.

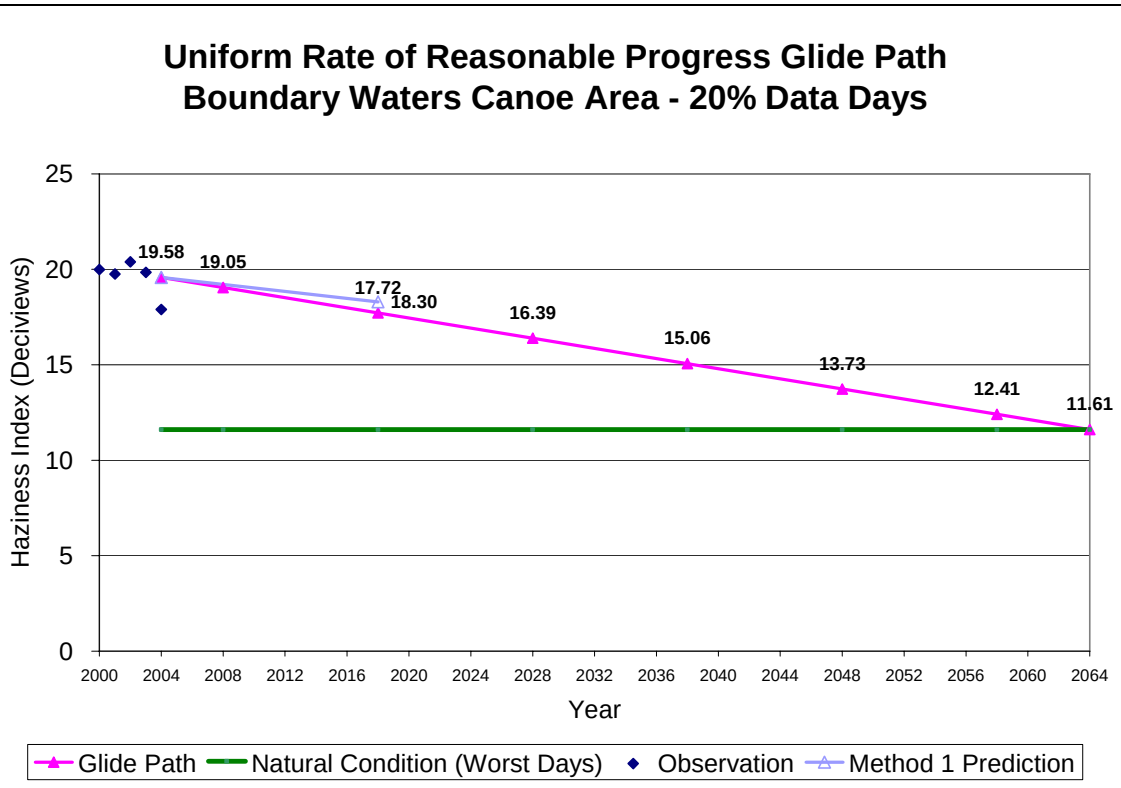

Figure D-4a. 2018 Visibility Projections and 2018 URP Glidepaths in deciview for Boundary Waters (BOWA), Minnesota and Worst 20% (W20%) days using 2002/2018 Base G CMAQ 36 km modeling results.

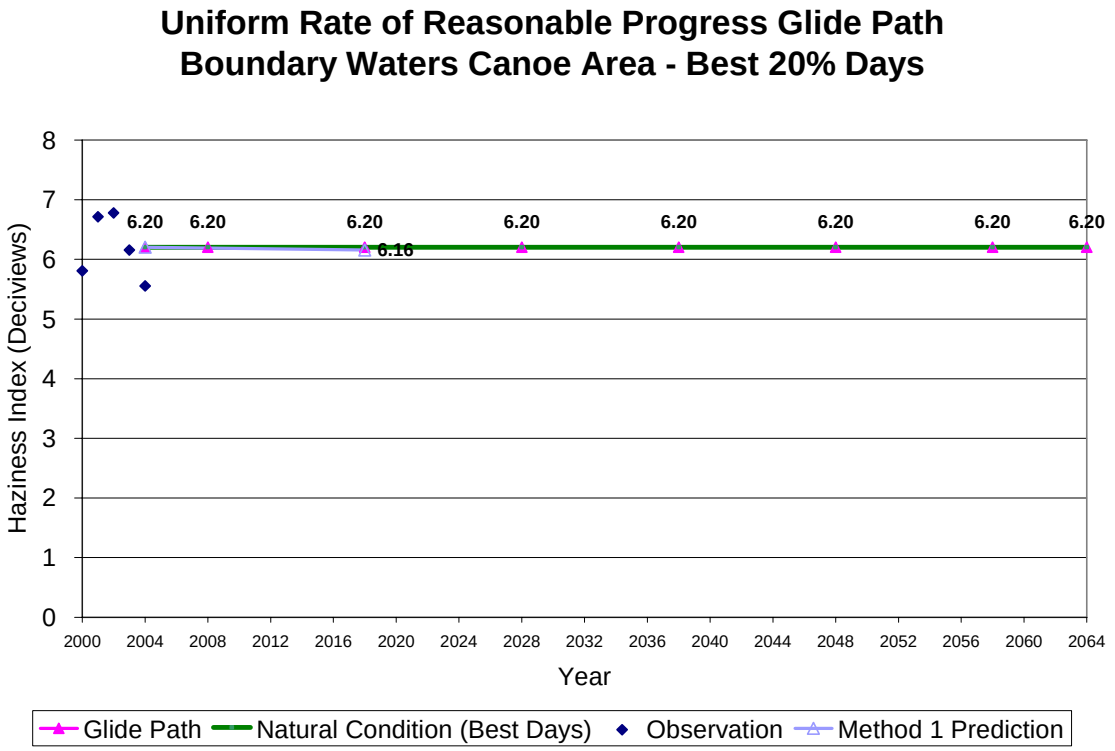

Figure D-4b. 2018 Visibility Projections and 2018 URP Glidepaths in deciview for Boundary Waters (BOWA), Minnesota and Best 20% (B20%) days using 2002/2018 Base G CMAQ 36 km modeling results.

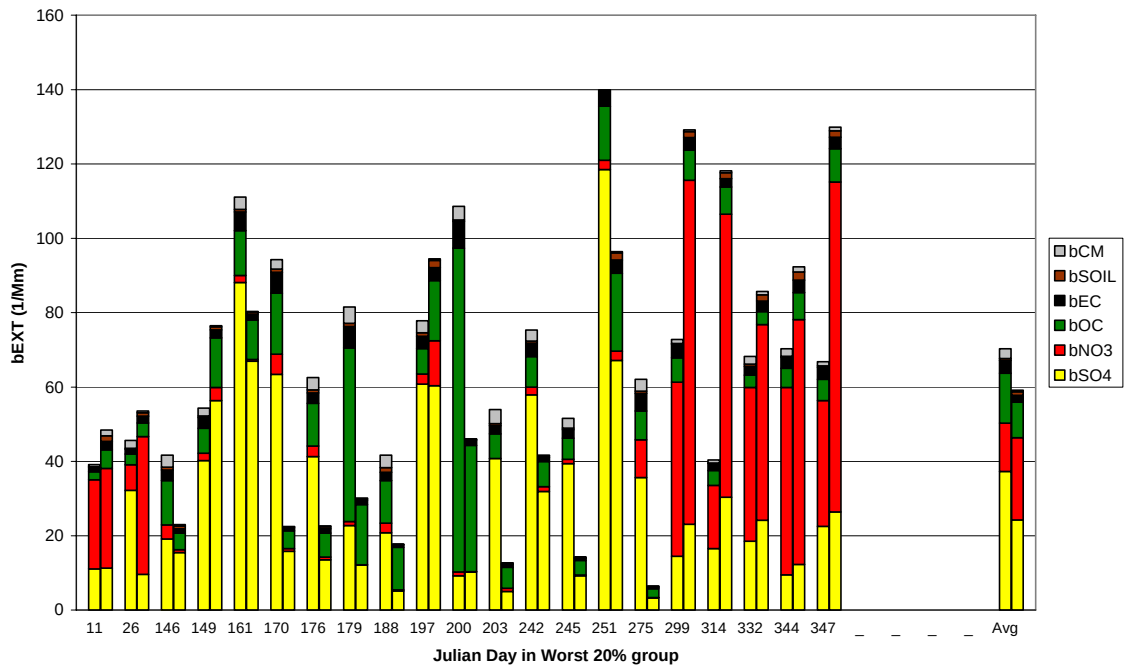

Figure D-4c. Comparison of observed (left) and 2002 Base G modeled (right) daily extinction for Boundary Waters (BOWA), Minnesota and Worst 20% (W20%) days in 2002.

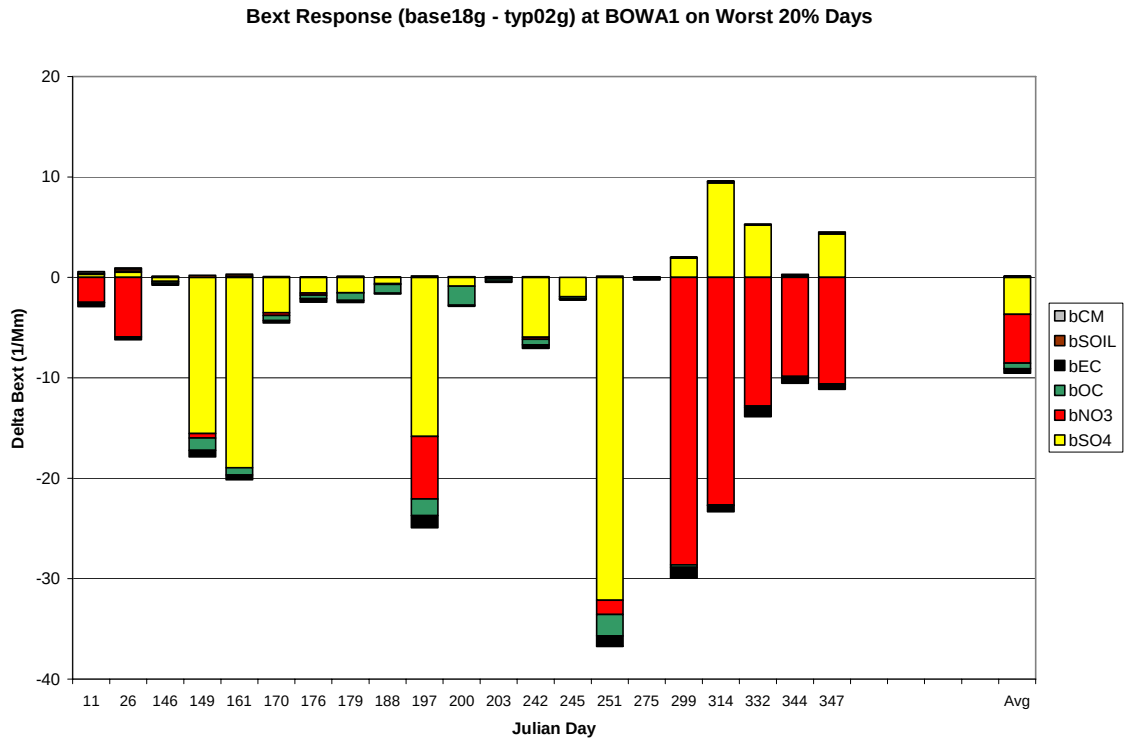

Figure D-4d. Differences in modeled 2002 and 2018 Base G CMAQ results (2018-2002) daily extinction for Boundary Waters (BOWA), Minnesota and Worst 20% (W20%) days in 2002.

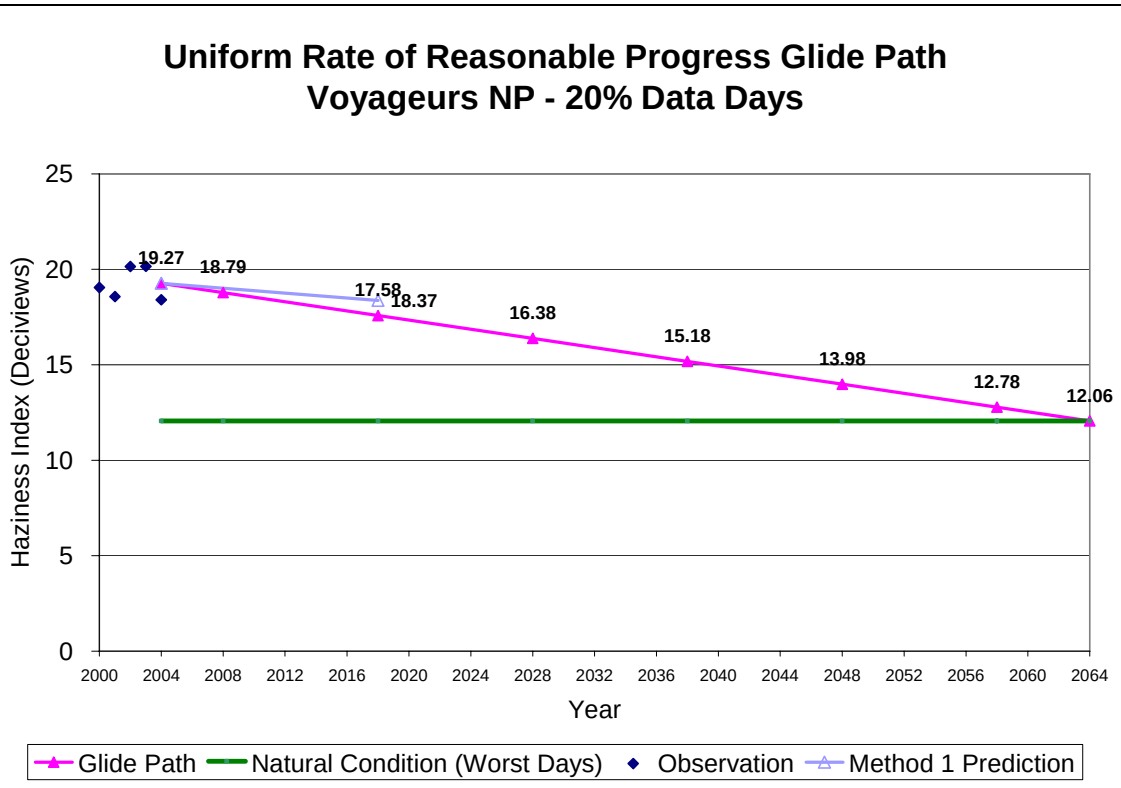

Figure D-5a. 2018 Visibility Projections and 2018 URP Glidepaths in deciview for Voyageurs (VOYA), Minnesota and Worst 20% (W20%) days using 2002/2018 Base G CMAQ 36 km modeling results.

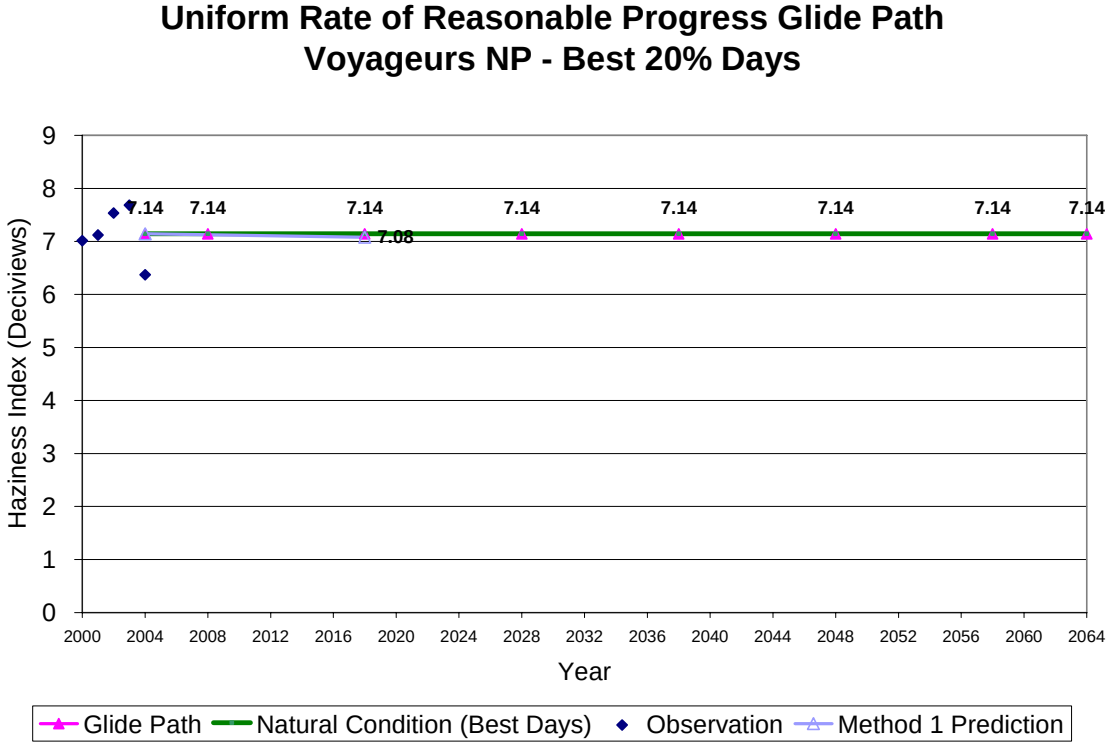

Figure D-5b. 2018 Visibility Projections and 2018 URP Glidepaths in deciview for Voyageurs (VOYA), Minnesota and Best 20% (B20%) days using 2002/2018 Base G CMAQ 36 km modeling results.

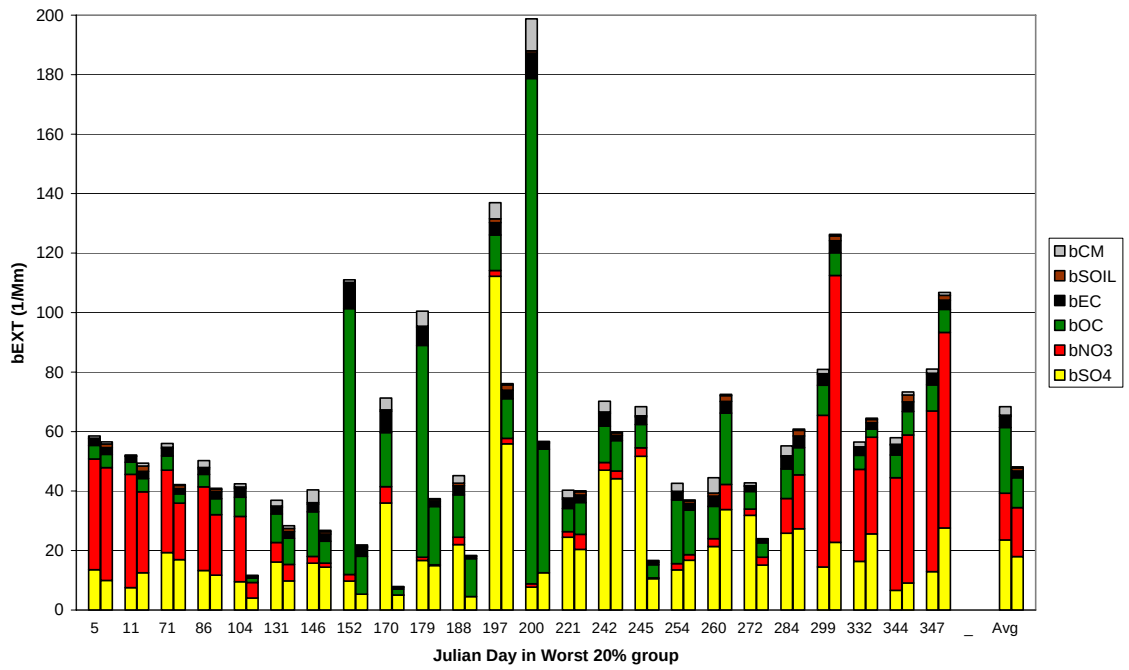

Figure D-5c. Comparison of observed (left) and 2002 Base G modeled (right) daily extinction for Voyageurs (VOYA), Minnesota and Worst 20% (W20%) days in 2002.

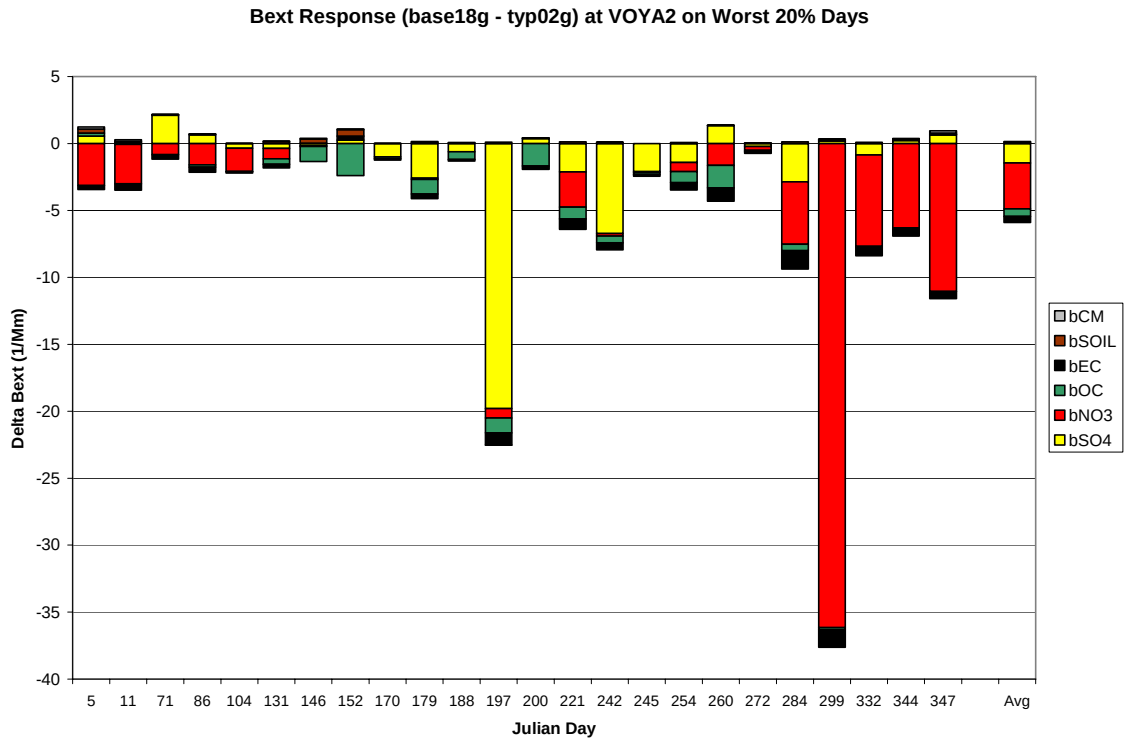

Figure D-5d. Differences in modeled 2002 and 2018 Base G CMAQ results (2018-2002) daily extinction for Voyageurs (VOYA), Minnesota and Worst 20% (W20%) days in 2002.

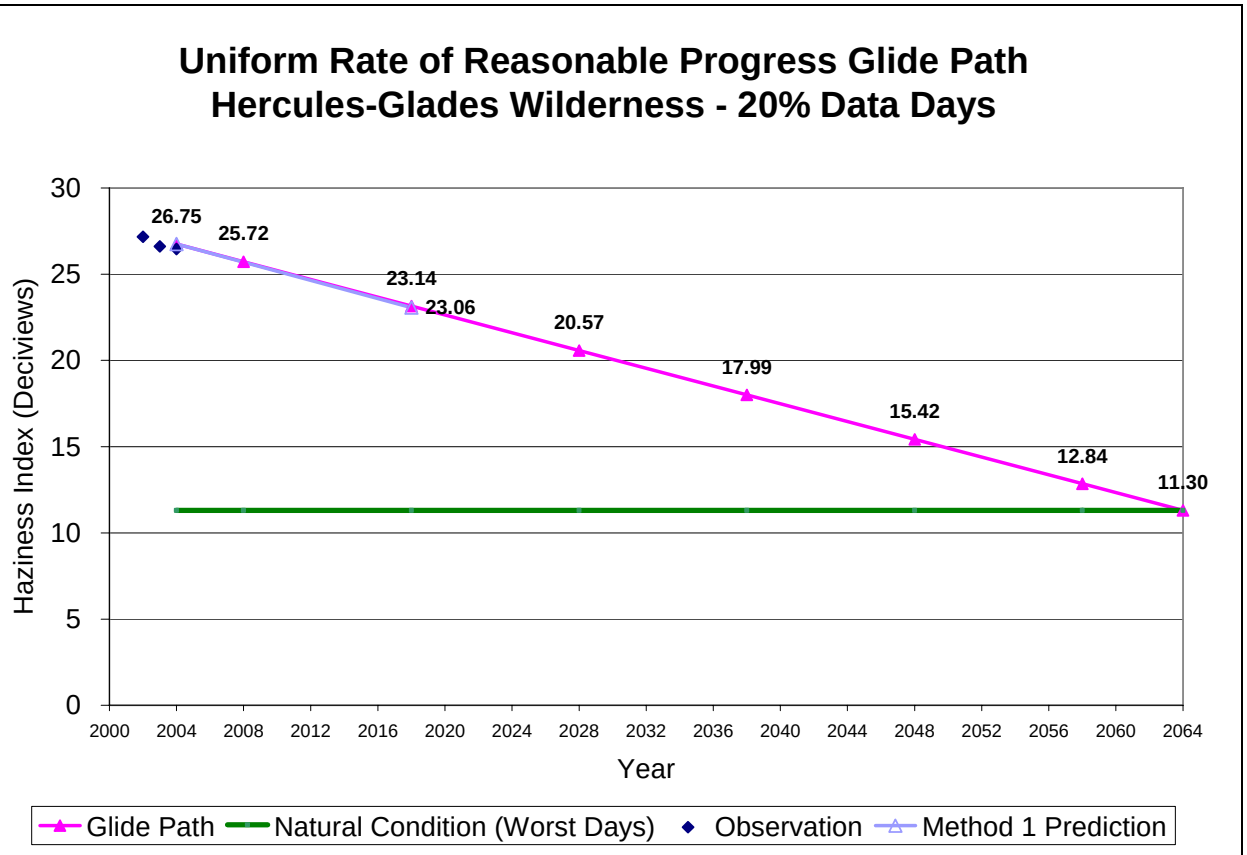

Figure D-6a. 2018 Visibility Projections and 2018 URP Glidepaths in deciview for Hercules-Glade (HEGL), Missouri and Worst 20% (W20%) days using 2002/2018 Base G CMAQ 36 km modeling results.

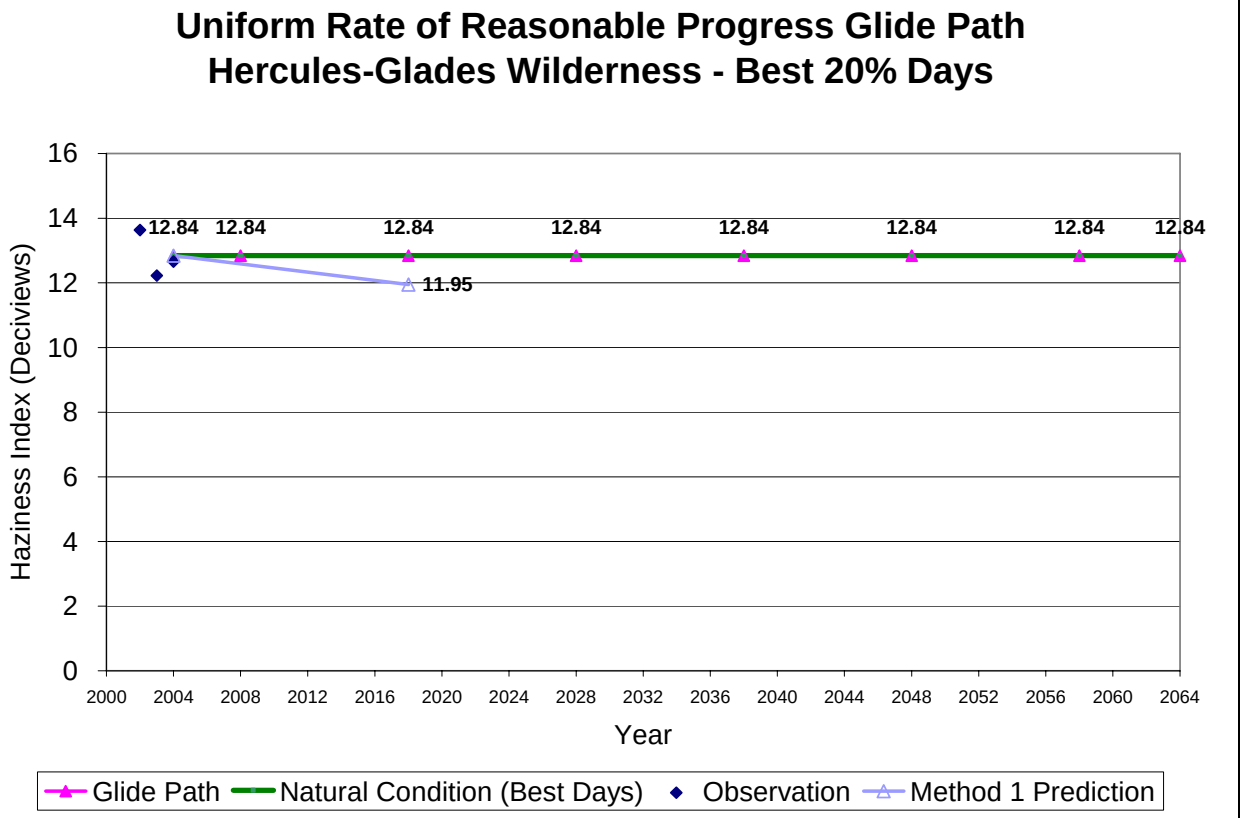

Figure D-6b. 2018 Visibility Projections and 2018 URP Glidepaths in deciview for Hercules-Glade (HEGL), Missouri and Best 20% (B20%) days using 2002/2018 Base G CMAQ 36 km modeling results.

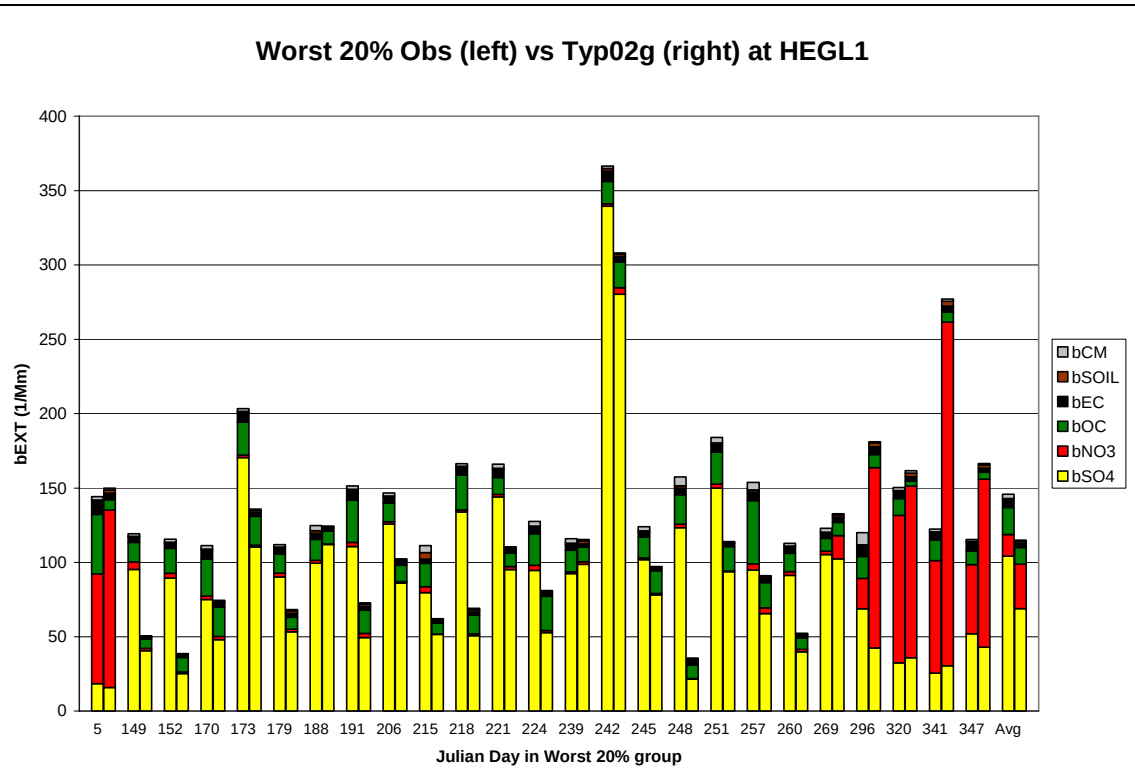

Figure D-6c. Comparison of observed (left) and 2002 Base G modeled (right) daily extinction for Hercules-Glade (HEGL), Missouri and Worst 20% (W20%) days in 2002.

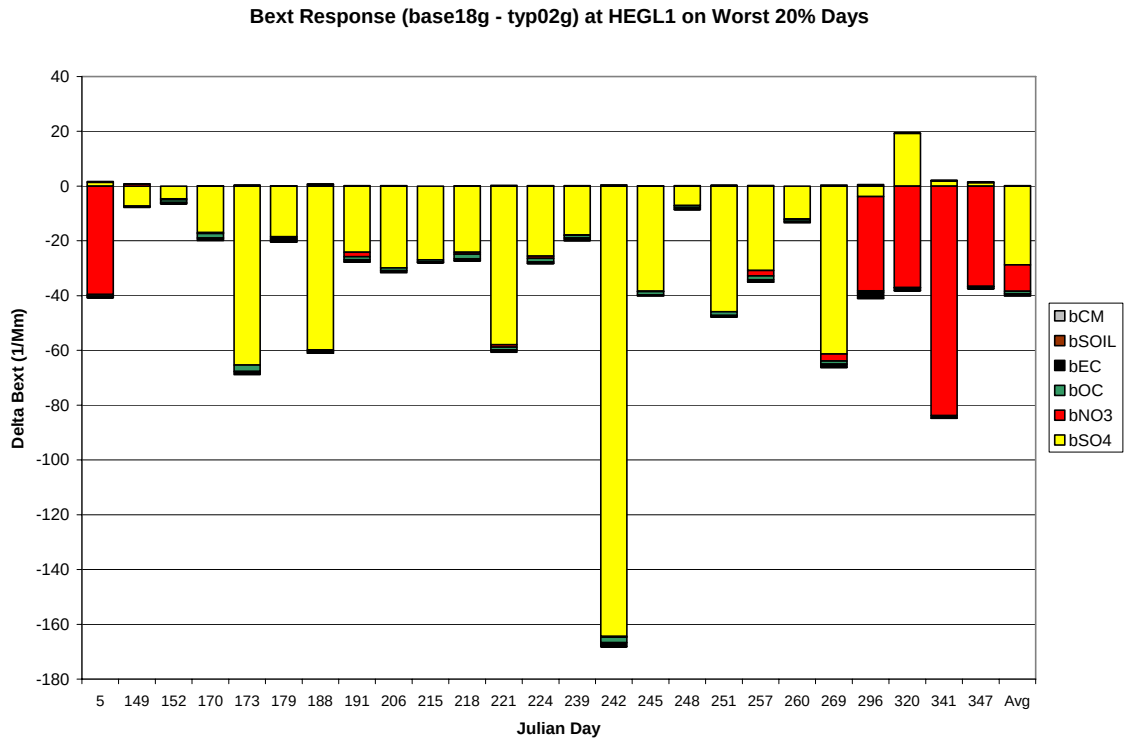

Figure D-6d. Differences in modeled 2002 and 2018 Base G CMAQ results (2018-2002) daily extinction for Hercules-Glade (HEGL), Missouri and Worst 20% (W20%) days in 2002.

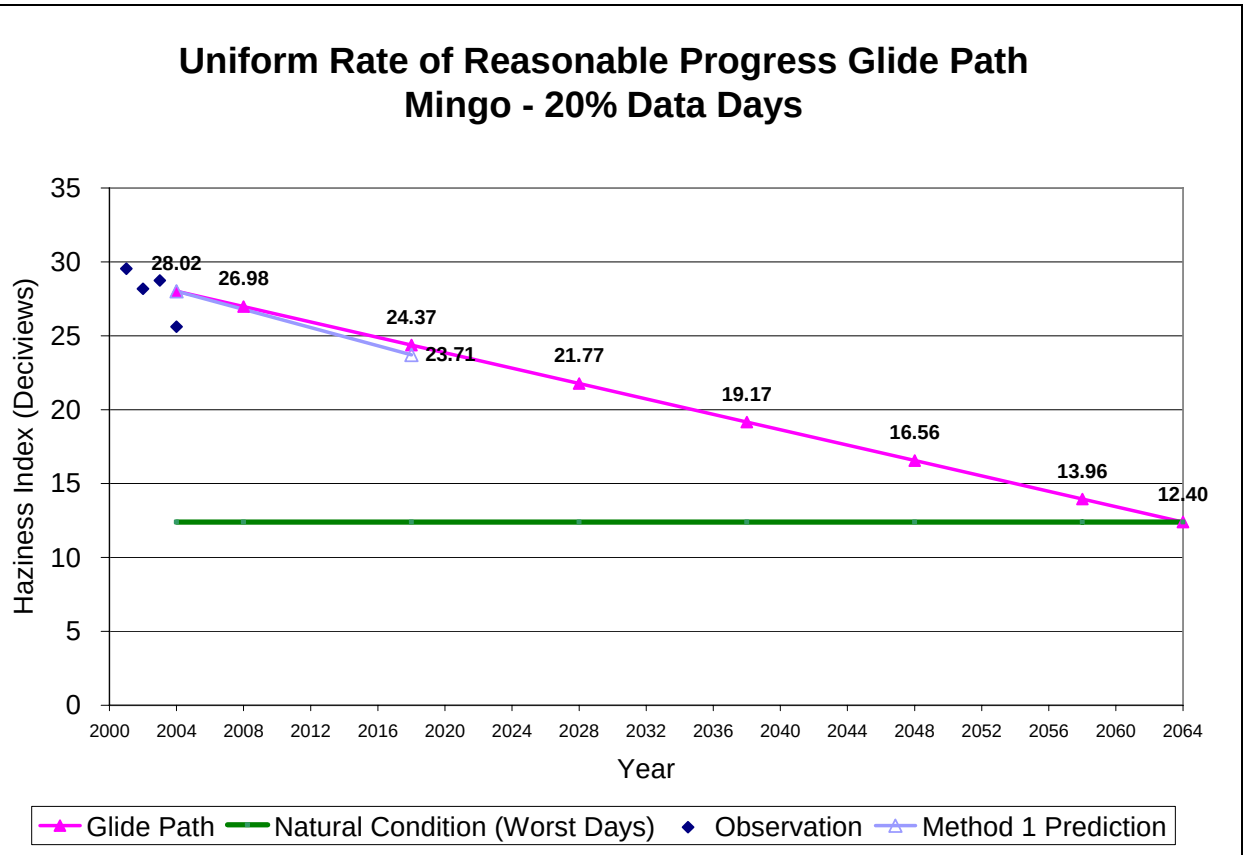

Figure D-7a. 2018 Visibility Projections and 2018 URP Glidepaths in deciview for Mingo (MING), Missouri and Worst 20% (W20%) days using 2002/2018 Base G CMAQ 36 km modeling results.

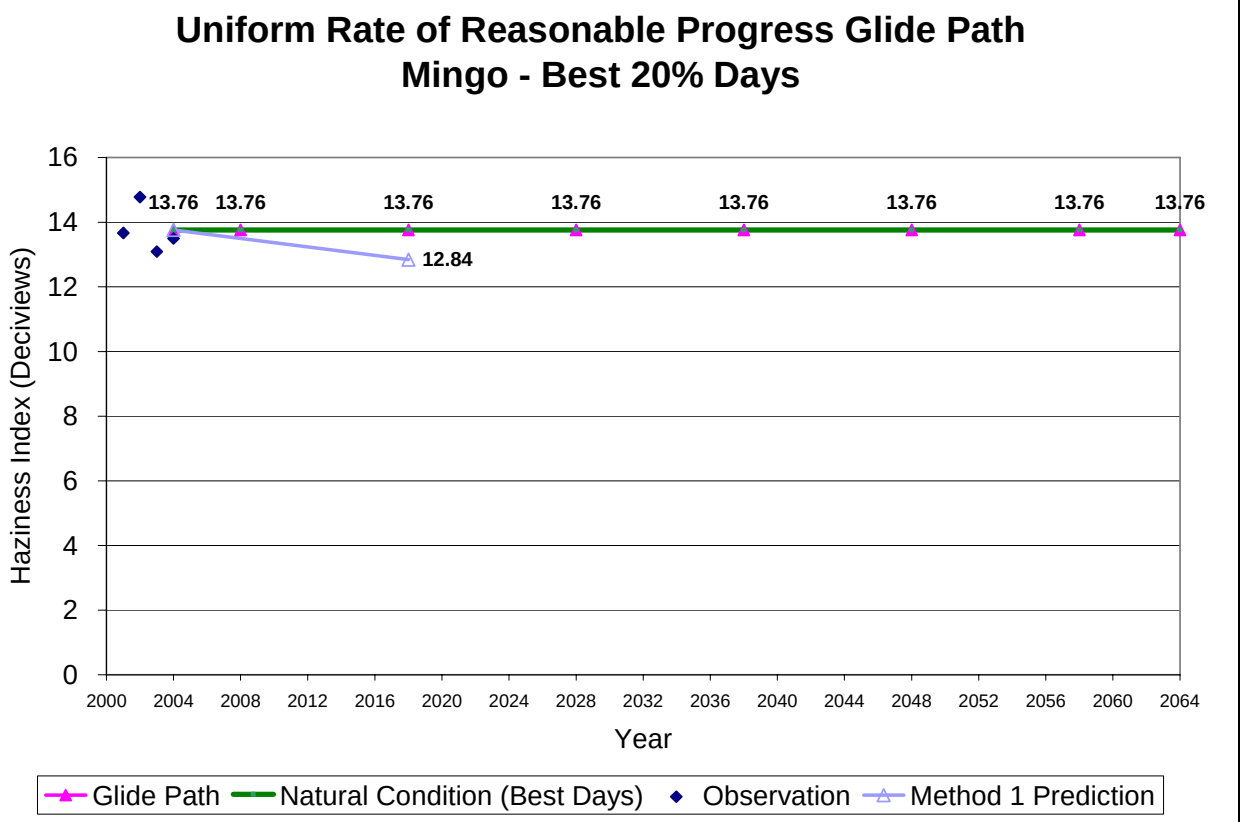

Figure D-7b. 2018 Visibility Projections and 2018 URP Glidepaths in deciview for Mingo (MING), Missouri and Best 20% (B20%) days using 2002/2018 Base G CMAQ 36 km modeling results.

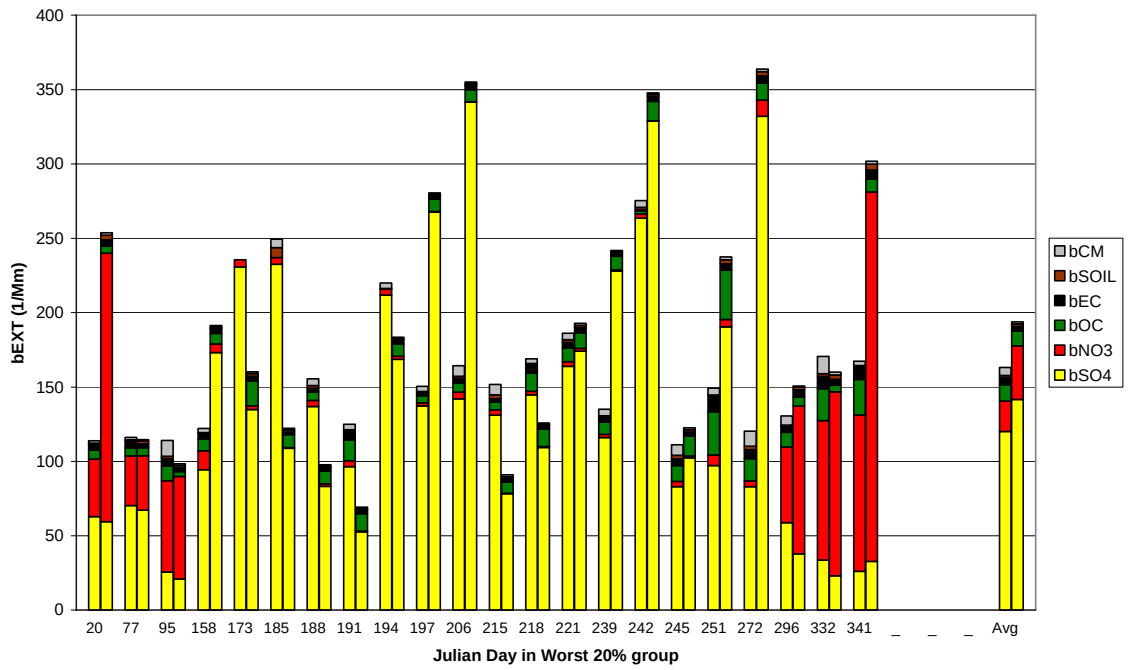

Figure D-7c. Comparison of observed (left) and 2002 Base G modeled (right) daily extinction for Mingo (MING), Missouri and Worst 20% (W20%) days in 2002.

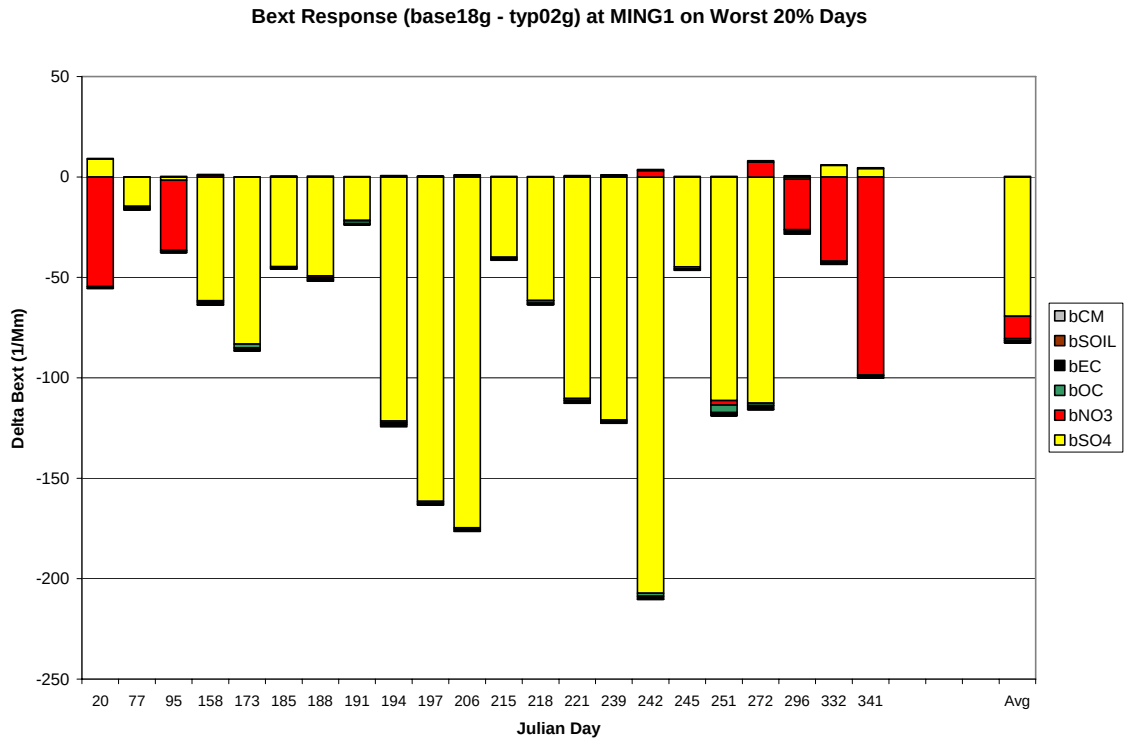

Figure D-7d. Differences in modeled 2002 and 2018 Base G CMAQ results (2018-2002) daily extinction for Mingo (MING), Missouri and Worst 20% (W20%) days in 2002.

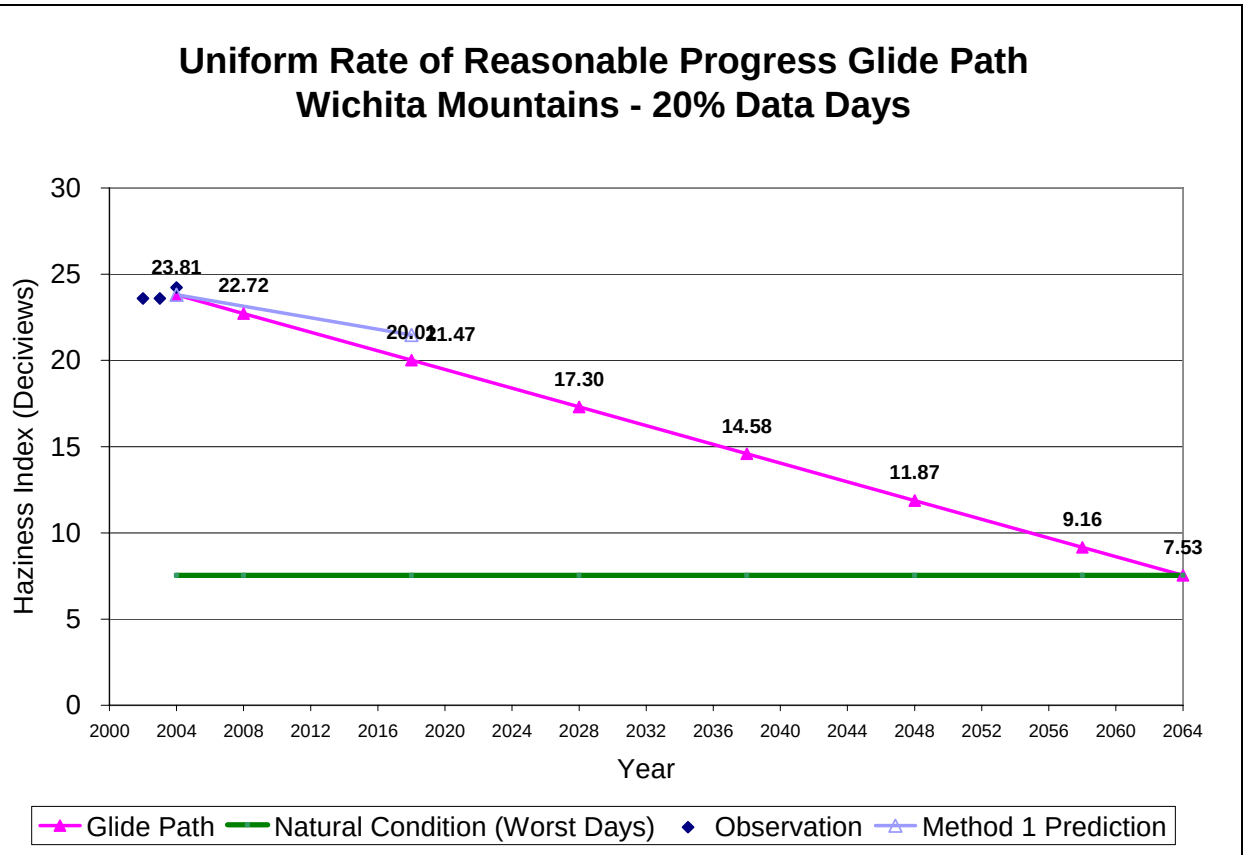

Figure D-8a. 2018 Visibility Projections and 2018 URP Glidepaths in deciview for Wichita Mountains (WIMO), Oklahoma and Worst 20% (W20%) days using 2002/2018 Base G CMAQ 36 km modeling results.

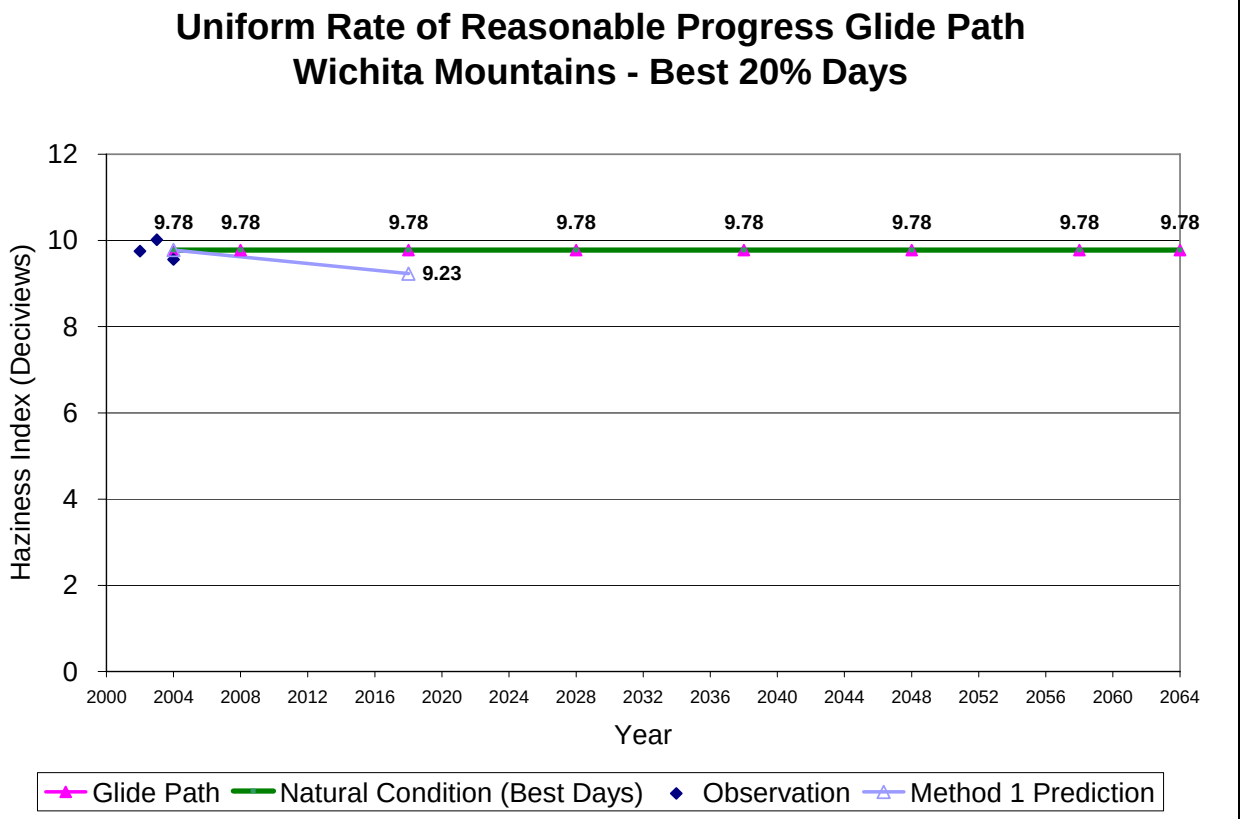

Figure D-8b. 2018 Visibility Projections and 2018 URP Glidepaths in deciview for Wichita Mountains (WIMO), Oklahoma and Best 20% (B20%) days using 2002/2018 Base G CMAQ 36 km modeling results.

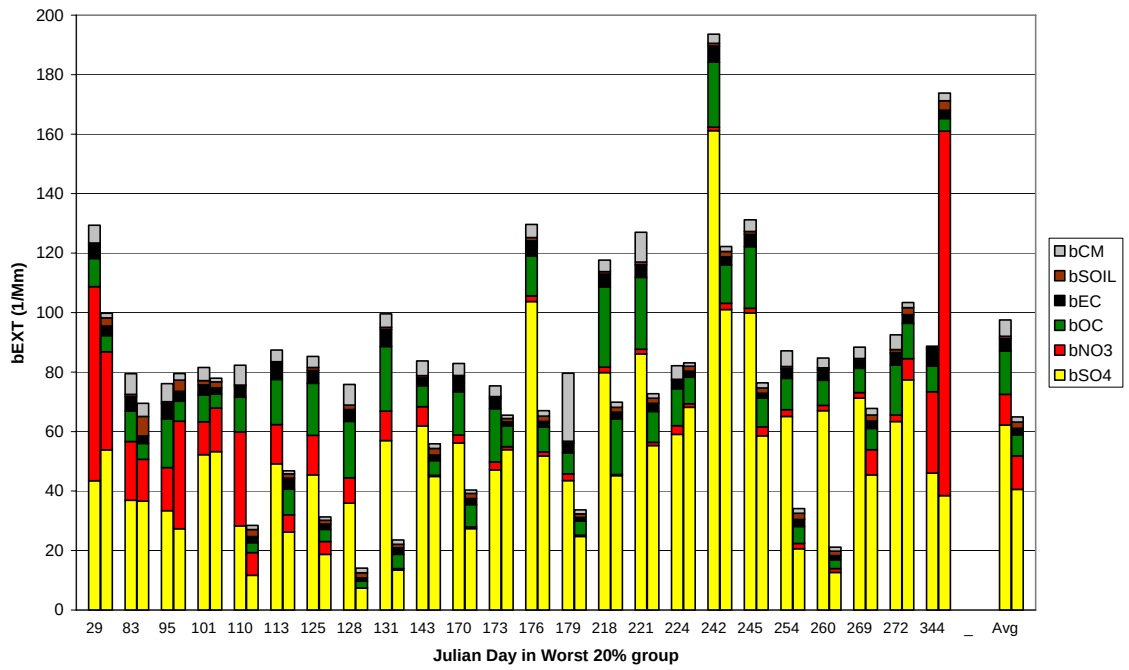

Figure D-8c. Comparison of observed (left) and 2002 Base G modeled (right) daily extinction for Wichita Mountains (WIMO), Oklahoma and Worst 20% (W20%) days in 2002.

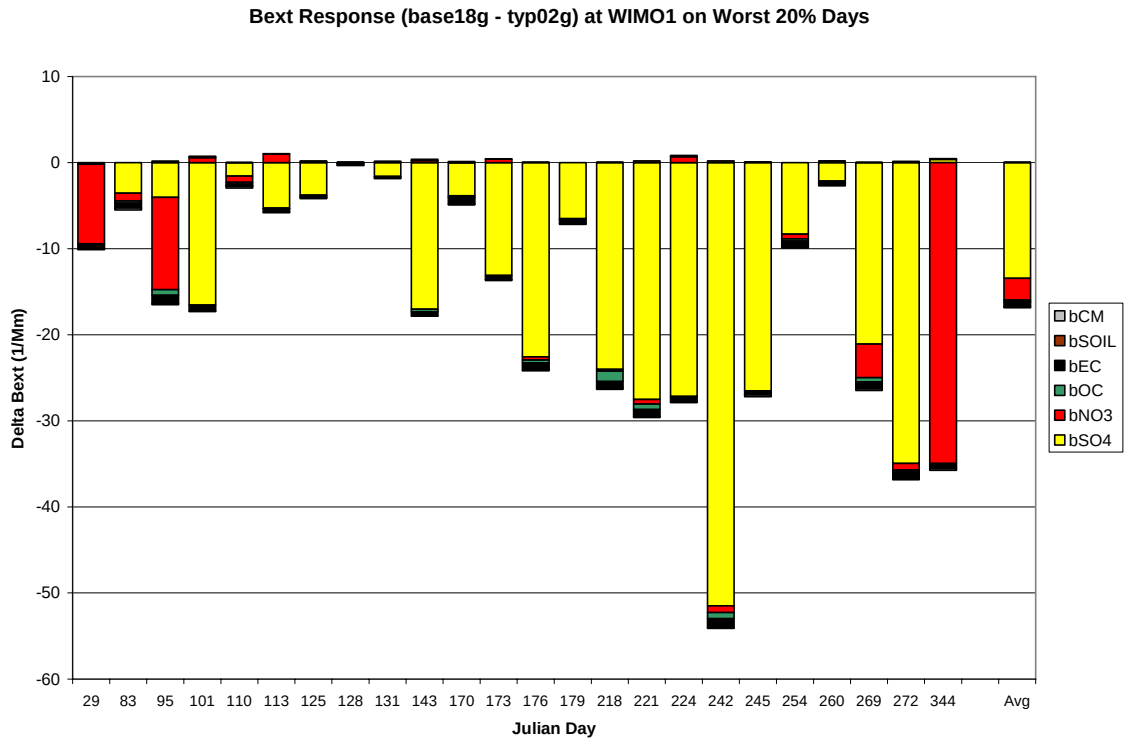

Figure D-8d. Differences in modeled 2002 and 2018 Base G CMAQ results (2018-2002) daily extinction for Wichita Mountains (WIMO), Oklahoma and Worst 20% (W20%) days in 2002.

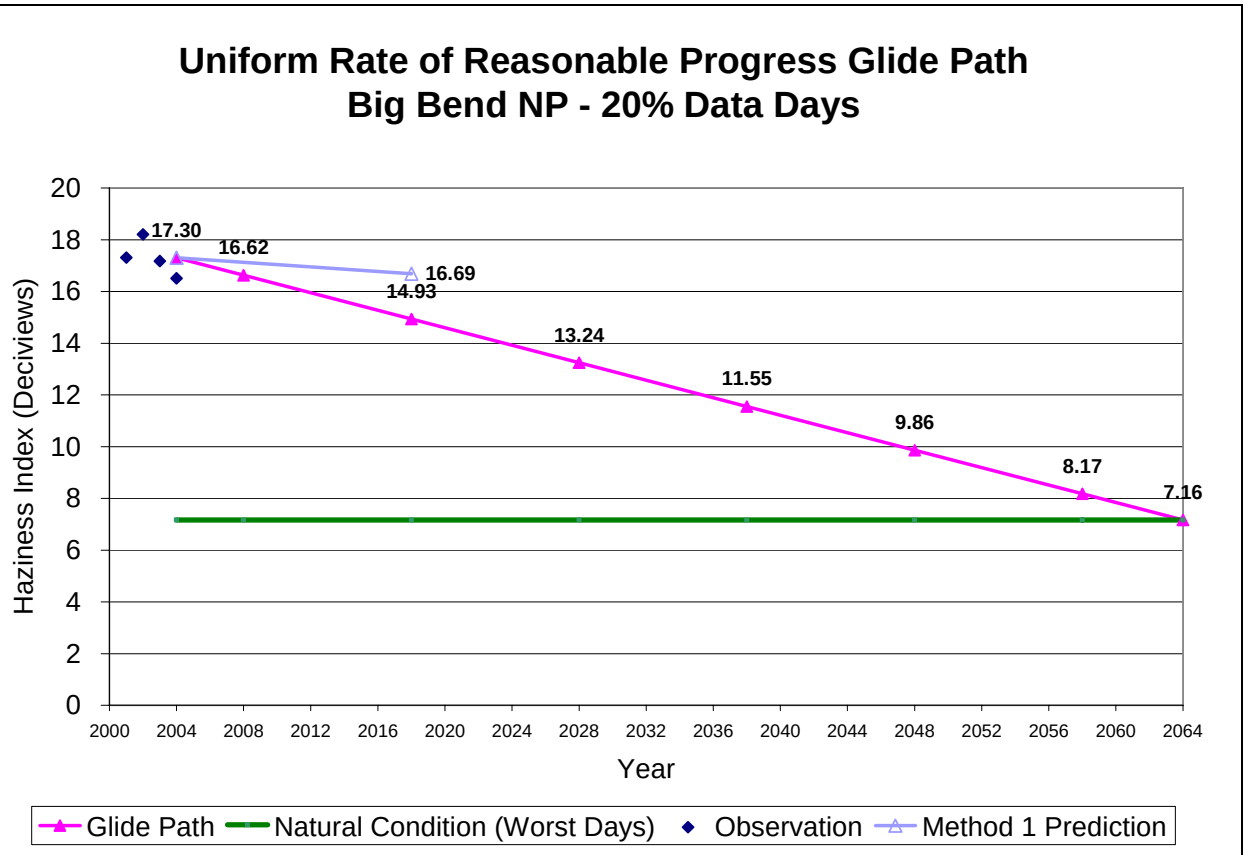

Figure D-9a. 2018 Visibility Projections and 2018 URP Glidepaths in deciview for Big Bend (BIBE), Texas and Worst 20% (W20%) days using 2002/2018 Base G CMAQ 36 km modeling results.

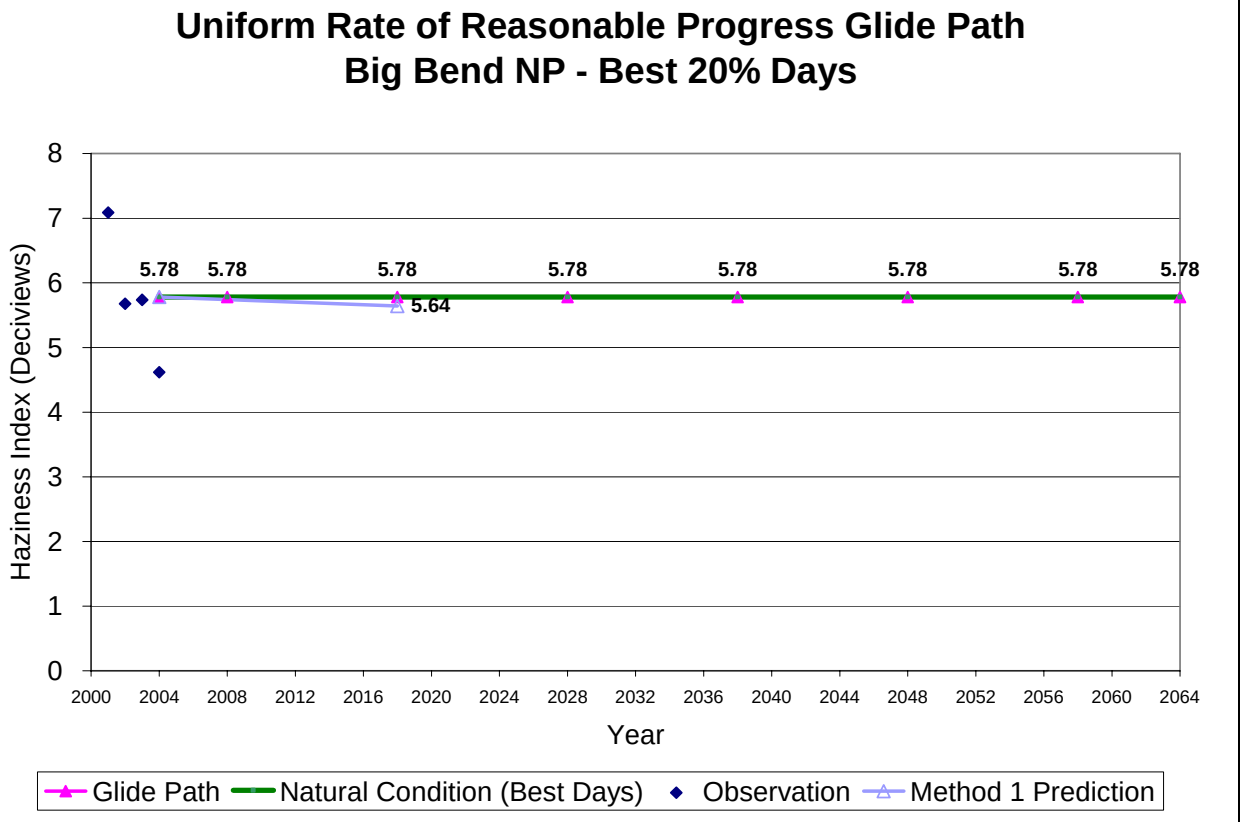

Figure D-9b. 2018 Visibility Projections and 2018 URP Glidepaths in deciview for Big Bend (BIBE), Texas and Best 20% (B20%) days using 2002/2018 Base G CMAQ 36 km modeling results.

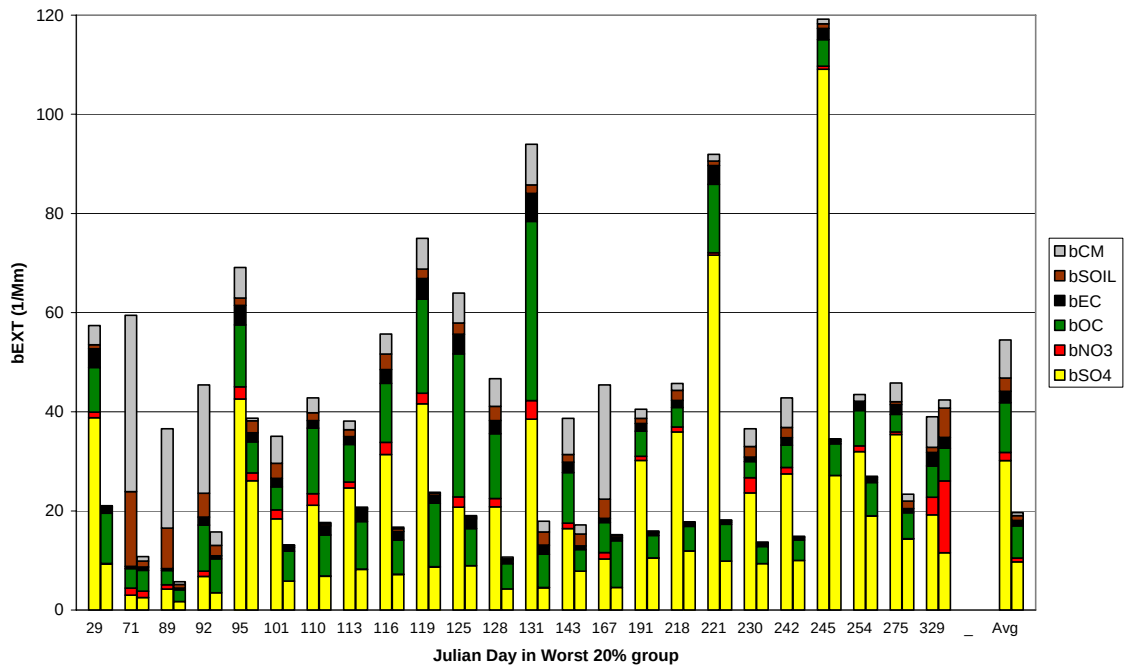

Figure D-9c. Comparison of observed (left) and 2002 Base G modeled (right) daily extinction for Big Bend (BIBE), Texas and Worst 20% (W20%) days in 2002.

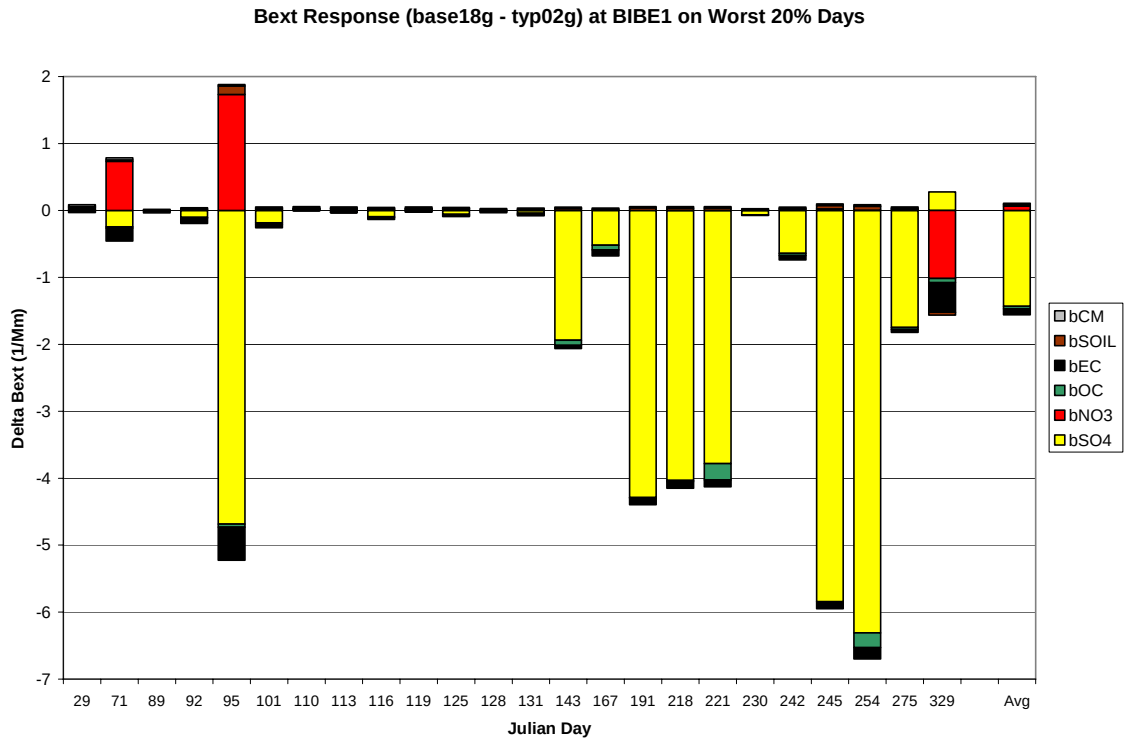

Figure D-9d. Differences in modeled 2002 and 2018 Base G CMAQ results (2018-2002) daily extinction for Big Bend (BIBE), Texas and Worst 20% (W20%) days in 2002.

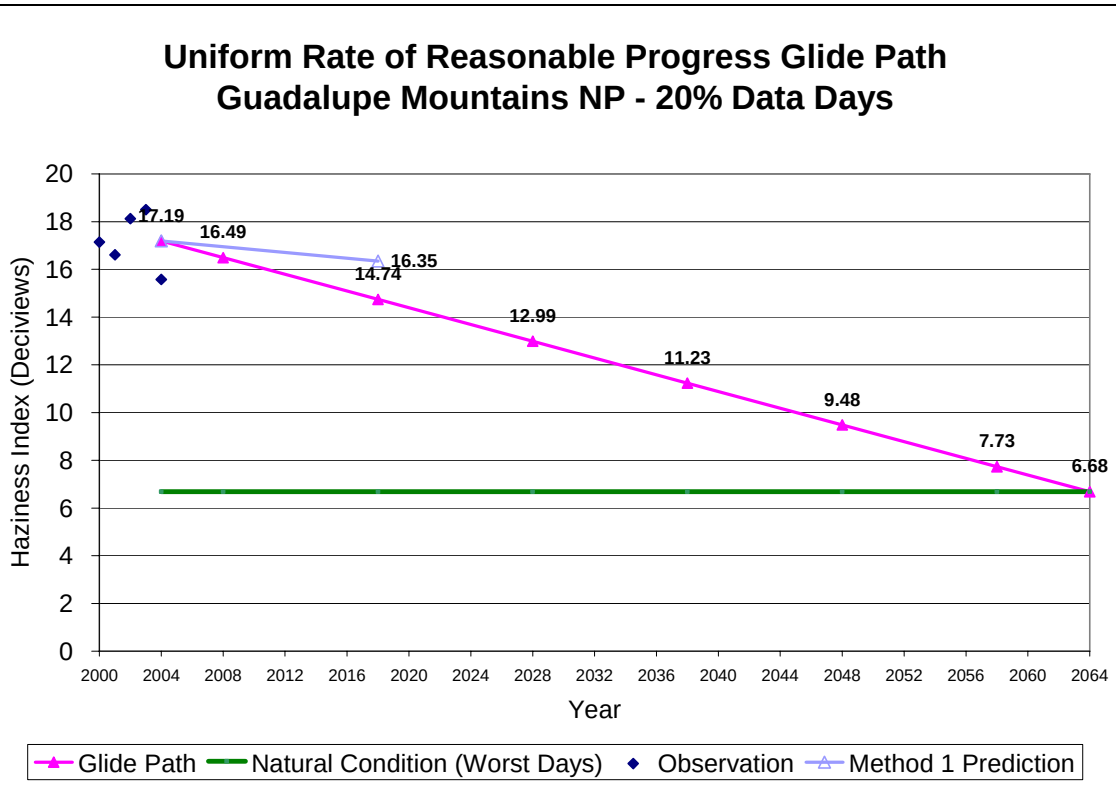

Figure D-10a. 2018 Visibility Projections and 2018 URP Glidepaths in deciview for Guadalupe Mountains (GUMO), Texas and Worst 20% (W20%) days using 2002/2018 Base G CMAQ 36 km modeling results.

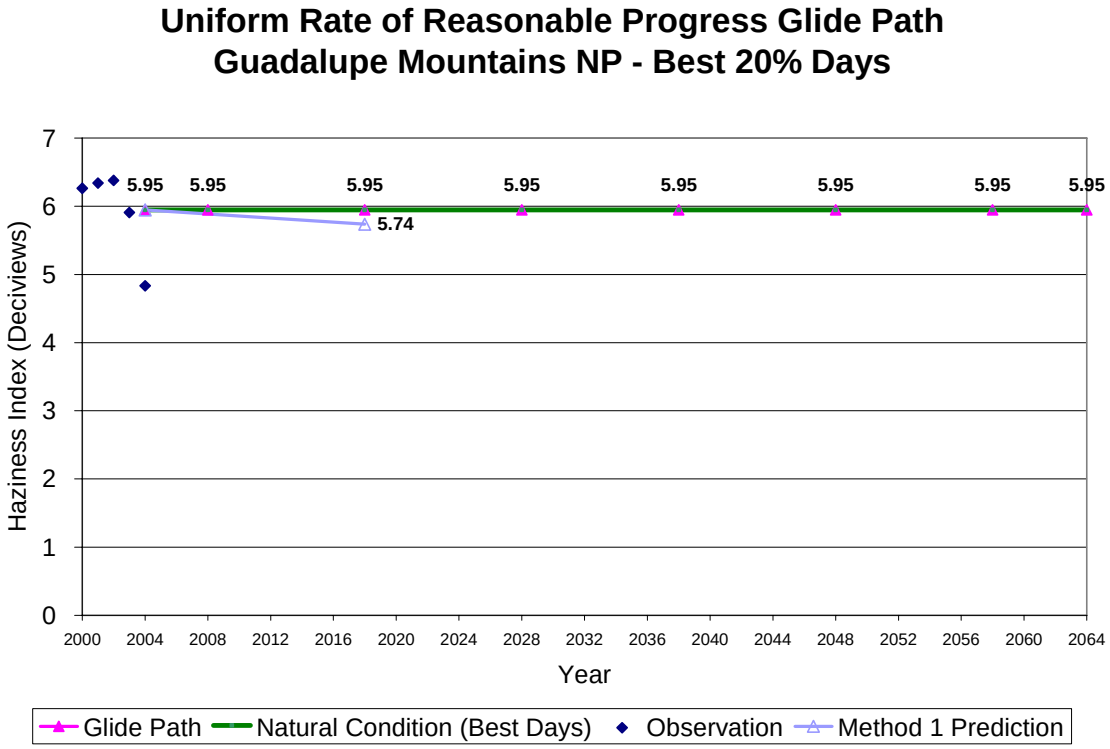

Figure D-10b. 2018 Visibility Projections and 2018 URP Glidepaths in deciview for Guadalupe Mountains (GUMO), Texas and Best 20% (B20%) days using 2002/2018 Base G CMAQ 36 km modeling results.

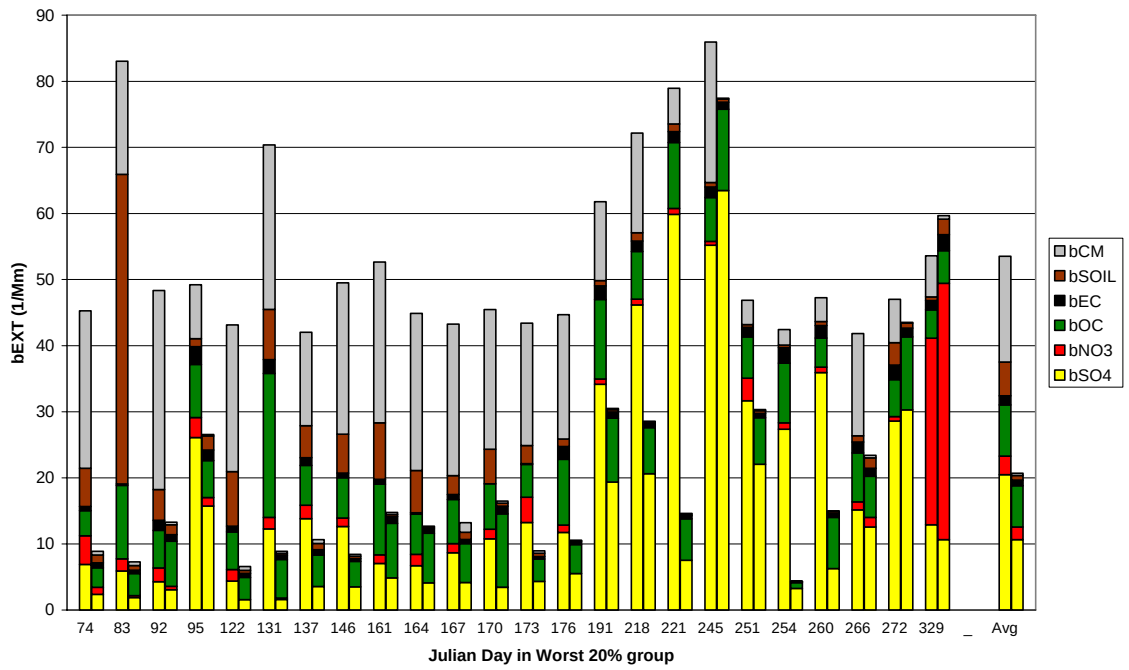

Figure D-10c. Comparison of observed (left) and 2002 Base G modeled (right) daily extinction for Guadalupe Mountains (GUMO), Texas and Worst 20% (W20%) days in 2002.

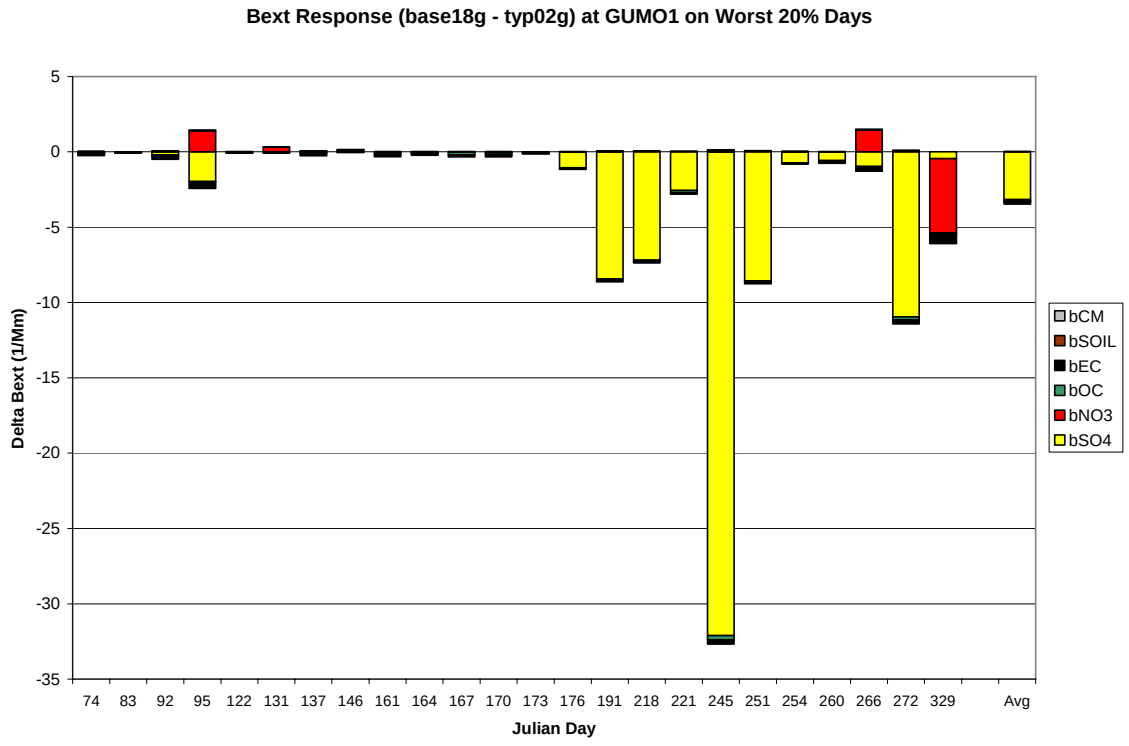

Figure D-10d. Differences in modeled 2002 and 2018 Base G CMAQ results (2018-2002) daily extinction for Guadalupe Mountains (GUMO), Texas and Worst 20% (W20%) days in 2002.

APPENDIX E

CAMx PM Source Apportionment Technology (PSAT) Extinction (Mm^{-1}) Contributions for the 2002 Worst and Best 20 Percent Days at CENRAP Class I Areas

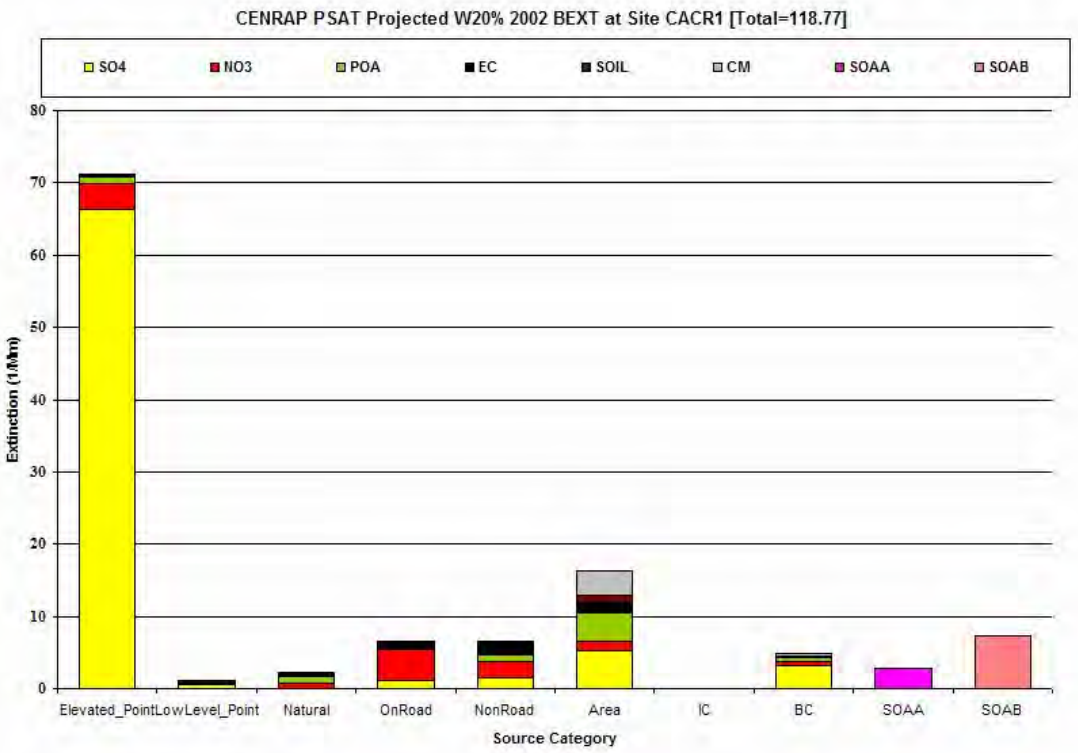

Figure E-1a. PSAT source categories by PM species contributions to the average 2000-2004 Baseline extinction (Mm^{-1}) for the Worst 20% visibility days at Caney Creek (CACR), Arkansas.

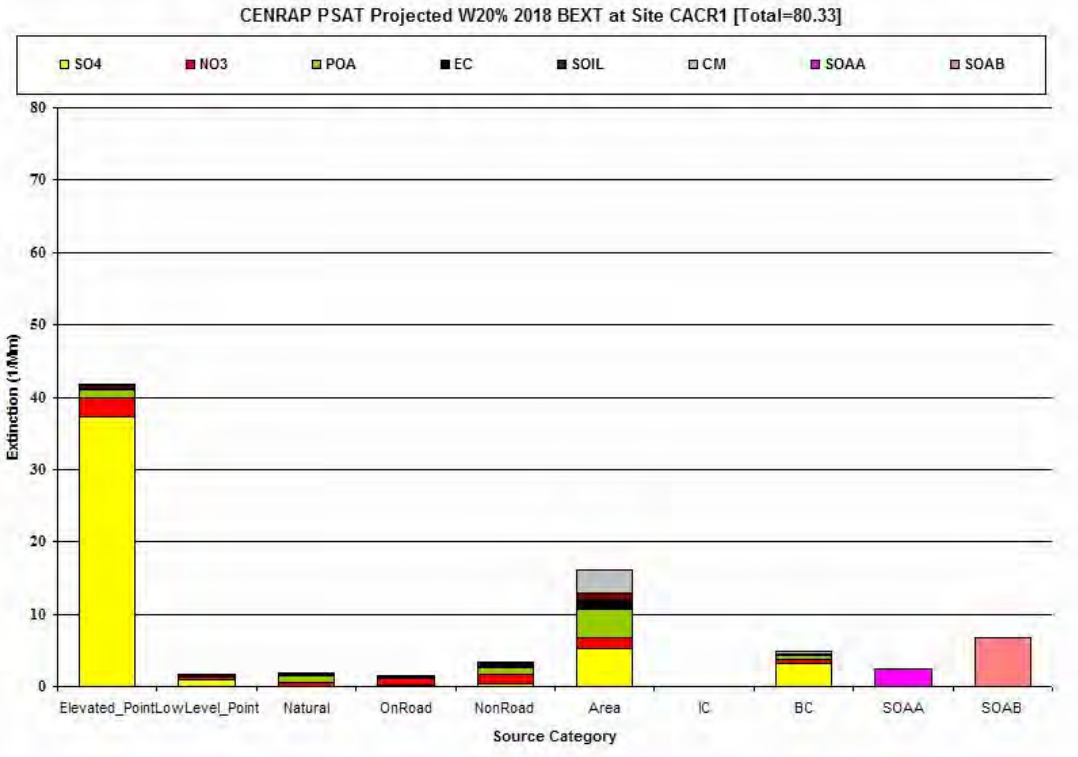

Figure E-1b. PSAT source category by PM species contributions to the average 2018 projected

extinction (Mm^{-1}) for the Worst 20% visibility days at Caney Creek (CACR), Arkansas.

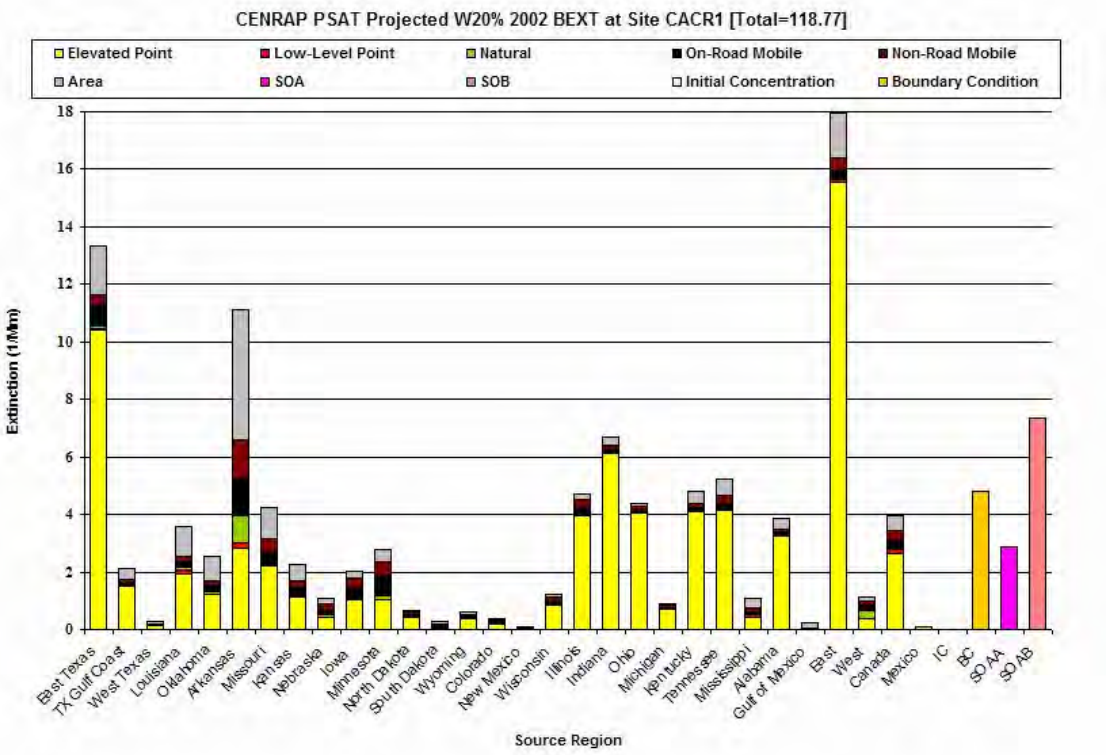

Figure E-1c. PSAT source region by source category contributions to the average 2000-2004 Baseline extinction (Mm^{-1}) for the Worst 20% visibility days at Caney Creek (CACR), Arkansas.

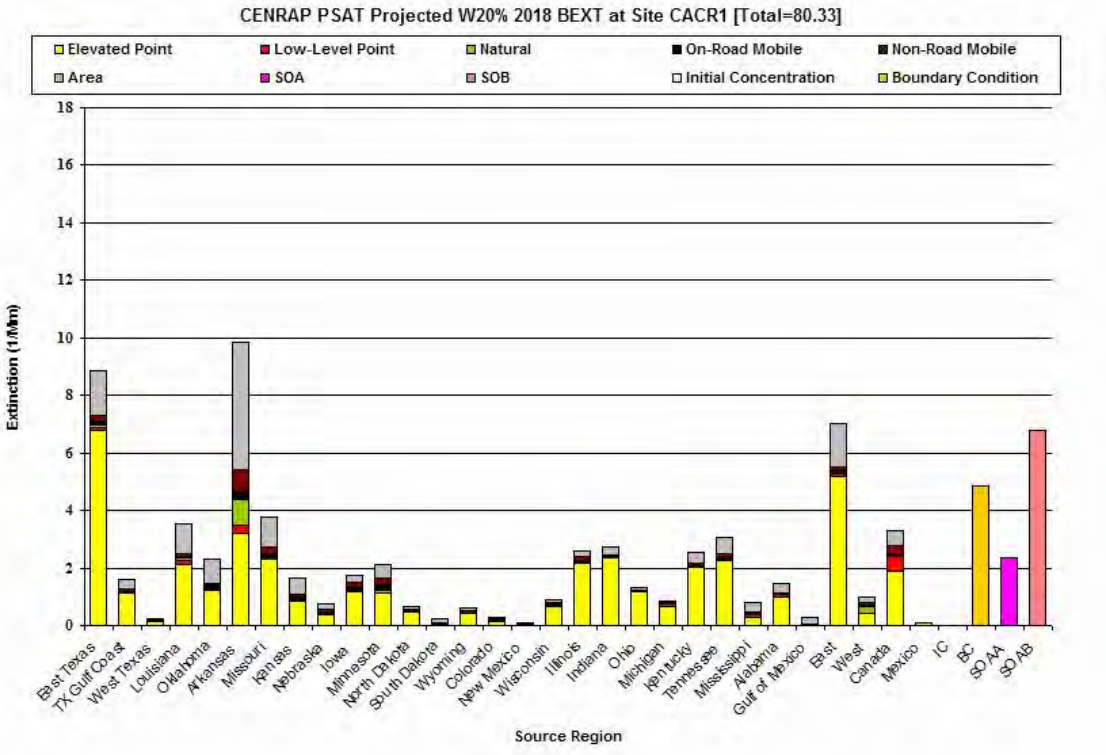

Figure E-1d. PSAT source region by source category contributions to the average 2018 extinction

(Mm^{-1}) for the Worst 20% visibility days at Caney Creek (CACR), Arkansas.

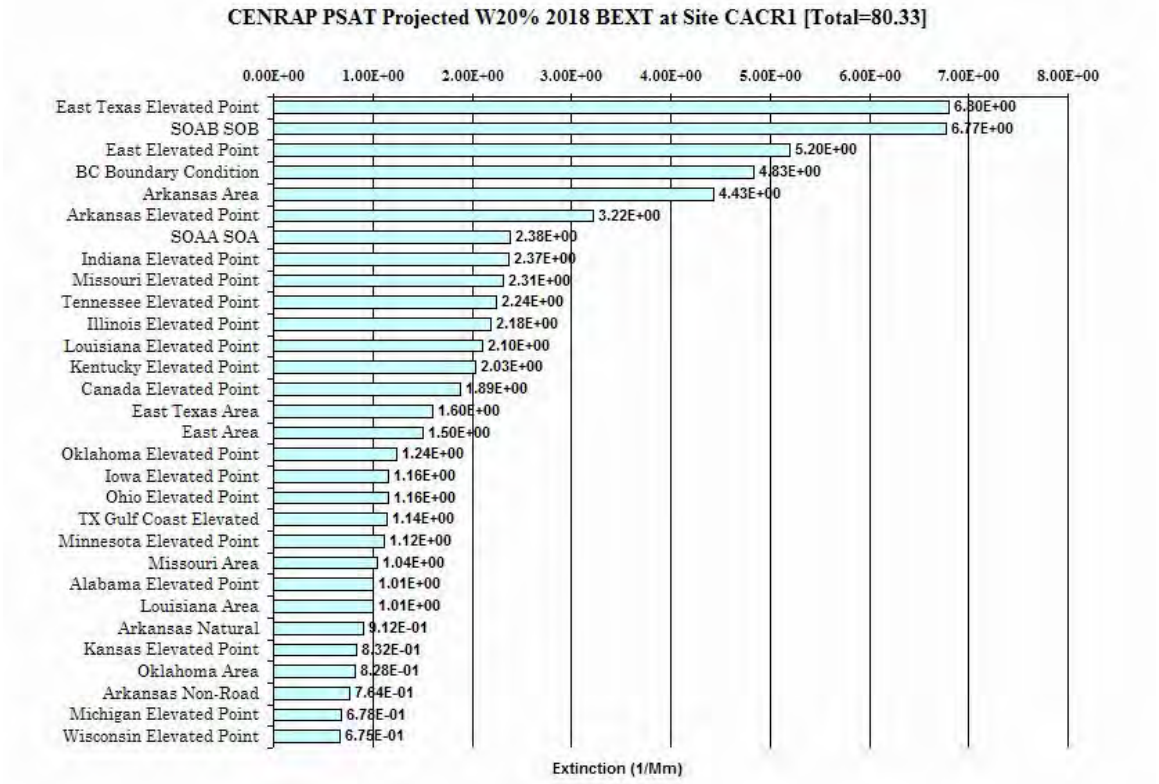

Figure E-1e. Ranked PSAT source region by source category contributions to the average 2018 extinction (Mm^{-1}) for the Worst 20% visibility days at Caney Creek (CACR), Arkansas

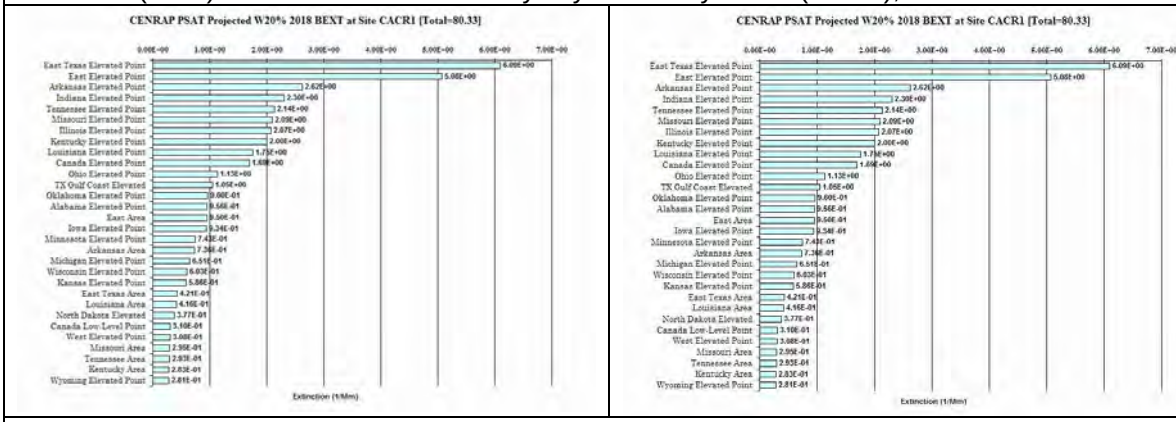

Figure E-1f. Ranked PSAT source region by source category contributions to the average 2018 SO4 (left) and NO3 (right) extinction (Mm^{-1}) for the Worst 20% visibility days at Caney Creek (CACR), Arkansas

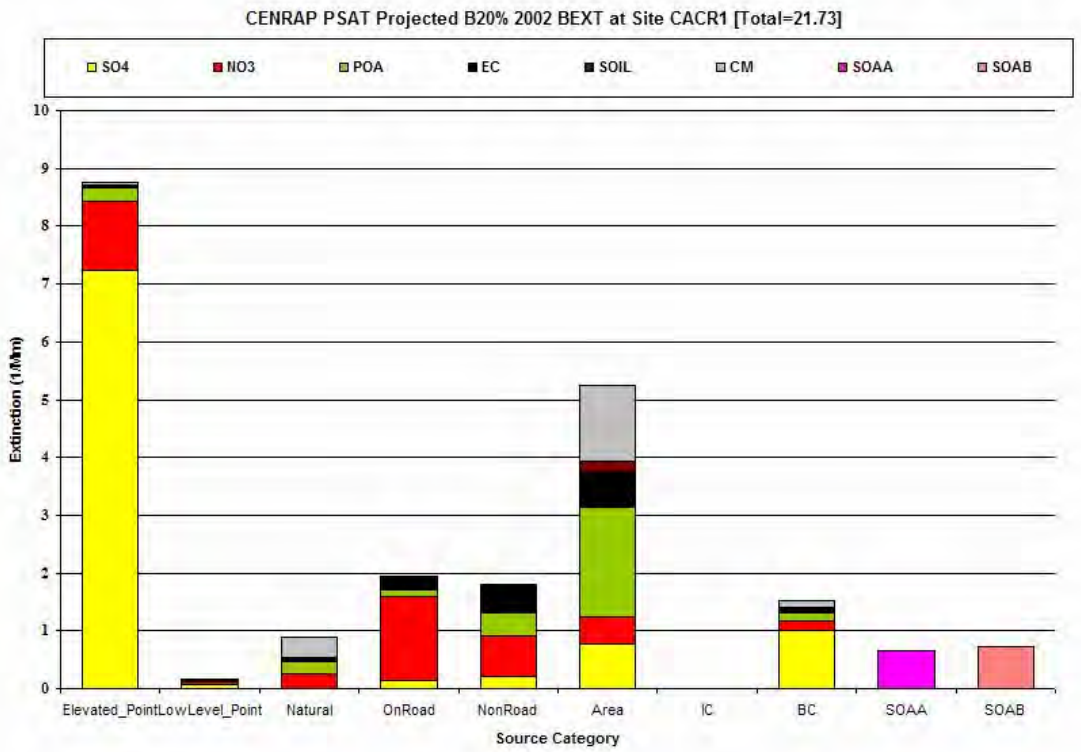

Figure E-1g. PSAT contributions by source category and PM species to the average 2000-2004 Baseline extinction (Mm^{-1}) for the Best 20% visibility days at Caney Creek (CACR), Arkansas.

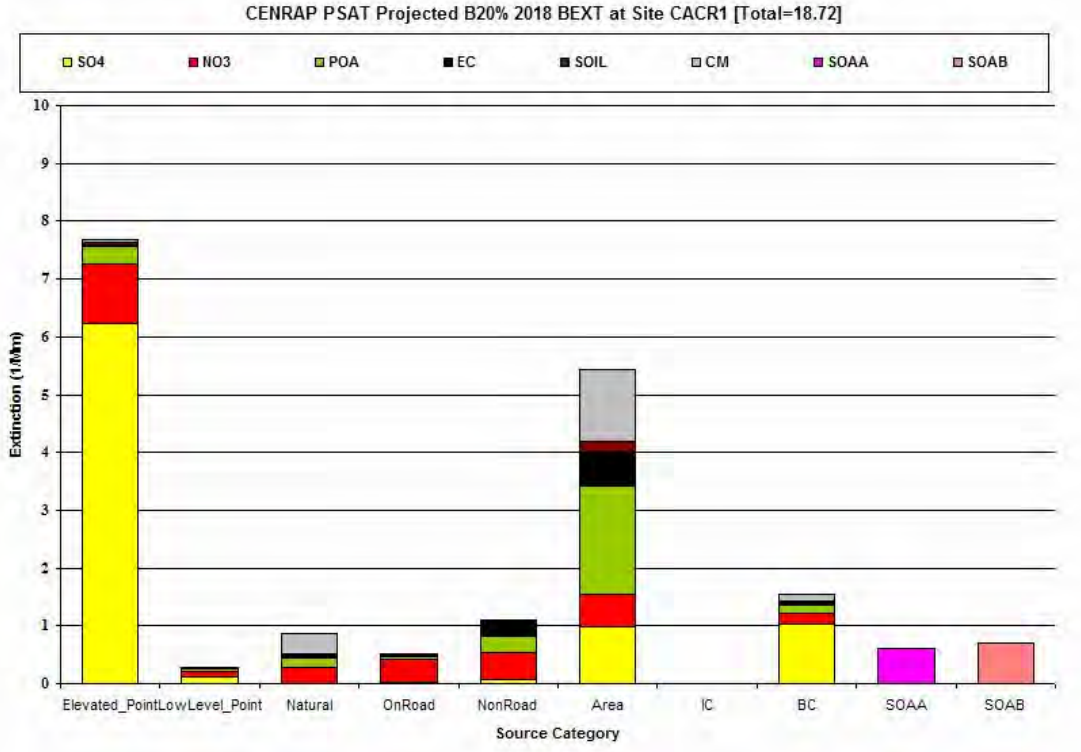

Figure E-1h. PSAT contributions by source category and PM species to the average 2018 extinction (Mm^{-1}) for the Best 20% visibility days at Caney Creek (CACR), Arkansas.

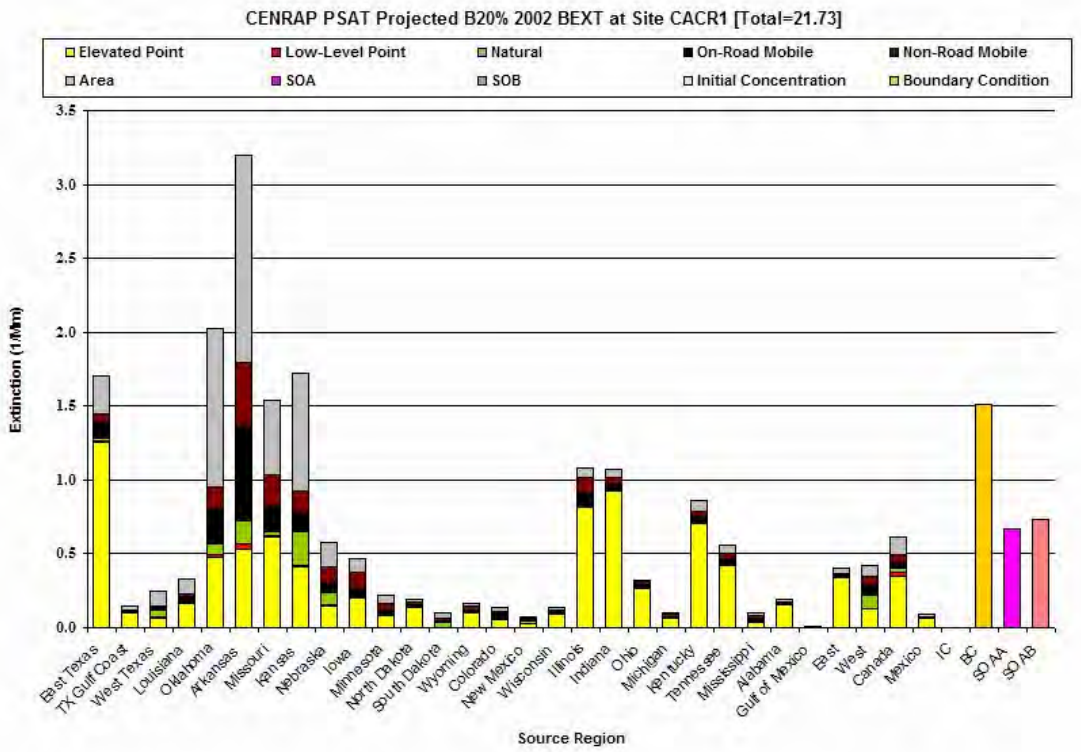

Figure E-1i. PSAT contributions by source region and source category to the average 2000-2004 Baseline extinction (Mm^{-1}) for the Best 20% visibility days at Caney Creek (CACR), Arkansas.

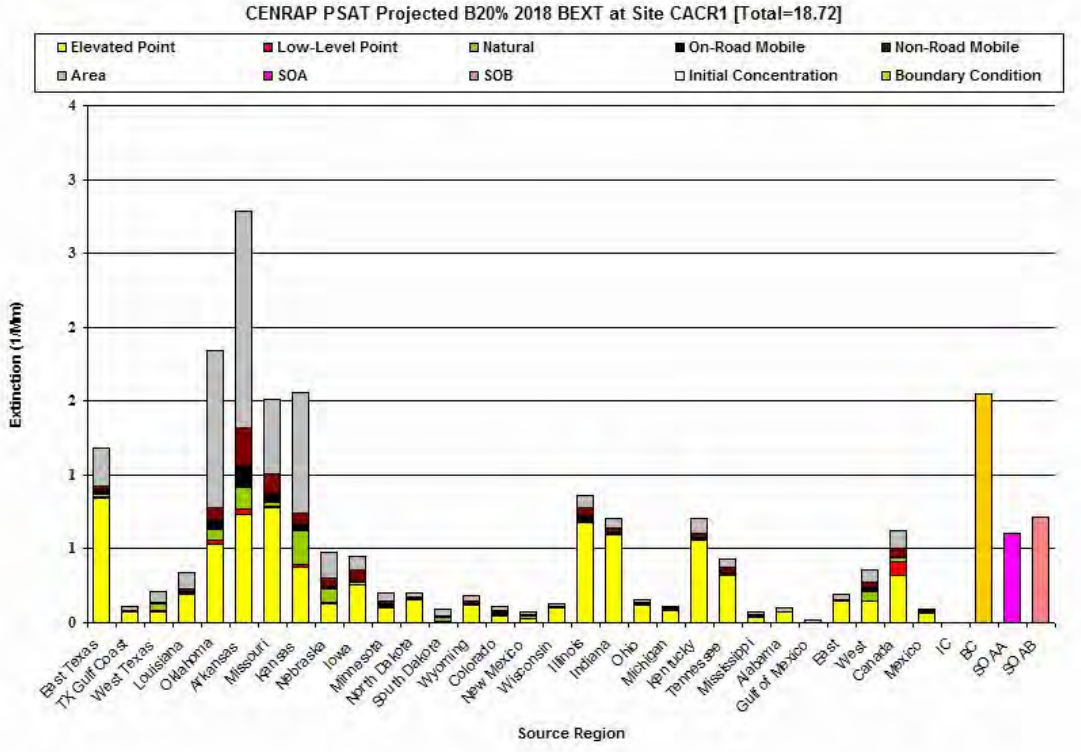

Figure E-1j. PSAT contributions by source region and source category to the average 2018 extinction (Mm^{-1}) for the Best 20% visibility days at Caney Creek (CACR), Arkansas.

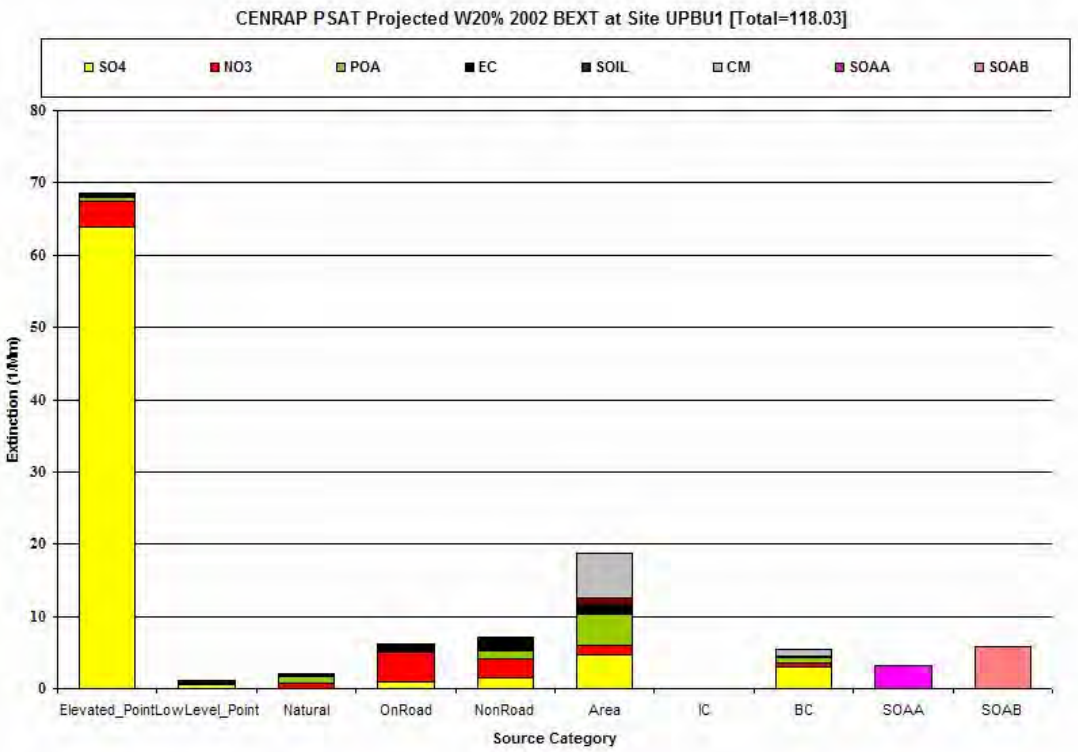

Figure E-2a. PSAT source categories by PM species contributions to the average 2000-2004 Baseline extinction (Mm^{-1}) for the Worst 20% visibility days at Upper Buffalo (UPBU), Arkansas.

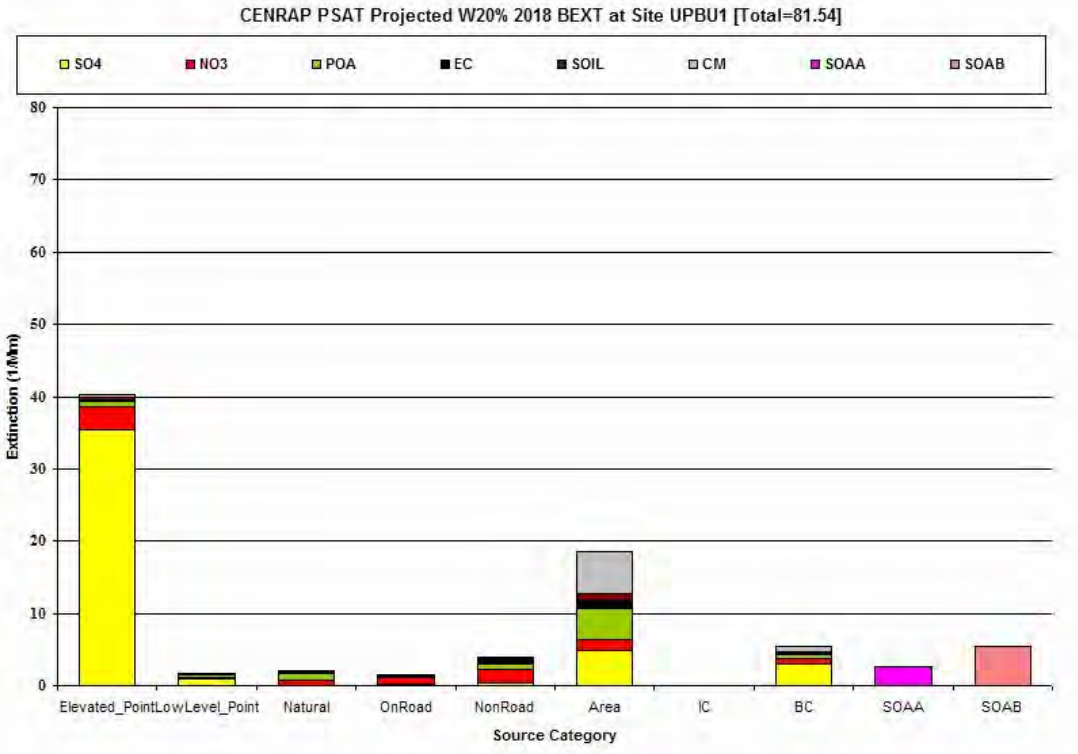

Figure E-2b. PSAT source category by PM species contributions to the average 2018 projected extinction (Mm^{-1}) for the Worst 20% visibility days at Upper Buffalo (UPBU), Arkansas.

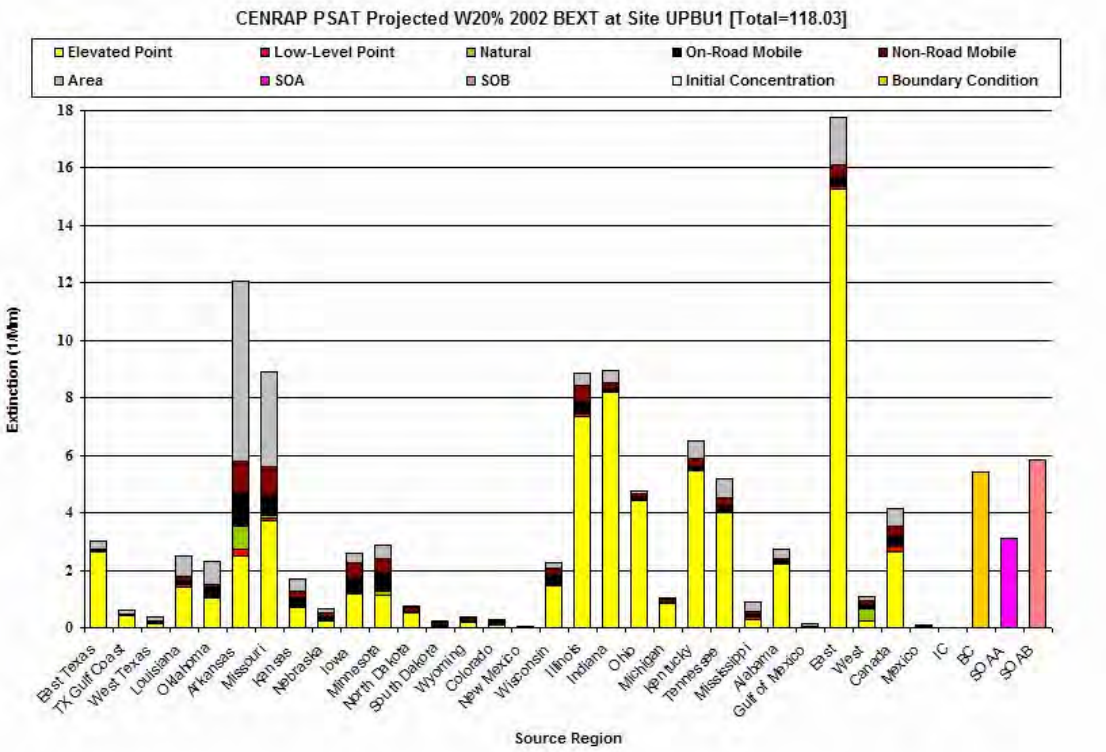

Figure E-2c. PSAT source region by source category contributions to the average 2000-2004 Baseline extinction (Mm^{-1}) for the Worst 20% visibility days at Upper Buffalo (UPBU), Arkansas.

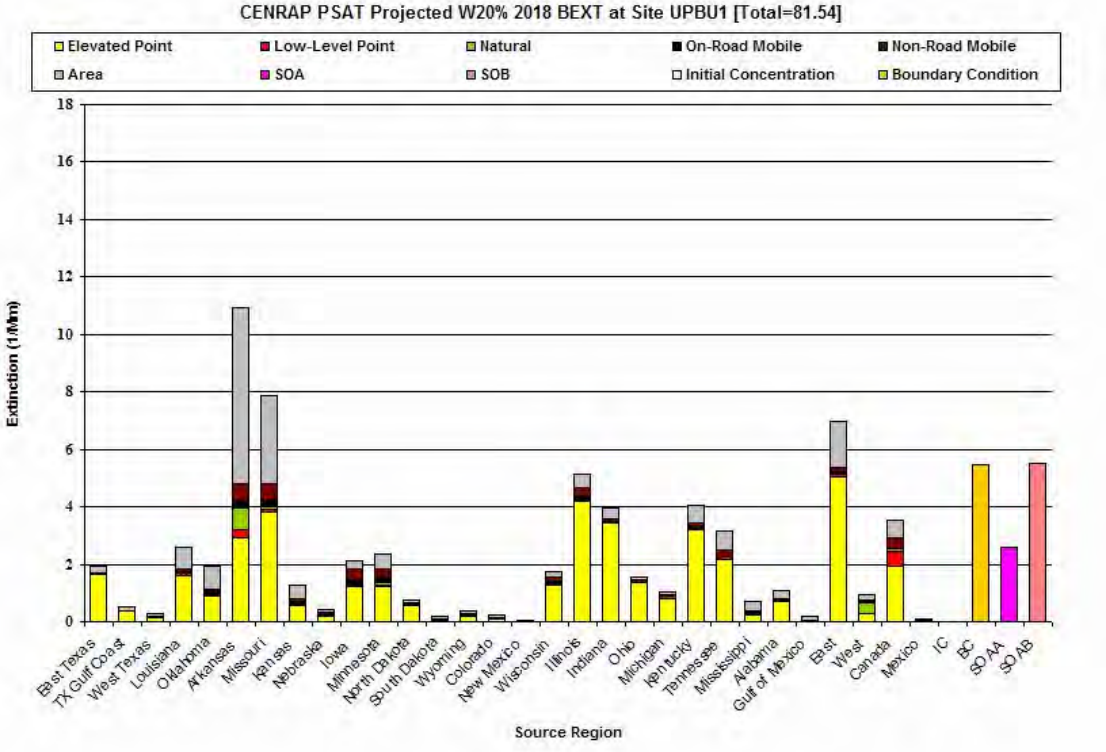

Figure E-2d. PSAT source region by source category contributions to the average 2018 extinction (Mm^{-1}) for the Worst 20% visibility days at Upper Buffalo (UPBU), Arkansas.

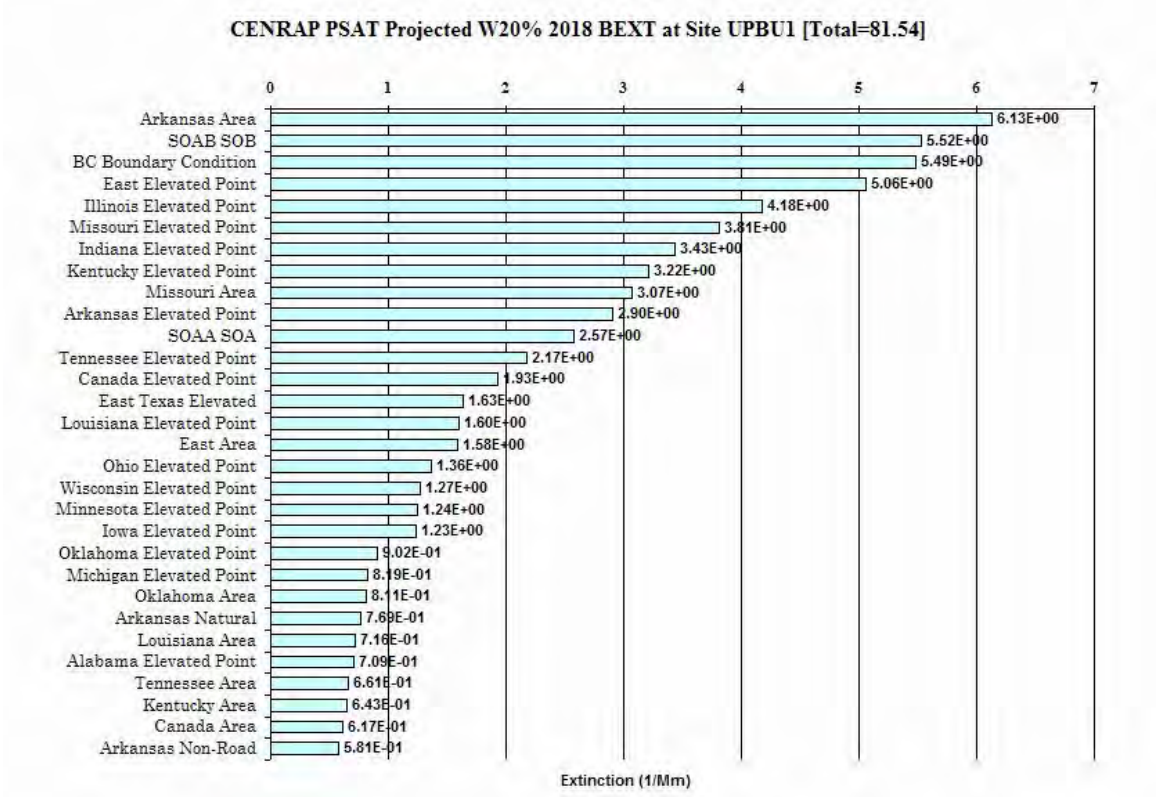

Figure E-2e. Ranked PSAT source region by source category contributions to the average 2018 extinction (Mm^{-1}) for the Worst 20% visibility days at Upper Buffalo (UPBU), Arkansas.

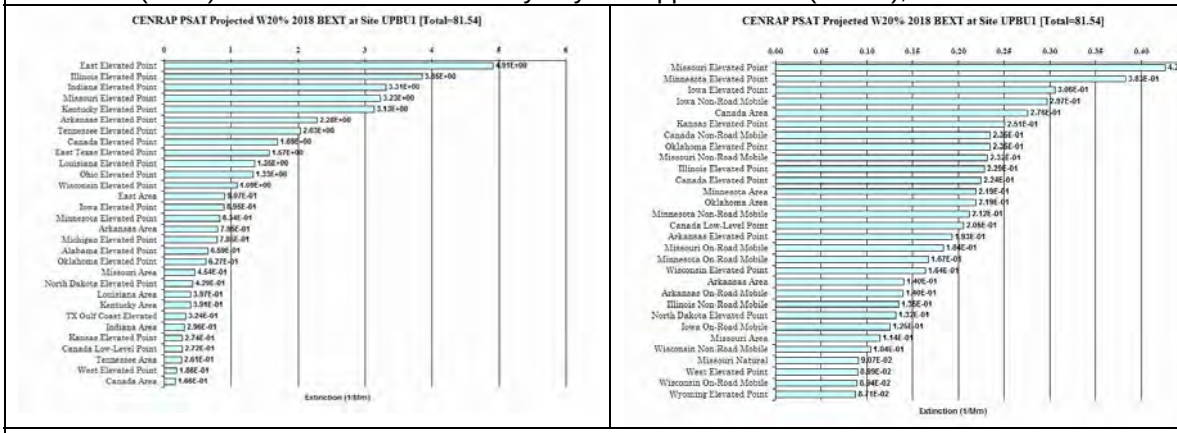

Figure E-2f. Ranked PSAT source region by source category contributions to the average 2018 SO4 (left) and NO3 (right) extinction (Mm^{-1}) for the Worst 20% visibility days at Upper Buffalo (UPBU), Arkansas.

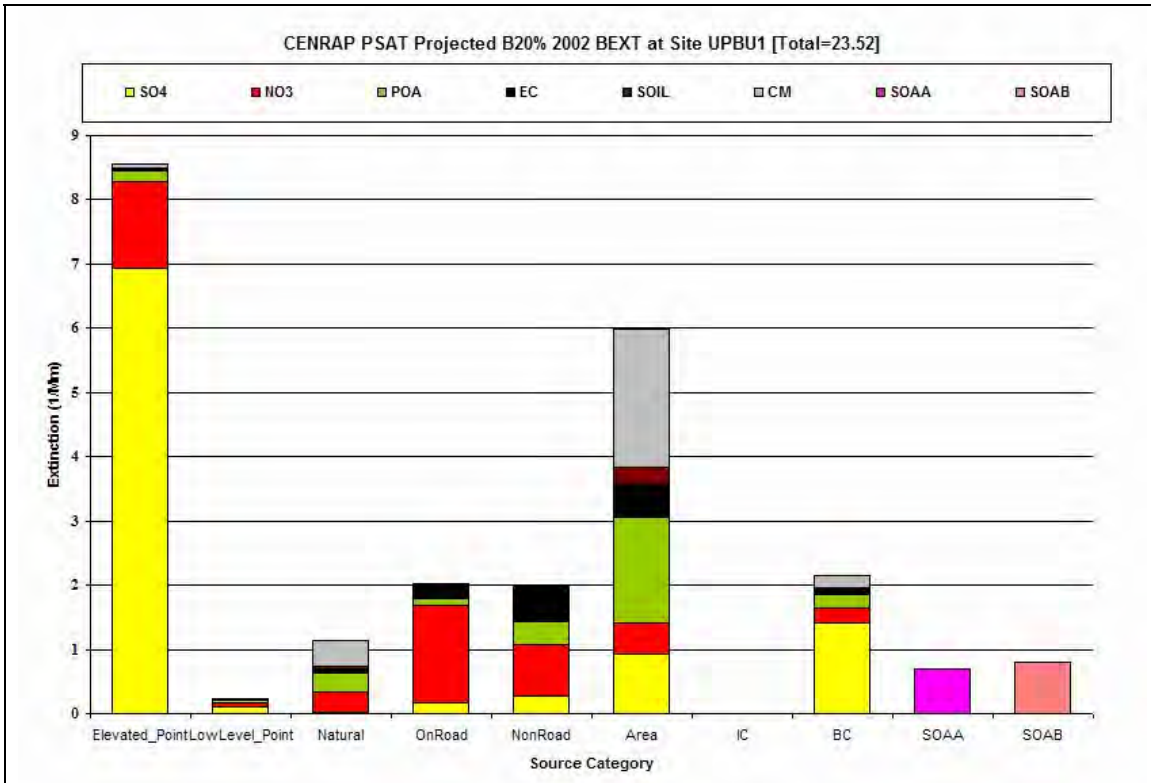

Figure E-2g. PSAT contributions by source category and PM species to the average 2000-2004 Baseline extinction (Mm^{-1}) for the Best 20% visibility days at Upper Buffalo (UPBU), Arkansas.

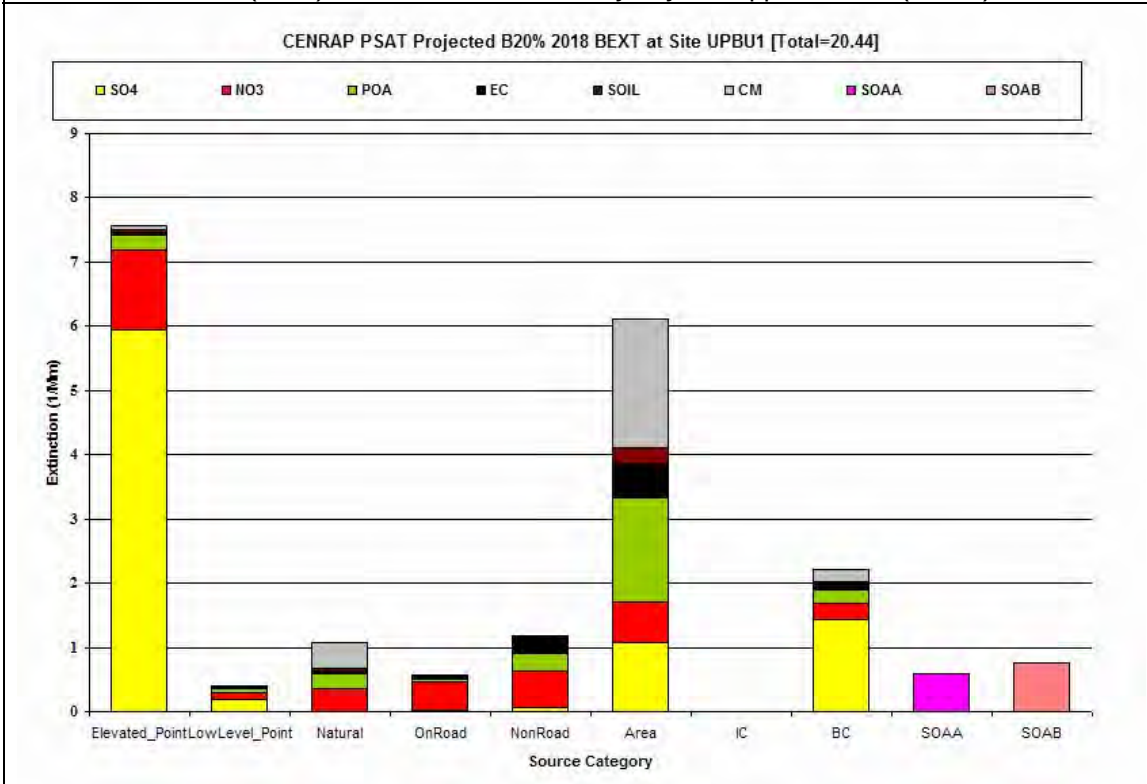

Figure E-2h. PSAT contributions by source category and PM species to the average 2018 extinction (Mm^{-1}) for the Best 20% visibility days at Upper Buffalo (UPBU), Arkansas.

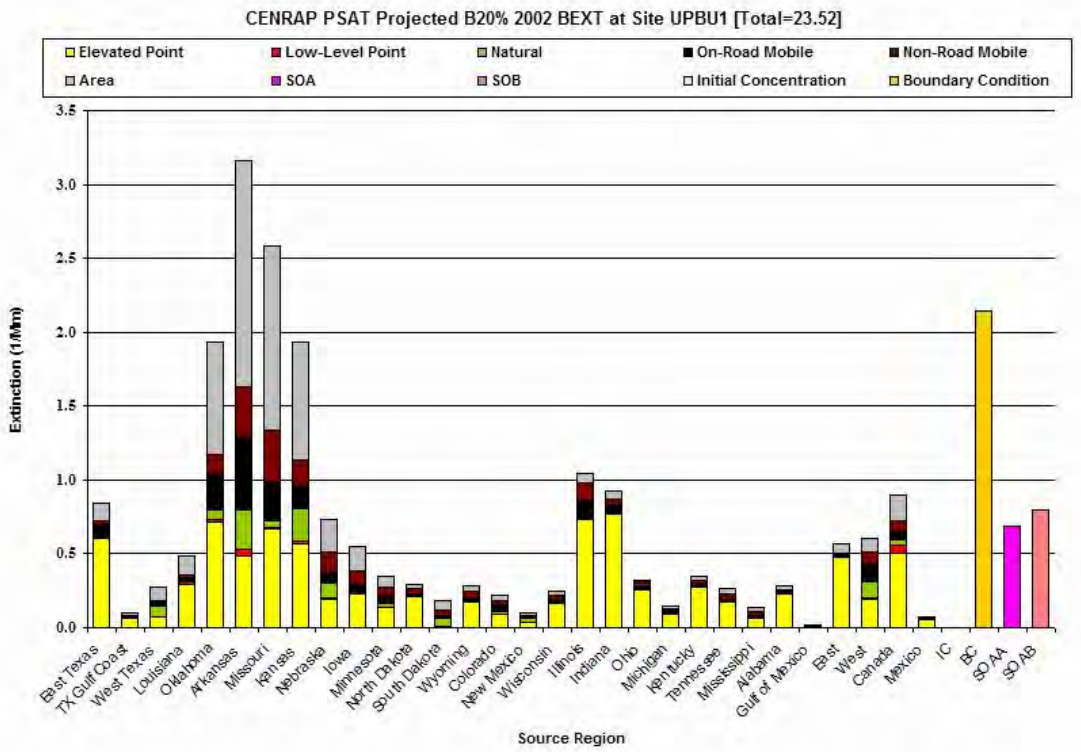

Figure E-2i. PSAT contributions by source region and source category to the average 2000-2004 Baseline extinction (Mm^{-1}) for the Best 20% visibility days at Upper Buffalo (UPBU), Arkansas.

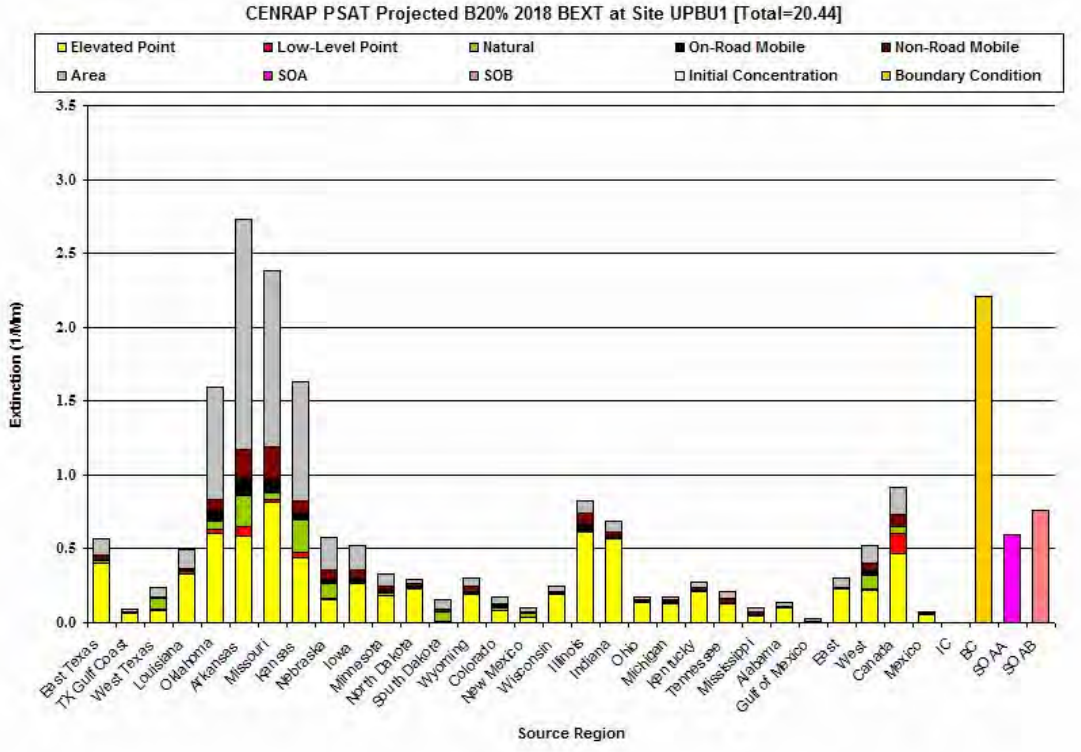

Figure E-2j. PSAT contributions by source region and source category to the average 2018 extinction (Mm^{-1}) for the Best 20% visibility days at Upper Buffalo (UPBU), Arkansas.

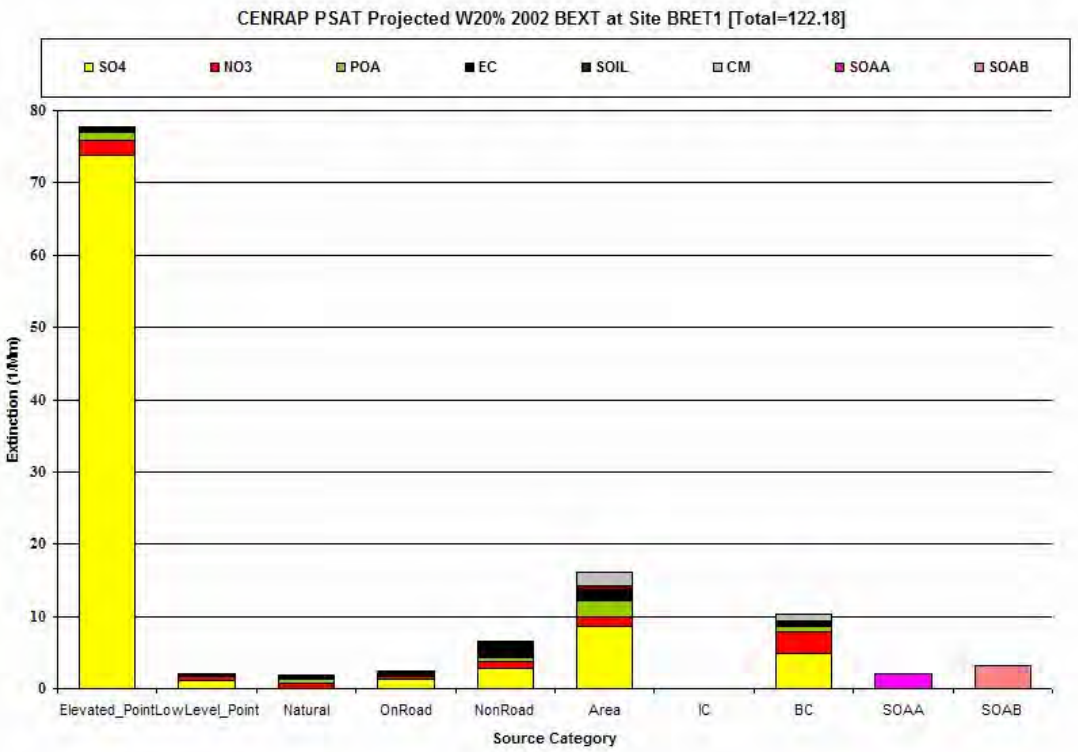

Figure E-3a. PSAT source categories by PM species contributions to the average 2000-2004 Baseline extinction (Mm^{-1}) for the Worst 20% visibility days at Breton Island (BRET), Louisiana.

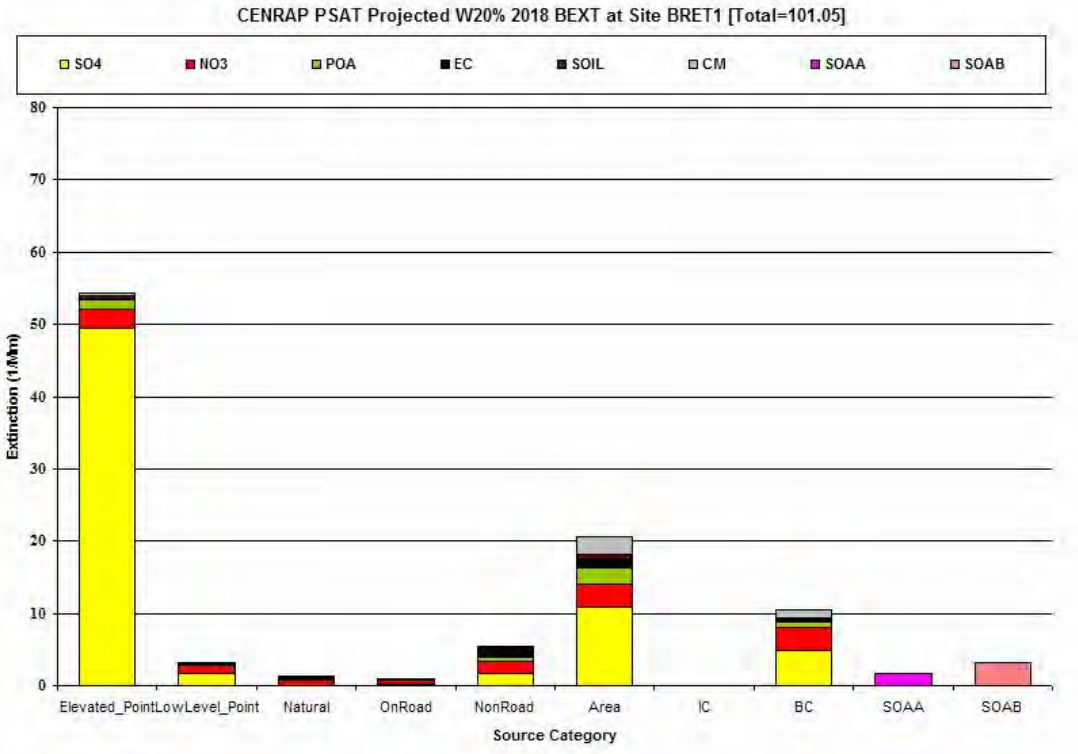

Figure E-3b. PSAT source category by PM species contributions to the average 2018 projected extinction (Mm^{-1}) for the Worst 20% visibility days at Breton Island (BRET), Louisiana.

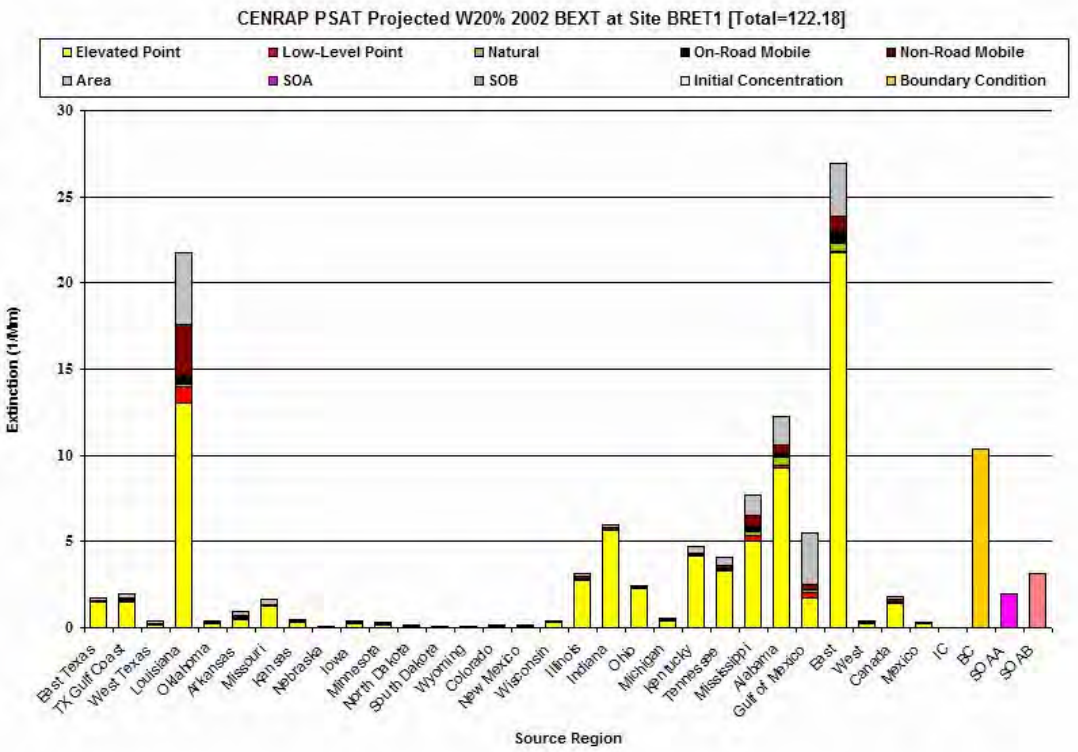

Figure E-3c. PSAT source region by source category contributions to the average 2000-2004 Baseline extinction (Mm^{-1}) for the Worst 20% visibility days at Breton Island (BRET), Louisiana.

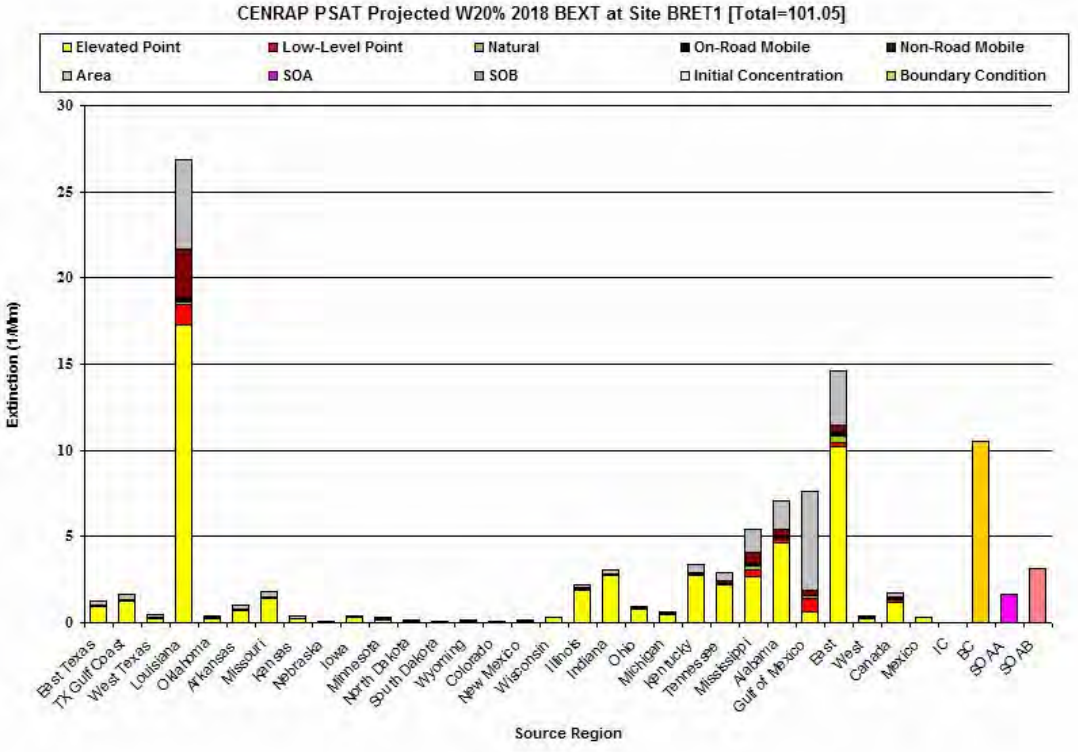

Figure E-3d. PSAT source region by source category contributions to the average 2018 extinction (Mm^{-1}) for the Worst 20% visibility days at Breton Island (BRET), Louisiana.

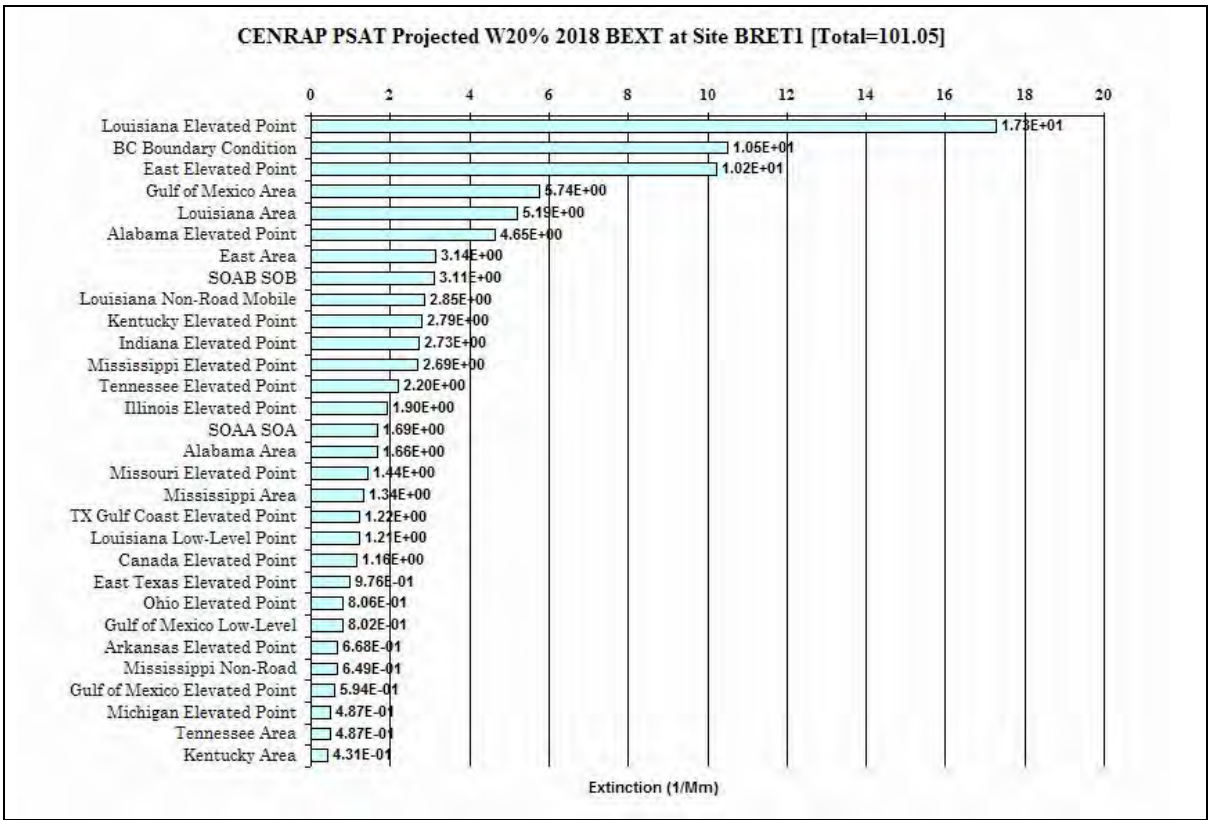

Figure E-3e. Ranked PSAT source region by source category contributions to the average 2018 extinction (Mm^{-1}) for the Worst 20% visibility days at Breton Island (BRET), Louisiana.

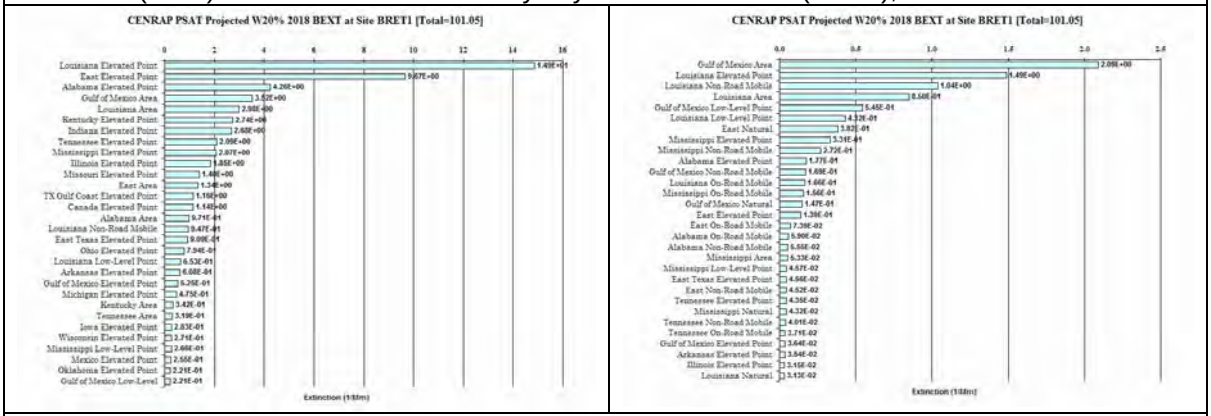

Figure E-3f. Ranked PSAT source region by source category contributions to the average 2018 SO4 (left) and NO3 (right) extinction (Mm^{-1}) for the Worst 20% visibility days at Breton Island (BRET), Louisiana.

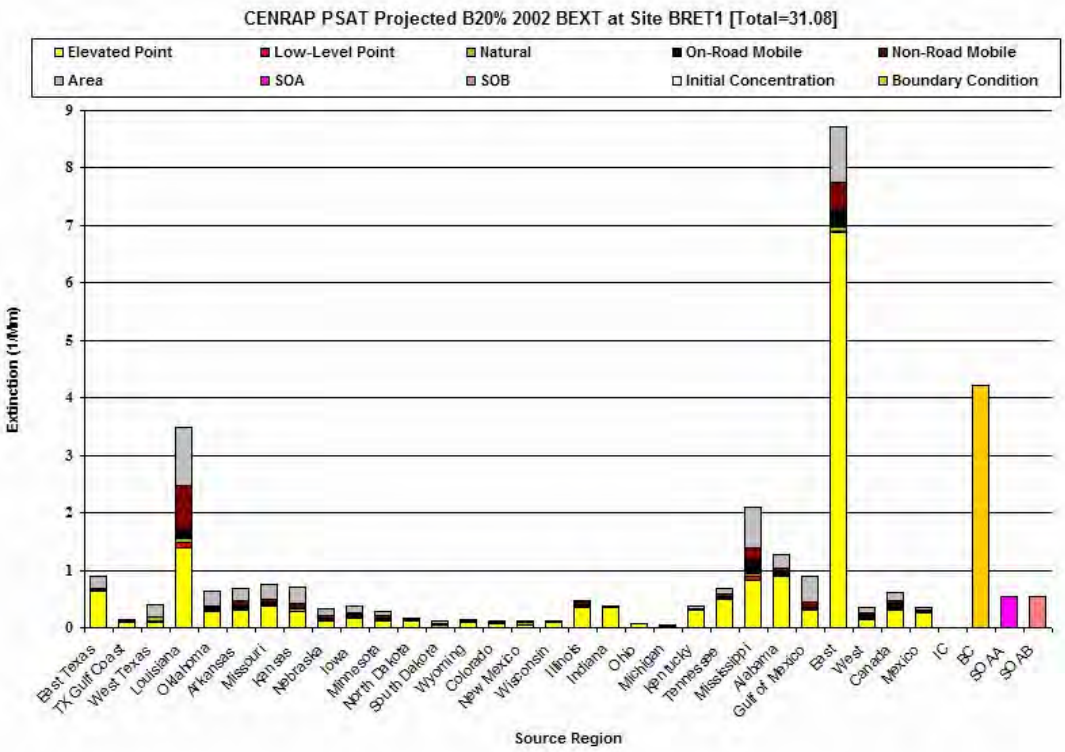

Figure E-3g. PSAT contributions by source category and PM species to the average 2000-2004 Baseline extinction (Mm^{-1}) for the Best 20% visibility days at Breton Island (BRET), Louisiana.

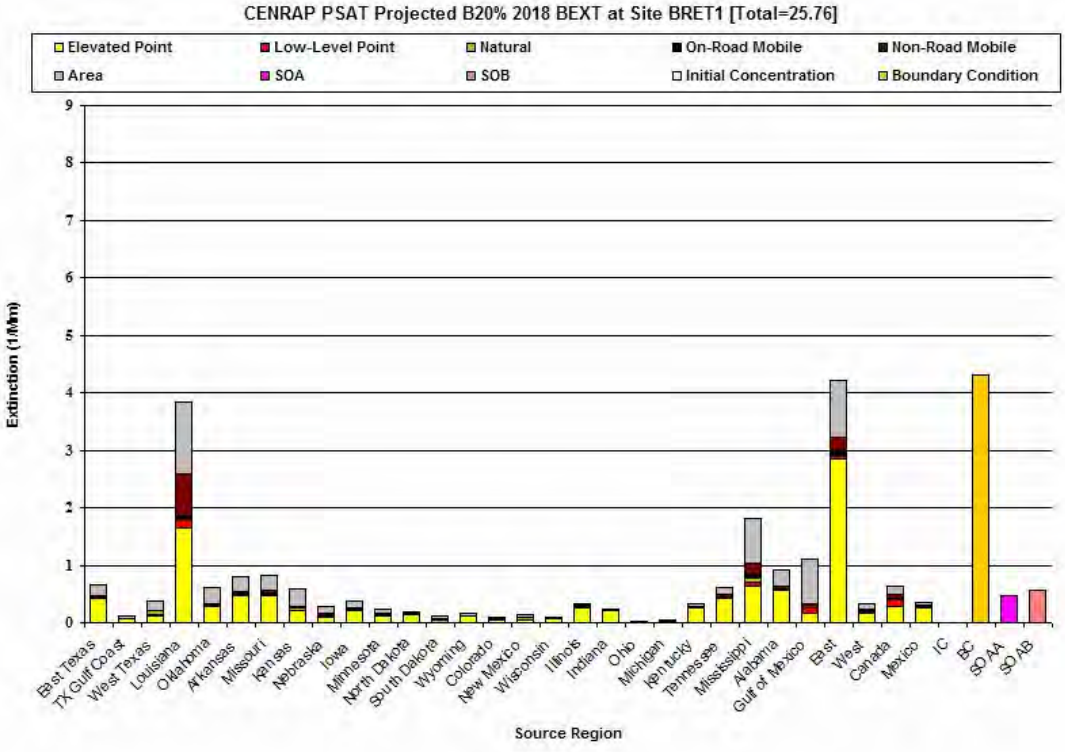

Figure E-3h. PSAT contributions by source category and PM species to the average 2018 extinction (Mm^{-1}) for the Best 20% visibility days at Breton Island (BRET), Louisiana.

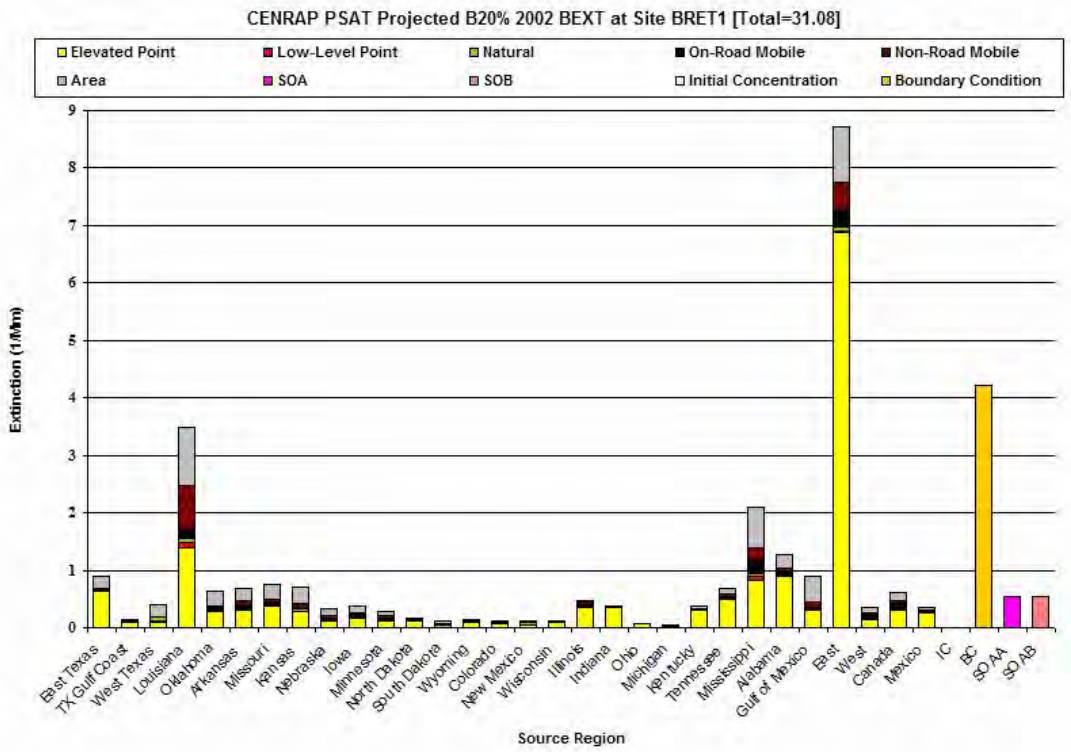

Figure E-3i. PSAT contributions by source region and source category to the average 2000-2004 Baseline extinction (Mm^{-1}) for the Best 20% visibility days at Breton Island (BRET), Louisiana.

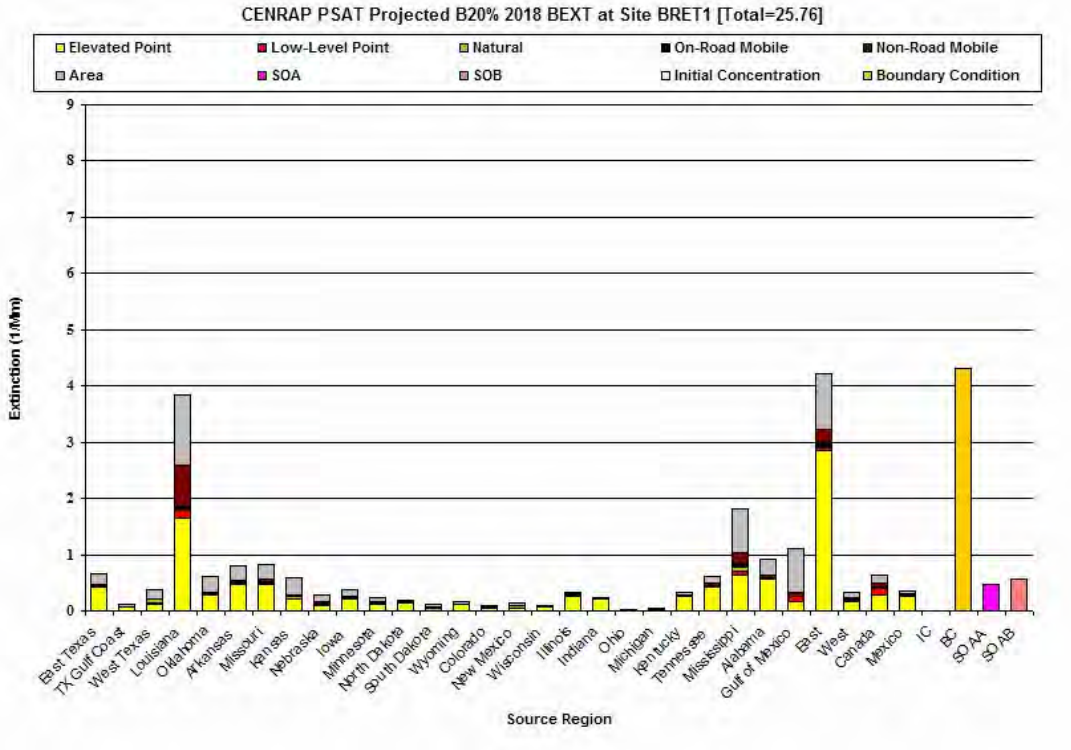

Figure E-3j. PSAT contributions by source region and source category to the average 2018 extinction (Mm^{-1}) for the Best 20% visibility days at Breton Island (BRET), Louisiana.

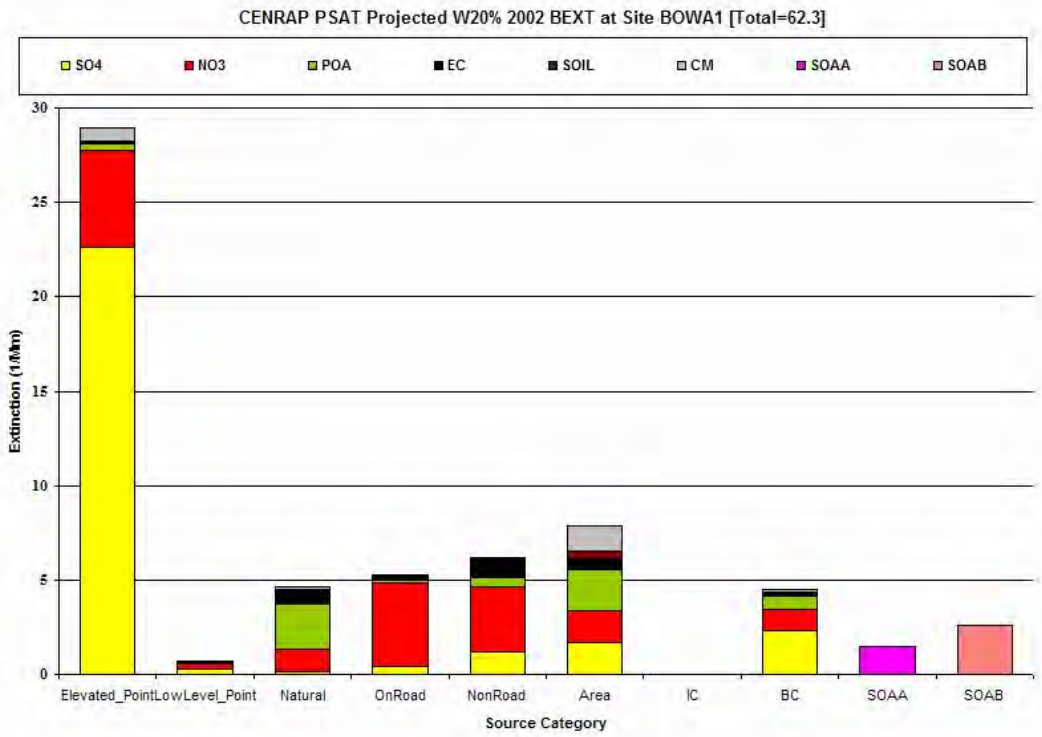

Figure E-4a. PSAT source categories by PM species contributions to the average 2000-2004 Baseline extinction (Mm^{-1}) for the Worst 20% visibility days at Boundary Waters (BOWA), Minnesota.

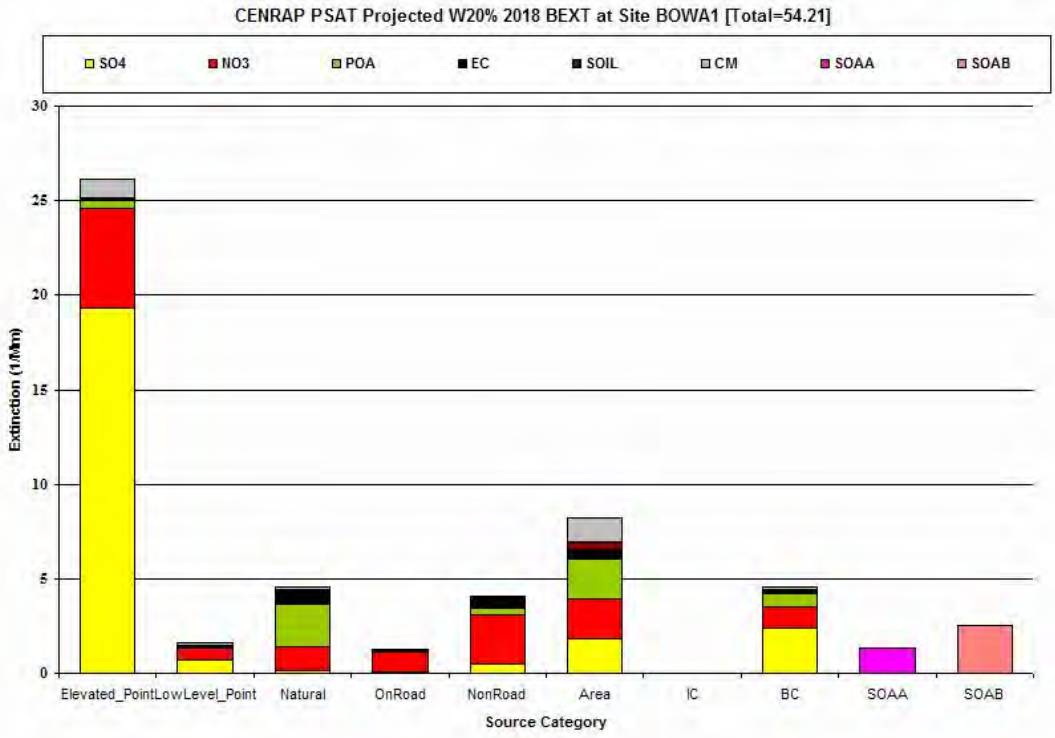

Figure E-4b. PSAT source category by PM species contributions to the average 2018 projected extinction (Mm^{-1}) for the Worst 20% visibility days at Boundary Waters (BOWA), Minnesota.

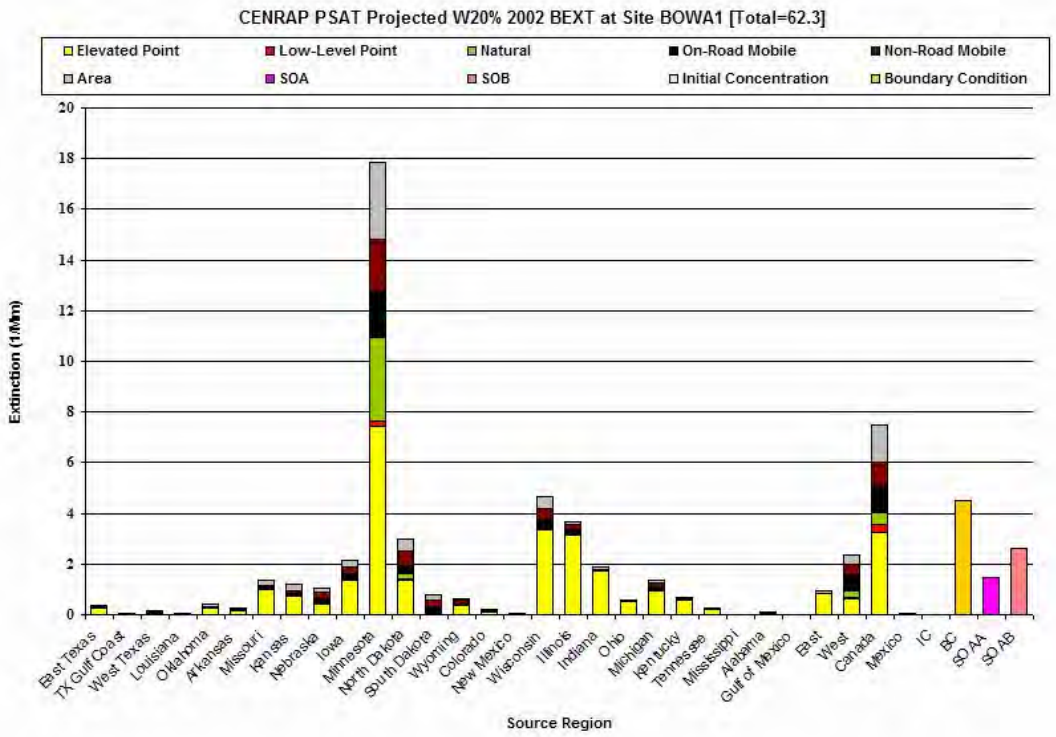

Figure E-4c. PSAT source region by source category contributions to the average 2000-2004 Baseline extinction (Mm^{-1}) for the Worst 20% visibility days at Boundary Waters (BOWA), Minnesota.

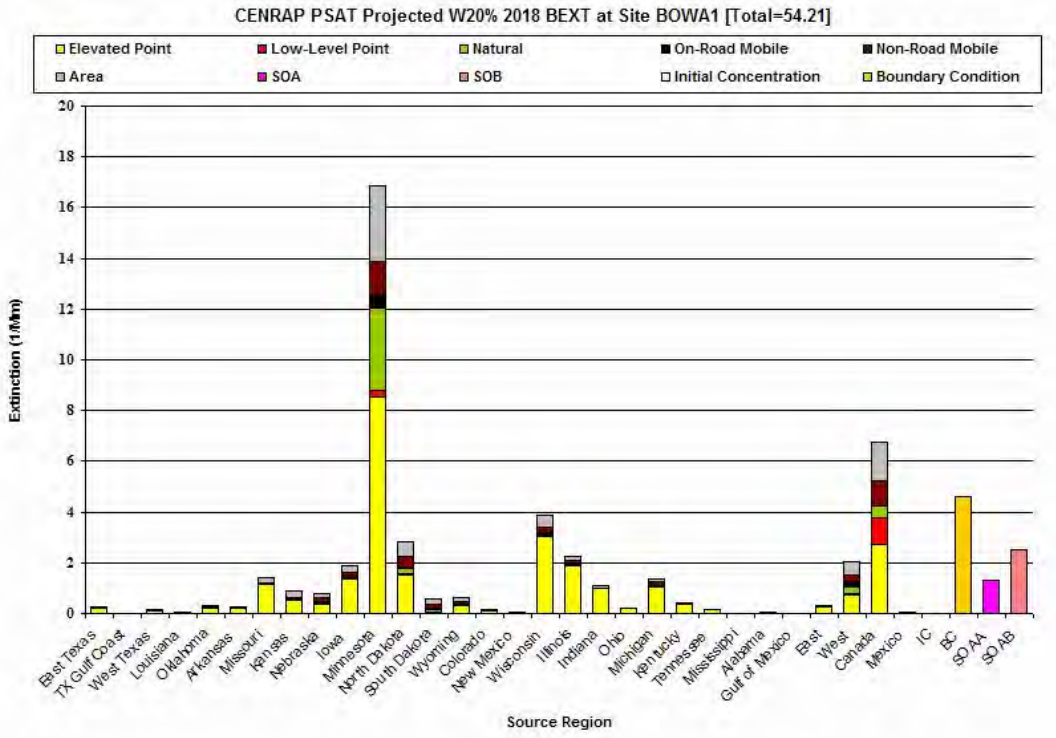

Figure E-4d. PSAT source region by source category contributions to the average 2018 extinction (Mm^{-1}) for the Worst 20% visibility days at Boundary Waters (BOWA), Minnesota.

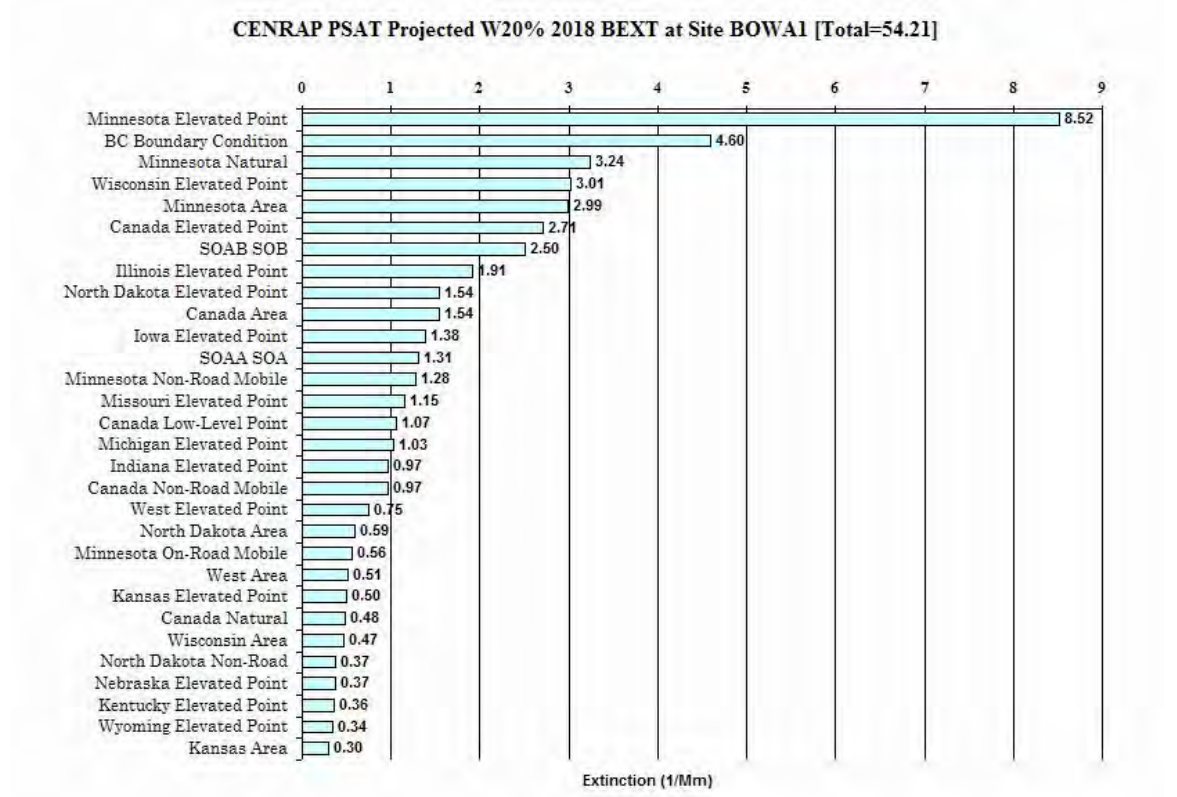

Figure E-4e. Ranked PSAT source region by source category contributions to the average 2018 extinction (Mm^{-1}) for the Worst 20% visibility days at Boundary Waters (BOWA), Minnesota.

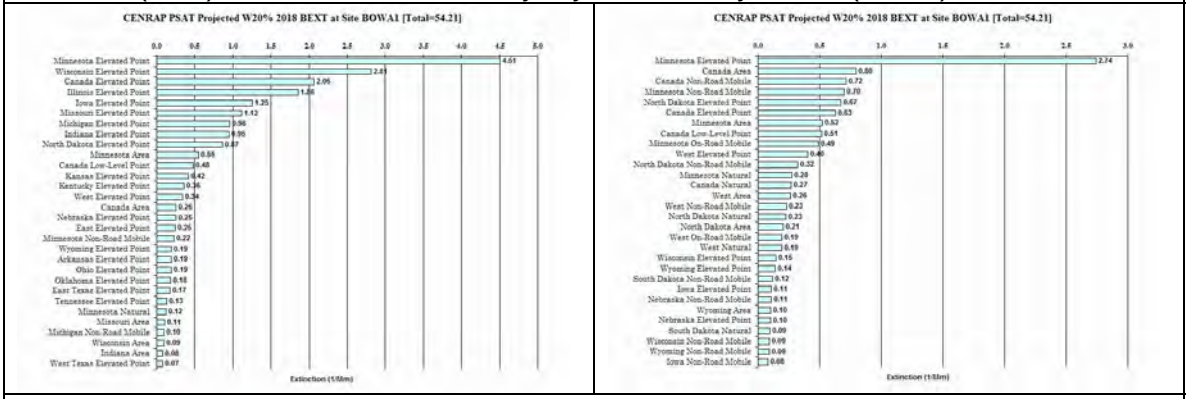

Figure E-4f. Ranked PSAT source region by source category contributions to the average 2018 SO4 (left) and NO3 (right) extinction (Mm^{-1}) for the Worst 20% visibility days at Boundary Waters (BOWA), Minnesota.

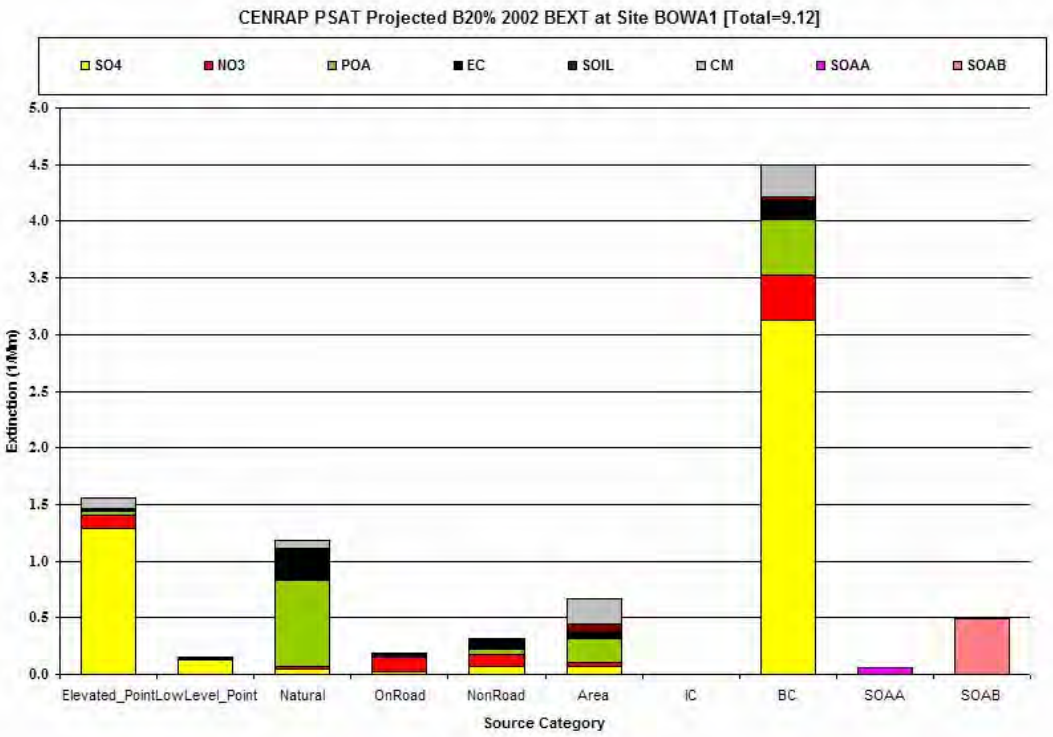

Figure E-4g. PSAT contributions by source category and PM species to the average 2000-2004 Baseline extinction (Mm^{-1}) for the Best 20% visibility days at Boundary Waters (BOWA), Minnesota.

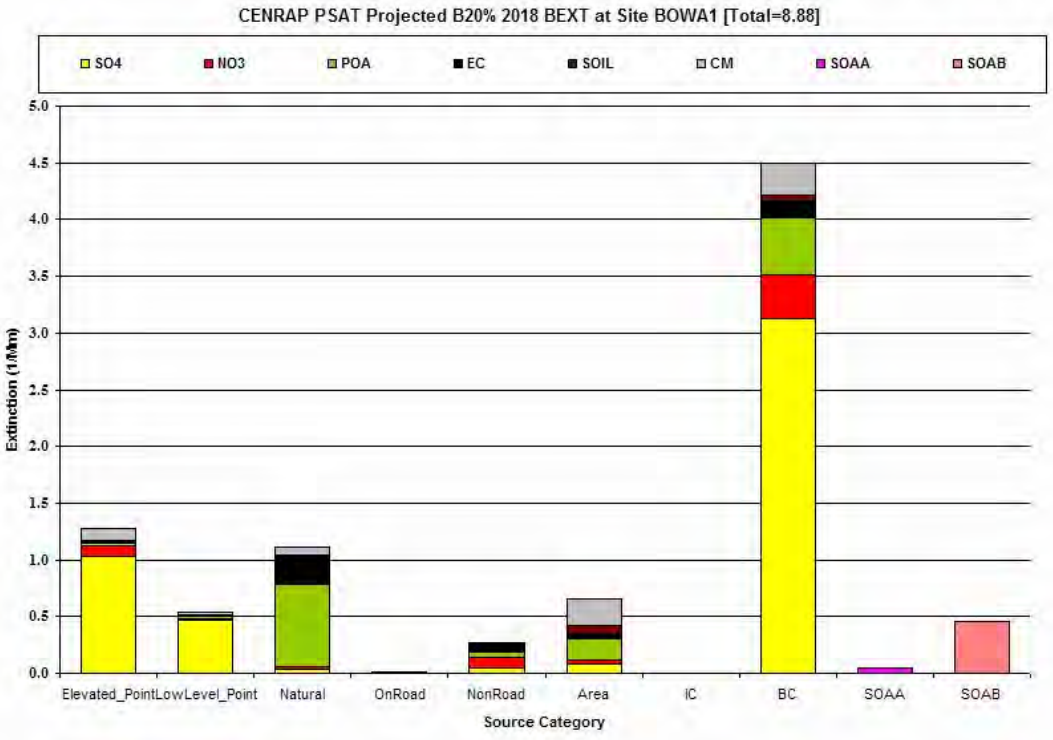

Figure E-4h. PSAT contributions by source category and PM species to the average 2018 extinction (Mm^{-1}) for the Best 20% visibility days at Boundary Waters (BOWA), Minnesota.

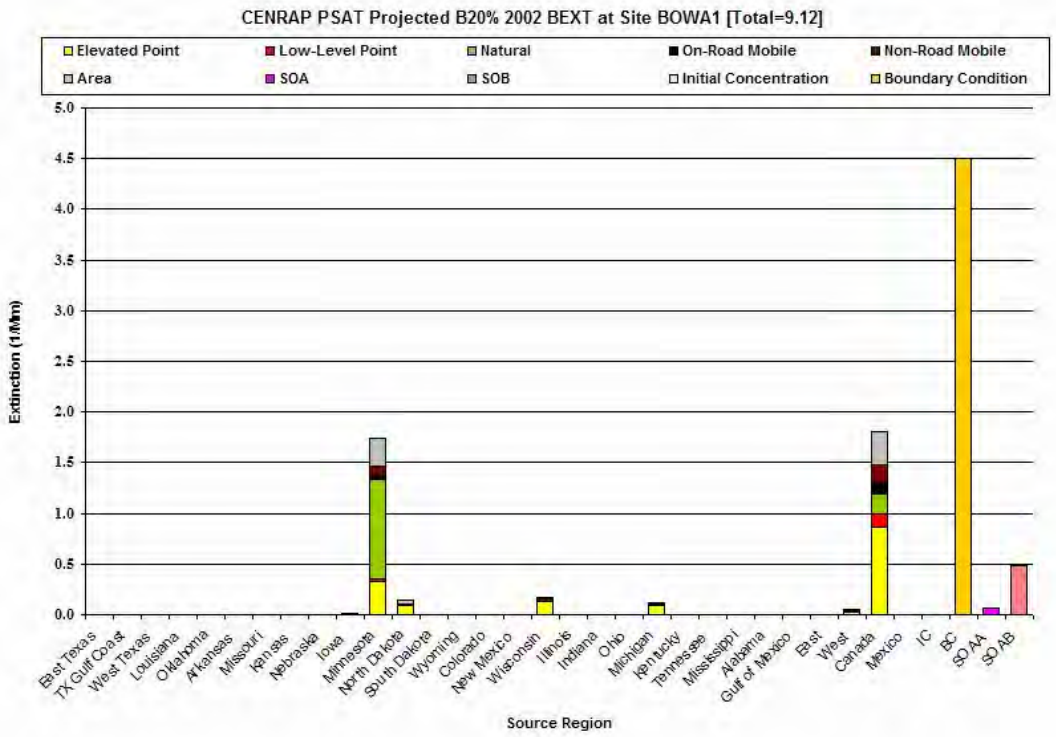

Figure E-4i. PSAT contributions by source region and source category to the average 2000-2004 Baseline extinction (Mm^{-1}) for the Best 20% visibility days at Boundary Waters (BOWA), Minnesota.

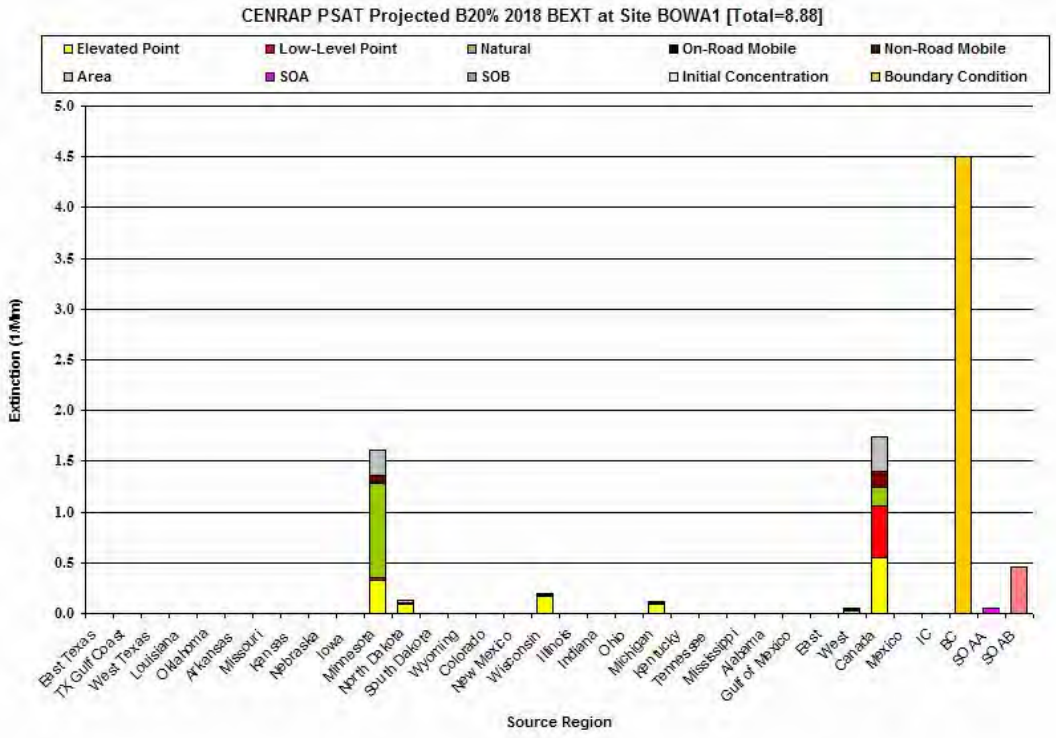

Figure E-4j. PSAT contributions by source region and source category to the average 2018 extinction (Mm^{-1}) for the Best 20% visibility days at Boundary Waters (BOWA), Minnesota.

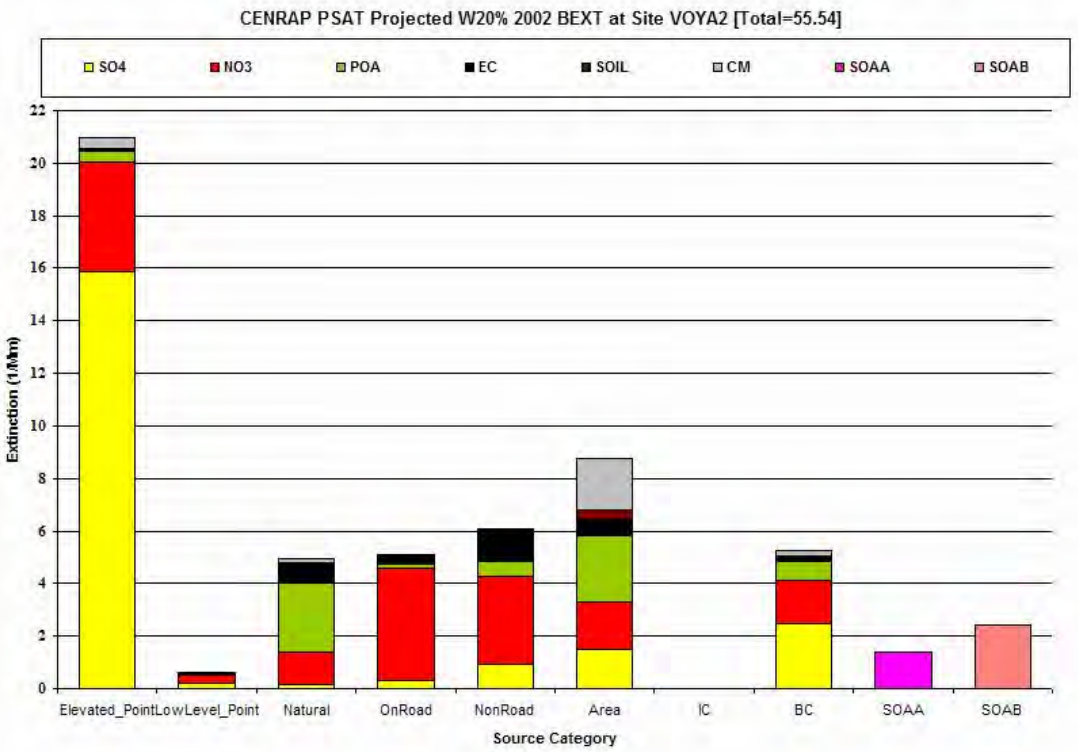

Figure E-5a. PSAT source categories by PM species contributions to the average 2000-2004 Baseline extinction (Mm^{-1}) for the Worst 20% visibility days at Voyageurs (VOYA), Minnesota.

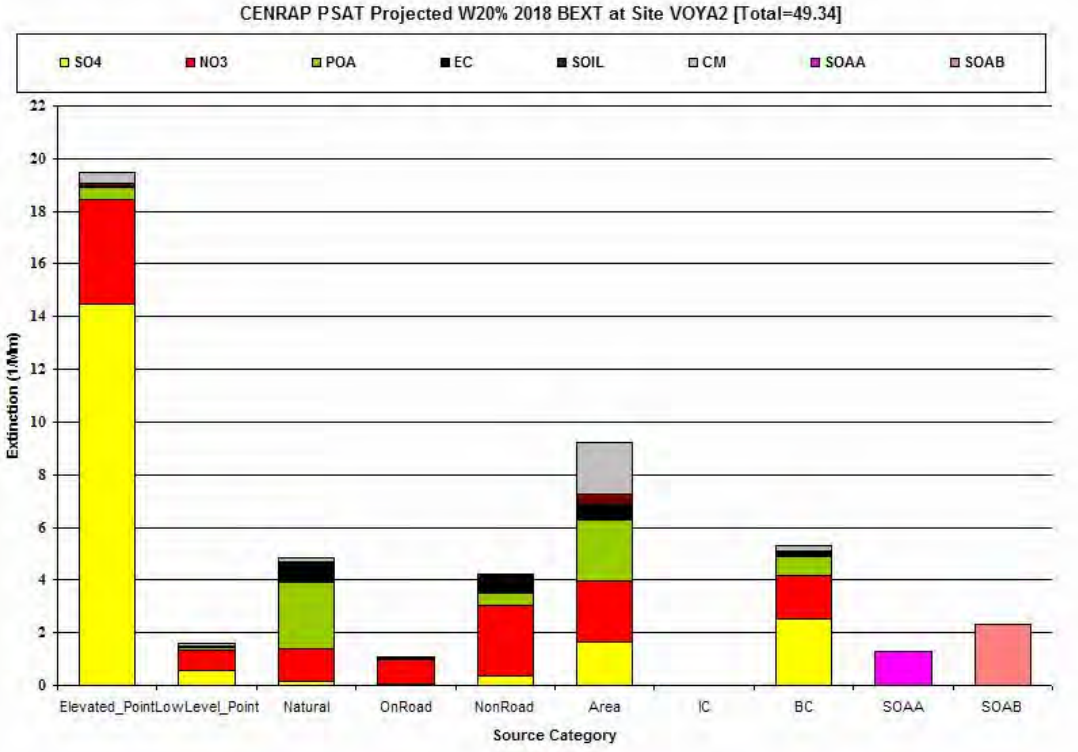

Figure E-5b. PSAT source category by PM species contributions to the average 2018 projected extinction (Mm^{-1}) for the Worst 20% visibility days at Voyageurs (VOYA), Minnesota.

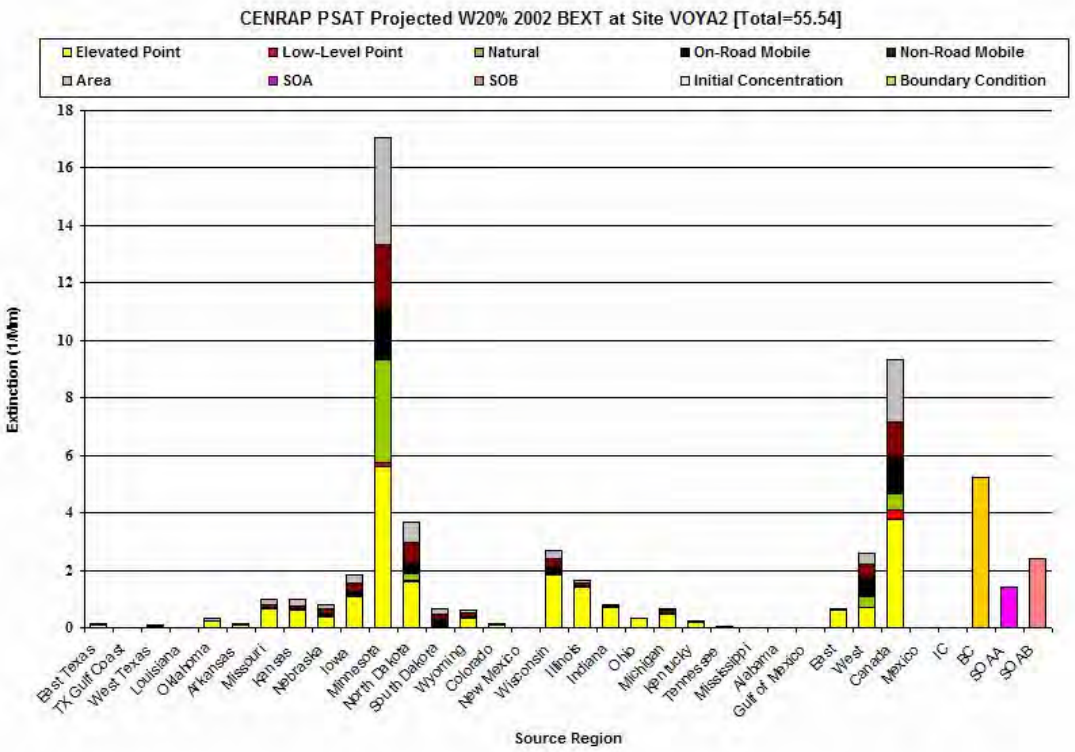

Figure E-5c. PSAT source region by source category contributions to the average 2000-2004 Baseline extinction (Mm^{-1}) for the Worst 20% visibility days at Voyageurs (VOYA), Minnesota.

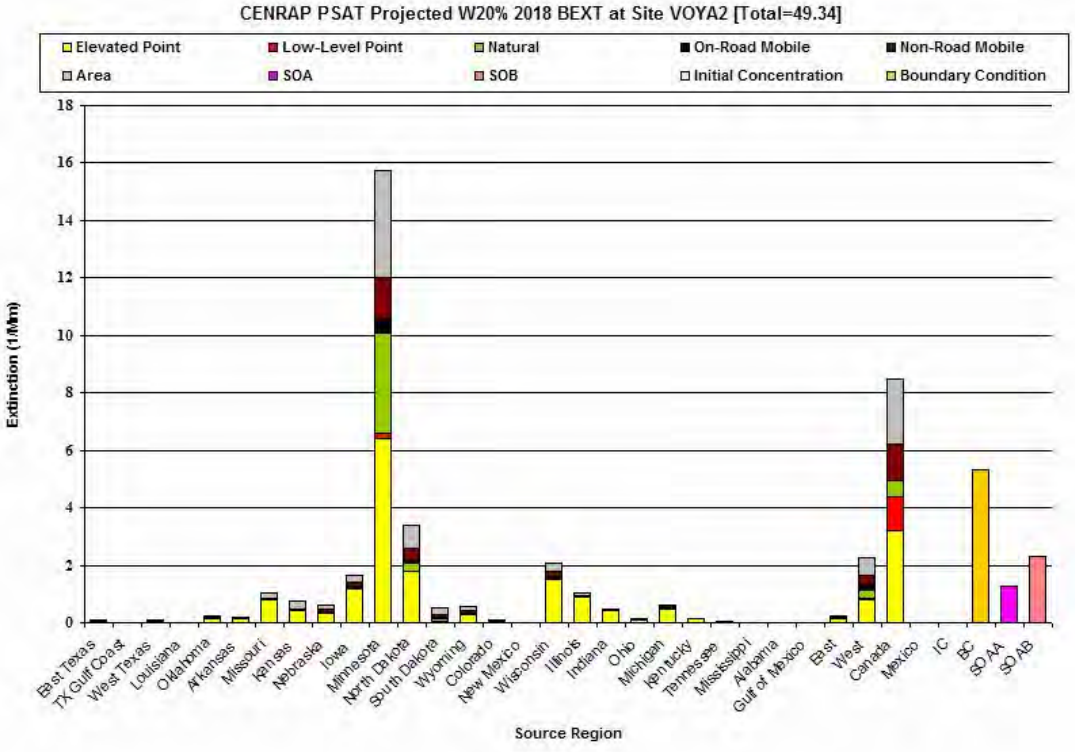

Figure E-5d. PSAT source region by source category contributions to the average 2018 extinction (Mm^{-1}) for the Worst 20% visibility days at Voyageurs (VOYA), Minnesota.

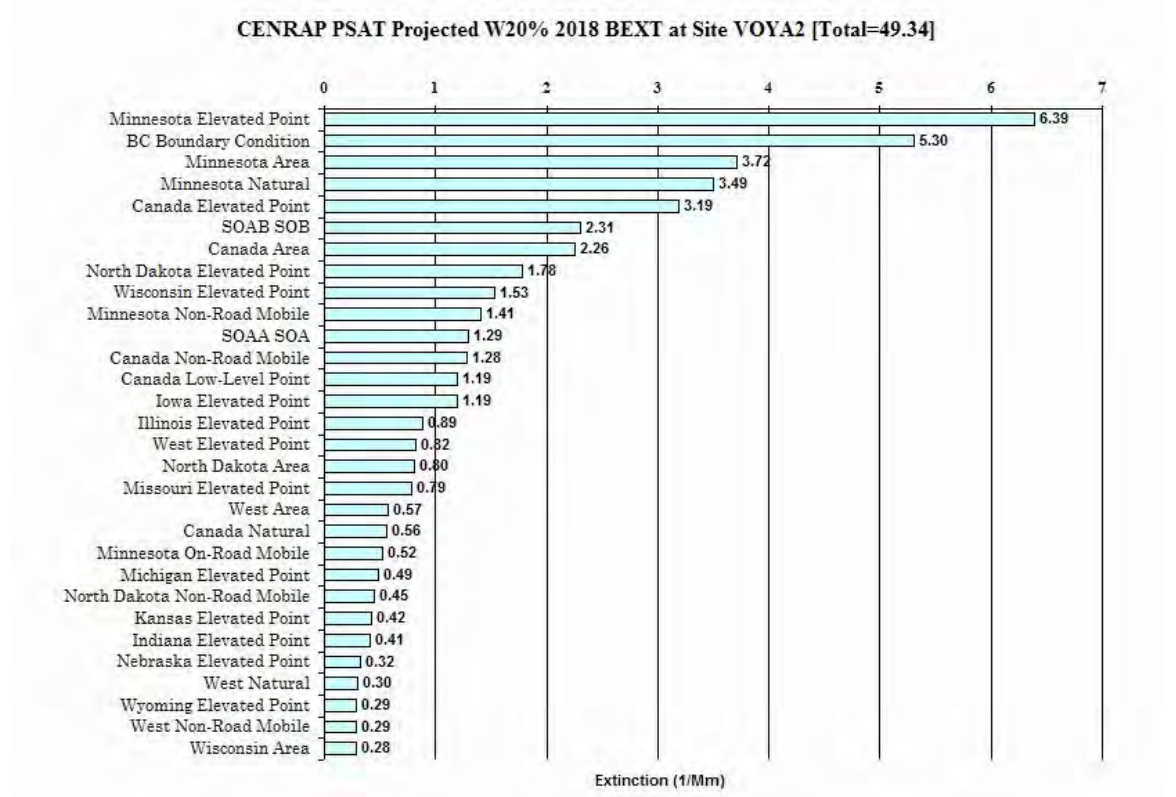

Figure E-5e. Ranked PSAT source region by source category contributions to the average 2018 extinction (Mm^{-1}) for the Worst 20% visibility days at Voyageurs (VOYA), Minnesota.

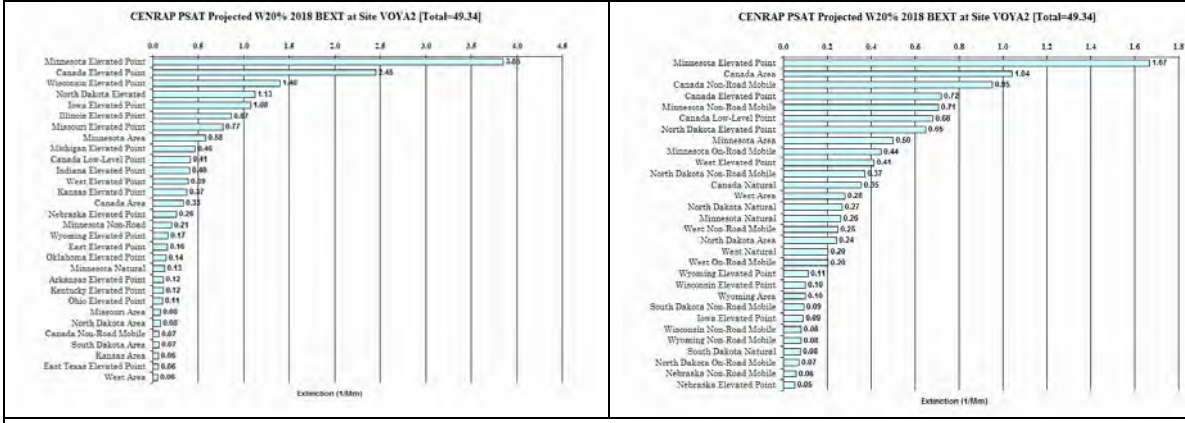

Figure E-5f. Ranked PSAT source region by source category contributions to the average 2018 SO4 (left) and NO3 (right) extinction (Mm^{-1}) for the Worst 20% visibility days at Voyageurs (VOYA), Minnesota.

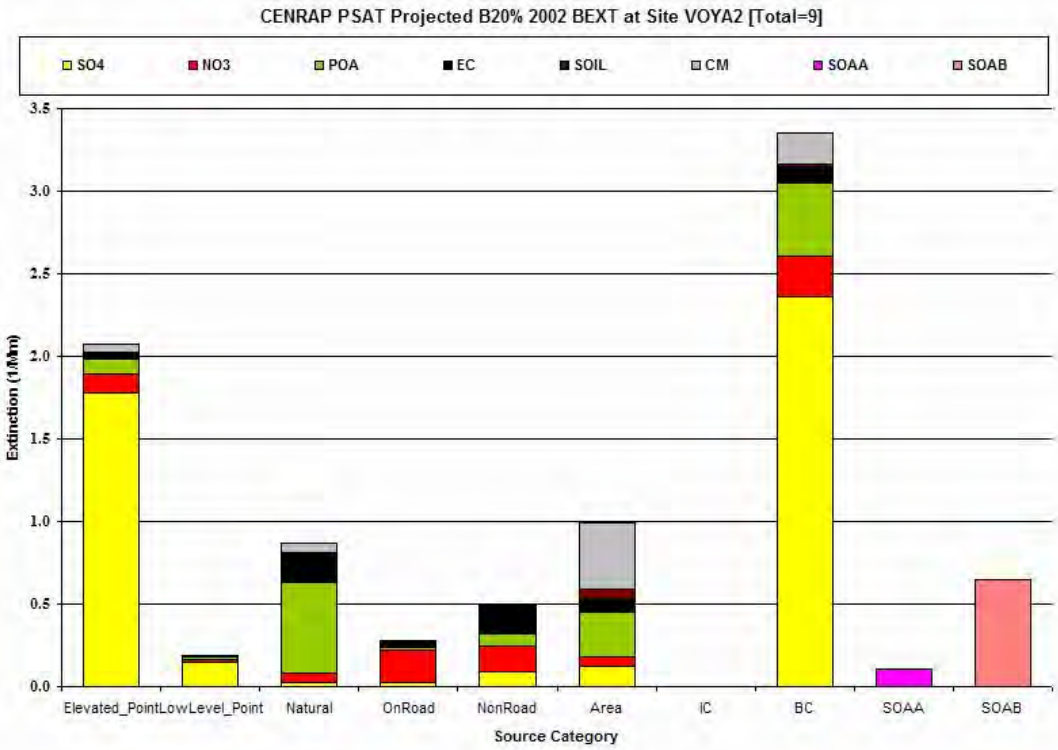

Figure E-5g. PSAT contributions by source category and PM species to the average 2000-2004 Baseline extinction (Mm^{-1}) for the Best 20% visibility days at Voyageurs (VOYA), Minnesota.

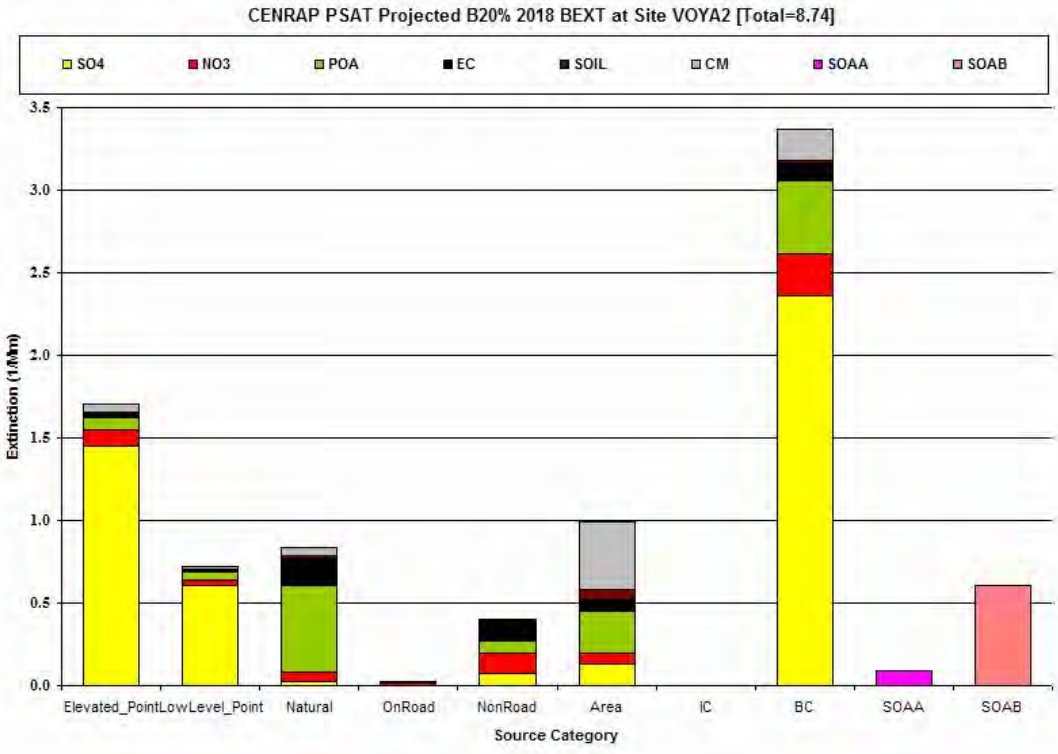

Figure E-5h. PSAT contributions by source category and PM species to the average 2018 extinction (Mm^{-1}) for the Best 20% visibility days at Voyageurs (VOYA), Minnesota.

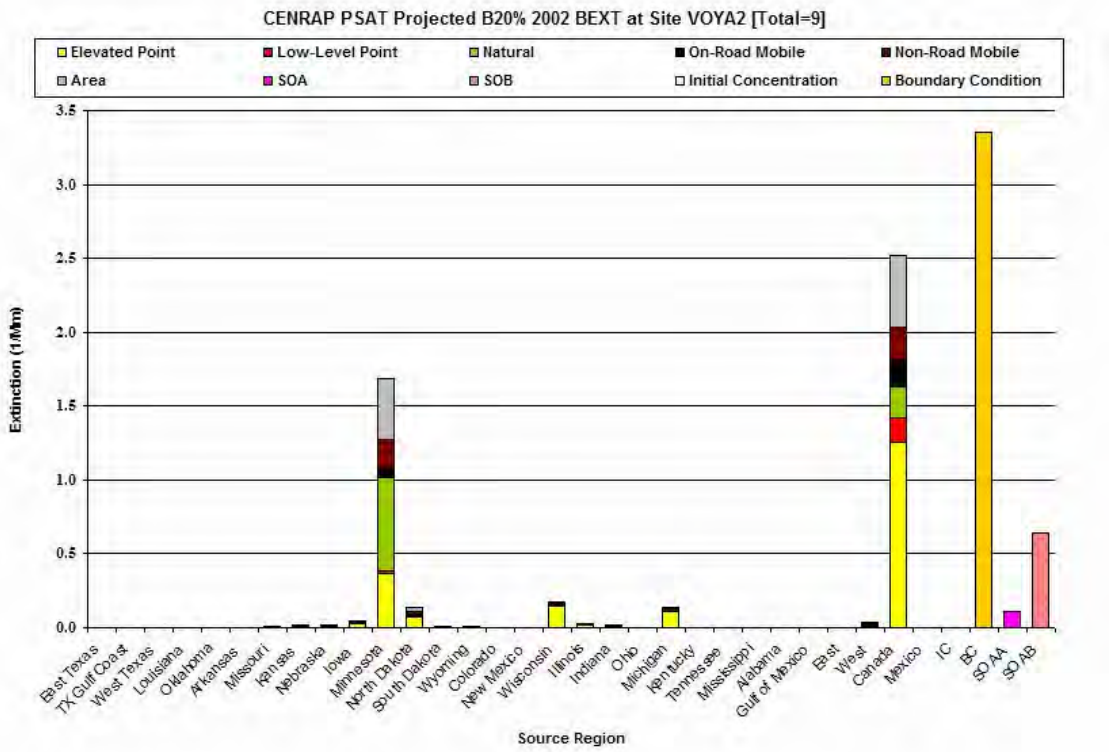

Figure E-5i. PSAT contributions by source region and source category to the average 2000-2004 Baseline extinction (Mm^{-1}) for the Best 20% visibility days at Voyageurs (VOYA), Minnesota.

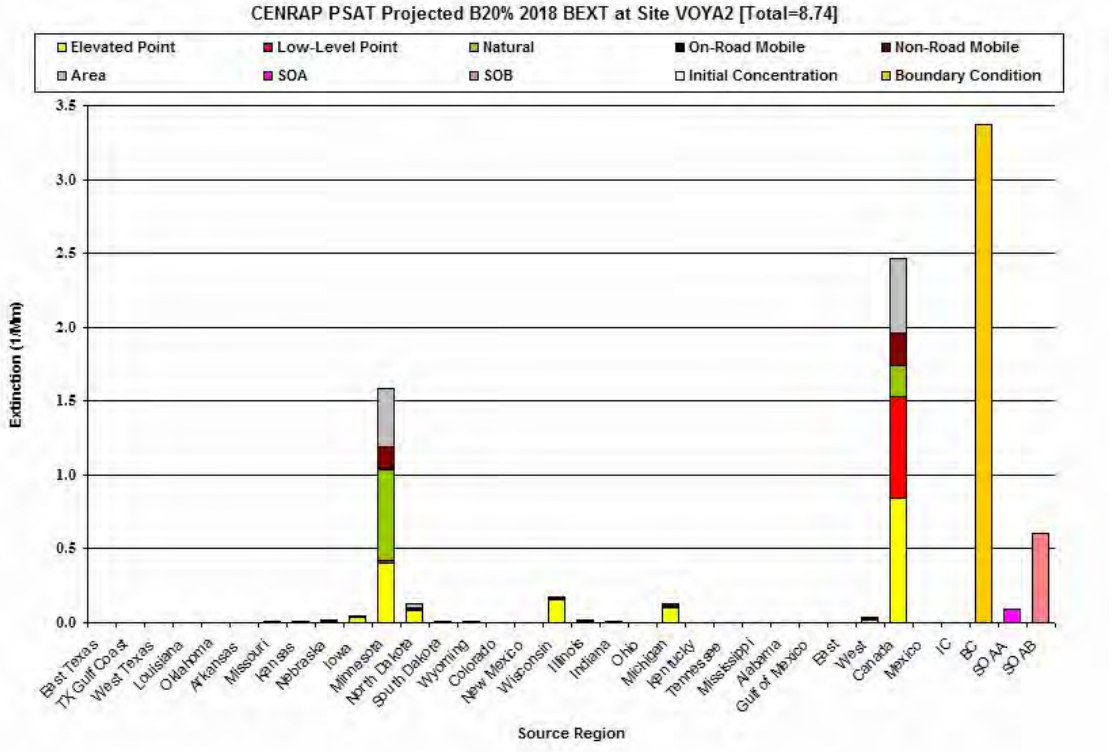

Figure E-5j. PSAT contributions by source region and source category to the average 2018 extinction (Mm^{-1}) for the Best 20% visibility days at Voyageurs (VOYA), Minnesota.

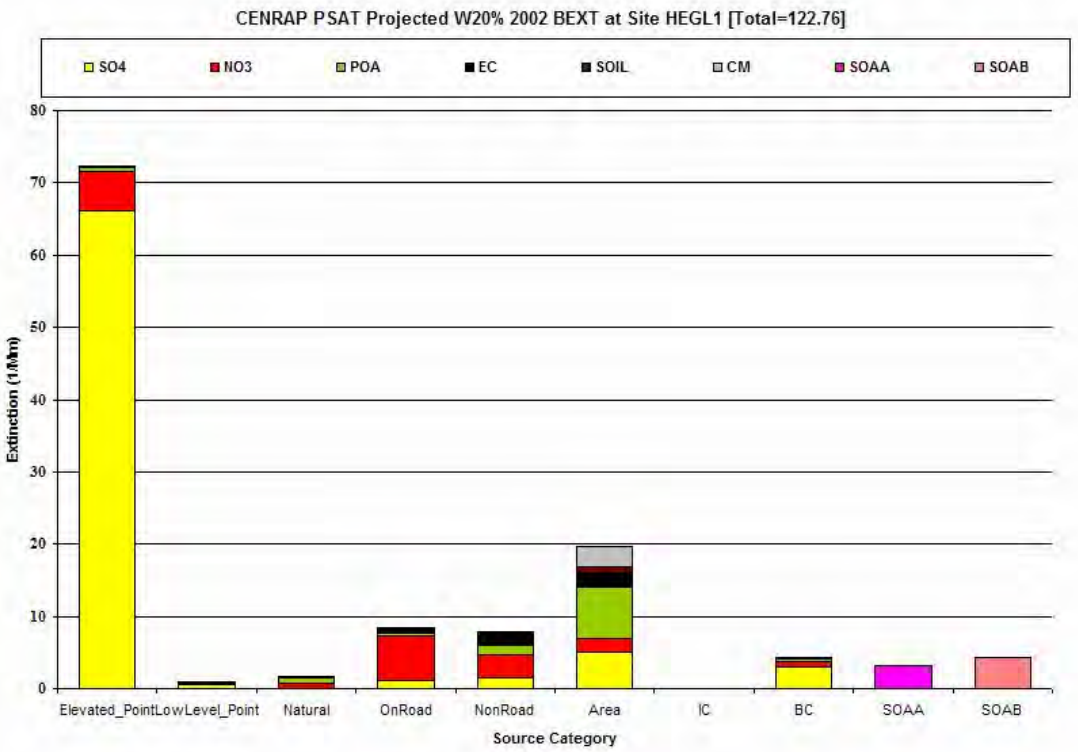

Figure E-6a. PSAT source categories by PM species contributions to the average 2000-2004 Baseline extinction (Mm^{-1}) for the Worst 20% visibility days at Hercules Glade (HEGL), Missouri.

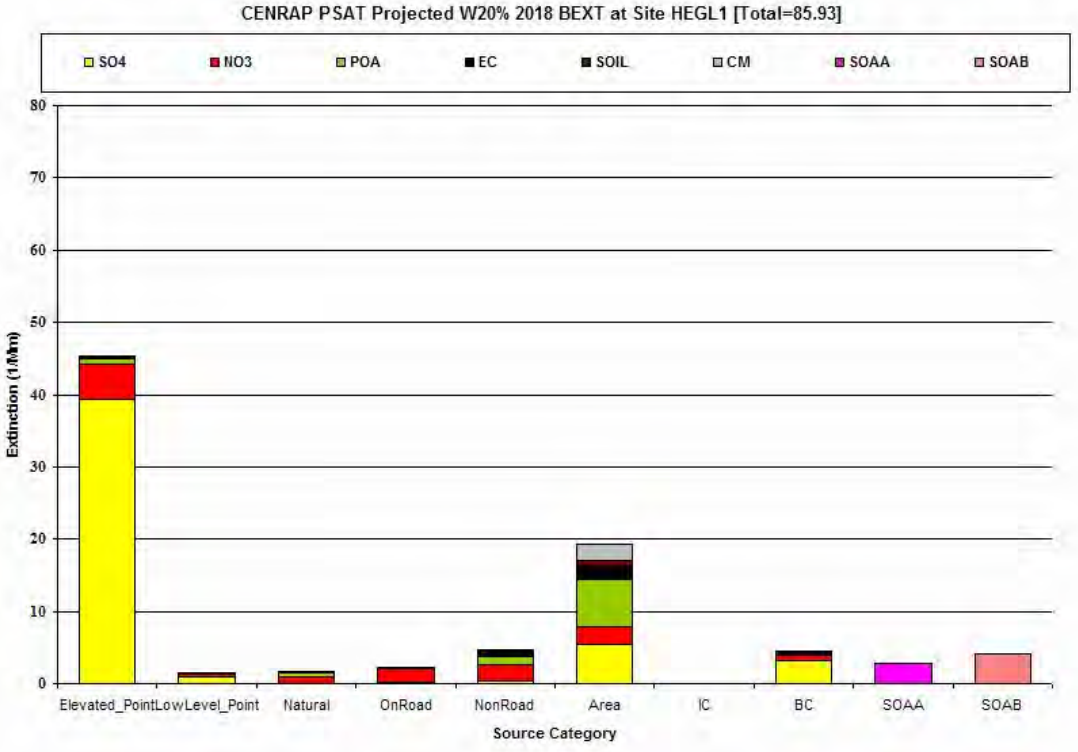

Figure E-6b. PSAT source category by PM species contributions to the average 2018 projected extinction (Mm^{-1}) for the Worst 20% visibility days at Hercules Glade (HEGL), Missouri.

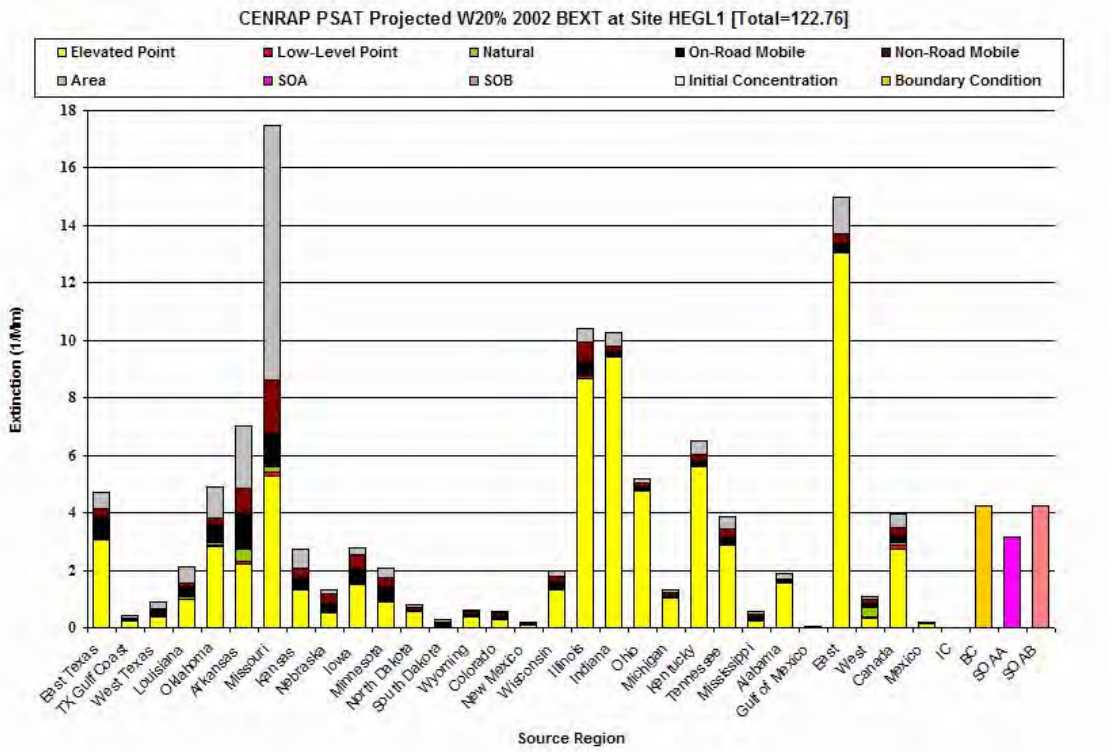

Figure E-6c. PSAT source region by source category contributions to the average 2000-2004 Baseline extinction (Mm^{-1}) for the Worst 20% visibility days at Hercules Glade (HEGL), Missouri.

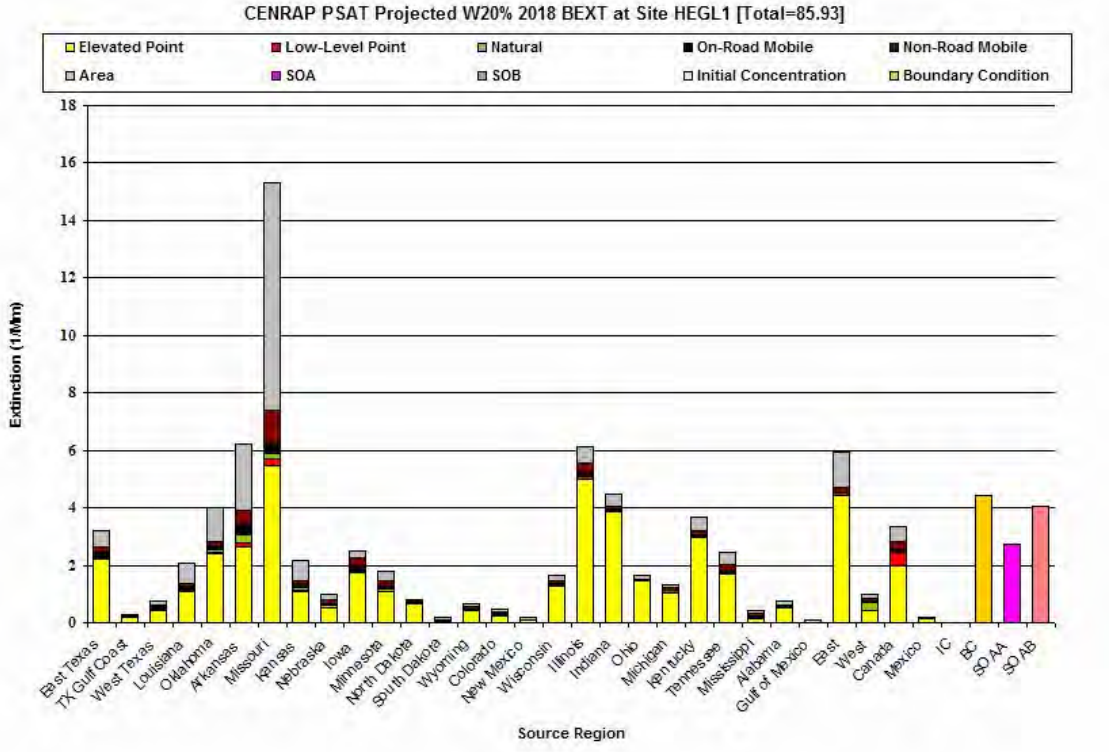

Figure E-6d. PSAT source region by source category contributions to the average 2018 extinction (Mm^{-1}) for the Worst 20% visibility days at Hercules Glade (HEGL), Missouri.

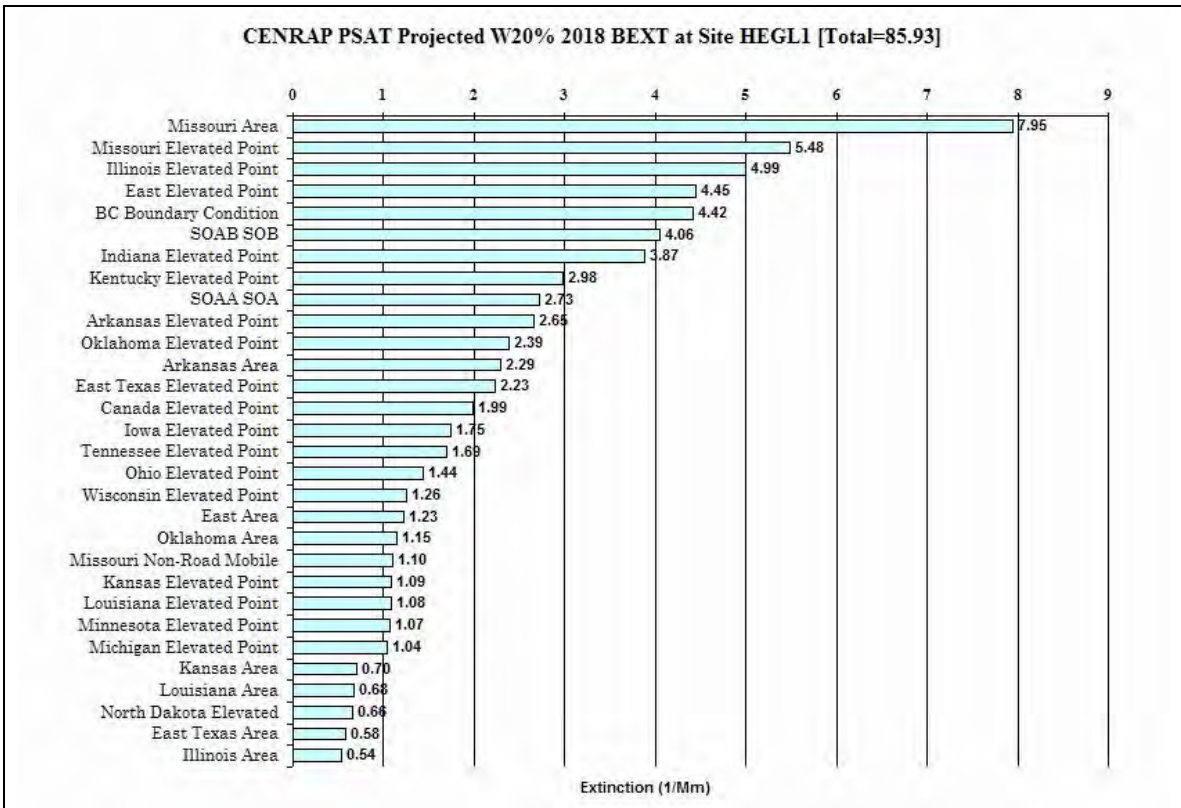

Figure E-6e. Ranked PSAT source region by source category contributions to the average 2018 extinction (Mm^{-1}) for the Worst 20% visibility days at Hercules Glade (HEGL), Missouri.

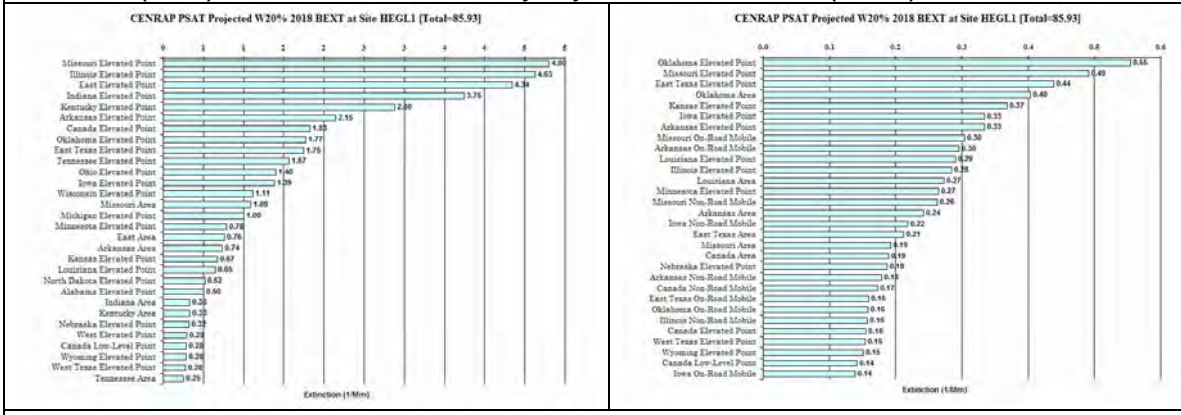

Figure E-6f. Ranked PSAT source region by source category contributions to the average 2018 SO4 (left) and NO3 (right) extinction (Mm^{-1}) for the Worst 20% visibility days at Hercules Glade (HEGL), Missouri.

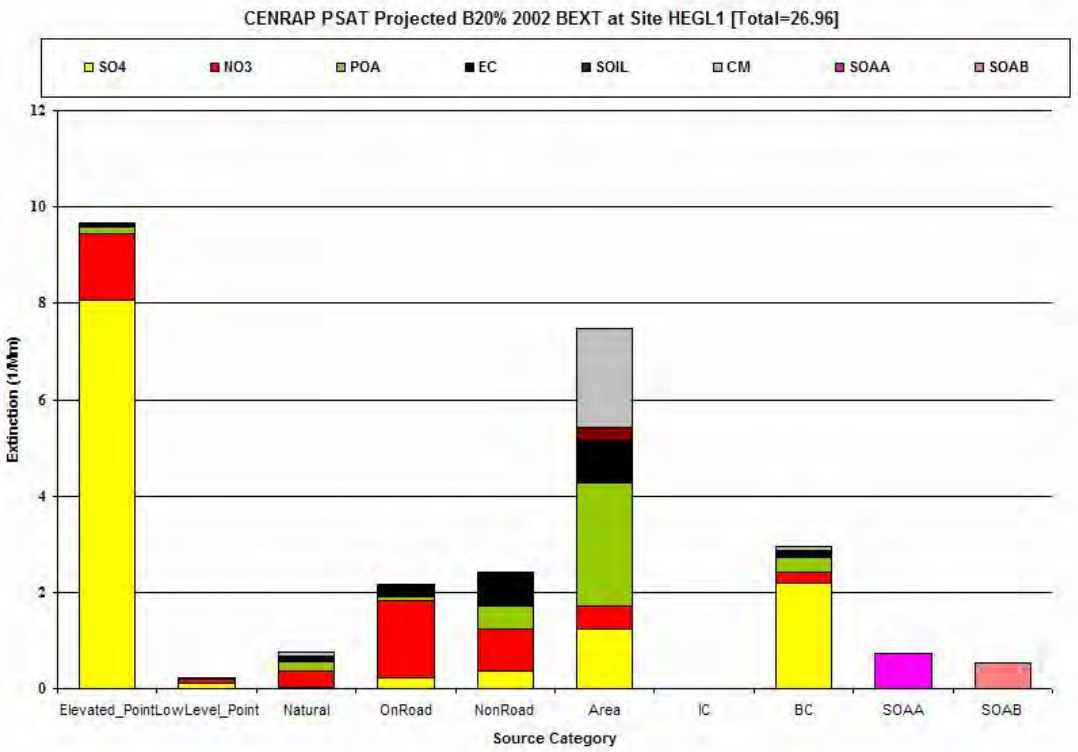

Figure E-6g. PSAT contributions by source category and PM species to the average 2000-2004 Baseline extinction (Mm^{-1}) for the Best 20% visibility days at Hercules Glade (HEGL), Missouri.

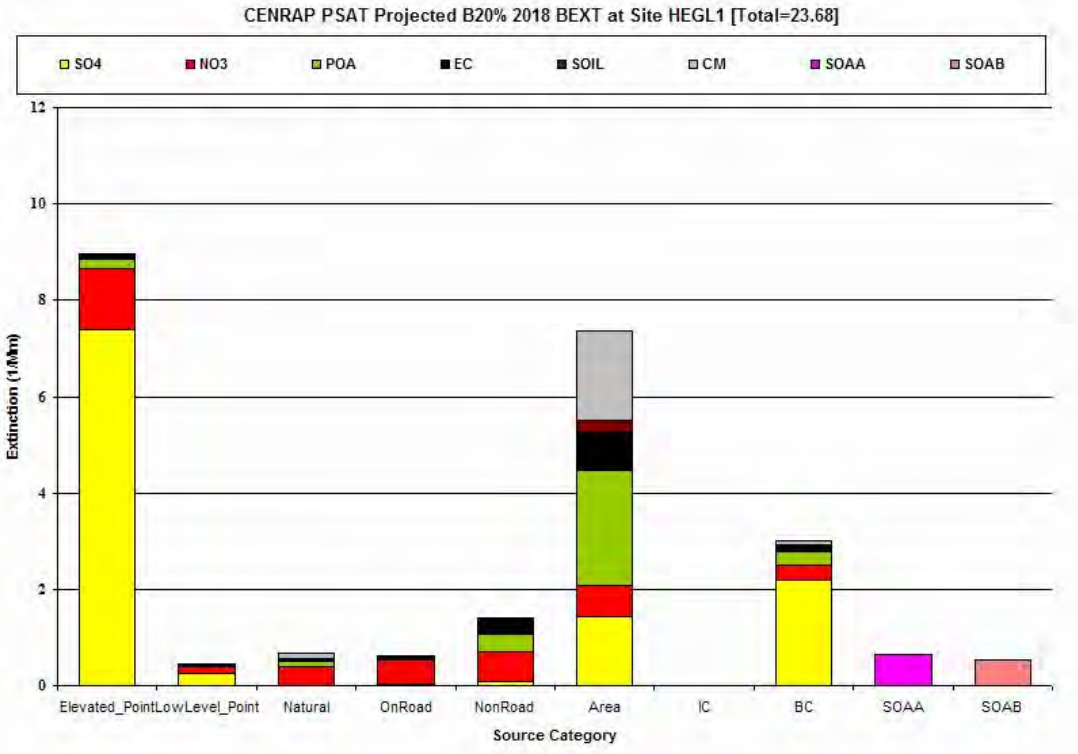

Figure E-6h. PSAT contributions by source category and PM species to the average 2018 extinction (Mm^{-1}) for the Best 20% visibility days at Hercules Glade (HEGL), Missouri.

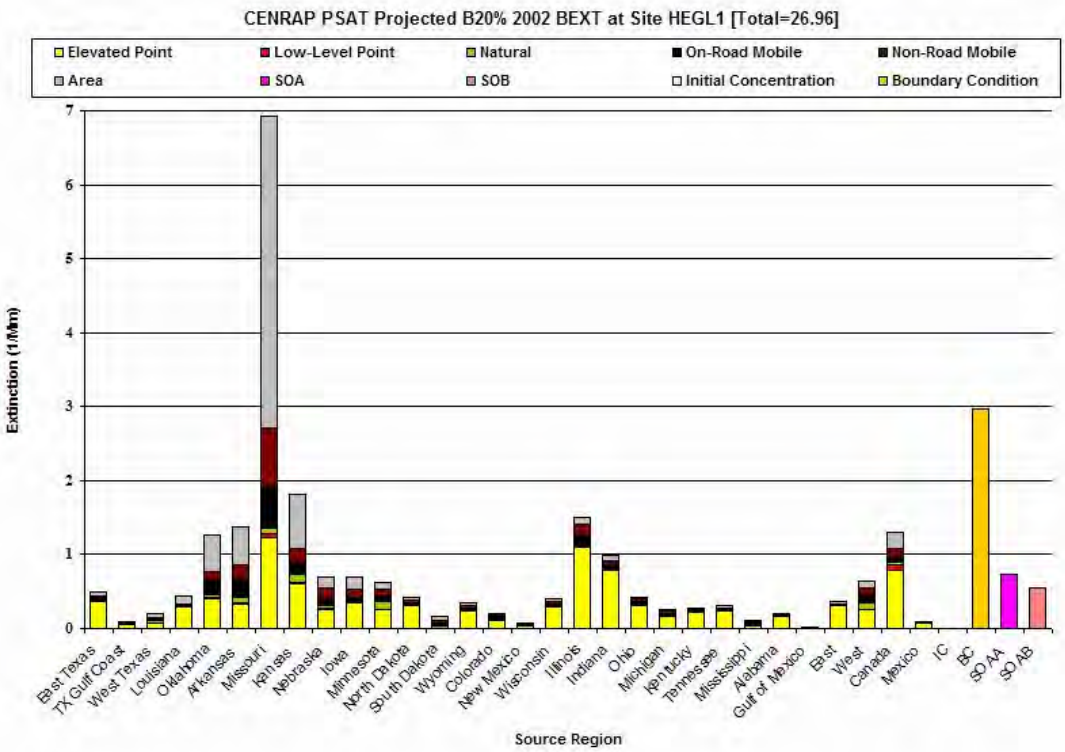

Figure E-6i. PSAT contributions by source region and source category to the average 2000-2004 Baseline extinction (Mm^{-1}) for the Best 20% visibility days at Hercules Glade (HEGL), Missouri.

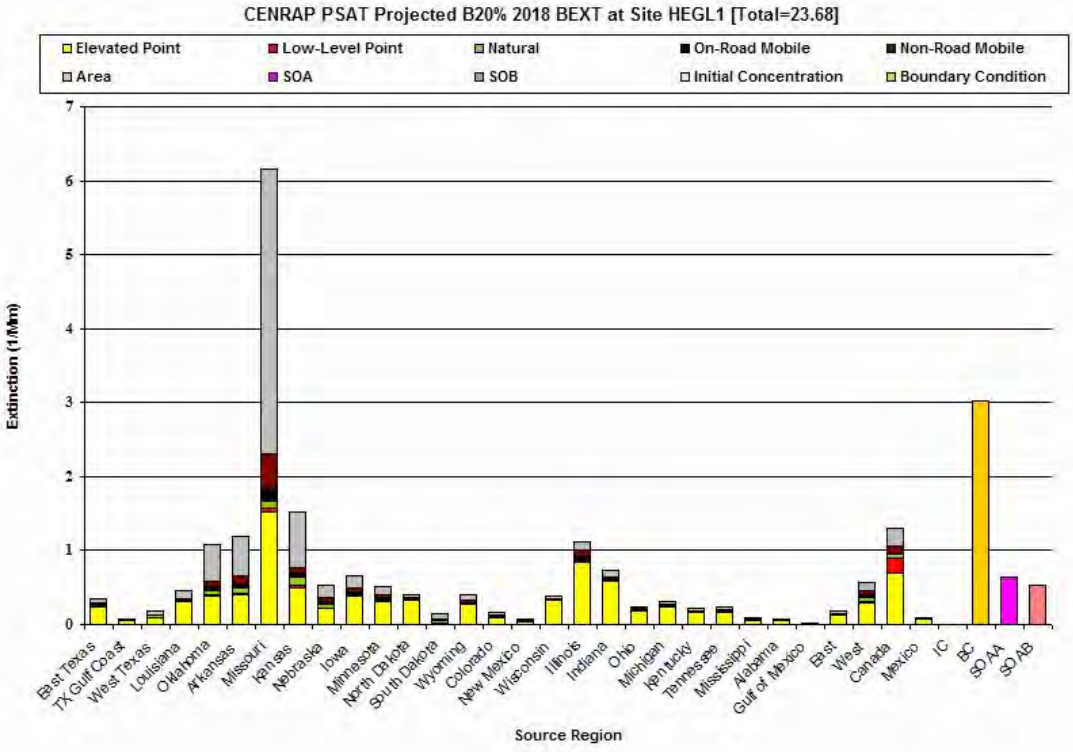

Figure E-6j. PSAT contributions by source region and source category to the average 2018 extinction (Mm^{-1}) for the Best 20% visibility days at Voyageurs Hercules Glade (HEGL), Missouri.

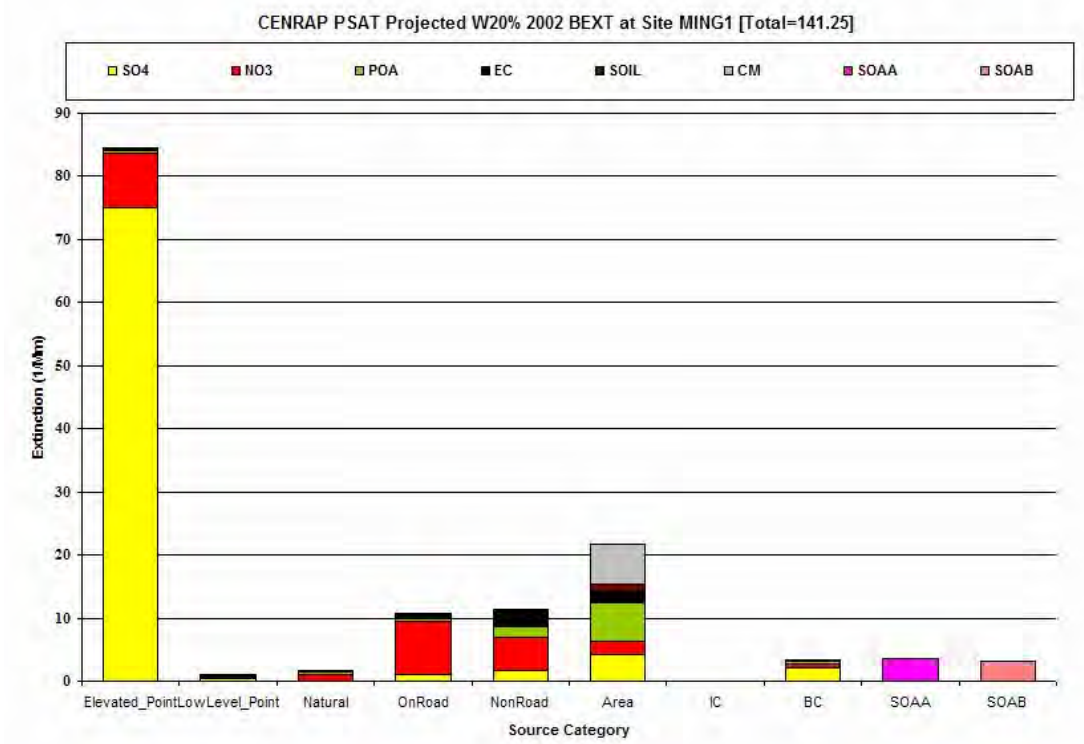

Figure E-7a. PSAT source categories by PM species contributions to the average 2000-2004 Baseline extinction (Mm^{-1}) for the Worst 20% visibility days at Mingo (MING), Missouri.

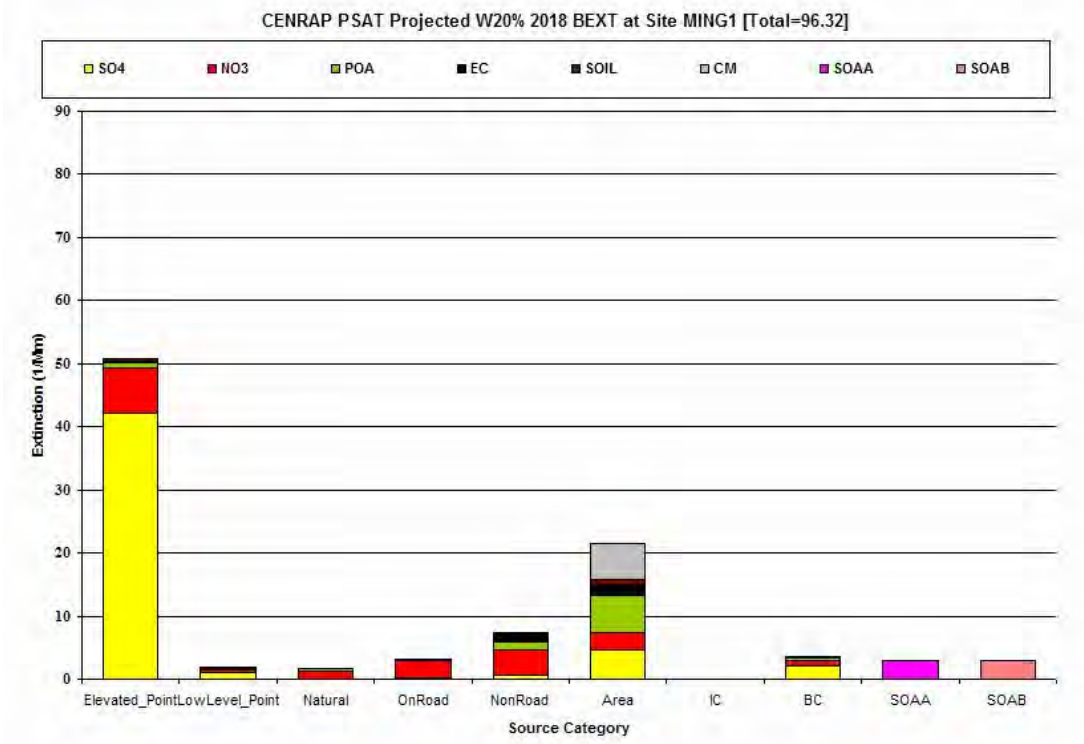

Figure E-7b. PSAT source category by PM species contributions to the average 2018 projected extinction (Mm^{-1}) for the Worst 20% visibility days at Mingo (MING), Missouri.

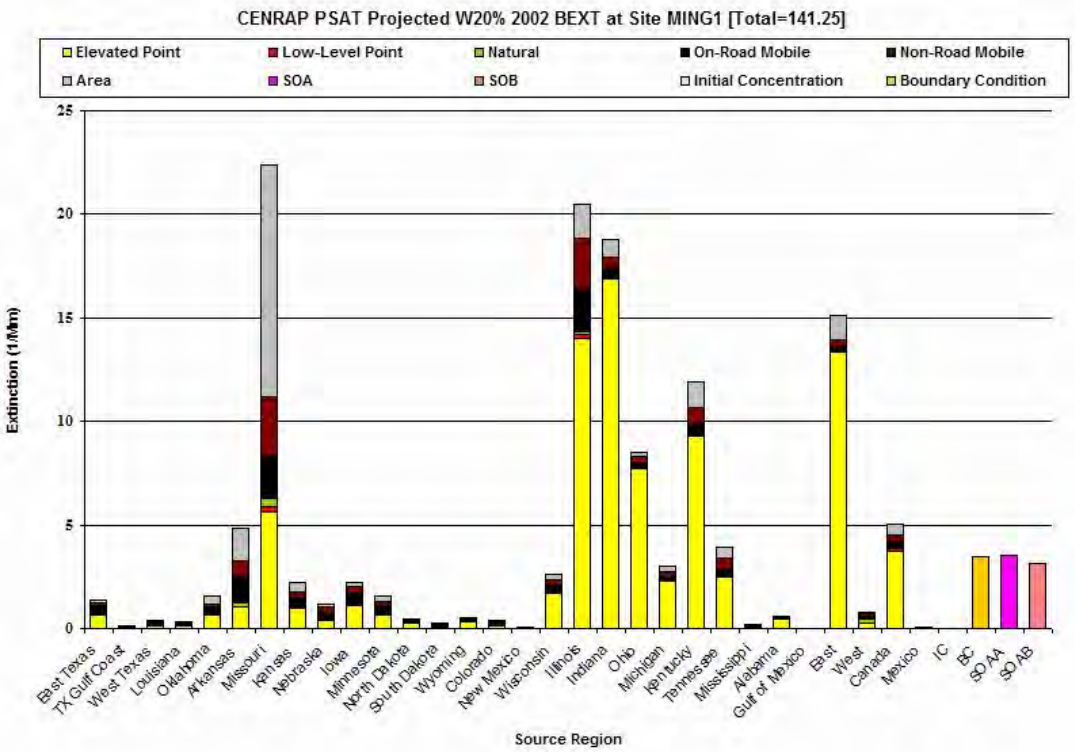

Figure E-7c. PSAT source region by source category contributions to the average 2000-2004 Baseline extinction (Mm^{-1}) for the Worst 20% visibility days at Mingo (MING), Missouri.

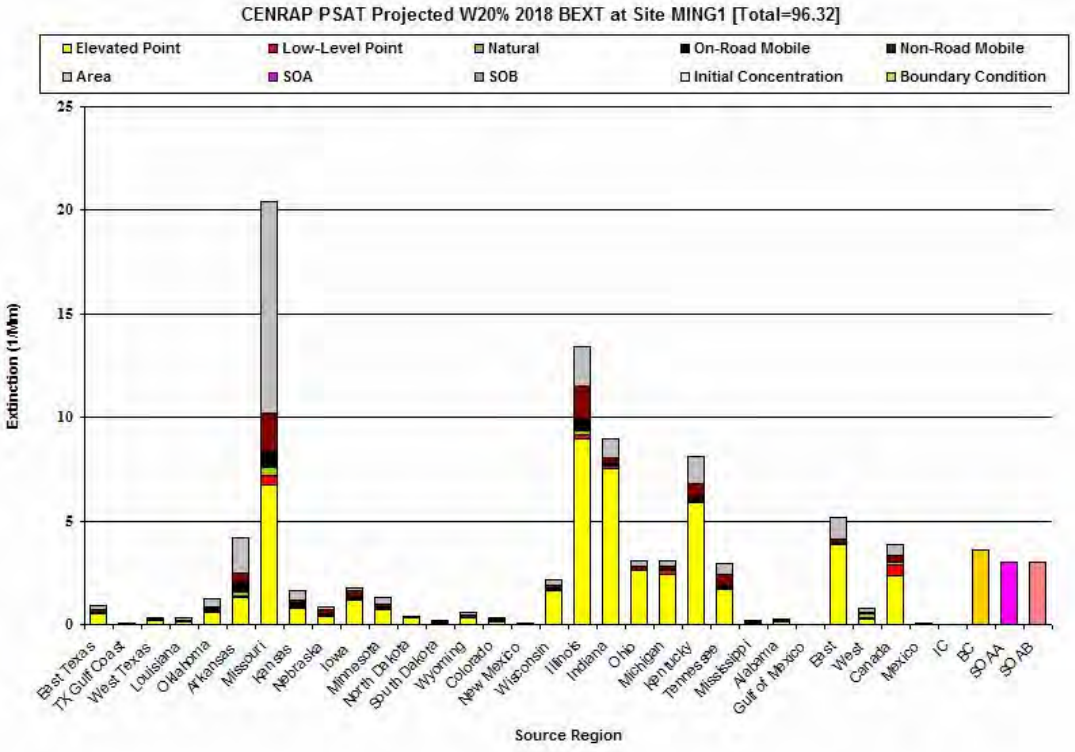

Figure E-7d. PSAT source region by source category contributions to the average 2018 extinction (Mm^{-1}) for the Worst 20% visibility days at Mingo (MING), Missouri.

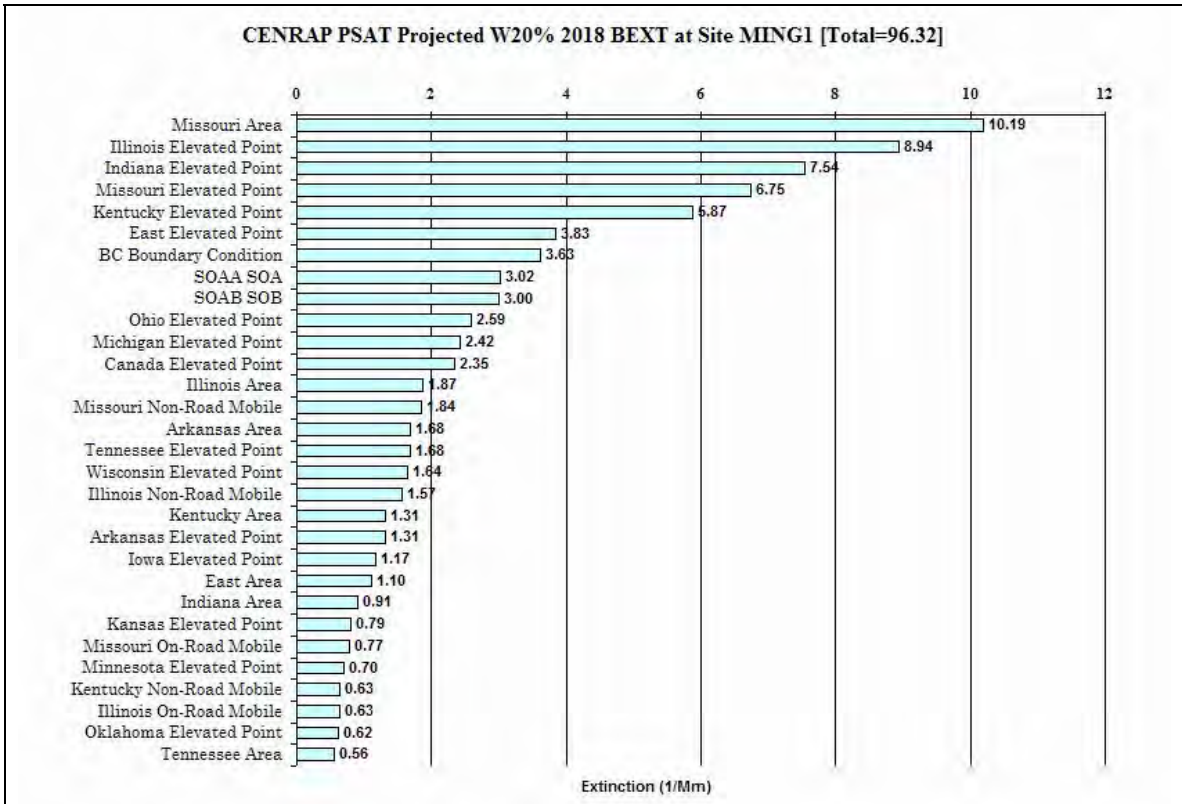

Figure E-7e. Ranked PSAT source region by source category contributions to the average 2018 extinction (Mm^{-1}) for the Worst 20% visibility days at Mingo (MING), Missouri.

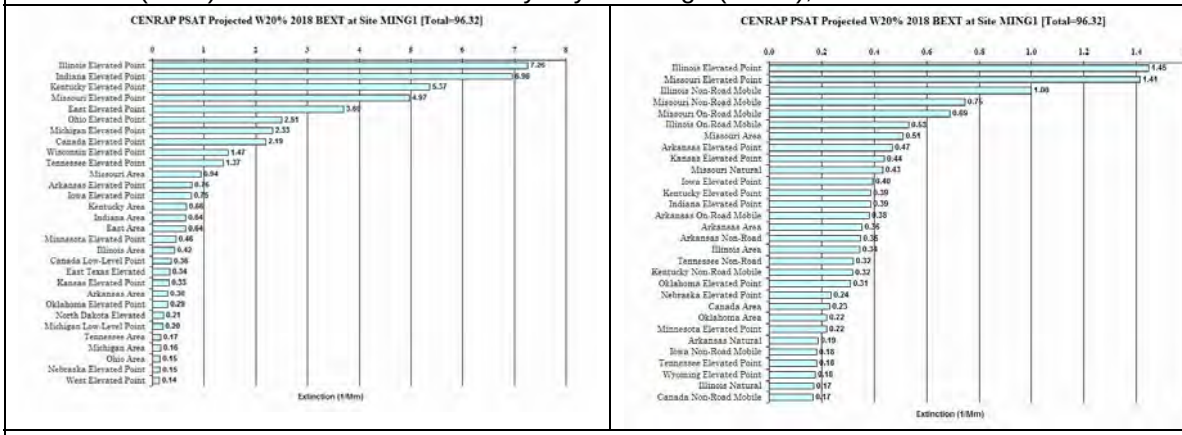

Figure E-7f. Ranked PSAT source region by source category contributions to the average 2018 SO4 (left) and NO3 (right) extinction (Mm^{-1}) for the Worst 20% visibility days at Mingo (MING), Missouri.

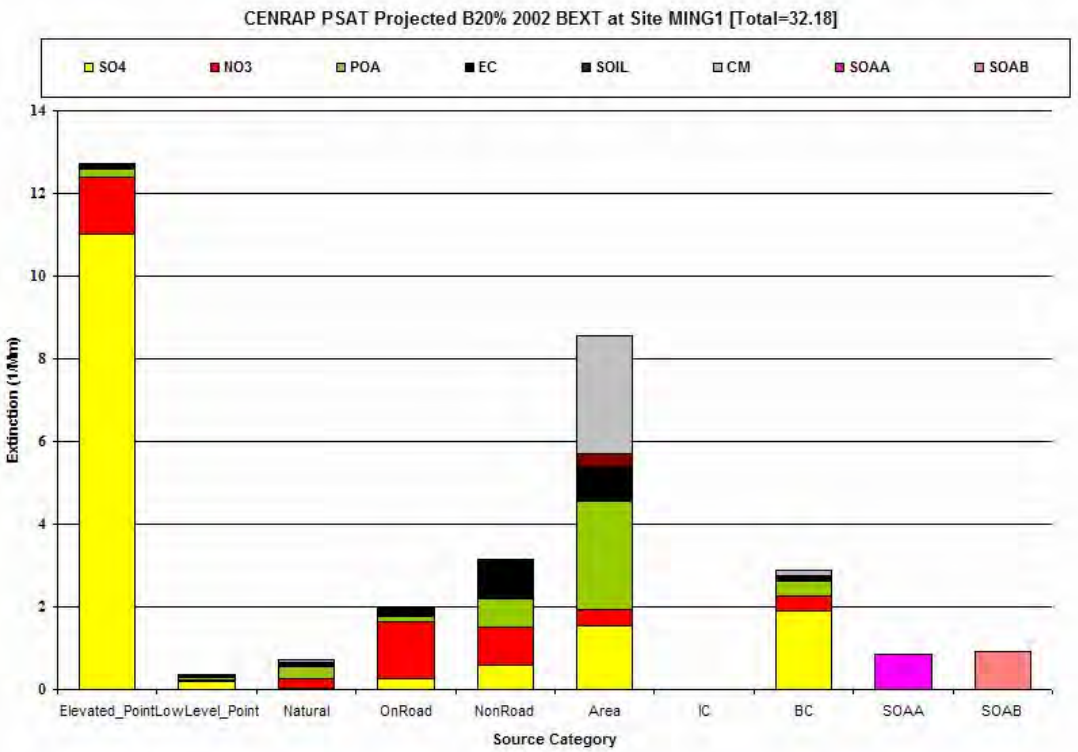

Figure E-7g. PSAT contributions by source category and PM species to the average 2000-2004 Baseline extinction (Mm^{-1}) for the Best 20% visibility days at Mingo (MING), Missouri.

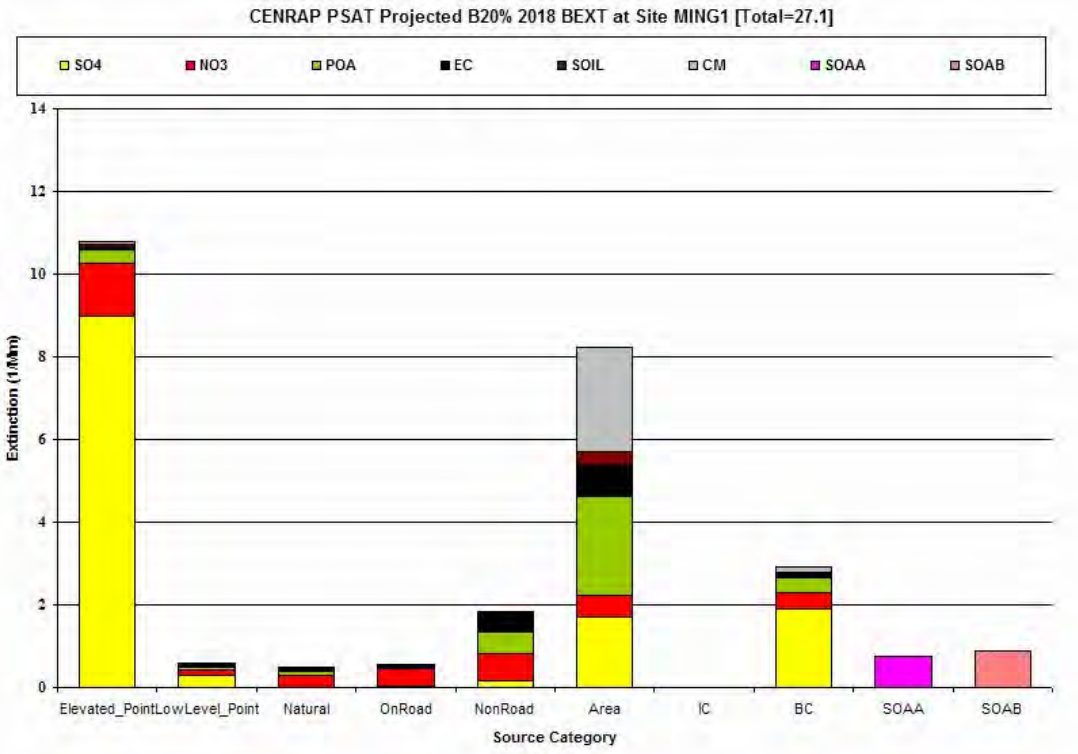

Figure E-7h. PSAT contributions by source category and PM species to the average 2018 extinction (Mm^{-1}) for the Best 20% visibility days at Mingo (MING), Missouri.

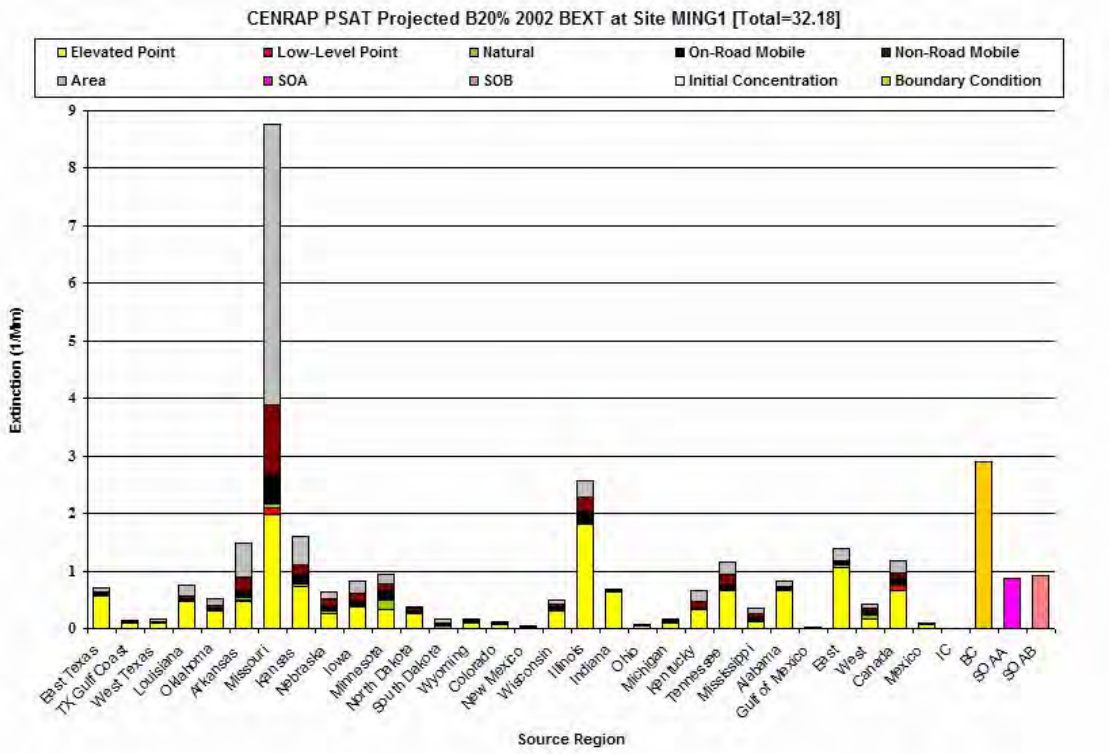

Figure E-7i. PSAT contributions by source region and source category to the average 2000-2004 Baseline extinction (Mm^{-1}) for the Best 20% visibility days at Mingo (MING), Missouri.

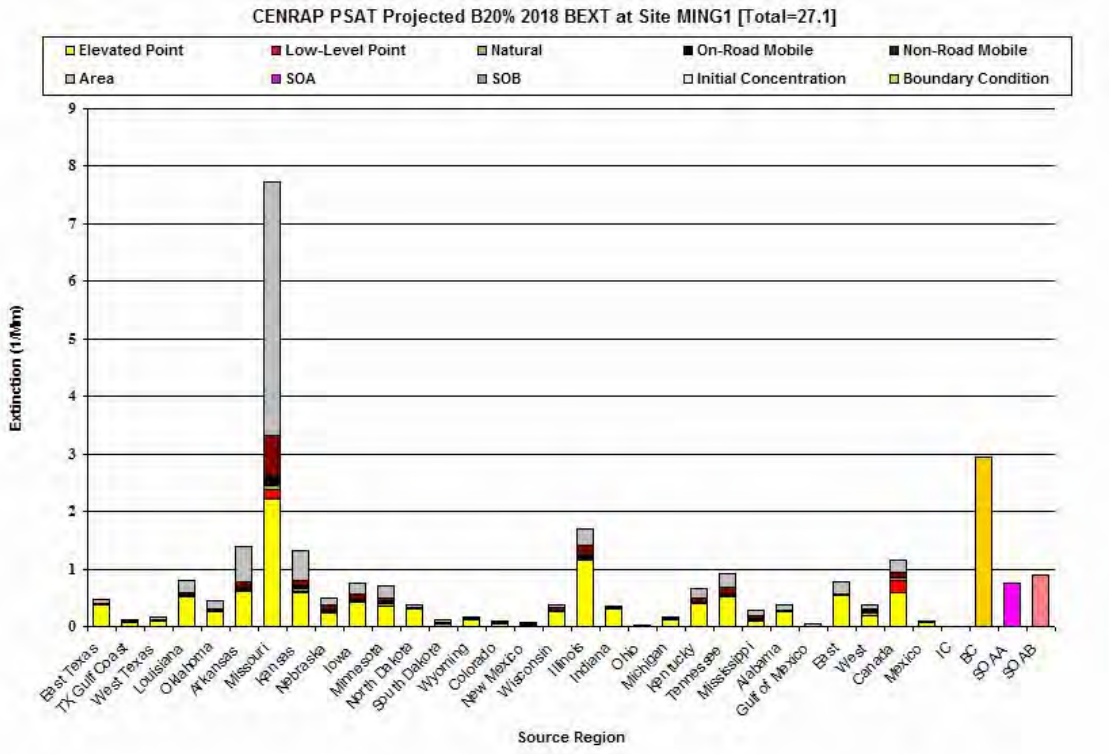

Figure E-7j. PSAT contributions by source region and source category to the average 2018 extinction (Mm^{-1}) for the Best 20% visibility days at Mingo (MING), Missouri.

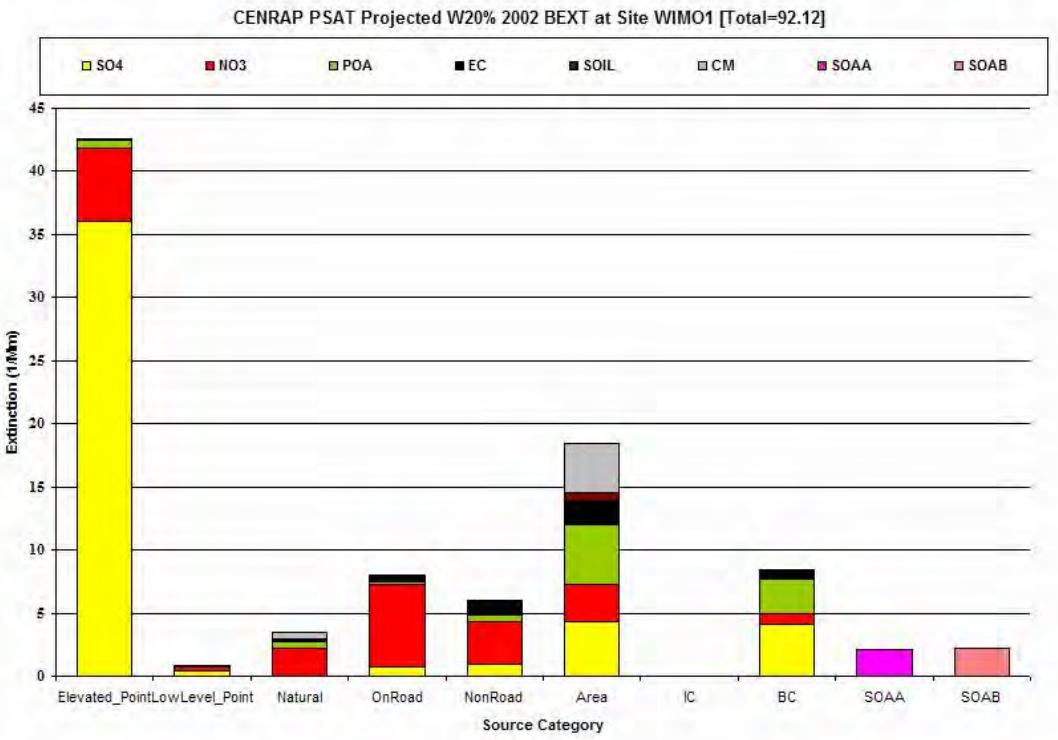

Figure E-8a. PSAT source categories by PM species contributions to the average 2000-2004 Baseline extinction (Mm^{-1}) for the Worst 20% visibility days at Wichita Mountains (WIMO), Oklahoma.

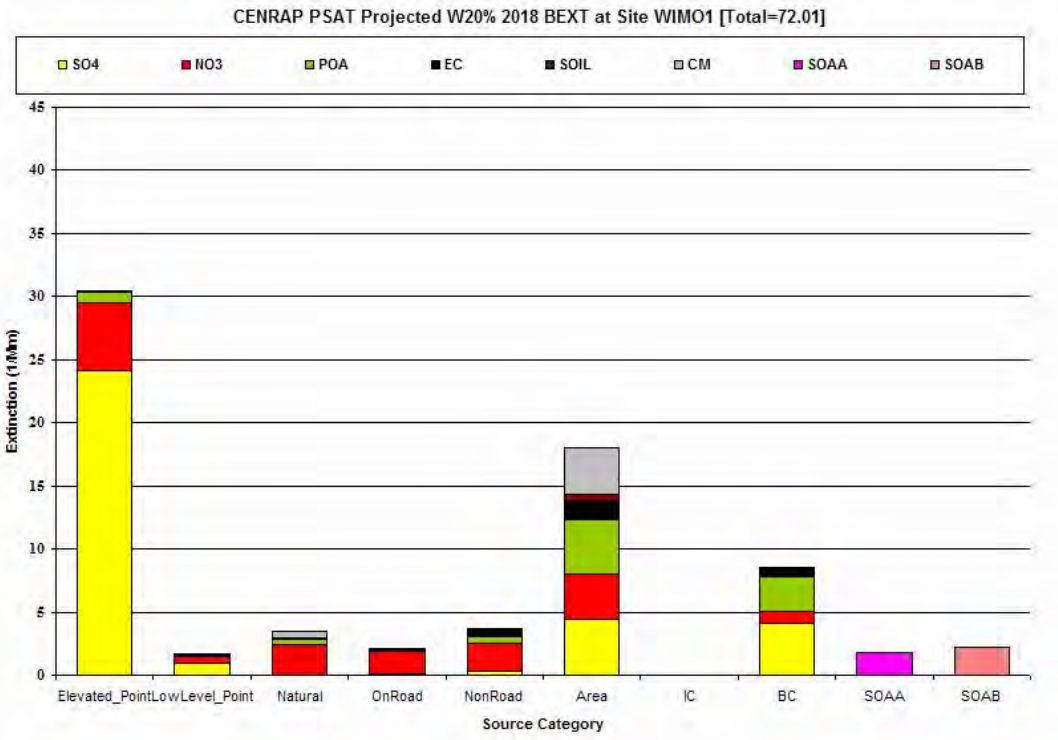

Figure E-8b. PSAT source category by PM species contributions to the average 2018 projected extinction (Mm^{-1}) for the Worst 20% visibility days at Wichita Mountains (WIMO), Oklahoma.

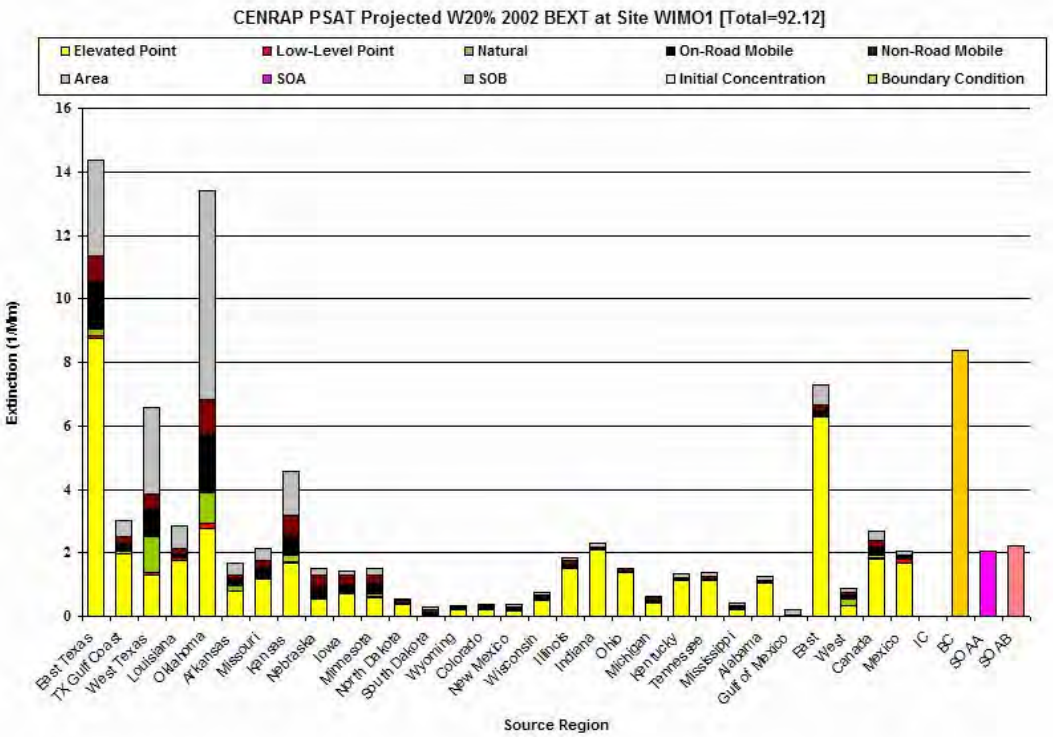

Figure E-8c. PSAT source region by source category contributions to the average 2000-2004 Baseline extinction (Mm^{-1}) for the Worst 20% visibility days at Wichita Mountains (WIMO), Oklahoma.

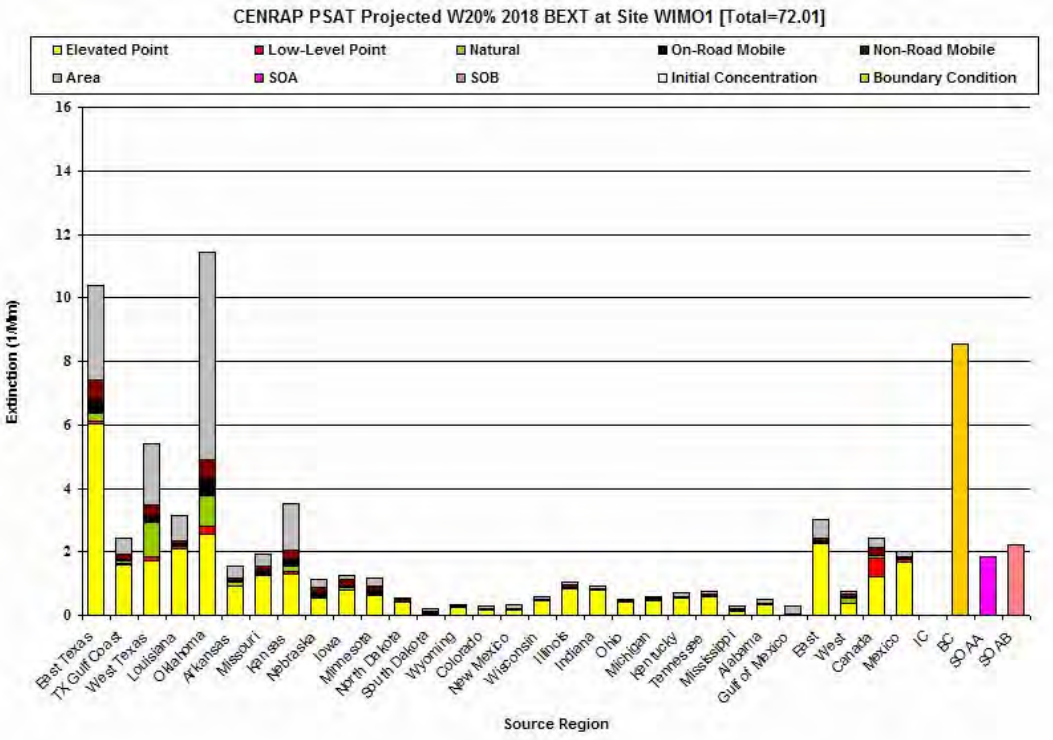

Figure E-8d. PSAT source region by source category contributions to the average 2018 extinction (Mm^{-1}) for the Worst 20% visibility days at Wichita Mountains (WIMO), Oklahoma.

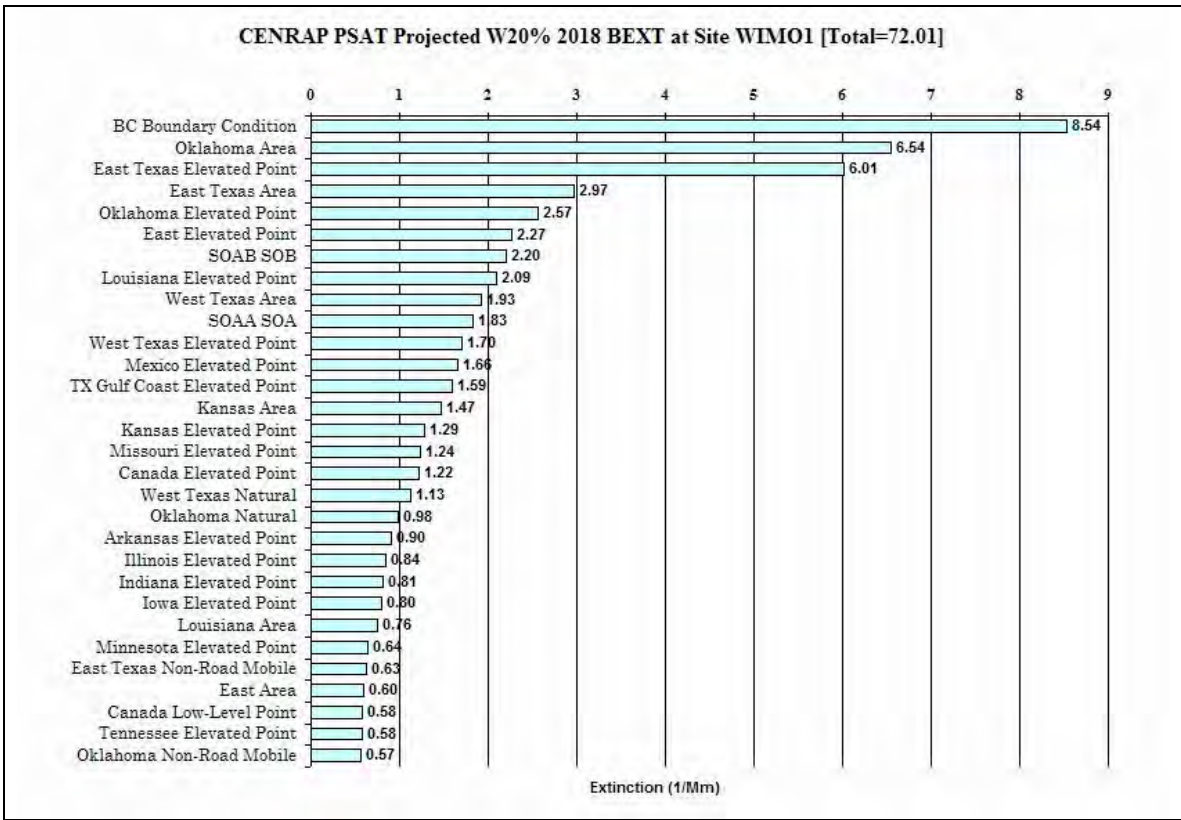

Figure E-8e. Ranked PSAT source region by source category contributions to the average 2018 extinction (Mm^{-1}) for the Worst 20% visibility days at Wichita Mountains (WIMO), Oklahoma.

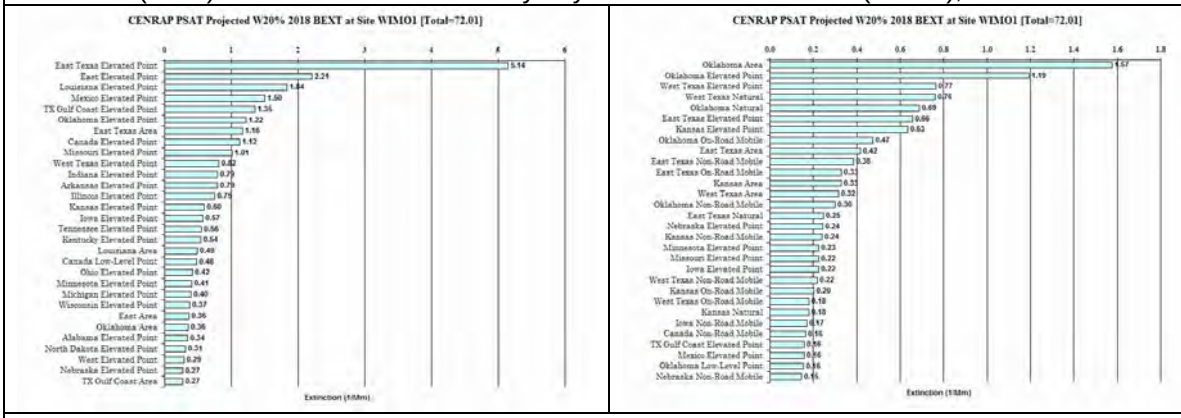

Figure E-8f. Ranked PSAT source region by source category contributions to the average 2018 SO4 (left) and NO3 (right) extinction (Mm^{-1}) for the Worst 20% visibility days at Wichita Mountains (WIMO), Oklahoma.

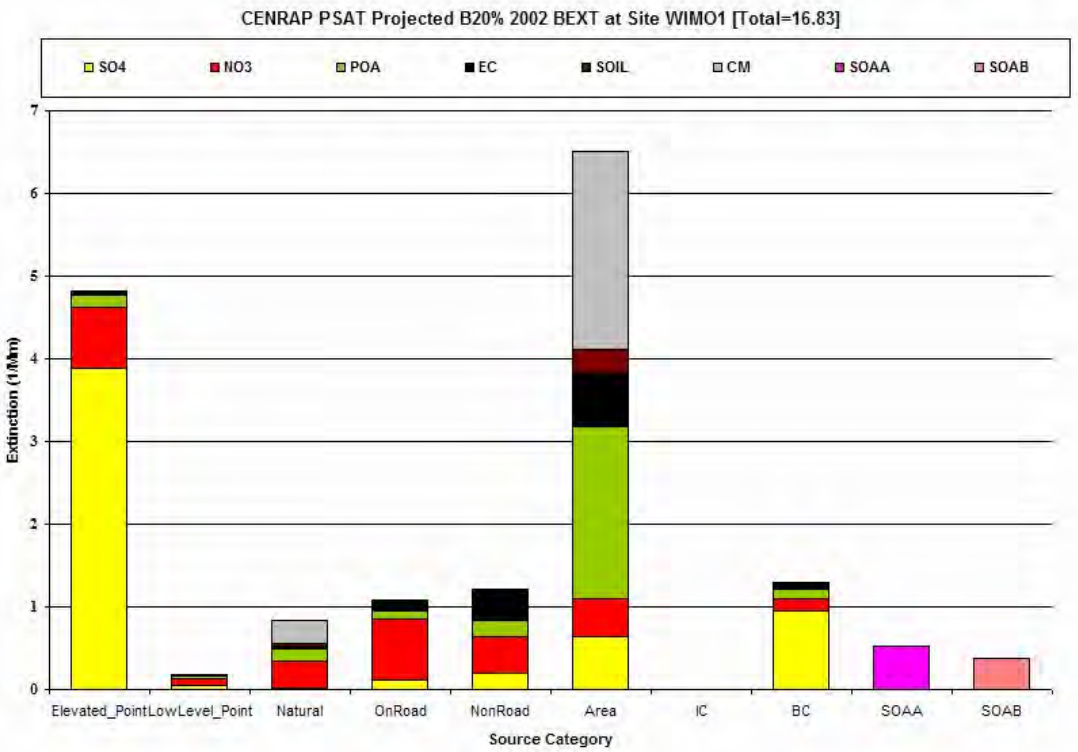

Figure E-8g. PSAT contributions by source category and PM species to the average 2000-2004 Baseline extinction (Mm^{-1}) for the Best 20% visibility days at Wichita Mountains (WIMO), Oklahoma.

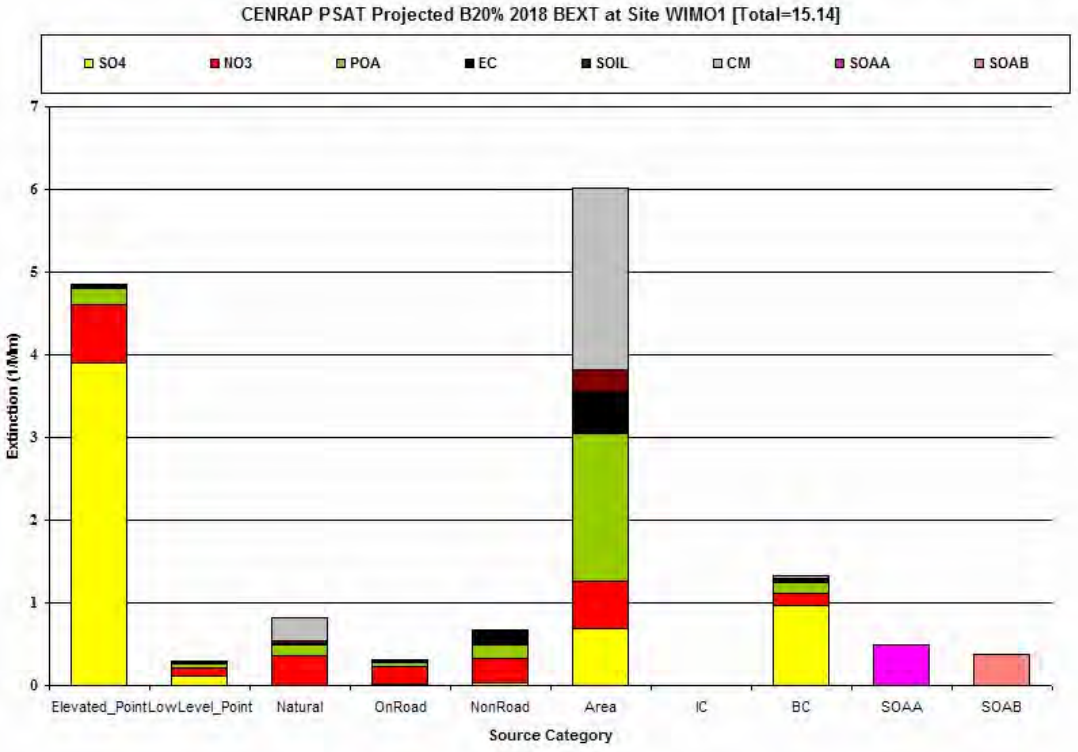

Figure E-8h. PSAT contributions by source category and PM species to the average 2018 extinction (Mm^{-1}) for the Best 20% visibility days at Wichita Mountains (WIMO), Oklahoma.

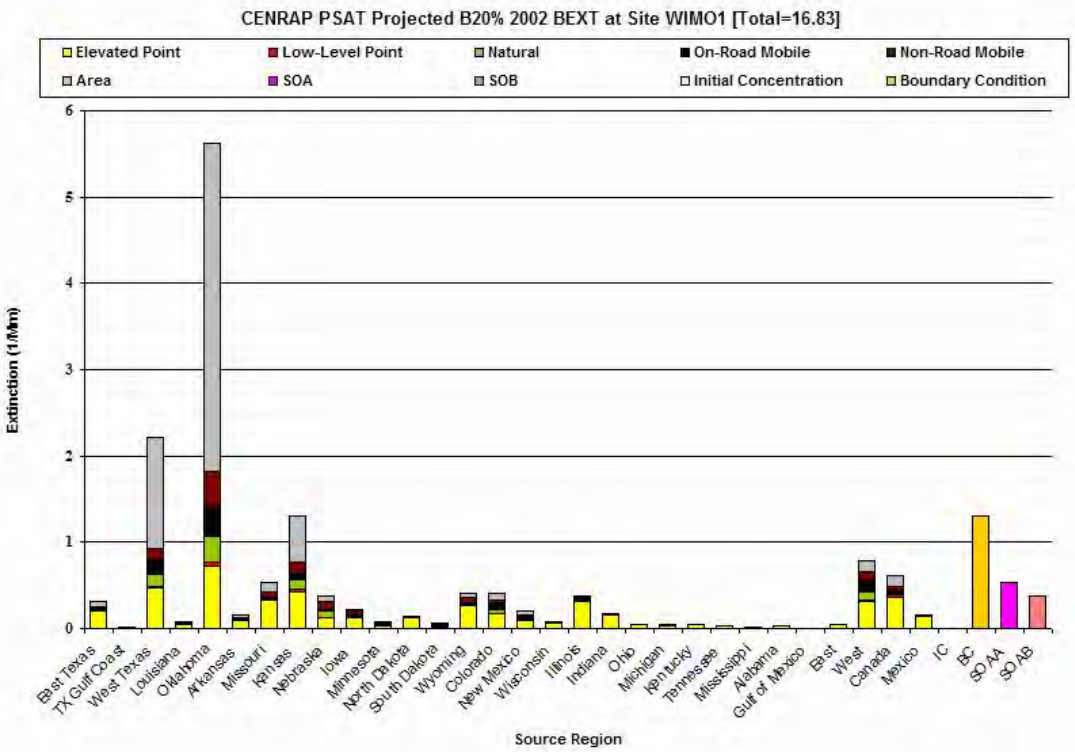

Figure E-8i. PSAT contributions by source region and source category to the average 2000-2004 Baseline extinction (Mm^{-1}) for the Best 20% visibility days at Wichita Mountains (WIMO), Oklahoma.

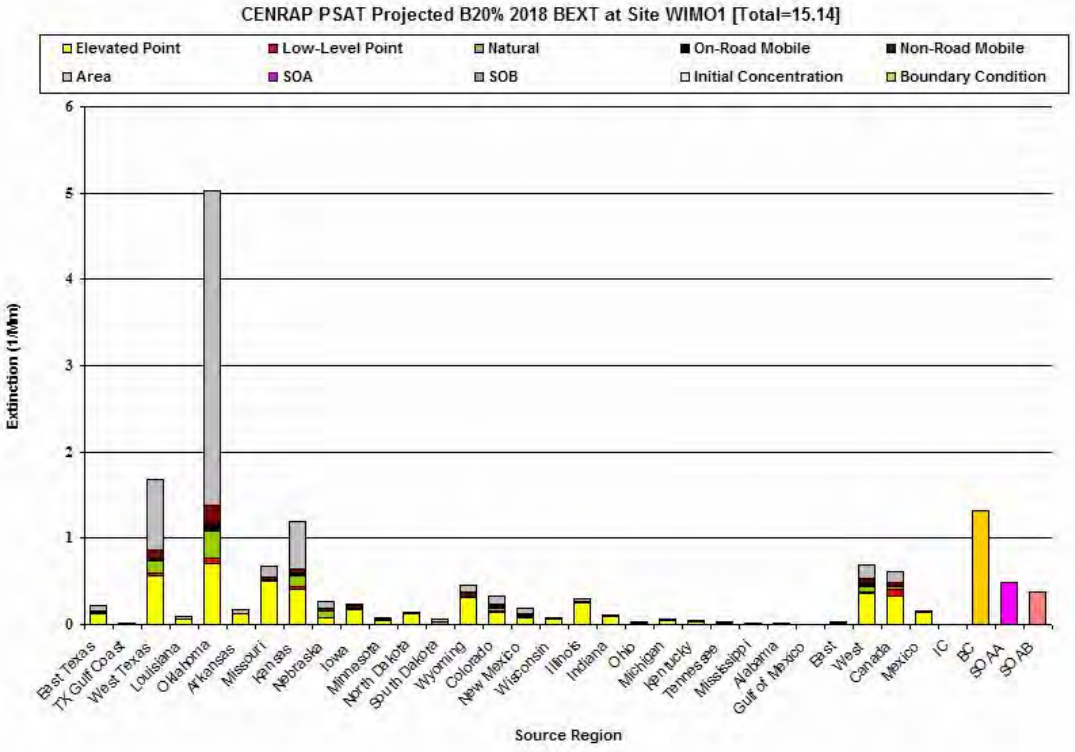

Figure E-8j. PSAT contributions by source region and source category to the average 2018 extinction (Mm^{-1}) for the Best 20% visibility days at Wichita Mountains (WIMO), Oklahoma.

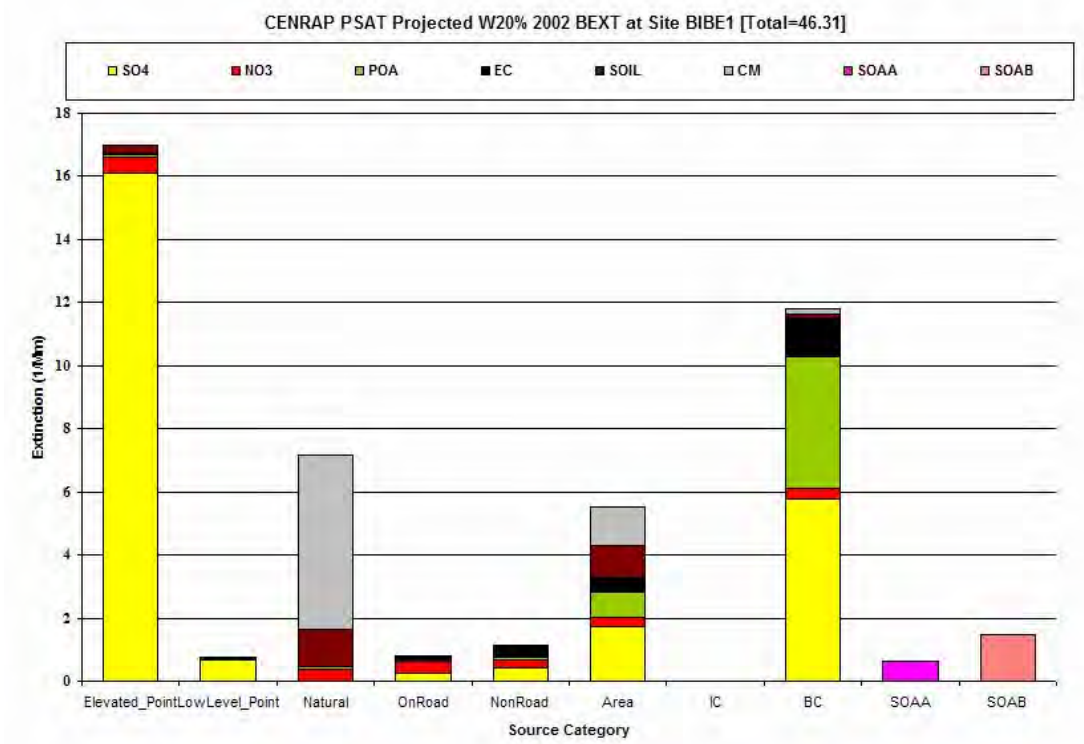

Figure E-9a. PSAT source categories by PM species contributions to the average 2000-2004 Baseline extinction (Mm^{-1}) for the Worst 20% visibility days at Big Bend (BIBE), Texas.

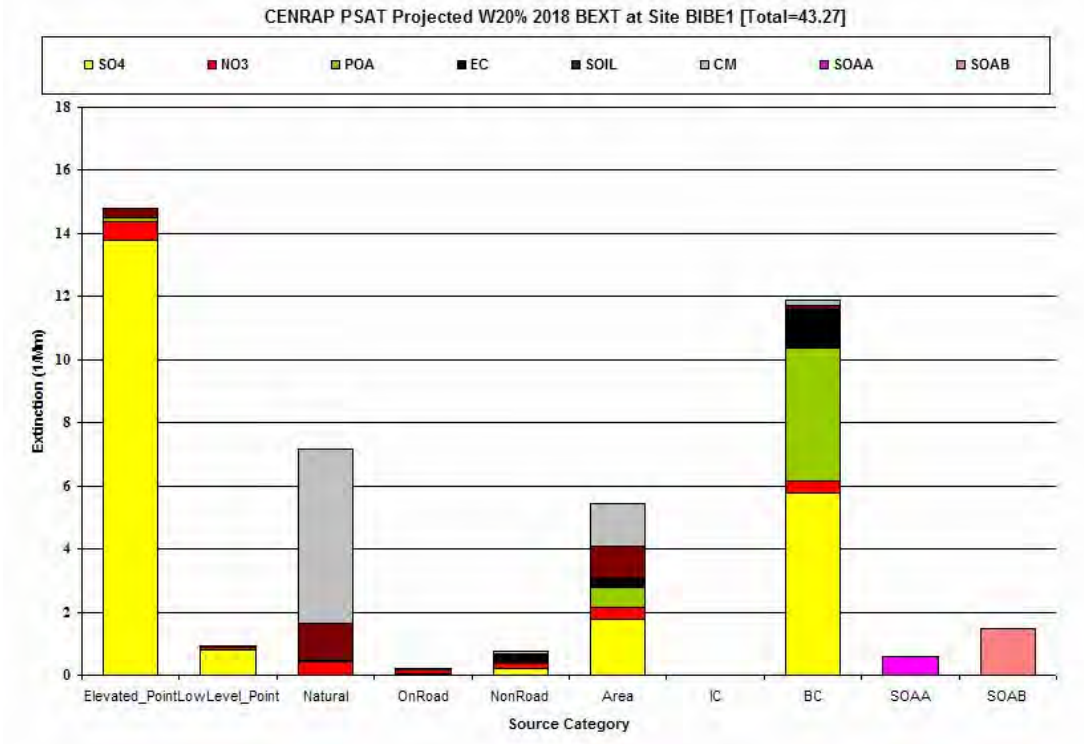

Figure E-9b. PSAT source category by PM species contributions to the average 2018 projected extinction (Mm^{-1}) for the Worst 20% visibility days at Big Bend (BIBE), Texas.

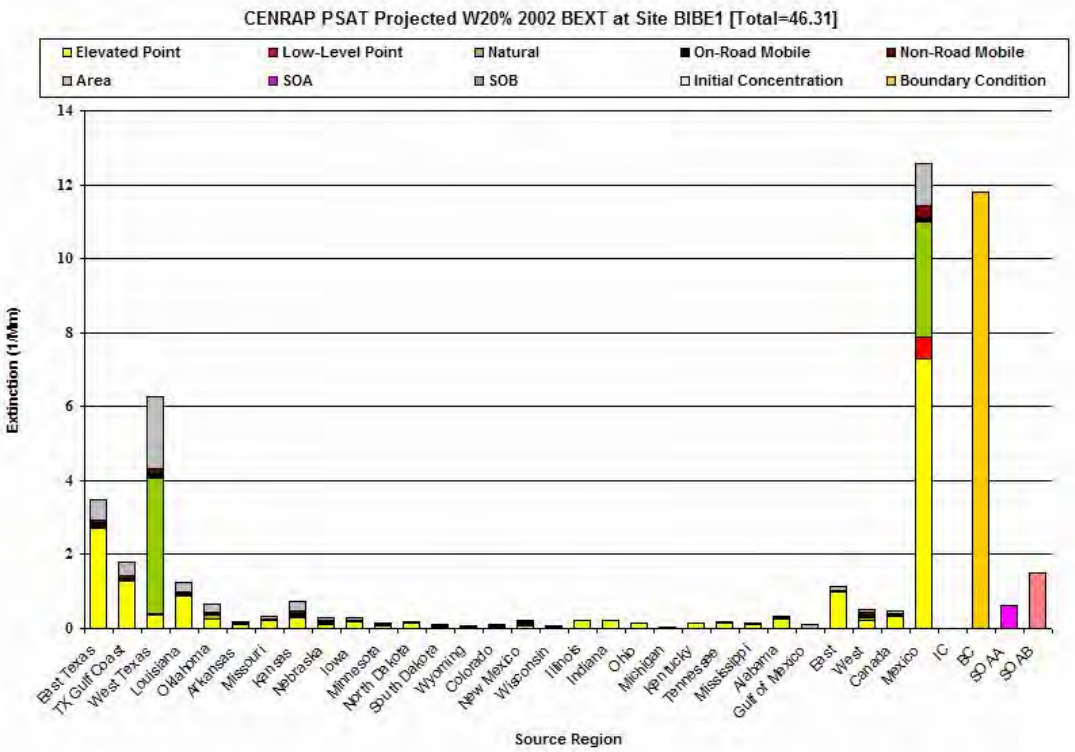

Figure E-9c. PSAT source region by source category contributions to the average 2000-2004 Baseline extinction (Mm^{-1}) for the Worst 20% visibility days at Big Bend (BIBE), Texas.

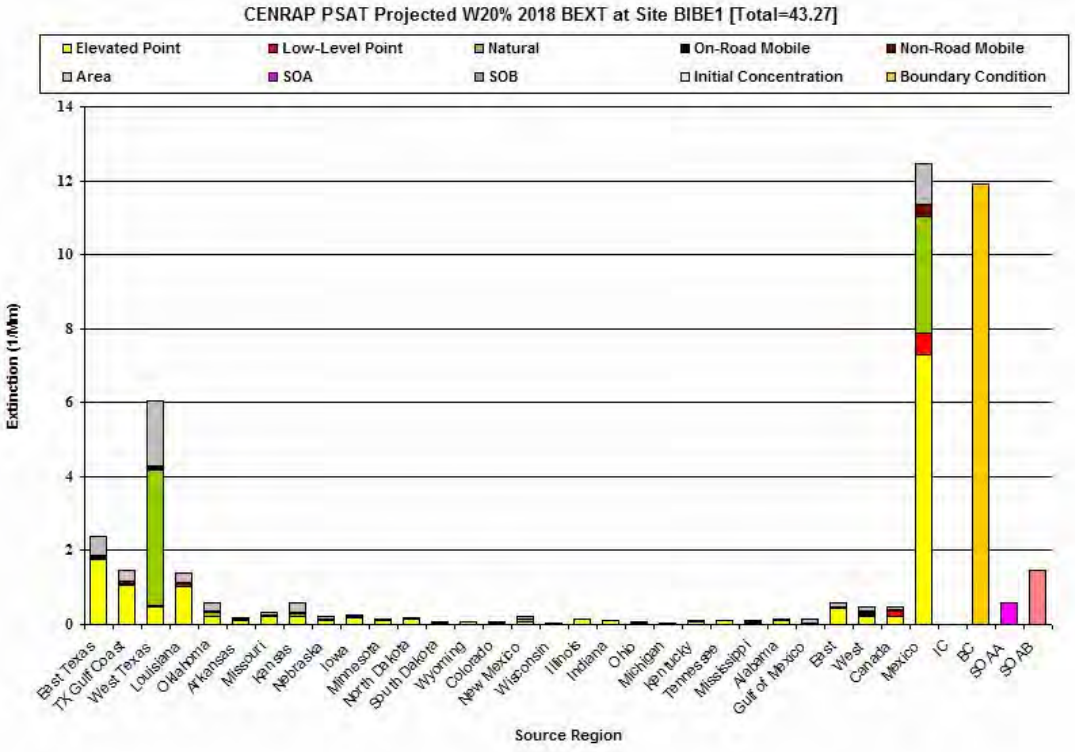

Figure E-9d. PSAT source region by source category contributions to the average 2018 extinction (Mm^{-1}) for the Worst 20% visibility days at Big Bend (BIBE), Texas.

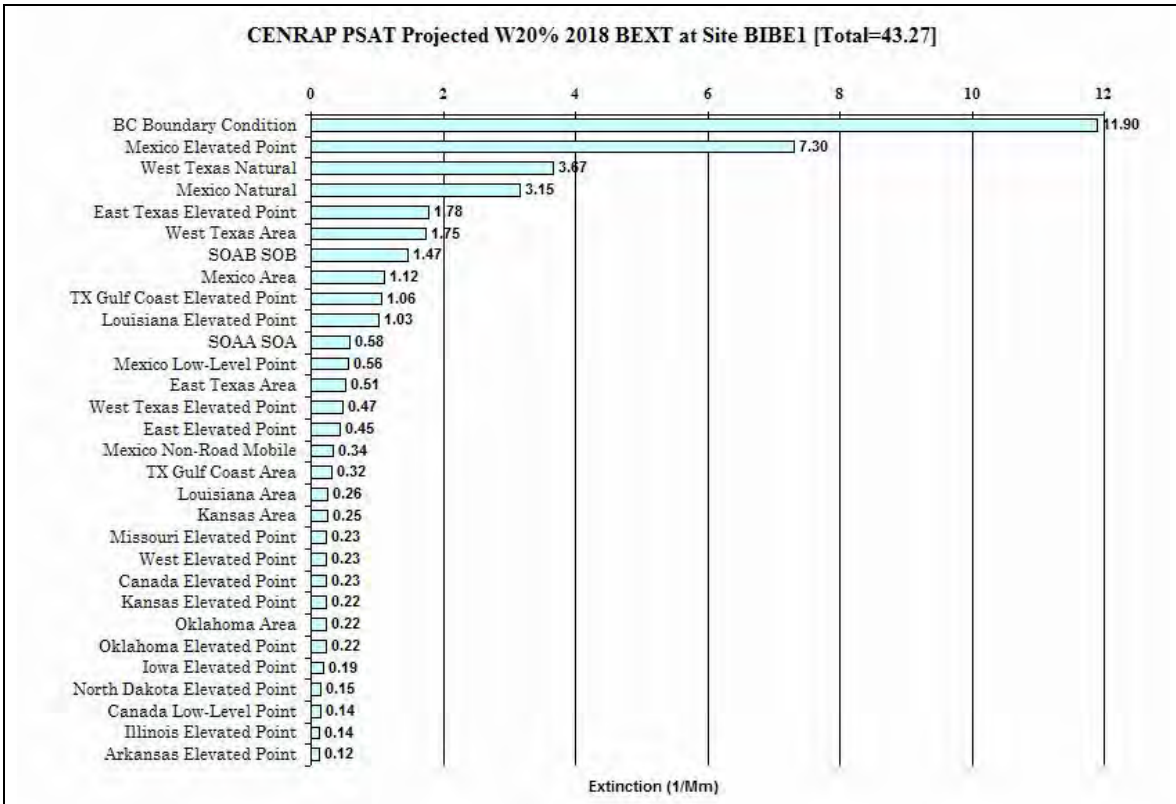

Figure E-9e. Ranked PSAT source region by source category contributions to the average 2018 extinction (Mm^{-1}) for the Worst 20% visibility days at Big Bend (BIBE), Texas.

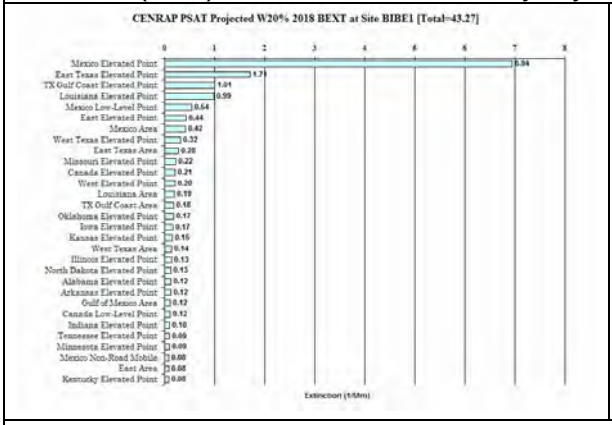

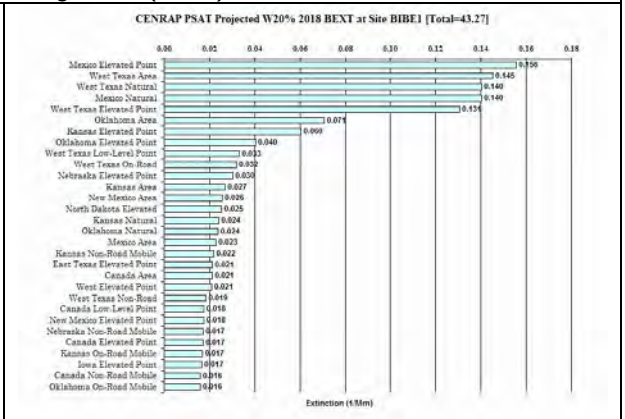

Figure E-9f. Ranked PSAT source region by source category contributions to the average 2018 SO4 (left) and NO3 (right) extinction (Mm^{-1}) for the Worst 20% visibility days at Big Bend (BIBE), Texas.

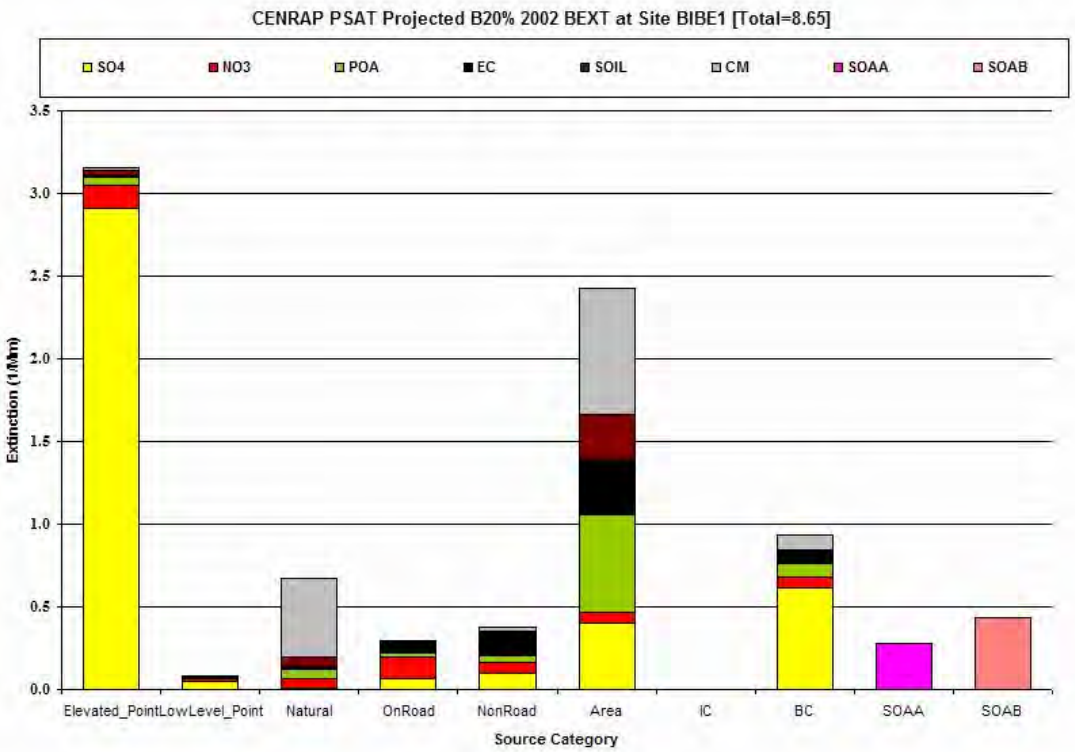

Figure E-9g. PSAT contributions by source category and PM species to the average 2000-2004 Baseline extinction (Mm^{-1}) for the Best 20% visibility days at Big Bend (BIBE), Texas.

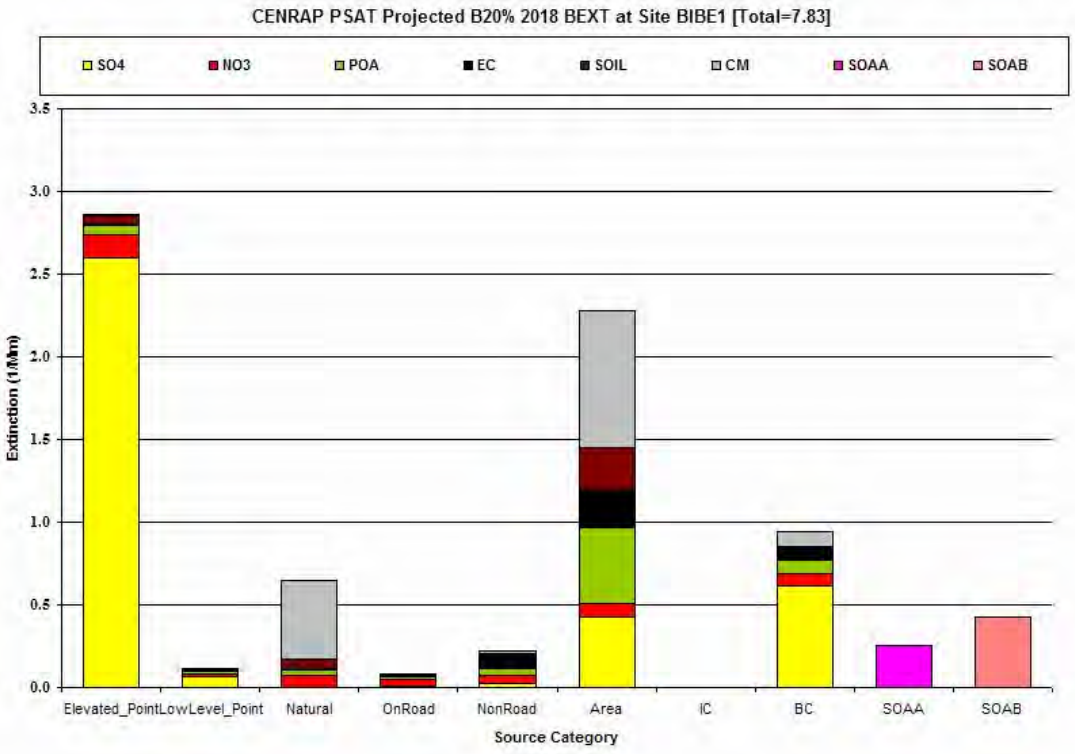

Figure E-9h. PSAT contributions by source category and PM species to the average 2018 extinction (Mm^{-1}) for the Best 20% visibility days at Big Bend (BIBE), Texas.

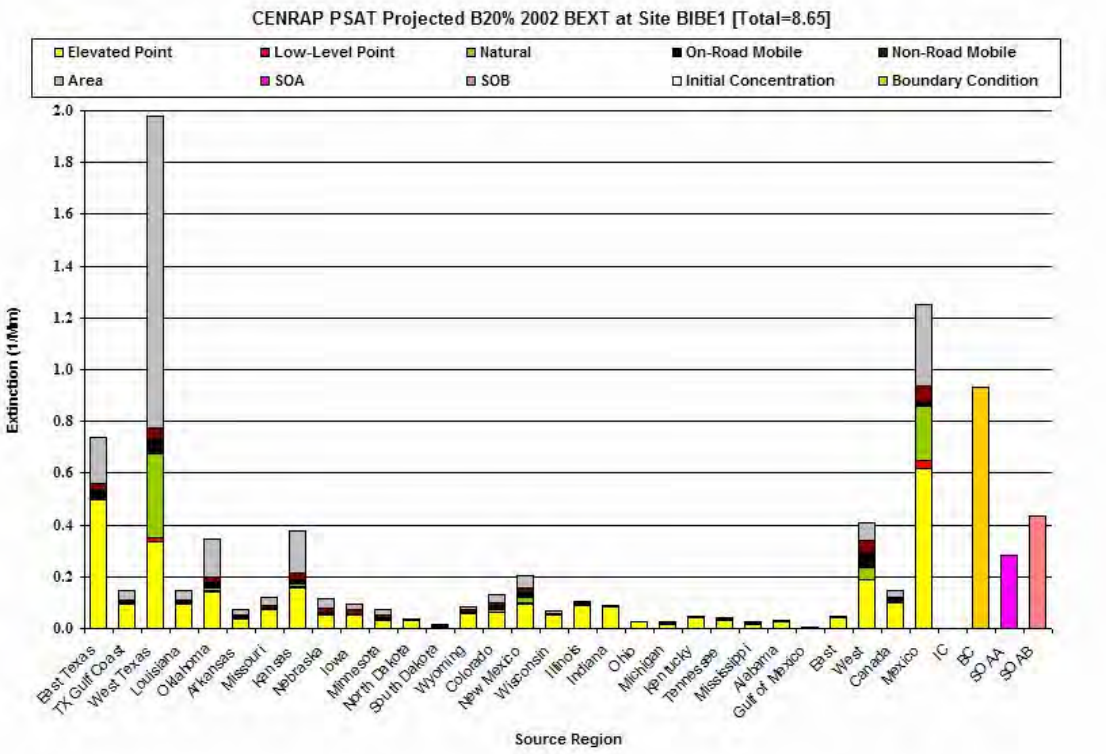

Figure E-9i. PSAT contributions by source region and source category to the average 2000-2004 Baseline extinction (Mm^{-1}) for the Best 20% visibility days Big Bend (BIBE), Texas.

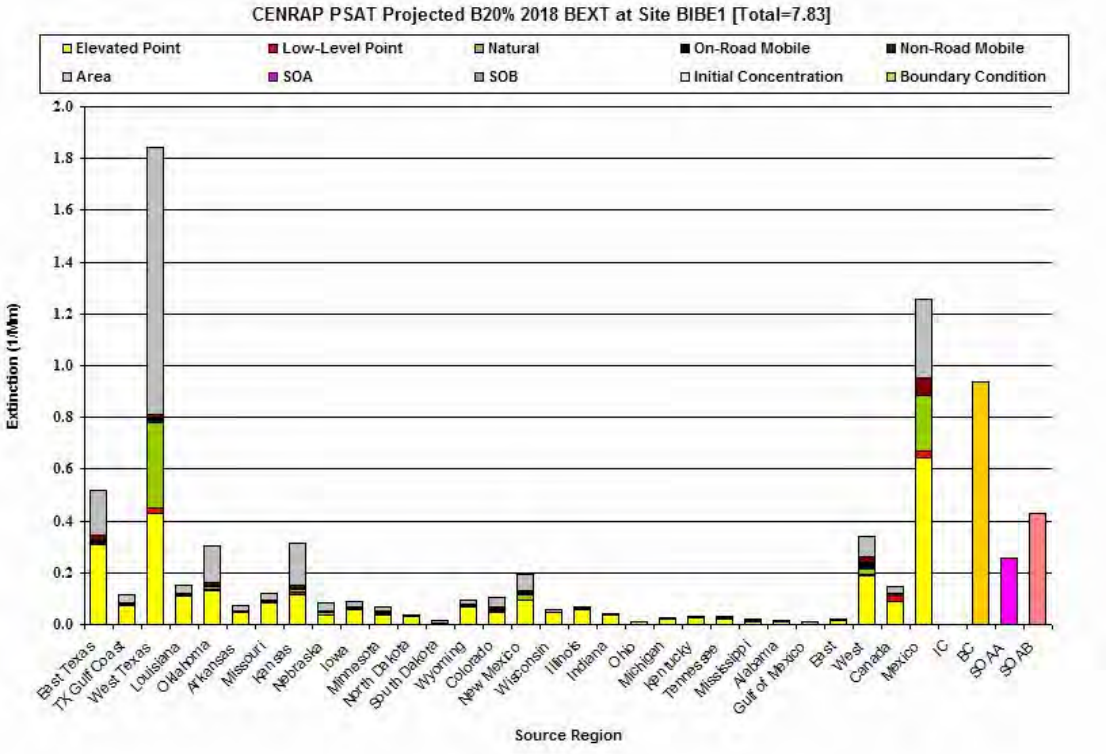

Figure E-9j. PSAT contributions by source region and source category to the average 2018 extinction (Mm^{-1}) for the Best 20% visibility days at Big Bend (BIBE), Texas.

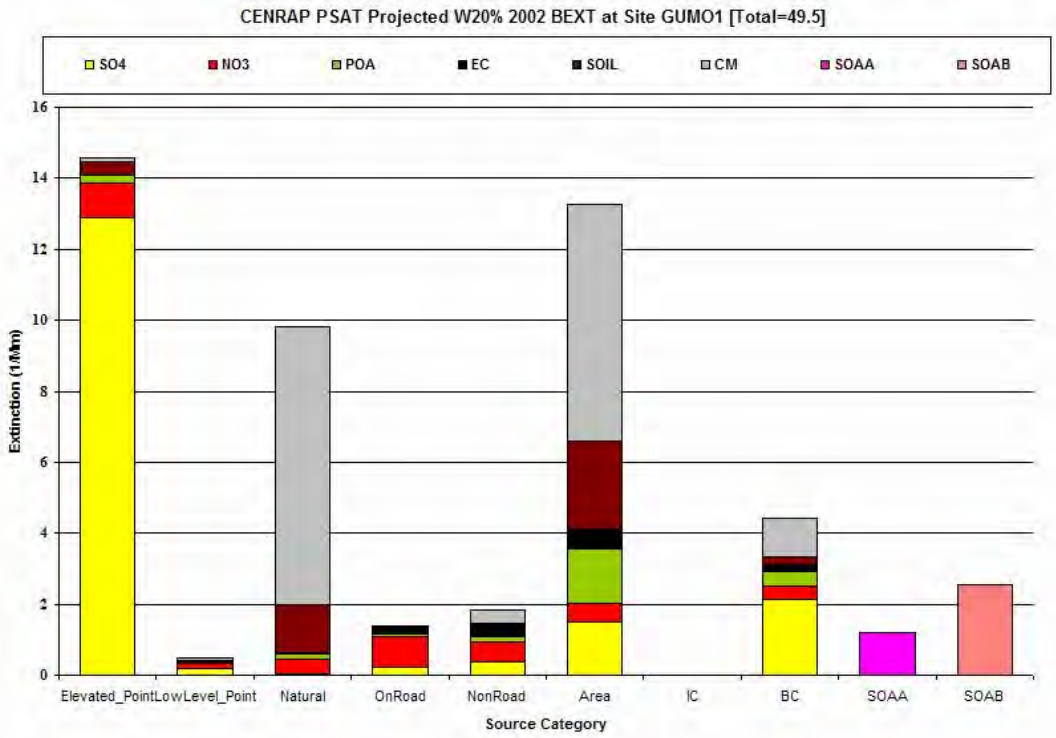

Figure E-10a. PSAT source categories by PM species contributions to the average 2000-2004 Baseline extinction (Mm^{-1}) for the Worst 20% visibility days at Big Bend (BIBE), Texas.

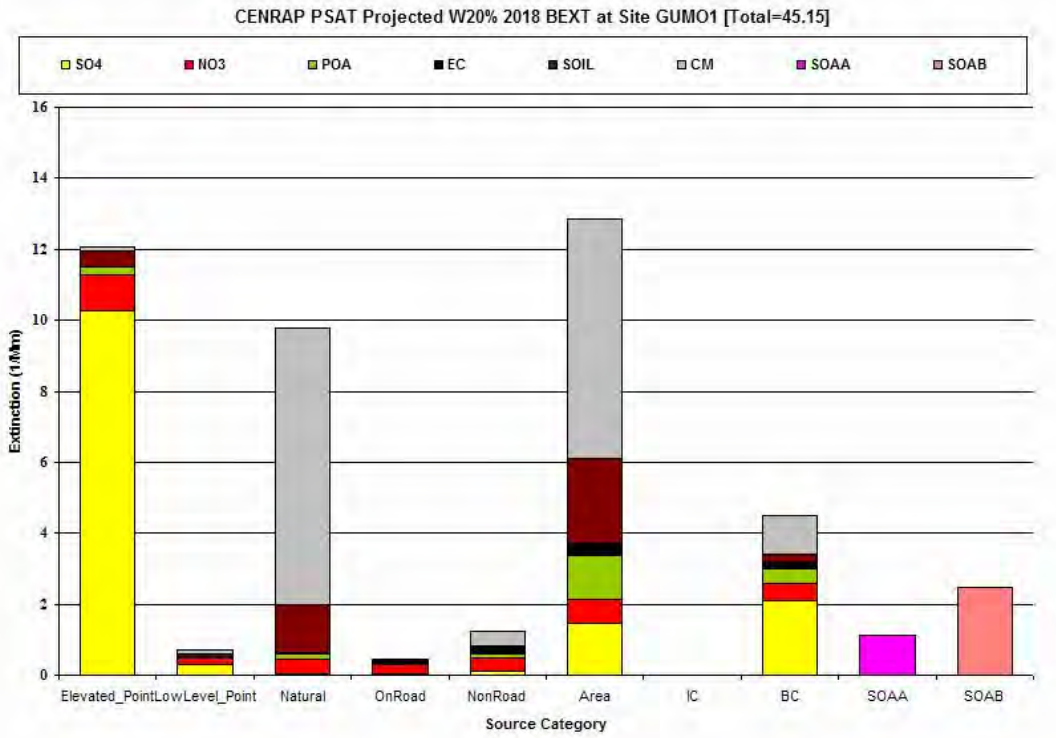

Figure E-10b. PSAT source category by PM species contributions to the average 2018 projected extinction (Mm^{-1}) for the Worst 20% visibility days at Big Bend (BIBE), Texas.

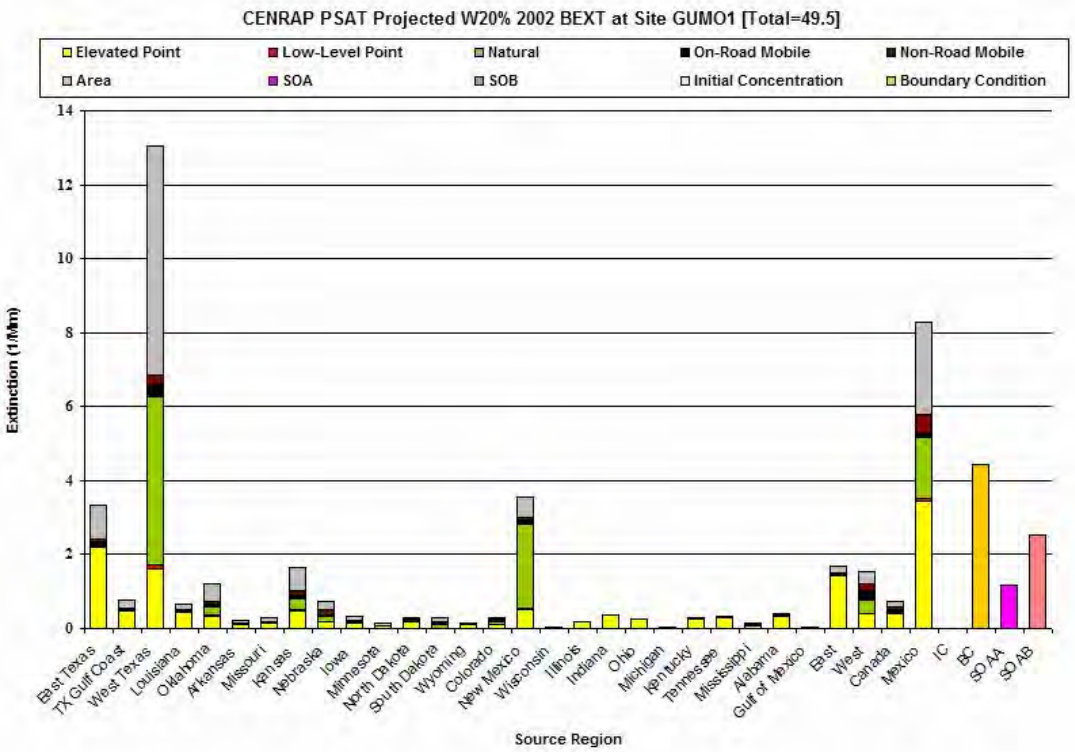

Figure E-10c. PSAT source region by source category contributions to the average 2000-2004 Baseline extinction (Mm^{-1}) for the Worst 20% visibility days at Big Bend (BIBE), Texas.

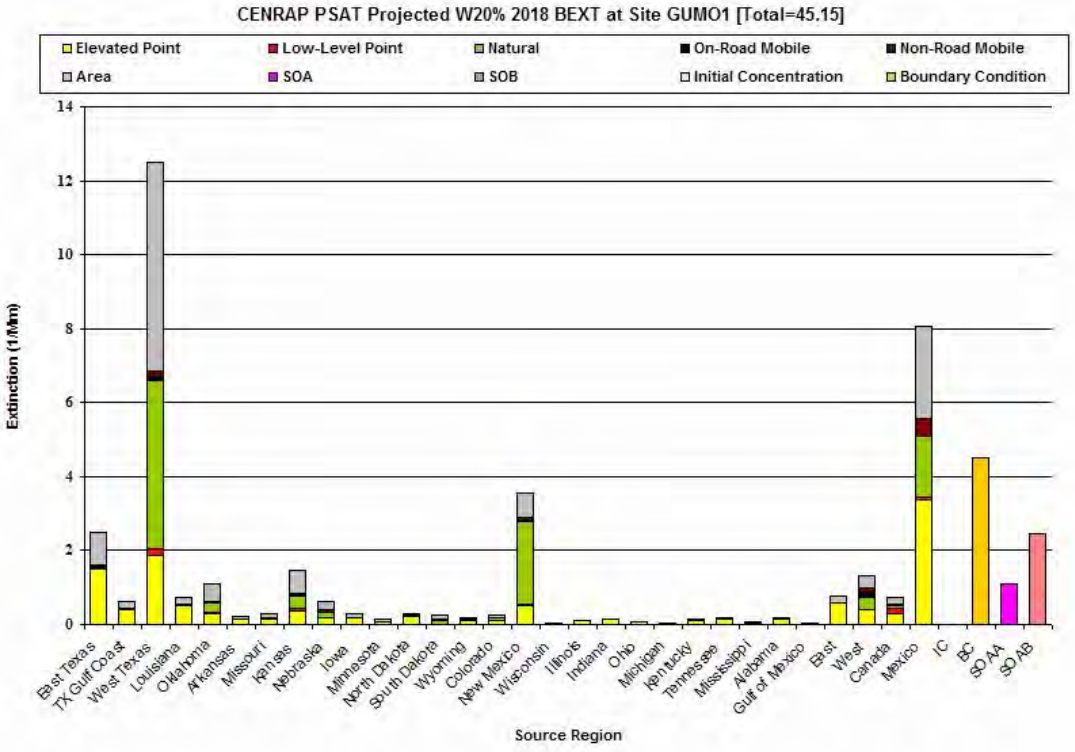

Figure E-10d. PSAT source region by source category contributions to the average 2018 extinction (Mm^{-1}) for the Worst 20% visibility days at Big Bend (BIBE), Texas.

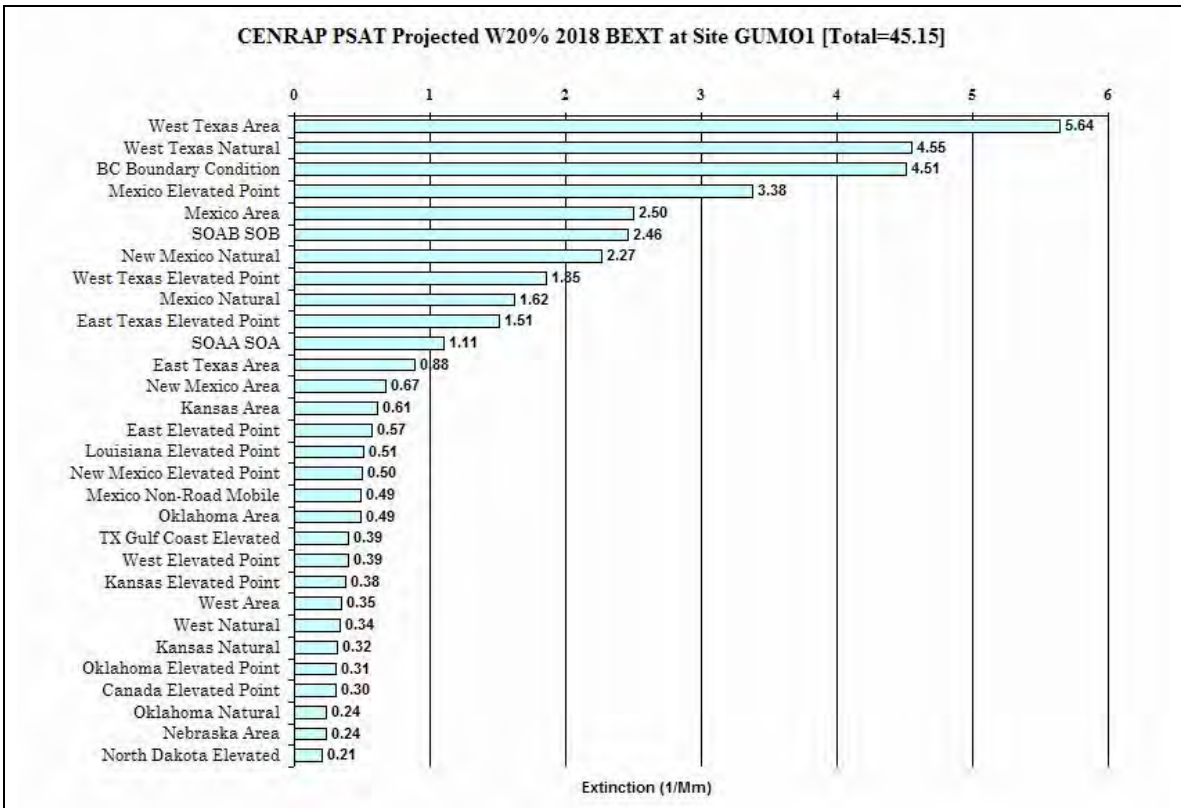

Figure E-10e. Ranked PSAT source region by source category contributions to the average 2018 extinction (Mm^{-1}) for the Worst 20% visibility days at Big Bend (BIBE), Texas.

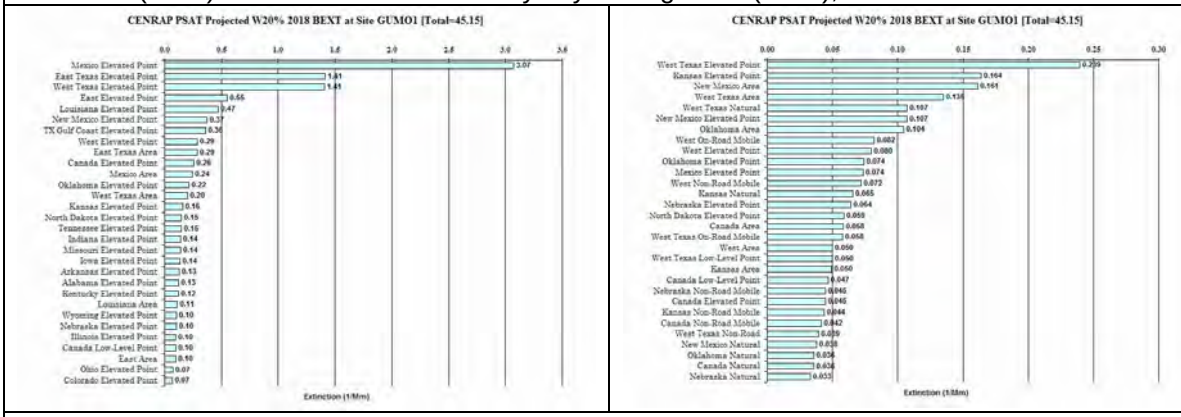

Figure E-10f. Ranked PSAT source region by source category contributions to the average 2018 SO4 (left) and NO3 (right) extinction (Mm^{-1}) for the Worst 20% visibility days at Big Bend (BIBE), Texas.

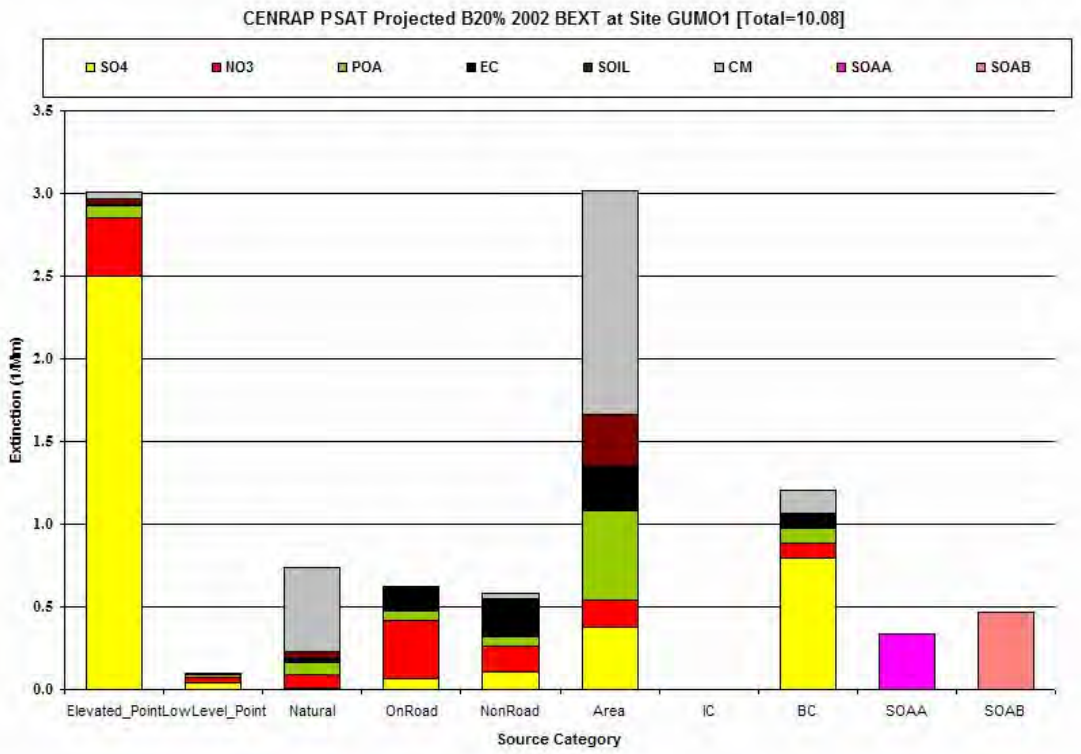

Figure E-10g. PSAT contributions by source category and PM species to the average 2000-2004 Baseline extinction (Mm^{-1}) for the Best 20% visibility days at Big Bend (BIBE), Texas.

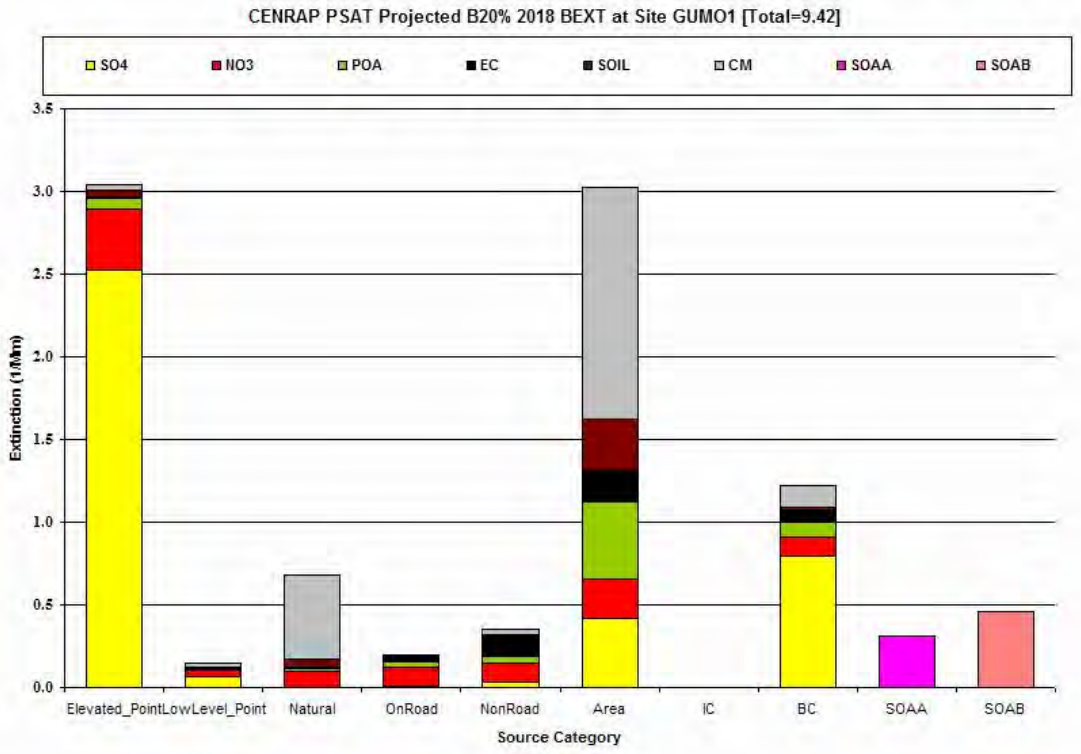

Figure E-10h. PSAT contributions by source category and PM species to the average 2018 extinction (Mm^{-1}) for the Best 20% visibility days at Big Bend (BIBE), Texas.

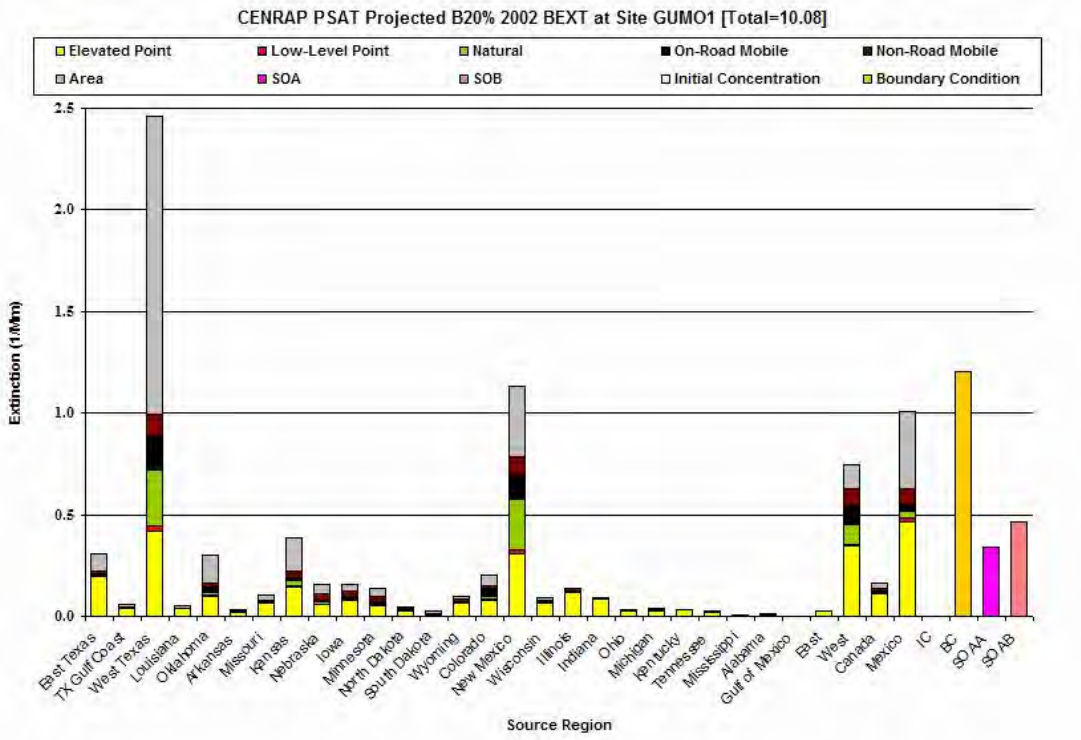

Figure E-10i. PSAT contributions by source region and source category to the average 2000-2004 Baseline extinction (Mm^{-1}) for the Best 20% visibility days Big Bend (BIBE), Texas.

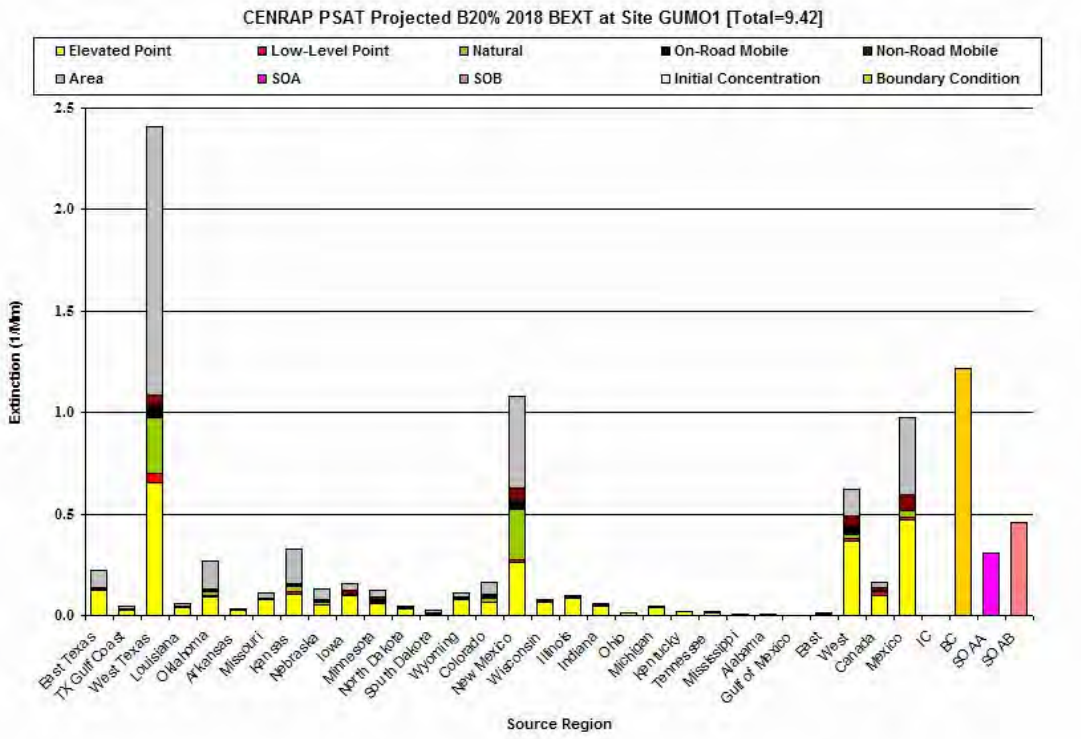

Figure E-10j. PSAT contributions by source region and source category to the average 2018 extinction (Mm^{-1}) for the Best 20% visibility days at Big Bend (BIBE), Texas.

APPENDIX F

Extinction and PM Species-Specific 2018 Visibility Projections and Comparisons with 2018 URP Points

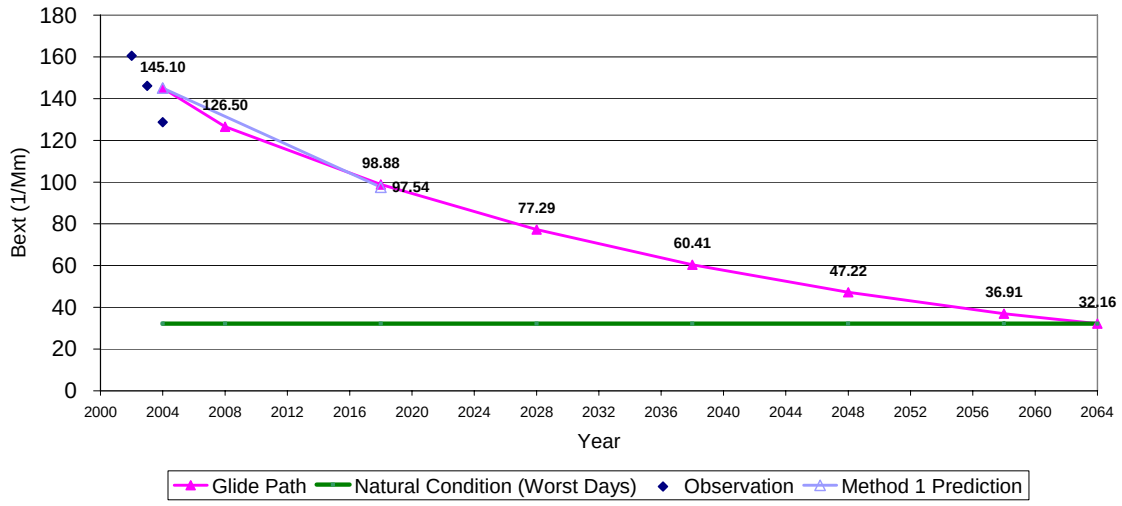

Figure F-1a. 2018 Visibility Projections and 2018 URP Glidepaths in extinction (Mm^{-1}) for Caney Creek (CACR), Arkansas and Worst 20% (W20%) days using 2002/2018 Base G CMAQ 36 km modeling results.

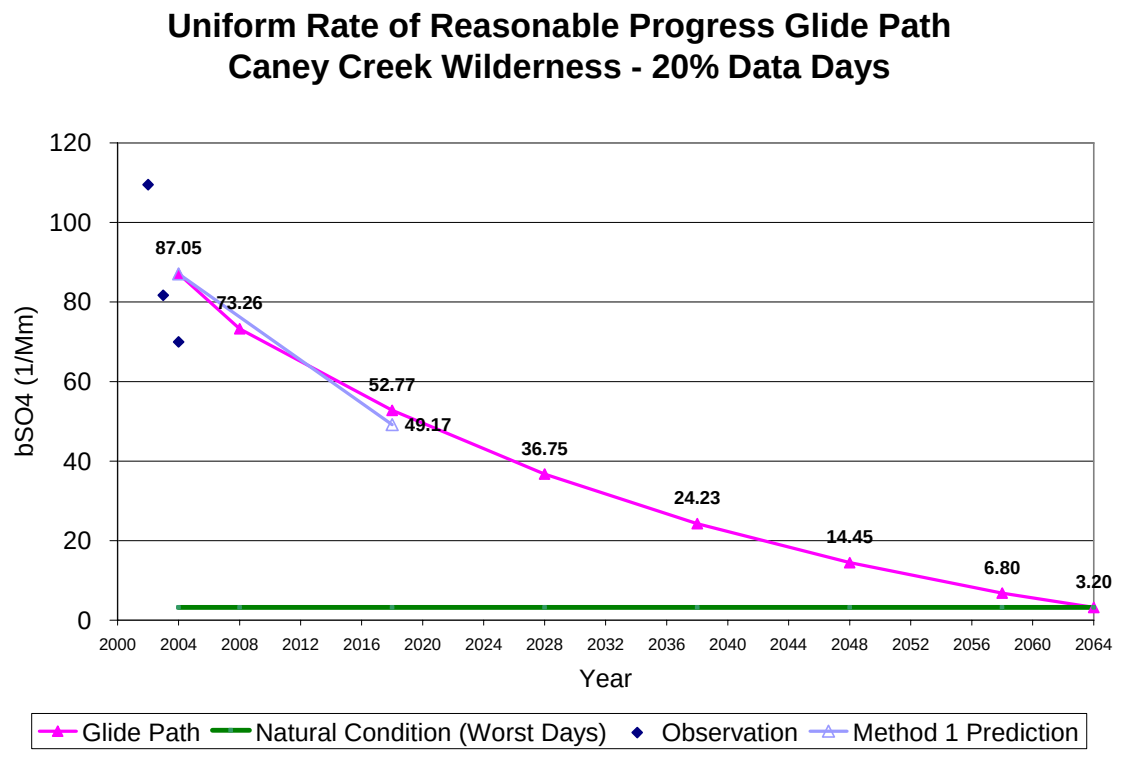

Figure F-1b. 2018 Visibility Projections and 2018 URP Glidepaths for Sulfate (SO4) in extinction (Mm^{-1}) for Caney Creek (CACR), Arkansas and Worst 20% (W20%) days using 2002/2018 Base G CMAQ 36 km modeling results.

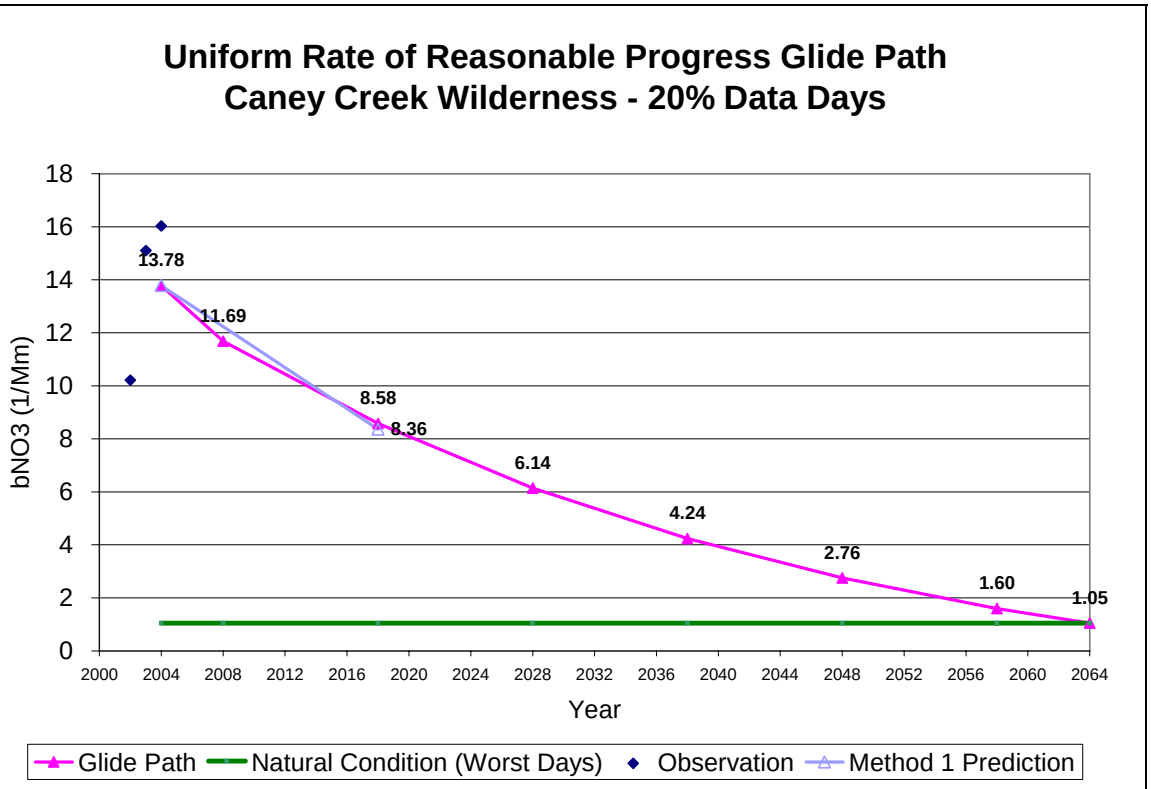

Figure F-1c. 2018 Visibility Projections and 2018 URP Glidepaths for Nitrate (NO3) in extinction (Mm^{-1}) for Caney Creek (CACR), Arkansas and Worst 20% (W20%) days using 2002/2018 Base G CMAQ 36 km modeling results.

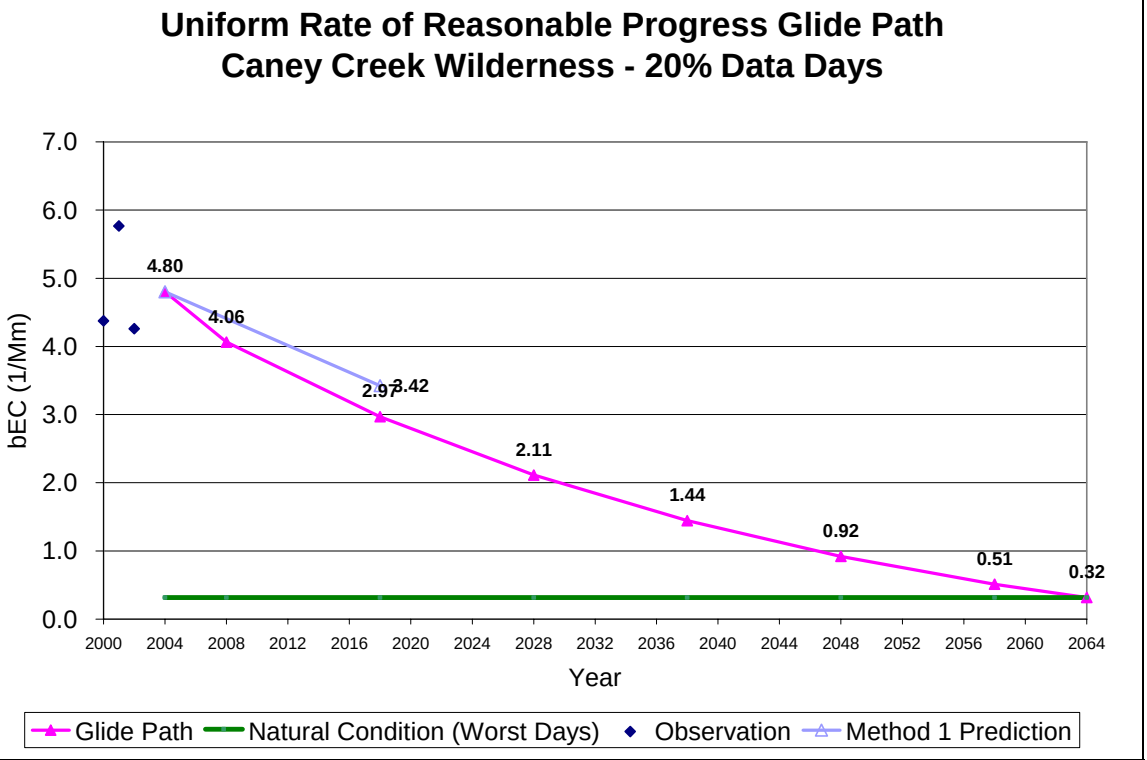

Figure F-1d. 2018 Visibility Projections and 2018 URP Glidepaths for Elemental Carbon (EC) in extinction (Mm^{-1}) for Caney Creek (CACR), Arkansas and Worst 20% (W20%) days using 2002/2018 Base G CMAQ 36 km modeling results.

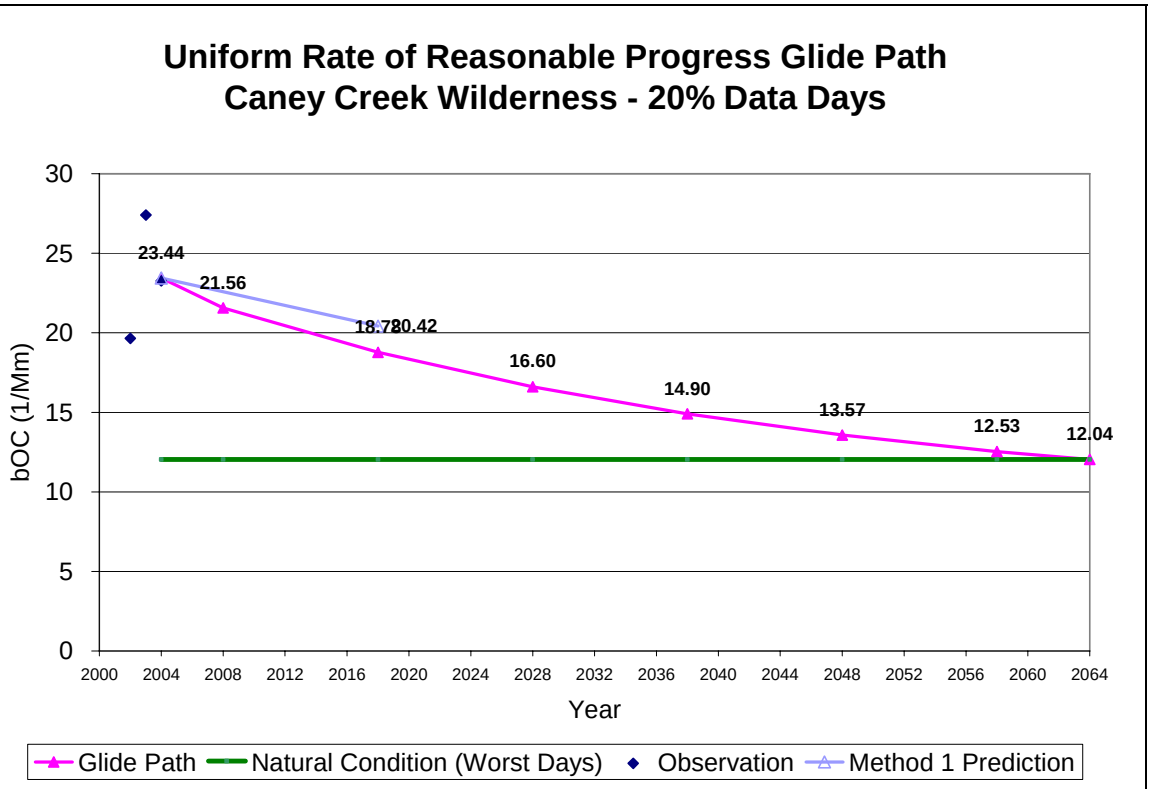

Figure F-1e. 2018 Visibility Projections and 2018 URP Glidepaths for Organic Mass Carbon (OMC) in extinction (Mm^{-1}) for Caney Creek (CACR), Arkansas and Worst 20% (W20%) days using 2002/2018 Base G CMAQ 36 km modeling results.

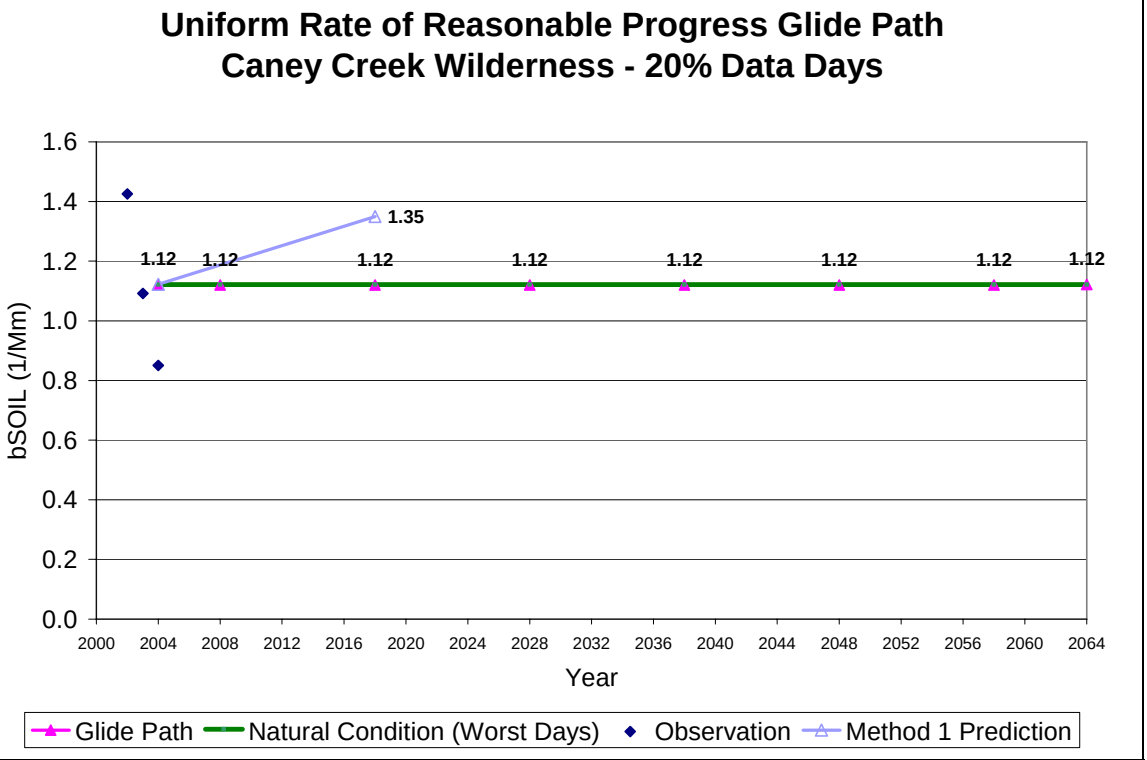

Figure F-1f. 2018 Visibility Projections and 2018 URP Glidepaths for Other Fine Particulate (SOIL) in extinction (Mm^{-1}) for Caney Creek (CACR), Arkansas and Worst 20% (W20%) days using 2002/2018 Base G CMAQ 36 km modeling results.

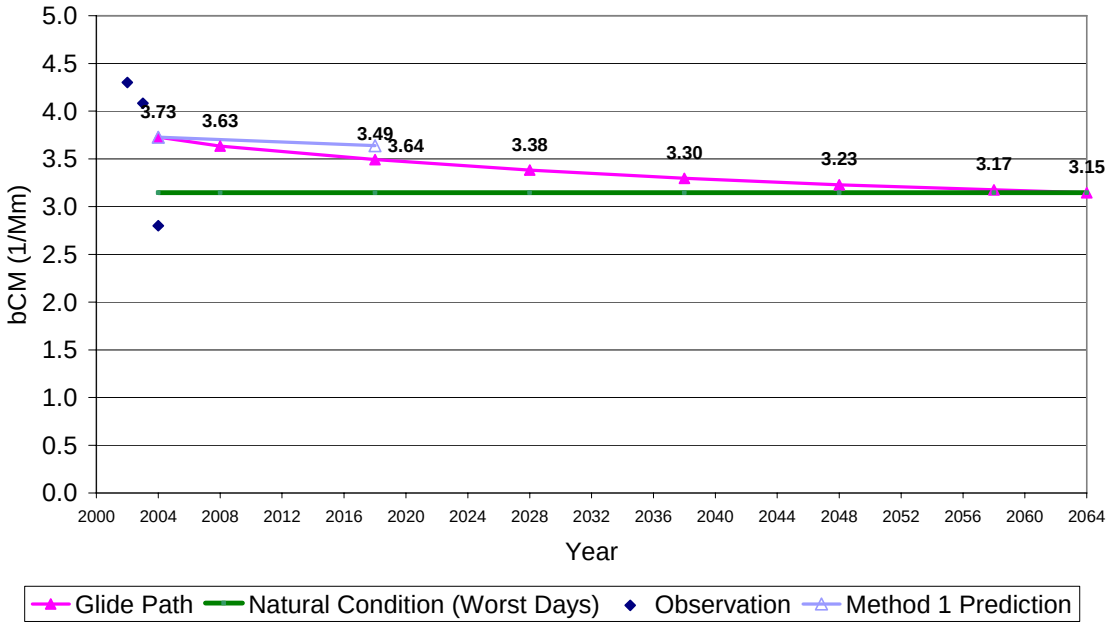

Figure F-1g. 2018 Visibility Projections and 2018 URP Glidepaths for Coarse Mass (CM) in extinction (Mm^{-1}) for Caney Creek (CACR), Arkansas and Worst 20% (W20%) days using 2002/2018 Base G CMAQ 36 km modeling results.

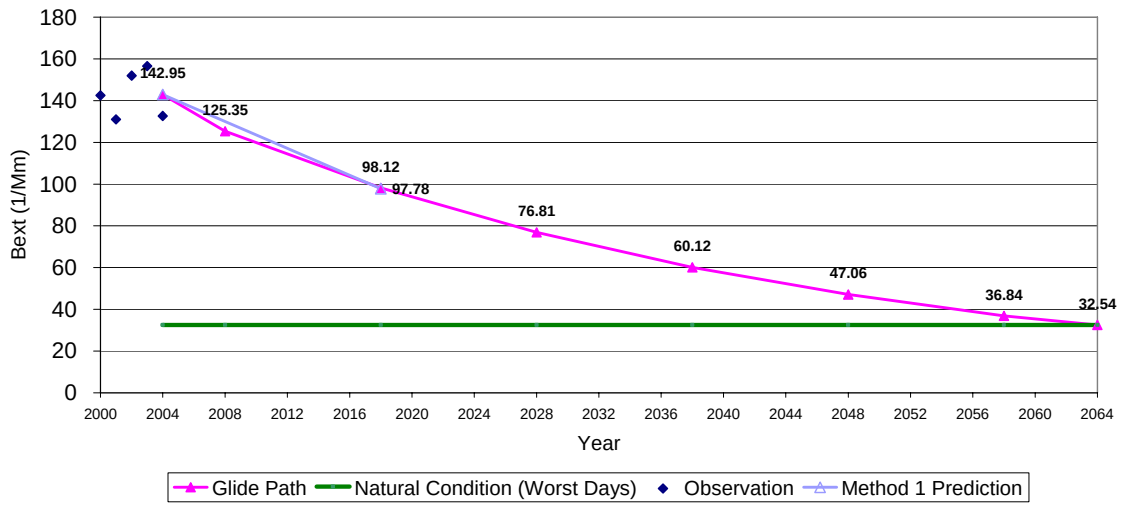

Figure F-2a. 2018 Visibility Projections and 2018 URP Glidepaths in extinction (Mm^{-1}) for Upper Buffalo (UPBU), Arkansas and Worst 20% (W20%) days using 2002/2018 Base G CMAQ 36 km modeling results.

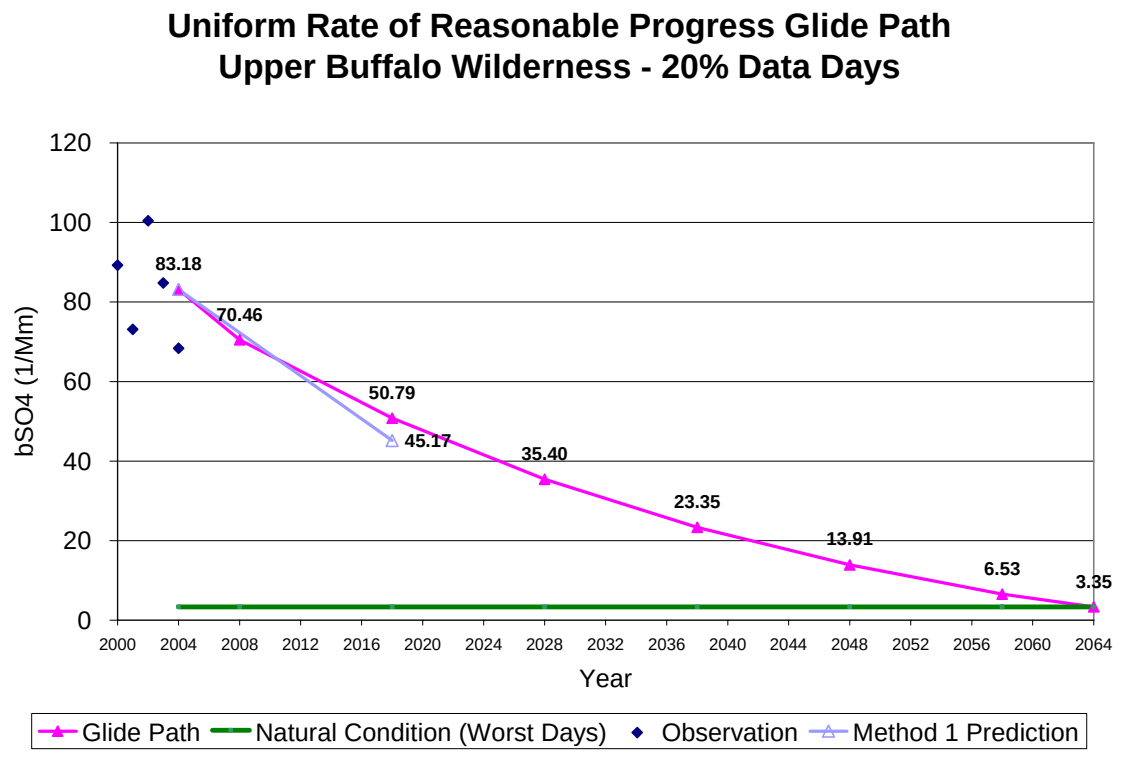

Figure F-2b. 2018 Visibility Projections and 2018 URP Glidepaths for Sulfate (SO4) in extinction (Mm^{-1}) for Upper Buffalo (UPBU), Arkansas and Worst 20% (W20%) days using 2002/2018 Base G CMAQ 36 km modeling results.

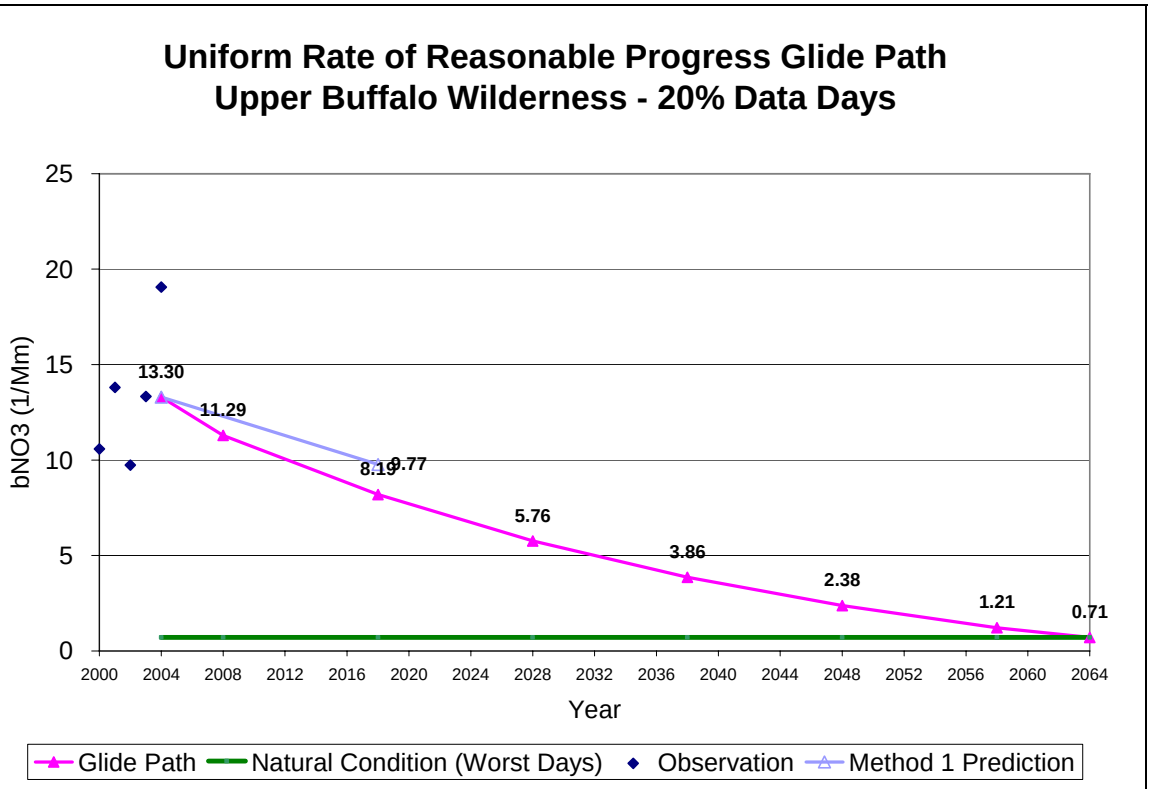

Figure F-2c. 2018 Visibility Projections and 2018 URP Glidepaths for Nitrate (NO3) in extinction (Mm^{-1}) for Upper Buffalo (UPBU), Arkansas and Worst 20% (W20%) days using 2002/2018 Base G CMAQ 36 km modeling results.

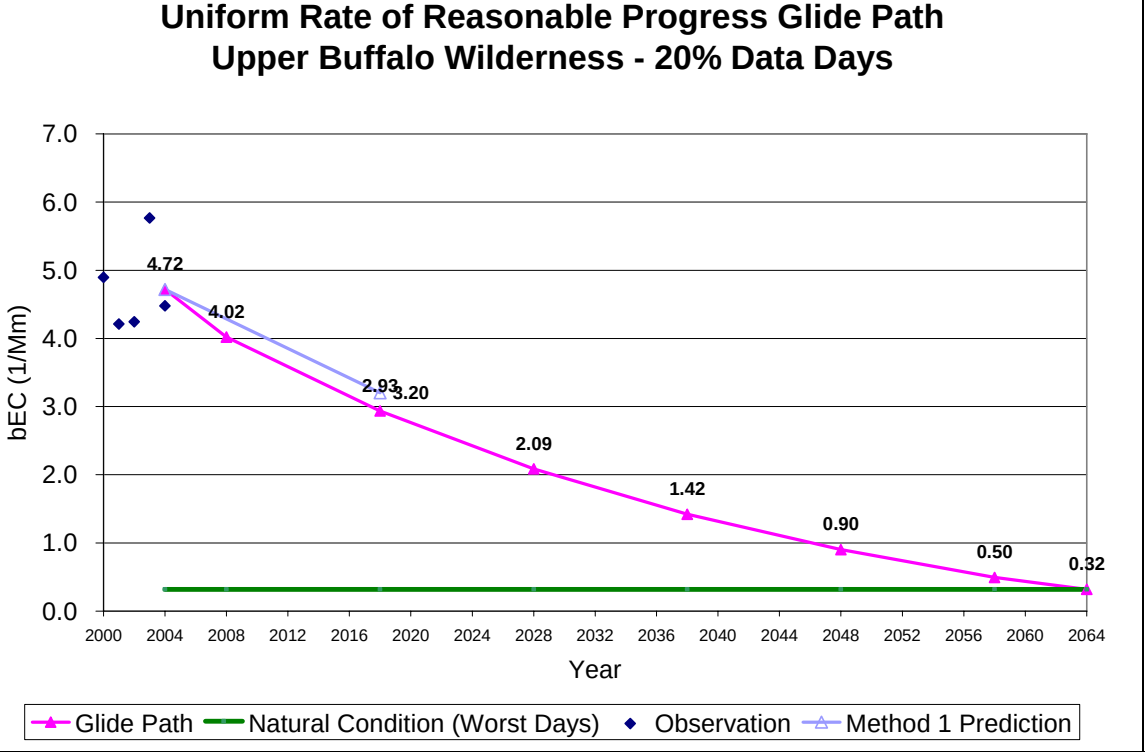

Figure F-2d. 2018 Visibility Projections and 2018 URP Glidepaths for Elemental Carbon (EC) in extinction (Mm^{-1}) for Upper Buffalo (UPBU), Arkansas and Worst 20% (W20%) days using 2002/2018 Base G CMAQ 36 km modeling results.

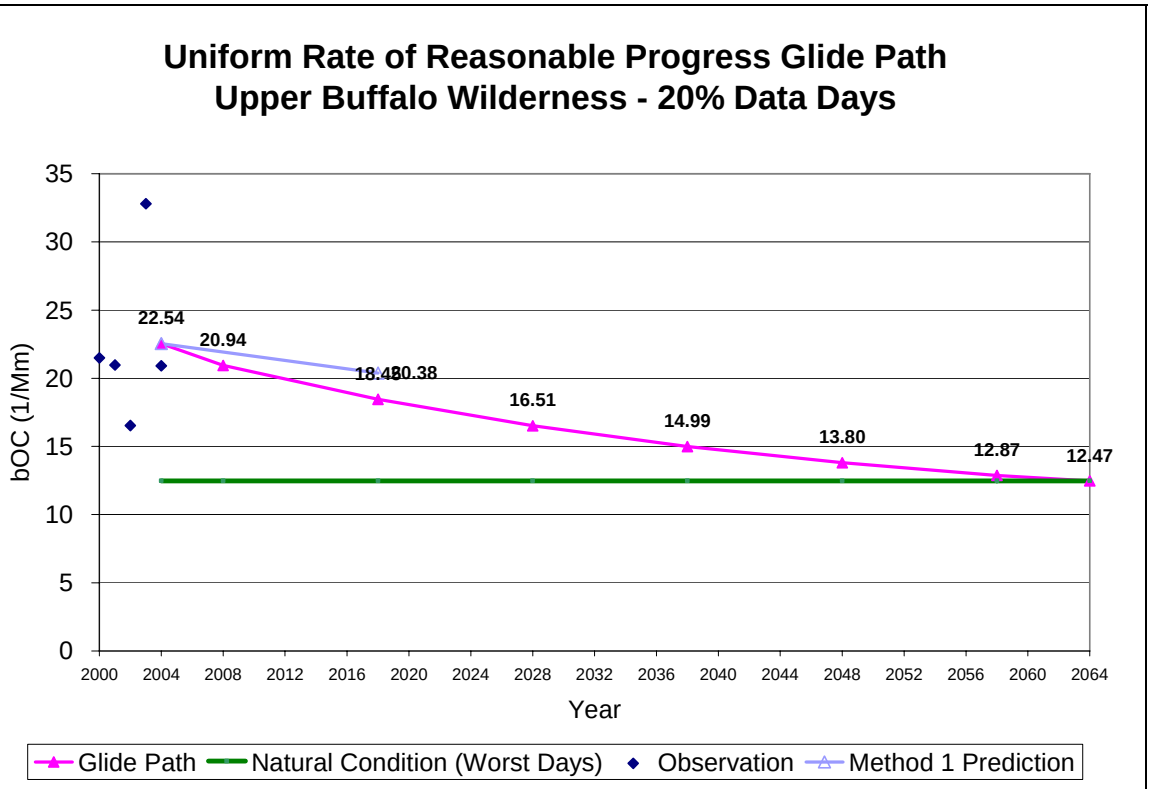

Figure F-2e. 2018 Visibility Projections and 2018 URP Glidepaths for Organic Mass Carbon (OMC) in extinction (Mm^{-1}) for Upper Buffalo (UPBU), Arkansas and Worst 20% (W20%) days using 2002/2018 Base G CMAQ 36 km modeling results.

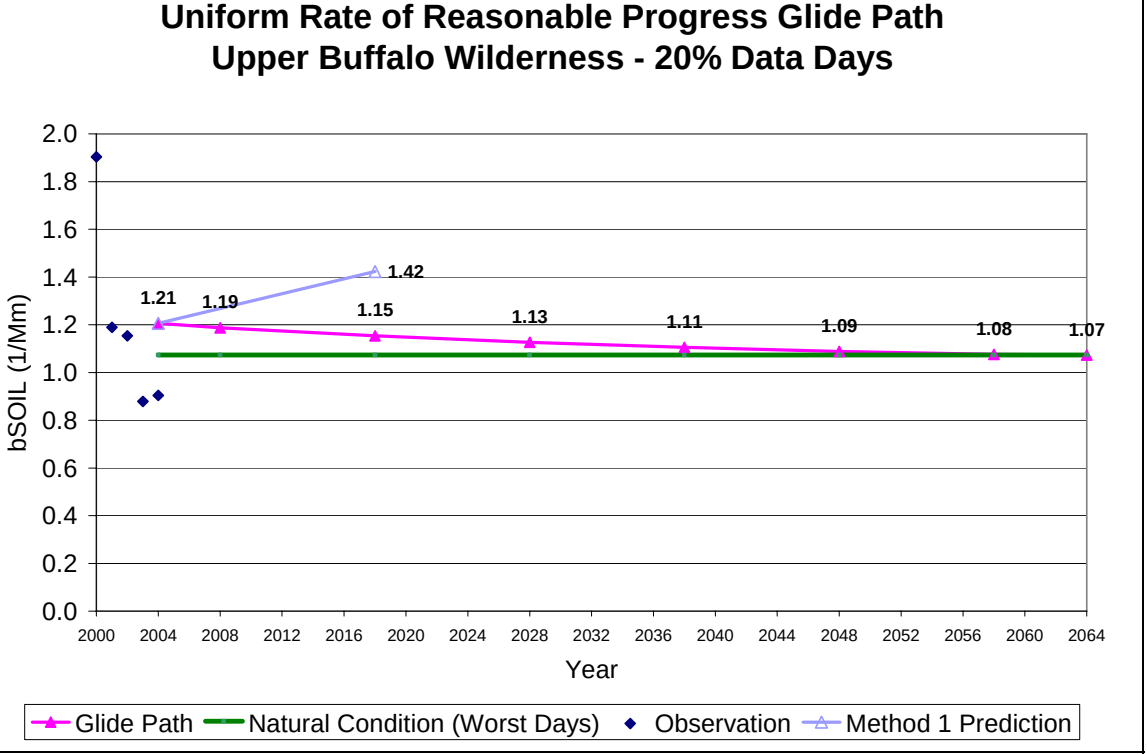

Figure F-2f. 2018 Visibility Projections and 2018 URP Glidepaths for Other Fine Particulate (SOIL) in extinction (Mm^{-1}) for Upper Buffalo (UPBU), Arkansas and Worst 20% (W20%) days using 2002/2018 Base G CMAQ 36 km modeling results.

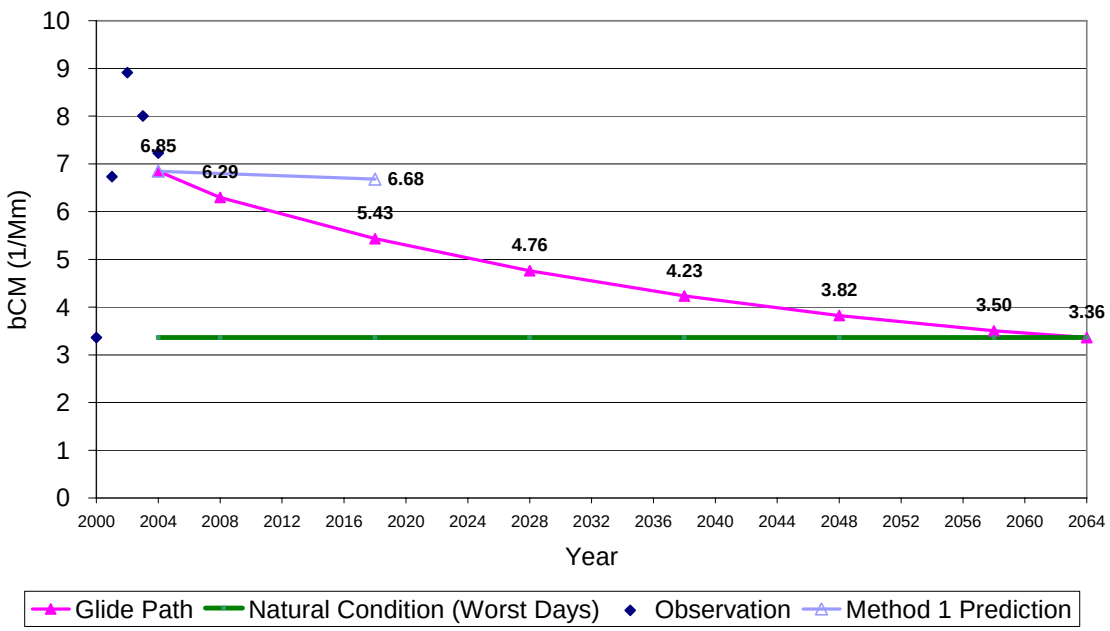

Figure F-2g. 2018 Visibility Projections and 2018 URP Glidepaths for Coarse Mass (CM) in extinction (Mm^{-1}) for Upper Buffalo (UPBU), Arkansas and Worst 20% (W20%) days using 2002/2018 Base G CMAQ 36 km modeling results.

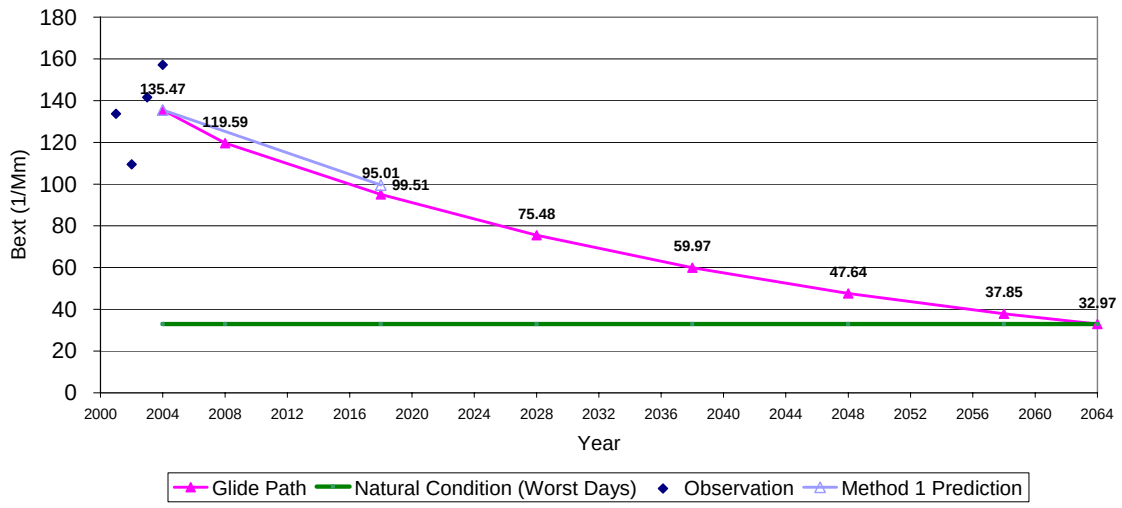

Figure F-3a. 2018 Visibility Projections and 2018 URP Glidepaths in extinction (Mm^{-1}) for Breton Island (BRET), Louisiana and Worst 20% (W20%) days using 2002/2018 Base G CMAQ 36 km modeling results.

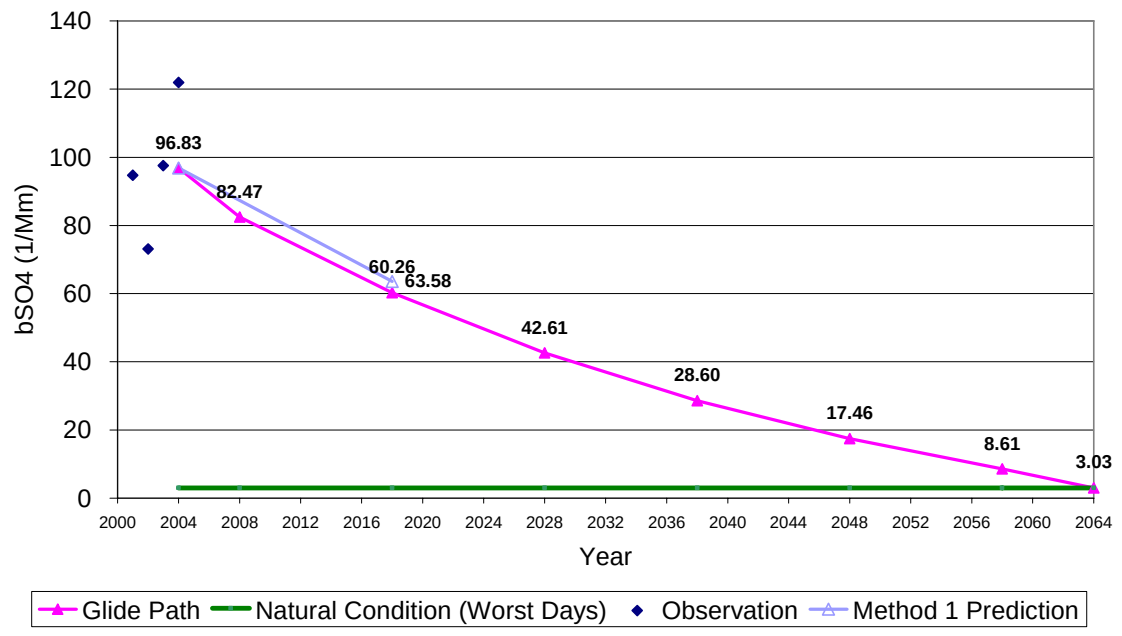

Figure F-3b. 2018 Visibility Projections and 2018 URP Glidepaths for Sulfate (SO4) in extinction (Mm^{-1}) for Breton Island (BRET), Louisiana and Worst 20% (W20%) days using 2002/2018 Base G CMAQ 36 km modeling results.

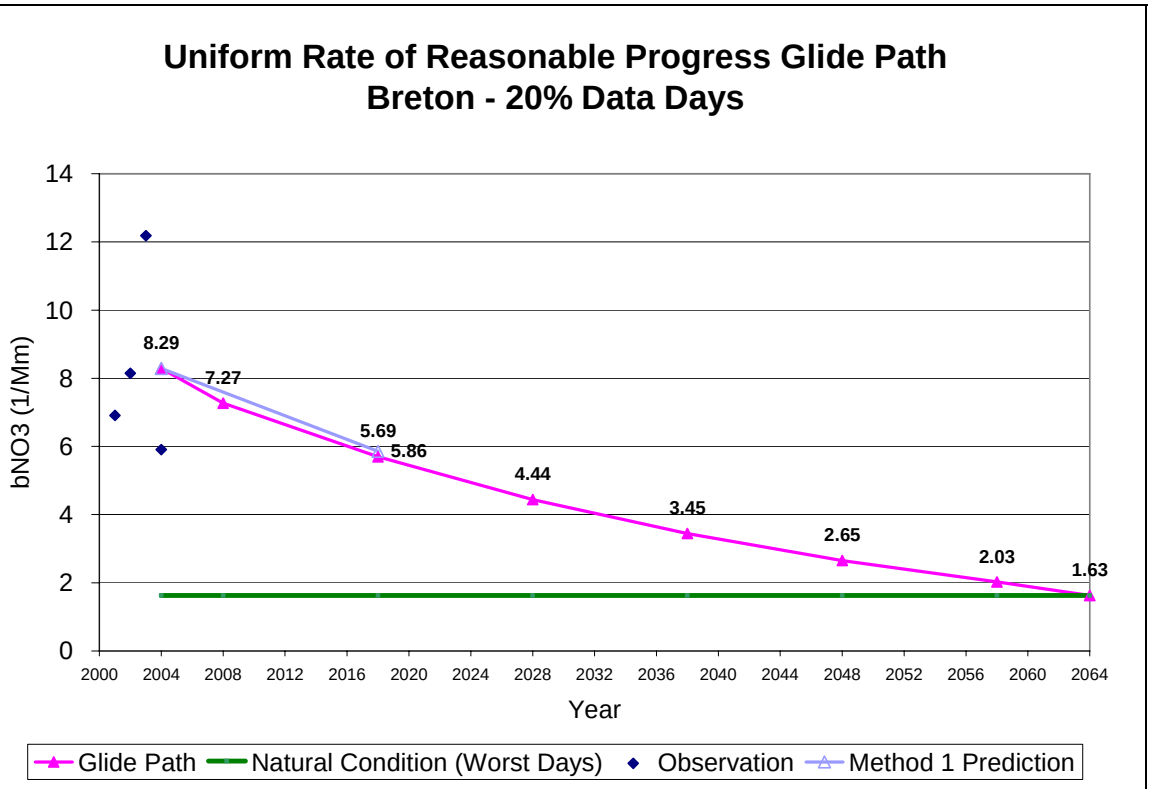

Figure F-3c. 2018 Visibility Projections and 2018 URP Glidepaths for Nitrate (NO3) in extinction (Mm^{-1}) for Breton Island (BRET), Louisiana and Worst 20% (W20%) days using 2002/2018 Base G CMAQ 36 km modeling results.

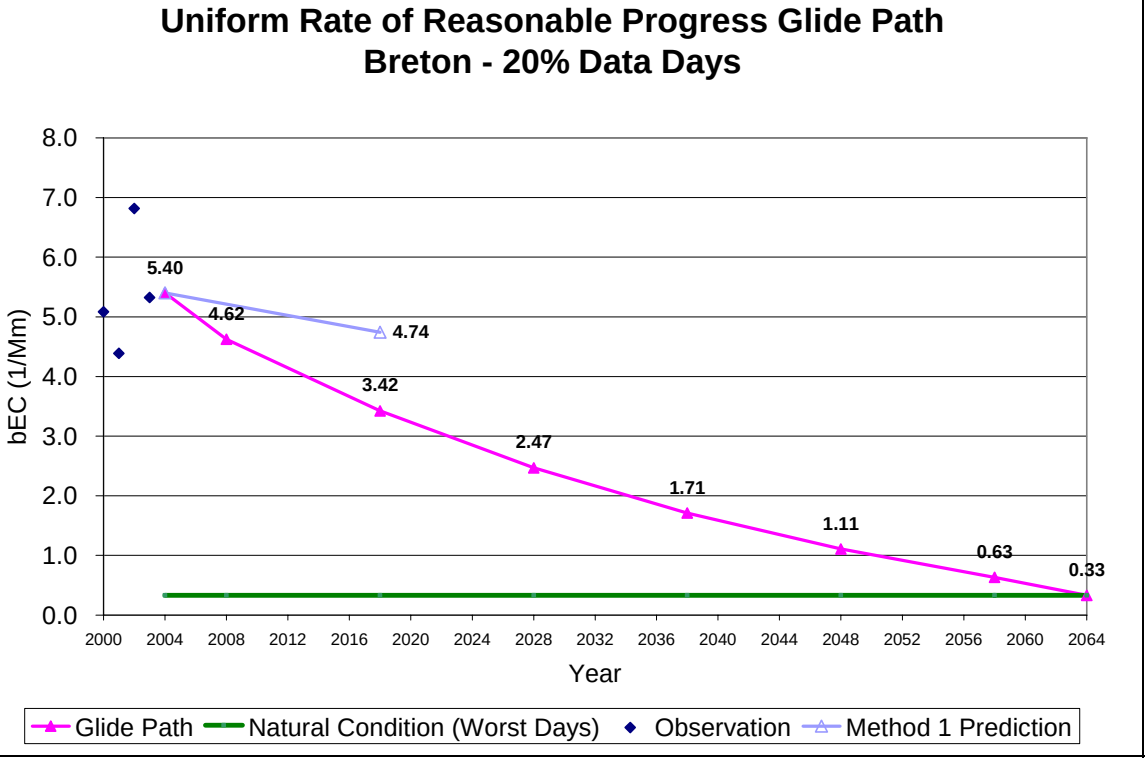

Figure F-3d. 2018 Visibility Projections and 2018 URP Glidepaths for Elemental Carbon (EC) in extinction (Mm^{-1}) for Breton Island (BRET), Louisiana and Worst 20% (W20%) days using 2002/2018 Base G CMAQ 36 km modeling results.

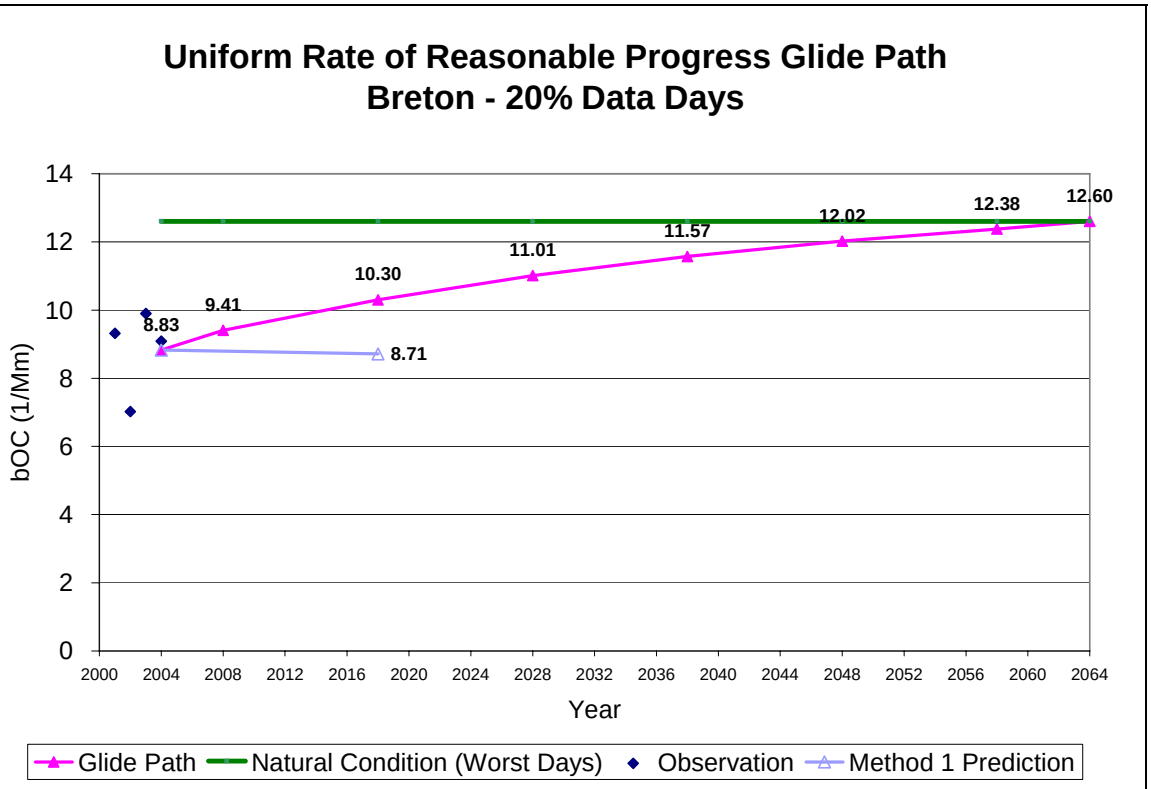

Figure F-3e. 2018 Visibility Projections and 2018 URP Glidepaths for Organic Mass Carbon (OMC) in extinction (Mm^{-1}) for Breton Island (BRET), Louisiana and Worst 20% (W20%) days using 2002/2018 Base G CMAQ 36 km modeling results.

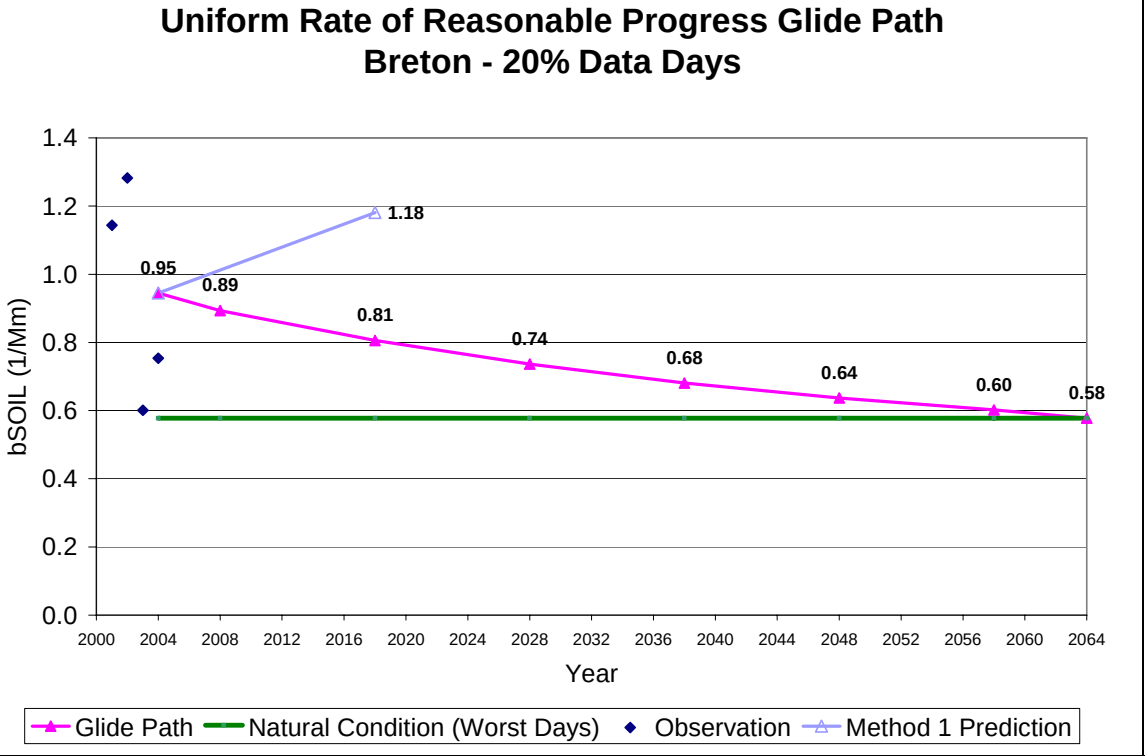

Figure F-3f. 2018 Visibility Projections and 2018 URP Glidepaths for Other Fine Particulate (SOIL) in extinction (Mm^{-1}) for Breton Island (BRET), Louisiana and Worst 20% (W20%) days using 2002/2018 Base G CMAQ 36 km modeling results.

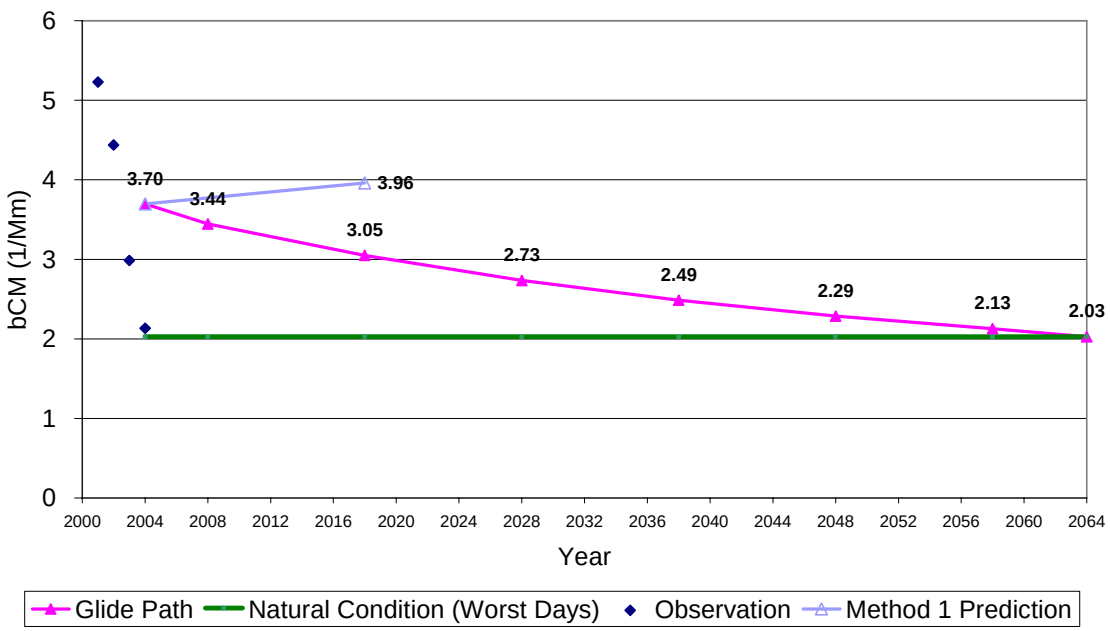

Figure F-3g. 2018 Visibility Projections and 2018 URP Glidepaths for Coarse Mass (CM) in extinction (Mm^{-1}) for Breton Island (BRET), Louisiana and Worst 20% (W20%) days using 2002/2018 Base G CMAQ 36 km modeling results.

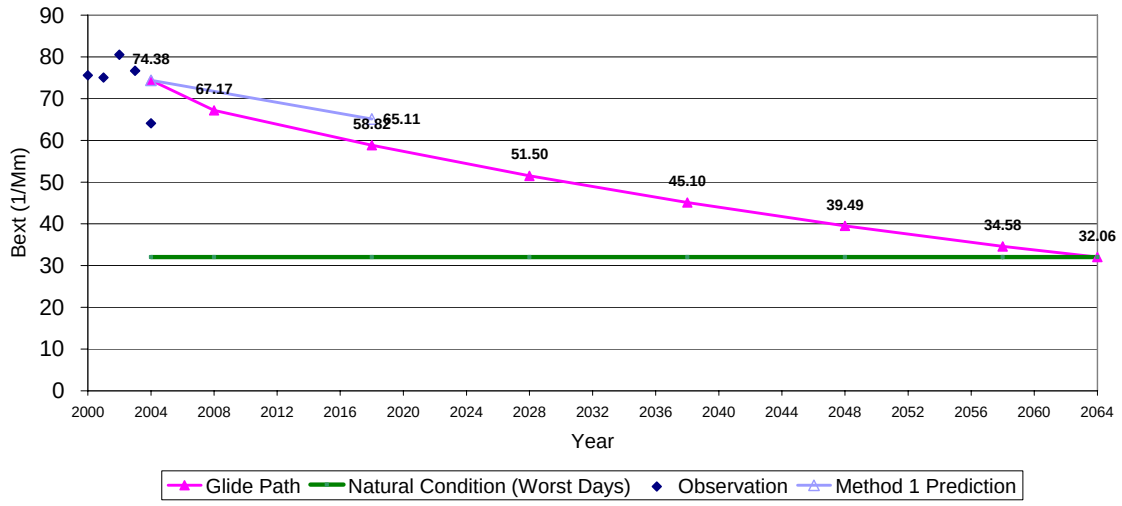

Figure F-4a. 2018 Visibility Projections and 2018 URP Glidepaths in extinction (Mm^{-1}) for Boundary Waters (BOWA), Minnesota and Worst 20% (W20%) days using 2002/2018 Base G CMAQ 36 km modeling results.

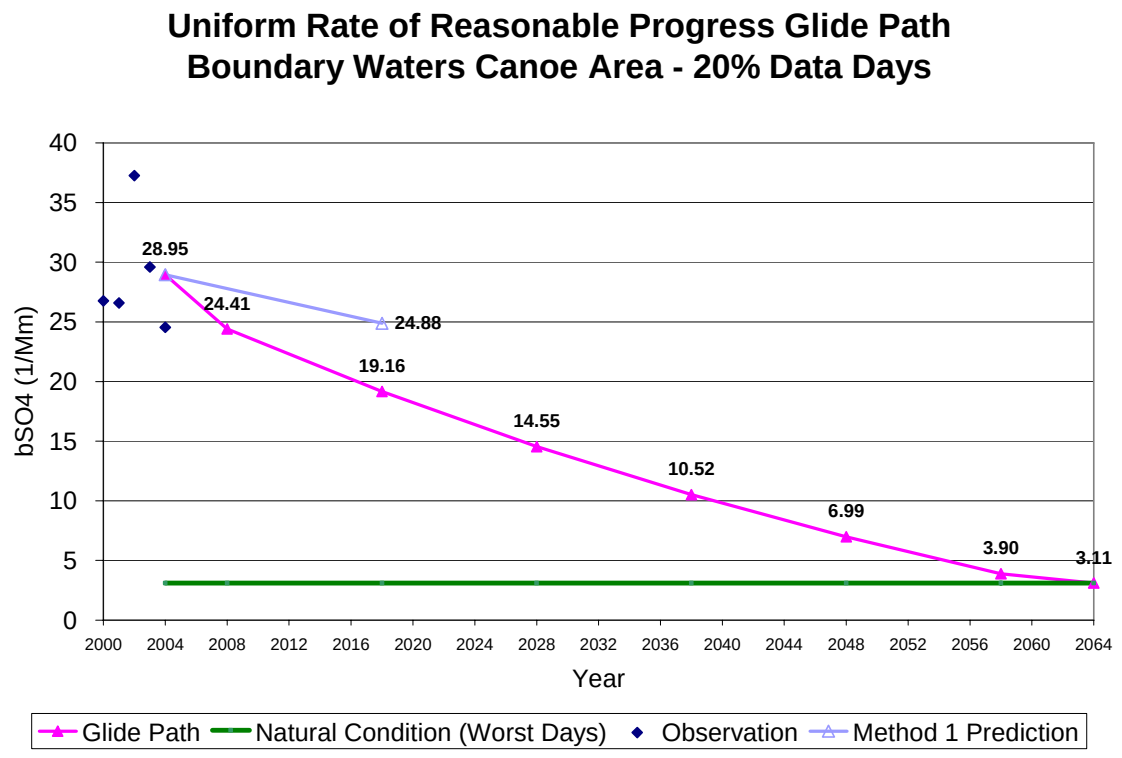

Figure F-4b. 2018 Visibility Projections and 2018 URP Glidepaths for Sulfate (SO4) in extinction (Mm^{-1}) for Boundary Waters (BOWA), Minnesota and Worst 20% (W20%) days using 2002/2018 Base G CMAQ 36 km modeling results.

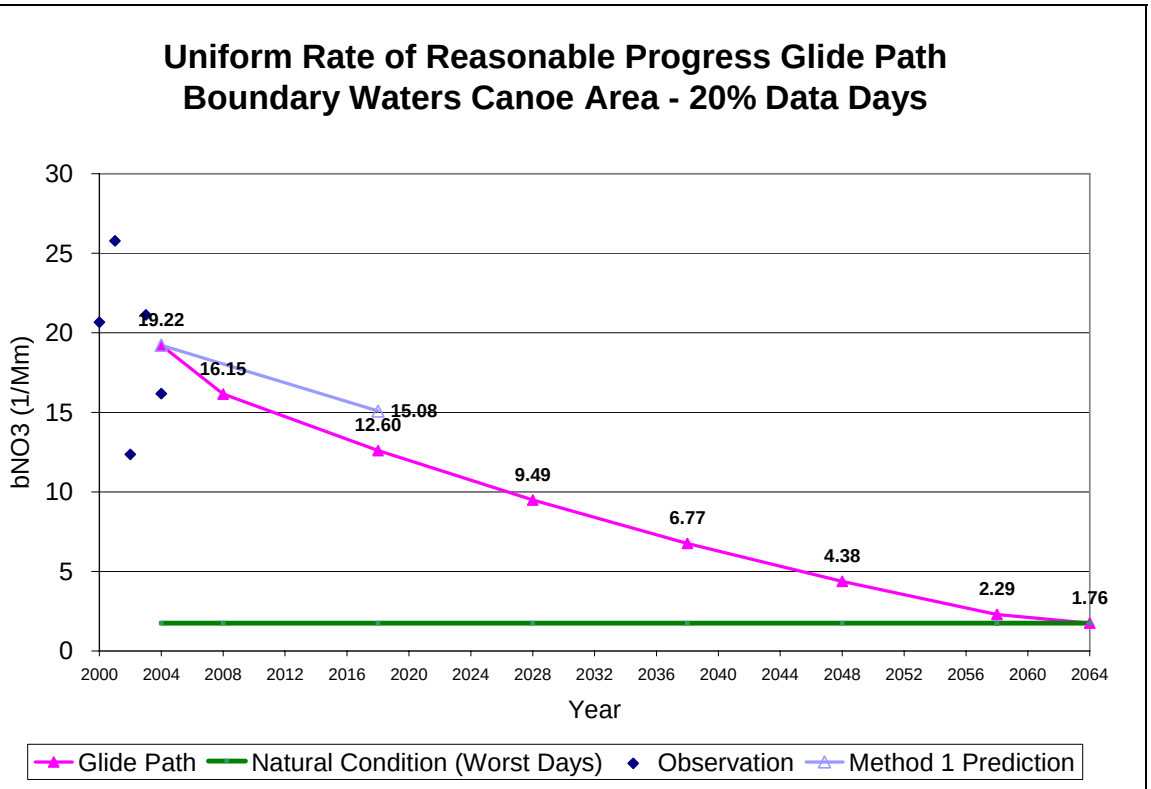

Figure F-4c. 2018 Visibility Projections and 2018 URP Glidepaths for Nitrate (NO3) in extinction (Mm^{-1}) for Boundary Waters (BOWA), Minnesota and Worst 20% (W20%) days using 2002/2018 Base G CMAQ 36 km modeling results.

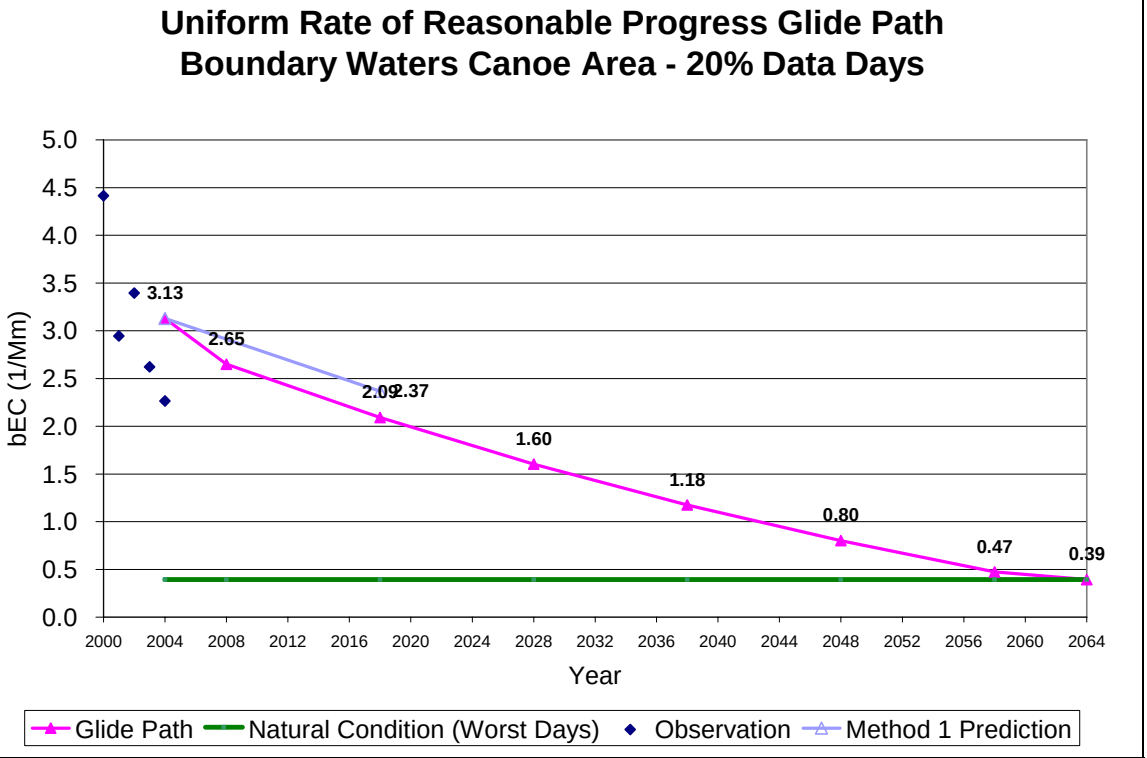

Figure F-4d. 2018 Visibility Projections and 2018 URP Glidepaths for Elemental Carbon (EC) in extinction (Mm^{-1}) for Boundary Waters (BOWA), Minnesota and Worst 20% (W20%) days using 2002/2018 Base G CMAQ 36 km modeling results.

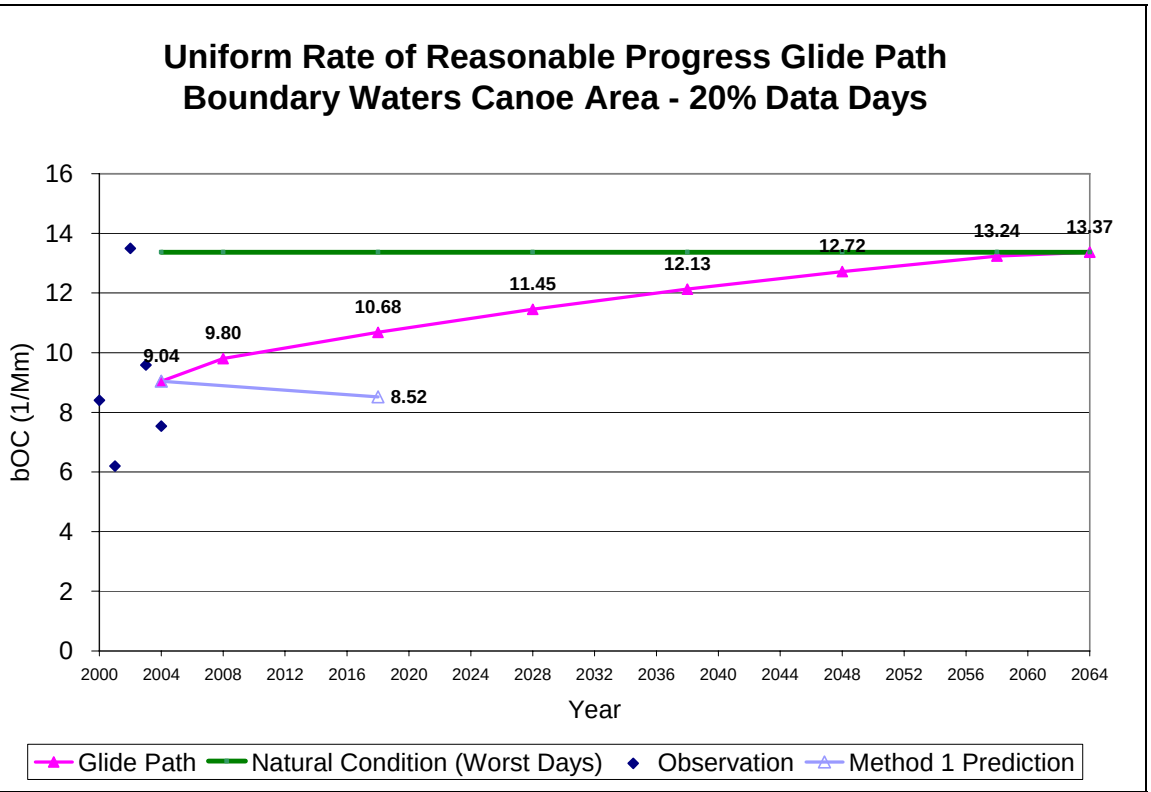

Figure F-4e. 2018 Visibility Projections and 2018 URP Glidepaths for Organic Mass Carbon (OMC) in extinction (Mm^{-1}) for Boundary Waters (BOWA), Minnesota and Worst 20% (W20%) days using 2002/2018 Base G CMAQ 36 km modeling results.

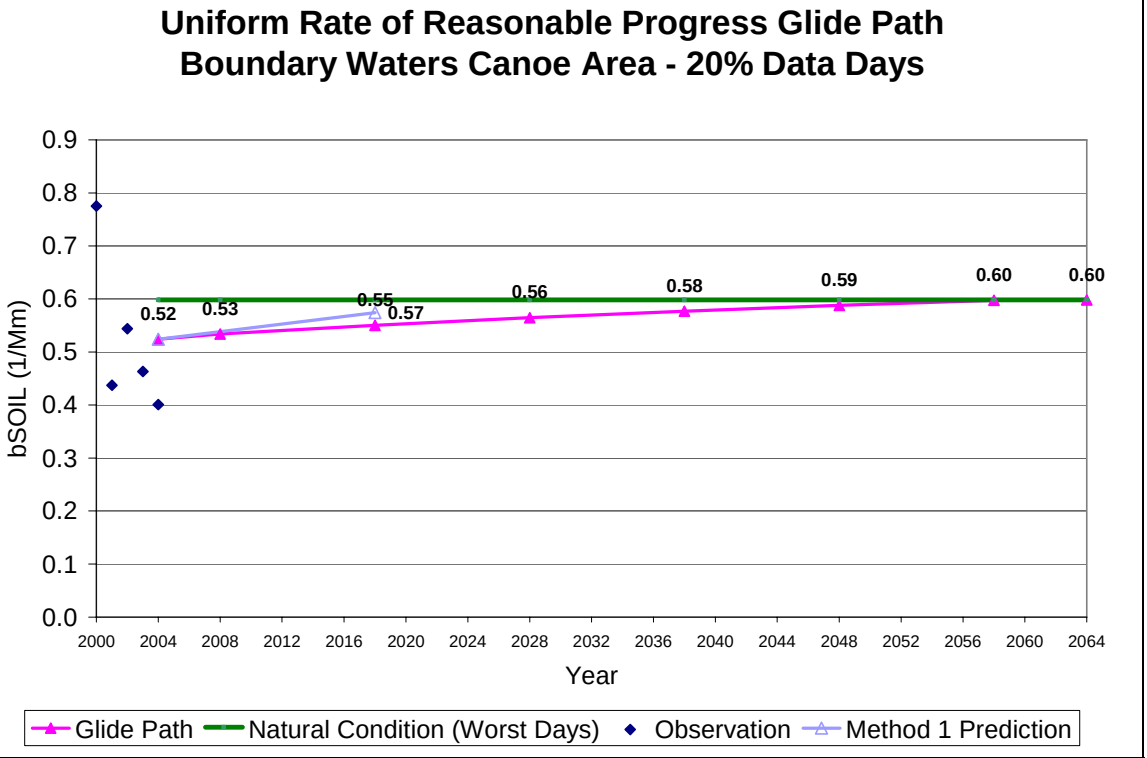

Figure F-4f. 2018 Visibility Projections and 2018 URP Glidepaths for Other Fine Particulate (SOIL) in extinction (Mm^{-1}) for Boundary Waters (BOWA), Minnesota and Worst 20% (W20%) days using 2002/2018 Base G CMAQ 36 km modeling results.

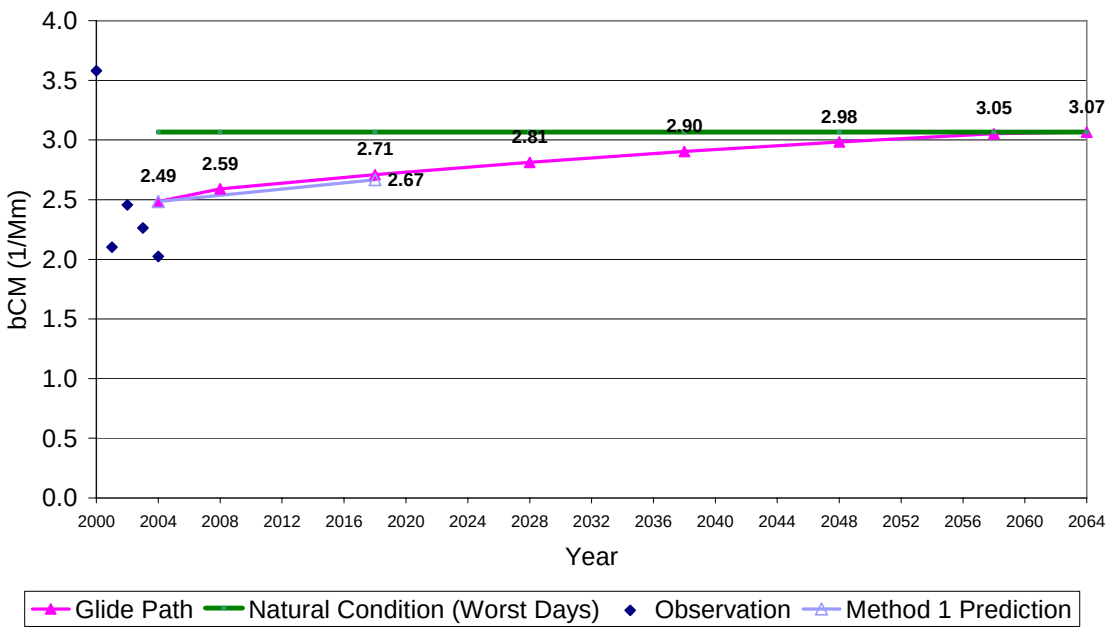

Figure F-4g. 2018 Visibility Projections and 2018 URP Glidepaths for Coarse Mass (CM) in extinction (Mm^{-1}) for Boundary Waters (BOWA), Minnesota and Worst 20% (W20%) days using 2002/2018 Base G CMAQ 36 km modeling results.

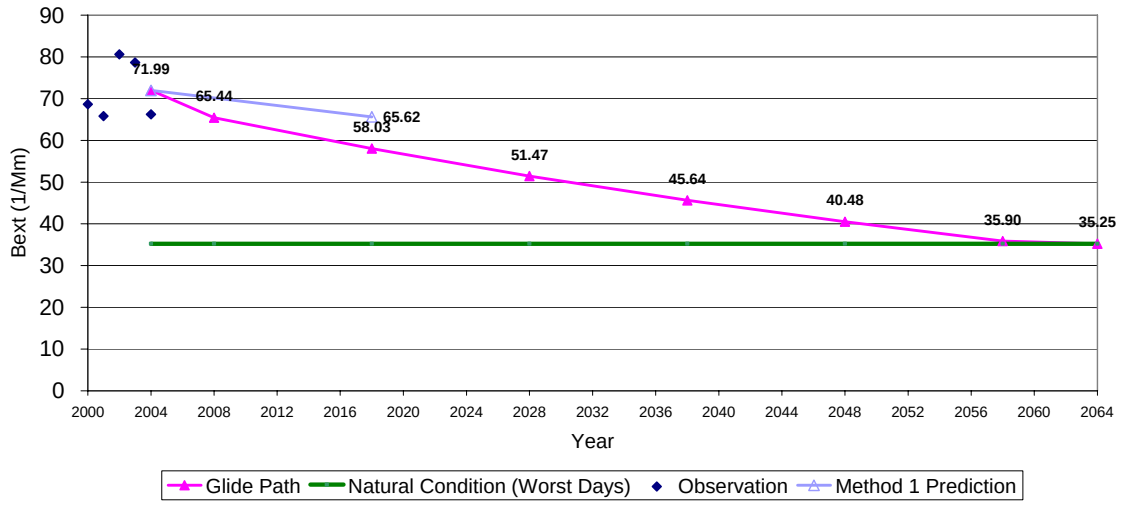

Figure F-5a. 2018 Visibility Projections and 2018 URP Glidepaths in extinction (Mm^{-1}) for Voyageurs (VOYA), Minnesota and Worst 20% (W20%) days using 2002/2018 Base G CMAQ 36 km modeling results.

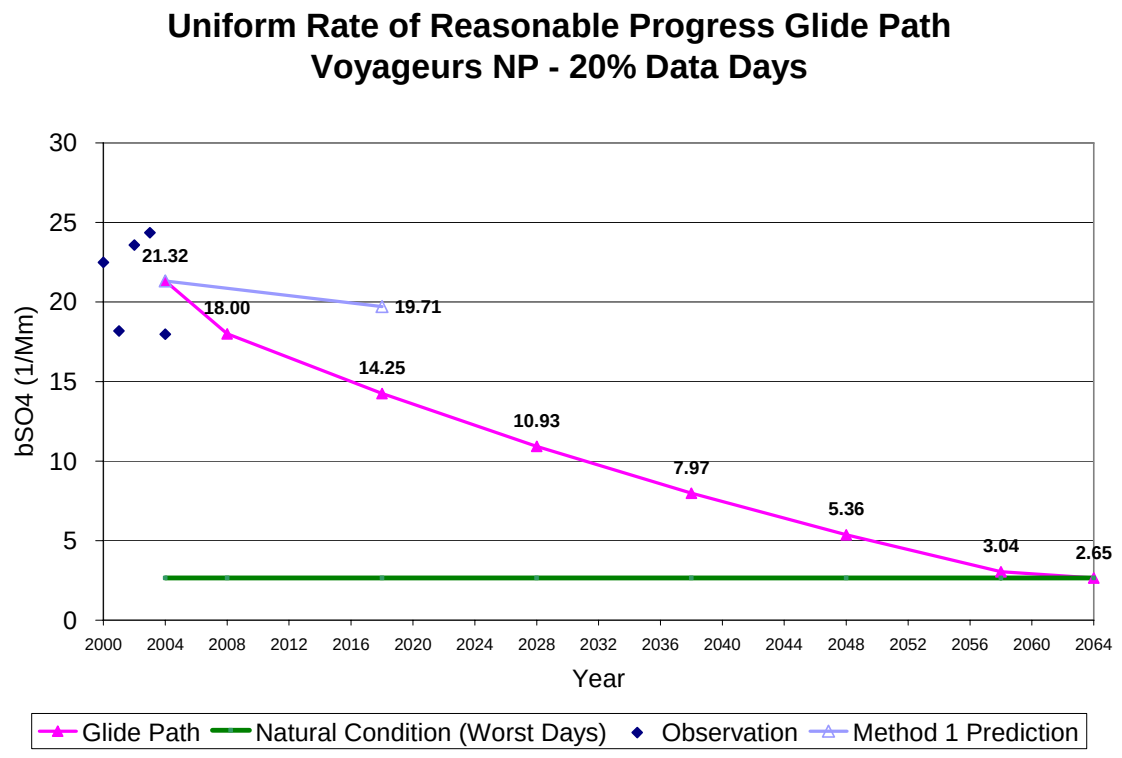

Figure F-5b. 2018 Visibility Projections and 2018 URP Glidepaths for Sulfate (SO4) in extinction (Mm^{-1}) for Voyageurs (VOYA), Minnesota and Worst 20% (W20%) days using 2002/2018 Base G CMAQ 36 km modeling results.

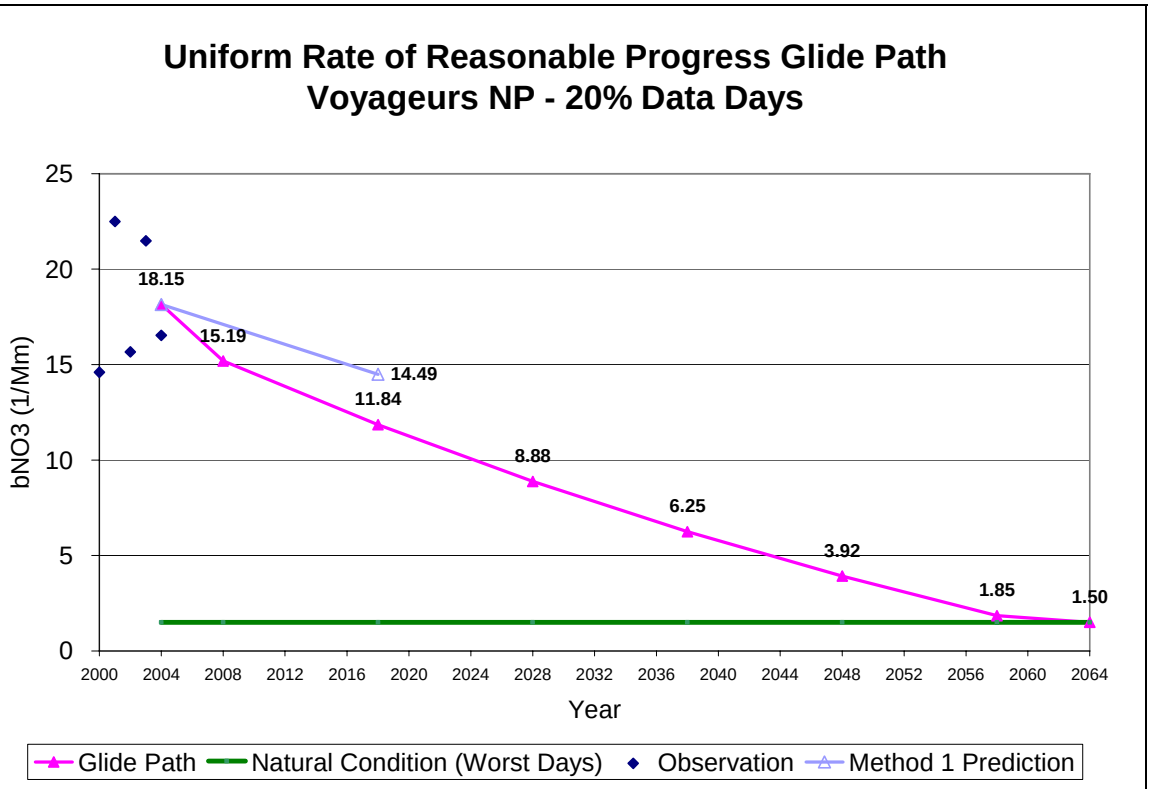

Figure F-5c. 2018 Visibility Projections and 2018 URP Glidepaths for Nitrate (NO3) in extinction (Mm^{-1}) for Voyageurs (VOYA), Minnesota and Worst 20% (W20%) days using 2002/2018 Base G CMAQ 36 km modeling results.

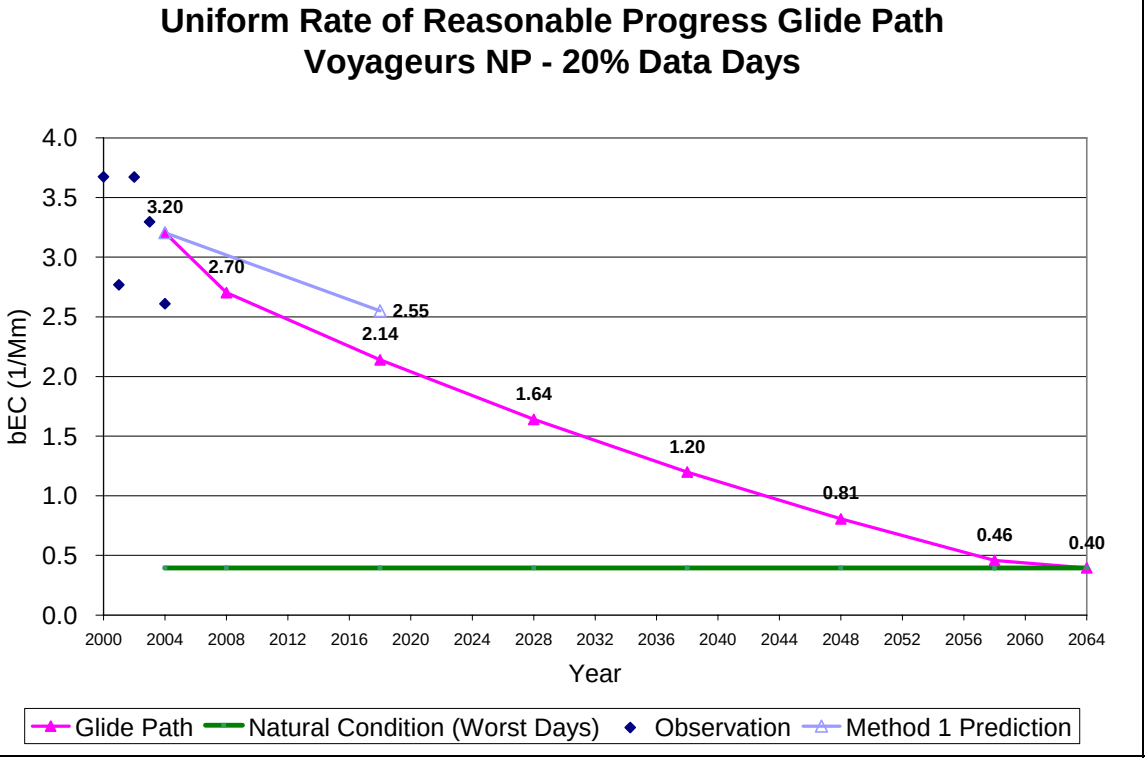

Figure F-5d. 2018 Visibility Projections and 2018 URP Glidepaths for Elemental Carbon (EC) in extinction (Mm^{-1}) for Voyageurs (VOYA), Minnesota and Worst 20% (W20%) days using 2002/2018 Base G CMAQ 36 km modeling results.

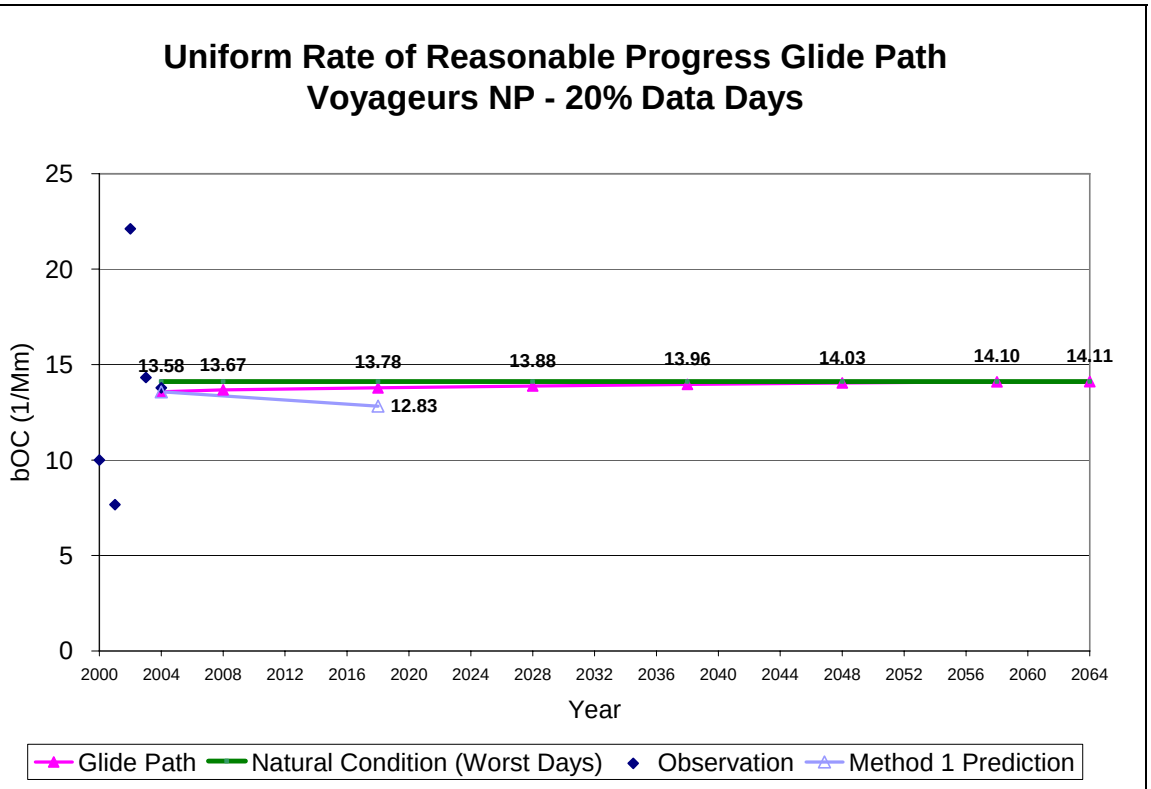

Figure F-5e. 2018 Visibility Projections and 2018 URP Glidepaths for Organic Mass Carbon (OMC) in extinction (Mm^{-1}) for Voyageurs (VOYA), Minnesota and Worst 20% (W20%) days using 2002/2018 Base G CMAQ 36 km modeling results.

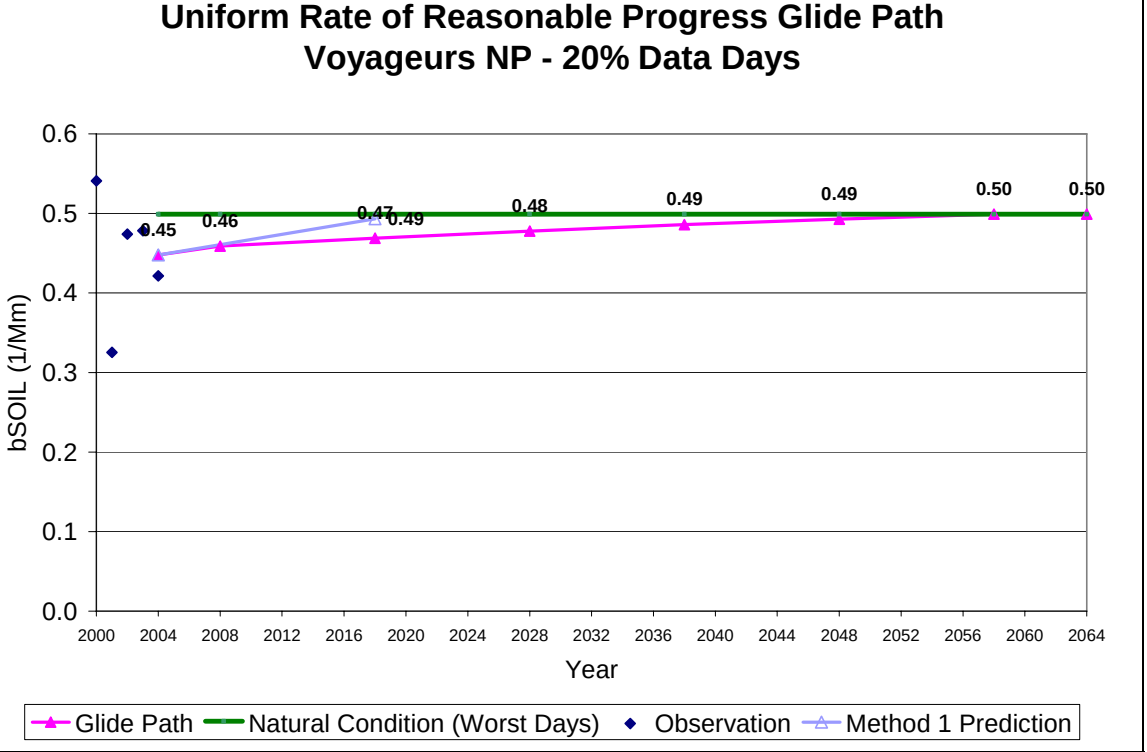

Figure F-5f. 2018 Visibility Projections and 2018 URP Glidepaths for Other Fine Particulate (SOIL) in extinction (Mm^{-1}) for Voyageurs (VOYA), Minnesota and Worst 20% (W20%) days using 2002/2018 Base G CMAQ 36 km modeling results.

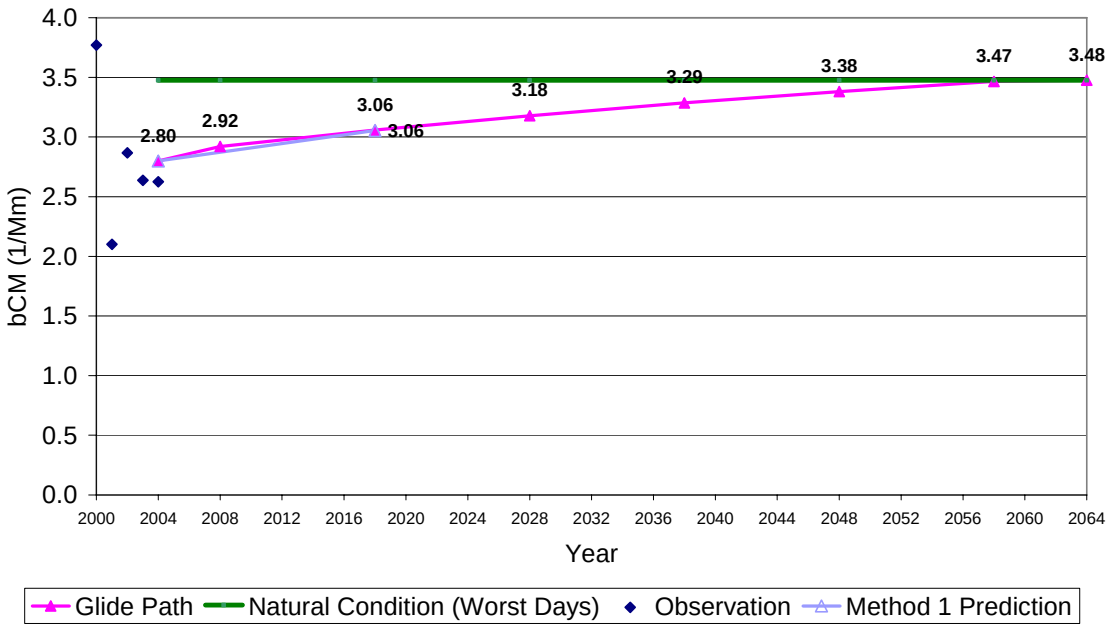

Figure F-5g. 2018 Visibility Projections and 2018 URP Glidepaths for Coarse Mass (CM) in extinction (Mm^{-1}) for Voyageurs (VOYA), Minnesota and Worst 20% (W20%) days using 2002/2018 Base G CMAQ 36 km modeling results.

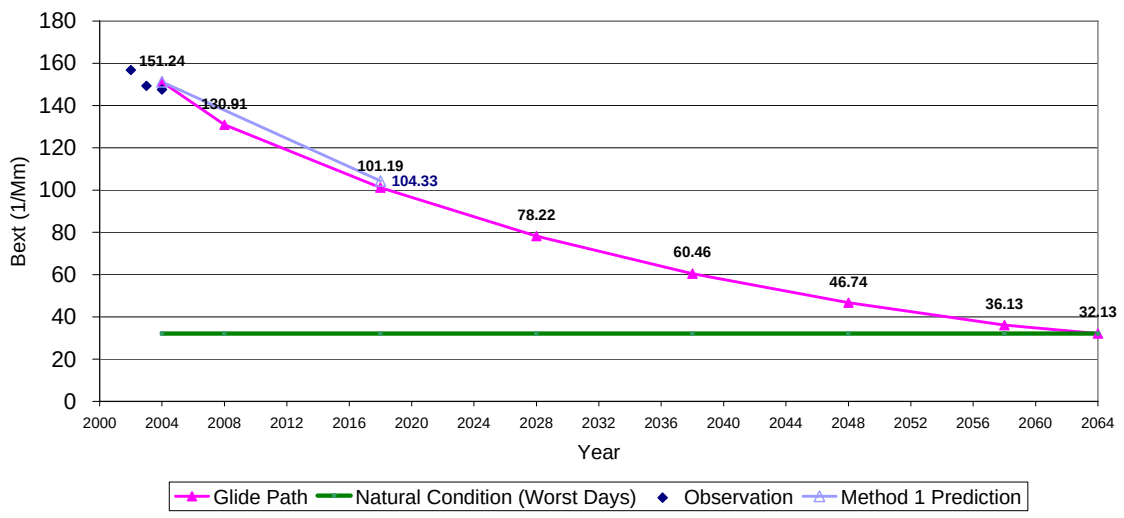

Figure F-6a. 2018 Visibility Projections and 2018 URP Glidepaths in extinction (Mm^{-1}) for Hercules-Glade (HEGL), Missouri and Worst 20% (W20%) days using 2002/2018 Base G CMAQ 36 km modeling results.

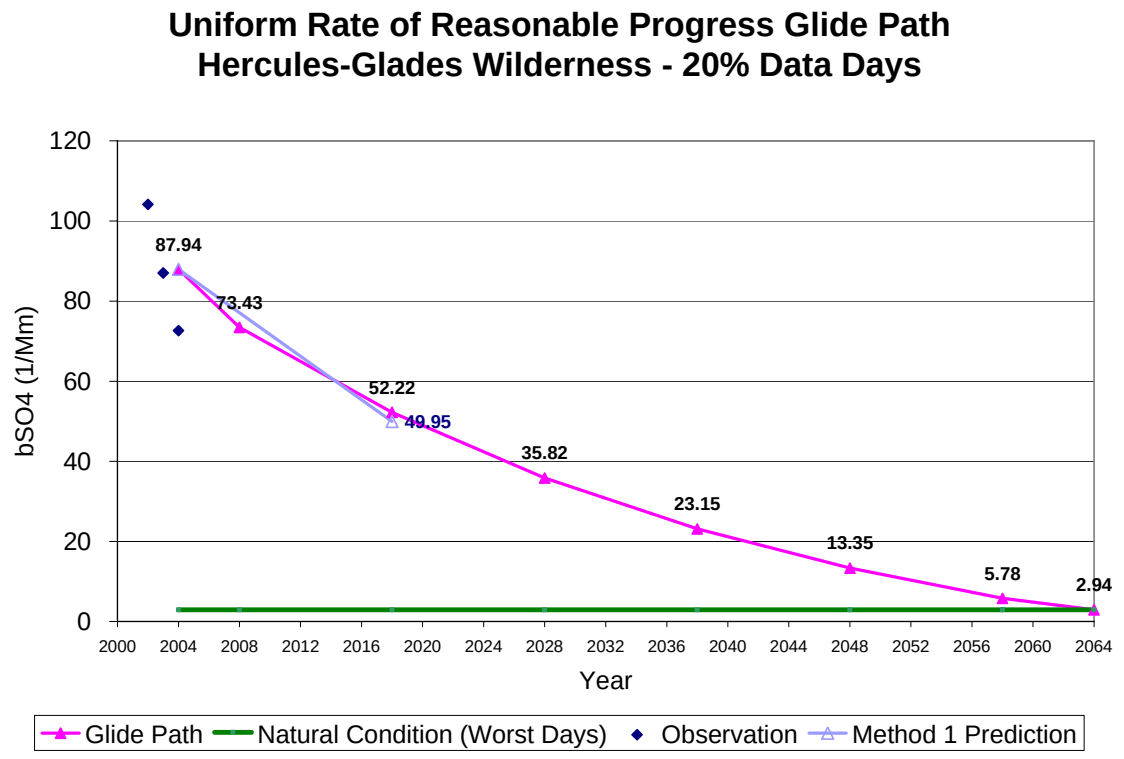

Figure F-6b. 2018 Visibility Projections and 2018 URP Glidepaths for Sulfate (SO4) in extinction (Mm^{-1}) for Hercules-Glade (HEGL), Missouri and Worst 20% (W20%) days using 2002/2018 Base G CMAQ 36 km modeling results.

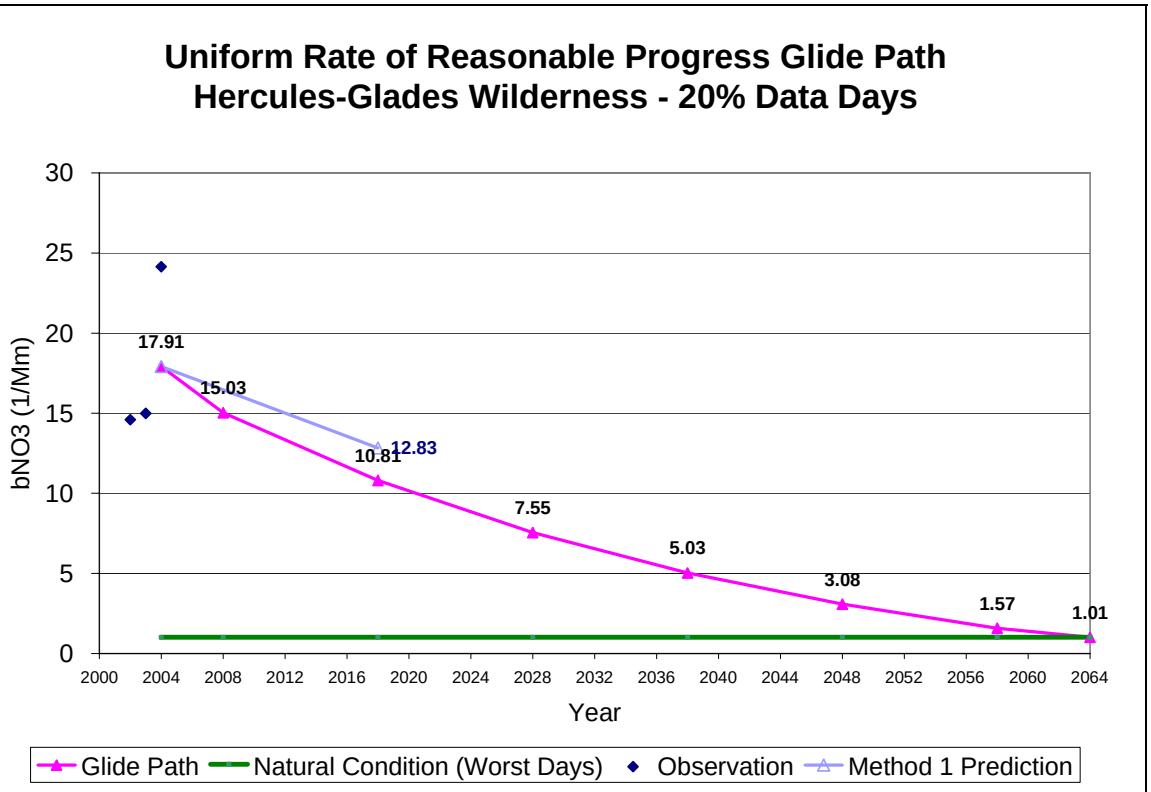

Figure F-6c. 2018 Visibility Projections and 2018 URP Glidepaths for Nitrate (NO3) in extinction (Mm^{-1}) for Hercules-Glade (HEGL), Missouri and Worst 20% (W20%) days using 2002/2018 Base G CMAQ 36 km modeling results.

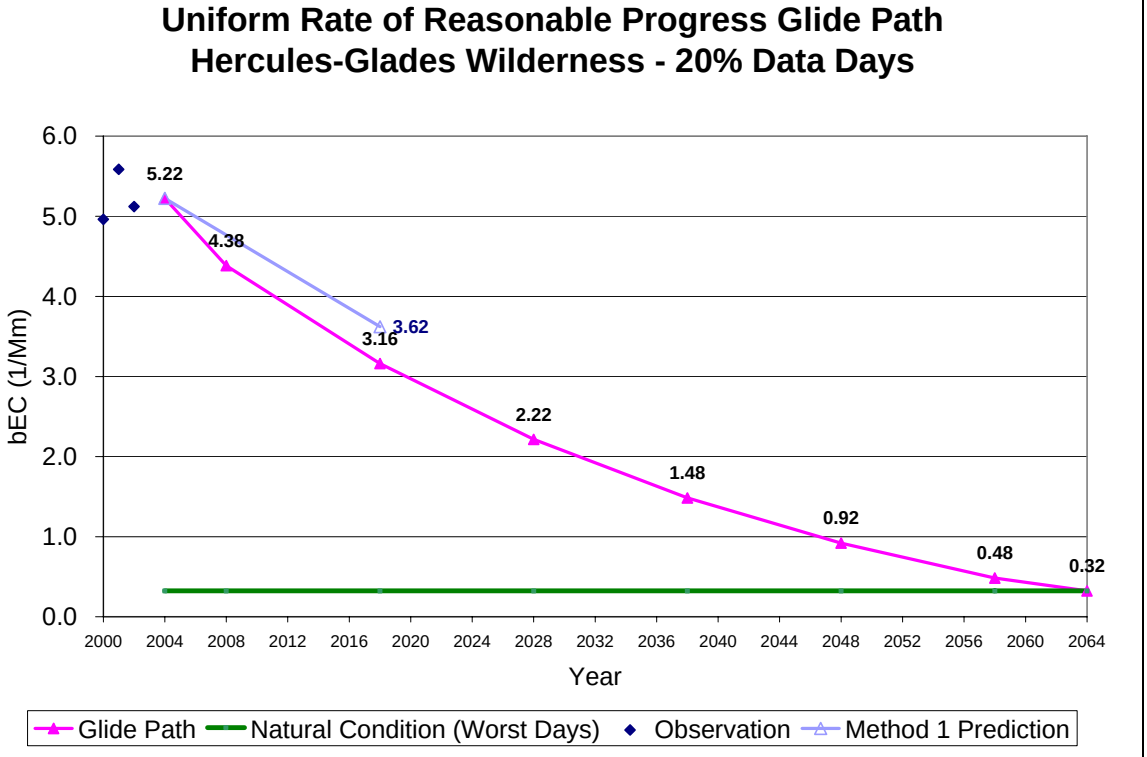

Figure F-6d. 2018 Visibility Projections and 2018 URP Glidepaths for Elemental Carbon (EC) in extinction (Mm^{-1}) for Hercules-Glade (HEGL), Missouri and Worst 20% (W20%) days using 2002/2018 Base G CMAQ 36 km modeling results.

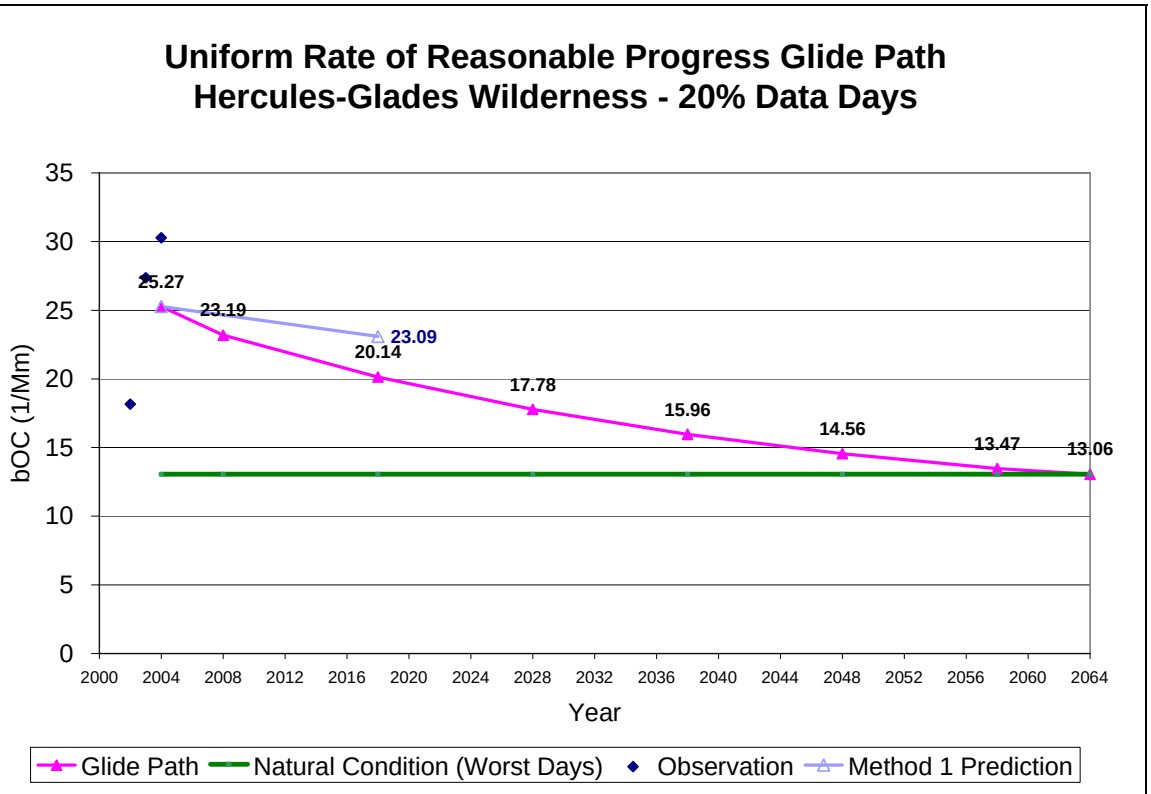

Figure F-6e. 2018 Visibility Projections and 2018 URP Glidepaths for Organic Mass Carbon (OMC) in extinction (Mm^{-1}) for Hercules-Glade (HEGL), Missouri and Worst 20% (W20%) days using 2002/2018 Base G CMAQ 36 km modeling results.

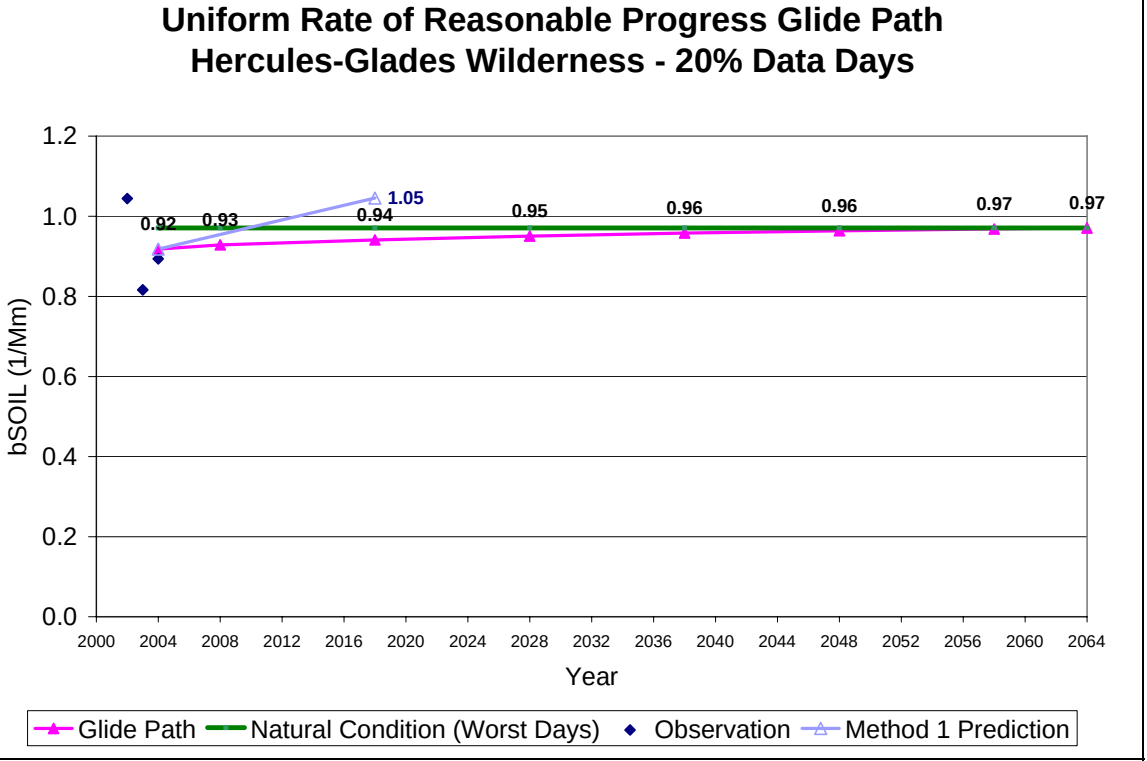

Figure F-6f. 2018 Visibility Projections and 2018 URP Glidepaths for Other Fine Particulate (SOIL) in extinction (Mm^{-1}) for Hercules-Glade (HEGL), Missouri and Worst 20% (W20%) days using 2002/2018 Base G CMAQ 36 km modeling results.

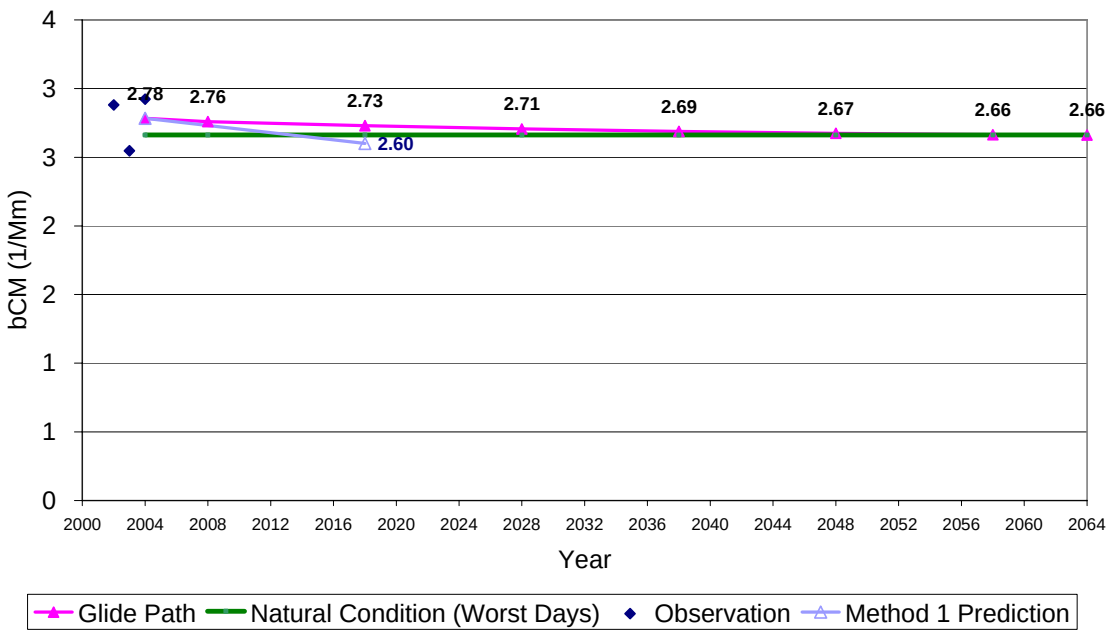

Figure F-6g. 2018 Visibility Projections and 2018 URP Glidepaths for Coarse Mass (CM) in extinction (Mm^{-1}) for Hercules-Glade (HEGL), Missouri and Worst 20% (W20%) days using 2002/2018 Base G CMAQ 36 km modeling results.

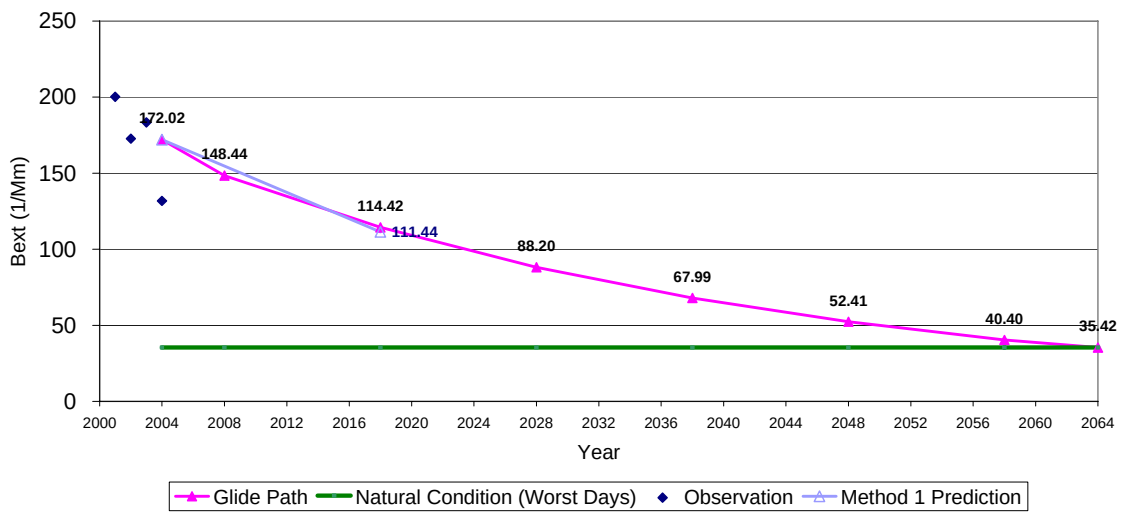

Figure F-7a. 2018 Visibility Projections and 2018 URP Glidepaths in extinction (Mm^{-1}) for Mingo (MING), Missouri and Worst 20% (W20%) days using 2002/2018 Base G CMAQ 36 km modeling results.

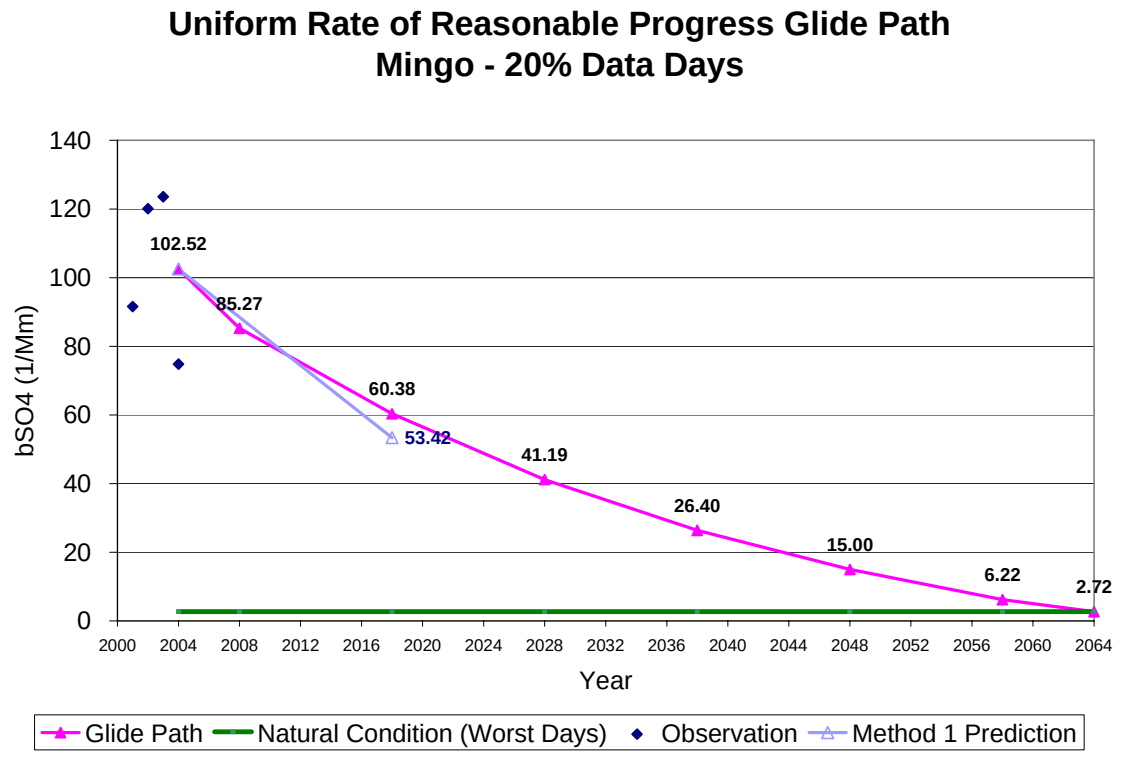

Figure F-7b. 2018 Visibility Projections and 2018 URP Glidepaths for Sulfate (SO4) in extinction (Mm^{-1}) for Mingo (MING), Missouri and Worst 20% (W20%) days using 2002/2018 Base G CMAQ 36 km modeling results.

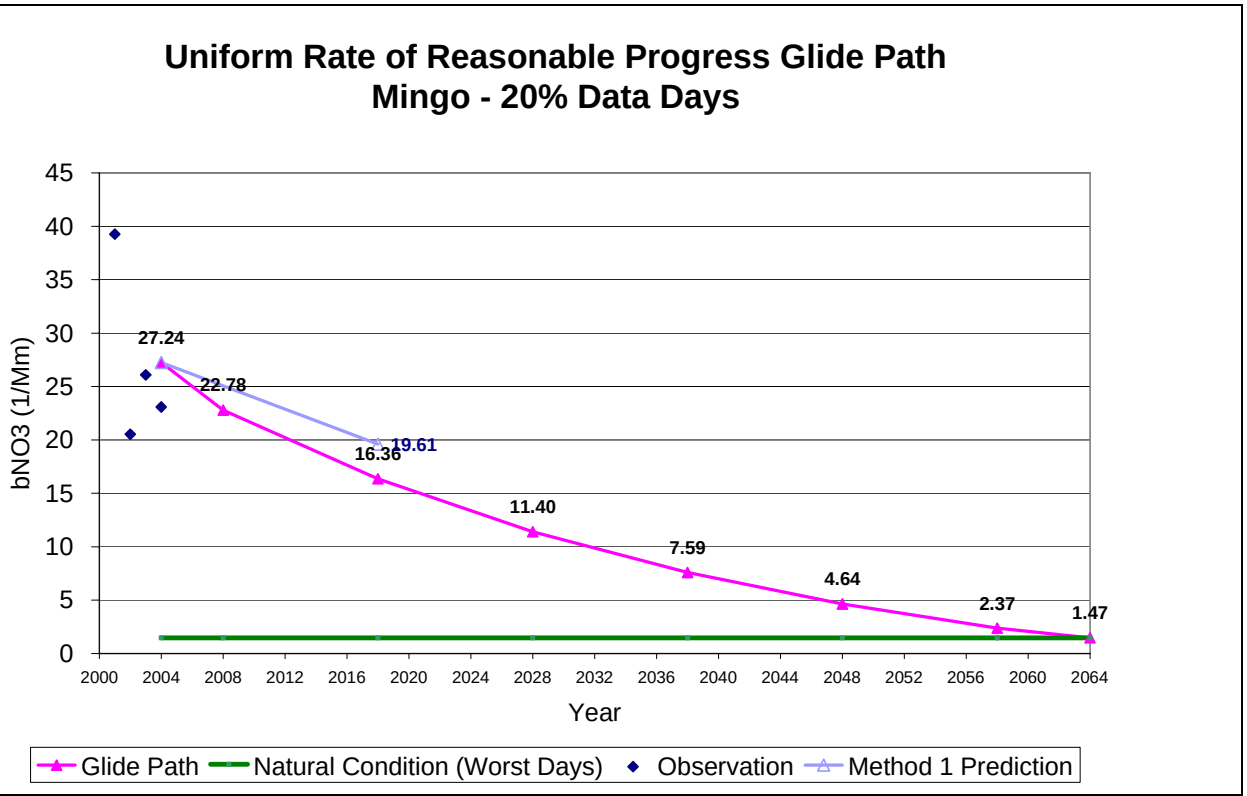

Figure F-7c. 2018 Visibility Projections and 2018 URP Glidepaths for Nitrate (NO3) in extinction (Mm^{-1}) for Mingo (MING), Missouri and Worst 20% (W20%) days using 2002/2018 Base G CMAQ 36 km modeling results.

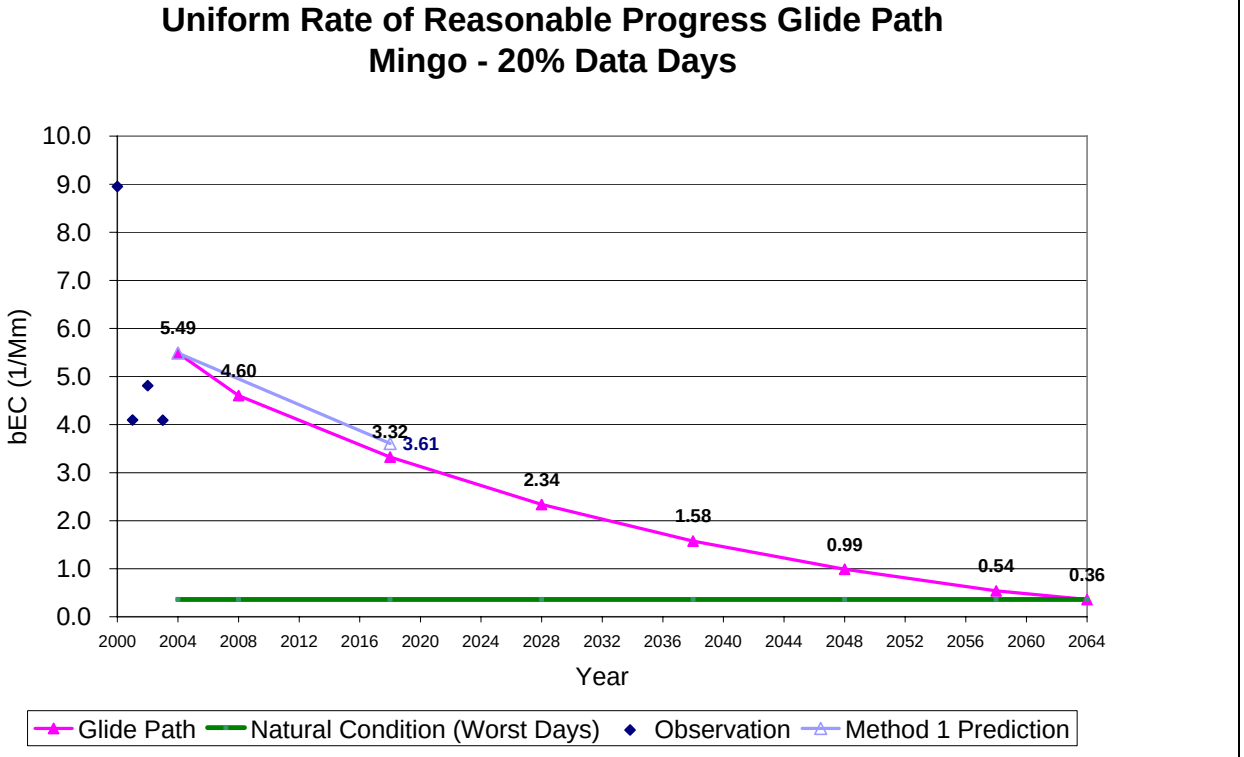

Figure F-7d. 2018 Visibility Projections and 2018 URP Glidepaths for Elemental Carbon (EC) in extinction (Mm^{-1}) for Mingo (MING), Missouri and Worst 20% (W20%) days using 2002/2018 Base G CMAQ 36 km modeling results.

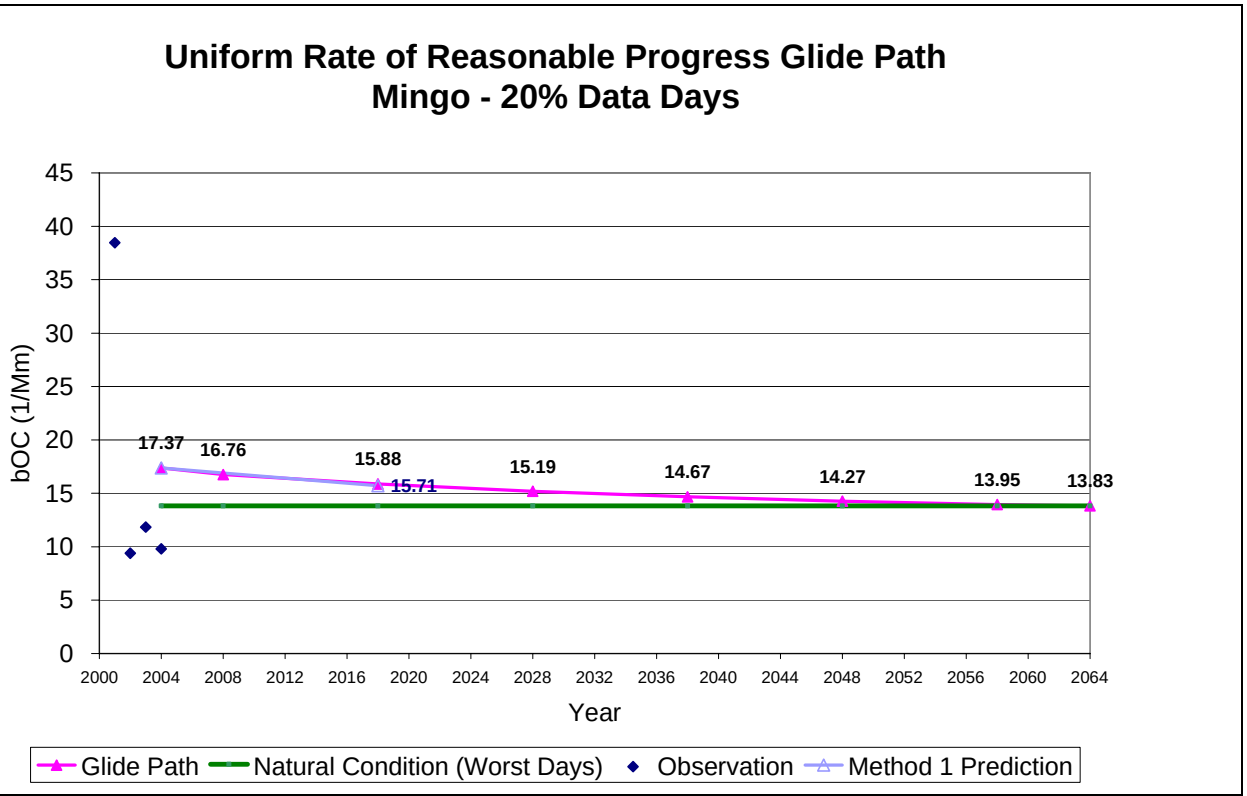

Figure F-7e. 2018 Visibility Projections and 2018 URP Glidepaths for Organic Mass Carbon (OMC) in extinction (Mm^{-1}) for Mingo (MING), Missouri and Worst 20% (W20%) days using 2002/2018 Base G CMAQ 36 km modeling results.

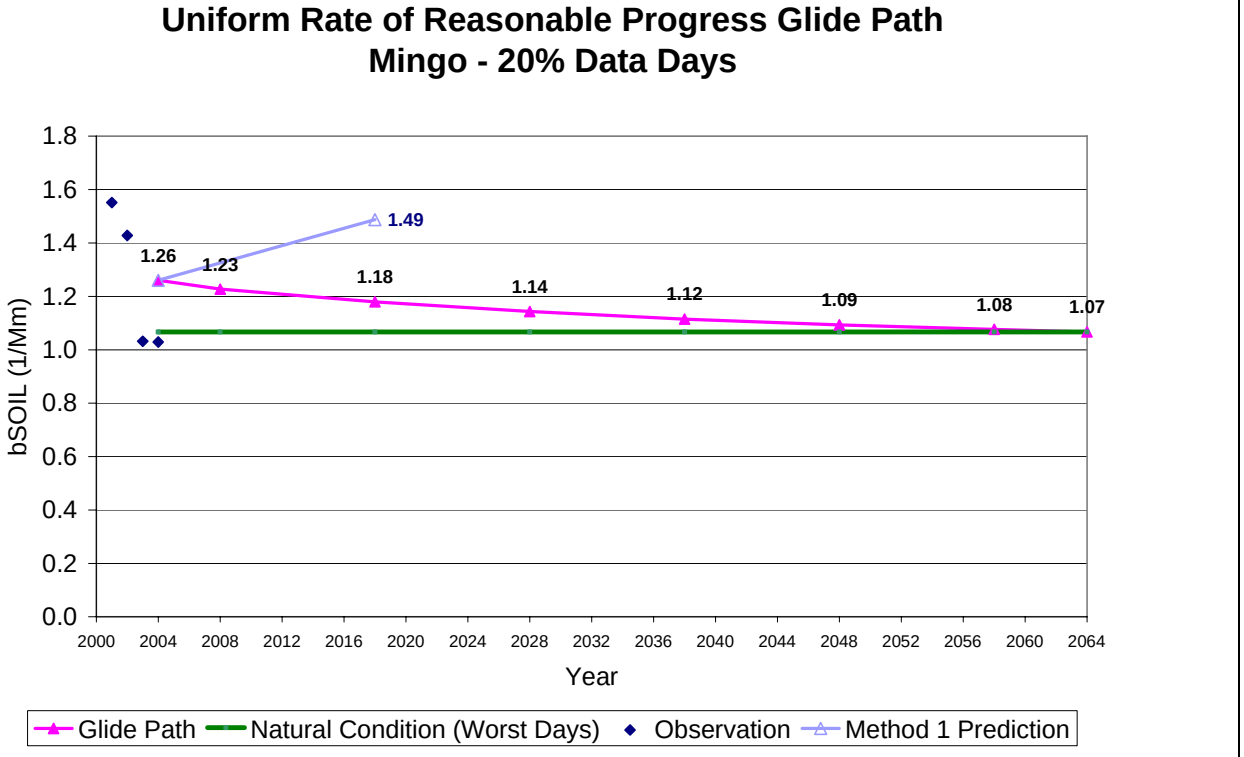

Figure F-7f. 2018 Visibility Projections and 2018 URP Glidepaths for Other Fine Particulate (SOIL) in extinction (Mm^{-1}) for Mingo (MING), Missouri and Worst 20% (W20%) days using 2002/2018 Base G CMAQ 36 km modeling results.

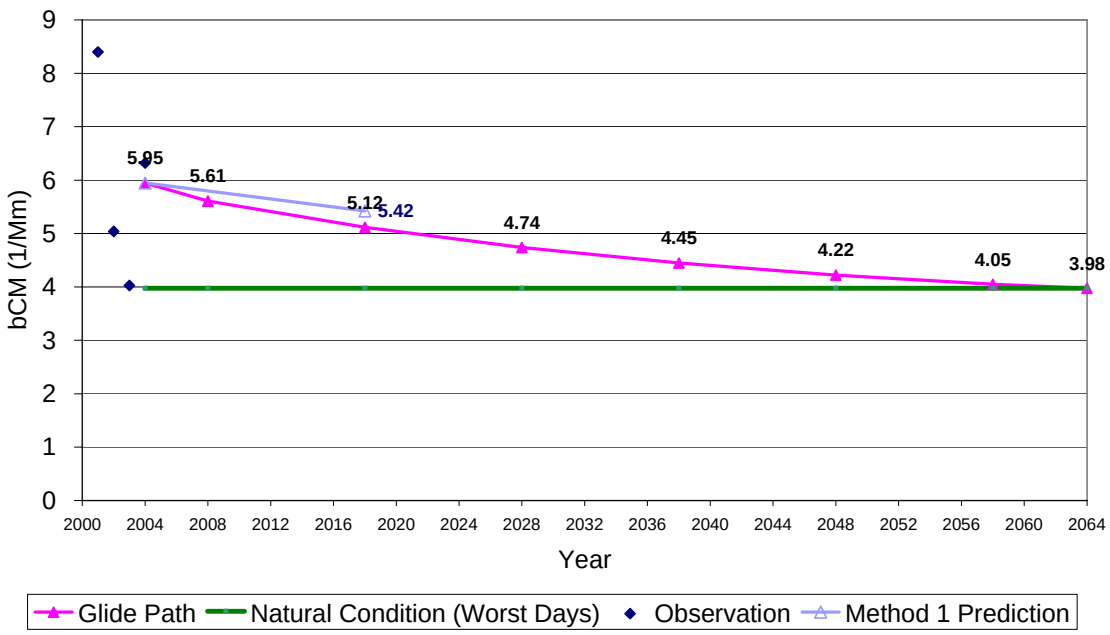

Figure F-7g. 2018 Visibility Projections and 2018 URP Glidepaths for Coarse Mass (CM) in extinction (Mm^{-1}) for Mingo (MING), Missouri and Worst 20% (W20%) days using 2002/2018 Base G CMAQ 36 km modeling results.

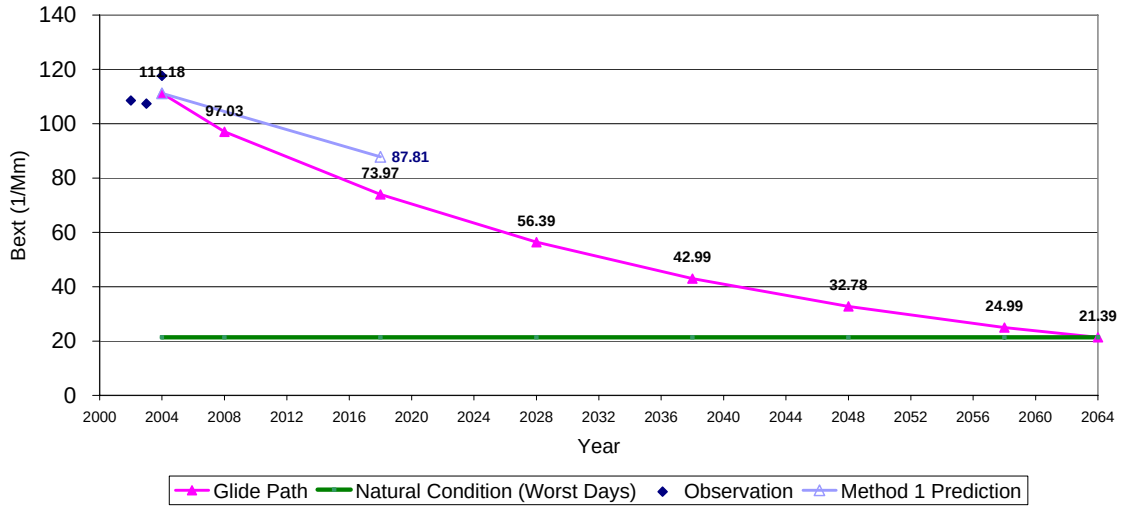

Figure F-8a. 2018 Visibility Projections and 2018 URP Glidepaths in extinction (Mm^{-1}) for Wichita Mountains (WIMO), Oklahoma and Worst 20% (W20%) days using 2002/2018 Base G CMAQ 36 km modeling results.

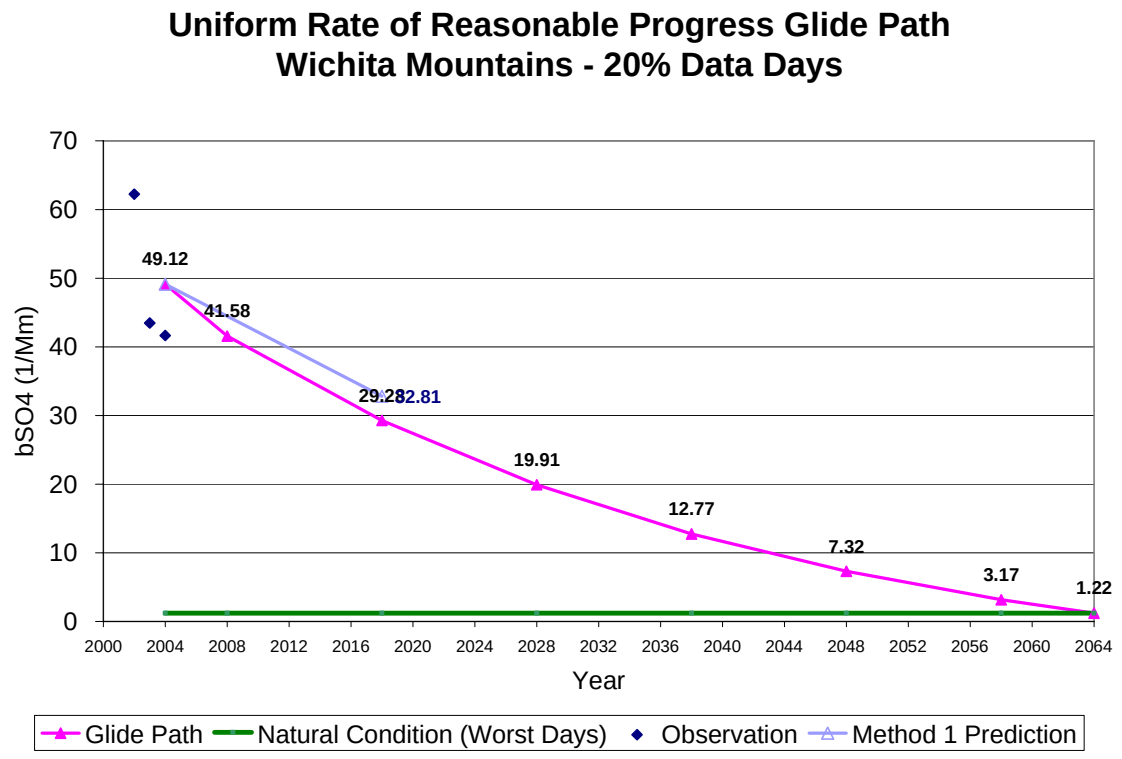

Figure F-8b. 2018 Visibility Projections and 2018 URP Glidepaths for Sulfate (SO4) in extinction (Mm^{-1}) for Wichita Mountains (WIMO), Oklahoma and Worst 20% (W20%) days using 2002/2018 Base G CMAQ 36 km modeling results.

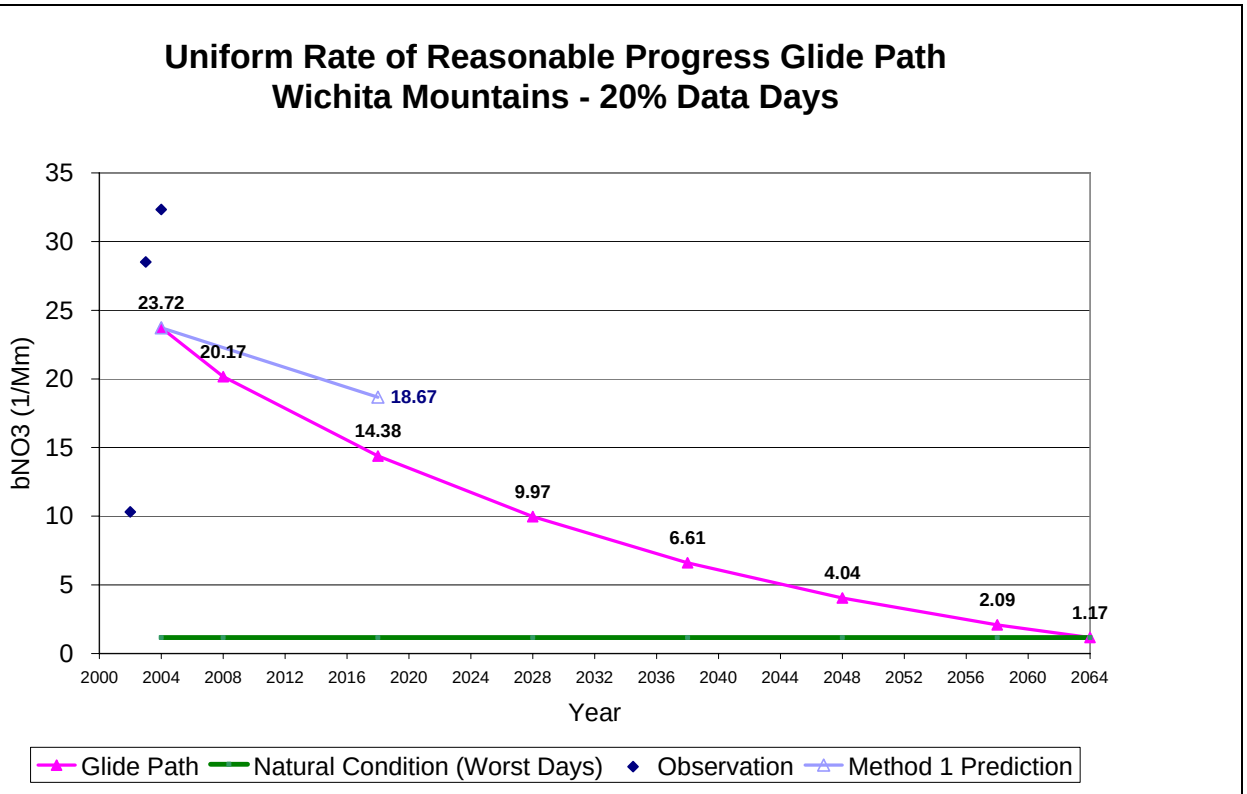

Figure F-8c. 2018 Visibility Projections and 2018 URP Glidepaths for Nitrate (NO3) in extinction (Mm^{-1}) for Wichita Mountains (WIMO), Oklahoma and Worst 20% (W20%) days using 2002/2018 Base G CMAQ 36 km modeling results.

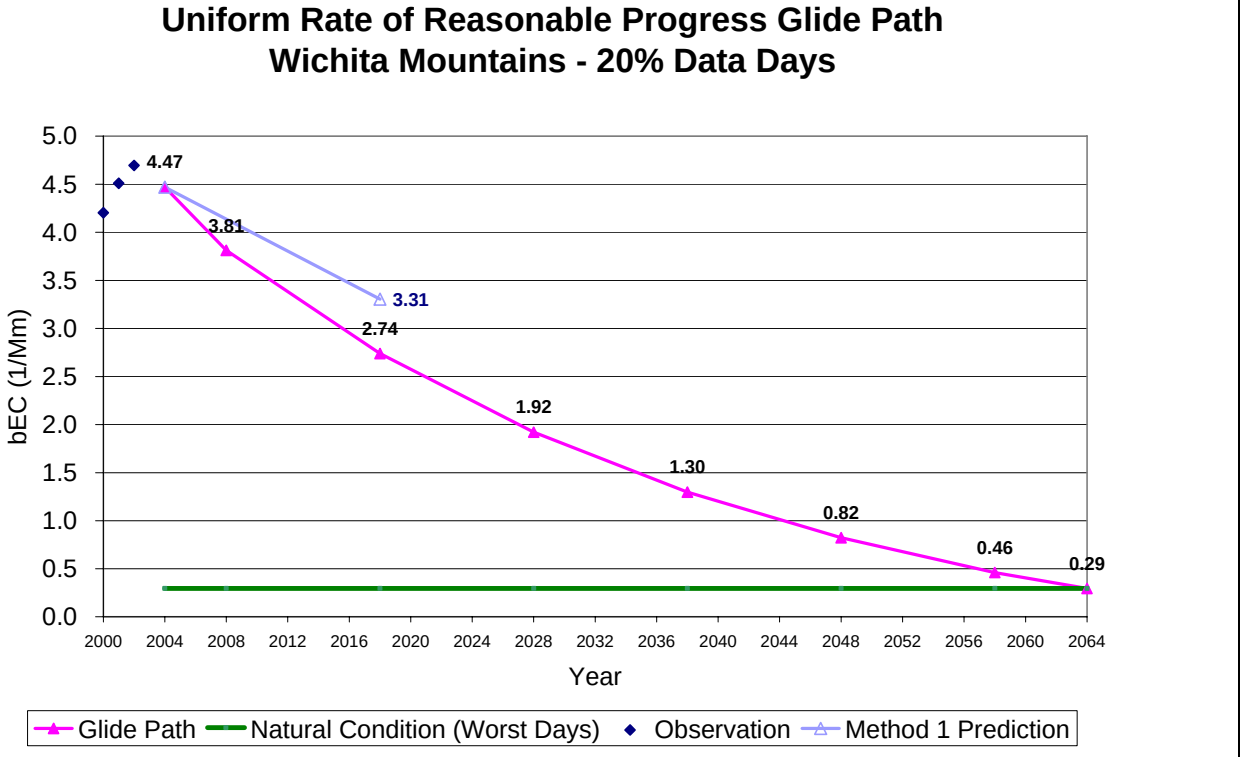

Figure F-8d. 2018 Visibility Projections and 2018 URP Glidepaths for Elemental Carbon (EC) in extinction (Mm^{-1}) for Wichita Mountains (WIMO), Oklahoma and Worst 20% (W20%) days using 2002/2018 Base G CMAQ 36 km modeling results.

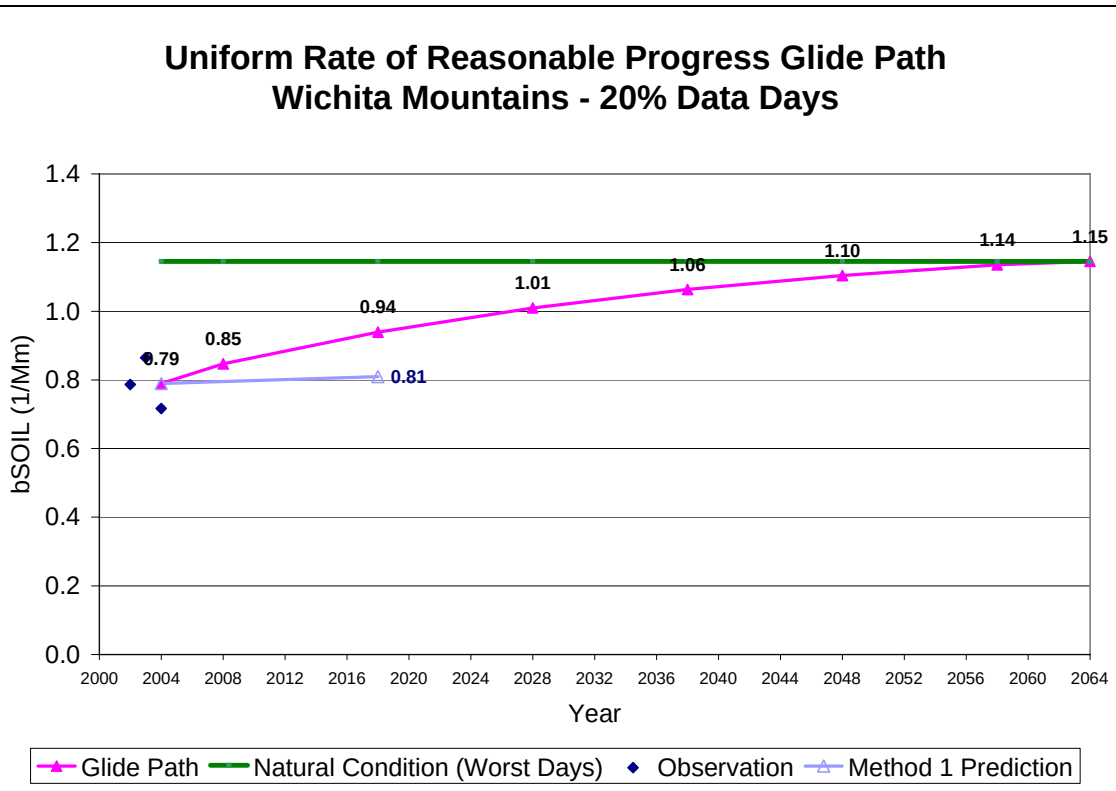

Figure F-8e. 2018 Visibility Projections and 2018 URP Glidepaths for Organic Mass Carbon (OMC) in extinction (Mm^{-1}) for Wichita Mountains (WIMO), Oklahoma and Worst 20% (W20%) days using 2002/2018 Base G CMAQ 36 km modeling results.

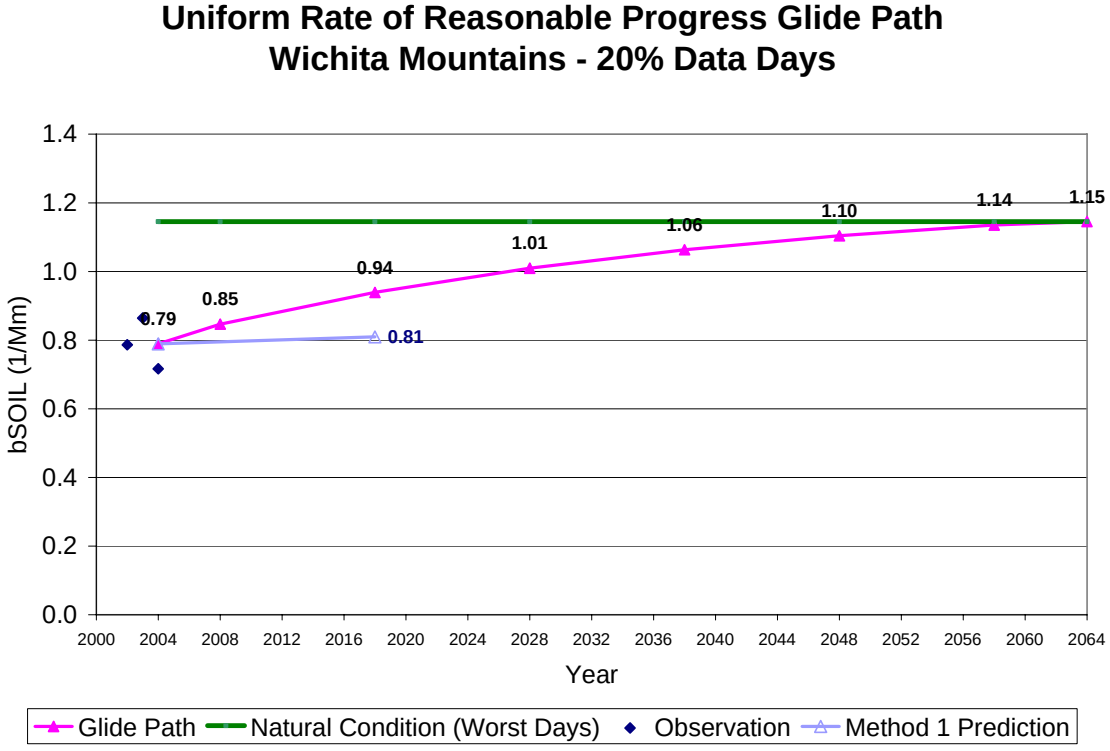

Figure F-8f. 2018 Visibility Projections and 2018 URP Glidepaths for Other Fine Particulate (SOIL) in extinction (Mm^{-1}) for Wichita Mountains (WIMO), Oklahoma and Worst 20% (W20%) days using 2002/2018 Base G CMAQ 36 km modeling results.

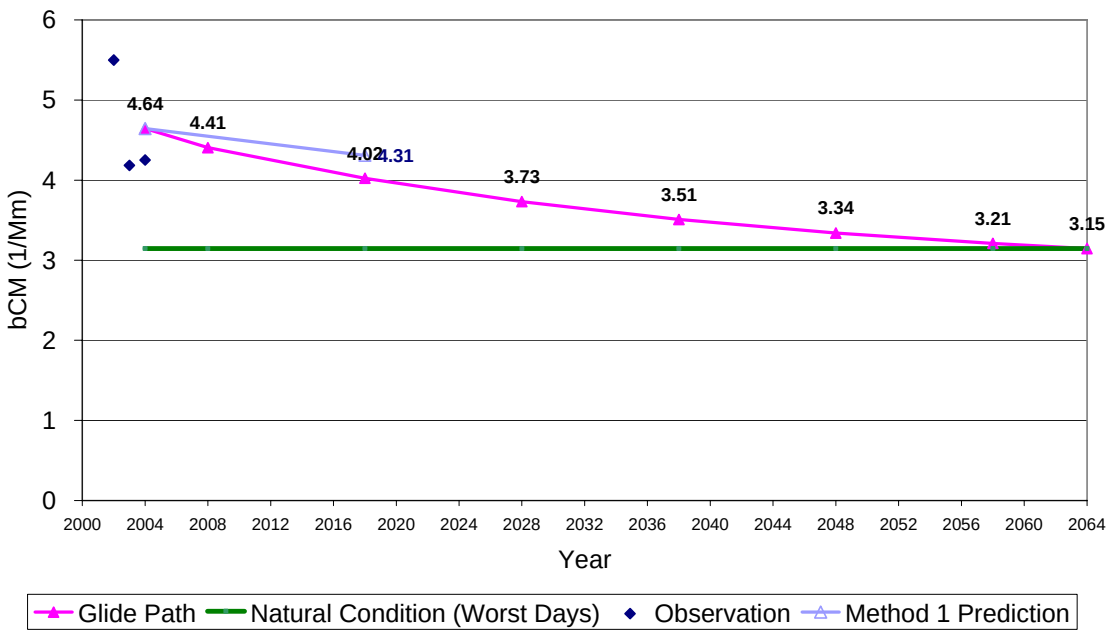

Figure F-8g. 2018 Visibility Projections and 2018 URP Glidepaths for Coarse Mass (CM) in extinction (Mm^{-1}) for Wichita Mountains (WIMO), Oklahoma and Worst 20% (W20%) days using 2002/2018 Base G CMAQ 36 km modeling results.

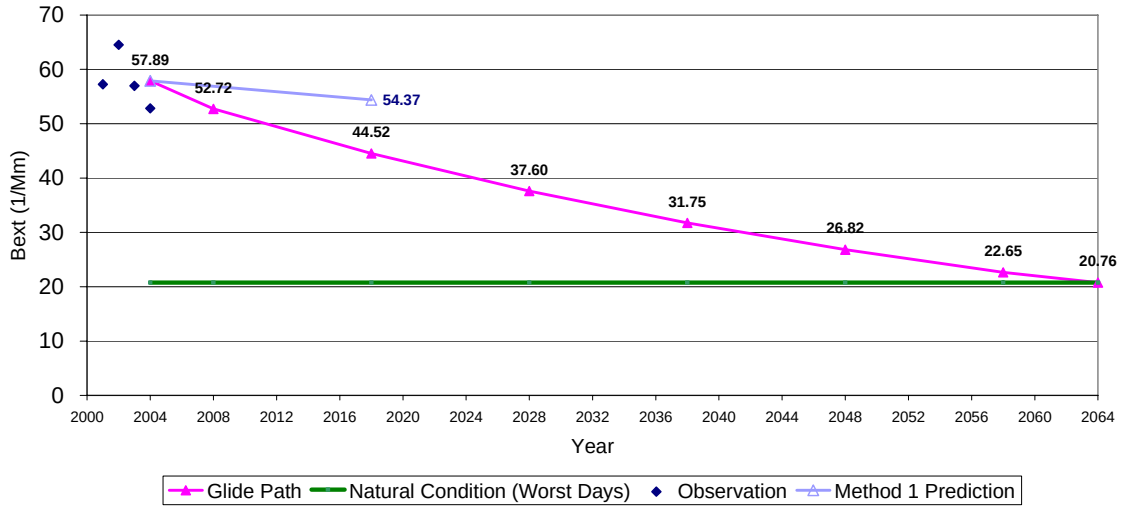

Figure F-9a. 2018 Visibility Projections and 2018 URP Glidepaths in extinction (Mm^{-1}) for Big Bend (BIBE), Texas and Worst 20% (W20%) days using 2002/2018 Base G CMAQ 36 km modeling results.

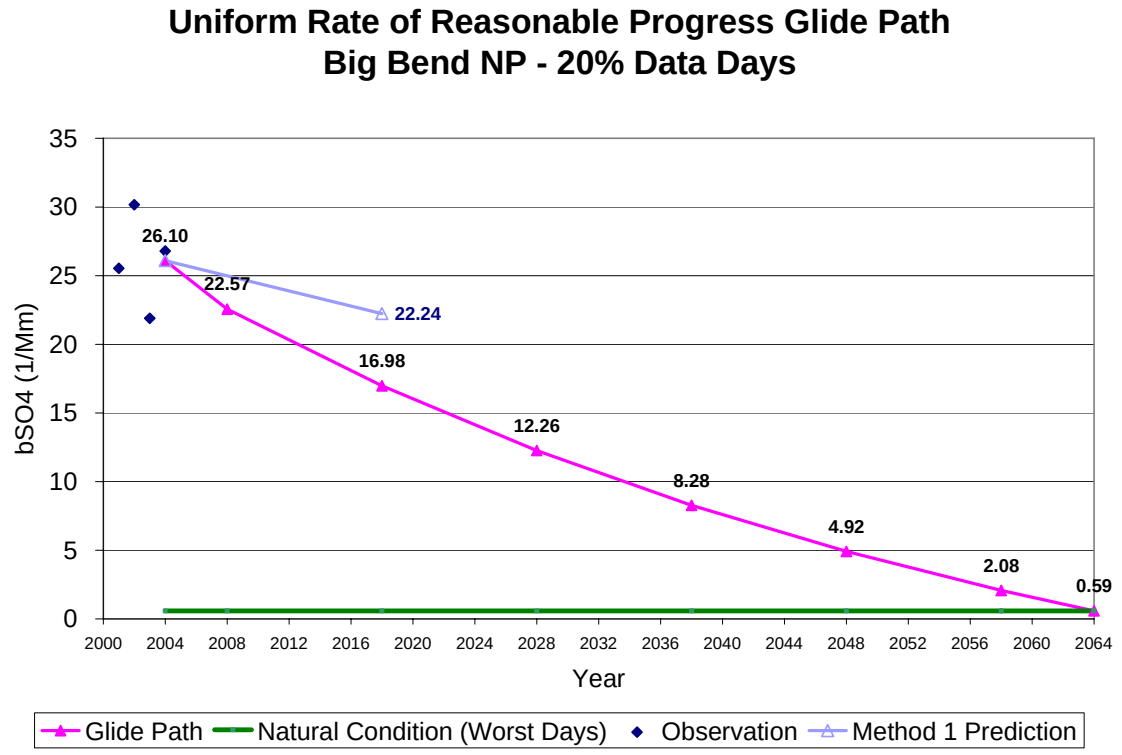

Figure F-9b. 2018 Visibility Projections and 2018 URP Glidepaths for Sulfate (SO4) in extinction (Mm^{-1}) for Big Bend (BIBE), Texas and Worst 20% (W20%) days using 2002/2018 Base G CMAQ 36 km modeling results.

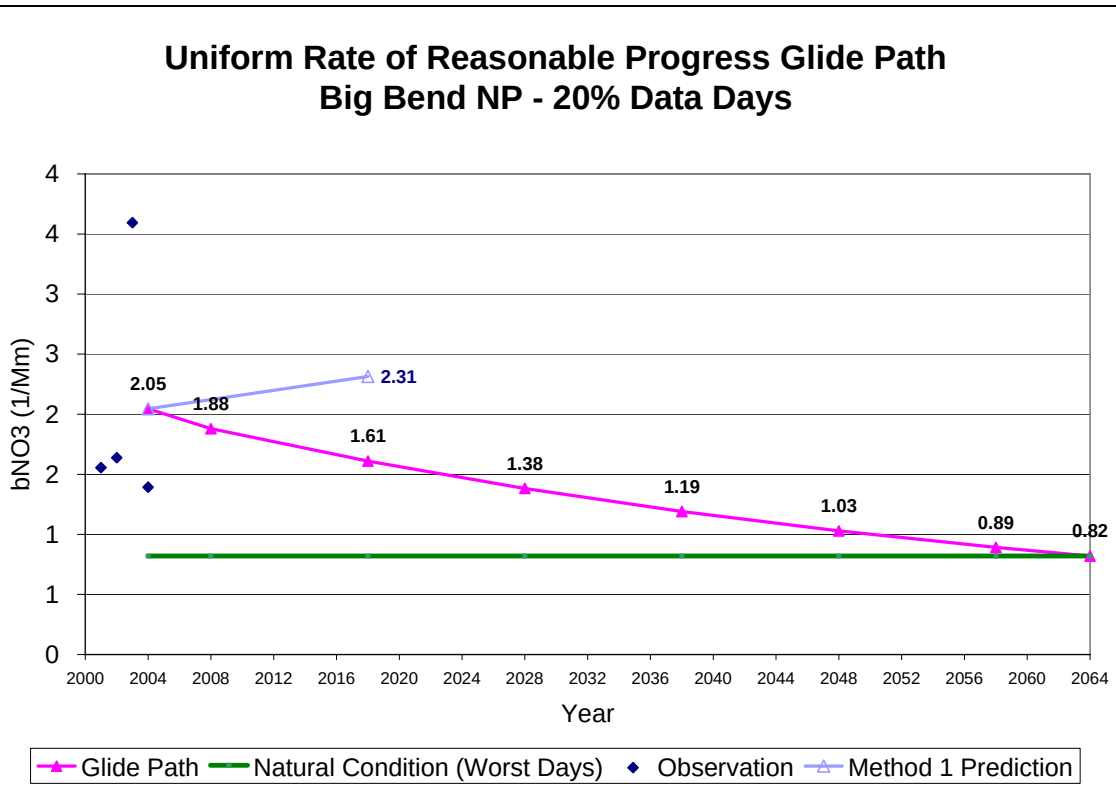

Figure F-9c. 2018 Visibility Projections and 2018 URP Glidepaths for Nitrate (NO3) in extinction (Mm^{-1}) for Big Bend (BIBE), Texas and Worst 20% (W20%) days using 2002/2018 Base G CMAQ 36 km modeling results.

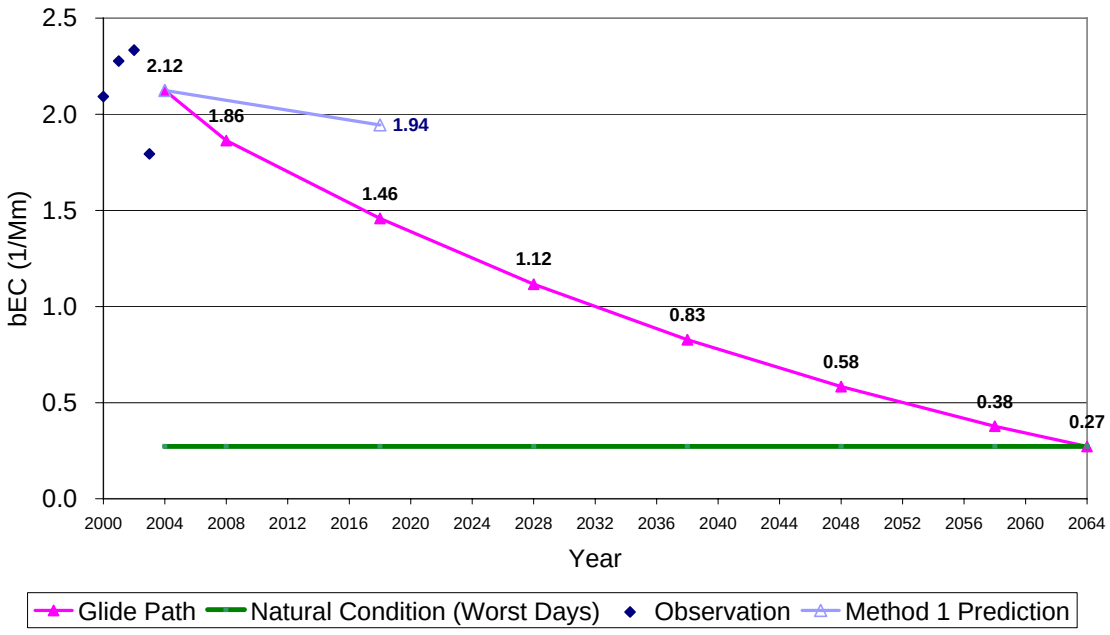

Figure F-9d. 2018 Visibility Projections and 2018 URP Glidepaths for Elemental Carbon (EC) in extinction (Mm^{-1}) for Big Bend (BIBE), Texas and Worst 20% (W20%) days using 2002/2018 Base G CMAQ 36 km modeling results.

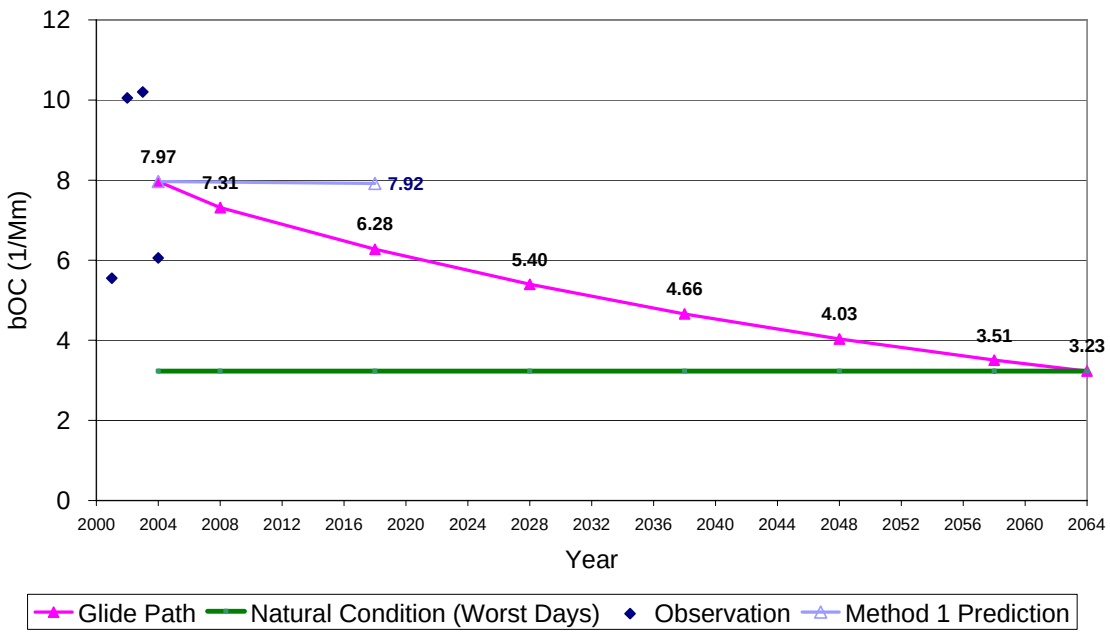

Figure F-9e. 2018 Visibility Projections and 2018 URP Glidepaths for Organic Mass Carbon (OMC) in extinction (Mm^{-1}) for Big Bend (BIBE), Texas and Worst 20% (W20%) days using 2002/2018 Base G CMAQ 36 km modeling results.

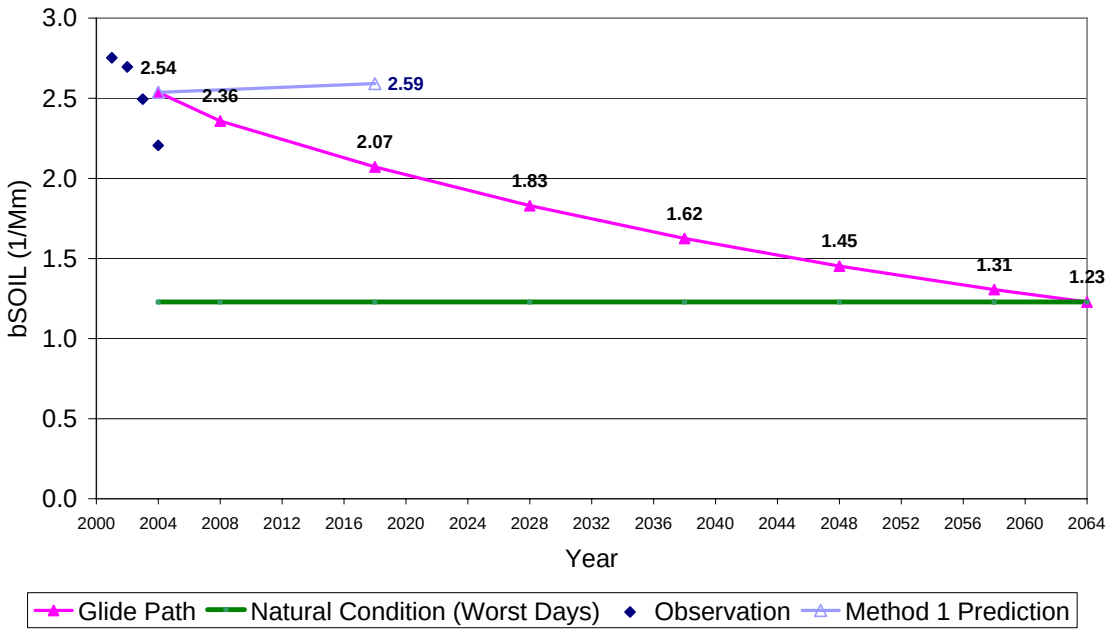

Figure F-9f. 2018 Visibility Projections and 2018 URP Glidepaths for Other Fine Particulate (SOIL) in extinction (Mm^{-1}) for Big Bend (BIBE), Texas and Worst 20% (W20%) days using 2002/2018 Base G CMAQ 36 km modeling results.

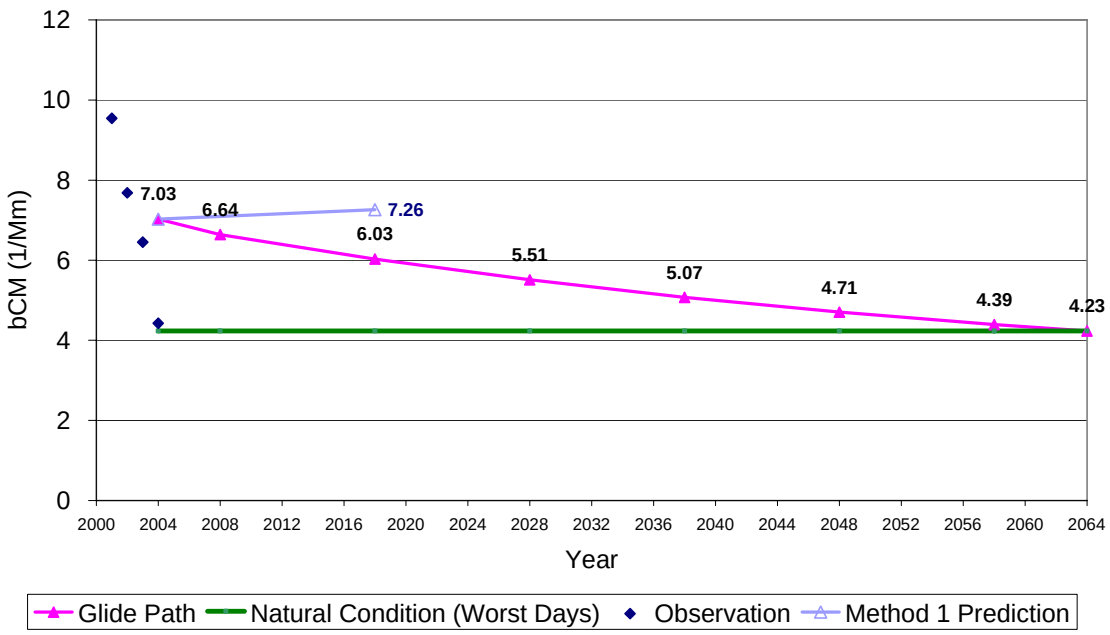

Figure F-9g. 2018 Visibility Projections and 2018 URP Glidepaths for Coarse Mass (CM) in extinction (Mm^{-1}) for Big Bend (BIBE), Texas and Worst 20% (W20%) days using 2002/2018 Base G CMAQ 36 km modeling results.

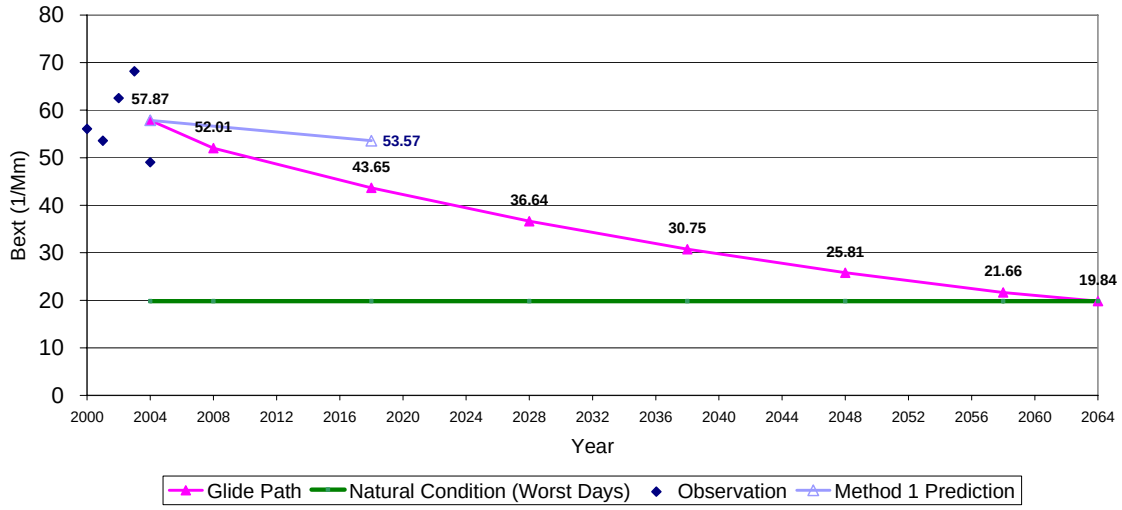

Figure F-10a. 2018 Visibility Projections and 2018 URP Glidepaths in extinction (Mm^{-1}) for Guadalupe Mountains (GUMO), Texas and Worst 20% (W20%) days using 2002/2018 Base G CMAQ 36 km modeling results.

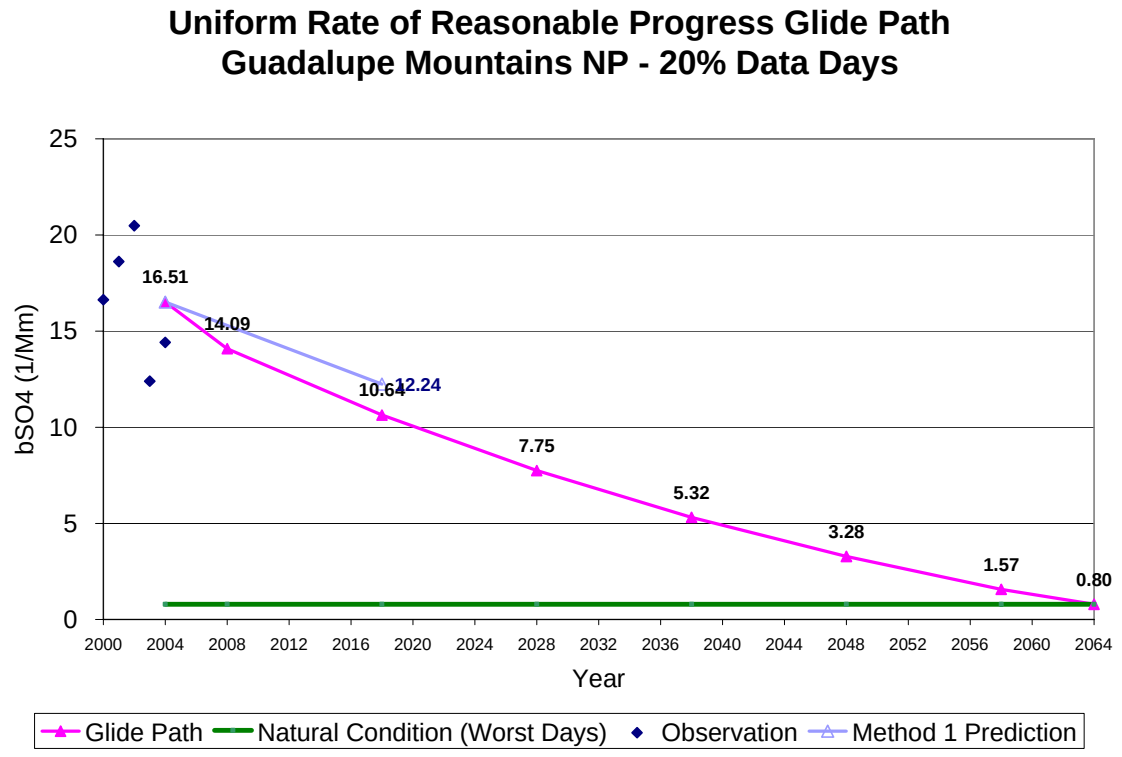

Figure F-10b. 2018 Visibility Projections and 2018 URP Glidepaths for Sulfate (SO4) in extinction (Mm^{-1}) for Guadalupe Mountains (GUMO), Texas and Worst 20% (W20%) days using 2002/2018 Base G CMAQ 36 km modeling results.

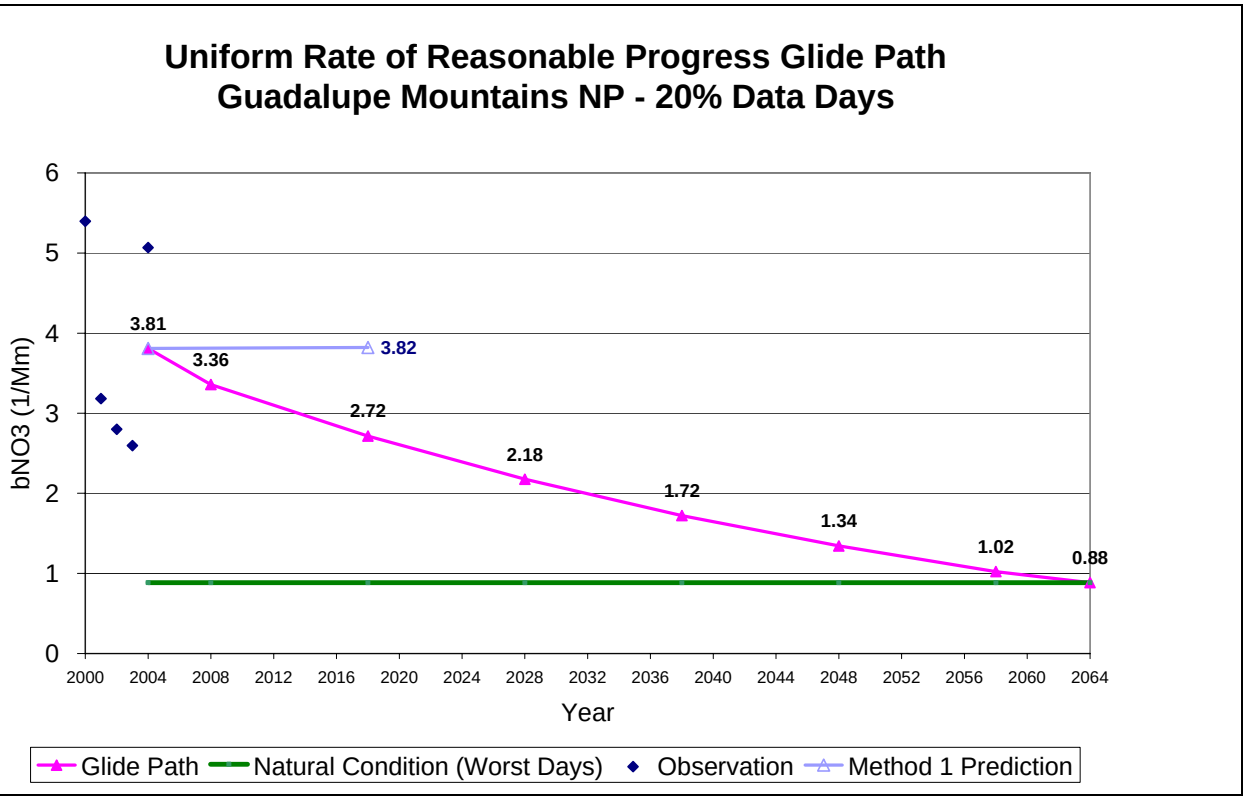

Figure F-10c. 2018 Visibility Projections and 2018 URP Glidepaths for Nitrate (NO3) in extinction (Mm^{-1}) for Guadalupe Mountains (GUMO), Texas and Worst 20% (W20%) days using 2002/2018 Base G CMAQ 36 km modeling results.

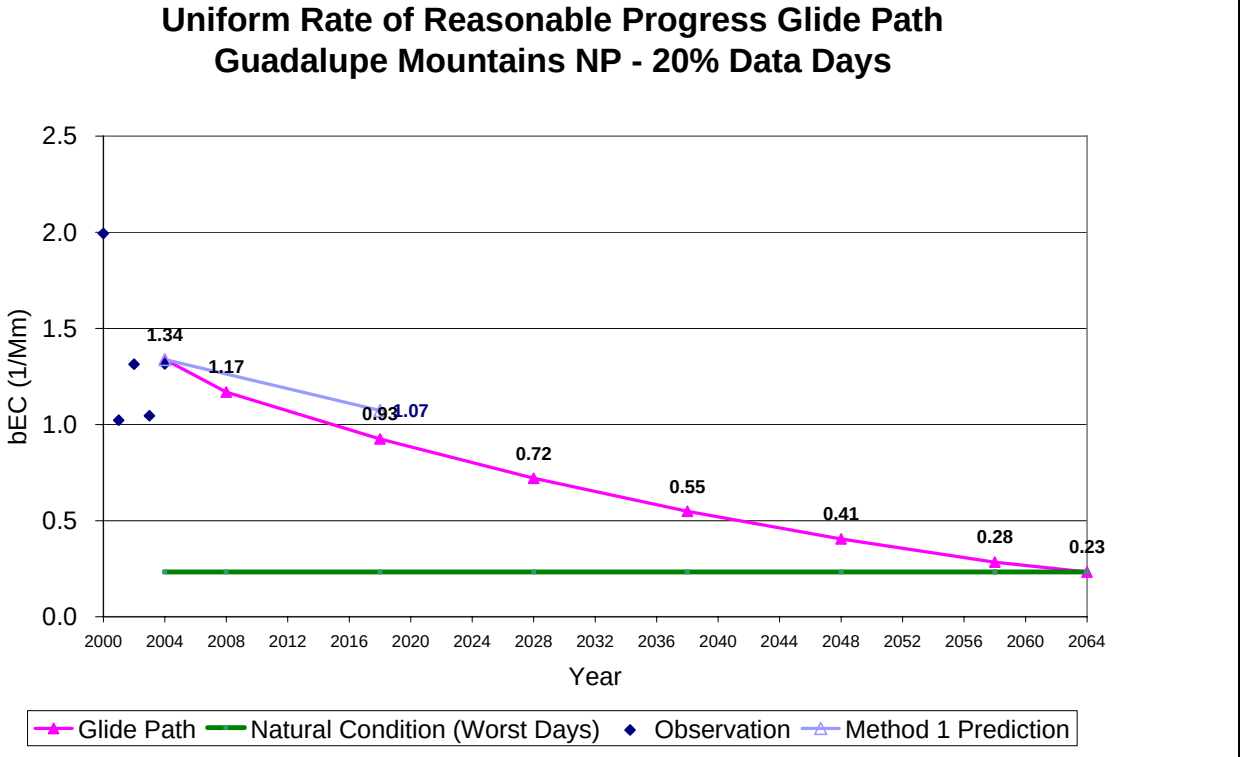

Figure F-10d. 2018 Visibility Projections and 2018 URP Glidepaths for Elemental Carbon (EC) in extinction (Mm^{-1}) for Guadalupe Mountains (GUMO), Texas and Worst 20% (W20%) days using 2002/2018 Base G CMAQ 36 km modeling results.

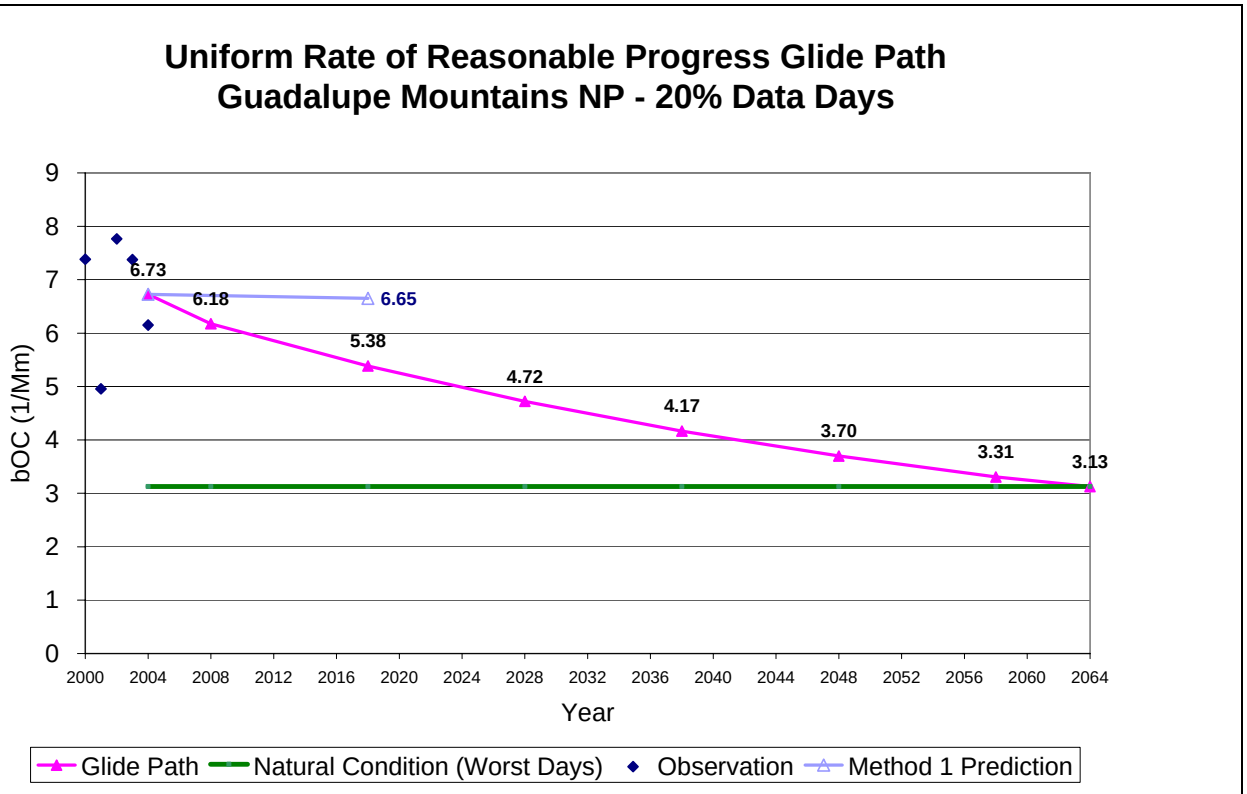

Figure F-10e. 2018 Visibility Projections and 2018 URP Glidepaths for Organic Mass Carbon (OMC) in extinction (Mm^{-1}) for Guadalupe Mountains (GUMO), Texas and Worst 20% (W20%) days using 2002/2018 Base G CMAQ 36 km modeling results.

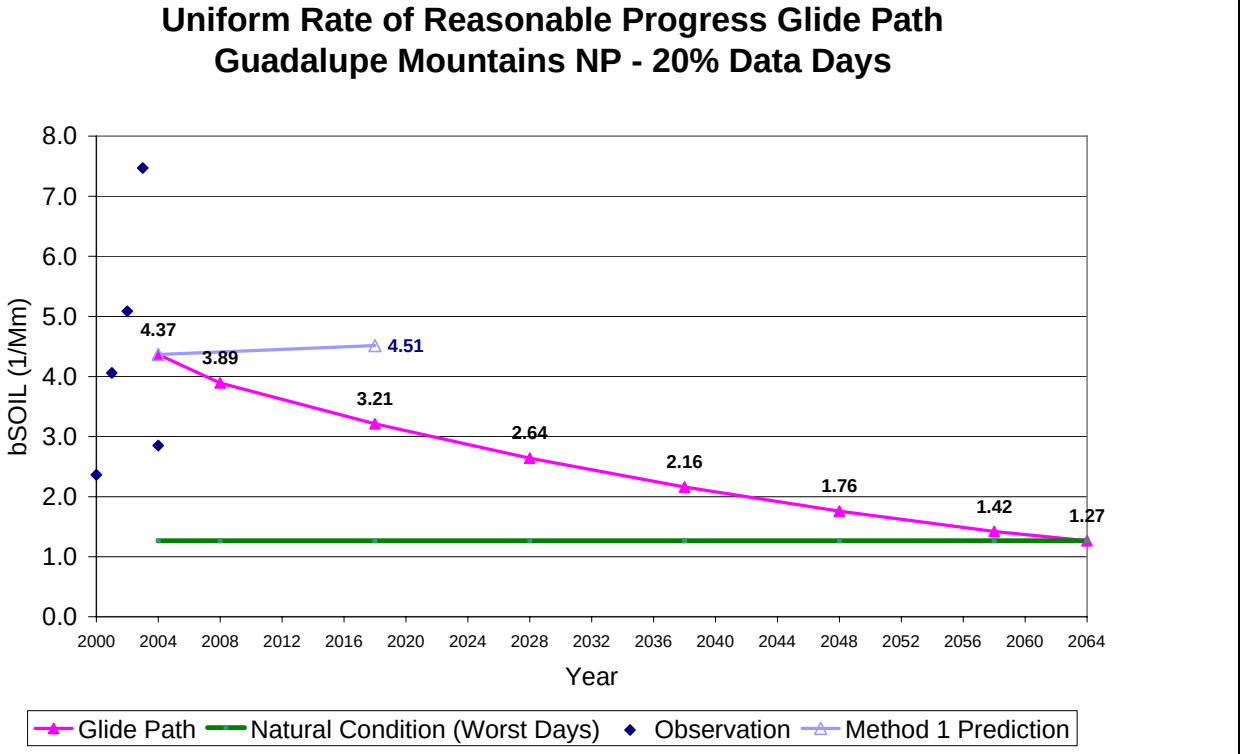

Figure F-10f. 2018 Visibility Projections and 2018 URP Glidepaths for Other Fine Particulate (SOIL) in extinction (Mm^{-1}) for Guadalupe Mountains (GUMO), Texas and Worst 20% (W20%) days using 2002/2018 Base G CMAQ 36 km modeling results.

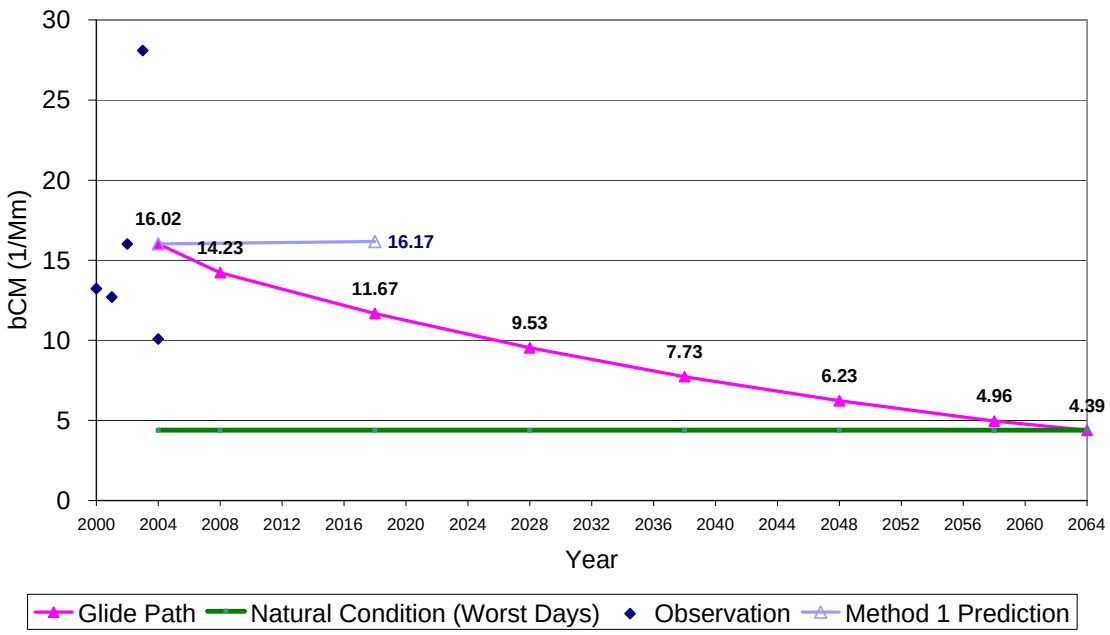

Figure F-10g. 2018 Visibility Projections and 2018 URP Glidepaths for Coarse Mass (CM) in extinction (Mm^{-1}) for Guadalupe Mountains (GUMO), Texas and Worst 20% (W20%) days using 2002/2018 Base G CMAQ 36 km modeling results.